Solar Signals – Possible correlations between the 11-Year Solar Sunspot Cycle and Earthquakes on Earth using the Fourier Transform

By Elizabeth C. Tyree

A Dissertation

Submitted to the Faculty

Of the

Worcester Polytechnic Institute

in fulfilment of the requirements for the

Degree of Masters of Science

In

Physics

August 2020

APPROVED:

_____

Professor Germano S. Iannacchione

_____

Professor Padmanabhan K. Aravind

_____

Professor David C. Medich

Acknowledgments:

I would like to thank and give my most sincere and deepest gratitude to my Advisor Germano S. Iannachione, my Mother Carmen, all of my family and closest friends, my spiritual family at the Cambridge Insight Meditation Center, who have all been on this long journey with me every step of the way. Thank you for your consistent and tireless support of me, this project, and my graduate journey. From the late night phone calls to bearing witness and supporting me through all of the ups and downs, and the countless moments along the way including the big, the small, the egregious, and the laughable ones; I thank you. A special thanks to my DSI Instructors, Outcomes Team, Fairy Godmother (you know who you are), Support and Frontlines Staff, and my Classmates at General Assembly Boston and East Coast Region. The tools I learned from you and endless encouragement have also helped to make this project possible. An extra special Thanks goes again to my Advisor Prof. Germano S. Iannacchione, I have no words to describe just how deeply grateful I am to you and how positively impactful to my life you have been. I am in your debt. Thank you!

EXECUTIVE SUMMARY:

Our understanding that the role sunspots play in earthquake activity remains both elusive and disputed. The hypothesis of this study is that the frequency and magnitude of earthquakes are influenced by changes in the slope of the solar sunspot cycle. Previous earthquake studies that have found sunspots and earthquakes to be uncorrelated, yet, in this study we will look for possible solar signals (periodicities) with respect to sunspots and the change in slope of the solar sunspot cycle using three global earthquake catalogs. Two catalogs are from the United States Geological Survey (USGS) including the Centennial Y2K Catalog, and the ANSS Comprehensive Earthquake Catalog (ComCat) and the Third catalog is the International Seismological Centre (ISC) catalog of earthquakes. Using statistical tools combined with signal analysis techniques such as the fourier transform, this study investigates if solar signals are contained in earthquake data. It is also the intent of this study to determine if earthquakes are correlated to the solar cycle, or at least help to provide another avenue for further study if the hypothesis of this thesis holds true.

Table of Contents

List of figures

List of Tables

Table 20: ISC, part 4 (Modern Era), 6 month averaged time series analysis results

Chapter 1: Introduction

Earthquakes are a powerful force of nature, that can cause a massive loss of life and property. Earthquakes range in intensity from the unnoticeable earthquakes that happen everyday globally to the massive and devastating that occur less frequently [1]. It is events like the 9.1 magnitude (Mw) Indian Ocean earthquake (a.k.a. the Sumatra earthquake) in 2004 [2] or the 9.2 Mw great Alaskan quake of 1964 [3] that have caused a great deal of damage and yet had very different outcomes in terms of loss of life. The Sumatra tsunami hit densely populated coastal areas in Indonesia, Sumatra, and parts of India causing over 230,000 people to be either dead or missing. This is very different compared to the Alaskan Earthquake and tsunami where only 131 people lost their lives [3]. This is because the Alaskan earthquake and tsunami did not affect densely populated areas like the Sumatra Earthquake. Fortunately the vast majority of earthquakes also will not trigger a tsunami, nor are they likely to be as large as these two. In fact, the vast majority of earthquakes are not even noticeable [1].

Although earthquakes are considered to be random and unpredictable [4], many continue to research ways to predict them [5, 6, 7]. It is important to continue to explore if earthquakes are influenced by other potential triggers, such as the solar sunspot cycle, even if the research into potential triggers may not lead to better earthquake prediction in the short term or near future. The continued research into potential earthquake triggers may still expand our understanding of earthquakes in ways not yet understood. What is understood is that there have been a number of studies examining various aspects of solar and/or space weather on earthquakes, including earth tides, lunar phases, solar wind, geomagnetic field, solar flares, climate change etc. [8, 9]. An

understanding of possible non-terrestrial influences on earthquakes however remains elusive. The hypothesis of this study is the frequency and magnitude of earthquakes on earth are influenced by changes in slope of the solar sunspot cycle, depending on which phase of the solar sunspot cycle the sun is in.

Mathematically, uncorrelated and statistically independent variables are orthogonal. If earthquakes are correlated to the slope (average number of sunspots/time) of the solar sunspot cycle, then that relationship may not necessarily be readily apparent. If earthquakes are related to the slope of the solar cycle, then they could be related but orthogonal like sin(x) and cos(x). If such a correlation were to exist, it would be informative and important to the field of earthquake science and prediction. Such a relationship would be suggestive of a solar (non-terrestrial) influence on earthquakes on earth even if a causal relationship is still unknown. The lack of historical data for global earthquakes of M7 or less is one of the challenges in attempting to determine if there is a possible correlation between earthquakes globally and changes in slope of 11-year solar cycle [10]. To overcome this and other differences including differences in time scales between sunspot indices and earthquake data, the investigation will also include converting earthquake magnitudes into an approximate total earthquake energy released globally per 2 days in Joules.

1.2 Literature Review

1.2.1 Sunspot Numbers

There are different types of solar and solar proxy data publicly available including solar irradiance, ice cores, sunspots, geomagnetic data, and solar flux. One of the most well known and established sources of solar data are sunspot records. When spectral analysis techniques are applied to sunspots or solar proxy data such as geomagnetic data, it is to identify periodicities contained within the data, or to investigate already known periodicities due to sunspot occurrence. However, the term ‘spectral analysis’ techniques when applied to earthquake data can mean something different. In the field of seismology, ‘spectral analysis’ can also refer to the spectral acceleration of an earthquake [11]. The terms ‘spectral acceleration’ is used to describe both the ground motion effects an individual earthquake has had on a structure, and the probability of another earthquake occurring in the future [12, 13]. When investigating solar periodicities within earthquake data, the terms ‘spectral analysis’ can also be confused with the ‘spectral analysis’ of earthquake body and surface waves which is something different [14]. This study will focus primarily on conducting spectral analysis of earthquake occurrence; Looking for solar like periodicities in earthquake data with each occurrence having equal weight using the Fourier transform.

To determine if there is a relationship between sunspots and earthquakes, it is important to understand what a sunspot is and what the solar periodicities (signals) contained in solar data are. A well-known solar signal contained in sunspot data is the 11-year solar sunspot cycle first noticed by Wolf in 1848 [15]. The 11-year sunspot cycle is half of the sun’s 22 year dynamo

cycle since every 11 years the sun undergoes a magnetic pole shift [16-18]. At the start of the 11-year solar sunspot cycle, there are few sunspots, which is known as the solar minimum. The sunspot cycle goes from solar minimum to maximum where there are the most observed counts of sunspot numbers per day and then back to minimum. A sunspot is a dark region on the surface of the sun where the sun's electromagnetic field is extremely active; so much so that the area becomes relatively cooler than the rest of the surrounding sun's surface [19]. While sunspots have been observed by many different cultures [20], it was Wolf who created a sunspot index and introduced it in 1848 [21][22]. Wolf described his sunspot number R_Z as,

$$R_Z = k(10g + n), \tag{1}$$

Where k is the observer correction factor for each observer, g is the number of sunspot groups identified, and n is the number of sunspots. Wolf's sunspot index (also known as the Zürich sunspot numbers) has been used extensively to study solar cycles since he introduced them [15]. However, Wolf's sunspot number is not the only measure of solar activity. Because Wolf's sunspot number had known irregularities for specific time periods, in 1998 Hoyt and Schatten introduced their group sunspot number R_G as an alternative to the Wolf sunspot number [23]. R_G is defined as,

$$R_G = \frac{1}{N} \sum_{i=1}^{N} k_i \, 12.08 g_i \,, \tag{2}$$

Where the number of observers is N, correction for the observer is k_i, and the number of sunspots the observer reported is g_i [21][23].

Irregularities during specific periods were not the only characteristic of using the Wolf sunspot numbers. Waldmeier in 1935 showed an inverse correlation between the rise time of the solar sunspot cycle and it's amplitude at peak sunspot number [24]. This inverse correlation is known as the Waldmeier effect [25]. It was Hathaway, Wilson, and Reichmann in 2002 who investigated if the Waldmeier effect was also present in Hoyt and Schatten' group sunspot numbers [21]. By investigating the Waldmeier effect in both Wolf numbers and group sunspot numbers Hathaway, Wilson, and Reichmann found that the effect was far weaker in the sunspot group numbers than in the Wolf numbers. The importance of the Waldmeier effect is that it has the potential to be used for solar cycle prediction [26]. However in 2008, Dikpati, Gilman, and De Toma who suggested that the Waldmeir effect may actually be an artifact of how Wolf defined his sunspot numbers in equation (1). They found that the Waldmeier effect is not at all present in sunspot area indexes and that, by smoothing both Wolf and the sunspot area numbers with a 13-rotation Gaussian running average, the Waldmeier effect remained in the Wolf's sunspot numbers with a correlation of $r = -0.71$, but was not in the sunspot area numbers with a correlation of $r = 10^{-4}$ [26].

Presently, Wolf numbers are called International Sunspot numbers [27], and there are at least two sources of official sunspot number data publicly available [28]. One source is the Solar Influences Data Analysis Center in Belgium providing the International Sunspot Numbers Version 2.0 (as revised in 2015). The other official source is the NOAA Sunspot numbers provided by the US National Oceanic and Atmospheric Administration [28].

1.2.2 Earthquakes

Earthquakes are caused when a crack in the earth's crusts releases elastic energy when the two sides of the crack slide past one another [29][30]. The crack in the earth's crust is referred to as a fault and the movement of a fault is called slip. The origin of the earthquake below ground is called a hypocenter and the point directly above the hypocenter on the earth's surface is the epicenter [31]. When an earthquake occurs, it releases energy in the form of heat due to friction, the breaking of rocks, and in the form of seismic waves known as body waves and surface waves [29]. Body waves travel through the earth's crust spreading from the hypocenter to the epicenter and come in two forms: primary (P) waves, also known as longitudinal or compressional waves and secondary (S) waves also known as shear or transverse waves [29][30][32]. When body waves reach the surface of the earth, some of them transform and become surface waves. There are two types of surface waves, Rayleigh and Love waves. In 1885, John William Strutt, 3rd Lord Rayleigh predicted earthquake surface waves [33]. A Rayleigh wave is a surface wave that rolls along the ground moving it up and down and rolling the earth like waves rolling on the ocean [30][34]. In 1911, a British mathematician Augustus Edward Hough Love discovered another type of surface wave called "Love waves" named after him [35]. Love waves travel from the epicenter in a transverse horizontal motion as they travel through the earth's surface.

Before Richter published what would later be known as the "Richter" scale also known as the "Gutenberg-Richter" scale, there were more subjective earthquake scales used to describe the intensity and destructiveness of an earthquake. Earthquake intensity is related to the impact of ground shaking on people, structures (such as buildings, cars, etc.), and the natural landscape

[34]; While earthquake magnitude is the amount of seismic energy released from the source of the earthquake [34]. With respect to intensity scales, distance from the epicenter is important. Thus an earthquake intensity scale measures the amount of damage caused by an earthquake with most damage being located around the epicenter. So one earthquake could be observed to have different amounts of damage depending on distance between the observer and the epicenter of the earthquake. This can result in an earthquake having more than one rating of intensity. An earthquake magnitude scale measures the size of the earthquake in the form of seismic energy released and is not dependent on the distance from the epicenter [29][34].

Intensity scales have been around for a very long time. The first known intensity scale was created by Italian physician Domenico Pignataro after a series of devastating earthquakes struck Reggio di Calabria, Italy from 1783 through 1786 [29]. Pignataro's intensity scale only had 5 levels of intensity: 'slight', 'moderate', 'strong', 'very strong', and 'violent' [29]. In general, intensity scales rely on the interpretations of human observers of an earthquake and the damage in its aftermath to determine the degree (or level) of earthquake intensity.

The first scale to be widely adopted was the Rossi-Forel scale (see Table # 1, on page # 20) [36]. Published in 1883, the Rossi-Forel scale had 10 degrees of intensity listed as roman numerals with 'I' for the lowest intensity and 'X' for the highest, and was a compromise between two independently created scales [36]. Italian seismologist Michele Stefano Conte de Rossi and Swiss Scientist (Limnologist) François-Alphonse Forel, had each created their own earthquake

intensity scales independent of each other; Rossi created his scale in 1874 and Forel in 1881 [36][37].

In 1902, Italian volcanologist Giuseppe Mercalli published his proposed changes to the Rossi-Forel scale in his book, “Sulle modificazioni proposte alla scala sismica De Rossi-Forel” [38]. This was actually Mercalli’s second intensity scale, his first was related to volcanos and was published in 1883, “Vulcani e fenomeni vulcanici in Italia” [36][39]. Mercalli’s changes to the Rossi-Forel scale in 1902 would be known as the Mercalli Scale. Soon after Mercalli, numerous people would make changes to and\or departures from the Mercalli scale in the creation of other scales. A few of the most notable changes were made by:

- Italian physicist, Prof. Adolfo Cancani in 1904, added two more categories to the Mercalli Scale expanding it from X to XII [40][41].
- German geophysicist, August Heinrich Sieberg in 1912 and 1923 completely rewrote the descriptions of the 12 degree Mercalli scale, overhauling them by greatly expanding them with more descriptive detail [36][41][42][43]. Sieberg’s changes to the scale became known as the Modified Mercalli scale (MM), Sieberg scale, and was also known as the Mercalli-Cancani-Sieberg (MCS) scale.
- American seismologists Harry Wood and Frank Neumann modified and refined the Sieberg scale in 1931. Wood and Neumann’s refinements to the scale (see Table # 1) were known as the Modified Mercalli Intensity scale of 1931 (MMI31) [44].

- Charles F. Richter would overhaul the MMI31 again in 1956, and published his new scale in his book Elementary Seismology in 1958 [45]. Richter added a series of building classes based on typography among other things, and his changes to the MMI31 are known as the Modified Mercalli scale of 1956 (MMI56) [36].

The MCS, MMI31 and MMI56 or variants of them are still in use today [36][43][47]. Intensity scales are no longer just used to characterize earthquake effects but are also used as a part of earthquake hazard prediction. Within the field of earthquake science there have been multiple earthquake intensity scales created and named ‘Modified Mercalli...’, not just the few mentioned herein. This has led to a lot of confusion and frustration surrounding the use of earthquake intensity scales. When reading reports using the Modified Mercalli scale it is not always clear which version of the scale is being used and referenced.

Table 1: Rossi-Forel scale and the Modified Mercalli Intensity Scale of 1931.

Degree #	Rossi–Forel scale [46]	Modified Mercalli Intensity Scale of 1931 (Abridged) [44]
I	Microseismic shocks recorded by a single seismograph, or by seismographs of the same model, but not putting seismographs of different patterns in motion; reported by experienced observers only.	Not felt except by a very few under especially favorable circumstances.
II	Shock recorded by several seismographs of different patterns; reported by a small number of persons who are at rest. "A very light shock."	Felt only by a few persons at rest, especially on upper floors of buildings. Delicately suspended objects may swing.
III	Shock reported by a number of persons who are at rest; duration or direction noted. "A shock;" "a light shock."	Felt quite noticeably indoors, especially on upper floors of buildings, but many people do not recognize it as an earthquake. Standing motor cars may rock slightly. Vibration like passing of truck. Duration estimated.
IV	Shock reported by persons in motion; shaking of movable objects, doors, and windows; cracking of ceilings. "Moderate;" "strong;" "sharp;" (sometimes) "light."	During the day felt indoors by many, outdoors by few. At night some awakened. Dishes, windows, doors disturbed; walls made cracking sound. Sensation like heavy truck striking building. Standing motor cars rocked noticeably.
V	Shock felt generally by every one ; furniture shaken; some bells rung; some clocks stopped; some sleepers waked. "Smart;" "strong;" "heavy;" "severe;" "sharp;" "quite violent."	Felt by nearly everyone; many awakened. Some dishes, windows, etc., broken ; a few instances of cracked plaster ; unstable objects overturned. Disturbance of trees, poles and other tall objects sometimes noticed. Pendulum clocks may stop.
VI	General awakening of sleepers; general ringing of bells; swinging of chandeliers; stopping of clocks; visible swaying of trees; some persons run out of buildings; window-glass broken. "Severe;" "a very severe;" "violent."	Felt by all ; many frightened and run outdoors. Some heavy furniture moved; a few instances of fallen plaster or damaged chimneys. Damage slight.
VII	Overturning of loose objects; fall of plaster; striking of church bells; general fright, without damage to buildings. " Nausea felt;" "violent;" "very violent."	Everybody runs outdoors. Damage negligible in buildings of good design and construction; slight to moderate in well-built ordinary structures; considerable in poorly built or badly designed structures ; some chimneys broken. Noticed by persons driving motor cars.

Table 1 Continued: Rossi-Forel scale and the Modified Mercalli Intensity Scale of 1931.

Degree #	Rossi–Forel scale [46] (Continued.)	Modified Mercalli Intensity Scale of 1931 (Abridged) [44] (Continued.)
VIII	Fall of chimneys; cracks in the walls of buildings.	Damage slight in specially designed structures; considerable in ordinary substantial buildings with partial collapse; great in poorly built structures. Panel walls thrown out of frame structures. Fall of chimneys, factory stacks, columns, monuments, walls. Heavy furniture overturned. Sand and mud ejected in small amounts. Changes in well water. Disturbed persons driving motor cars.
IX	Partial or total destruction of some buildings.	Damage considerable in specially designed structures; well designed frame structures thrown out of plumb; great in substantial buildings, with partial collapse. Buildings shifted off foundations. Ground cracked conspicuously. Underground pipes broken.
X	Great disasters; overturning of rocks; fissures in the surface of the earth; mountain slides.	Some well-built wooden structures destroyed; most masonry and frame structures destroyed with foundations; ground badly cracked. Rails bent. Landslides considerable from river banks and steep slopes. Shifted sand and mud. Water splashed (slopped) over banks.
XI	N/A	Few, if any (masonry), structures remain standing. Bridges destroyed. Broad fissures in ground. Underground pipe lines completely out of service. Earth slumps and land slips in soft ground. Rails bent greatly.
XII	N/A	Damage total. Waves seen on ground surfaces. Lines of sight and level distorted. Objects thrown upward into the air.

In 1995, R. M. W. Musson, G. Grunthal, and M. Stucchi opined about this confusion in their paper, “Comment on ‘The 17 August 1991 Honeydew Earthquake: a Case for Revising the Modified Mercalli Scale in Sparsely Populated Areas’ by Dengler and McPherson”.

> “The use of the phrases "Mercalli scale" and "Modified Mercalli scale" is becoming hopelessly confused. So far as we are aware the following variants are in print: Wood and Neumann (1931, two versions), Richter (1958), Eiby (1965), Brazee (1978), Principia (1982), NZSEE (1991), and now Dengler and McPherson (1993)--eight different scales, all claiming to be "Modified Mercalli," all quite different and none resembling the actual work of Mercalli. This confusion needs to be ended.”
> -R. M. W. Musson, G. Grunthal, and M. Stucchi [48]

Even though intensity scales may have similarities between them, their subjective nature at times can make it hard to reliably convert an intensity rating for an earthquake from one scale into that of another scale [43]. There is no universal earthquake intensity scale in use today and sadly the same is true for earthquake magnitude, albeit for different reasons. As mentioned earlier, earthquake magnitude is a measurement of the earthquake’s size in the form of seismic wave energy released. Seismic waves only make up about 1% to 10% of the energy an earthquake releases [32]. Unlike earthquake intensity, magnitude is an empirical based calculation on a logarithmic scale [32]. In general, when the media is speaking to the public about an earthquake event, earthquakes are commonly reported as being on the Richter scale, named after its creator Richter who first proposed it in 1935 [49][50]. When Richter later created the MMI56 he also wanted to name it the ‘Richter scale’ but didn’t because it would cause confusion [36].

The Richter scale is also known as local magnitude ($\mathbf{M_L}$) because it was defined for earthquakes located in southern California that were recorded using a Wood-Anderson seismograph which had a limited range of about 1000km [29, 30]. Local magnitude could not be applied to earthquakes that occured at teleseismic distances (> 1000km) away from the

seismograph. Ricter's magnitude formula uses the difference in arrival times between the P and S waves, along with the max amplitude of the S-wave (measured in thousandths of a millimeter) on the seismograph to calculate an estimated magnitude (size) of an earthquake [29][32]. Thus Richter defined his scale based on the amplitude of ground motion displacement of an earthquake [32].

With respect to earthquake magnitude, the field of seismology has since mostly moved away from using the Richter scale in favor of other ways of calculating the size of an earthquake [51]. Today, like intensity scales, Richter magnitude $\mathbf{M_L}$ is still calculated for some earthquakes and used in earthquake hazard analysis [32].

When an earthquake occurs the total energy released causes heat from friction, the cracking of rocks, and the generation of seismic waves [29][30][32]. There is no one scale that can describe the overall depth and complexity of an earthquake event or the total energy released during an earthquake [30][51][50]. Therefore the magnitude of an earthquake is only an estimated means of quantifying the size of an earthquake based on the measurement of seismic waves [50]. Unfortunately not all magnitude scales represent or describe the same aspects of an earthquake with respect to seismic waves [52]. This along with changes in technology and the development of new scales, can sometimes lead to difficulty in comparing the magnitude of earthquakes that occur in different geographical locations and/or are measured using different magnitude scales [51].

The purpose of Richter's local magnitude in 1935 was to provide an objective energy measurement for earthquakes in southern California as listed by the Seismological Laboratory in Pasadena [50]. Richter's local magnitude was never applicable to earthquakes of all sizes in all locations [29]. Regardless, the local magnitude scale served as the basis for all other magnitude scales created after it [50]. Each scale attempts to address or overcome the shortcomings of previous scales [52]. In 1945, German-American Seismologist Beno Gutenberg in a series of papers proposed extending the magnitude concept to include maximum body and surface-wave amplitude measurements at teleseismic distances [53, 54, 55]. Gutenberg was Richter's colleague and a collaborator at California Institute of Technology [56][57]. Their work from 1945 through 1956 resulted in the creation of two new magnitude scales based on teleseismic observations of earthquakes made by Gutenberg and Richter [50][58][59]. The two new scales were surface-wave magnitude ($\mathbf{M_S}$) and body wave-magnitude ($\mathbf{m_B}$). Gutenberg and Richter considered all three scales $\mathbf{M_L}$, $\mathbf{M_S}$, and $\mathbf{m_B}$ to be equal to one another initially [53, 54, 55]. After further analysis it was acknowledged that there were differences in the results each scale gave and in 1955 in Gutenberg and Richter's second paper that year they provided empirical relations for converting between them [60].

As the use of $\mathbf{M_L}$, $\mathbf{M_S}$, $\mathbf{m_B}$, and variations of them expanded there was also an already existing need for more quality seismological data for research [61]. The need for more seismological understanding and research combined with the need to detect and identify underground nuclear explosions, led to the conception of a global seismic network in the 1959 meeting at the Panel of Seismic Improvement [62]. Created in the early 1960's with the support

of the United States Department of Defense, the World-Wide Standardized Seismograph Network (known as WWSSN) formally launched in 1964 with over 120 new seismograph stations [61, 62, 63]. The WWSSN was supported by Project Vela Uniform, a research program managed by the Defense Advanced Research Projects Agency (DARPA) [61]. The purpose of the WWSSN was not to servale underground nuclear explosions but was to increase seismological research, but having the support of the US Military made it initially hard for some to believe the intentions of the WWSSN were purely for research purposes [62].

Before the 1960's $\mathbf{m}_B$ was determined using longer-period instruments with periods ranging from 0.5s to 12s, but after WWSSN was implemented how $\mathbf{m}_B$ was determined changed [51][52]. The WWSSN separated the frequency spectrum into two bands (short-period and long-period), and used a period of 0.75s on the shorter-period instruments to reduce the background noise due to microseisms generated by ocean waves having periods ranging from 3 to 9 seconds [52] [62]. Even though the equation to calculate body-wave magnitude did not change, the result was that earthquake $\mathbf{m}_B$ magnitudes based on the older longer-period instruments to be about 0.3 to 0.6 units higher than the new WWSSN body-wave magnitudes denoted as $\mathbf{m_b}$ with a period of 0.75s [52]. By the 1970's the WWSSN combined with previous seismic networks had increased earthquake detection from about 1000 events a year pre-WWSSN to over 5000 events per year [62].

Even though $\mathbf{m_b}$ was adopted widely and mostly replaced $\mathbf{m_B}$ after WWSSN was launched, $\mathbf{m_B}$ was still used in the former Soviet Union, China, and in a lot of eastern European countries [64]. The WWSSN was instrumental in greatly expanding the reach and access to

seismological data and research, and yet the predominate earthquake magnitude scales of local magnitude ($\mathbf{M_L}$), body-wave ($\mathbf{m_b}$), and surface-wave scales ($\mathbf{M_S}$) and those created later that were based on them were not without their limitations. All three magnitude scales saturate for above certain magnitudes as shown in Table # 2, and fail to accurately provide magnitude values for very large earthquakes (M > 8) [65].

Table 2: List of common earthquake magnitude scales with respective periods and saturation limits.

#	Magnitude Scale	Saturation	Period (s)	References
1	$\mathbf{M_L}$	M > 6.5	0.1 - 3	[51], [32]
2	$\mathbf{M_S}$	M > 8	~ 20	[51], [32]
3	$\mathbf{m_B}$	M > 8	0.5 ~ 12	[51], [66]
4	$\mathbf{m_b}$	M > 7	0.75	[32], [62]
5	$\mathbf{M_W}$	N/A	10 - ∞	[51]

Separately, $\mathbf{m}_B$ values for one earthquake could vary from station to station not just due to differences in instrumentation type, but also could be due to a variety of other factors including but not limited to failing to apply local station corrections, magnitude scales being based on different source parameters, regional geological differences in the earth's crust, fault type (dip slip vs strike slip), etc. [52]. For example, Chung and Bernreuter in their paper from 1980 discussed how a $5\mathbf{m}_B$ earthquake on the east coast of the United States of America (USA) is not equal to a $5\mathbf{m}_B$ on the west coast of the USA [52]. Even though both of these earthquakes are calculated to be $5\mathbf{m_B}$, the east coast USA earthquake is actually larger in magnitude than the west coast earthquake by about $\Delta\mathbf{m_B} \simeq ⅓$ due to regional differences in the upper mantle of the earth's crust [52]. The earthquakes that occur on the west coast of the USA are more attenuated

than on the east coast due to this. Chung and Bernreuter explained in some detail how certain types of regional differences in the United States can impact earthquake magnitude calculations for $\mathbf{M_L}$, $\mathbf{M_S}$, $\mathbf{m_B}$, and a few others. While both $\mathbf{M_S}$ and $\mathbf{m_B}$ were meant to be used universally, the limits of these scales can lead to considerable error if used in that way [52]. Similarly, Bormann and Di Giancomo pointed out in 2011, since the creation of $\mathbf{M_S}$ and $\mathbf{m_B}$ there have been numerous magnitude scales created after them, and while some are based on them, these other scales are measured with different bandwidth and period ranges and often have been based on "incompatible procedures" [66][67][68].

The closest thing to a universal earthquake magnitude scale currently in use is the Moment Magnitude scale ($\mathbf{M_W}$). The $\mathbf{M_W}$ scale is based on moment magnitude $\mathbf{M_O}$ which is defined as the product of the fault displacement and the force causing the fault displacement [32]. First introduced by Hiroo Kanamori in 1977 in his paper, "The Energy Release of Great Earthquakes" [69][32]. Shortly thereafter Thomas C. Hanks and Kanamori in 1979 and Kanamori again in 1983, refined $\mathbf{M_W}$ further. Bormann and Di Giancomo also commented that the $\mathbf{M_W}$ scale is often considered to be the only physically well defined, non-saturating magnitude scale [66]. Because of this and the limitations of magnitude scales in general, it has become widespread practice to convert local and teleseismic magnitudes into the $\mathbf{M_W}$ scale [66][70]. Since it is not always possible to convert directly from one magnitude scale to another, often scales are converted by using some form of empirical regression [66][70][71]. However, this approach is not suitable for all research purposes as explained in the next section [66].

1.2.3 The Historical Period vs. The Modern Era of Earthquake data

The limitations of earthquake magnitude scales are not self-evident nor intuitive. Seismologists tend to acknowledge how confusing the science and nomenclature can be [48][52][72]. When it comes to utilizing earthquake catalogs for analysis, there are many considerations one might think about when handling the magnitude data. The WWSSN was in operation from 1964 with 13 digital stations (DWWSSN) by the 1970's until both were replaced by the Global Seismographic Network (GSN) in 1986 [73]. The GSN continues to operate to this day [73].

The impact that the WWSSN had on seismological research and earthquake magnitude data has been profound [74]. With respect to earthquake data, the pre-WWSSN period before 1964 is often referred to as the historical period, and the time after 1964 when the WWSSN was launched as the modern period [75][76]. As stated earlier, the WWSSN greatly helped to increase earthquake detection. As a result, the increasing number of earthquakes over time contained in many earthquake catalogs are due to advances in technology [77][78][79][80]. The USGS has a page on their website, "Why are we having so many earthquakes?..." acknowledging the increasing earthquake trend contained in their ComCat earthquake catalog, used in this study, is due to advances in technology [81]. While the USGS did not specifically mention the increase of seismograph stations in its online explanation in print, the USGS does mention it in the audio recorded version of, "Why are we having so many earthquakes?..." [77]. The British Geological Survey also addresses this topic on their website [79]. Love and Thomas in 2013 (citing Engdahl and Villasenor, 2002 [75]) also pointed out that that there was an excess of $7.0 \leq M < 7.5$

earthquakes contained in the historical period of the USGS National Earthquake Information Center database, and that this increase was thought to be non-geophysical [82][75]. When looking at both the historical and modern periods combined from 1900 to the present, most catalogs may only be complete for earthquakes above 7.5M and larger [75]. Love and Thomas also mentioned that the USGS dataset was biased towards smaller earthquakes but that pertained to the modern era [82]. Utilizing data from only after the WWSSN was launched was something Stein, Okal, and Wiens in their 1988 paper, "Application of Modern Techniques to Analysis of Historical Earthquakes", warned against doing, for not using data from both the historical and modern periods could lead to "erroneous results" [83]. Stein et al, mentioned this in their paper because in the years after the WWSSN was launched, some researchers started to only use data only from after the early 1960's and ignored data from the historical period [83]. The scientific details of most earthquake events pre-WWSSN are not well known due to the limitations of technology available at the time those earthquakes occurred [75]. However there is ongoing work to make earthquake catalogs more complete by adding more sources of earthquake epicenter and magnitude information.

When looking at earthquake catalogs it is not uncommon to find numerous different earthquake magnitudes reported using different earthquake scales. Global catalogs can contain earthquakes from various seismic networks both global and regional and are reported on a variety of magnitude scales. Each magnitude scale has its own range of validity, usefulness, and limitations. While some researchers choose to convert earthquake magnitudes into a single scale, this approach is considered too simple when evaluating earthquake hazards [66]. Another

approach sometimes employed within earthquake catalogs and research is to use a scheme of complementary magnitudes where certain magnitudes are preferred over others based on a set of criteria and modern measurement techniques [66][75][84]. This practice of reporting multiple magnitudes but having a prefered magnitude allows researchers to investigate certain seismic hazards, and depending on the magnitude scale, depth, and earthquake size, some scales are near equivalent to each other in certain situations. For example, $\mathbf{M_W}$ and $\mathbf{M_S}$ can both be used for shallow < 60km earthquakes [75].

1.2.4 Sunspots & Earthquakes

There has been a very long standing interest and curiosity about the relationship between sunspots and earthquakes. In 1920, H. H. Turner, identified two periods of earthquake occurrence to be 14.8 months and 78 years respectively [85]. Turner claimed the two earthquake periods were related to the solar cycle using sunspot data, earthquake data from a catalog of destructive earthquakes, and a catalog of Chinese earthquakes. There have been many conflicting reports about earthquakes being correlated or influenced by solar or lunar effects. For example, in 1964 Knopoff and later Simpson in 1967 investigated earth tides as a possible triggering mechanism for earthquakes. Yet both found no correlation between the two[86][87]. At the time, Knopoff used Fourier analysis where each earthquake occurrence had equal weight and a data set containing 24 years of earthquakes from 1934 to 1957 from the Pasadena, CA earthquake network. Simpson used earthquake data from January 1950 through June 1963. Later in 1972, Shlien repeated Knopoff's analysis, this time with respect to semidiurnal tides and found a

possible tidal effect on earthquakes but only specifically in the year of 1966 and only for the South-Western United States and Tonga Japan [88].

Some studies will try to look for evidence of lunar or solar influences on earthquakes by either focusing on earthquakes globally, focusing on a specific region on earth, or both. In 1986, Palumbo proposed an adjusted Chapman-Miller method for determining lunar and solar daily components of earthquakes [89][90]. Palumbo focused on the Italian Peninsula for earthquakes from 1900 to 1983 ($M \geq 5$, where M = Magnitude) and compared the results with earthquakes globally, concluding that there were tidal (lunar) influences present but only for earthquakes on the Italian Peninsula. Palumbo could not find evidence of lunar tidal effects on earthquakes globally. In 1999, Shaltout, Tadros, and Mesiha also focused their investigation on both North African and earthquakes globally. Using a power spectra analysis and Kalman filter on the spectra, they found solar like signals of 1.01 years and 5.5 years in both global ($M \geq 5$) and in the North African earthquake data ($M \geq 5$, Cairo, Egypt & $M \geq 4$ Alger, Algeria) [14]. They also found a an 11 year signal but only in the North African data [14]. Both Palumbo and Shaltout, Tadros, and Mesiha used global earthquake datasets and did not find the same results when compared regionally.

When looking at more recent research into the solar or lunar triggering of earthquakes, this lack of agreement widens. In 2004, Cochran et al, found a correlation between shallow-dipping thrust earthquake events and strong earth tides [91]. Cochran found this correlation by calculating a tidal-stress time series for earthquakes and tested the significance of

their results using both Schuster's test and a binomial test. Two years after Cochran, Odintsov et al [92], found an increase in earthquake activity during solar maximums for years 1900 to 1999 than during lower solar activity for earthquakes $M \geq 7$ for both the Gleissberg and 11-year solar cycles. Odintsov used a Student's t-test to test the significance of their results and claimed to have a significant p-value of less than 0.05. Odintsov also found the variations in seismic activity relative to solar activity are the same as the variations in geomagnetic activity and concluded the factors influencing them both were probably the same. In 2012, Chen, Chen, and Xu did not find any correlations between lunisolar tides and earthquakes, but did however find a correlation between the 2011 Christchurch, New Zealand earthquake sequence and solid tides [93]. Chen et al also found the larger Christchurch aftershocks were mainly triggered by semidiurnal solid tides; and found for earthquakes worldwide since 1900 with magnitudes greater than 7M, were also mainly triggered by the semidiurnal sold tides [93]. In a stark contrast, Love and Thomas published in 2013 a deep dive into some of the approaches previously used to claim a correlation between earthquakes on earth and solar wind, geomagnetic activity, and sunspots [82]. Love and Thomas also conducted their own investigation into sunspots and earthquakes using a Student's t-test and Chi square test. Ultimately, Love and Thomas could not rule out the possibility that sunspots may influence earthquakes but did concluded if any influences were to exist that they were insignificant. In a similar vein, Hough most recently (2018) investigated both possible solar and lunar influences on earthquakes [94]. Hough titled her work, "Do large (magnitude ≥ 8) global earthquakes occur on preferred days of the calendar year or lunar cycle?" and then summarized the findings with a one word abstract, "No" [94].

If there are any solar periodicities to be found in earthquake data, it is important to take a look at what periodicities have already been previously identified in solar data. Table # 3 on the next page displays a very short sampling of previously identified solar periodicities. For brevity, only a few data sources and analysis methods are mentioned per periodicity found even if other data and analysis methods were also used. This table is by no means a complete or exhaustive list; it is but only a sampling of identified solar periodicities from 4 studies.

Table 3: A sampling of previously found solar periodicities.

#	Data Type	Periodicity Found	Analysis Method	Reference
1	Various	90 +/- 10 years	Various methods used, A study Wolf-Gleissberg Cycles	Yousef (2000, September) [8]
2	Monthly Sunspots, and Global Surface Temperature	55 years	Meyer wavelet	Li et al, (2018) [95]
3	Monthly Mean Sunspots	28 +/- 2 years	Instantly maximal wavelet skeleton spectra	Polygiannakis et al (2003) [96]
4	Monthly Mean Sunspots	24 +/- 2 years	Instantly maximal wavelet skeleton spectra	Polygiannakis et al (2003) [96]
5	Monthly Mean Sunspots	19 +/- 1 years	Instantly maximal wavelet skeleton spectra	Polygiannakis et al (2003) [96]
6	Monthly Mean Sunspots	13 +/- 1 years	Instantly maximal wavelet skeleton spectra	Polygiannakis et al (2003) [96]
7	Monthly Mean Sunspots	10.8 +/- 0.8 years	Instantly maximal wavelet skeleton spectra	Polygiannakis et al (2003) [96]
8	Monthly Mean Sunspots	8.8 +/- 0.7 years	Instantly maximal wavelet skeleton spectra	Polygiannakis et al (2003) [96]
9	Monthly Mean Sunspots	5.6 +/- 0.4 years	Instantly maximal wavelet skeleton spectra	Polygiannakis et al (2003) [96]
10	Monthly Mean Sunspots	3.8 +/- 0.2 years	Instantly maximal wavelet skeleton spectra	Polygiannakis et al (2003) [96]
11	Monthly Mean Sunspots	1.4 +/- 0.1 years	Instantly maximal wavelet skeleton spectra	Polygiannakis et al (2003) [96]
12	Monthly Mean Sunspots	1.07 +/- 0.08 years	Instantly maximal wavelet skeleton spectra	Polygiannakis et al (2003) [96]
13	Monthly Mean Sunspots	0.97 +/- 0.06 years	Instantly maximal wavelet skeleton spectra	Polygiannakis et al (2003) [96]
14	Daily Sunspots, Geomagnetic Indices	27 days +/- 1 day	Welch averaged periodogram, Linear phase finite impulse response, and more.	Mursula & Zieger (1996) [97]
15	Daily Sunspots, Geomagnetic Indices	13.5 +/- 0.5 days	Welch averaged periodogram, and Linear phase finite impulse response , and more.	Mursula & Zieger (1996) [97]

The 90 year periodicity listed in table # 1, is the 80 to 100 year range of the Wolf-Gleissberg cycle as discussed by Yousef [8] in investigation the Wolf-Gleissberg cycle in various terrestrial or climate related datasets including but not limited to solar irradiance, cosmogenic isotopes, global temperature, winter herring off the coast of Western Norway, and others. Li et al used the International Sunspot Number version 2.0 (yearly and monthly) and applied a continuous wavelet transform followed by the orthonormal discrete Meyer wavelet transform [95]. Li et al employed this kind of analysis because it allows for better detection of intermittent and/or nonstationary periodicities like the 22 year and 55 year solar signals they detected (among other) signals using these methods. Polygiannakis et al, also used a wavelet transform [96]. In their approach they decomposed the solar cycle into “signal-like” and “noise-like” components, this allowed them to create two independent “skeleton spectra” from the overall wavelet spectrum. Utilizing the two skeleton spectra allowed Polygiannakis et al, to detect periodicities in the time-series that would otherwise be undetectable using the traditional Fourier transform alone. They calculated the theoretical values they expected to find in the maximal wavelet skeleton spectrum and the theoretical values matched their observations using monthly averaged sunspot data. Their observed periodicities from 0.97 years to 28 years were included in Table # 1. Of the Polygiannakis et al results included in Table # 1, the 5.6 year and 3.8 year periodicities are considered to be harmonics reflecting the asymmetrical average rise and fall (decline) of the solar cycle. Polygiannakis et al also speculates that the 8.8 year and 13 year periodicities are related to the 11-year signal and maybe due to a mode-splitting effect while the 0.97, 1.07, and the 1.4 year periodicities are likely to be harmonics of the sun’s 2-year quasi-biennial oscillation [96].

The last two entries in Table #1 are the 27 day and the 13.5 day periodicities came from Mursula and Zieger [97]. Mursula and Zieger used multiple datasets including hourly averaged heliospheric data (including solar wind speed, temperature, etc.), daily sunspot numbers and geomagnetic indices. Using a Welch averaged periodogram method, followed by a linear phase finite impulse response bandpass filter, and other analysis treatments not discussed here, Mursula and Zieger claimed they were able to study the temporal structure of the 27 day and the 13.5 day periodicities. They concluded that the 13.5 day periodicity occurs during a two section interplanetary magnetic field structure.

Chapter 2: Data and Methodologies

2.1 Datasets

2.1.1 Solar Datasets

As mentioned in the previous chapter, there are different types of solar and solar proxy data publicly available. Carrasco et al, created a new and updated normalized sunspot-area series with data indices going back as far as 1932 [98]. Carrasco et al bridged the data gap between two sunspot area datasets by using the International Sunspot Number series version 2.0 to bridge the gap in sunspot-area from 1868 to 1874 [98]. However, Carrasco et al's new solar-area dataset ends in 2008, while the International Sunspot Numbers continued to be tabulated to the present.

This study uses daily sunspots and yearly mean sunspot numbers (International Sunspot Numbers version 2.0) from the Sunspot Index and Long-term Solar Observations (SILSO) Royal Observatory of Belgium, Brussels. The use of daily and yearly sunspot numbers was chosen for this study for multiple reasons. Using sunspots for spectral analysis eliminates the likelihood of any potential periodicities found in sunspot data are anything but solar related periodicities, artifacts, or just high amplitude noise. The length of the historical daily sunspot record from the SILSO in Belgium is consistent and runs from 1818 to the present as seen in Figure # 1 [99]. The yearly mean sunspot data goes back even farther to 1700. This study uses a little over 100 years' worth of earthquake magnitude and occurrence data from 3 sources. It was important when conducting a spectral analysis using the Fast Fourier transform to have as much consistent and continuous data on the same time scale as possible. Therefore the use of daily and yearly sunspot numbers were chosen for this analysis to use with earthquake data.

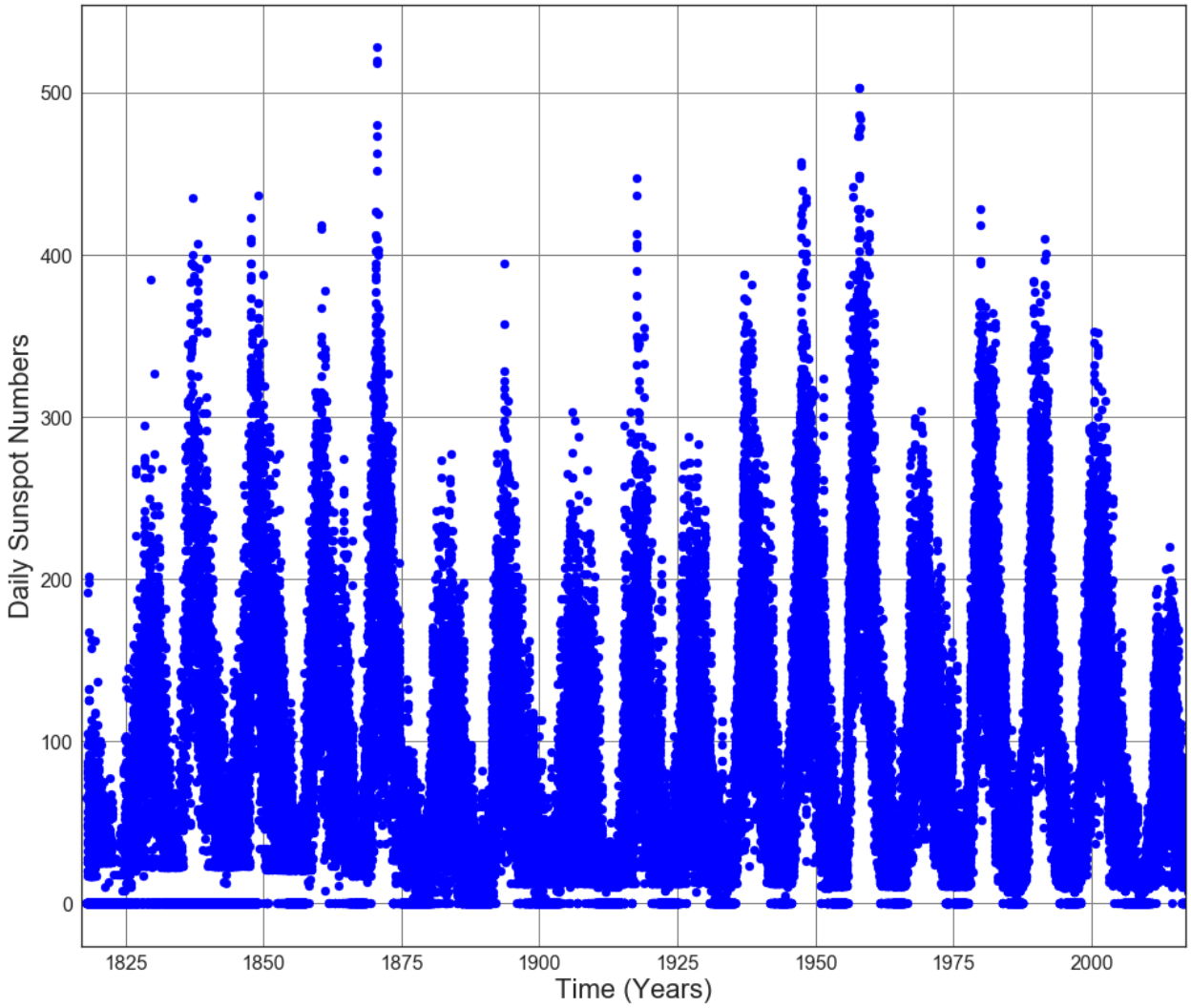

Figure 1: Daily Sunspot Numbers from the SILSO, version 2.0, 1818 to 2018 [99].

Both types of sunspot data yearly and daily were replaced with a new and improved version 2.0 in 2015 [100]. The difference is a change in sunspot observer from Wolf and using Wolf numbers, to his assistant Wolfer who also recorded sunspot numbers alongside Wolf. The differences between Wolf and Wolfer's sunspot observations have helped to address the known irregularities in the Wolf sunspot numbers. The entire sunspot data series has been revised and

replaced with the new series, version 2.0. It is worth noting that the Waldmeir effect is still present in version 2.0 sunspots as it was in the original Wolf sunspot number series [98]. The Waldmeir effect is, “the inverse correlation between the rise time and the maximum amplitude of a cycle”[98]. Also, both types of sunspot data utilize “-1” as a data flag for missing data. All sunspot number data flags were first converted to zero before use.

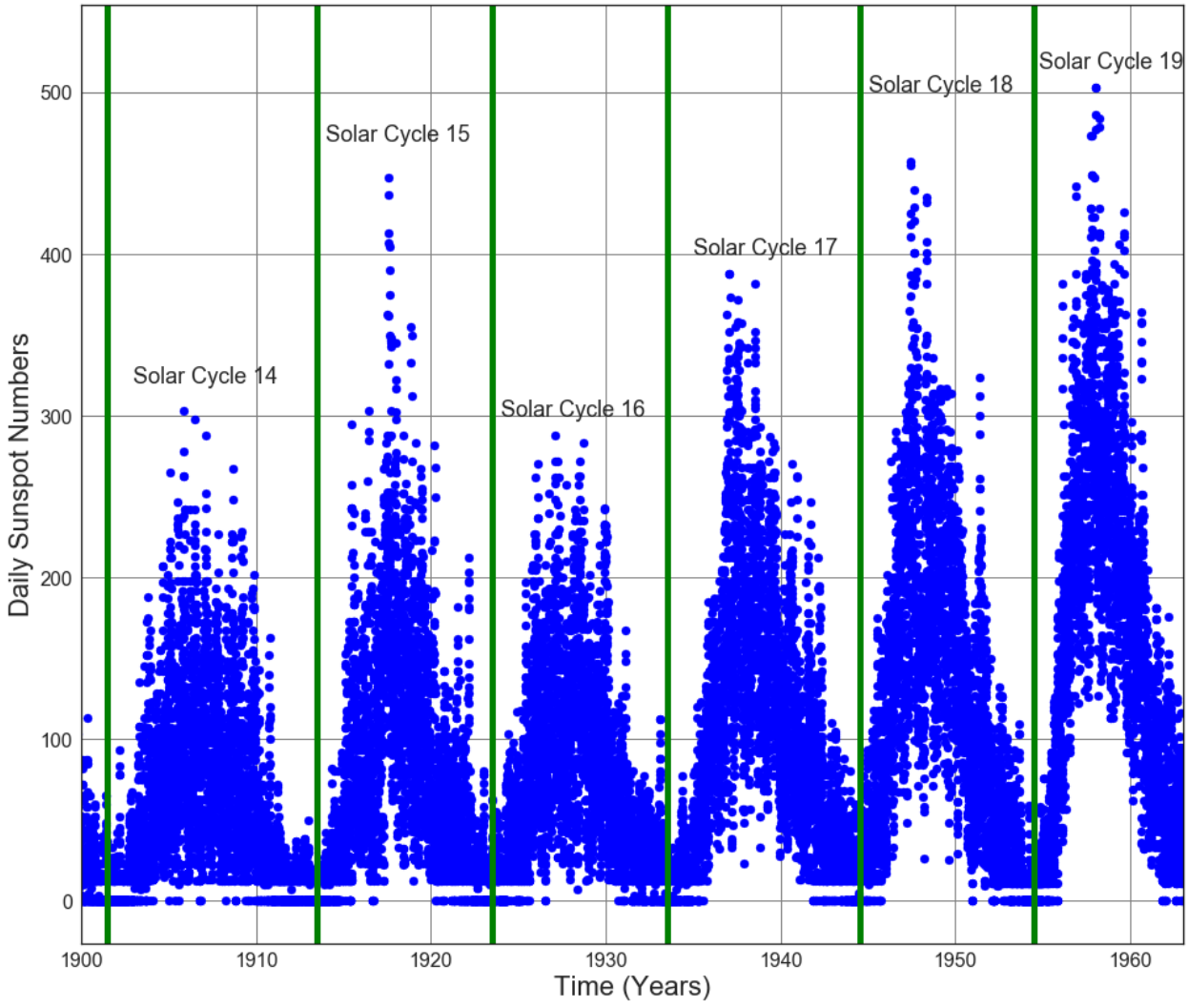

Figure 2: Scatter plot of Daily Sunspot Numbers from the SILSO, version 2.0, Pre-WWSSN Era (historical period) 1900 to 1963 labeled with their respective solar cycle number [44].

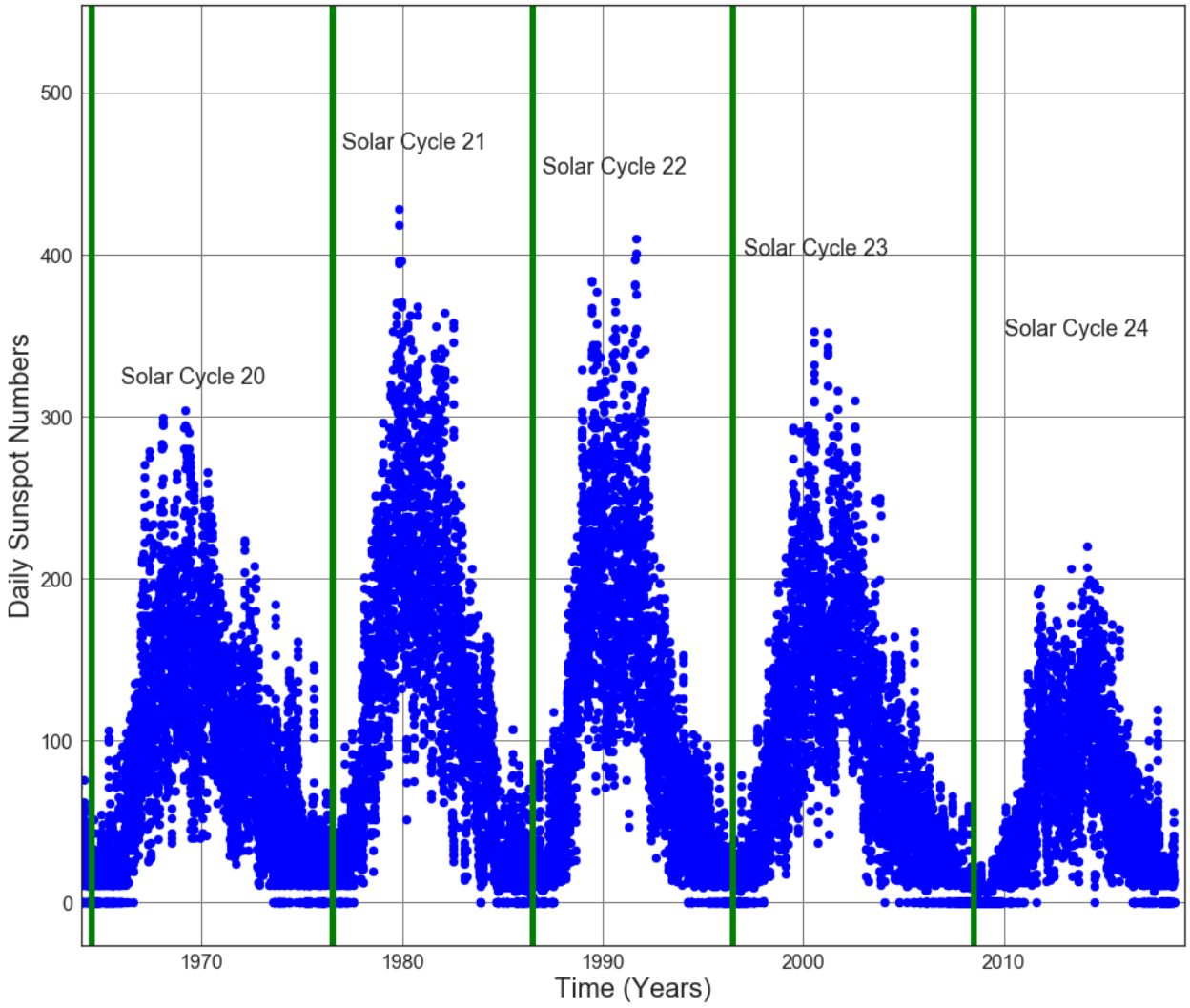

Figure 3: Scatter plot of Daily Sunspot Numbers from the SILSO, version 2.0, Post-WWSSN (modern era) from 1964 to 2018 labeled with their respective solar cycle number [99].

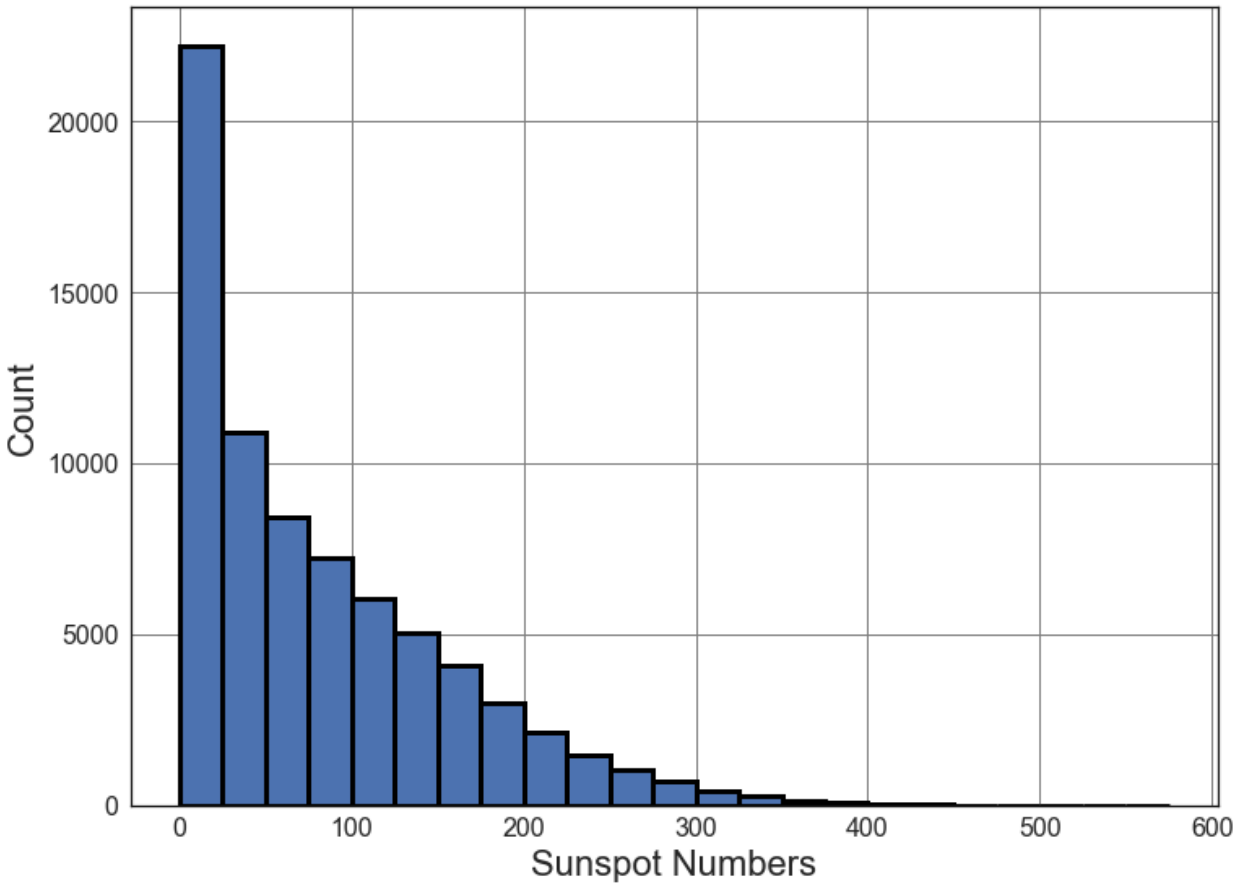

Figure 4: Histogram of Daily Sunspot Numbers contained in the SILSO dataset, version 2.0, from 1818 to 2018 [99].

2.1.2 Earthquake Datasets

For simplicity, all earthquakes in this study are treated as if they were reported on the same scale without regard to the type of scale calculation used. For example, a 6.7 M_W and a 5.4 M_B earthquake are treated as 6.7 M and 5.4 M respectively, where M = magnitude.

The approach is to look for possible solar cycle signals (periodicities) with respect to sunspots in multiple global earthquake catalogs with a focus on earthquake occurrence first and earthquake magnitude second. Two of the earthquake catalogs are from the United States Geological Survey (USGS), the USGS Centennial Y2K Catalog (Centennial) and the USGS

Reviewed ANSS Comprehensive Earthquake Catalog (ComCat). The third earthquake catalog is from the International Seismological Centre (ISC) Reviewed earthquake Bulletin. Using three global earthquake datasets allows for comparison of potential periodicities if found in one dataset against the other two. If periodicities are found in one dataset and not in another, the potential periodicity may not be a real or due to some other effect. Of the following earthquake catalogs, both the Centennial Y2K and the ISC lists many reported magnitudes per earthquake recorded. For the Centennial Y2K catalog, the first magnitude listed is the prefered magnitude [101], but for the ISC catalog which magnitude in the list is the prefered one was initially not clear. For this reason, only the largest magnitude for each earthquake listed is used in this study for the ISC Catalog. The USGS ComCat catalog is the only one of the three catalogs where selecting the largest listed magnitude per earthquake is not an issue, because it only lists one magnitude per earthquake.

A. The Centennial catalog

The Centennial Y2K catalog is an updated version of the original Centennial catalog by Engdahl and Villaseñor in 2002 [75, 101, 102]. The Centennial Y2K catalog is a global collection of instrumentally recorded earthquakes of the 20th century [75]. Originally spanning 1900 to 1999, the Centennial is occasionally updated and as of this study spans 1900 to September 30, 2007. The lowest earthquake magnitude contained in the updated Centennial Y2K is 5.5M starting in 1964 (see figures # 5 and # 6). From 1900 to 1963 the lowest magnitude contained is 6.5M as seen in Figure # 5 on the next page. There also appears to be a gap in the

data for magnitude 5.5M through 5.7M starting from around the year 2000 to the end of the dataset in 2014. It is unknown if the apparent gap is due to catalog curation or something else.

It was initially assumed that the earthquake magnitude data was evenly distributed over the dataset from 1900 to 2007 with the exception of earthquakes less than 6.5M. Exploring the Centennial dataset revealed that the dataset is unbalanced with most of the data contained in the dataset being collected after 1964 (see figures # 7 and # 8). While the increase in earthquake data after 1964 might seem obvious from Figure # 5, the degree to which this is the case was not initially clear. As shown in figure # 7, there is an exponential increase in the number of earthquakes after 1964 coinciding with the launch of the WWSSN. It is assumed for the purposes of this study that the sudden increasing trend in earthquakes starting in 1964 is due to the WWSSN increasing the number of earthquakes detected, and is not due to a global increase in earthquakes.

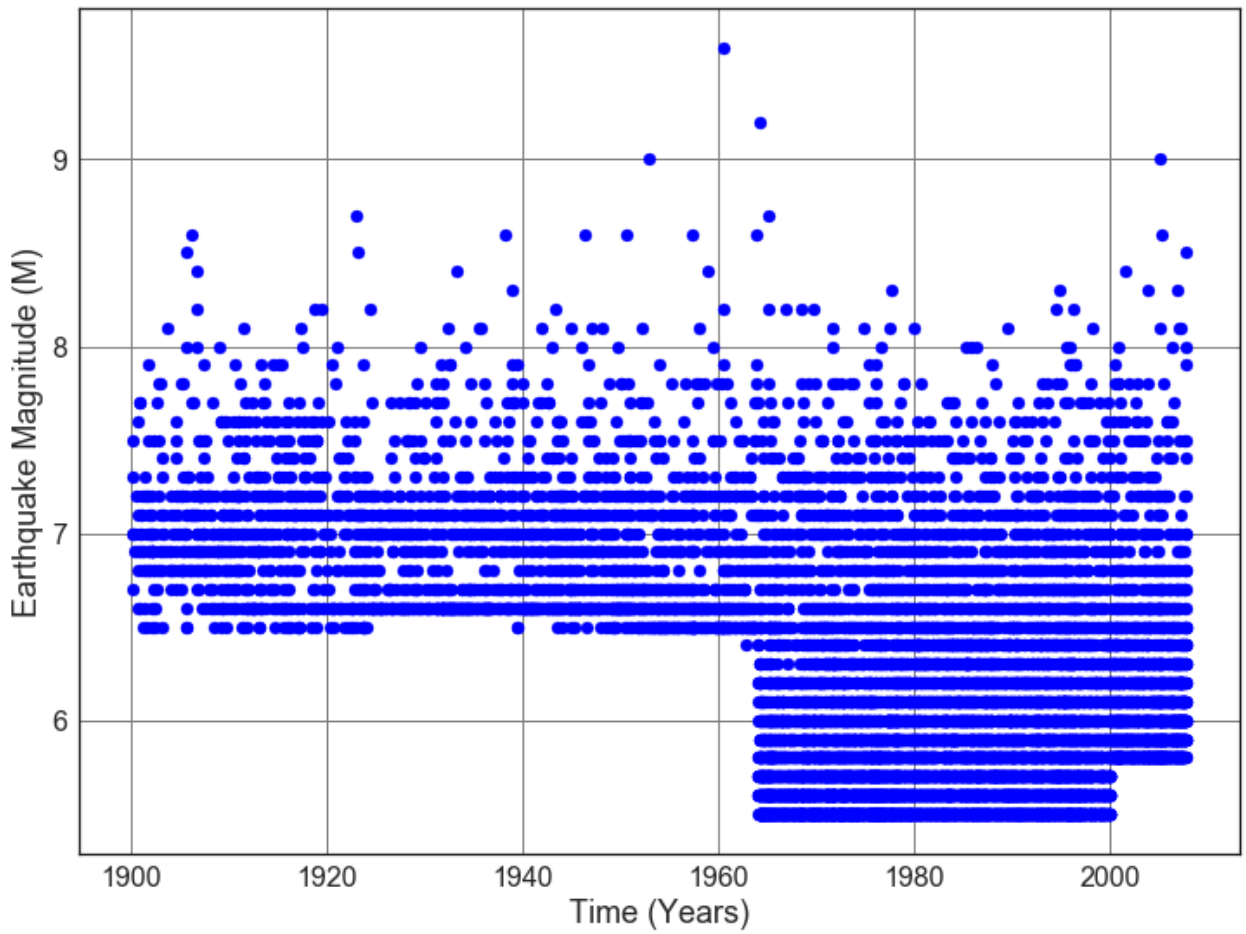

Figure 5: Scatter plot of Earthquake Magnitude vs. Time from the USGS Centennial catalog, from 1900 to 2007. The catalog only contains earthquakes 5.5M and larger. The smallest earthquakes contained in the Centennial is 6.5M until about 1963.

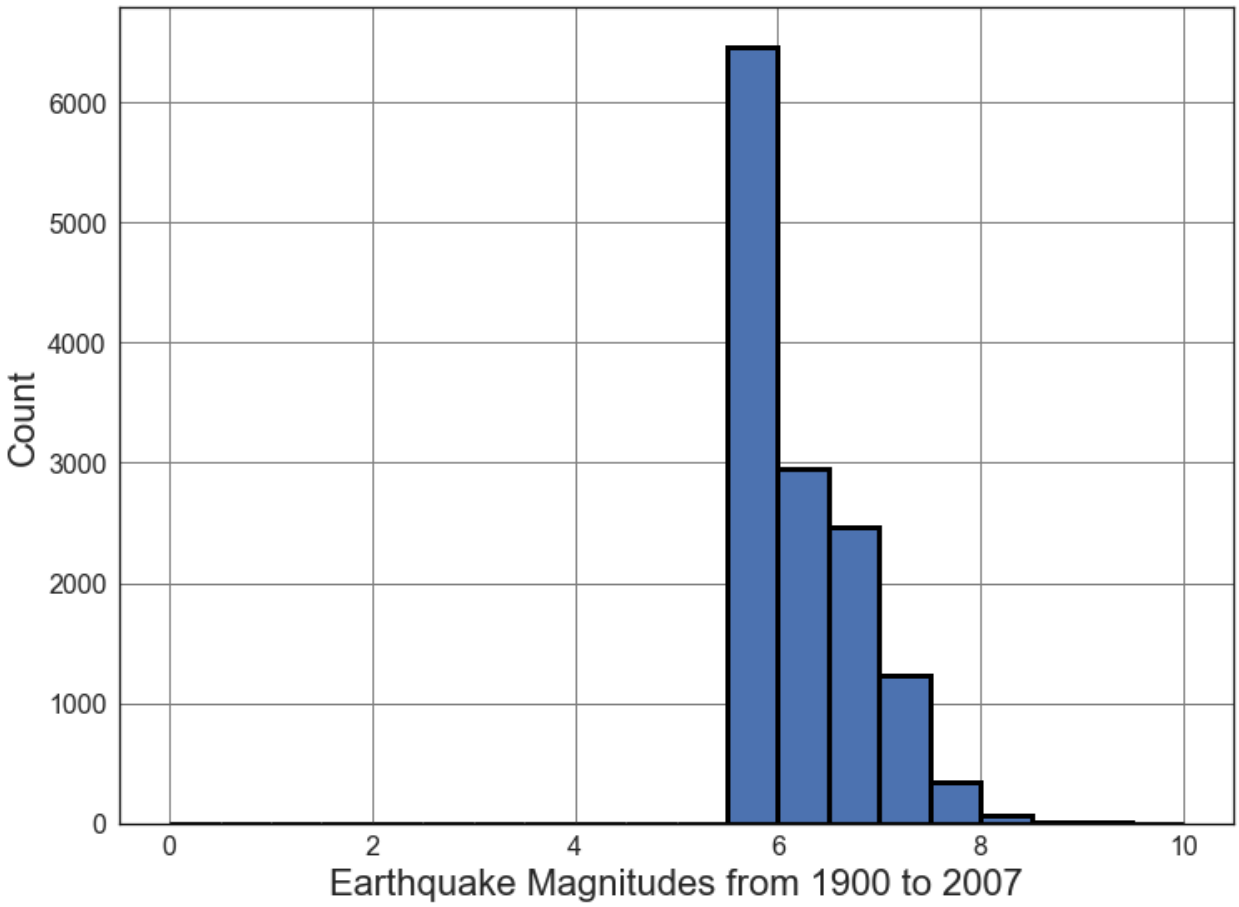

Figure 6: Histogram of Earthquake Magnitudes from the USGS Centennial catalog, from 1900 to 2007. The catalog only contains earthquakes 5.5M and larger.

Since the Centennial catalog only contains earthquakes of 5.5M and larger, it was not possible to compare the dataset to the ISC or USGS datasets with respect to moderate or smaller earthquakes. However, earthquakes 6.5M and larger were more evenly distributed from 1900 to 2007 and were utilized for part # 1 of the time series analysis discussed later in this report. While not directly shown in figure # 5 or in the histogram in figure # 6, nearly half (47.74%) of the Centennial dataset are earthquakes between 5.5M and 6M (see figure # 8). Earthquakes magnitude 9M and above are not plotted because there are only four of them contained in the data set from 1900 to 2007.

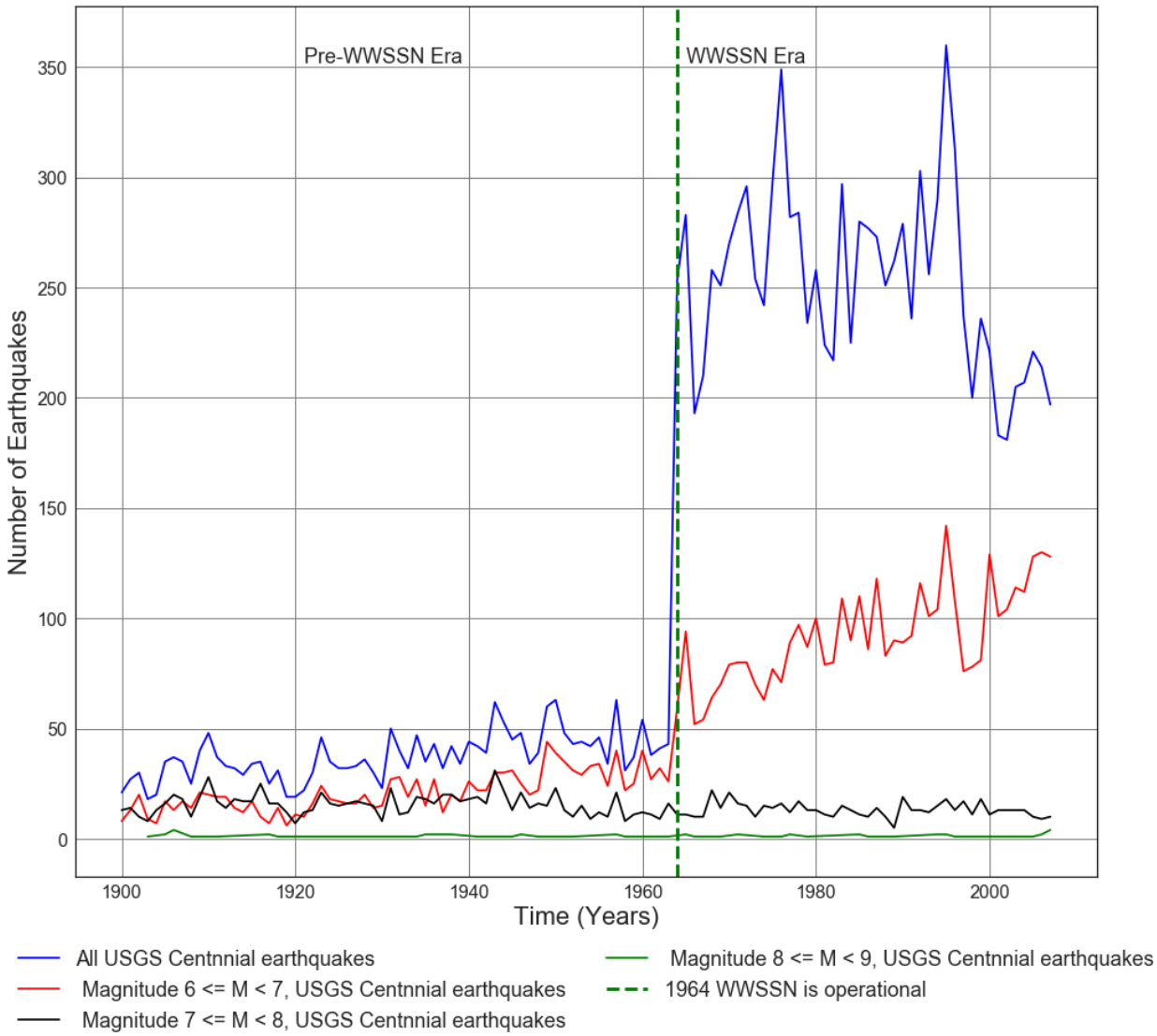

Figure 7: Plot of earthquakes per year for the USGS Centennial catalog, from 1900 to 2007. The catalog only contains earthquakes 5.5M and larger. The smallest earthquakes contained in the Centennial is 6.5M until about 1963. In 1964, the number of earthquakes increased coinciding with when the WWSSN was launched.

Figures # 5, # 7, and # 8 show that the catalog is dominated by data from after 1964 (82.3%). The smallest earthquakes contained in the Centennial is 6.5M until about 1963. In 1964, the number of earthquakes increased coinciding with when the WWSSN was launched.

Aside from the unbalanced nature of the dataset, exploratory data analysis of the dataset also revealed that one earthquake in the Centennial dataset did not have a complete timestamp. In order to create an approximate fractional time stamp (to be discussed later in the Methodologies section), all earthquakes in the dataset must have both a date and a time. There was one earthquake contained in the Centennial Y2K dataset that had only year and month listed but no day and time information. This earthquake took place in 1911 in the month of July, with a magnitude of 6.5 and icat = BJI. BJI is the identifier used for the China Earthquake Networks Center in Beijing, China. Using the latitude (glat) and the longitude (glon) given for this earthquake references a place in 加扎拉古, Zayu, Nyingchi, China. This earthquake in China was not contained in the ISC dataset nor the USGS ComCat dataset. Since another reference for this earthquake could not be found, a date of July, 1, 1911, at midnight (00:00 hrs) was assigned to this earthquake.

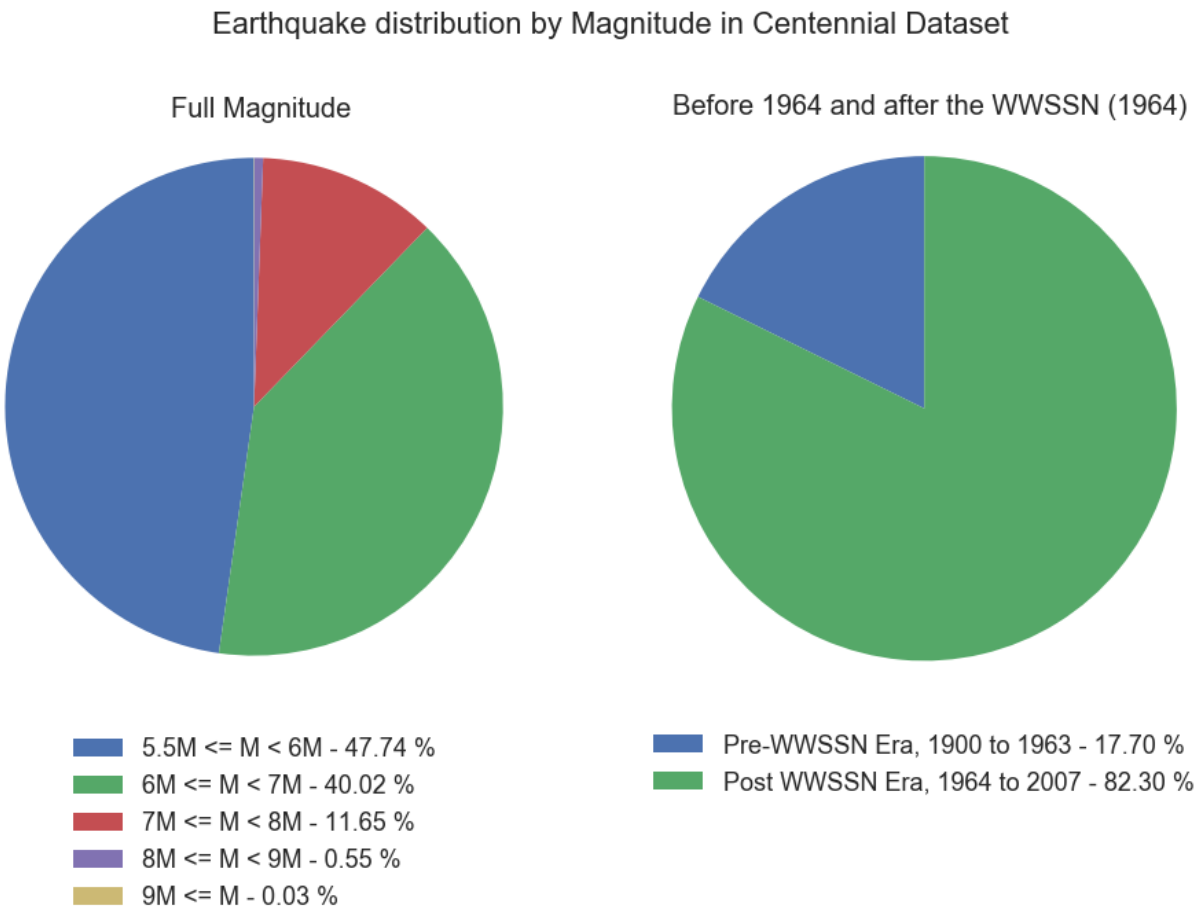

Figure 8: Pie chart of Earthquakes contained in the USGS Centennial catalog. The pie chart on the right shows the percentage of earthquakes contained in the dataset from before 1964 and after when the WWSSN was launched. The pie chart on the left shows the percentage of earthquakes by magnitude category in the catalog.

B. The USGS ANSS Comprehensive Earthquake Catalog (ComCat)

The United States Geological Survey (USGS) Advanced National Seismic System (ANSS) Comprehensive Earthquake Catalog (ComCat), henceforth USGS, USGS earthquake catalog or USGS ComCat for short, is an earthquake catalog meant to eventually replace the world-wide ANSS Composite Catalog that is hosted by the Northern California Data Center

[103]. At the time the data for this study was acquired, not all of the historic regional seismic network catalogs had been fully loaded yet in the ANSS ComCat catalog [103,104]. The USGS ComCat dataset contains earthquakes from 1900 to 2017. While earthquakes with magnitudes less than 2M were available for download, only earthquakes equal to 2M and larger were downloaded and for this study.

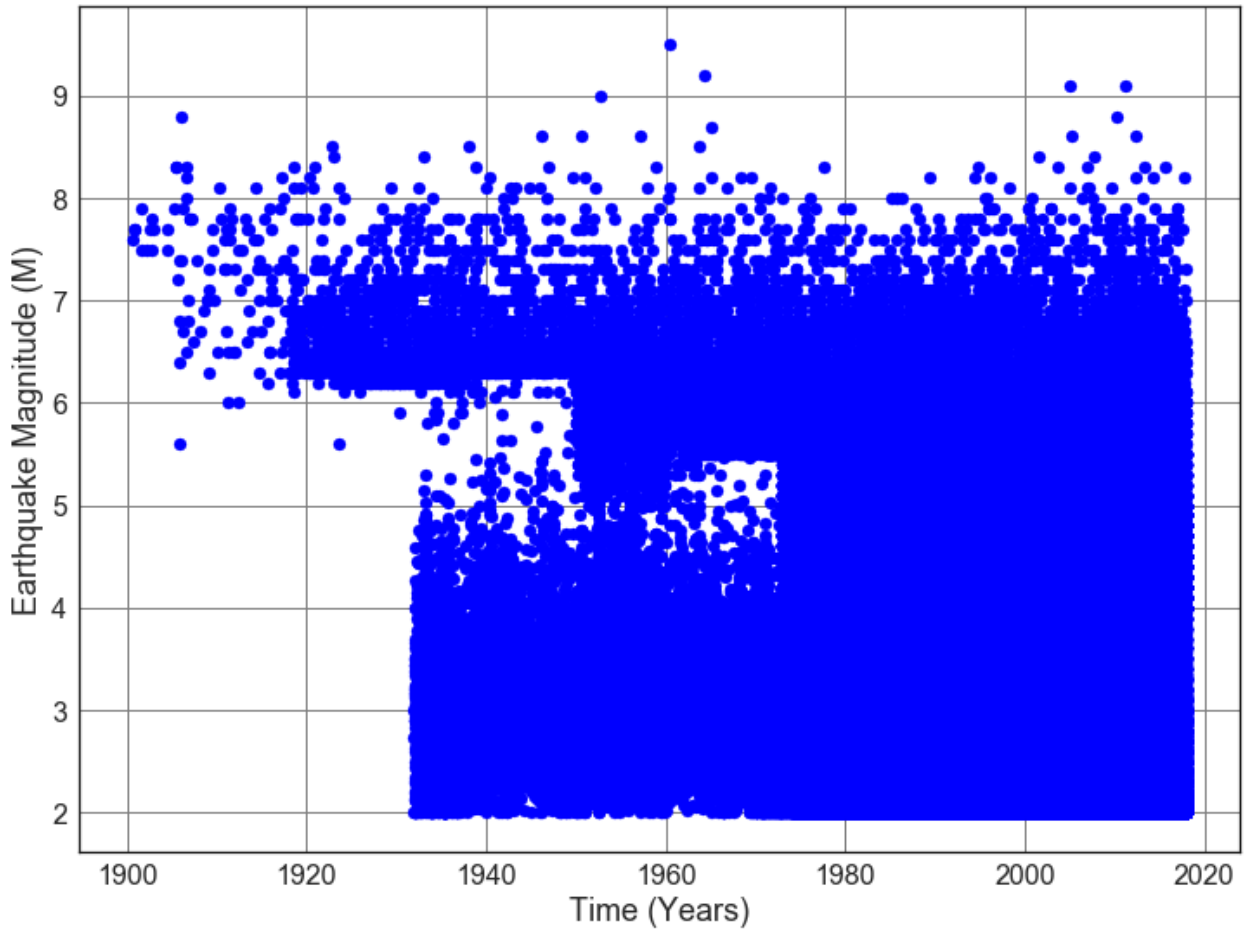

Figure 9: Scatter plot of Earthquake Magnitude vs. Time from the USGS the ANSS Comprehensive Earthquake Catalog (ComCat), from 1900 to 2017. Only earthquakes 2M and larger were used for this study.

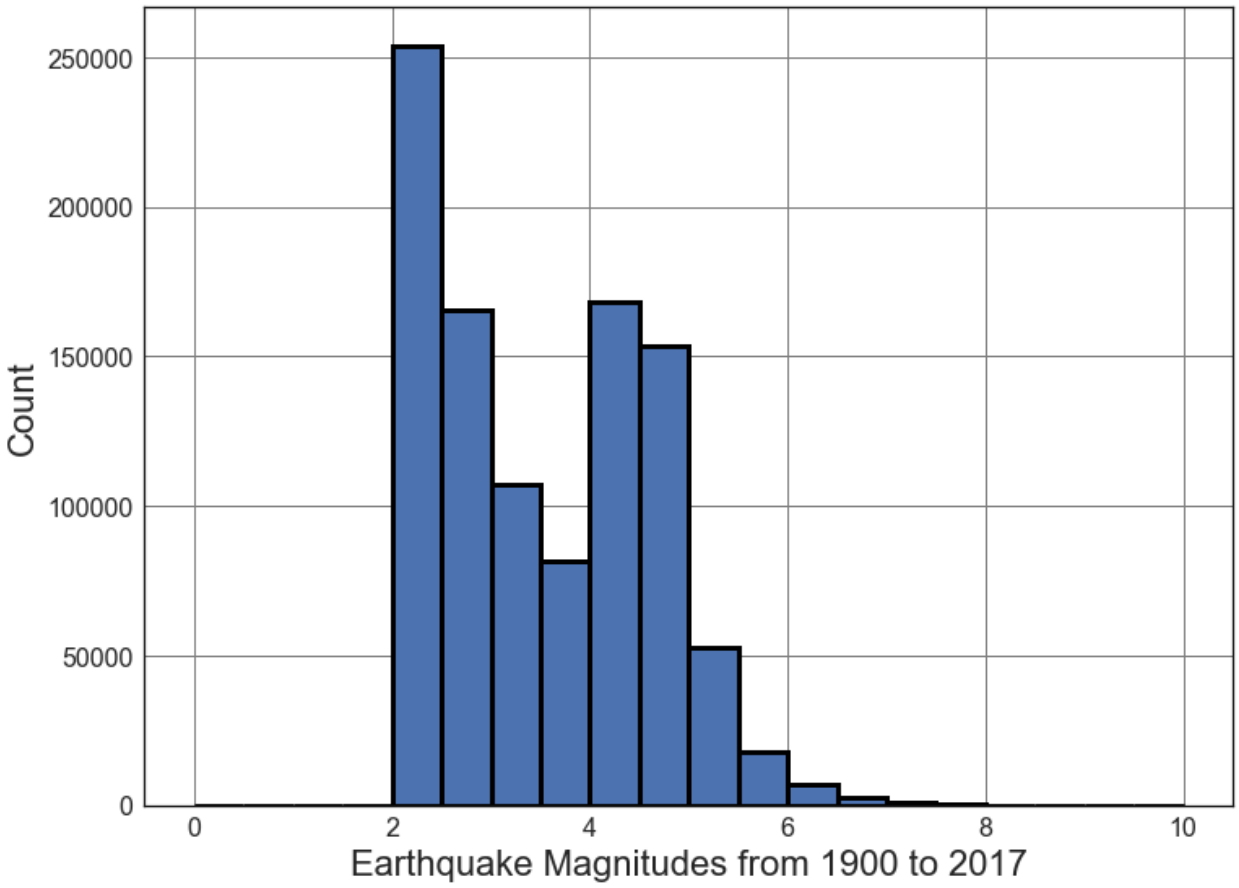

Figure 10: Histogram plot of Earthquake Magnitude vs. Time from the USGS the ANSS Comprehensive Earthquake Catalog (ComCat), from 1900 to 2017. Only earthquakes 2M and larger were utilized for this study.

In exploring the USGS dataset, the histogram in figure # 10 shows a bimodal distribution of earthquake magnitudes. It is assumed that the bimodal distribution of earthquake magnitudes is likely due to a combination of missing earthquake data from the historical period and advancements in technology resulting in more earthquakes of all magnitudes being recorded in the modern era. Figure # 9 shows that there is almost no data for <6M earthquakes until about the mid 1930's. The dataset looks sparse for earthquakes between 6M and 7.5M until about the 1920's. Figure #9 also shows for earthquakes ~4.5M to ~6M from the 1930's into the 1970's,

that there are two regions where the earthquake data looks sparse. The USGS dataset also has an increasing upward trend in the number of earthquakes recorded starting around the 1970's as shown in figure # 11.

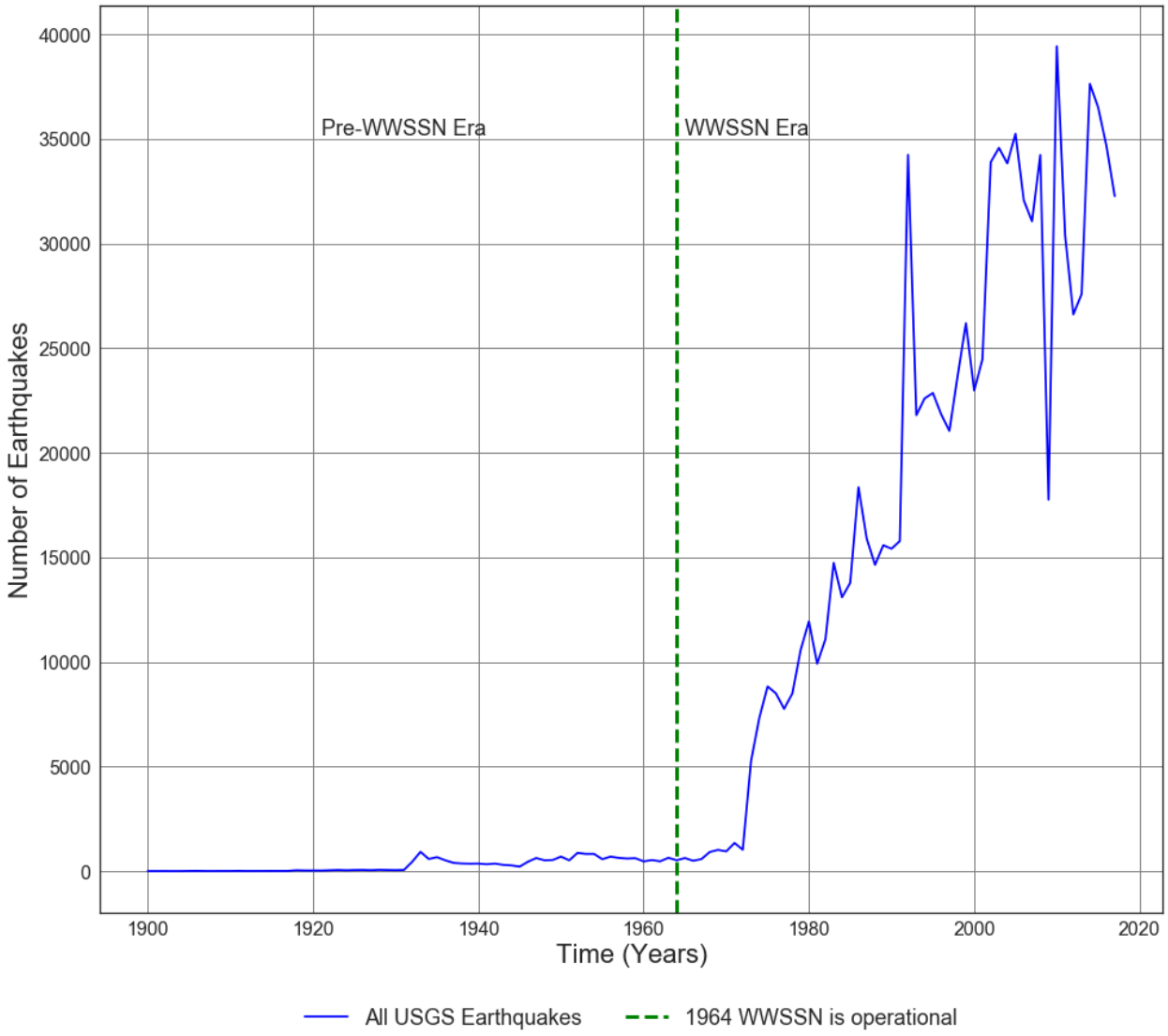

Figure 11: Plot of earthquakes per year for all earthquakes contained within the USGS catalog.

Looking at earthquakes of magnitude 6M and above, earthquakes between 6M and 7M were not evenly distributed from 1900 to 2007 as shown in figure # 12. Figure # 12 also shows that earthquakes between 6M and 7M in the USGS dataset had an order of magnitude increase

starting around the mid to late 1940's. Earthquakes magnitude 9M and above are not plotted because there are only 5 of them contained in the data set from 1900 to 2017.

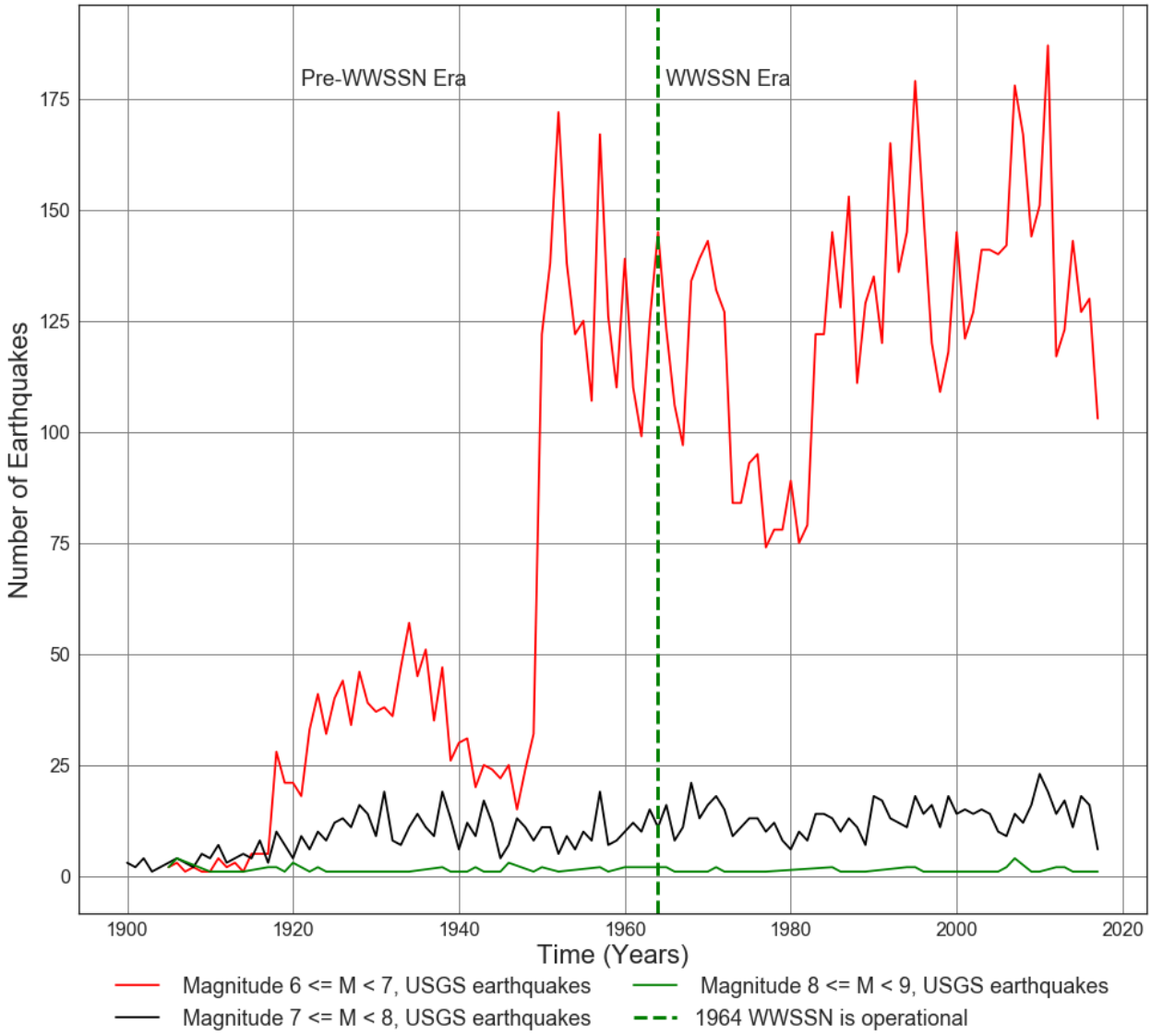

Figure 12: Plot of USGS magnitudes 6M, 7M, and 8M per year for 1900 to 2017.

Data for moderate and smaller earthquakes (M < 6M) start in the 1930's for the USGS dataset and dramatically increase in the 1970's as shown in figure # 13. Figures # 13 and #14

also shows the dataset mostly consisting of earthquakes less than 5M and that 98% percent of all earthquakes in the USGS data occurs after 1964.

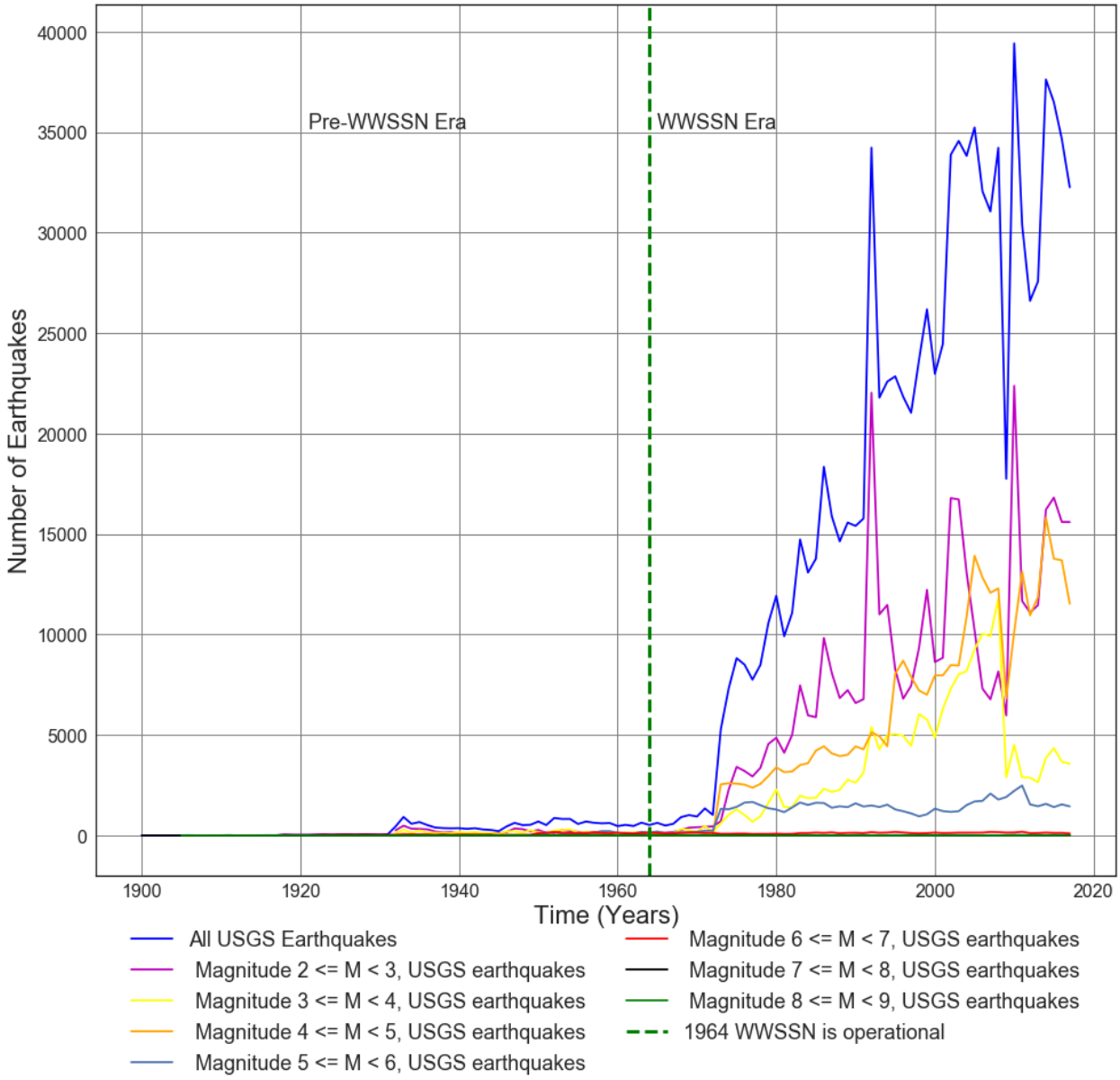

Figure 13: Plot of USGS magnitudes per year for 1900 to 2017.

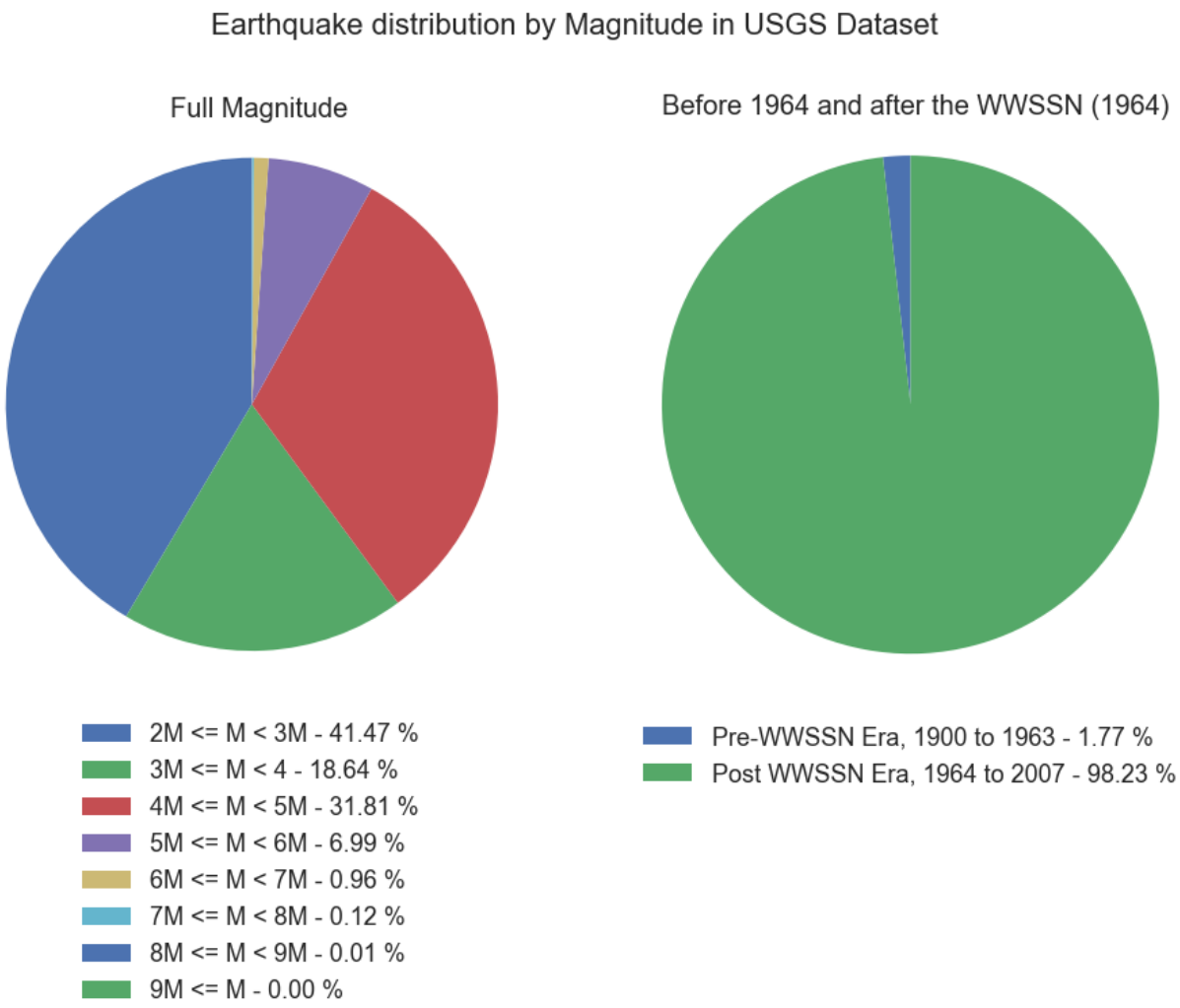

Figure 14: Pie chart of Earthquakes contained in the USGS catalog. The pie chart on the right shows that only 1.77% of earthquakes contained in the dataset are from before 1964 and 98.23% are from after when the WWSSN was launched. The pie chart on the left shows the percentage of earthquakes by magnitude category in the catalog with 60% of the data consisting of earthquakes < 4M, and 92% consisting of earthquakes less than 5M.

C. The Bulletin of The International Seismological Centre (ISC)

The Bulletin of the International Seismological Centre (ISC) henceforth referred to as ISC, is considered to be the definitive record of the Earth's seismicity [105]. The ISC earthquake dataset used in this study was downloaded in 2017 from the ISC Bulletin website for all

reviewed earthquake magnitudes globally and spans from January 1904 to September 30, 2014 [106]. This is before the rebuild for the period 1964 to 1984 was completed in 2019, and also before the ISC's dataset rebuild for the period 1985 to 2010 was completed in 2020 [107].

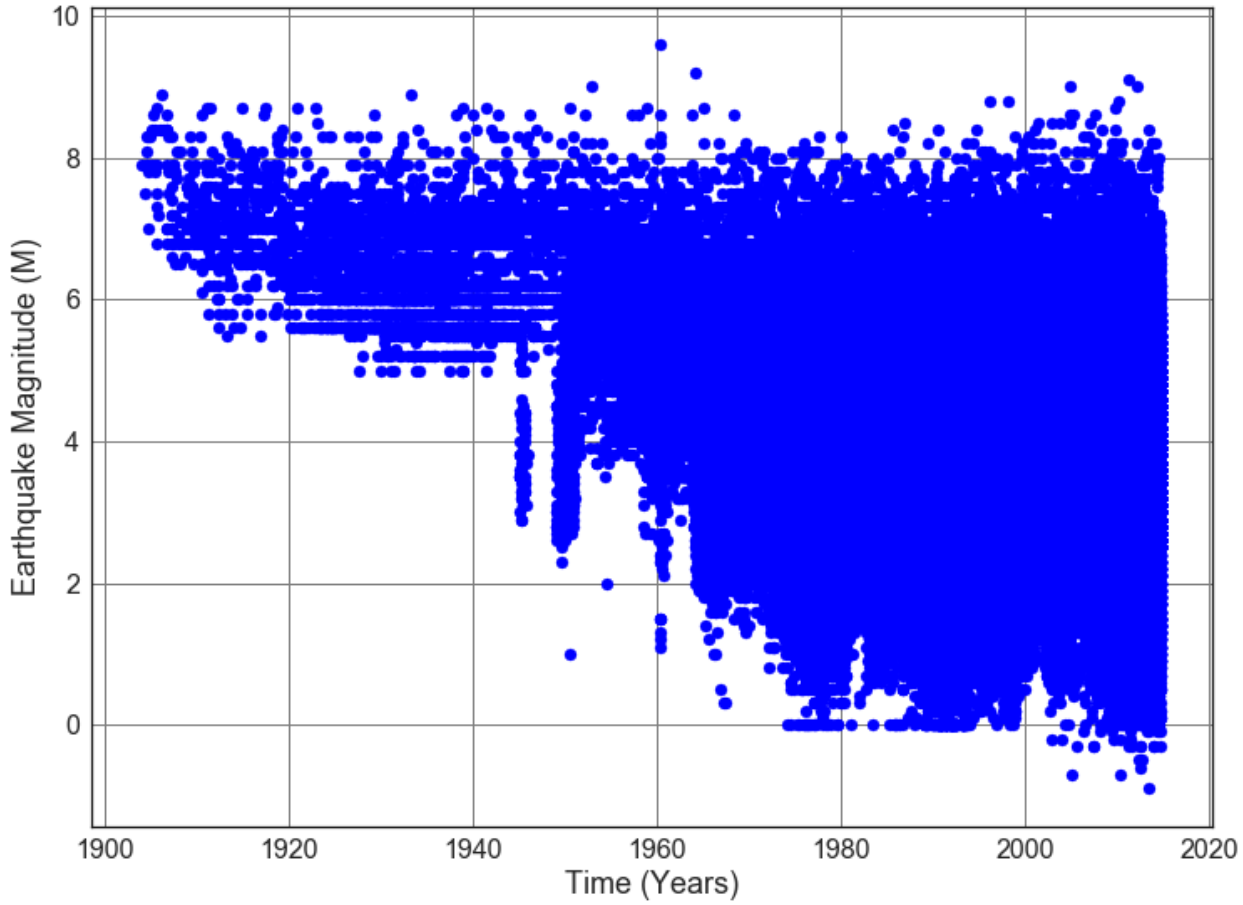

Figure 15: Scatter plot of Reviewed Max Magnitude Earthquakes vs. Time from the International Seismological Centre (ISC) catalog of earthquakes from 1904 to 2014.

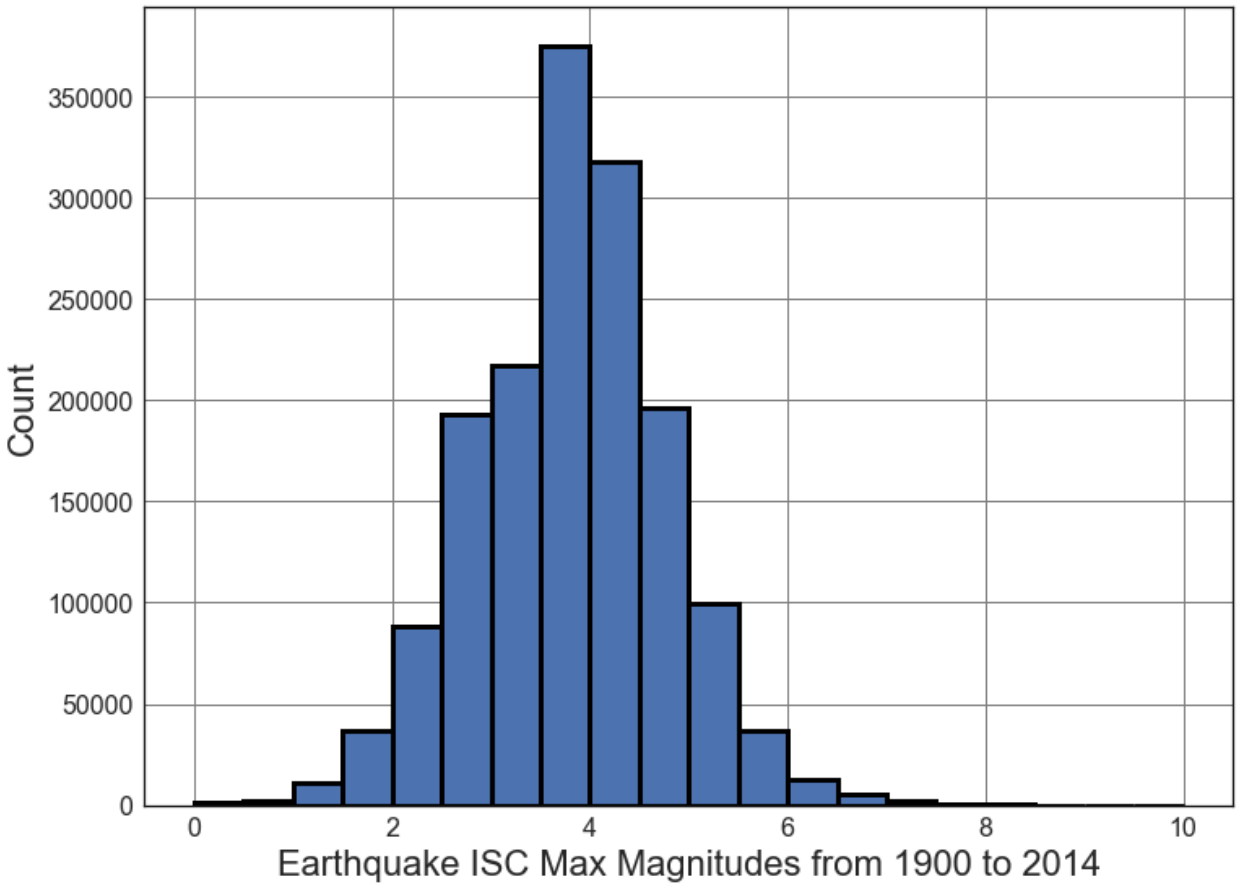

Figure 16: Scatter plot of Reviewed Max Magnitude Earthquakes vs. Time from the International Seismological Centre (ISC) catalog of earthquakes from 1904 to 2014.

Since reviewed earthquakes of all magnitudes were downloaded from the ISC Bulletin, this also includes earthquakes of negative magnitudes as seen in the lower right hand corner of Figure # 15. Because the earthquake magnitude scales are logarithmic an earthquake of -1M is just an earthquake 1000 times smaller than an earthquake of 0M and is so small that it is unfelt by humans [108].

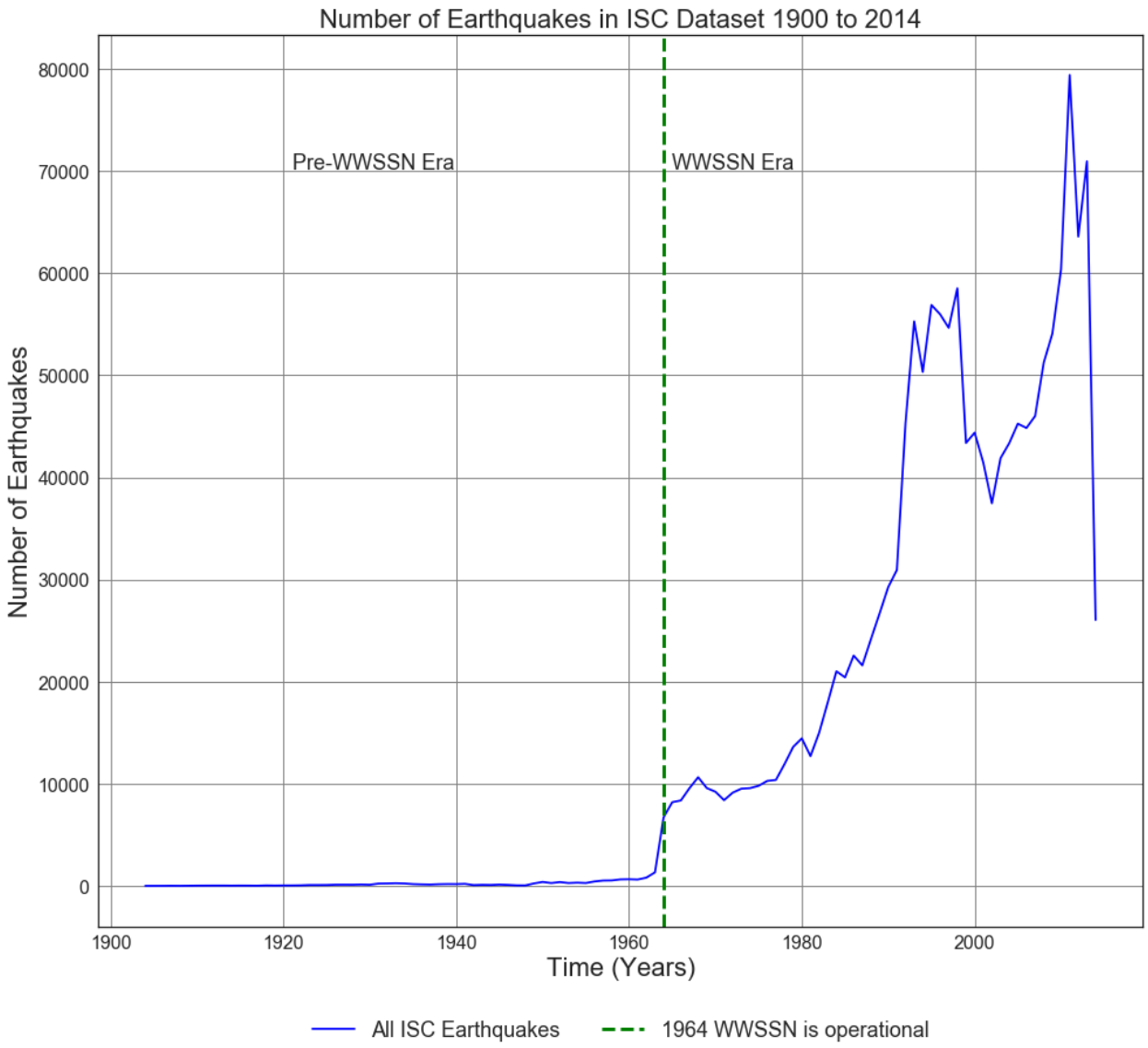

Figure 17: Plot of earthquakes per year for reviewed earthquakes contained within the ISC catalog from 1900 to 2014.

The ISC dataset is the largest of the three used for this study with 1,595,107 earthquakes. In this dataset there are no earthquakes between 5.5M and 6M listed until the 1910's, and most of the moderate and small earthquake events are from after 1964 as shown in figure # 15. While figure # 15 shows that there are earthquakes contained within the dataset before 1964, figure # 17 clearly shows that the majority of the dataset consists of earthquakes from after 1964 and has an

increasing upward trend coinciding with the launch of the WWSSN. When looking at earthquakes 6M and larger there is also an upward overall increasing trend for earthquakes from 6M and to less than 7M as shown in figure # 18 although it starts earlier than 1964. Earthquakes 7M and 8M seem to be more evenly distributed from 1900 to 2014.

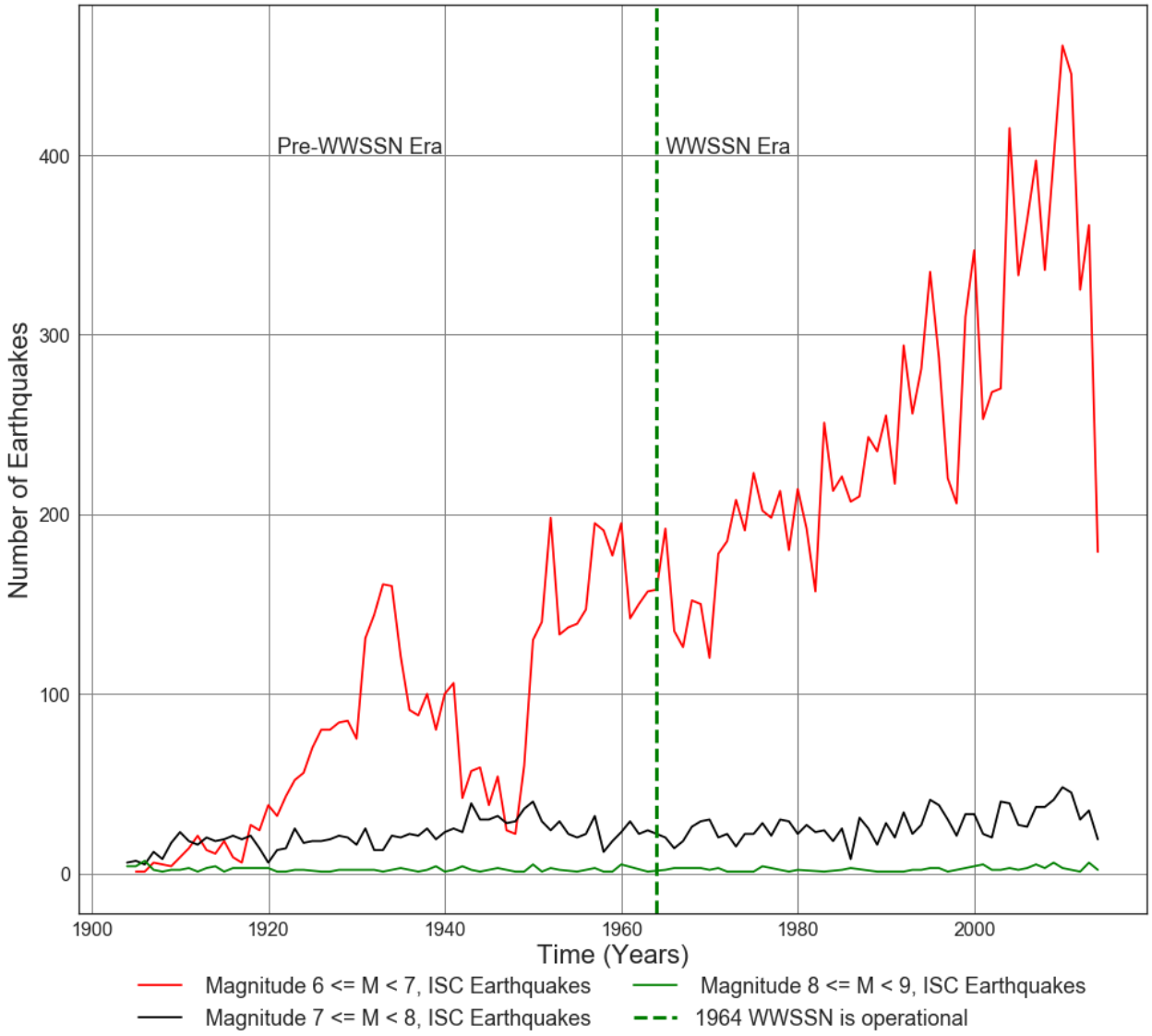

Figure 18: Plot of ISC magnitudes 6M, 7M, and 8M per year for 1900 to 2014.

In taking a more close up visual inspection of ISC earthquakes 4M and greater, figure # 19 shows that the ISC dataset is unevenly distributed and sparse for earthquakes between 5M and 7M until the 1950's.

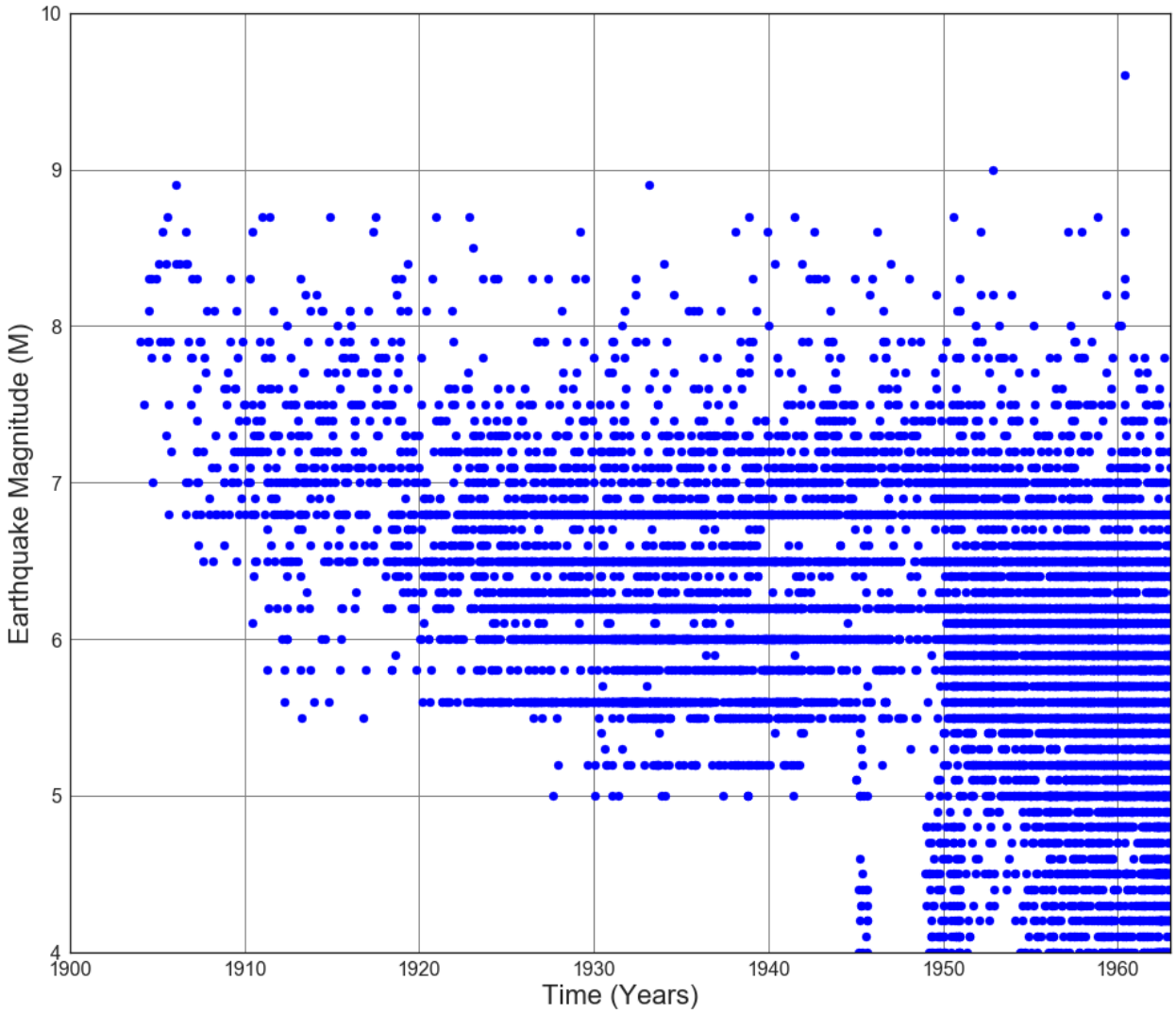

Figure 19: Scatter Plot of ISC magnitudes 4M and larger per year for 1904 to 1963.

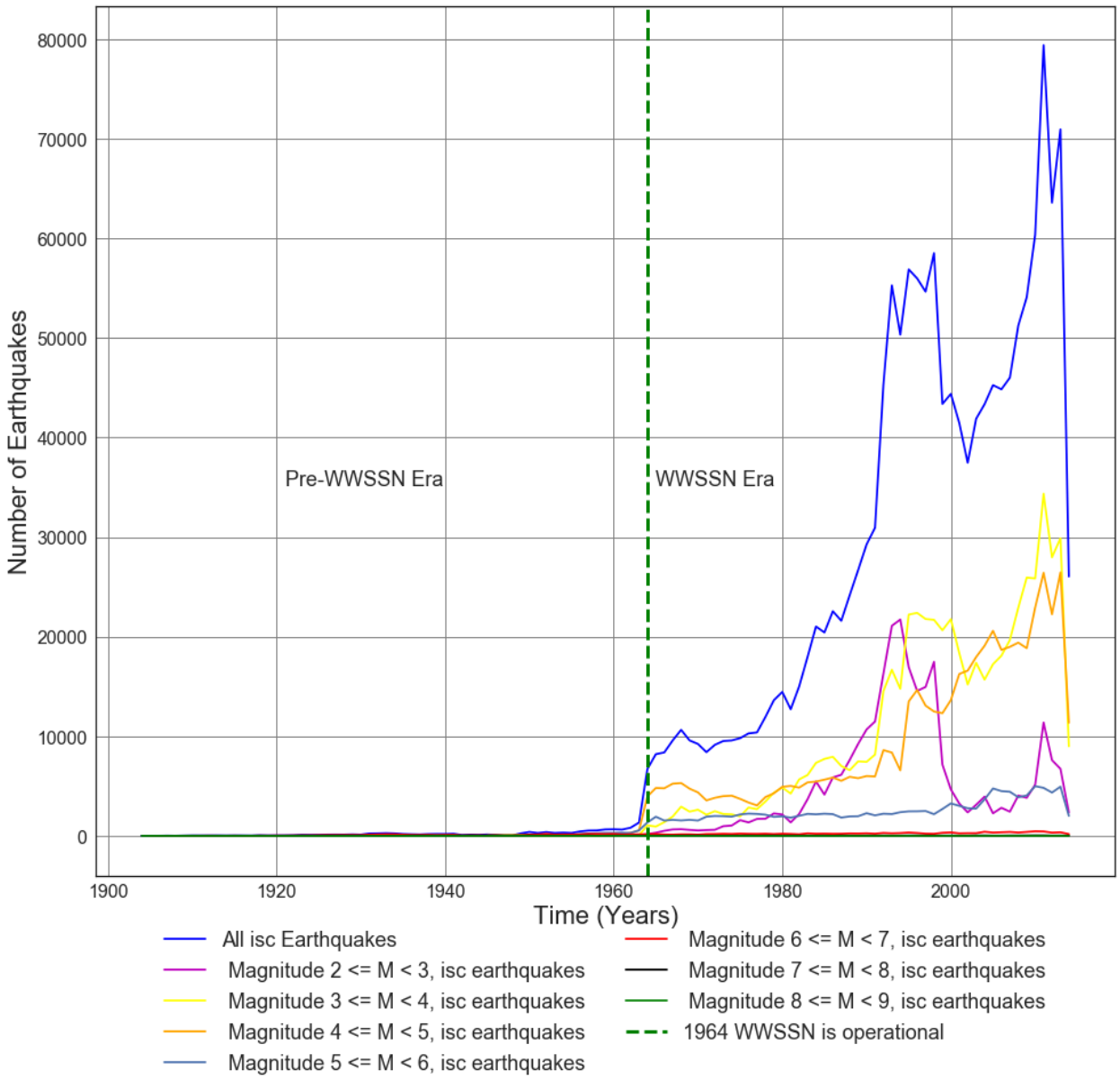

Figure 20: Plot of ISC magnitudes 2M, 3M, 4M, and 5M per year for 1900 to 2014.

Moderate and smaller earthquakes plotted in figure # 20 also shows that the ISC dataset mostly contains small and medium earthquakes occurring after 1964, and all of them with increasing trends per year. Figure # 21 shows the distribution of magnitudes contained within the ISC dataset with over ~90% of the dataset consisting of earthquakes of magnitude 5M or less, and less than 1% of the data is from before 1964.

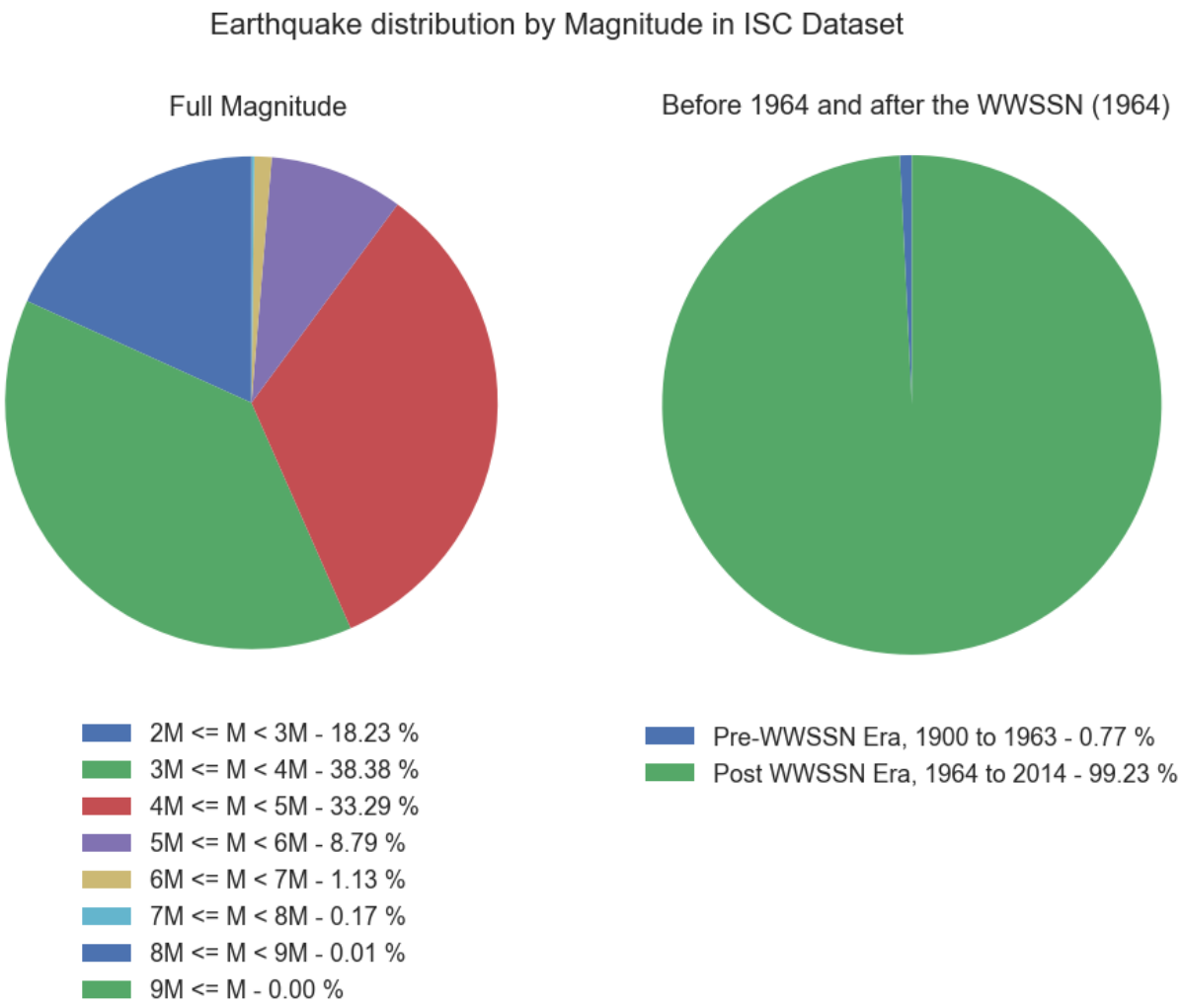

Figure 21: Pie chart of Earthquakes greater than 2M contained in the ISC catalog. Earthquakes less than 2M were excluded. The pie chart on the right shows that less than 1% of earthquakes contained in the dataset are from before 1964 and 99% are from after 1964 coinciding with when the WWSSN was launched. The pie chart on the left shows the percentage of earthquakes by magnitude category in the catalog with 60% of the catalog consisting of earthquakes < 4M and ~ 90% of the data consisting of earthquakes < 5M.

2.2 Methodologies

The hypothesis of this study is that earthquakes are related to the change in slope of the solar cycle and thus may have an orthogonal relationship to the sunspot cycle in a similar way that cos(x) is orthogonal and yet related to sin(x). Within this study, the period of time between solar cycle minimum to when the cycle reaches its highest point during solar maximum is referred to as the 'rise', 'rise side' or the 'rise phase' of the sunspot cycle. The time between when the highest point during the solar maximum has been reached and sunspots are decreasing back down to the lowest point during solar minimum is referred to as the 'decline', 'decline side' or the 'decline phase'.

As previously discussed, all three earthquake datasets have increasing numbers of earthquakes starting either right after or within 10 years of 1964. The only visually consistent magnitude range across all three earthquake catalogs spanning from the 1900's into the 2000's are earthquakes 7.5M and larger. Based on this, the first half of this study will primarily focus earthquakes 7.5M and larger. Earthquakes 6.5M and larger were also given the same treatment as 7.5M and larger for comparison and exploratory purposes with a few caveats. The caveats are that the 6.5M and larger magnitude category while containing more data than the 7.5M and larger, is not as evenly distributed, is incomplete (missing earthquakes) from the time period of 1900 to 1964 for all three datasets, and depending on the time period may contain non geophysical trends due to advancements or limitations of seismological technology of the time.

The analysis for this study is divided into multiple parts each with its own focus. Parts 1, 2, 3, and 4 are focused on time series analysis of sunspots and earthquakes 7.5M and larger in the time domain only, and utilize linear-least squares, Pearson's R correlation with p-value,

Shapiro-Wilk test, and Quartile-Quartile (Q-Q) plots to help determine the significance of any possible linear correlation.

Part 1 investigates the possibility of a connection between earthquakes and the change in slope of the solar cycle, but only with earthquakes and annual sunspot numbers grouped with respect to the whole rise and decline phases of the solar cycle. Part 2 using daily sunspot numbers grouped into 6 month (182 days) long averages, and investigates if there is a possible correlation between sunspots and earthquakes using the change in slope of the solar sunspot cycle over the 1900 to 2000's data range. Part 3 repeats the analysis of part 2, but only for the historical period (pre-WWSSN Era) of 1900 through 1963. Part 4 also repeats the analysis of 2 but for the modern period from 1964 into the 2000's. Part 5 starts the spectral analysis aspect of this study using the real fast fourier transform (RFFT) on magnitude categories of earthquake data using the whole earthquake dataset. The Magnitude spectrum results of the RFFT on earthquake data are compared to known solar periodicities found in the literature review.

2.2.1: Part 1 - Time Series Analysis - The Rise and Decline of the Solar Sunspot Cycle.

Using yearly mean sunspot numbers, each solar cycle was identified from 1700 to 2008. The starting point for each solar cycle was the first non-zero year from which the years following had increasing sunspot numbers (SN). Since the first solar cycle Wolf identified started in 1755 (solar cycle 1), the first five solar cycles were given letter names A, B, C, D, and E as presented in table 2. The starting year of the solar sunspot number rise and decline phases were also identified for each solar cycle. The solar cycle slope was calculated for each rise and decline phase using,

$$Solar\ cycle\ slope = \frac{SN_{Min} - SN_{Max}}{Year_{Min} - Year_{Max}} \quad . \tag{3}$$

Where,

SN_{Min} = Sunspot number at the start of the solar cycle or at solar cycle minimum.

SN_{Max} = Sunspot number at the height of the solar cycle maximum.

$Year_{Min}$ = Solar sunspot cycle start year or minimum.

$Year_{Max}$ = Solar sunspot cycle maximum year.

For the rise phase $Year_{Min}$ and SN_{Min} corresponded to the start of the solar cycle. For the decline phase $Year_{Min}$ and SN_{Min} corresponded to the solar minimum = the year before the start of the next solar cycle. The corresponding slope year was also calculated with,

$$Slope\ year = \frac{Year_{Min} + Year_{Max}}{2} \tag{4}$$

Table 4: List of solar cycle sunspot numbers (SN) start years for the rise and decline phase, with the slope (m) calculated for each phase from 1700 to 1755.

Solar Cycle	Cycle phase	Min year	Min SN	Max year	Max SN	Slope year	Slope (m)
Solar cycle A	Rise	1700	8.3	1705	96.7	1702.5	17.7
Solar cycle A	Decline	1712	0	1705	96.7	1708.5	-13.8
Solar cycle B	Rise	1712	0	1717	105	1714.5	21.0
Solar cycle B	Decline	1723	18.3	1717	105	1720.0	-14.5
Solar cycle C	Rise	1723	18.3	1727	203.3	1725.0	46.3
Solar cycle C	Decline	1733	8.3	1727	203.3	1730.0	-32.5
Solar cycle D	Rise	1733	8.3	1738	185	1735.5	35.3
Solar cycle D	Decline	1744	8.3	1738	185	1741.0	-29.5
Solar cycle E	Rise	1744	8.3	1750	139	1747.0	21.8
Solar cycle E	Decline	1755	16	1750	139	1752.5	-24.6

The slopes were calculated for each solar cycle rise and decline from 1700 to the solar maximum of cycle # 24 in 2008. For each earthquake dataset, the average number of earthquakes per rise and decline phase of the solar cycle was calculated starting with solar cycle # 14 in 1901. For solar cycles such as # 14 and # 22 that are double peaked at solar maximum, the first peak is used in calculating the solar slope over the rise phase and the second peak is used to calculate the slope over the decline phase as shown in the table below. The sunspots between the double peaks were ignored and are not included in the slope calculations.

Table 5: List of sunspot number (SN) solar cycles with their respective minimum year, maximum year, minimum sunspot number (Min SN), maximum sunspot number (Max SN), the slope, and the calculated midpoint of the cycle side (SN slope year).

Solar cycle	Cycle side	Min year	Min SN	Max year	Max SN	SN slope year	SN slope (m)
Solar cycle 14	Rise	1901	4.6	1905	105.5	1903	25.2
Solar cycle 14	Decline	1913	2.4	1907	102.8	1910	-16.7
Solar cycle 15	Rise	1913	2.4	1917	173.6	1915	42.8
Solar cycle 15	Decline	1923	9.7	1917	173.6	1920	-27.3
Solar cycle 16	Rise	1923	9.7	1928	129.7	1925.5	24
Solar cycle 16	Decline	1933	9.2	1928	129.7	1930.5	-24.1
Solar cycle 17	Rise	1933	9.2	1937	190.6	1935	45.4
Solar cycle 17	Decline	1944	16.1	1937	190.6	1940.5	-24.9
Solar cycle 18	Rise	1944	16.1	1947	214.7	1945.5	66.2
Solar cycle 18	Decline	1954	6.6	1947	214.7	1950.5	-29.7
Solar cycle 19	Rise	1954	6.6	1957	269.3	1955.5	87.6
Solar cycle 19	Decline	1964	15	1957	269.3	1960.5	-36.3
Solar cycle 20	Rise	1964	15	1968	150	1966	33.8
Solar cycle 20	Decline	1976	18.4	1968	150	1972	-16.5
Solar cycle 21	Rise	1976	18.4	1979	220.1	1977.5	67.2
Solar cycle 21	Decline	1986	14.8	1979	220.1	1982.5	-29.3
Solar cycle 22	Rise	1986	14.8	1989	211.1	1987.5	65.4
Solar cycle 22	Decline	1996	11.6	1991	203.3	1993.5	-38.3
Solar cycle 23	Rise	1996	11.6	2000	173.9	1998	40.6
Solar cycle 23	Decline	2008	4.2	2000	173.9	2004	-21.2
Solar cycle 24	Rise	2008	4.2	2014	113.3	2011	18.2

With respect to the earthquake catalogs, there were some differences between the 3 of them. To make sure the earthquake data across all three datasets were handled the same way with respect to time, the time stamp for all three catalogs needed to be standardized. First the

datetime-stamps were standardized into an estimated fractional year using midnight January 1st, 1900 as the baseline start year. The date and timestamp for each earthquake was converted to the total number of seconds from the 1900 baseline. Then an approximate fractal year was calculated without consideration for leap years. For this study a year was defined as 365.2422 days. The approximate fractional year was calculated using the following equation,

$$Fractional\ year = 1900 + \frac{\left(\frac{Earthquake\ occurrence\ time\ in\ seconds\ from\ 1900}{86400\ seconds\ in\ a\ day}\right)}{365.2422\ days\ in\ a\ year} \quad (5)$$

For each earthquake dataset, the earthquakes were then divided into earthquake (EQ) magnitude (M) categories for exploratory purposes as shown in Table # 6.

Table 6: Earthquake magnitude categories. Note the Cennteinal Y2K catalog only contained earthquakes of magnitude 5.5M and larger so analysis for categories < 5.5M could not be done.

#	Earthquake Magnitude Category	#	Earthquake Magnitude Category
1	7.5M and up (7.5 ≤ EQs)	**12**	3.5M to 4M (3.5M ≤ EQs < 4M)
2	2M (2M ≤ EQs < 3M)	**13**	4M to 4.5M (4M ≤ EQs < 4.5M)
3	3M (3M ≤ EQs < 4M)	**14**	4.5M to 5M (4.5M ≤ EQs < 5M)
4	4M (4M ≤ EQs < 5M)	**15**	5M to 5.5M (5M ≤ EQs < 5.5M)
5	5M (5M ≤ EQs < 6M)	**16**	5.5M to 6M (5.5M ≤ EQs < 6M)
6	6M (6M ≤ EQs < 7M)	**17**	6M to 6.5M (6M ≤ EQs < 6.5M)
7	7M (7M ≤ EQs < 8M)	**18**	6.5M to 7M (6.5M ≤ EQs < 7M)
8	8M (8M ≤ EQs < 9M)	**19**	7M to 7.5M (7M ≤ EQs < 7.5M)
9	2M to 2.5M (2M ≤ EQs < 2.5M)	**20**	7.5M to7M (7.5M ≤ EQs < 8M)
10	2.5M to 3M (2.5M ≤ EQs < 3M)	**21**	8M to 8.5M (8M ≤ EQs < 8.5M)
11	3M to 3.5M (3M ≤ EQs < 3.5M)	**22**	8.5M to 9M (8.5M ≤ EQs < 9M)

The average number of earthquakes and standard deviation for the rise phase of the solar cycle were calculated for earthquakes 7.5M and larger for each dataset using equations 6, 7, and

8. Equations 9, 10, and 11 were used to calculate the average number of earthquakes and standard deviation for the decline phase of the solar cycle.

For the rise phase:

$$E_{qRise} = \sum_{n \geq R_{Min}}^{n < R_{Max}} E_q(n) \quad (6)$$

Where, E_{qRise} = Number of earthquakes during the rise phase of the solar cycle, n = year, $E_q(n)$ = Number of earthquakes during year n, R_{Max} = Solar rise maximum year, and R_{Min} = Solar rise start year.

$$\overline{E}_{qRise} = \frac{E_{qRise}}{N_R} \quad (7)$$

Where, $\overline{E}_{qRise}$ = Average number of earthquakes during the rise phase, N_R = Total number of years for rise phase. The standard deviation was calculated using,

$$\mathrm{Std}_{\mathrm{EqR}} = \sqrt{\frac{\Sigma (E_{qRise} - \overline{E}_{qRise})^2}{(N_R - 1)}} \quad (8)$$

Where, $\mathrm{Std}_{\mathrm{EqR}}$ = Standard deviation of $\overline{E}_{qRise}$.

For the decline phase:

$$E_{qDecline} = \sum_{n \geq R_{Max}}^{n < D_{Min}} E_q(n) \quad (9)$$

Where, $E_{qDecline}$ = Number of earthquakes during the decline phase of the solar cycle, n = year, $E_q(n)$ = Number of earthquakes during year n, and R_{Max} = Solar rise maximum year (this is the beginning of the decline phase). D_{Min} = Solar rise start year for the next solar cycle.

$$\overline{E}_{qDecline} = \frac{E_{qDecline}}{N_D} \quad (10)$$

Where, $\overline{E}_{qDecline}$ = Average number of earthquakes during the decline phase, N_D = Total number of years for decline phase. The standard deviation was calculated using,

$$\mathrm{Std}_{EqD} = \sqrt{\frac{\Sigma (E_{qDecline} - \overline{E}_{qDecline})^2}{(N_D - 1)}} \quad (11)$$

Where,

Std_{EqD} = Standard deviation of $\overline{E}_{qDecline}$.

Then scatter plots of 7.5M and up earthquakes vs. time were generated in order to look for any visually obvious gaps in the data for any periods of time. The next aspect of part 1 consists of first summing the total number of earthquakes per year from 1900 into the 2000's and then plotting earthquakes per year vs. time. Then using a linear least squares approximation to model a trend line of best fit,

$$y = mx + b. \quad (12)$$

Where y is the number of earthquakes, m is the slope (earthquakes/year), x is time in years, and b is the y-intercept. The slope m was calculated using,

$$m = \frac{\Sigma(x - \bar{x})(y - \bar{y})}{\Sigma(x - \bar{x})^2}, \quad (13)$$

and the y-intercept b was calculated using,

$$b = \bar{y} - m\bar{x}. \quad (14)$$

Where $\bar{y}$ is the average number of earthquakes contained in the the dataset, and $\bar{x}$ is the average time in years.

Once the line of best fit was calculated, it was then used to mean center the earthquake data. The original earthquake data was plotted in green and the mean centered data with the overall linear trend removed was plotted in black. Then the average number of earthquakes per rise and decline phase of the solar cycle for both original and detrended data were calculated and compared against the slope of the solar sunspot cycle in the following ways for both original and detrended data:

1. Using overlay plots:
    a. The averaged 7.5M and up earthquake data was plotted with the change in slope m of the solar cycle for visual inspection.
    b. Then the positive solar slope data points along with their corresponding (with respect to time) earthquake data points were separated from the negative slope valued data and were overlaid with corresponding earthquake data for visual inspection.

    c. Then the absolute value of the solar cycle slope was plotted with the earthquake data.
2. Scatter plots with a line of best fit, Pearson's R correlation and associated p-value were generated for steps 'a' through 'c' of # 1 above.
    a. For each scatter plot with line of best fit, another plot of the resulting residuals were also plotted.

Pearson's R correlation can assess the strength of a linear correlation between two independent variables assuming a relationship exists. Pearson's R correlation and p-value can help assess to what degree earthquakes are linearly related to the change in slope of the solar cycle, while the R^2 value indicates what percentage of the correlation is explained by the line of best fit. If a non-linear correlation were to exist between the variables, then Pearson's R correlation with its associated p-value may not reflect that. Pearson's R correlation also assumes that there are no outliers, homoscedasticity (meaning the variance is relatively the same for all all values around the line of best fit), and that the data sample follows a normal distribution even if the overall population is not normally distributed. However, the hypothesis of this study assumes that sunspots and earthquakes are orthogonal and yet possibly correlated in a similar way to how sin(x) and cos(x) are related, and thus are not linearly correlated. So to help assess if the Pearson's R and p-values are evaluating a normally distributed sample, the residuals of the resulting linear line of best fit were tested using the Shapiro-Wilk test (W) for normality [109]. To help assess if the Shapiro-Wilk test was accurate and if Pearson's R coefficient were also

evaluating a linear relationship, the residuals of the line of best fit were ranked and plotted against theoretical normally distributed values on a Quartile-Quartile plot [110].

The Shapiro-Wilk test statistic W is calculated using:

$$\mathrm{W} = \frac{\left(\sum_{i=1}^{n} a_i x_{(i)}\right)^2}{\sum_{i=1}^{n} (x_i - \bar{x})^2} \quad , \tag{15}$$

where $x_{(i)}$ are the sampled values in order from the smallest $x_{(1)}$ to the largest $x_{(n)}$, with the constants a_i are "generated from the means, variances, and covariances, of the order statistics of a sample size n from a normal distribution." [109][111][112]

The W statistic ranges between 0 and 1, and the closer W is to 1, then it means the data sample came from a normal distribution with W=1 being the perfect theoretical normal distribution. In this case it would mean that the residuals are normally distributed, and thus both data samples from earthquake and sunspot data used are also normally distributed. If the p-value for the Shapiro-Wilk test statistic W is $p > 0.05$ it means that the distribution of the residuals does not significantly differ from a normal distribution. If $p < 0.05$ then the sample did not likely come from a normal distribution.

The Shapiro-Wilk test result and p-value are listed on the corresponding Quartile-Quartile plot of the residuals for each scatter plot.

2.2.2: Part 2: Time Series Analysis - Earthquakes and Solar Sunspot Cycle Comparison.

For part 2, the earthquake dataset was divided into equally spaced one day increments of time. The daily sunspot data are already in this format. Zeros were used to fill the gaps on days where either there was missing data or an earthquake did not occur. Then both the daily sunspot numbers and daily earthquake counts were averaged over six month increments with the instantaneous solar slope m being calculated as:

$$S_m = \frac{\Delta SN_A}{\Delta SN_T} = \frac{SN_A(i) - SN_A(i+2)}{SN_T(i) - SN_T(i+2)}$$, where SN_A = Average Sunspot number, (16)

SN_T = Corresponding time of average sunspot number in years, and i = the 6th month period of interest. The instantaneous slope was averaged using,

$$S_{mAve} = \frac{S_m(i-1) - S_m(i+1)}{2}$$, where i = the 6th month period of interest. (16)

Once the 6 month averages were calculated for the slope of the solar cycle and for earthquakes, then the 6 month averaged number of earthquakes of the solar cycle were calculated and compared against the slope of the solar sunspot cycle in the following ways for both original and detrended data:

3. Using overlay plots:
    a. The averaged 7.5M and up earthquake data was plotted with the change in slope m of the solar cycle for visual inspection.
    b. Then the absolute value of the solar cycle slope was plotted with the earthquake data.

The rest of the procedure for part 2 is identical to part 1 with respect to scatter plots, calculating Pearson's R squared coefficient, residuals, Shapiro-Wilk test, and Q-Q plots.

2.2.3: Part 3: Time Series Analysis - Earthquakes and Sunspot Cycle Slope Comparison 1900 through 1963 (Historical Period).

The procedure for part 3 is identical to part 2, except the date range is 1900 through 2007.

2.2.4: Part 4: Time Series Analysis - Earthquakes and Sunspot Cycle Slope Comparison 1964 through 2000's (Modern Era).

The procedure for part 4 is identical to parts 2 and 3, except the date range is 1964 through 2007.

2.2.5: Part 5: Spectral Analysis - Earthquakes and Sunspots, Comparing the fft of their two day counts and slopes.

Instead of focusing primarily on magnitude 7.5M and up earthquakes. Part 5 utilizes the whole earthquake dataset from 1900 to 2000's for the FFT without care or redguard that the datasets may be incomplete for most magnitudes, dominated by smaller earthquakes, and\or contains non-geophysical trends due to advancements in technology. Each dataset is divided into the following magnitude categories as shown in table # 7.

Table 7: Earthquake magnitude categories. Note the Cennteinal Y2K catalog only contained earthquakes of magnitude 5.5M and larger so analysis for categories < 5.5M could not be done.

#	Earthquake Magnitude Category	#	Earthquake Magnitude Category
1	All Earthquakes in dataset	**13**	4M (4M ≤ EQs < 5M)
2	7.5M and up (7.5M ≤ EQs)	**14**	5M (5M ≤ EQs < 6M)
3	6.5M and up (6.5M ≤ EQs)	**15**	6M (6M ≤ EQs < 7M)
4	8M and up (8M ≤ EQs)	**16**	7M (7M ≤ EQs < 8M)
5	7M and up (7M ≤ EQs)	**17**	8M (8M ≤ EQs < 9M)
6	6M and up (6M ≤ EQs)	**18**	9M down (EQs < 9M)
7	5M and up (5M ≤ EQs)	**19**	8M down (EQs < 8M)
8	4M and up (4M ≤ EQs)	**20**	7M down (EQs < 7M)
9	3M and up (3M ≤ EQs)	**21**	6M down (EQs < 6M)
10	2M and up (2M ≤ EQs)	**22**	5M down (EQs < 5M)
11	2M (2M ≤ EQs < 3M)	**23**	4M down (EQs < 4M)
12	3M (3M ≤ EQs < 4M)	**24**	3M down (EQs < 3M)

Before dividing the earthquake data into magnitude categories, the seismic energy (E) released for each earthquake was estimated using the following energy equations substituting M for magnitude [66]:

For earthquakes ≥ 5.5M,

$$E = 10^{4.8+1.5M}, \quad (18)$$

and for earthquakes < 5.5M,

$$E = 10^{2.4M-1.2}, \quad (19)$$

where M = earthquake magnitude, and E = total seismic earthquake energy released in Joules. Equation 18 is only good for medium to large earthquakes, and equation 19 assumes a range of $2.0 \leq \mathbf{m_B} < 8.0$ [66]. Since this study is using these equations as a rough estimate of seismic energy released, M was also substituted for $\mathbf{m_B}$ and applied to earthquakes less than 2M.

After the estimated earthquake energy was calculated, then the dataset was divided into magnitude categories. The data also had to be divided into equally spaced one day increments of time because the FFT requires the data be continuous and without any gaps. In order to achieve a continuous earthquake dataset suitable for the FFT, zeros were used to fill the gaps (similar to part 2) on days where either there was missing data or an earthquake did not occur. The total earthquake energy released per day was approximated by summing up all of the calculated energies for all earthquake occurrences per day within each magnitude category. Once the data was in a continuous format, then the instantaneous change in slope was calculated for both sunspots and earthquakes, resulting in 2 data series for the solar data:

1) Total Sunspot number per day,
2) Slope m of daily sunspot number.

And 4 data series for each magnitude category:

3) Earthquake occurrence per day,
4) Estimated energy released per day,

5) The slope of daily earthquake occurrence,

6) The slope of daily energy released.

Then all six of the above series were averaged over two day increments and the real FFT was used to transform each of the six data series from the time domain into the frequency domain.

The equation used for the FFT method of computing the discrete fourier transform (DST) is [113][114],

$$A_n = \sum_{k=0}^{N-1} X_k \, exp(-2\pi jnk/N) \tag{20}$$

Where,

X_k is the kth sample of the time series consisting of N samples,

$$j = \sqrt{-1}\,. \tag{21}$$

Inverse Fourier transform is,

$$X_k = \sum_{k=0}^{N-1} A_n \, exp(2\pi jnk/N) \quad . \tag{22}$$

This study uses the real FFT (RFFT) taking advantage of the symmetrical nature of the FFT, and it outputs only the first half of the symmetrical transformation. Since both the sunspot numbers and earthquake data are real valued, using the RFFT variant of the FFT saves computation time and is easier to plot.

The magnitude of the RFFT is,

$$\text{Magnitude of } A_n = |A_n|\,. \tag{23}$$

The Magnitude was then averaged together across all three (ISC, Centennial, and USGS ComCat) for the following magnitude categories as listed in the table below.

Table 8: The earthquake magnitude categories that had their Magnitude spectra averaged together across all three of the earthquake datasets ISC, Centennial, and USGS ComCat*. Note the Cennteinal Y2K catalog only contained earthquakes of magnitude 5.5M and larger, that is why it was excluded from averaging with the other magnitude categories that are not on this list.*

#	**Earthquake Magnitude Category**	#	**Earthquake Magnitude Category**
1	All Earthquakes in dataset	**7**	5M and up (5M ≤ EQs)
2	7.5M and up (7.5M ≤ EQs)	**8**	5M (5M ≤ EQs < 6M)
3	6.5M and up (6.5M ≤ EQs)	**9**	6M (6M ≤ EQs < 7M)
4	8M and up (8M ≤ EQs)	**10**	7M (7M ≤ EQs < 8M)
5	7M and up (7M ≤ EQs)	**11**	8M (8M ≤ EQs < 9M)
6	6M and up (6M ≤ EQs)		

The other magnitude categories were averaged between the USGS Comcat and the ISC datasets except for earthquakes 2M down. No earthquakes below 2M were downloaded from the USGS ComCat online catalog. The magnitude of the averaged spectra was compared to the magnitude of the spectra of the earthquake datasets for all magnitude categories and finally against the solar cycle for both the two day average and two day averaged slope in order to compare it against known periodicities from the literature review.

Chapter 3: Results

3.1 Time Series Results

The results in this section are organized in order and pertain only to the magnitude category of earthquakes 7.5M and larger, starting with a summary of part 1 of the time series analysis and ending with a sampling of 16 plots out of 88 from part 5 spectral analysis. Sections 3.1.1 through 3.1.4 are organized in an identical manner. First a summary table containing the statistical results of that part of the analysis. Due to the large number of plots, only a selection of related plots based on the last line of each table are included herein, with the remaining plots located in the appendix. Earthquakes 6.5M and larger were given the same treatment as 7.5M and larger for parts 1 to 4 of the time series analysis, and their plots are also located in the appendix.

The figure names within each table are abridged from their full name. Instead of the normal convention of figure numbers being continuous within the body of a report, this section breaks with that convention and instead uses the exact figure number as found within the appendix for each figure in the table and the accompanying plots that follow it. The letter contained within the figure number denotes which section of the appendix the plot can be found in as well as which earthquake dataset was used for the analysis. The letters in the figure numbers have the following meanings:

B = Centennial Earthquake dataset, with plots found in Appendix section B.

C = USGS ComCat Earthquake dataset, with plots found in Appendix section C.

D = ISC Earthquake dataset, with plots found in Appendix section D.

E = Magnitude of averaged earthquake spectra, with plots found in Appendix section E.

F = Comparison of Magnitude of averaged earthquake spectra to ISC, USGS, and Centennial datasets (Not shown in this section), with plots found in Appendix section F.

This convention was used in order to make finding the respective plots in association with each table easier within this large document. Each line in the table represents only 1 of 4 plots, each based on the associated statistics found in their respective row, and these statistics are repeated within the figure caption of 3 out of the 4 associated plots.

It is also worth noting that many plots “with earthquake trend removed” will have some sort of negative number of earthquakes, or a negative average number of earthquakes. This is a result of averaging earthquakes over time, calculating a linear line of best fit, and then removing the linear trendline from the data, and thus causing the transformed data to be centered about zero. In nature, there is no such thing as 0.5 of an earthquake, or an average of -1.5 earthquakes. The overall point of these plots is to use them as a tool to help determine how non-geophysical trends once removed from the data, impact correlation analysis between sunspots and earthquakes. The analysis assumes the non-geophysical trends contained in the earthquake data are overall linear.

3.1.1 Time Series Results Part 1

Table 9: USGS Centennial, part 1 (1900-2007) time series analysis results, where y = 7.5M and larger earthquake data, and x = solar data.

Figure name	p value	r value	r sqrd	y average	y std	m slope	b intercept	x average	x std
Figure # B1.15: SN Slope (m). Associated Plots: B1.5, B1.16, B1.17.	0.0562	-0.4450	0.1981	3.9591	1.0865	-0.0116	4.0860	10.98	41.86
Figure # B1.18: SN Slope (m) notrend. Associated Plots: B1.6, B1.19, B1.20.	0.0406	-0.4734	0.2241	-0.1409	0.9348	-0.0106	-0.0248	10.98	41.86
Figure # B1.21: SN Slope rise phase. Associated Plots: B1.11, B1.22, B1.23.	0.9062	-0.0430	0.0018	3.4444	1.1831	-0.0102	3.9798	52.56	19.00
Figure # B1.21: SN Slope decline phase. Associated Plots: B1.13, B1.22, B1.23.	0.4270	0.2837	0.0805	4.4223	0.7281	0.0296	5.2050	-26.43	6.97
Figure # B1.24: SN Slope rise phase notrend. Associated Plots: B1.12, B1.25, B1.26.	0.2415	-0.4354	0.1895	-0.5648	0.9443	-0.0216	0.5721	52.56	19.00
Figure # B1.24: SN Slope decline phase notrend. Associated Plots: B1.14, B1.25, B1.26.	0.2778	0.3807	0.1449	0.2406	0.7421	0.0405	1.3112	-26.43	6.97
Figure # B1.27: SN Slope Absolute value. Associated Plots: B1.7, B1.28, B1.29	0.0688	-0.4262	0.1817	3.9591	1.0865	-0.0242	4.8973	38.81	19.15
Figure # B1.30: SN Slope Absolute value notrend. Associated Plots: B1.8, B1.31, B1.32.	0.0131	-0.5576	0.3109	-0.1409	0.9348	-0.0272	0.9152	38.81	19.15

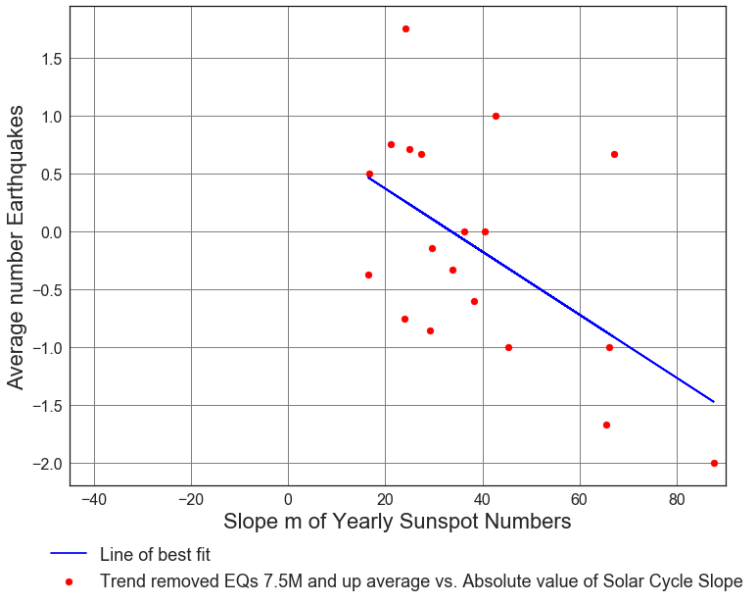

Figure B1.30: Scatter Plot of Absolute Slope Magnitude of the Solar cycle (from 1900 to 2014) vs. Trend removed Average number of 7.5M and up Earthquakes. Line of best fit, y = -0.02722x + (0.9152), mean x = 38.81 +/- 19.15, mean y = -0.1409 +/- 0.9348, R = -0.5576, R squared = 0.3109, p-value = 0.01312.

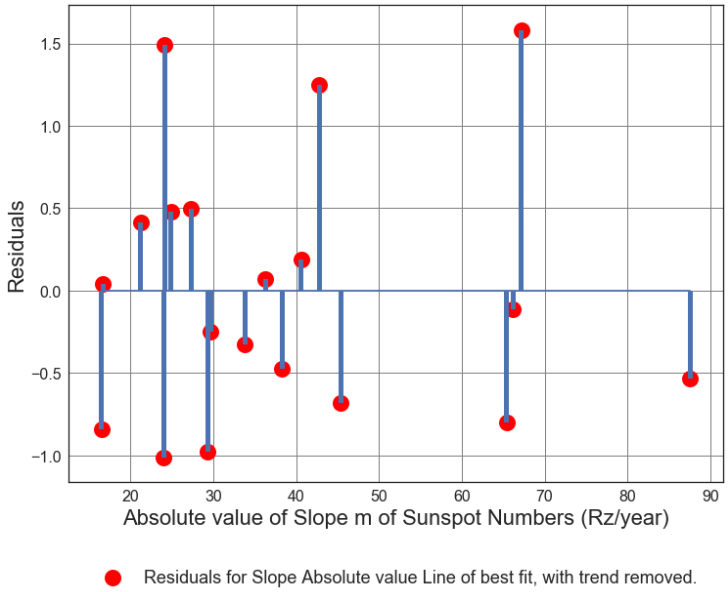

Figure B1.31: Scatter Plot of Absolute Slope Magnitude of the Solar cycle (from 1900 to 2014) vs. Trend removed Average number of 7.5M and up Earthquakes. Line of best fit, y = -0.02722x + (0.9152), mean x = 38.81 +/- 19.15, mean y = -0.1409 +/- 0.9348, R = -0.5576, R squared = 0.3109, p-value = 0.01312.

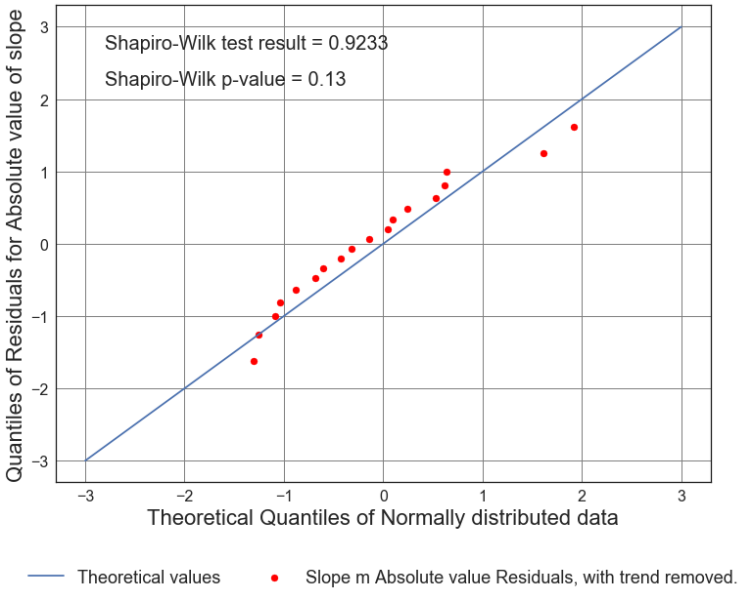

Figure B1.32: Scatter Plot of Absolute Slope Magnitude of the Solar cycle (from 1900 to 2014) vs. Trend removed Average number of 7.5M and up Earthquakes. Line of best fit, y = -0.02722x + (0.9152), mean x = 38.81 +/- 19.15, mean y = -0.1409 +/- 0.9348, R = -0.5576, R squared = 0.3109, p-value = 0.01312.

Table 10: USGS ComCat, part 1 (1900-2007) time series analysis results, where y = 7.5M and larger earthquake data, and x = solar data.

Figure name	p value	r value	r sqrd	y average	y std	m slope	b intercept	x average	x std
Figure # C1.15: SN Slope (m). Associated Plots: C1.5, B1.16, C1.17.	0.3262	-0.2381	0.0567	3.7591	1.2218	-0.0070	3.8355	10.98	41.86
Figure # C1.18: SN Slope (m) notrend. Associated Plots: C1.6, C1.19, C1.20.	0.3937	-0.2076	0.0431	-0.0651	0.8932	-0.0044	-0.0164	10.98	41.86
Figure # C1.21: SN Slope rise phase. Associated Plots: C1.11, C1.22, C1.23.	0.7950	-0.0945	0.0089	3.4815	1.2202	-0.0163	4.3397	52.56	19.00
Figure # C1.21: SN Slope decline phase. Associated Plots: C1.13, C1.22, C1.23.	0.5152	0.2340	0.0548	4.0090	1.1682	0.0392	5.0452	-26.43	6.97
Figure # C1.24: SN Slope rise phase notrend. Associated Plots: C1.12, C1.25, C1.26.	0.5065	-0.2558	0.0654	-0.2593	0.7354	-0.0099	0.2609	52.56	19.00
Figure # C1.24: SN Slope decline phase notrend. Associated Plots: C1.14, C1.25, C1.26.	0.3494	0.3315	0.1099	0.1096	0.9821	0.0467	1.3435	-26.43	6.97
Figure # C1.27: SN Slope Absolute value. Associated Plots: C1.7, C1.28, C1.29	0.1979	-0.3091	0.0955	3.7591	1.2218	-0.0197	4.5243	38.81	19.15
Figure # C1.30: SN Slope Absolute value notrend. Associated Plots: C1.8, C1.31, C1.32.	0.1976	-0.3093	0.0957	-0.0651	0.8932	-0.0144	0.4946	38.81	19.15

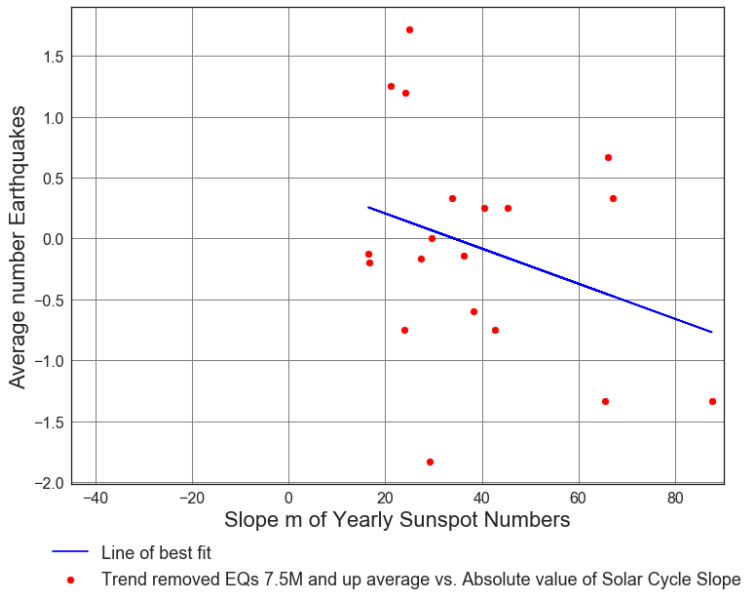

Figure C1.30: Scatter Plot of Absolute Slope Magnitude of the Solar cycle (from 1900 to 2014) vs. Trend removed Average number of 7.5M and up Earthquakes. Line of best fit, y = -0.01442x + (0.4946), mean x = 38.81 +/- 19.15, mean y = -0.0651 +/- 0.8932, R = -0.3093, R squared = 0.09566, p-value = 0.1976.

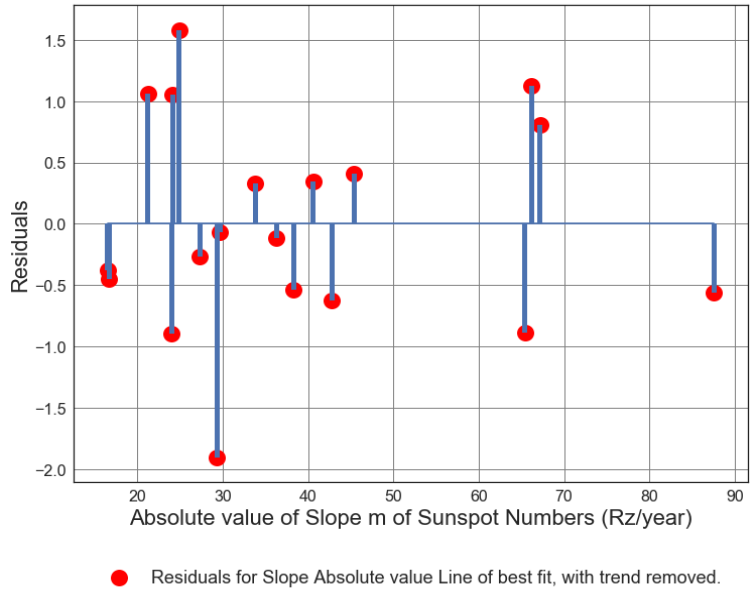

Figure C1.31: Scatter Plot of Absolute Slope Magnitude of the Solar cycle (from 1900 to 2014) vs. Trend removed Average number of 7.5M and up Earthquakes. Line of best fit, y = -0.01442x + (0.4946), mean x = 38.81 +/- 19.15, mean y = -0.0651 +/- 0.8932, R = -0.3093, R squared = 0.09566, p-value = 0.1976.

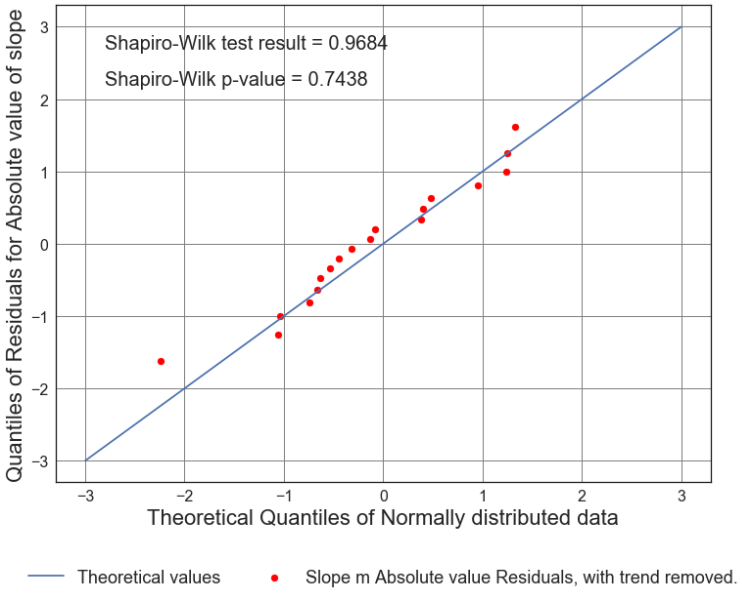

Figure C1.32: Scatter Plot of Absolute Slope Magnitude of the Solar cycle (from 1900 to 2014) vs. Trend removed Average number of 7.5M and up Earthquakes. Line of best fit, y = -0.01442x + (0.4946), mean x = 38.81 +/- 19.15, mean y = -0.0651 +/- 0.8932, R = -0.3093, R squared = 0.09566, p-value = 0.1976.

Table 11: ISC, part 1 (1900-2007) time series analysis results, where y = 7.5M and larger earthquake data, and x = solar data.

Figure name	p value	r value	r sqrd	y average	y std	m slope	b intercept	x average	x std
Figure # D1.15: SN Slope (m). Associated Plots: D1.5, D1.16, D1.17.	0.1003	-0.3884	0.1509	7.3669	2.0935	-0.0194	7.5802	10.98	41.86
Figure # D1.18: SN Slope (m) notrend. Associated Plots: D1.6, D1.19, D1.20.	0.0502	-0.4552	0.2072	-0.4840	1.6695	-0.0182	-0.2845	10.98	41.86
Figure # D1.21: SN Slope rise phase. Associated Plots: D1.11, D1.22, D1.23.	0.5950	-0.1921	0.0369	6.4815	2.3153	-0.0081	6.9079	52.56	19.00
Figure # D1.21: SN Slope decline phase. Associated Plots: D1.13, D1.22, D1.23.	0.8080	0.0885	0.0078	8.1637	1.4705	0.0187	8.6567	-26.43	6.97
Figure # D1.24: SN Slope rise phase notrend. Associated Plots: D1.12, D1.25, D1.26.	0.6163	-0.1944	0.0378	-1.2778	1.9798	-0.0202	-0.2136	52.56	19.00
Figure # D1.24: SN Slope decline phase notrend. Associated Plots: D1.14, D1.25, D1.26.	0.1990	0.4437	0.1969	0.2305	0.8307	0.0528	1.6273	-26.43	6.97
Figure # D1.27: SN Slope Absolute value. Associated Plots: D1.7, D1.28, D1.29	0.1820	-0.3198	0.1023	7.3669	2.0935	-0.0350	8.7233	38.81	19.15
Figure # D1.30: SN Slope Absolute value notrend. Associated Plots: D1.8, D1.31, D1.32.	0.0487	-0.4579	0.2096	-0.4840	1.6695	-0.0399	1.0648	38.81	19.15

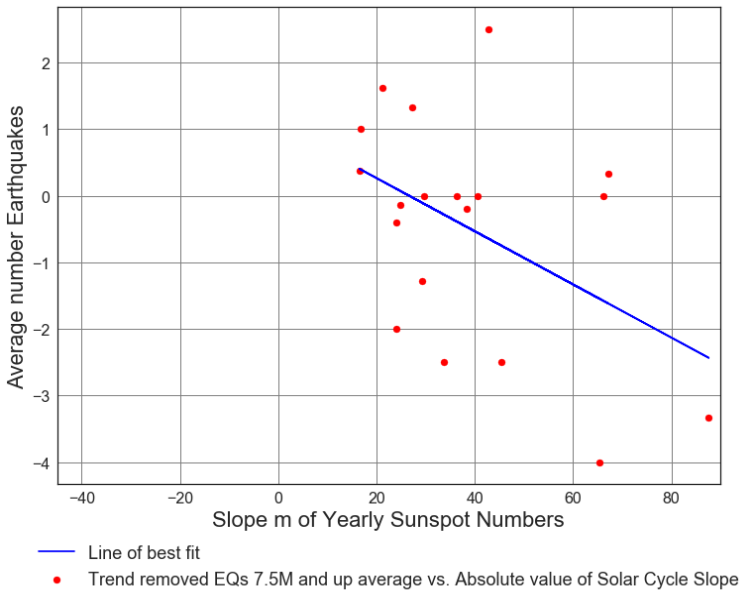

Figure D1.30: Scatter Plot of Absolute Slope Magnitude of the Solar cycle (from 1900 to 2014) vs. Trend removed Average number of 7.5M and up Earthquakes. Line of best fit, y = -0.03991x + (1.065), mean x = 38.81 +/- 19.15, mean y = -0.484 +/- 1.669, R = -0.4579, R squared = 0.2096, p-value = 0.04869.

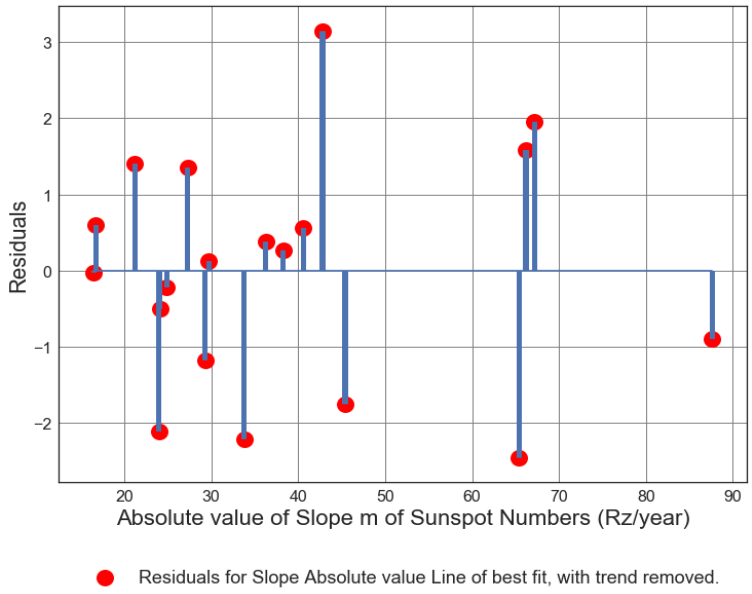

Figure D1.31: Scatter Plot of Absolute Slope Magnitude of the Solar cycle (from 1900 to 2014) vs. Trend removed Average number of 7.5M and up Earthquakes. Line of best fit, y = -0.03991x + (1.065), mean x = 38.81 +/- 19.15, mean y = -0.484 +/- 1.669, R = -0.4579, R squared = 0.2096, p-value = 0.04869.

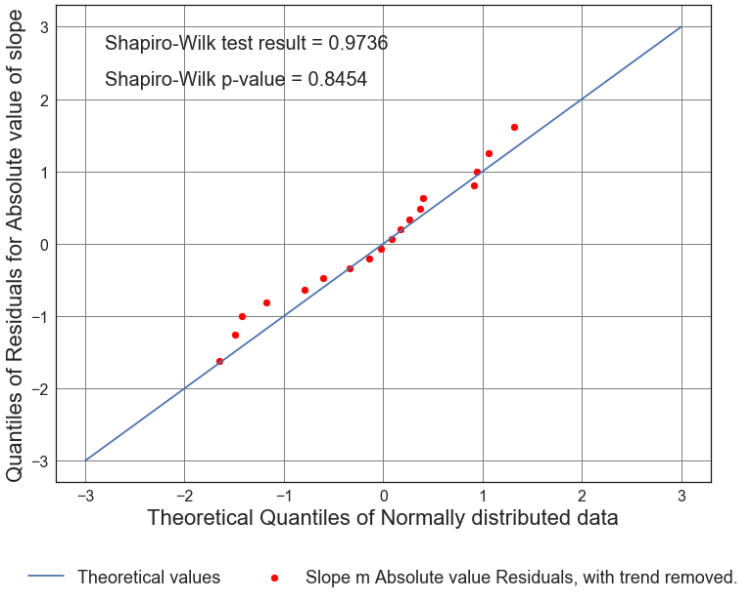

Figure D1.32: Scatter Plot of Absolute Slope Magnitude of the Solar cycle (from 1900 to 2014) vs. Trend removed Average number of 7.5M and up Earthquakes. Line of best fit, y = -0.03991x + (1.065), mean x = 38.81 +/- 19.15, mean y = -0.484 +/- 1.669, R = -0.4579, R squared = 0.2096, p-value = 0.04869.

3.1.2 Time Series Results Part 2

Table 12: USGS Centennial, part 2 (1900-2007), 6 month averaged time series analysis results, where y = 7.5M and larger earthquake data, and x = solar data.

Figure name	p value	r value	r sqrd	y average	y std	m slope	b intercept	x average	x std
Figure # B2.5: SN Slope vs average Eqs. Associated Plots: B2.1, B2.6, B2.7.	0.0026	-0.2038	0.0416	1.9421	1.0058	-0.0053	1.9418	-0.0701	38.33
Figure # B2.8: SN Slope vs average Eqs notrend. Associated Plots: B2.2, B2.9, B2.10.	0.0032	-0.1996	0.0398	-0.0008	1.0034	-0.0052	-0.0012	-0.0701	38.33
Figure # B2.11: Absolute value SN Slope vs average Eqs. Associated Plots: B2.3, B2.12, B2.13.	0.0461	-0.1359	0.0185	1.9421	1.0058	-0.0059	2.1243	30.66	23.00
Figure # B2.14: Absolute value SN Slope vs average Eqs notrend. Associated Plots: B2.4, B2.15, B2.16.	0.0311	-0.1467	0.0215	-0.0008	1.0034	-0.0064	0.1954	30.66	23.00

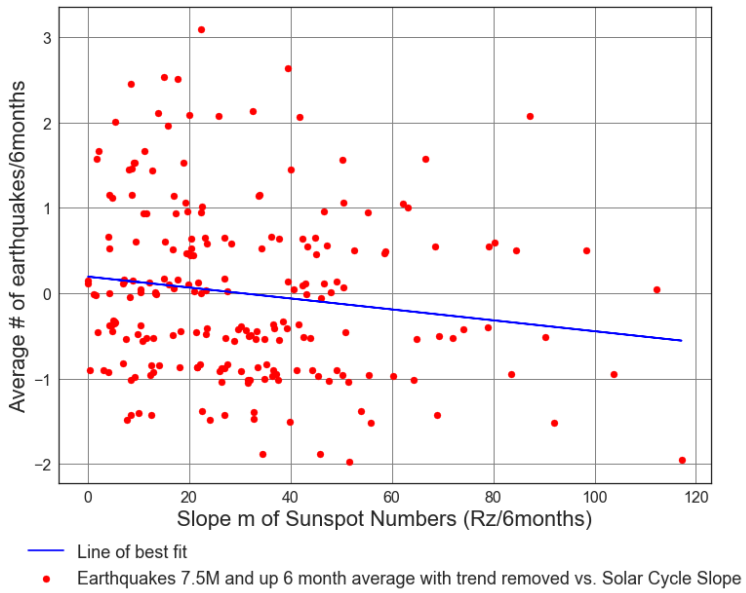

Figure B2.14: Scatter Plot of Solar cycle absolute value slope (from 1900 to 2007) vs. Average number of 7.5M and up Earthquakes/6months with trend removed. Line of best fit, y = -0.006401x + (0.1954), mean x = 30.66 +/- 23.0, mean y = -0.0008213 +/- 1.003, R = -0.1467, R squared = 0.02153, p-value = 0.03111.

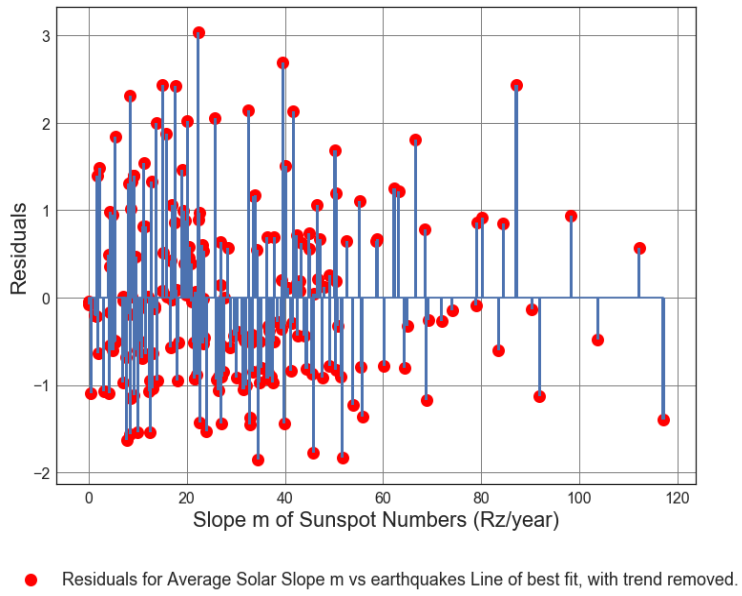

Figure B2.15: Scatter Plot of Solar cycle absolute value slope (from 1900 to 2007) vs. Average number of 7.5M and up Earthquakes/6months with trend removed. Line of best fit, y = -0.006401x + (0.1954), mean x = 30.66 +/- 23.0, mean y = -0.0008213 +/- 1.003, R = -0.1467, R squared = 0.02153, p-value = 0.03111.

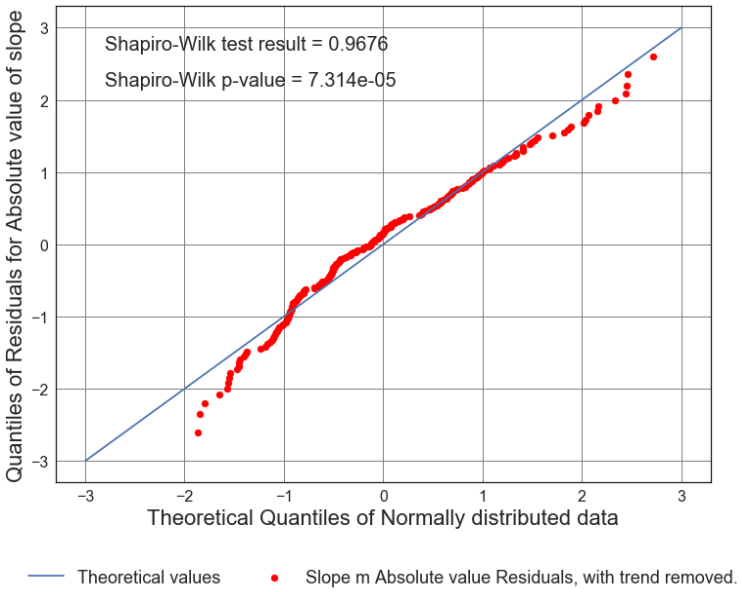

Figure B2.16: Scatter Plot of Solar cycle absolute value slope (from 1900 to 2007) vs. Average number of 7.5M and up Earthquakes/6months with trend removed. Line of best fit, y = -0.006401x + (0.1954), mean x = 30.66 +/- 23.0, mean y = -0.0008213 +/- 1.003, R = -0.1467, R squared = 0.02153, p-value = 0.03111.

Table 13: USGS ComCat, part 2 (1900-2007), 6 month averaged time series analysis results, where y = 7.5M and larger earthquake data, and x = solar data.

Figure name	p value	r value	r sqrd	y average	y std	m slope	b intercept	x average	x std
Figure # C2.5: SN Slope vs average Eqs. Associated Plots: C2.1, C2.6, C2.7.	0.0449	-0.1366	0.0187	1.8356	1.0832	-0.0039	1.8354	-0.0701	38.33
Figure #CB2.8: SN Slope vs average Eqs notrend. Associated Plots: C2.2, C2.9, C2.10.	0.0688	-0.1240	0.0154	-0.0004	1.0543	-0.0034	-0.0007	-0.0701	38.33
Figure # C2.11: Absolute value SN Slope vs average Eqs. Associated Plots: C2.3, C2.12, C2.13.	0.0081	-0.1798	0.0323	1.8356	1.0832	-0.0085	2.0953	30.66	23.00
Figure # C2.14: Absolute value SN Slope vs average Eqs notrend. Associated Plots: C2.4, C2.15, C2.16.	0.0011	-0.2206	0.0487	-0.0004	1.0543	-0.0101	0.3096	30.66	23.00

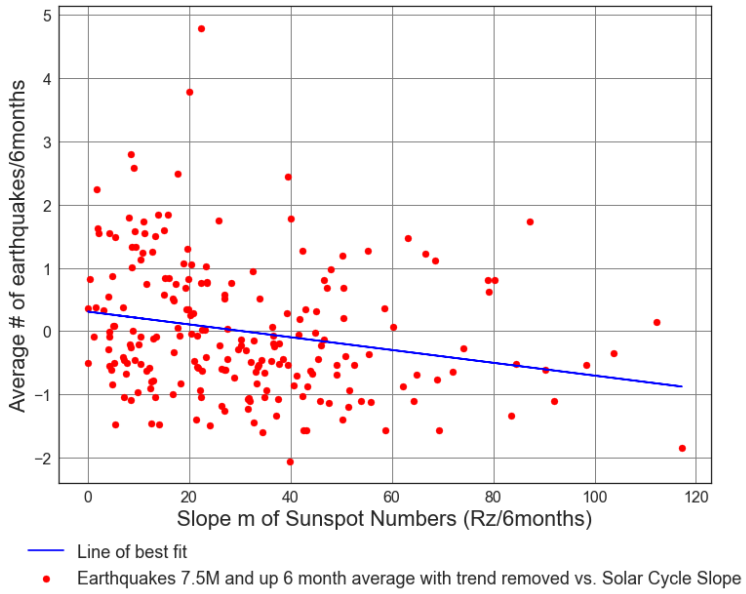

Figure C2.14: Scatter Plot of Solar cycle absolute value slope (from 1900 to 2017) vs. Average number of 7.5M and up Earthquakes/6months with trend removed. Line of best fit, y = -0.01011x + (0.3096), mean x = 30.66 +/- 23.0, mean y = -0.0004389 +/- 1.054, R = -0.2206, R squared = 0.04867, p-value = 0.0011.

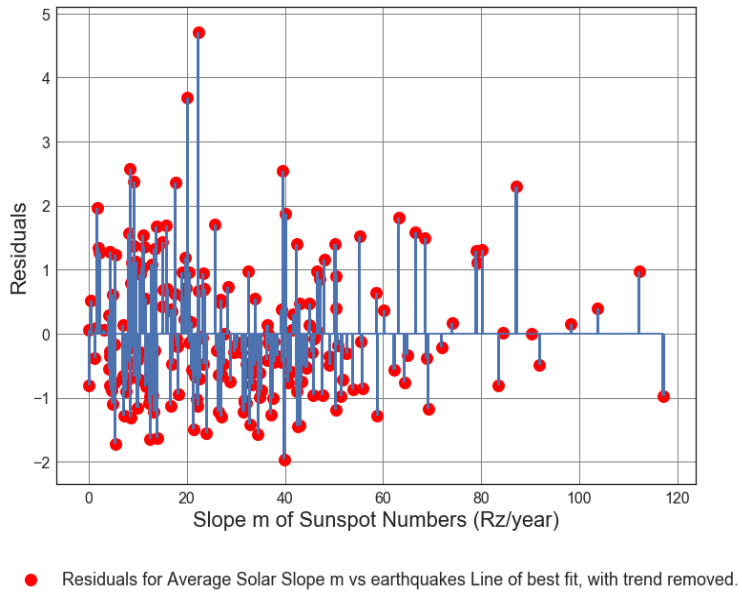

Figure C2.15: Scatter Plot of Solar cycle absolute value slope (from 1900 to 2017) vs. Average number of 7.5M and up Earthquakes/6months with trend removed. Line of best fit, y = -0.01011x + (0.3096), mean x = 30.66 +/- 23.0, mean y = -0.0004389 +/- 1.054, R = -0.2206, R squared = 0.04867, p-value = 0.0011.

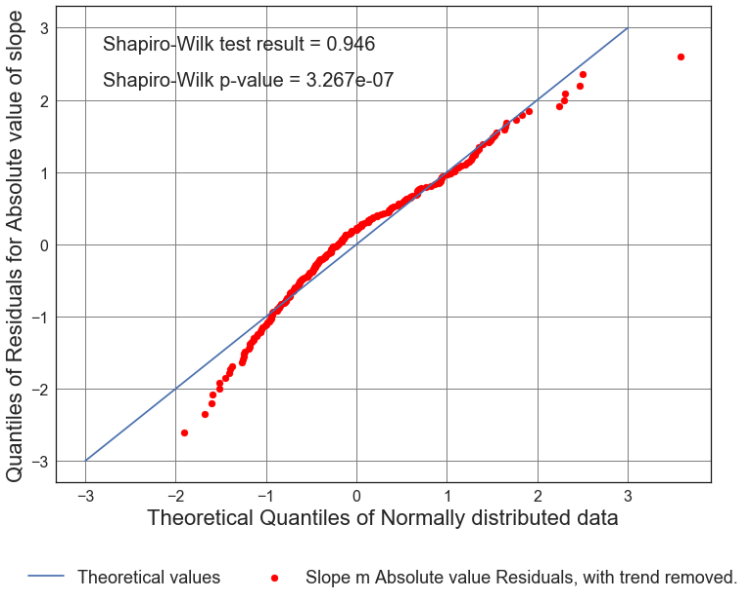

Figure C2.16: Scatter Plot of Solar cycle absolute value slope (from 1900 to 2017) vs. Average number of 7.5M and up Earthquakes/6months with trend removed. Line of best fit, y = -0.01011x + (0.3096), mean x = 30.66 +/- 23.0, mean y = -0.0004389 +/- 1.054, R = -0.2206, R squared = 0.04867, p-value = 0.0011.

Table 14: ISC, part 2 (1900-2007), 6 month averaged time series analysis results, where y = 7.5M and larger earthquake data, and x = solar data.

Figure name	p value	r value	r sqrd	y average	y std	m slope	b intercept	x average	x std
Figure # D2.5: SN Slope vs average Eqs. Associated Plots: D2.1, D2.6, D2.7.	0.0042	-0.1943	0.0378	3.7269	1.7445	-0.0088	3.7262	-0.0701	38.33
Figure # D2.8: SN Slope vs average Eqs notrend. Associated Plots: D2.2, D2.9, D2.10.	0.0078	-0.1806	0.0326	0.0121	1.6332	-0.0077	0.0115	-0.0701	38.33
Figure # D2.11: Absolute value SN Slope vs average Eqs. Associated Plots: D2.3, D2.12, D2.13.	0.0718	-0.1227	0.0151	3.7269	1.7445	-0.0093	4.0123	30.66	23.00
Figure # B2.14: Absolute value SN Slope vs average Eqs notrend. Associated Plots: D2.4, D2.15, D2.16.	0.0050	-0.1904	0.0362	0.0121	1.6332	-0.0135	0.4266	30.66	23.00

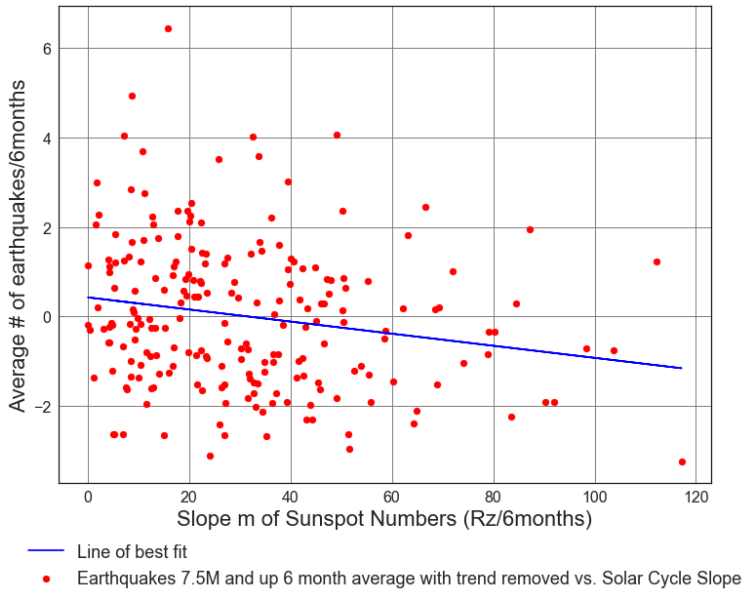

Figure D2.14: Scatter Plot of Solar cycle absolute value slope (from 1900 to 2017) vs. Average number of 7.5M and up Earthquakes/6months with trend removed. Line of best fit, y = -0.01352x + (0.4266), mean x = 30.66 +/- 23.0, mean y = 0.01209 +/- 1.633, R = -0.1904, R squared = 0.03625, p-value = 0.004991.

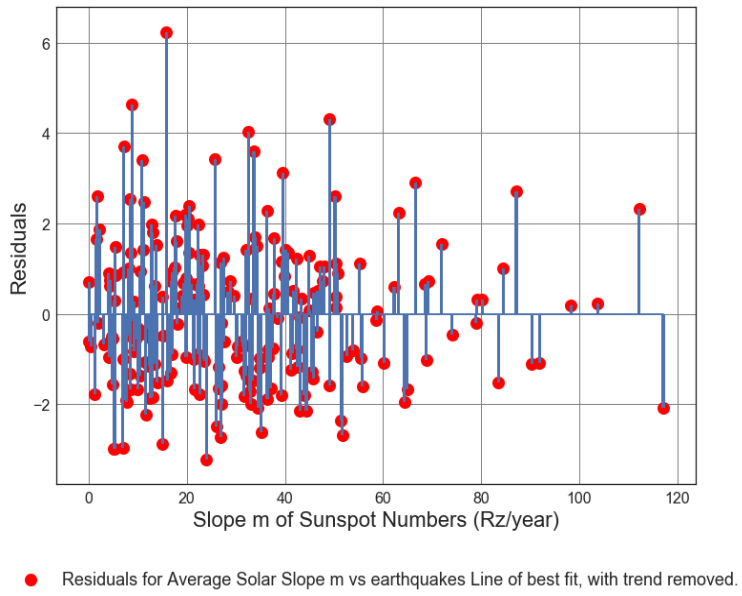

Figure D2.15: Scatter Plot of Solar cycle absolute value slope (from 1900 to 2017) vs. Average number of 7.5M and up Earthquakes/6months with trend removed. Line of best fit, y = -0.01352x + (0.4266), mean x = 30.66 +/- 23.0, mean y = 0.01209 +/- 1.633, R = -0.1904, R squared = 0.03625, p-value = 0.004991.

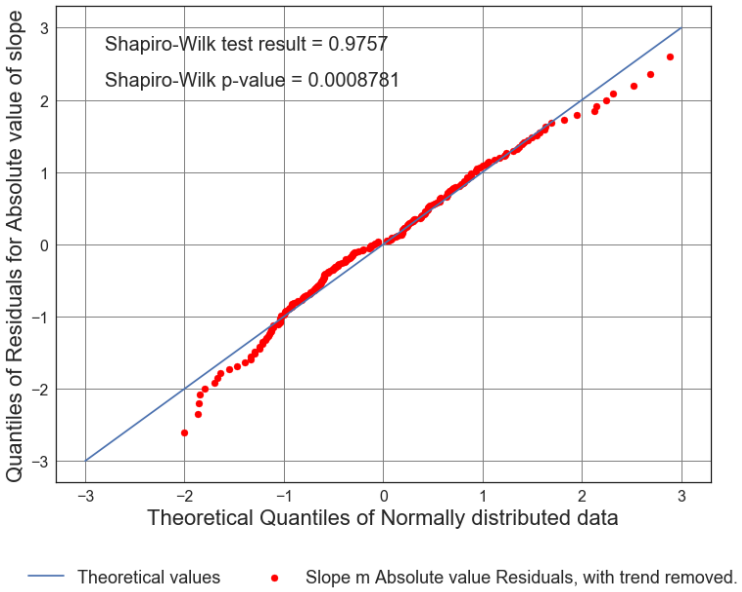

Figure D2.16: Scatter Plot of Solar cycle absolute value slope (from 1900 to 2017) vs. Average number of 7.5M and up Earthquakes/6months with trend removed. Line of best fit, y = -0.01352x + (0.4266), mean x = 30.66 +/- 23.0, mean y = 0.01209 +/- 1.633, R = -0.1904, R squared = 0.03625, p-value = 0.004991.

3.1.3 Time Series Results Part 3

Table 15: USGS Centennial, part 3 (PreWWSSN), 6 month averaged time series analysis results, where y = 7.5M and larger earthquake data, and x = solar data.

Figure name	p value	r value	r sqrd	y average	y std	m slope	b intercept	x average	x std
Figure # B3.5: SN Slope vs average Eqs. Associated Plots: B3.1, B3.6, B3.7.	0.0054	-0.2464	0.0607	1.8770	0.9994	-0.0064	1.8794	0.3737	38.55
Figure # B3.8: SN Slope vs average Eqs notrend. Associated Plots: B3.2, B3.9, B3.10.	0.0045	-0.2515	0.0632	-0.0003	0.9980	-0.0065	0.0022	0.3737	38.55
Figure # B3.11: Absolute value SN Slope vs average Eqs. Associated Plots: B3.3, B3.12, B3.13.	0.7259	-0.0315	0.0010	1.8770	0.9994	-0.0013	1.9175	30.43	23.66
Figure # B3.14: Absolute value SN Slope vs average Eqs notrend. Associated Plots: B3.4, B3.15, B3.16.	0.9082	-0.0104	0.0001	-0.0003	0.9980	-0.0004	0.0131	30.43	23.66

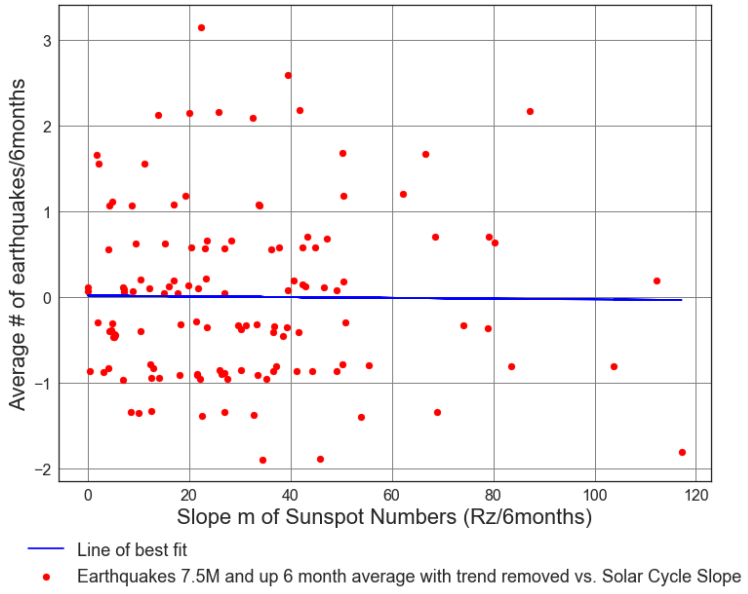

Figure B3.14: Scatter Plot of Solar cycle absolute value slope (from 1900 to 1964) vs. Average number of 7.5M and up Earthquakes/6months with trend removed. Line of best fit, y = -0.0004375x + (0.01306), mean x = 30.43 +/- 23.66, mean y = -0.0002525 +/- 0.998, R = -0.01037, R squared = 0.0001076, p-value = 0.9082.

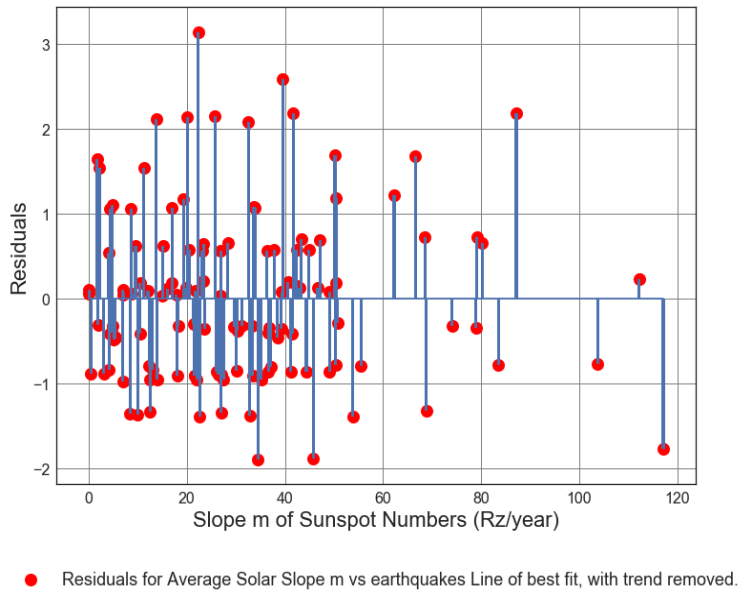

Figure B3.15: Scatter Plot of Solar cycle absolute value slope (from 1900 to 1964) vs. Average number of 7.5M and up Earthquakes/6months with trend removed. Line of best fit, y = -0.0004375x + (0.01306), mean x = 30.43 +/- 23.66, mean y = -0.0002525 +/- 0.998, R = -0.01037, R squared = 0.0001076, p-value = 0.9082.

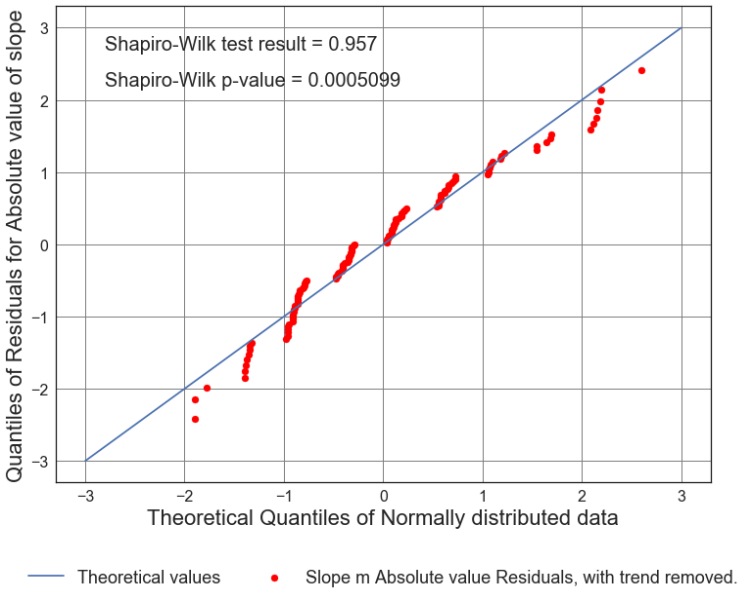

Figure B3.16: Scatter Plot of Solar cycle absolute value slope (from 1900 to 1964) vs. Average number of 7.5M and up Earthquakes/6months with trend removed. Line of best fit, y = -0.0004375x + (0.01306), mean x = 30.43 +/- 23.66, mean y = -0.0002525 +/- 0.998, R = -0.01037, R squared = 0.0001076, p-value = 0.9082.

Table 16: USGS ComCat, part 3 (PreWWSSN), 6 month averaged time series analysis results, where y = 7.5M and larger earthquake data, and x = solar data.

Figure name	p value	r value	r sqrd	y average	y std	m slope	b intercept	x average	x std
Figure # C3.5: SN Slope vs average Eqs. Associated Plots: C3.1, C3.6, C3.7.	0.0105	-0.2273	0.0517	1.6786	1.0283	-0.0061	1.6808	0.3737	38.55
Figure # C3.8: SN Slope vs average Eqs notrend. Associated Plots: C3.2, C3.9, C3.10.	0.0153	-0.2157	0.0465	-0.0008	1.0154	-0.0057	0.0013	0.3737	38.55
Figure # C3.11: Absolute value SN Slope vs average Eqs. Associated Plots: C3.3, C3.12, C3.13.	0.5834	-0.0493	0.0024	1.6786	1.0283	-0.0021	1.7438	30.43	23.66
Figure # C3.14: Absolute value SN Slope vs average Eqs notrend. Associated Plots: C3.4, C3.15, C3.16.	0.2021	-0.1144	0.0131	-0.0008	1.0154	-0.0049	0.1486	30.43	23.66

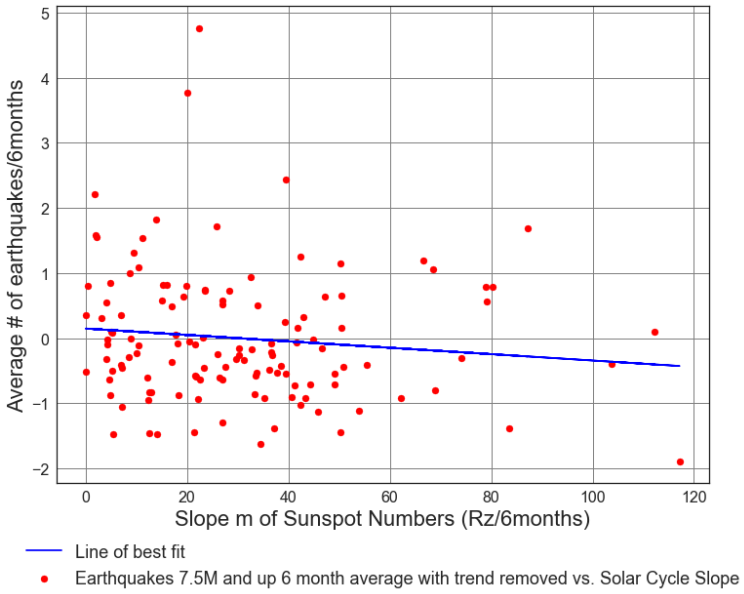

Figure C3.14: Scatter Plot of Solar cycle absolute value slope (from 1900 to 1964) vs. Average number of 7.5M and up Earthquakes/6months with trend removed. Line of best fit, y = -0.004909x + (0.1486), mean x = 30.43 +/- 23.66, mean y = -0.0008086 +/- 1.015, R = -0.1144, R squared = 0.01309, p-value = 0.2021.

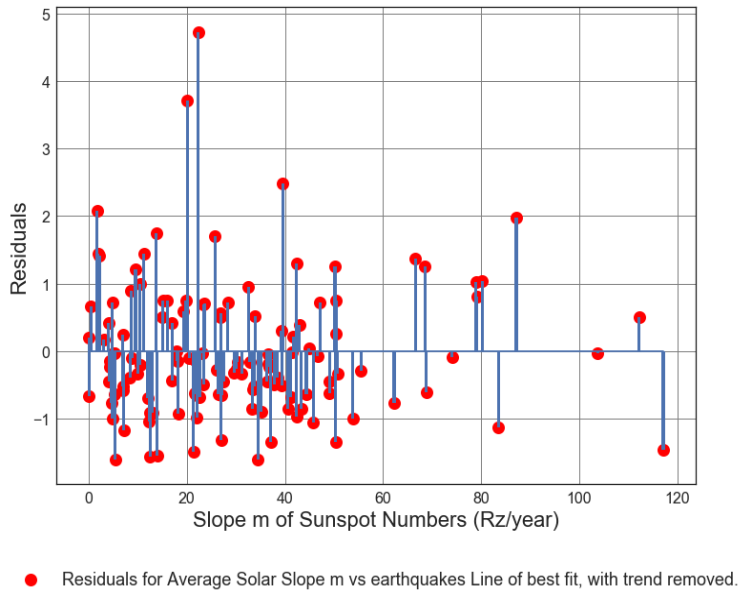

Figure C3.15: Scatter Plot of Solar cycle absolute value slope (from 1900 to 1964) vs. Average number of 7.5M and up Earthquakes/6months with trend removed. Line of best fit, y = -0.004909x + (0.1486), mean x = 30.43 +/- 23.66, mean y = -0.0008086 +/- 1.015, R = -0.1144, R squared = 0.01309, p-value = 0.2021.

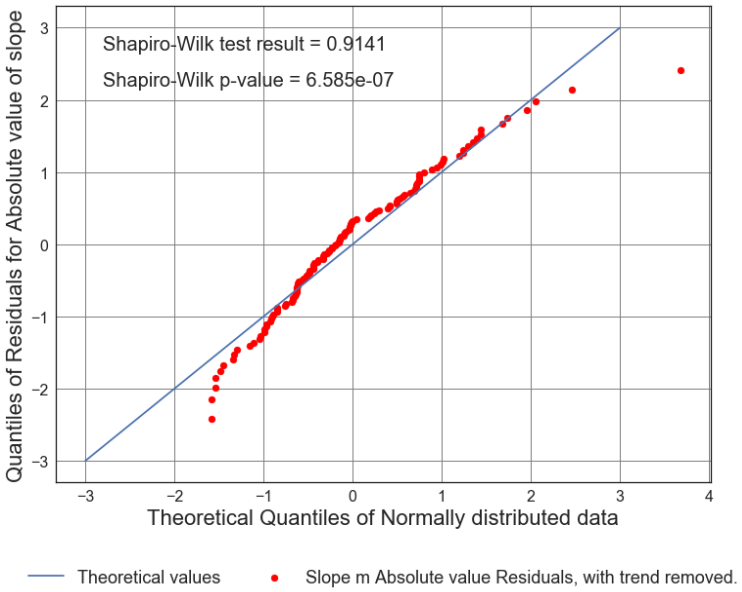

Figure C3.16: Scatter Plot of Solar cycle absolute value slope (from 1900 to 1964) vs. Average number of 7.5M and up Earthquakes/6months with trend removed. Line of best fit, y = -0.004909x + (0.1486), mean x = 30.43 +/- 23.66, mean y = -0.0008086 +/- 1.015, R = -0.1144, R squared = 0.01309, p-value = 0.2021.

Table 17: ISC, part 3 (PreWWSSN), 6 month averaged time series analysis results, where y = earthquake data, and x = solaTable 18: USGS Centennial, part 4 (Modern Era), 6 month averaged time series analysis results, where y = 7.5M and larger earthquake data, and x = solar data.r data.

Figure name	p value	r value	r sqrd	y average	y std	m slope	b intercept	x average	x std
Figure # D3.5: SN Slope vs average Eqs. Associated Plots: D3.1, D3.6, D3.7.	0.1217	-0.1386	0.0192	3.2778	1.5768	-0.0057	3.2799	0.3737	38.55
Figure # D3.8: SN Slope vs average Eqs notrend. Associated Plots: D3.2, D3.9, D3.10.	0.1542	-0.1277	0.0163	0.0231	1.5694	-0.0052	0.0250	0.3737	38.55
Figure # D3.11: Absolute value SN Slope vs average Eqs. Associated Plots: D3.3, D3.12, D3.13.	0.8564	0.0163	0.0003	3.2778	1.5768	0.0011	3.2448	30.43	23.66
Figure # B3.14: Absolute value SN Slope vs average Eqs notrend. Associated Plots: D3.4, D3.15, D3.16.	0.6974	-0.0350	0.0012	0.0231	1.5694	-0.0023	0.0937	30.43	23.66

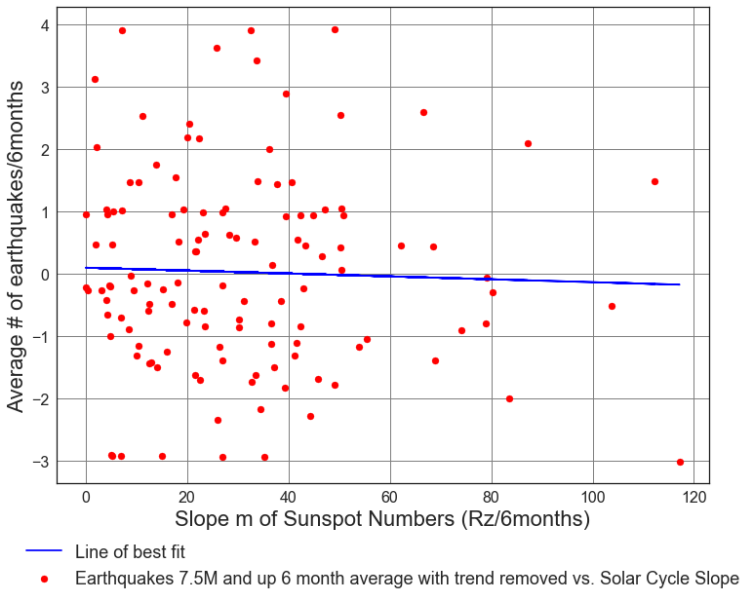

Figure D3.14: Scatter Plot of Solar cycle absolute value slope (from 1900 to 1964) vs. Average number of 7.5M and up Earthquakes/6months with trend removed. Line of best fit, y = -0.00232x + (0.09368), mean x = 30.43 +/- 23.66, mean y = 0.02308 +/- 1.569, R = -0.03498, R squared = 0.001223, p-value = 0.6974.

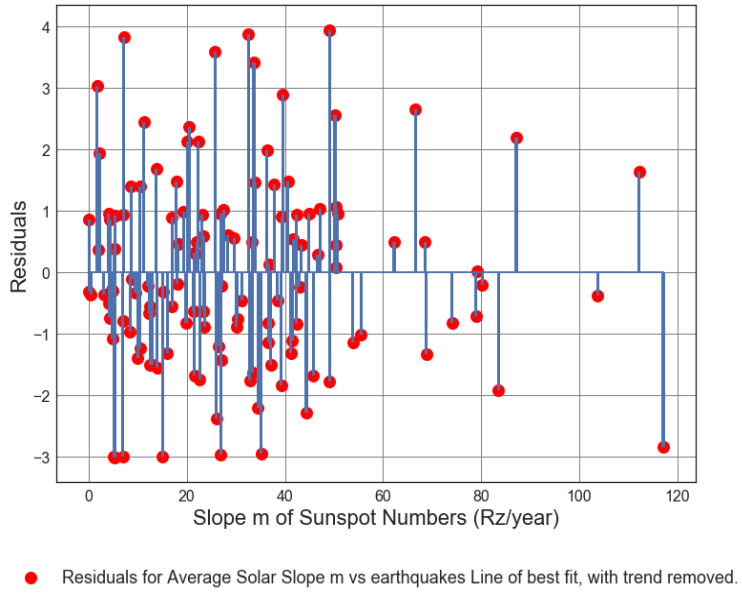

Figure D3.15: Scatter Plot of Solar cycle absolute value slope (from 1900 to 1964) vs. Average number of 7.5M and up Earthquakes/6months with trend removed. Line of best fit, y = -0.00232x + (0.09368), mean x = 30.43 +/- 23.66, mean y = 0.02308 +/- 1.569, R = -0.03498, R squared = 0.001223, p-value = 0.6974.

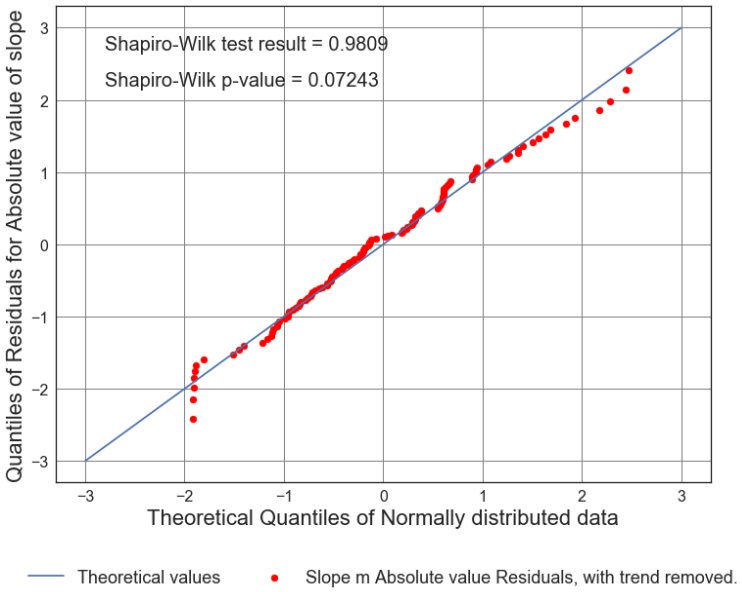

Figure D3.16: Scatter Plot of Solar cycle absolute value slope (from 1900 to 1964) vs. Average number of 7.5M and up Earthquakes/6months with trend removed. Line of best fit, y = -0.00232x + (0.09368), mean x = 30.43 +/- 23.66, mean y = 0.02308 +/- 1.569, R = -0.03498, R squared = 0.001223, p-value = 0.6974.

3.1.4 Time Series Results Part 4

Table 18: USGS Centennial, part 4 (Modern Era), 6 month averaged time series analysis results, where y = 7.5M and larger earthquake data, and x = solar data.

Figure name	p value	r value	r sqrd	y average	y std	m slope	b intercept	x average	x std
Figure # B4.5: SN Slope vs average Eqs. Associated Plots: B4.1, B4.6, B4.7.	0.1993	-0.1374	0.0189	2.0056	0.9787	-0.0035	2.0038	-0.5303	38.19
Figure # B4.8: SN Slope vs average Eqs notrend. Associated Plots: B4.2, B4.9, B4.10.	0.3085	-0.1092	0.0119	0.0000	0.9620	-0.0027	-0.0015	-0.5303	38.19
Figure # B4.11: Absolute value SN Slope vs average Eqs. Associated Plots: B4.3, B4.12, B4.13.	0.0067	-0.2857	0.0816	2.0056	0.9787	-0.0127	2.3999	31.16	22.09
Figure # B4.14: Absolute value SN Slope vs average Eqs notrend. Associated Plots: B4.4, B4.15, B4.16.	0.0061	-0.2884	0.0832	0.0000	0.9620	-0.0126	0.3912	31.16	22.09

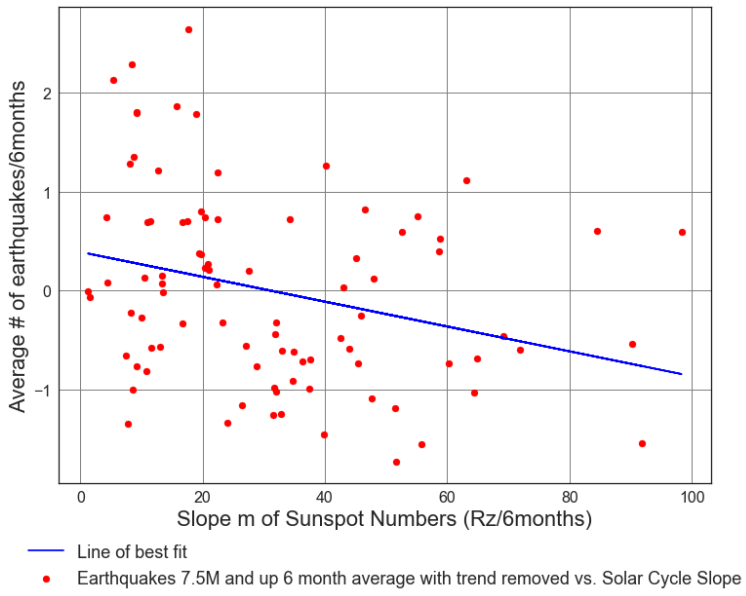

Figure B4.14: Scatter Plot of Solar cycle absolute value slope (from 1964 to 2007) vs. Average number of 7.5M and up Earthquakes/6months with trend removed. Line of best fit, y = -0.01256x + (0.3912), mean x = 31.16 +/- 22.09, mean y = -3.313e-15 +/- 0.962, R = -0.2884, R squared = 0.08317, p-value = 0.006131.

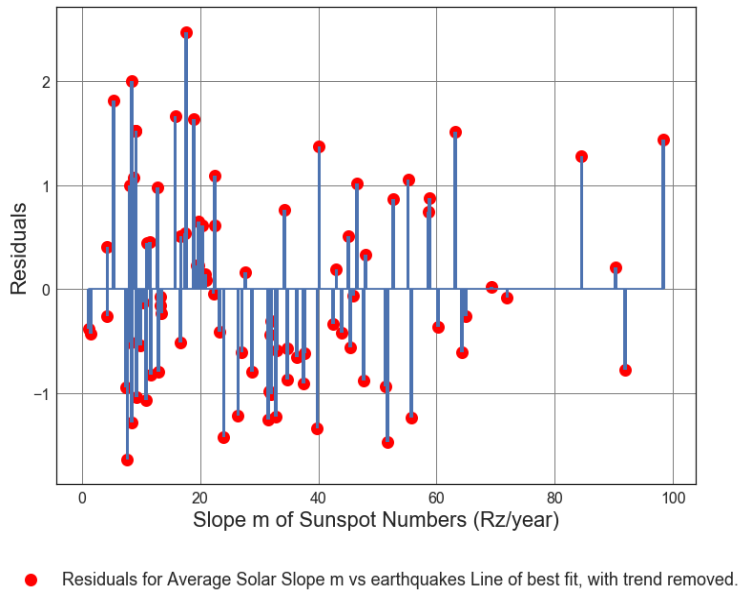

Figure B4.15: Scatter Plot of Solar cycle absolute value slope (from 1964 to 2007) vs. Average number of 7.5M and up Earthquakes/6months with trend removed. Line of best fit, y = -0.01256x + (0.3912), mean x = 31.16 +/- 22.09, mean y = -3.313e-15 +/- 0.962, R = -0.2884, R squared = 0.08317, p-value = 0.006131.

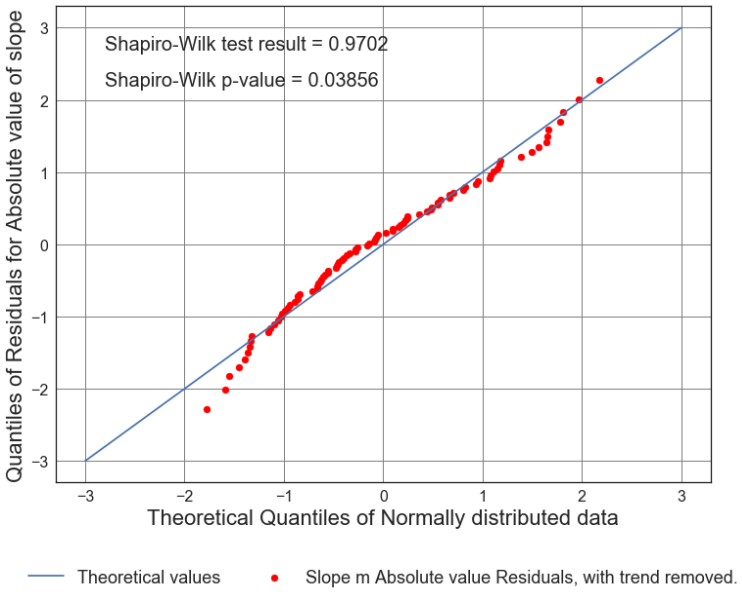

Figure B4.16: Scatter Plot of Solar cycle absolute value slope (from 1964 to 2007) vs. Average number of 7.5M and up Earthquakes/6months with trend removed. Line of best fit, y = -0.01256x + (0.3912), mean x = 31.16 +/- 22.09, mean y = -3.313e-15 +/- 0.962, R = -0.2884, R squared = 0.08317, p-value = 0.006131.

Table 19: USGS ComCat, part 4 (Modern Era), 6 month averaged time series analysis results, where y = 7.5M and larger earthquake data, and x = solar data.

Figure name	p value	r value	r sqrd	y average	y std	m slope	b intercept	x average	x std
Figure # C4.5: SN Slope vs average Eqs. Associated Plots: C4.1, C4.6, C4.7.	0.9067	-0.0126	0.0002	2.0393	1.1148	-0.0004	2.0391	-0.5303	38.19
Figure # C4.8: SN Slope vs average Eqs notrend. Associated Plots: C4.2, C4.9, C4.10.	0.8402	0.0217	0.0005	0.0000	1.0906	0.0006	0.0003	-0.5303	38.19
Figure # C4.11: Absolute value SN Slope vs average Eqs. Associated Plots: C4.3, C4.12, C4.13.	0.0004	-0.3668	0.1345	2.0393	1.1148	-0.0185	2.6160	31.16	22.09
Figure # C4.14: Absolute value SN Slope vs average Eqs notrend. Associated Plots: C4.4, C4.15, C4.16.	0.0003	-0.3724	0.1387	0.0000	1.0906	-0.0184	0.5728	31.16	22.09

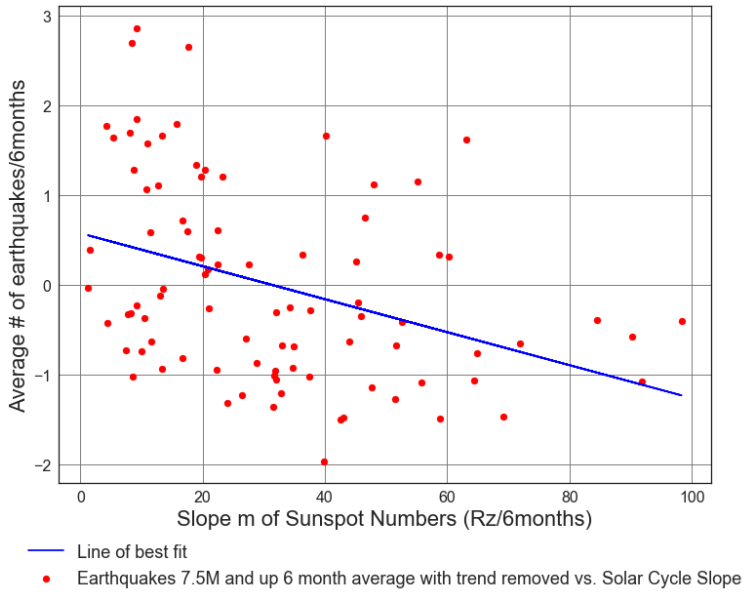

Figure C4.14: Scatter Plot of Solar cycle absolute value slope (from 1964 to 2017) vs. Average number of 7.5M and up Earthquakes/6months with trend removed. Line of best fit, y = -0.01838x + (0.5728), mean x = 31.16 +/- 22.09, mean y = 1.836e-15 +/- 1.091, R = -0.3724, R squared = 0.1387, p-value = 0.000326.

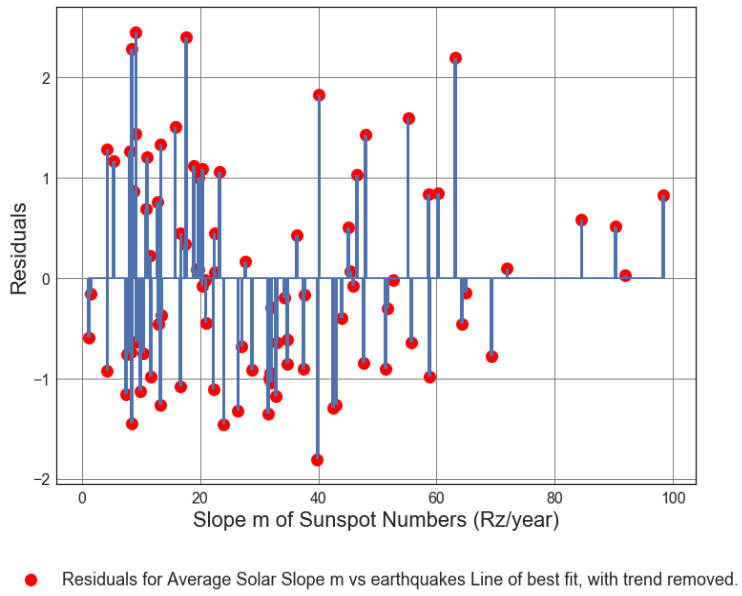

Figure C4.15: Scatter Plot of Solar cycle absolute value slope (from 1964 to 2017) vs. Average number of 7.5M and up Earthquakes/6months with trend removed. Line of best fit, y = -0.01838x + (0.5728), mean x = 31.16 +/- 22.09, mean y = 1.836e-15 +/- 1.091, R = -0.3724, R squared = 0.1387, p-value = 0.000326.

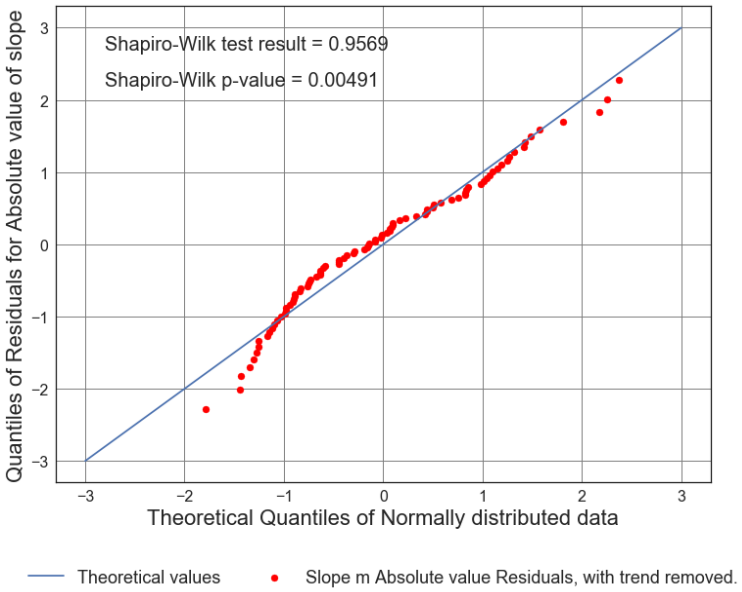

Figure C4.16: Scatter Plot of Solar cycle absolute value slope (from 1964 to 2017) vs. Average number of 7.5M and up Earthquakes/6months with trend removed. Line of best fit, y = -0.01838x + (0.5728), mean x = 31.16 +/- 22.09, mean y = 1.836e-15 +/- 1.091, R = -0.3724, R squared = 0.1387, p-value = 0.000326.

Table 20: ISC, part 4 (Modern Era), 6 month averaged time series analysis results, where y = 7.5M and larger earthquake data, and x = solar data.

Figure name	p value	r value	r sqrd	y average	y std	m slope	b intercept	x average	x std
Figure # D4.5: SN Slope vs average Eqs. Associated Plots:	0.0085	-0.2775	0.0770	4.3539	1.7835	-0.0130	4.3471	-0.5303	38.19
Figure # D4.8: SN Slope vs average Eqs notrend. Associated Plots:	0.0266	-0.2351	0.0553	0.0000	1.6694	-0.0103	-0.0054	-0.5303	38.19
Figure # D4.11: Absolute value SN Slope vs average Eqs. Associated Plots:	0.0014	-0.3333	0.1111	4.3539	1.7835	-0.0269	5.1922	31.16	22.09
Figure # D4.14: Absolute value SN Slope vs average Eqs notrend. Associated Plots:	0.0007	-0.3516	0.1236	0.0000	1.6694	-0.0266	0.8277	31.16	22.09

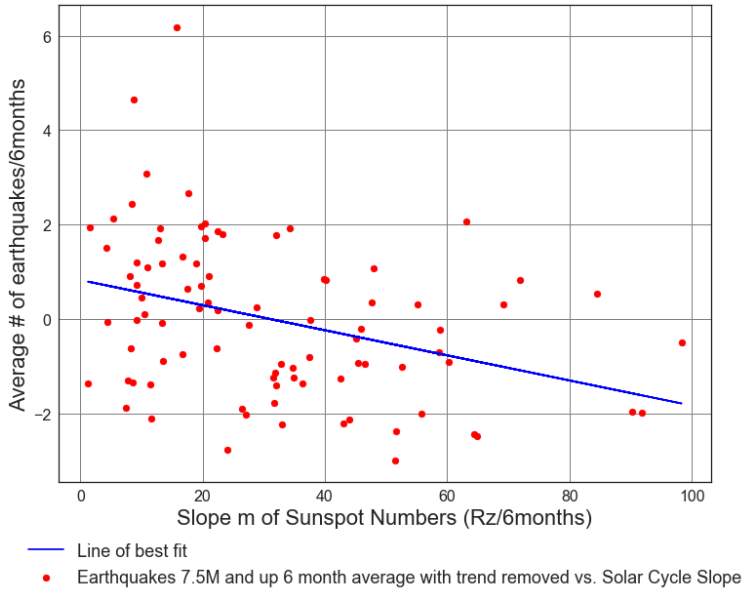

Figure D4.14: Scatter Plot of Solar cycle absolute value slope (from 1964 to 2017) vs. Average number of 7.5M and up Earthquakes/6months with trend removed. Line of best fit, y = -0.02656x + (0.8277), mean x = 31.16 +/- 22.09, mean y = -1.277e-15 +/- 1.669, R = -0.3516, R squared = 0.1236, p-value = 0.0007294.

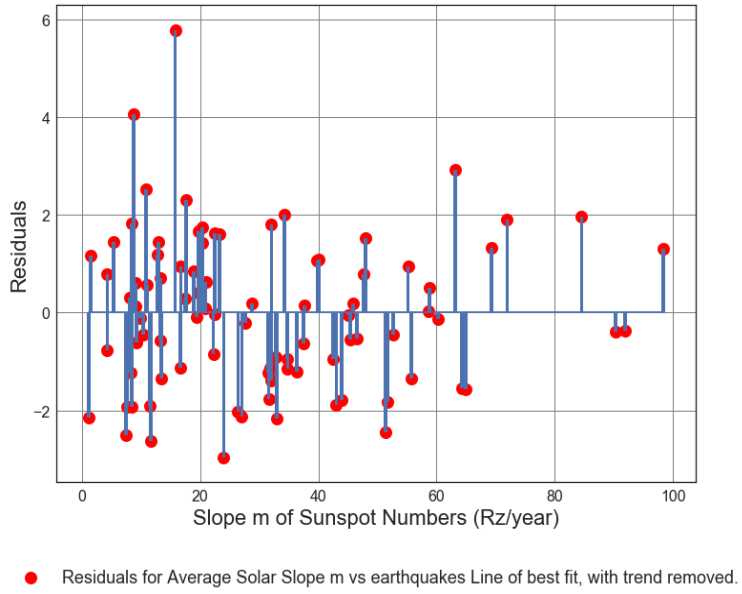

Figure D4.15: Scatter Plot of Solar cycle absolute value slope (from 1964 to 2017) vs. Average number of 7.5M and up Earthquakes/6months with trend removed. Line of best fit, y = -0.02656x + (0.8277), mean x = 31.16 +/- 22.09, mean y = -1.277e-15 +/- 1.669, R = -0.3516, R squared = 0.1236, p-value = 0.0007294.

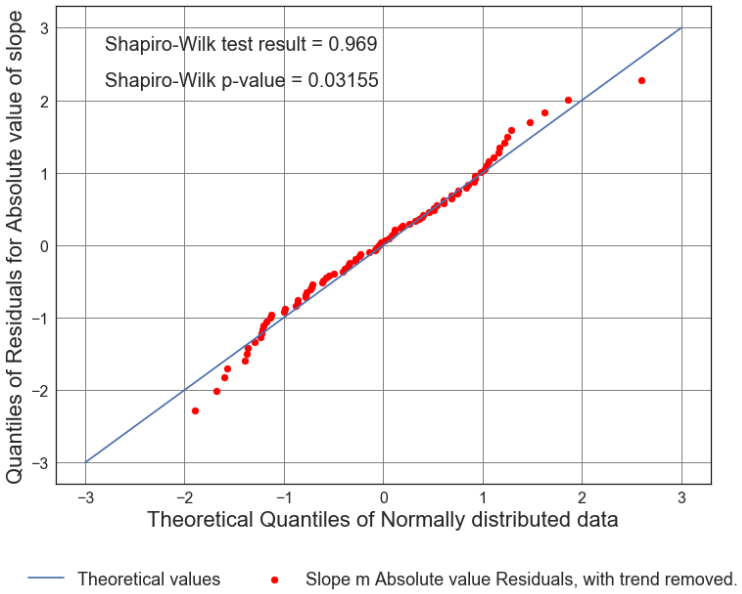

Figure D4.16: Scatter Plot of Solar cycle absolute value slope (from 1964 to 2017) vs. Average number of 7.5M and up Earthquakes/6months with trend removed. Line of best fit, y = -0.02656x + (0.8277), mean x = 31.16 +/- 22.09, mean y = -1.277e-15 +/- 1.669, R = -0.3516, R squared = 0.1236, p-value = 0.0007294.

3.2.1 Spectral Analysis Results Part 5

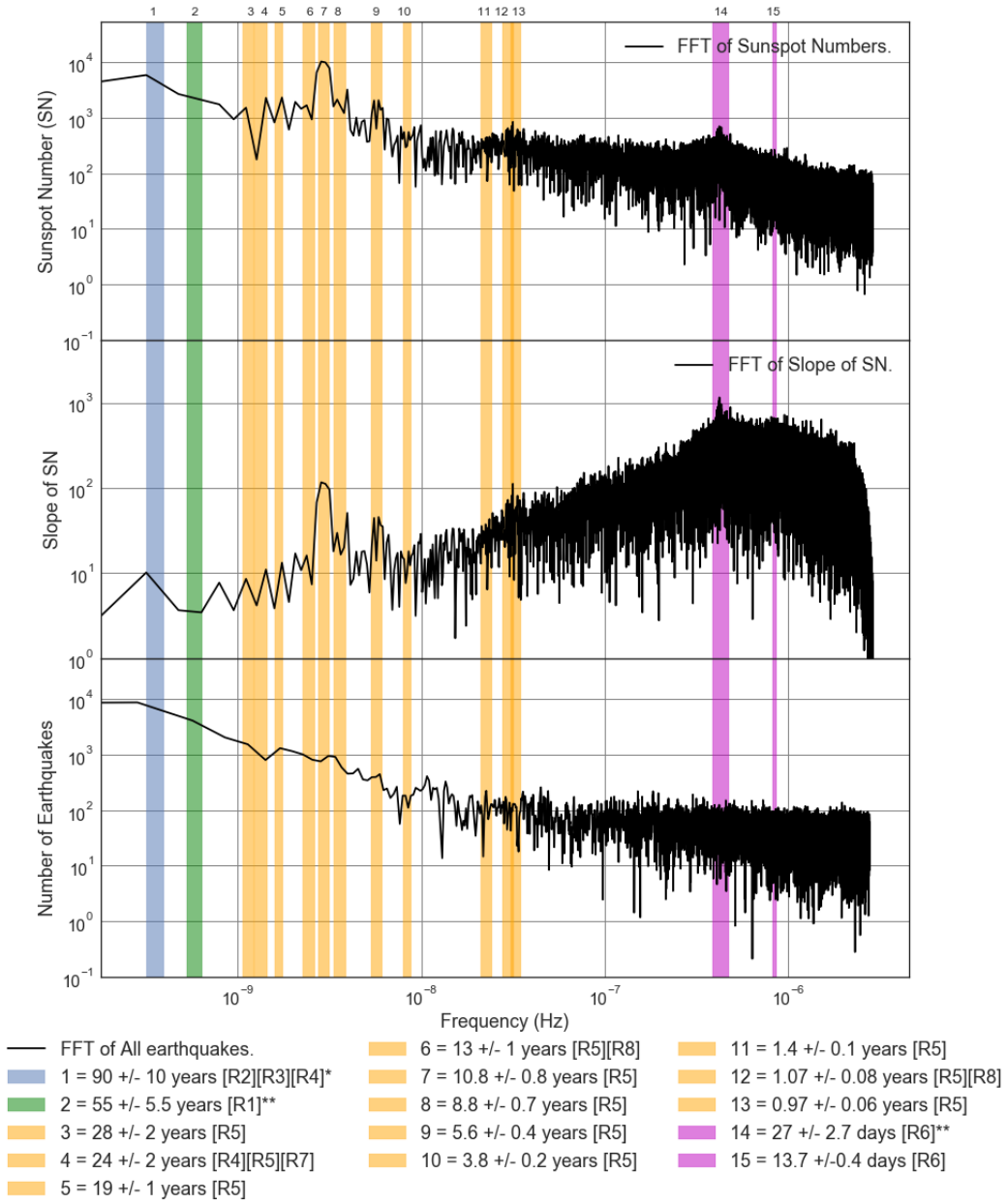

Figure E1.1: FFT Loglog Comparison Plot of number of Averaged All Earthquakes, Sunspot number (SN) and slope from 1818 to 2017. Additional meaning of the legend colors: Blue = Various Analysis techniques, Green = Meyer wavelet, Orange = Instantly maximal wavelet skeleton spectra, Magenta = Periodram and Linear phase finite impulse response.

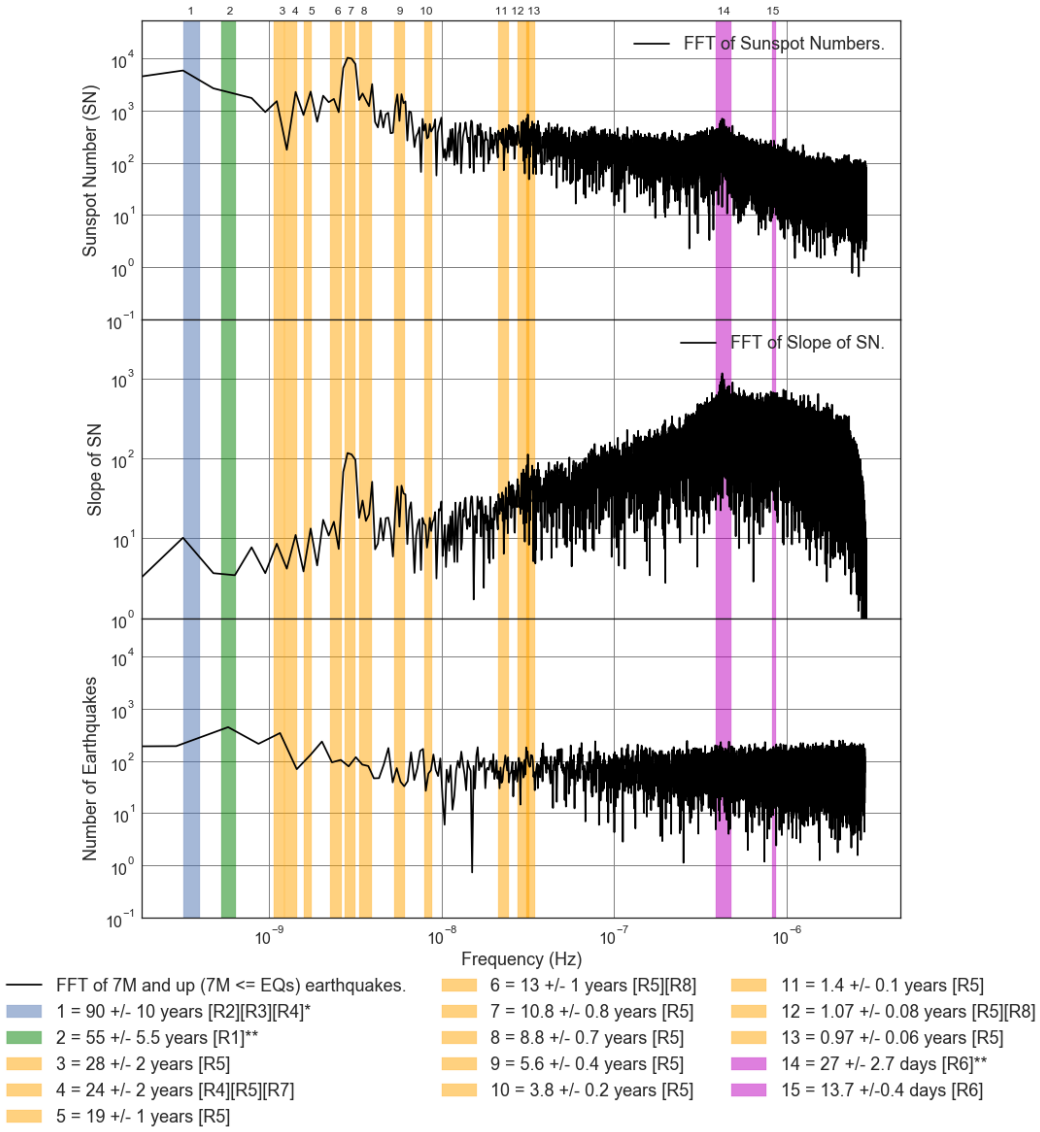

Figure E1.5: FFT Loglog Comparison Plot of number of Averaged 7M and up (7M <= EQs) Earthquakes, Sunspot number (SN) and slope from 1818 to 2017. Additional meaning of the legend colors: Blue = Various Analysis techniques, Green = Meyer wavelet, Orange = Instantly maximal wavelet skeleton spectra, Magenta = Periodram and Linear phase finite impulse response.

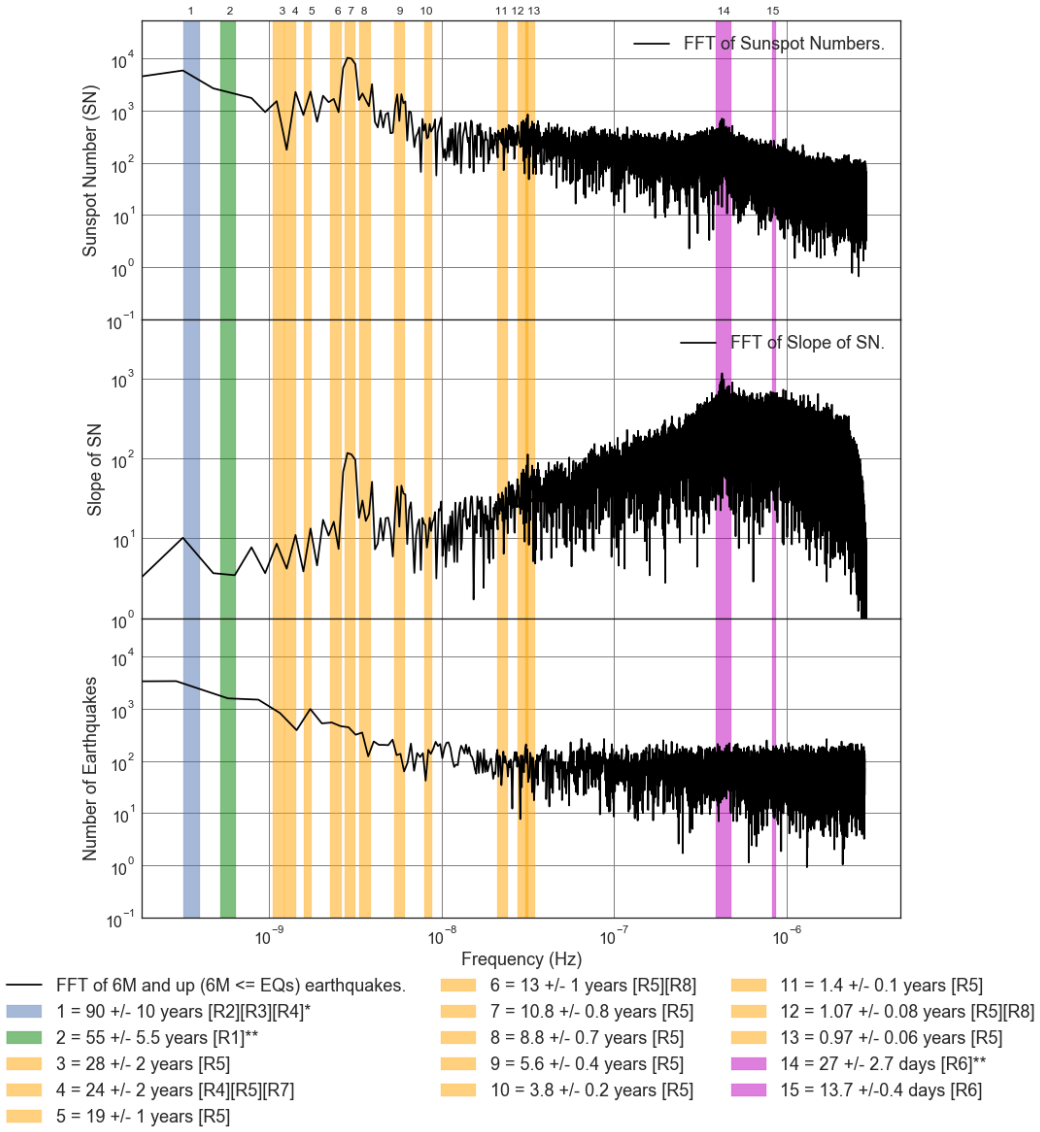

Figure E1.6: FFT Loglog Comparison Plot of number of Averaged 6M and up (6M <= EQs) Earthquakes, Sunspot number (SN) and slope from 1818 to 2017. Additional meaning of the legend colors: Blue = Various Analysis techniques, Green = Meyer wavelet, Orange = Instantly maximal wavelet skeleton spectra, Magenta = Periodram and Linear phase finite impulse response.

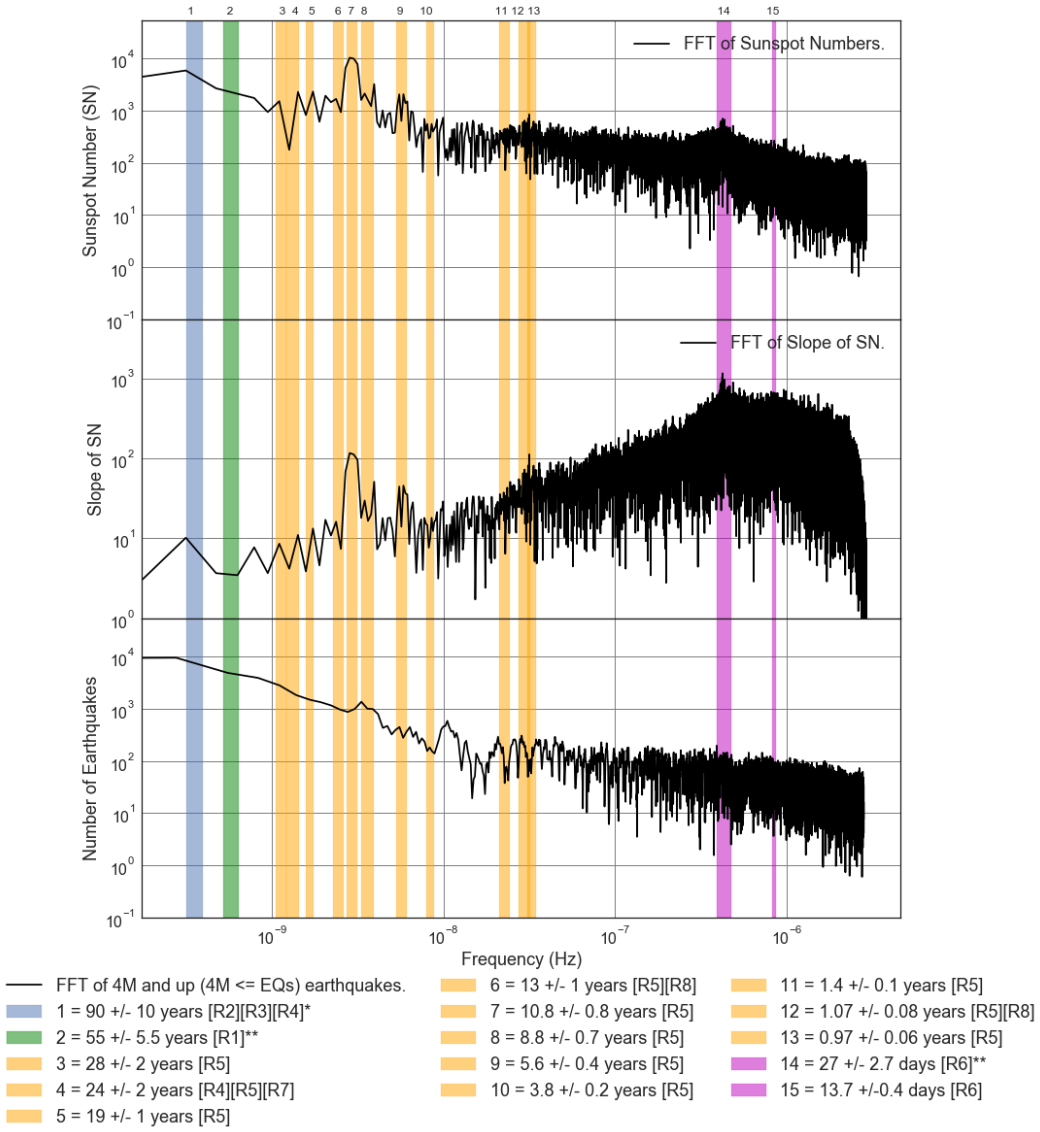

Figure E1.8: FFT Loglog Comparison Plot of number of Averaged 4M and up (4M <= EQs) Earthquakes, Sunspot number (SN) and slope from 1818 to 2017. Additional meaning of the legend colors: Blue = Various Analysis techniques, Green = Meyer wavelet, Orange = Instantly maximal wavelet skeleton spectra, Magenta = Periodram and Linear phase finite impulse response.

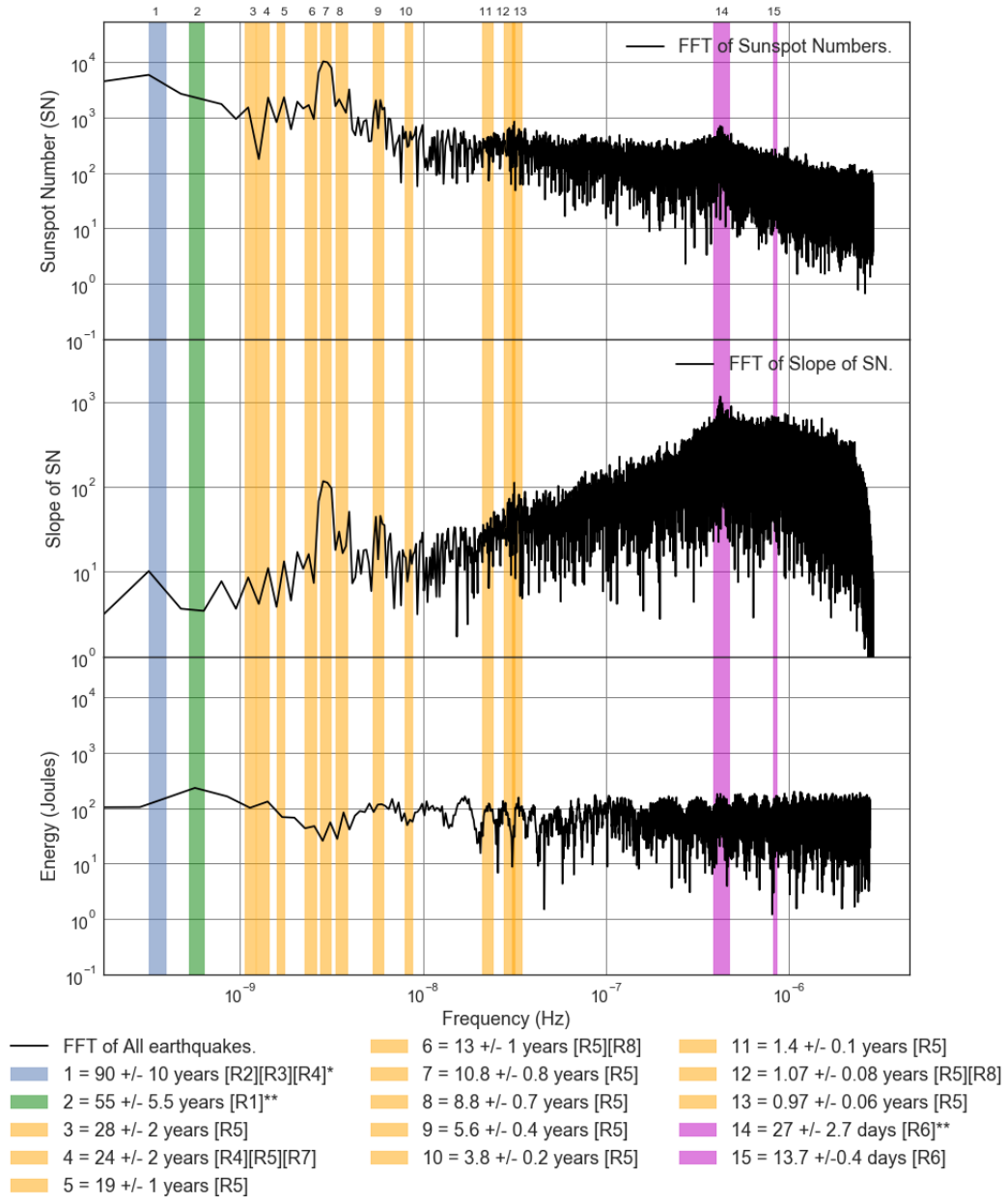

Figure E1.25: FFT Loglog Comparison Plot of Averaged All Earthquake (EQ) total energy released, 2 Day Sunspot number and slope from 1818 to 2017. Additional meaning of the legend colors: Blue = Various Analysis techniques, Green = Meyer wavelet, Orange = Instantly maximal wavelet skeleton spectra, Magenta = Periodram and Linear phase finite impulse response.

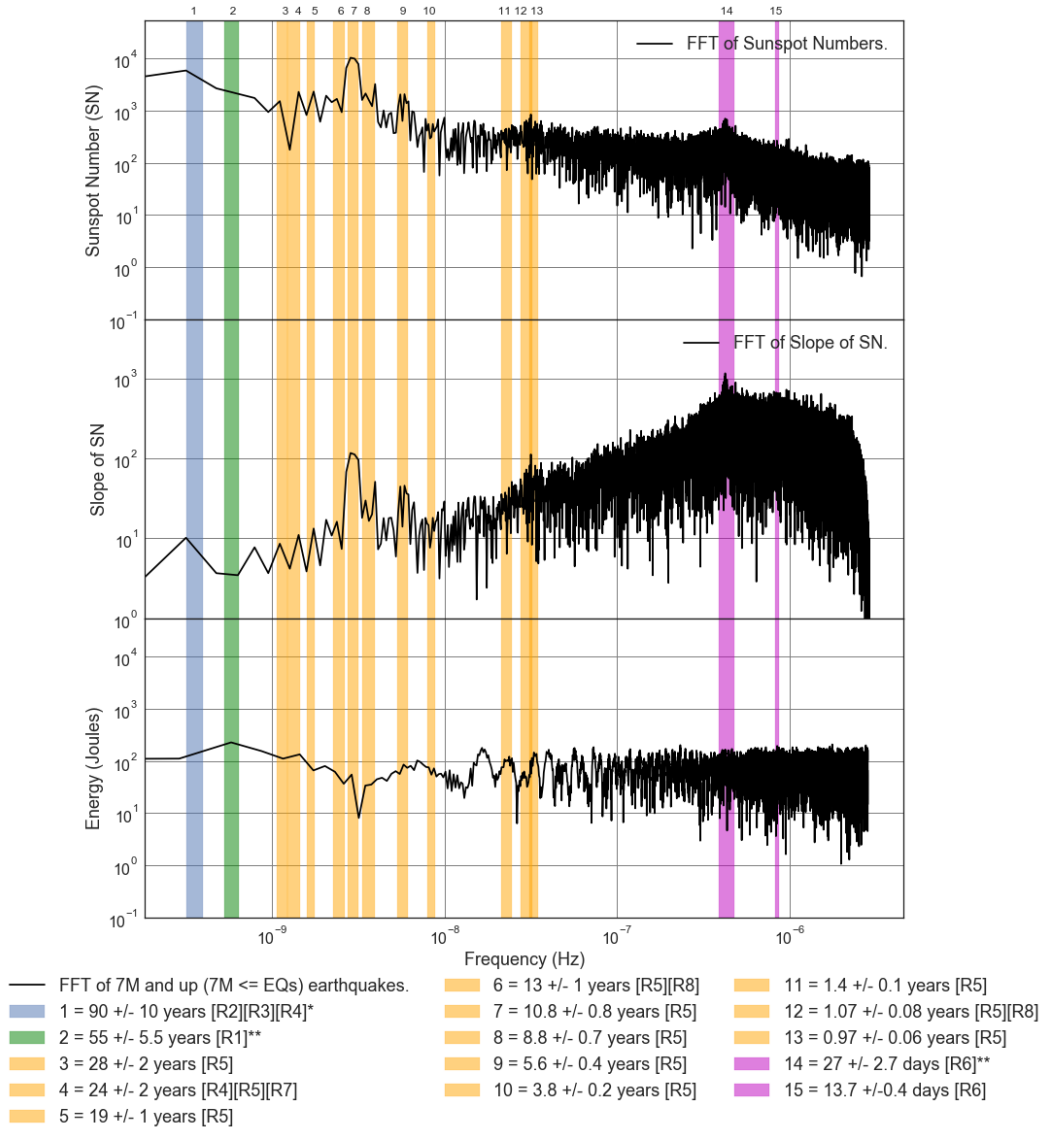

Figure E1.29: FFT Loglog Comparison Plot of Averaged 7M and up (7M <= EQs) Earthquake (EQ) total energy released, 2 Day Sunspot number and slope from 1818 to 2017. Additional meaning of the legend colors: Blue = Various Analysis techniques, Green = Meyer wavelet, Orange = Instantly maximal wavelet skeleton spectra, Magenta = Periodram and Linear phase finite impulse response.

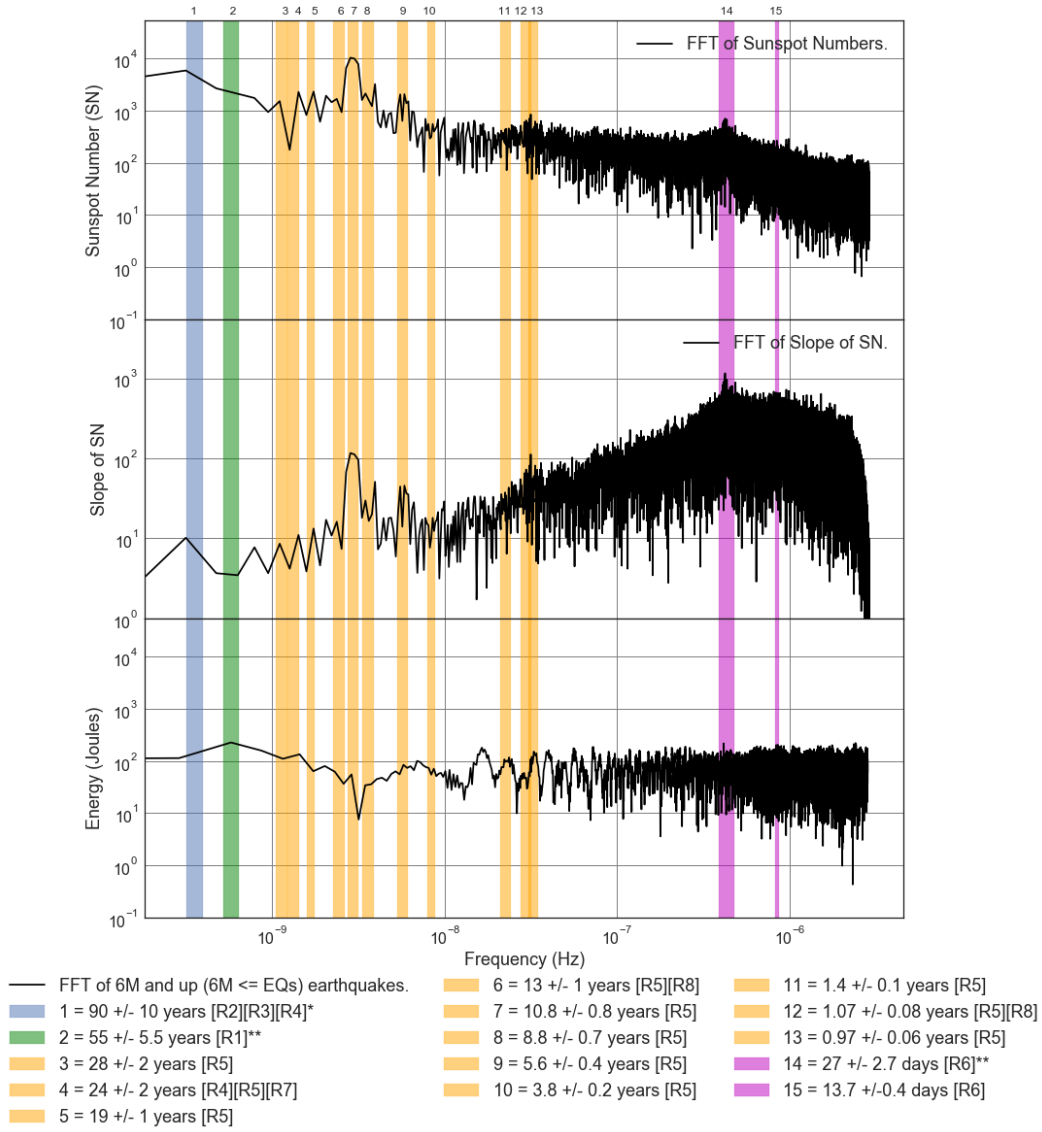

Figure E1.30: FFT Loglog Comparison Plot of Averaged 6M and up (6M <= EQs) Earthquake (EQ) total energy released, 2 Day Sunspot number and slope from 1818 to 2017. Additional meaning of the legend colors: Blue = Various Analysis techniques, Green = Meyer wavelet, Orange = Instantly maximal wavelet skeleton spectra, Magenta = Periodram and Linear phase finite impulse response.

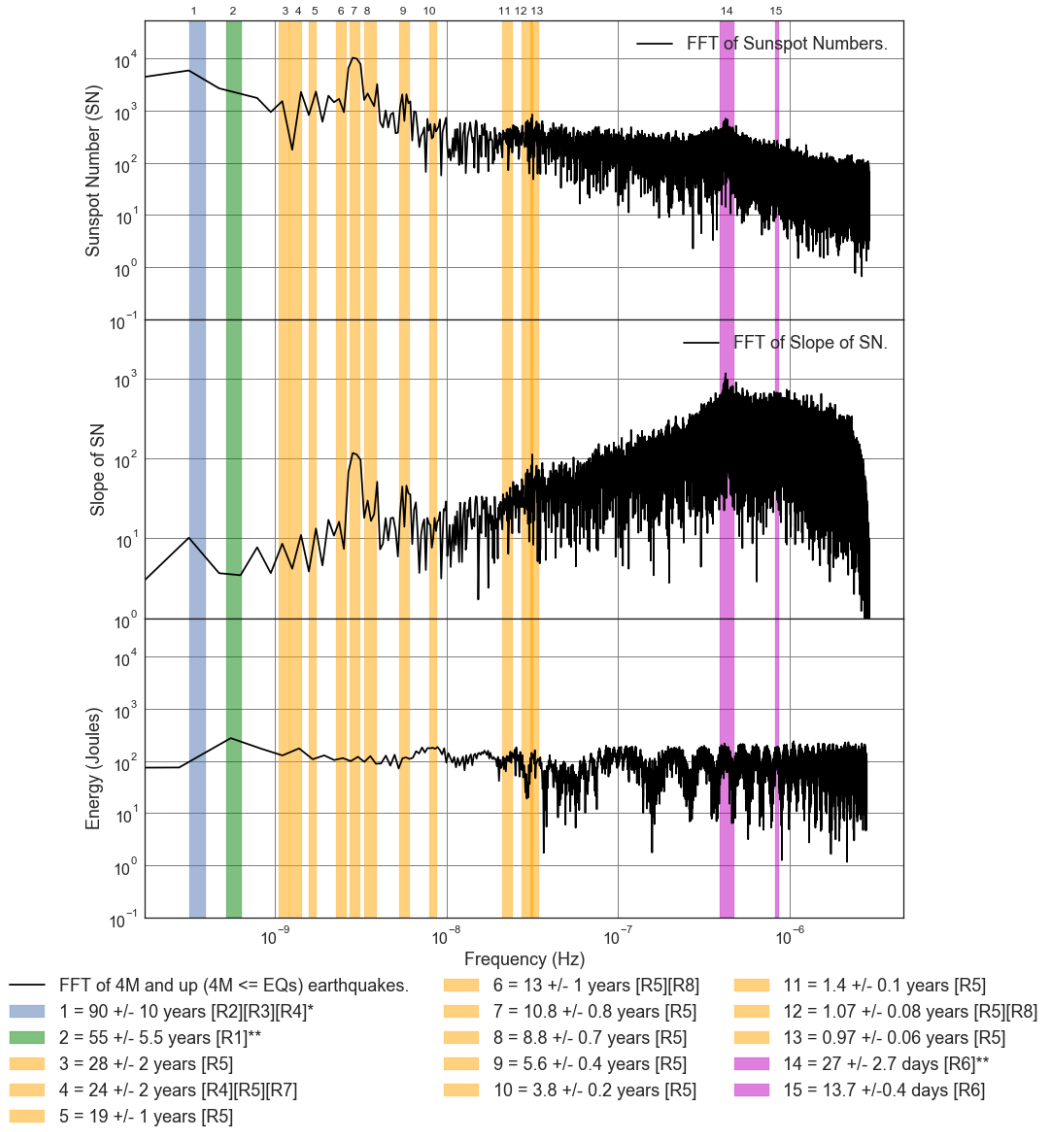

Figure E1.32: FFT Loglog Comparison Plot of Averaged 4M and up (4M <= EQs) Earthquake (EQ) total energy released, 2 Day Sunspot number and slope from 1818 to 2017. Additional meaning of the legend colors: Blue = Various Analysis techniques, Green = Meyer wavelet, Orange = Instantly maximal wavelet skeleton spectra, Magenta = Periodram and Linear phase finite impulse response.

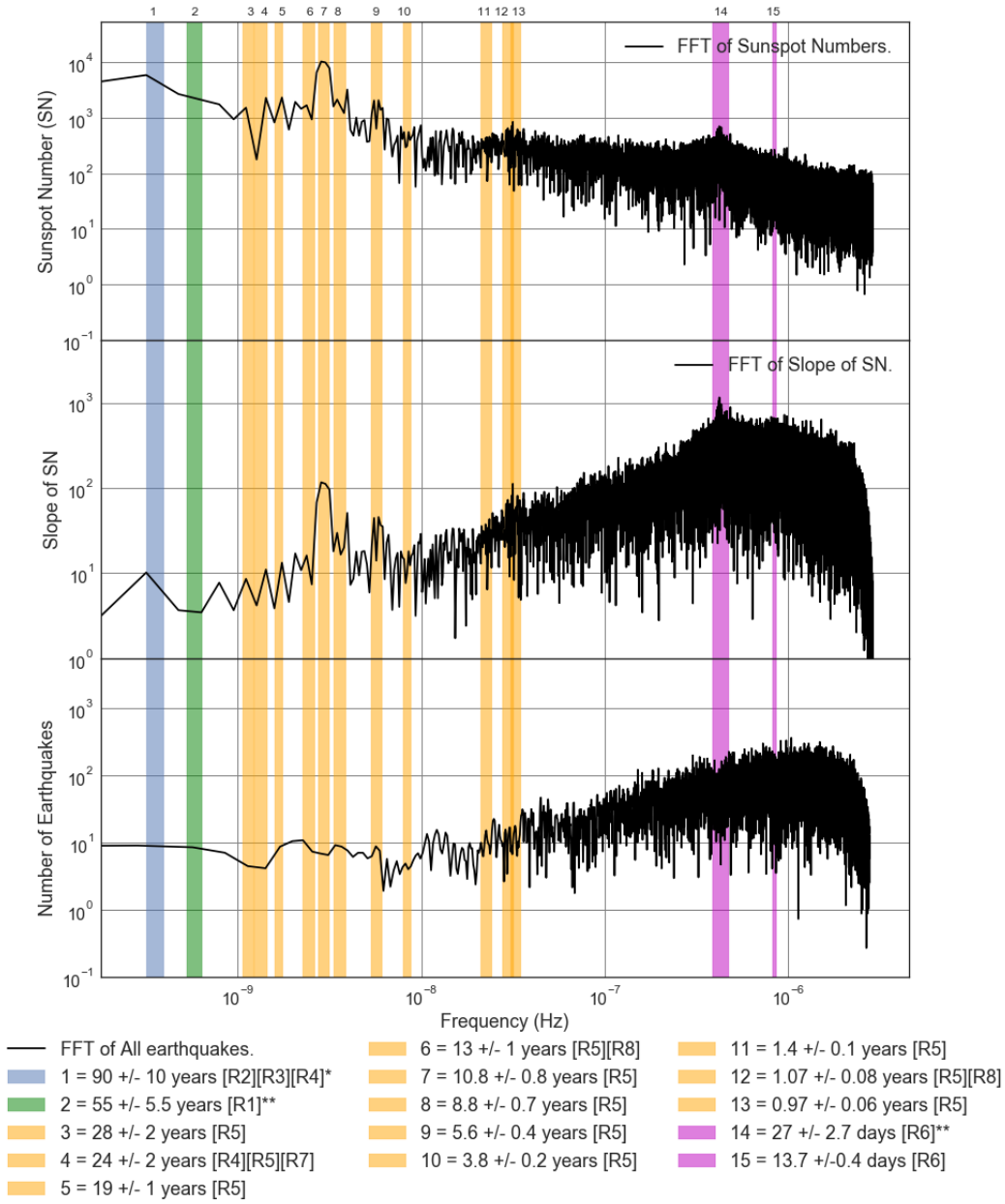

Figure E2.1: FFT Loglog Comparison Plot: Slope of Averaged All Earthquake counts, Sunspot number (SN) and slope from 1818 to 2017. Additional meaning of the legend colors: Blue = Various Analysis techniques, Green = Meyer wavelet, Orange = Instantly maximal wavelet skeleton spectra, Magenta = Periodram and Linear phase finite impulse response.

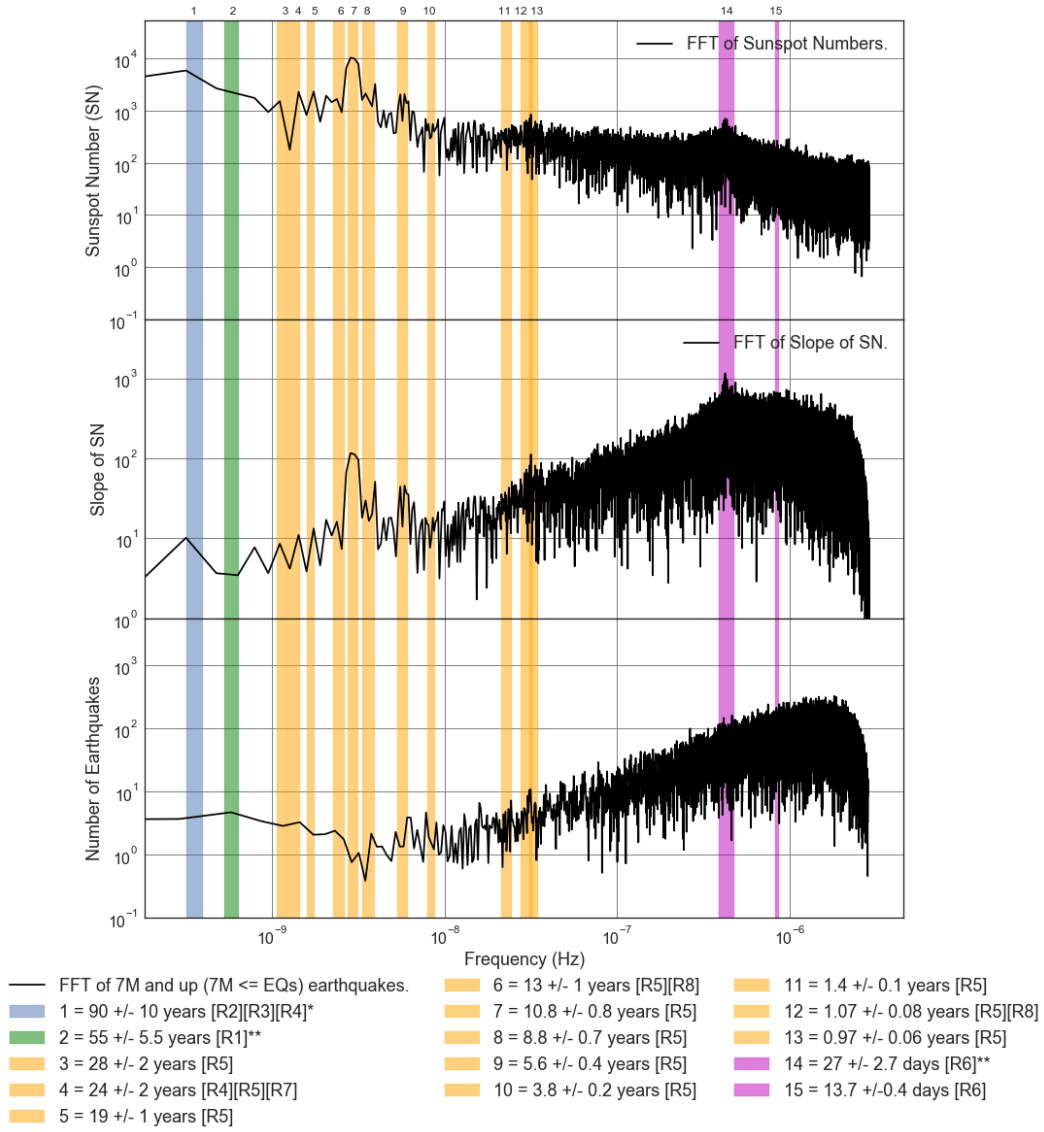

Figure E2.5: FFT Loglog Comparison Plot: Slope of Averaged 7M and up (7M <= EQs) Earthquake counts, Sunspot number (SN) and slope from 1818 to 2017. Additional meaning of the legend colors: Blue = Various Analysis techniques, Green = Meyer wavelet, Orange = Instantly maximal wavelet skeleton spectra, Magenta = Periodram and Linear phase finite impulse response.

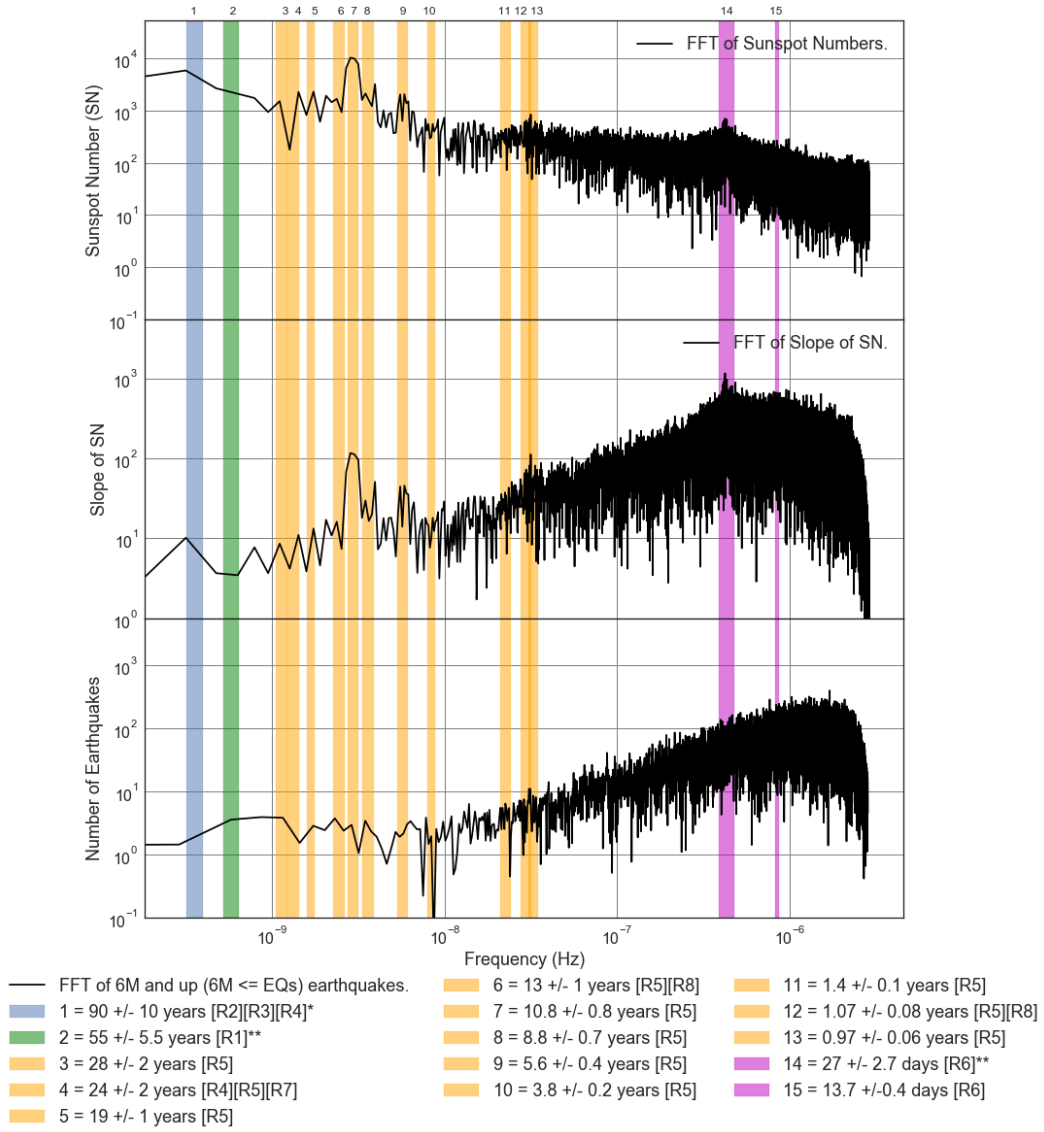

Figure E2.6: FFT Loglog Comparison Plot: Slope of Averaged 6M and up (6M <= EQs) Earthquake counts, Sunspot number (SN) and slope from 1818 to 2017. Additional meaning of the legend colors: Blue = Various Analysis techniques, Green = Meyer wavelet, Orange = Instantly maximal wavelet skeleton spectra, Magenta = Periodram and Linear phase finite impulse response.

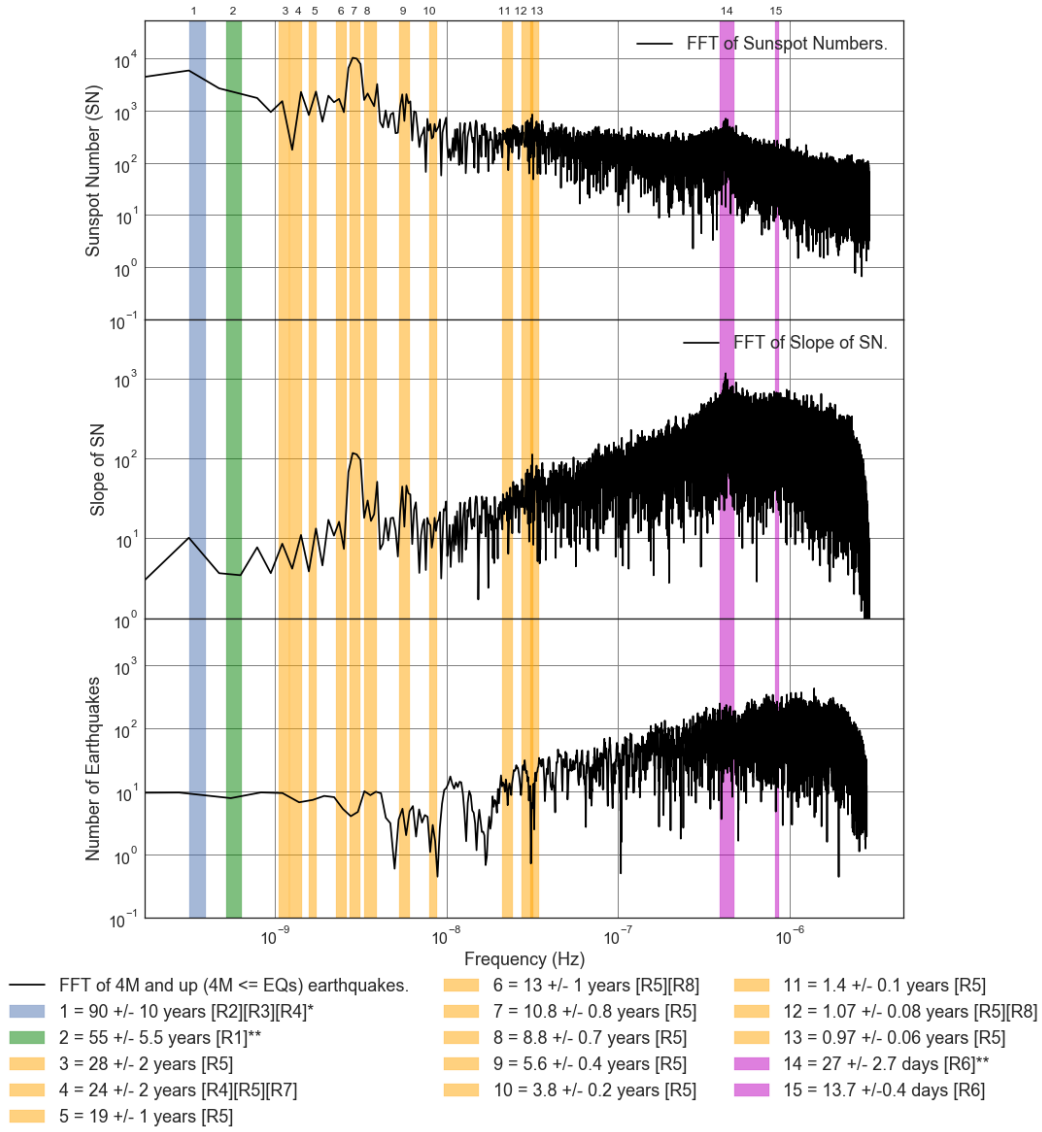

Figure E2.8: FFT Loglog Comparison Plot: Slope of Averaged 4M and up (4M <= EQs) Earthquake counts, Sunspot number (SN) and slope from 1818 to 2017. Additional meaning of the legend colors: Blue = Various Analysis techniques, Green = Meyer wavelet, Orange = Instantly maximal wavelet skeleton spectra, Magenta = Periodram and Linear phase finite impulse response.

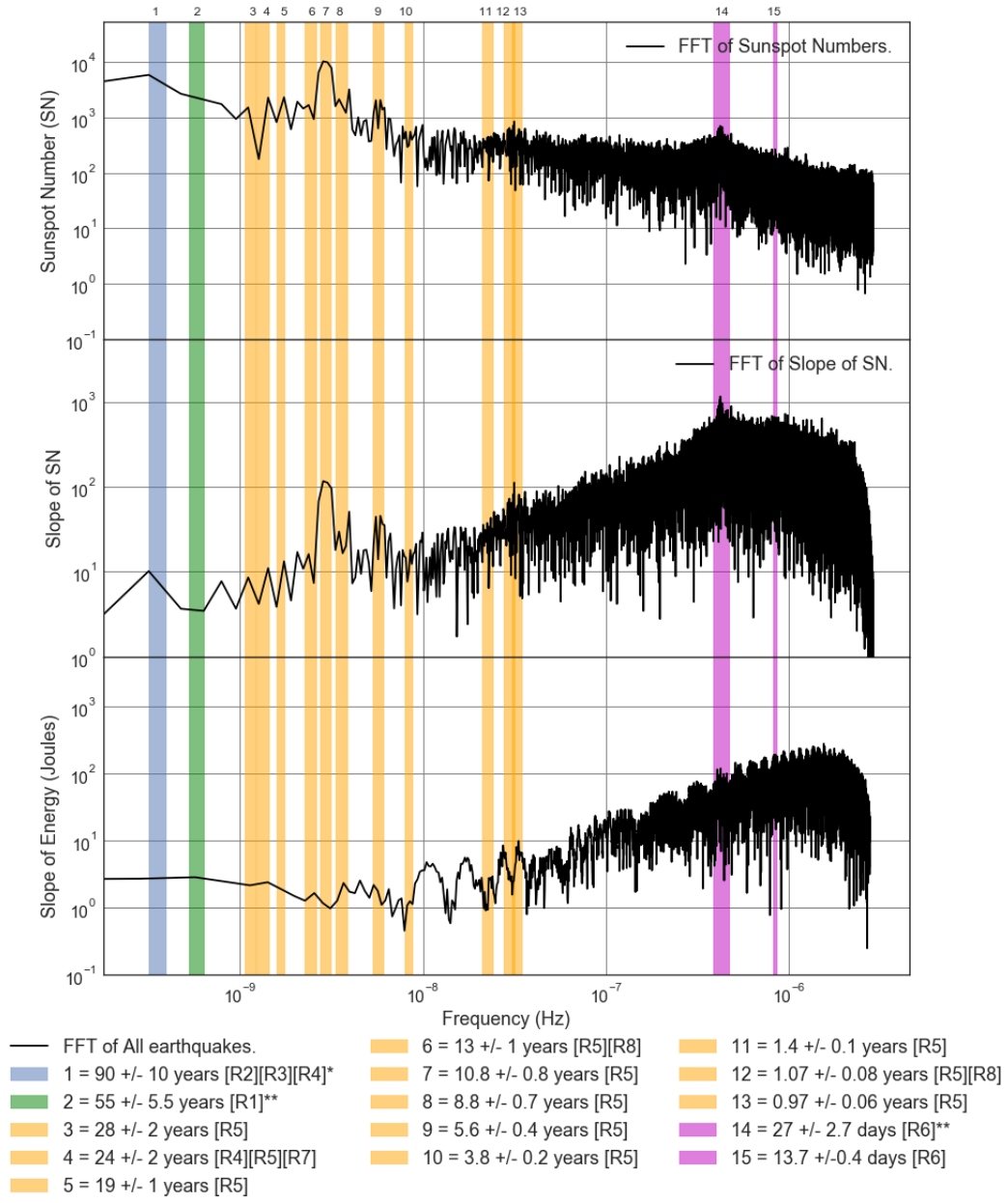

Figure E2.25: FFT Loglog Comparison Plot: Slope of Averaged All Earthquake (EQ) total energy released, 2 Day Sunspot number and slope from 1818 to 2017. Additional meaning of the legend colors: Blue = Various Analysis techniques, Green = Meyer wavelet, Orange = Instantly maximal wavelet skeleton spectra, Magenta = Periodram and Linear phase finite impulse response.

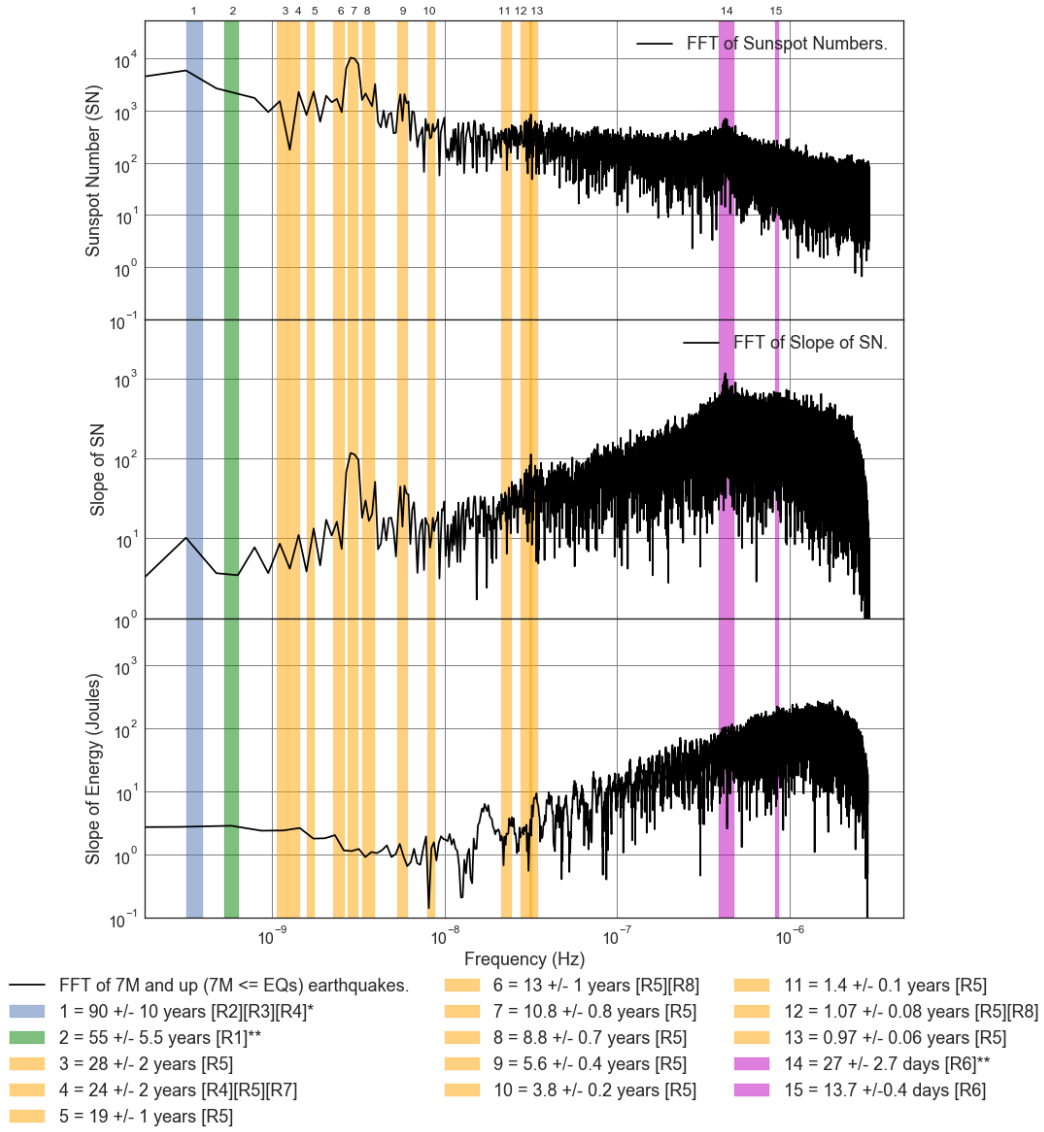

Figure E2.29: FFT Loglog Comparison Plot: Slope of Averaged 7M and up (7M <= EQs) Earthquake (EQ) total energy released, 2 Day Sunspot number and slope from 1818 to 2017. Additional meaning of the legend colors: Blue = Various Analysis techniques, Green = Meyer wavelet, Orange = Instantly maximal wavelet skeleton spectra, Magenta = Periodram and Linear phase finite impulse response.

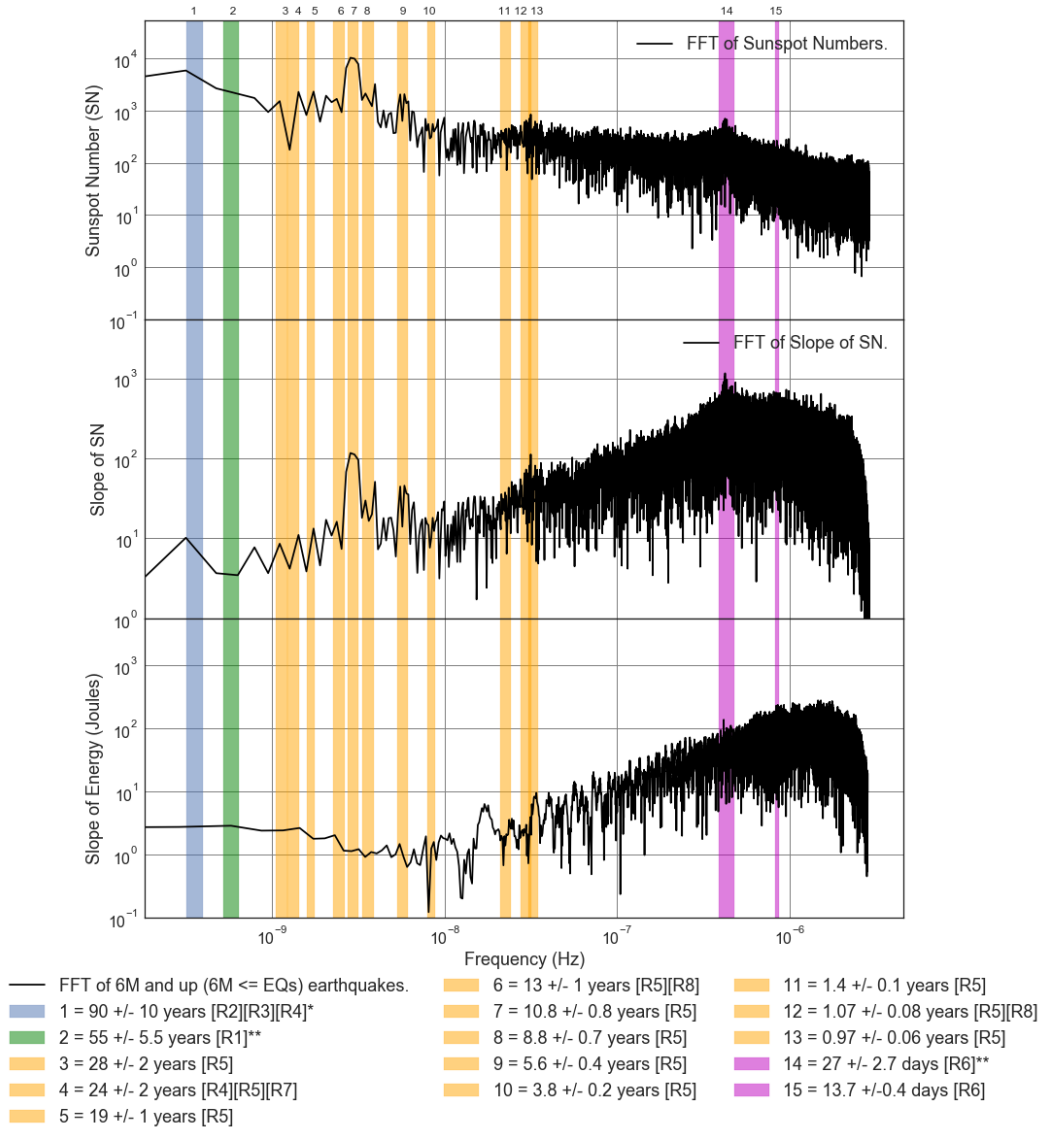

Figure E2.30: FFT Loglog Comparison Plot: Slope of Averaged 6M and up (6M <= EQs) Earthquake (EQ) total energy released, 2 Day Sunspot number and slope from 1818 to 2017. Additional meaning of the legend colors: Blue = Various Analysis techniques, Green = Meyer wavelet, Orange = Instantly maximal wavelet skeleton spectra, Magenta = Periodram and Linear phase finite impulse response.

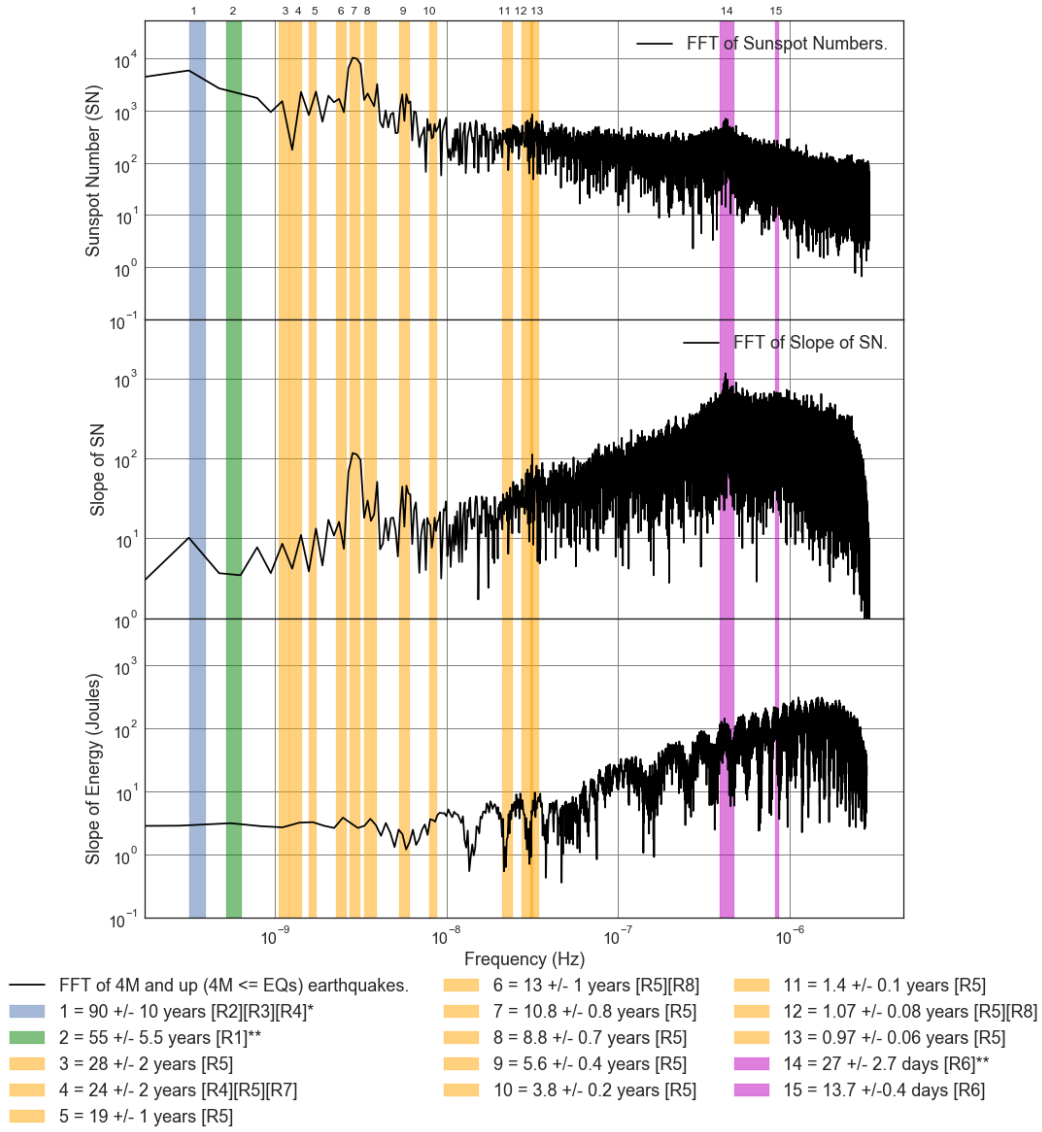

Figure E2.32: FFT Loglog Comparison Plot: Slope of Averaged 4M and up (4M <= EQs) Earthquake (EQ) total energy released, 2 Day Sunspot number and slope from 1818 to 2017. Additional meaning of the legend colors: Blue = Various Analysis techniques, Green = Meyer wavelet, Orange = Instantly maximal wavelet skeleton spectra, Magenta = Periodram and Linear phase finite impulse response.

Chapter 4: Discussion

This section refers to figures that are not just in the results of chapter 3, but also heavily refers to figures that are only found in the appendix. The summary tables in chapter 3 however only exist in chapter 3 and are not reproduced in the appendix.

In this chapter, each part of the analysis is initially discussed in its own section but not fully in isolation from the other parts. Therefore the first 5 sections of the discussion 4.1.1 through 4.1.4, and 4.2.1 are all discussed in a focused manner and may have a few comparisons to each other. Discussion section 4.3.1 incorporates all parts of the analysis into a much larger conversation and compares and contrasts the results of all sections in a larger context. As a part of the larger discussion some of the results for the magnitude category 6.5M and larger are also included.

4.1.1 Time Series Part 1 - Discussion

In looking at the summary tables for the results of part 1 of the analysis, the only aspects of the analysis that resulted in significant or near significant p-values for Pearson's R correlation were found when comparing the sunspot number (SN) slope (m) to the average number of earthquakes and for comparing the solar absolute value of the slope with earthquakes. This was only true for the Centennial and ISC datasets. For these respective figures, removing the overall linear trend from the earthquake data (see tables # 9 and # 11 for figures B1.15, B1.27, D1.15, and D1.27) was enough to shift the results from being not significant to significant with low to moderate anti-correlation values for R (see figures B1.18, B1.30, D1.18, and D1.30).

The low to at times moderate anti-correlated behavior is evident when looking at figures B1.5 to B1.8 in the appendix, through most of the historical period. The anti correlated behavior starts around or shortly after 1920 and the pattern stops abruptly after 1960 during the time when WWSSN is launched. Also, there were no significant p-values with respect to the Pearson's R correlation for the USGS ComCat dataset with respect to part 1 of the analysis (see table # 10). With that said, across all three earthquake datasets the Shapiro-Wilk test result and p-value were significant ($p_W > 0.5$) for nearly all plots where it was calculated in part 1 of the analysis except for figure D1.23 Solar Rise phase slope vs average # of earthquakes. For figure D1.23, W = 0.8333 strongly suggested the residuales were normally distributed but with $p_W = 0.04819$, p_W could not confirm the W statistic. This would otherwise suggest the data was normally distributed for all plots except this one. Since p_W is close to 0.05, the residuals may still be normally distributed with this particular p_W being an outlier. The Q-Q plots also looked somewhat normal but it was hard to tell if the residuals of the linear best fit line were truly distributed similarly to a normal distribution, or if they only looked that way due to having a smaller sample size.

In examining all of the residual plots, there was no discernable overall tube shape to show the residuals are uniformly dispersed about their respective lines of best fit. When looking at the scatter plots, the data points look very dispersed about a very flat trendline with little to no discernable trend. The one figure that visually looked the closest to having an overall relatively uniform tube shape with respect to its residuals was figure D1.23. In general, this lack of uniform

tube shape suggests that homoscedasticity is not preserved but again the lack of overall uniformity might be attributed to the analysis having a smaller sample size of < 20 data points.

In the context of the hypothesis of this study that earthquakes and the solar sunspot cycle maybe related orthogonally, in looking at the results of part 1 of the time series analysis in isolation, it is important to note that nearly all of the linear line of best fit slopes are very small or near zero. In addition, most of the values for R^2 are also very low to near 0, these results likely mean one of two mutually exclusive outcomes. Either, 1) there is a non-linear relationship between SN slope (m) including its absolute value and earthquakes, therefore Pearson's R and R^2 cannot fully describe such a relationship and can only confirm orthogonality. Or 2) there is no obvious relationship between sunspots and earthquakes and the low to moderate R correlations found between SN slope (m) vs the average number of earthquakes, and the absolute value of the SN slope (m) vs the average number of earthquakes are just due to random chance and are not real.

4.1.2 Time Series Part 2 - Discussion

In looking at the results of part 2 of the analysis, the summary tables give the statistics for 6 month averaged earthquakes vs the SN slope (m), and also for 6 month averaged earthquakes vs. the absolute value of SN slope (m) both for the time period of 1900 to 2007. Nearly all of the p-values for Pearson's R correlation were significant (within 95% confidence) or were just outside of the 95% confidence range but were still within 90% confidence across all three earthquake datasets. However, all of the Pearson's R correlations were low ranging between -0.221 to -0.122, resulting in very small values for R^2. All of the Shapiro-Wilk test results gave a

strong indication that the residuals from the linear lines of best fit were normally distributed, but all of their respective p_W values were near zero and failed to confirm it across all three earthquake datasets (see figures B2.7, B2.10, B2.13, C2.7, C2.10, C2.13, D2.7, D2.10, and D2.13). The scatter plots of SN slope (m) vs. Average # of earthquakes both with and without the trend in figures B2.5, B2.8, C2.5, and C2.8 show a loose (not quite spherical) grouping of the data into two groups. The first grouping of data points ranges from $x = -75$ to $x \approx 22$, and the second grouping from $x \approx 22$ to $x \approx 110$. It is easier to see this grouping of points when looking at their residuals in figures B2.6, B2.9, C2.6, and C2.9, in these plots homoscedasticity is not preserved and the grouping of the data is suggestive but alone are not definitive of a nonlinear relationship between sunspots and earthquakes. For the ISC dataset in figures D2.6, and D2.9, this loose grouping of data is replaced with a nonuniform ovalish-like shape where homoscedasticity is still not preserved.

For SN slope (m) vs. average # of earthquakes before the trend was removed, across all three datasets (see tables # 12, 13, and 14), the R-value while still low showed a slightly higher correlation with a slightly more significant p-value than after removing the trend. While for the absolute value of SN slope (m) vs. average # of earthquakes, the R and p-values were slightly more significant after the trend was removed, and this was consistent for all three datasets (see tables # 12, 13, and 14). Also with respect to the absolute value of SN slope (m) vs. average # of earthquakes, while it was not necessarily obvious in the scatter plots (see figures B2.14, C2.14, and D2.14), homoscedasticity was not preserved and was more visible in the plot of residuals (see figures B2.15, C2.15, and D2.15).

The scatter plots in figures B2.5, B2.8, D2.5, and D2.8 show a loose (not quite spherical) grouping of the data into two groups, the first one ranging from x = -75 to x = 25, and the second from x = 25 to x ≈ 110. It is easier to see this grouping of points when looking at their residuals in figures B2.6, B2.9, D2.6, and D2.9.

4.1.3 Time Series Part 3 - Discussion

Part 3 of the time series analysis only uses earthquake data from the historical period (pre-WWSSN) from 1900 to the end of 1963. Across all three datasets, the p-values with respect to the pearson's r correlation were all significantly lower for SN slope (m) vs. average number of earthquakes both with and without trend removed, but were only significant within 95% confidence for the USGS Centennial and USGS ComCat datasets (see tables # 15, 16, and 17). The Pearson's R values for the SN slope (m) vs. average number of earthquakes showed a low negative correlation of R ≈ 0.2 for both with and without trend removed for the Centennial and USGS ComCat datasets (see table # 15 and 16).

The Q-Q plots and the Shapiro-Wilk test statistics reported that the residuals were normally distributed but the p_W values were only significant for the ISC dataset with the one exception of figure D3.13, where $p_W = 0.0342$ (absolute value of SN slope (m) vs. average # of earthquakes). For the Centennial and USGS ComCat datasets, p_W values were near zero, but Shapiro-Wilk test statistic W was still near equal to 1. The residuals for all three datasets showed heteroscedastic behavior and both the Centennial and the USGS ComCat data residuals showed similar data grouping behavior between x = -75 to x ≈ 22 for the SN slope (m) vs. average

number of earthquakes both with and without trend removed as displayed in part 2 of the analysis (see figures B2.6, B2.9, B3.6, B3.9, C2.6, C2.9, C3.6, and C3.9). The residuals for the ISC earthquake data were also similar to their respective counterparts in part 2 of the time series analysis.

4.1.4 Time Series Part 4 - Discussion

Part 4 of the time series analysis uses earthquake data from the modern period (post-WWSSN) from 1964 into the 2000's. The results of part 4 are curiously different from part 3. Across all three datasets, for the absolute value of SN slope (m) vs. average number of earthquakes, both with and without the trend removed, had p-values that were all significant to within 98% confidence, with the pearson's R values ranging from R = -0.37 to R = -0.29 (see tables # 18, 19, and 20). The ISC dataset (see table # 20) was the only one where all of the p-values in the table were significant. It is also worth noting, that the loose grouping of data points as observed in analysis parts 2 and 3 for the residuals of SN slope (m) vs. Average # earthquakes both with and without the trend removed, were now consistently observed across all three earthquake datasets (the Centennial, USGS ComCat, and the ISC), see figures B4.6, B4.9, C4.6, C4.9, D4.6, and D4.9. The first grouping of data points still ranges from x = -75 to x ≈ 22, but the second grouping from x ≈ 22 to x ≈ 100. All of the Shapiro-Wilk tests results were near equal to 1, but only figure B4.13 had a p_W value that was significant, with $p_W = 0.06$. There were no significant p_W values for the USGS ComCat and ISC datasets. The Q-Q plots of residuals all look like they are more or less following a normal distribution.

4.2.1 Spectral Analysis Part 5 - Discussion

Averaging the RFFT spectra of all three datasets gave interesting results but did not yield a peak that towered obviously above its surrounding noise. Instead there were some very weak yet intriguing peaks, or possible peaks with most being difficult to differentiate from the surrounding noise. The first thing that stood out about the magnitude of the earthquake (EQ) count spectra compared to the sunspot number spectra, was similarity in their overall shape and magnitude of the spectra, especially how similar the noise was between the two. In looking at figure E1.1 (all averaged EQ), it was almost as if someone took the solar sunspot data and filtered out most of the notable features but left in all of the noise and instead left only a small bump like peak between bands # 7 and # 8, 10.8 +/- 0.8 years and 8.8 +/- 0.7 years respectively. To understand why the rfft of all earthquakes in figure E1.1 looks the way it does, refer to figure F1.1 (rfft of all EQ for each dataset) in the appendix. The magnitude of averaged earthquake spectra as shown in E1.1 is also shown at the bottom of figure F1.1 with a magnitude plot of the earthquake spectra for each dataset averaged into it plotted directly above. Figure F1.1 shows that the USGS ComCat dataset has a small peak at about where band #7 is (10.8 +/- 0.8 years) had the color bars been plotted over it.

Most of the magnitude of the averaged earthquake spectra plots looked unremarkable but there were a few recurring themes. For example, of the plots listed in the results section, E1.5 (7M ≤ EQ's), E1.25 (all EQ total energy), E1.29 (7M ≤ EQ total energy), E1.30 (6M ≤ EQ's total energy), and E1.32 (4M ≤ EQ's) all had a small peak at 55 +/- 5.5 years. However, of these figures mentioned, only in figures E1.5, E1.25, E1.30, and E1.32 did this peak at 55 +/- 5.5 years rise only slightly above the noise while E1.29 was at the noise level. Also E1.5, had another

small peak slightly above the noise at band # 3 (28 +/- 2 years), E1.6 (6M ≤ EQ's) had a small peak at band # 5 (19 +/- 1 years), E1.8 (4M ≤ EQ's) had a small but more prominent peak between bands # 7 and # 8 (10.8 +/- 0.8 years and 8.8 +/- 0.7 years respectively). However the peak at band # 4 (24 +/- 2 years) in figures E1.25, E1.30, and E1.32 did not rise even slightly above the noise and therefore was not really counted as a peak. Of these figures mentioned above, E1.25, E1.29, E1.30, and E1.32 are all the rfft magnitude of total earthquake energy released.

Also, it is worth reiterating that for magnitude categories 9M down, 8M down, 7M down, etc. all exclude the Centennial earthquake data from the averaging of the spectra because it does not contain any earthquakes below 5.5M. However, when possible the Centennial rfft magnitude data is still plotted for comparison purposes. Such is the case with figure E1.43 rfft of total energy released (Joules) for earthquakes less than 8M (found only in appendix E1). There is a weak but noticeable peak whose apex is close to the right edge of band # 5 (19 +/- 1 years). This peak is taller than the noise immediately to the right of it but it does not rise above the noise overall, making it harder to discern what it is. Because it does rise above the noise in it's immediate vicinity for the purposes of this study it is considered to be a very weak peak. In order to have a better understanding of why this plot looks the way it does see figure F1.43 (EQ's < 8M total energy released), as it is an average of the USGS Comcat and ISC spectra shown there.

One of the more noticeable but still small peaks can be seen in between bands # 12 (1.07 +/- 0.08 years) and # 13 (0.97 +/- 0.06 years) on E1.47 (EQ's < 4M total energy released) and E2.27 (EQ's < 4M slope of total energy released). It was a curious and unexpected find to see a

peak located at approximately 1 year in the rfft plot of total energy released and in the rfft plot of it's slope.

4.3.1 Overall - Discussion

It would be easy to look at the results of any one of the time series analysis sections in isolation from the rest, and be dismissive of any correlation found. However, when looked at collectively that is harder to do. The same grouping patterns found in parts 2, 3, and 4 of the analysis for earthquakes 7.5M and larger are only evident in some of the corresponding 6.5M and larger plots (see figures B2.22, B2.25, and C2.25). Since none of the data sets are considered complete for earthquakes 6.5M and larger for the historical period, it is important to keep that in mind while considering results for that magnitude range that contains data from during that time period. All of the residual plots for 6.5M and larger for all of the time series analysis sections showed that homoscedasticity was not preserved. The R values for 6.5M and up earthquakes were mostly very low and at times near zero. However, the results 6.5M and up at times proved to have significant p-values and similar R values for the ISC and USGS datasets. This was particularly true for part 4 of the time series analysis. Please see figures C4.21, C4.25, C4.27, C30, D4.21, D4.27, and D4.30 .

Chapter 5: Conclusions

In considering the results of the analysis both the time series and spectral analysis, and that nearly all of the residual plots showed heteroscedastic behavior while nearly the slope ‘m’ of all of the lines of best fit were either small or near zero, it is the conclusion of this study that the results indicate a non-linear, orthogonal, anti-correlated relationship between the change in slope of the solar cycle and earthquakes 7.5M and larger. In addition, because both part 1 and part 4 of the time series analysis showed a moderate negative correlation between 7.5M and larger earthquakes and the absolute value of SN slope (m), but part 1 averaged the number of earthquakes over the entire rise and decline phases, while part 4 only averaged earthquakes over a fix window of every 6 months (defined here as 182 days), it is possible that what is appearing in this paper as a at times low to moderate anticorrelation between sunspot solar cycle slope, and earthquakes may suggest the frequency of earthquakes 7.5M and larger are actually a response to the curvature (concave/convex nature) of the change in slope of the solar cycle. Some of this behavior is easier to see on the line plots in part 3 and 4 of the analysis. It would explain the higher yet still moderate anti-correlation behavior seen in parts 1, and 4, between the average number of earthquakes and the absolute value of the SN slope. More research in this area would need to be conducted in order to confirm or reject this finding.

Also, it was surprising to see weak solar-like periodicities in the rfft of earthquake energy and at times the slope of earthquake energy, suggesting that there may be a solar influence in the cumulative amount of seismic energy released for earthquakes.

It is also evident that there are non-geophysical trends contained within all three earthquake datasets for 7.5M and larger earthquakes. These trend(s) contained in the historical

period are different from those found during the modern period. Thus likely interfering in some way with many statistical studies of earthquakes 7.5M and larger when the data used spans from 1900 into the modern era. The non-geophysical trends are also likely helping to obscure statistical evidence of any relationship between sunspots and earthquakes especially since the presence of these trends and the change in behaviour during the modern era were not obvious when earthquakes 7.5M and larger were plotted over time.

Great care should be used whenever a statistical tool requiring homoscedasticity and/or normally distributed data is used with respect to sunspots and earthquakes, as these tools may likely give misleading or confusing results. Based on the results of this paper, it is more understandable why some researchers might find a correlation between sunspots and earthquakes and some don't depending on multiple factors such as: The completeness of the earthquake dataset, non-geophysical trends, the time span of the dataset (historical vs modern, or both), and the statistical tools.

The conclusions of this paper with respect to finding a correlation between solar cycle slope and earthquakes, are given as suggestive because both the ISC and the USGS ComCat datasets were being overhauled and updated during the time that the data for this study was acquired. It is unknown what if any impact that may have had on the results of this study. However, most recently (July 2020), a study conducted by Marchitelli et al, also found a high correlation between earthquakes and solar wind. Specifically, Marchitelli et al found a statistically significant correlation, "between large world wide earthquakes and the proton density near the magnetosphere, due to solar wind".

VI. References

[1] USGS Earthquake Facts. Retrieved April 4, 2019, from https://earthquake.usgs.gov/learn/facts.php

[2] Sumatra, Indonesia Earthquake and Tsunami, 26 December 2004. Retrieved April 4, 2019, from https://www.ngdc.noaa.gov/hazard/26dec2004.html

[3] 1964 M9.2 Great Alaskan Earthquake. Retrieved April 4, 2019, from https://earthquake.alaska.edu/earthquakes/notable/1964-m92-great-alaskan-earthquake

[4] Geller, R. J., Jackson, D. D., Kagan, Y. Y., & Mulargia, F. (1997). Earthquakes cannot be predicted. *Science*, *275*(5306), 1616-1616.

[5] Mogi, K. (1985). Earthquake prediction. United States.

[6] Yin, X. C., Wang, Y. C., Peng, K. Y., Bai, Y. L., Wang, H. T., & Yin, X. F. (2000). Development of a new approach to earthquake prediction: Load/Unload Response Ratio (LURR) theory. In *Microscopic and Macroscopic Simulation: Towards Predictive Modelling of the Earthquake Process* (pp. 2365-2383). Birkhäuser, Basel.

[7] Varotsos, P., & Lazaridou, M. (1991). Latest aspects of earthquake prediction in Greece based on seismic electric signals. *Tectonophysics*, *188*(3-4), 321-347.

[8] Yousef, S. M. (2000, September). The solar Wolf-Gleissberg cycle and its influence on the Earth. In Proceedings of the international conference on the environmental hazards mitigation, Cairo University, Cairo.

[9] Viterito, A. (2016). The correlation of seismic activity and recent global warming. *J. Earth Sci. Clim. Change*, *7*, 345.

[10] Hough, S. E. (2013). Missing great earthquakes. *Journal of Geophysical Research: Solid Earth*, *118*(3), 1098-1108.

[11] Baker, J. W., & Cornell, C. A. (2006). Which spectral acceleration are you using?. *Earthquake Spectra*, *22*(2), 293-312.

[12] Housner, G. W., Martel, R. R., & Alford, J. L. (1953). Spectrum analysis of strong-motion earthquakes. *Bulletin of the Seismological Society of America*, *43*(2), 97-119.

[13] Alford, J. L., Housner, G. W., & Martel, R. R. (1964). Spectrum analyses of strong-motion earthquakes.

[14] Shaltout, M. A. M., Tadros, M. T. Y., & Mesiha, S. L. (1999). Power spectra analysis for world-wide and North Africa historical earthquakes data in relation to sunspots periodicities. *Renewable energy*, *17*(4), 499-507.

[15] Wolf, R. (1853). On the periodic return of the minimum of sun-sport; the agreement between those periods and the variations of magnetic declination. *The London, Edinburgh, and Dublin Philosophical Magazine and Journal of Science*, *5*(29), 67-67.

[16] Love, J. J., & Rigler, E. J. (2012). Sunspot random walk and 22−year variation. *Geophysical Research Letters*, *39*(10).

[17] Leighton, R. B. (1969). A magneto-kinematic model of the solar cycle. *The Astrophysical Journal*, *156*, 1.

[18] Babcock, H. W. (1961). The Topology of the Sun's Magnetic Field and the 22-YEAR Cycle. *The Astrophysical Journal*, *133*, 572.

[19] Schüssler, M., & Vögler, A. (2006). Magnetoconvection in a sunspot umbra. *The Astrophysical Journal Letters*, *641*(1), L73.

[20] Vaquero, J. M. (2007). Historical sunspot observations: a review. *Advances in Space Research*, *40*(7), 929-941.

[21] Hathaway, D. H., Wilson, R. M., & Reichmann, E. J. (2002). Group sunspot numbers: Sunspot cycle characteristics. *Solar Physics*, *211*(1-2), 357-370.

[22] Kiepenheuer, K. O. (1953). Solar activity. *The Sun*, 322.

[23] Hoyt, D. V., & Schatten, K. H. (1998). Group sunspot numbers: A new solar activity reconstruction. *Solar physics*, *179*(1), 189-219.

[24] Waldmeier, M. (1935). Neue eigenschaften der sonnenfleckenkurve. *Astronomische Mitteilungen der Eidgenössischen Sternwarte Zurich*, *14*, 105-136.

[25] Waldmeier, M. (1939). Die zonenwanderung der sonnenflecken. *Astronomische Mitteilungen der Eidgenössischen Sternwarte Zurich*, *14*, 470-481.

[26] Dikpati, M., Gilman, P. A., & De Toma, G. (2008). The waldmeier effect: an artifact of the definition of wolf sunspot number?. *The Astrophysical Journal Letters*, *673*(1), L99.

[27] Aparicio, A. J. P., Vaquero, J. M., & Gallego, M. C. (2012). The proposed “Waldmeier discontinuity”: How does it affect to sunspot cycle characteristics?. *Journal of Space Weather and Space Climate*, *2*, A12.

[28] The Sunspot Cycle (updated on 03/15/2017). Retrieved on 04/16/2019, from https://solarscience.msfc.nasa.gov/SunspotCycle.shtml

[29] Robinson, A. (2013). *Earthquake: nature and culture*. Reaktion Books.

[30] Scholz, C. H. (2019). *The mechanics of earthquakes and faulting*. Cambridge university press.

[31] Armentrout, D., & Armentrout, P. (2014). *Earthquakes*. Retrieved from https://ebookcentral-proquest-com.ezpxy-web-p-u01.wpi.edu

[32] Estrada, H., & Lee, L. (2017). *Introduction to earthquake engineering* . Boca Raton ;: CRC Press, Taylor & Francis Group.

[33] Humphrey, A. T. (1992). Lord Rayleigh-the last of the great Victorian polymaths. *GEC review*, *7*(3), 167-79.

[34] Sen, T. K. (2009). *Fundamentals of seismic loading on structures*. John Wiley & Sons.

[35] Love, A. E. H. (2015). *Some Problems of Geodynamics*. Cambridge University Press.

[36] Musson, R., Grünthal, G., & Stucchi, M. (2010). The comparison of macroseismic intensity scales. Journal of Seismology, 14(2), 413–428. https://doi.org/10.1007/s10950-009-9172-0

[37] Allaby, M. (2013). A dictionary of geology and earth sciences (4th ed.). Oxford: Oxford University Press.

[38] Mercalli, G. (1902). *Sulle modificazioni proposte alla scala sismica De Rossi-Forel* (Vol. 8). Società tipografica modenese.

[39] Mercalli, G. (1883). *Vulcani e fenomeni vulcanici in Italia* (Vol. 3). A. Forni.

[40] J. M. (1904). Prof. Adolfo Cancani. Nature, 70(1806), 128–129. https://doi.org/10.1038/070128a0

[41] Ranke, U. (2016). Natural disaster risk management: Geosciences and social responsibility (pp. 1–514). https://doi.org/10.1007/978-3-319-20675-2

[42] Chauhan, Lincoln K. (2017). Basics Of Geophysics. RED'SHINE Publication. Pvt. Ltd.

[43] Musson, R. M., & Cecić, I. (2012). Intensity and intensity scales. *New manual of seismological observatory practice*, *2*, 1-41.

[44] Wood, H. O., & Neumann, F. (1931). Modified Mercalli intensity scale of 1931. *Bulletin of the Seismological Society of America*, *21*(4), 277-283.

[45] Richter, C. F. (1958). Elementary Seismology, WH. *Fleeman and Company, San*.

[46] C. D. P. (1895). The Rossi-forel Scale of Earthquake Intensity. *Publications of the Astronomical Society of the Pacific*, *7*(41), 123–125. Retrieved from www.jstor.org/stable/40670542

[47] Dowrick, D. J. (1996). The Modified Mercalli earthquake intensity scale. *Bulletin of the New Zealand Society for Earthquake Engineering*, *29*(2), 92-106.

[48] Musson, R. M. W., Grunthal, G., & Stucchi, M. (1995). Comment on "the 17 August 1991 Honeydew earthquake: a case for revising the Modified Mercalli scale in sparsely populated areas" by Dengler and McPherson. *Bulletin of the Seismological Society of America*, *85*(4), 1266-1267.

[49] Richter, C. F. (1935). An instrumental earthquake magnitude scale. *Bulletin of the Seismological Society of America*, *25*(1), 1-32.

[50] Ellsworth, W. L. (1990). Earthquake history, 1769-1989. *United States Geological Survey, Professional Paper;(USA)*, *1515*.

[51] Kanamori, H. (1983). Magnitude scale and quantification of earthquakes. *Tectonophysics*, *93*(3-4), 185-199.

[52] Chung, D. H., & Bernreuter, D. L. (1981). Regional relationships among earthquake magnitude scales. *Reviews of Geophysics*, *19*(4), 649-663.

[53] Gutenberg, B. (1945). Amplitudes of surface waves and magnitudes of shallow earthquakes. *Bulletin of the Seismological Society of America*, *35*(1), 3-12.

[54] Gutenberg, B. (1945). Amplitudes of P, PP, and S and magnitude of shallow earthquakes. *Bulletin of the Seismological Society of America*, *35*(2), 57-69.

[55] Gutenberg, B. (1945). Magnitude determination for deep-focus earthquakes. *Bulletin of the Seismological Society of America*, *35*(3), 117-130.

[56] Wilford, John Noble (1985). "Charles Richter, Quake Expert, Dies", New York Times, October 1, 1985, Section B, Page 7. Retrieved from: https://www.nytimes.com/1985/10/01/obituaries/charles-richter-quake-expert-dies.html

[57] Jeffreys, Harold (1960). "Beno Gutenberg (obituary)". Quarterly Journal of the Royal Astronomical Society, Vol. 1, p.239. Retrieved from: http://articles.adsabs.harvard.edu//full/1960QJRAS...1..239./0000239.000.html

[58] Gutenberg, B., & Richter, C. F. (1954). Seismicity of the Earth, 310 pp. *Princeton University Press, Princeton, NJ*, *235*, 1-15.

[59] Gutenberg, B., & Richter, C. F. (1956). Earthquake magnitude, intensity, energy, and acceleration: (Second paper). *Bulletin of the seismological society of America*, *46*(2), 105-145.

[60] Gutenberg, B., & Richter, C. F. (1955). Magnitude and energy of earthquakes. *Nature*, *176*(4486), 795-795.

[61] Peterson, J., & Hutt, C. R. (2014). *World-wide standardized seismograph network: A data users guide* (p. 82). US Department of the Interior, US Geological Survey.

[62] Oliver, J., & Murphy, L. (1971). WWNSS: Seismology's global network of observing stations. *Science*, *174*(4006), 254-261.

[63] Michigan Univ Ann Arbor Inst Of Science And Technology. (1964). HANDBOOK: WORLD-WIDE STANDARD SEISMOGRAPH NETWORK. Retrieved from http://www.dtic.mil/docs/citations/AD0439691
Document Retrieved from: http://ds.iris.edu/seismo-archives/info/stations/WWSSN1964.pdf

[64] Bormann, P., & Saul, J. (2008). The new IASPEI standard broadband magnitude m B. *Seismological Research Letters*, *79*(5), 698-705.

[65] Hanks, T. C., Kanamori, H. (1979) A moment magnitude scale. Journal of Geophysical Research: Solid Earth, 84(B5), 2348–2350. https://doi.org/10.1029/JB084iB05p02348

[66] Peter Bormann, Domenico Giacomo. The moment magnitude and the energy magnitude : common roots and differences. Journal of Seismology, Springer Verlag, 2010, 15 (2), pp.411-427. 10.1007/s10950-010-9219-2. hal-00646919

[67] Bormann, Peter & Liu, Ruifeng & Ren, Xiao & Gutdeutsch, Rudolf & Kaiser, Diethelm & Castellaro, Silvia. (2007). Chinese National Network Magnitudes, Their Relation to NEIC Magnitudes, and Recommendations for New IASPEI Magnitude Standards. Bulletin of the Seismological Society of America. 97. 114-127. 10.1785/0120060078.

[68] Bormann P., Saul J. (2009) Earthquake Magnitude. In: Meyers R. (eds) Encyclopedia of Complexity and Systems Science. Springer, New York, NY

[69] Kanamori, H. (1977). The energy release in great earthquakes. *Journal of geophysical research*, *82*(20), 2981-2987.

[70] Grünthal, G., & Wahlström, R. (2003). An M w based earthquake catalogue for central, northern and northwestern Europe using a hierarchy of magnitude conversions. *Journal of seismology*, *7*(4), 507-531.

[71] Liu, R., Chen, Y., Ren, X., Xu, Z., Sun, L., Yang, H., … Ren, K. (2007). Comparison between different earthquake magnitudes determined by China Seismograph Network. Acta Seismologica Sinica, 20(5), 497–506. https://doi.org/10.1007/s11589-007-0497-x

[72] Bormann, P. (2015). Are new data suggesting a revision of the current M w and M e scaling formulas?. *Journal of Seismology*, *19*(4), 989-1002.

[73] Butler, R., Lay, T., Creager, K., Earl, P., Fischer, K., Gaherty, J., ... & Tromp, J. (2004). The Global Seismographic Network surpasses its design goal. *Eos, Transactions American Geophysical Union*, *85*(23), 225-229.

[74] Ambraseys, N. N., & Douglas, J. (2004). Magnitude calibration of north Indian earthquakes. *Geophysical Journal International*, *159*(1), 165-206.

[75] Engdahl, E. R., Villaseñor, A. (2002). Global seismicity: 1900-1999. *International handbook of earthquake and engineering seismology*, 665-690.

[76] Engdahl, E. R., van der Hilst, R., & Buland, R. (1998). Global teleseismic earthquake relocation with improved travel times and procedures for depth determination. *Bulletin of the Seismological Society of America*, *88*(3), 722-743.

[77] Audio recording: “Why are we having so many earthquakes? Has earthquake activity been increasing?” United States Geological Survey. Retrieved on 05/21/2020. From https://www.usgs.gov/media/audio/why-are-we-having-so-many-earthquakes-has-earthquake-activity-been-increasing

[78] “Is earthquake activity increasing?” British Geological Survey. Retrieved on 05/21/2020. From https://earthquakes.bgs.ac.uk/research/earthquakeActivity.html

[79] “Is earthquake activity increasing?” British Geological Survey. Retrieved on 05/21/2020. From https://earthquakes.bgs.ac.uk/research/earthquakeActivity.html

[80] Dunbar, P., Stroker, K., & McCullough, H. (2010). Do the 2010 Haiti and Chile earthquakes and tsunamis indicate increasing trends?. *Geomatics, Natural Hazards and Risk*, *1*(2), 95-114.

[81] “Why are we having so many earthquakes? Has naturally occurring earthquake activity been increasing? Does this mean a big one is going to hit? OR We haven't had any earthquakes in a long time; does this mean that the pressure is building up for a big one?” United States Geological Survey. Retrieved on 05/21/2020. From https://www.usgs.gov/faqs/why-are-we-having-so-many-earthquakes-has-naturally-occurring-earthquake-activity-been?qt-news_science_products=0#qt-news_science_products

[82] Love, J. J., & Thomas, J. N. (2013). Insignificant solar−terrestrial triggering of earthquakes. *Geophysical Research Letters*, *40*(6), 1165-1170.

[83] Stein, S., Okal, E. A., & Wiens, D. A. (1988). Application of modern techniques to analysis of historical earthquakes. *Historical Seismograms and Earthquakes of the World*, 85-104.

[84] Di Giacomo, D., & Storchak, D. A. (2016). A scheme to set preferred magnitudes in the ISC Bulletin. *Journal of Seismology*, *20*(2), 555-567.

[85] Alter, D. (1920). Possible Connection between Sunspots and Earthquakes. *Science*, *51*(1324), 486-487.

[86] Knopoff, L. (1964). Earth tides as a triggering mechanism for earthquakes. *Bulletin of the Seismological Society of America*, *54*(6A), 1865-1870.

[87] Simpson, J. F. (1967). Earth tides as a triggering mechanism for earthquakes. *Earth and Planetary Science Letters*, *2*(5), 473-478.

[88] Shlien, S. (1972). Earthquake-tide correlation. *Geophysical Journal International*, *28*(1), 27-34.

[89] Palumbo, A. (1986). Lunar and solar tidal components in the occurrence of earthquakes in Italy. *Geophysical Journal International*, *84*(1), 93-99.

[90] Chapman, S., & Miller, J. C. P. (1940). The statistical determination of lunar daily variations in geomagnetic and meteorological elements. *Geophysical Supplements to the Monthly Notices of the Royal Astronomical Society*, *4*(9), 649-669.

[91] Cochran, E. S., Vidale, J. E., & Tanaka, S. (2004). Earth tides can trigger shallow thrust fault earthquakes. *Science*, *306*(5699), 1164-1166.

[92] Odintsov, S., Boyarchuk, K., Georgieva, K., Kirov, B., & Atanasov, D. (2006). Long-period trends in global seismic and geomagnetic activity and their relation to solar activity. *Physics and Chemistry of the Earth, Parts A/B/C*, *31*(1-3), 88-93.

[93] Chen, L., Chen, J. G., & Xu, Q. H. (2012). Correlations between solid tides and worldwide earthquakes M S≥ 7.0 since 1900. *Natural Hazards and Earth System Sciences*, *12*(3), 587-590.

[94] Hough, S. E. (2018). Do large (magnitude≥ 8) global earthquakes occur on preferred days of the calendar year or lunar cycle?. *Seismological Research Letters*.

[95] Li, Z., Yue, J., Xiang, Y., Chen, J., Bian, Y., & Chen, H. (2018). Multiresolution Analysis of the Relationship of Solar Activity, Global Temperatures, and Global Warming. *Advances in Meteorology*, *2018*.

[96] Polygiannakis, J., Preka-Papadema, P., & Moussas, X. (2003). On signal–noise decomposition of time-series using the continuous wavelet transform: application to sunspot index. *Monthly Notices of the Royal Astronomical Society*, *343*(3), 725-734.

[97] Mursula, K., & Zieger, B. (1996). The 13.5−day periodicity in the Sun, solar wind, and geomagnetic activity: The last three solar cycles. *Journal of Geophysical Research: Space Physics*, *101*(A12), 27077-27090.

[98] Carrasco, V. M. S., Vaquero, J. M., Gallego, M. C., & Sánchez-Bajo, F. (2016). A normalized sunspot-area series starting in 1832: An update. *Solar Physics*, *291*(9-10), 2931-2940.

[99] Daily Sunspot Numbers, Years: 1818-2018, SILSO, World Data Center - Sunspot Number and Long-term Solar Observations, Royal Observatory of Belgium, on-line Sunspot Number catalogue: http://www.sidc.be/SILSO/

[100] Sunspot Number Version 2.0: new data and conventions, Retrieved April 14, 2019, from http://www.sidc.be/silso/newdataset

[101] Centennial Earthquake Catalog: Files. Accessed on 4/18/2019, from https://earthquake.usgs.gov/data/centennial/centennial_README.rtf

[102] Centennial Earthquake Catalog. Accessed on 04/17/2019, from https://earthquake.usgs.gov/data/centennial/

[103] ANSS Comprehensive Earthquake Catalog (ComCat) Documentation. Retrieved on 05/05/2019, from https://earthquake.usgs.gov/data/comcat/

[104] ANSS Composite Catalog Search, Retrieved on 05/05/2019, from http://www.quake.geo.berkeley.edu/anss/catalog-search.html

[105] The Bulletin of the International Seismological Centre. Retrieved on 05/05/2019, from http://isc-mirror.iris.washington.edu/iscbulletin/

[106] International Seismological Centre, *On-line Bulletin*, http://www.isc.ac.uk, Internatl. Seismol. Cent., Thatcham, United Kingdom, 2017.
http://doi.org/10.31905/D808B830

[107] ISC Bulletin: bulletin search. Retrieved on 05/05/2019, from http://isc-mirror.iris.washington.edu/iscbulletin/search/bulletin/

[108] How can an earthquake have a negative magnitude? Retrieved on 05/05/2019, from https://www.usgs.gov/faqs/how-can-earthquake-have-a-negative-magnitude?qt-news_science_products=0#qt-news_science_products

[109] NIST/SEMATECH e-Handbook of Statistical Methods, https://www.itl.nist.gov/div898/handbook/prc/section2/prc213.htm Retreived 05/06/2020.

[110] Bhatt, Bhavesh (2019). Quantile (Q-Q) Plots from Scratch In Pandas. [Video] YouTube. Uploaded on 02/17/2019. https://youtu.be/JfnHsWhGRBk

[111] Shapiro, S. S., & Wilk, M. B. (1965). An analysis of variance test for normality (complete samples). *Biometrika*, *52*(3/4), 591-611.

[112] Pearson, A. V., and Hartley, H. O. (1972). Biometrica Tables for Statisticians, Vol 2, (Table 15) Cambridge, England, Cambridge University Press.

[113] Cooley, J. W., & Tukey, J. W. (1965). An algorithm for the machine calculation of complex Fourier series. *Mathematics of computation*, *19*(90), 297-301.

[114] Bluestein, L. (1970). A linear filtering approach to the computation of discrete Fourier transform. IEEE Transactions on Audio and Electroacoustics, 18(4), 451–455. https://doi.org/10.1109/TAU.1970.1162132

[115] Vercruyssen, M., & Hendrick, H. W. (2011). *Behavioral research and analysis: an introduction to statistics within the context of experimental design*. CRC Press.

[116] Magiya, Joseph (2019). Pearson Coefficient of Correlation Explained. Retrieved June 23, 2020, from https://towardsdatascience.com/pearson-coefficient-of-correlation-explained-369991d93404

[117] Pearson Product-Moment Correlation. Retrieved June 23, 2020, from https://statistics.laerd.com/statistical-guides/pearson-correlation-coefficient-statistical-guide.php

[118] Marchitelli, V., Harabaglia, P., Troise, C. *et al.* On the correlation between solar activity and large earthquakes worldwide. *Sci Rep* 10, 11495 (2020). https://doi.org/10.1038/s41598-020-67860-3

VII. Appendix

Appendix A

Table A1: List of solar cycle slope per rise and decline phase from 1700 to 2008.

Solar Cycle	cycle side	min year	min sn	max year	max sn	slope year	slope_m	Note
Solar cycle A	Rise	1700	8.3	1705	96.7	1702.5	17.7	
Solar cycle A	Decline	1712	0	1705	96.7	1708.5	-13.8	
Solar cycle B	Rise	1712	0	1717	105	1714.5	21.0	
Solar cycle B	Decline	1723	18.3	1717	105	1720.0	-14.5	
Solar cycle C	Rise	1723	18.3	1727	203.3	1725.0	46.3	
Solar cycle C	Decline	1733	8.3	1727	203.3	1730.0	-32.5	
Solar cycle D	Rise	1733	8.3	1738	185	1735.5	35.3	
Solar cycle D	Decline	1744	8.3	1738	185	1741.0	-29.5	
Solar cycle E	Rise	1744	8.3	1750	139	1747.0	21.8	
Solar cycle E	Decline	1755	16	1750	139	1752.5	-24.6	
Solar cycle 1	Rise	1755	16	1761	143.2	1758.0	21.2	
Solar cycle 1	Decline	1766	19	1761	143.2	1763.5	-24.8	
Solar cycle 2	Rise	1766	19	1769	176.8	1767.5	52.6	
Solar cycle 2	Decline	1775	11.7	1769	176.8	1772.0	-27.5	
Solar cycle 3	Rise	1775	11.7	1778	257.3	1776.5	81.9	
Solar cycle 3	Decline	1784	17	1778	257.3	1781.0	-40.1	
Solar cycle 4	Rise	1784	17	1787	220	1785.5	67.7	
Solar cycle 4	Decline	1798	6.8	1787	220	1792.5	-19.4	
Solar cycle 5	Rise	1798	6.8	1802	75	1800.0	17.1	Double Peak
Solar cycle 5	Decline	1810	0	1804	79.2	1807.0	-13.2	Double Peak
Solar cycle 6	Rise	1810	0	1816	76.3	1813.0	12.7	
Solar cycle 6	Decline	1823	2.2	1816	76.3	1819.5	-10.6	
Solar cycle 7	Rise	1823	2.2	1830	117.4	1826.5	16.5	
Solar cycle 7	Decline	1833	13.4	1830	117.4	1831.5	-34.7	
Solar cycle 8	Rise	1833	13.4	1837	227.3	1835.0	53.5	
Solar cycle 8	Decline	1843	18.1	1837	227.3	1840.0	-34.9	
Solar cycle 9	Rise	1843	18.1	1848	208.3	1845.5	38.0	
Solar cycle 9	Decline	1856	8.2	1848	208.3	1852.0	-25.0	
Solar cycle 10	Rise	1856	8.2	1860	182.2	1858.0	43.5	
Solar cycle 10	Decline	1867	13.9	1860	182.2	1863.5	-24.0	
Solar cycle 11	Rise	1867	13.9	1870	232	1868.5	72.7	

Solar cycle 11	Decline	1878	5.7	1870	232	1874.0	-28.3	
Solar cycle 12	Rise	1878	5.7	1883	106.1	1880.5	20.1	
Solar cycle 12	Decline	1889	10.4	1883	106.1	1886.0	-16.0	
Solar cycle 13	Rise	1889	10.4	1893	142	1891.0	32.9	
Solar cycle 13	Decline	1901	4.6	1893	142	1897.0	-17.2	Eq's start in 1904, Eq's that occurred during max year are included in the rise and not the decline of the solar cycle.
Solar cycle 14	Rise	1901	4.6	1905	105.5	1903.0	25.2	Double Peak
Solar cycle 14	Decline	1913	2.4	1907	102.8	1910.0	-16.7	Double Peak
Solar cycle 15	Rise	1913	2.4	1917	173.6	1915.0	42.8	
Solar cycle 15	Decline	1923	9.7	1917	173.6	1920.0	-27.3	
Solar cycle 16	Rise	1923	9.7	1928	129.7	1925.5	24.0	
Solar cycle 16	Decline	1933	9.2	1928	129.7	1930.5	-24.1	
Solar cycle 17	Rise	1933	9.2	1937	190.6	1935.0	45.4	
Solar cycle 17	Decline	1944	16.1	1937	190.6	1940.5	-24.9	
Solar cycle 18	Rise	1944	16.1	1947	214.7	1945.5	66.2	
Solar cycle 18	Decline	1954	6.6	1947	214.7	1950.5	-29.7	
Solar cycle 19	Rise	1954	6.6	1957	269.3	1955.5	87.6	
Solar cycle 19	Decline	1964	15	1957	269.3	1960.5	-36.3	
Solar cycle 20	Rise	1964	15	1968	150	1966.0	33.8	
Solar cycle 20	Decline	1976	18.4	1968	150	1972.0	-16.5	
Solar cycle 21	Rise	1976	18.4	1979	220.1	1977.5	67.2	
Solar cycle 21	Decline	1986	14.8	1979	220.1	1982.5	-29.3	
Solar cycle 22	Rise	1986	14.8	1989	211.1	1987.5	65.4	Double Peak

Solar cycle 22	Decline	1996	11.6	1991	203.3	1993.5	-38.3	Double Peak
Solar cycle 23	Rise	1996	11.6	2000	173.9	1998.0	40.6	
Solar cycle 23	Decline	2008	4.2	2000	173.9	2004.0	-21.2	
Solar cycle 24	Rise	2008	4.2	2014	113.3	2011.0	18.2	
Solar cycle 24	Decline							

Appendix B1: USGS Centennial Time Series Analysis Part 1 - Average # of Earthquakes per Rise and Decline of Solar cycle slope.

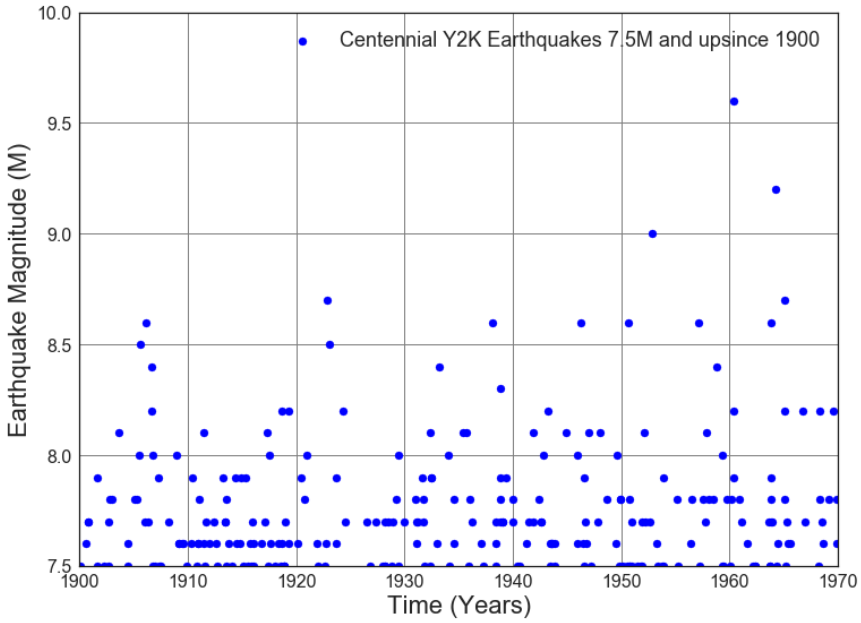

Figure B1.1: Scatter plot of Centennial Y2K earthquakes 7.5M and up magnitudes 1900 to 1970

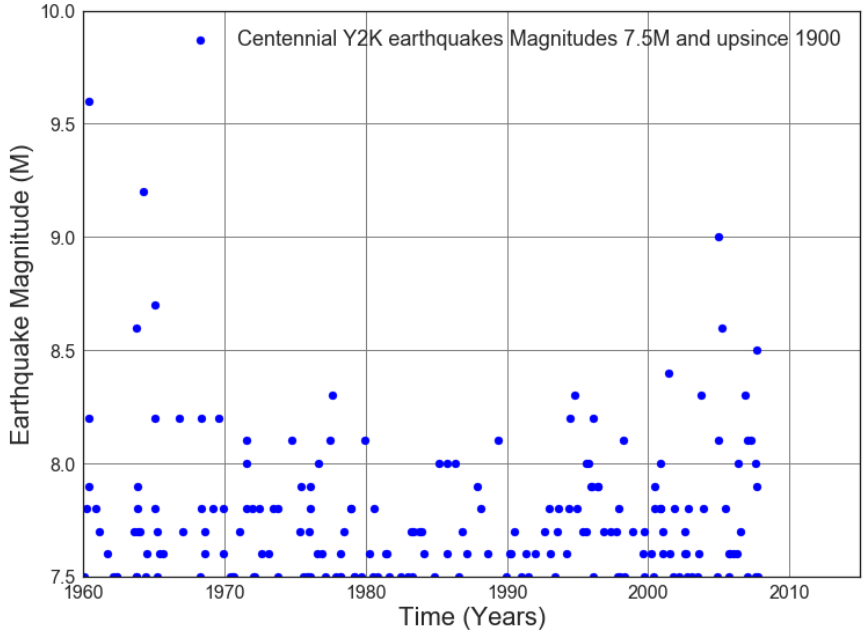

Figure B1.2: Scatter plot of Centennial Y2K Max EQs 7.5M and up Magnitudes 1960 to 2007

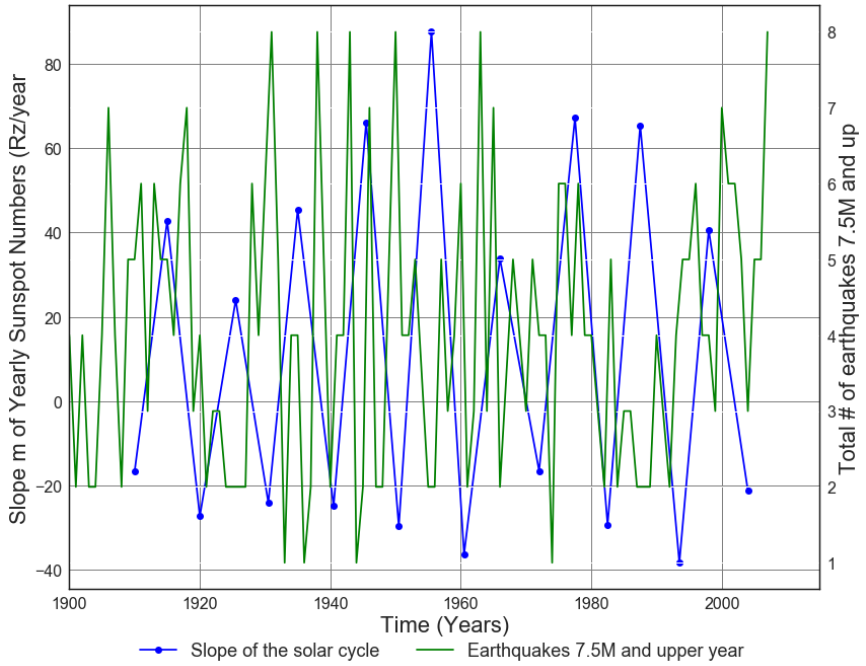

Figure B1.3: Slope of Solar cycle from 1900 to 2014 vs. Average number of 7.5M and up Earthquakes.

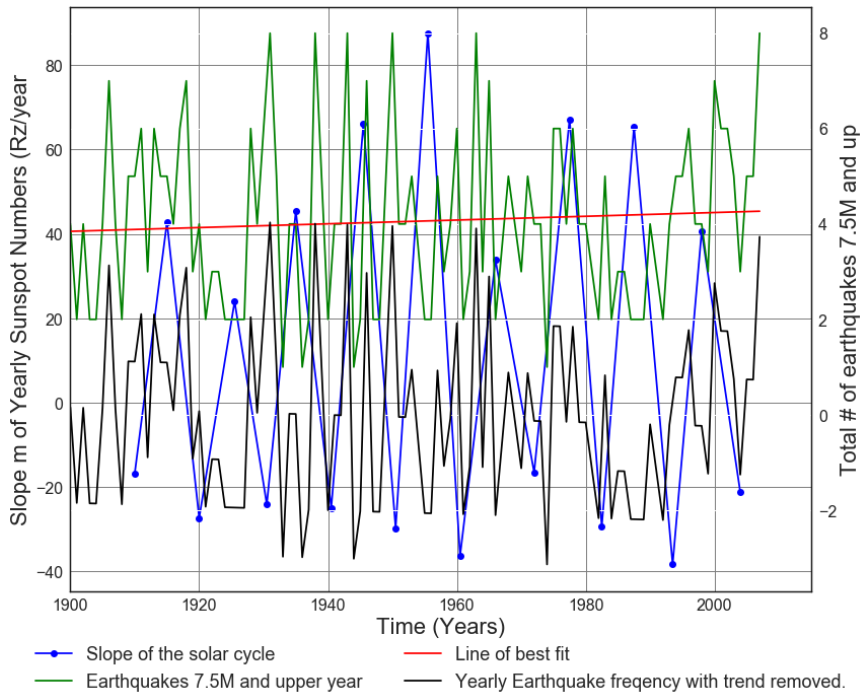

Figure B1.4: Slope of Solar cycle from 1900 to 2014 vs. Average number of 7.5M and up Earthquakes. Line of best fit, y = 0.003944x + (-3.648), mean x = 1.954e+03 +/- 31.53, mean y = 4.058 +/- 1.818

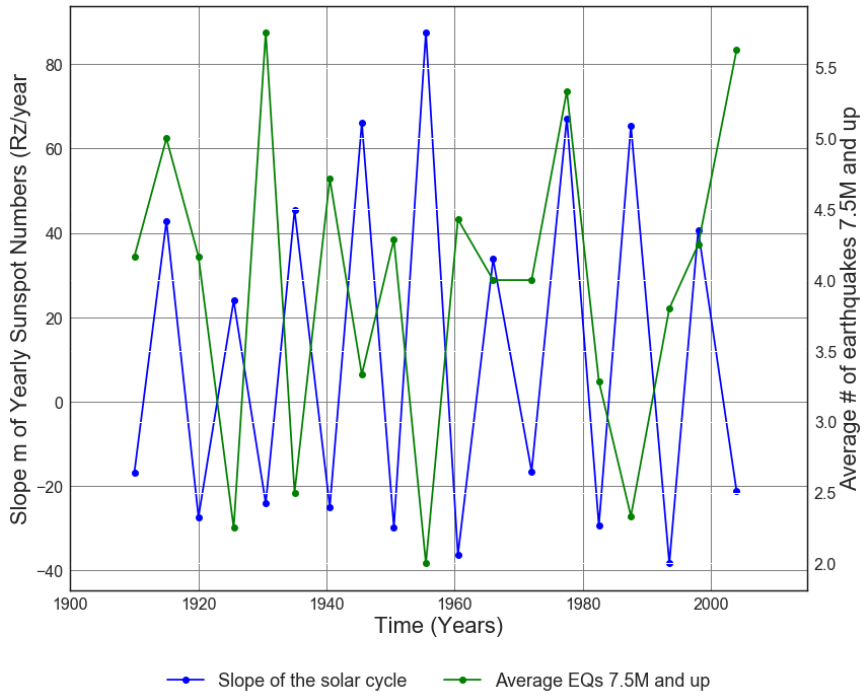

Figure B1.5: Slope of Solar cycle from 1900 to 2014 vs. Average number of 7.5M and up Earthquakes.

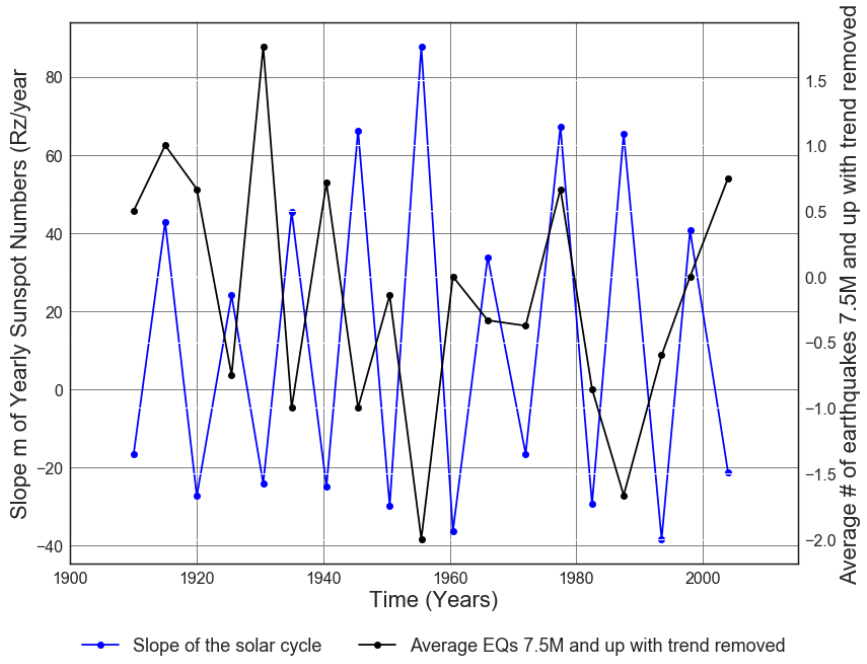

Figure B1.6: Slope of Solar cycle from 1900 to 2014 vs. Average number of 7.5M and up earthquakes.

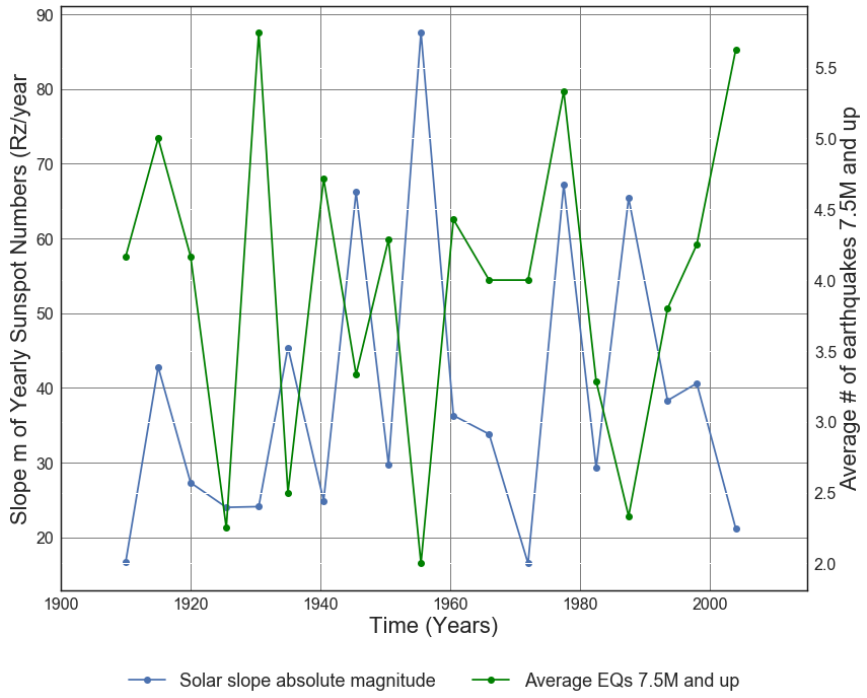

Figure B1.7: Absolute value of Solar cycle slope from 1900 to 2014 vs. Average number of 7.5M and up Earthquakes.

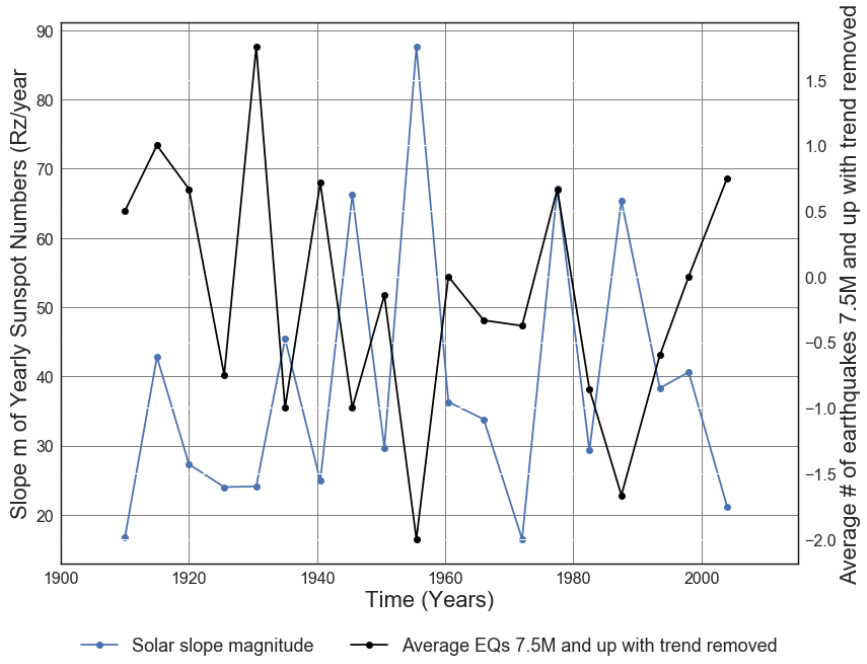

Figure B1.8: Absolute value of solar cycle slope from 1900 to 2014 vs. Average number of 7.5M and up Earthquakes with trend removed.

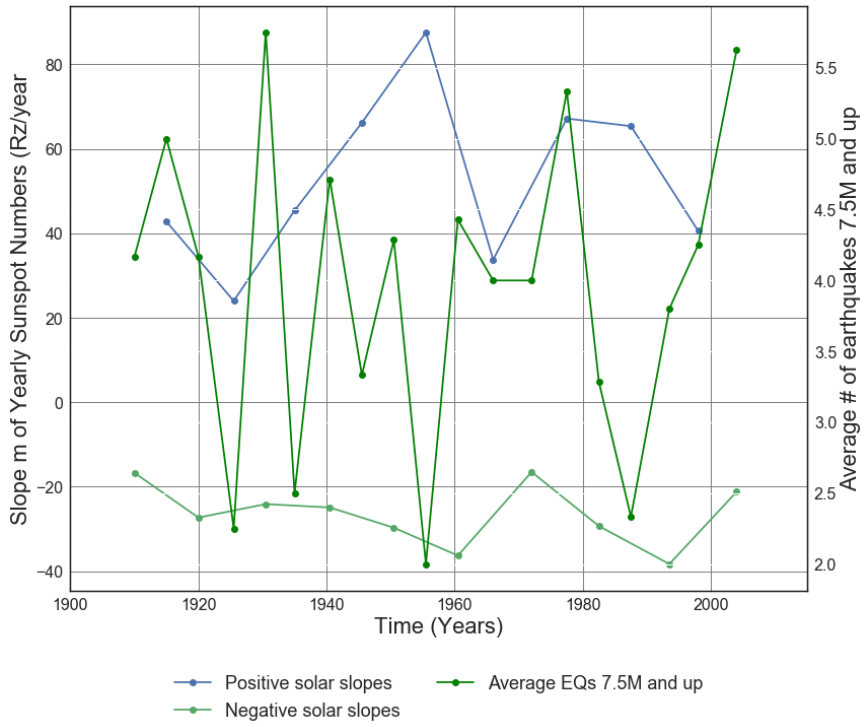

Figure B1.9: Positive and negative solar cycle slopes from 1900 to 2014 vs. Average number of 7.5M and up Earthquakes.

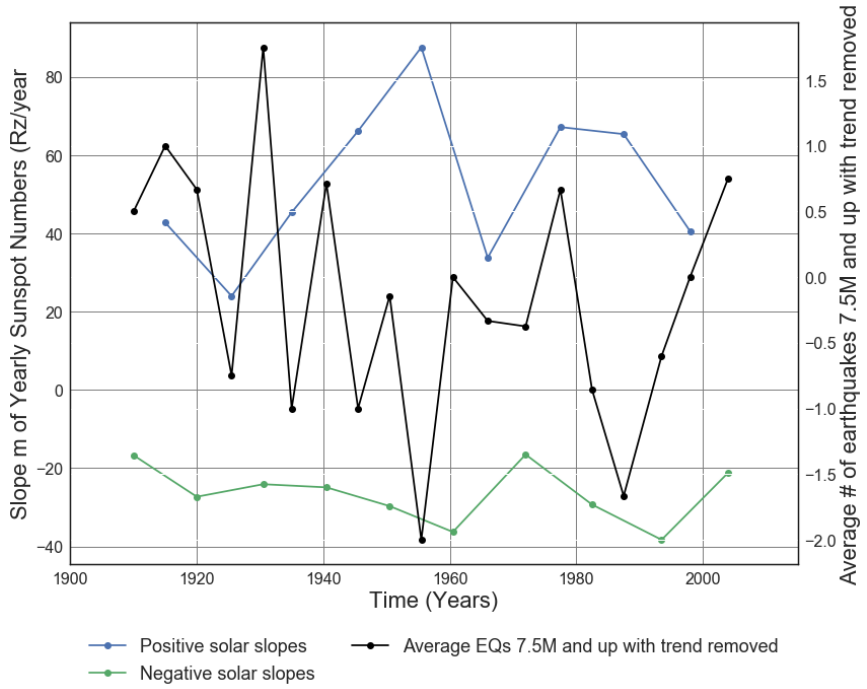

Figure B1.10: Positive and negative solar cycle slopes from 1900 to 2014 vs. Average number of 7.5M and up Earthquakes with trend removed.

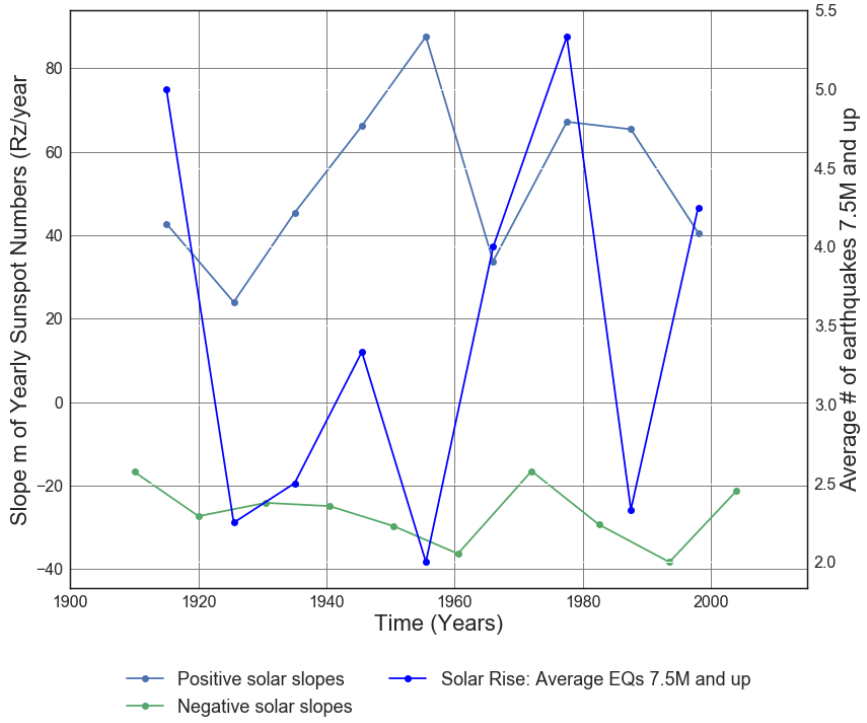

Figure B1.11: Positive and negative solar cycle slopes from 1900 to 2014 vs. Solar Rise: Average number of 7.5M and up Earthquakes.

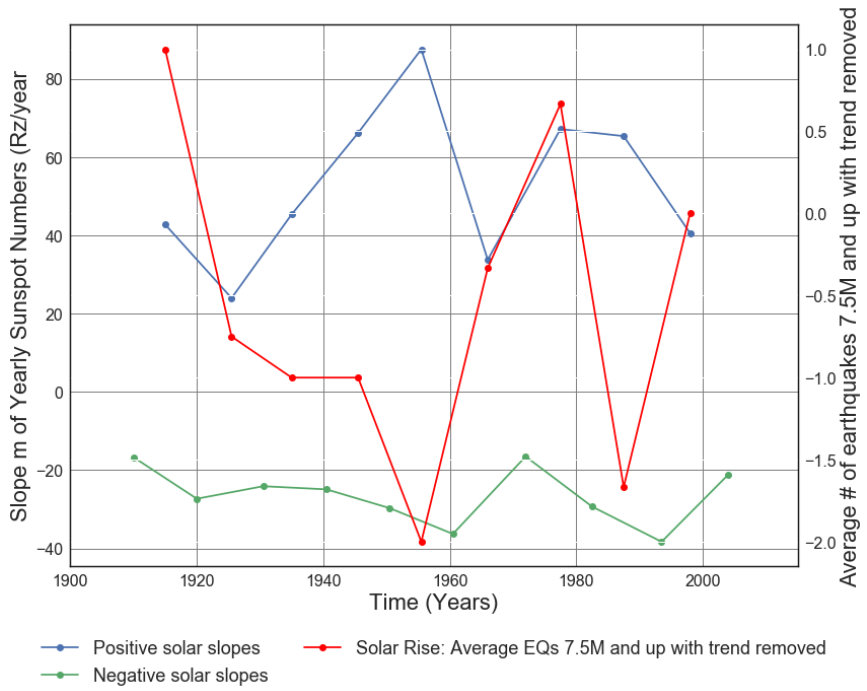

Figure B1.12: Positive and negative solar cycle slopes from 1900 to 2014 vs. Solar Rise: Average number of 7.5M and up Earthquakes with trend removed.

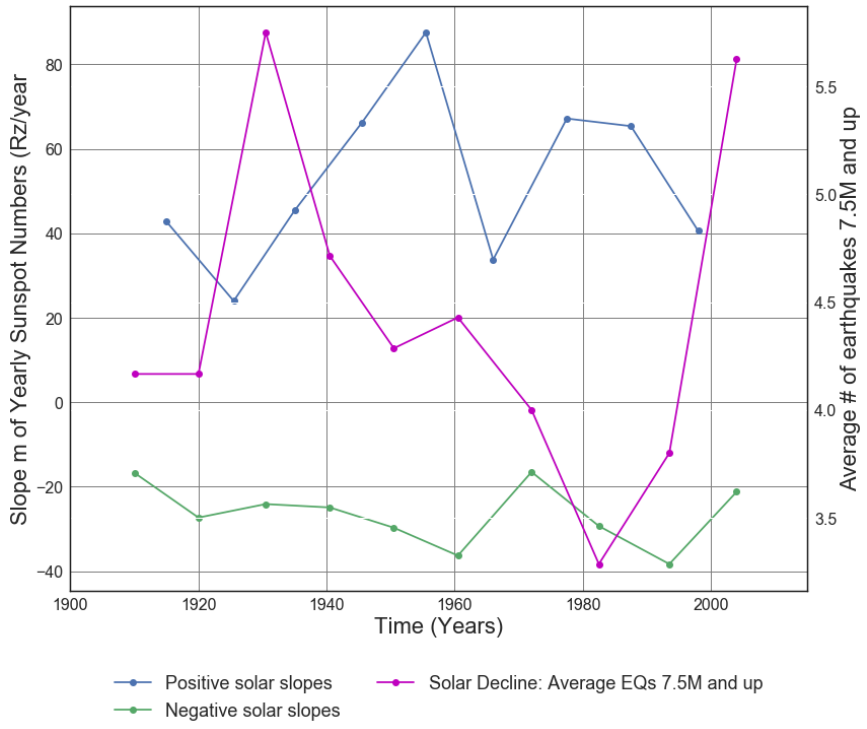

Figure B1.13: Positive and negative solar cycle slopes from 1900 to 2014 vs. Solar Decline: Average number of 7.5M and up Earthquakes.

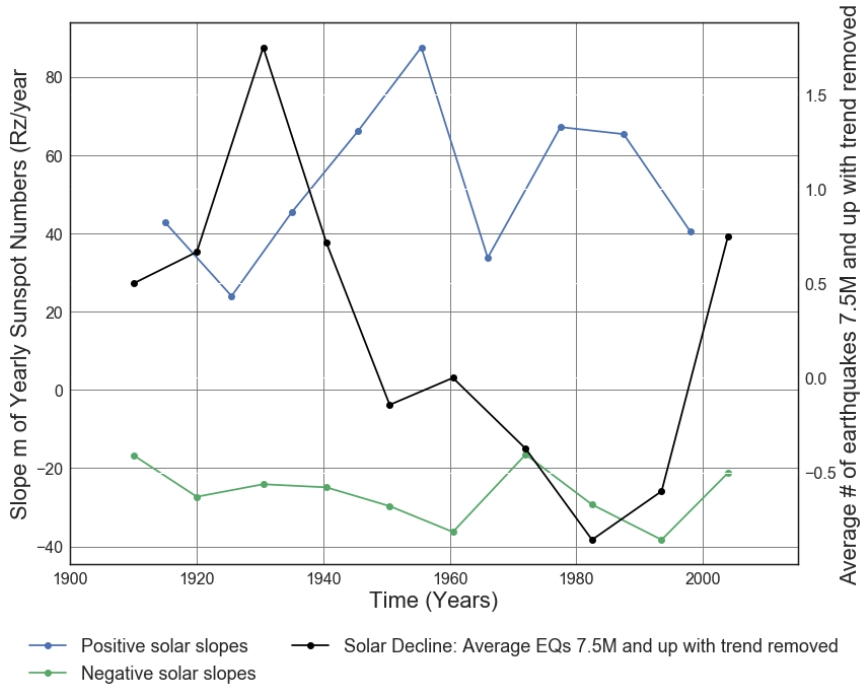

Figure B1.14: Positive and negative solar cycle slopes from 1900 to 2014 vs. Solar Rise: Average number of 7.5M and up Earthquakes.

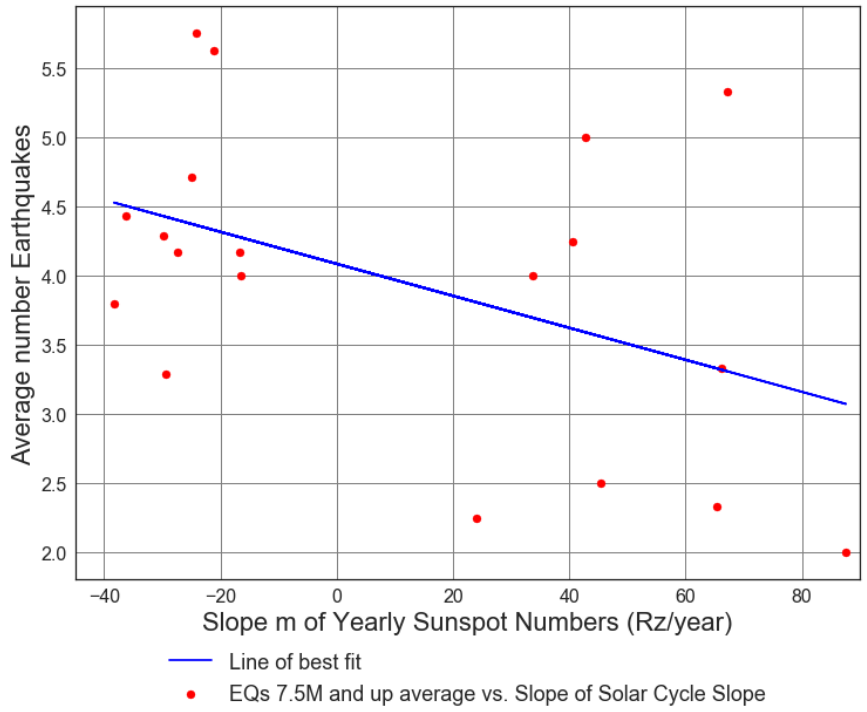

Figure B1.15: Scatter Plot of Slope m of Solar cycle (from 1900 to 2014) vs. Average number of 7.5M and up Earthquakes. Line of best fit, y = -0.01155x + (4.086), mean x = 10.98 +/- 41.86, mean y = 3.959 +/- 1.086, R = -0.445, R squared = 0.1981, p-value = 0.05621.

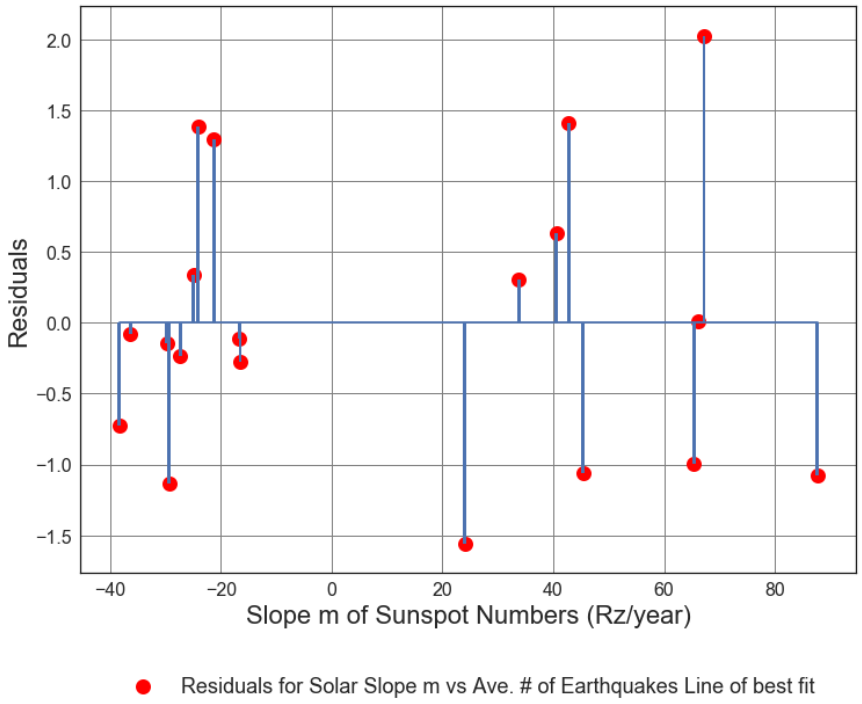

Figure B1.16: Residuals Plot of Average Solar Cycle Slope m (from 1900 to 2014) vs. Average number of 7.5M and up Earthquakes. Line of best fit, y = -0.01155x + (4.086), mean x = 10.98 +/- 41.86, mean y = 3.959 +/- 1.086, R = -0.445, R squared = 0.1981, p-value = 0.05621.

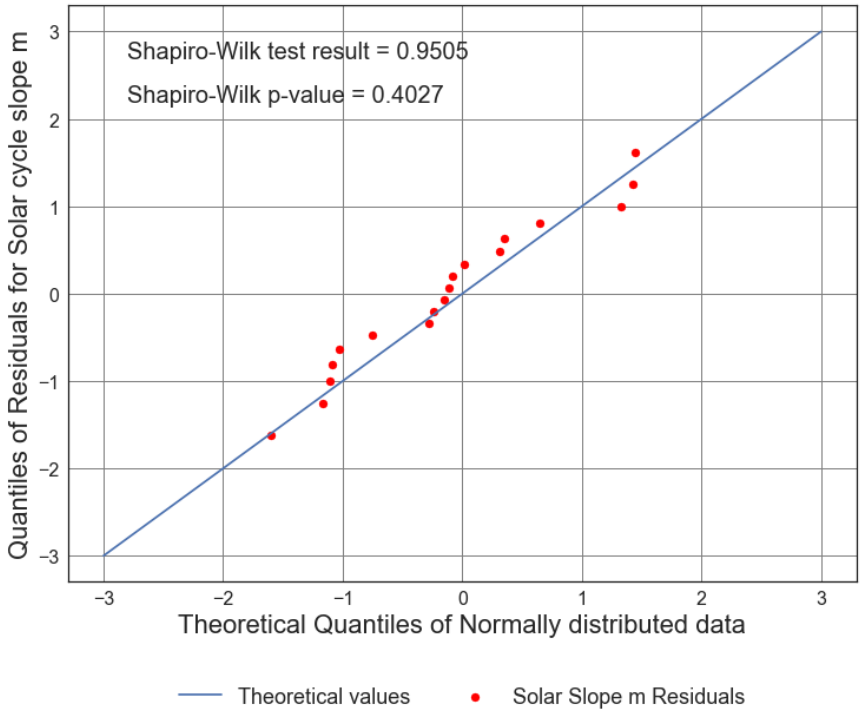

Figure B1.17: Quantile-Quantile Plot of the resisuales of Slope of Solar cycle m (from 1900 to 2014) vs. Average number of 7.5M and up Earthquakes. Line of best fit, y = -0.01155x + (4.086), mean x = 10.98 +/- 41.86, mean y = 3.959 +/- 1.086, R = -0.445, R squared = 0.1981, p-value = 0.05621.

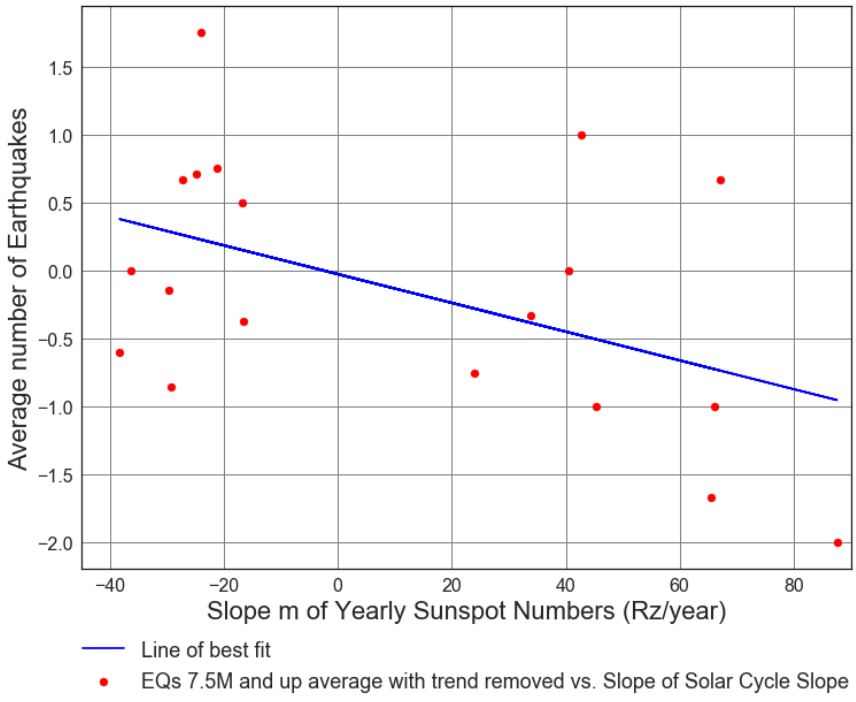

Figure B1.18: Scatter Plot of Slope m of Solar cycle (from 1900 to 2014) vs. Average number of 7.5M and up Earthquakes with trend removed. Line of best fit, y = -0.01057x + (-0.02478), mean x = 10.98 +/- 41.86, mean y = -0.1409 +/- 0.9348, R = -0.4734, R squared = 0.2241, p-value = 0.04064.

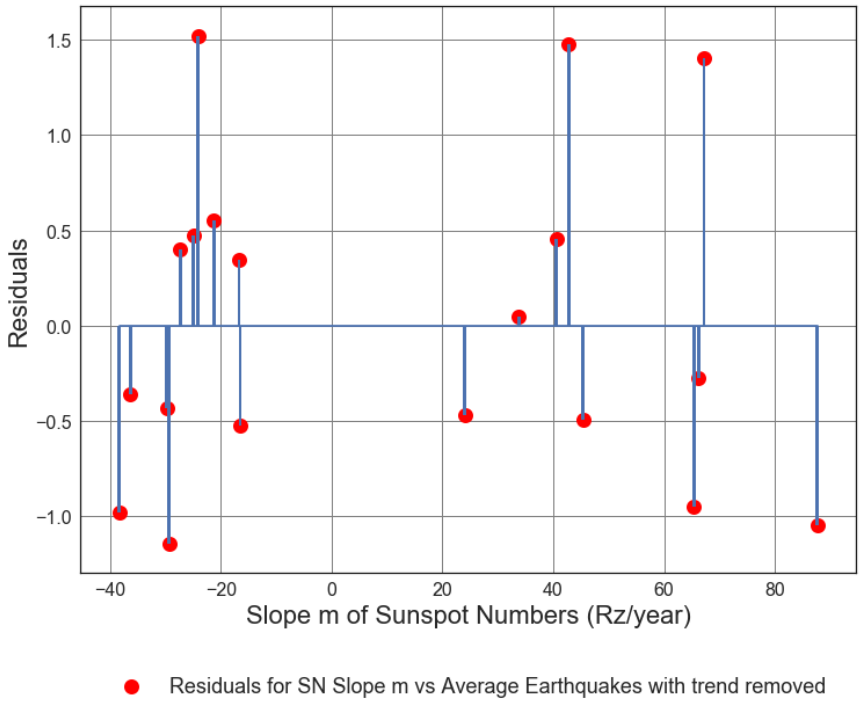

Figure B1.19: Residuals Plot of the Slope of Solar cycle (from 1900 to 2014) vs. Average number of 7.5M and up Earthquakes with trend removed. Line of best fit, y = -0.01057x + (-0.02478), mean x = 10.98 +/- 41.86, mean y = -0.1409 +/- 0.9348, R = -0.4734, R squared = 0.2241, p-value = 0.04064.

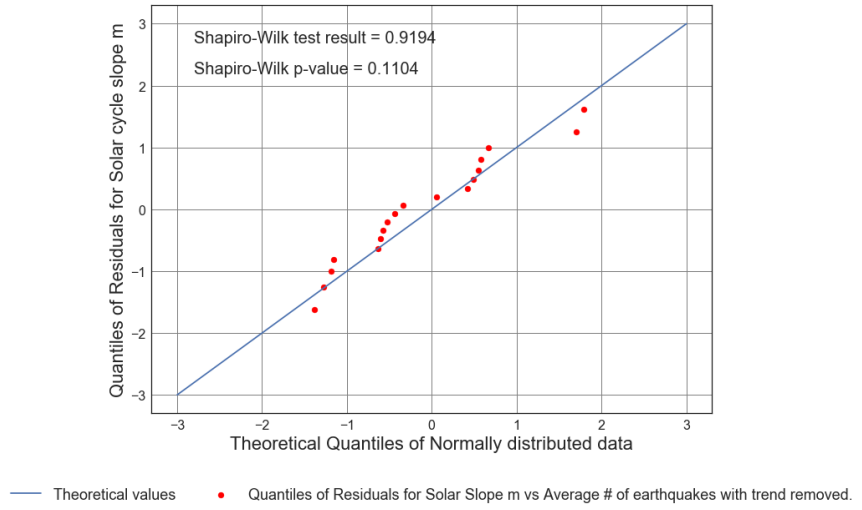

Figure B1.20: Scatter Plot of Absolute Magnitude of the Slope of Solar cycle (from 1900 to 2014) vs. Average number of 7.5M and up Earthquakes. Line of best fit, y = -0.01057x + (-0.02478), mean x = 10.98 +/- 41.86, mean y = -0.1409 +/- 0.9348, R = -0.4734, R squared = 0.2241, p-value = 0.04064.

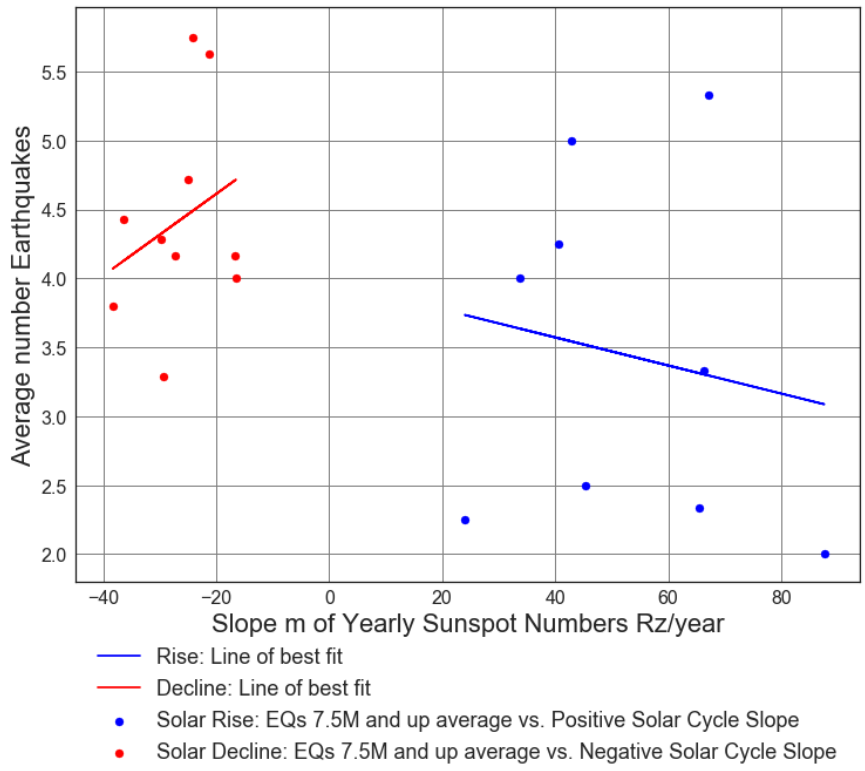

Figure B1.21: Scatter Plot of Slope of Solar cycle (from 1900 to 2014) vs. Average number of 7.5M and up Earthquakes. Rise: Line of best fit, y = -0.01019x + (3.98), mean x = 52.56 +/- 19.0, mean y = 3.444 +/- 1.183, R = -0.04297, R squared = 0.001847, p-value = 0.9062. Decline: Line of best fit, y = 0.02962x + 5.205, mean x = -26.43 +/- 6.974, mean y = 4.422 +/- 0.7281, R = 0.2837, R squared = 0.08048, p-value = 0.427.

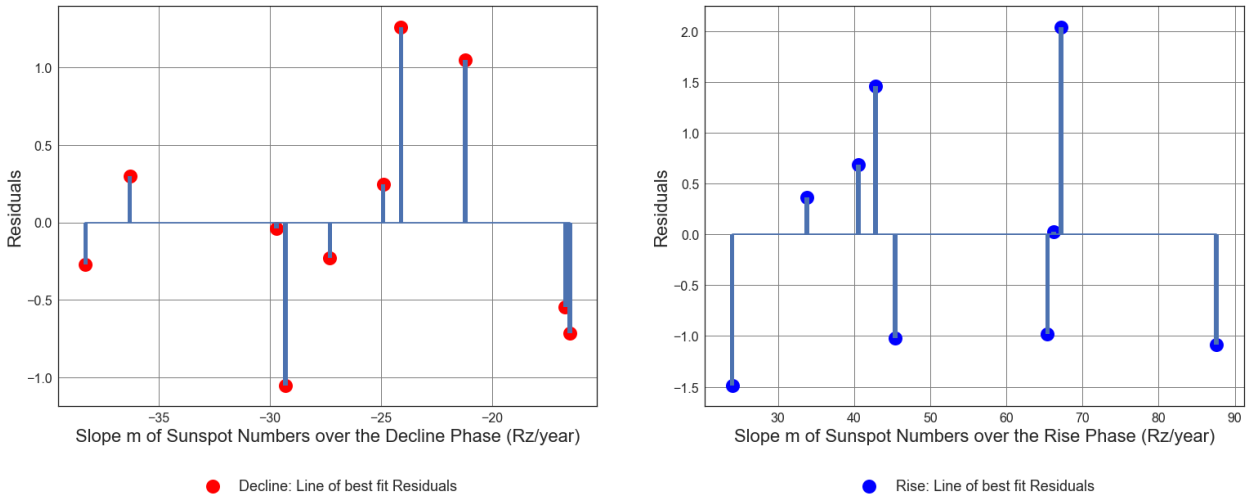

Figure B1.22: Residuals centered about zero, plot of Slope of Solar cycle (from 1900 to 2014) vs. Average number of 7.5M and up Earthquakes. Rise: Line of best fit, y = -0.01019x + (3.98), mean x = 52.56 +/- 19.0, mean y = 3.444 +/- 1.183, R = -0.04297, R squared = 0.001847, p-value = 0.9062. Decline: Line of best fit, y = 0.02962x + 5.205, mean x = -26.43 +/- 6.974, mean y = 4.422 +/- 0.7281, R = 0.2837, R squared = 0.08048, p-value = 0.427.

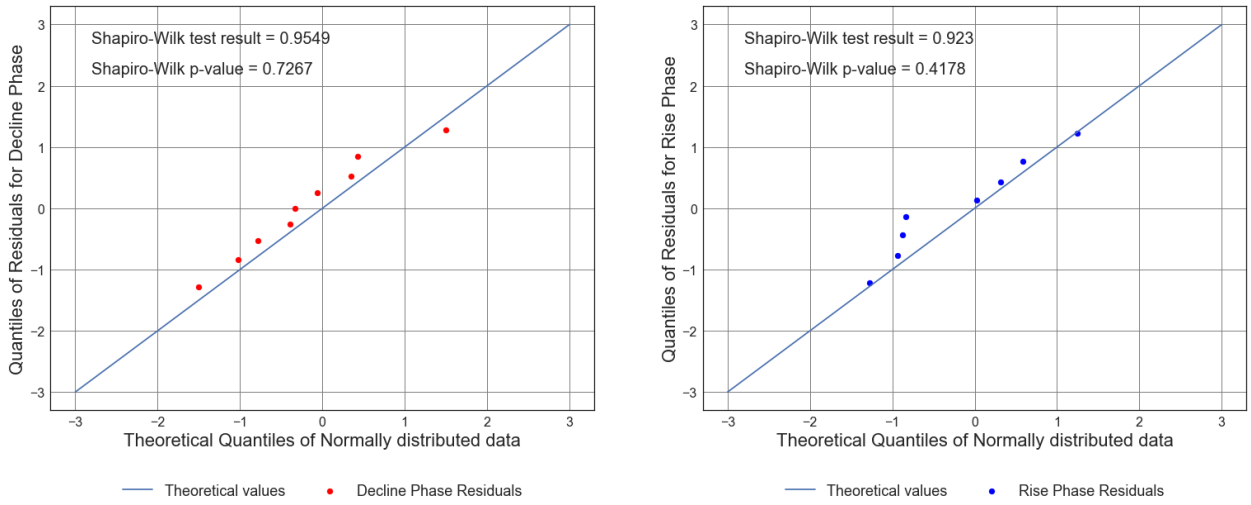

Figure B1.23: Quartile-Quartile Plot of Residuals for the Rise and Decline phase Slope of Solar cycle (from 1900 to 2014) vs. Average number of 7.5M and up Earthquakes. Rise: Line of best fit, y = -0.01019x + (3.98), mean x = 52.56 +/- 19.0, mean y = 3.444 +/- 1.183, R = -0.04297, R squared = 0.001847, p-value = 0.9062. Decline: Line of best fit, y = 0.02962x + 5.205, mean x = -26.43 +/- 6.974, mean y = 4.422 +/- 0.7281, R = 0.2837, R squared = 0.08048, p-value = 0.427.

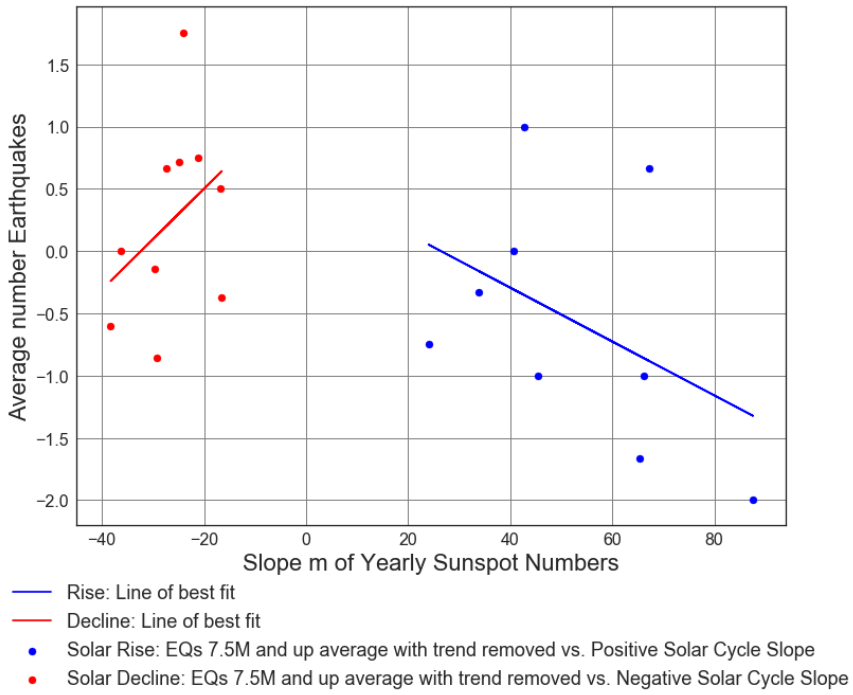

Figure B1.24: Scatter Plot of Slope of Solar cycle (from 1900 to 2014) vs. with trend removed Average number of 7.5M and up Earthquakes. Rise: Line of best fit, y = -0.02163x + (0.5721), mean x = 52.56 +/- 19.0, mean y = -0.5648 +/- 0.9443, R = -0.4354, R squared = 0.1895, p-value = 0.2415. Decline: Line of best fit, y = 0.04051x + 1.311, mean x = -26.43 +/- 6.974, mean y = 0.2406 +/- 0.7421, R = 0.3807, R squared = 0.1449, p-value = 0.2778.

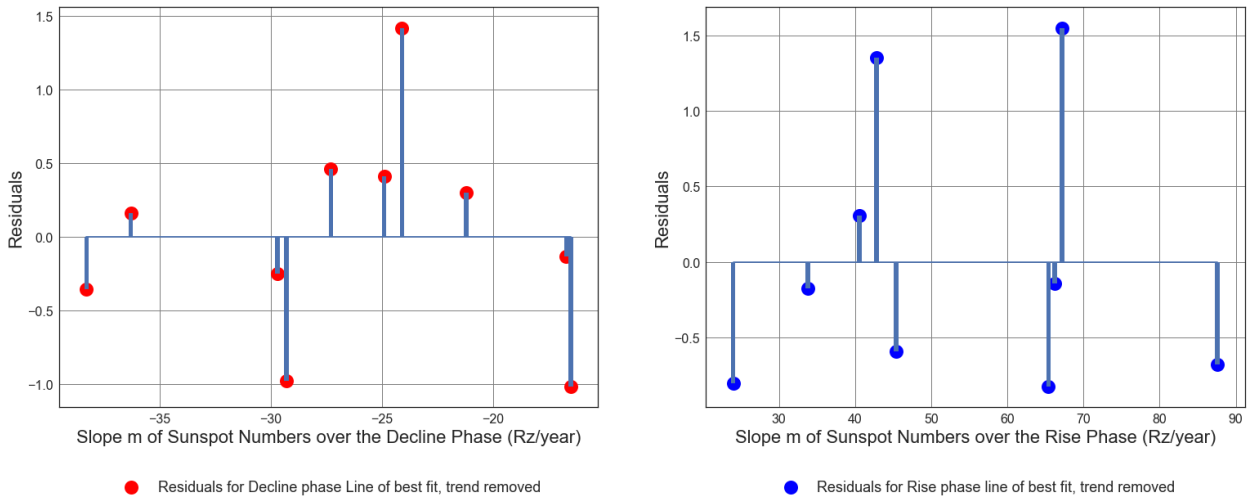

Figure B1.25: Residuals centered about zero, plot of Slope of Solar cycle (from 1900 to 2014) vs. Average number of 7.5M and up Earthquakes with trend removed. Rise: Line of best fit, y = -0.02163x + (0.5721), mean x = 52.56 +/- 19.0, mean y = -0.5648 +/- 0.9443, R = -0.4354, R squared = 0.1895, p-value = 0.2415. Decline: Line of best fit, y = 0.04051x + 1.311, mean x = -26.43 +/- 6.974, mean y = 0.2406 +/- 0.7421, R = 0.3807, R squared = 0.1449, p-value = 0.2778.

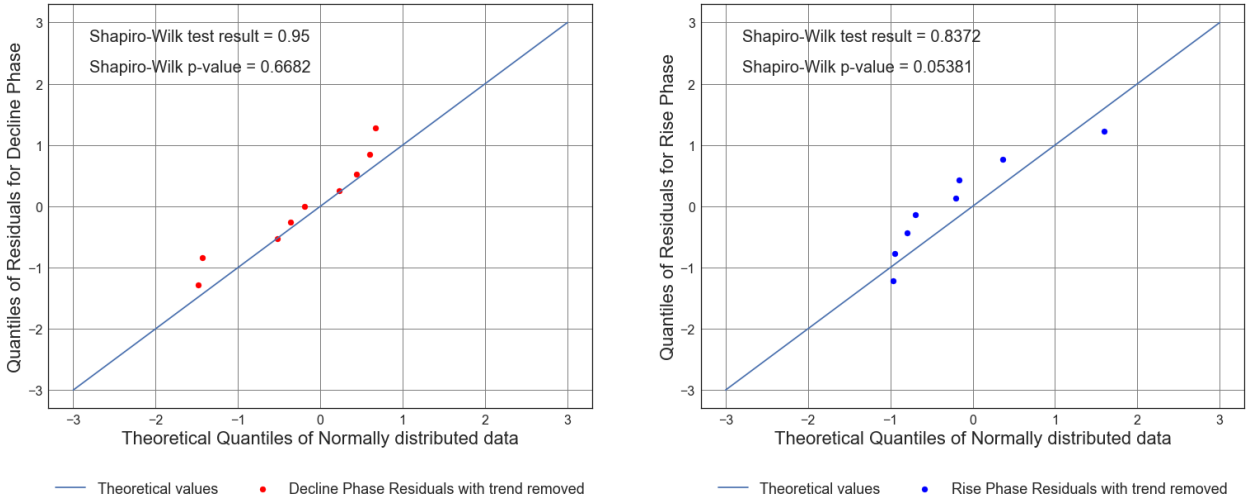

Figure B1.26: Quartile-Quartile Plot of Residuals for the Rise and Decline phase Slope of Solar cycle (from 1900 to 2014) vs. Average number of 7.5M and up Earthquakes with trend removed. Rise: Line of best fit, y = -0.02163x + (0.5721), mean x = 52.56 +/- 19.0, mean y = -0.5648 +/- 0.9443, R = -0.4354, R squared = 0.1895, p-value = 0.2415. Decline: Line of best fit, y = 0.04051x + 1.311, mean x = -26.43 +/- 6.974, mean y = 0.2406 +/- 0.7421, R = 0.3807, R squared = 0.1449, p-value = 0.2778.

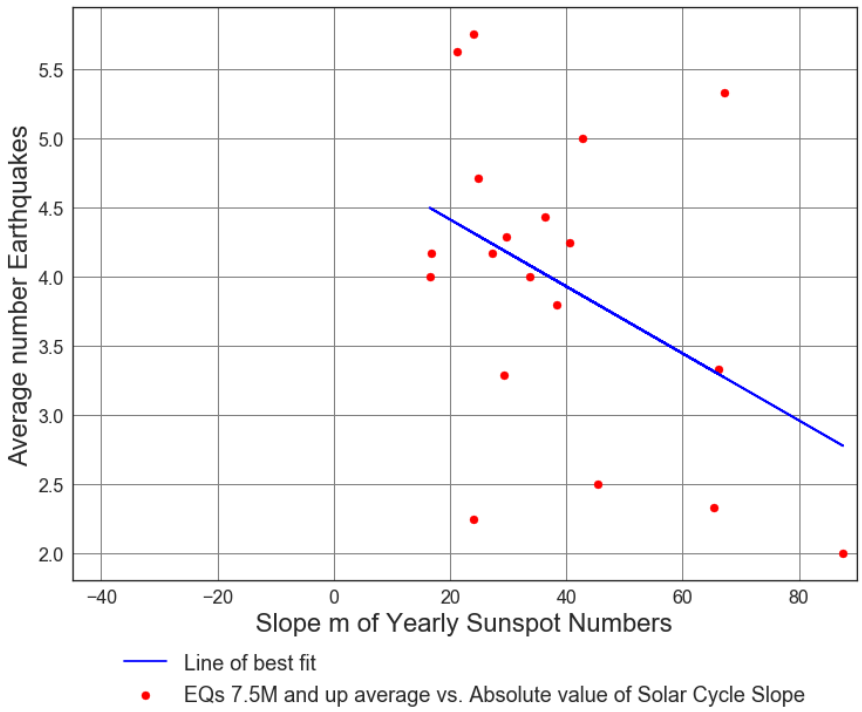

Figure B1.27: Scatter Plot of Absolute Magnitude of the Slope of Solar cycle (from 1900 to 2014) vs. Average number of 7.5M and up Earthquakes. Line of best fit, y = -0.02418x + (4.897), mean x = 38.81 +/- 19.15, mean y = 3.959 +/- 1.086, R = -0.4262, R squared = 0.1817, p-value = 0.0688.

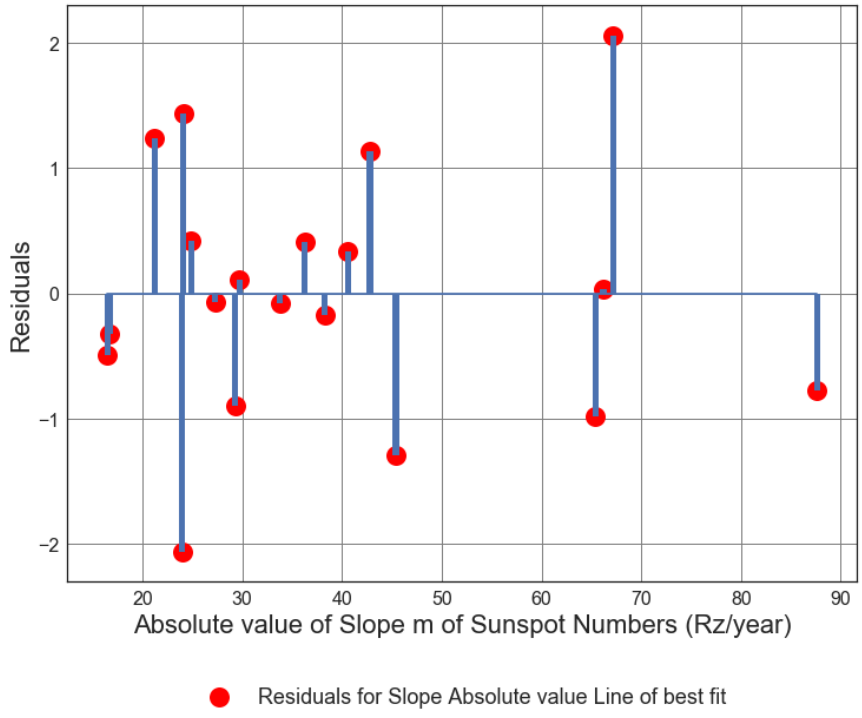

Figure B1.28: Residuals Plot of Absolute Magnitude of the Slope of Solar cycle (from 1900 to 2014) vs. Average number of 7.5M and up Earthquakes. Line of best fit, y = -0.02418x + (4.897), mean x = 38.81 +/- 19.15, mean y = 3.959 +/- 1.086, R = -0.4262, R squared = 0.1817, p-value = 0.0688.

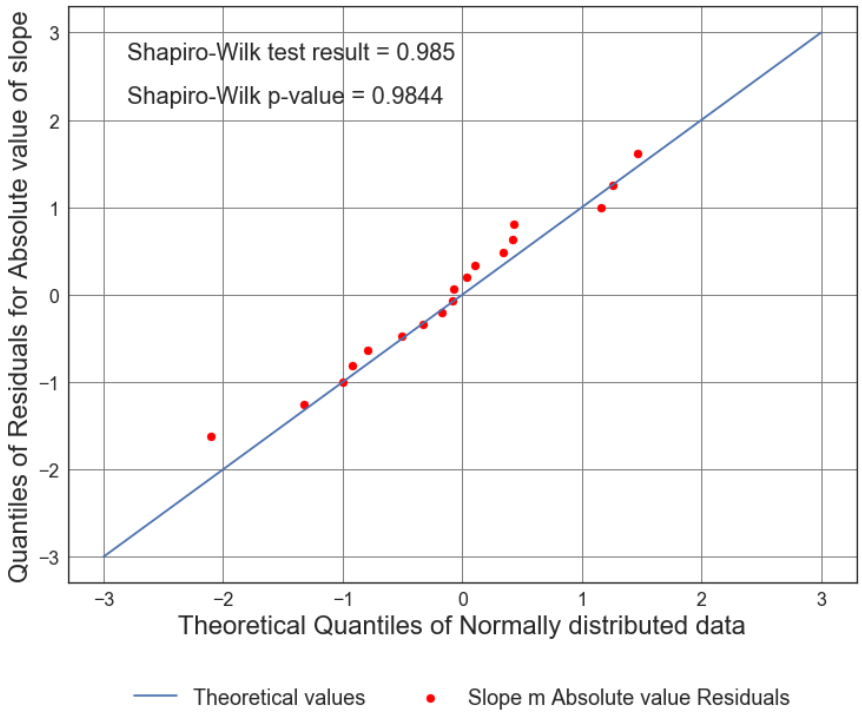

Figure B1.29: Scatter Plot of Absolute Magnitude of the Slope of Solar cycle (from 1900 to 2014) vs. Average number of 7.5M and up Earthquakes. Line of best fit, y = -0.02418x + (4.897), mean x = 38.81 +/- 19.15, mean y = 3.959 +/- 1.086, R = -0.4262, R squared = 0.1817, p-value = 0.0688.

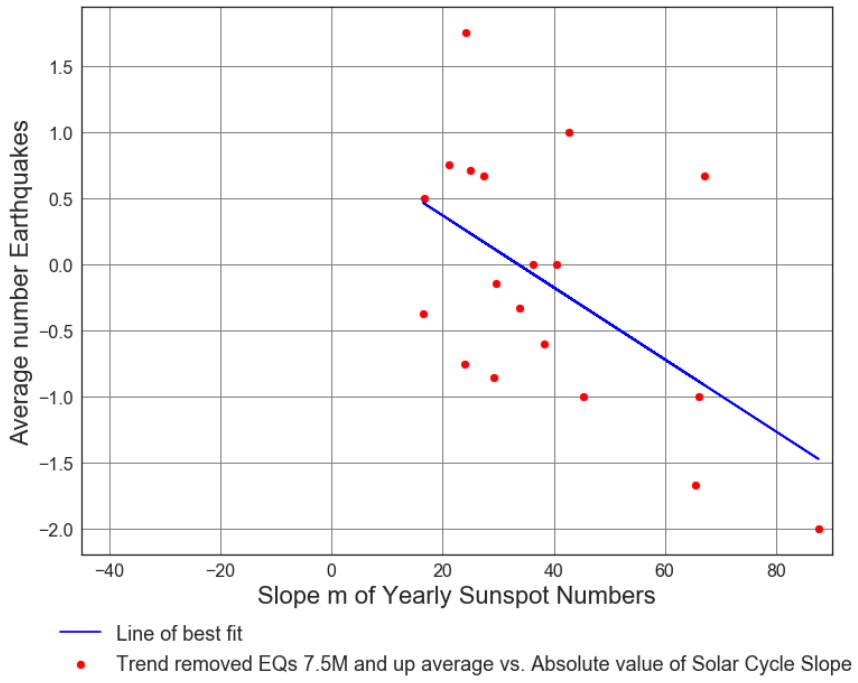

Figure B1.30: Scatter Plot of Absolute Slope Magnitude of the Solar cycle (from 1900 to 2014) vs. Trend removed Average number of 7.5M and up Earthquakes. Line of best fit, y = -0.02722x + (0.9152), mean x = 38.81 +/- 19.15, mean y = -0.1409 +/- 0.9348, R = -0.5576, R squared = 0.3109, p-value = 0.01312.

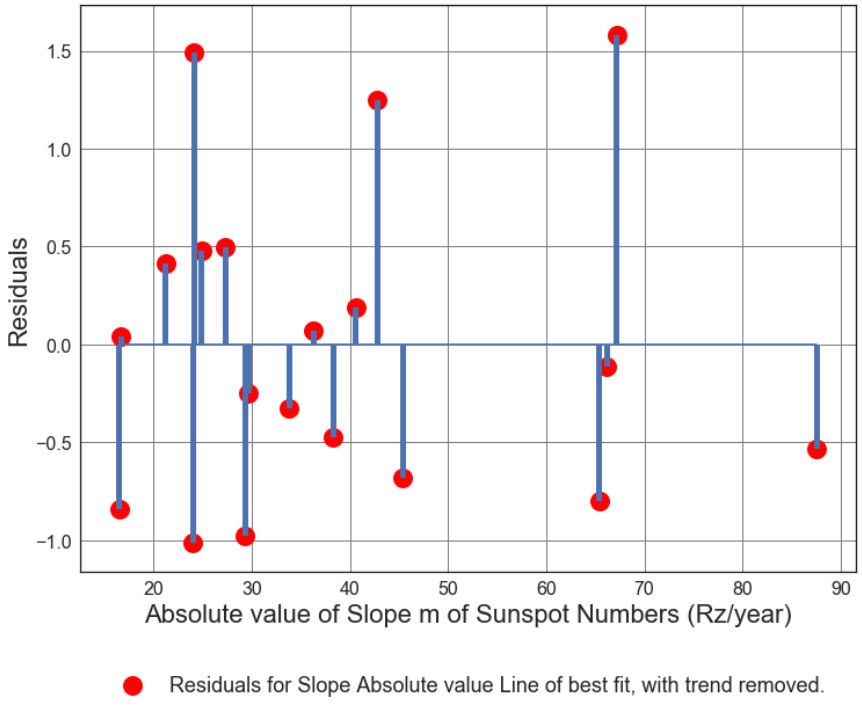

Figure B1.31: Scatter Plot of Absolute Slope Magnitude of the Solar cycle (from 1900 to 2014) vs. Trend removed Average number of 7.5M and up Earthquakes. Line of best fit, y = -0.02722x + (0.9152), mean x = 38.81 +/- 19.15, mean y = -0.1409 +/- 0.9348, R = -0.5576, R squared = 0.3109, p-value = 0.01312.

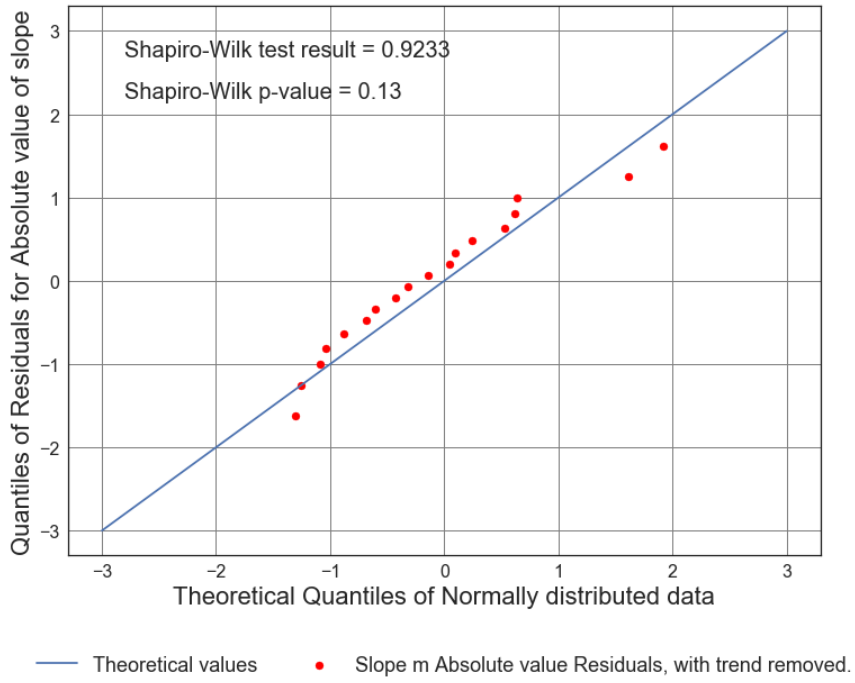

Figure B1.32: Scatter Plot of Absolute Slope Magnitude of the Solar cycle (from 1900 to 2014) vs. Trend removed Average number of 7.5M and up Earthquakes. Line of best fit, y = -0.02722x + (0.9152), mean x = 38.81 +/- 19.15, mean y = -0.1409 +/- 0.9348, R = -0.5576, R squared = 0.3109, p-value = 0.01312.

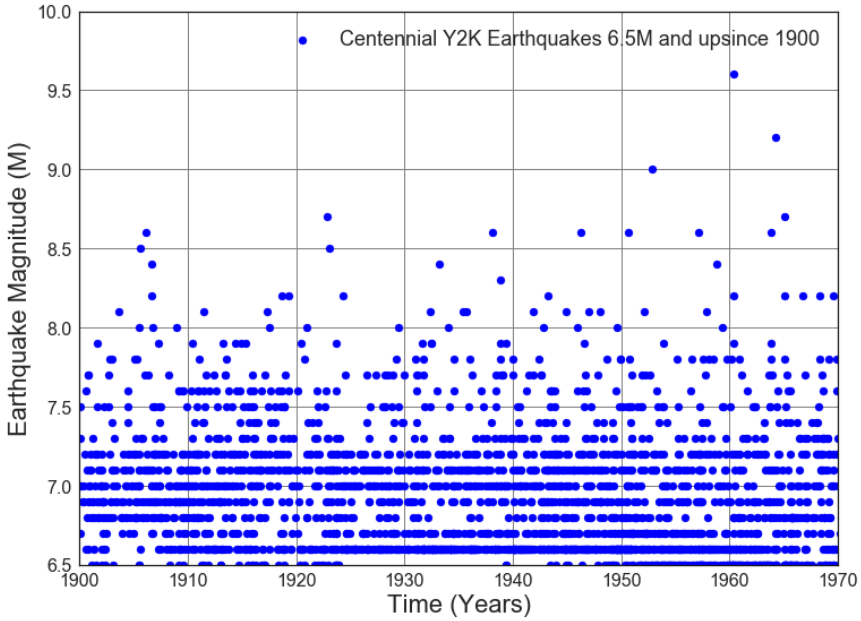

Figure B1.33: Scatter plot of Centennial Y2K earthquakes 6.5M and up magnitudes 1900 to 1970

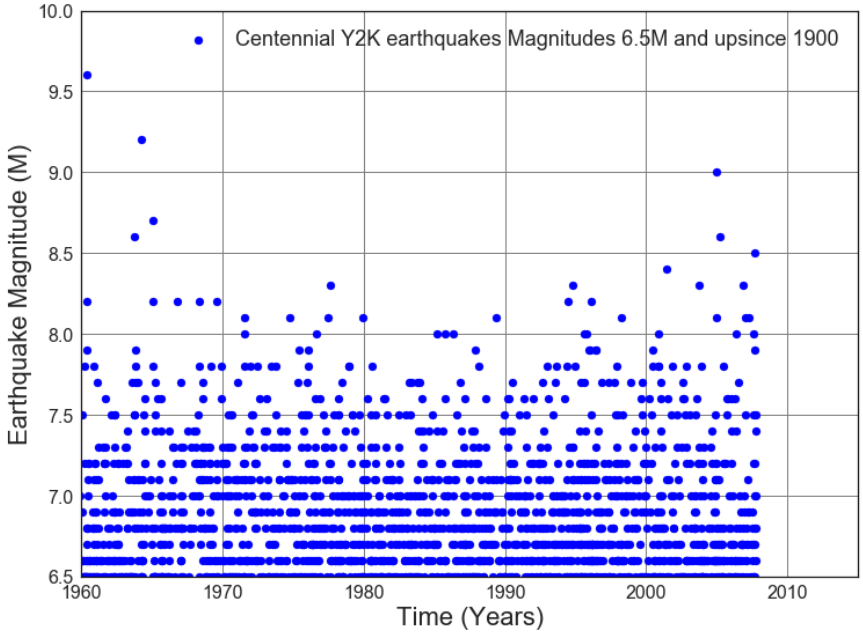

Figure B1.34: Scatter plot of Centennial Y2K Max EQs 6.5M and up Magnitudes 1960 to 2007

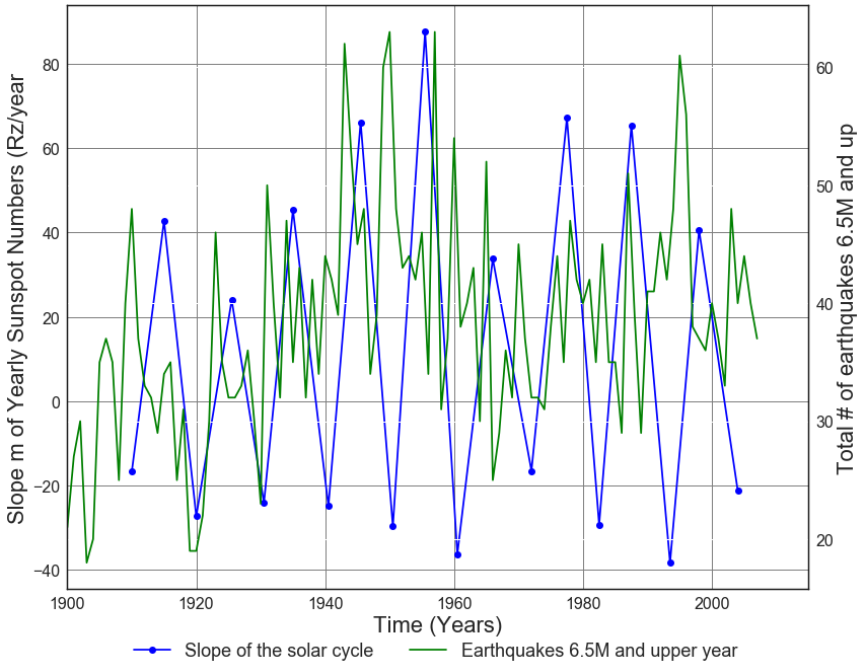

Figure B1.35: Slope of Solar cycle from 1900 to 2014 vs. Average number of 6.5M and up Earthquakes.

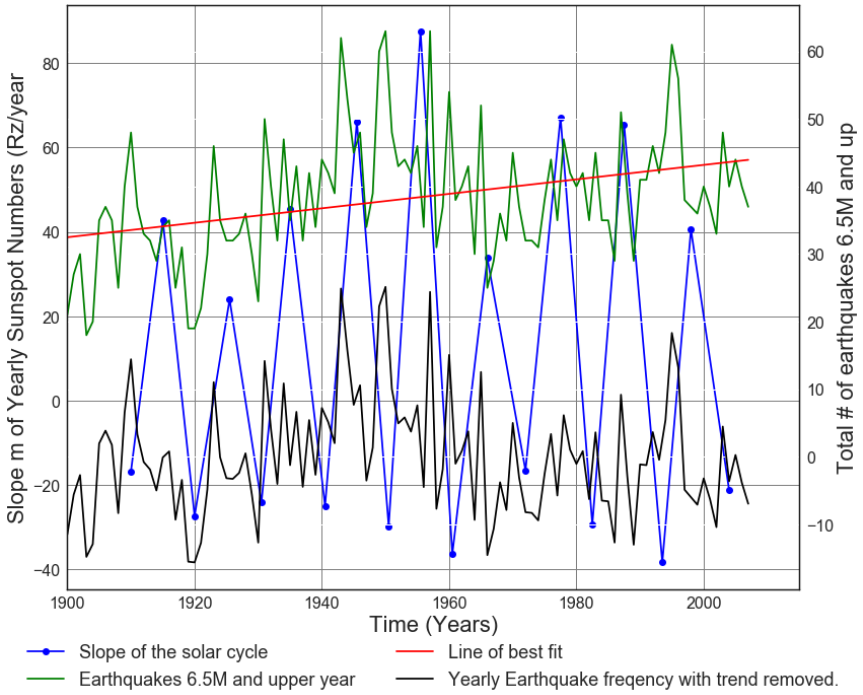

Figure B1.36: Slope of Solar cycle from 1900 to 2014 vs. Average number of 6.5M and up Earthquakes. Line of best fit, y = 0.1071x + (-170.9), mean x = 1.954e+03 +/- 31.18, mean y = 38.22 +/- 9.433

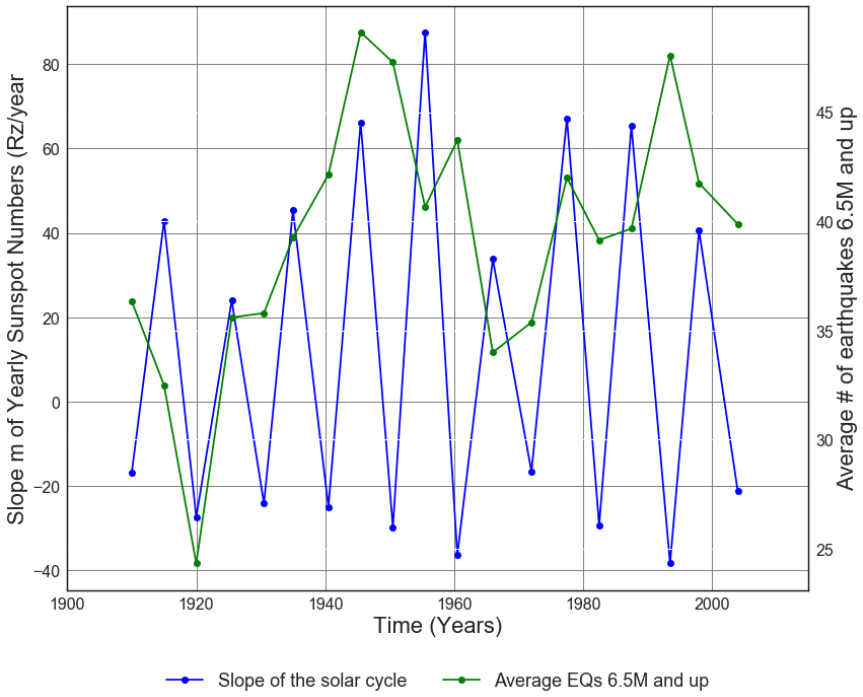

Figure B1.37: Slope of Solar cycle from 1900 to 2014 vs. Average number of 6.5M and up Earthquakes.

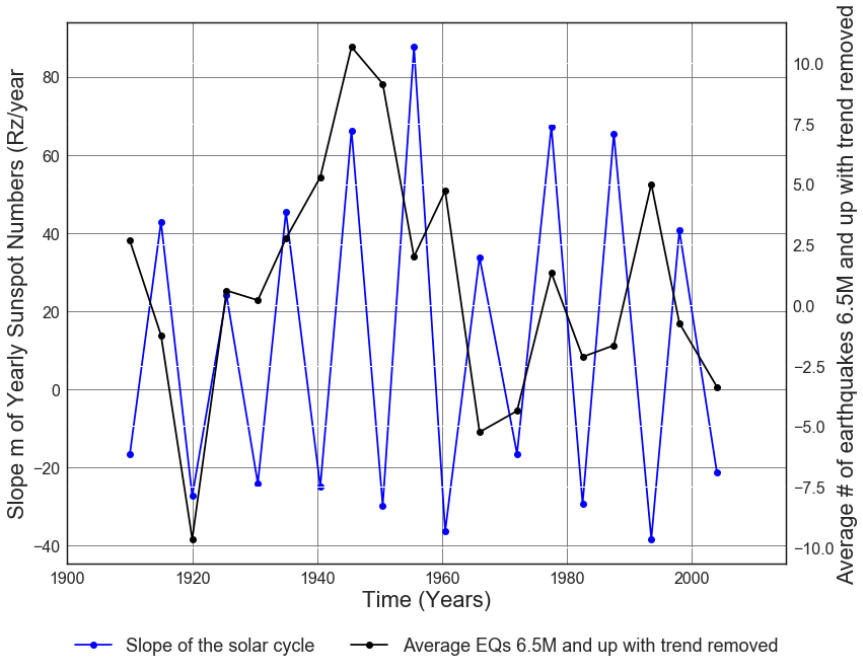

Figure B1.38: Slope of Solar cycle from 1900 to 2014 vs. Average number of 6.5M and up earthquakes.

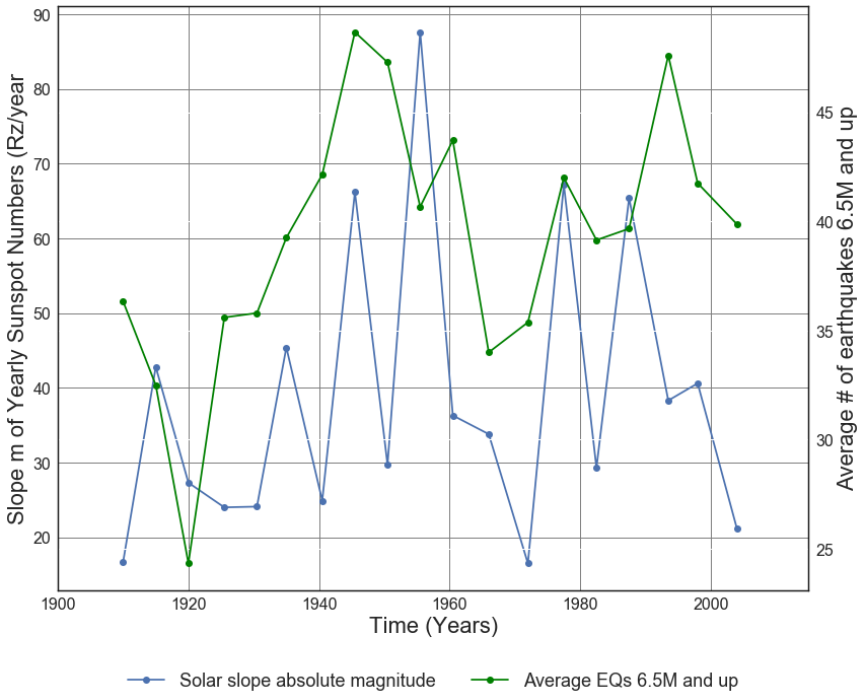

Figure B1.39: Absolute value of Solar cycle slope from 1900 to 2014 vs. Average number of 6.5M and up Earthquakes.

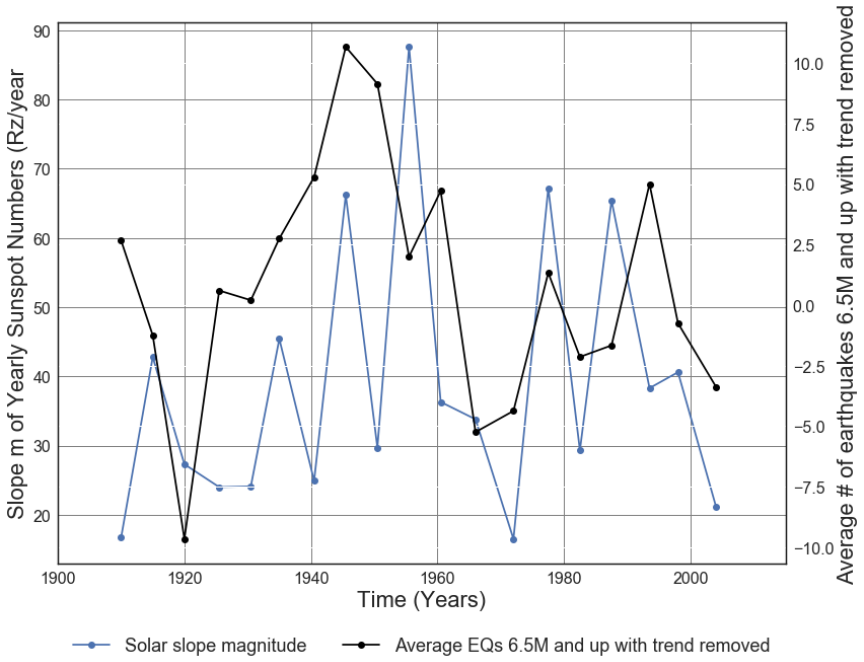

Figure B1.40: Absolute value of solar cycle slope from 1900 to 2014 vs. Average number of 6.5M and up Earthquakes with trend removed.

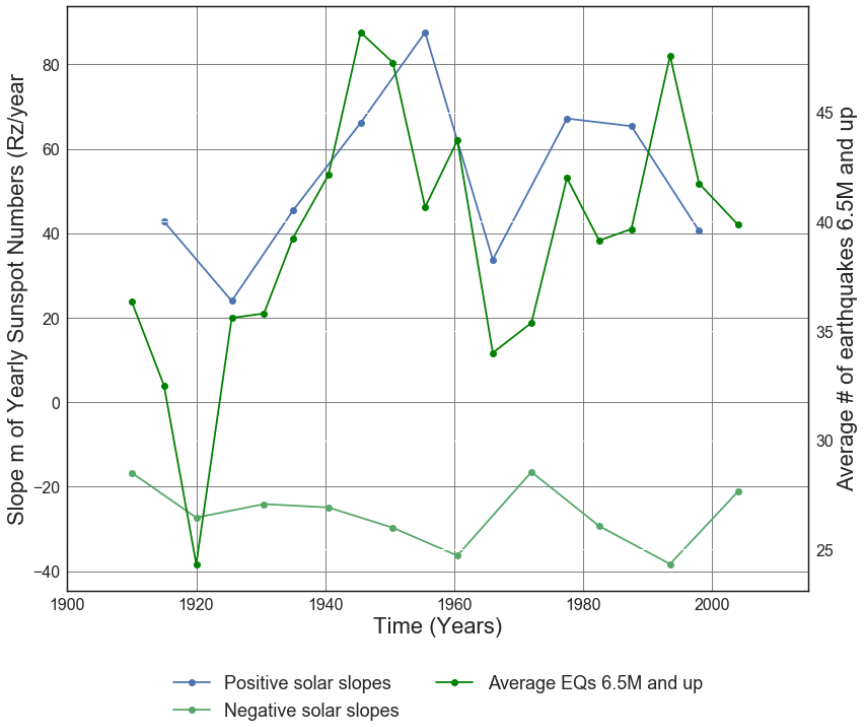

Figure B1.41: Positive and negative solar cycle slopes from 1900 to 2014 vs. Average number of 6.5M and up Earthquakes.

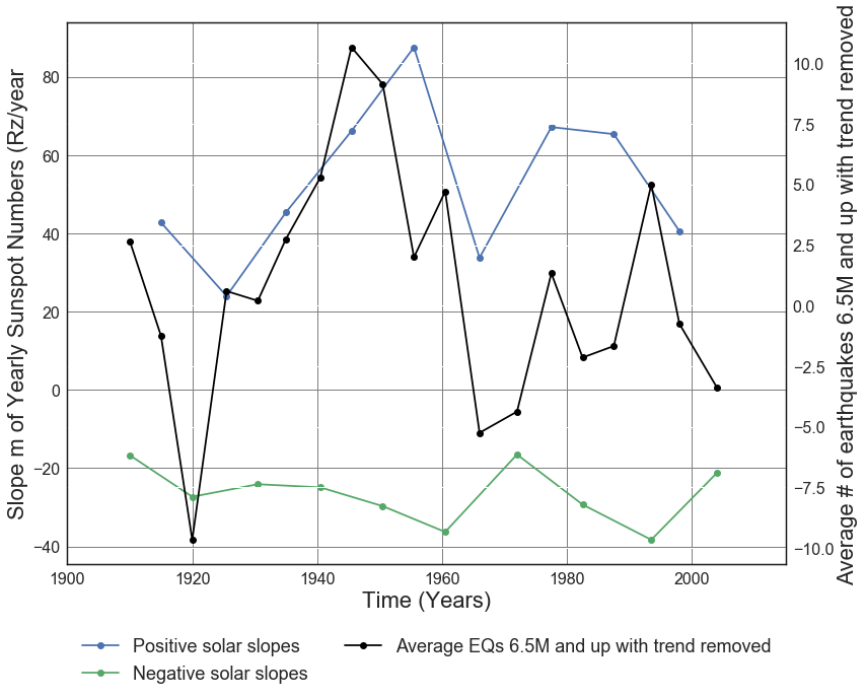

Figure B1.42: Positive and negative solar cycle slopes from 1900 to 2014 vs. Average number of 6.5M and up Earthquakes with trend removed.

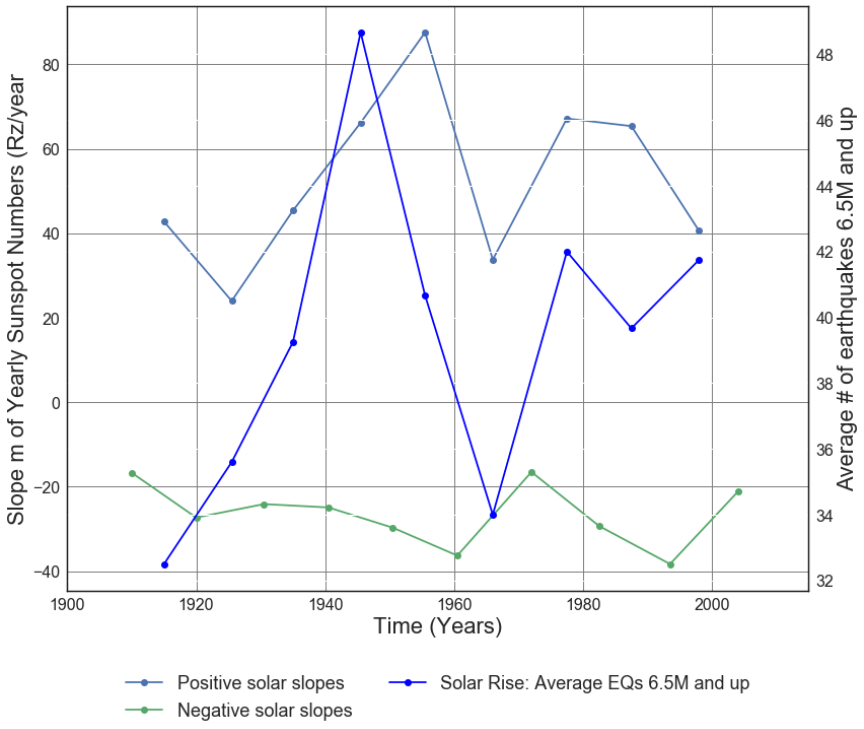

Figure B1.43: Positive and negative solar cycle slopes from 1900 to 2014 vs. Solar Rise: Average number of 6.5M and up Earthquakes.

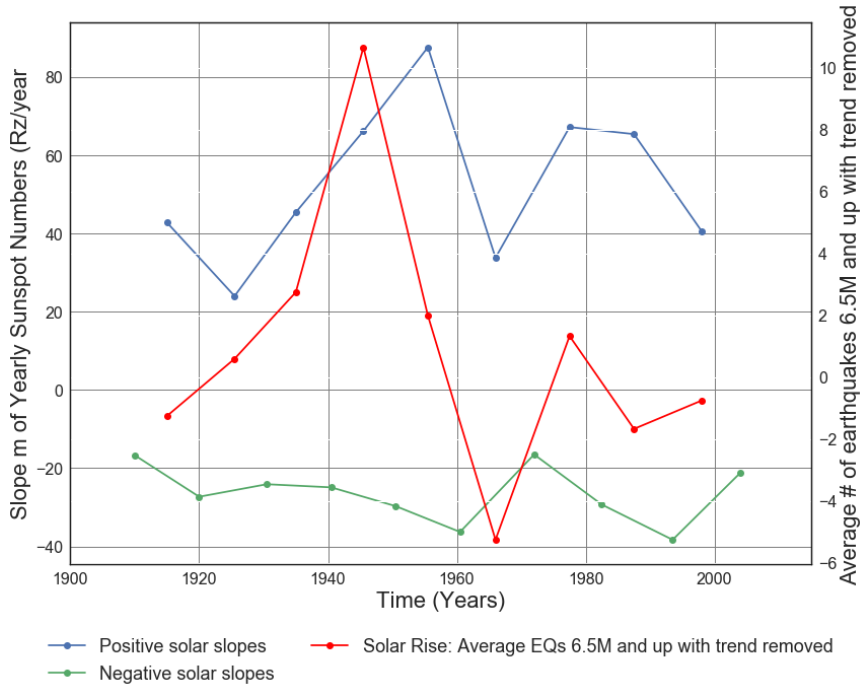

Figure B1.44: Positive and negative solar cycle slopes from 1900 to 2014 vs. Solar Rise: Average number of 6.5M and up Earthquakes with trend removed.

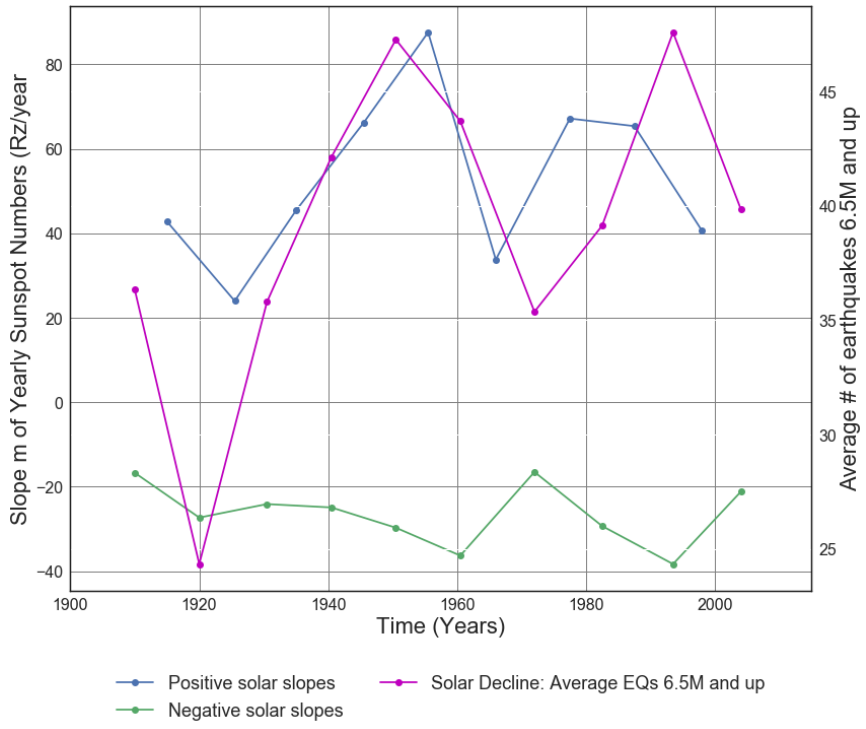

Figure B1.45: Positive and negative solar cycle slopes from 1900 to 2014 vs. Solar Decline: Average number of 6.5M and up Earthquakes.

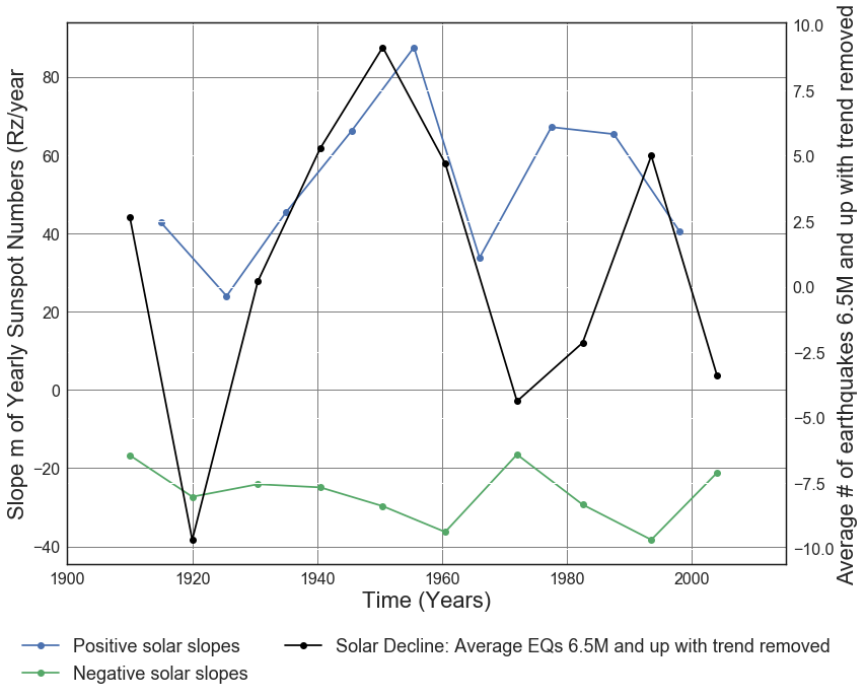

Figure B1.46: Positive and negative solar cycle slopes from 1900 to 2014 vs. Solar Rise: Average number of 6.5M and up Earthquakes.

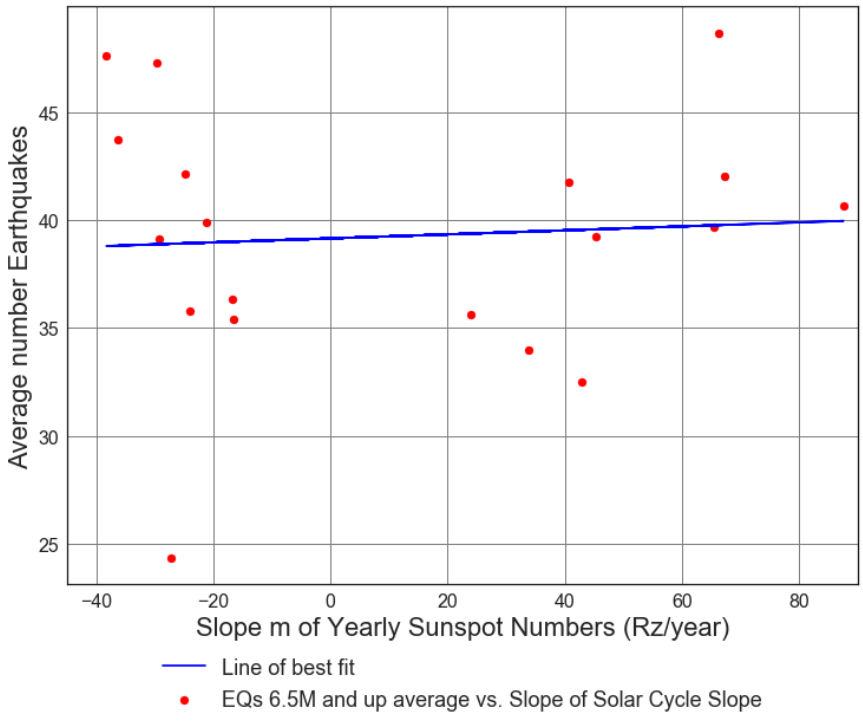

Figure B1.47: Scatter Plot of Slope m of Solar cycle (from 1900 to 2014) vs. Average number of 6.5M and up Earthquakes. Line of best fit, y = 0.009251x + (39.15), mean x = 10.98 +/- 41.86, mean y = 39.25 +/- 5.676, R = 0.06823, R squared = 0.004655, p-value = 0.7814.

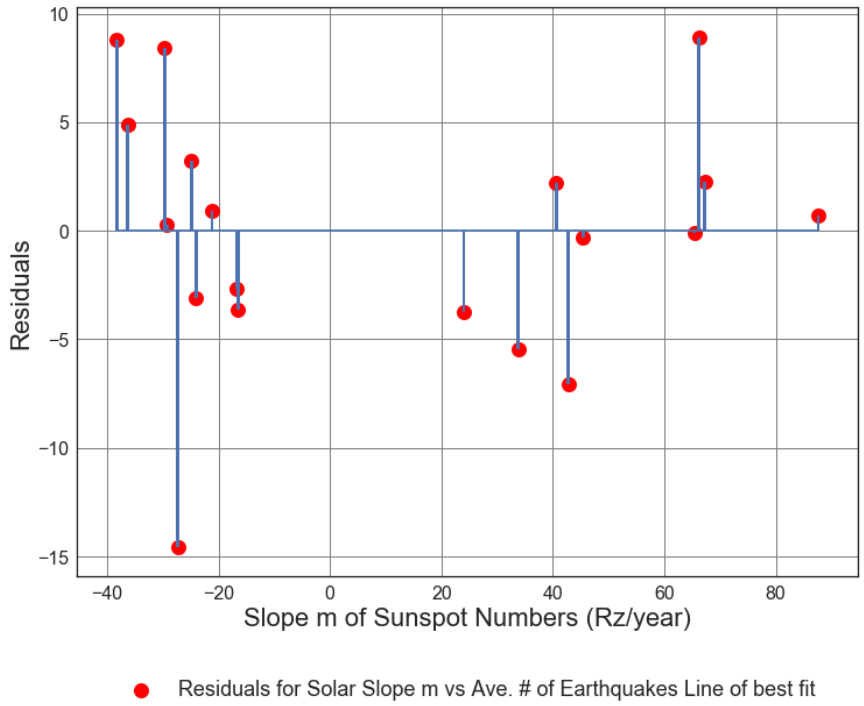

Figure B1.48: Residuals Plot of Average Solar Cycle Slope m (from 1900 to 2014) vs. Average number of 6.5M and up Earthquakes. Line of best fit, y = 0.009251x + (39.15), mean x = 10.98 +/- 41.86, mean y = 39.25 +/- 5.676, R = 0.06823, R squared = 0.004655, p-value = 0.7814.

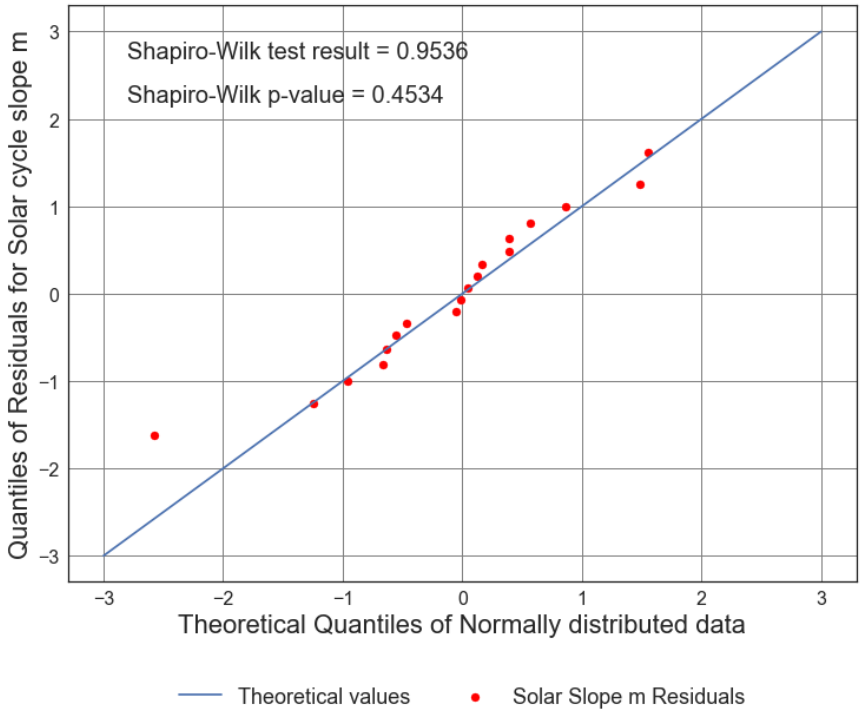

Figure B1.49: Quantile-Quantile Plot of the resisuales of Slope of Solar cycle m (from 1900 to 2014) vs. Average number of 6.5M and up Earthquakes. Line of best fit, y = 0.009251x + (39.15), mean x = 10.98 +/- 41.86, mean y = 39.25 +/- 5.676, R = 0.06823, R squared = 0.004655, p-value = 0.7814.

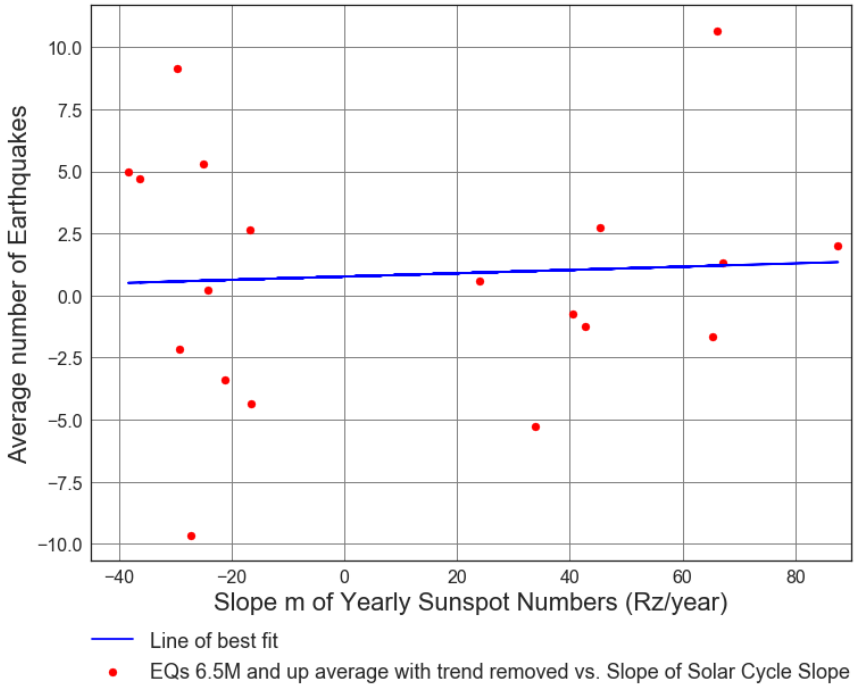

Figure B1.50: Scatter Plot of Slope m of Solar cycle (from 1900 to 2014) vs. Average number of 6.5M and up Earthquakes with trend removed. Line of best fit, y = 0.006627x + (0.7632), mean x = 10.98 +/- 41.86, mean y = 0.836 +/- 4.818, R = 0.05757, R squared = 0.003314, p-value = 0.8149.

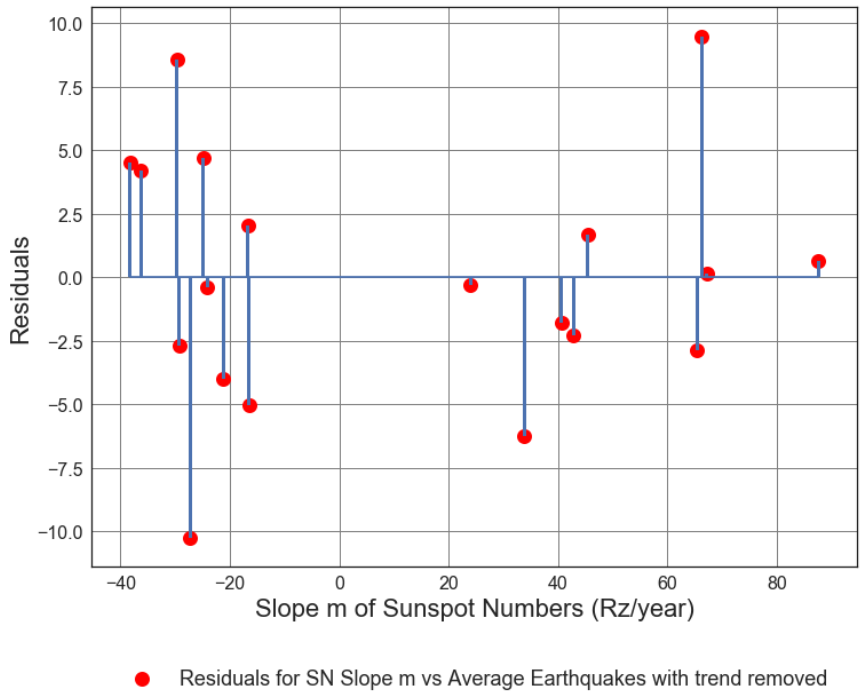

Figure B1.51: Residuals Plot of the Slope of Solar cycle (from 1900 to 2014) vs. Average number of 6.5M and up Earthquakes with trend removed. Line of best fit, y = 0.006627x + (0.7632), mean x = 10.98 +/- 41.86, mean y = 0.836 +/- 4.818, R = 0.05757, R squared = 0.003314, p-value = 0.8149.

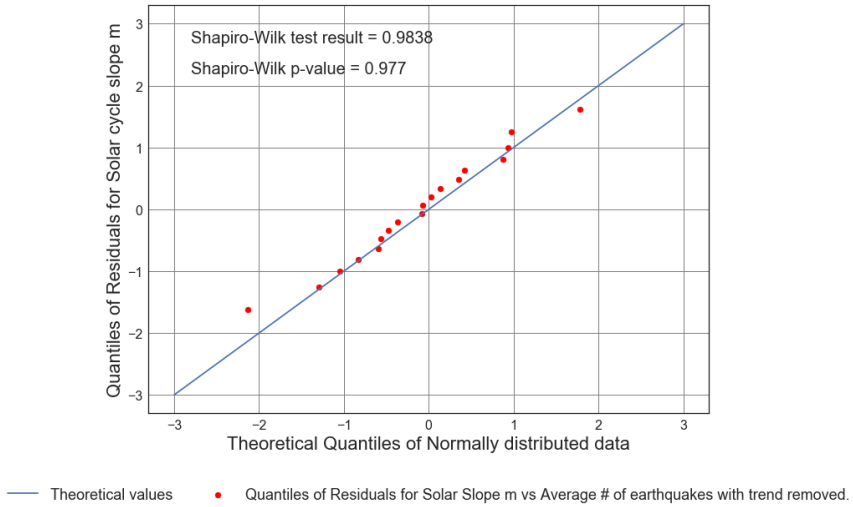

Figure B1.52: Scatter Plot of Absolute Magnitude of the Slope of Solar cycle (from 1900 to 2014) vs. Average number of 6.5M and up Earthquakes. Line of best fit, y = 0.006627x + (0.7632), mean x = 10.98 +/- 41.86, mean y = 0.836 +/- 4.818, R = 0.05757, R squared = 0.003314, p-value = 0.8149.

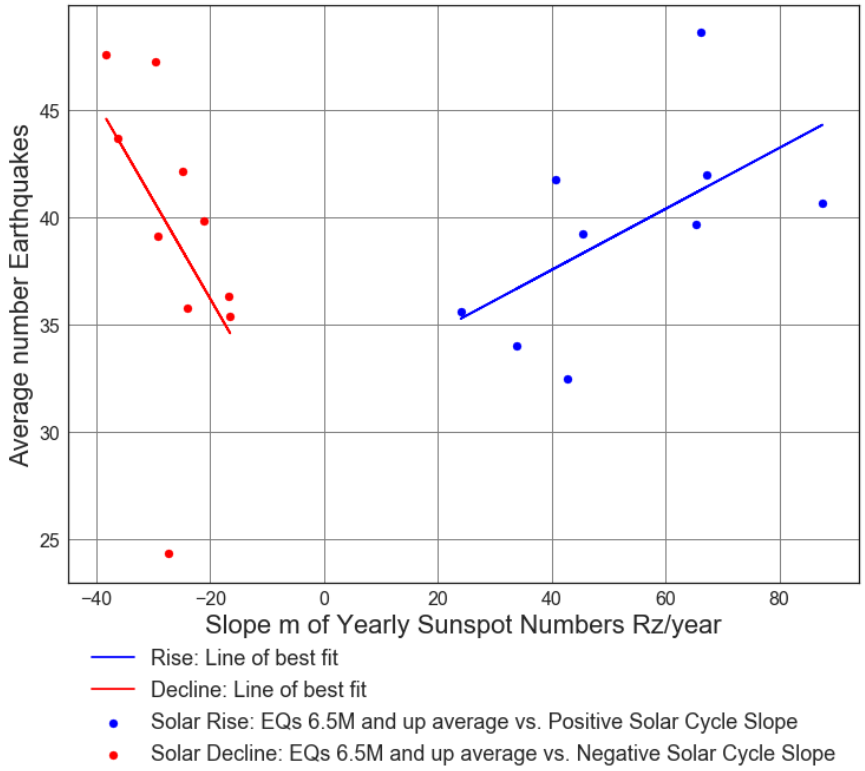

Figure B1.53: Scatter Plot of Slope of Solar cycle (from 1900 to 2014) vs. Average number of 6.5M and up Earthquakes. Rise: Line of best fit, y = 0.1423x + (31.87), mean x = 52.56 +/- 19.0, mean y = 39.34 +/- 4.607, R = 0.6674, R squared = 0.4454, p-value = 0.03501. Decline: Line of best fit, y = -0.4592x + 27.02, mean x = -26.43 +/- 6.974, mean y = 39.16 +/- 6.487, R = -0.4937, R squared = 0.2437, p-value = 0.147.

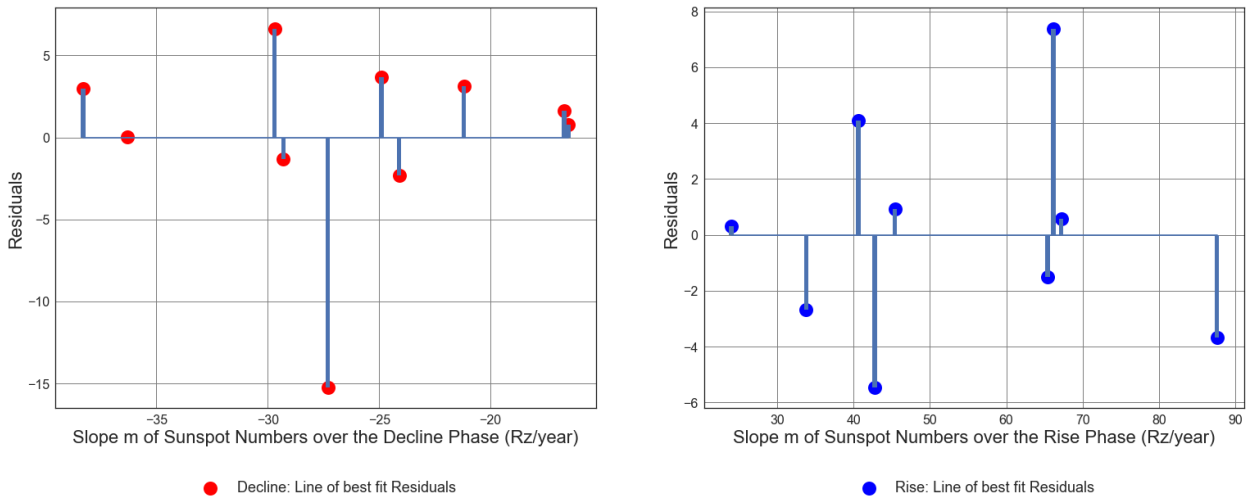

Figure B1.54: Residuals centered about zero, plot of Slope of Solar cycle (from 1900 to 2014) vs. Average number of 6.5M and up Earthquakes. Rise: Line of best fit, y = 0.1423x + (31.87), mean x = 52.56 +/- 19.0, mean y = 39.34 +/- 4.607, R = 0.6674, R squared = 0.4454, p-value = 0.03501. Decline: Line of best fit, y = -0.4592x + 27.02, mean x = -26.43 +/- 6.974, mean y = 39.16 +/- 6.487, R = -0.4937, R squared = 0.2437, p-value = 0.147.

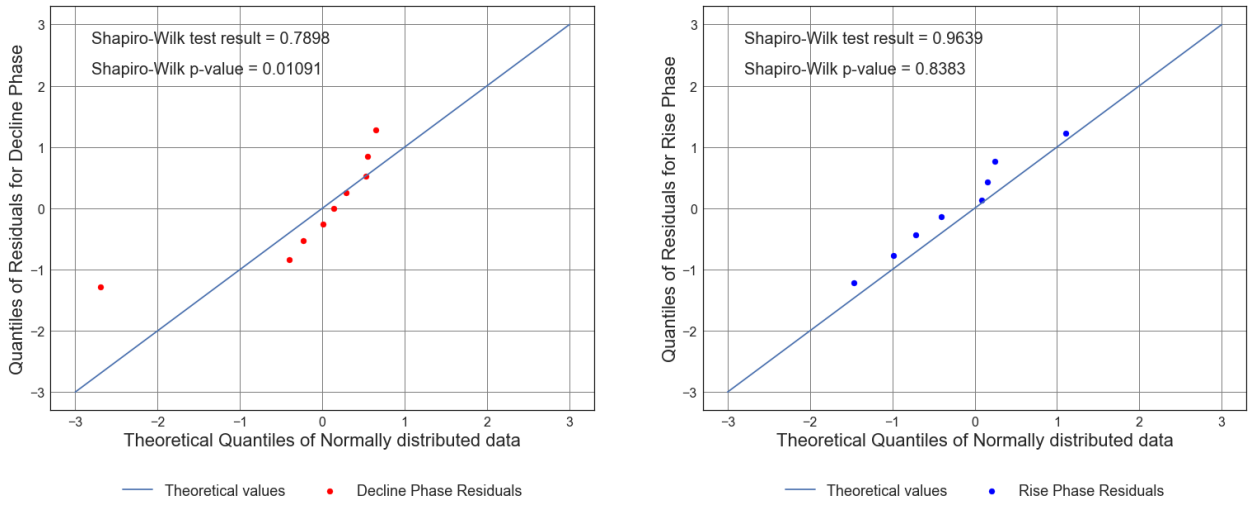

Figure B1.55: Quartile-Quartile Plot of Residuals for the Rise and Decline phase Slope of Solar cycle (from 1900 to 2014) vs. Average number of 6.5M and up Earthquakes. Rise: Line of best fit, y = 0.1423x + (31.87), mean x = 52.56 +/- 19.0, mean y = 39.34 +/- 4.607, R = 0.6674, R squared = 0.4454, p-value = 0.03501. Decline: Line of best fit, y = -0.4592x + 27.02, mean x = -26.43 +/- 6.974, mean y = 39.16 +/- 6.487, R = -0.4937, R squared = 0.2437, p-value = 0.147.

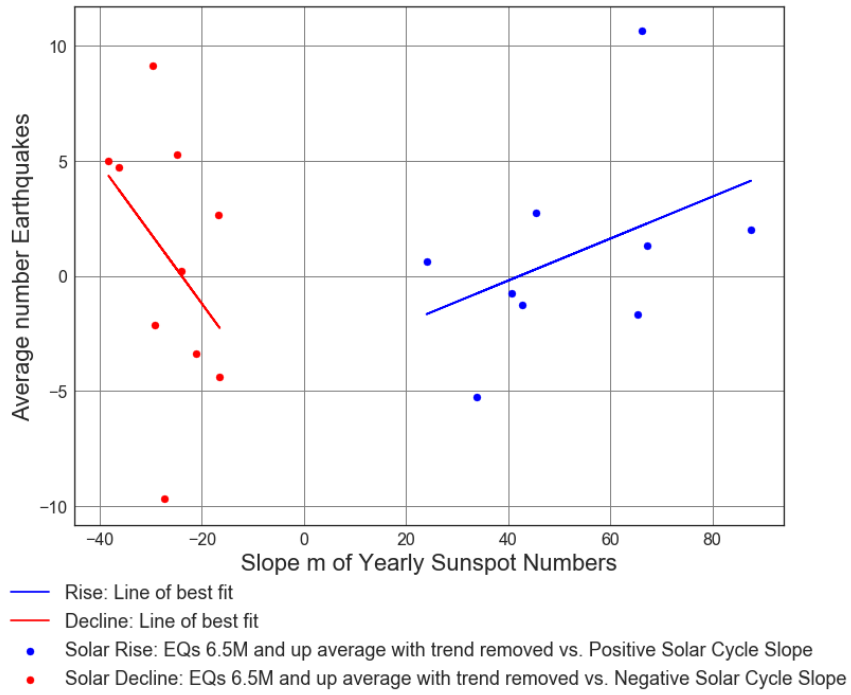

Figure B1.56: Scatter Plot of Slope of Solar cycle (from 1900 to 2014) vs. with trend removed Average number of 6.5M and up Earthquakes. Rise: Line of best fit, y = 0.09124x + (-3.858), mean x = 52.56 +/- 19.0, mean y = 0.937 +/- 4.11, R = 0.4219, R squared = 0.178, p-value = 0.258. Decline: Line of best fit, y = -0.3039x + -7.287, mean x = -26.43 +/- 6.974, mean y = 0.745 +/- 5.375, R = -0.3943, R squared = 0.1555, p-value = 0.2595.

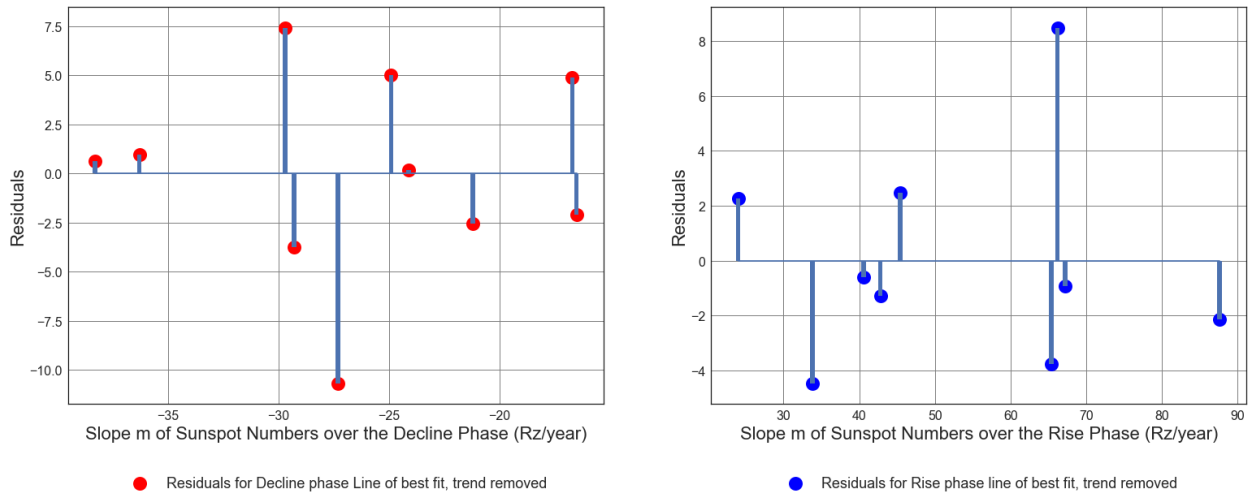

Figure B1.57: Residuals centered about zero, plot of Slope of Solar cycle (from 1900 to 2014) vs. Average number of 6.5M and up Earthquakes with trend removed. Rise: Line of best fit, y = 0.09124x + (-3.858), mean x = 52.56 +/- 19.0, mean y = 0.937 +/- 4.11, R = 0.4219, R squared = 0.178, p-value = 0.258. Decline: Line of best fit, y = -0.3039x + -7.287, mean x = -26.43 +/- 6.974, mean y = 0.745 +/- 5.375, R = -0.3943, R squared = 0.1555, p-value = 0.2595.

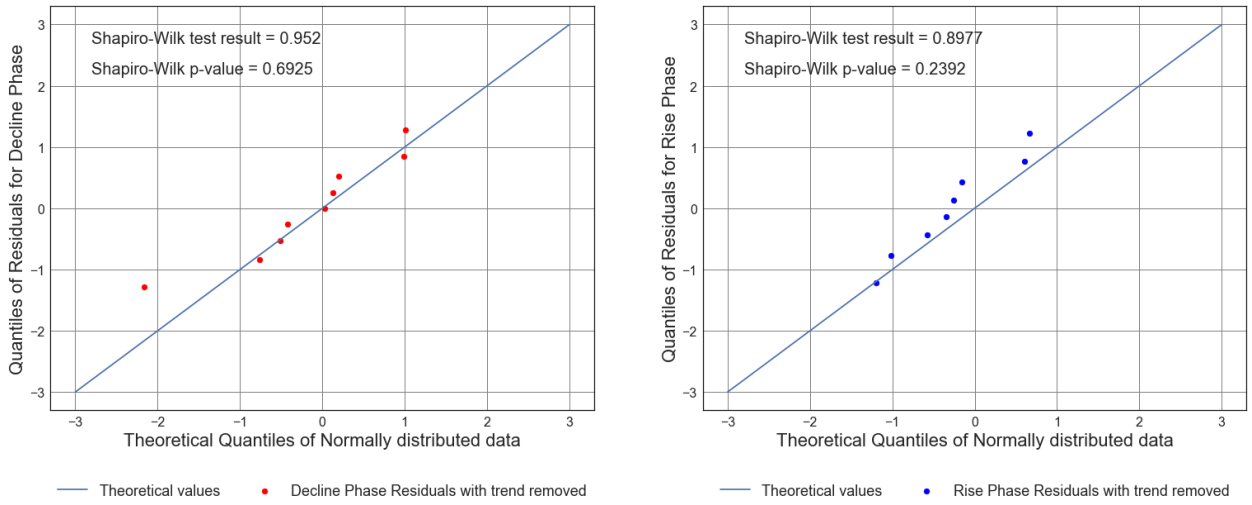

Figure B1.58: Quartile-Quartile Plot of Residuals for the Rise and Decline phase Slope of Solar cycle (from 1900 to 2014) vs. Average number of 6.5M and up Earthquakes with trend removed. Rise: Line of best fit, y = 0.09124x + (-3.858), mean x = 52.56 +/- 19.0, mean y = 0.937 +/- 4.11, R = 0.4219, R squared = 0.178, p-value = 0.258. Decline: Line of best fit, y = -0.3039x + -7.287, mean x = -26.43 +/- 6.974, mean y = 0.745 +/- 5.375, R = -0.3943, R squared = 0.1555, p-value = 0.2595.

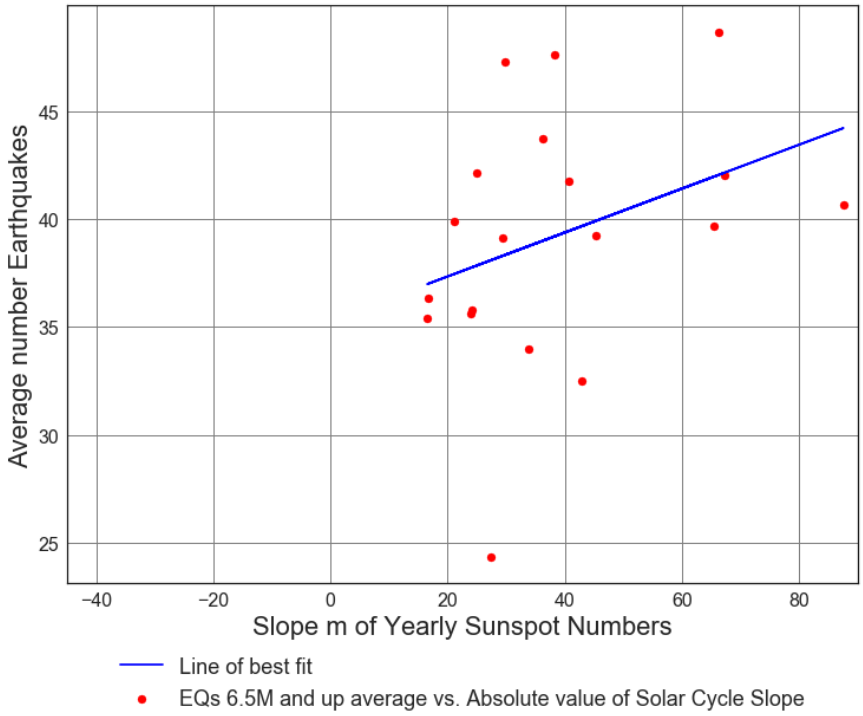

Figure B1.59: Scatter Plot of Absolute Magnitude of the Slope of Solar cycle (from 1900 to 2014) vs. Average number of 6.5M and up Earthquakes. Line of best fit, y = 0.1017x + (35.3), mean x = 38.81 +/- 19.15, mean y = 39.25 +/- 5.676, R = 0.3431, R squared = 0.1177, p-value = 0.1504.

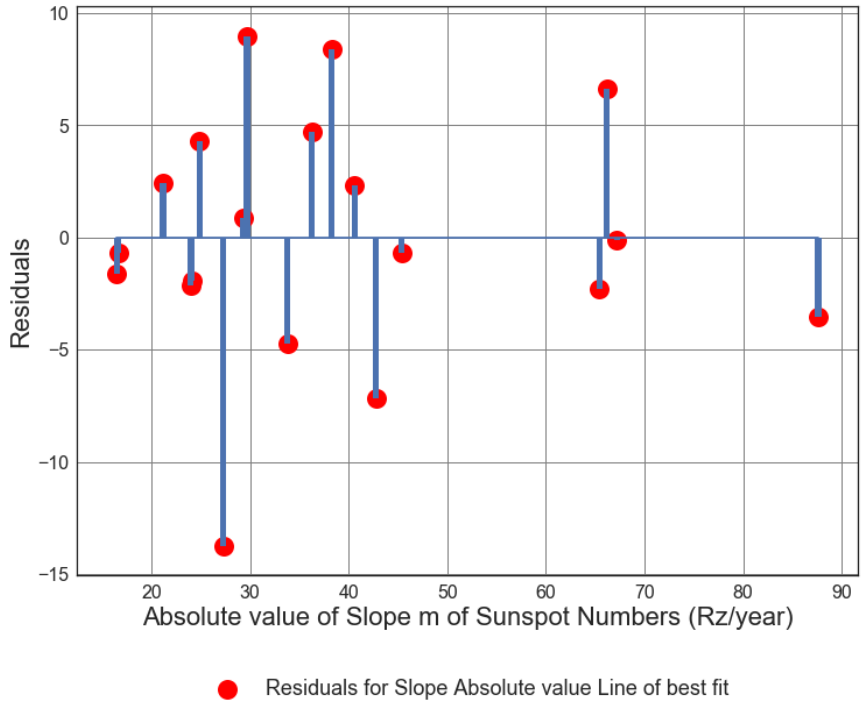

Figure B1.60: Residuals Plot of Absolute Magnitude of the Slope of Solar cycle (from 1900 to 2014) vs. Average number of 6.5M and up Earthquakes. Line of best fit, y = 0.1017x + (35.3), mean x = 38.81 +/- 19.15, mean y = 39.25 +/- 5.676, R = 0.3431, R squared = 0.1177, p-value = 0.1504.

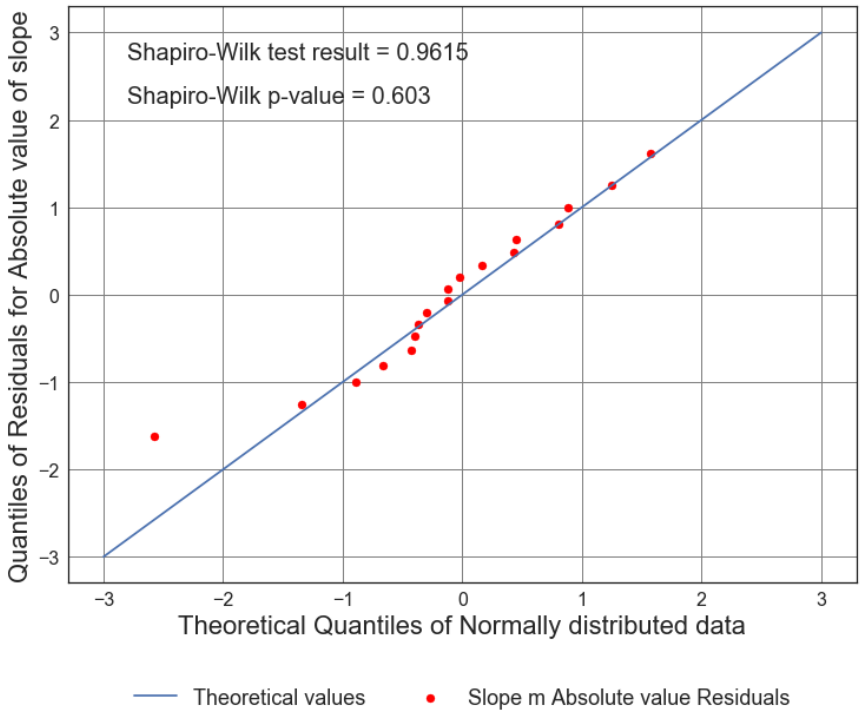

Figure B1.61: Scatter Plot of Absolute Magnitude of the Slope of Solar cycle (from 1900 to 2014) vs. Average number of 6.5M and up Earthquakes. Line of best fit, y = 0.1017x + (35.3), mean x = 38.81 +/- 19.15, mean y = 39.25 +/- 5.676, R = 0.3431, R squared = 0.1177, p-value = 0.1504.

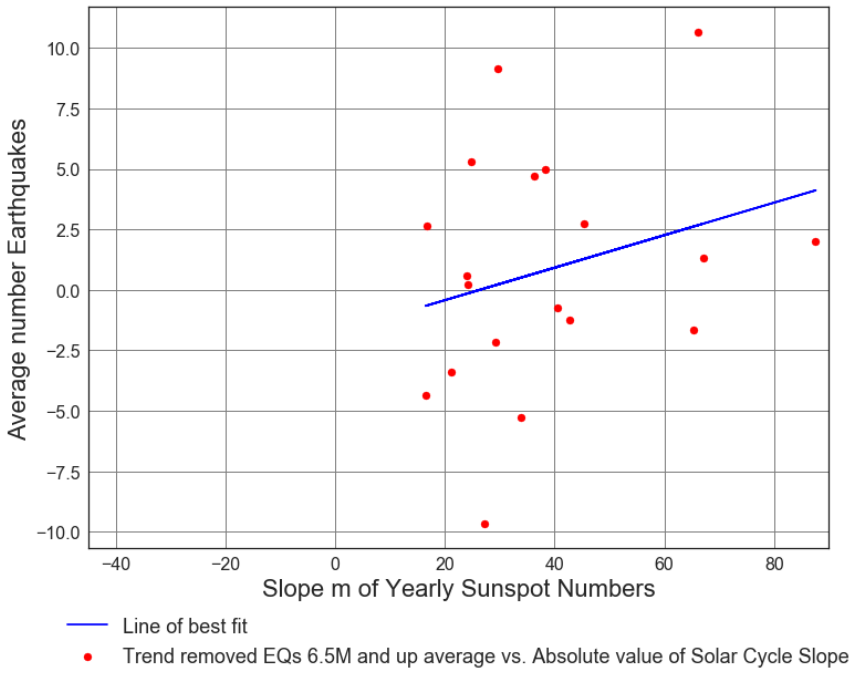

Figure B1.62: Scatter Plot of Absolute Slope Magnitude of the Solar cycle (from 1900 to 2014) vs. Trend removed Average number of 6.5M and up Earthquakes. Line of best fit, y = 0.06717x + (-1.771), mean x = 38.81 +/- 19.15, mean y = 0.836 +/- 4.818, R = 0.267, R squared = 0.07128, p-value = 0.2692.

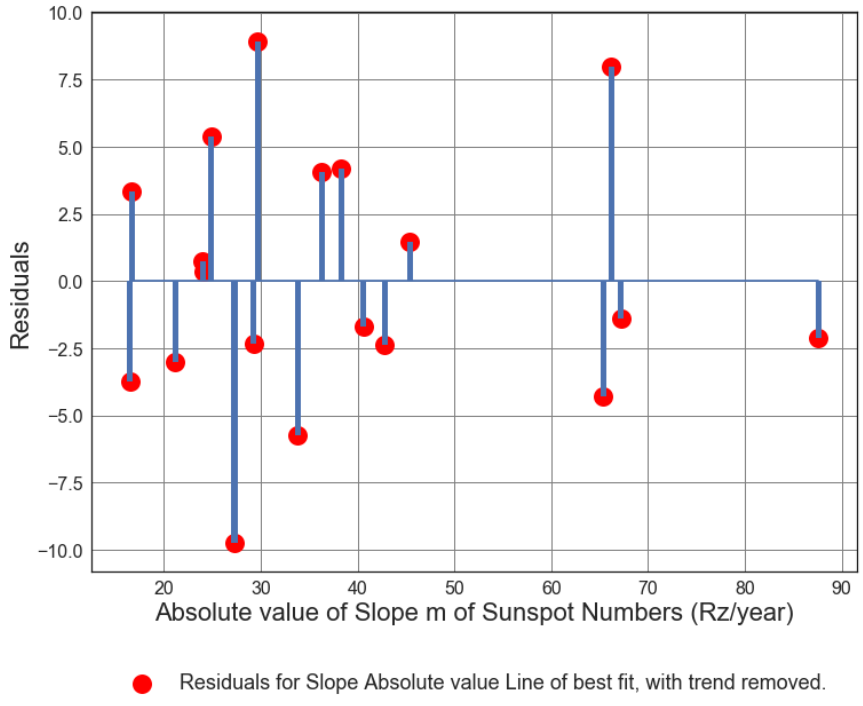

Figure B1.63: Scatter Plot of Absolute Slope Magnitude of the Solar cycle (from 1900 to 2014) vs. Trend removed Average number of 6.5M and up Earthquakes. Line of best fit, y = 0.06717x + (-1.771), mean x = 38.81 +/- 19.15, mean y = 0.836 +/- 4.818, R = 0.267, R squared = 0.07128, p-value = 0.2692.

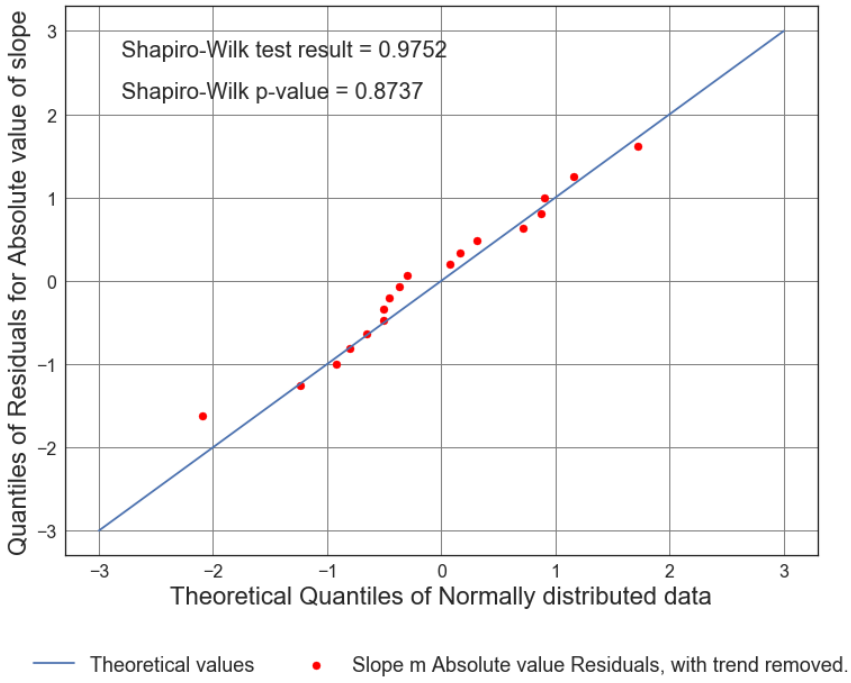

Figure B1.64: Scatter Plot of Absolute Slope Magnitude of the Solar cycle (from 1900 to 2014) vs. Trend removed Average number of 6.5M and up Earthquakes. Line of best fit, y = 0.06717x + (-1.771), mean x = 38.81 +/- 19.15, mean y = 0.836 +/- 4.818, R = 0.267, R squared = 0.07128, p-value = 0.2692.

Appendix B2: USGS Centennial Time Series Analysis Part 2 - Six Month Averaged Earthquake and Sunspot Data.

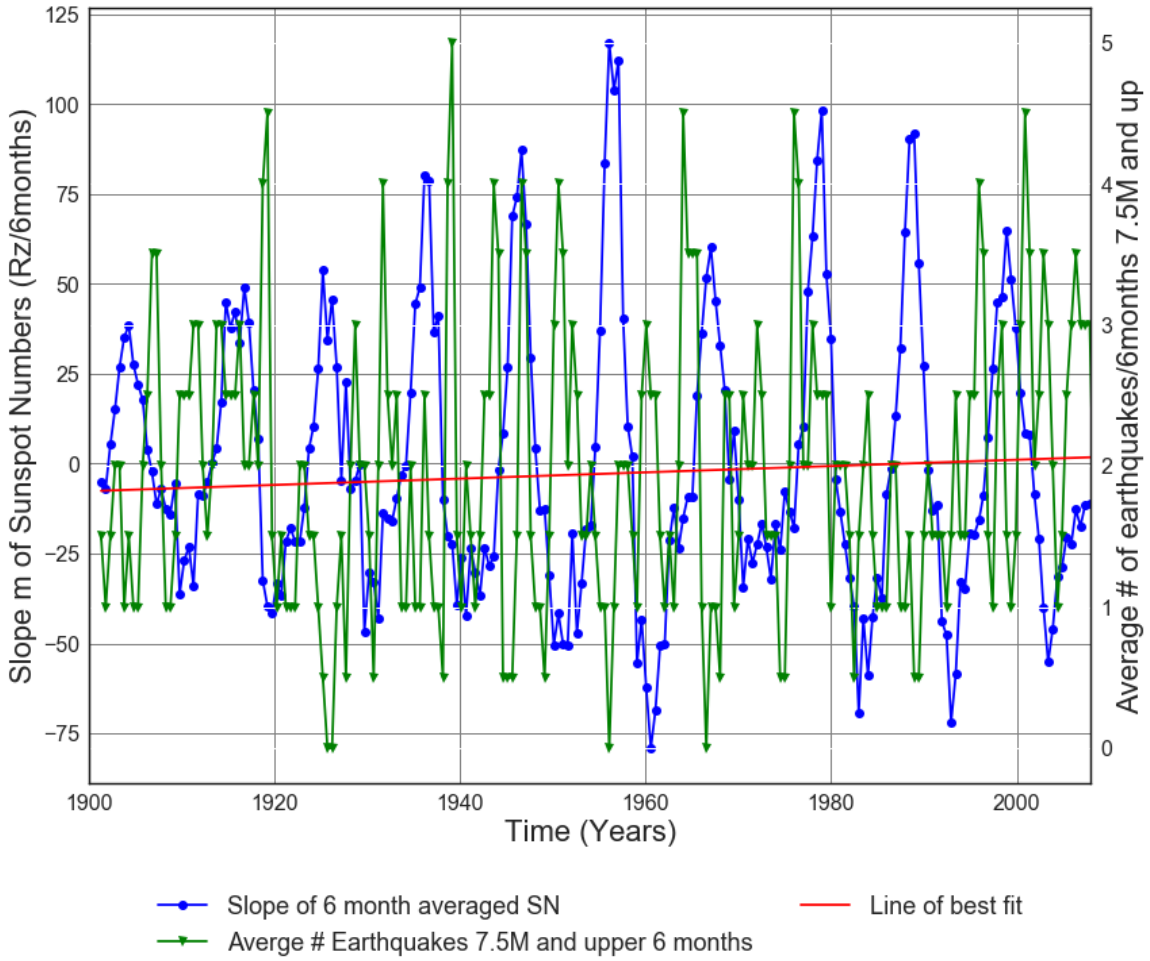

Figure B2.1: Slope of Solar cycle from 1900 to 2007 vs. Average number of 7.5M and up Earthquakes.

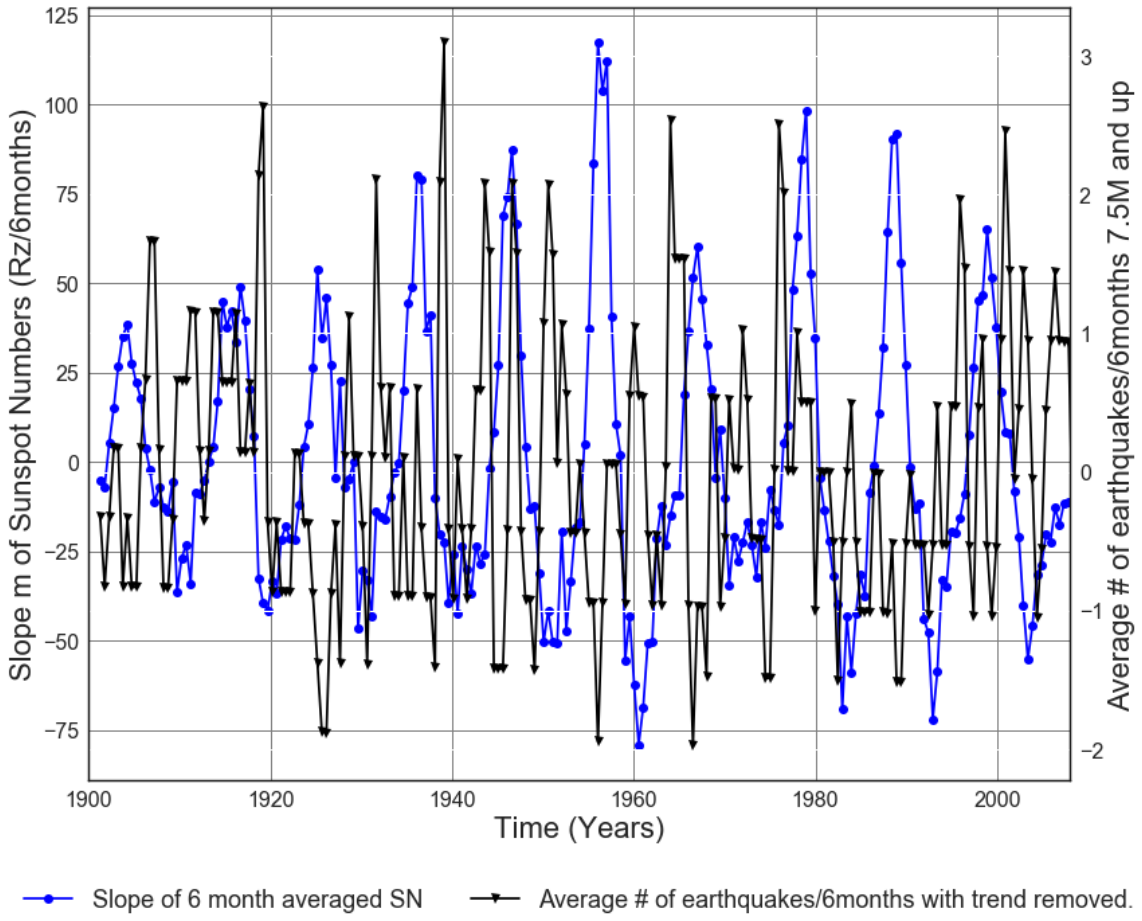

Figure B2.2: Slope of 6 month averaged SN 1900 to 2007 vs. Average number of 7.5M and up Earthquakes with trend removed. Line of best fit, y = 0.002226x + (-2.409), mean x = 1.955e+03 +/- 31.21, mean y = 1.942 +/- 1.004

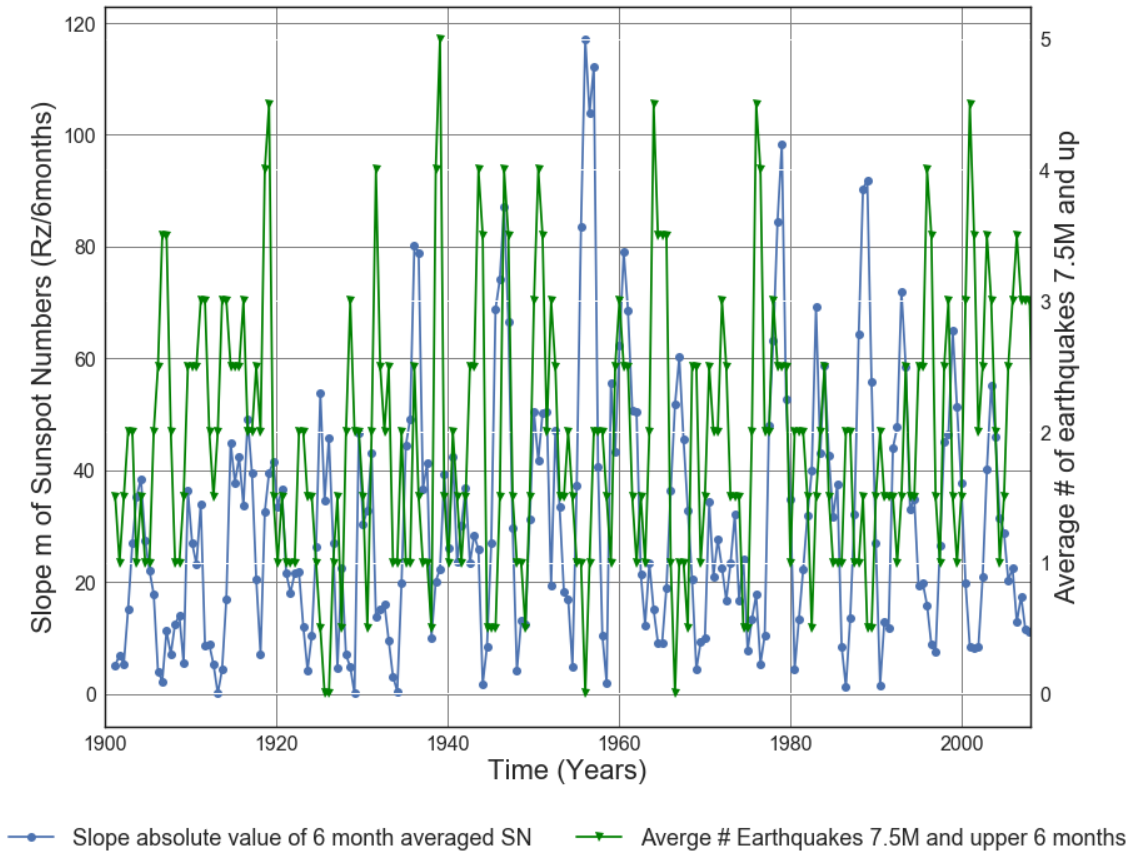

Figure B2.3: Slope Absolute value of Solar cycle from 1900 to 2007 vs. Average number of 7.5M and up Earthquakes.

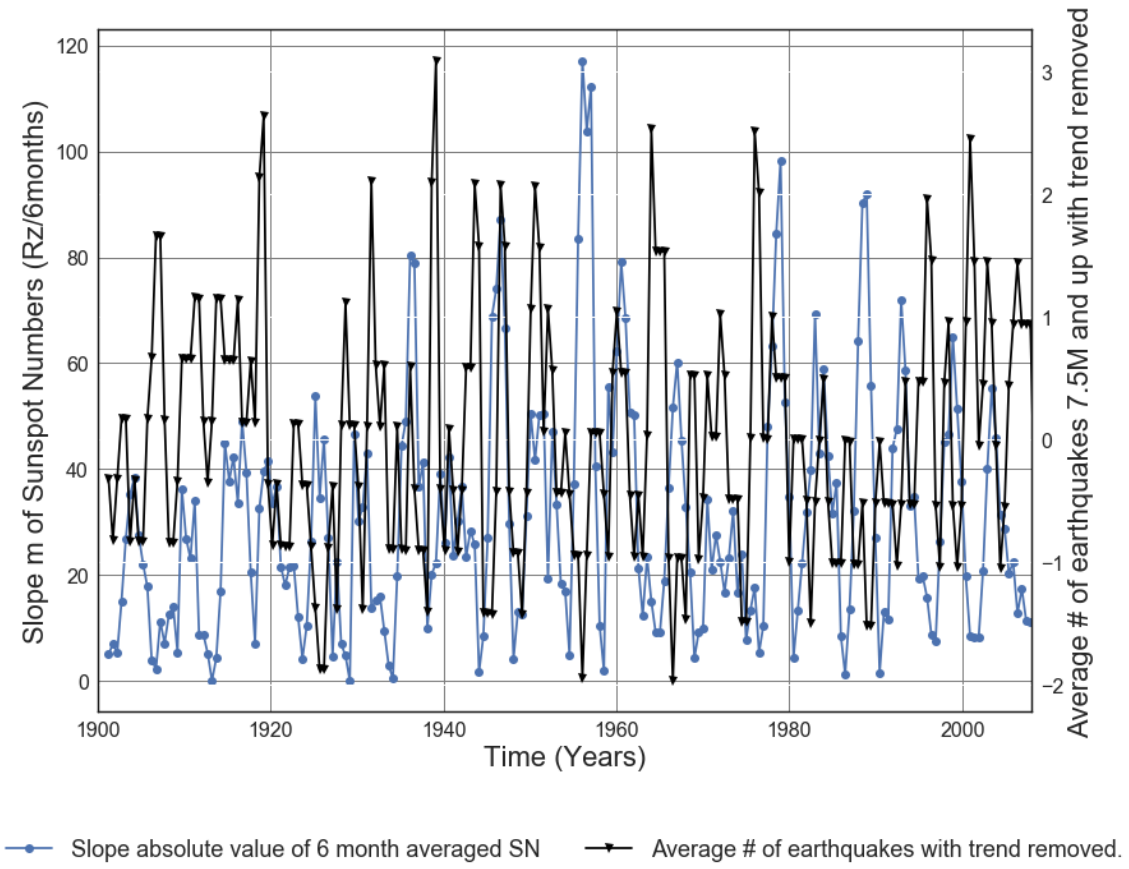

Figure B2.4: Slope Absolute value of Solar cycle from 1900 to 2007 vs. Average number of 7.5M and up earthquakes with trend removed.

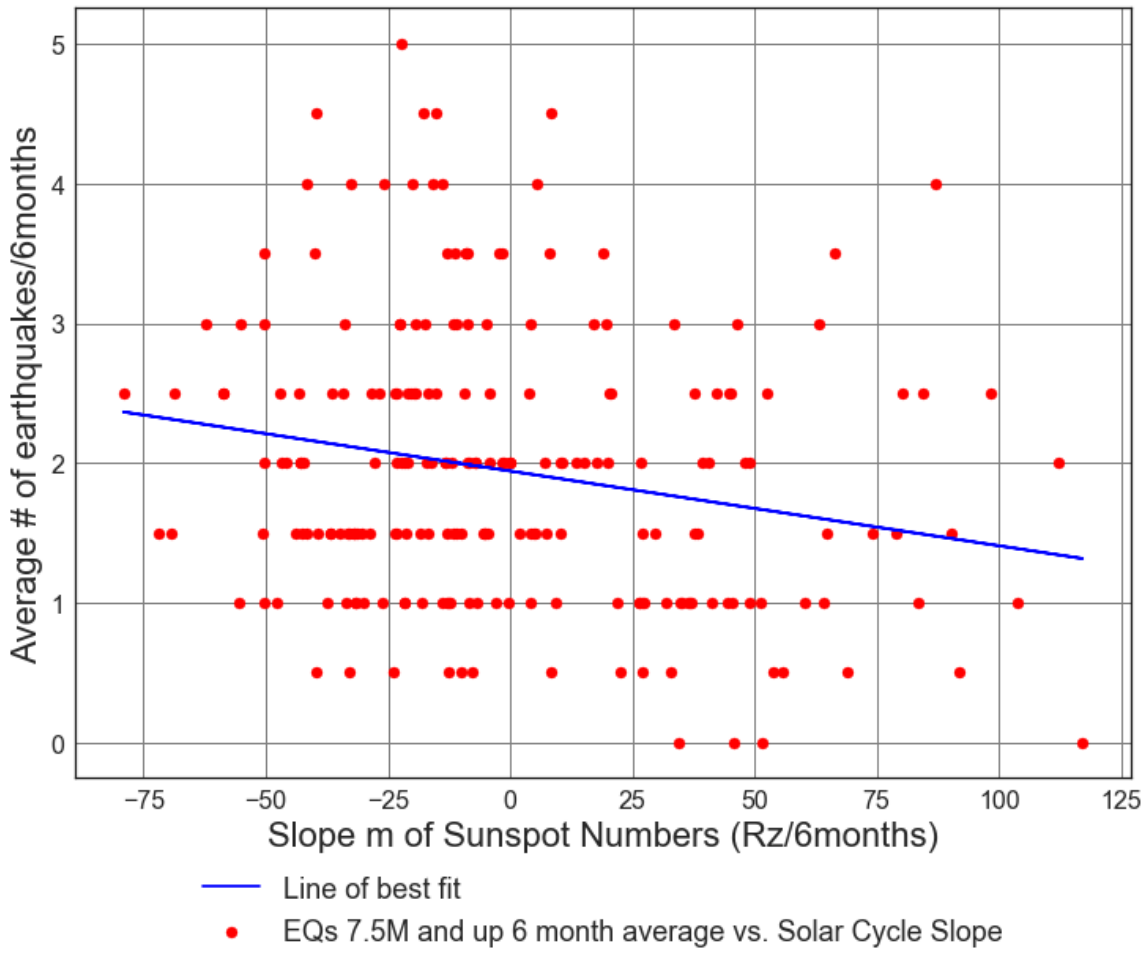

Figure B2.5: Scatter Plot of Solar cycle slope (from 1900 to 2007) vs. Average number of 7.5M and up Earthquakes/6months. Line of best fit, y = -0.005349x + (1.942), mean x = -0.07013 +/- 38.33, mean y = 1.942 +/- 1.006, R = -0.2038, R squared = 0.04155, p-value = 0.002611.

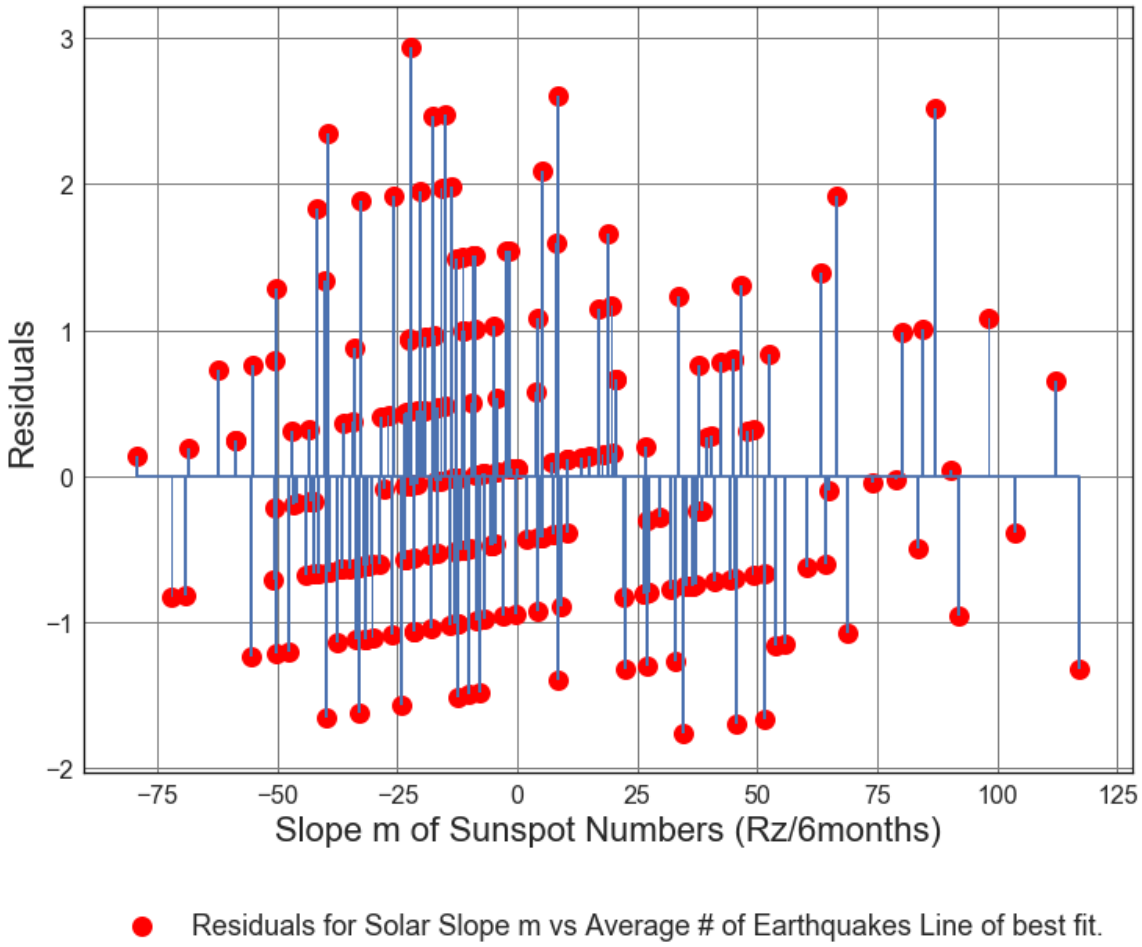

Figure B2.6: Residuals Plot of Solar cycle slope (from 1900 to 2007) vs. Average number of 7.5M and up Earthquakes/6months. Line of best fit, y = -0.005349x + (1.942), mean x = -0.07013 +/- 38.33, mean y = 1.942 +/- 1.006, R = -0.2038, R squared = 0.04155, p-value = 0.002611.

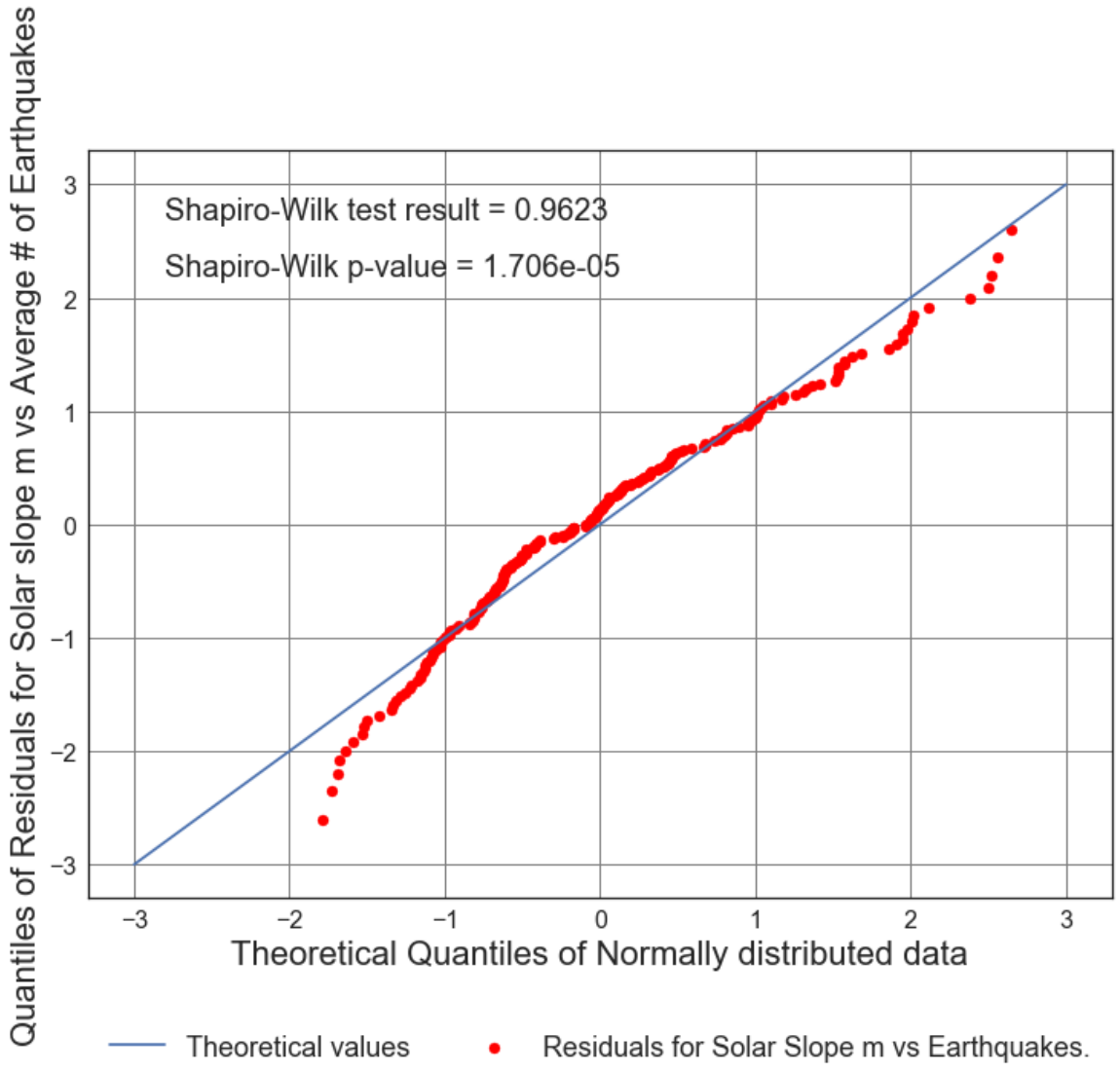

Figure B2.7: Residuals Plot of Solar cycle slope (from 1900 to 2007) vs. Average number of 7.5M and up Earthquakes/6months. Line of best fit, y = -0.005349x + (1.942), mean x = -0.07013 +/- 38.33, mean y = 1.942 +/- 1.006, R = -0.2038, R squared = 0.04155, p-value = 0.002611.

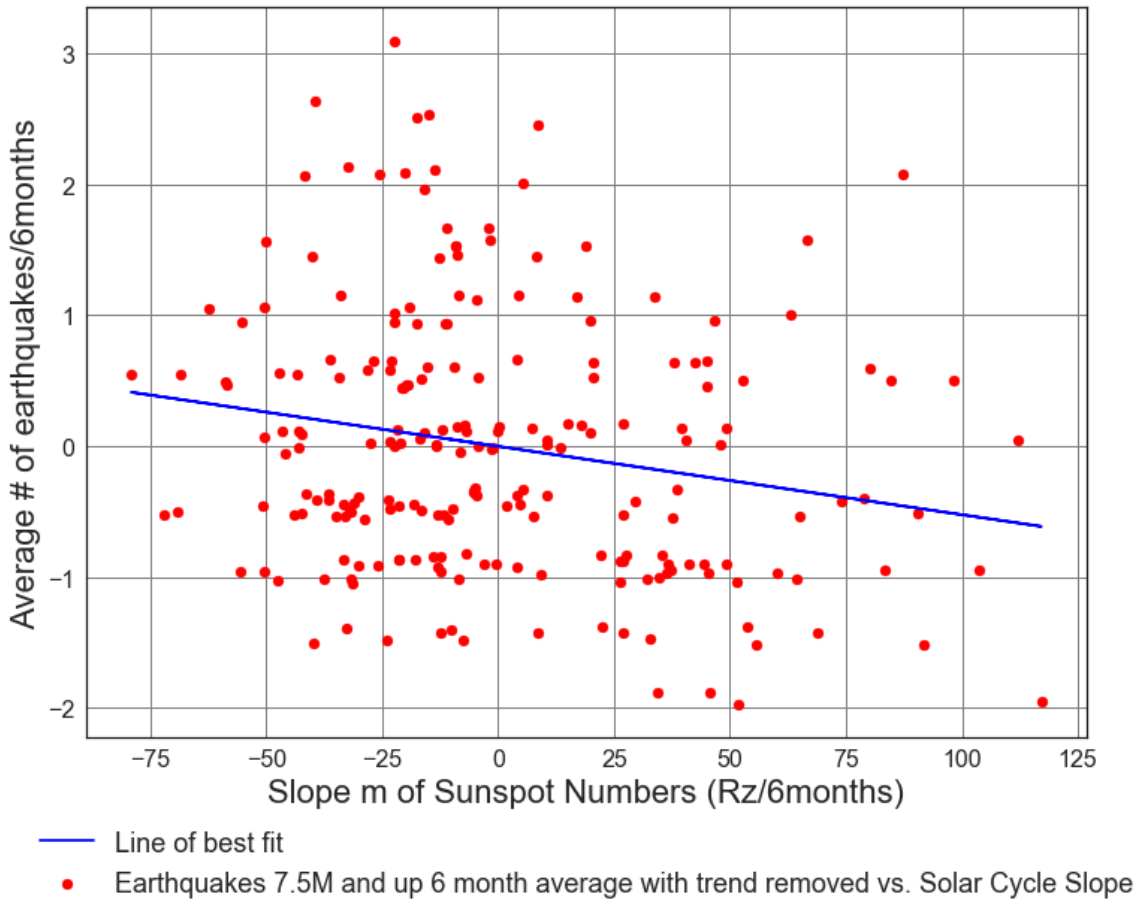

Figure B2.8: Scatter Plot of Solar cycle slope (from 1900 to 2007) vs. Average number of 7.5M and up Earthquakes/6months with trend removed. Line of best fit, y = -0.005224x + (-0.001188), mean x = -0.07013 +/- 38.33, mean y = -0.0008213 +/- 1.003, R = -0.1996, R squared = 0.03983, p-value = 0.003223.

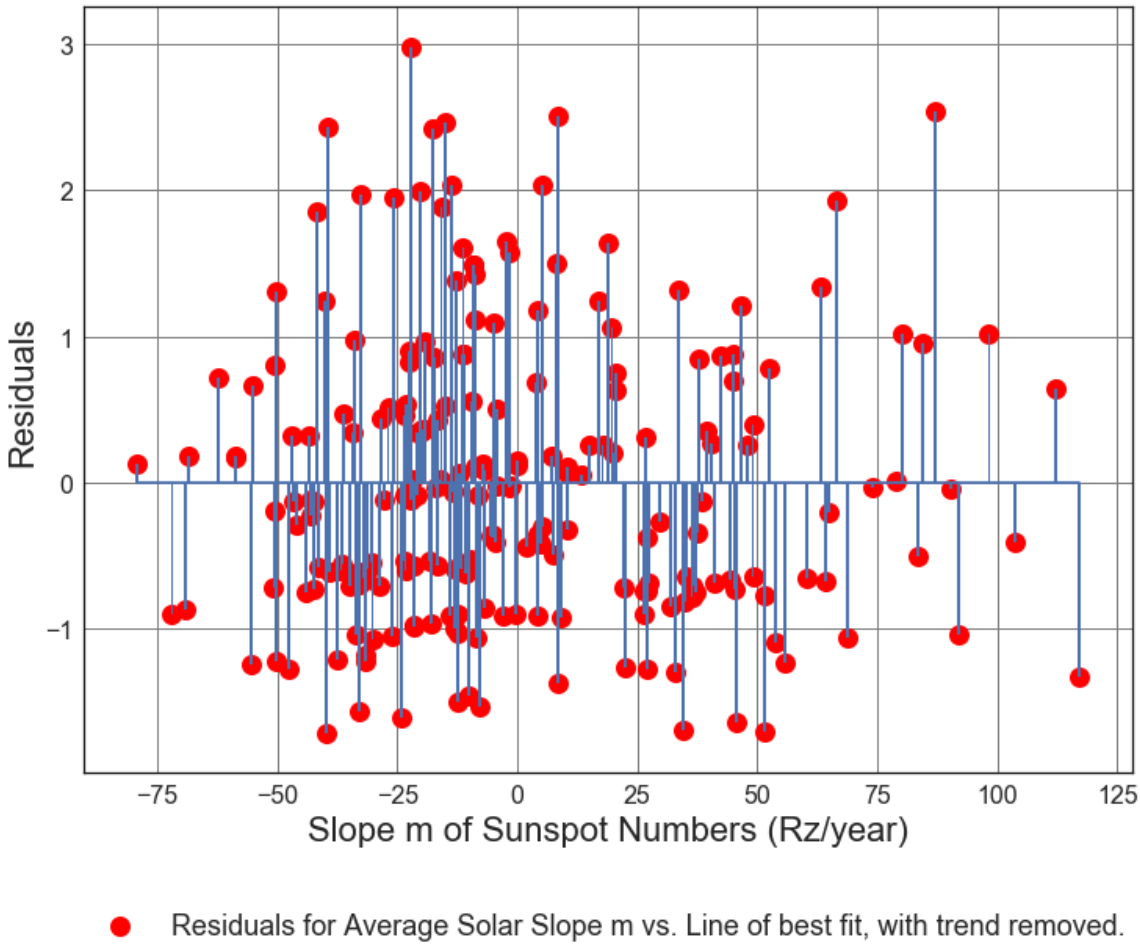

Figure B2.9: Scatter Plot of Solar cycle slope (from 1900 to 2007) vs. Average number of 7.5M and up Earthquakes/6months with trend removed. Line of best fit, y = -0.005224x + (-0.001188), mean x = -0.07013 +/- 38.33, mean y = -0.0008213 +/- 1.003, R = -0.1996, R squared = 0.03983, p-value = 0.003223.

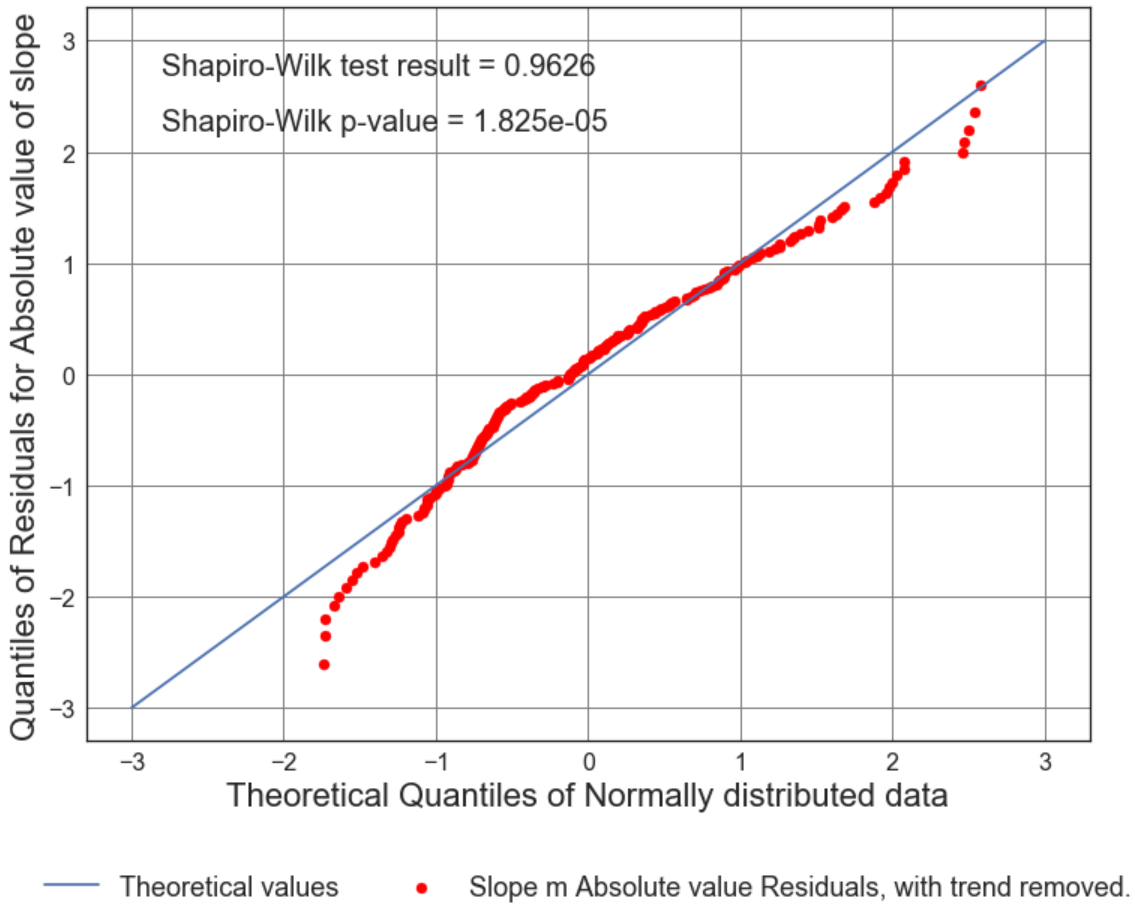

Figure B2.10: Scatter Plot of Solar cycle slope (from 1900 to 2007) vs. Average number of 7.5M and up Earthquakes/6months with trend removed. Line of best fit, y = -0.005224x + (-0.001188), mean x = -0.07013 +/- 38.33, mean y = -0.0008213 +/- 1.003, R = -0.1996, R squared = 0.03983, p-value = 0.003223.

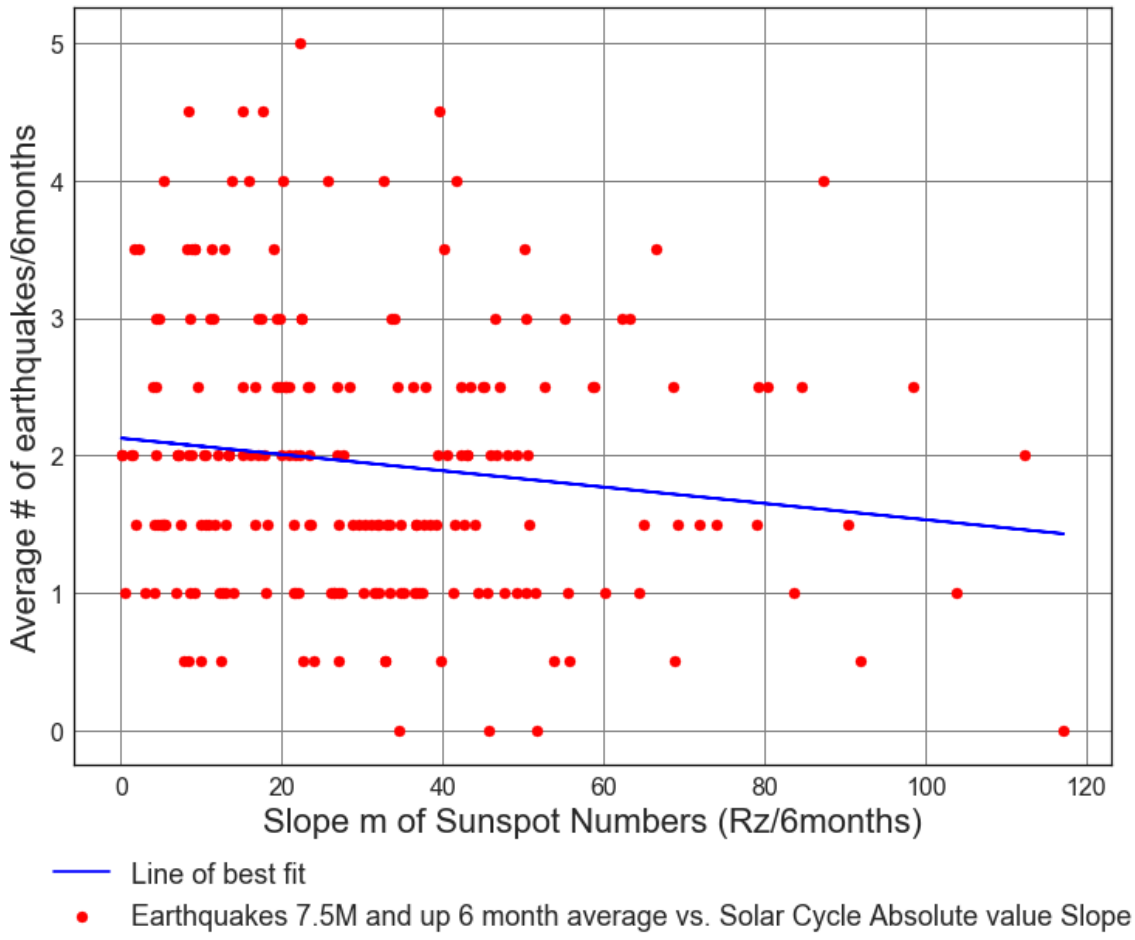

Figure B2.11: Scatter Plot of Solar cycle slope (from 1900 to 2007) vs. Average number of 7.5M and up Earthquakes/6months. Line of best fit, y = -0.005942x + (2.124), mean x = 30.66 +/- 23.0, mean y = 1.942 +/- 1.006, R = -0.1359, R squared = 0.01846, p-value = 0.04608.

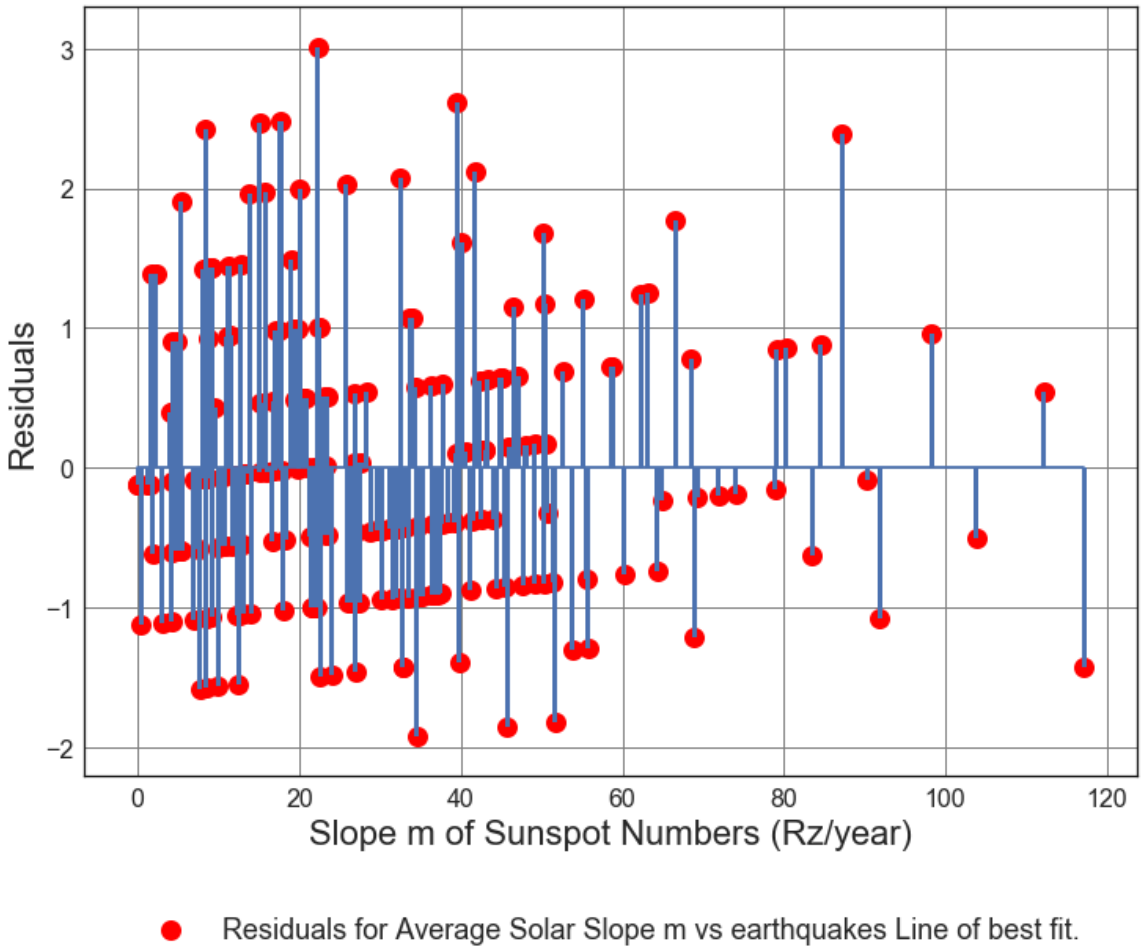

Figure B2.12: Scatter Plot of Solar cycle slope (from 1900 to 2007) vs. Average number of 7.5M and up Earthquakes/6months. Line of best fit, y = -0.005942x + (2.124), mean x = 30.66 +/- 23.0, mean y = 1.942 +/- 1.006, R = -0.1359, R squared = 0.01846, p-value = 0.04608.

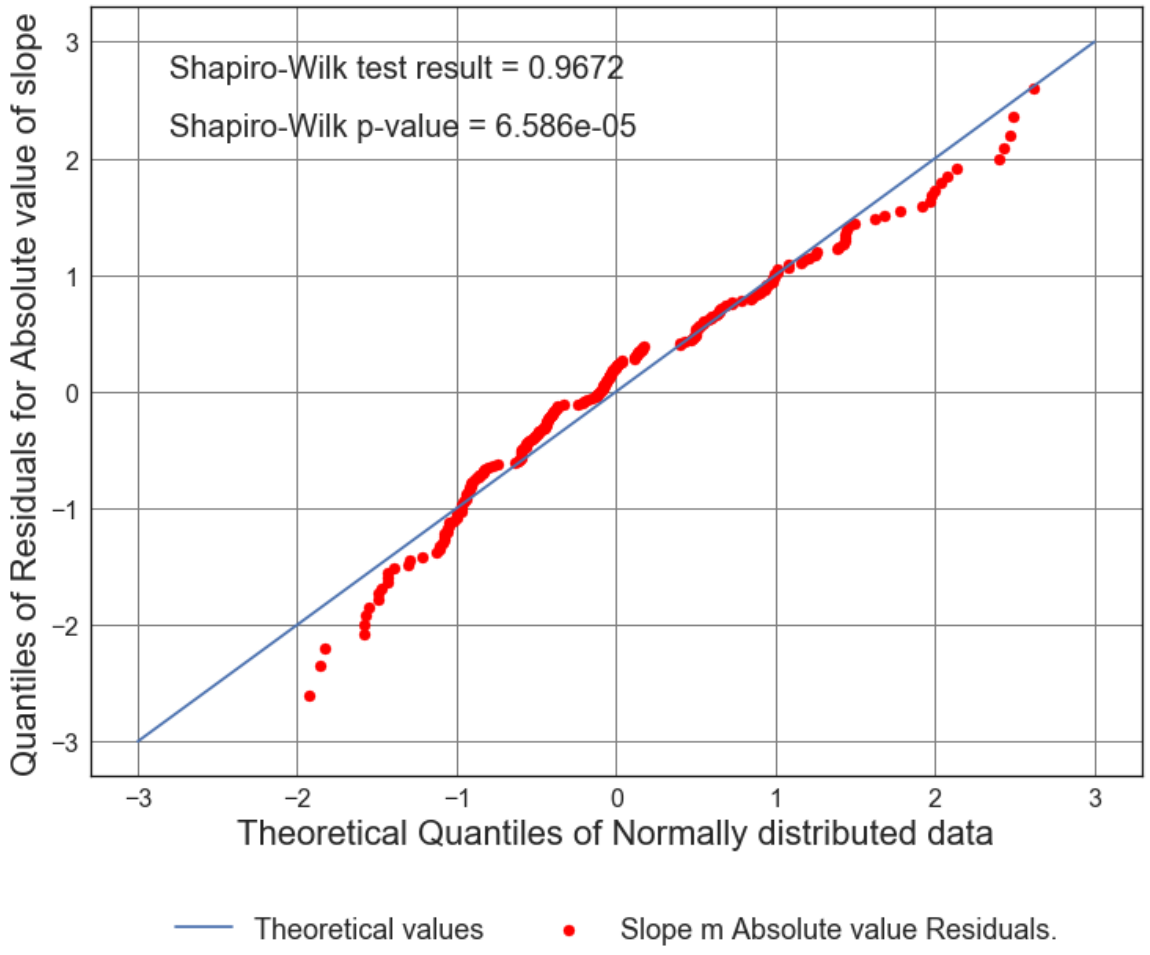

Figure B2.13: Scatter Plot of Solar cycle slope (from 1900 to 2007) vs. Average number of 7.5M and up Earthquakes/6months. Line of best fit, y = -0.005942x + (2.124), mean x = 30.66 +/- 23.0, mean y = 1.942 +/- 1.006, R = -0.1359, R squared = 0.01846, p-value = 0.04608.

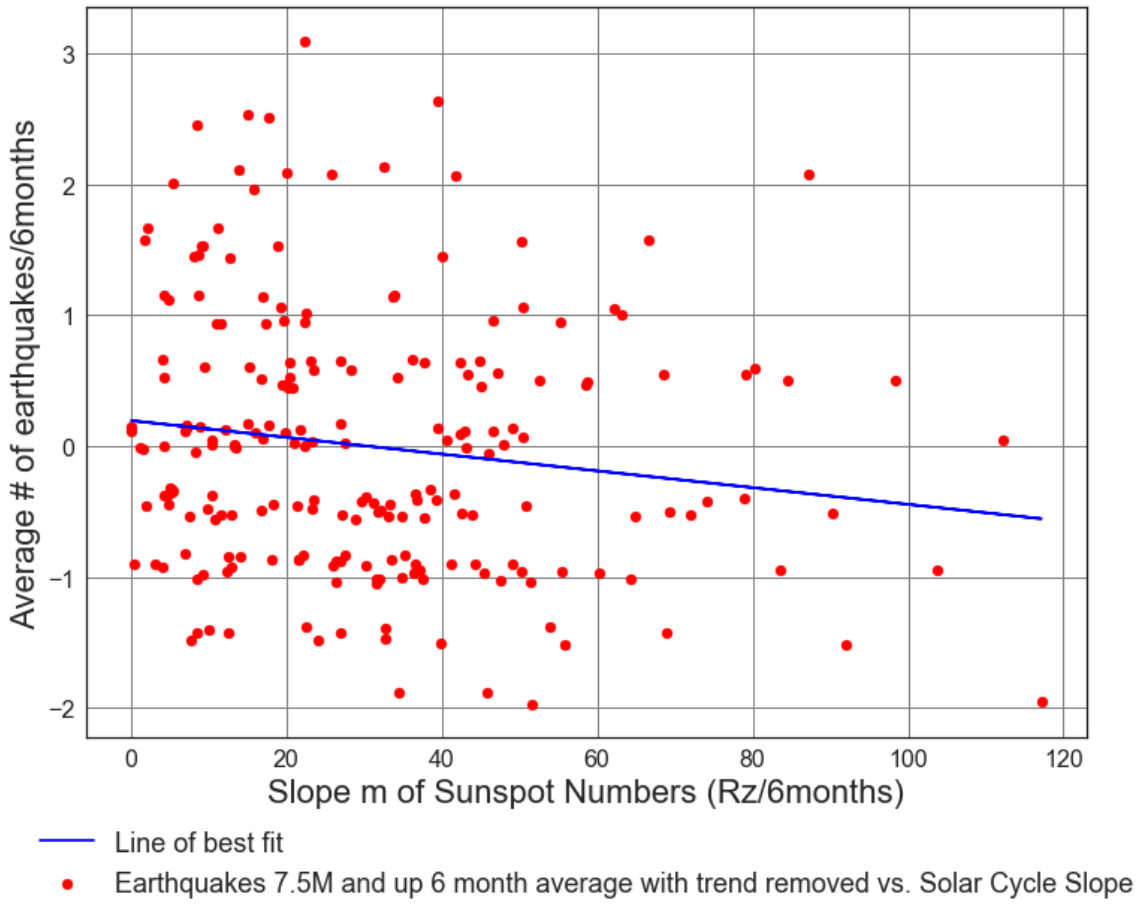

Figure B2.14: Scatter Plot of Solar cycle absolute value slope (from 1900 to 2007) vs. Average number of 7.5M and up Earthquakes/6months with trend removed. Line of best fit, y = -0.006401x + (0.1954), mean x = 30.66 +/- 23.0, mean y = -0.0008213 +/- 1.003, R = -0.1467, R squared = 0.02153, p-value = 0.03111.

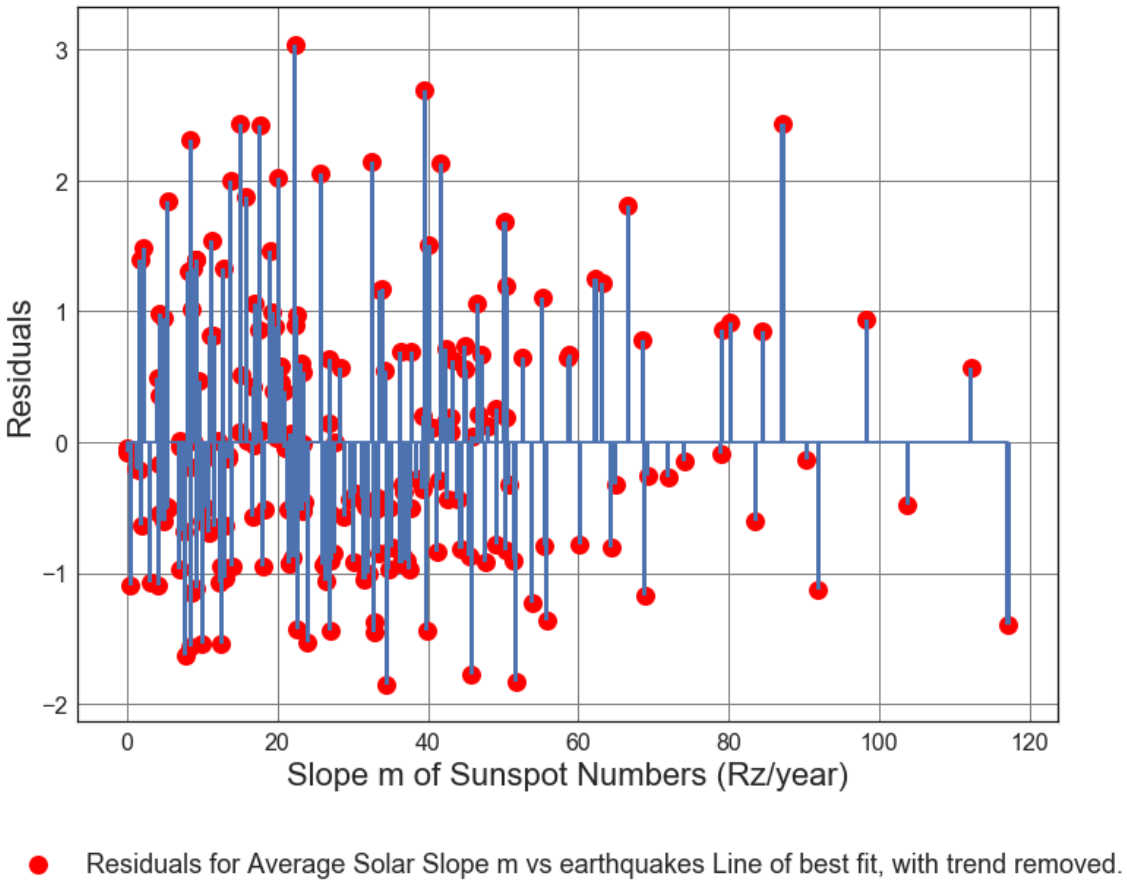

Figure B2.15: Scatter Plot of Solar cycle absolute value slope (from 1900 to 2007) vs. Average number of 7.5M and up Earthquakes/6months with trend removed. Line of best fit, y = -0.006401x + (0.1954), mean x = 30.66 +/- 23.0, mean y = -0.0008213 +/- 1.003, R = -0.1467, R squared = 0.02153, p-value = 0.03111.

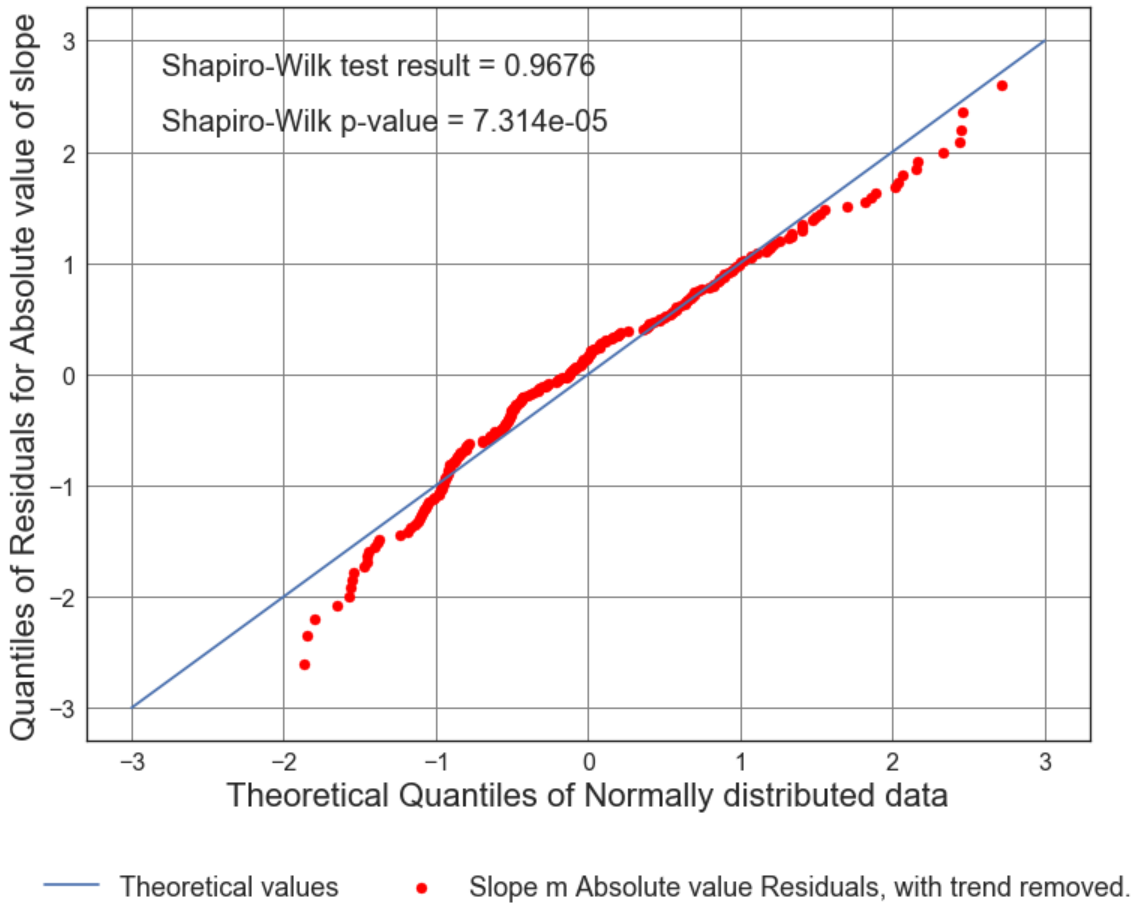

Figure B2.16: Scatter Plot of Solar cycle absolute value slope (from 1900 to 2007) vs. Average number of 7.5M and up Earthquakes/6months with trend removed. Line of best fit, y = -0.006401x + (0.1954), mean x = 30.66 +/- 23.0, mean y = -0.0008213 +/- 1.003, R = -0.1467, R squared = 0.02153, p-value = 0.03111.

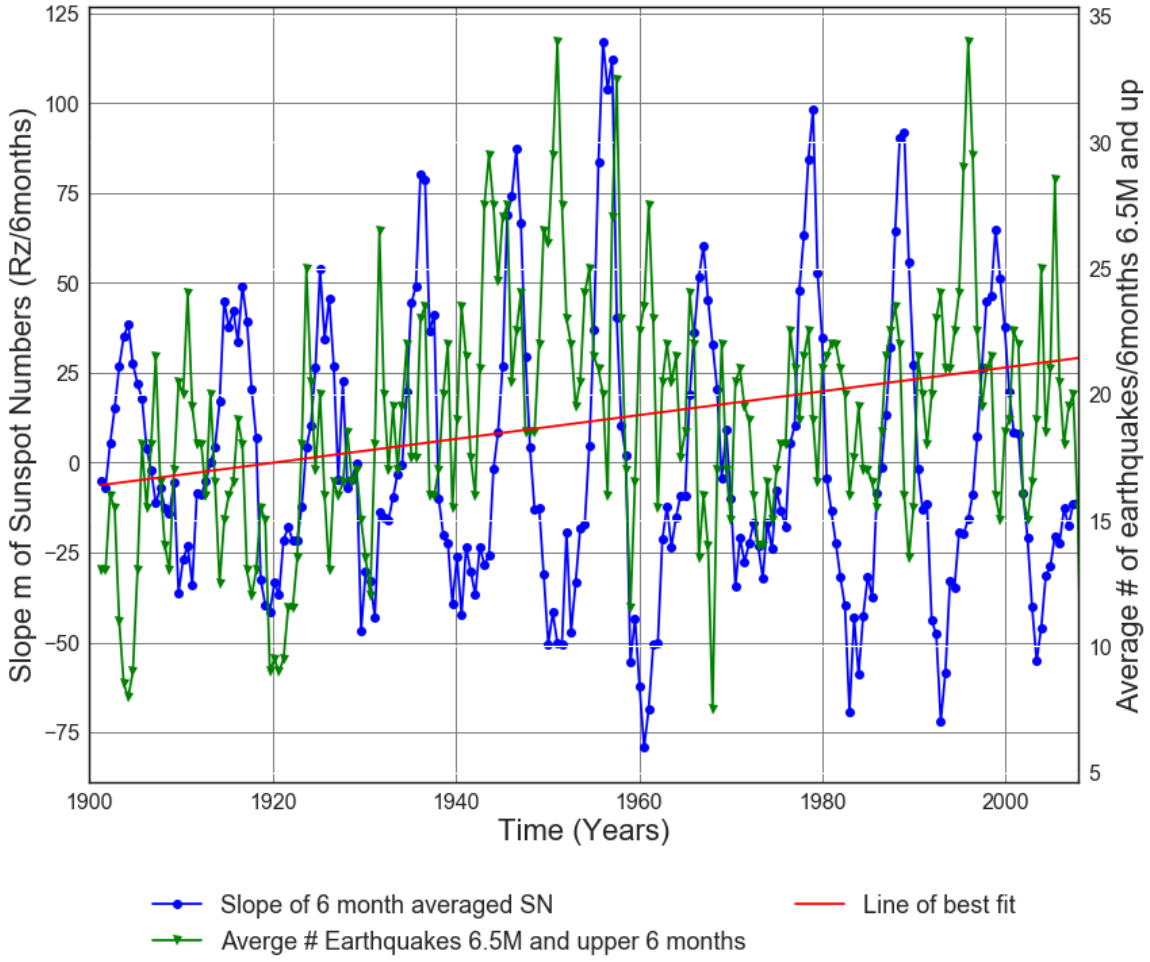

Figure B2.17: Slope of Solar cycle from 1900 to 2007 vs. Average number of 6.5M and up Earthquakes.

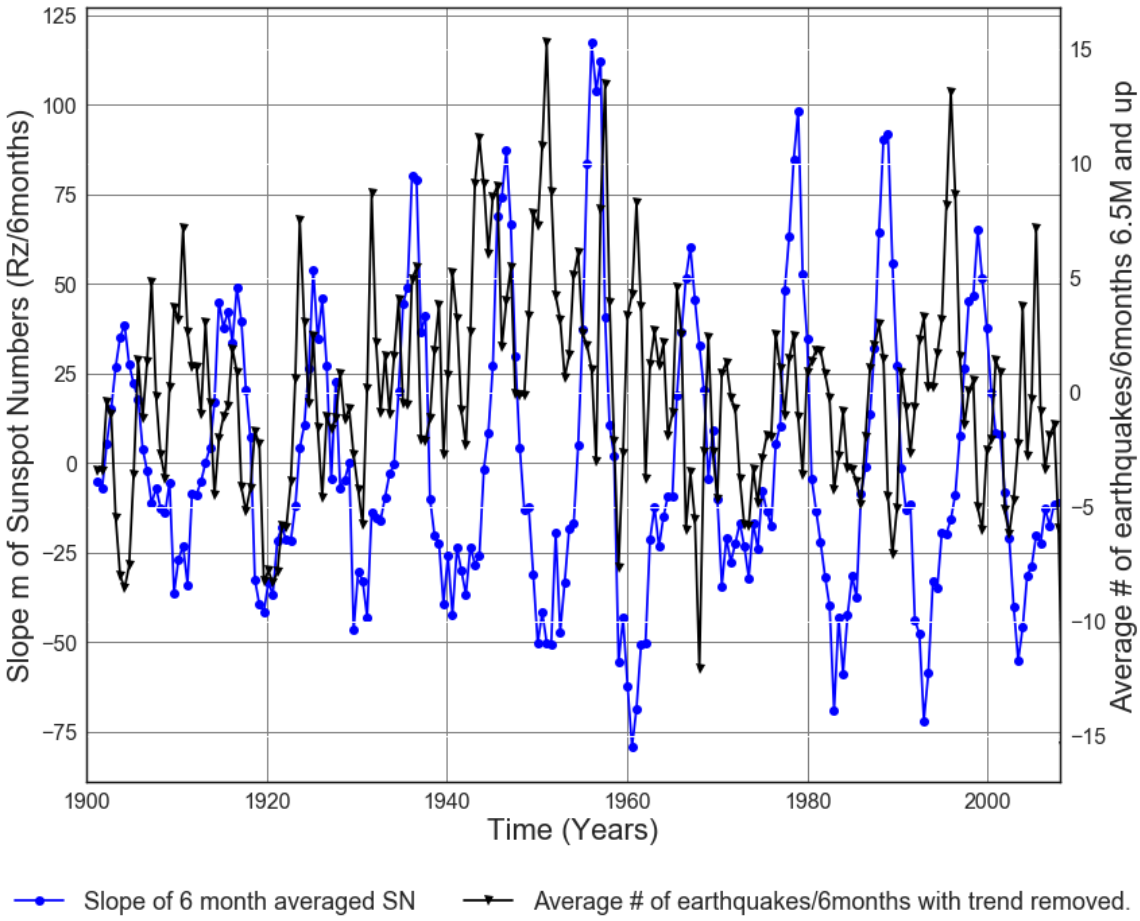

Figure B2.18: Slope of 6 month averaged SN 1900 to 2007 vs. Average number of 6.5M and up Earthquakes with trend removed. Line of best fit, y = 0.04729x + (-73.52), mean x = 1.955e+03 +/- 31.21, mean y = 18.92 +/- 4.796

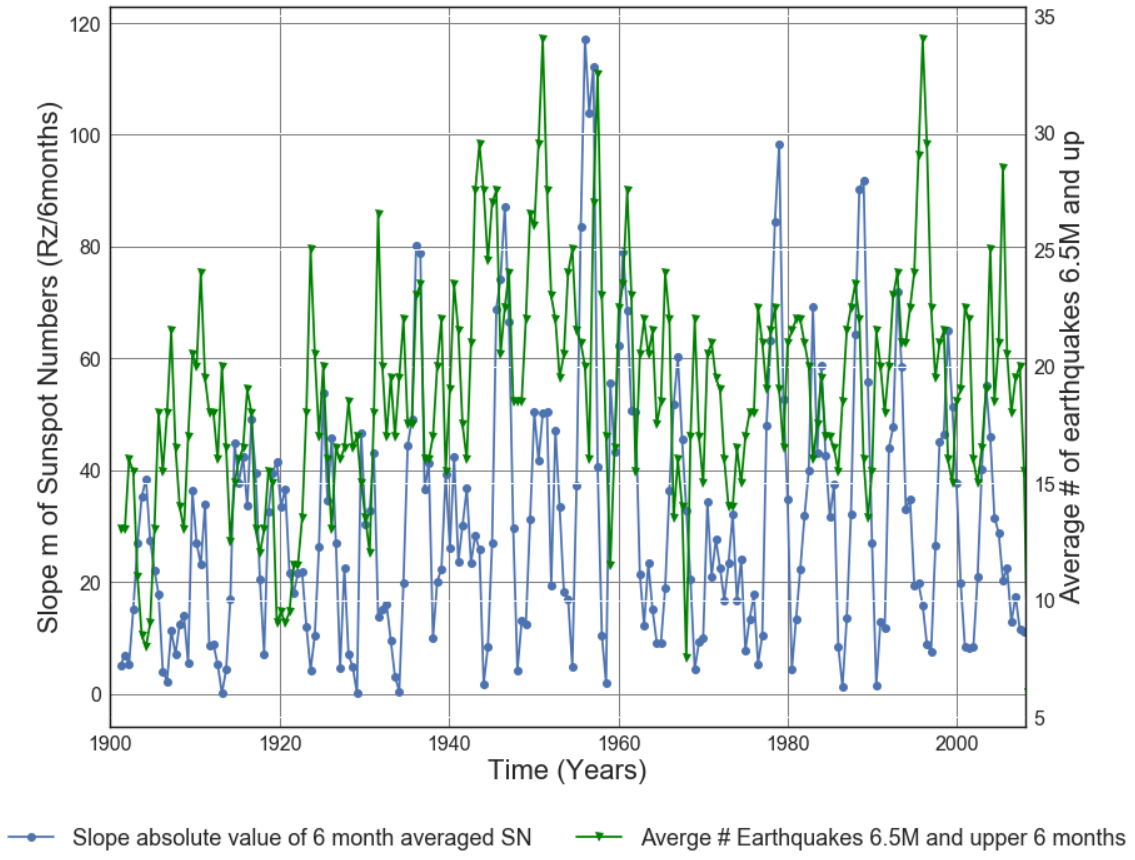

Figure B2.19: Slope Absolute value of Solar cycle from 1900 to 2007 vs. Average number of 6.5M and up Earthquakes.

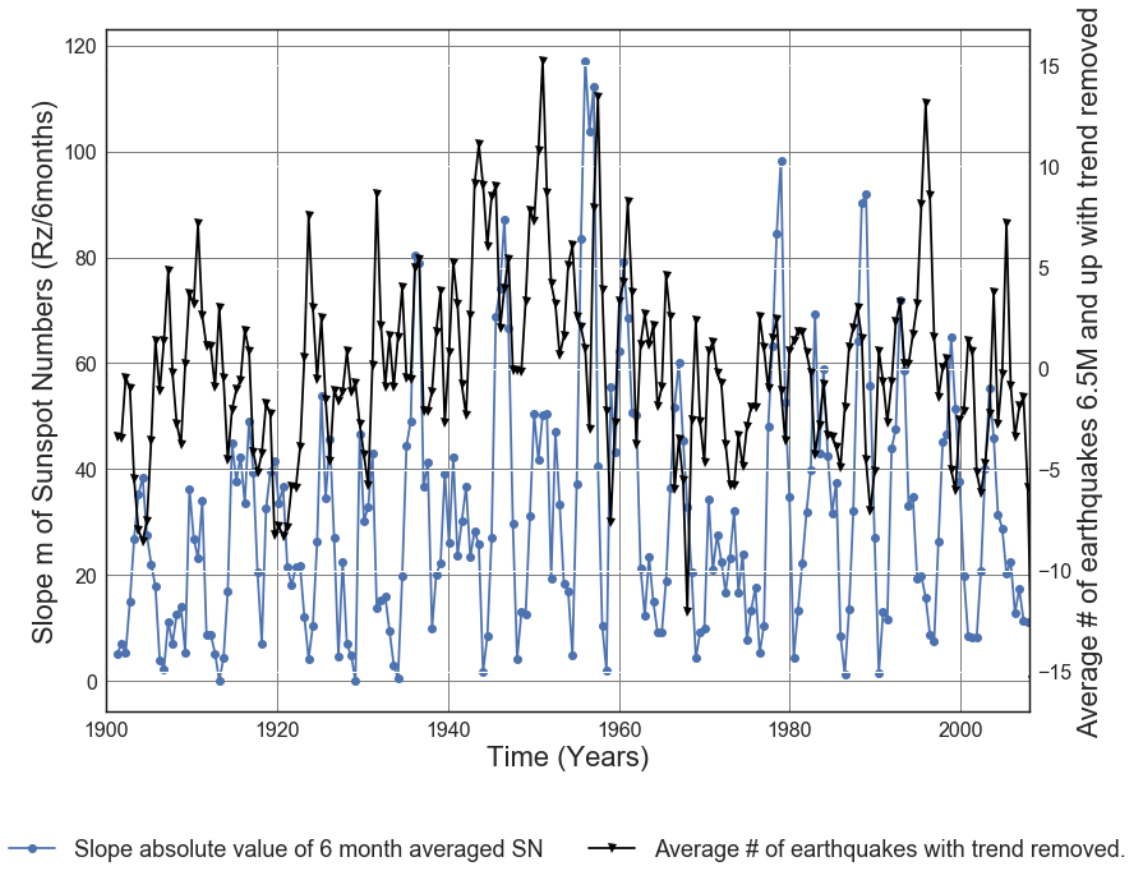

Figure B2.20: Slope Absolute value of Solar cycle from 1900 to 2007 vs. Average number of 6.5M and up earthquakes with trend removed.

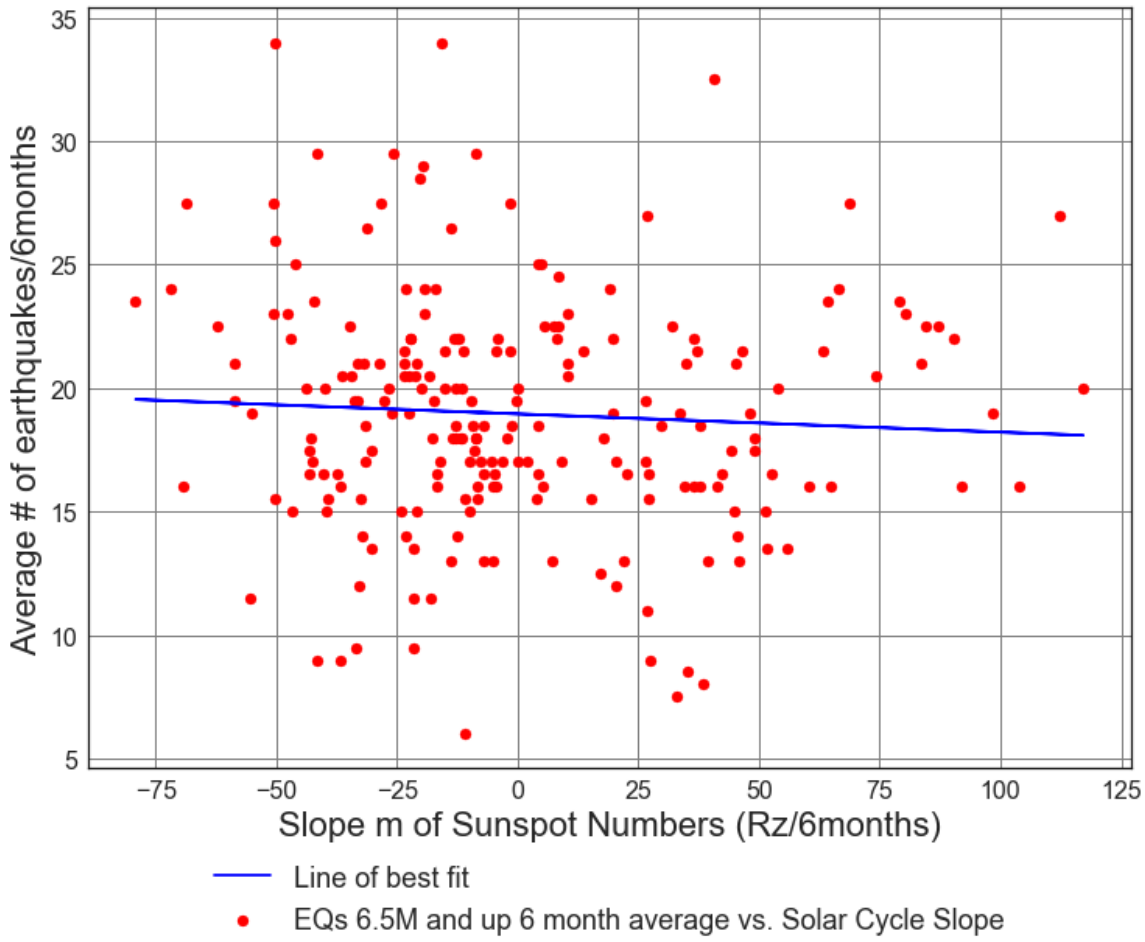

Figure B2.21: Scatter Plot of Solar cycle slope (from 1900 to 2007) vs. Average number of 6.5M and up Earthquakes/6months. Line of best fit, y = -0.007396x + (18.96), mean x = -0.07013 +/- 38.33, mean y = 18.96 +/- 4.773, R = -0.05939, R squared = 0.003527, p-value = 0.3851.

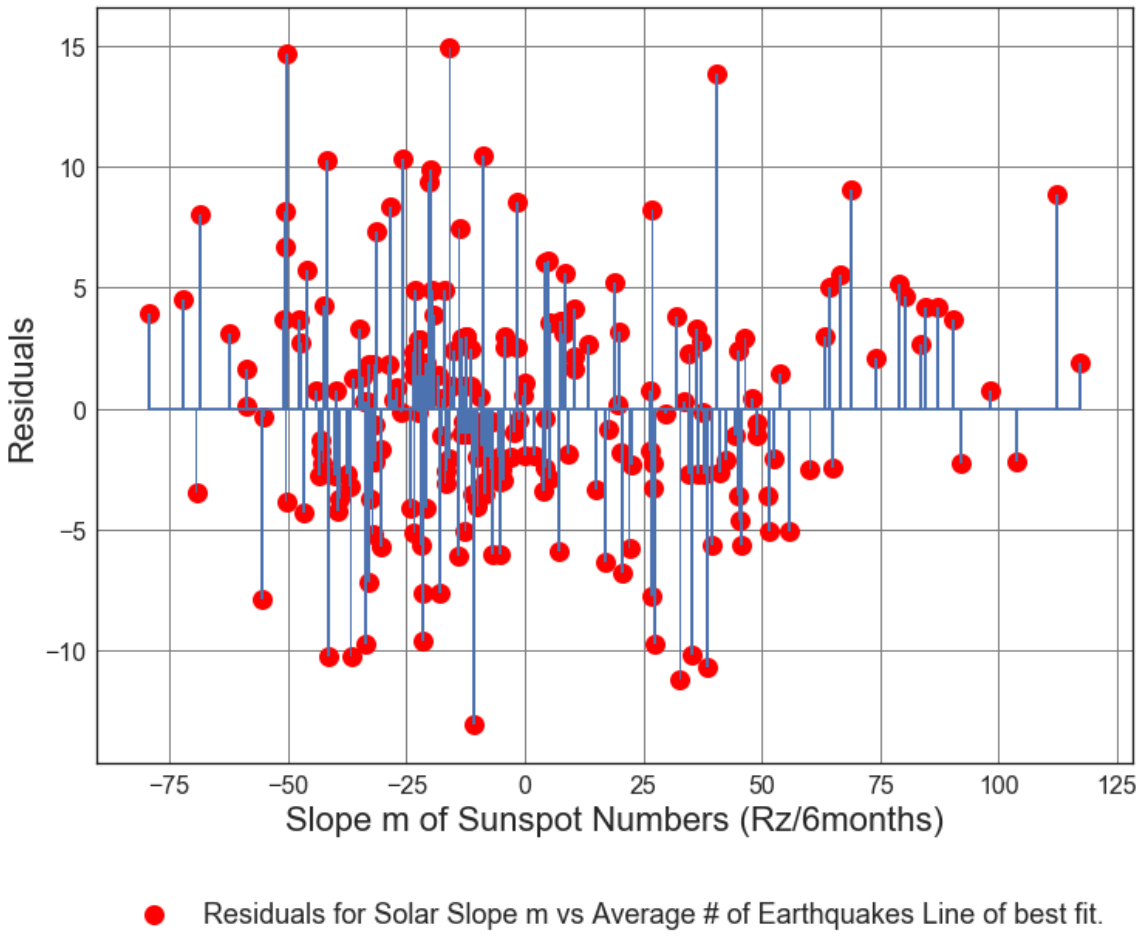

Figure B2.22: Residuals Plot of Solar cycle slope (from 1900 to 2007) vs. Average number of 6.5M and up Earthquakes/6months. Line of best fit, y = -0.007396x + (18.96), mean x = -0.07013 +/- 38.33, mean y = 18.96 +/- 4.773, R = -0.05939, R squared = 0.003527, p-value = 0.3851.

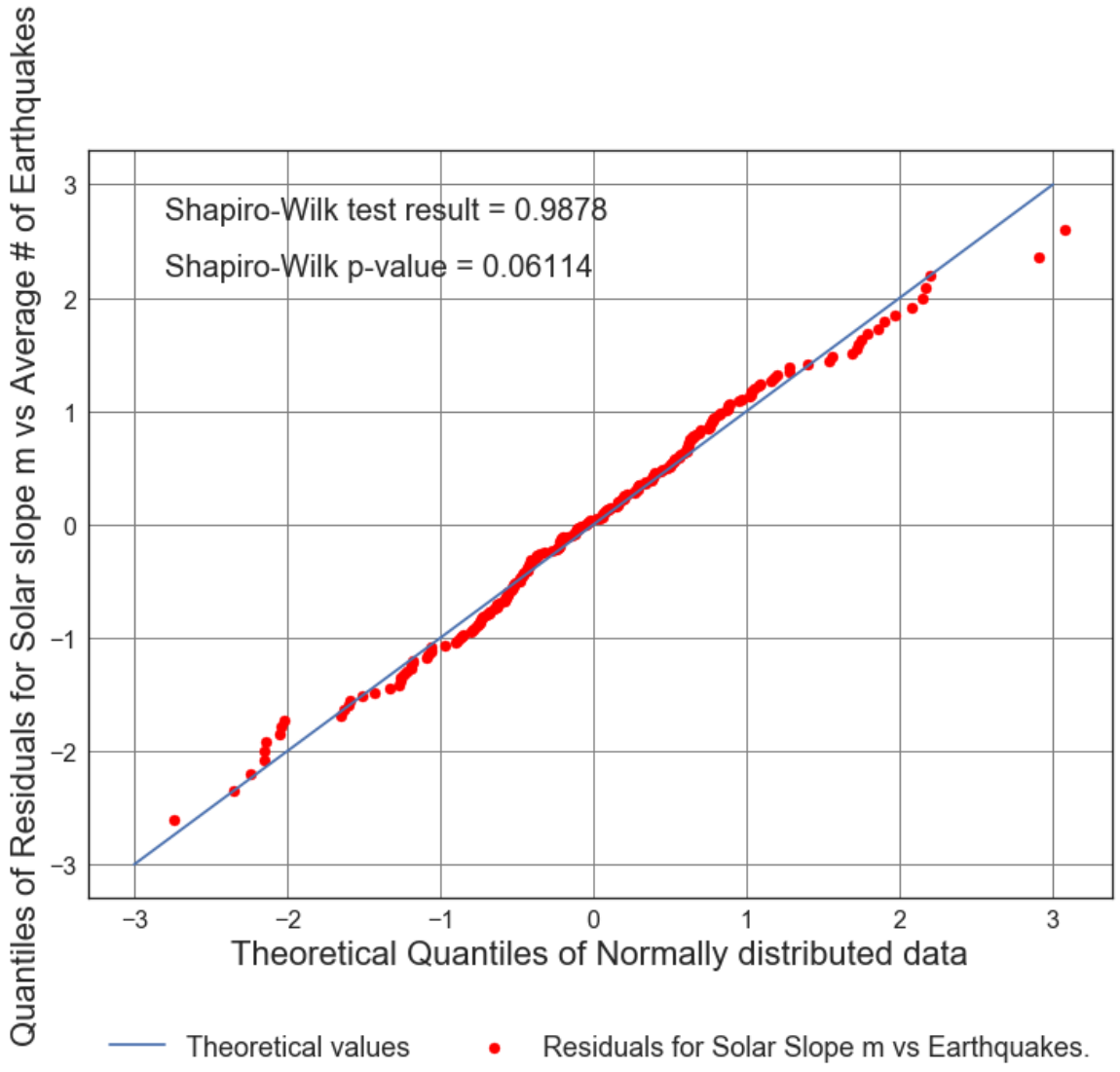

Figure B2.23: Residuals Plot of Solar cycle slope (from 1900 to 2007) vs. Average number of 6.5M and up Earthquakes/6months. Line of best fit, y = -0.007396x + (18.96), mean x = -0.07013 +/- 38.33, mean y = 18.96 +/- 4.773, R = -0.05939, R squared = 0.003527, p-value = 0.3851.

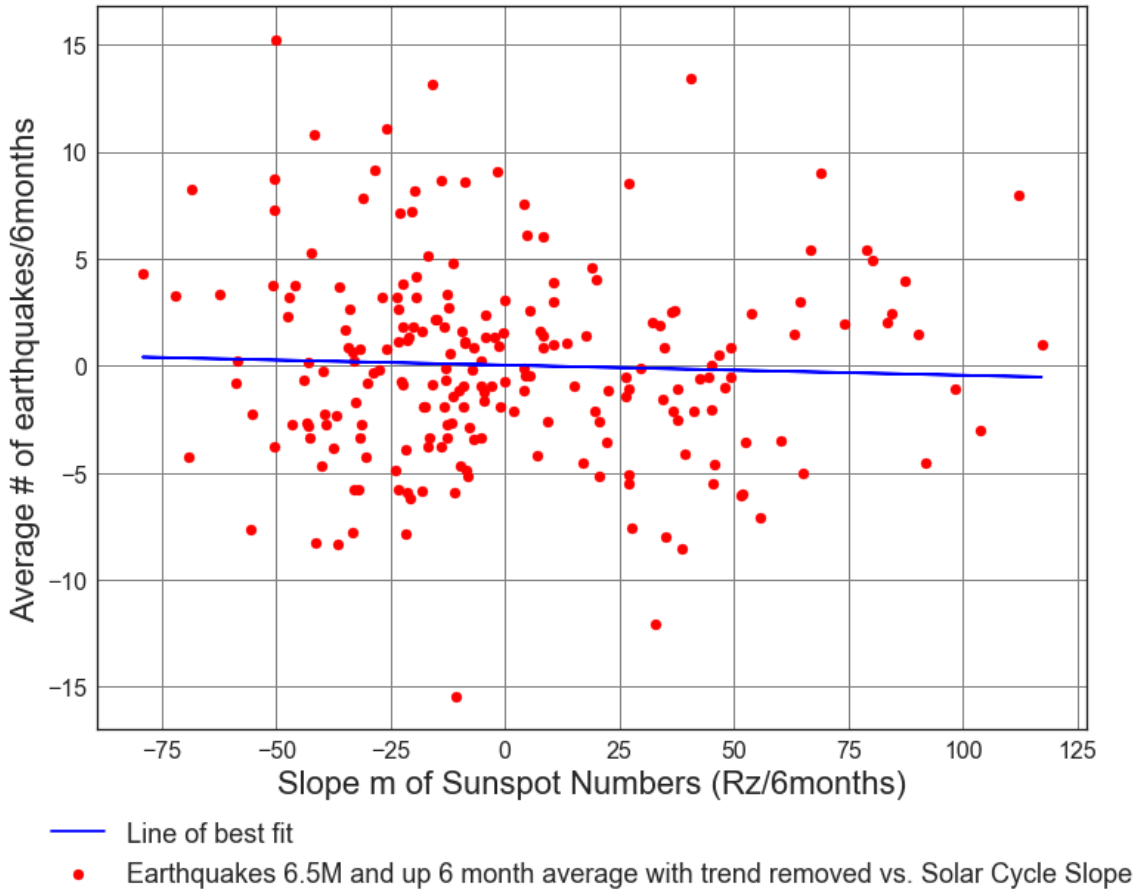

Figure B2.24: Scatter Plot of Solar cycle slope (from 1900 to 2007) vs. Average number of 6.5M and up Earthquakes/6months with trend removed. Line of best fit, y = -0.004737x + (0.02686), mean x = -0.07013 +/- 38.33, mean y = 0.0272 +/- 4.557, R = -0.03984, R squared = 0.001588, p-value = 0.5603.

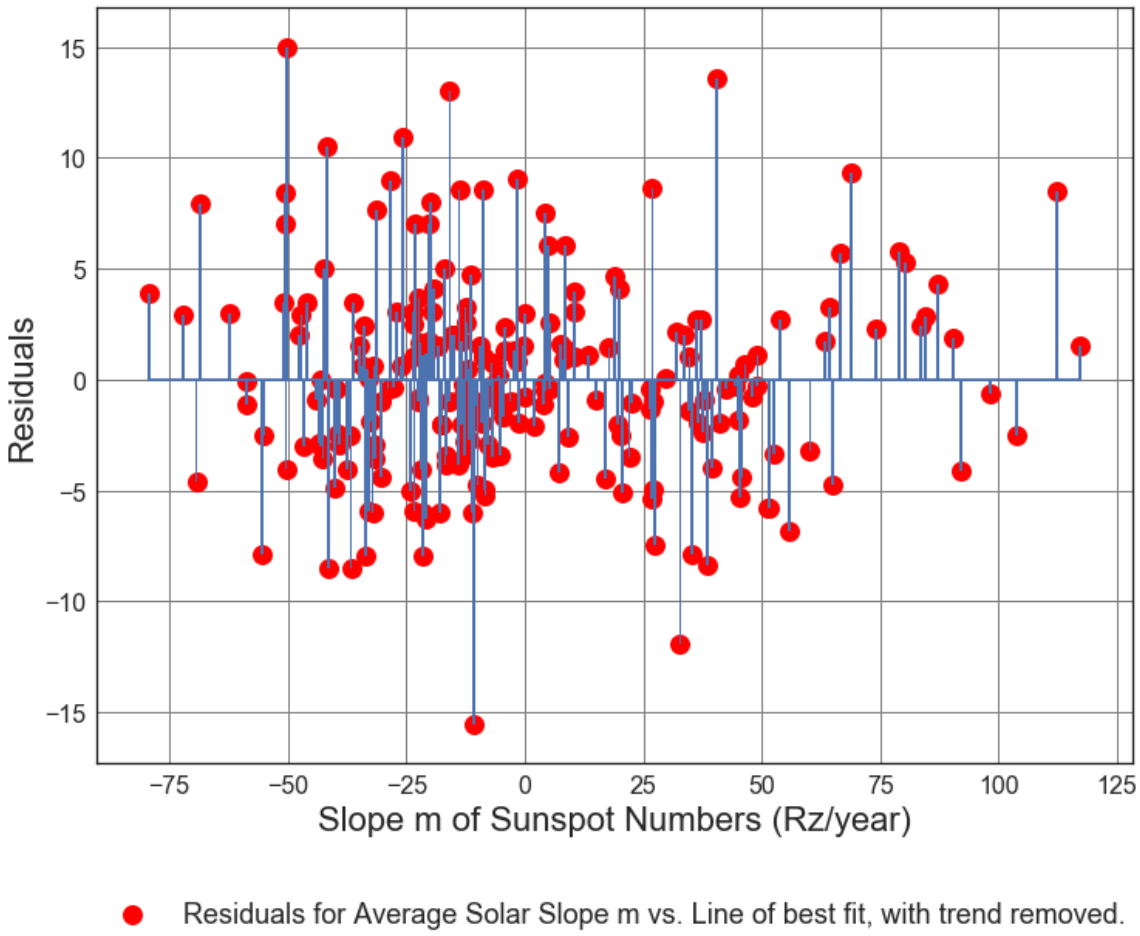

Figure B2.25: Scatter Plot of Solar cycle slope (from 1900 to 2007) vs. Average number of 6.5M and up Earthquakes/6months with trend removed. Line of best fit, y = -0.004737x + (0.02686), mean x = -0.07013 +/- 38.33, mean y = 0.0272 +/- 4.557, R = -0.03984, R squared = 0.001588, p-value = 0.5603.

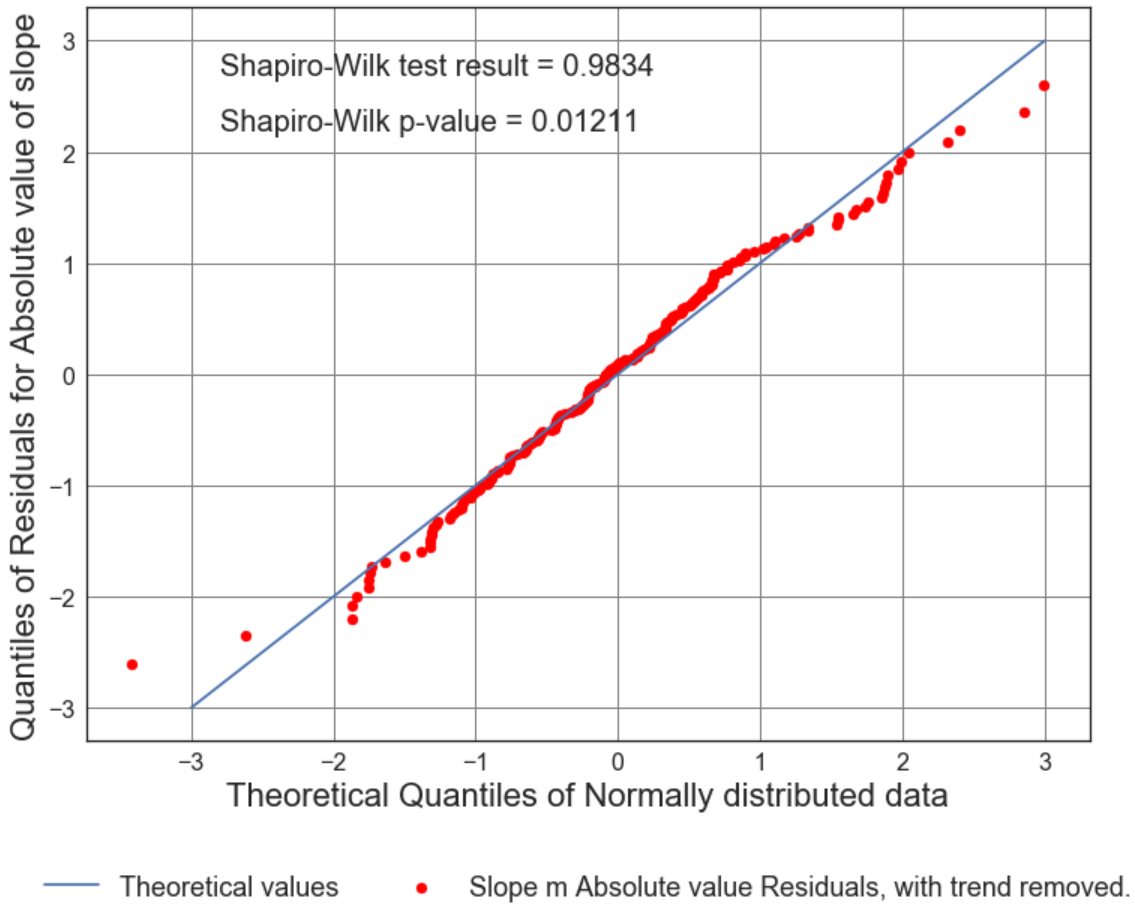

Figure B2.26: Scatter Plot of Solar cycle slope (from 1900 to 2007) vs. Average number of 6.5M and up Earthquakes/6months with trend removed. Line of best fit, y = -0.004737x + (0.02686), mean x = -0.07013 +/- 38.33, mean y = 0.0272 +/- 4.557, R = -0.03984, R squared = 0.001588, p-value = 0.5603.

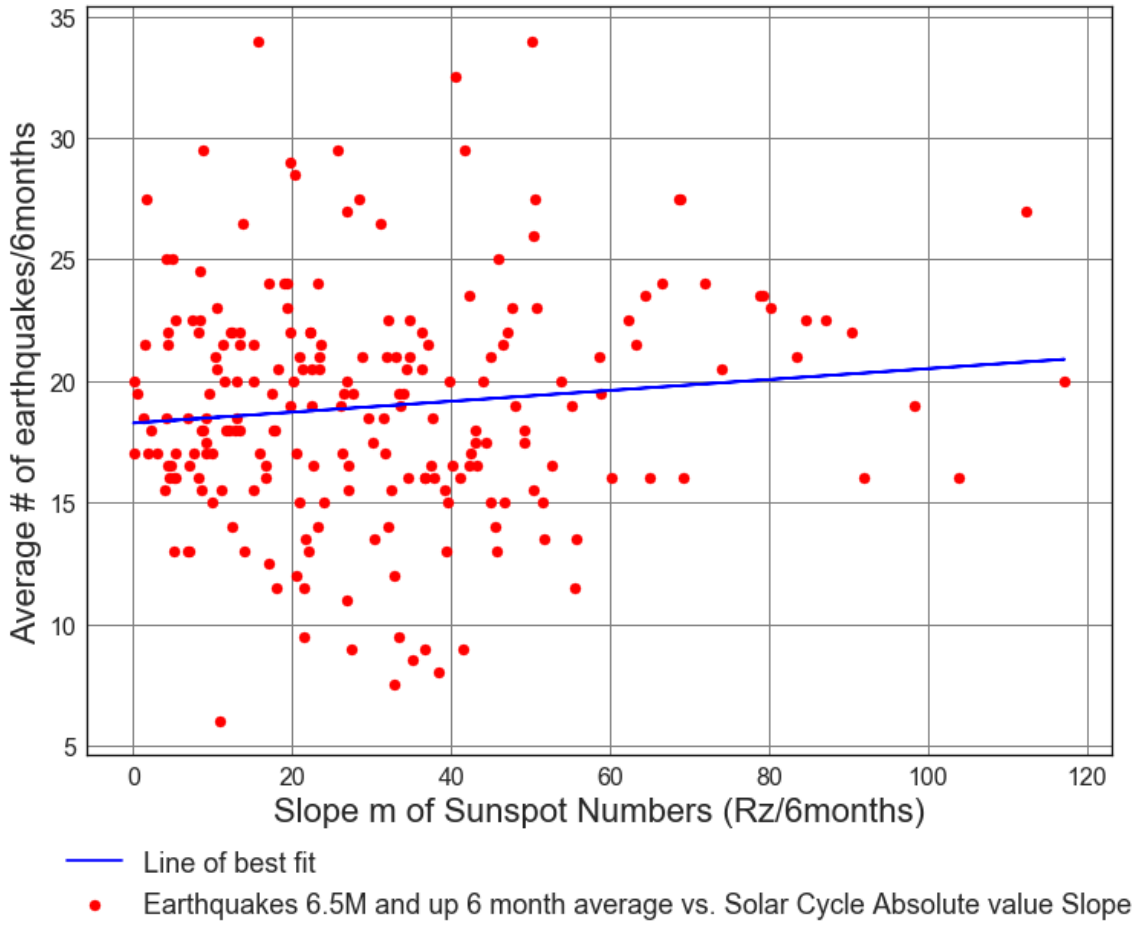

Figure B2.27: Scatter Plot of Solar cycle slope (from 1900 to 2007) vs. Average number of 6.5M and up Earthquakes/6months. Line of best fit, y = 0.0224x + (18.27), mean x = 30.66 +/- 23.0, mean y = 18.96 +/- 4.773, R = 0.108, R squared = 0.01166, p-value = 0.1136.

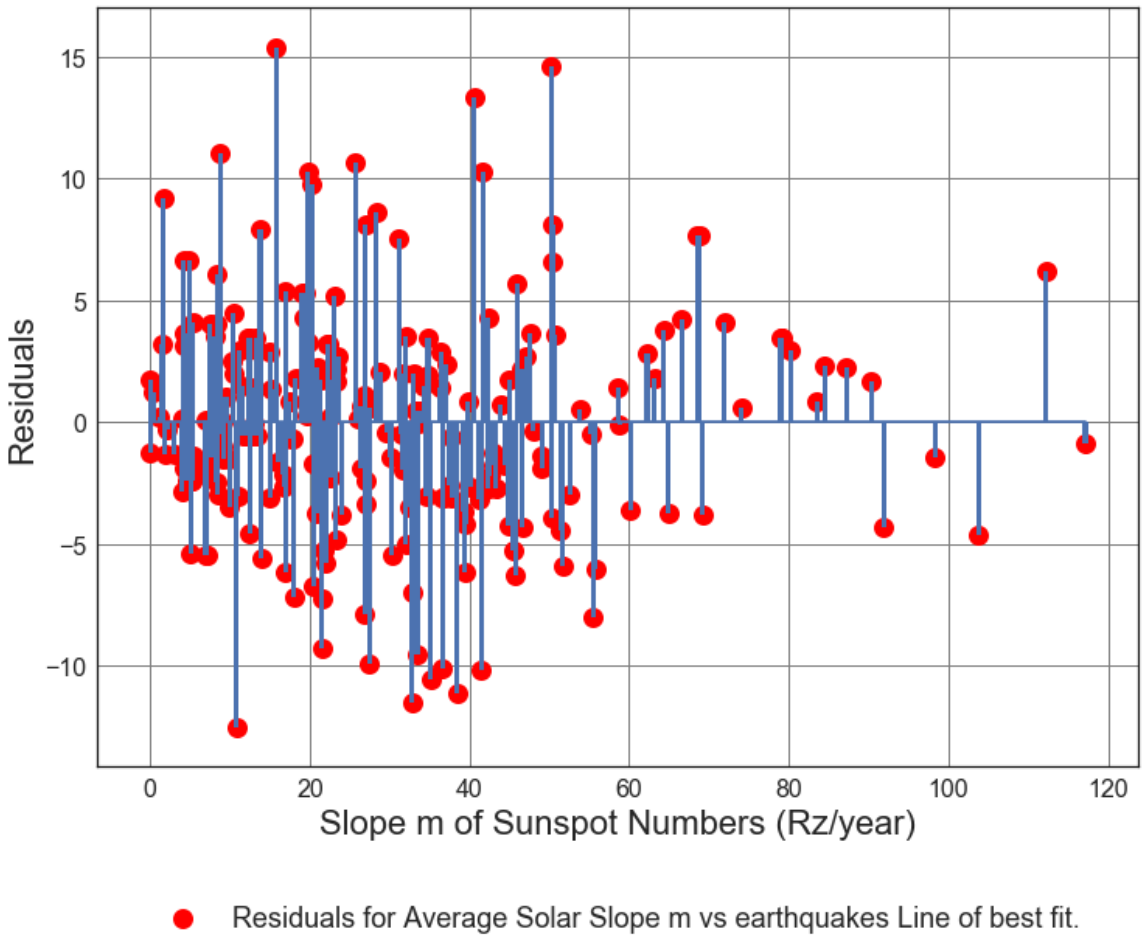

Figure B2.28: Scatter Plot of Solar cycle slope (from 1900 to 2007) vs. Average number of 6.5M and up Earthquakes/6months. Line of best fit, y = 0.0224x + (18.27), mean x = 30.66 +/- 23.0, mean y = 18.96 +/- 4.773, R = 0.108, R squared = 0.01166, p-value = 0.1136.

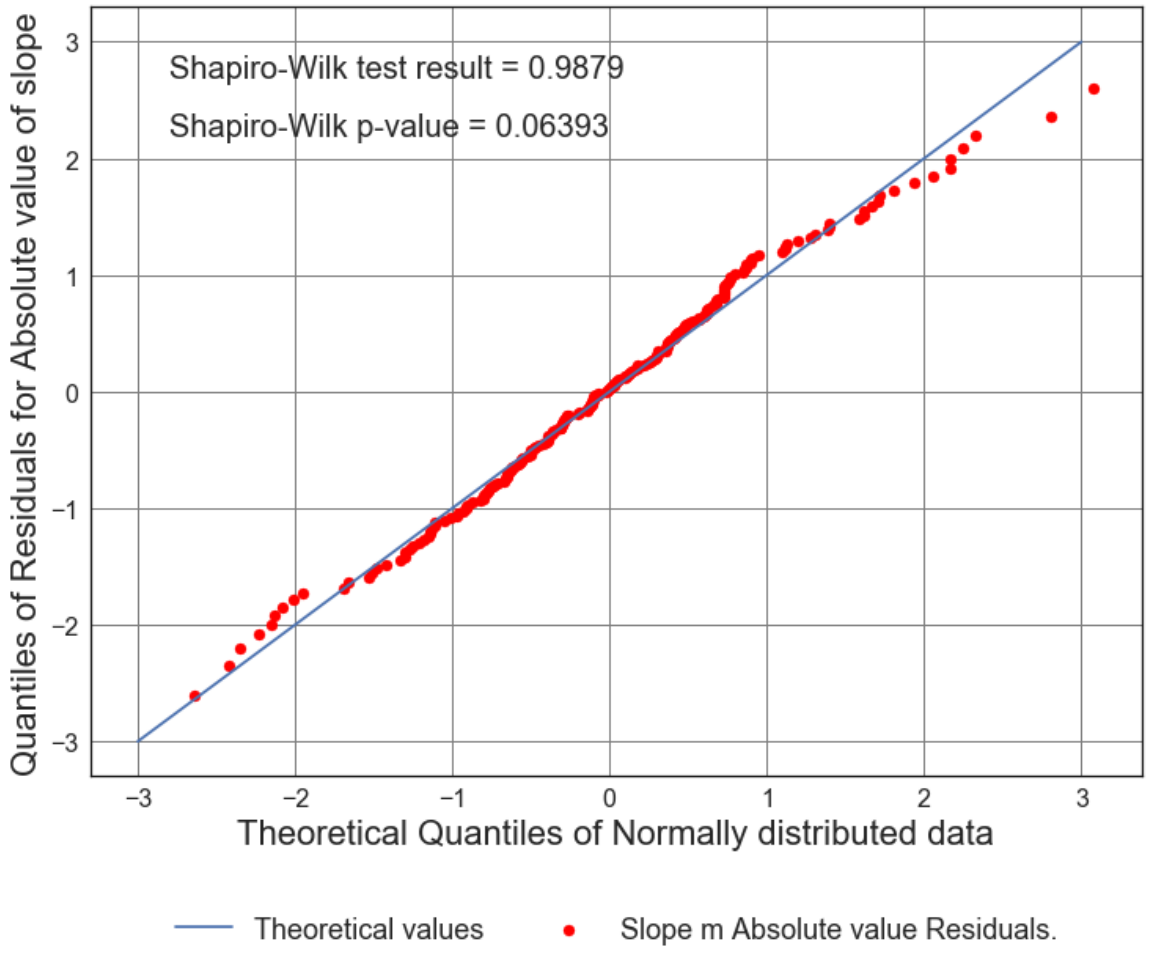

Figure B2.29: Scatter Plot of Solar cycle slope (from 1900 to 2007) vs. Average number of 6.5M and up Earthquakes/6months. Line of best fit, y = 0.0224x + (18.27), mean x = 30.66 +/- 23.0, mean y = 18.96 +/- 4.773, R = 0.108, R squared = 0.01166, p-value = 0.1136.

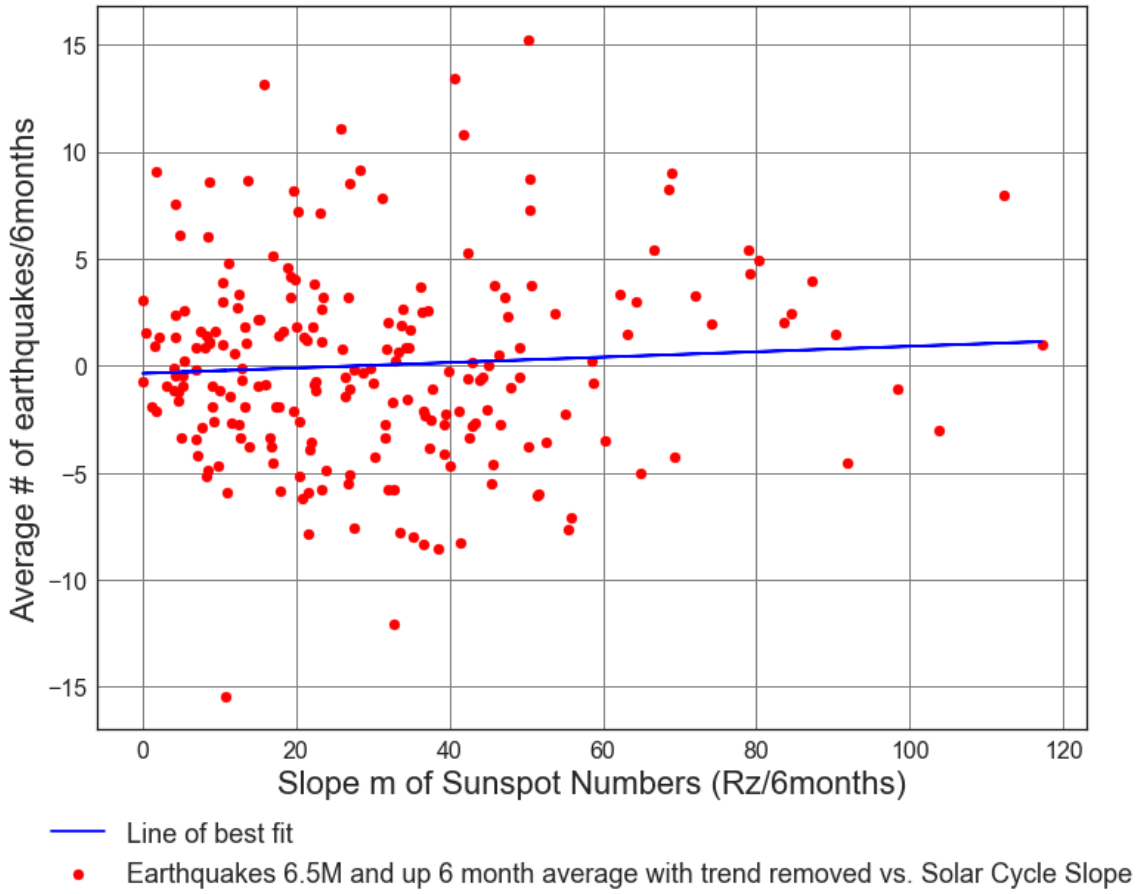

Figure B2.30: Scatter Plot of Solar cycle absolute value slope (from 1900 to 2007) vs. Average number of 6.5M and up Earthquakes/6months with trend removed. Line of best fit, y = 0.01266x + (-0.3609), mean x = 30.66 +/- 23.0, mean y = 0.0272 +/- 4.557, R = 0.06389, R squared = 0.004082, p-value = 0.3501.

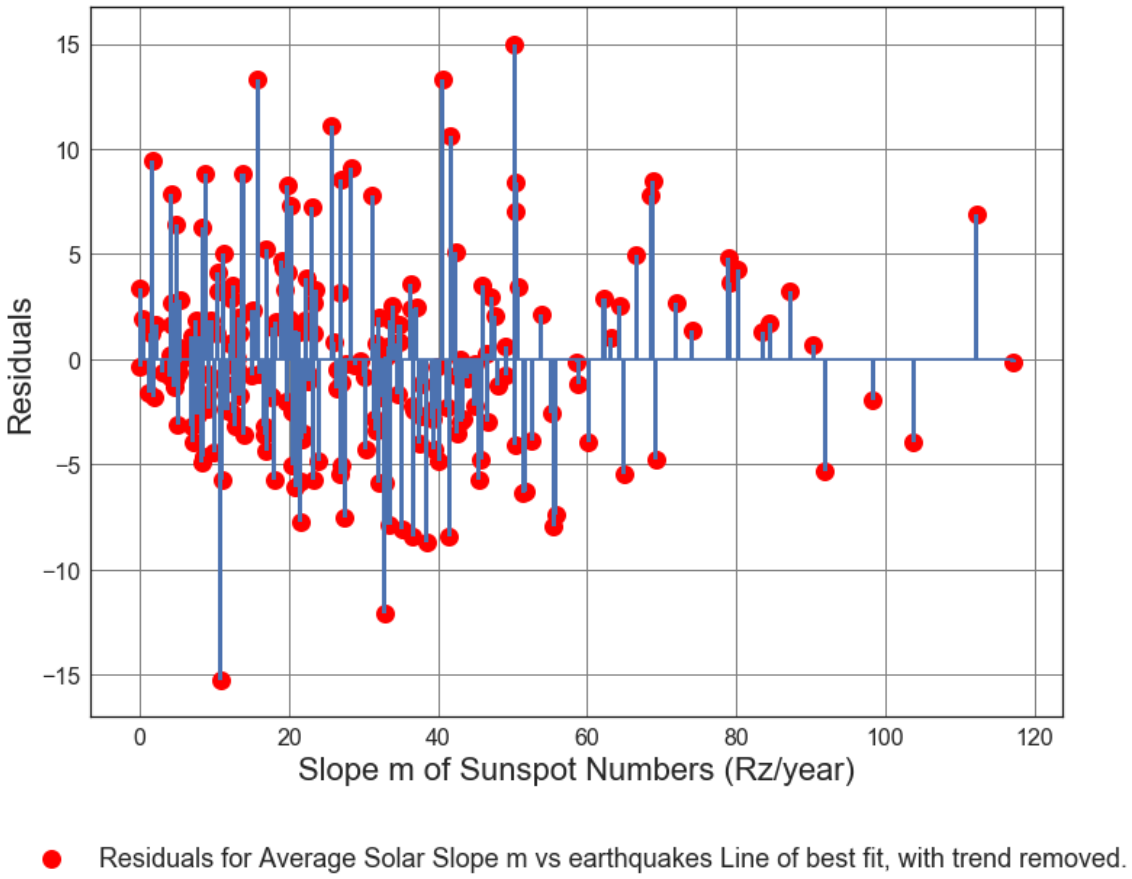

Figure B2.31: Scatter Plot of Solar cycle absolute value slope (from 1900 to 2007) vs. Average number of 6.5M and up Earthquakes/6months with trend removed. Line of best fit, y = 0.01266x + (-0.3609), mean x = 30.66 +/- 23.0, mean y = 0.0272 +/- 4.557, R = 0.06389, R squared = 0.004082, p-value = 0.3501.

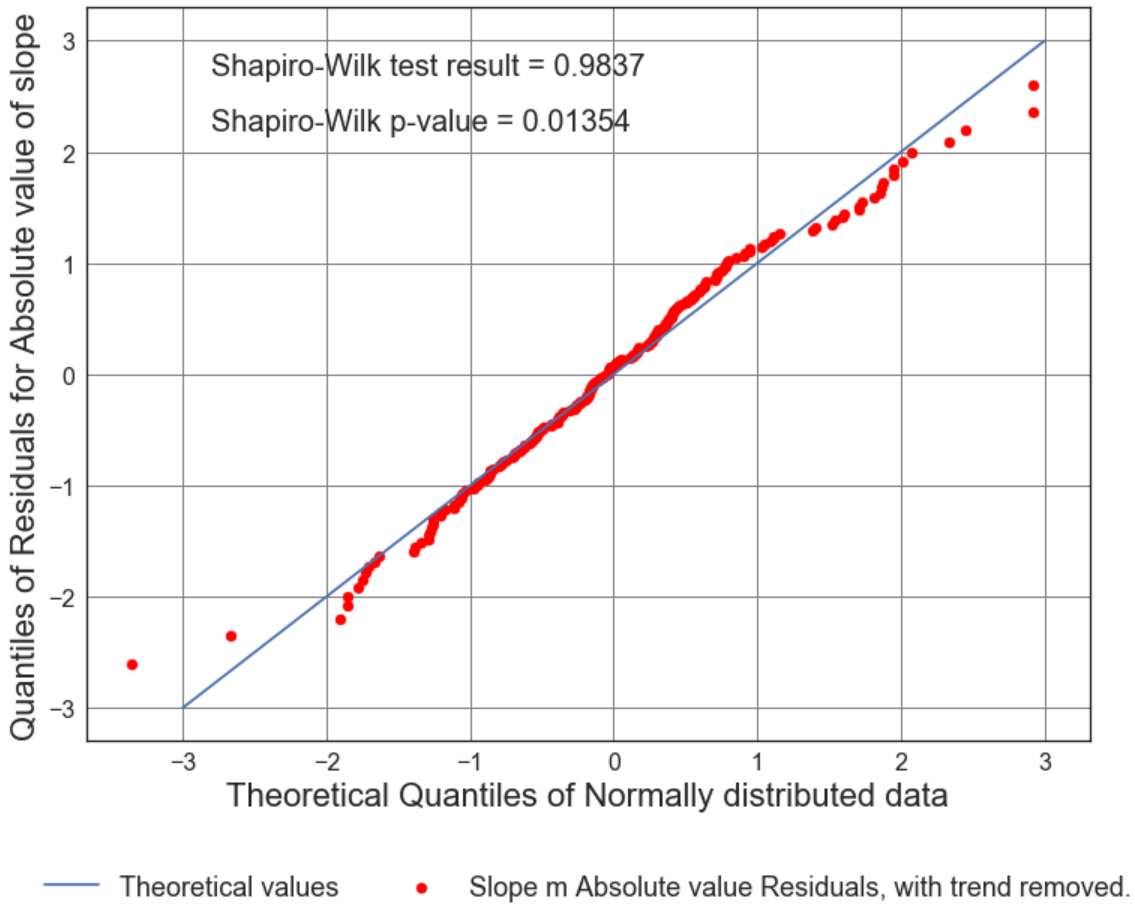

Figure B2.32: Scatter Plot of Solar cycle absolute value slope (from 1900 to 2007) vs. Average number of 6.5M and up Earthquakes/6months with trend removed. Line of best fit, y = 0.01266x + (-0.3609), mean x = 30.66 +/- 23.0, mean y = 0.0272 +/- 4.557, R = 0.06389, R squared = 0.004082, p-value = 0.3501.

Appendix B3: USGS Centennial Time Series Analysis Part 3 - Pre 1964 (Historical period) Six Month Averaged Earthquake and Sunspot Data.

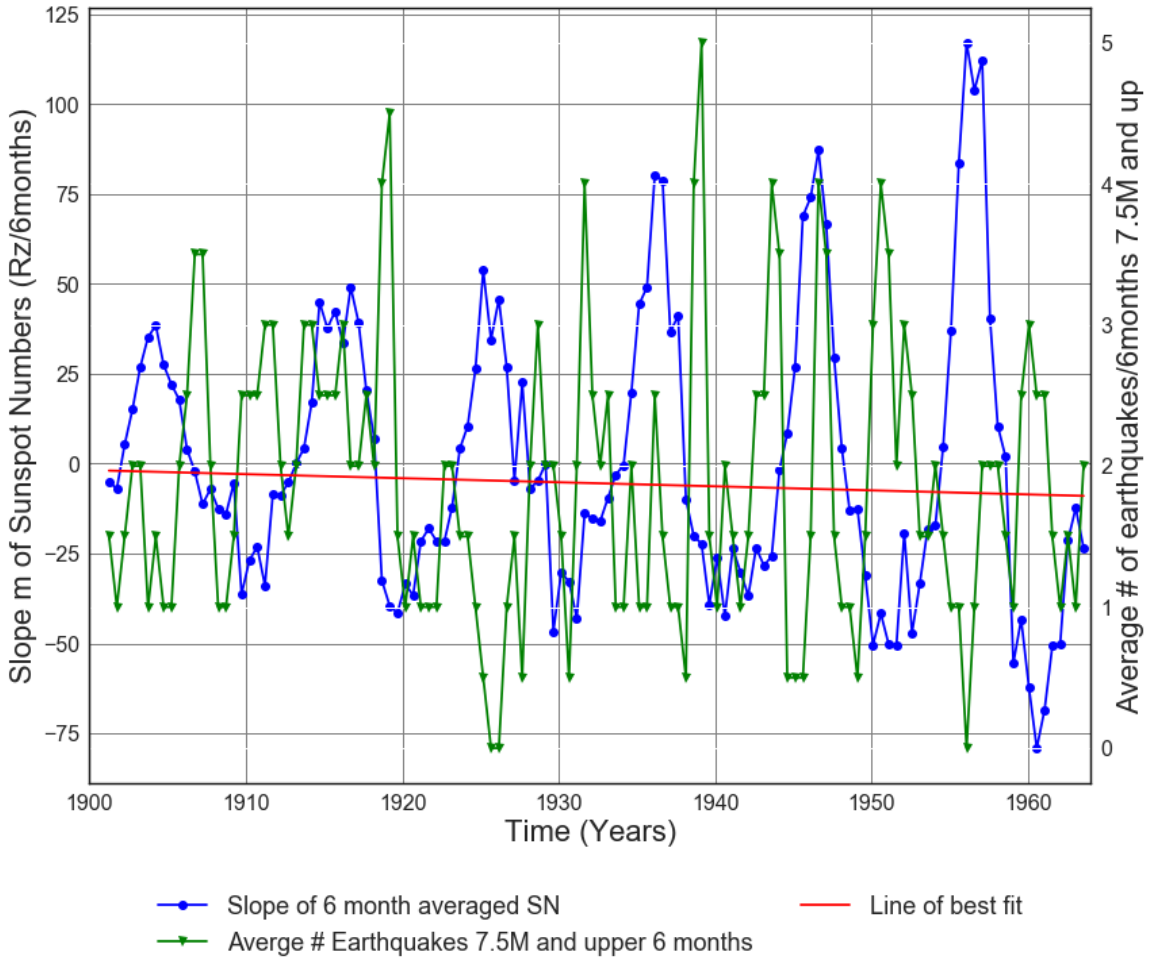

Figure B3.1: Slope of Solar cycle from 1900 to 1964 vs. Average number of 7.5M and up Earthquakes.

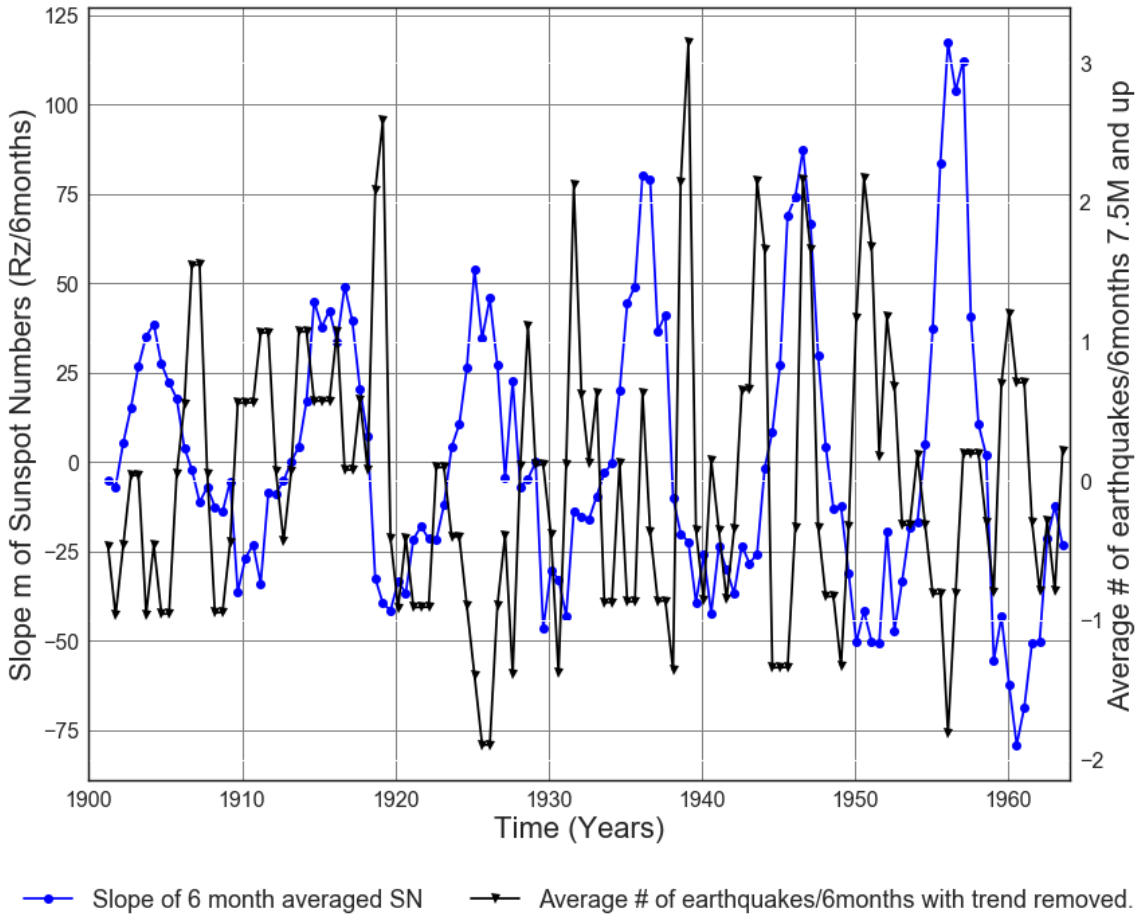

Figure B3.2: Slope of 6 month averaged SN 1900 to 1964 vs. Average number of 7.5M and up Earthquakes with trend removed. Line of best fit, y = -0.002874x + (7.432), mean x = 1.932e+03 +/- 18.27, mean y = 1.878 +/- 0.9955

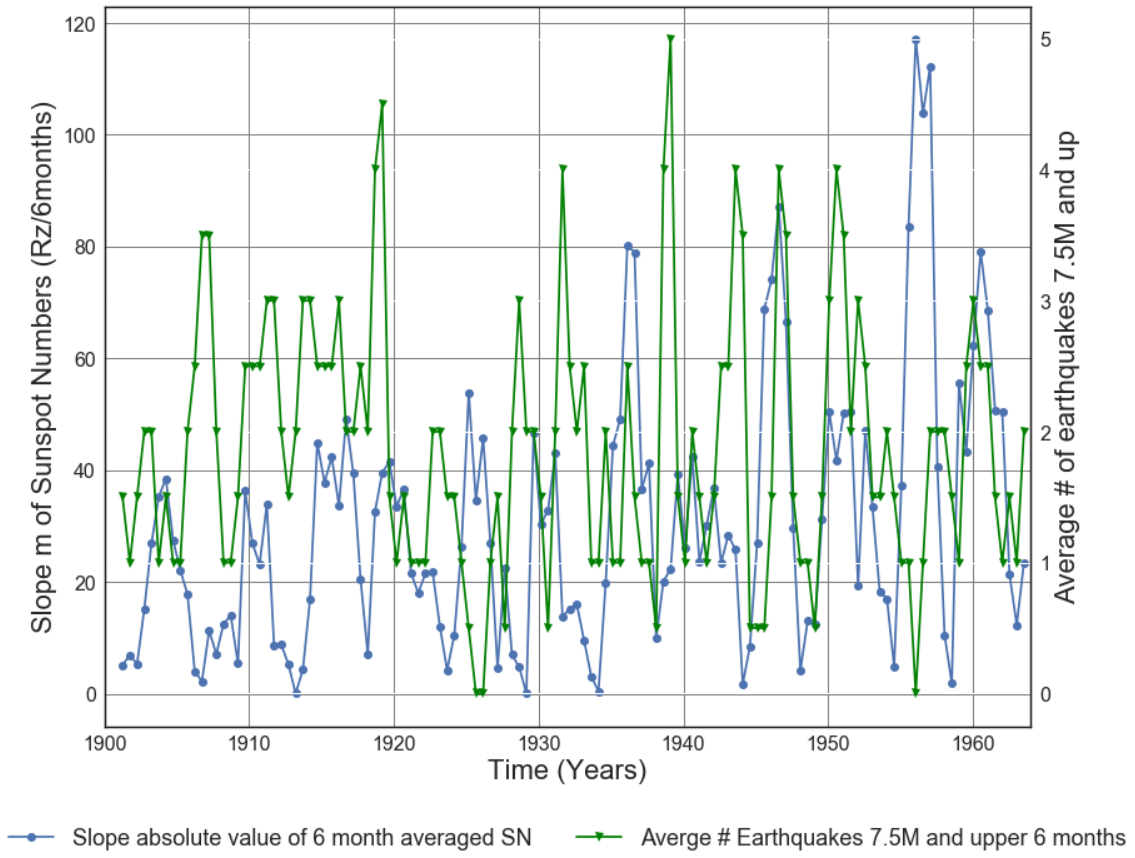

Figure B3.3: Slope Absolute value of Solar cycle from 1900 to 1964 vs. Average number of 7.5M and up Earthquakes.

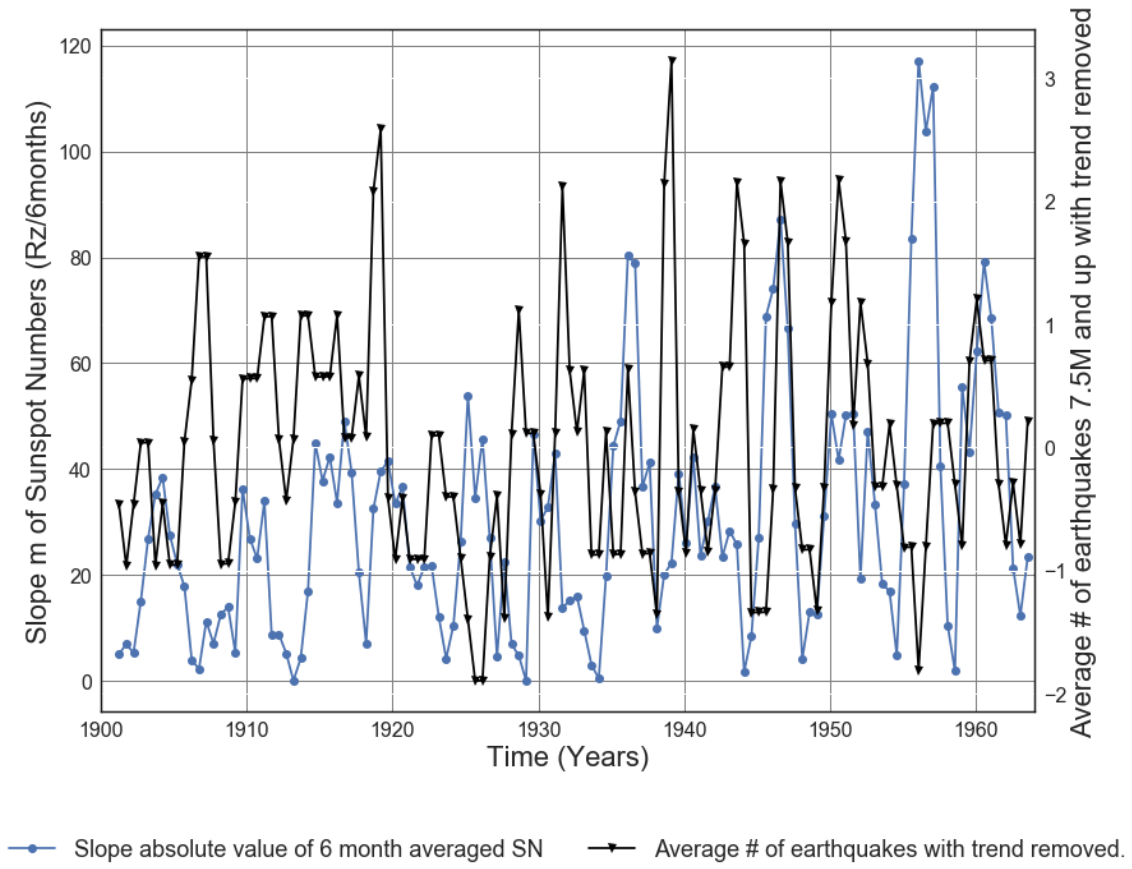

Figure B3.4: Slope Absolute value of Solar cycle from 1900 to 1964 vs. Average number of 7.5M and up earthquakes with trend removed.

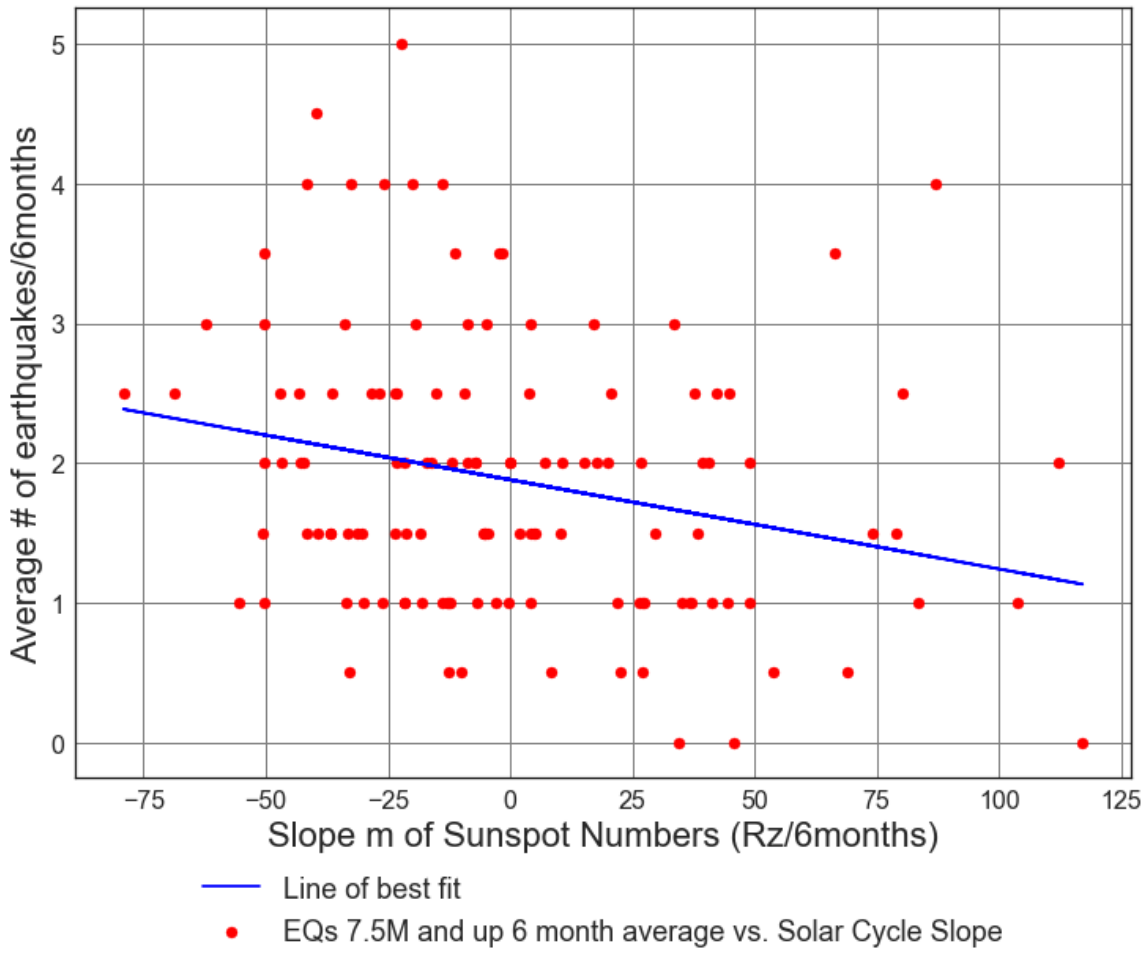

Figure B3.5: Scatter Plot of Solar cycle slope (from 1900 to 1964) vs. Average number of 7.5M and up Earthquakes/6months. Line of best fit, y = -0.006387x + (1.879), mean x = 0.3737 +/- 38.55, mean y = 1.877 +/- 0.9994, R = -0.2464, R squared = 0.0607, p-value = 0.005418.

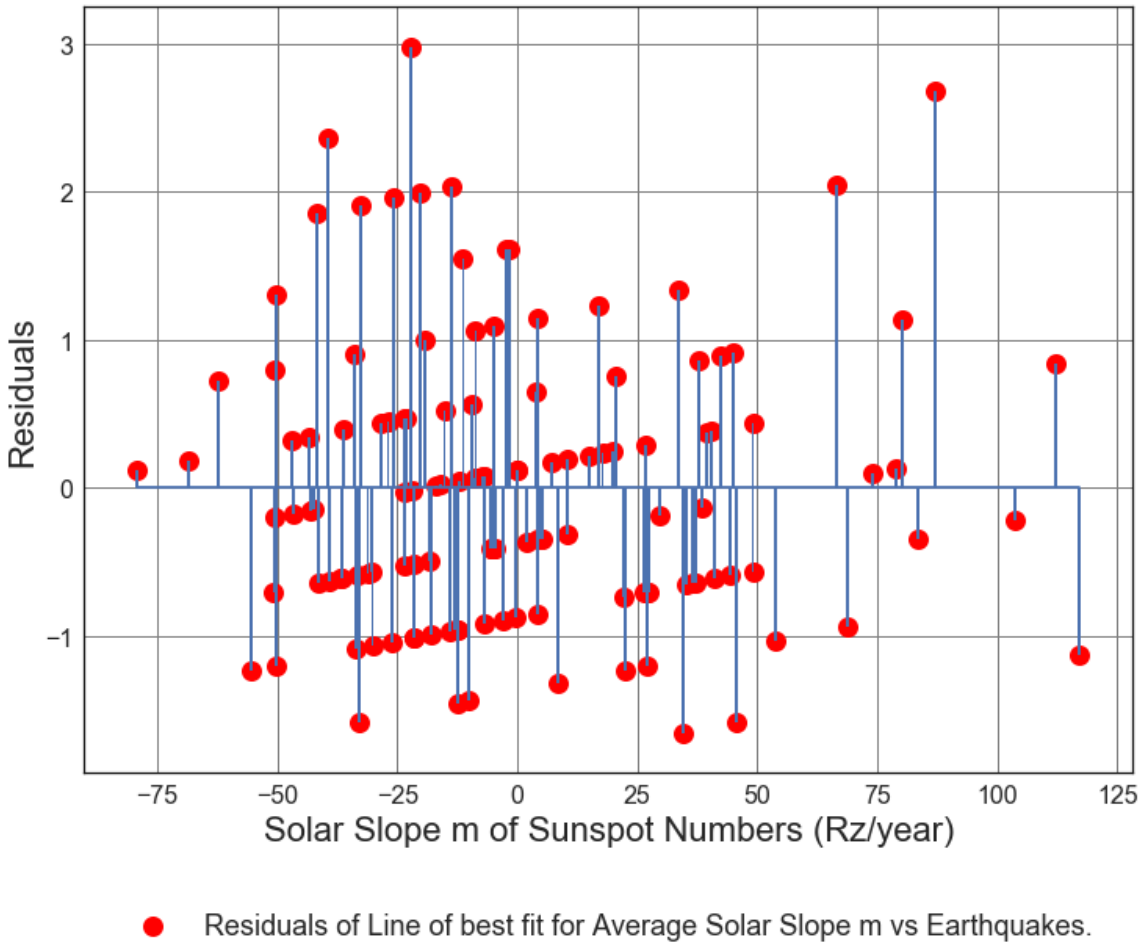

Figure B3.6: Residuals Plot of Solar cycle slope (from 1900 to 1964) vs. Average number of 7.5M and up Earthquakes/6months. Line of best fit, y = -0.006387x + (1.879), mean x = 0.3737 +/- 38.55, mean y = 1.877 +/- 0.9994, R = -0.2464, R squared = 0.0607, p-value = 0.005418.

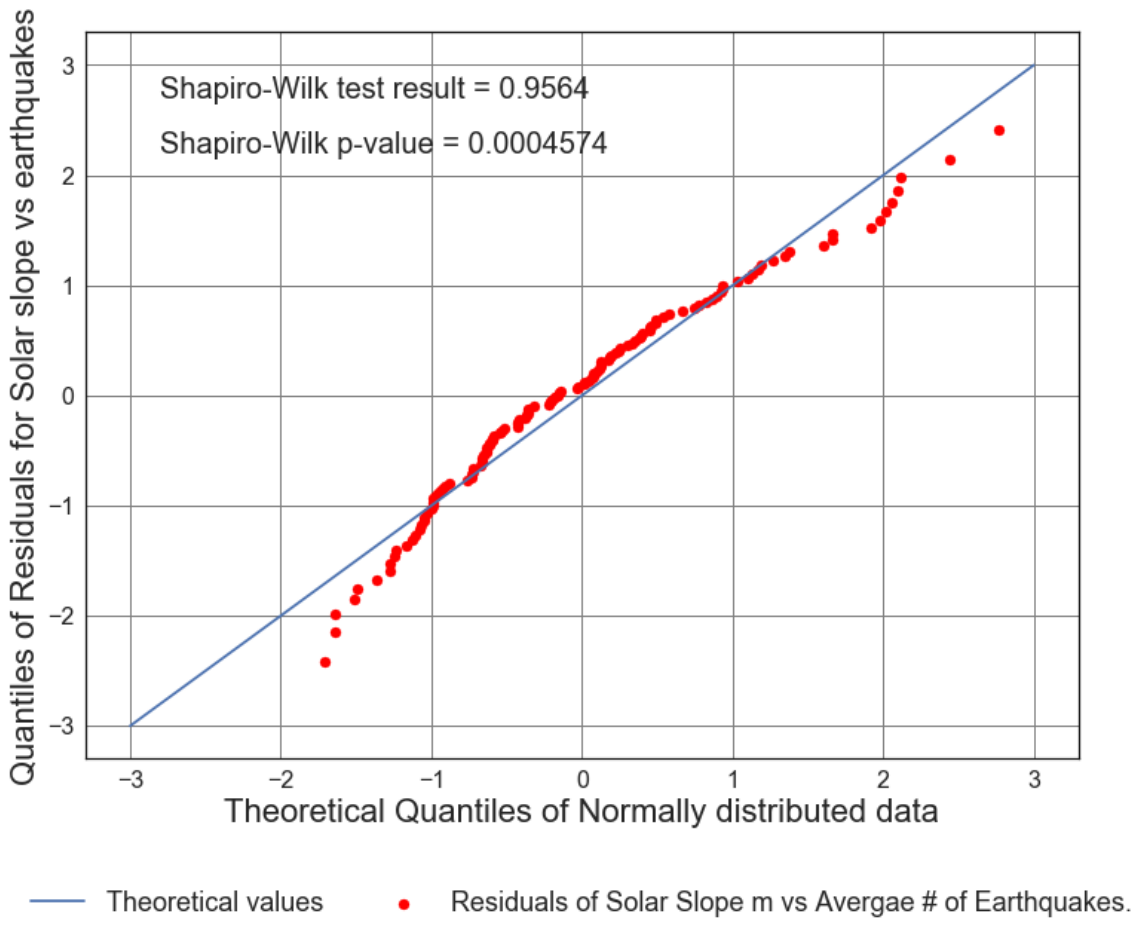

Figure B3.7: Residuals Plot of Solar cycle slope (from 1900 to 1964) vs. Average number of 7.5M and up Earthquakes/6months. Line of best fit, y = -0.006387x + (1.879), mean x = 0.3737 +/- 38.55, mean y = 1.877 +/- 0.9994, R = -0.2464, R squared = 0.0607, p-value = 0.005418.

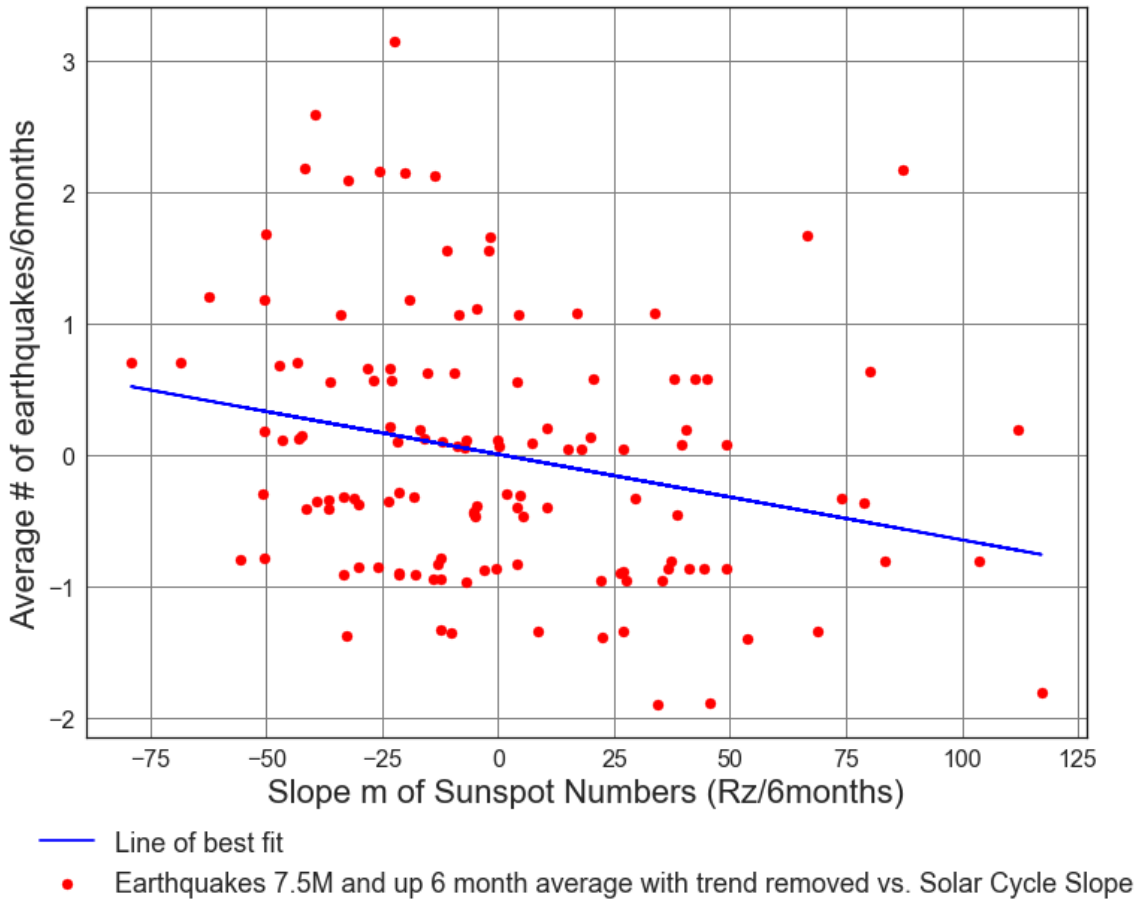

Figure B3.8: Scatter Plot of Solar cycle slope (from 1900 to 1964) vs. Average number of 7.5M and up Earthquakes/6months with trend removed. Line of best fit, y = -0.006511x + (0.002181), mean x = 0.3737 +/- 38.55, mean y = -0.0002525 +/- 0.998, R = -0.2515, R squared = 0.06324, p-value = 0.004503.

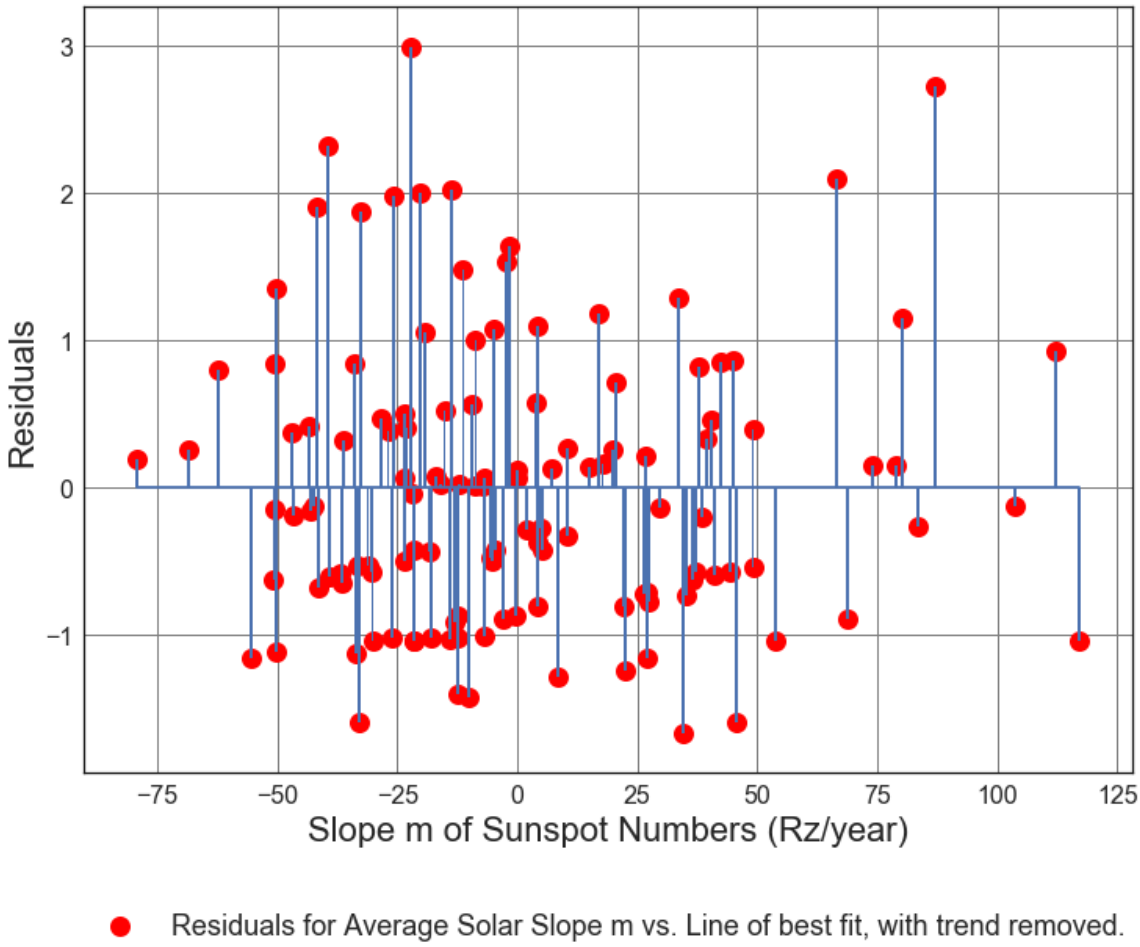

Figure B3.9: Scatter Plot of Solar cycle slope (from 1900 to 1964) vs. Average number of 7.5M and up Earthquakes/6months with trend removed. Line of best fit, y = -0.006511x + (0.002181), mean x = 0.3737 +/- 38.55, mean y = -0.0002525 +/- 0.998, R = -0.2515, R squared = 0.06324, p-value = 0.004503.

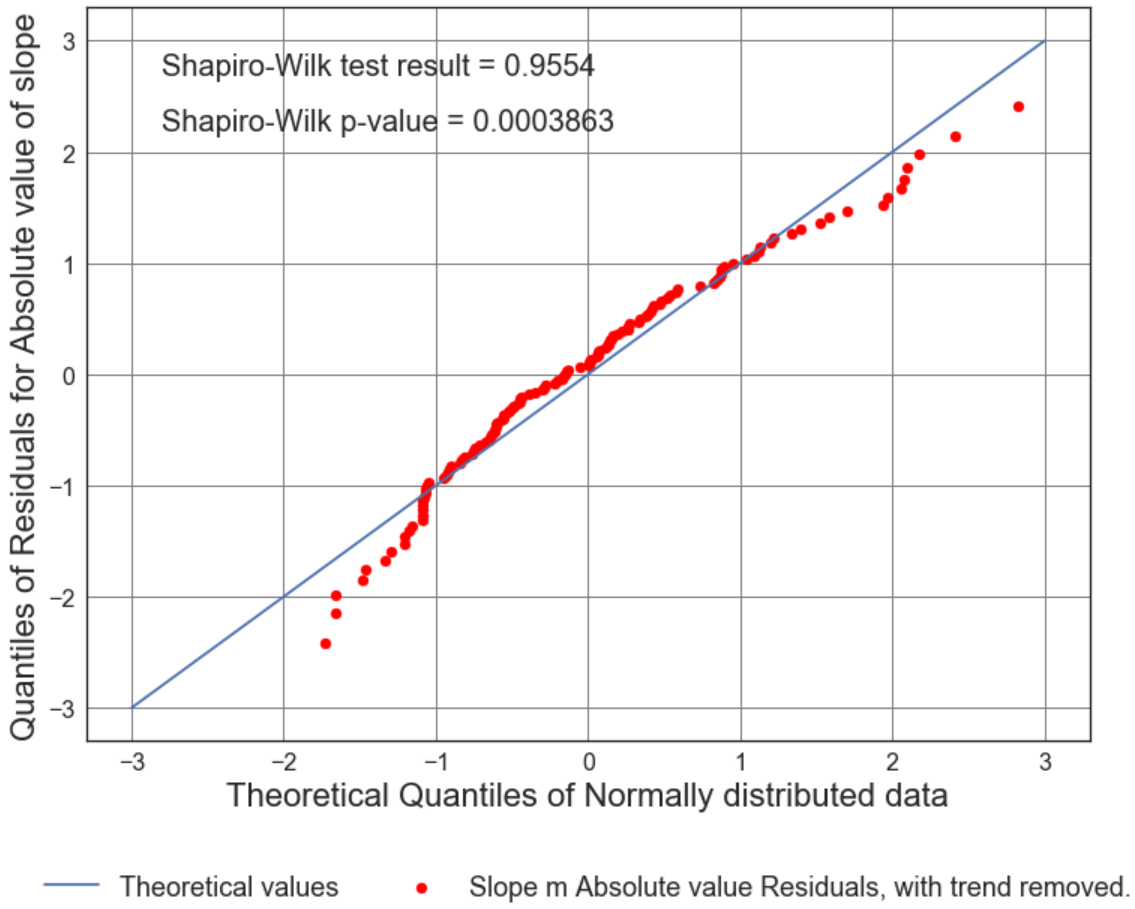

Figure B3.10: Scatter Plot of Solar cycle slope (from 1900 to 1964) vs. Average number of 7.5M and up Earthquakes/6months with trend removed. Line of best fit, y = -0.006511x + (0.002181), mean x = 0.3737 +/- 38.55, mean y = -0.0002525 +/- 0.998, R = -0.2515, R squared = 0.06324, p-value = 0.004503.

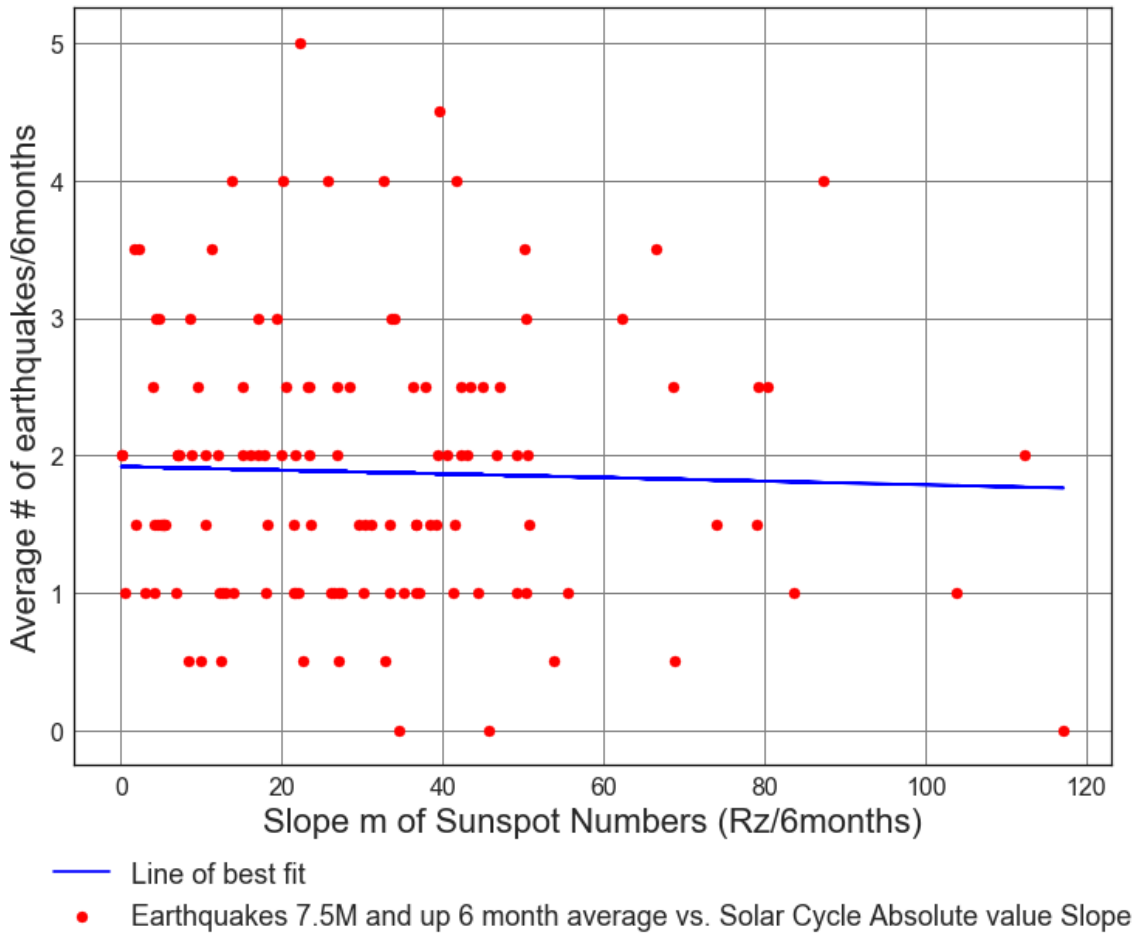

Figure B3.11: Scatter Plot of Solar cycle slope (from 1900 to 1964) vs. Average number of 7.5M and up Earthquakes/6months. Line of best fit, y = -0.001332x + (1.918), mean x = 30.43 +/- 23.66, mean y = 1.877 +/- 0.9994, R = -0.03154, R squared = 0.0009947, p-value = 0.7259.

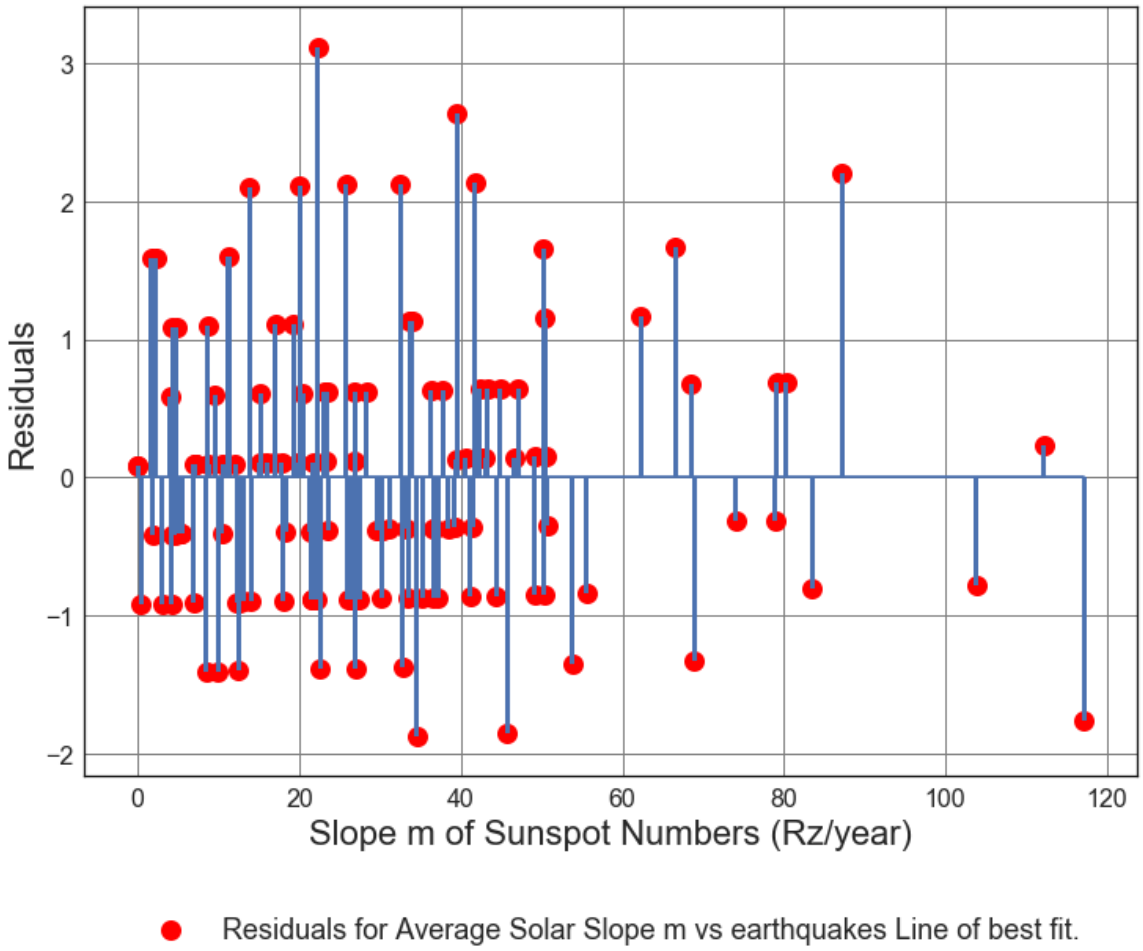

Figure B3.12: Scatter Plot of Solar cycle slope (from 1900 to 1964) vs. Average number of 7.5M and up Earthquakes/6months. Line of best fit, y = -0.001332x + (1.918), mean x = 30.43 +/- 23.66, mean y = 1.877 +/- 0.9994, R = -0.03154, R squared = 0.0009947, p-value = 0.7259.

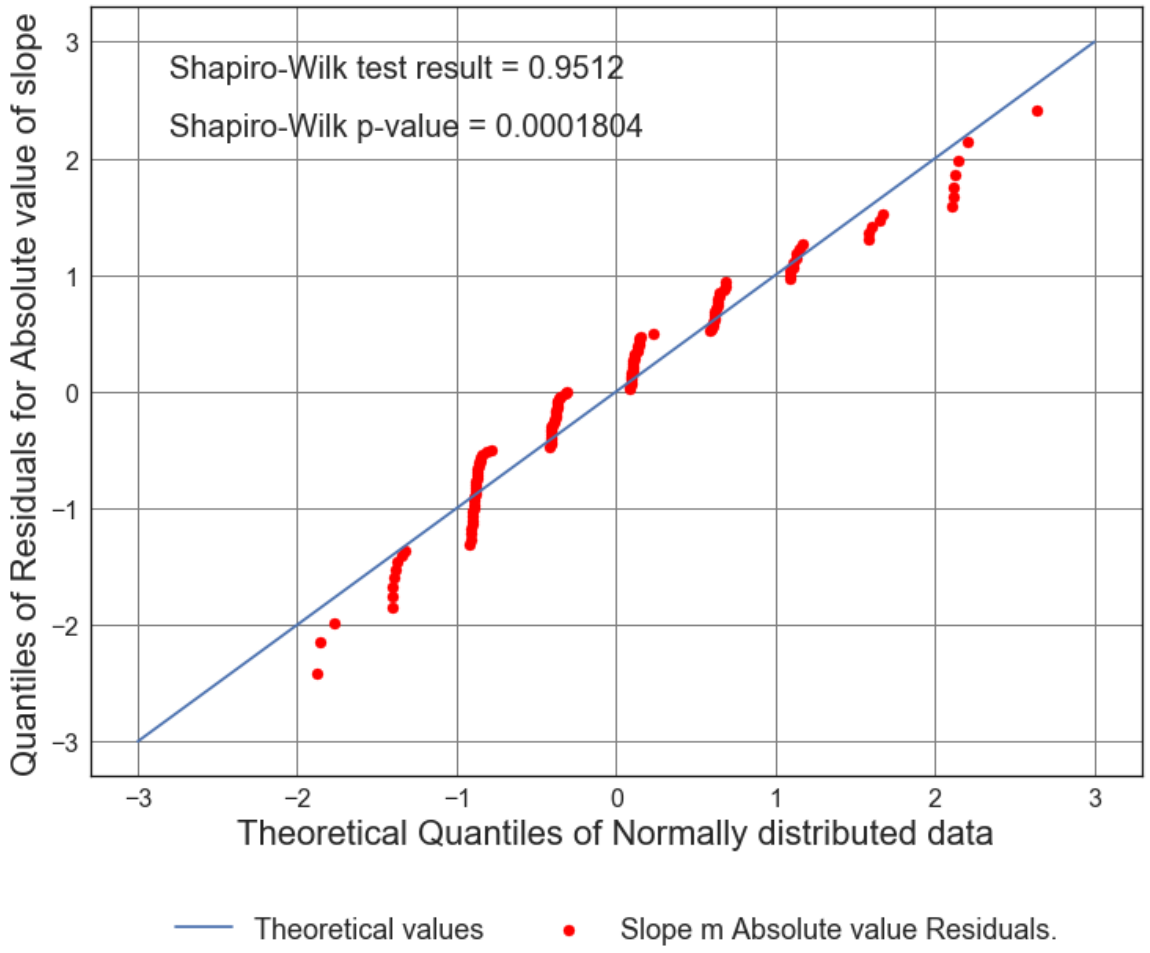

Figure B3.13: Scatter Plot of Solar cycle slope (from 1900 to 1964) vs. Average number of 7.5M and up Earthquakes/6months. Line of best fit, y = -0.001332x + (1.918), mean x = 30.43 +/- 23.66, mean y = 1.877 +/- 0.9994, R = -0.03154, R squared = 0.0009947, p-value = 0.7259.

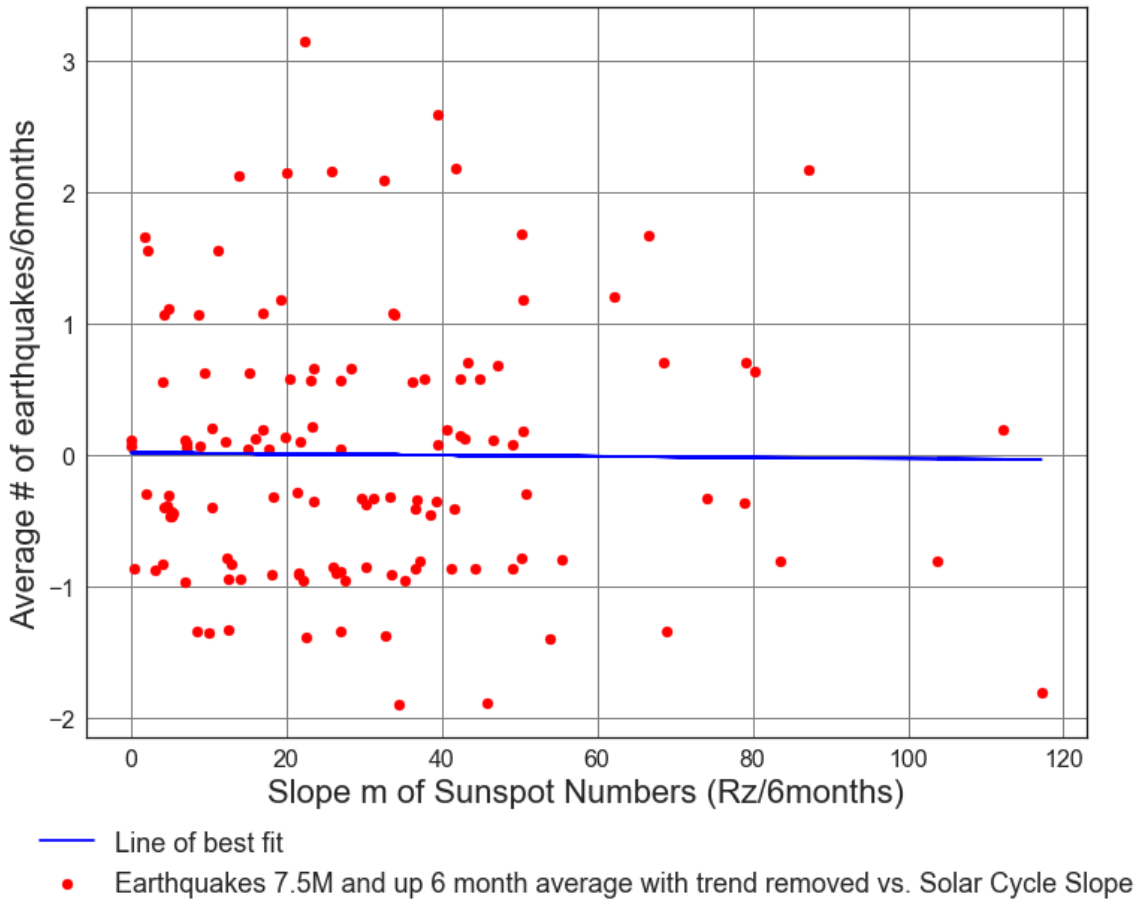

Figure B3.14: Scatter Plot of Solar cycle absolute value slope (from 1900 to 1964) vs. Average number of 7.5M and up Earthquakes/6months with trend removed. Line of best fit, y = -0.0004375x + (0.01306), mean x = 30.43 +/- 23.66, mean y = -0.0002525 +/- 0.998, R = -0.01037, R squared = 0.0001076, p-value = 0.9082.

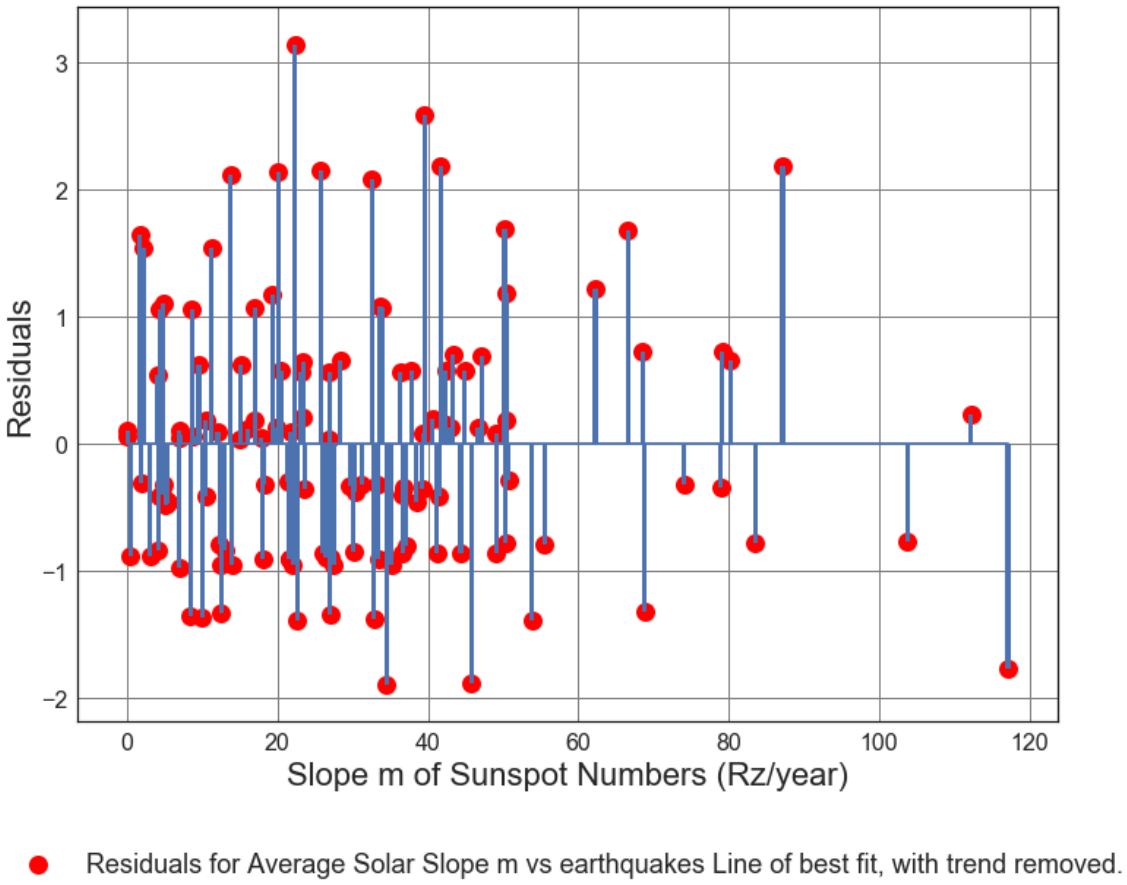

Figure B3.15: Scatter Plot of Solar cycle absolute value slope (from 1900 to 1964) vs. Average number of 7.5M and up Earthquakes/6months with trend removed. Line of best fit, y = -0.0004375x + (0.01306), mean x = 30.43 +/- 23.66, mean y = -0.0002525 +/- 0.998, R = -0.01037, R squared = 0.0001076, p-value = 0.9082.

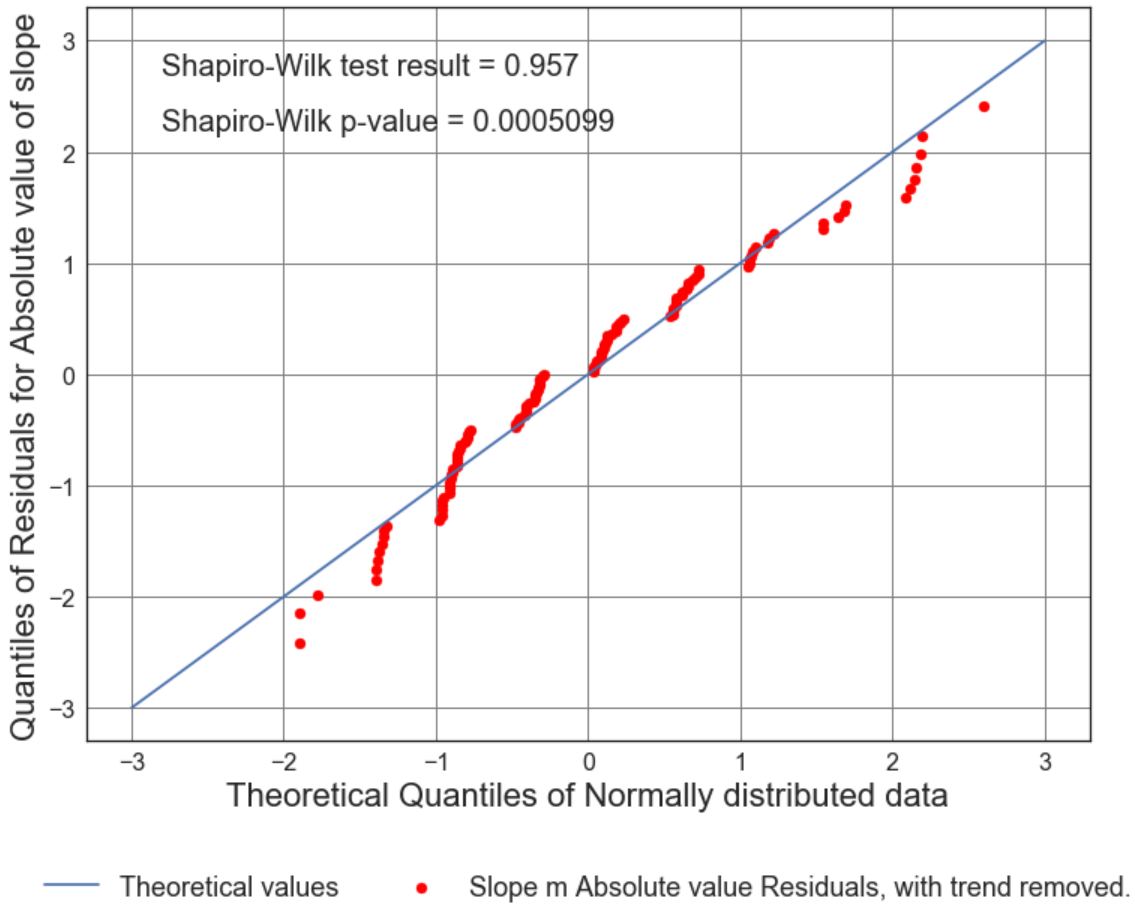

Figure B3.16: Scatter Plot of Solar cycle absolute value slope (from 1900 to 1964) vs. Average number of 7.5M and up Earthquakes/6months with trend removed. Line of best fit, y = -0.0004375x + (0.01306), mean x = 30.43 +/- 23.66, mean y = -0.0002525 +/- 0.998, R = -0.01037, R squared = 0.0001076, p-value = 0.9082.

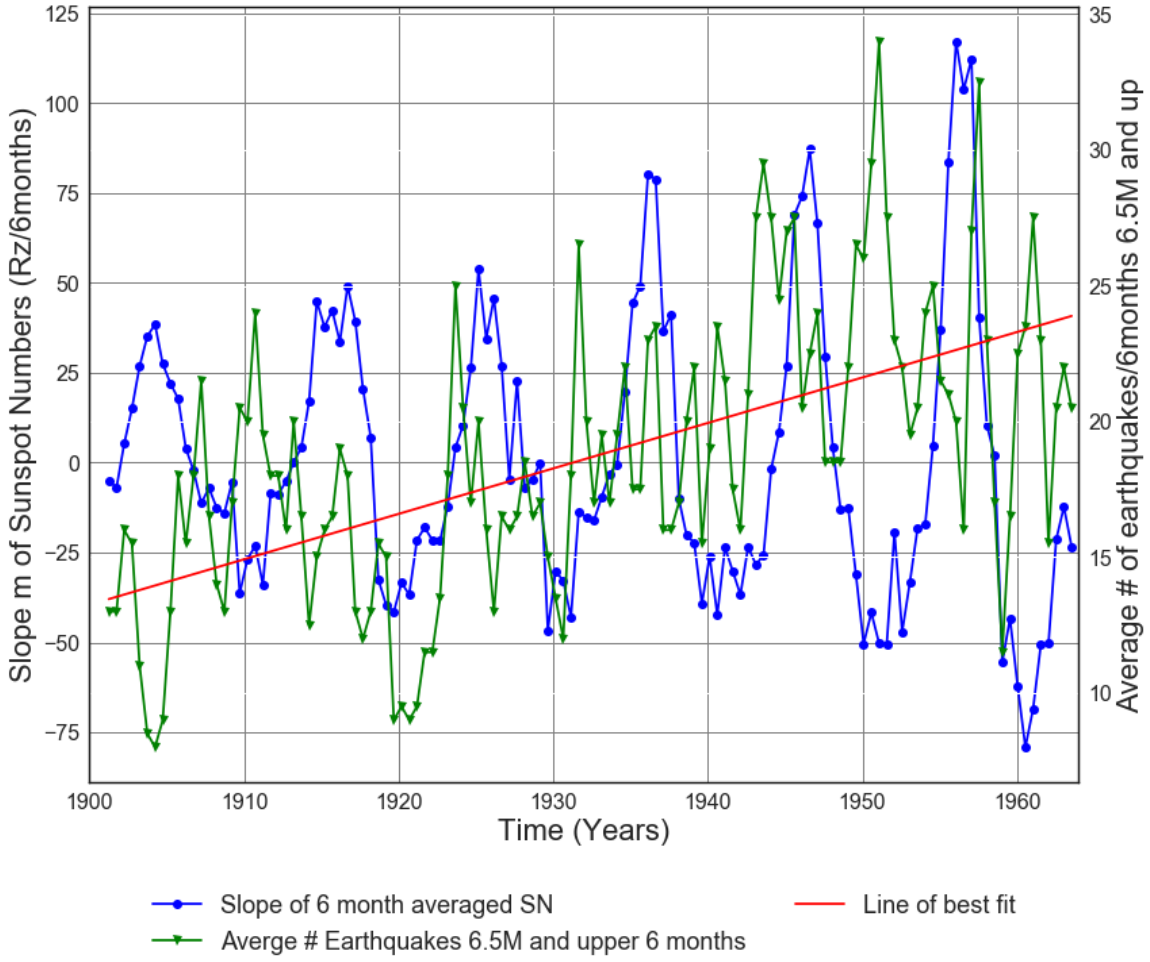

Figure B3.17: Slope of Solar cycle from 1900 to 1964 vs. Average number of 6.5M and up Earthquakes.

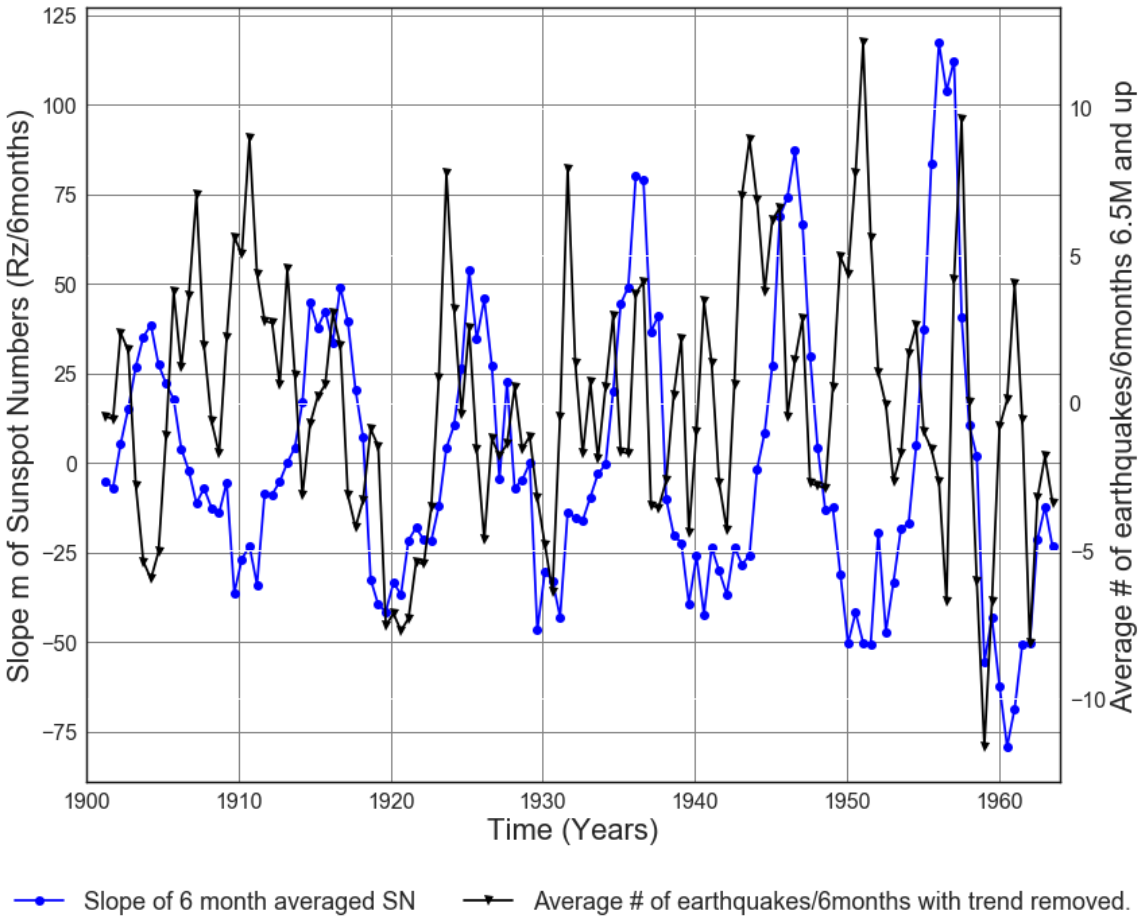

Figure B3.18: Slope of 6 month averaged SN 1900 to 1964 vs. Average number of 6.5M and up Earthquakes with trend removed. Line of best fit, y = 0.1675x + (-305.0), mean x = 1.932e+03 +/- 18.27, mean y = 18.63 +/- 5.213

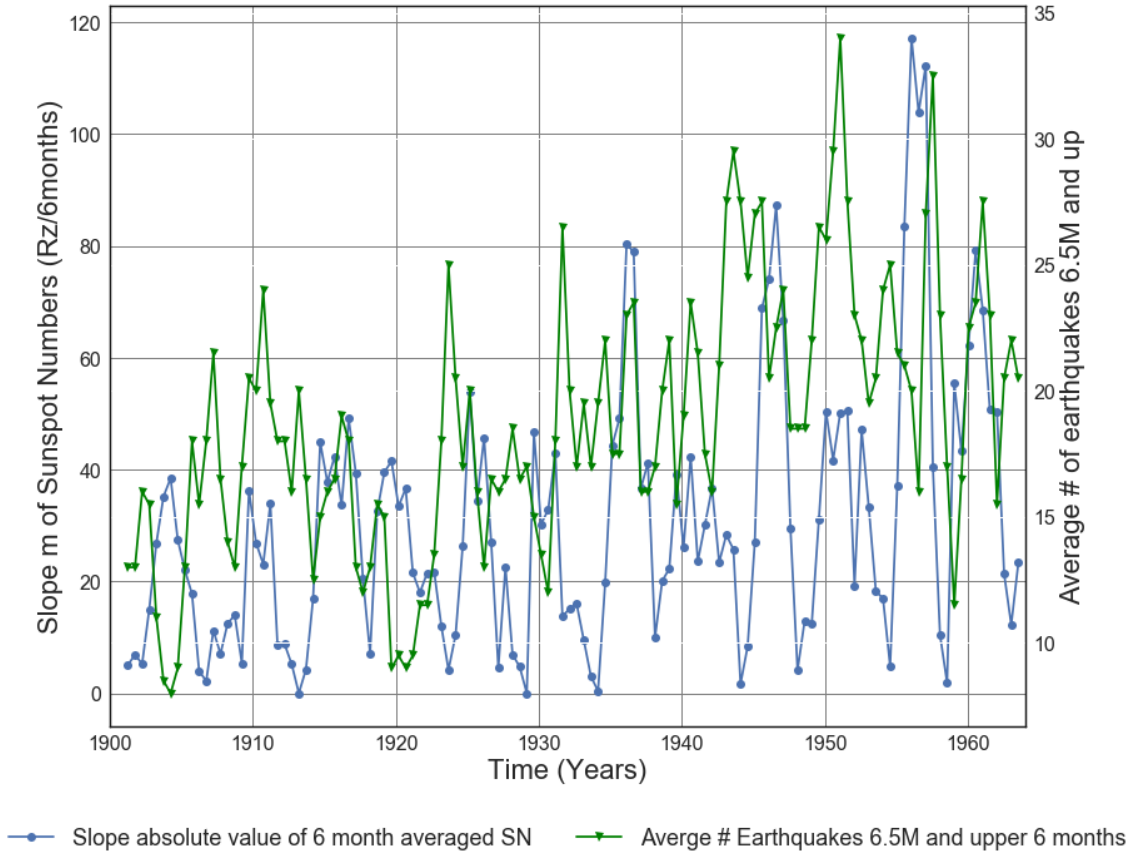

Figure B3.19: Slope Absolute value of Solar cycle from 1900 to 1964 vs. Average number of 6.5M and up Earthquakes.

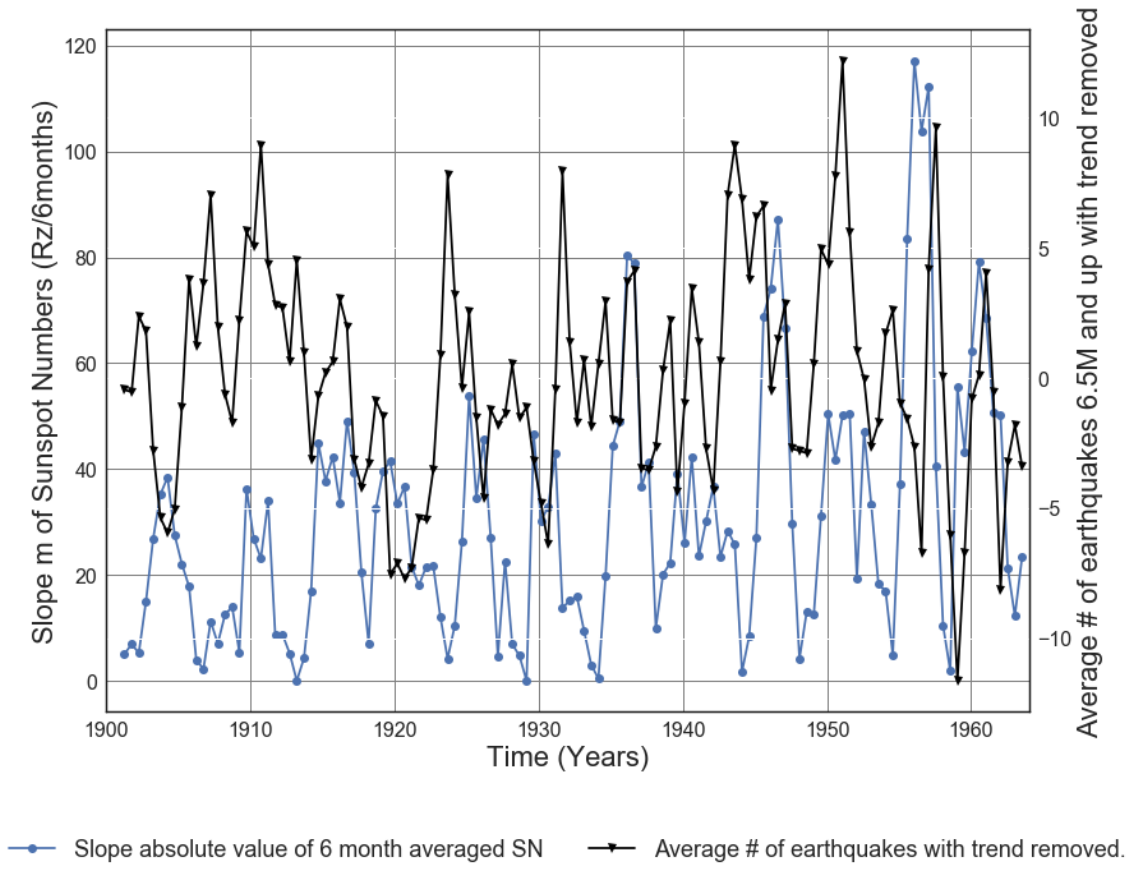

Figure B3.20: Slope Absolute value of Solar cycle from 1900 to 1964 vs. Average number of 6.5M and up earthquakes with trend removed.

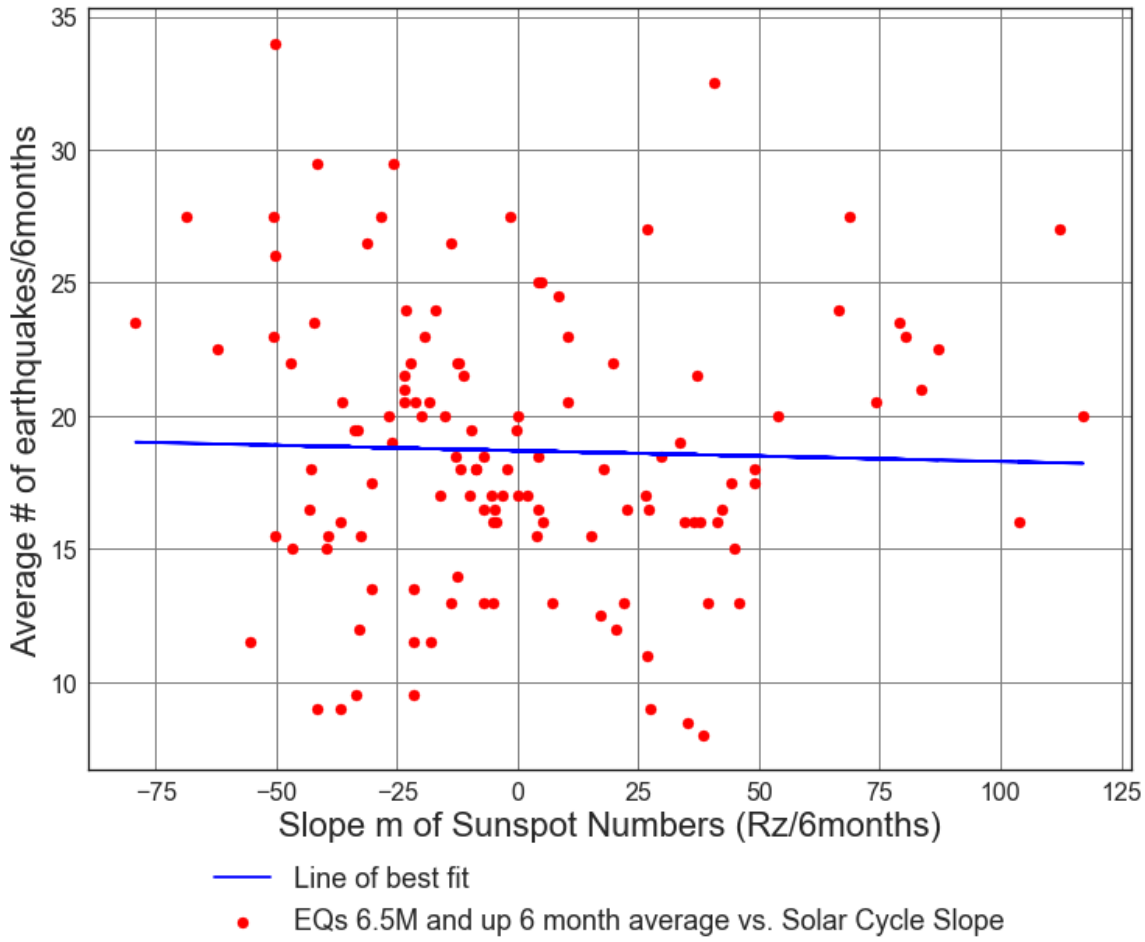

Figure B3.21: Scatter Plot of Solar cycle slope (from 1900 to 1964) vs. Average number of 6.5M and up Earthquakes/6months. Line of best fit, y = -0.004072x + (18.7), mean x = 0.3737 +/- 38.55, mean y = 18.69 +/- 5.183, R = -0.03028, R squared = 0.0009171, p-value = 0.7364.

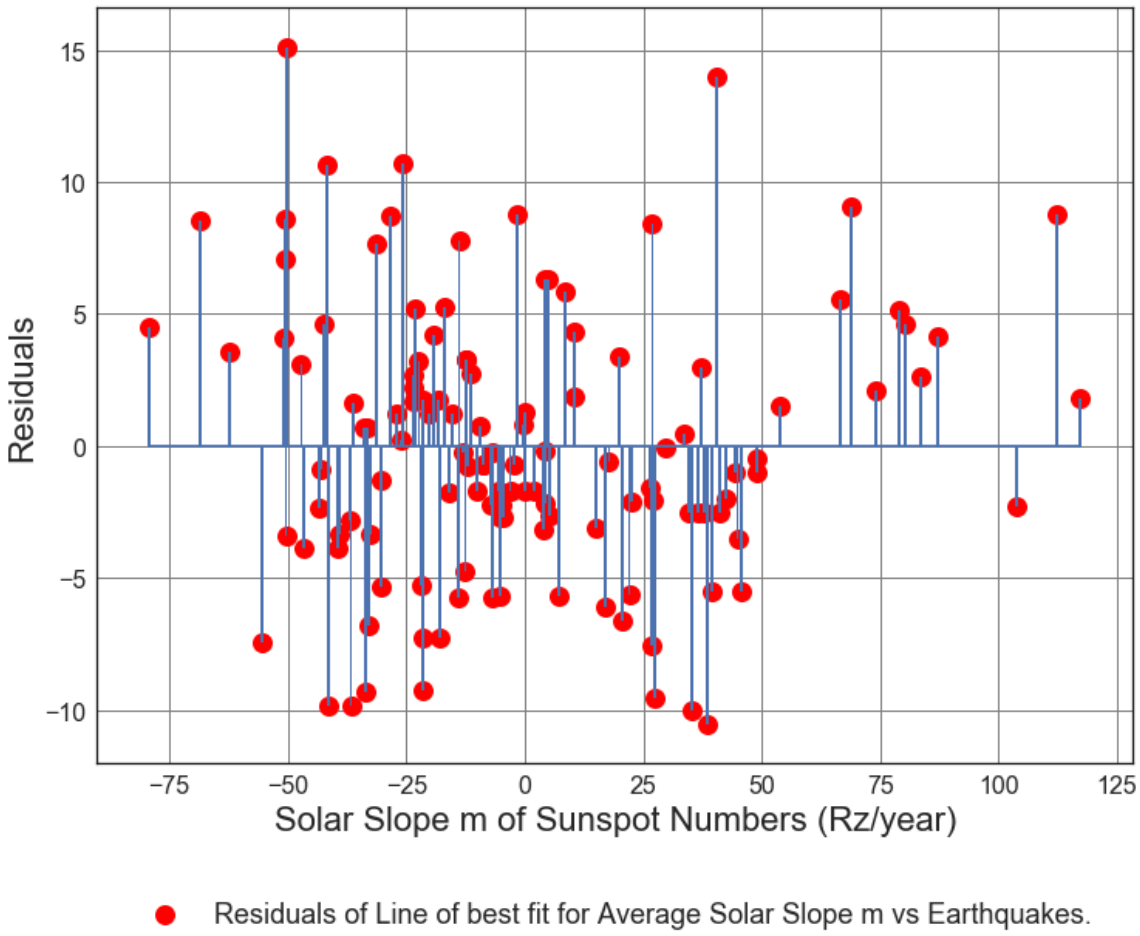

Figure B3.22: Residuals Plot of Solar cycle slope (from 1900 to 1964) vs. Average number of 6.5M and up Earthquakes/6months. Line of best fit, y = -0.004072x + (18.7), mean x = 0.3737 +/- 38.55, mean y = 18.69 +/- 5.183, R = -0.03028, R squared = 0.0009171, p-value = 0.7364.

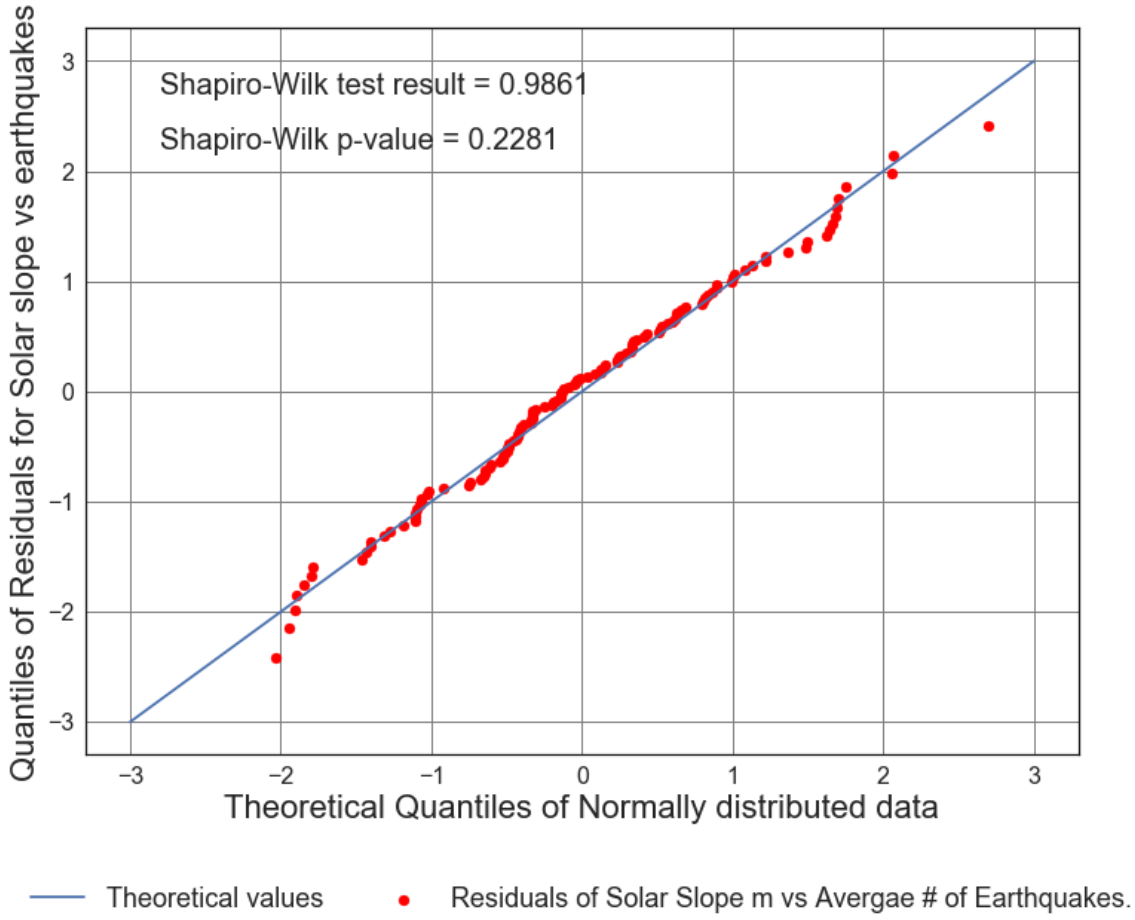

Figure B3.23: Residuals Plot of Solar cycle slope (from 1900 to 1964) vs. Average number of 6.5M and up Earthquakes/6months. Line of best fit, y = -0.004072x + (18.7), mean x = 0.3737 +/- 38.55, mean y = 18.69 +/- 5.183, R = -0.03028, R squared = 0.0009171, p-value = 0.7364.

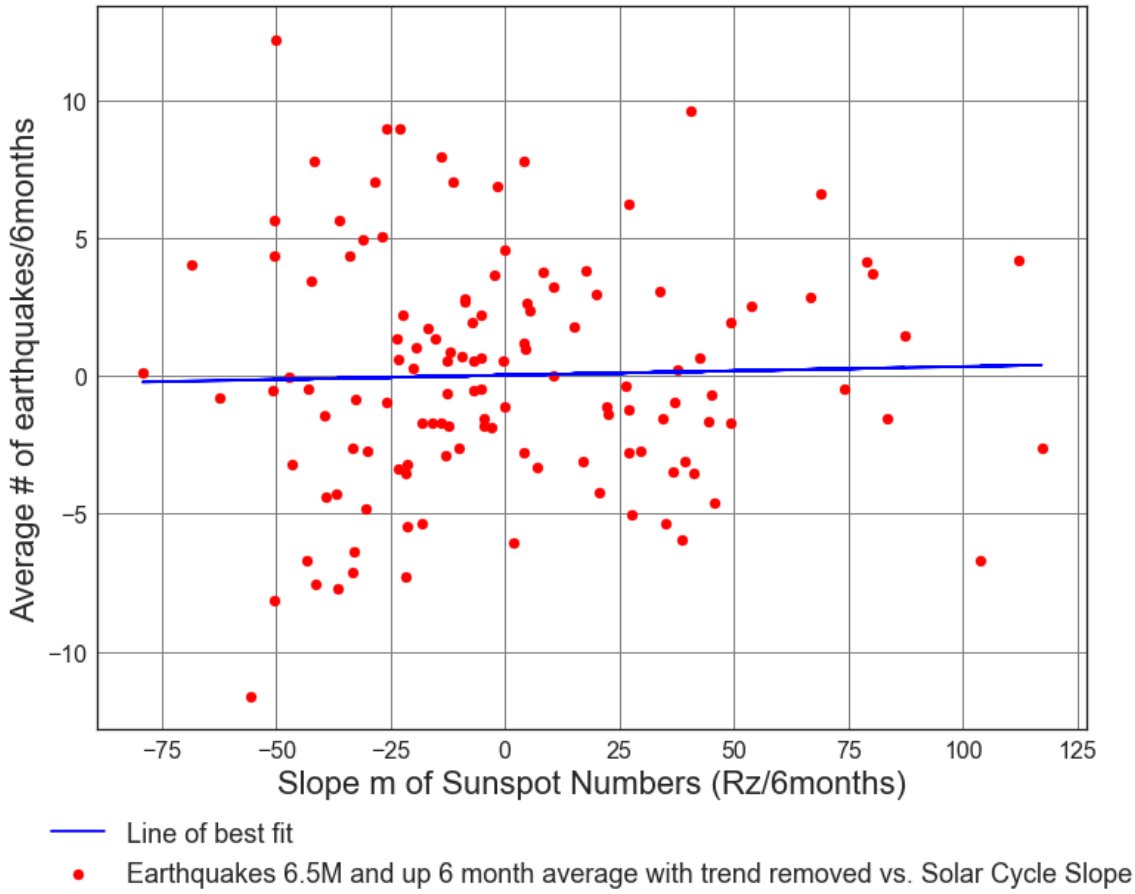

Figure B3.24: Scatter Plot of Solar cycle slope (from 1900 to 1964) vs. Average number of 6.5M and up Earthquakes/6months with trend removed. Line of best fit, y = 0.003132x + (0.02162), mean x = 0.3737 +/- 38.55, mean y = 0.02279 +/- 4.229, R = 0.02855, R squared = 0.000815, p-value = 0.751.

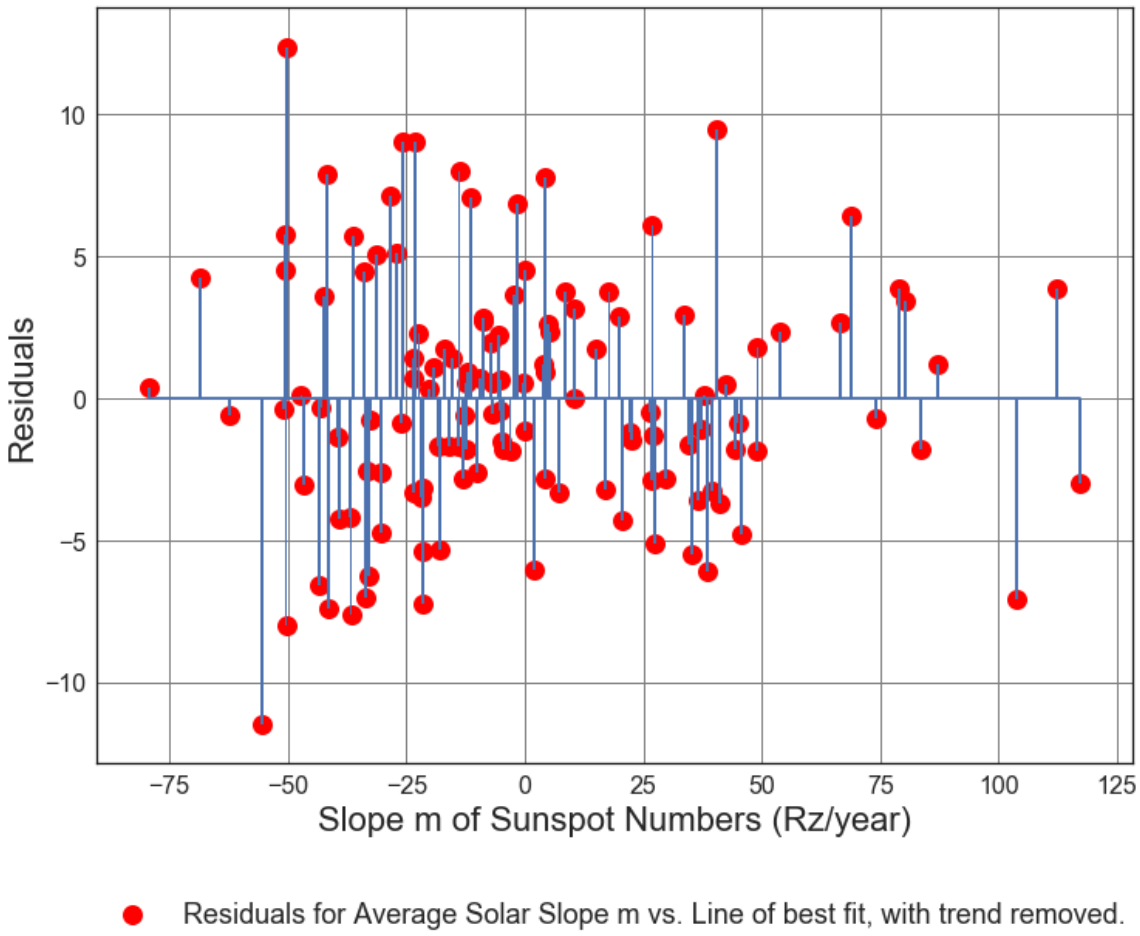

Figure B3.25: Scatter Plot of Solar cycle slope (from 1900 to 1964) vs. Average number of 6.5M and up Earthquakes/6months with trend removed. Line of best fit, y = 0.003132x + (0.02162), mean x = 0.3737 +/- 38.55, mean y = 0.02279 +/- 4.229, R = 0.02855, R squared = 0.000815, p-value = 0.751.

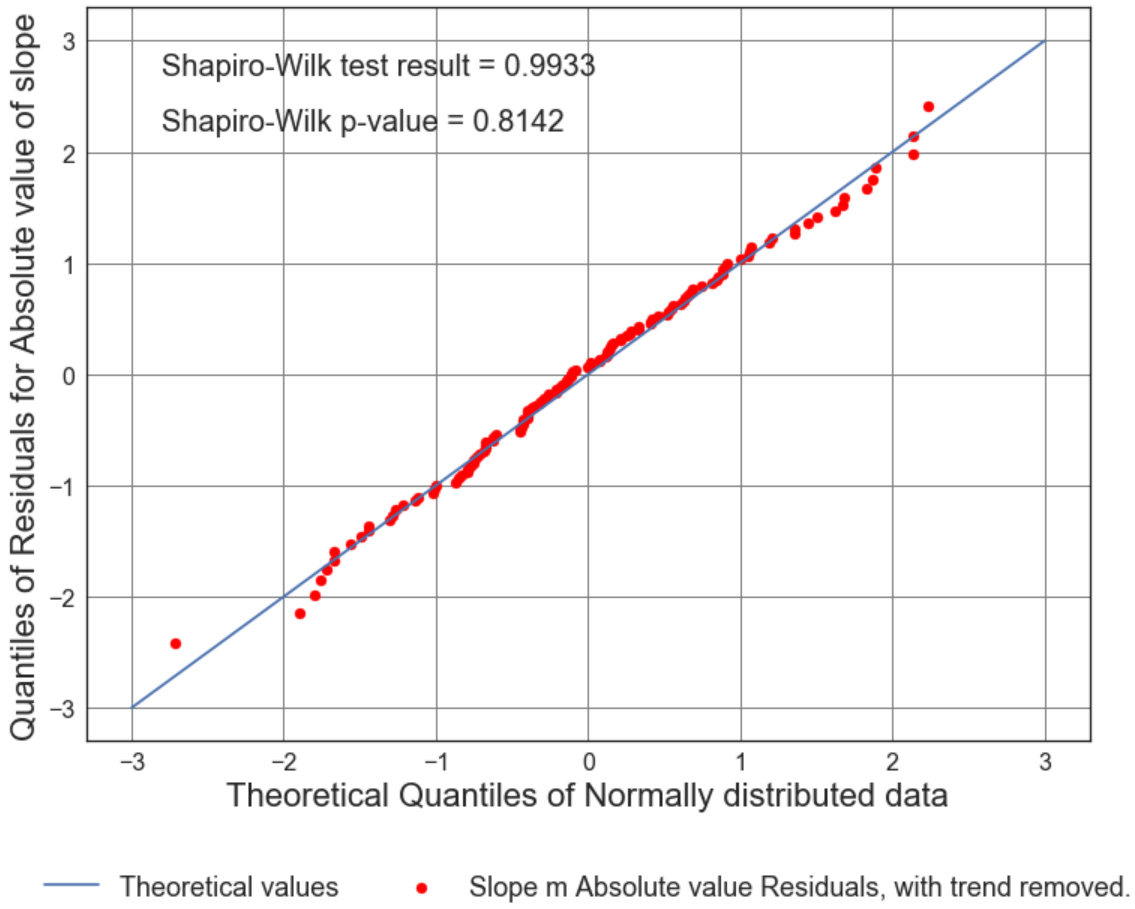

Figure B3.26: Scatter Plot of Solar cycle slope (from 1900 to 1964) vs. Average number of 6.5M and up Earthquakes/6months with trend removed. Line of best fit, y = 0.003132x + (0.02162), mean x = 0.3737 +/- 38.55, mean y = 0.02279 +/- 4.229, R = 0.02855, R squared = 0.000815, p-value = 0.751.

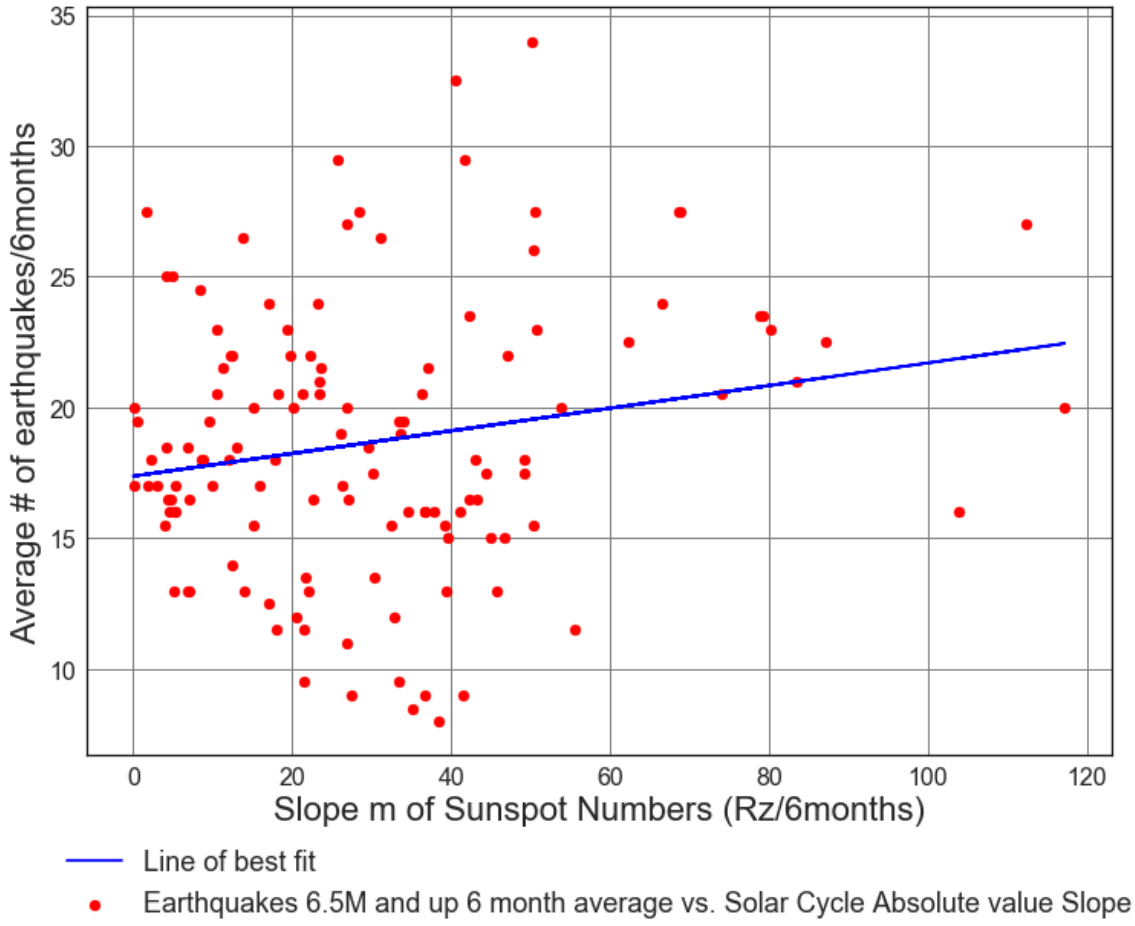

Figure B3.27: Scatter Plot of Solar cycle slope (from 1900 to 1964) vs. Average number of 6.5M and up Earthquakes/6months. Line of best fit, y = 0.04329x + (17.38), mean x = 30.43 +/- 23.66, mean y = 18.69 +/- 5.183, R = 0.1977, R squared = 0.03908, p-value = 0.02651.

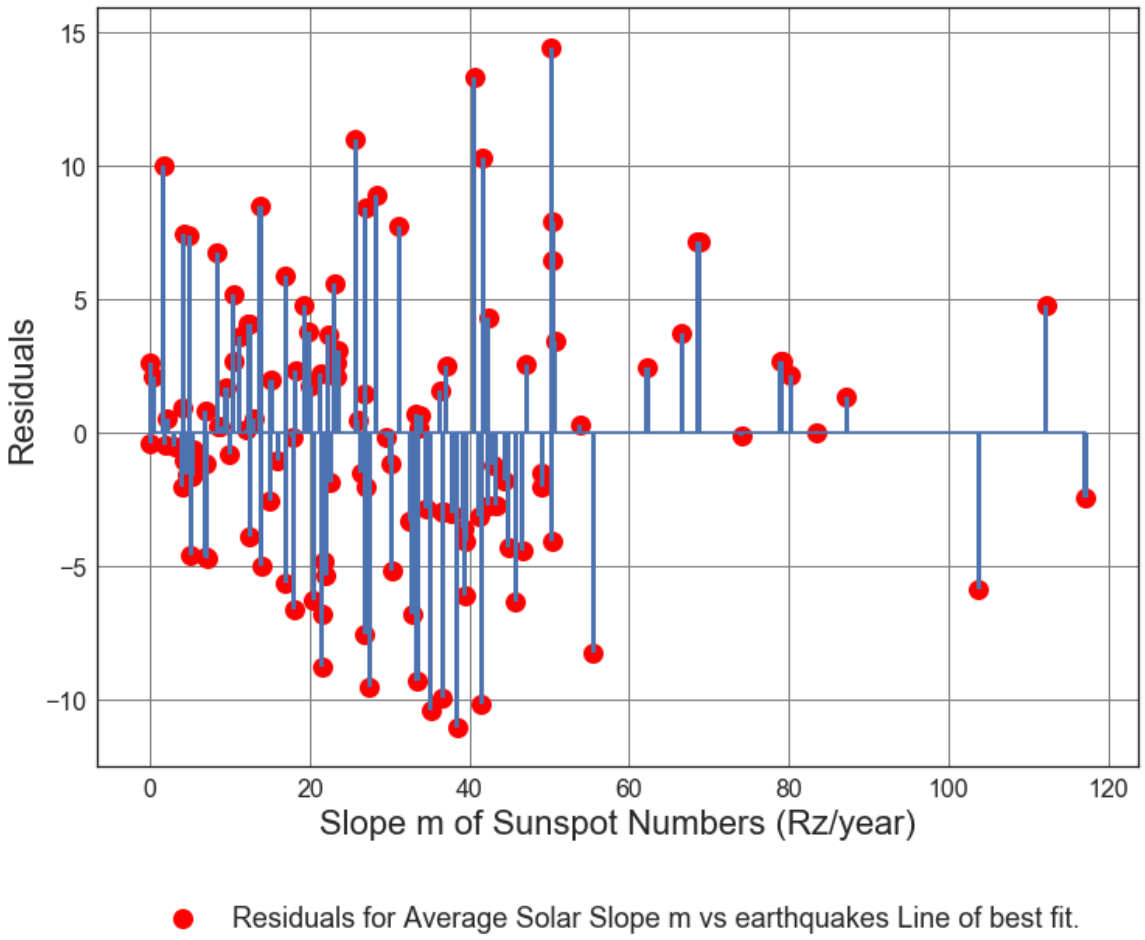

Figure B3.28: Scatter Plot of Solar cycle slope (from 1900 to 1964) vs. Average number of 6.5M and up Earthquakes/6months. Line of best fit, y = 0.04329x + (17.38), mean x = 30.43 +/- 23.66, mean y = 18.69 +/- 5.183, R = 0.1977, R squared = 0.03908, p-value = 0.02651.

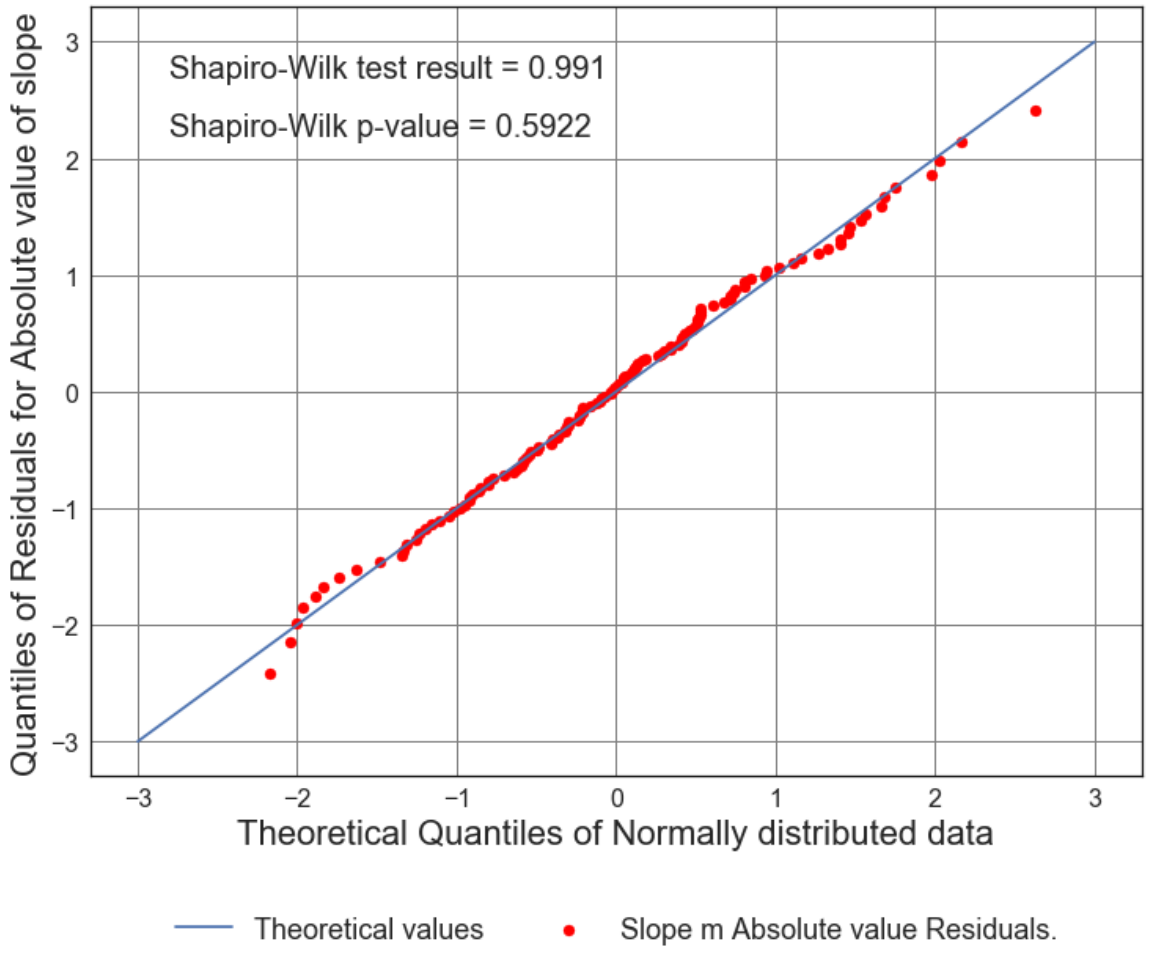

Figure B3.29: Scatter Plot of Solar cycle slope (from 1900 to 1964) vs. Average number of 6.5M and up Earthquakes/6months. Line of best fit, y = 0.04329x + (17.38), mean x = 30.43 +/- 23.66, mean y = 18.69 +/- 5.183, R = 0.1977, R squared = 0.03908, p-value = 0.02651.

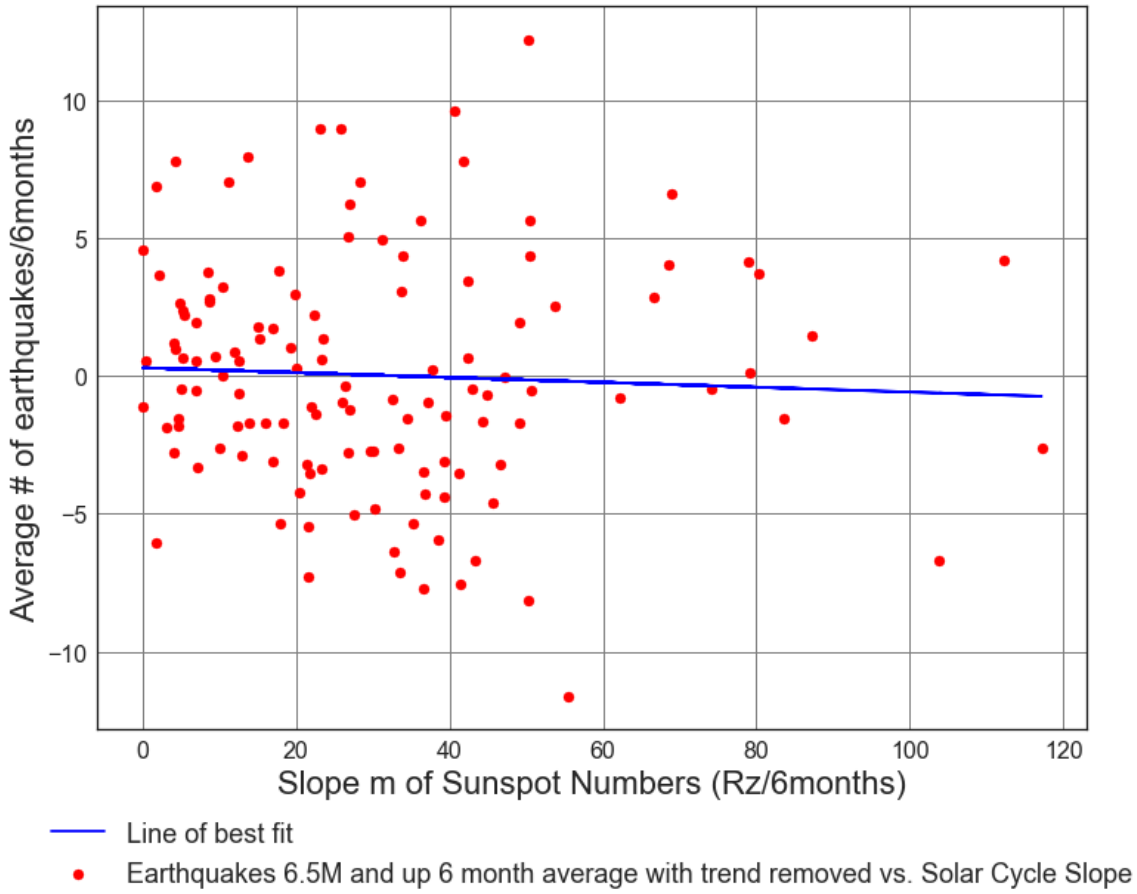

Figure B3.30: Scatter Plot of Solar cycle absolute value slope (from 1900 to 1964) vs. Average number of 6.5M and up Earthquakes/6months with trend removed. Line of best fit, y = -0.008831x + (0.2915), mean x = 30.43 +/- 23.66, mean y = 0.02279 +/- 4.229, R = -0.04941, R squared = 0.002441, p-value = 0.5827.

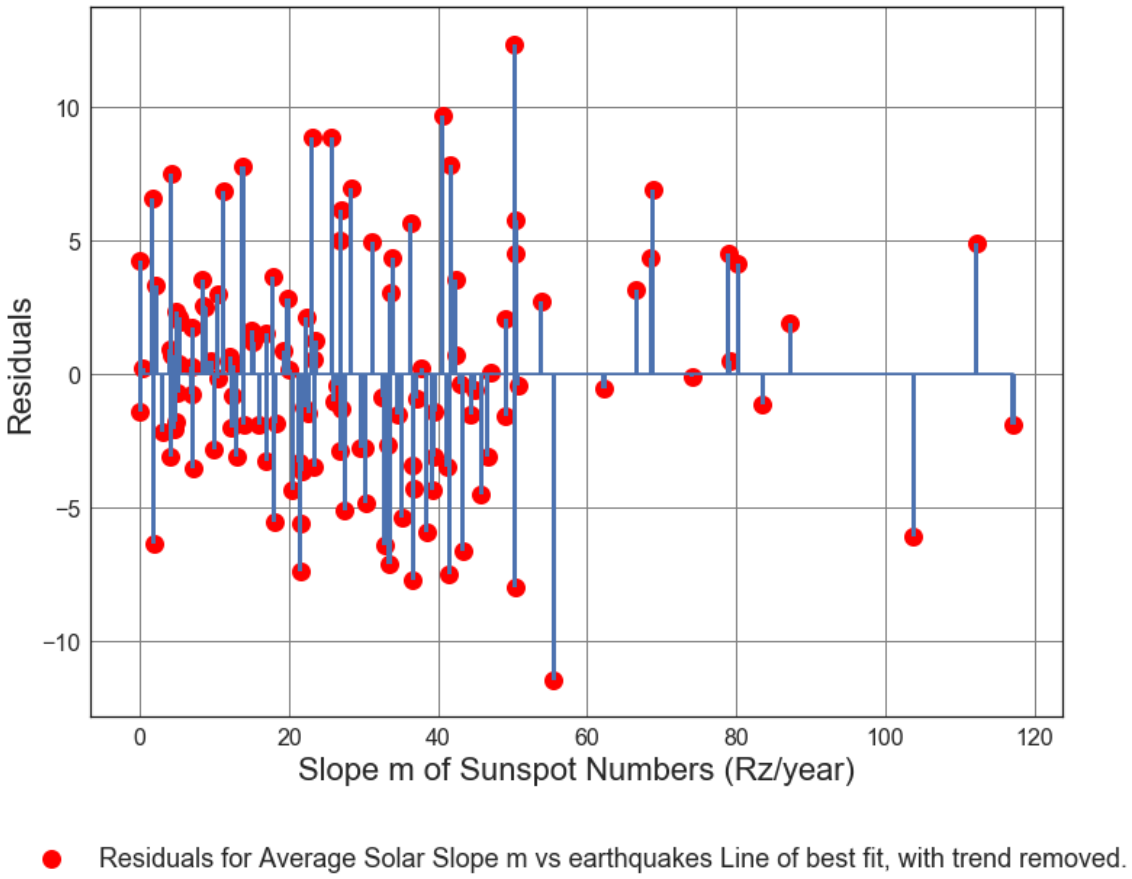

Figure B3.31: Scatter Plot of Solar cycle absolute value slope (from 1900 to 1964) vs. Average number of 6.5M and up Earthquakes/6months with trend removed. Line of best fit, y = -0.008831x + (0.2915), mean x = 30.43 +/- 23.66, mean y = 0.02279 +/- 4.229, R = -0.04941, R squared = 0.002441, p-value = 0.5827.

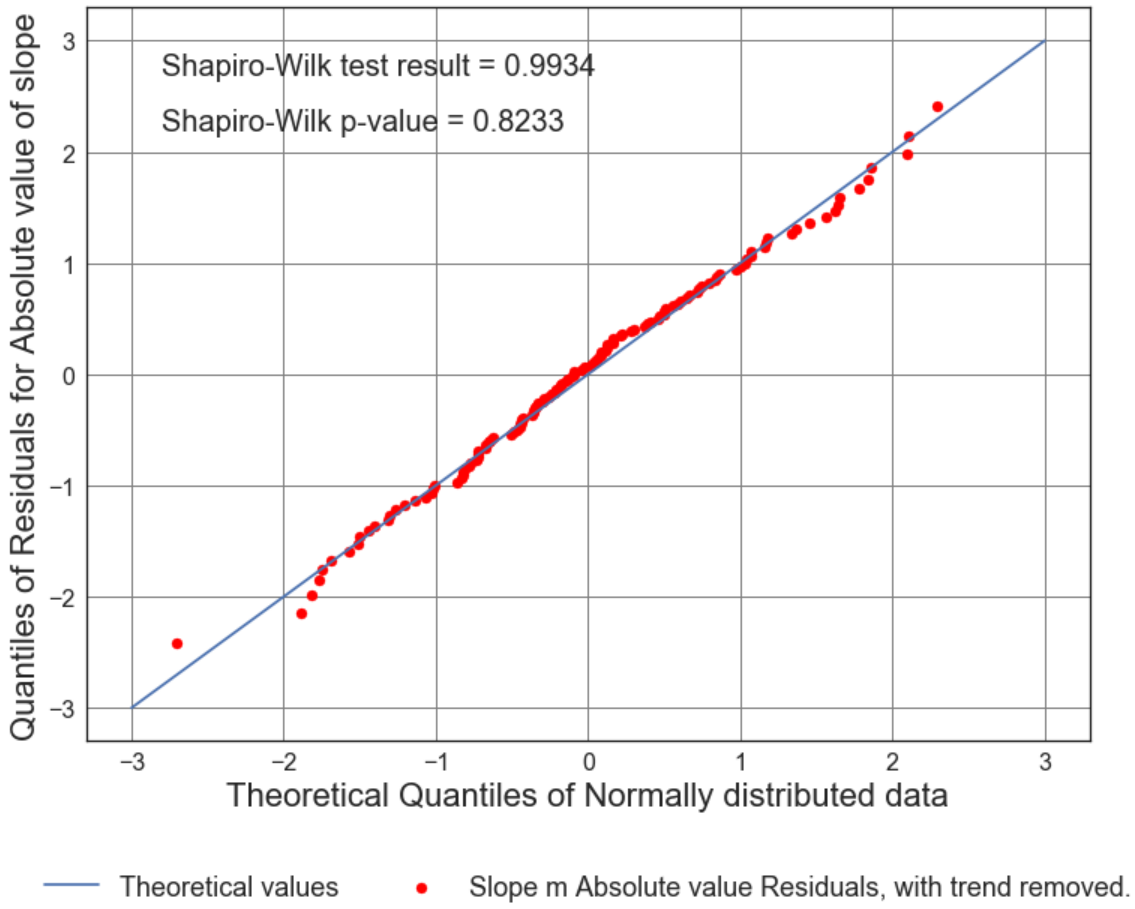

Figure B3.32: Scatter Plot of Solar cycle absolute value slope (from 1900 to 1964) vs. Average number of 6.5M and up Earthquakes/6months with trend removed. Line of best fit, y = -0.008831x + (0.2915), mean x = 30.43 +/- 23.66, mean y = 0.02279 +/- 4.229, R = -0.04941, R squared = 0.002441, p-value = 0.5827.

Appendix B4: USGS Centennial Time Series Analysis Part 4 - Modern Era Post 1964 Six Month Averaged Earthquake and Sunspot Data.

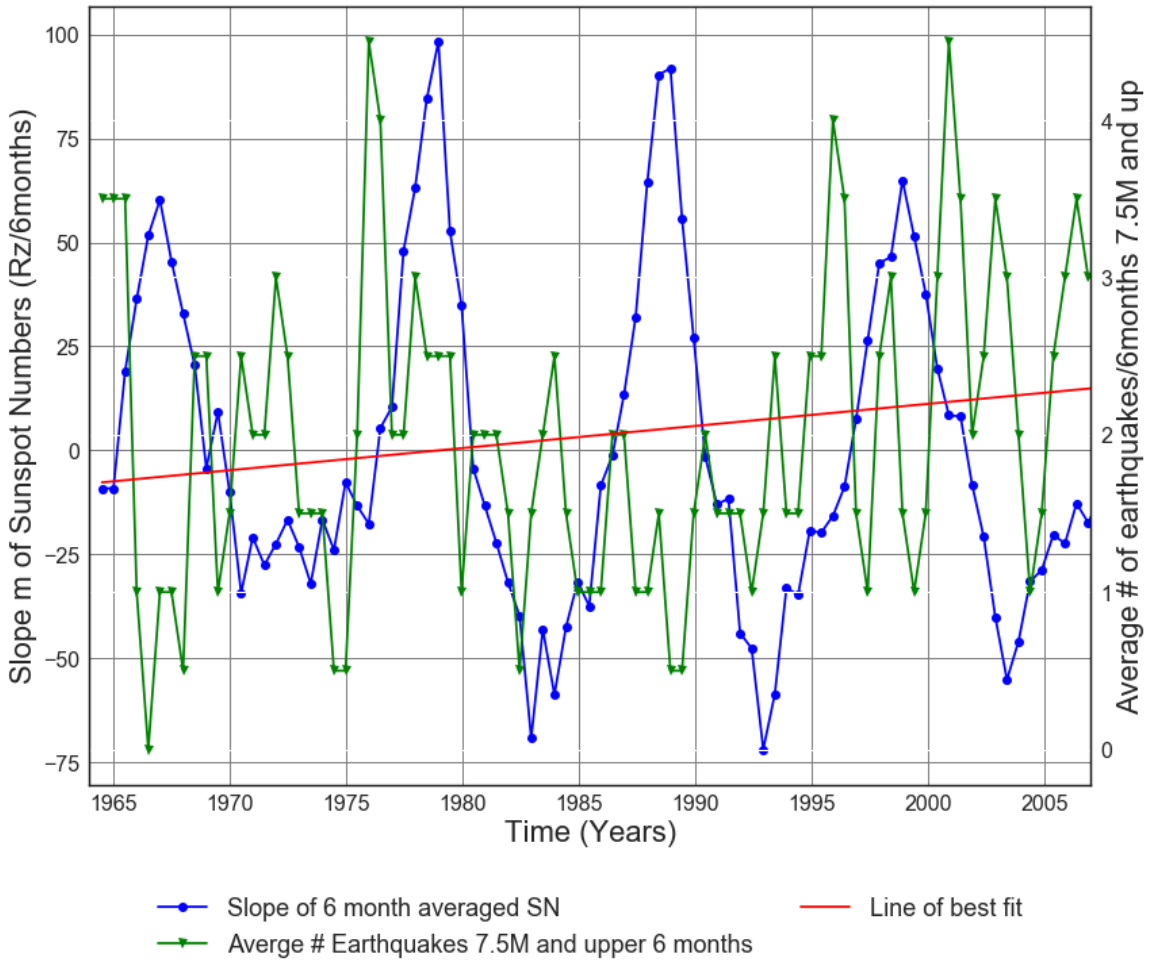

Figure B4.1: Slope of Solar cycle from 1964 to 2007 vs. Average number of 7.5M and up Earthquakes.

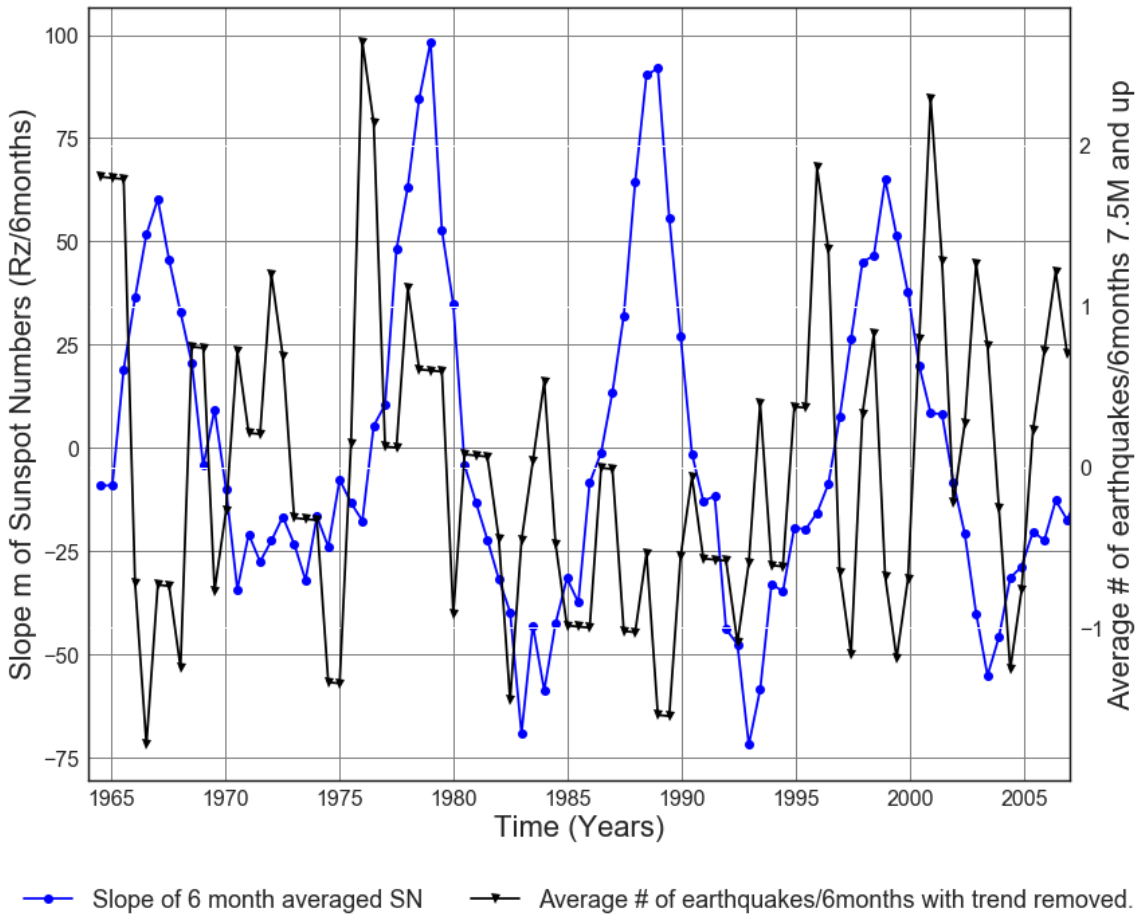

Figure B4.2: Slope of 6 month averaged SN 1964 to 2007 vs. Average number of 7.5M and up Earthquakes with trend removed. Line of best fit, y = 0.01408x + (-25.96), mean x = 1.986e+03 +/- 12.8, mean y = 2.006 +/- 0.9787

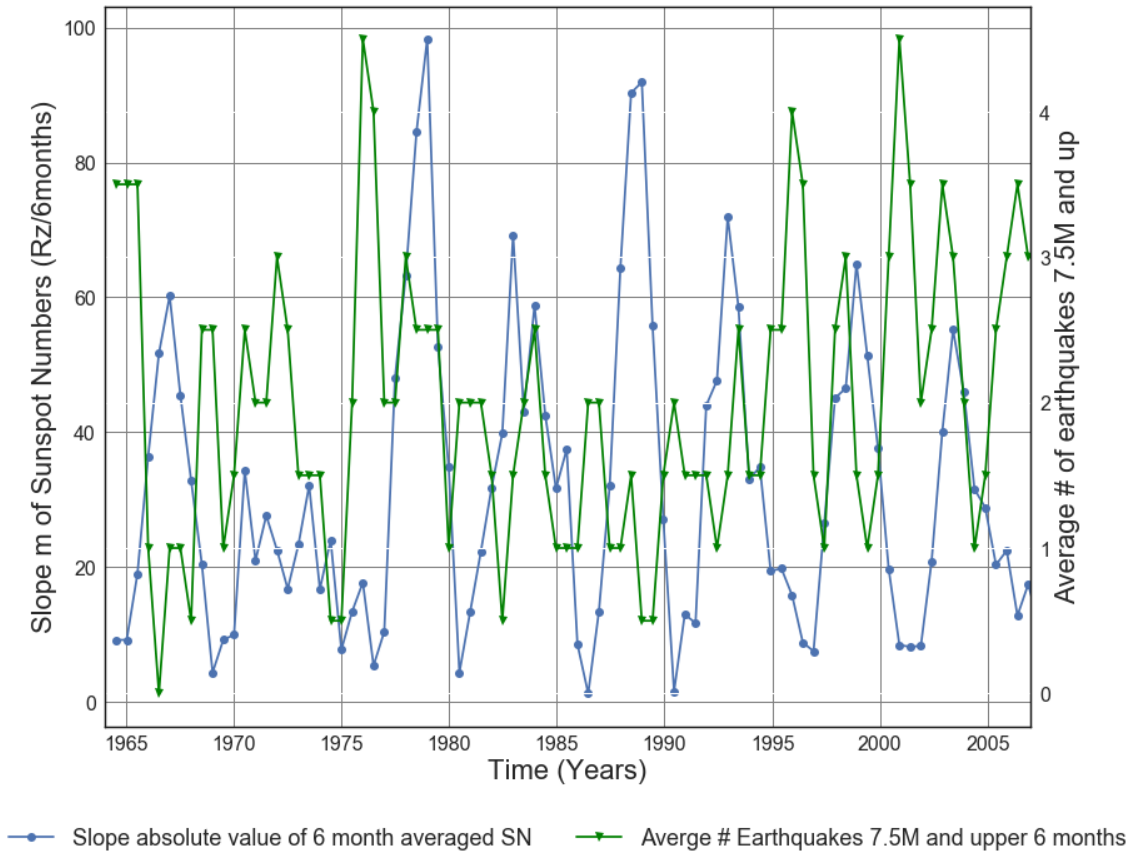

Figure B4.3: Slope Absolute value of Solar cycle from 1964 to 2007 vs. Average number of 7.5M and up Earthquakes.

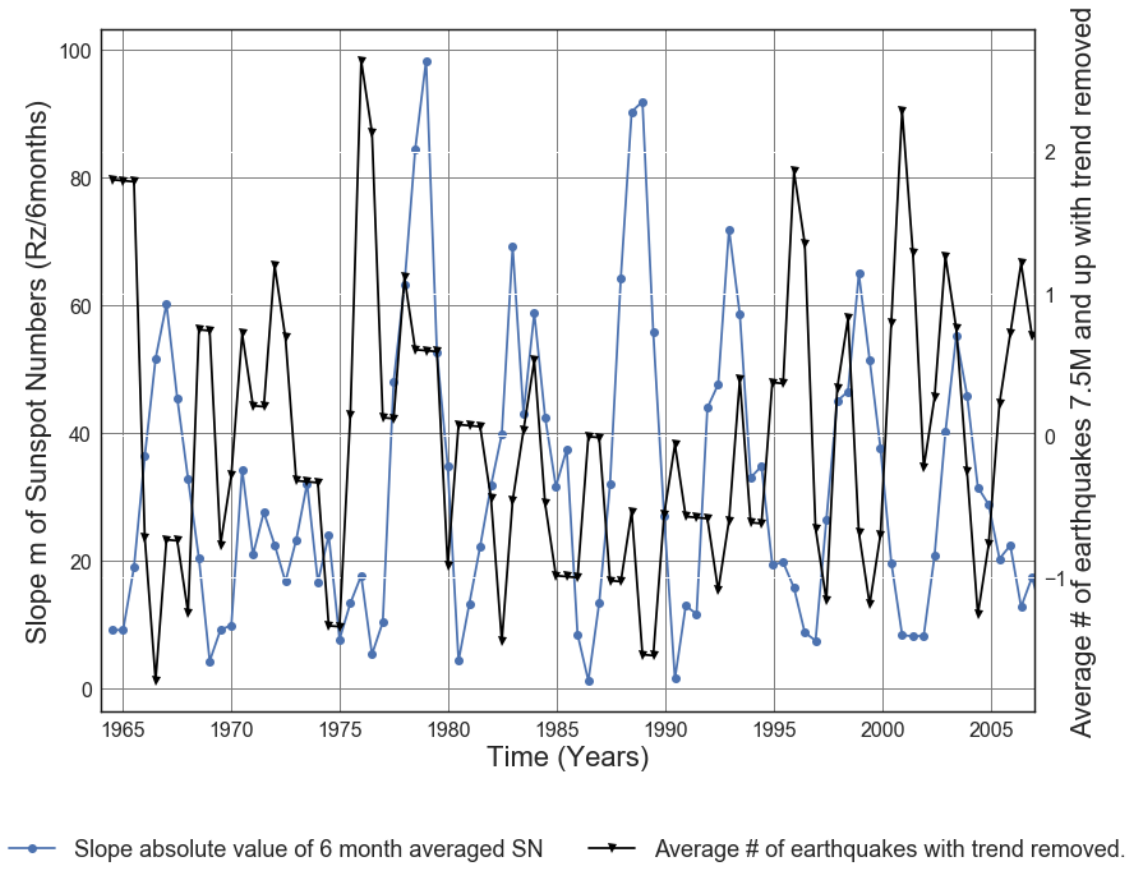

Figure B4.4: Slope Absolute value of Solar cycle from 1964 to 2007 vs. Average number of 7.5M and up earthquakes with trend removed.

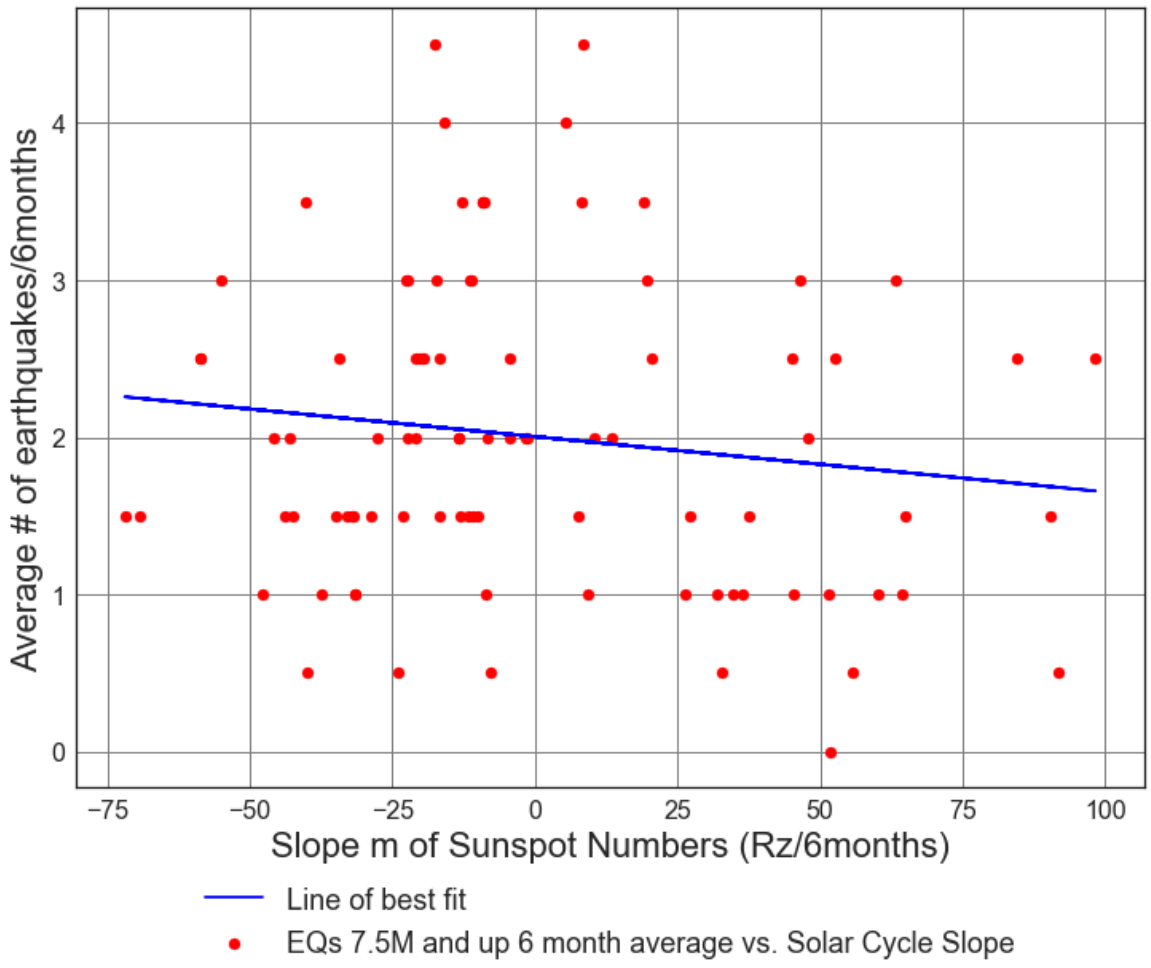

Figure B4.5: Scatter Plot of Solar cycle slope (from 1964 to 2007) vs. Average number of 7.5M and up Earthquakes/6months. Line of best fit, y = -0.00352x + (2.004), mean x = -0.5303 +/- 38.19, mean y = 2.006 +/- 0.9787, R = -0.1374, R squared = 0.01887, p-value = 0.1993.

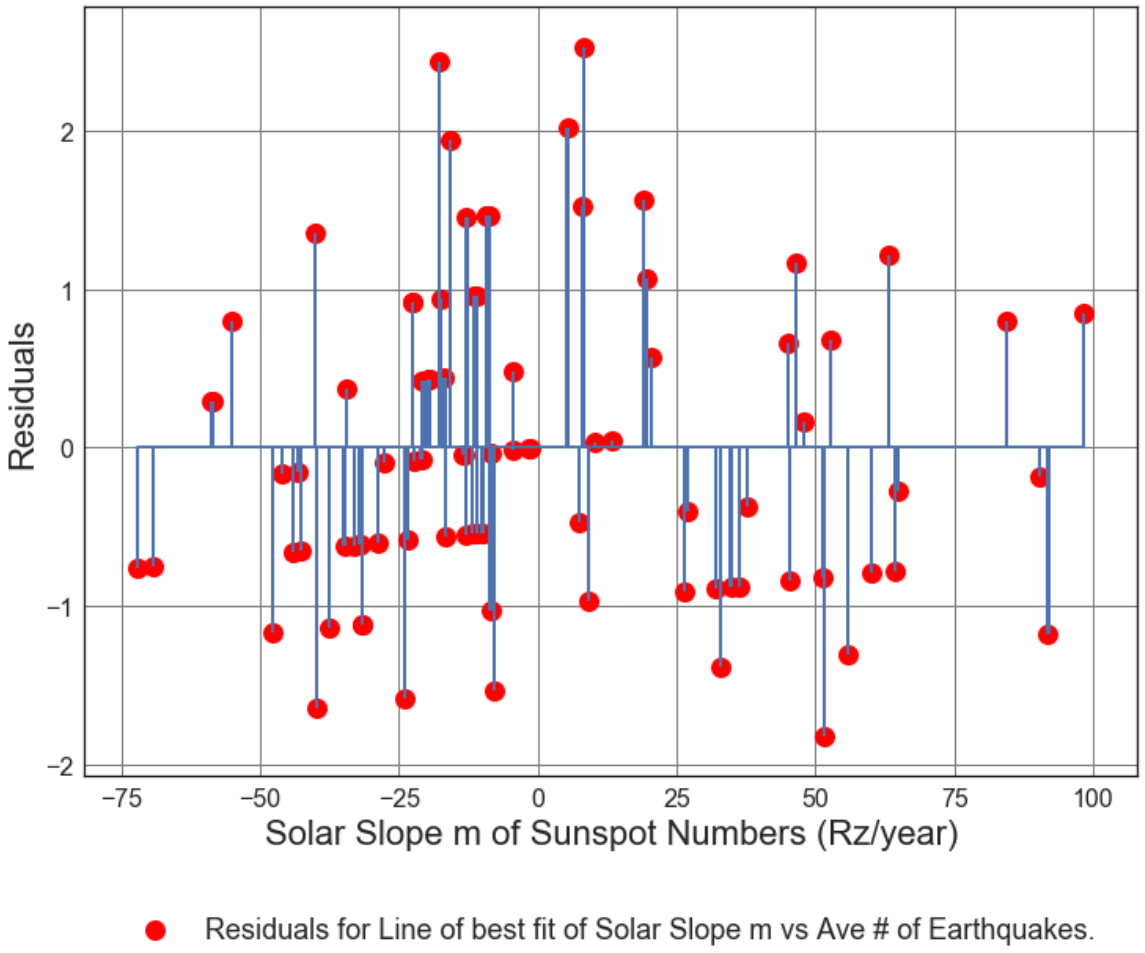

Figure B4.6: Residuals Plot of Solar cycle slope (from 1964 to 2007) vs. Average number of 7.5M and up Earthquakes/6months. Line of best fit, y = -0.00352x + (2.004), mean x = -0.5303 +/- 38.19, mean y = 2.006 +/- 0.9787, R = -0.1374, R squared = 0.01887, p-value = 0.1993.

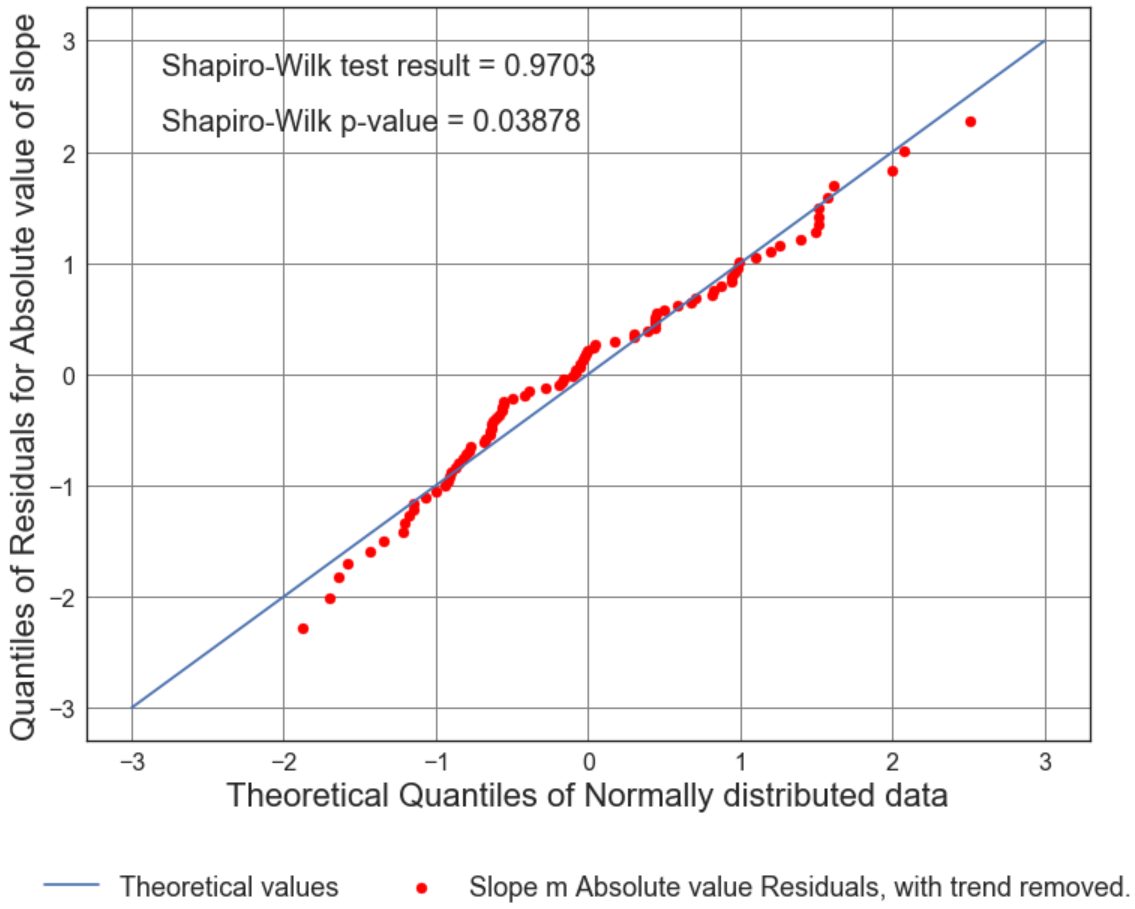

Figure B4.7: Residuals Plot of Solar cycle slope (from 1964 to 2007) vs. Average number of 7.5M and up Earthquakes/6months. Line of best fit, y = -0.00352x + (2.004), mean x = -0.5303 +/- 38.19, mean y = 2.006 +/- 0.9787, R = -0.1374, R squared = 0.01887, p-value = 0.1993.

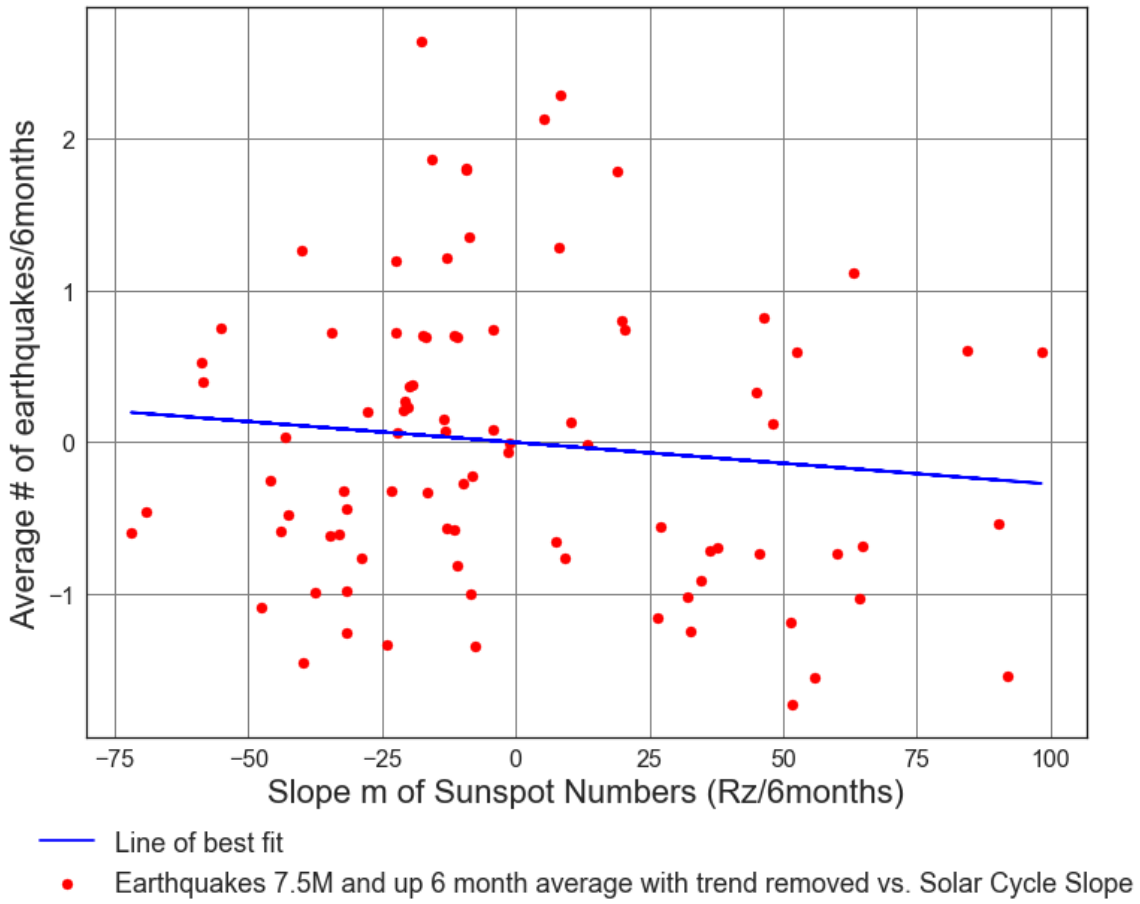

Figure B4.8: Scatter Plot of Solar cycle slope (from 1964 to 2007) vs. Average number of 7.5M and up Earthquakes/6months with trend removed. Line of best fit, y = -0.00275x + (-0.001458), mean x = -0.5303 +/- 38.19, mean y = -3.313e-15 +/- 0.962, R = -0.1092, R squared = 0.01192, p-value = 0.3085.

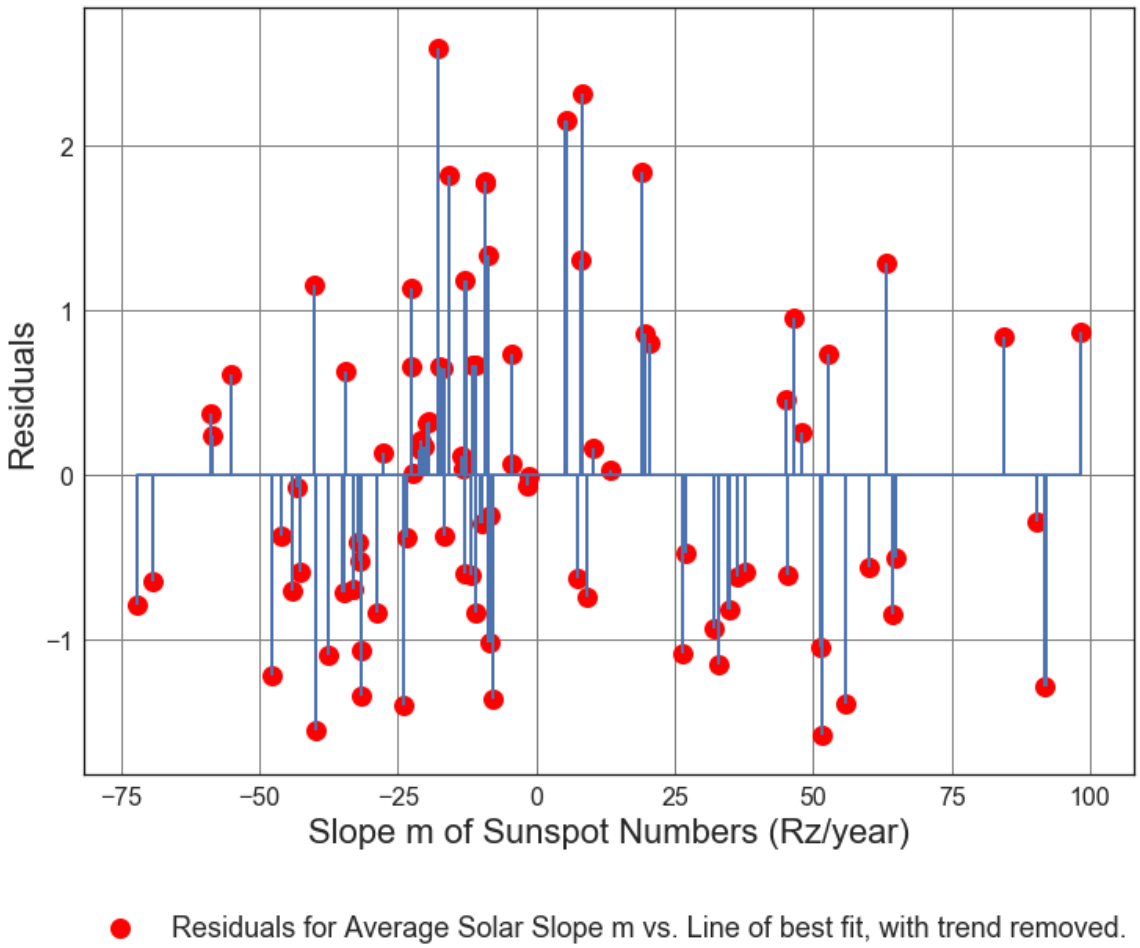

Figure B4.9: Scatter Plot of Solar cycle slope (from 1964 to 2007) vs. Average number of 7.5M and up Earthquakes/6months with trend removed. Line of best fit, y = -0.00275x + (-0.001458), mean x = -0.5303 +/- 38.19, mean y = -3.313e-15 +/- 0.962, R = -0.1092, R squared = 0.01192, p-value = 0.3085.

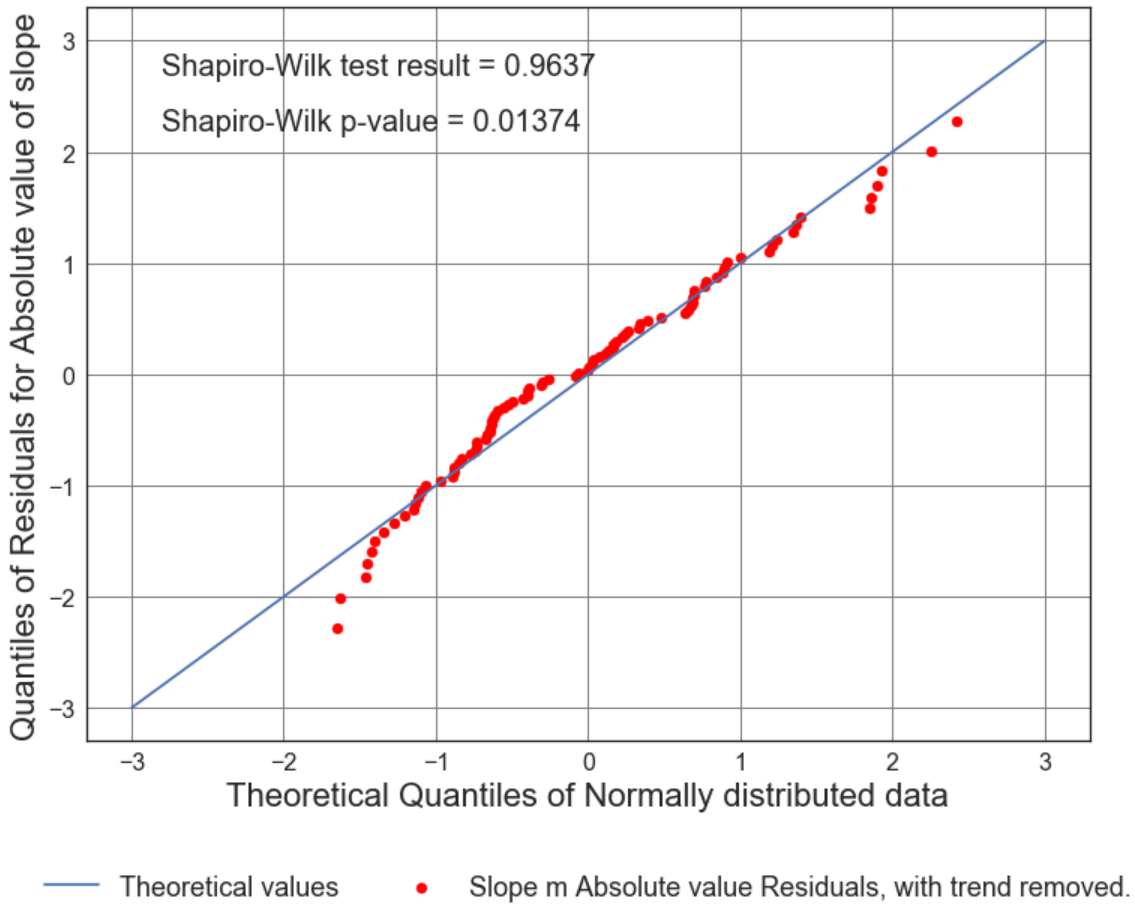

Figure B4.10: Scatter Plot of Solar cycle slope (from 1964 to 2007) vs. Average number of 7.5M and up Earthquakes/6months with trend removed. Line of best fit, y = -0.00275x + (-0.001458), mean x = -0.5303 +/- 38.19, mean y = -3.313e-15 +/- 0.962, R = -0.1092, R squared = 0.01192, p-value = 0.3085.

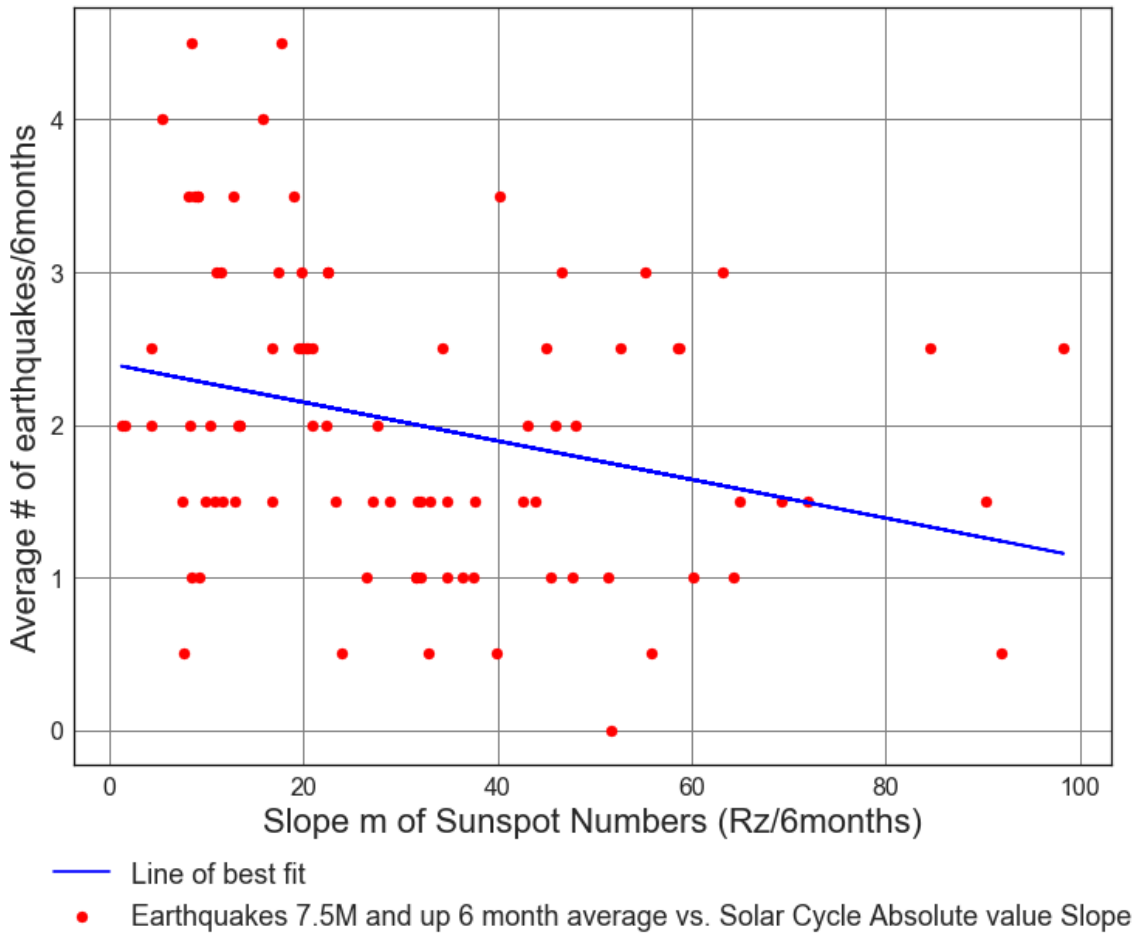

Figure B4.11: Scatter Plot of Solar cycle slope (from 1964 to 2007) vs. Average number of 7.5M and up Earthquakes/6months. Line of best fit, y = -0.01265x + (2.4), mean x = 31.16 +/- 22.09, mean y = 2.006 +/- 0.9787, R = -0.2857, R squared = 0.0816, p-value = 0.006655.

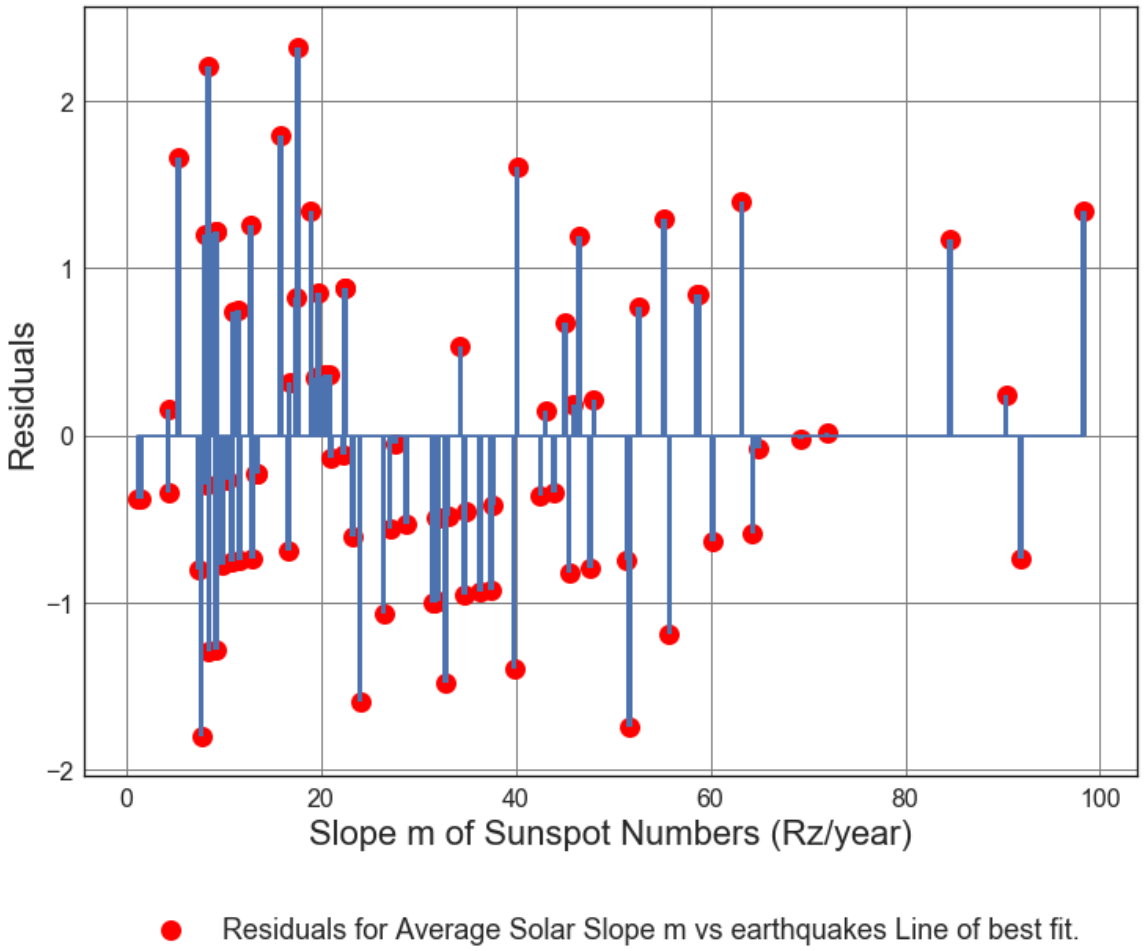

Figure B4.12: Scatter Plot of Solar cycle slope (from 1964 to 2007) vs. Average number of 7.5M and up Earthquakes/6months. Line of best fit, y = -0.01265x + (2.4), mean x = 31.16 +/- 22.09, mean y = 2.006 +/- 0.9787, R = -0.2857, R squared = 0.0816, p-value = 0.006655.

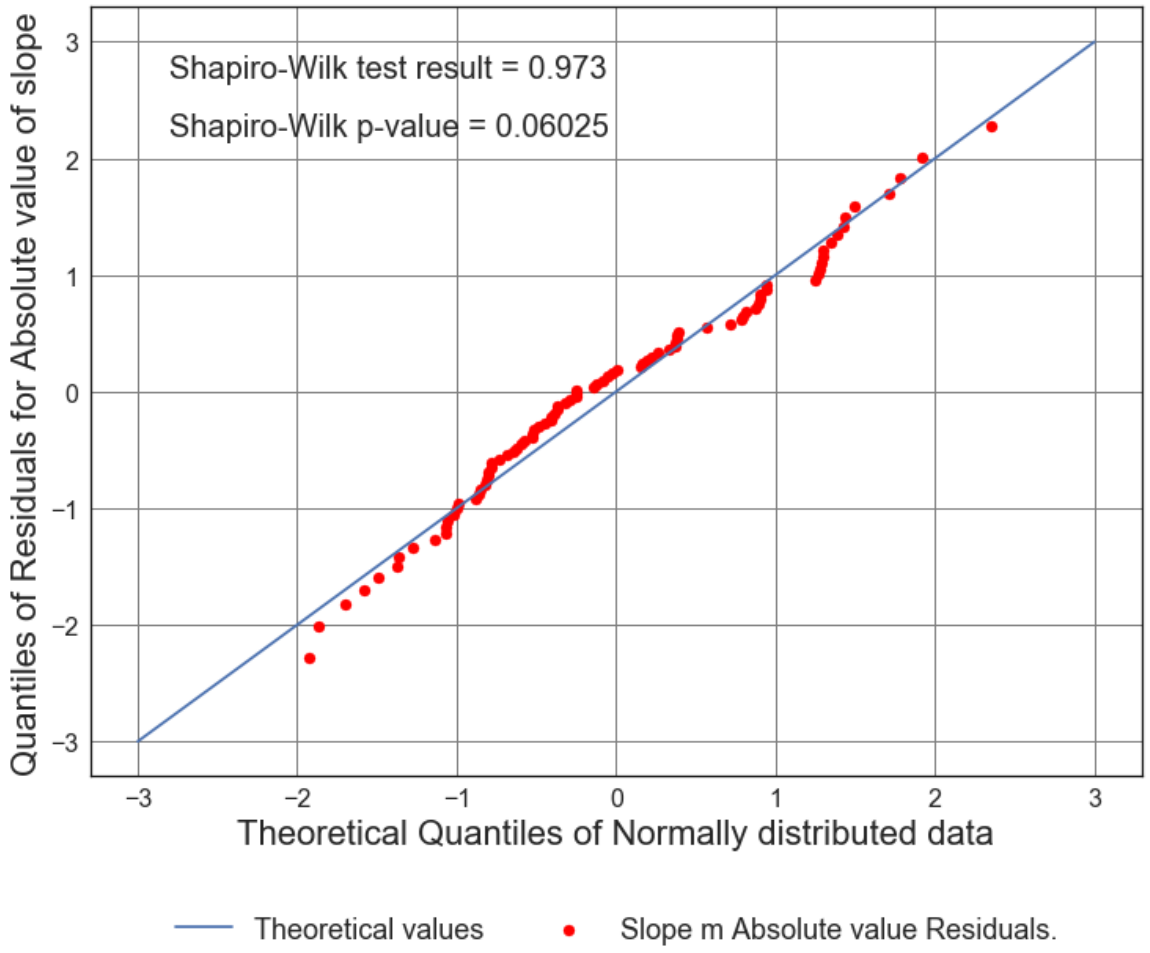

Figure B4.13: Scatter Plot of Solar cycle slope (from 1964 to 2007) vs. Average number of 7.5M and up Earthquakes/6months. Line of best fit, y = -0.01265x + (2.4), mean x = 31.16 +/- 22.09, mean y = 2.006 +/- 0.9787, R = -0.2857, R squared = 0.0816, p-value = 0.006655.

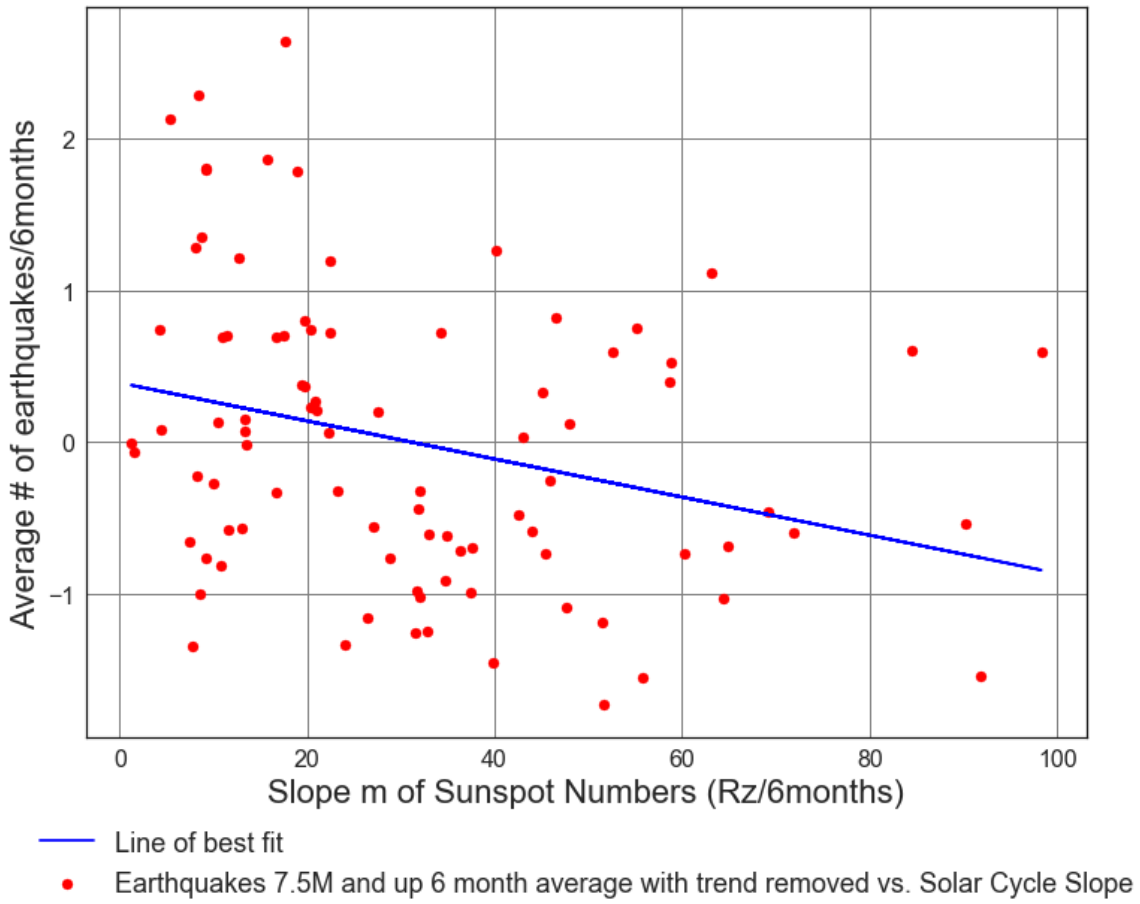

Figure B4.14: Scatter Plot of Solar cycle absolute value slope (from 1964 to 2007) vs. Average number of 7.5M and up Earthquakes/6months with trend removed. Line of best fit, y = -0.01256x + (0.3912), mean x = 31.16 +/- 22.09, mean y = -3.313e-15 +/- 0.962, R = -0.2884, R squared = 0.08317, p-value = 0.006131.

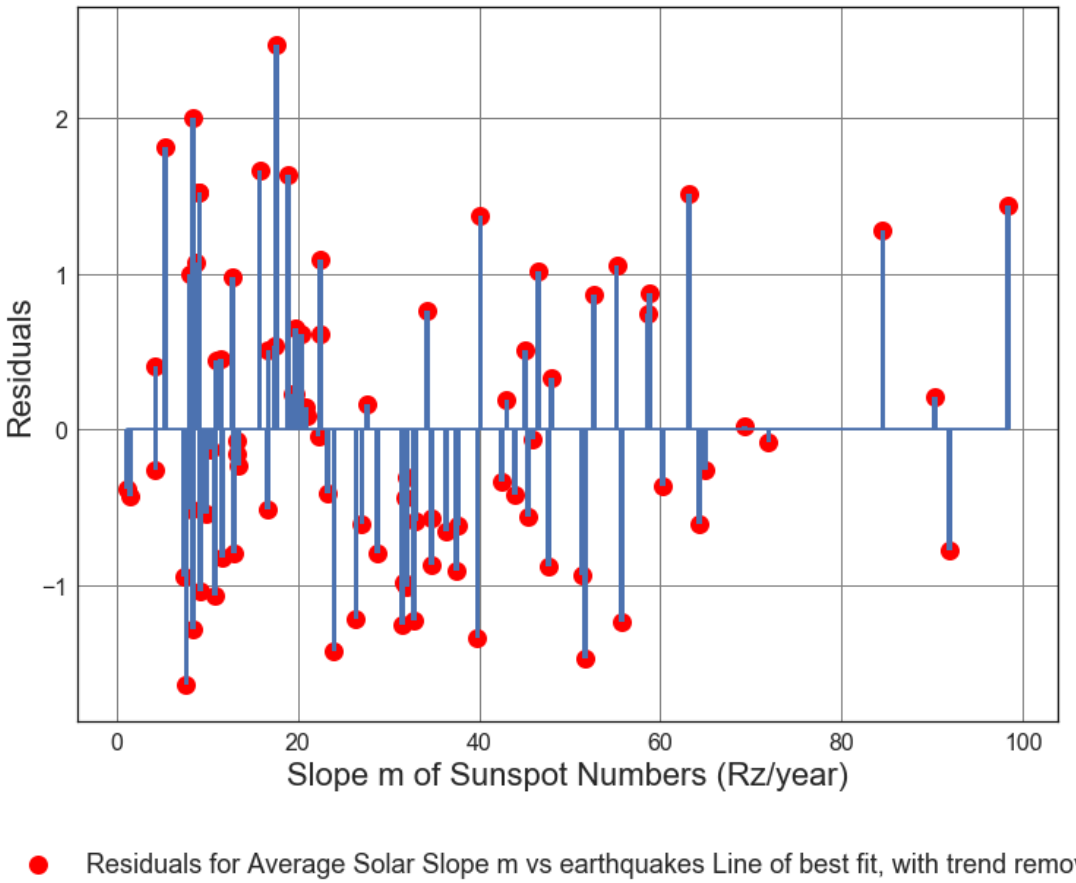

Figure B4.15: Scatter Plot of Solar cycle absolute value slope (from 1964 to 2007) vs. Average number of 7.5M and up Earthquakes/6months with trend removed. Line of best fit, y = -0.01256x + (0.3912), mean x = 31.16 +/- 22.09, mean y = -3.313e-15 +/- 0.962, R = -0.2884, R squared = 0.08317, p-value = 0.006131.

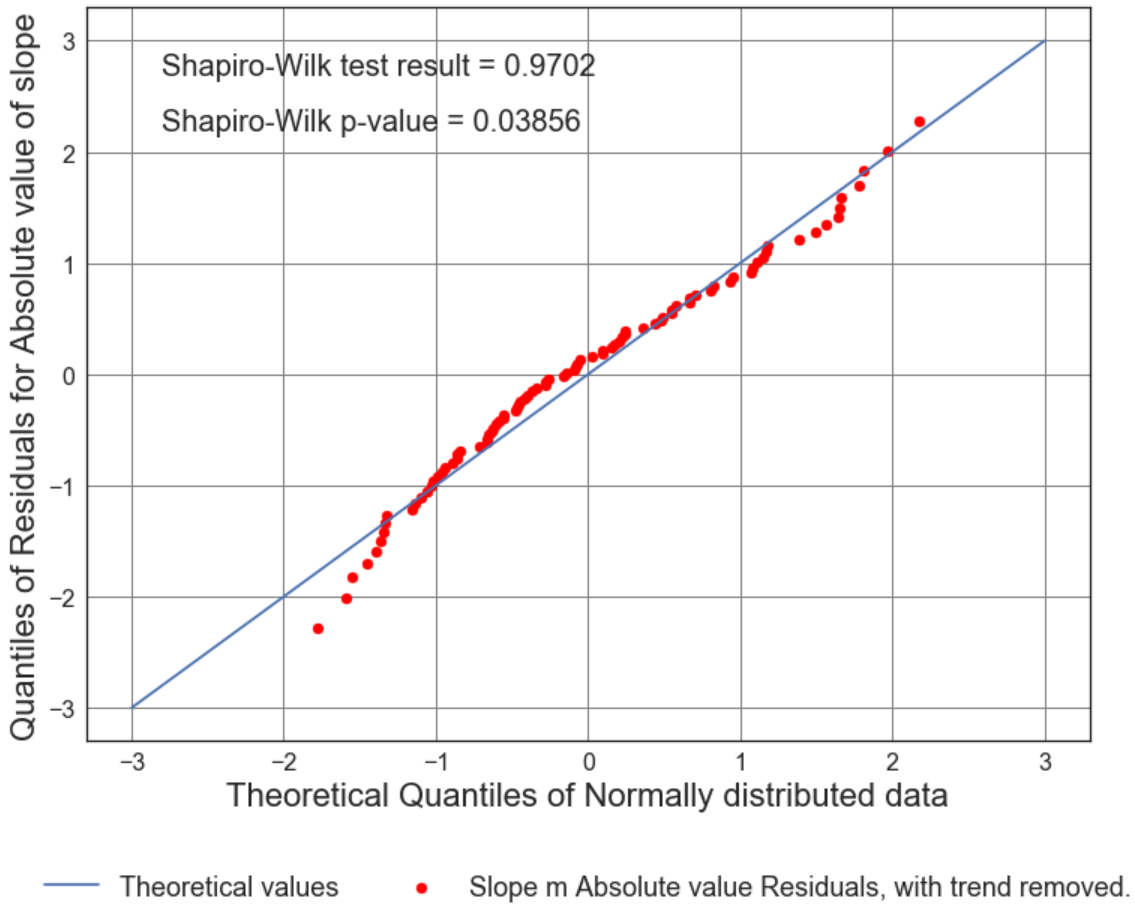

Figure B4.16: Scatter Plot of Solar cycle absolute value slope (from 1964 to 2007) vs. Average number of 7.5M and up Earthquakes/6months with trend removed. Line of best fit, y = -0.01256x + (0.3912), mean x = 31.16 +/- 22.09, mean y = -3.313e-15 +/- 0.962, R = -0.2884, R squared = 0.08317, p-value = 0.006131.

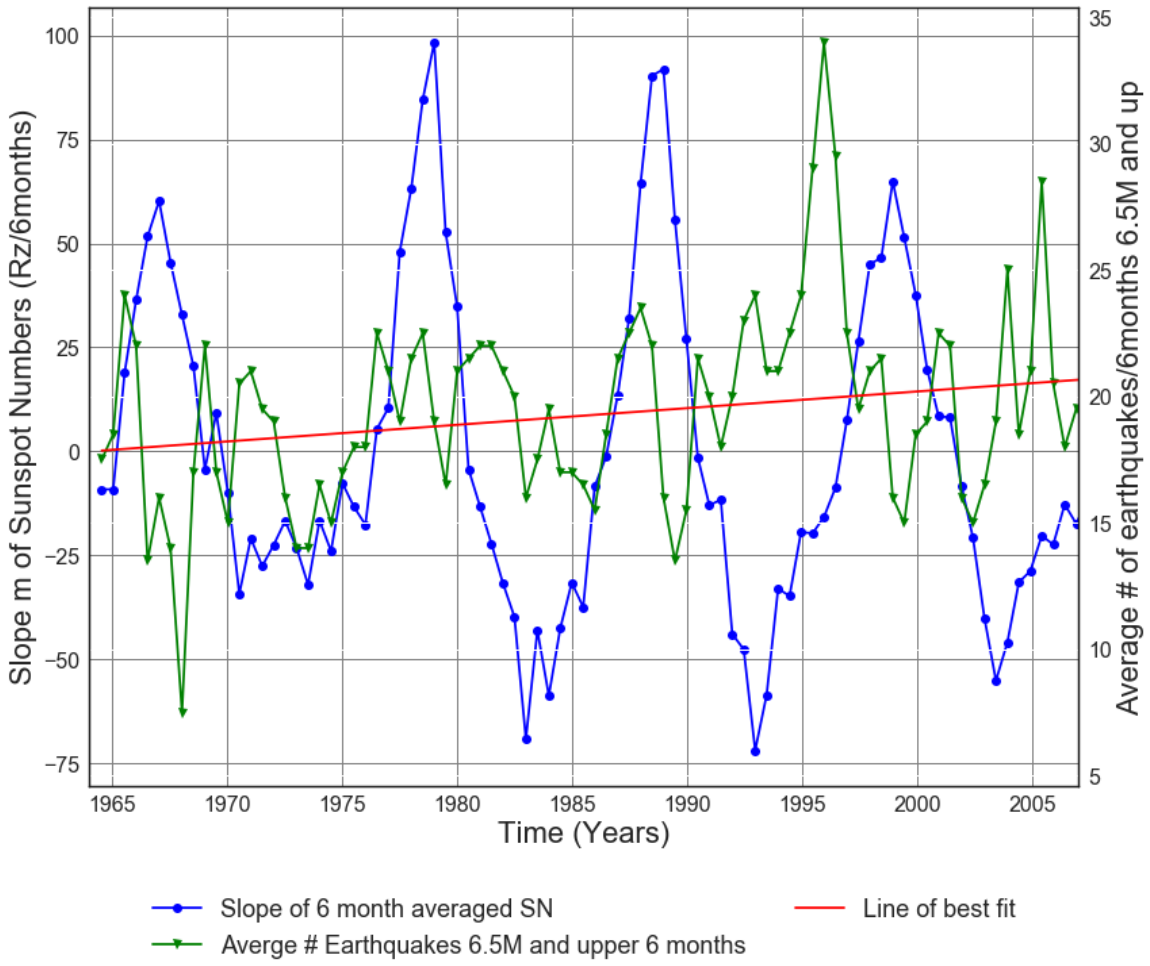

Figure B4.17: Slope of Solar cycle from 1964 to 2007 vs. Average number of 6.5M and up Earthquakes.

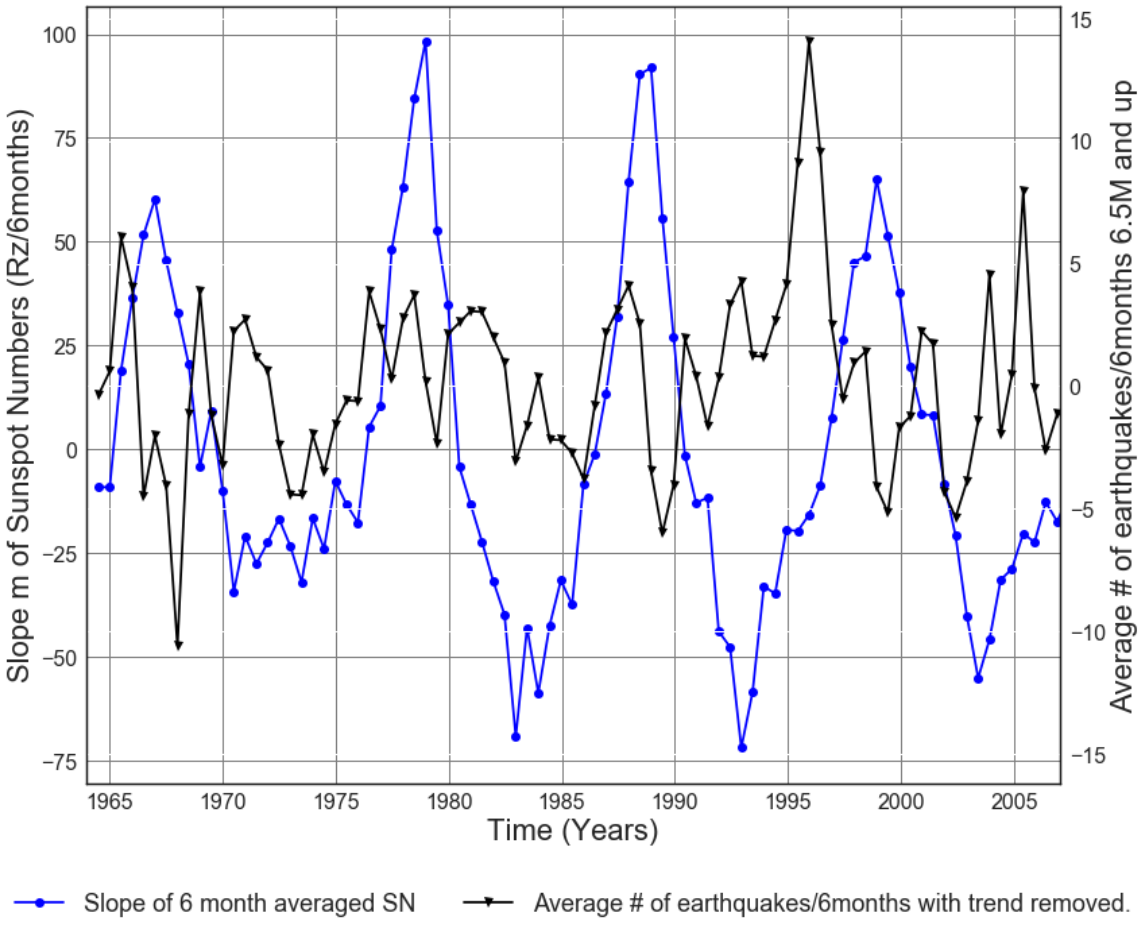

Figure B4.18: Slope of 6 month averaged SN 1964 to 2007 vs. Average number of 6.5M and up Earthquakes with trend removed. Line of best fit, y = 0.06594x + (-111.7), mean x = 1.986e+03 +/- 12.8, mean y = 19.3 +/- 4.12

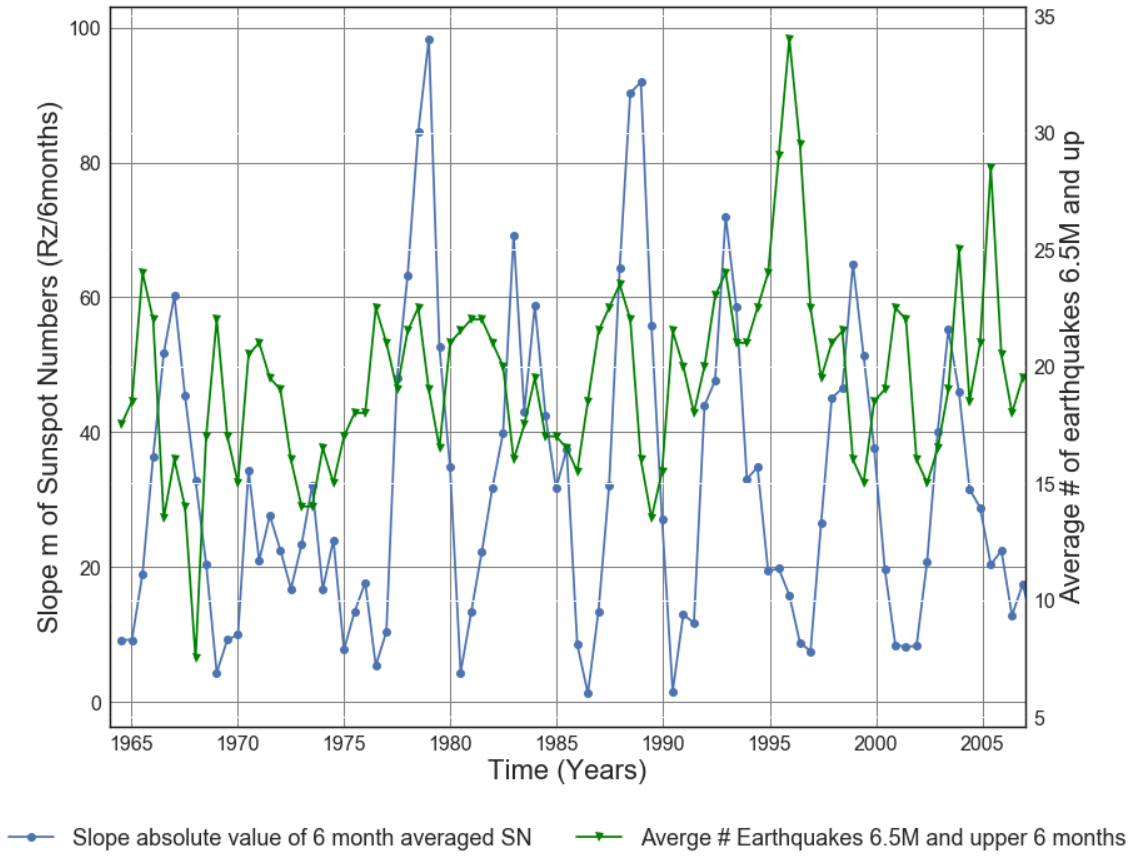

Figure B4.19: Slope Absolute value of Solar cycle from 1964 to 2007 vs. Average number of 6.5M and up Earthquakes.

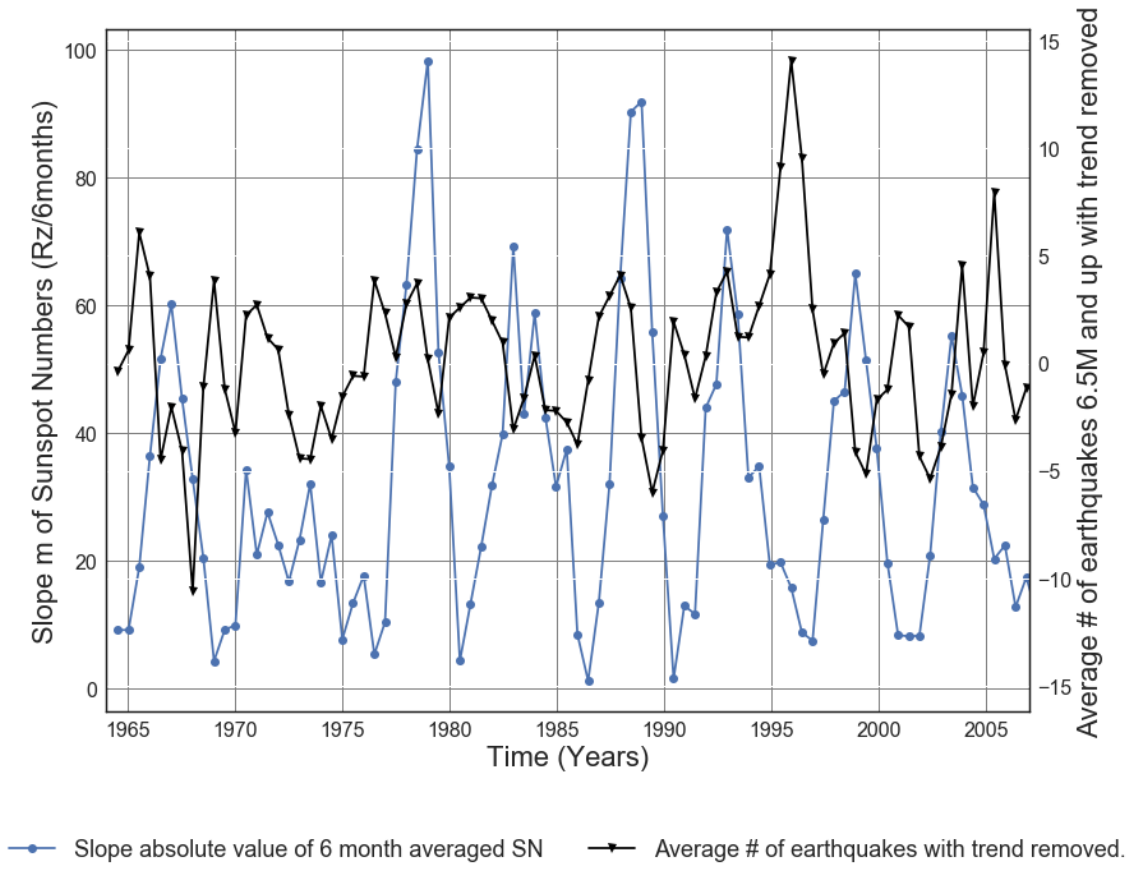

Figure B4.20: Slope Absolute value of Solar cycle from 1964 to 2007 vs. Average number of 6.5M and up earthquakes with trend removed.

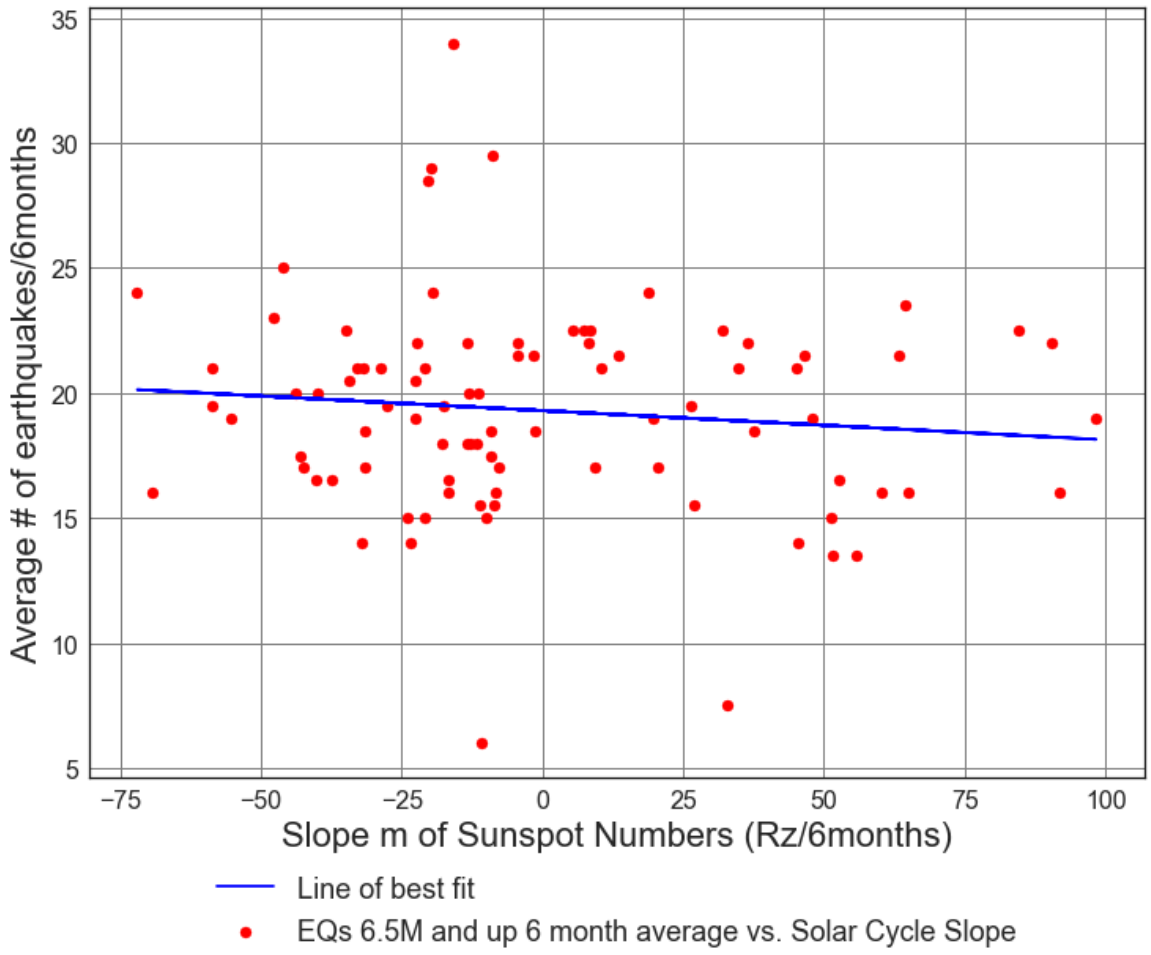

Figure B4.21: Scatter Plot of Solar cycle slope (from 1964 to 2007) vs. Average number of 6.5M and up Earthquakes/6months. Line of best fit, y = -0.01169x + (19.3), mean x = -0.5303 +/- 38.19, mean y = 19.3 +/- 4.12, R = -0.1084, R squared = 0.01174, p-value = 0.3121.

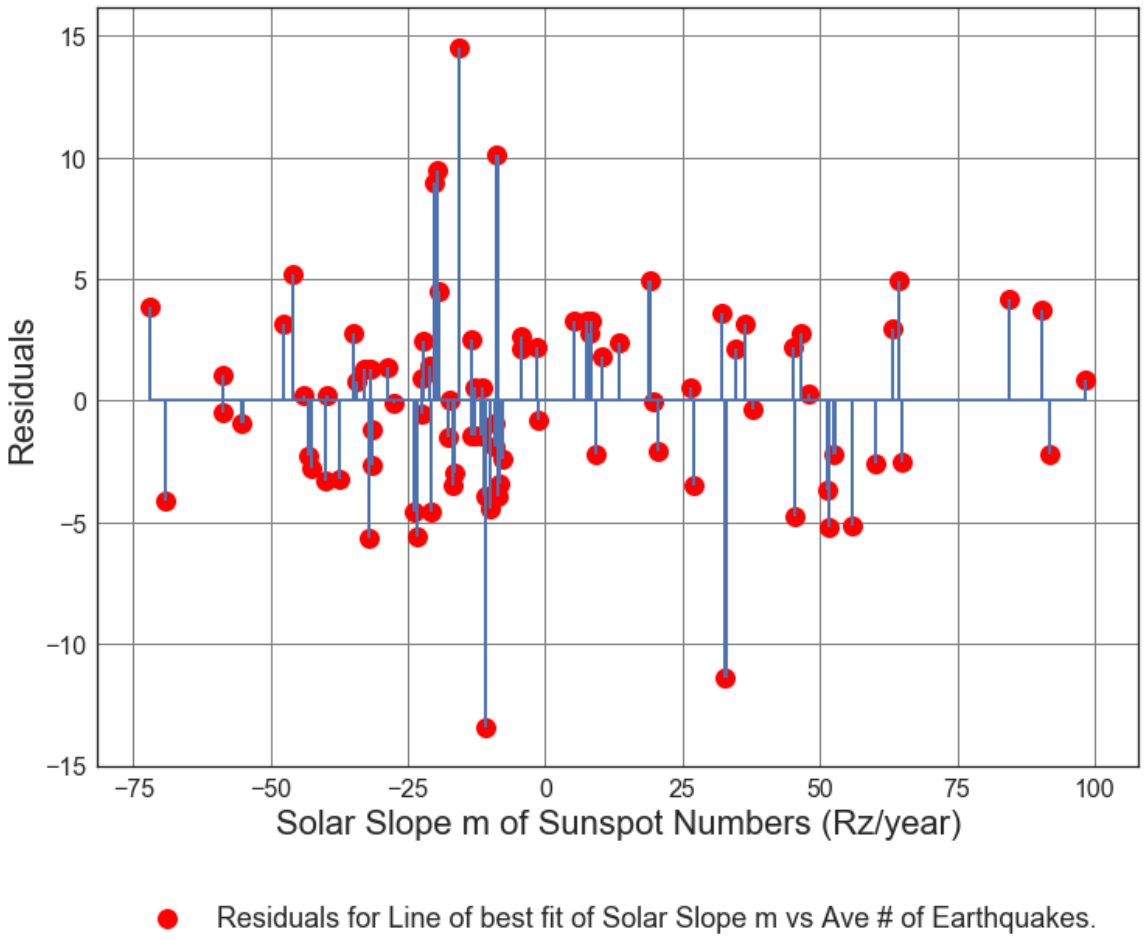

Figure B4.22: Residuals Plot of Solar cycle slope (from 1964 to 2007) vs. Average number of 6.5M and up Earthquakes/6months. Line of best fit, y = -0.01169x + (19.3), mean x = -0.5303 +/- 38.19, mean y = 19.3 +/- 4.12, R = -0.1084, R squared = 0.01174, p-value = 0.3121.

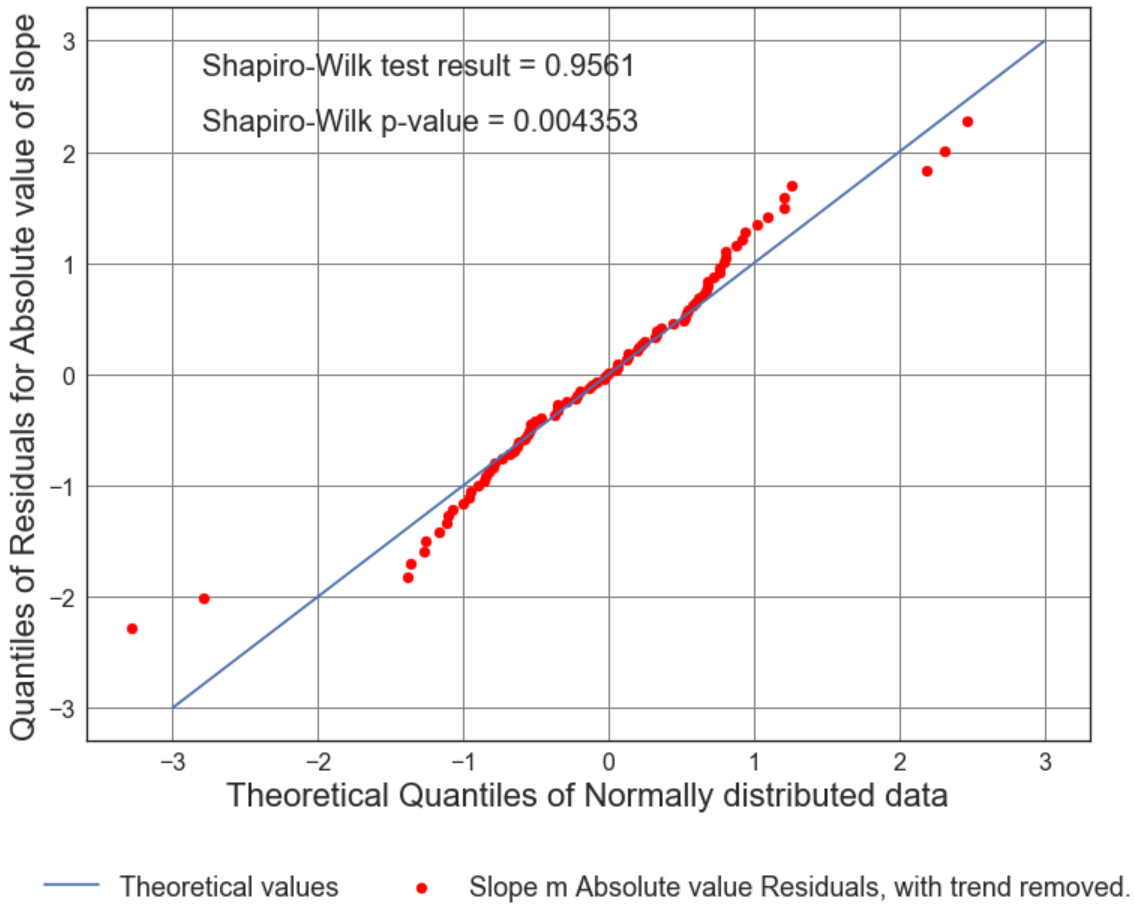

Figure B4.23: Residuals Plot of Solar cycle slope (from 1964 to 2007) vs. Average number of 6.5M and up Earthquakes/6months. Line of best fit, y = -0.01169x + (19.3), mean x = -0.5303 +/- 38.19, mean y = 19.3 +/- 4.12, R = -0.1084, R squared = 0.01174, p-value = 0.3121.

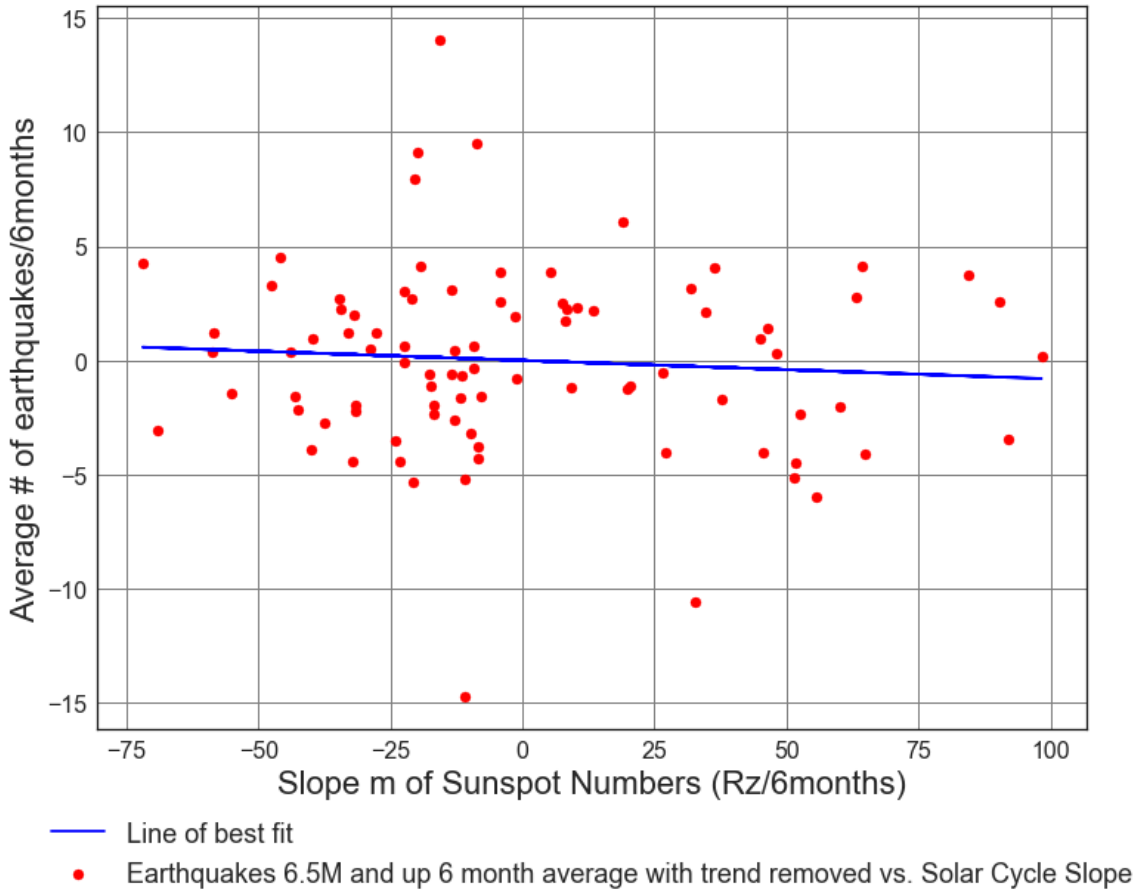

Figure B4.24: Scatter Plot of Solar cycle slope (from 1964 to 2007) vs. Average number of 6.5M and up Earthquakes/6months with trend removed. Line of best fit, y = -0.008083x + (-0.004286), mean x = -0.5303 +/- 38.19, mean y = -1.437e-15 +/- 4.033, R = -0.07655, R squared = 0.00586, p-value = 0.4758.

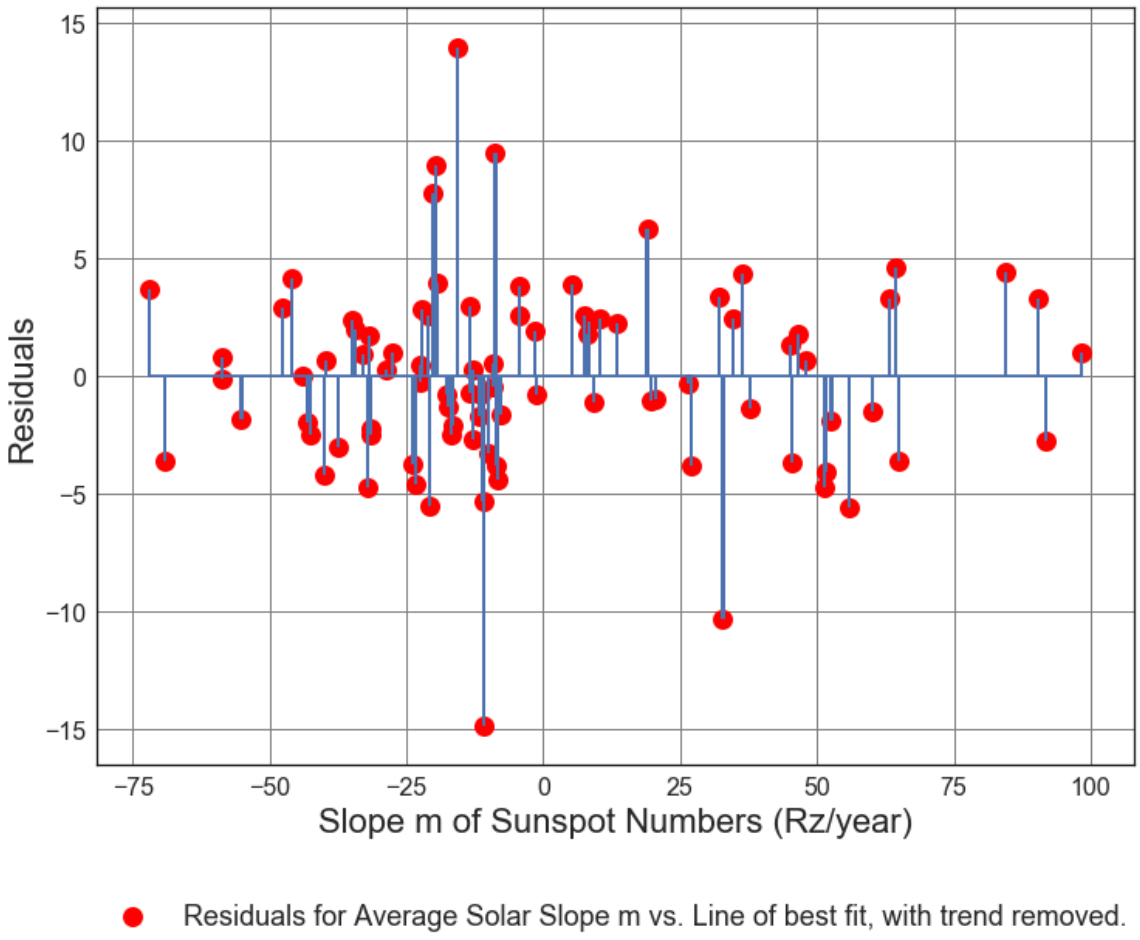

Figure B4.25: Scatter Plot of Solar cycle slope (from 1964 to 2007) vs. Average number of 6.5M and up Earthquakes/6months with trend removed. Line of best fit, y = -0.008083x + (-0.004286), mean x = -0.5303 +/- 38.19, mean y = -1.437e-15 +/- 4.033, R = -0.07655, R squared = 0.00586, p-value = 0.4758.

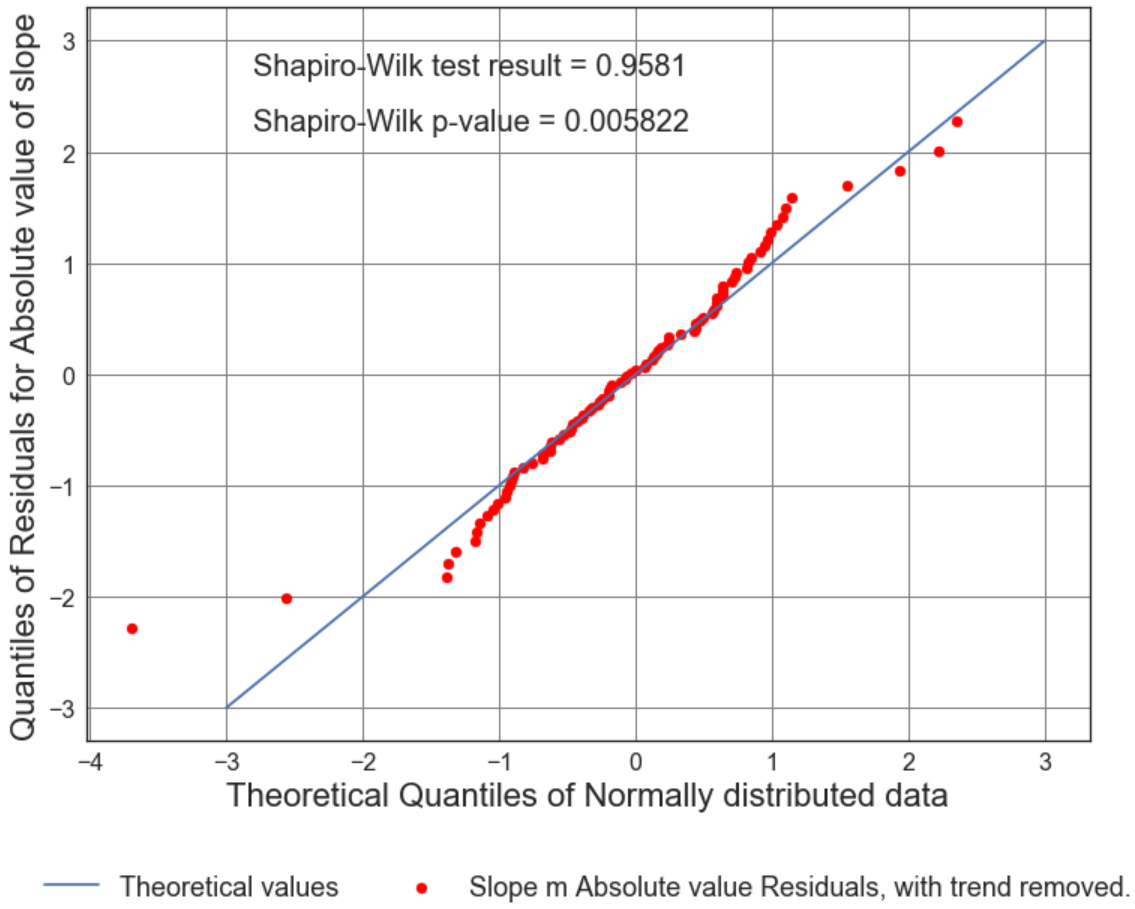

Figure B4.26: Scatter Plot of Solar cycle slope (from 1964 to 2007) vs. Average number of 6.5M and up Earthquakes/6months with trend removed. Line of best fit, y = -0.008083x + (-0.004286), mean x = -0.5303 +/- 38.19, mean y = -1.437e-15 +/- 4.033, R = -0.07655, R squared = 0.00586, p-value = 0.4758.

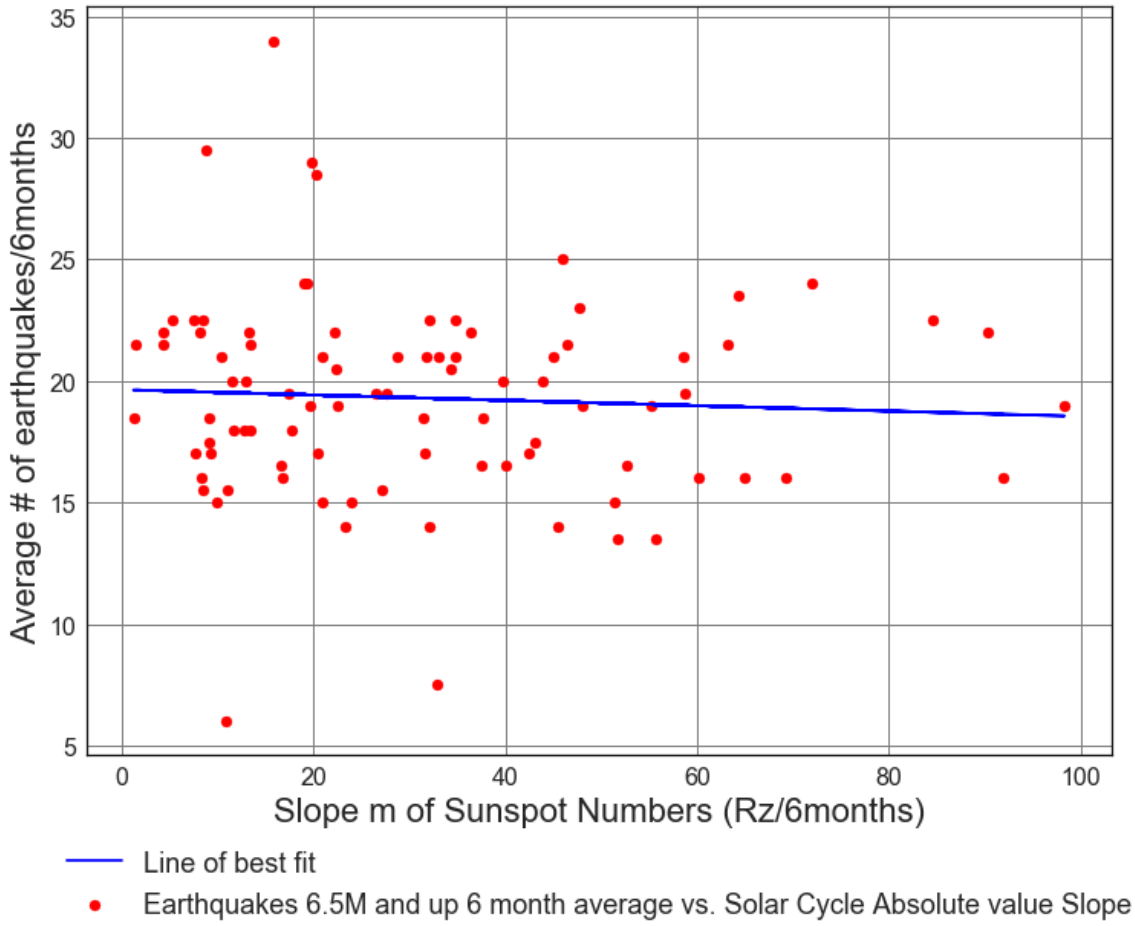

Figure B4.27: Scatter Plot of Solar cycle slope (from 1964 to 2007) vs. Average number of 6.5M and up Earthquakes/6months. Line of best fit, y = -0.01099x + (19.65), mean x = 31.16 +/- 22.09, mean y = 19.3 +/- 4.12, R = -0.05894, R squared = 0.003474, p-value = 0.5832.

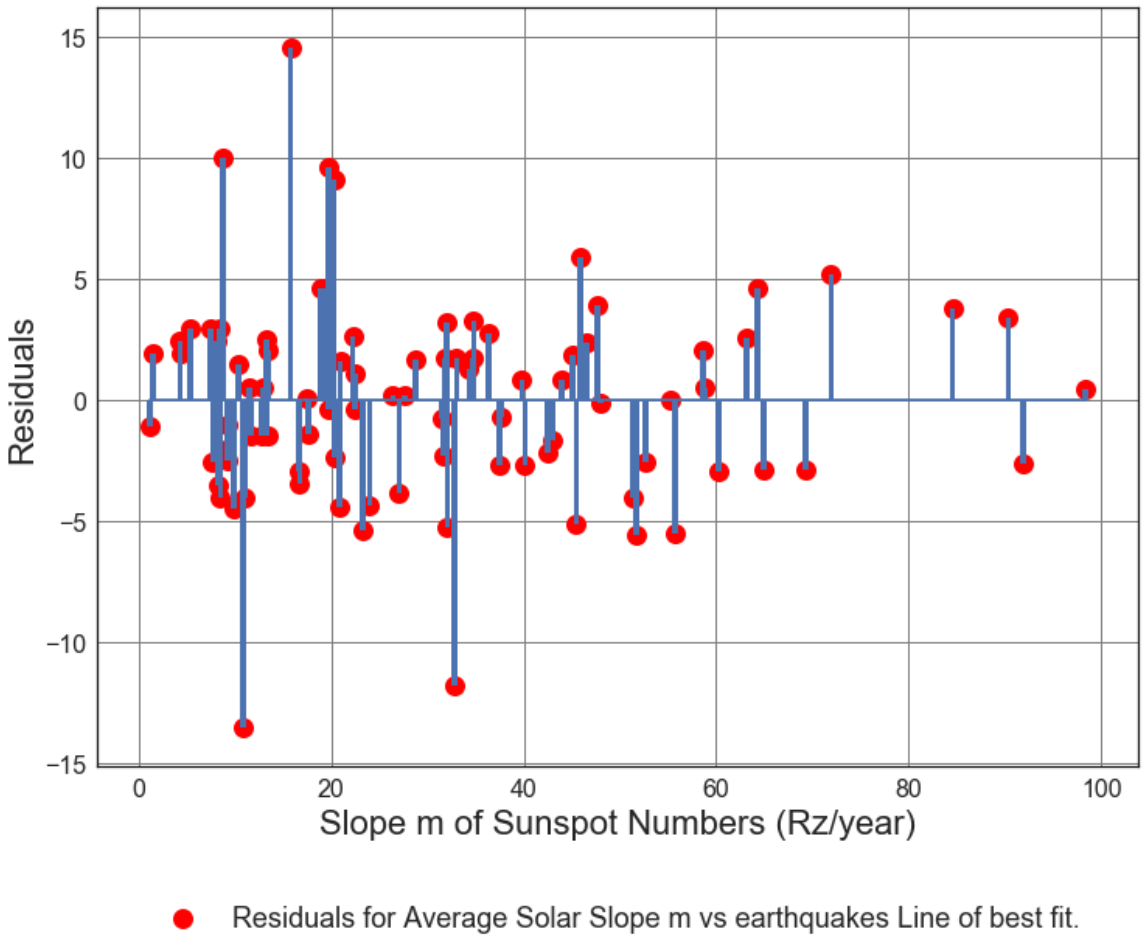

Figure B4.28: Scatter Plot of Solar cycle slope (from 1964 to 2007) vs. Average number of 6.5M and up Earthquakes/6months. Line of best fit, y = -0.01099x + (19.65), mean x = 31.16 +/- 22.09, mean y = 19.3 +/- 4.12, R = -0.05894, R squared = 0.003474, p-value = 0.5832.

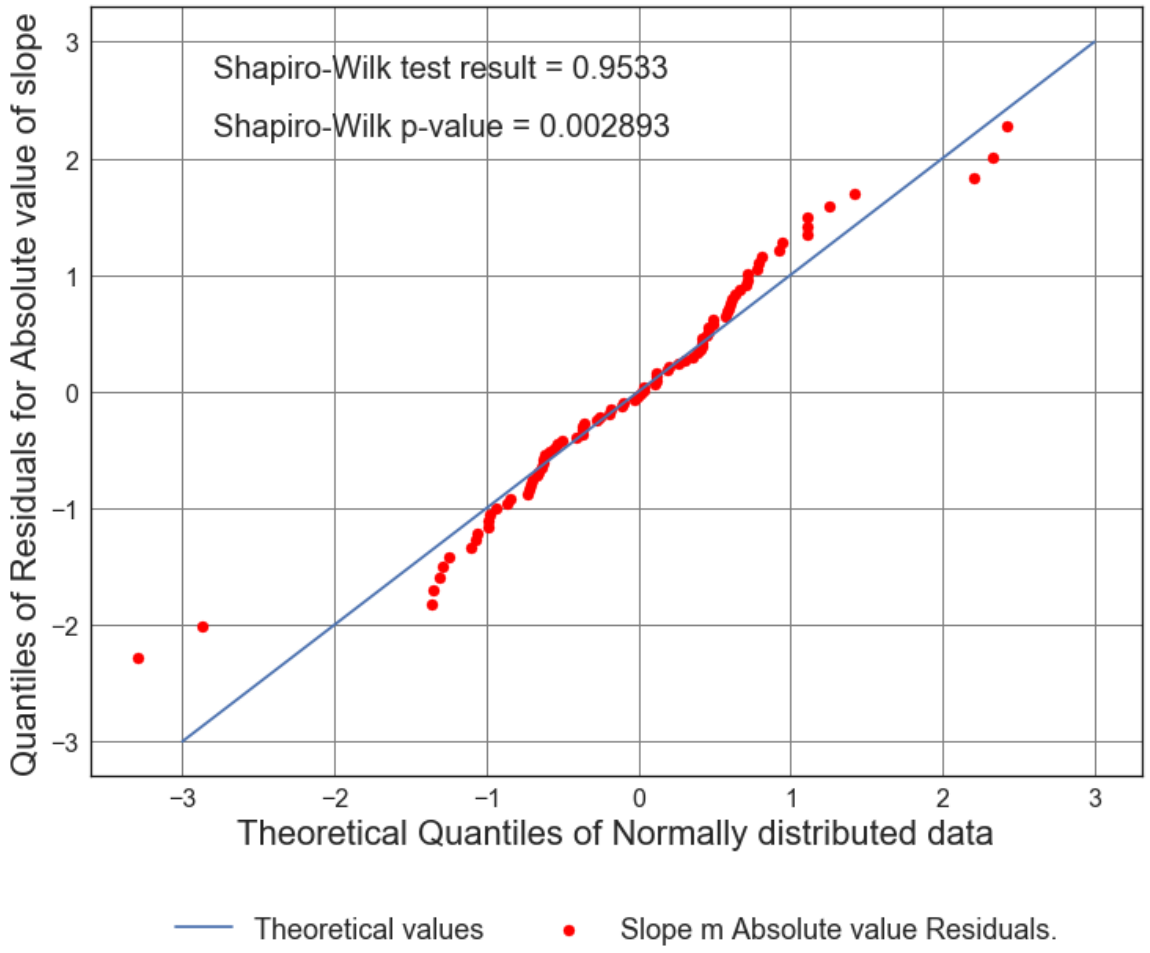

Figure B4.29: Scatter Plot of Solar cycle slope (from 1964 to 2007) vs. Average number of 6.5M and up Earthquakes/6months. Line of best fit, y = -0.01099x + (19.65), mean x = 31.16 +/- 22.09, mean y = 19.3 +/- 4.12, R = -0.05894, R squared = 0.003474, p-value = 0.5832.

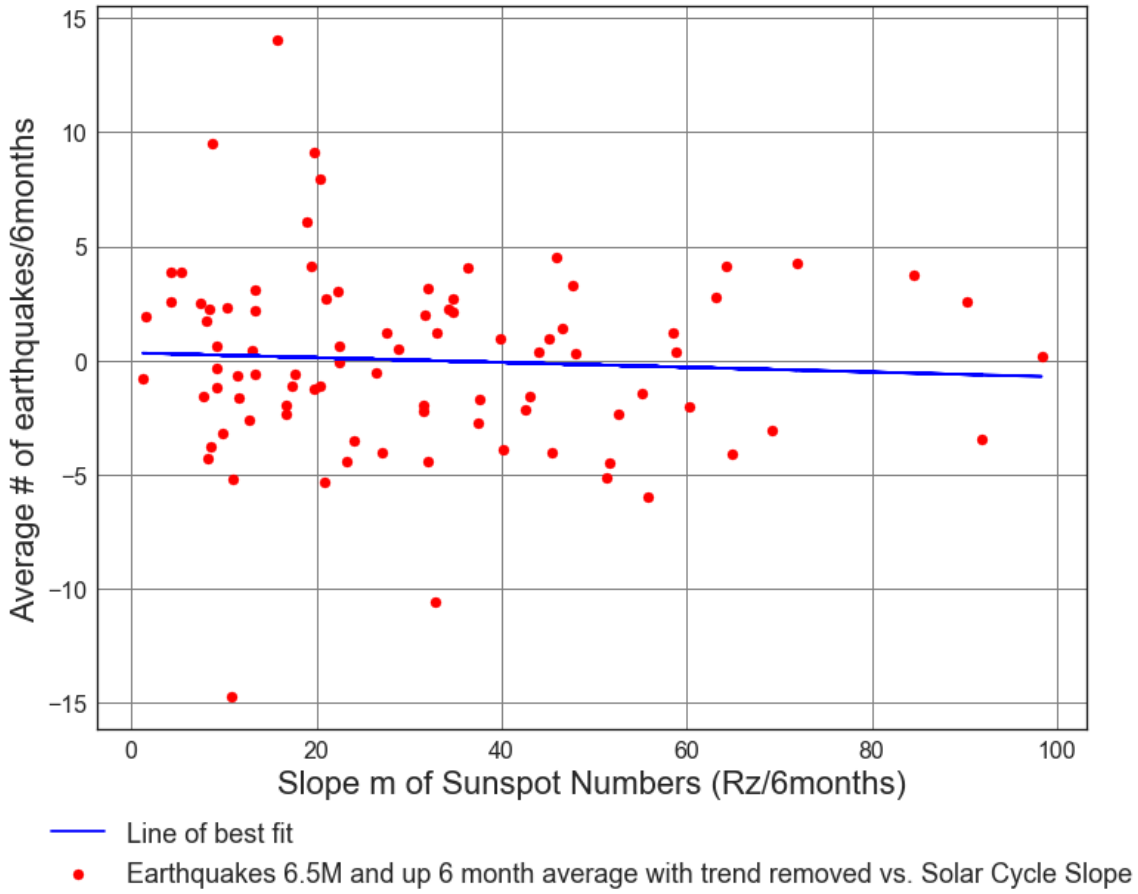

Figure B4.30: Scatter Plot of Solar cycle absolute value slope (from 1964 to 2007) vs. Average number of 6.5M and up Earthquakes/6months with trend removed. Line of best fit, y = -0.01053x + (0.3282), mean x = 31.16 +/- 22.09, mean y = -1.437e-15 +/- 4.033, R = -0.05771, R squared = 0.003331, p-value = 0.5911.

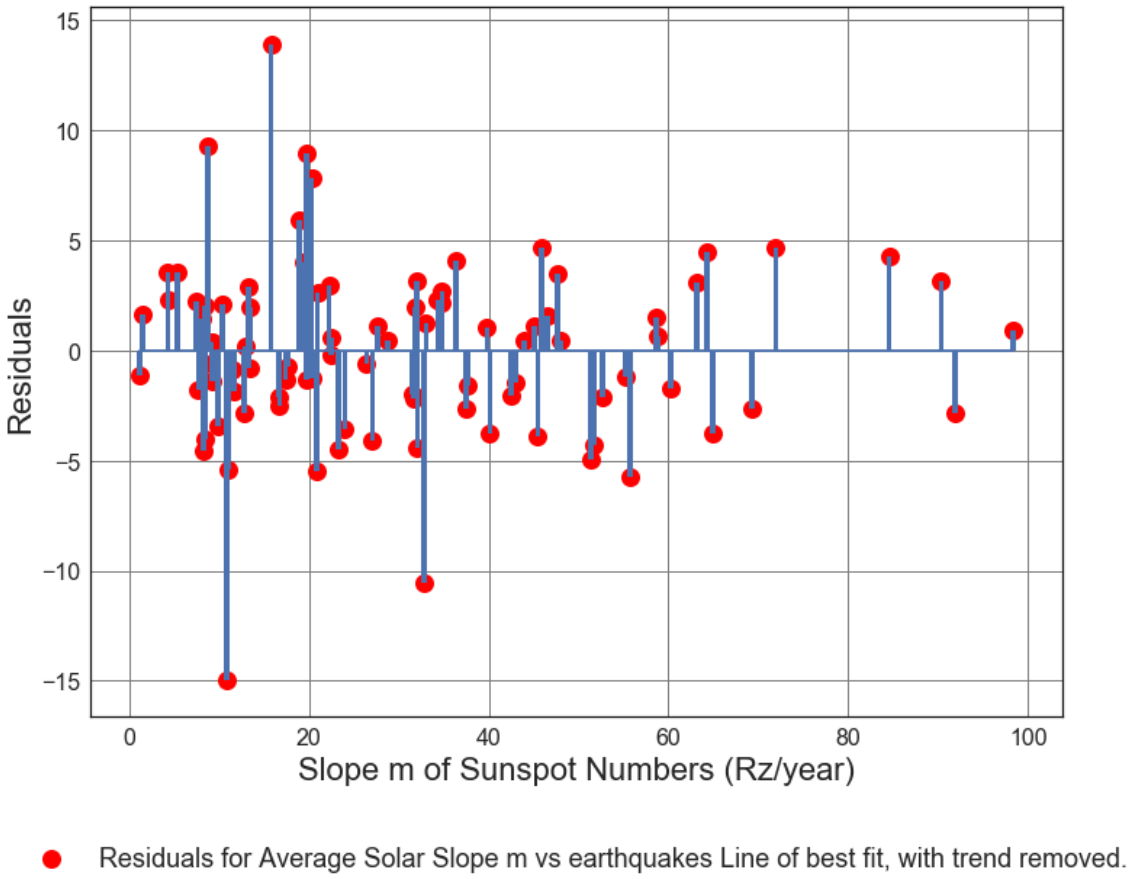

Figure B4.31: Scatter Plot of Solar cycle absolute value slope (from 1964 to 2007) vs. Average number of 6.5M and up Earthquakes/6months with trend removed. Line of best fit, y = -0.01053x + (0.3282), mean x = 31.16 +/- 22.09, mean y = -1.437e-15 +/- 4.033, R = -0.05771, R squared = 0.003331, p-value = 0.5911.

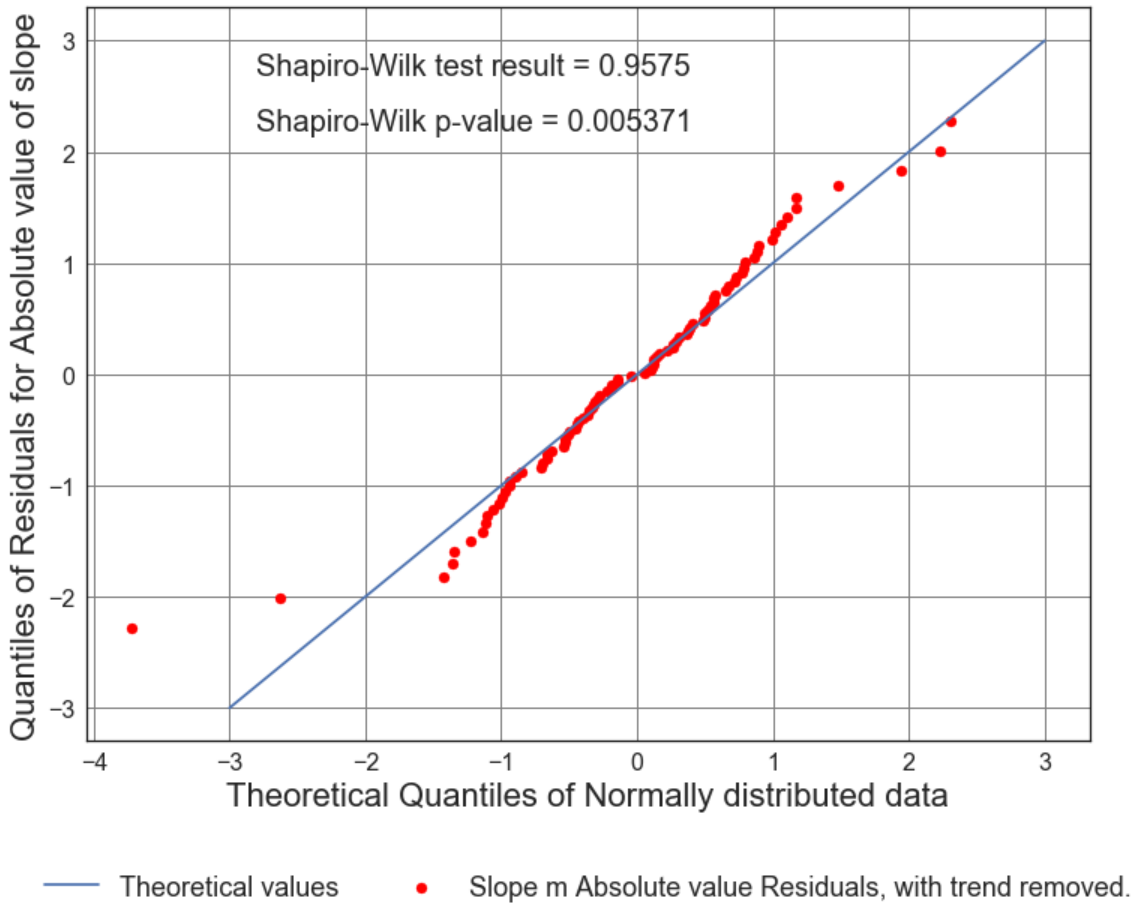

Figure B4.32: Scatter Plot of Solar cycle absolute value slope (from 1964 to 2007) vs. Average number of 6.5M and up Earthquakes/6months with trend removed. Line of best fit, y = -0.01053x + (0.3282), mean x = 31.16 +/- 22.09, mean y = -1.437e-15 +/- 4.033, R = -0.05771, R squared = 0.003331, p-value = 0.5911.

Appendix C1: USGS ComCat Time Series Analysis Part 1 - Average # of Earthquakes per Rise and Decline of Solar cycle slope.

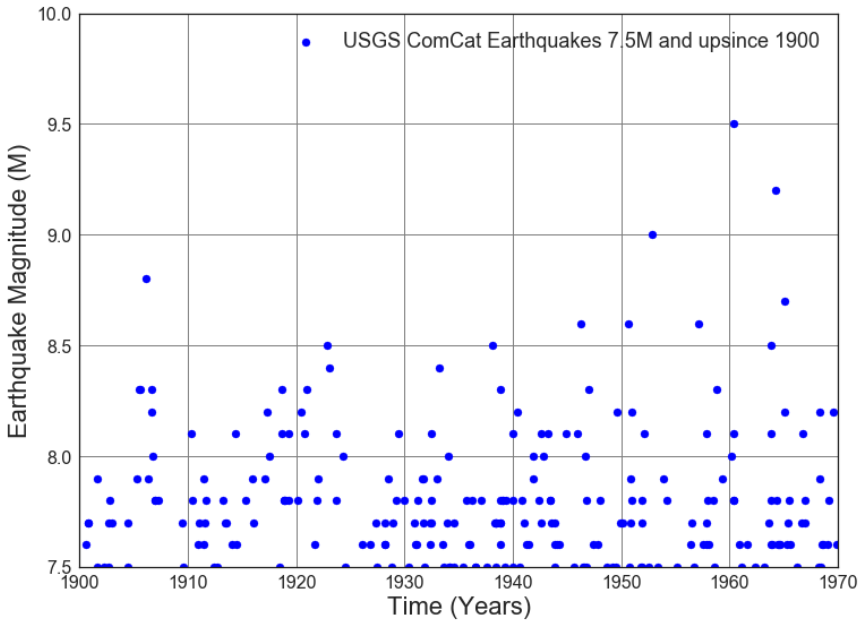

Figure C1.1: Scatter plot of USGS ComCat earthquakes 7.5M and up magnitudes 1900 to 1970

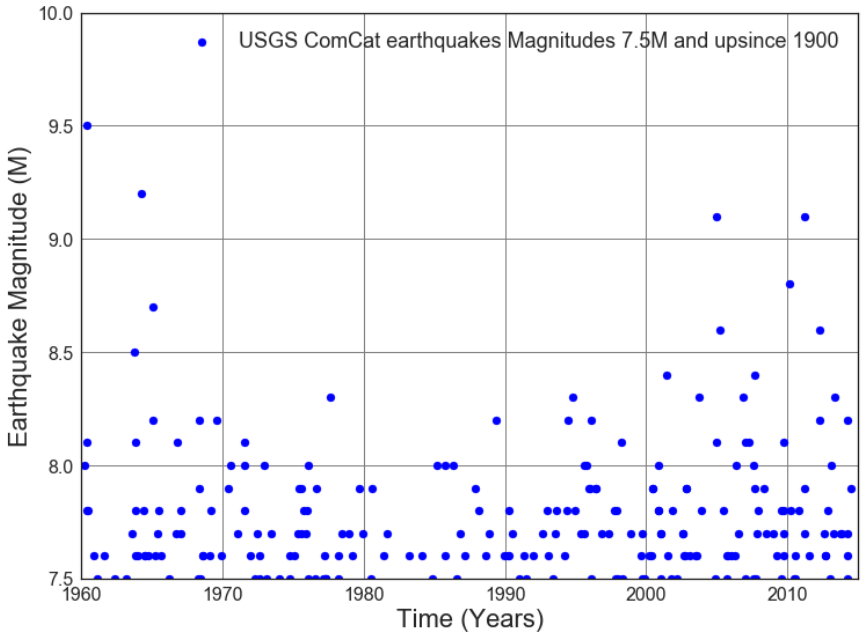

Figure C1.2: Scatter plot of USGS ComCat earthquakes 7.5M and up Magnitudes 1960 to 2017

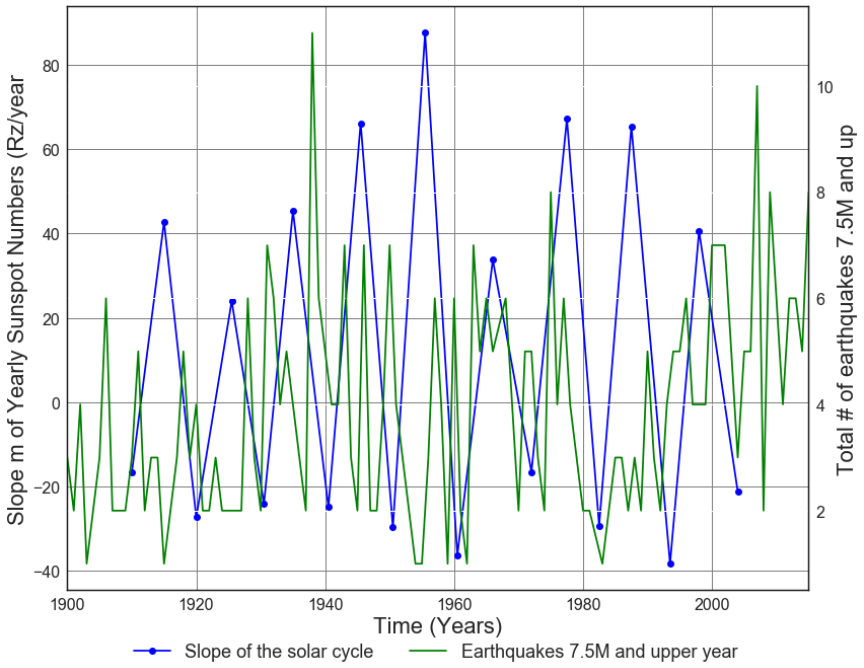

Figure C1.3: Slope of Solar cycle from 1900 to 2014 vs. Average number of 7.5M and up Earthquakes.

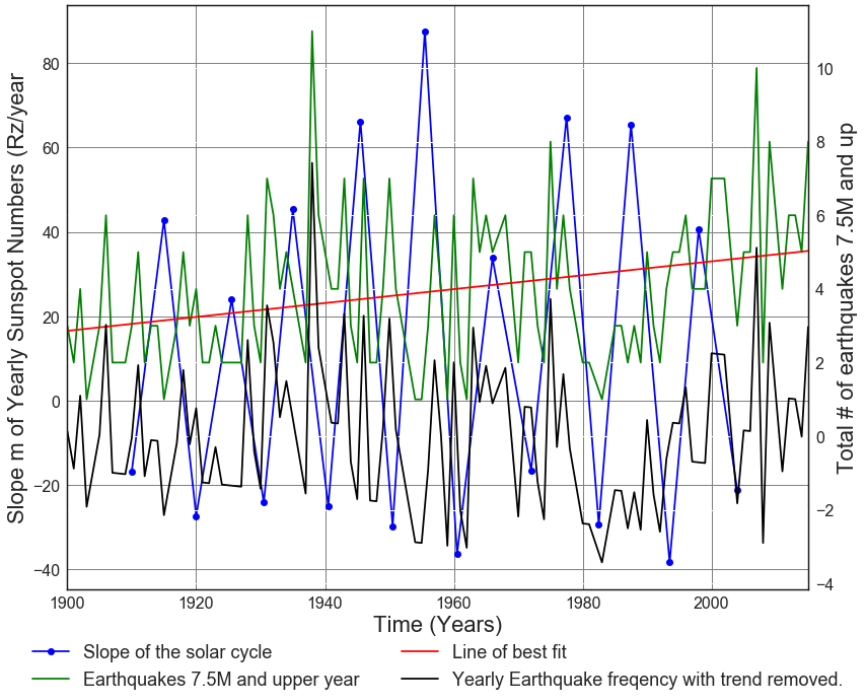

Figure C1.4: Slope of Solar cycle from 1900 to 2014 vs. Average number of 7.5M and up Earthquakes. Line of best fit, y = 0.01887x + (-32.99), mean x = 1.959e+03 +/- 34.1, mean y = 3.974 +/- 2.037

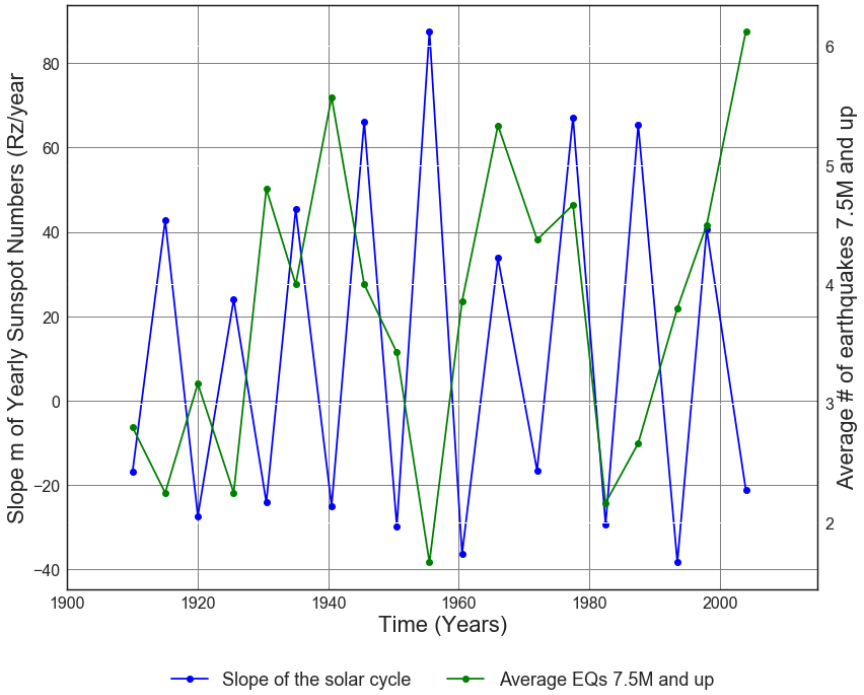

Figure C1.5: Slope of Solar cycle from 1900 to 2014 vs. Average number of 7.5M and up Earthquakes.

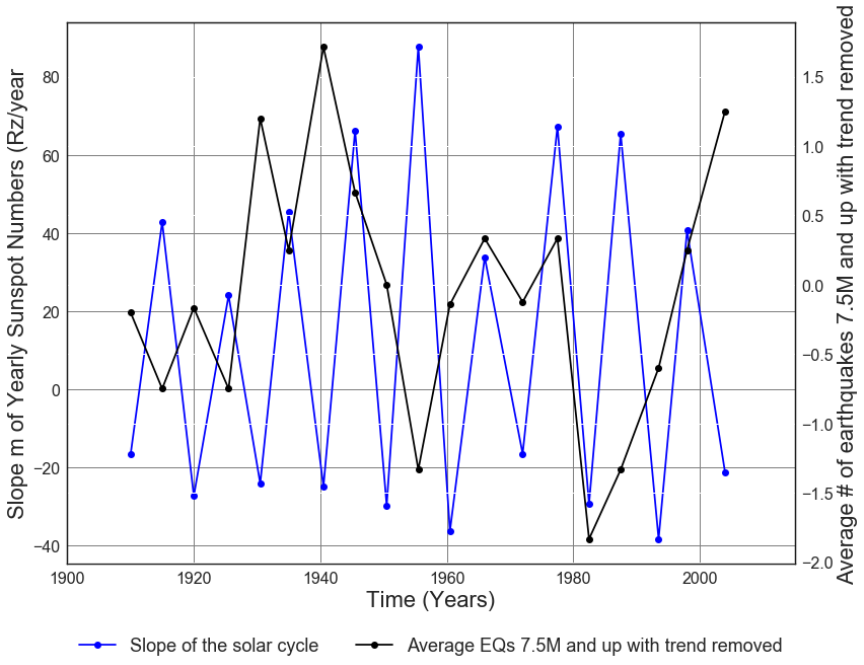

Figure C1.6: Slope of Solar cycle from 1900 to 2014 vs. Average number of 7.5M and up earthquakes.

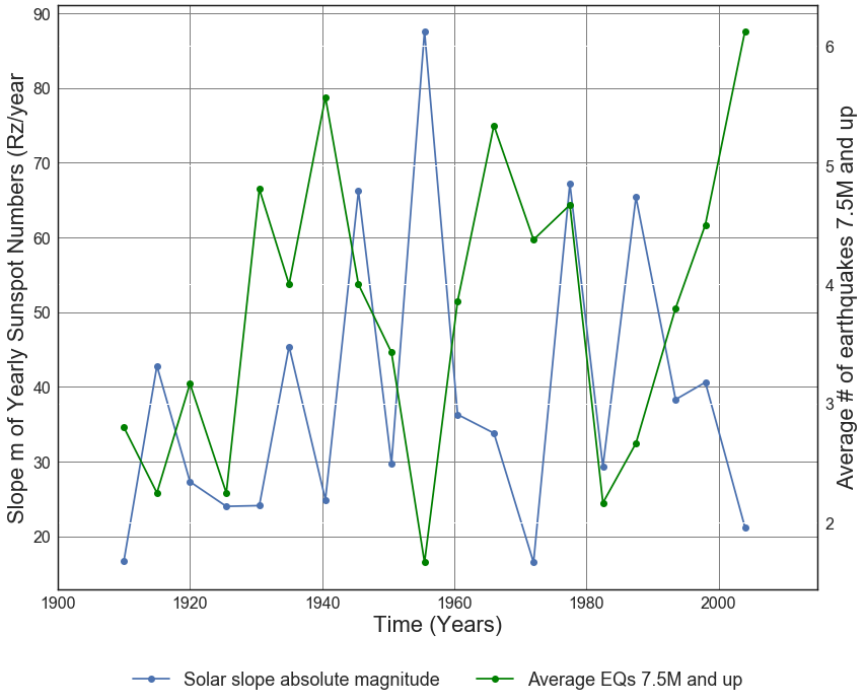

Figure C1.7: Absolute value of Solar cycle slope from 1900 to 2014 vs. Average number of 7.5M and up Earthquakes.

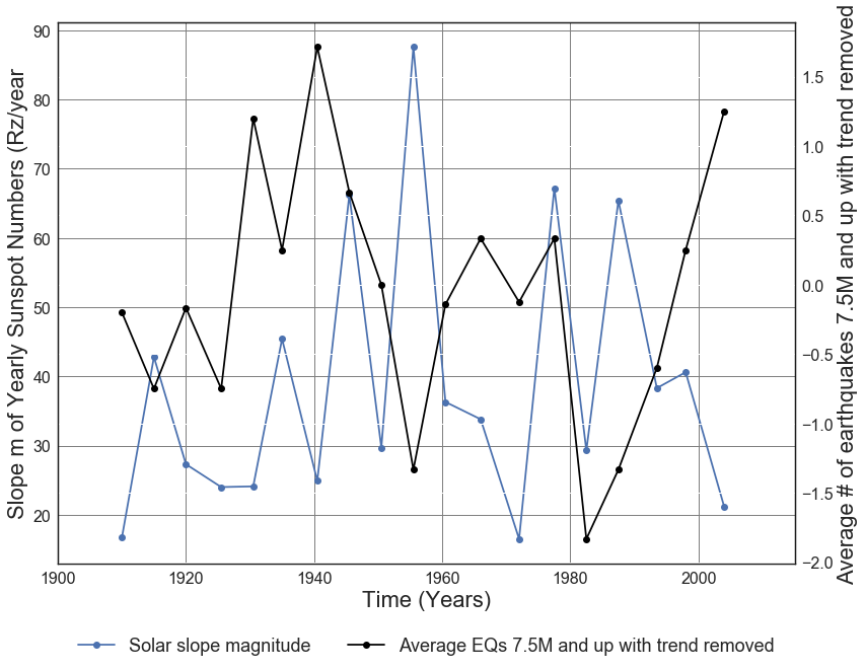

Figure C1.8: Absolute value of solar cycle slope from 1900 to 2014 vs. Average number of 7.5M and up Earthquakes with trend removed.

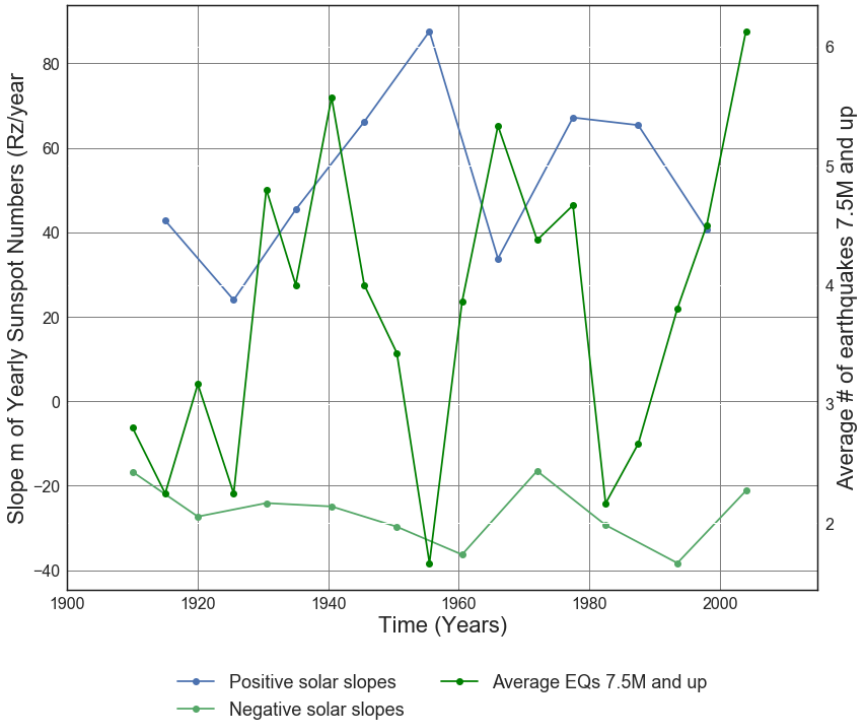

Figure C1.9: Positive and negative solar cycle slopes from 1900 to 2014 vs. Average number of 7.5M and up Earthquakes.

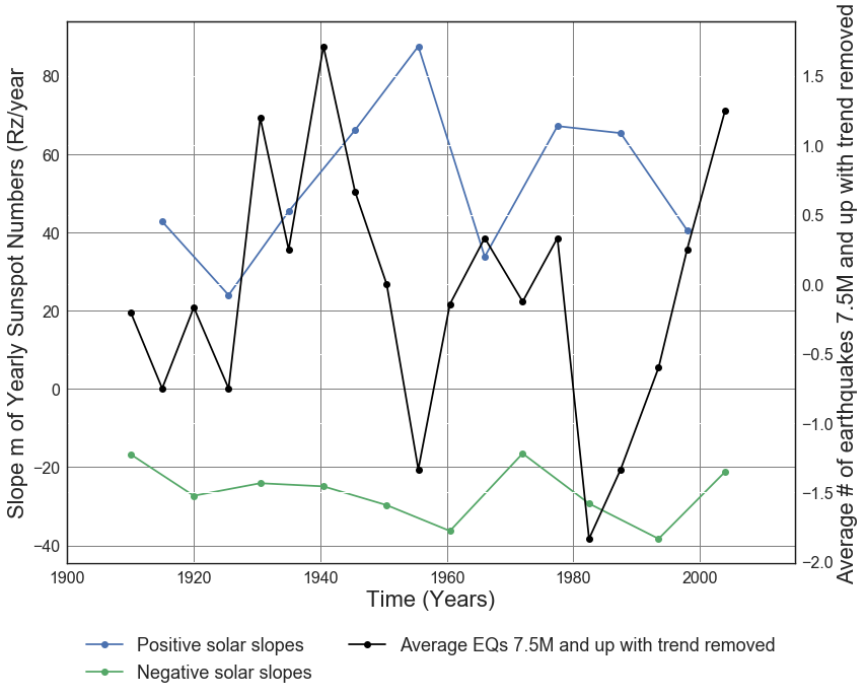

Figure C1.10: Positive and negative solar cycle slopes from 1900 to 2014 vs. Average number of 7.5M and up Earthquakes with trend removed.

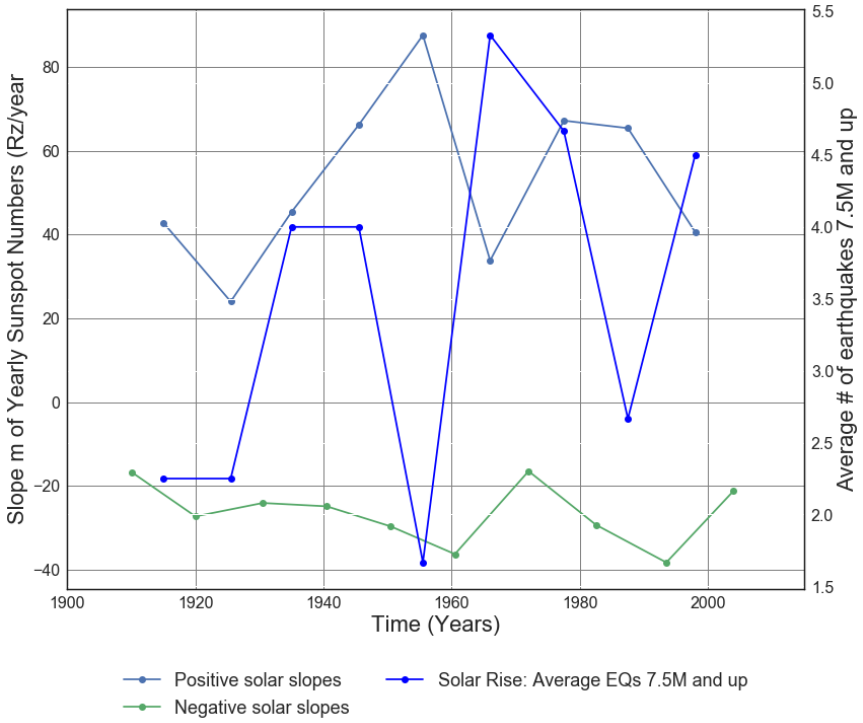

Figure C1.11: Positive and negative solar cycle slopes from 1900 to 2014 vs. Solar Rise: Average number of 7.5M and up Earthquakes.

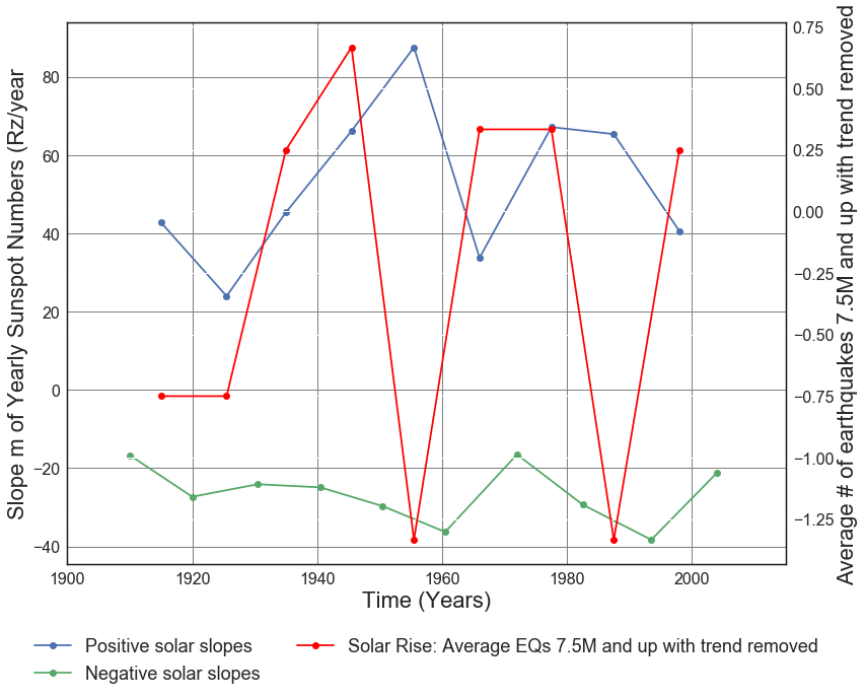

Figure C1.12: Positive and negative solar cycle slopes from 1900 to 2014 vs. Solar Rise: Average number of 7.5M and up Earthquakes with trend removed.

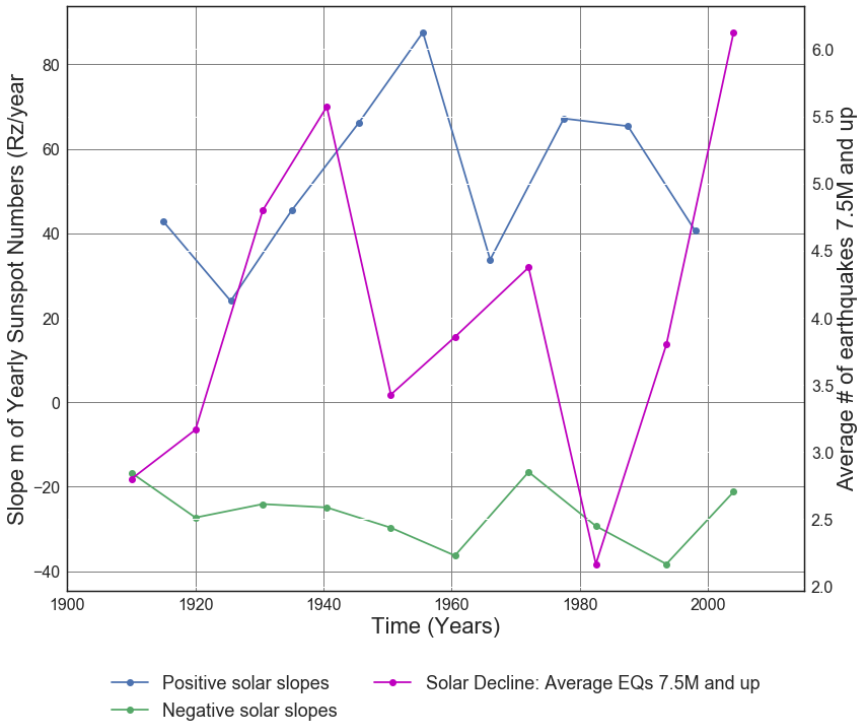

Figure C1.13: Positive and negative solar cycle slopes from 1900 to 2014 vs. Solar Decline: Average number of 7.5M and up Earthquakes.

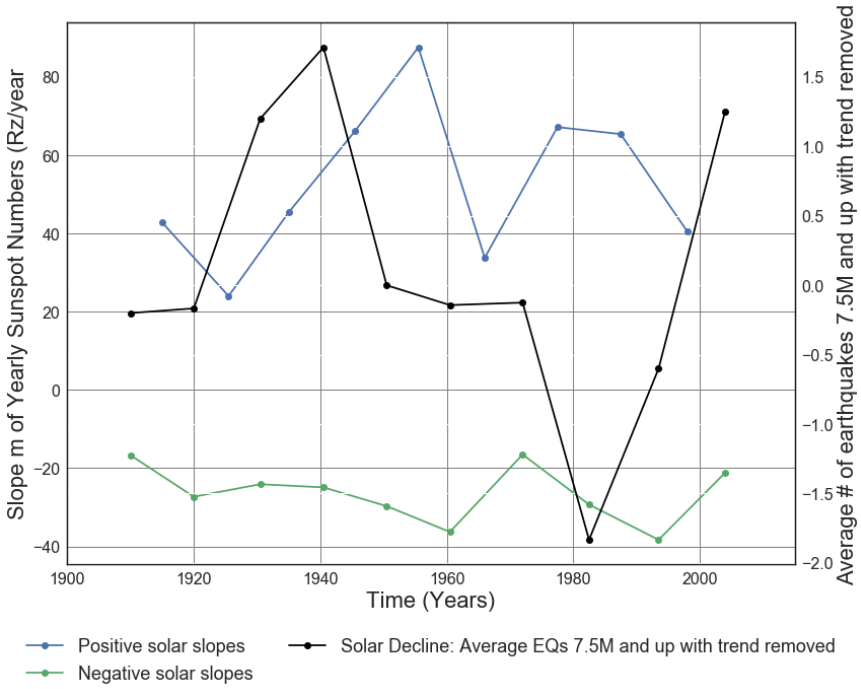

Figure C1.14: Positive and negative solar cycle slopes from 1900 to 2014 vs. Solar Rise: Average number of 7.5M and up Earthquakes.

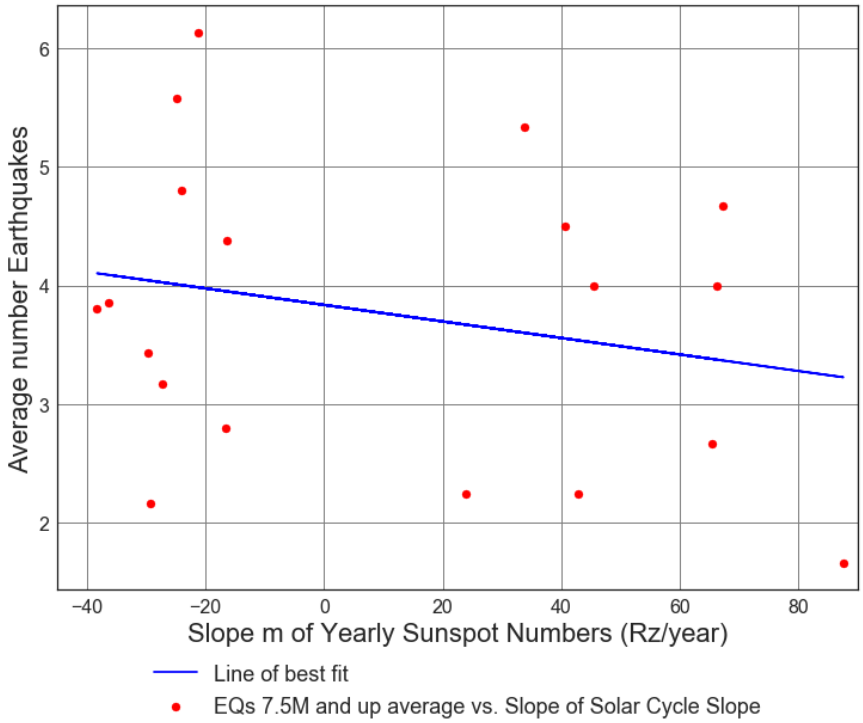

Figure C1.15: Scatter Plot of Slope m of Solar cycle (from 1900 to 2014) vs. Average number of 7.5M and up Earthquakes. Line of best fit, y = -0.006951x + (3.835), mean x = 10.98 +/- 41.86, mean y = 3.759 +/- 1.222, R = -0.2381, R squared = 0.0567, p-value = 0.3262.

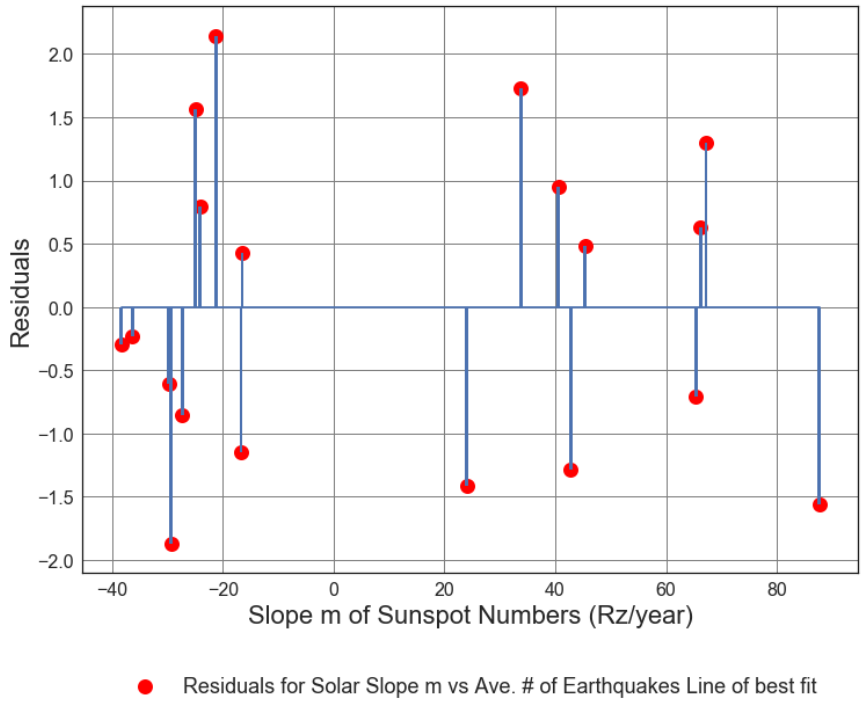

Figure C1.16: Residuals Plot of Average Solar Cycle Slope m (from 1900 to 2007) vs. Average number of 7.5M and up Earthquakes. Line of best fit, y = -0.006951x + (3.835), mean x = 10.98 +/- 41.86, mean y = 3.759 +/- 1.222, R = -0.2381, R squared = 0.0567, p-value = 0.3262.

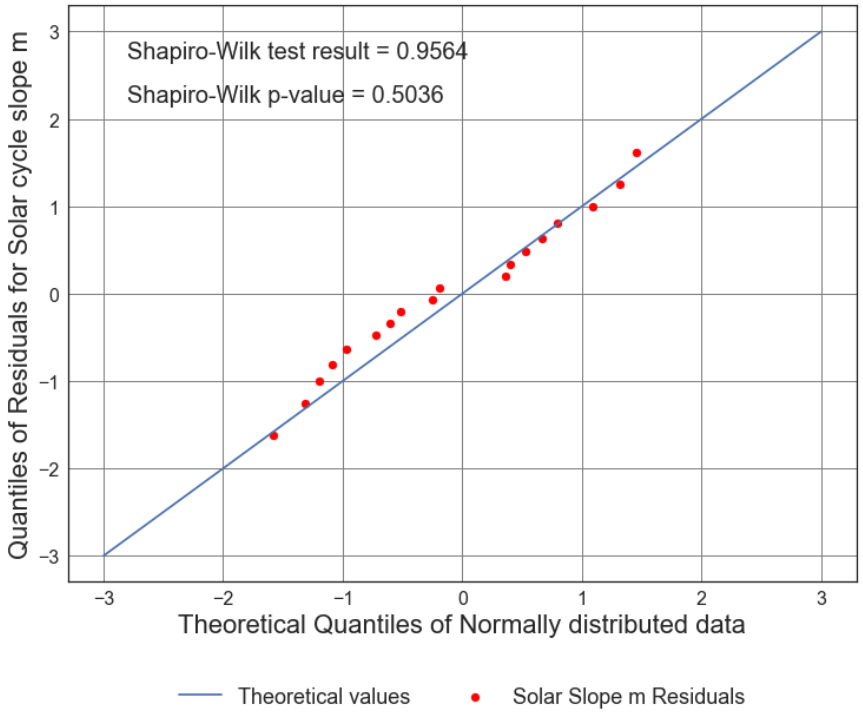

Figure C1.17: Quantile-Quantile Plot of the resisuals of Slope of Solar cycle m (from 1900 to 2014) vs. Average number of 7.5M and up Earthquakes. Line of best fit, y = -0.006951x + (3.835), mean x = 10.98 +/- 41.86, mean y = 3.759 +/- 1.222, R = -0.2381, R squared = 0.0567, p-value = 0.3262.

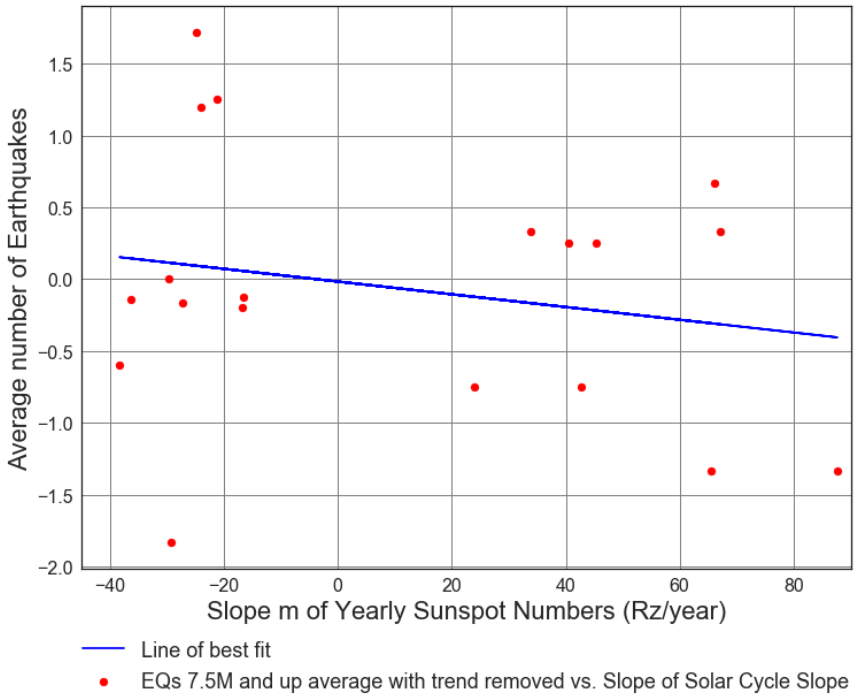

Figure C1.18: Scatter Plot of Slope m of Solar cycle (from 1900 to 2014) vs. Average number of 7.5M and up Earthquakes with trend removed. Line of best fit, y = -0.00443x + (-0.01643), mean x = 10.98 +/- 41.86, mean y = -0.0651 +/- 0.8932, R = -0.2076, R squared = 0.04311, p-value = 0.3937.

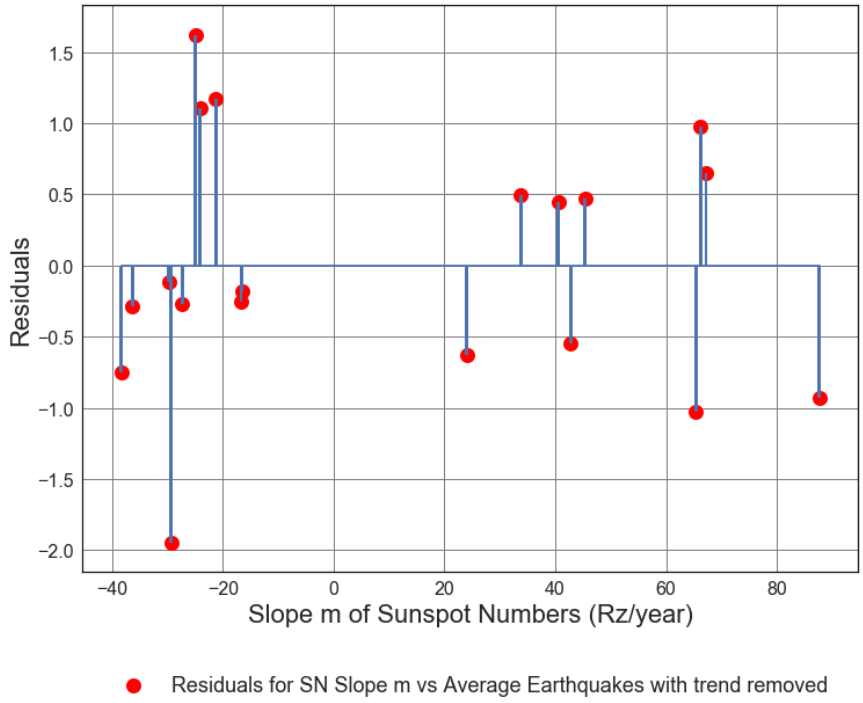

Figure C1.19: Residuals Plot of the Slope of Solar cycle (from 1900 to 2014) vs. Average number of 7.5M and up Earthquakes with trend removed. Line of best fit, y = -0.00443x + (-0.01643), mean x = 10.98 +/- 41.86, mean y = -0.0651 +/- 0.8932, R = -0.2076, R squared = 0.04311, p-value = 0.3937.

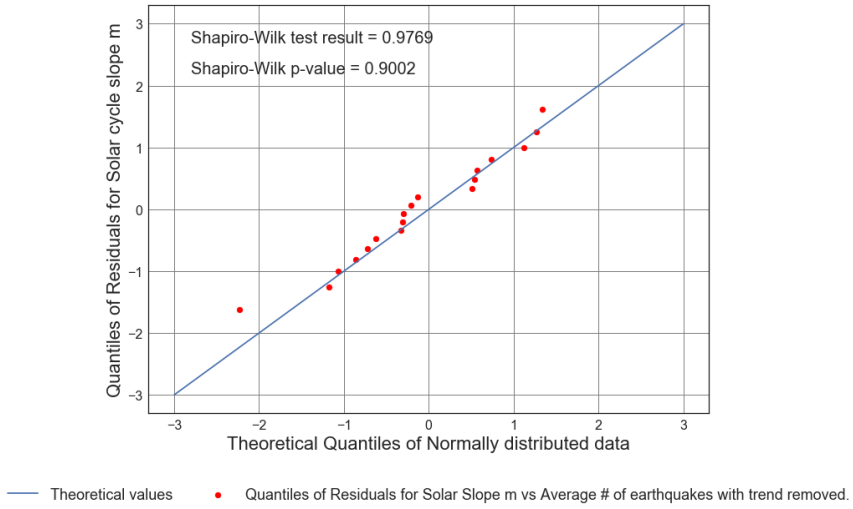

Figure C1.20: Scatter Plot of Absolute Magnitude of the Slope of Solar cycle (from 1900 to 2014) vs. Average number of 7.5M and up Earthquakes. Line of best fit, y = -0.00443x + (-0.01643), mean x = 10.98 +/- 41.86, mean y = -0.0651 +/- 0.8932, R = -0.2076, R squared = 0.04311, p-value = 0.3937.

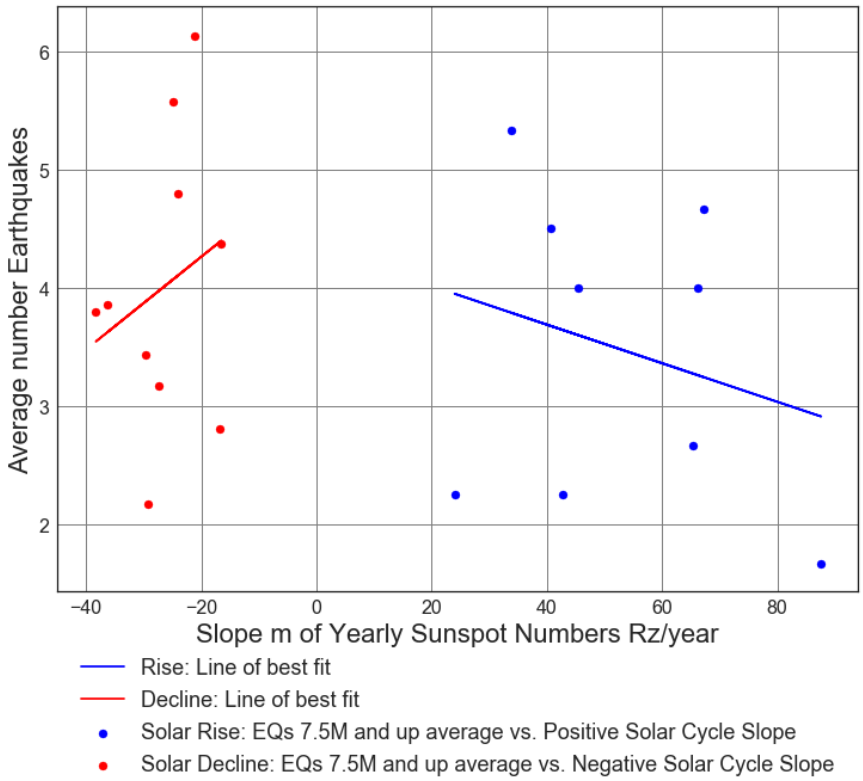

Figure C1.21: Scatter Plot of Slope of Solar cycle (from 1900 to 2014) vs. Average number of 7.5M and up Earthquakes. Rise: Line of best fit, y = -0.01633x + (4.34), mean x = 52.56 +/- 19.0, mean y = 3.481 +/- 1.22, R = -0.09454, R squared = 0.008938, p-value = 0.795. Decline: Line of best fit, y = 0.0392x + 5.045, mean x = -26.43 +/- 6.974, mean y = 4.009 +/- 1.168, R = 0.234, R squared = 0.05478, p-value = 0.5152.

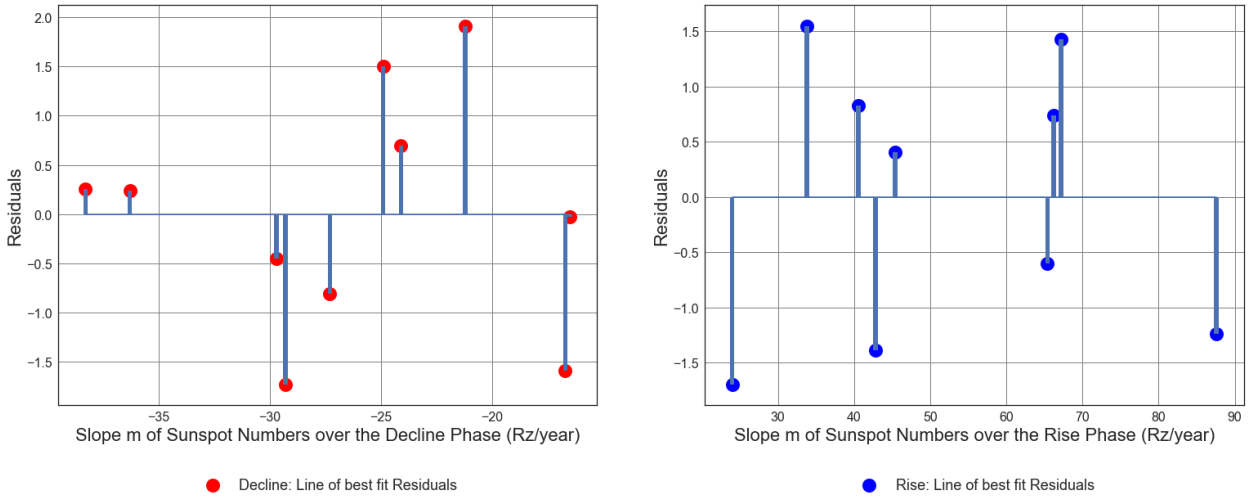

Figure C1.22: Residuals centered about zero, plot of Slope of Solar cycle (from 1900 to 2014) vs. Average number of 7.5M and up Earthquakes. Rise: Line of best fit, y = -0.01633x + (4.34), mean x = 52.56 +/- 19.0, mean y = 3.481 +/- 1.22, R = -0.09454, R squared = 0.008938, p-value = 0.795. Decline: Line of best fit, y = 0.0392x + 5.045, mean x = -26.43 +/- 6.974, mean y = 4.009 +/- 1.168, R = 0.234, R squared = 0.05478, p-value = 0.5152.

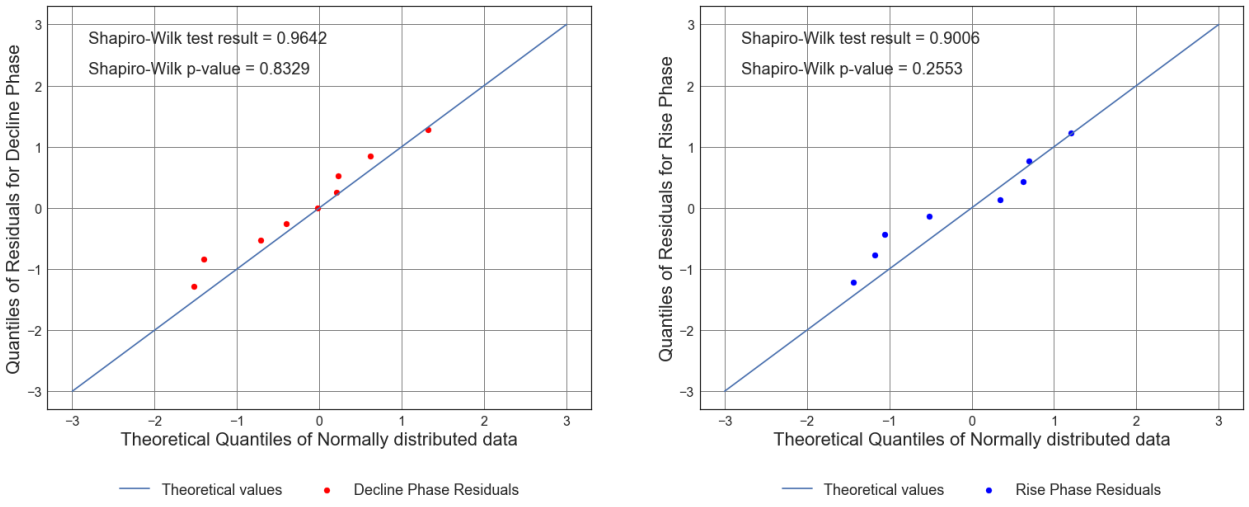

Figure C1.23: Quartile-Quartile Plot of Residuals for the Rise and Decline phase Slope of Solar cycle (from 1900 to 2014) vs. Average number of 7.5M and up Earthquakes. Rise: Line of best fit, y = -0.01633x + (4.34), mean x = 52.56 +/- 19.0, mean y = 3.481 +/- 1.22, R = -0.09454, R squared =

0.008938, p-value = 0.795. Decline: Line of best fit, y = 0.0392x + 5.045, mean x = -26.43 +/- 6.974, mean y = 4.009 +/- 1.168, R = 0.234, R squared = 0.05478, p-value = 0.5152.

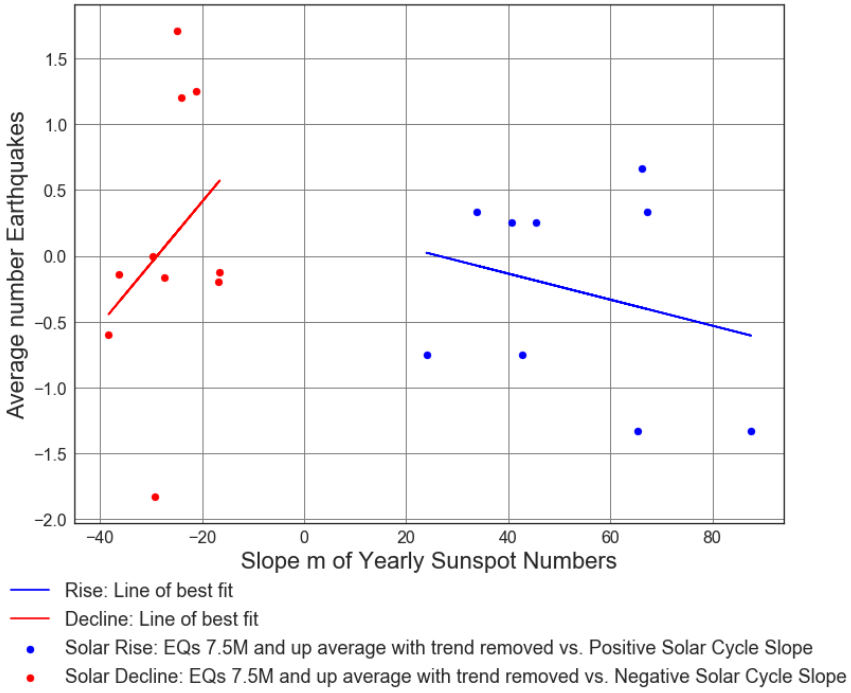

Figure C1.24: Scatter Plot of Slope of Solar cycle (from 1900 to 2014) vs. with trend removed Average number of 7.5M and up Earthquakes. Rise: Line of best fit, y = -0.009898x + (0.2609), mean x = 52.56 +/- 19.0, mean y = -0.2593 +/- 0.7354, R = -0.2558, R squared = 0.06542, p-value = 0.5065. Decline: Line of best fit, y = 0.04669x + 1.344, mean x = -26.43 +/- 6.974, mean y = 0.1096 +/- 0.9821, R = 0.3315, R squared = 0.1099, p-value = 0.3494.

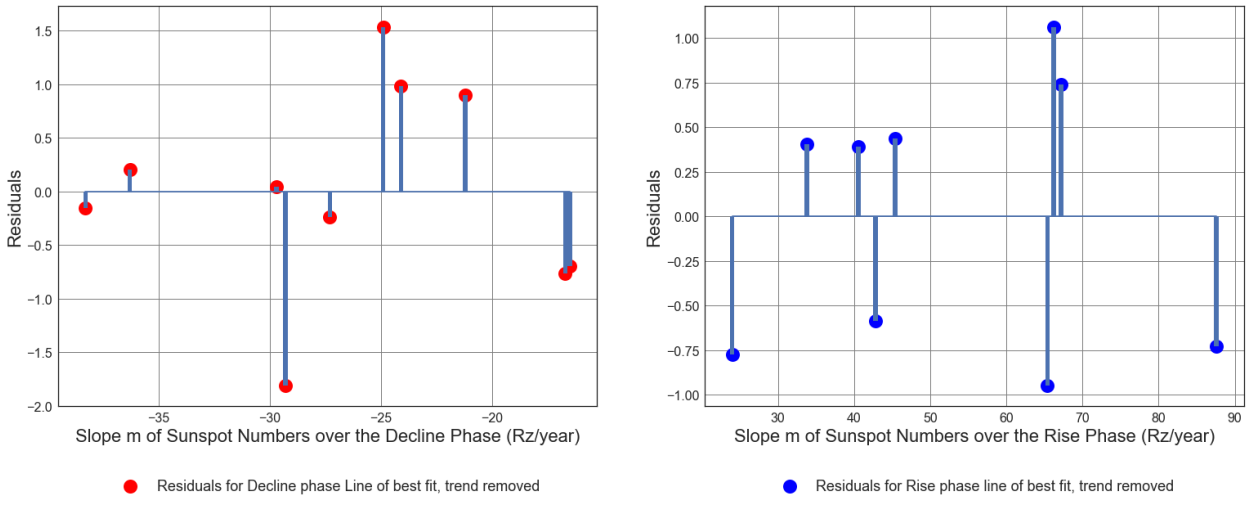

Figure C1.25: Residuals centered about zero, plot of Slope of Solar cycle (from 1900 to 2014) vs. Average number of 7.5M and up Earthquakes with trend removed. Rise: Line of best fit, y =

-0.009898x + (0.2609), mean x = 52.56 +/- 19.0, mean y = -0.2593 +/- 0.7354, R = -0.2558, R squared = 0.06542, p-value = 0.5065. Decline: Line of best fit, y = 0.04669x + 1.344, mean x = -26.43 +/- 6.974, mean y = 0.1096 +/- 0.9821, R = 0.3315, R squared = 0.1099, p-value = 0.3494.

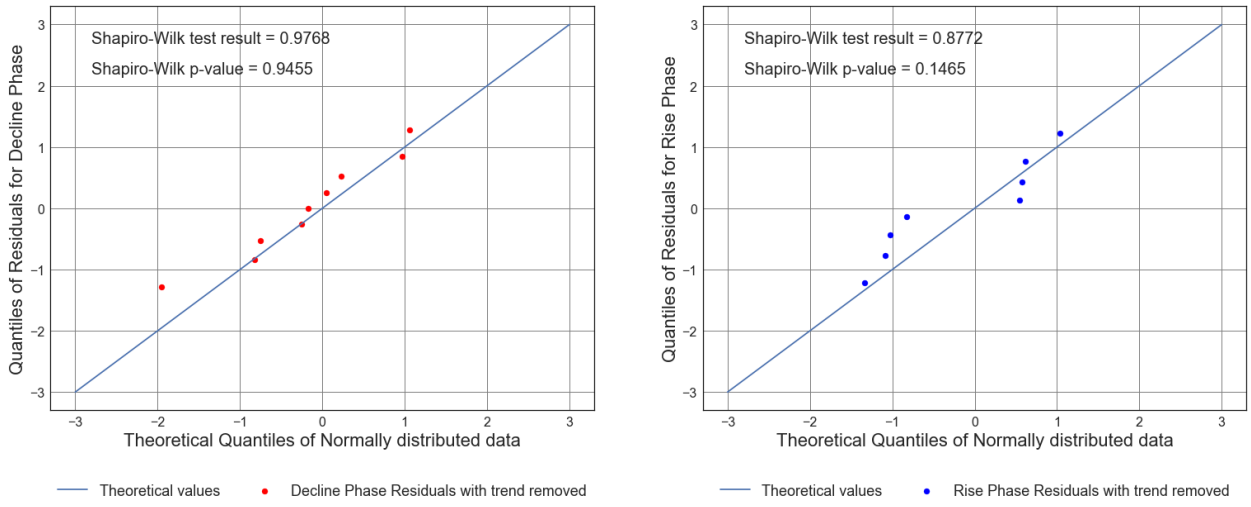

Figure C1.26: Quartile-Quartile Plot of Residuals for the Rise and Decline phase Slope of Solar cycle (from 1900 to 2014) vs. Average number of 7.5M and up Earthquakes with trend removed. Rise: Line of best fit, y = -0.009898x + (0.2609), mean x = 52.56 +/- 19.0, mean y = -0.2593 +/- 0.7354, R = -0.2558, R squared = 0.06542, p-value = 0.5065. Decline: Line of best fit, y = 0.04669x + 1.344, mean x = -26.43 +/- 6.974, mean y = 0.1096 +/- 0.9821, R = 0.3315, R squared = 0.1099, p-value = 0.3494.

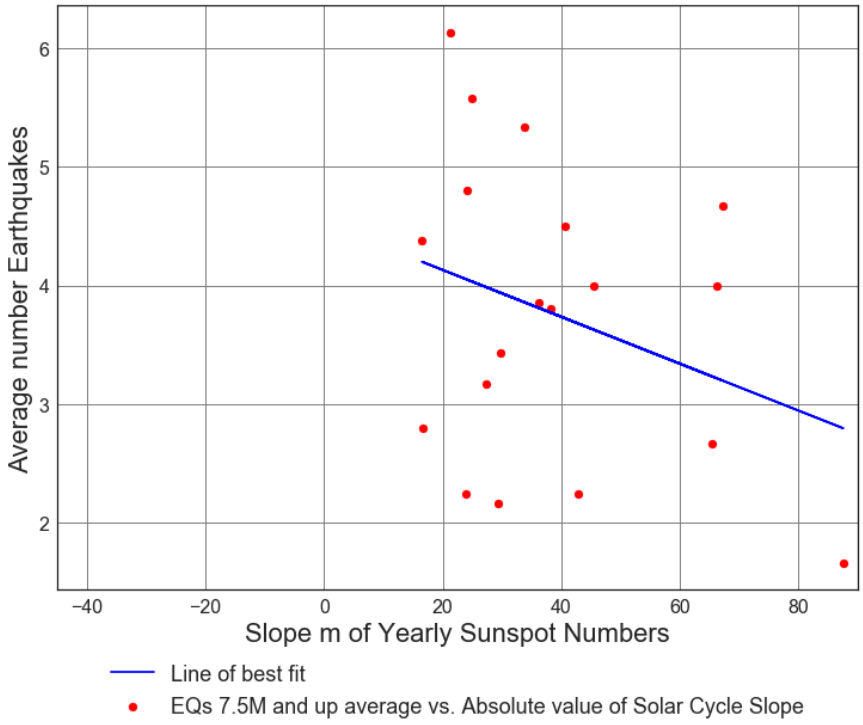

Figure C1.27: Scatter Plot of Absolute value of the Slope of Solar cycle (from 1900 to 2014) vs. Average number of 7.5M and up Earthquakes. Line of best fit, y = -0.01972x + (4.524), mean x = 38.81 +/- 19.15, mean y = 3.759 +/- 1.222, R = -0.3091, R squared = 0.09554, p-value = 0.1979.

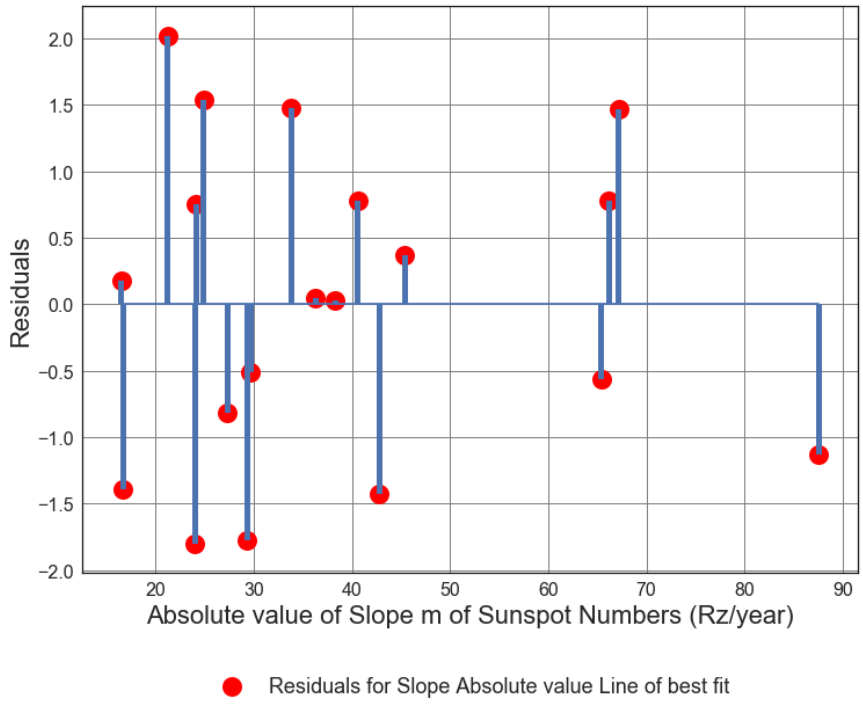

Figure C1.28: Residuals Plot of Absolute Magnitude of the Slope of Solar cycle (from 1900 to 2014) vs. Average number of 7.5M and up Earthquakes. Line of best fit, y = -0.01972x + (4.524), mean x = 38.81 +/- 19.15, mean y = 3.759 +/- 1.222, R = -0.3091, R squared = 0.09554, p-value = 0.1979.

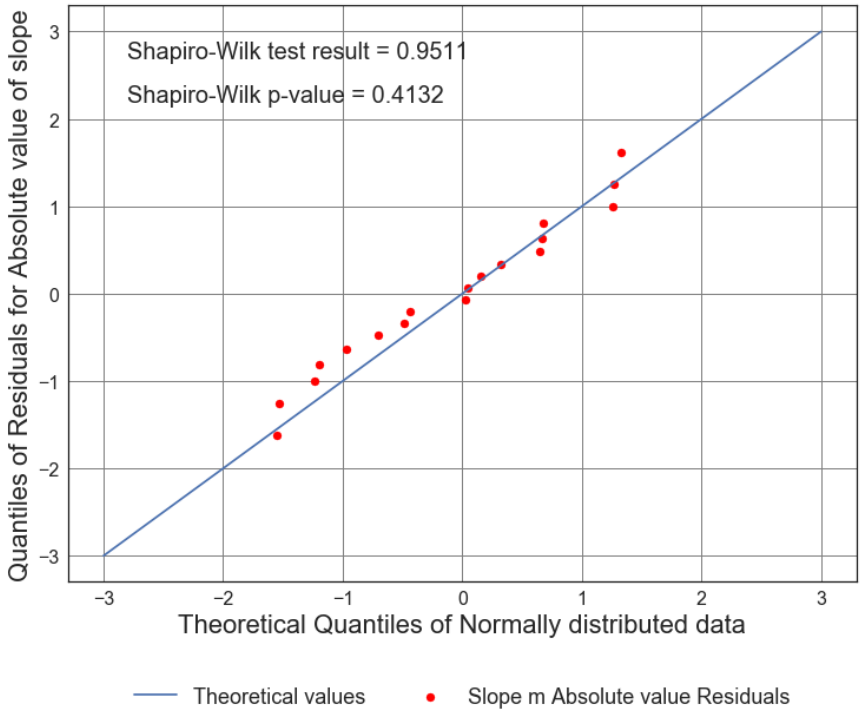

Figure C1.29: Scatter Plot of Absolute Magnitude of the Slope of Solar cycle (from 1900 to 2014) vs. Average number of 7.5M and up Earthquakes. Line of best fit, y = -0.01972x + (4.524), mean x = 38.81 +/- 19.15, mean y = 3.759 +/- 1.222, R = -0.3091, R squared = 0.09554, p-value = 0.1979.

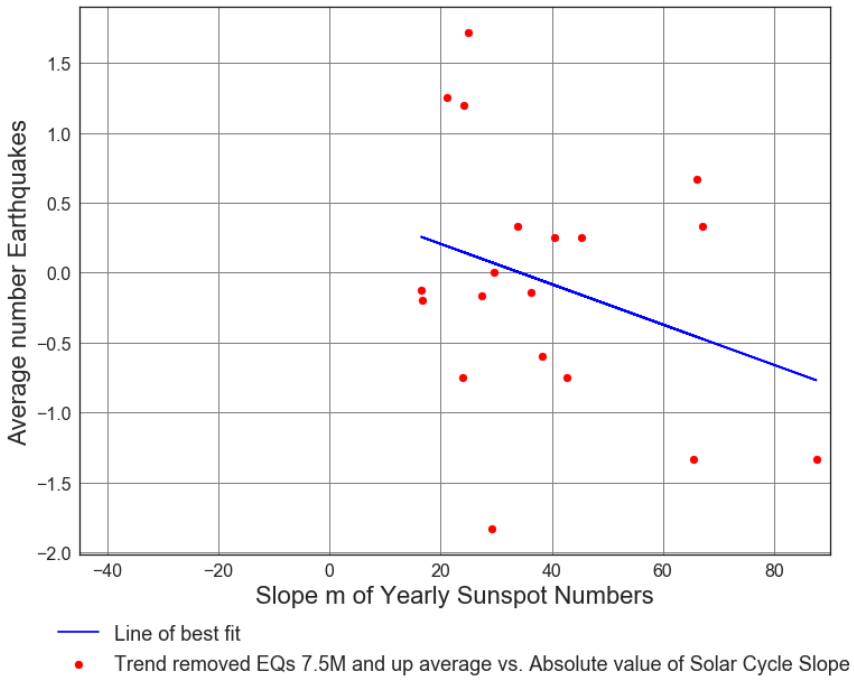

Figure C1.30: Scatter Plot of Absolute Slope Magnitude of the Solar cycle (from 1900 to 2014) vs. Trend removed Average number of 7.5M and up Earthquakes. Line of best fit, y = -0.01442x + (0.4946), mean x = 38.81 +/- 19.15, mean y = -0.0651 +/- 0.8932, R = -0.3093, R squared = 0.09566, p-value = 0.1976.

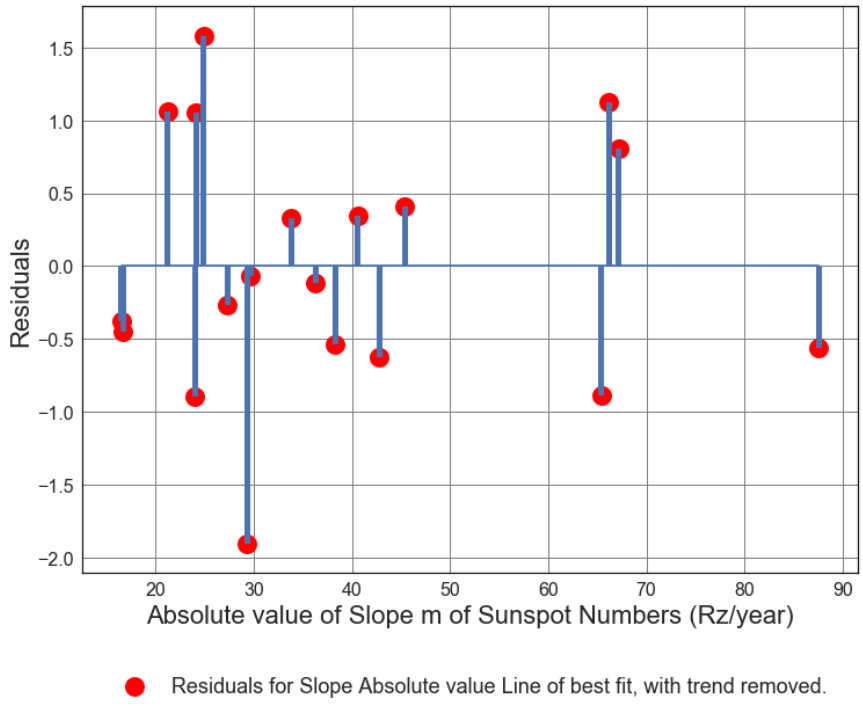

Figure C1.31: Scatter Plot of Absolute Slope Magnitude of the Solar cycle (from 1900 to 2014) vs. Trend removed Average number of 7.5M and up Earthquakes. Line of best fit, y = -0.01442x + (0.4946), mean x = 38.81 +/- 19.15, mean y = -0.0651 +/- 0.8932, R = -0.3093, R squared = 0.09566, p-value = 0.1976.

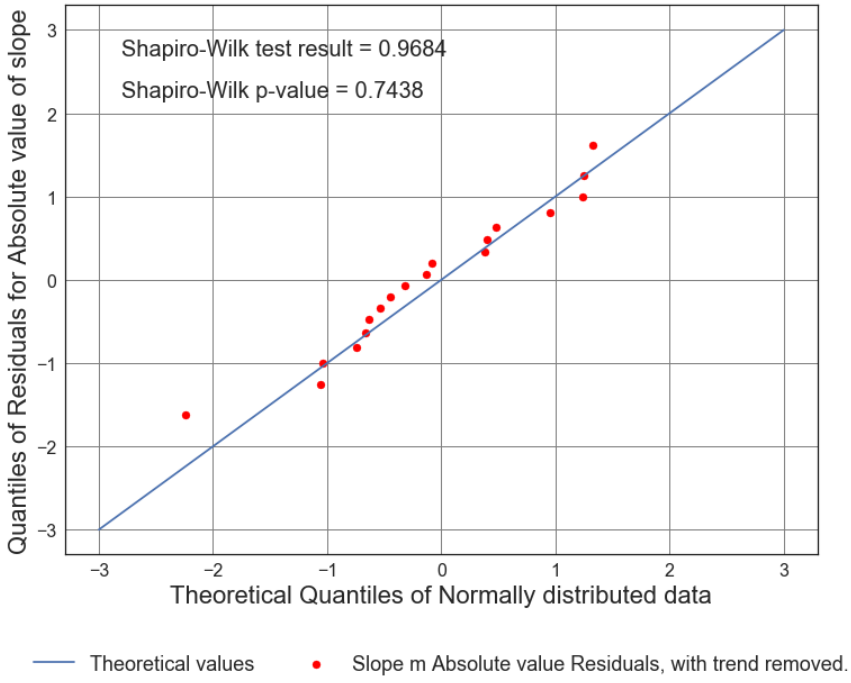

Figure C1.32: Scatter Plot of Absolute Slope Magnitude of the Solar cycle (from 1900 to 2014) vs. Trend removed Average number of 7.5M and up Earthquakes. Line of best fit, y = -0.01442x + (0.4946), mean x = 38.81 +/- 19.15, mean y = -0.0651 +/- 0.8932, R = -0.3093, R squared = 0.09566, p-value = 0.1976.

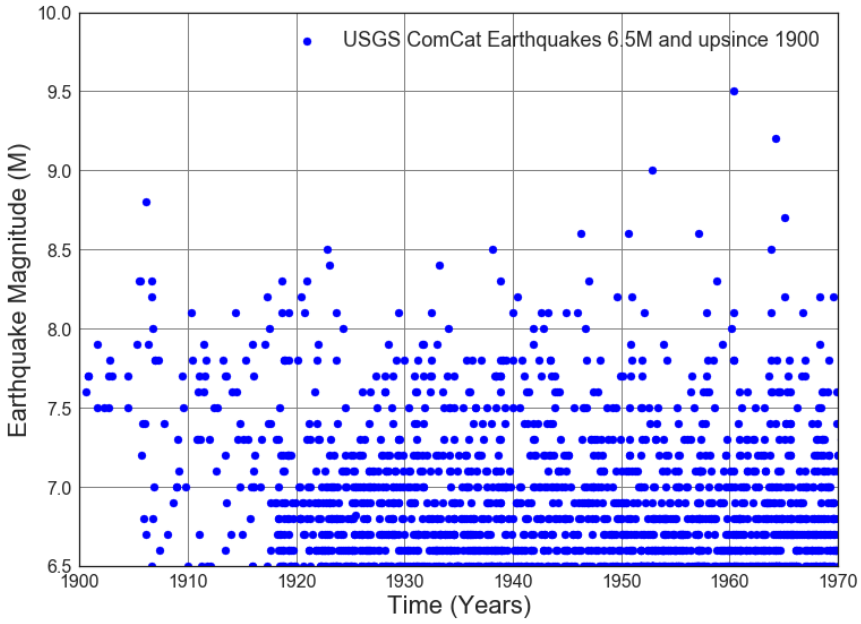

Figure C1.33: Scatter plot of USGS ComCat earthquakes 6.5M and up magnitudes 1900 to 1970

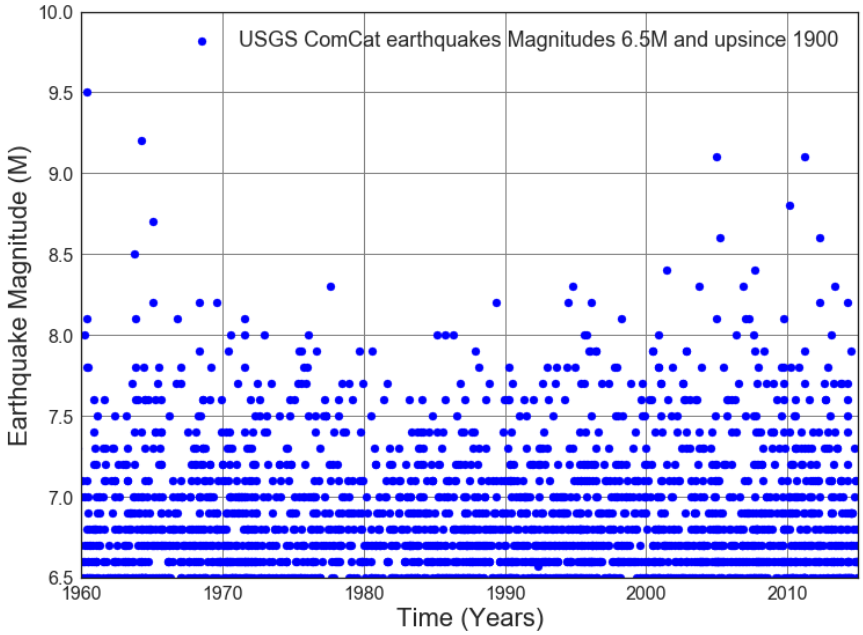

Figure C1.34: Scatter plot of USGS ComCat earthquakes 6.5M and up Magnitudes 1960 to 2017

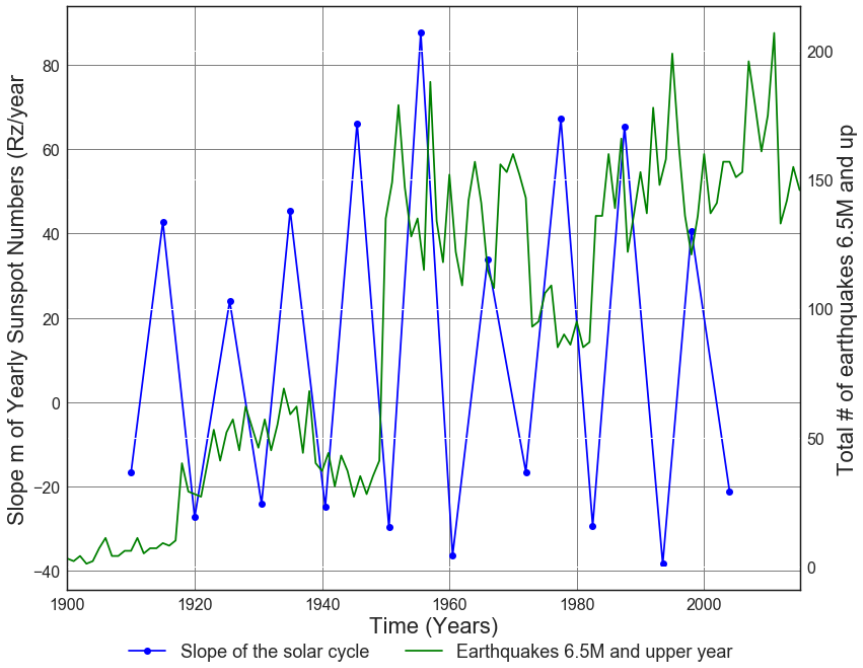

Figure C1.35: Slope of Solar cycle from 1900 to 2014 vs. Average number of 6.5M and up Earthquakes.

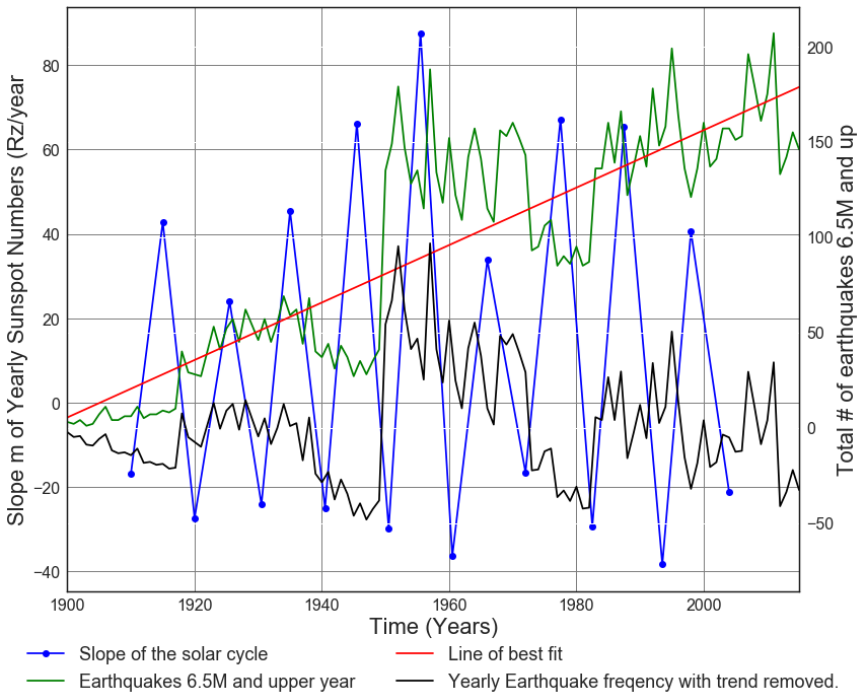

Figure C1.36: Slope of Solar cycle from 1900 to 2014 vs. Average number of 6.5M and up Earthquakes. Line of best fit, y = 1.507x + (-2.859e+03), mean x = 1.958e+03 +/- 34.06, mean y = 93.55 +/- 59.49

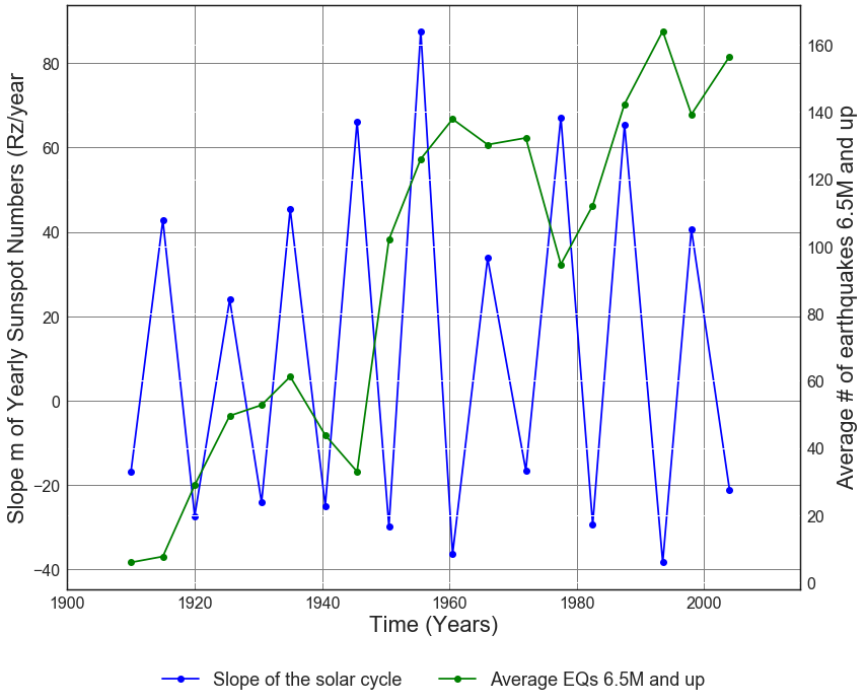

Figure C1.37: Slope of Solar cycle from 1900 to 2014 vs. Average number of 6.5M and up Earthquakes.

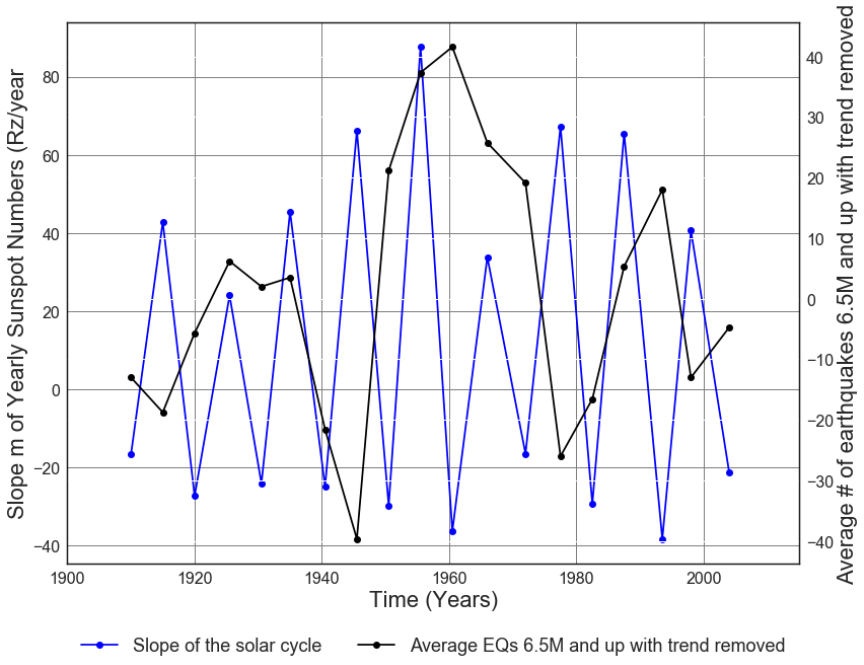

Figure C1.38: Slope of Solar cycle from 1900 to 2014 vs. Average number of 6.5M and up earthquakes.

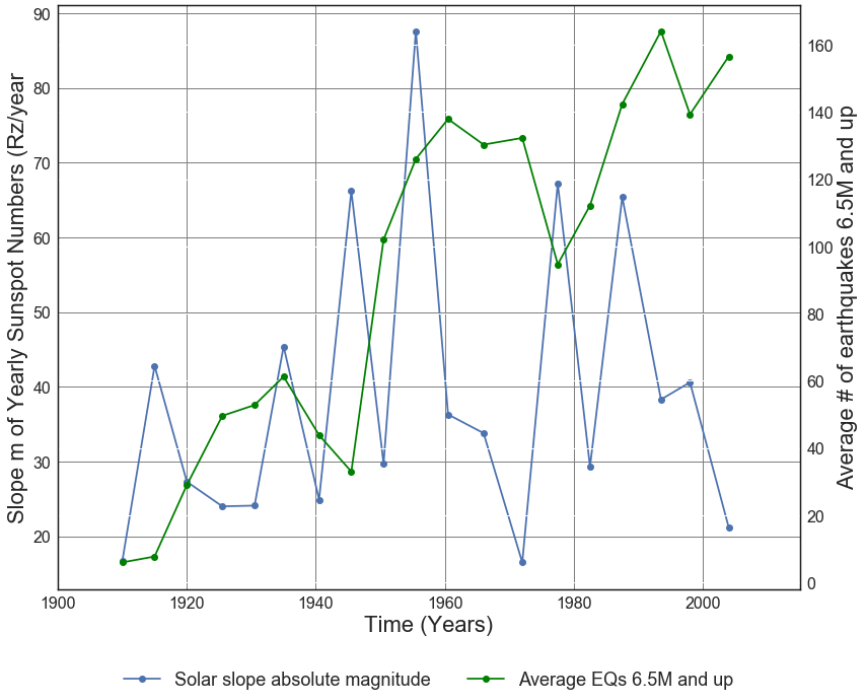

Figure C1.39: Absolute value of Solar cycle slope from 1900 to 2014 vs. Average number of 6.5M and up Earthquakes.

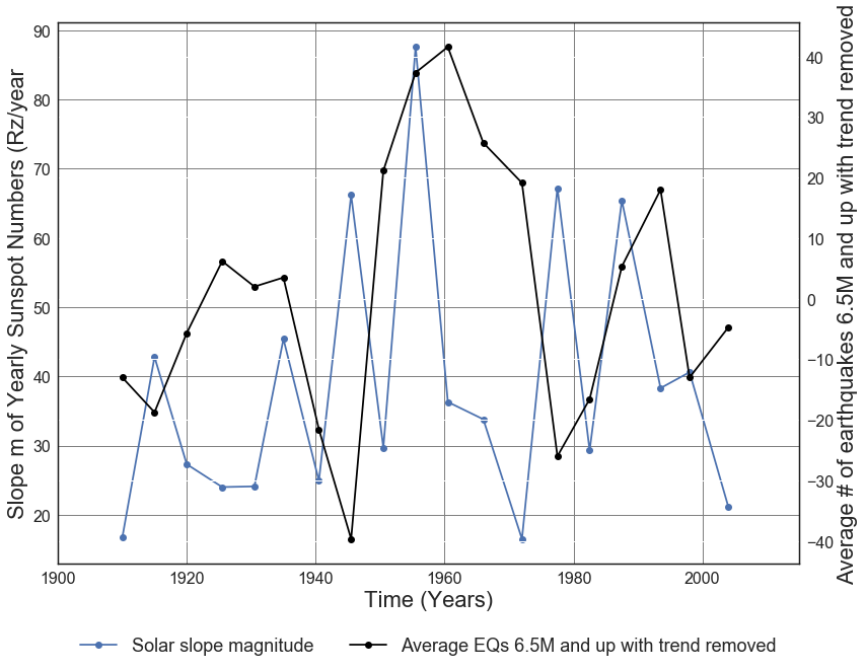

Figure C1.40: Absolute value of solar cycle slope from 1900 to 2014 vs. Average number of 6.5M and up Earthquakes with trend removed.

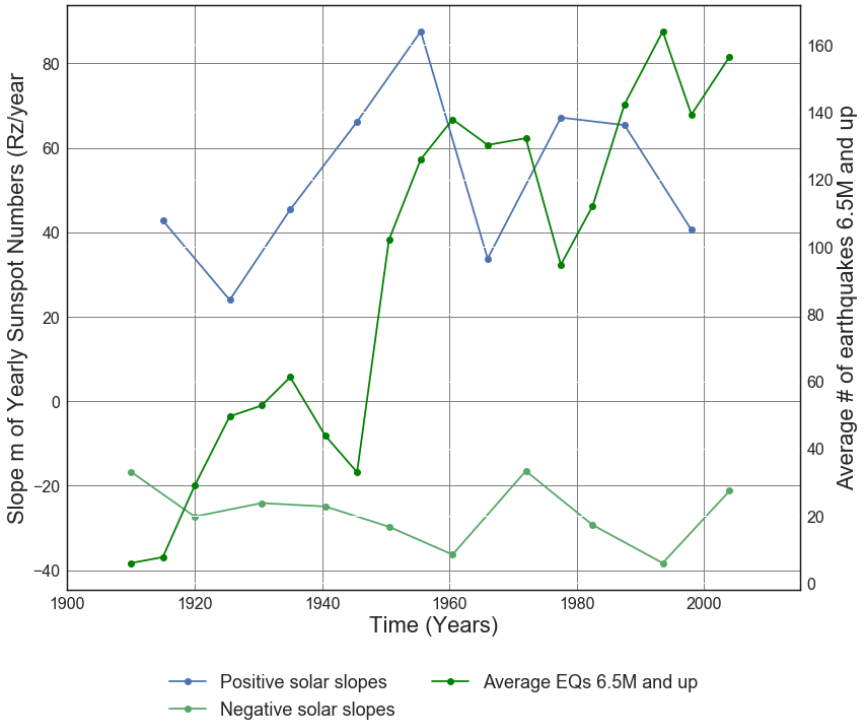

Figure C1.41: Positive and negative solar cycle slopes from 1900 to 2014 vs. Average number of 6.5M and up Earthquakes.

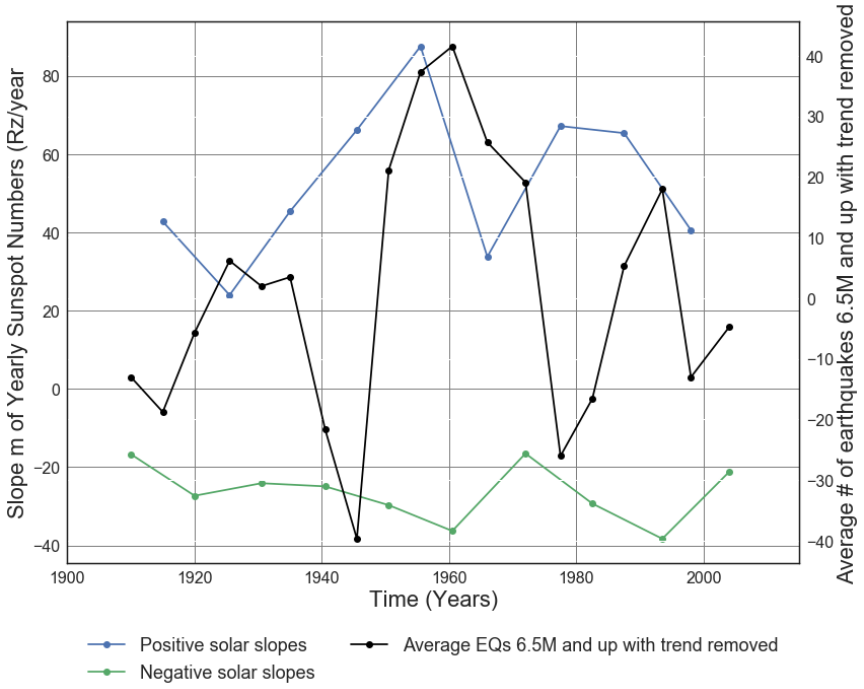

Figure C1.42: Positive and negative solar cycle slopes from 1900 to 2014 vs. Average number of 6.5M and up Earthquakes with trend removed.

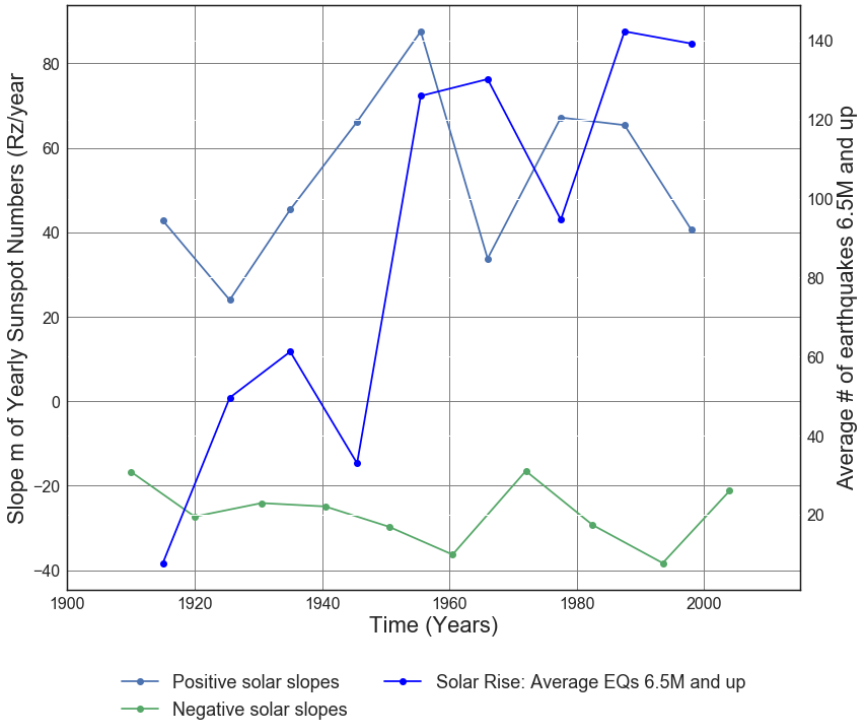

Figure C1.43: Positive and negative solar cycle slopes from 1900 to 2014 vs. Solar Rise: Average number of 6.5M and up Earthquakes.

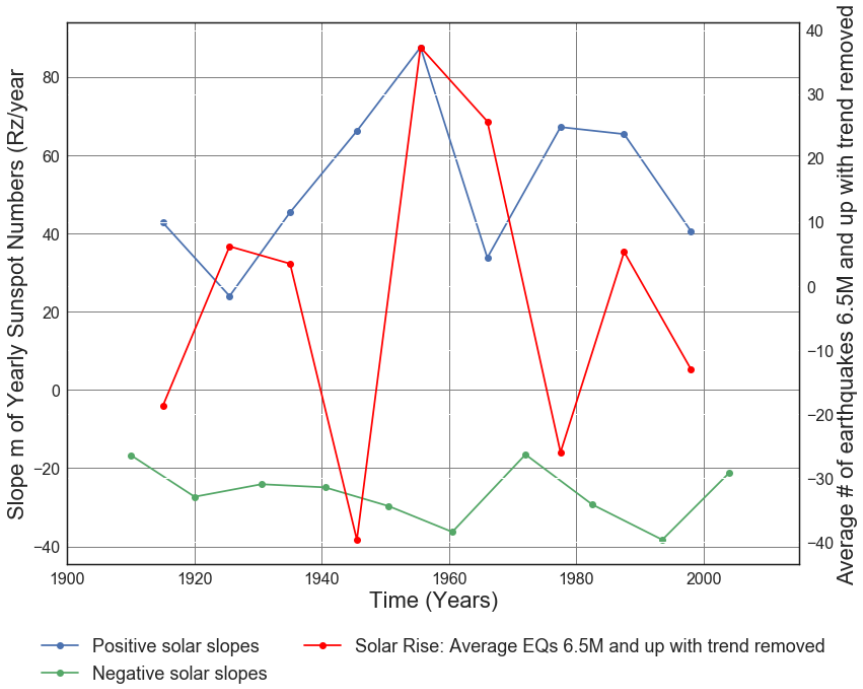

Figure C1.44: Positive and negative solar cycle slopes from 1900 to 2014 vs. Solar Rise: Average number of 6.5M and up Earthquakes with trend removed.

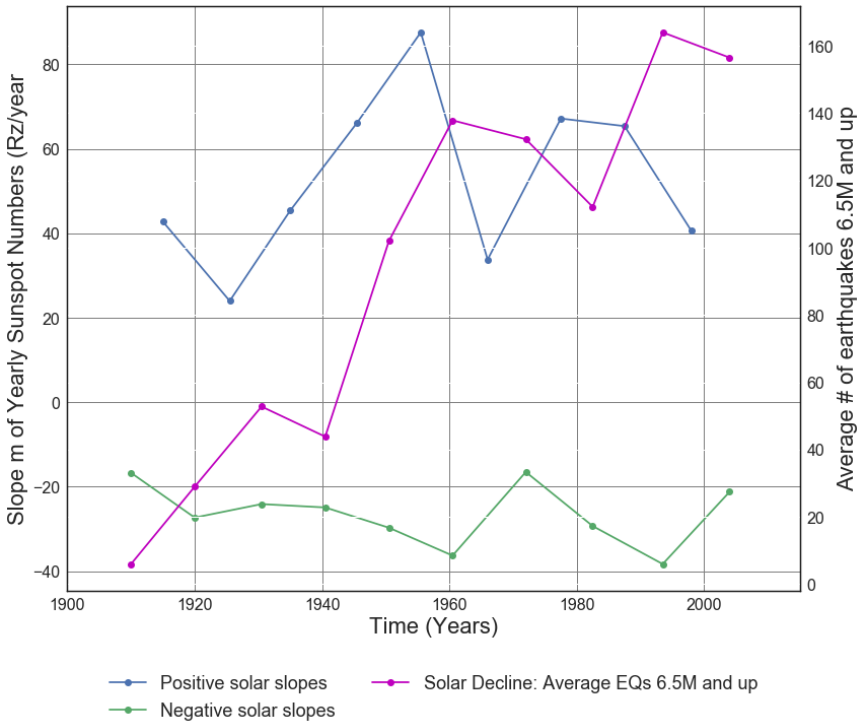

Figure C1.45: Positive and negative solar cycle slopes from 1900 to 2014 vs. Solar Decline: Average number of 6.5M and up Earthquakes.

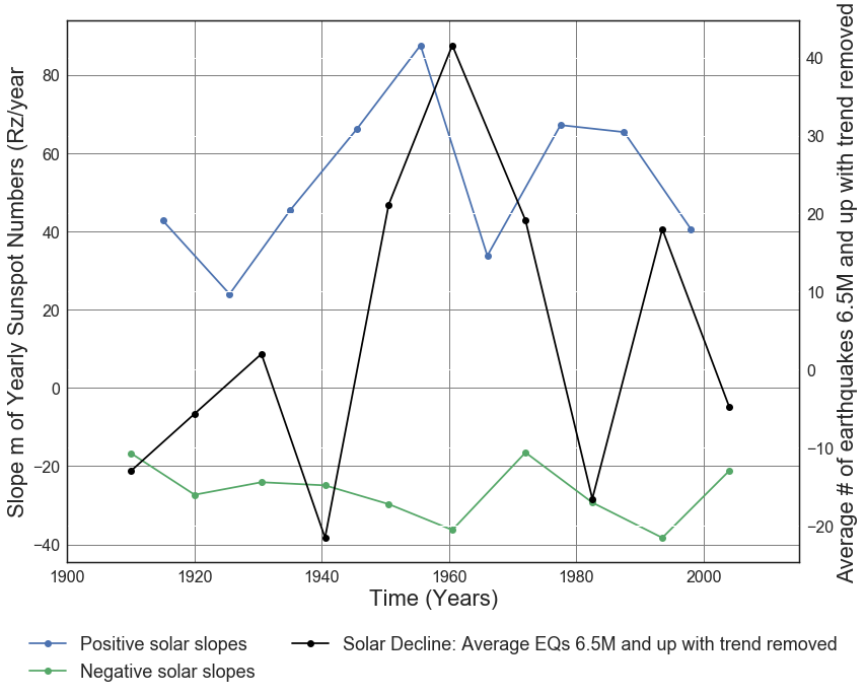

Figure C1.46: Positive and negative solar cycle slopes from 1900 to 2014 vs. Solar Rise: Average number of 6.5M and up Earthquakes.

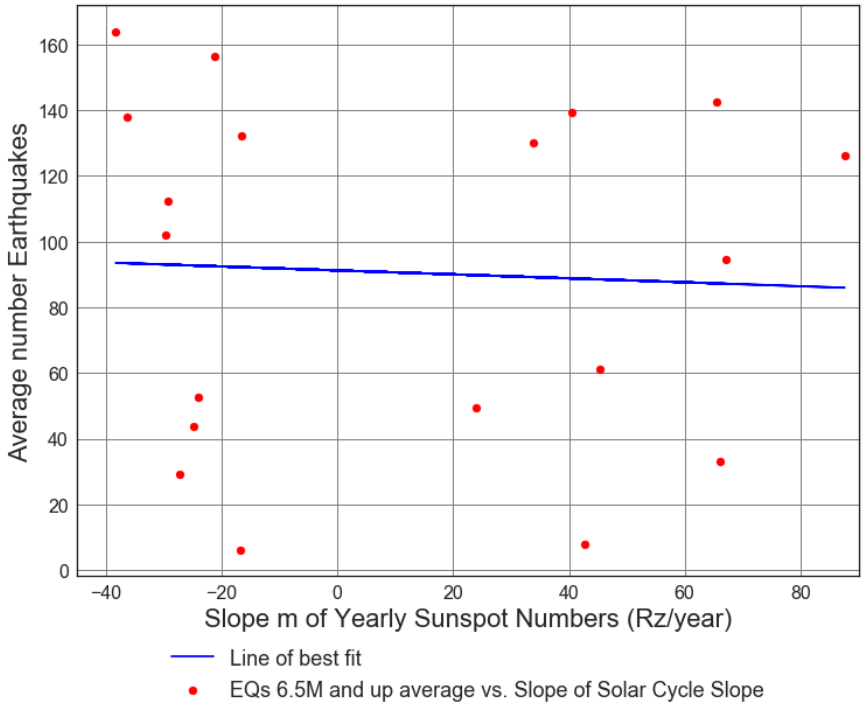

Figure C1.47: Scatter Plot of Slope m of Solar cycle (from 1900 to 2014) vs. Average number of 6.5M and up Earthquakes. Line of best fit, y = -0.0602x + (91.21), mean x = 10.98 +/- 41.86, mean y = 90.55 +/- 51.02, R = -0.04939, R squared = 0.002439, p-value = 0.8409.

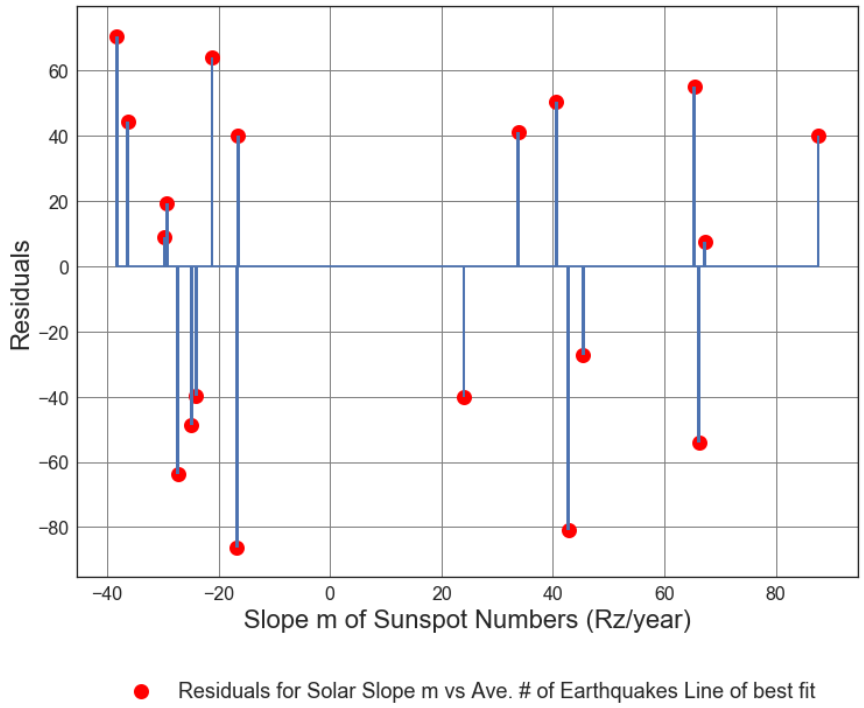

Figure C1.48: Residuals Plot of Average Solar Cycle Slope m (from 1900 to 2007) vs. Average number of 6.5M and up Earthquakes. Line of best fit, y = -0.0602x + (91.21), mean x = 10.98 +/- 41.86, mean y = 90.55 +/- 51.02, R = -0.04939, R squared = 0.002439, p-value = 0.8409.

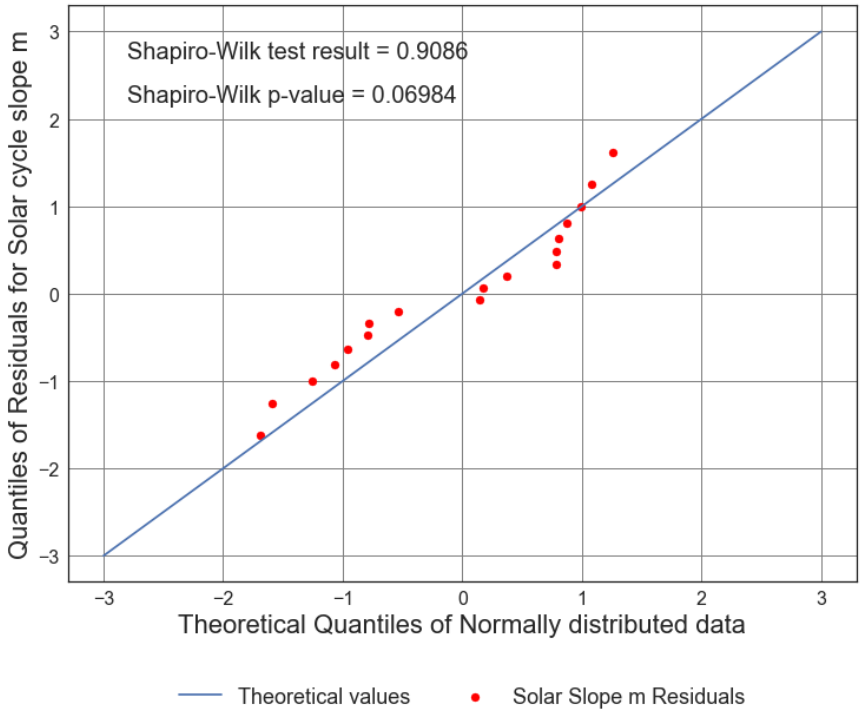

Figure C1.49: Quantile-Quantile Plot of the resisuals of Slope of Solar cycle m (from 1900 to 2014) vs. Average number of 6.5M and up Earthquakes. Line of best fit, y = -0.0602x + (91.21), mean x = 10.98 +/- 41.86, mean y = 90.55 +/- 51.02, R = -0.04939, R squared = 0.002439, p-value = 0.8409.

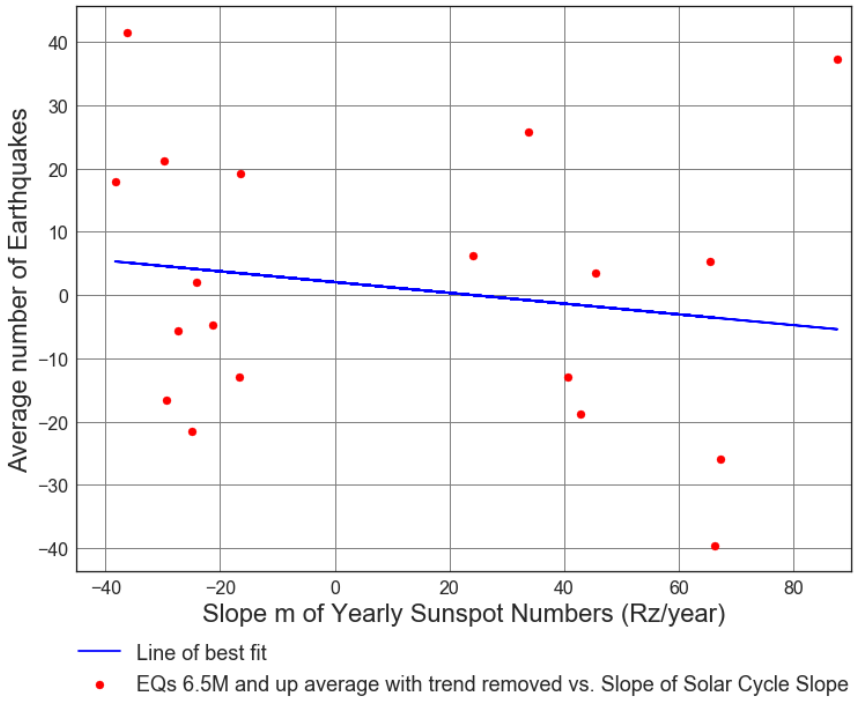

Figure C1.50: Scatter Plot of Slope m of Solar cycle (from 1900 to 2014) vs. Average number of 6.5M and up Earthquakes with trend removed. Line of best fit, y = -0.08506x + (2.039), mean x = 10.98 +/- 41.86, mean y = 1.104 +/- 21.42, R = -0.1662, R squared = 0.02764, p-value = 0.4964.

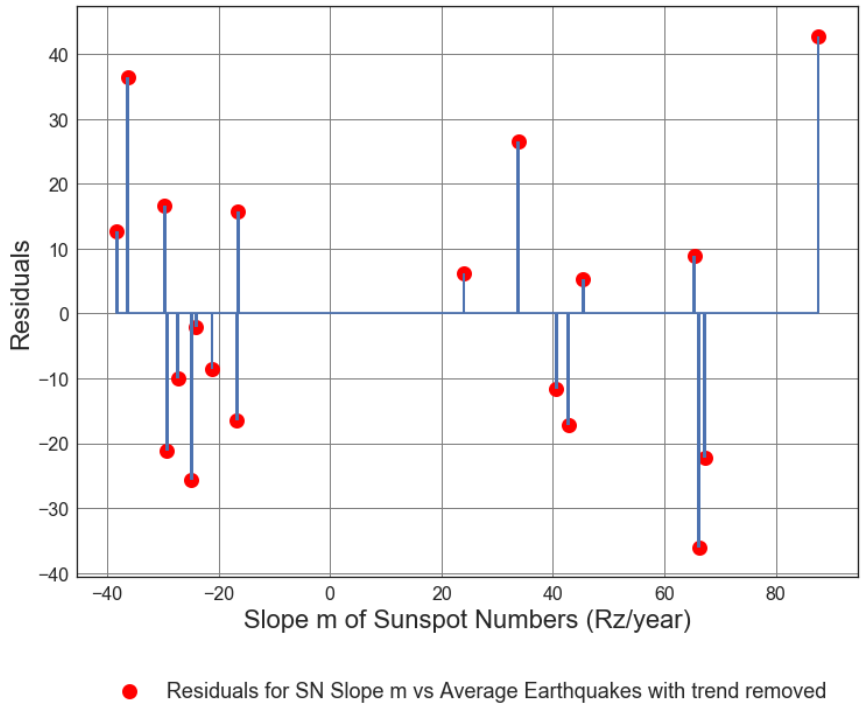

Figure C1.51: Residuals Plot of the Slope of Solar cycle (from 1900 to 2014) vs. Average number of 6.5M and up Earthquakes with trend removed. Line of best fit, y = -0.08506x + (2.039), mean x = 10.98 +/- 41.86, mean y = 1.104 +/- 21.42, R = -0.1662, R squared = 0.02764, p-value = 0.4964.

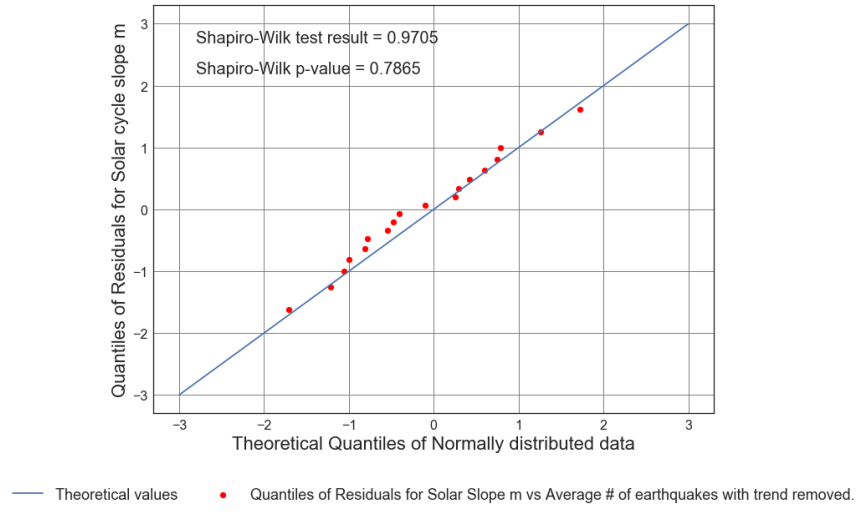

Figure C1.52: Scatter Plot of Absolute Magnitude of the Slope of Solar cycle (from 1900 to 2014) vs. Average number of 6.5M and up Earthquakes. Line of best fit, y = -0.08506x + (2.039), mean x = 10.98 +/- 41.86, mean y = 1.104 +/- 21.42, R = -0.1662, R squared = 0.02764, p-value = 0.4964.

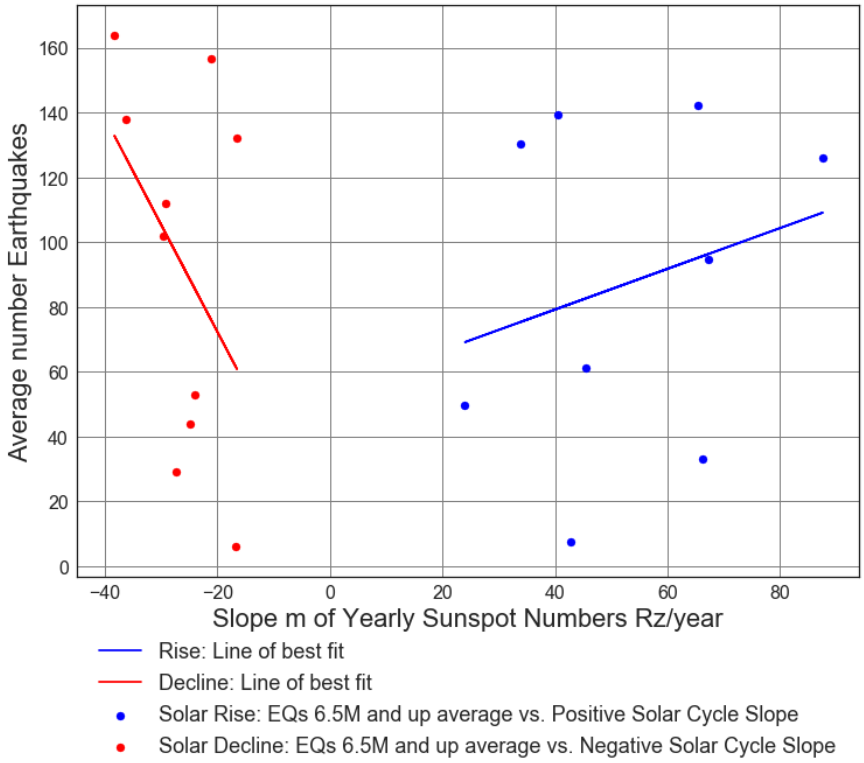

Figure C1.53: Scatter Plot of Slope of Solar cycle (from 1900 to 2014) vs. Average number of 6.5M and up Earthquakes. Rise: Line of best fit, y = 0.6284x + (54.1), mean x = 52.56 +/- 19.0, mean y = 87.12 +/- 47.73, R = 0.4016, R squared = 0.1613, p-value = 0.25. Decline: Line of best fit, y = -3.305x + 6.281, mean x = -26.43 +/- 6.974, mean y = 93.64 +/- 53.63, R = -0.4298, R squared = 0.1847, p-value = 0.2151.

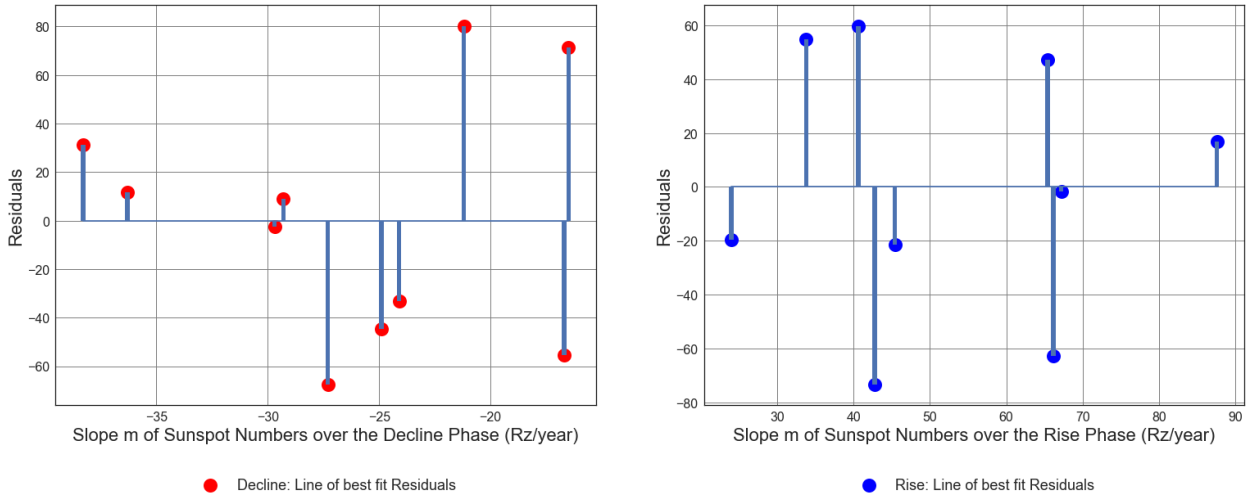

Figure C1.54: Residuals centered about zero, plot of Slope of Solar cycle (from 1900 to 2014) vs. Average number of 6.5M and up Earthquakes. Rise: Line of best fit, y = 0.6284x + (54.1), mean x = 52.56 +/- 19.0, mean y = 87.12 +/- 47.73, R = 0.4016, R squared = 0.1613, p-value = 0.25. Decline: Line of best fit, y = -3.305x + 6.281, mean x = -26.43 +/- 6.974, mean y = 93.64 +/- 53.63, R = -0.4298, R squared = 0.1847, p-value = 0.2151.

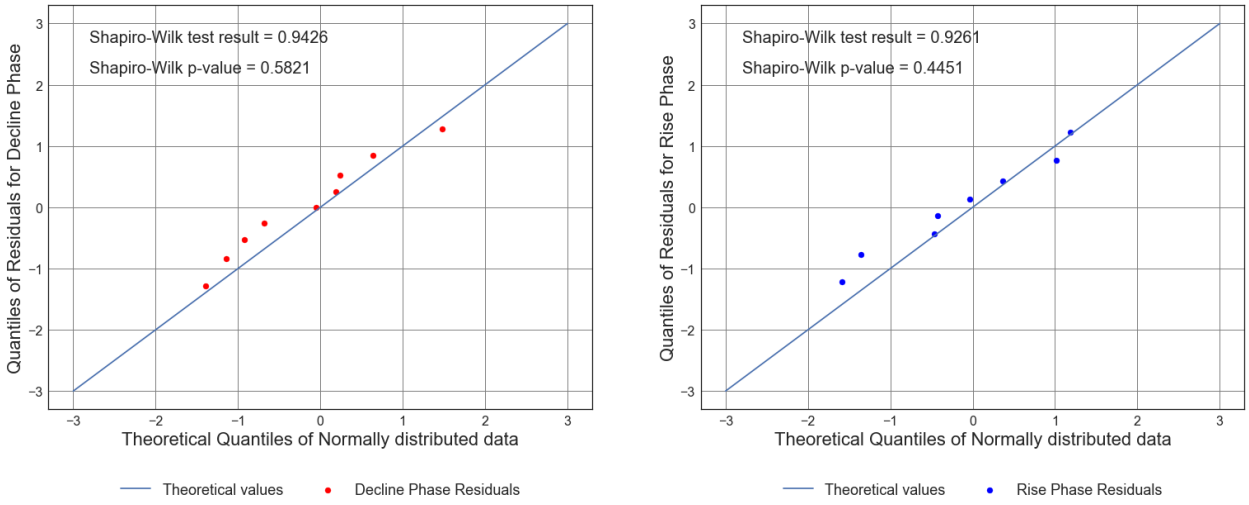

Figure C1.55: Quartile-Quartile Plot of Residuals for the Rise and Decline phase Slope of Solar cycle (from 1900 to 2014) vs. Average number of 6.5M and up Earthquakes. Rise: Line of best fit, y = 0.6284x + (54.1), mean x = 52.56 +/- 19.0, mean y = 87.12 +/- 47.73, R = 0.4016, R squared = 0.1613, p-value = 0.25. Decline: Line of best fit, y = -3.305x + 6.281, mean x = -26.43 +/- 6.974, mean y = 93.64 +/- 53.63, R = -0.4298, R squared = 0.1847, p-value = 0.2151.

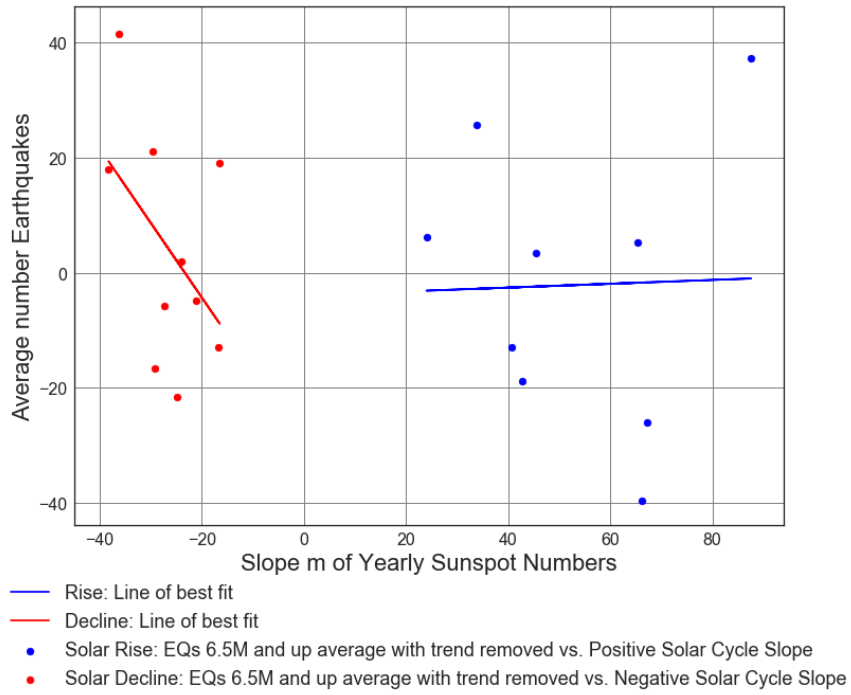

Figure C1.56: Scatter Plot of Slope of Solar cycle (from 1900 to 2014) vs. with trend removed Average number of 6.5M and up Earthquakes. Rise: Line of best fit, y = 0.03327x + (-3.893), mean x = 52.56 +/- 19.0, mean y = -2.144 +/- 23.25, R = 0.0272, R squared = 0.0007396, p-value = 0.9446. Decline: Line of best fit, y = -1.296x + -30.23, mean x = -26.43 +/- 6.974, mean y = 4.028 +/- 19.16, R = -0.4718, R squared = 0.2226, p-value = 0.1686.

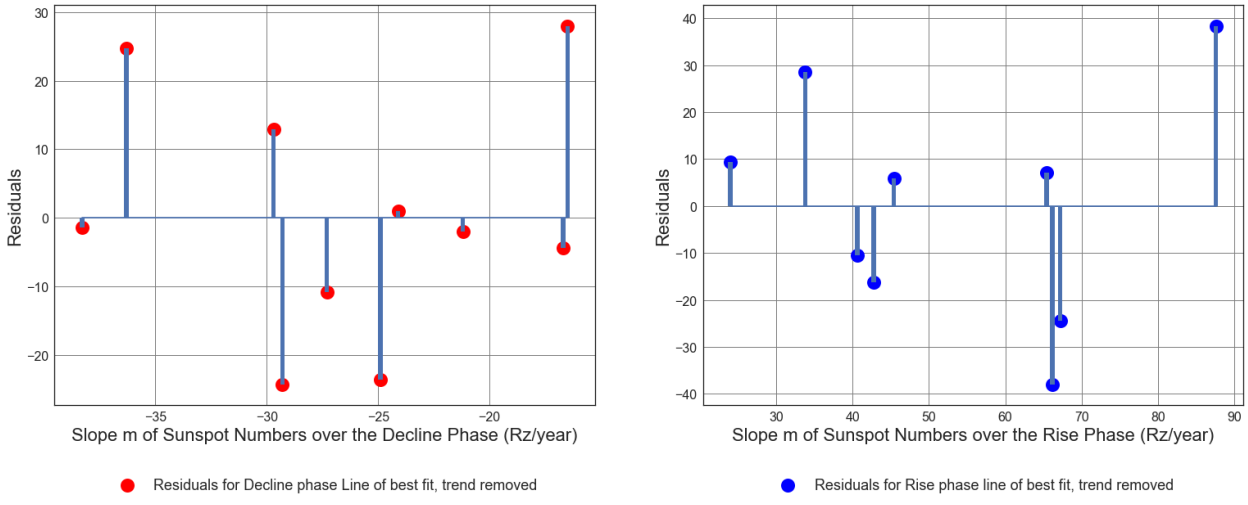

Figure C1.57: Residuals centered about zero, plot of Slope of Solar cycle (from 1900 to 2014) vs. Average number of 6.5M and up Earthquakes with trend removed. Rise: Line of best fit, y = 0.03327x + (-3.893), mean x = 52.56 +/- 19.0, mean y = -2.144 +/- 23.25, R = 0.0272, R squared =

0.0007396, p-value = 0.9446. Decline: Line of best fit, y = -1.296x + -30.23, mean x = -26.43 +/- 6.974, mean y = 4.028 +/- 19.16, R = -0.4718, R squared = 0.2226, p-value = 0.1686.

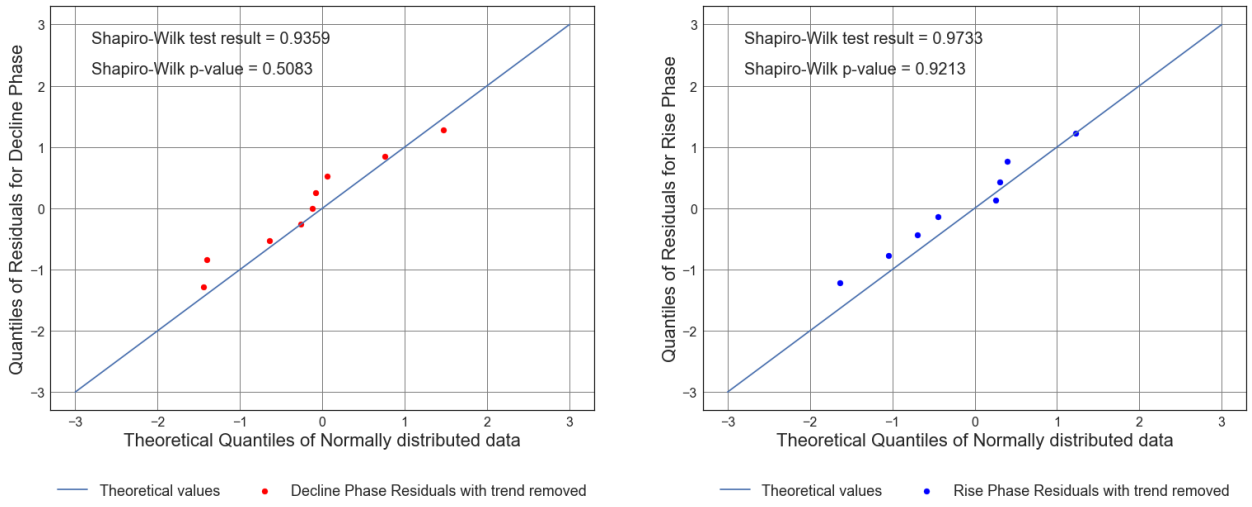

Figure C1.58: Quartile-Quartile Plot of Residuals for the Rise and Decline phase Slope of Solar cycle (from 1900 to 2014) vs. Average number of 6.5M and up Earthquakes with trend removed. Rise: Line of best fit, y = 0.03327x + (-3.893), mean x = 52.56 +/- 19.0, mean y = -2.144 +/- 23.25, R = 0.0272, R squared = 0.0007396, p-value = 0.9446. Decline: Line of best fit, y = -1.296x + -30.23, mean x = -26.43 +/- 6.974, mean y = 4.028 +/- 19.16, R = -0.4718, R squared = 0.2226, p-value = 0.1686.

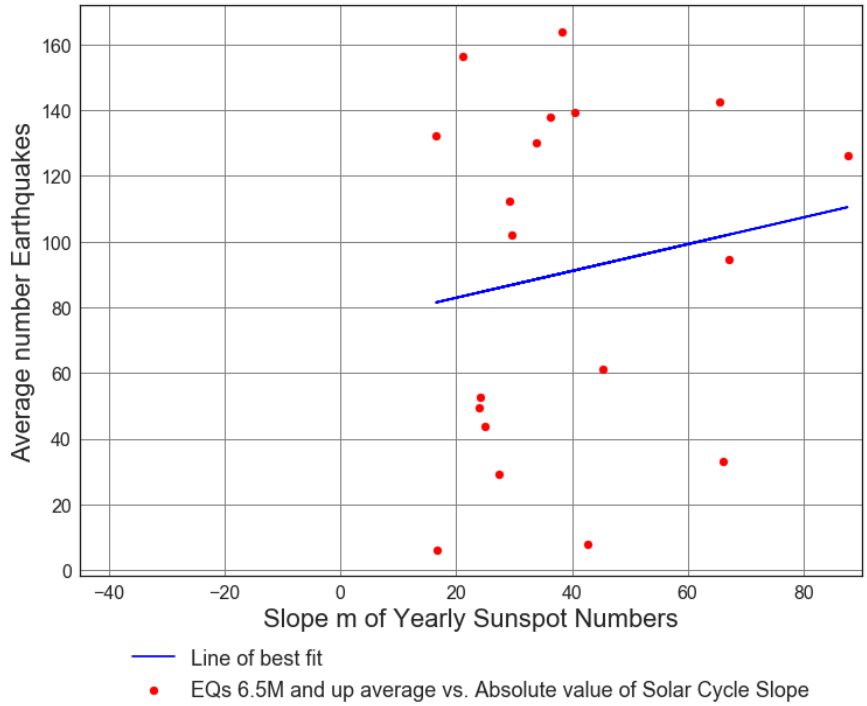

Figure C1.59: Scatter Plot of Absolute value of the Slope of Solar cycle (from 1900 to 2014) vs. Average number of 6.5M and up Earthquakes. Line of best fit, y = 0.408x + (74.72), mean x = 38.81 +/- 19.15, mean y = 90.55 +/- 51.02, R = 0.1531, R squared = 0.02345, p-value = 0.5314.

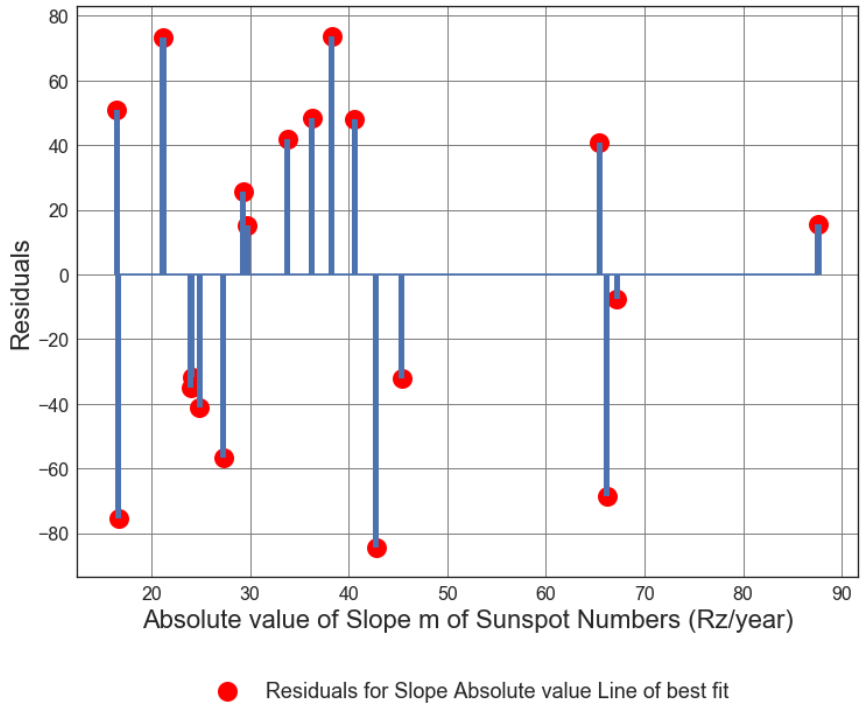

Figure C1.60: Residuals Plot of Absolute Magnitude of the Slope of Solar cycle (from 1900 to 2014) vs. Average number of 6.5M and up Earthquakes. Line of best fit, y = 0.408x + (74.72), mean x = 38.81 +/- 19.15, mean y = 90.55 +/- 51.02, R = 0.1531, R squared = 0.02345, p-value = 0.5314.

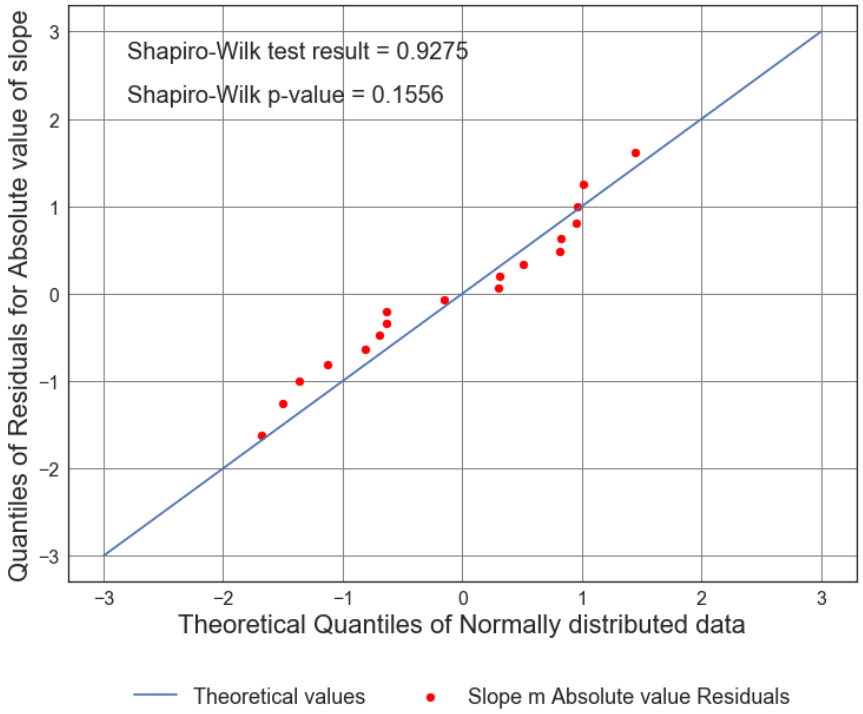

Figure C1.61: Scatter Plot of Absolute Magnitude of the Slope of Solar cycle (from 1900 to 2014) vs. Average number of 6.5M and up Earthquakes. Line of best fit, y = 0.408x + (74.72), mean x = 38.81 +/- 19.15, mean y = 90.55 +/- 51.02, R = 0.1531, R squared = 0.02345, p-value = 0.5314.

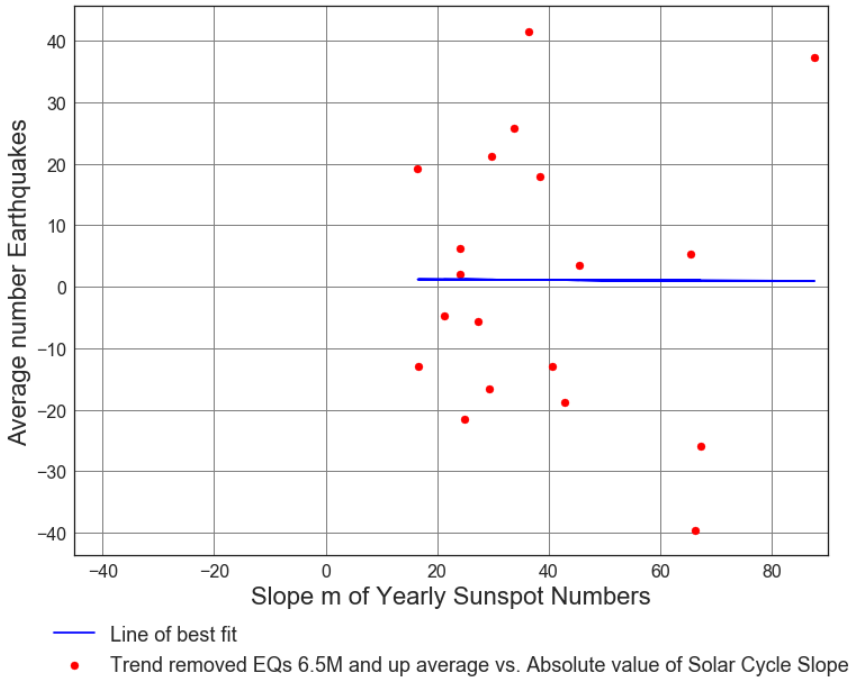

Figure C1.62: Scatter Plot of Absolute Slope Magnitude of the Solar cycle (from 1900 to 2014) vs. Trend removed Average number of 6.5M and up Earthquakes. Line of best fit, y = -0.003635x + (1.245), mean x = 38.81 +/- 19.15, mean y = 1.104 +/- 21.42, R = -0.00325, R squared = 1.056e-05, p-value = 0.9895.

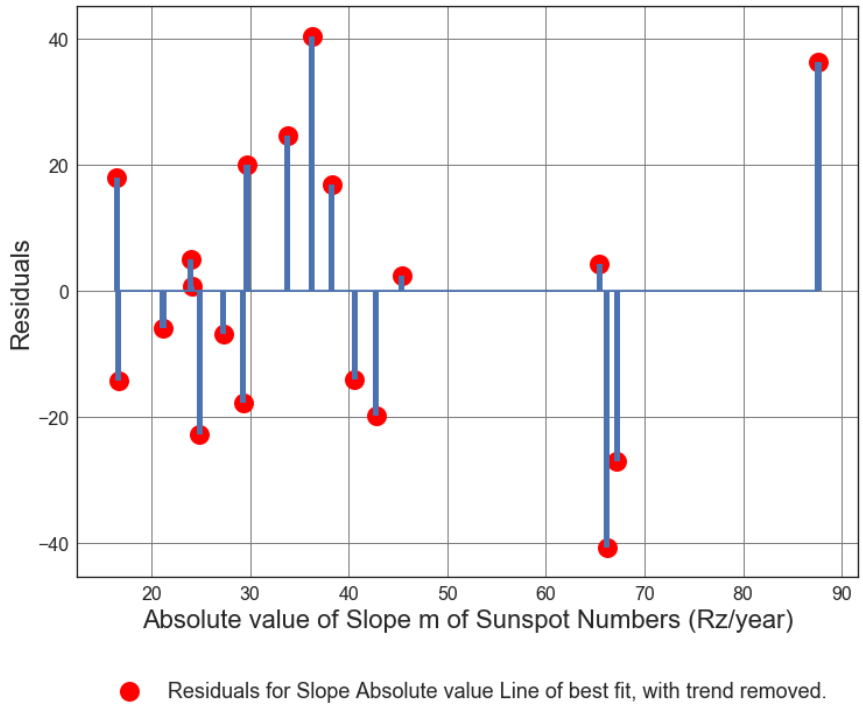

Figure C1.63: Scatter Plot of Absolute Slope Magnitude of the Solar cycle (from 1900 to 2014) vs. Trend removed Average number of 6.5M and up Earthquakes. Line of best fit, y = -0.003635x + (1.245), mean x = 38.81 +/- 19.15, mean y = 1.104 +/- 21.42, R = -0.00325, R squared = 1.056e-05, p-value = 0.9895.

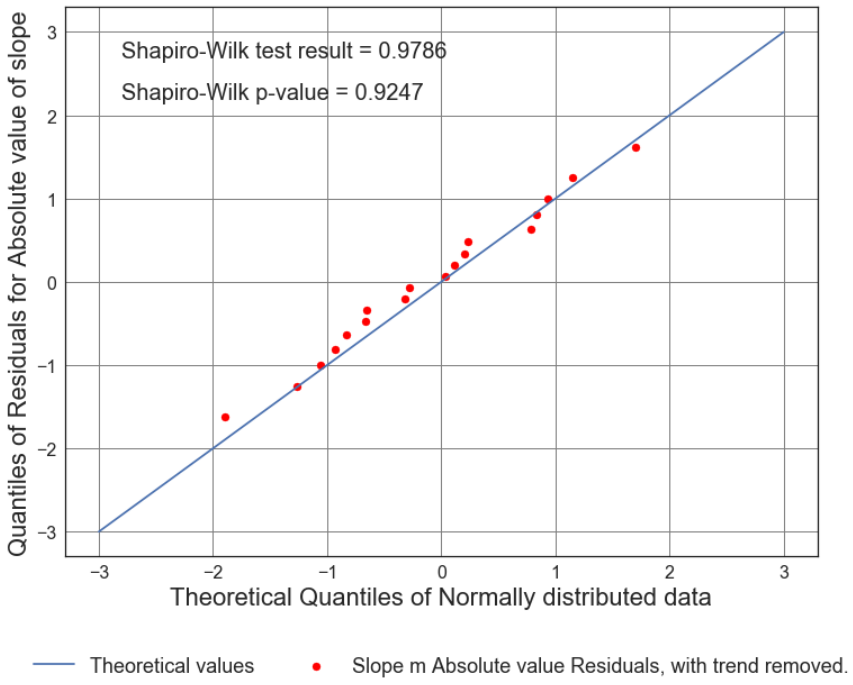

Figure C1.64: Scatter Plot of Absolute Slope Magnitude of the Solar cycle (from 1900 to 2014) vs. Trend removed Average number of 6.5M and up Earthquakes. Line of best fit, y = -0.003635x + (1.245), mean x = 38.81 +/- 19.15, mean y = 1.104 +/- 21.42, R = -0.00325, R squared = 1.056e-05, p-value = 0.9895.

Appendix C2: USGS ComCat Time Series Analysis Part 2 - Six Month Averaged Earthquake and Sunspot Data.

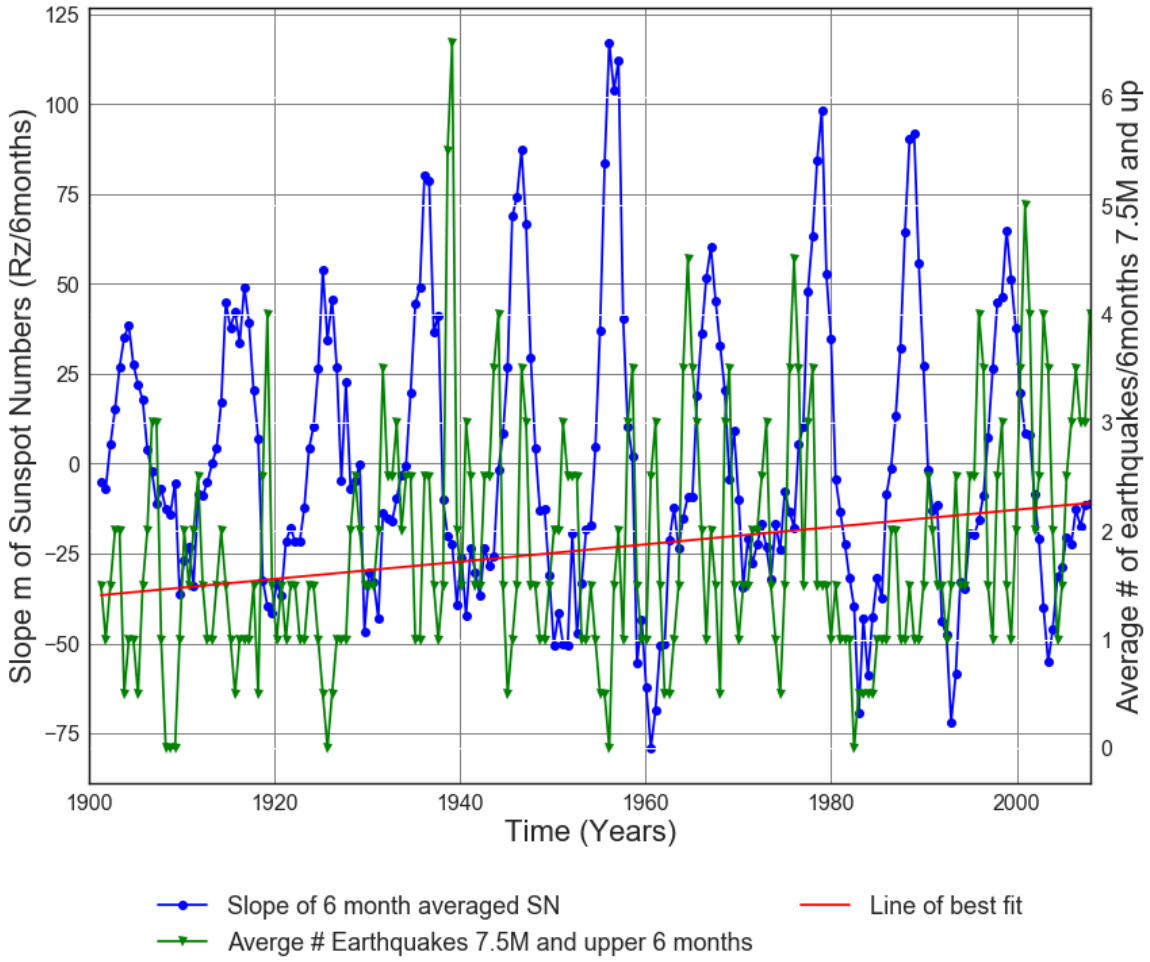

Figure C2.1: Slope of Solar cycle from 1900 to 2017 vs. Average number of 7.5M and up Earthquakes.

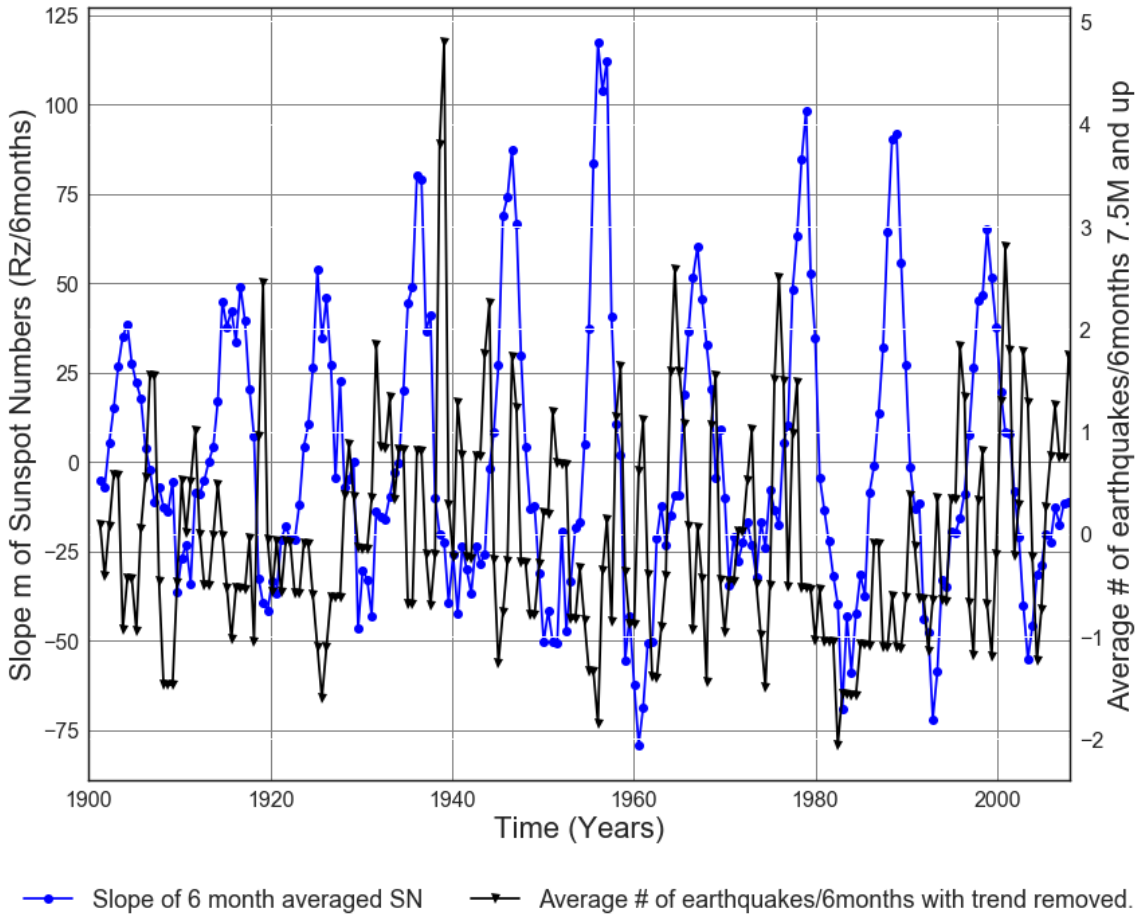

Figure C2.2: Slope of 6 month averaged SN 1900 to 2017 vs. Average number of 7.5M and up Earthquakes with trend removed. Line of best fit, y = 0.00797x + (-13.74), mean x = 1.955e+03 +/- 31.21, mean y = 1.834 +/- 1.081

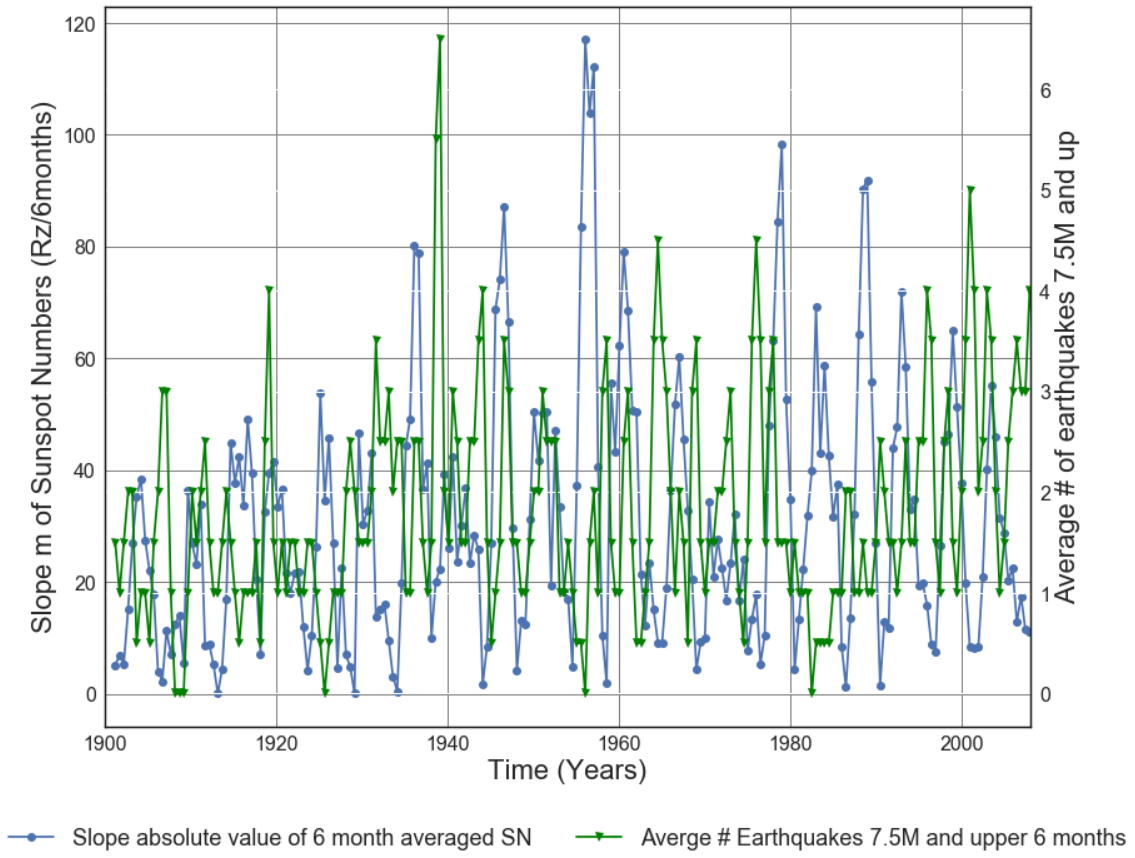

Figure C2.3: Slope Absolute value of Solar cycle from 1900 to 2017 vs. Average number of 7.5M and up Earthquakes.

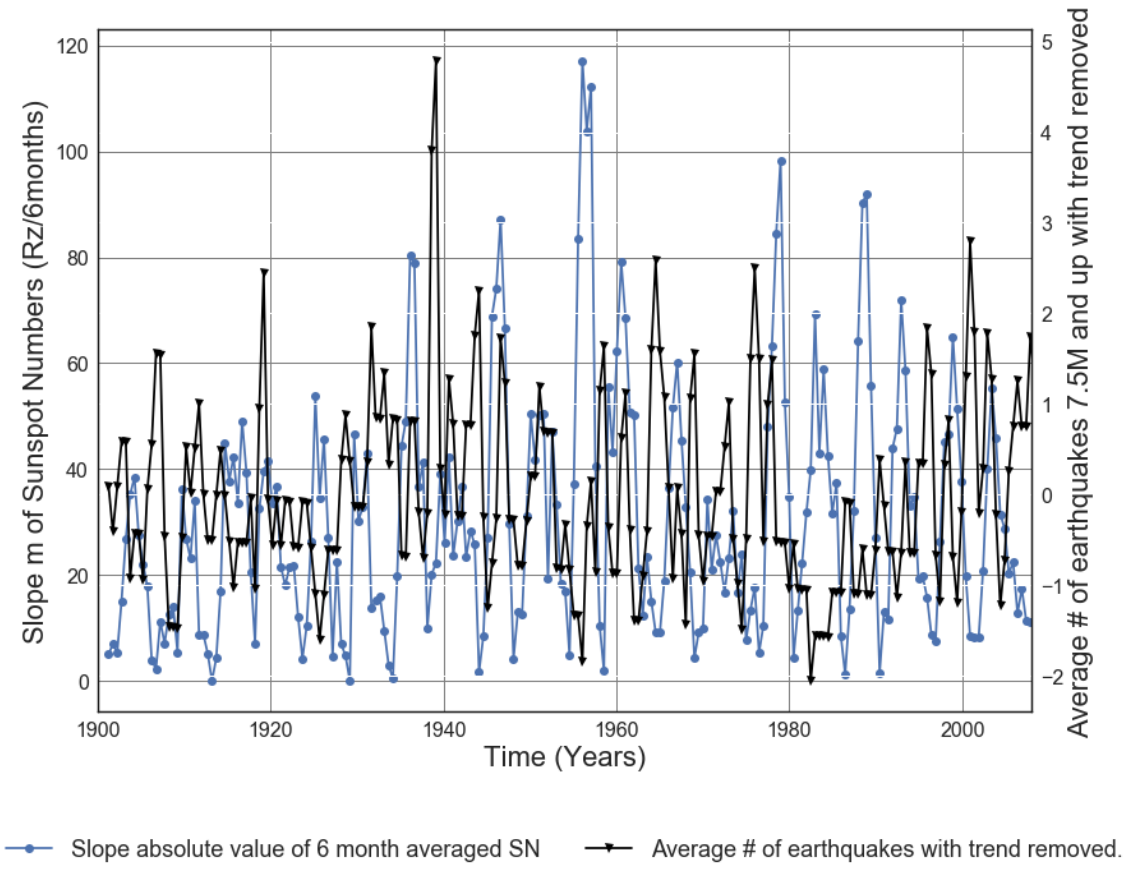

Figure C2.4: Slope Absolute value of Solar cycle from 1900 to 2017 vs. Average number of 7.5M and up earthquakes with trend removed.

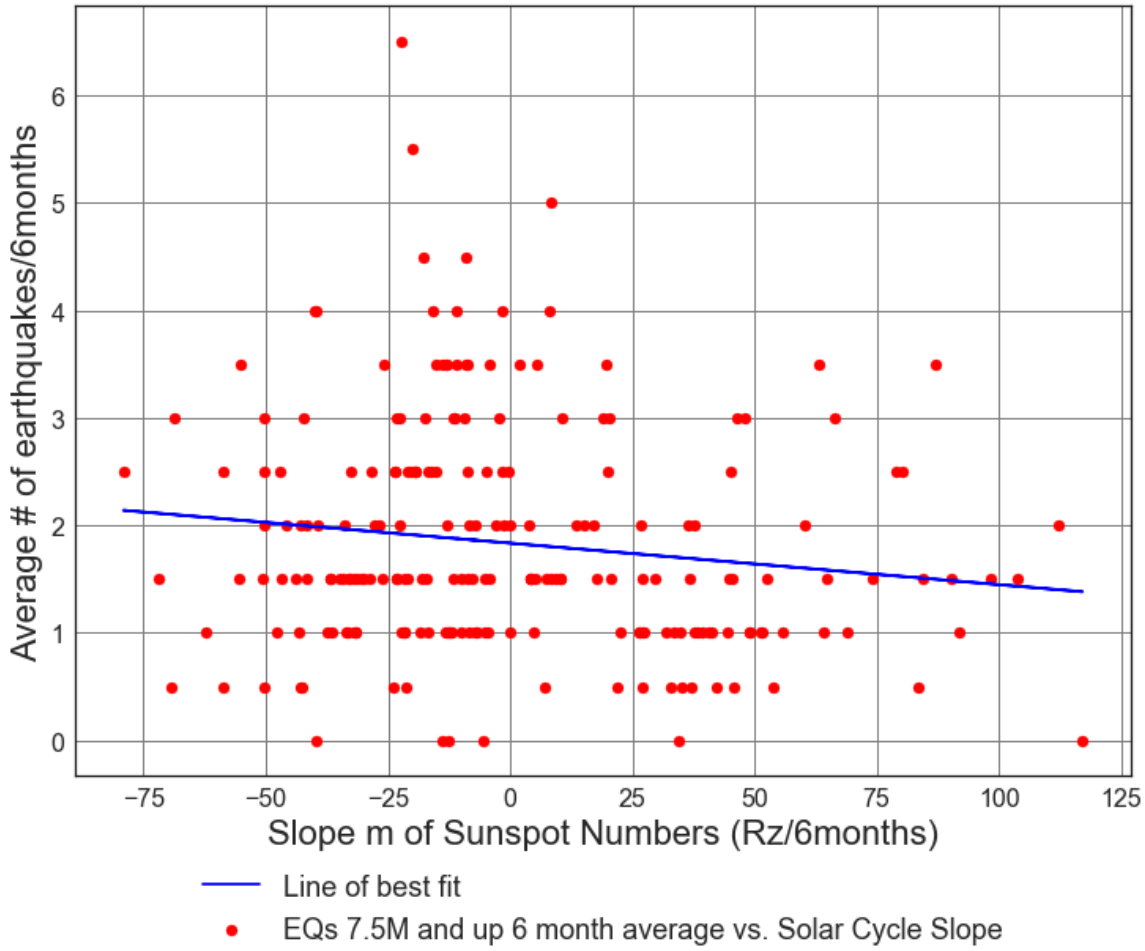

Figure C2.5: Scatter Plot of Solar cycle slope (from 1900 to 2017) vs. Average number of 7.5M and up Earthquakes/6months. Line of best fit, y = -0.00386x + (1.835), mean x = -0.07013 +/- 38.33, mean y = 1.836 +/- 1.083, R = -0.1366, R squared = 0.01866, p-value = 0.04493.

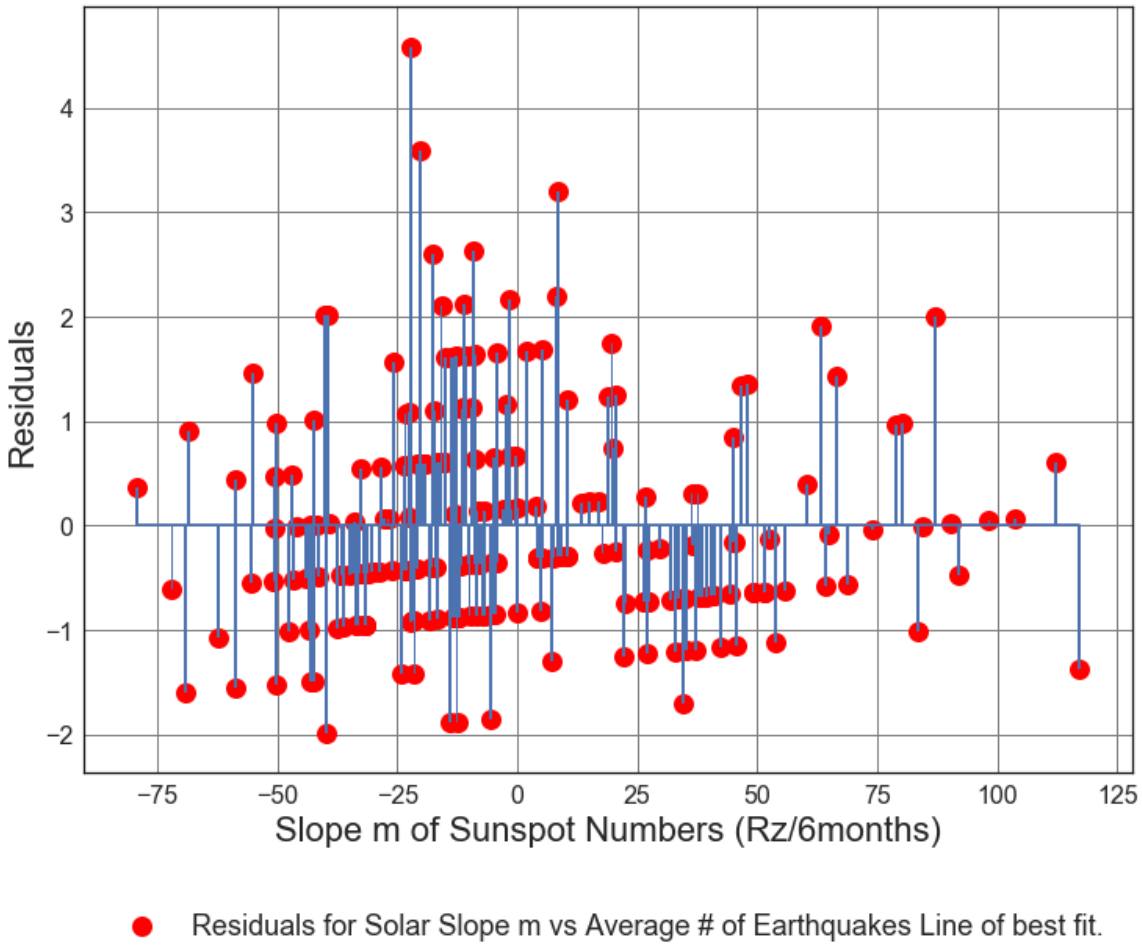

Figure C2.6: Residuals Plot of Solar cycle slope (from 1900 to 2017) vs. Average number of 7.5M and up Earthquakes/6months. Line of best fit, y = -0.00386x + (1.835), mean x = -0.07013 +/- 38.33, mean y = 1.836 +/- 1.083, R = -0.1366, R squared = 0.01866, p-value = 0.04493.

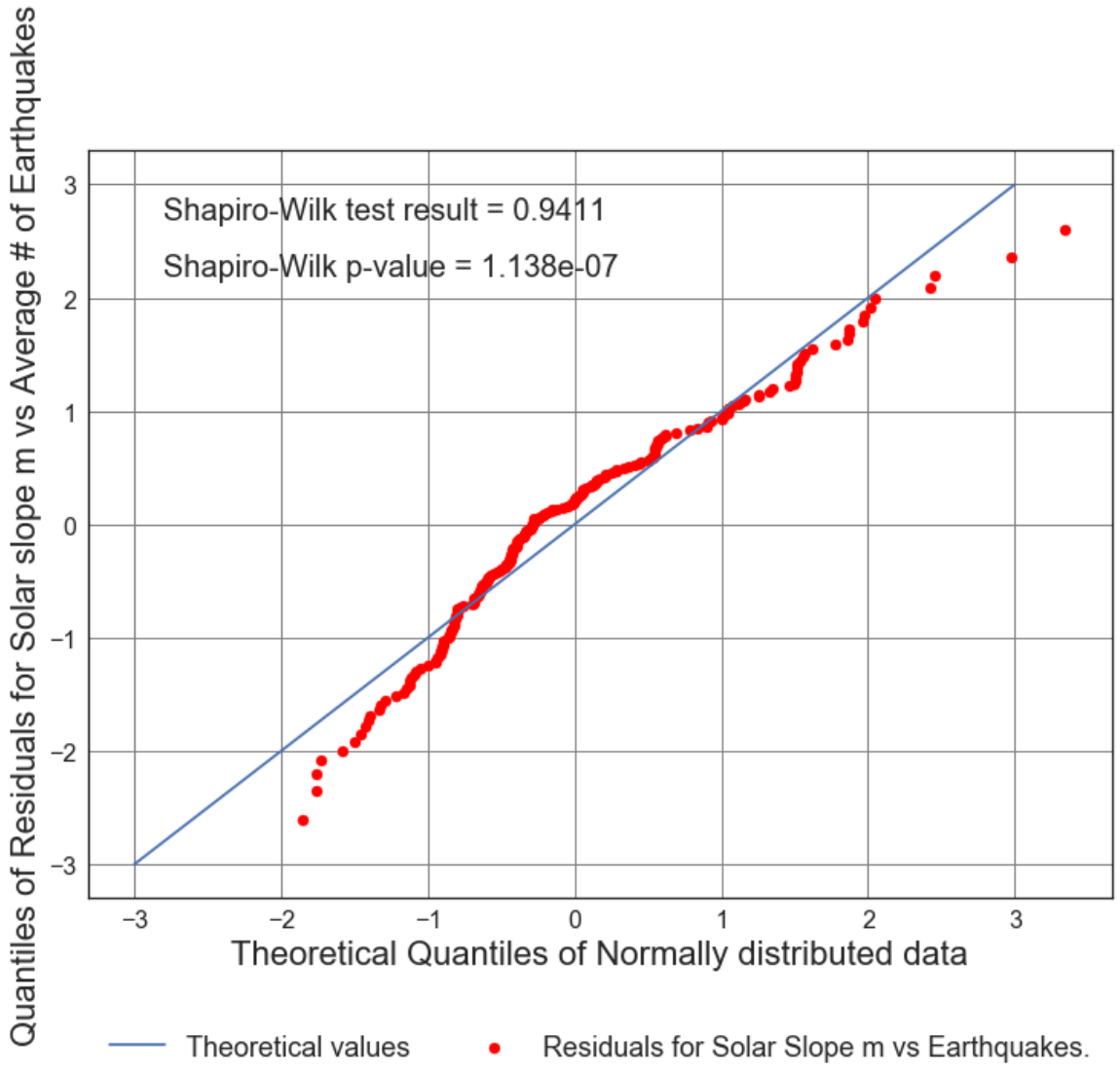

Figure C2.7: Residuals Plot of Solar cycle slope (from 1900 to 2017) vs. Average number of 7.5M and up Earthquakes/6months. Line of best fit, y = -0.00386x + (1.835), mean x = -0.07013 +/- 38.33, mean y = 1.836 +/- 1.083, R = -0.1366, R squared = 0.01866, p-value = 0.04493.

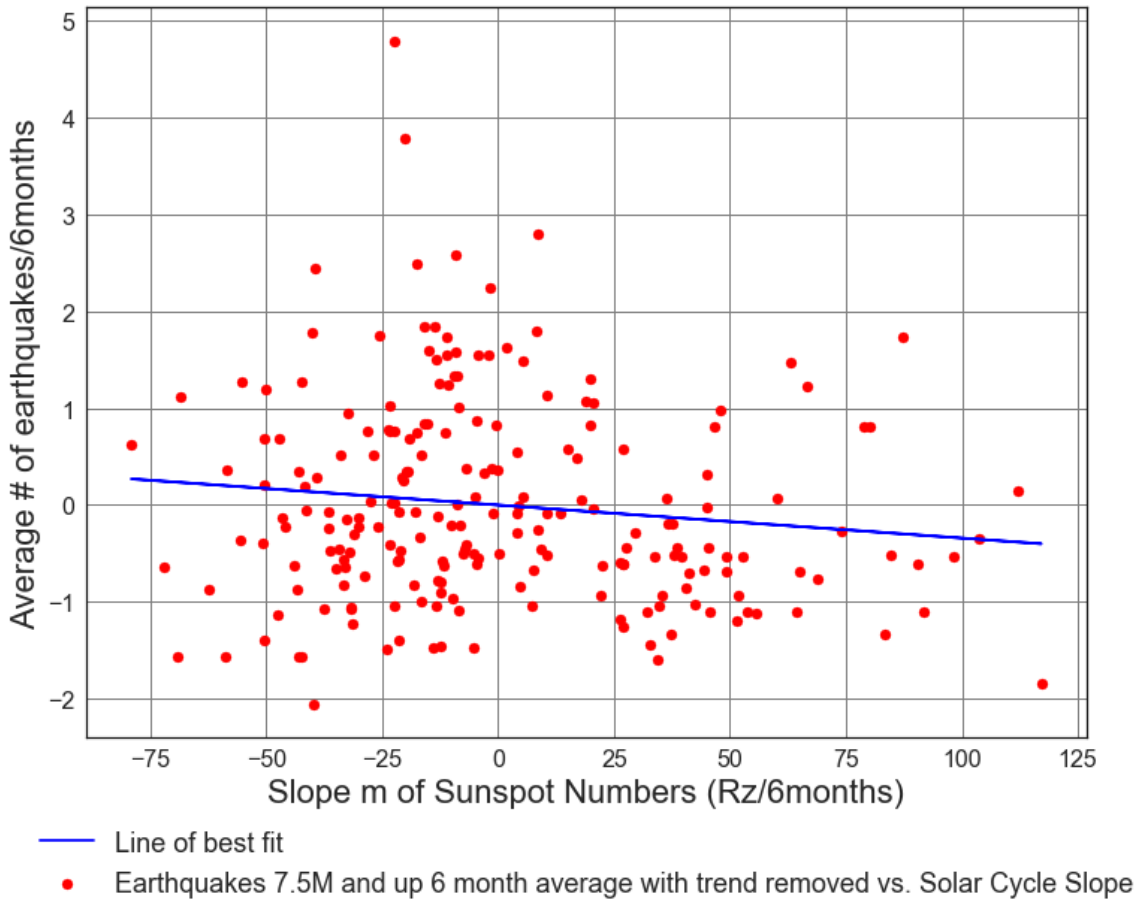

Figure C2.8: Scatter Plot of Solar cycle slope (from 1900 to 2017) vs. Average number of 7.5M and up Earthquakes/6months with trend removed. Line of best fit, y = -0.003412x + (-0.0006782), mean x = -0.07013 +/- 38.33, mean y = -0.0004389 +/- 1.054, R = -0.124, R squared = 0.01539, p-value = 0.06883.

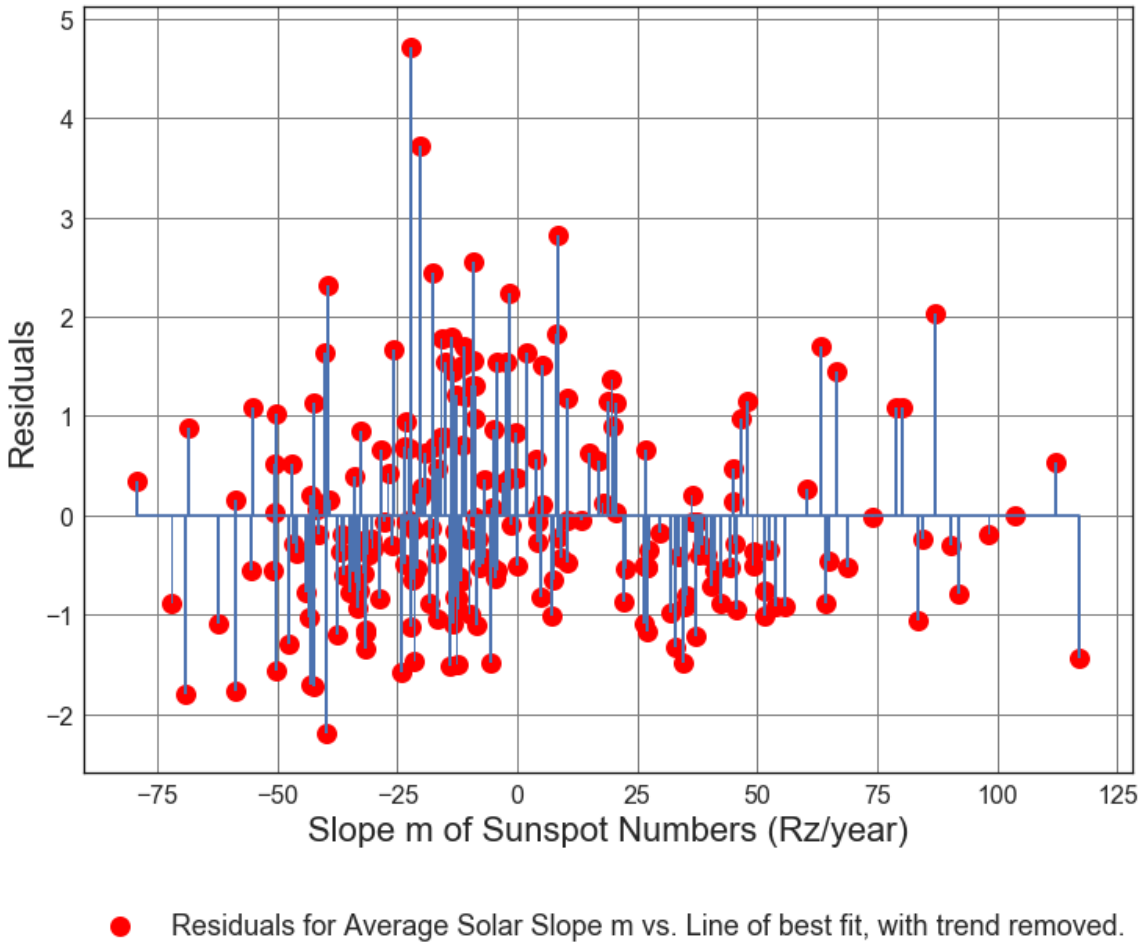

Figure C2.9: Scatter Plot of Solar cycle slope (from 1900 to 2017) vs. Average number of 7.5M and up Earthquakes/6months with trend removed. Line of best fit, y = -0.003412x + (-0.0006782), mean x = -0.07013 +/- 38.33, mean y = -0.0004389 +/- 1.054, R = -0.124, R squared = 0.01539, p-value = 0.06883.

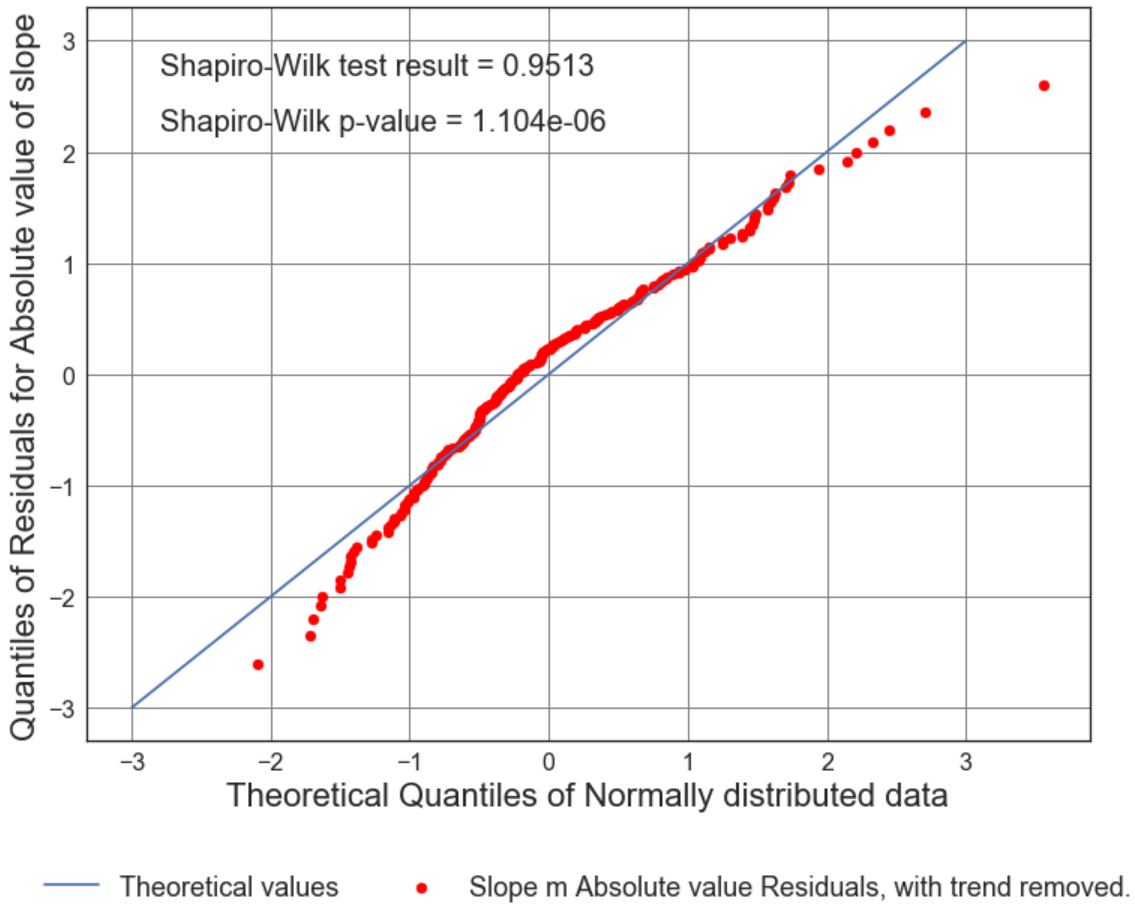

Figure C2.10: Scatter Plot of Solar cycle slope (from 1900 to 2017) vs. Average number of 7.5M and up Earthquakes/6months with trend removed. Line of best fit, y = -0.003412x + (-0.0006782), mean x = -0.07013 +/- 38.33, mean y = -0.0004389 +/- 1.054, R = -0.124, R squared = 0.01539, p-value = 0.06883.

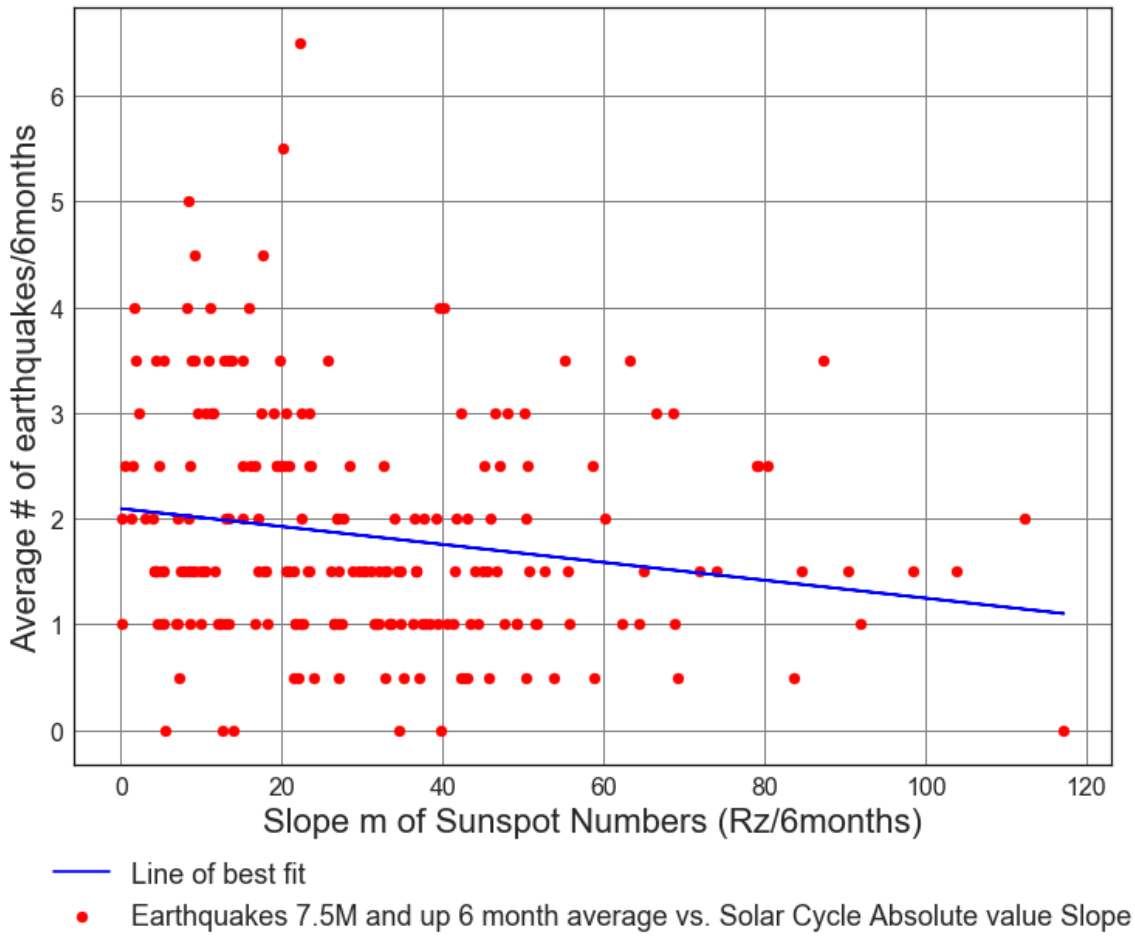

Figure C2.11: Scatter Plot of Solar cycle slope (from 1900 to 2017) vs. Average number of 7.5M and up Earthquakes/6months. Line of best fit, y = -0.008469x + (2.095), mean x = 30.66 +/- 23.0, mean y = 1.836 +/- 1.083, R = -0.1798, R squared = 0.03234, p-value = 0.008063.

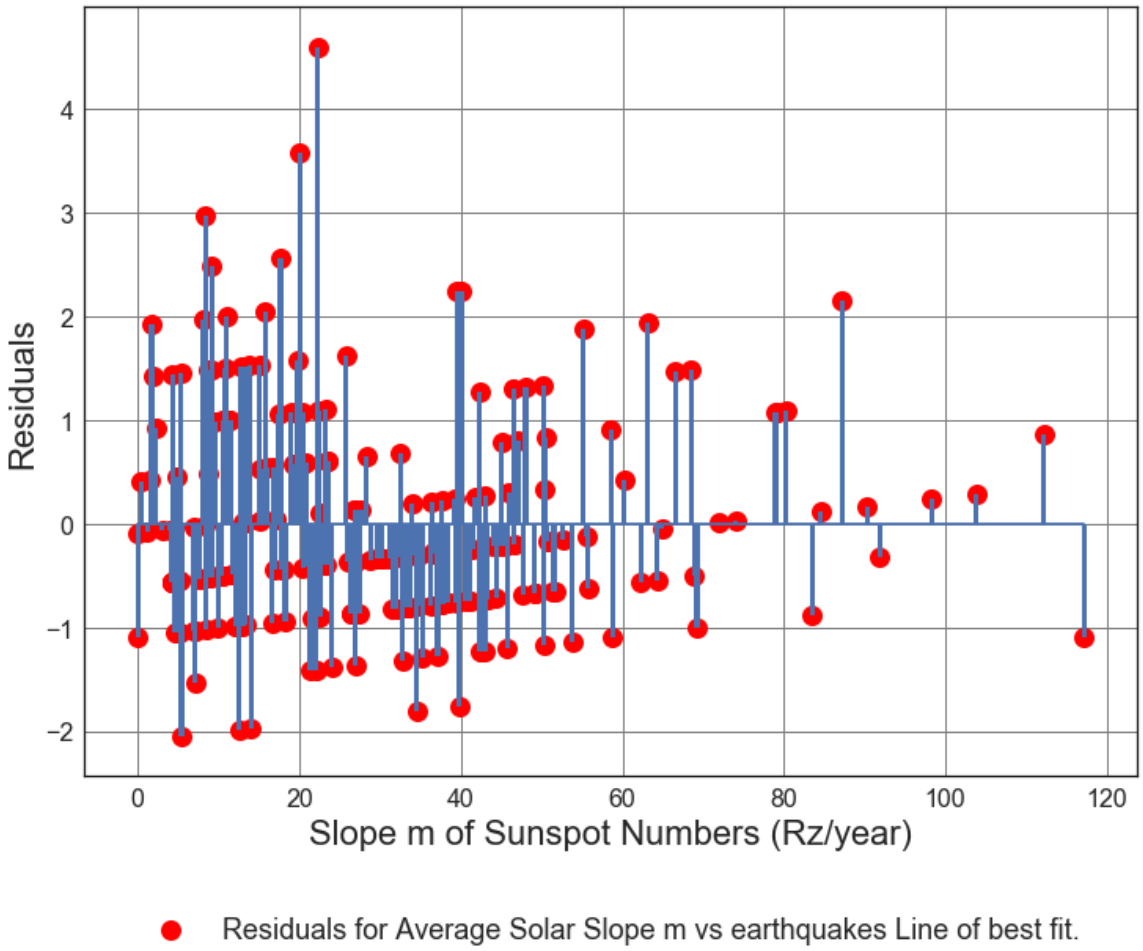

Figure C2.12: Scatter Plot of Solar cycle slope (from 1900 to 2017) vs. Average number of 7.5M and up Earthquakes/6months. Line of best fit, y = -0.008469x + (2.095), mean x = 30.66 +/- 23.0, mean y = 1.836 +/- 1.083, R = -0.1798, R squared = 0.03234, p-value = 0.008063.

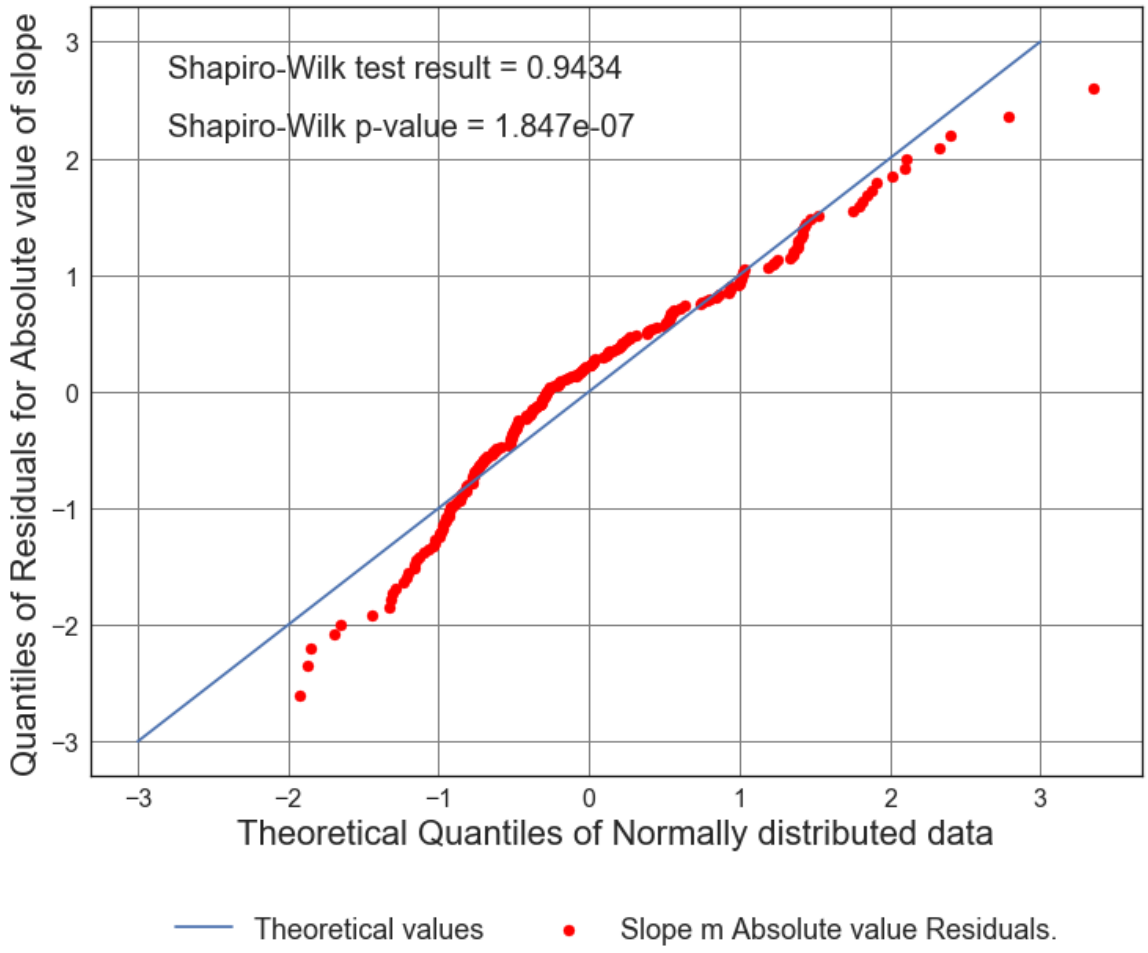

Figure C2.13: Scatter Plot of Solar cycle slope (from 1900 to 2017) vs. Average number of 7.5M and up Earthquakes/6months. Line of best fit, y = -0.008469x + (2.095), mean x = 30.66 +/- 23.0, mean y = 1.836 +/- 1.083, R = -0.1798, R squared = 0.03234, p-value = 0.008063.

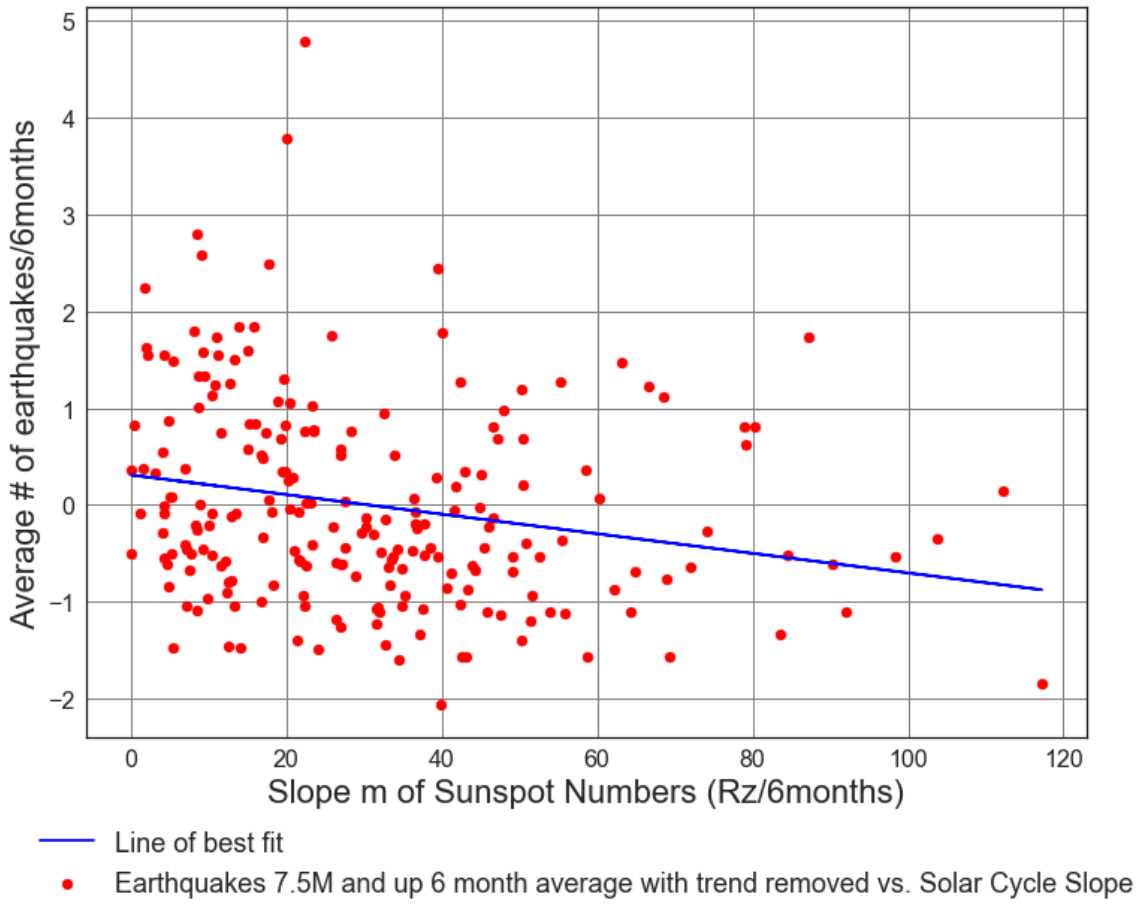

Figure C2.14: Scatter Plot of Solar cycle absolute value slope (from 1900 to 2017) vs. Average number of 7.5M and up Earthquakes/6months with trend removed. Line of best fit, y = -0.01011x + (0.3096), mean x = 30.66 +/- 23.0, mean y = -0.0004389 +/- 1.054, R = -0.2206, R squared = 0.04867, p-value = 0.0011.

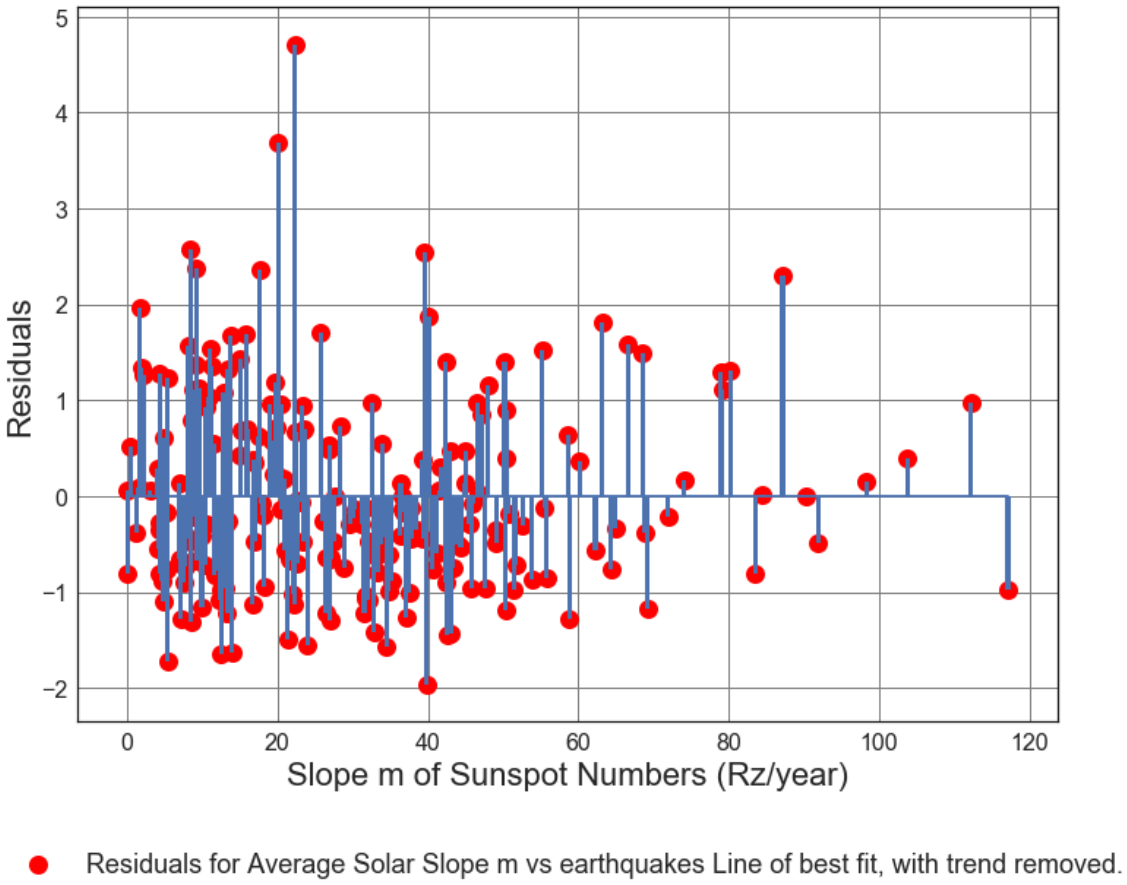

Figure C2.15: Scatter Plot of Solar cycle absolute value slope (from 1900 to 2017) vs. Average number of 7.5M and up Earthquakes/6months with trend removed. Line of best fit, y = -0.01011x + (0.3096), mean x = 30.66 +/- 23.0, mean y = -0.0004389 +/- 1.054, R = -0.2206, R squared = 0.04867, p-value = 0.0011.

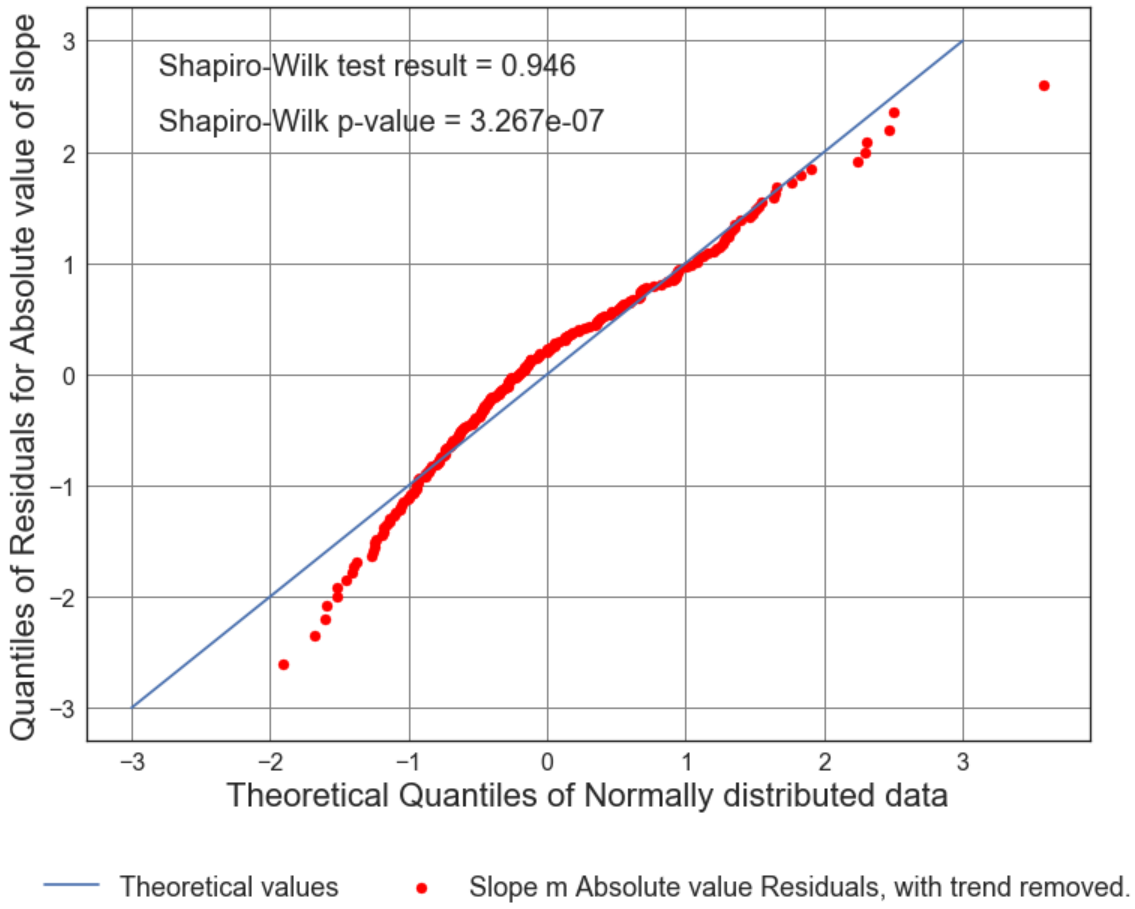

Figure C2.16: Scatter Plot of Solar cycle absolute value slope (from 1900 to 2017) vs. Average number of 7.5M and up Earthquakes/6months with trend removed. Line of best fit, y = -0.01011x + (0.3096), mean x = 30.66 +/- 23.0, mean y = -0.0004389 +/- 1.054, R = -0.2206, R squared = 0.04867, p-value = 0.0011.

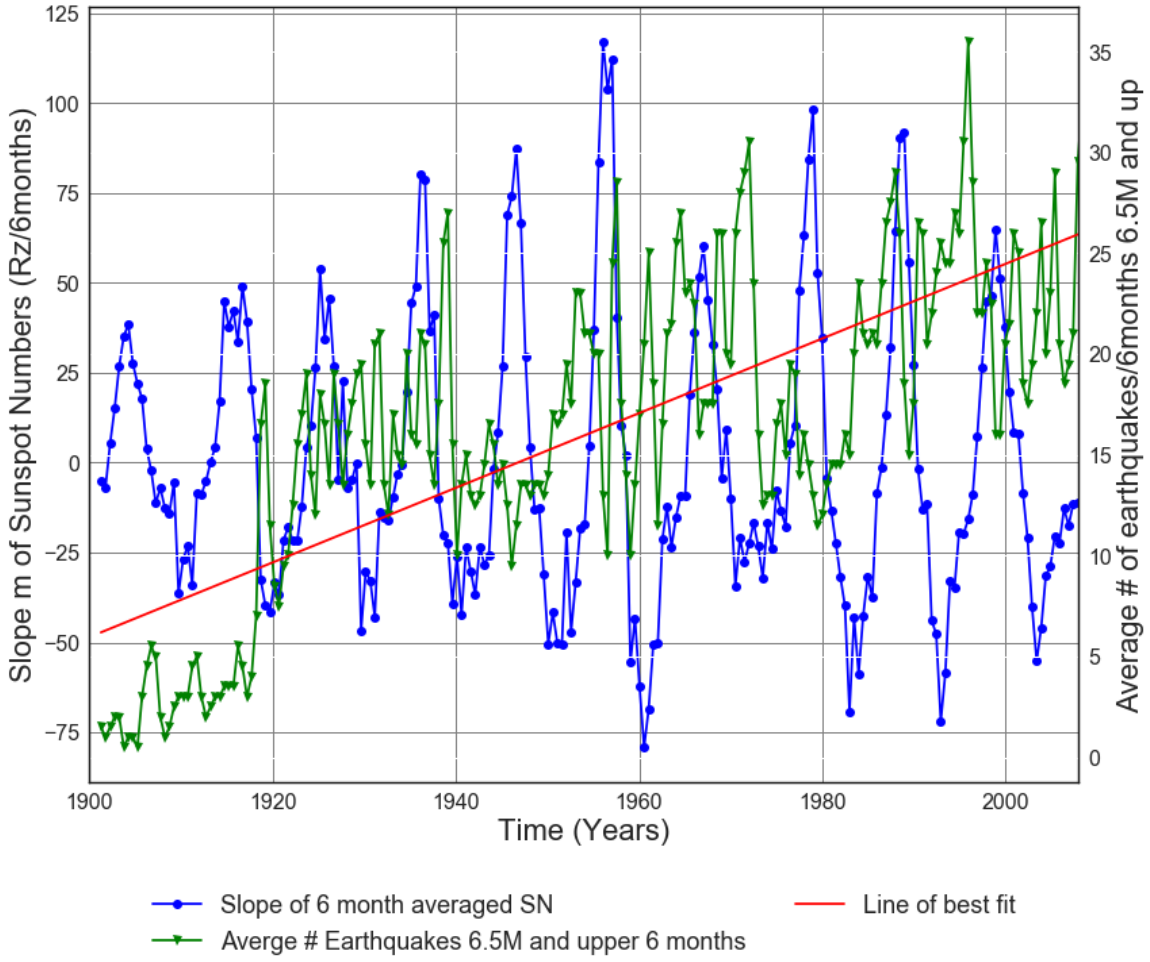

Figure C2.17: Slope of Solar cycle from 1900 to 2017 vs. Average number of 6.5M and up Earthquakes.

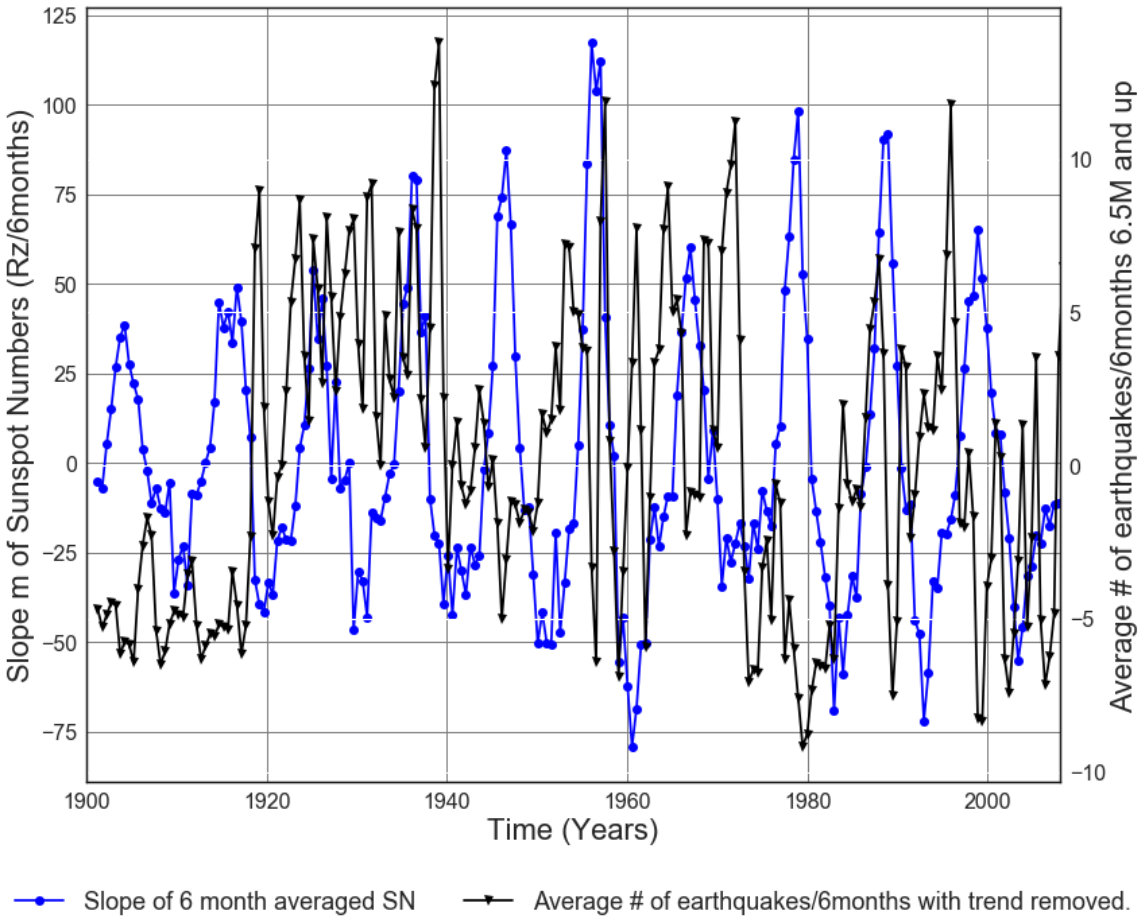

Figure C2.18: Slope of 6 month averaged SN 1900 to 2017 vs. Average number of 6.5M and up Earthquakes with trend removed. Line of best fit, y = 0.1851x + (-345.8), mean x = 1.955e+03 +/- 31.21, mean y = 16.06 +/- 7.702

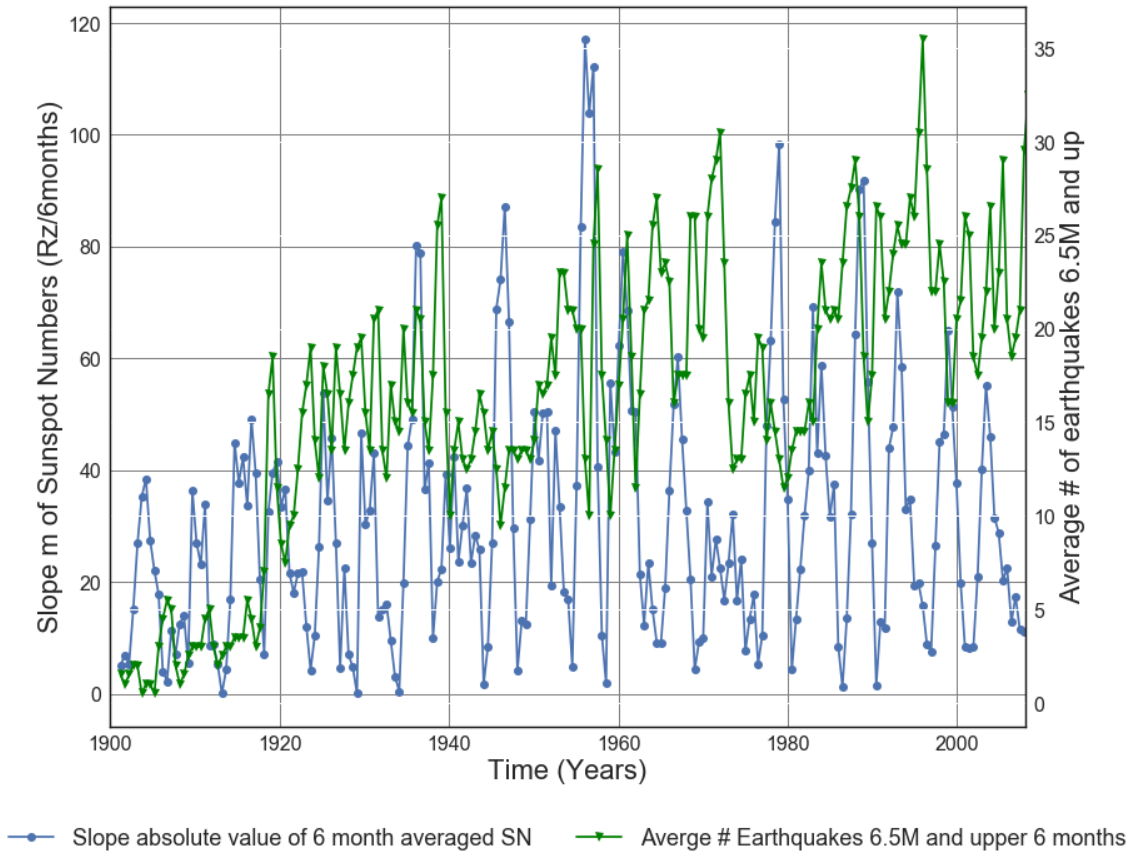

Figure C2.19: Slope Absolute value of Solar cycle from 1900 to 2017 vs. Average number of 6.5M and up Earthquakes.

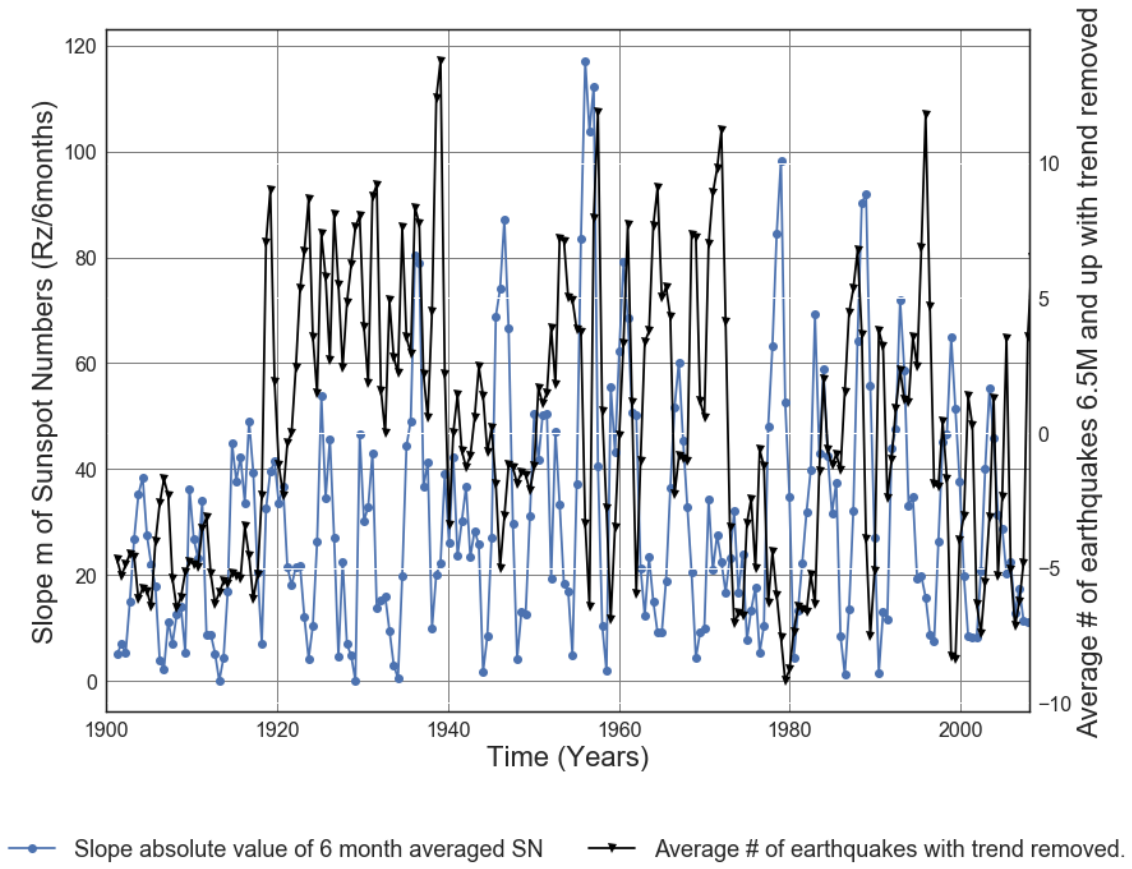

Figure C2.20: Slope Absolute value of Solar cycle from 1900 to 2017 vs. Average number of 6.5M and up earthquakes with trend removed.

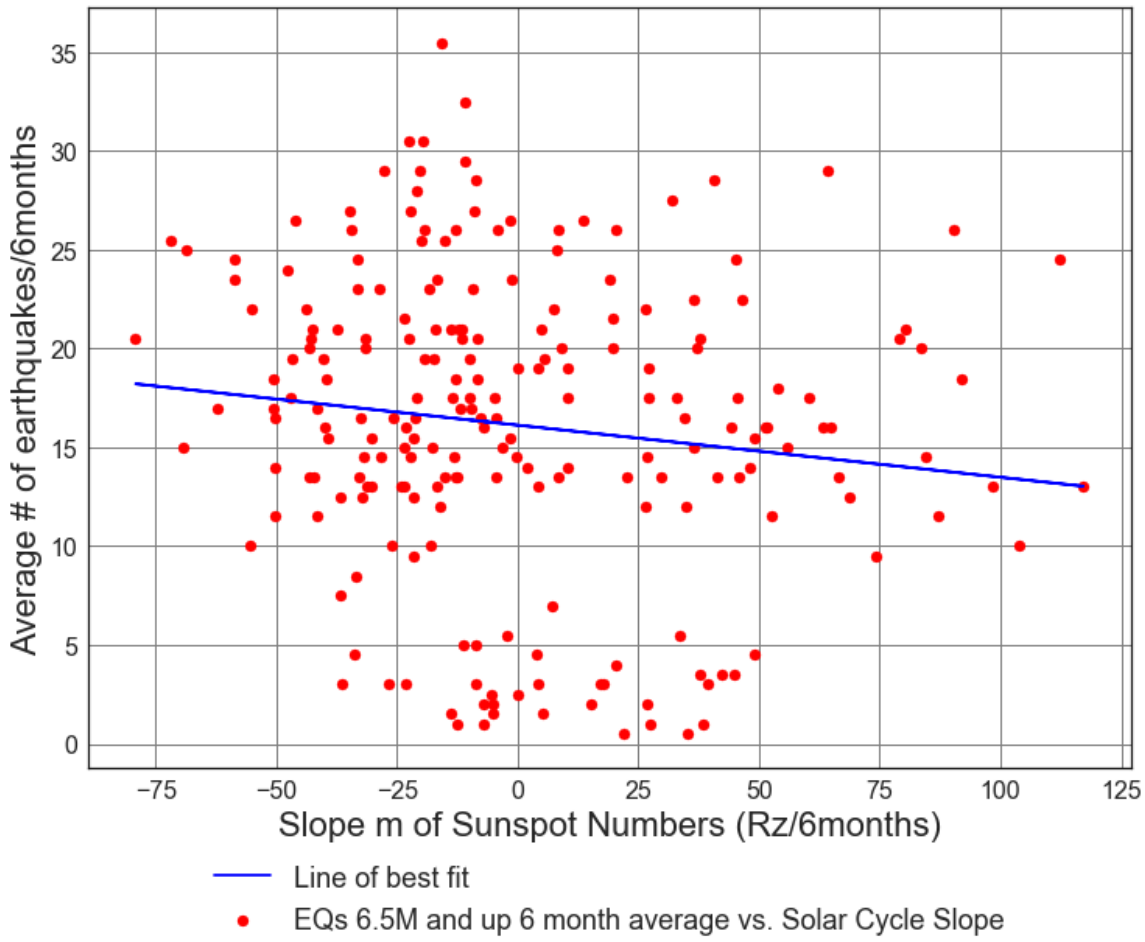

Figure C2.21: Scatter Plot of Solar cycle slope (from 1900 to 2017) vs. Average number of 6.5M and up Earthquakes/6months. Line of best fit, y = -0.02638x + (16.13), mean x = -0.07013 +/- 38.33, mean y = 16.13 +/- 7.656, R = -0.1321, R squared = 0.01744, p-value = 0.05259.

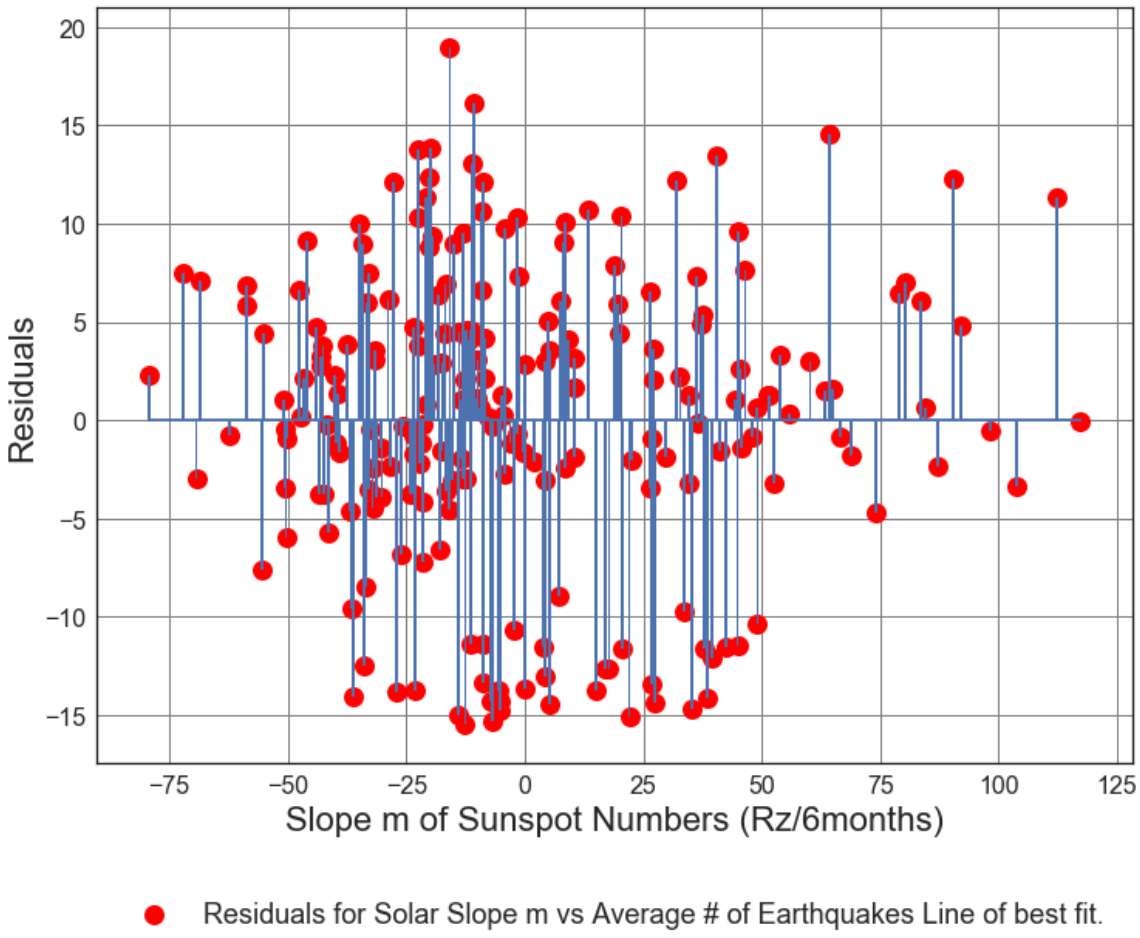

Figure C2.22: Residuals Plot of Solar cycle slope (from 1900 to 2017) vs. Average number of 6.5M and up Earthquakes/6months. Line of best fit, y = -0.02638x + (16.13), mean x = -0.07013 +/- 38.33, mean y = 16.13 +/- 7.656, R = -0.1321, R squared = 0.01744, p-value = 0.05259.

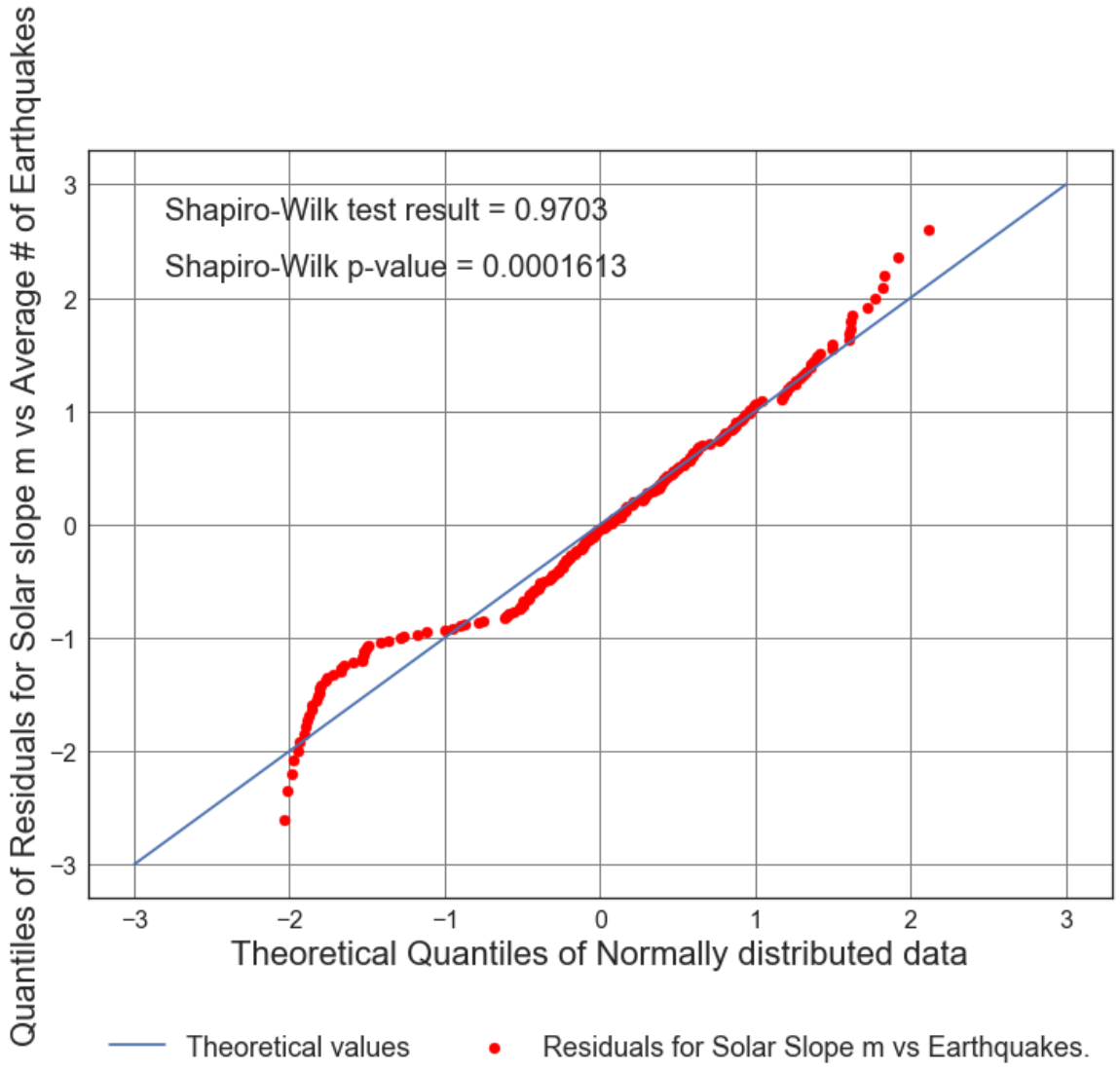

Figure C2.23: Residuals Plot of Solar cycle slope (from 1900 to 2017) vs. Average number of 6.5M and up Earthquakes/6months. Line of best fit, y = -0.02638x + (16.13), mean x = -0.07013 +/- 38.33, mean y = 16.13 +/- 7.656, R = -0.1321, R squared = 0.01744, p-value = 0.05259.

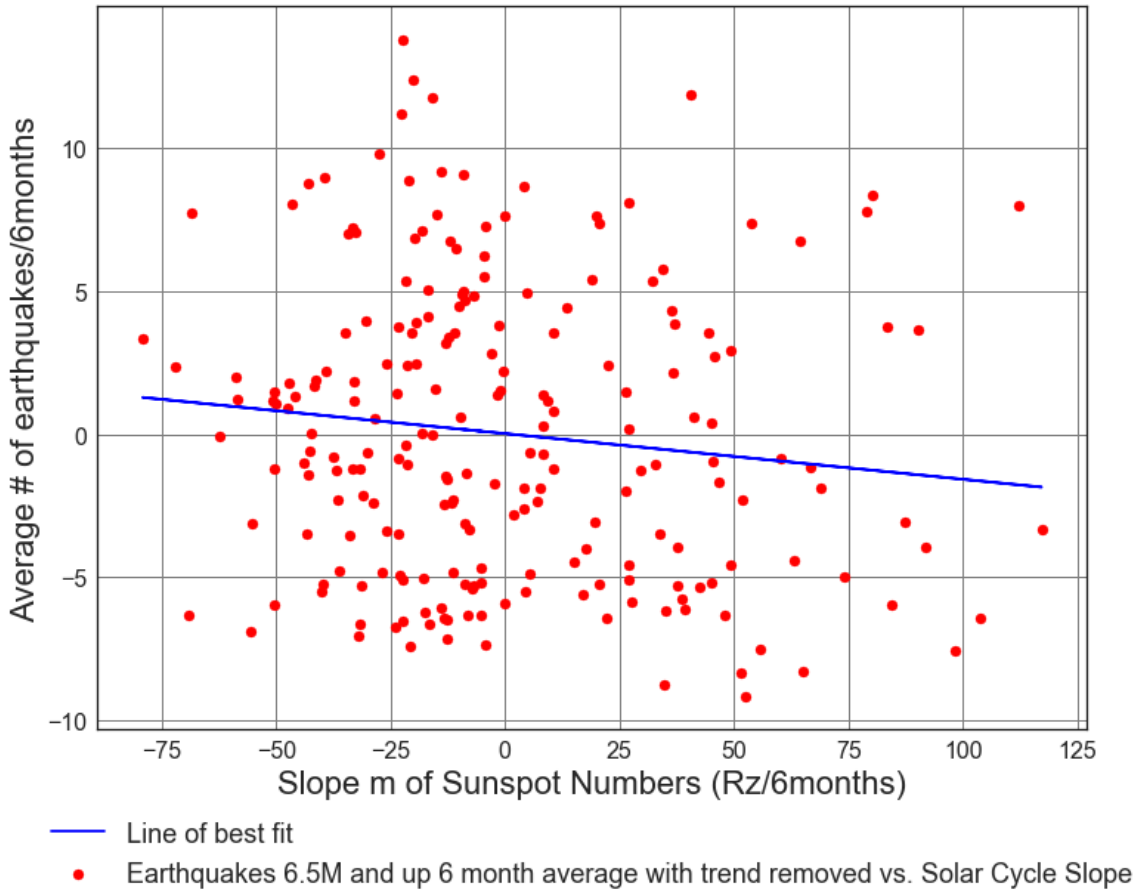

Figure C2.24: Scatter Plot of Solar cycle slope (from 1900 to 2017) vs. Average number of 6.5M and up Earthquakes/6months with trend removed. Line of best fit, y = -0.01597x + (0.02018), mean x = -0.07013 +/- 38.33, mean y = 0.0213 +/- 5.095, R = -0.1201, R squared = 0.01444, p-value = 0.07808.

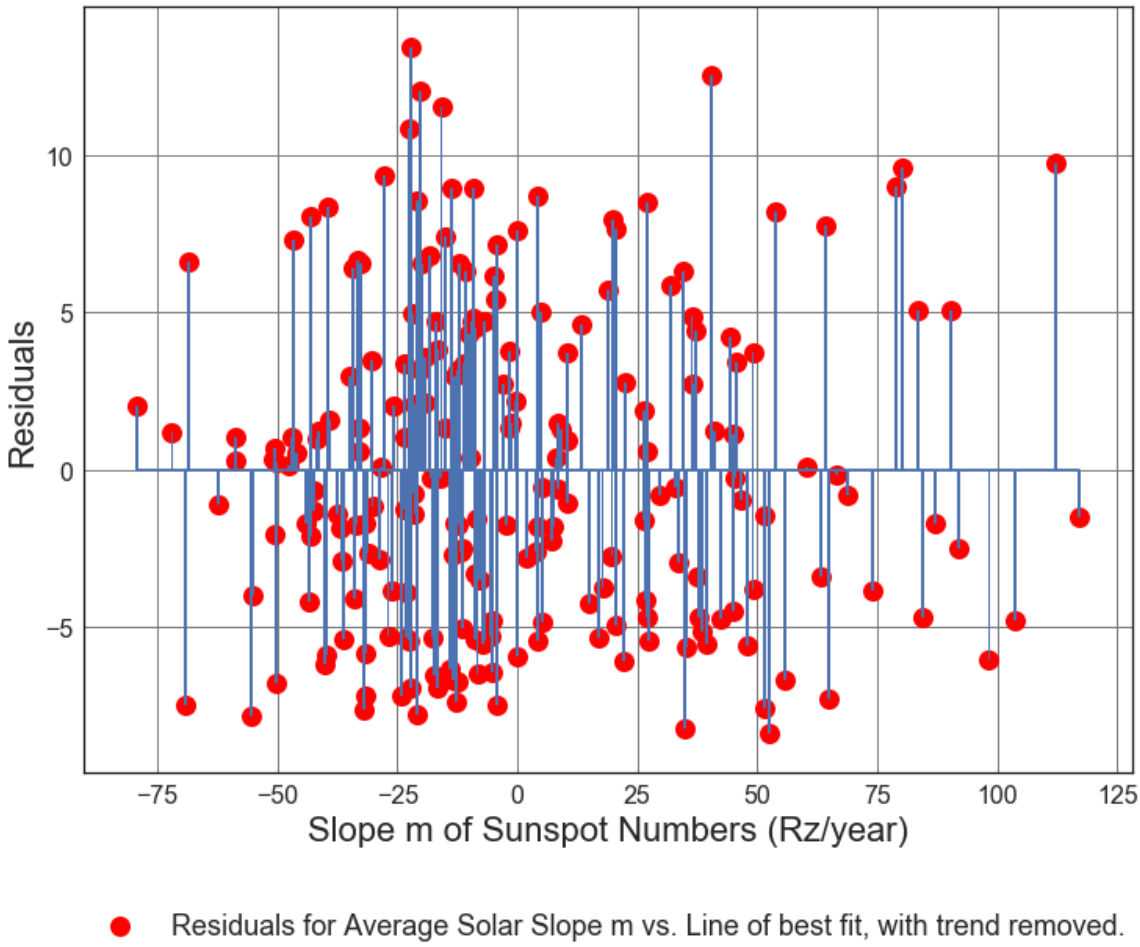

Figure C2.25: Scatter Plot of Solar cycle slope (from 1900 to 2017) vs. Average number of 6.5M and up Earthquakes/6months with trend removed. Line of best fit, y = -0.01597x + (0.02018), mean x = -0.07013 +/- 38.33, mean y = 0.0213 +/- 5.095, R = -0.1201, R squared = 0.01444, p-value = 0.07808.

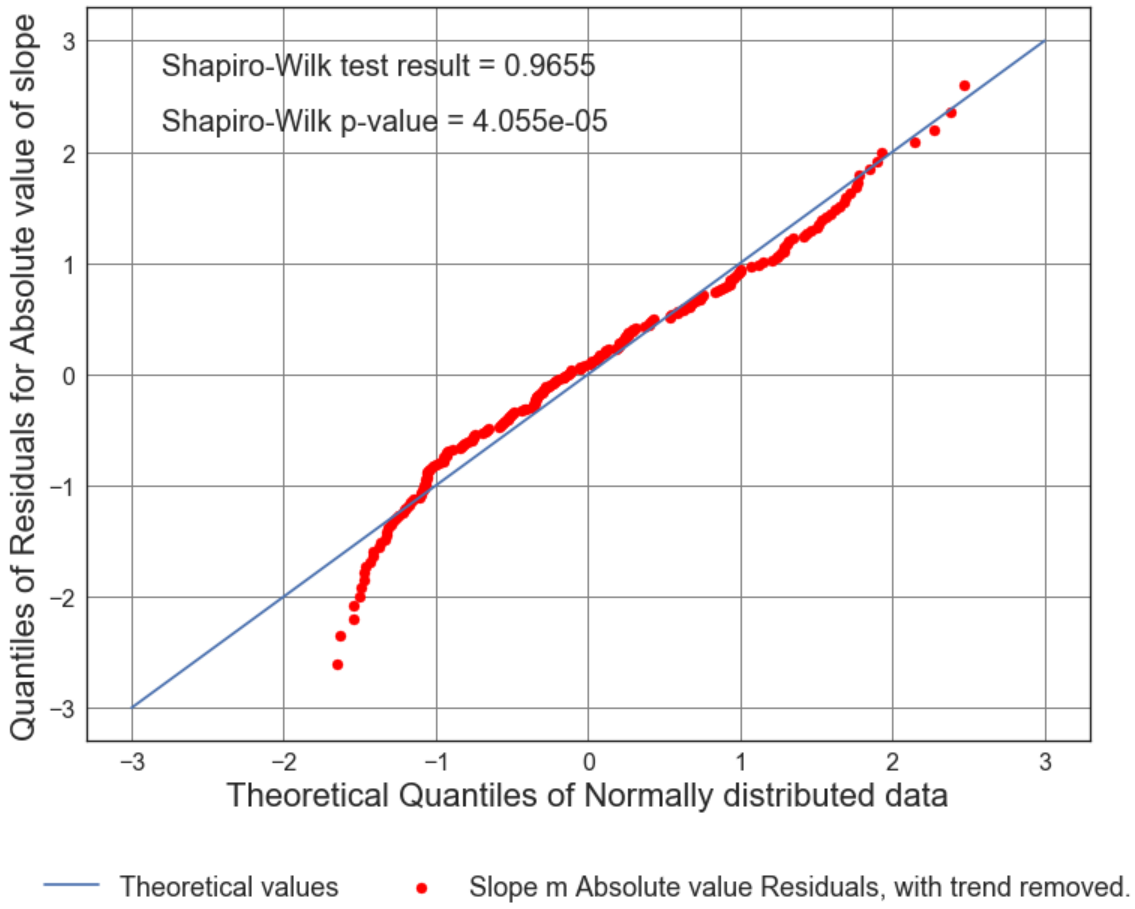

Figure C2.26: Scatter Plot of Solar cycle slope (from 1900 to 2017) vs. Average number of 6.5M and up Earthquakes/6months with trend removed. Line of best fit, y = -0.01597x + (0.02018), mean x = -0.07013 +/- 38.33, mean y = 0.0213 +/- 5.095, R = -0.1201, R squared = 0.01444, p-value = 0.07808.

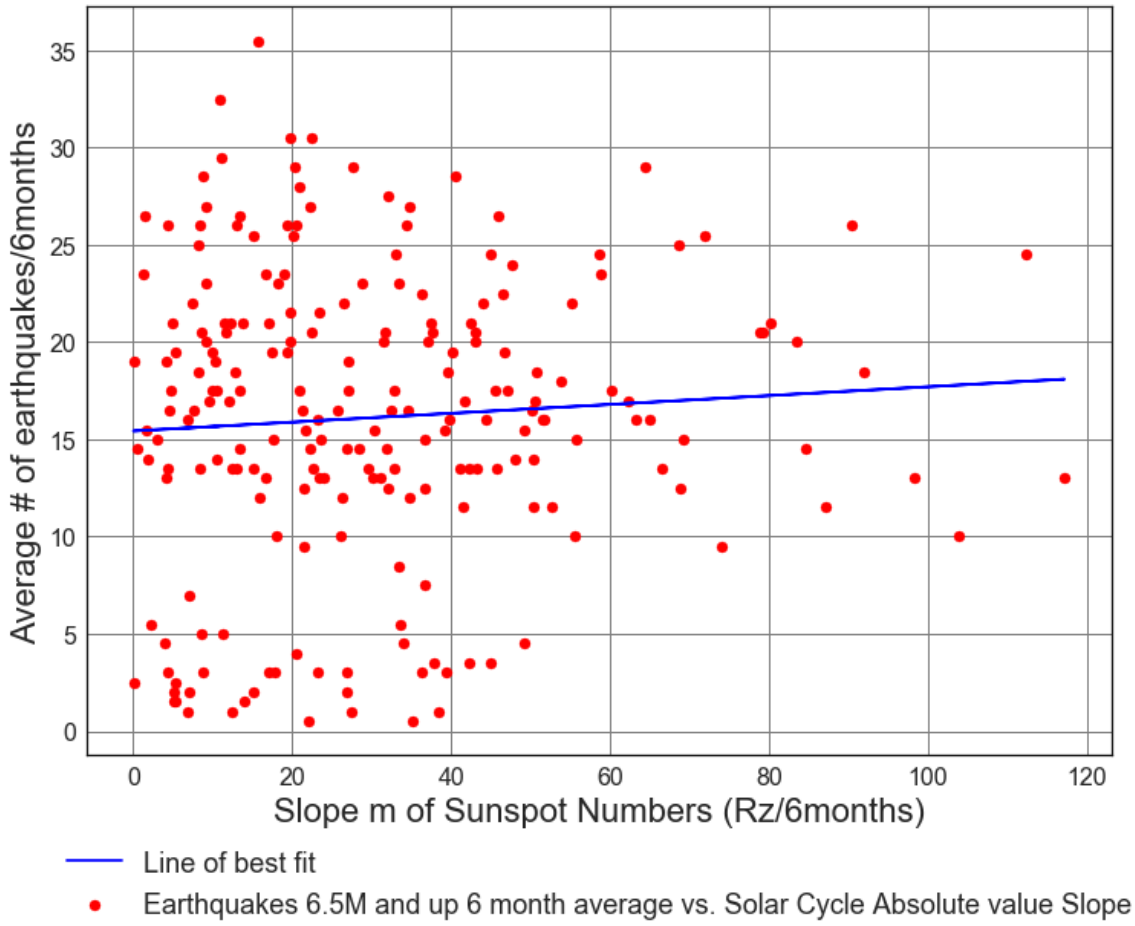

Figure C2.27: Scatter Plot of Solar cycle slope (from 1900 to 2017) vs. Average number of 6.5M and up Earthquakes/6months. Line of best fit, y = 0.02274x + (15.43), mean x = 30.66 +/- 23.0, mean y = 16.13 +/- 7.656, R = 0.06833, R squared = 0.004669, p-value = 0.3175.

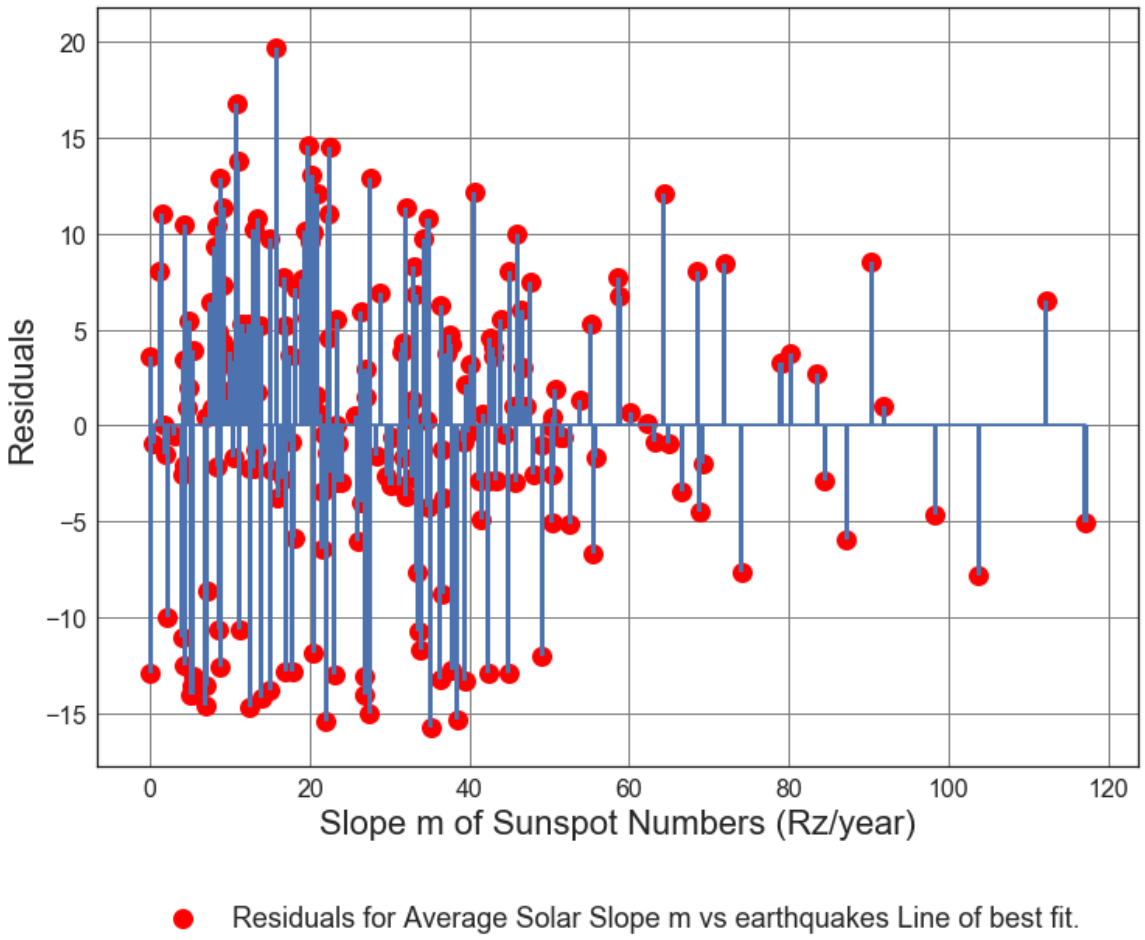

Figure C2.28: Scatter Plot of Solar cycle slope (from 1900 to 2017) vs. Average number of 6.5M and up Earthquakes/6months. Line of best fit, y = 0.02274x + (15.43), mean x = 30.66 +/- 23.0, mean y = 16.13 +/- 7.656, R = 0.06833, R squared = 0.004669, p-value = 0.3175.

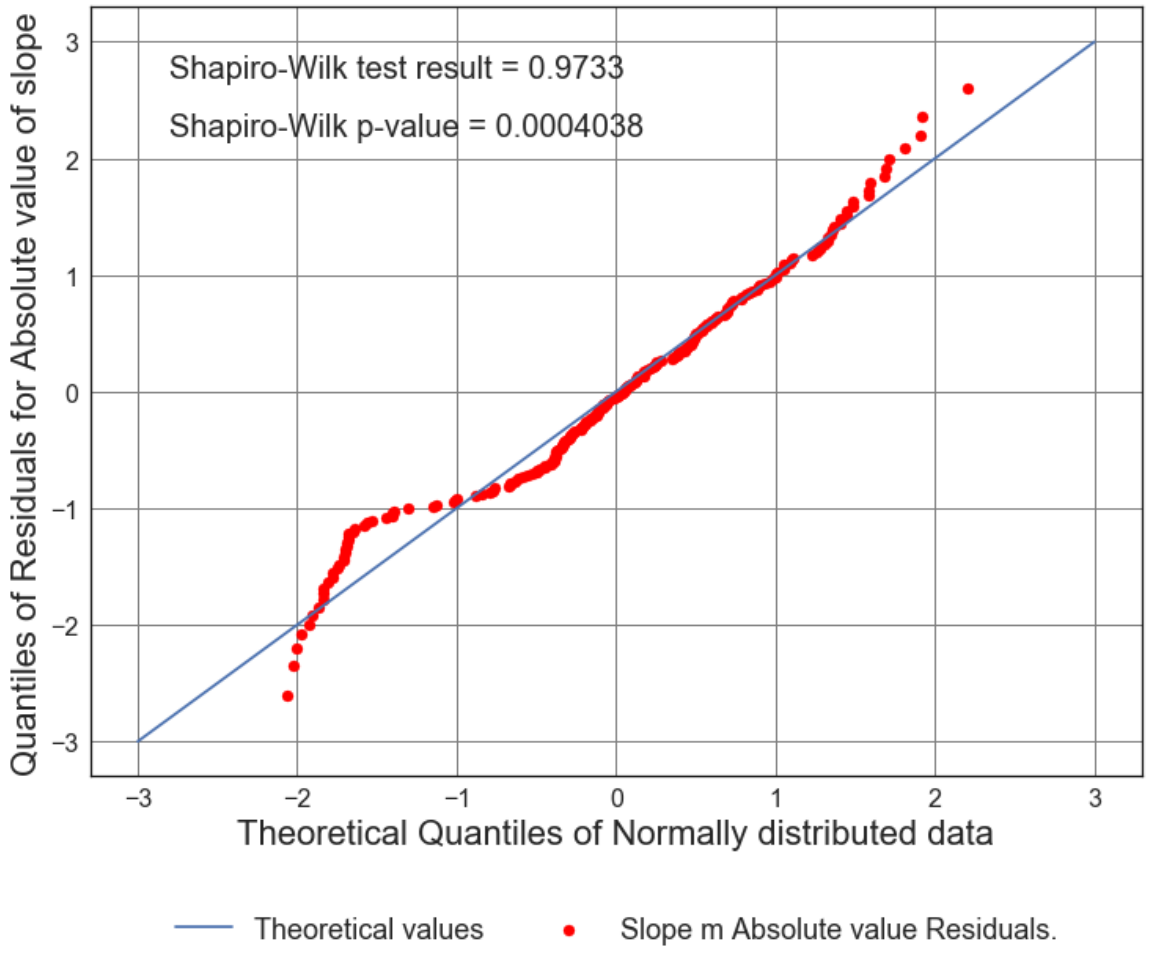

Figure C2.29: Scatter Plot of Solar cycle slope (from 1900 to 2017) vs. Average number of 6.5M and up Earthquakes/6months. Line of best fit, y = 0.02274x + (15.43), mean x = 30.66 +/- 23.0, mean y = 16.13 +/- 7.656, R = 0.06833, R squared = 0.004669, p-value = 0.3175.

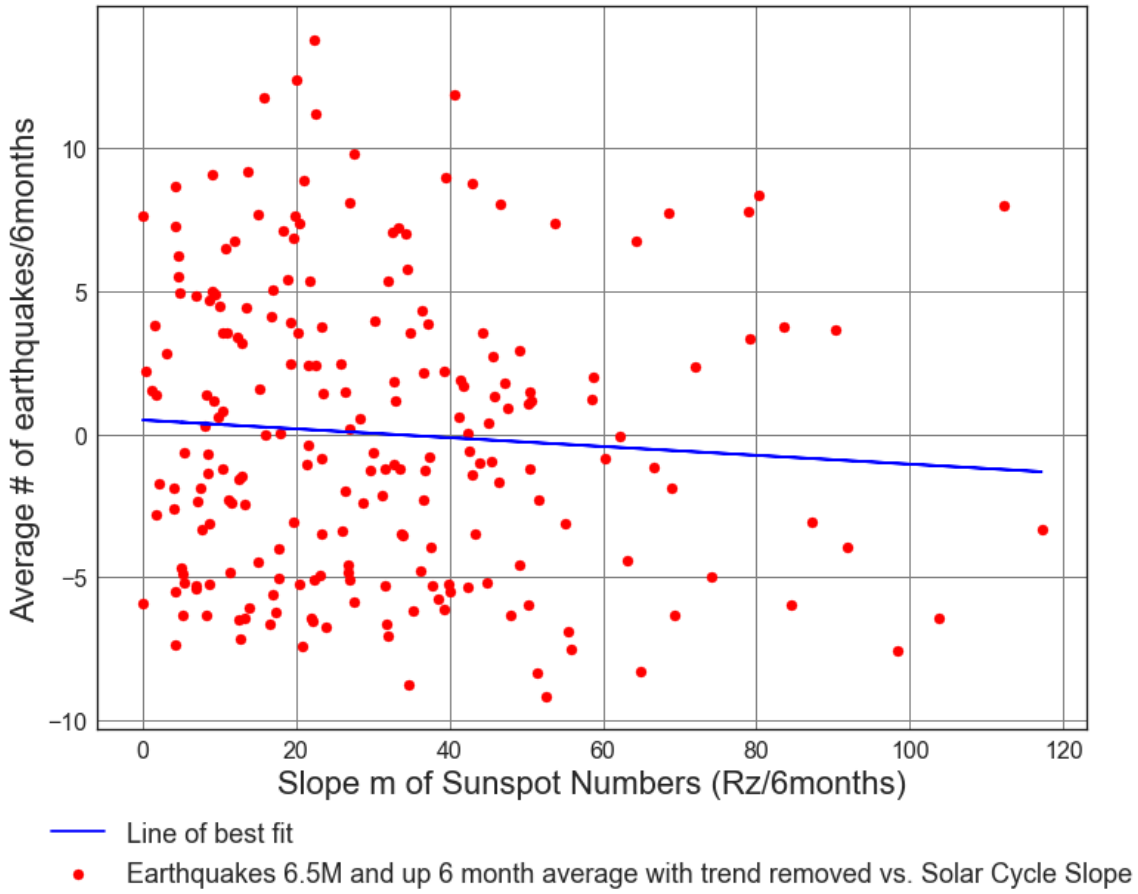

Figure C2.30: Scatter Plot of Solar cycle absolute value slope (from 1900 to 2017) vs. Average number of 6.5M and up Earthquakes/6months with trend removed. Line of best fit, y = -0.01541x + (0.4938), mean x = 30.66 +/- 23.0, mean y = 0.0213 +/- 5.095, R = -0.06956, R squared = 0.004839, p-value = 0.3088.

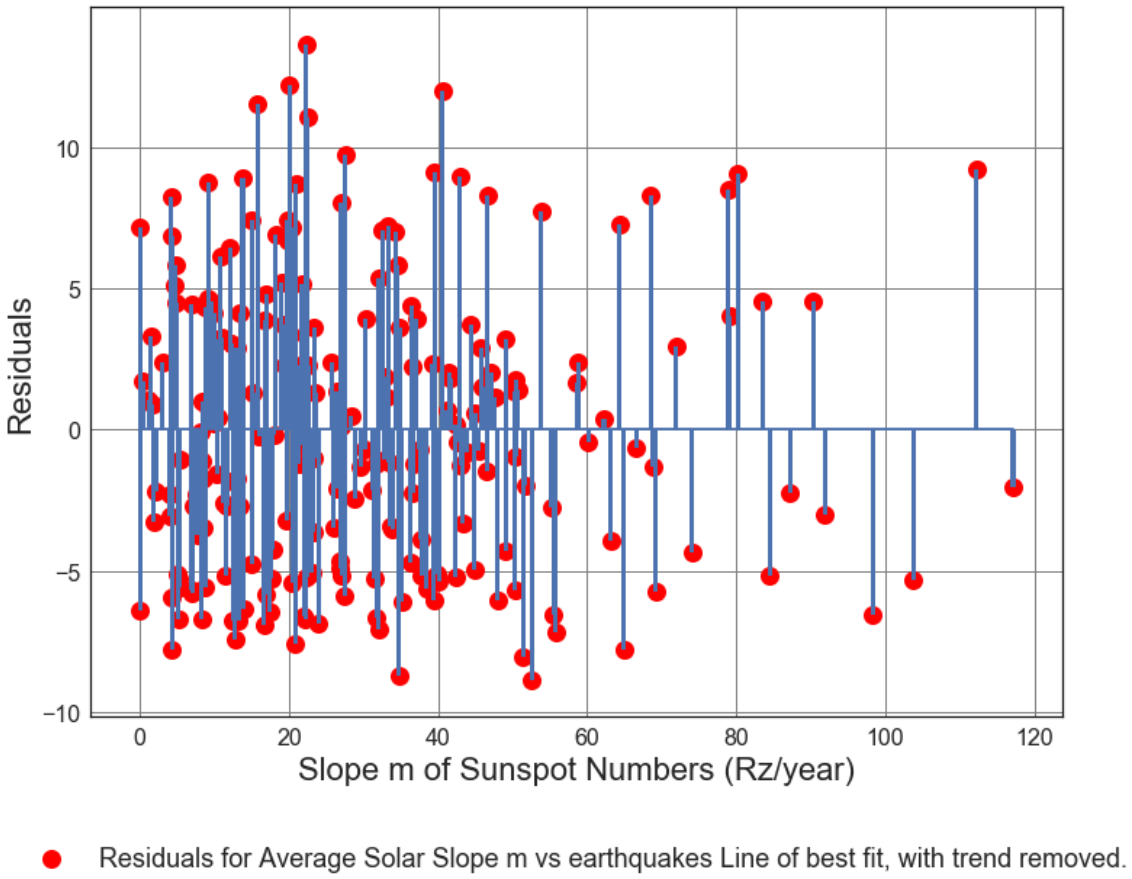

Figure C2.31: Scatter Plot of Solar cycle absolute value slope (from 1900 to 2017) vs. Average number of 6.5M and up Earthquakes/6months with trend removed. Line of best fit, y = -0.01541x + (0.4938), mean x = 30.66 +/- 23.0, mean y = 0.0213 +/- 5.095, R = -0.06956, R squared = 0.004839, p-value = 0.3088.

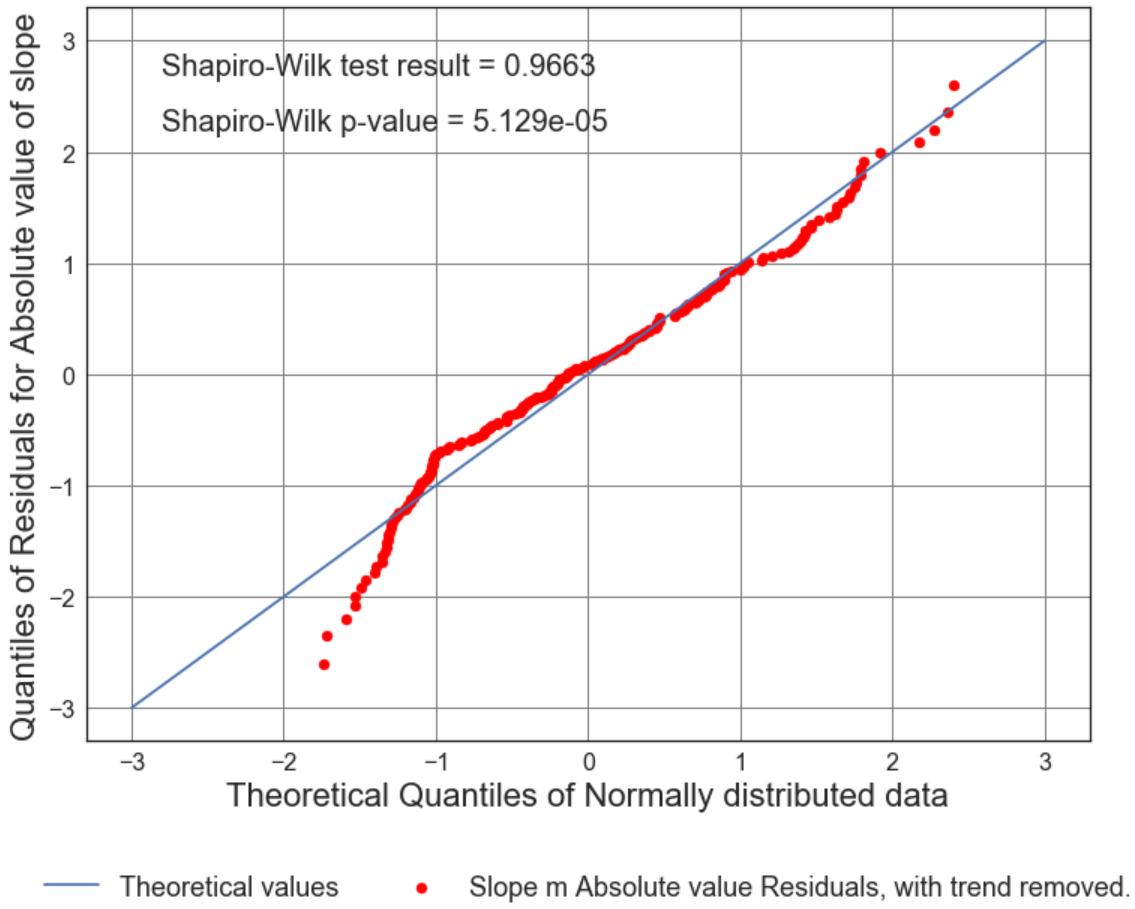

Figure C2.32: Scatter Plot of Solar cycle absolute value slope (from 1900 to 2017) vs. Average number of 6.5M and up Earthquakes/6months with trend removed. Line of best fit, y = -0.01541x + (0.4938), mean x = 30.66 +/- 23.0, mean y = 0.0213 +/- 5.095, R = -0.06956, R squared = 0.004839, p-value = 0.3088.

Appendix C3: USGS Centennial Time Series Analysis Part 3 - Pre 1964 (Historical period) Six Month Averaged Earthquake and Sunspot Data.

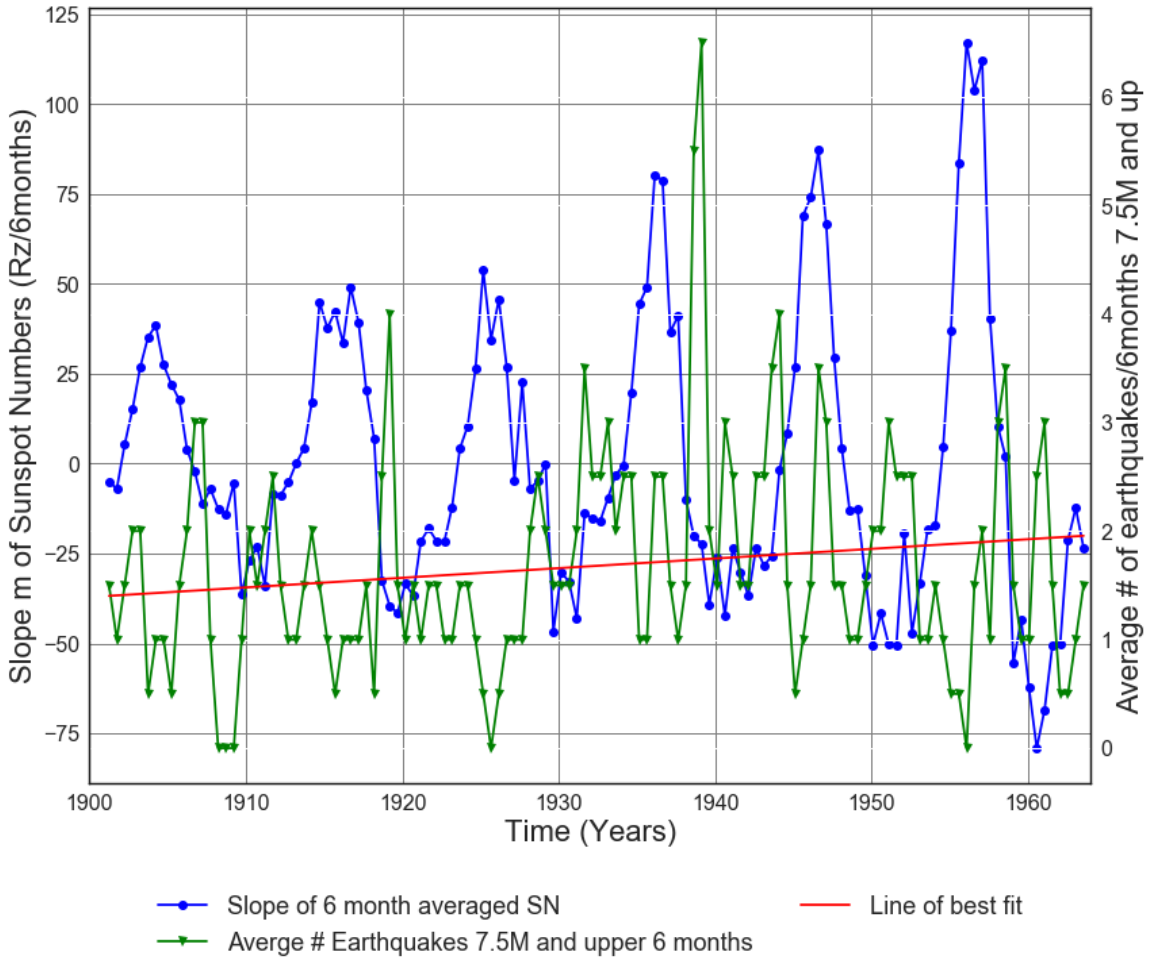

Figure C3.1: Slope of Solar cycle from 1900 to 1964 vs. Average number of 7.5M and up Earthquakes.

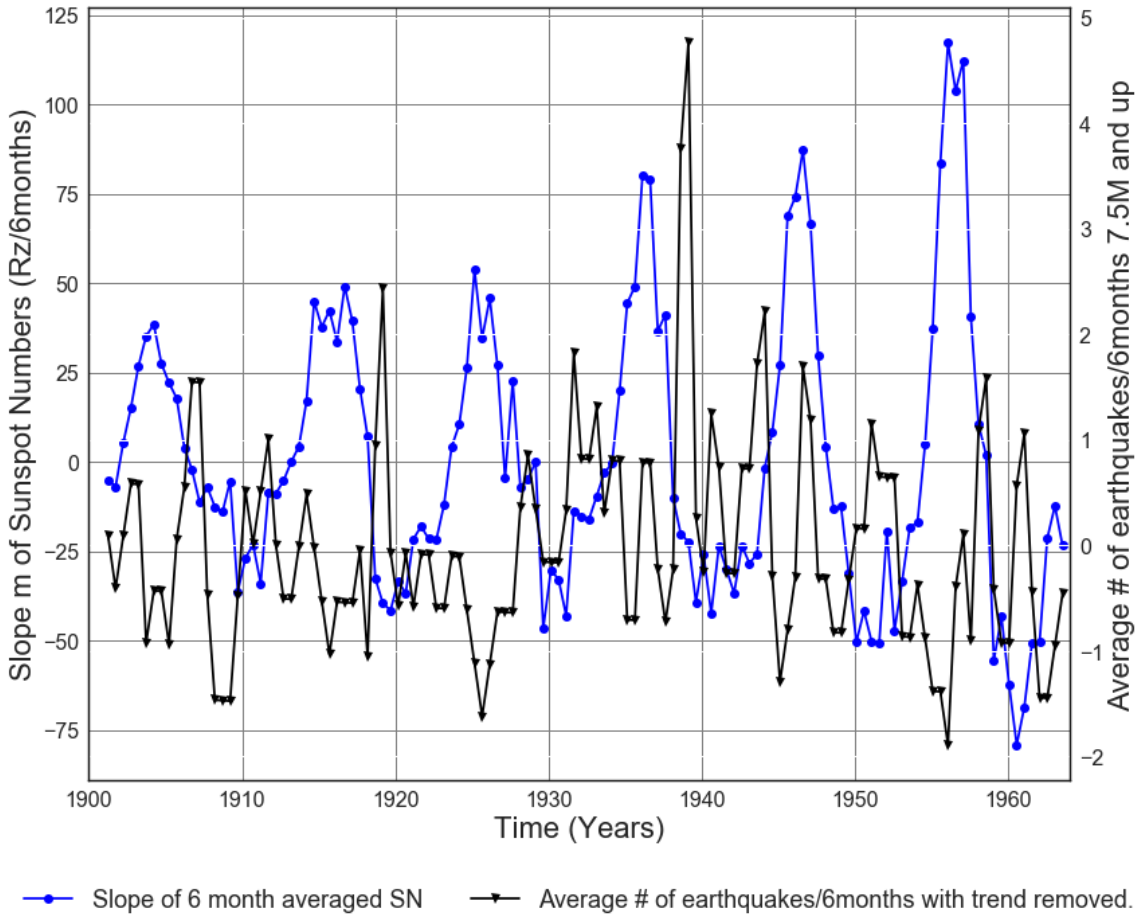

Figure C3.2: Slope of 6 month averaged SN 1900 to 1964 vs. Average number of 7.5M and up Earthquakes with trend removed. Line of best fit, y = 0.008889x + (-15.5), mean x = 1.932e+03 +/- 18.27, mean y = 1.677 +/- 1.024

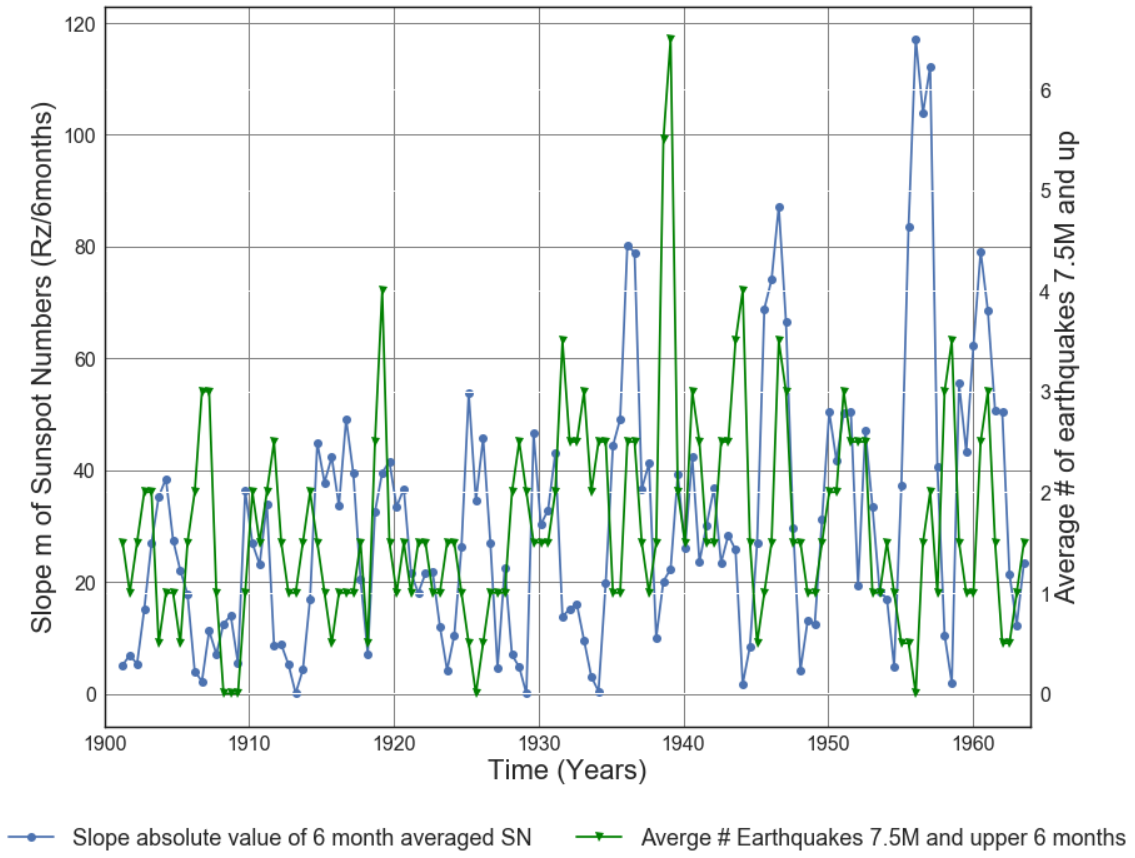

Figure C3.3: Slope Absolute value of Solar cycle from 1900 to 1964 vs. Average number of 7.5M and up Earthquakes.

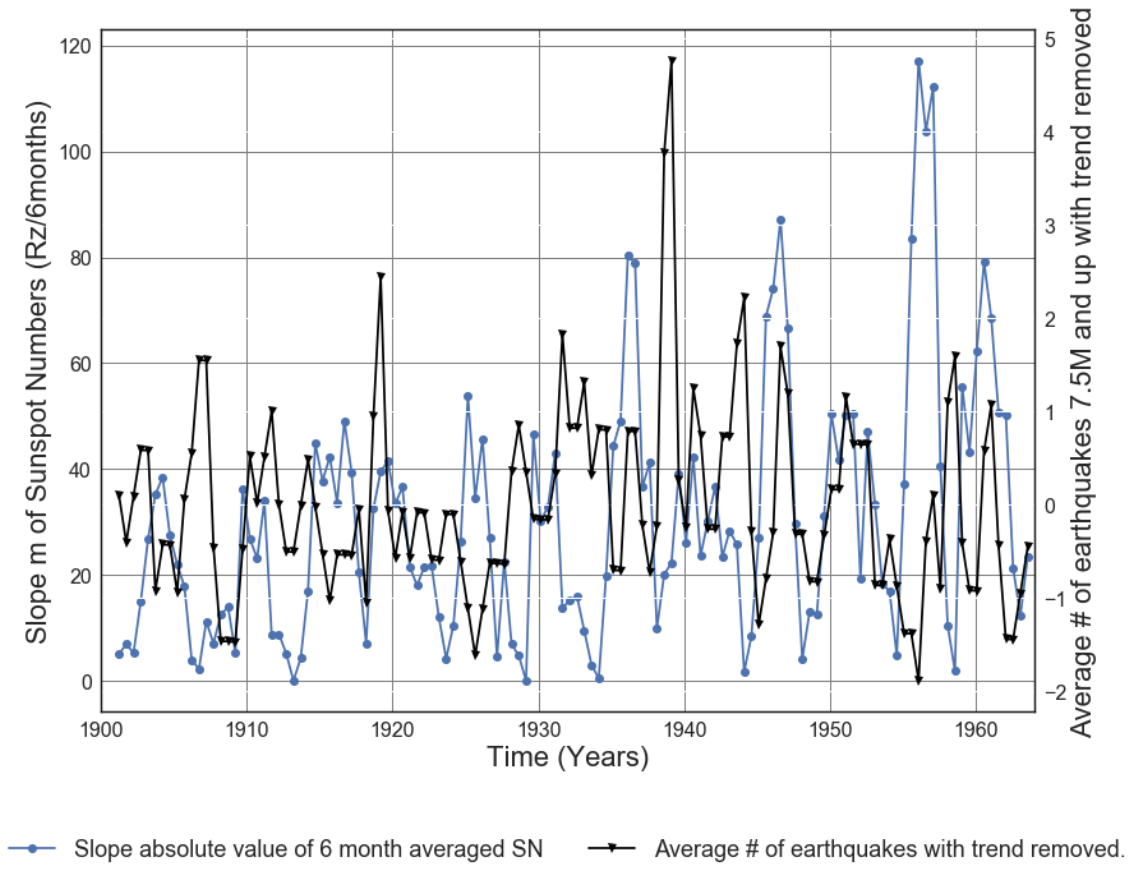

Figure C3.4: Slope Absolute value of Solar cycle from 1900 to 1964 vs. Average number of 7.5M and up earthquakes with trend removed.

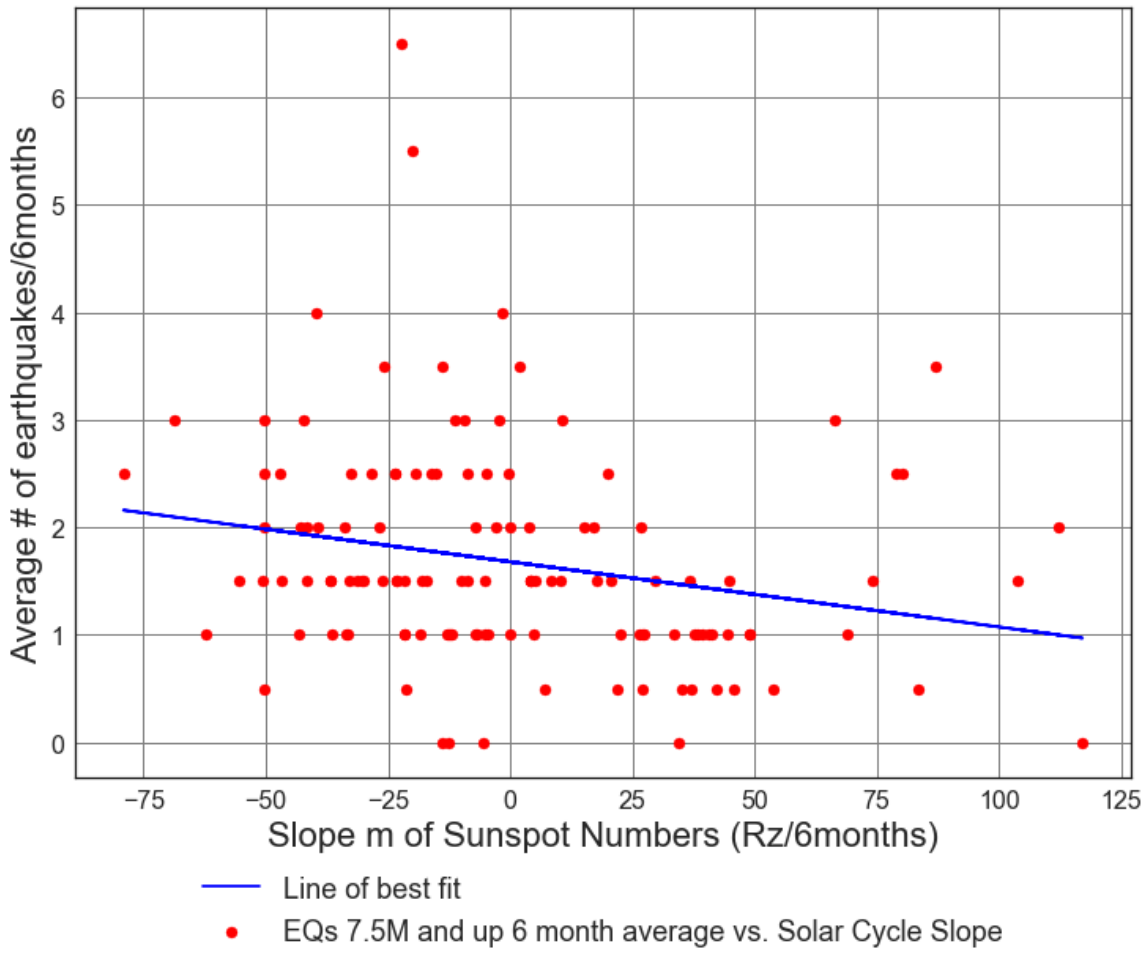

Figure C3.5: Scatter Plot of Solar cycle slope (from 1900 to 1964) vs. Average number of 7.5M and up Earthquakes/6months. Line of best fit, y = -0.006063x + (1.681), mean x = 0.3737 +/- 38.55, mean y = 1.679 +/- 1.028, R = -0.2273, R squared = 0.05165, p-value = 0.01049.

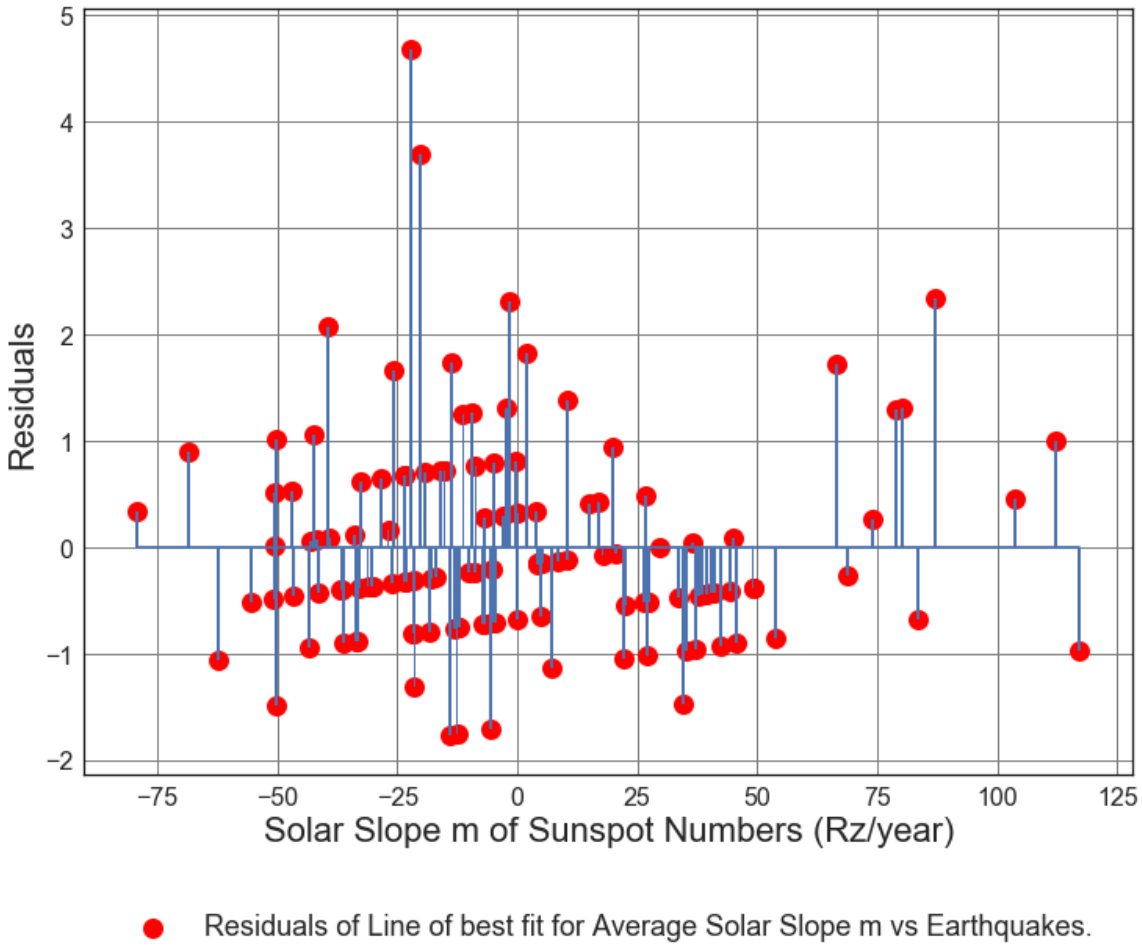

Figure C3.6: Residuals Plot of Solar cycle slope (from 1900 to 1964) vs. Average number of 7.5M and up Earthquakes/6months. Line of best fit, y = -0.006063x + (1.681), mean x = 0.3737 +/- 38.55, mean y = 1.679 +/- 1.028, R = -0.2273, R squared = 0.05165, p-value = 0.01049.

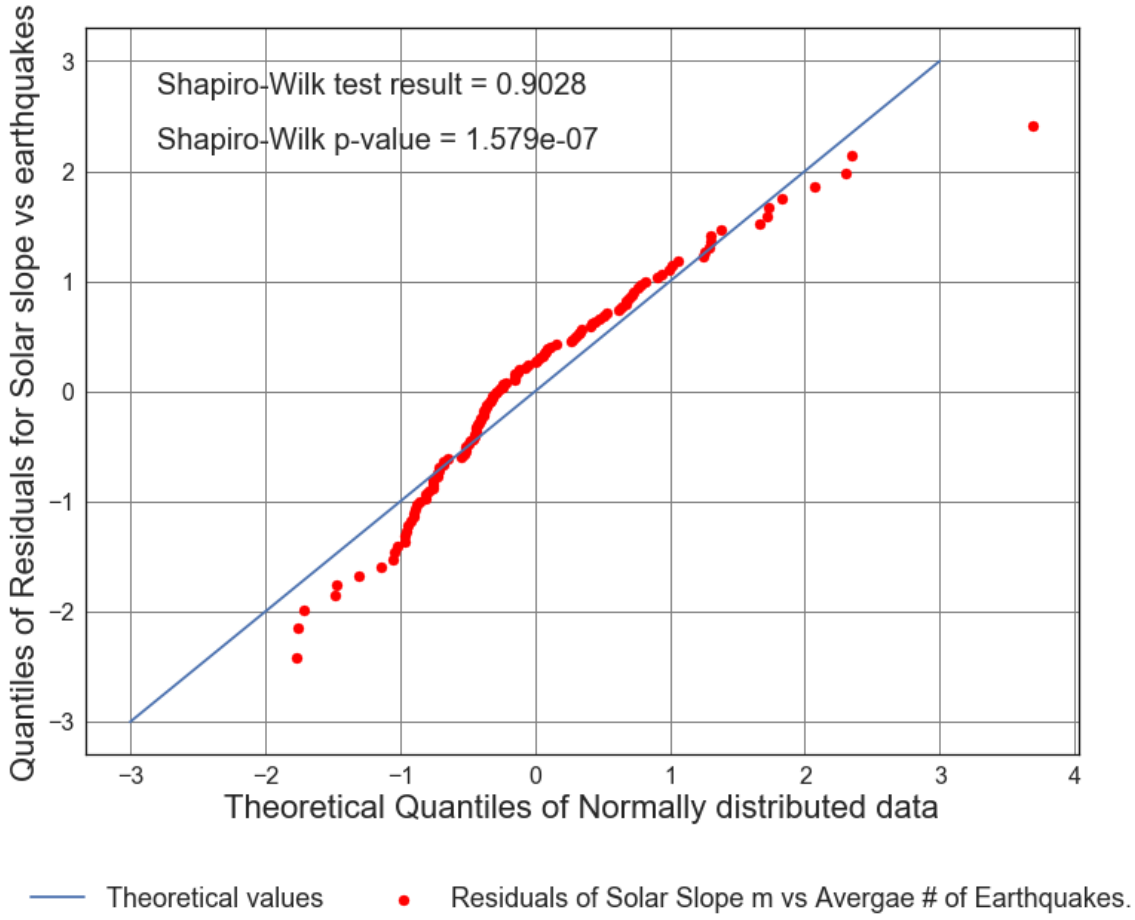

Figure C3.7: Residuals Plot of Solar cycle slope (from 1900 to 1964) vs. Average number of 7.5M and up Earthquakes/6months. Line of best fit, y = -0.006063x + (1.681), mean x = 0.3737 +/- 38.55, mean y = 1.679 +/- 1.028, R = -0.2273, R squared = 0.05165, p-value = 0.01049.

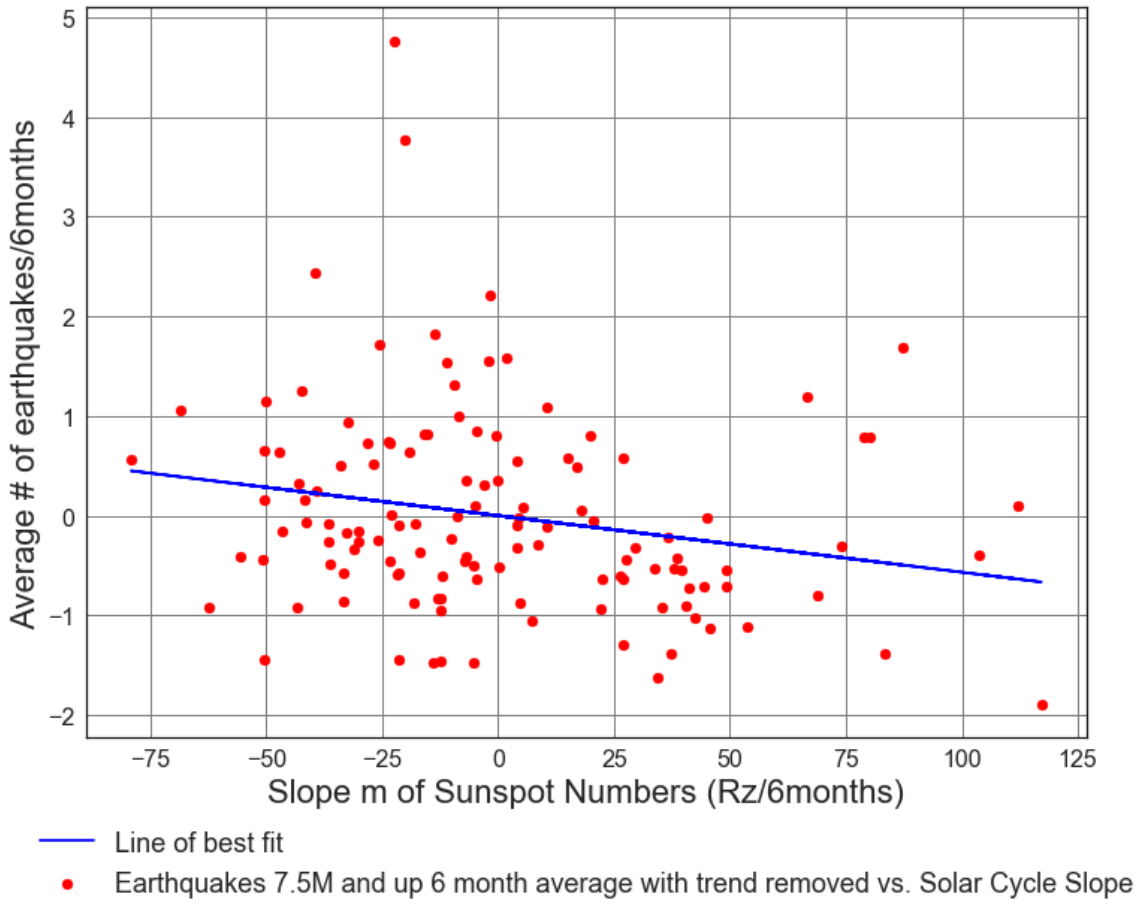

Figure C3.8: Scatter Plot of Solar cycle slope (from 1900 to 1964) vs. Average number of 7.5M and up Earthquakes/6months with trend removed. Line of best fit, y = -0.00568x + (0.001314), mean x = 0.3737 +/- 38.55, mean y = -0.0008086 +/- 1.015, R = -0.2157, R squared = 0.04651, p-value = 0.0153.

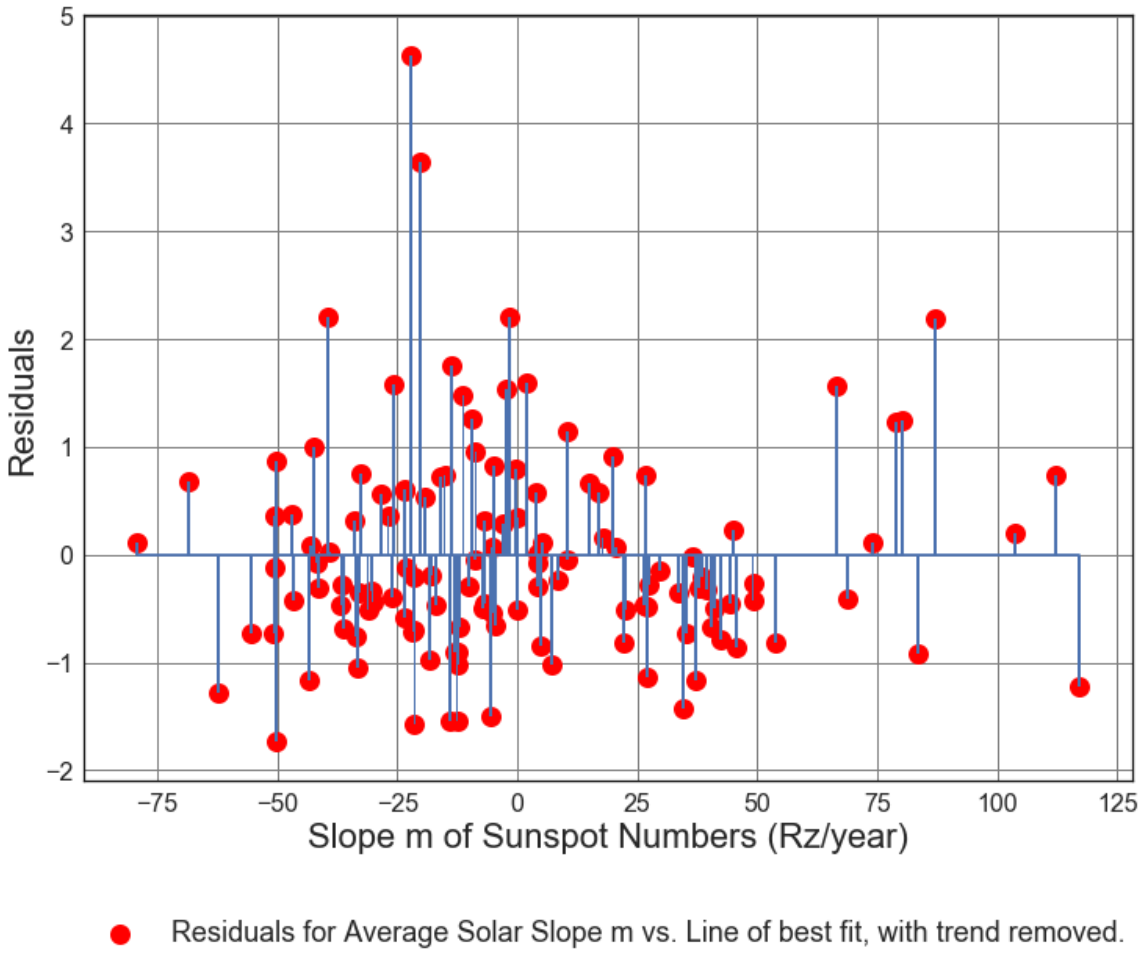

Figure C3.9: Scatter Plot of Solar cycle slope (from 1900 to 1964) vs. Average number of 7.5M and up Earthquakes/6months with trend removed. Line of best fit, y = -0.00568x + (0.001314), mean x = 0.3737 +/- 38.55, mean y = -0.0008086 +/- 1.015, R = -0.2157, R squared = 0.04651, p-value = 0.0153.

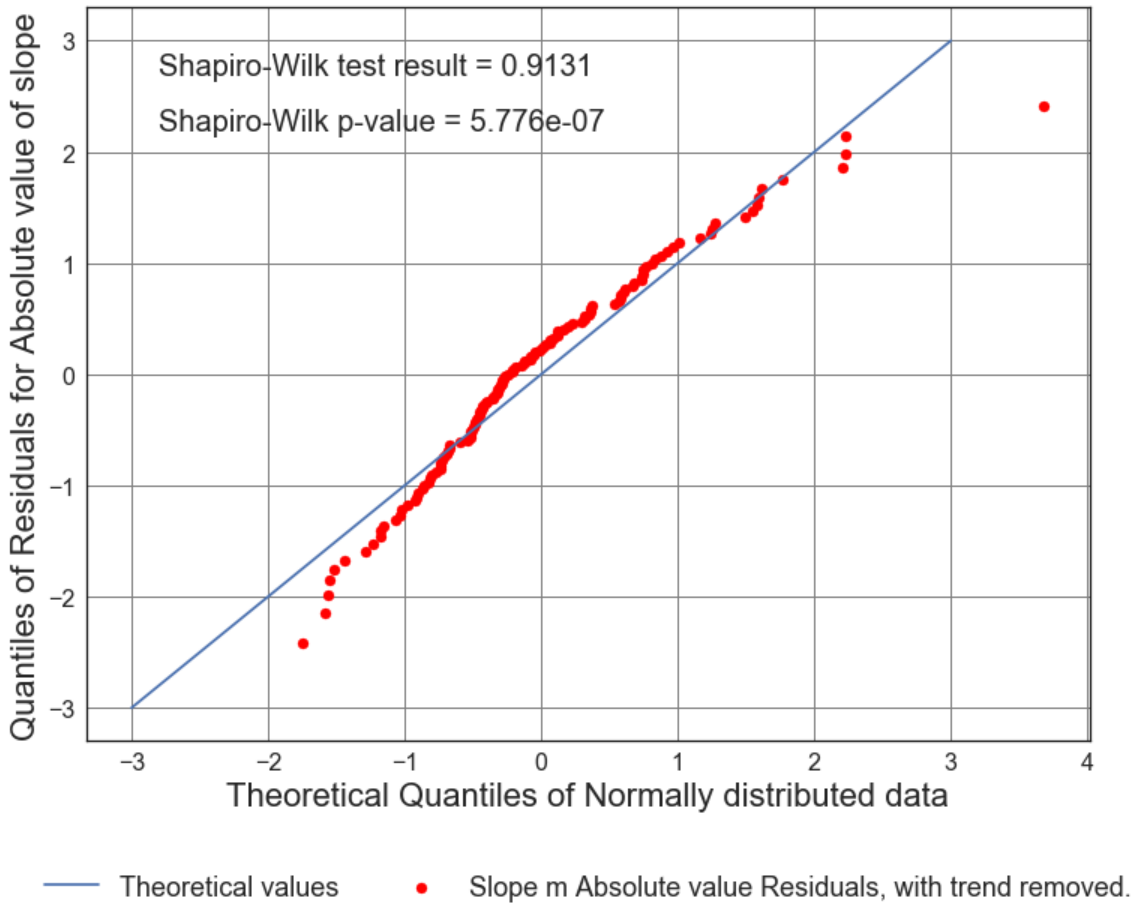

Figure C3.10: Scatter Plot of Solar cycle slope (from 1900 to 1964) vs. Average number of 7.5M and up Earthquakes/6months with trend removed. Line of best fit, y = -0.00568x + (0.001314), mean x = 0.3737 +/- 38.55, mean y = -0.0008086 +/- 1.015, R = -0.2157, R squared = 0.04651, p-value = 0.0153.

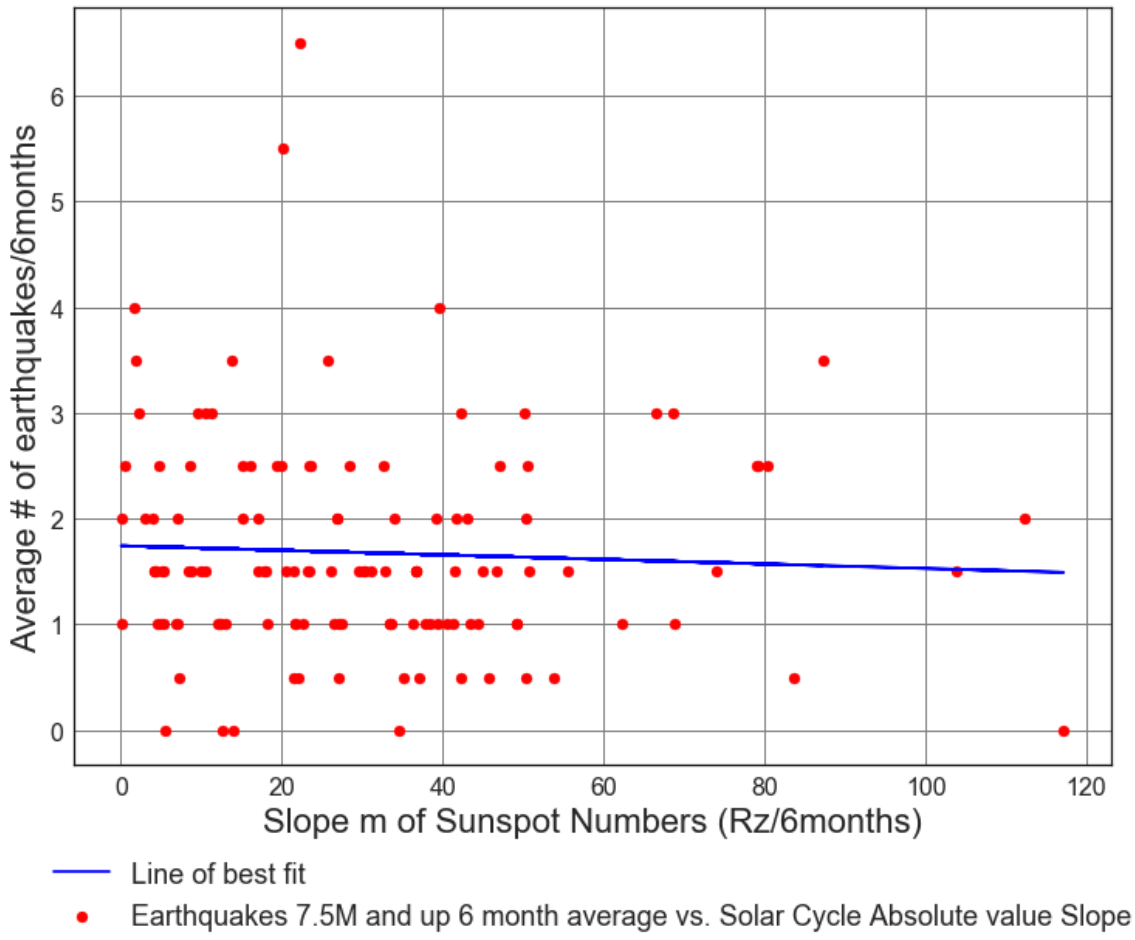

Figure C3.11: Scatter Plot of Solar cycle slope (from 1900 to 1964) vs. Average number of 7.5M and up Earthquakes/6months. Line of best fit, y = -0.002143x + (1.744), mean x = 30.43 +/- 23.66, mean y = 1.679 +/- 1.028, R = -0.04932, R squared = 0.002432, p-value = 0.5834.

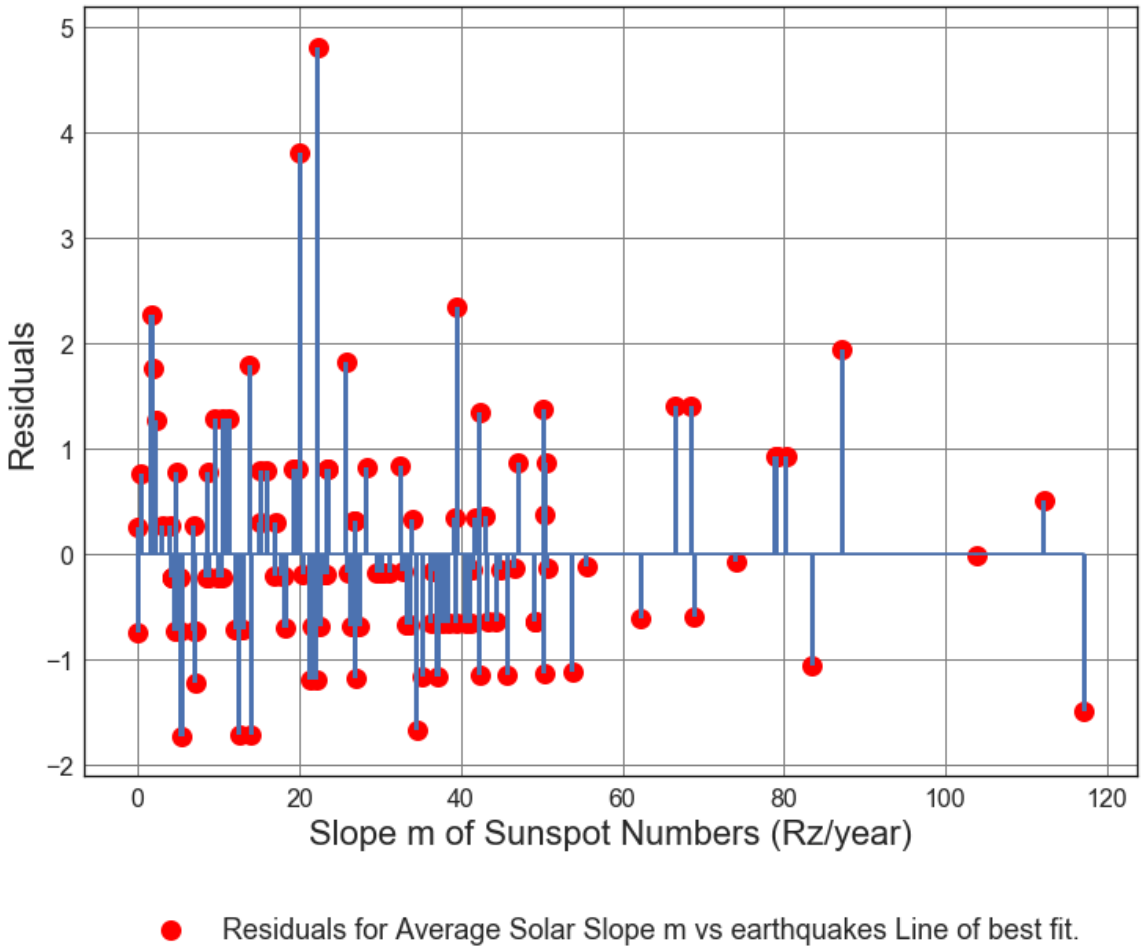

Figure C3.12: Scatter Plot of Solar cycle slope (from 1900 to 1964) vs. Average number of 7.5M and up Earthquakes/6months. Line of best fit, y = -0.002143x + (1.744), mean x = 30.43 +/- 23.66, mean y = 1.679 +/- 1.028, R = -0.04932, R squared = 0.002432, p-value = 0.5834.

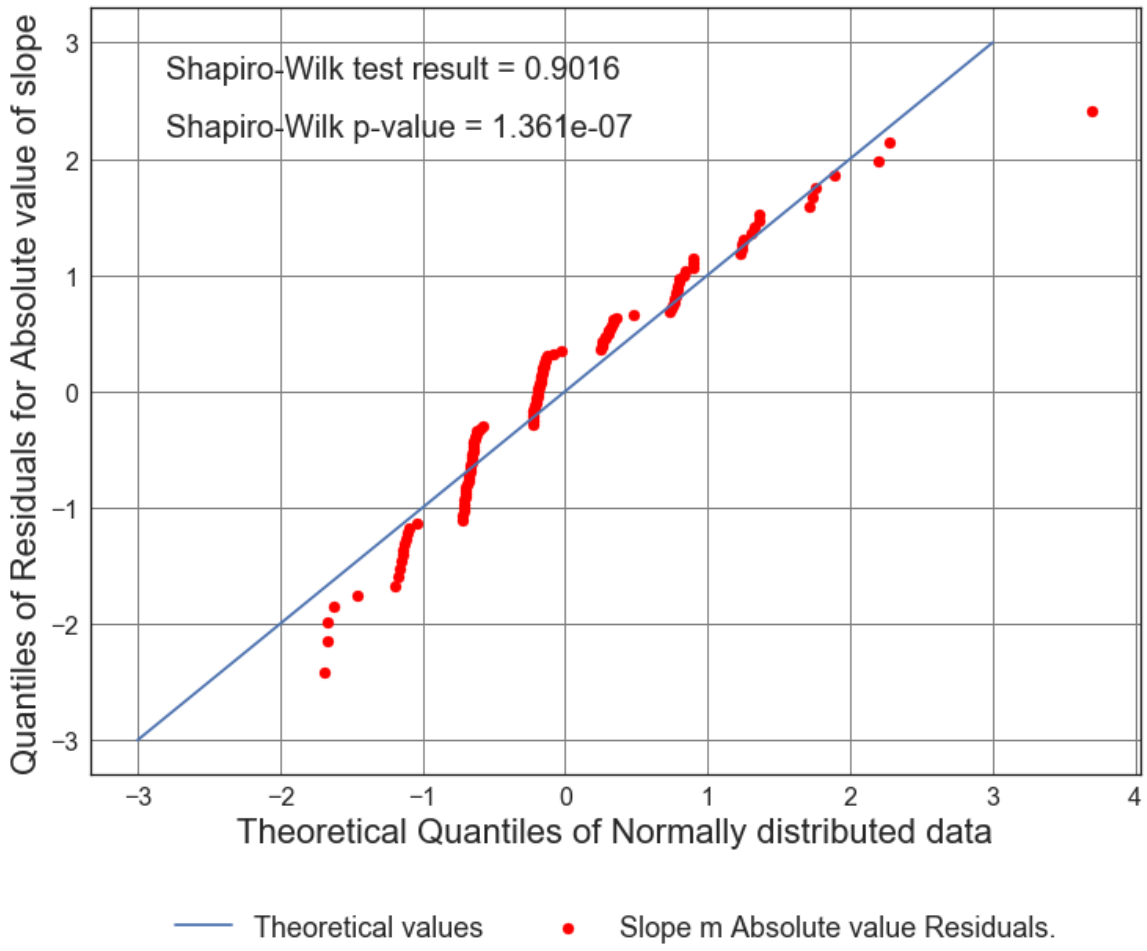

Figure C3.13: Scatter Plot of Solar cycle slope (from 1900 to 1964) vs. Average number of 7.5M and up Earthquakes/6months. Line of best fit, y = -0.002143x + (1.744), mean x = 30.43 +/- 23.66, mean y = 1.679 +/- 1.028, R = -0.04932, R squared = 0.002432, p-value = 0.5834.

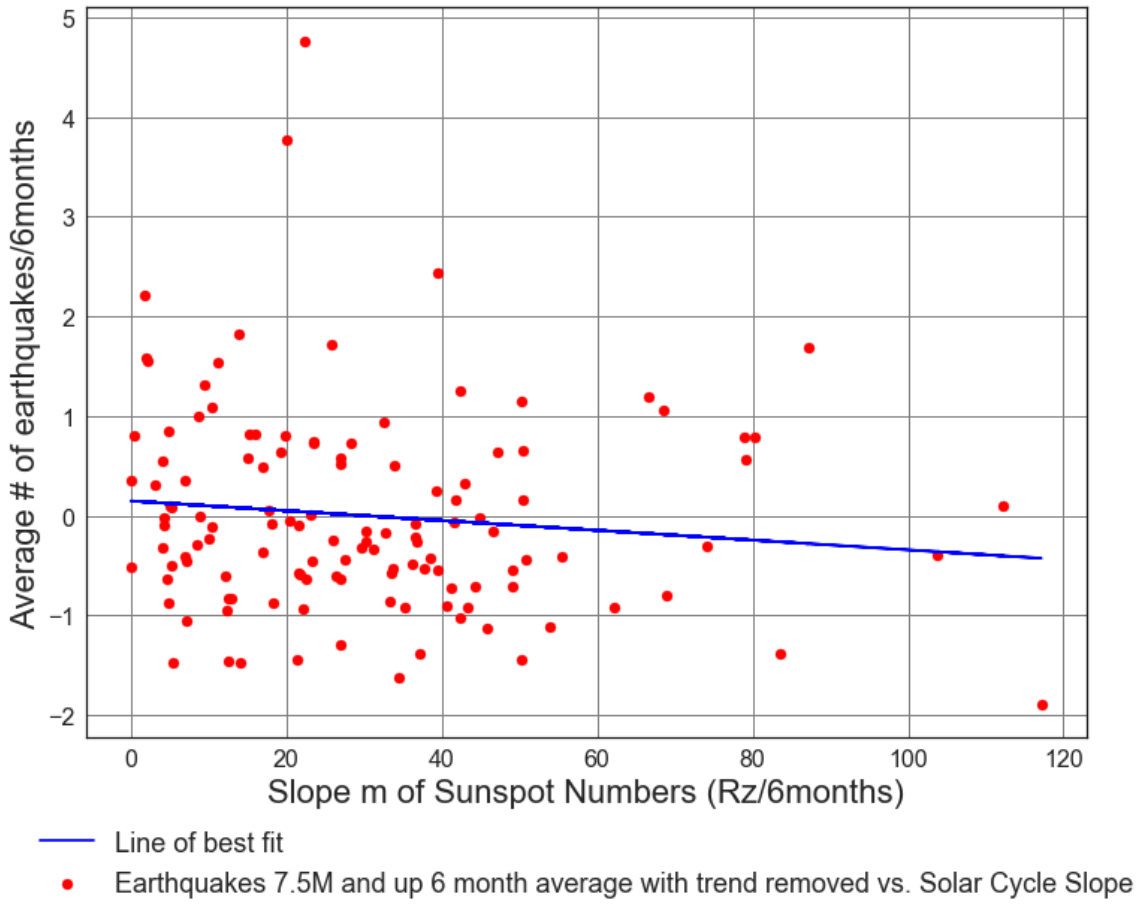

Figure C3.14: Scatter Plot of Solar cycle absolute value slope (from 1900 to 1964) vs. Average number of 7.5M and up Earthquakes/6months with trend removed. Line of best fit, y = -0.004909x + (0.1486), mean x = 30.43 +/- 23.66, mean y = -0.0008086 +/- 1.015, R = -0.1144, R squared = 0.01309, p-value = 0.2021.

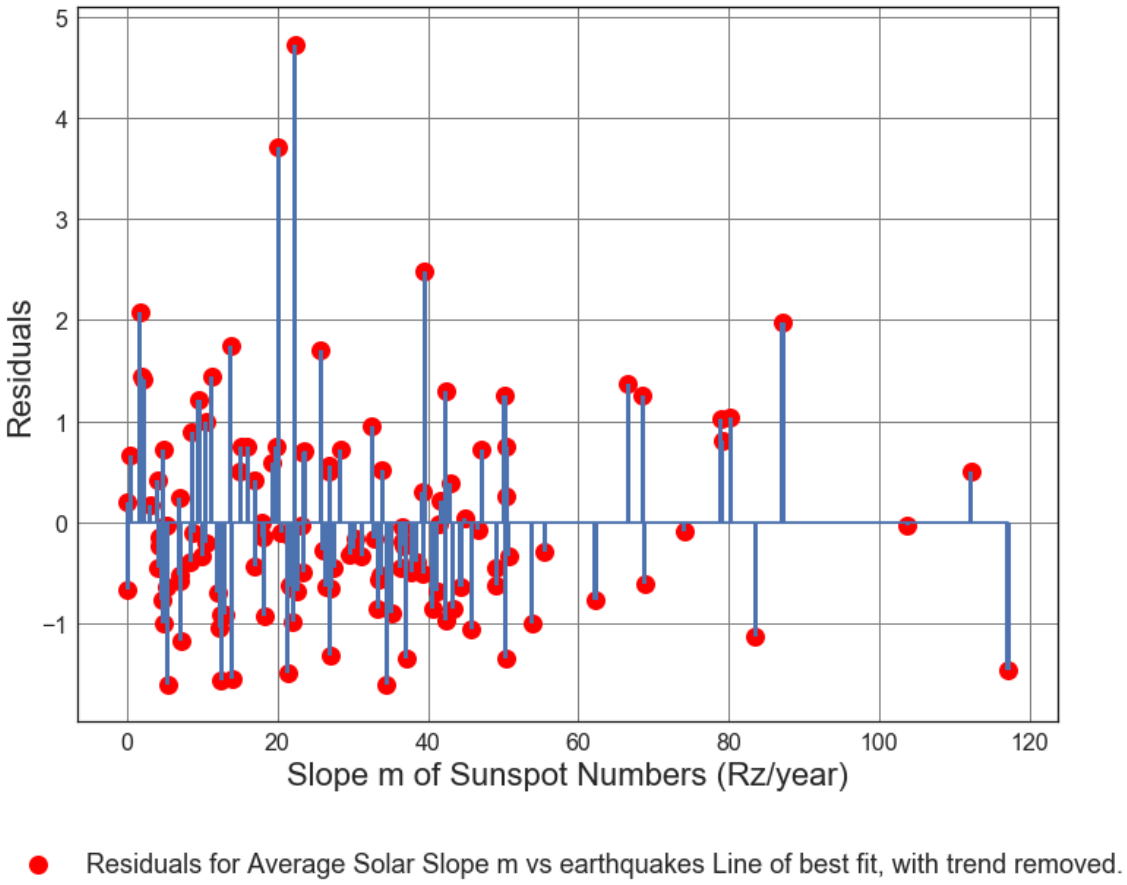

Figure C3.15: Scatter Plot of Solar cycle absolute value slope (from 1900 to 1964) vs. Average number of 7.5M and up Earthquakes/6months with trend removed. Line of best fit, y = -0.004909x + (0.1486), mean x = 30.43 +/- 23.66, mean y = -0.0008086 +/- 1.015, R = -0.1144, R squared = 0.01309, p-value = 0.2021.

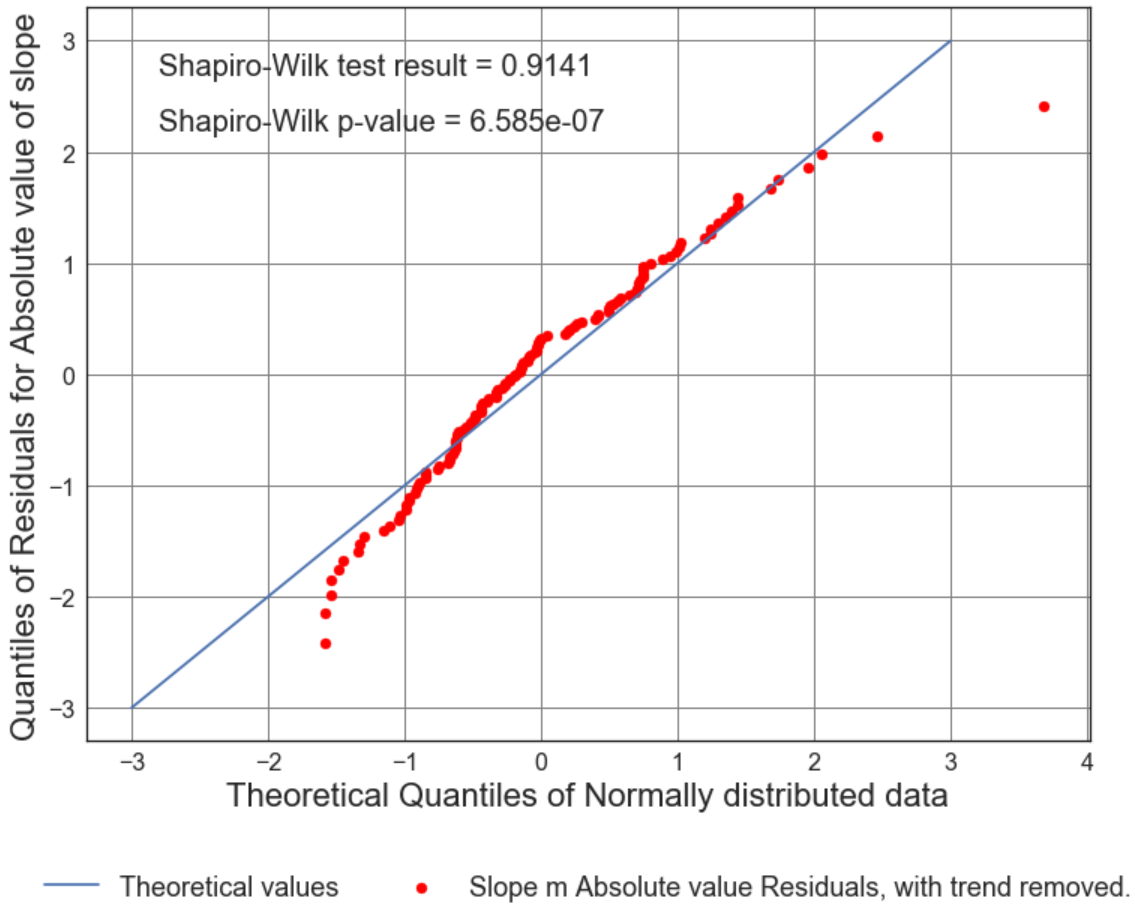

Figure C3.16: Scatter Plot of Solar cycle absolute value slope (from 1900 to 1964) vs. Average number of 7.5M and up Earthquakes/6months with trend removed. Line of best fit, y = -0.004909x + (0.1486), mean x = 30.43 +/- 23.66, mean y = -0.0008086 +/- 1.015, R = -0.1144, R squared = 0.01309, p-value = 0.2021.

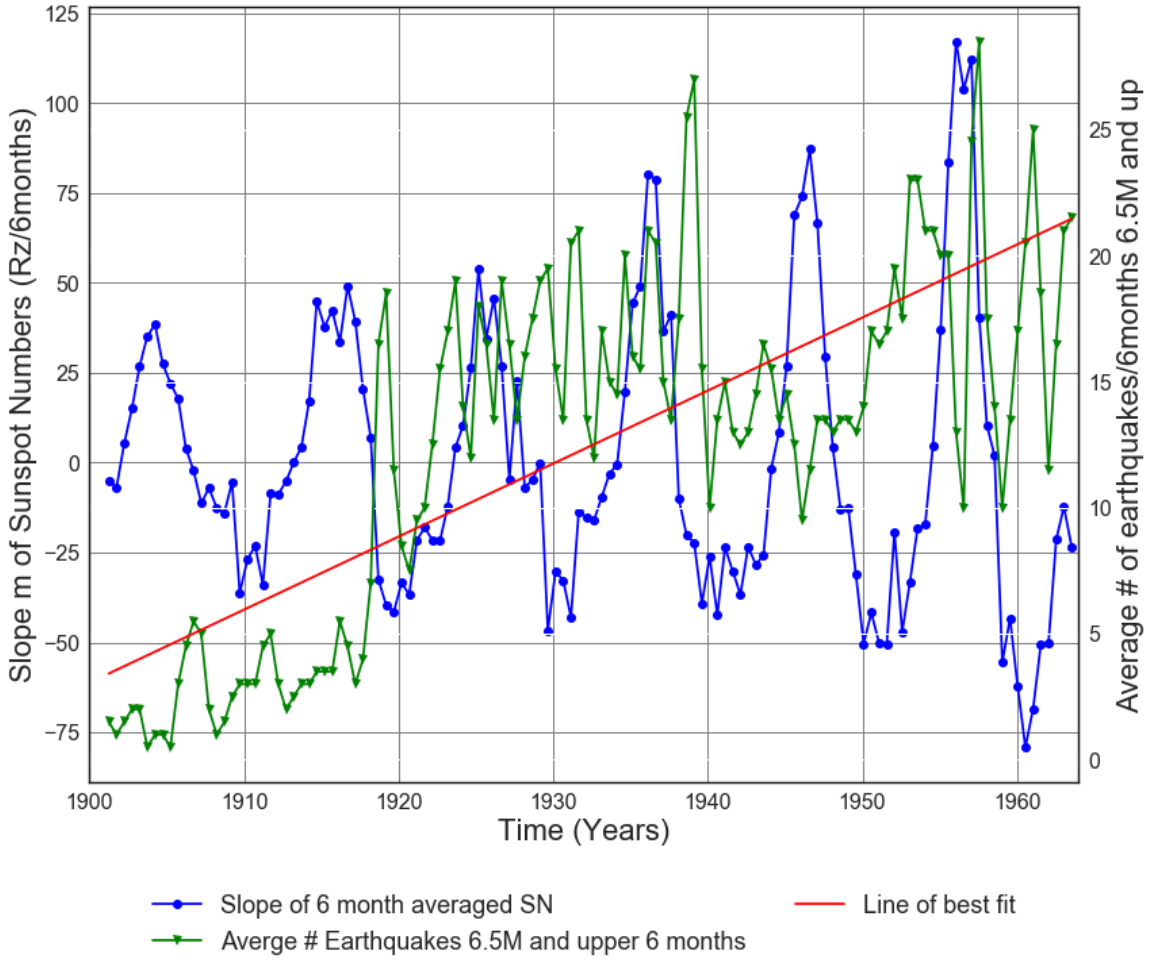

Figure C3.17: Slope of Solar cycle from 1900 to 1964 vs. Average number of 6.5M and up Earthquakes.

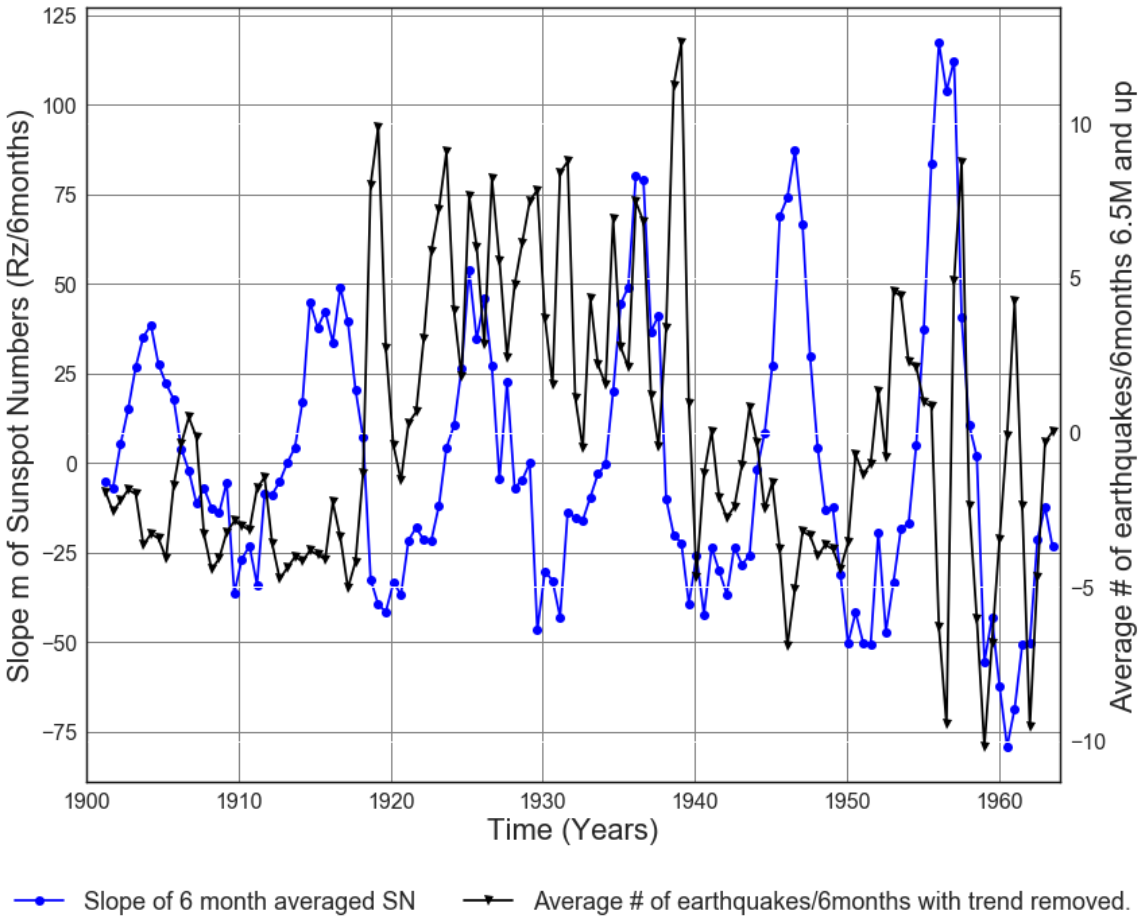

Figure C3.18: Slope of 6 month averaged SN 1900 to 1964 vs. Average number of 6.5M and up Earthquakes with trend removed. Line of best fit, y = 0.2898x + (-547.5), mean x = 1.932e+03 +/- 18.27, mean y = 12.37 +/- 6.988

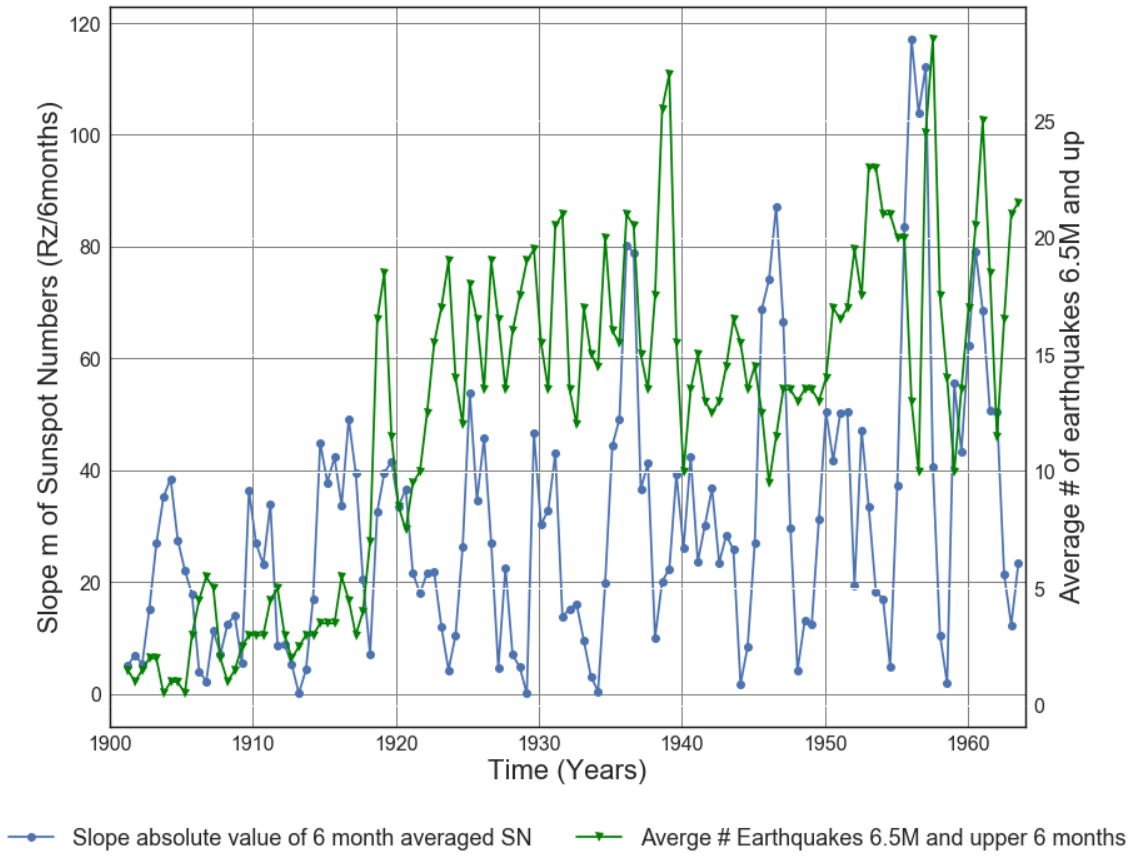

Figure C3.19: Slope Absolute value of Solar cycle from 1900 to 1964 vs. Average number of 6.5M and up Earthquakes.

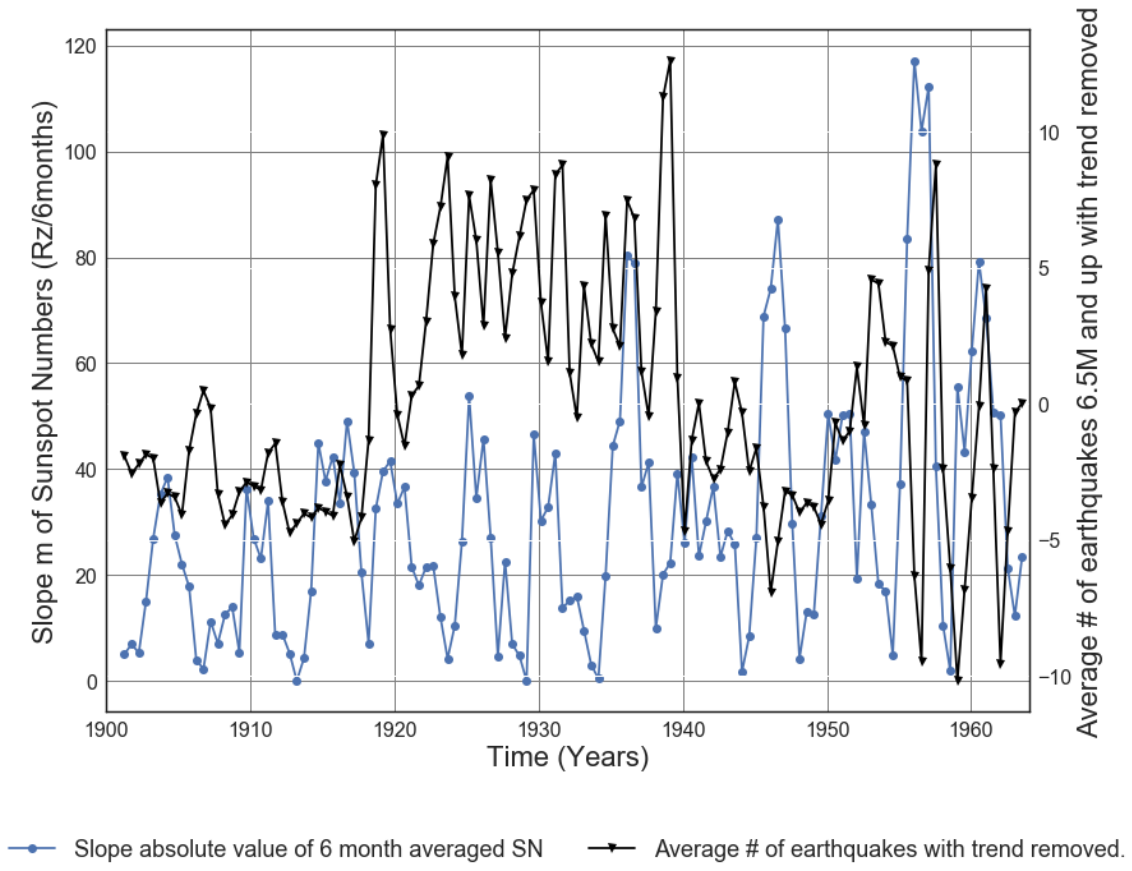

Figure C3.20: Slope Absolute value of Solar cycle from 1900 to 1964 vs. Average number of 6.5M and up earthquakes with trend removed.

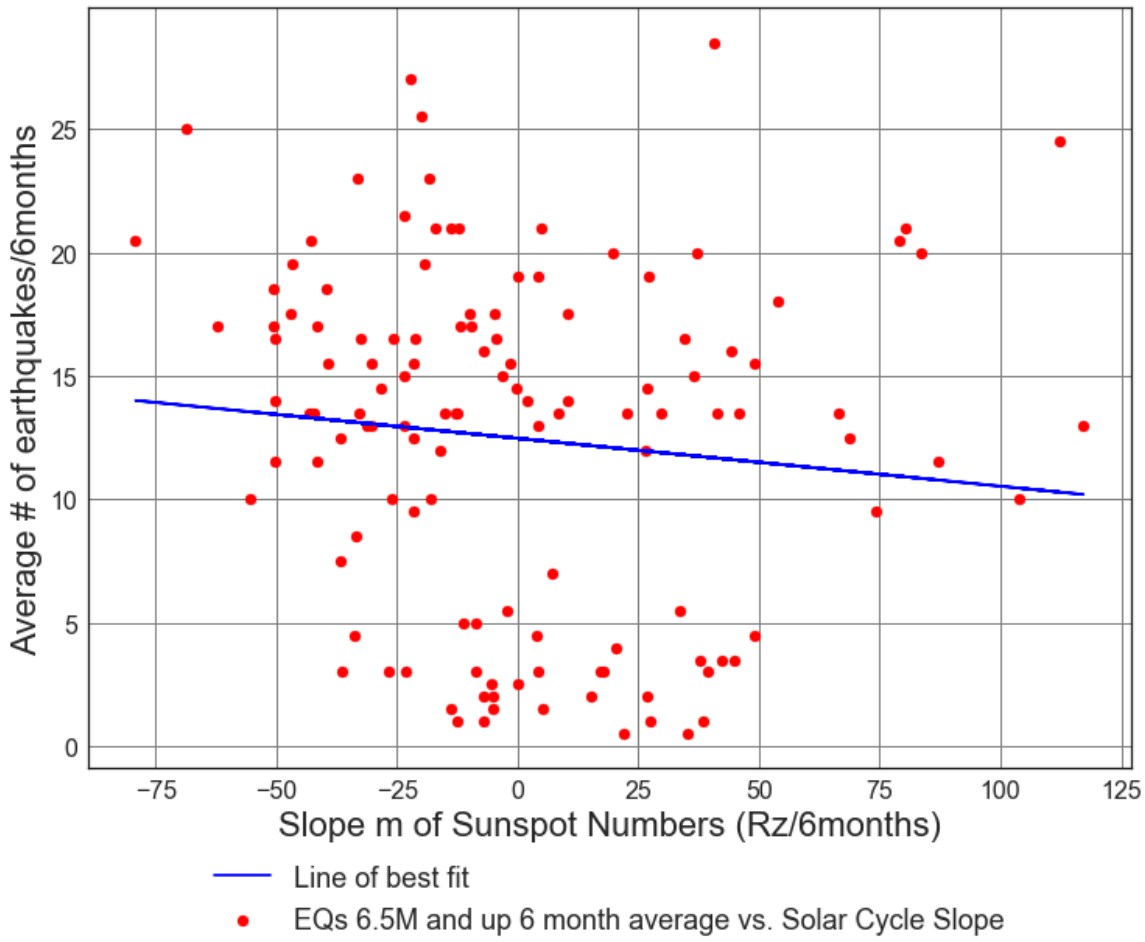

Figure C3.21: Scatter Plot of Solar cycle slope (from 1900 to 1964) vs. Average number of 6.5M and up Earthquakes/6months. Line of best fit, y = -0.01939x + (12.47), mean x = 0.3737 +/- 38.55, mean y = 12.46 +/- 6.948, R = -0.1076, R squared = 0.01157, p-value = 0.2305.

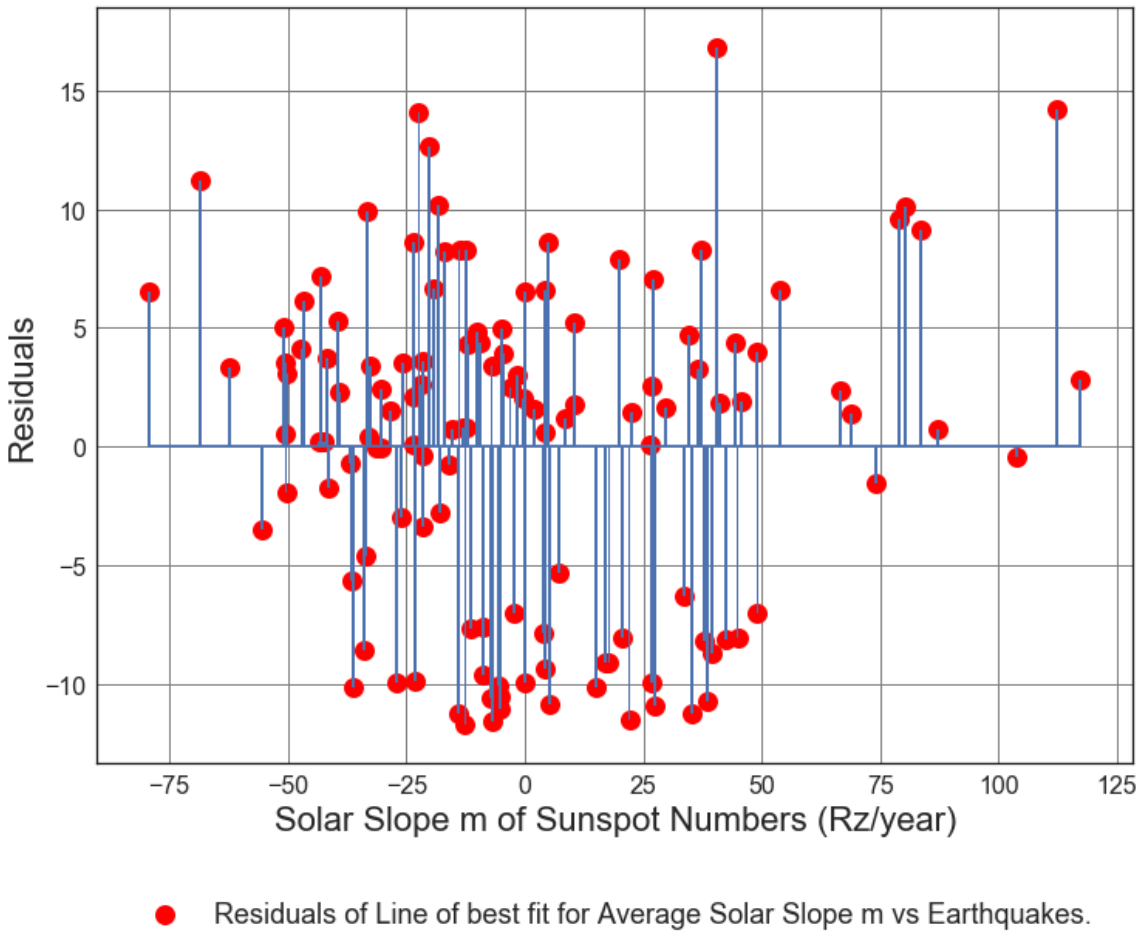

Figure C3.22: Residuals Plot of Solar cycle slope (from 1900 to 1964) vs. Average number of 6.5M and up Earthquakes/6months. Line of best fit, y = -0.01939x + (12.47), mean x = 0.3737 +/- 38.55, mean y = 12.46 +/- 6.948, R = -0.1076, R squared = 0.01157, p-value = 0.2305.

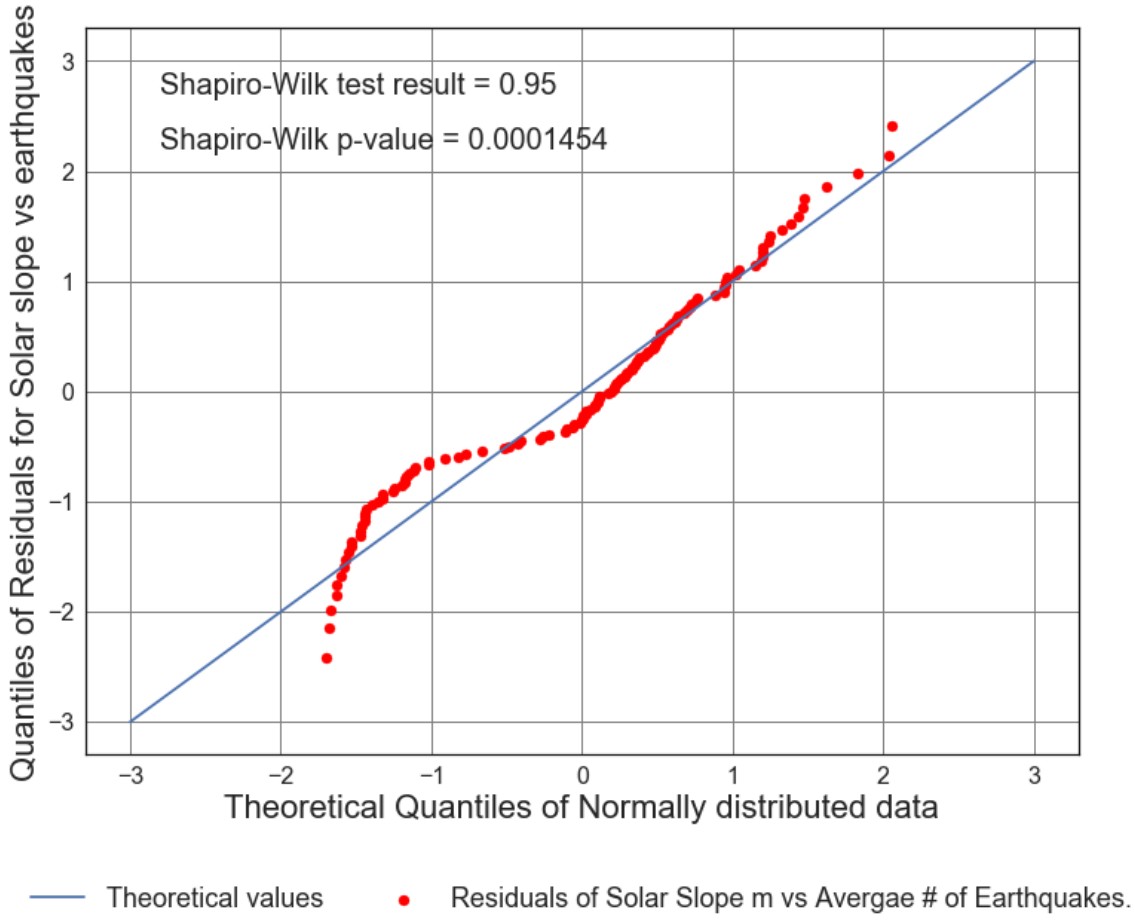

Figure C3.23: Residuals Plot of Solar cycle slope (from 1900 to 1964) vs. Average number of 6.5M and up Earthquakes/6months. Line of best fit, y = -0.01939x + (12.47), mean x = 0.3737 +/- 38.55, mean y = 12.46 +/- 6.948, R = -0.1076, R squared = 0.01157, p-value = 0.2305.

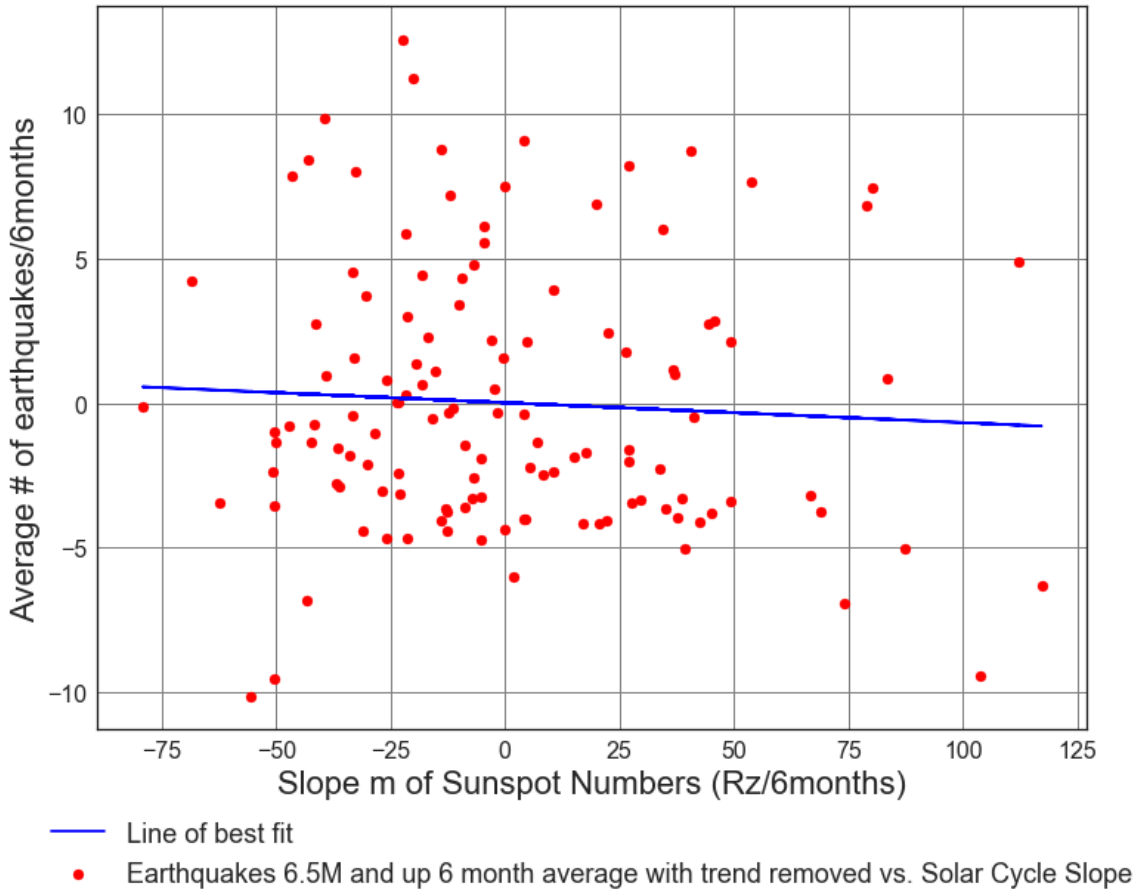

Figure C3.24: Scatter Plot of Solar cycle slope (from 1900 to 1964) vs. Average number of 6.5M and up Earthquakes/6months with trend removed. Line of best fit, y = -0.006927x + (0.01669), mean x = 0.3737 +/- 38.55, mean y = 0.0141 +/- 4.577, R = -0.05835, R squared = 0.003405, p-value = 0.5163.

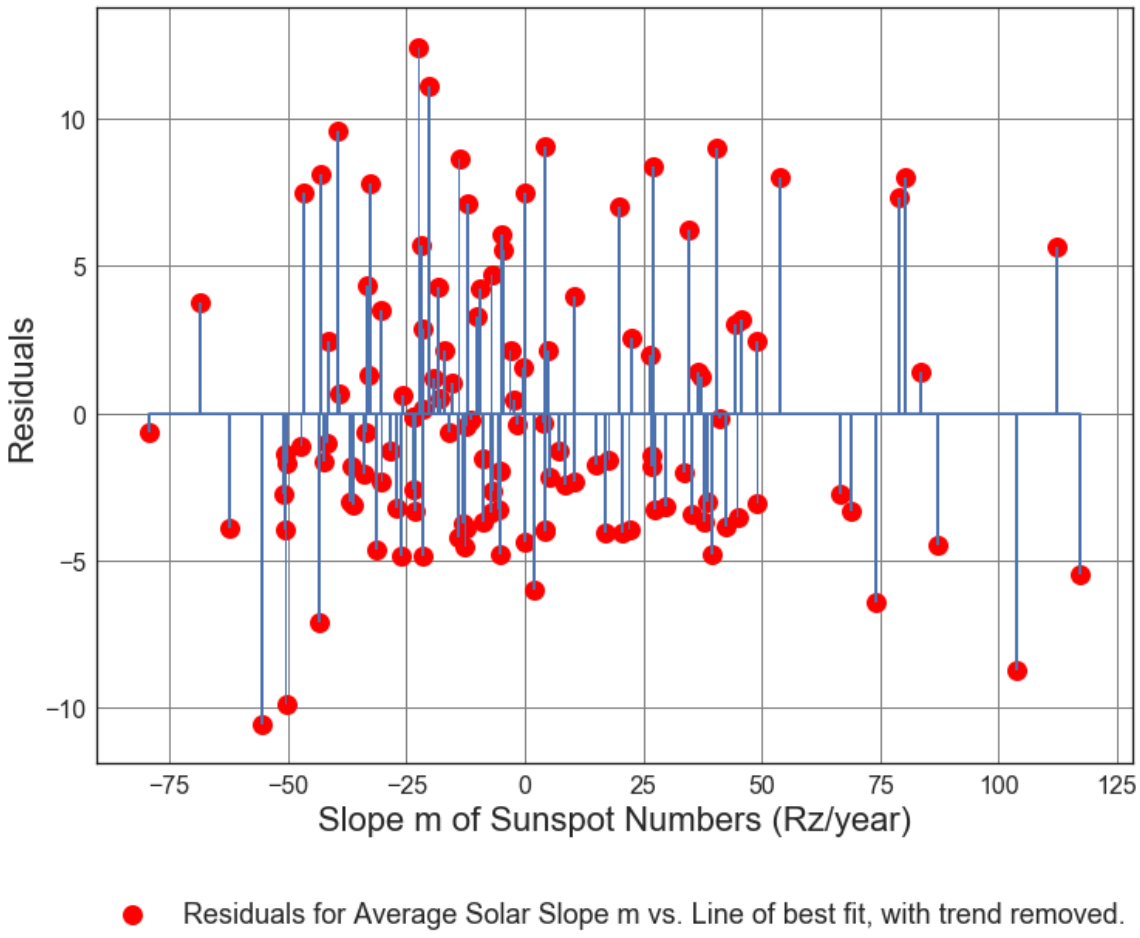

Figure C3.25: Scatter Plot of Solar cycle slope (from 1900 to 1964) vs. Average number of 6.5M and up Earthquakes/6months with trend removed. Line of best fit, y = -0.006927x + (0.01669), mean x = 0.3737 +/- 38.55, mean y = 0.0141 +/- 4.577, R = -0.05835, R squared = 0.003405, p-value = 0.5163.

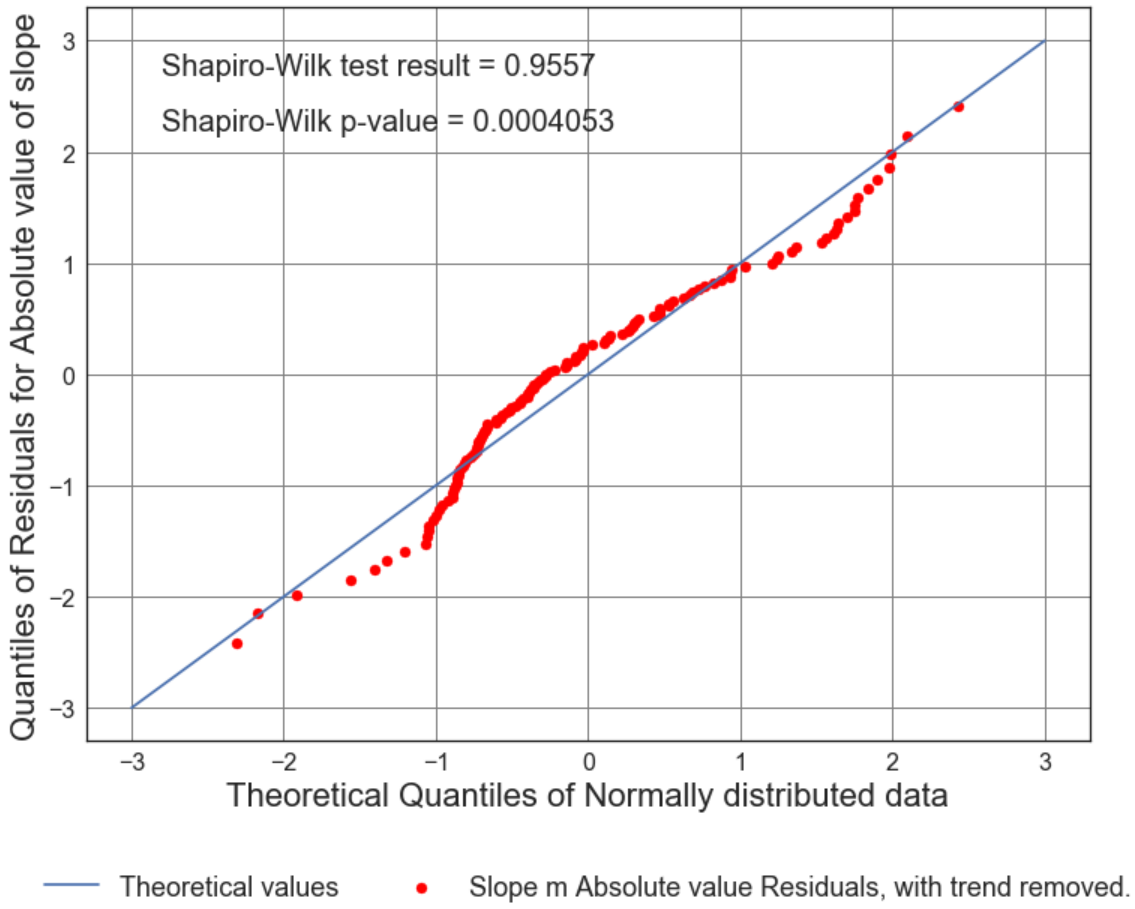

Figure C3.26: Scatter Plot of Solar cycle slope (from 1900 to 1964) vs. Average number of 6.5M and up Earthquakes/6months with trend removed. Line of best fit, y = -0.006927x + (0.01669), mean x = 0.3737 +/- 38.55, mean y = 0.0141 +/- 4.577, R = -0.05835, R squared = 0.003405, p-value = 0.5163.

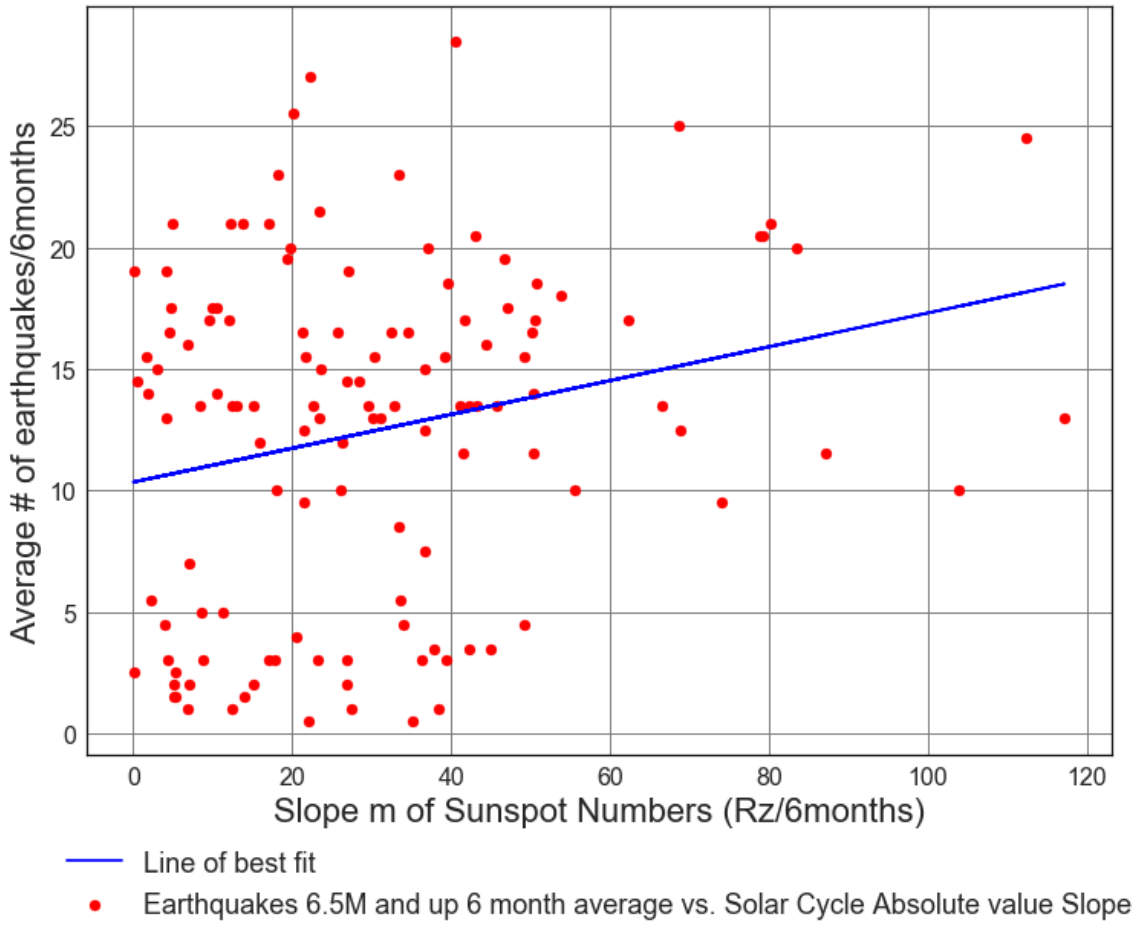

Figure C3.27: Scatter Plot of Solar cycle slope (from 1900 to 1964) vs. Average number of 6.5M and up Earthquakes/6months. Line of best fit, y = 0.06964x + (10.34), mean x = 30.43 +/- 23.66, mean y = 12.46 +/- 6.948, R = 0.2372, R squared = 0.05626, p-value = 0.007492.

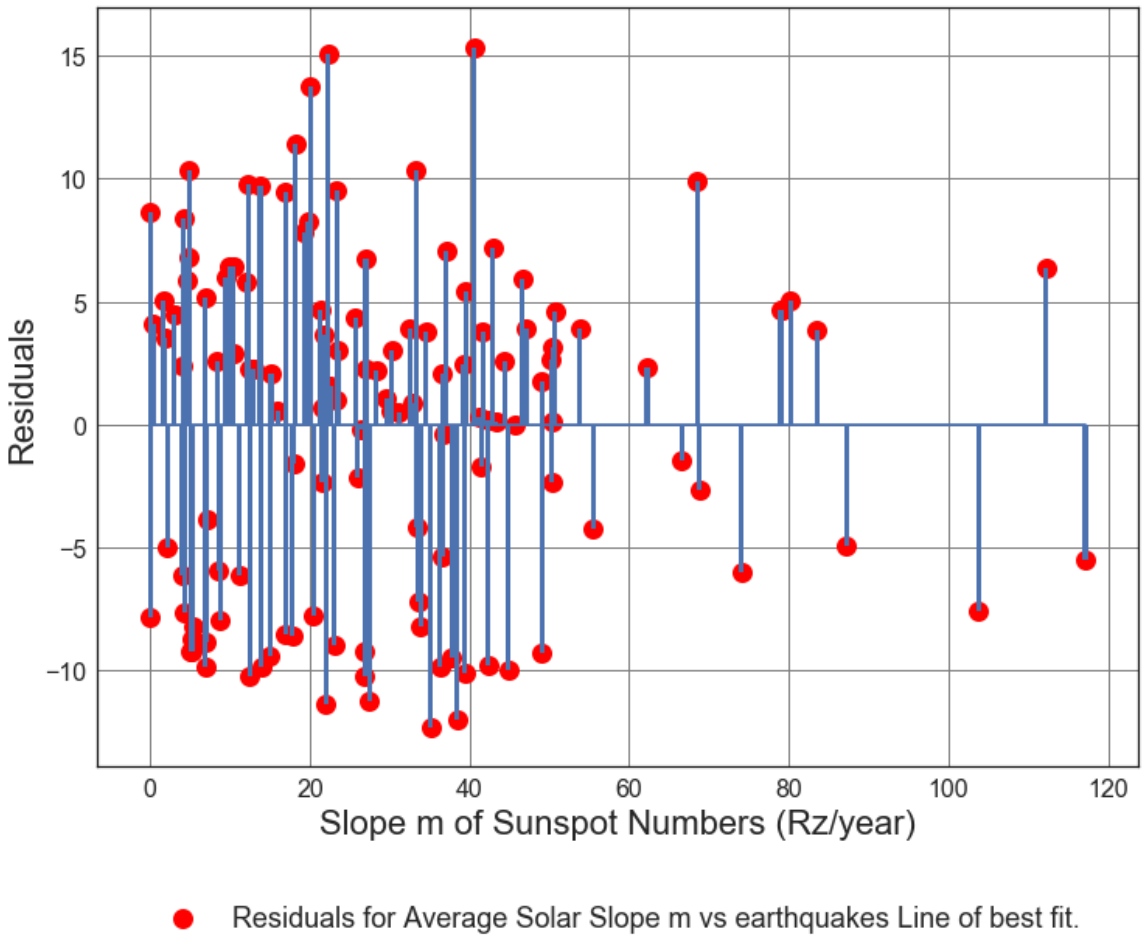

Figure C3.28: Scatter Plot of Solar cycle slope (from 1900 to 1964) vs. Average number of 6.5M and up Earthquakes/6months. Line of best fit, y = 0.06964x + (10.34), mean x = 30.43 +/- 23.66, mean y = 12.46 +/- 6.948, R = 0.2372, R squared = 0.05626, p-value = 0.007492.

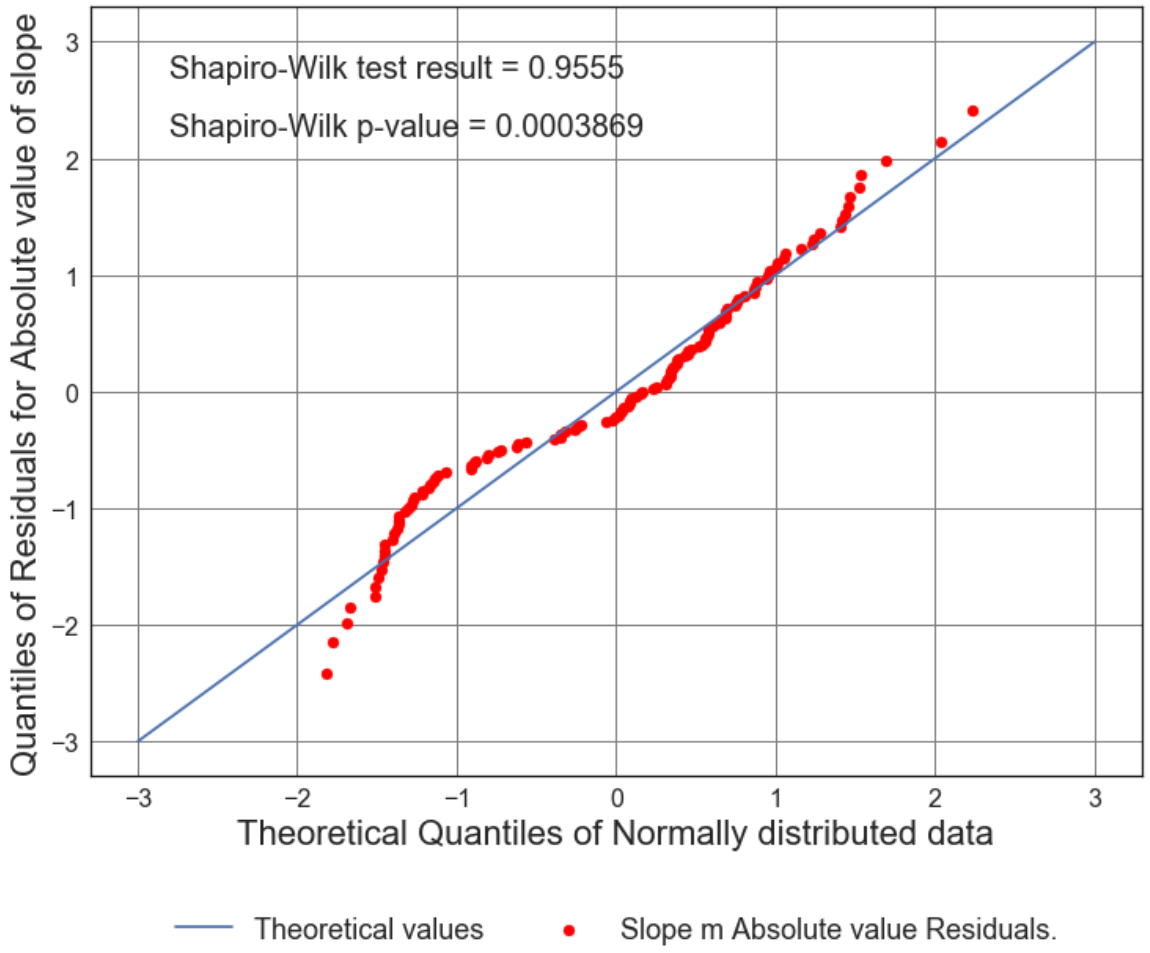

Figure C3.29: Scatter Plot of Solar cycle slope (from 1900 to 1964) vs. Average number of 6.5M and up Earthquakes/6months. Line of best fit, y = 0.06964x + (10.34), mean x = 30.43 +/- 23.66, mean y = 12.46 +/- 6.948, R = 0.2372, R squared = 0.05626, p-value = 0.007492.

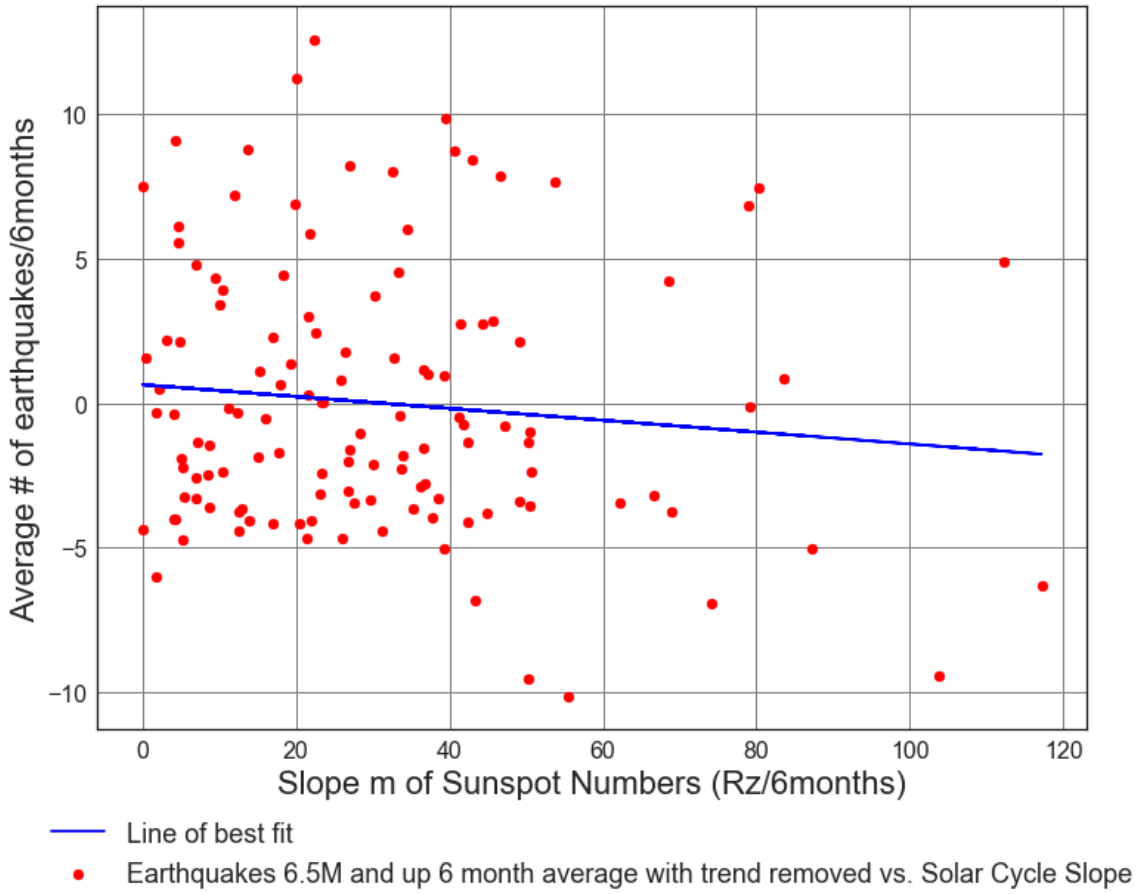

Figure C3.30: Scatter Plot of Solar cycle absolute value slope (from 1900 to 1964) vs. Average number of 6.5M and up Earthquakes/6months with trend removed. Line of best fit, y = -0.02054x + (0.6392), mean x = 30.43 +/- 23.66, mean y = 0.0141 +/- 4.577, R = -0.1062, R squared = 0.01128, p-value = 0.2366.

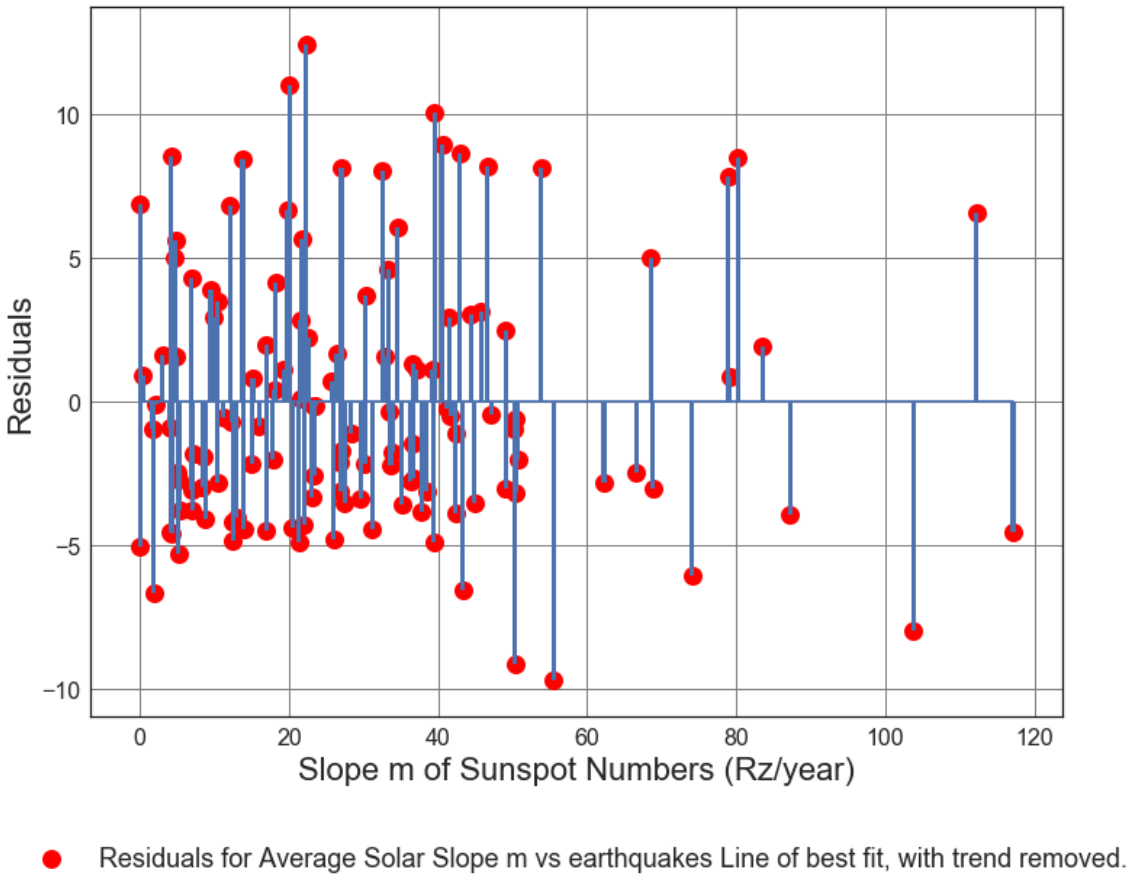

Figure C3.31: Scatter Plot of Solar cycle absolute value slope (from 1900 to 1964) vs. Average number of 6.5M and up Earthquakes/6months with trend removed. Line of best fit, y = -0.02054x + (0.6392), mean x = 30.43 +/- 23.66, mean y = 0.0141 +/- 4.577, R = -0.1062, R squared = 0.01128, p-value = 0.2366.

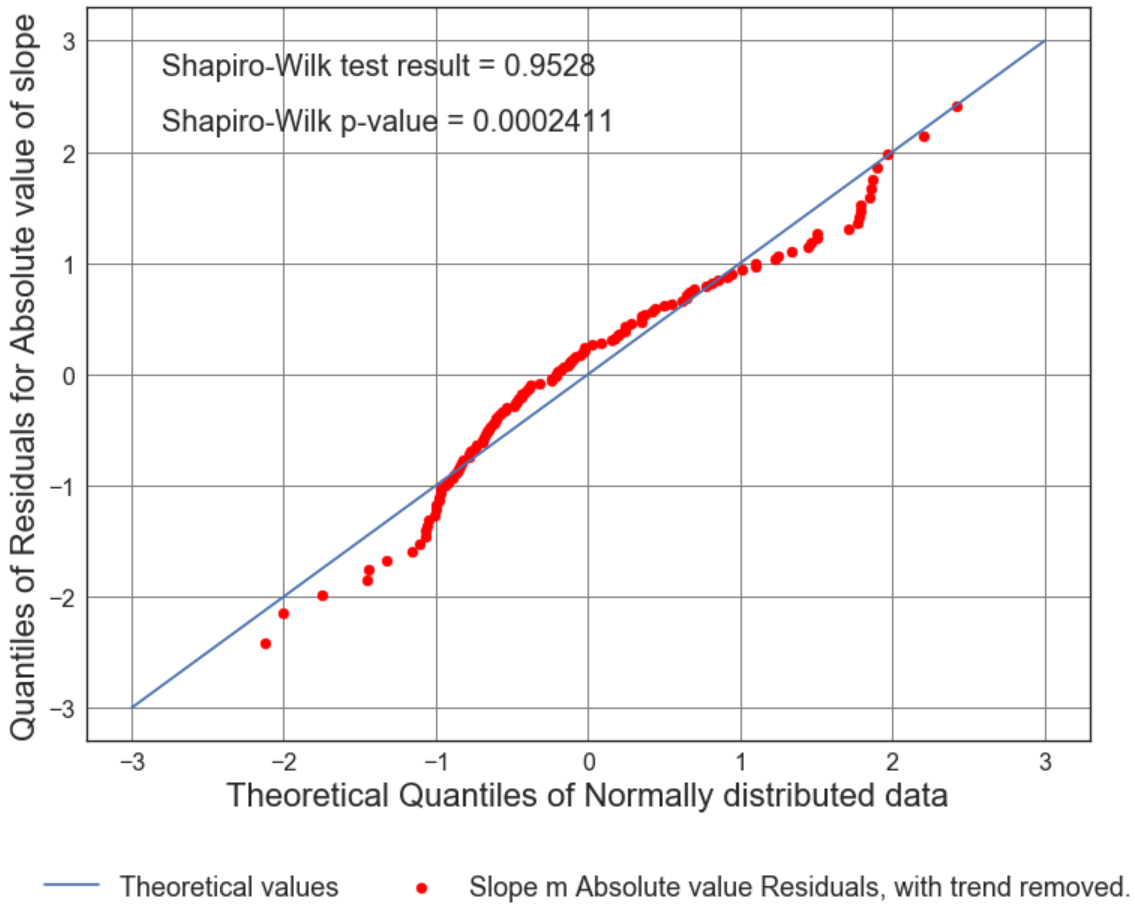

Figure C3.32: Scatter Plot of Solar cycle absolute value slope (from 1900 to 1964) vs. Average number of 6.5M and up Earthquakes/6months with trend removed. Line of best fit, y = -0.02054x + (0.6392), mean x = 30.43 +/- 23.66, mean y = 0.0141 +/- 4.577, R = -0.1062, R squared = 0.01128, p-value = 0.2366.

Appendix C4: USGS Centennial Time Series Analysis Part 4 - Modern Era Post 1964 Six Month Averaged Earthquake and Sunspot Data.

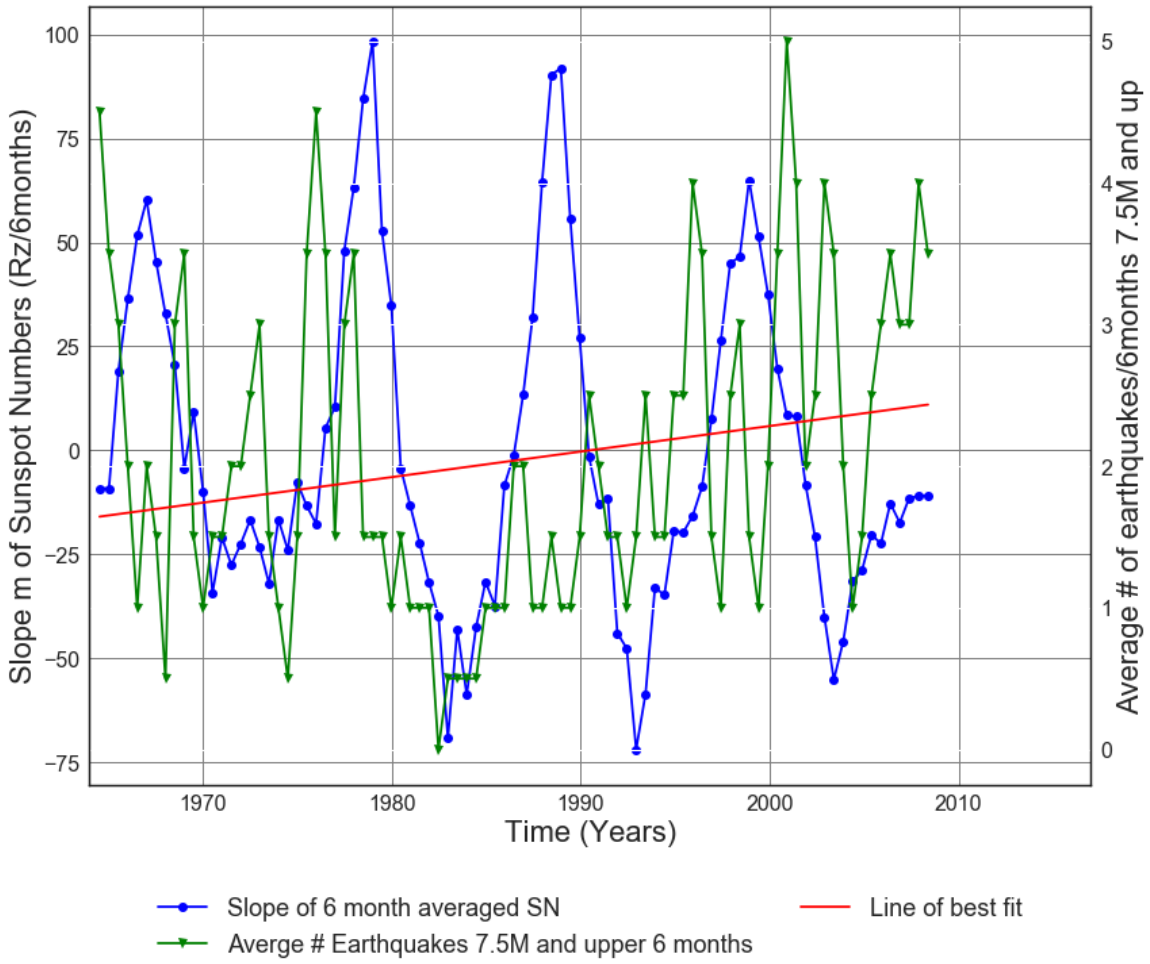

Figure C4.1: Slope of Solar cycle from 1964 to 2017 vs. Average number of 7.5M and up Earthquakes.

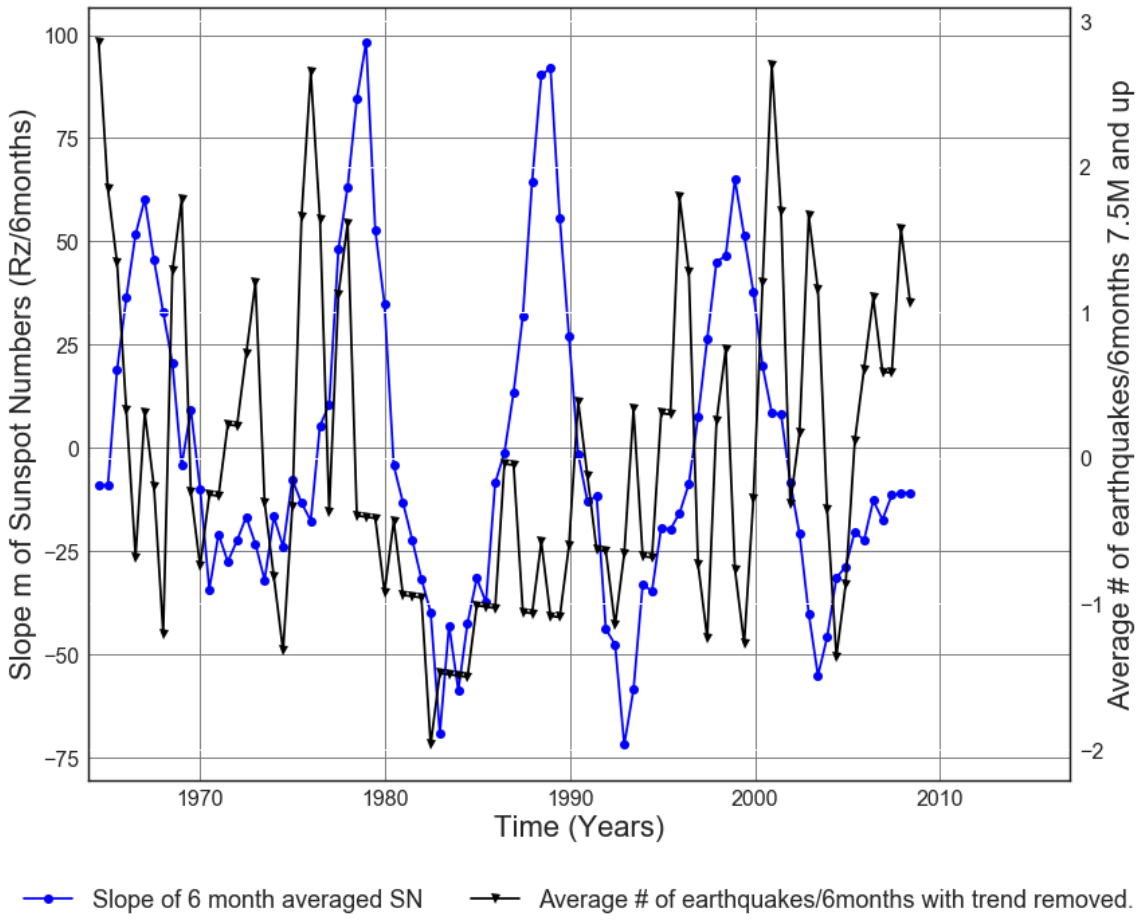

Figure C4.2: Slope of 6 month averaged SN 1964 to 2017 vs. Average number of 7.5M and up Earthquakes with trend removed. Line of best fit, y = 0.01804x + (-33.79), mean x = 1.986e+03 +/- 12.8, mean y = 2.039 +/- 1.115

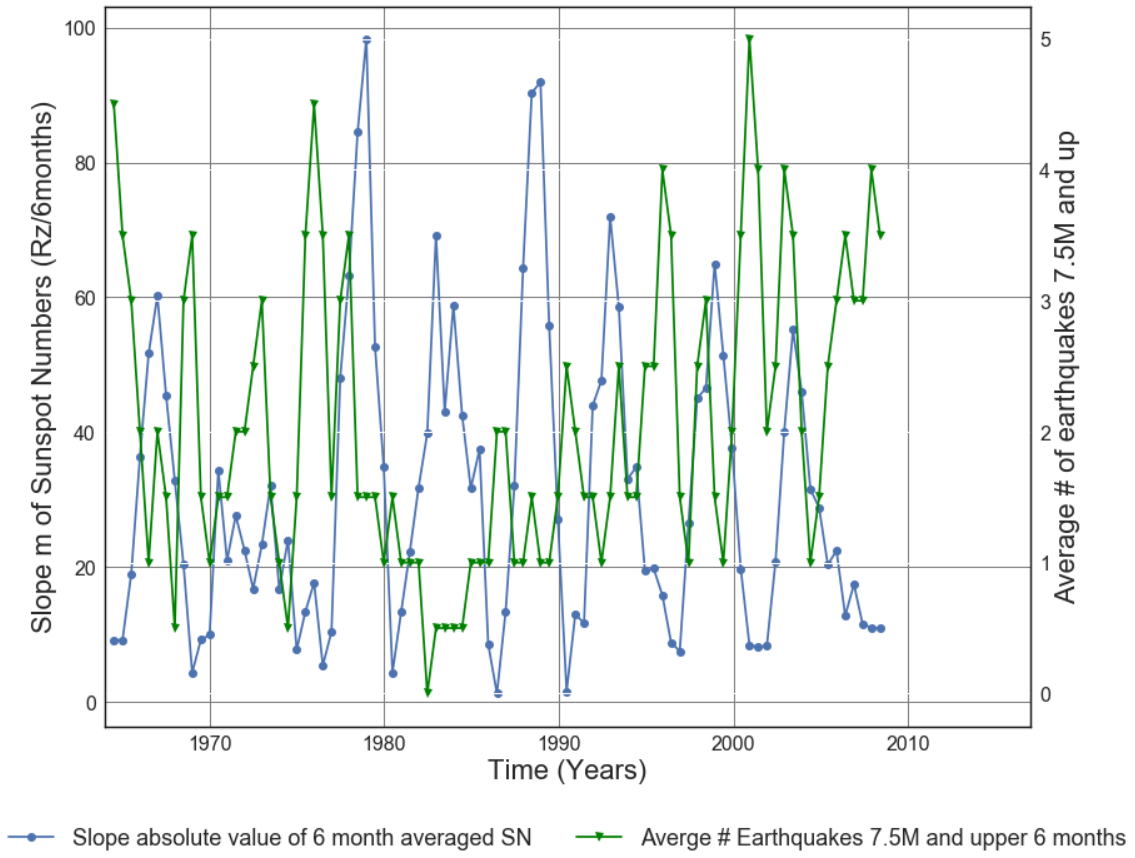

Figure C4.3: Slope Absolute value of Solar cycle from 1964 to 2017 vs. Average number of 7.5M and up Earthquakes.

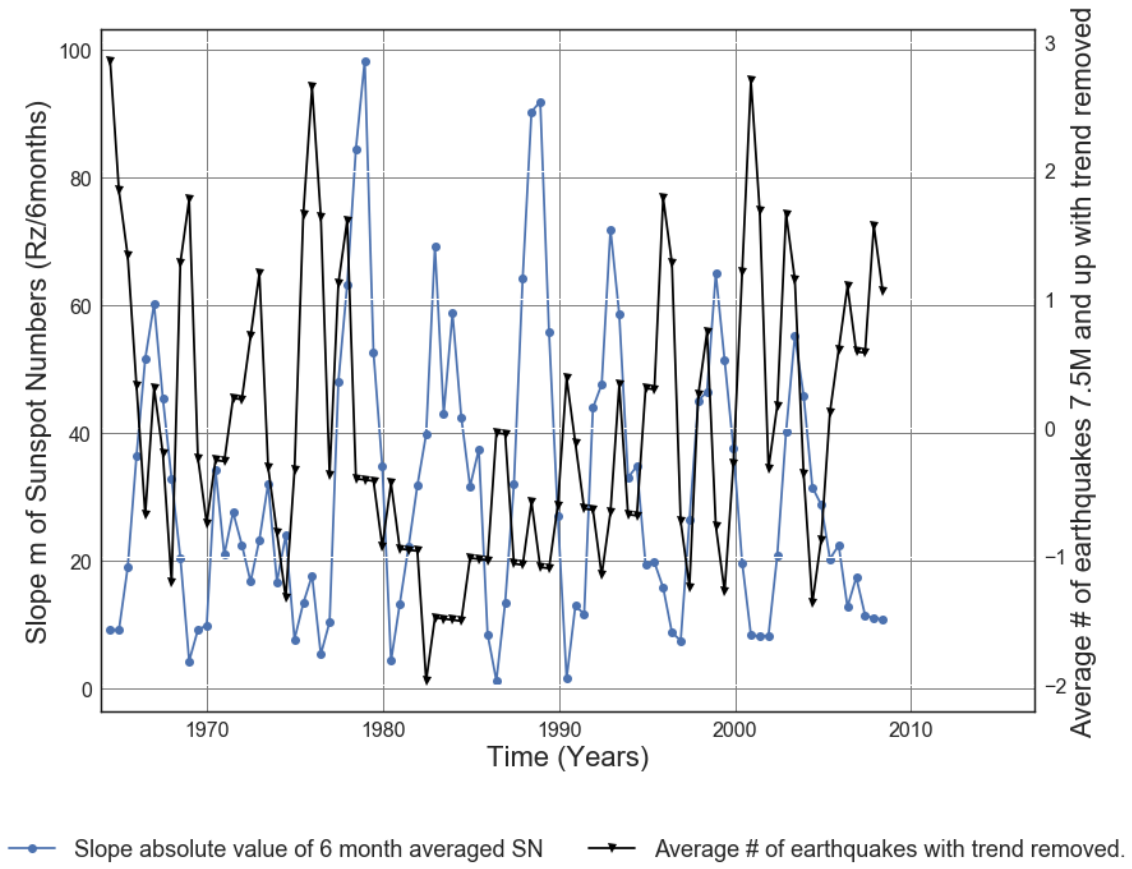

Figure C4.4: Slope Absolute value of Solar cycle from 1964 to 2017 vs. Average number of 7.5M and up earthquakes with trend removed.

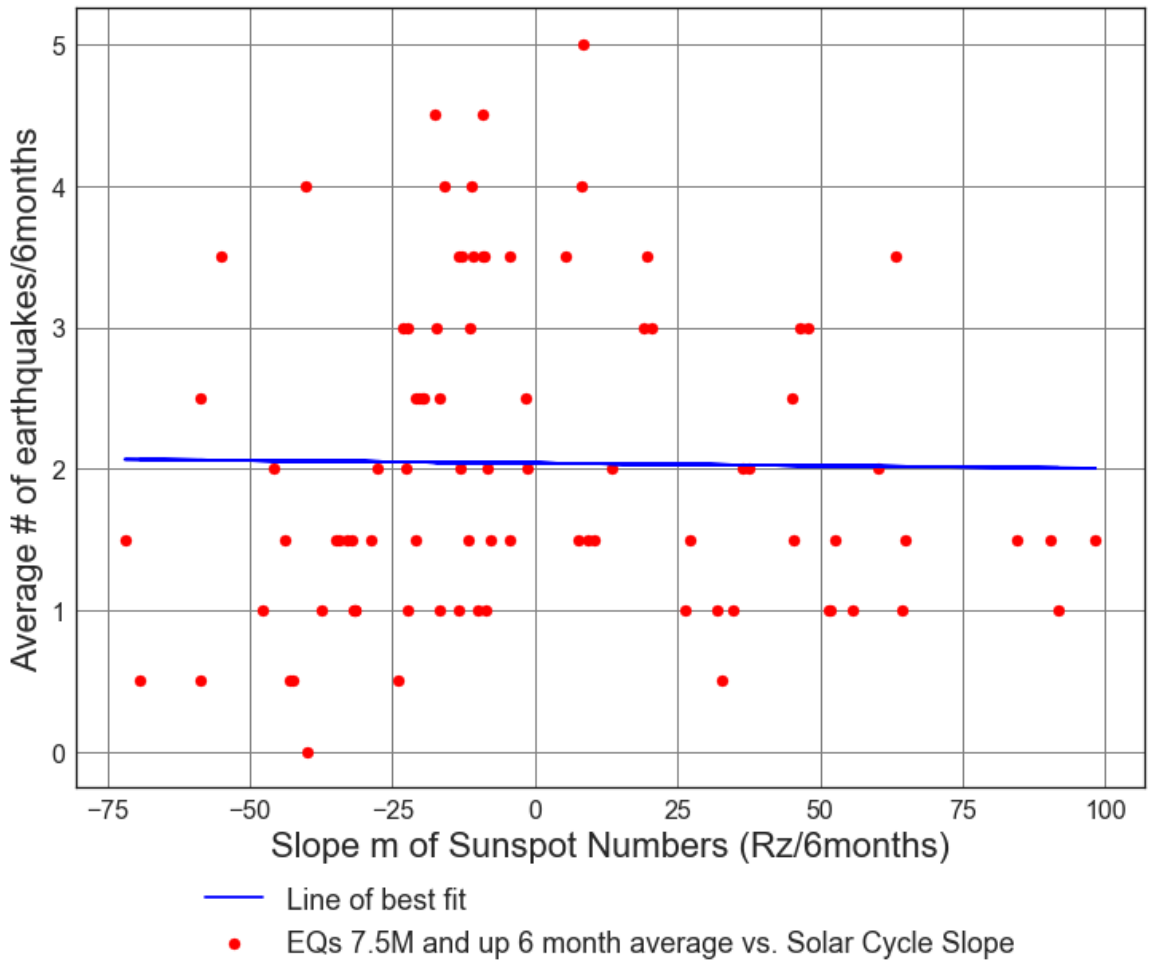

Figure C4.5: Scatter Plot of Solar cycle slope (from 1964 to 2017) vs. Average number of 7.5M and up Earthquakes/6months. Line of best fit, y = -0.0003677x + (2.039), mean x = -0.5303 +/- 38.19, mean y = 2.039 +/- 1.115, R = -0.0126, R squared = 0.0001587, p-value = 0.9067.

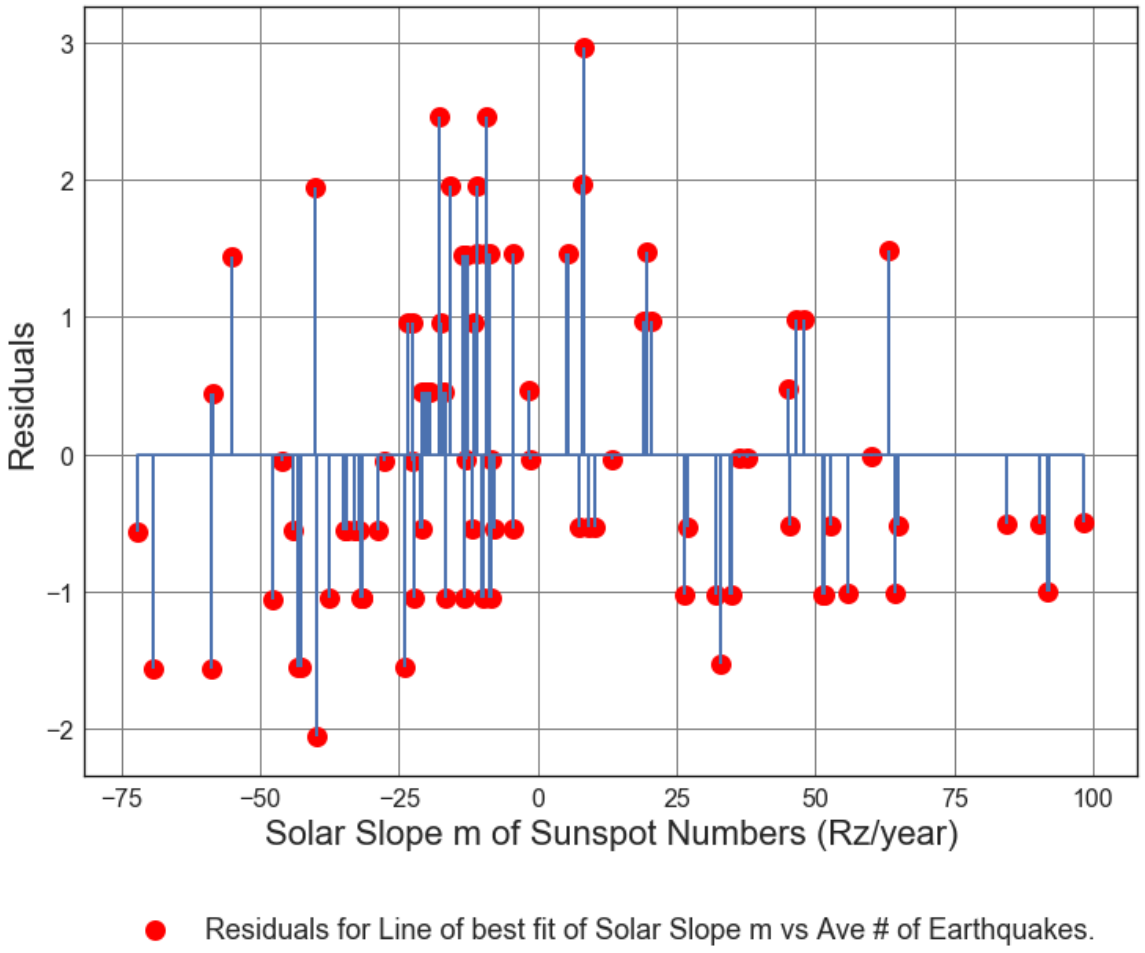

Figure C4.6: Residuals Plot of Solar cycle slope (from 1964 to 2017) vs. Average number of 7.5M and up Earthquakes/6months. Line of best fit, y = -0.0003677x + (2.039), mean x = -0.5303 +/- 38.19, mean y = 2.039 +/- 1.115, R = -0.0126, R squared = 0.0001587, p-value = 0.9067.

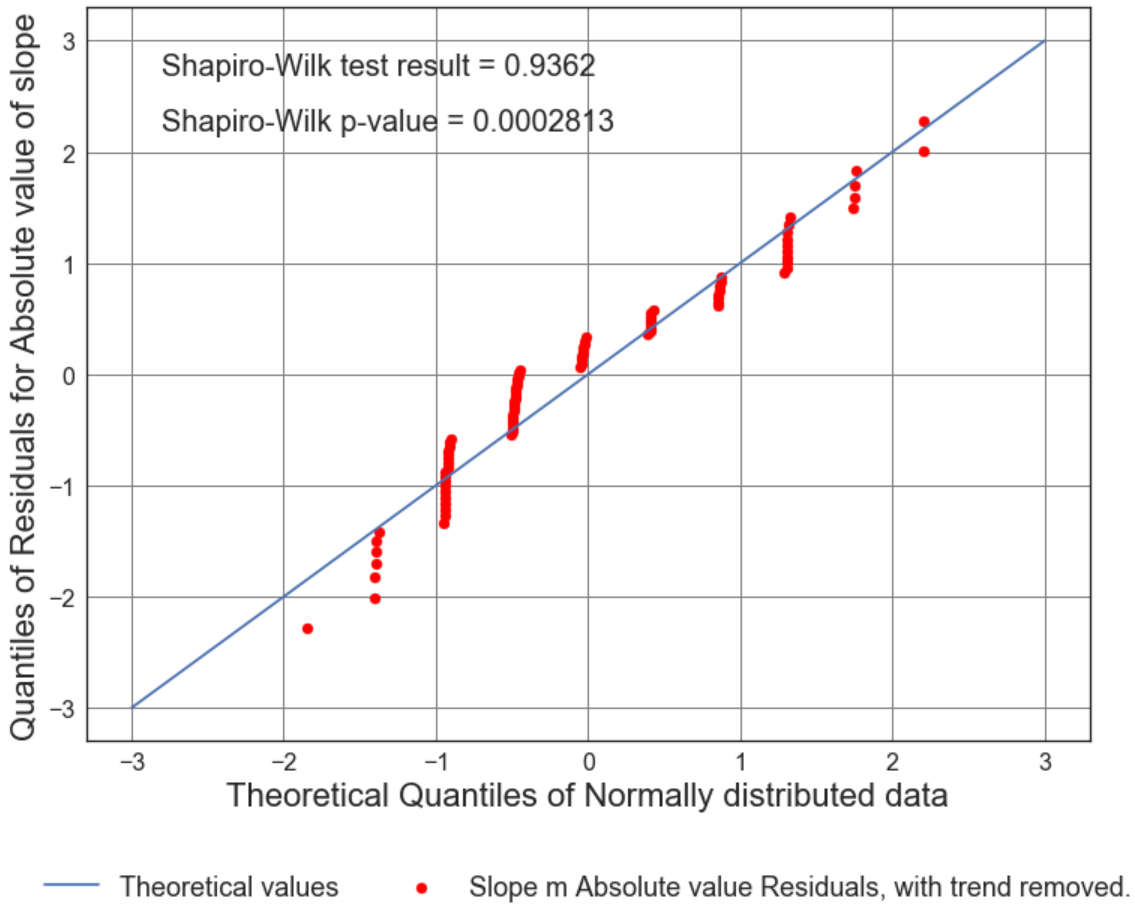

Figure C4.7: Residuals Plot of Solar cycle slope (from 1964 to 2017) vs. Average number of 7.5M and up Earthquakes/6months. Line of best fit, y = -0.0003677x + (2.039), mean x = -0.5303 +/- 38.19, mean y = 2.039 +/- 1.115, R = -0.0126, R squared = 0.0001587, p-value = 0.9067.

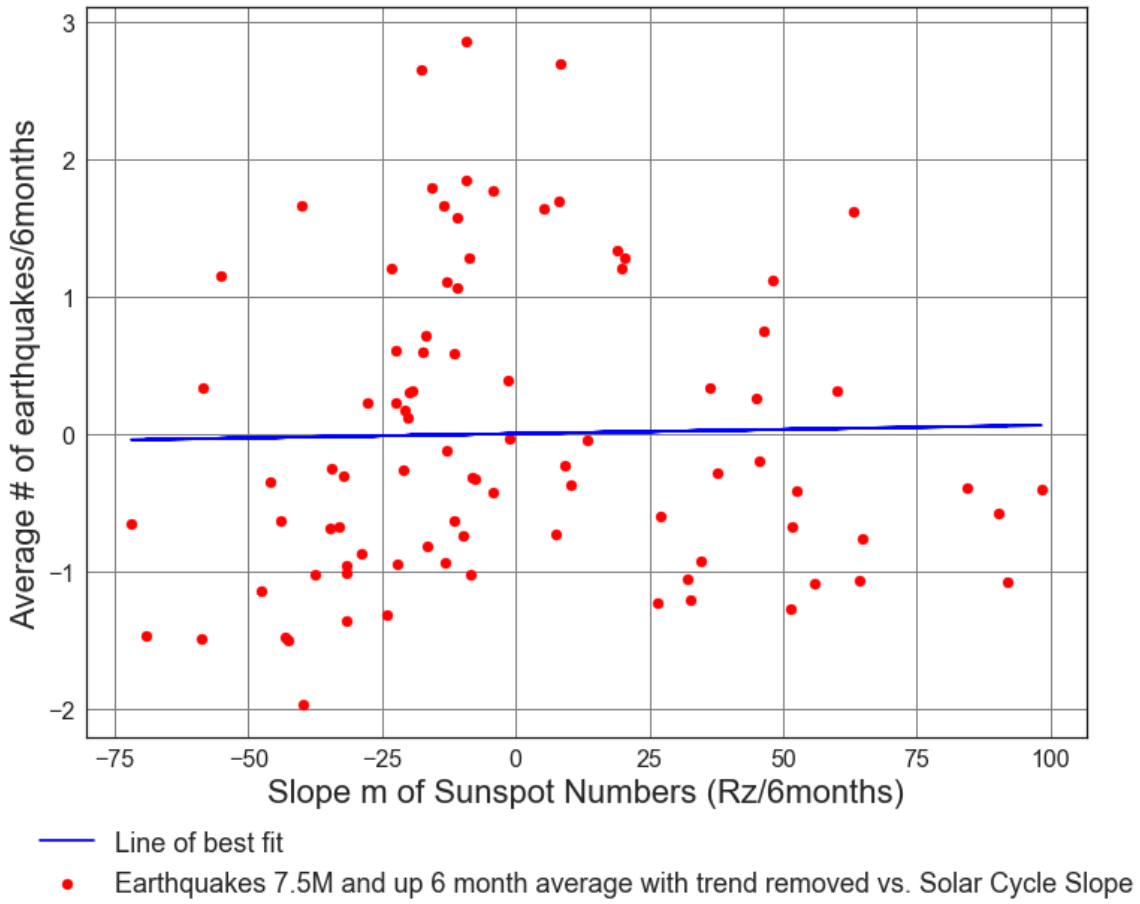

Figure C4.8: Scatter Plot of Solar cycle slope (from 1964 to 2017) vs. Average number of 7.5M and up Earthquakes/6months with trend removed. Line of best fit, y = 0.0006192x + (0.0003284), mean x = -0.5303 +/- 38.19, mean y = 1.836e-15 +/- 1.091, R = 0.02168, R squared = 0.0004702, p-value = 0.8402.

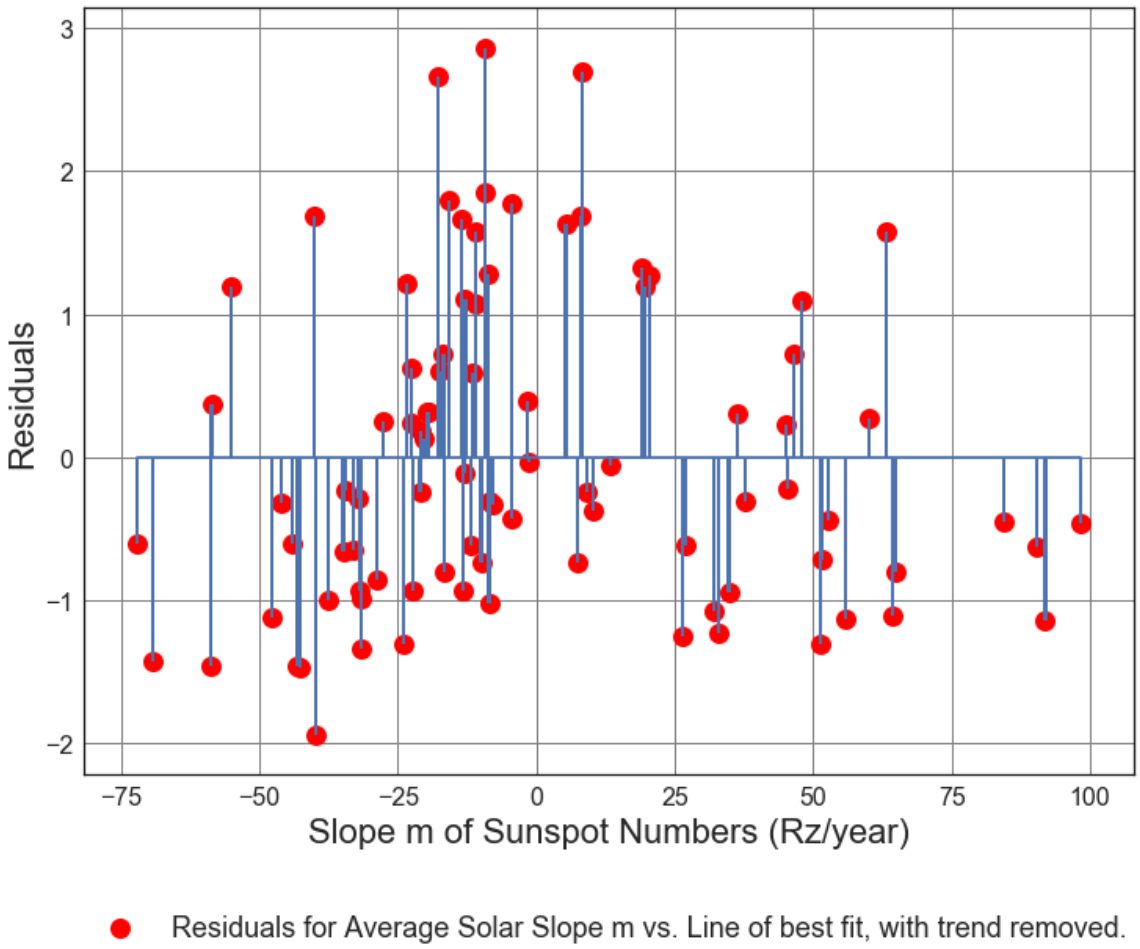

Figure C4.9: Scatter Plot of Solar cycle slope (from 1964 to 2017) vs. Average number of 7.5M and up Earthquakes/6months with trend removed. Line of best fit, y = 0.0006192x + (0.0003284), mean x = -0.5303 +/- 38.19, mean y = 1.836e-15 +/- 1.091, R = 0.02168, R squared = 0.0004702, p-value = 0.8402.

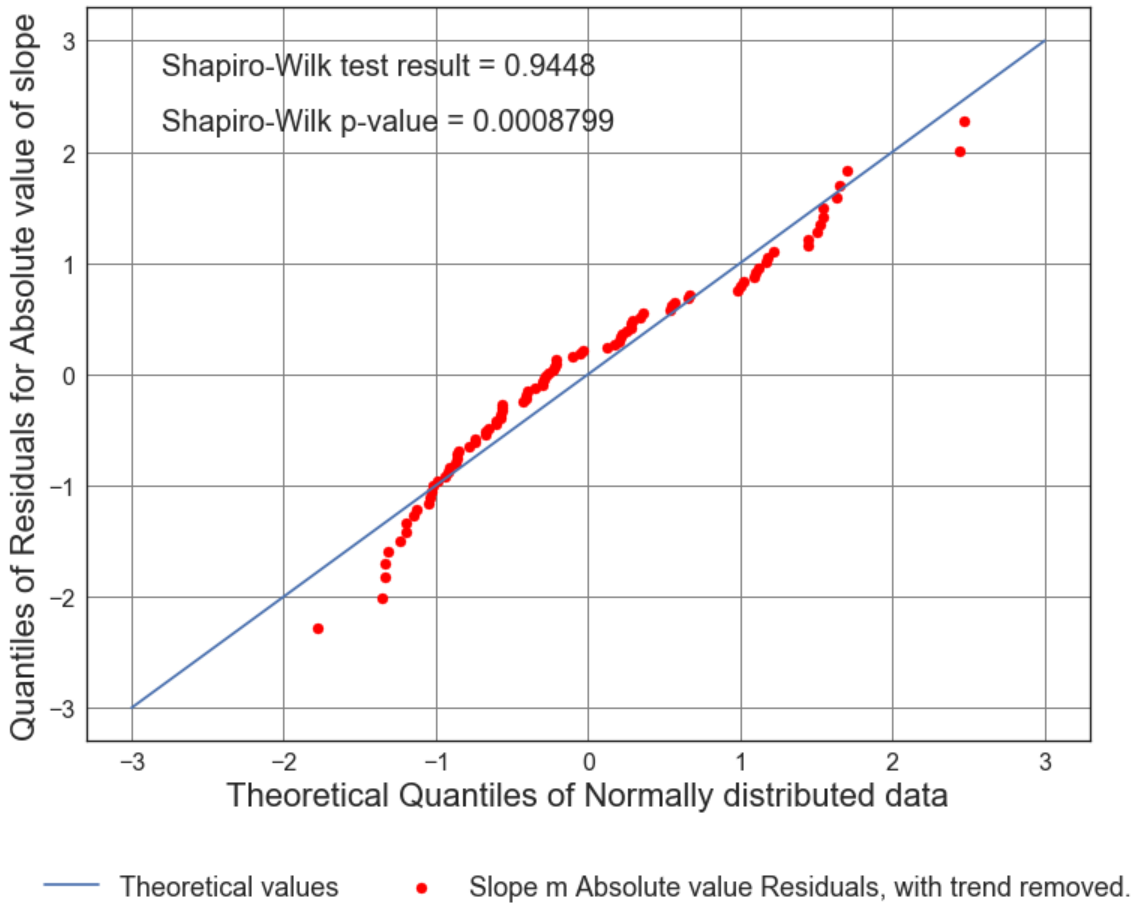

Figure C4.10: Scatter Plot of Solar cycle slope (from 1964 to 2017) vs. Average number of 7.5M and up Earthquakes/6months with trend removed. Line of best fit, y = 0.0006192x + (0.0003284), mean x = -0.5303 +/- 38.19, mean y = 1.836e-15 +/- 1.091, R = 0.02168, R squared = 0.0004702, p-value = 0.8402.

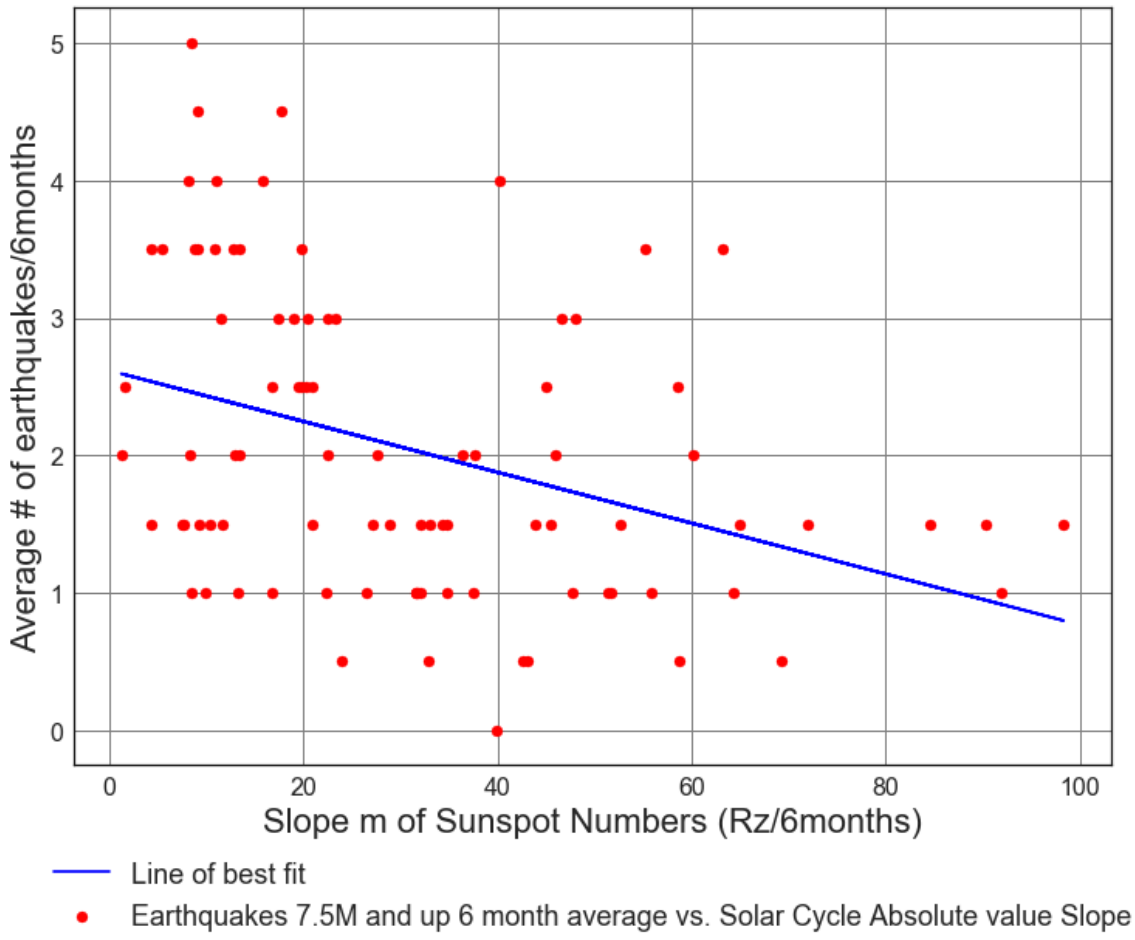

Figure C4.11: Scatter Plot of Solar cycle slope (from 1964 to 2017) vs. Average number of 7.5M and up Earthquakes/6months. Line of best fit, y = -0.01851x + (2.616), mean x = 31.16 +/- 22.09, mean y = 2.039 +/- 1.115, R = -0.3668, R squared = 0.1345, p-value = 0.0004069.

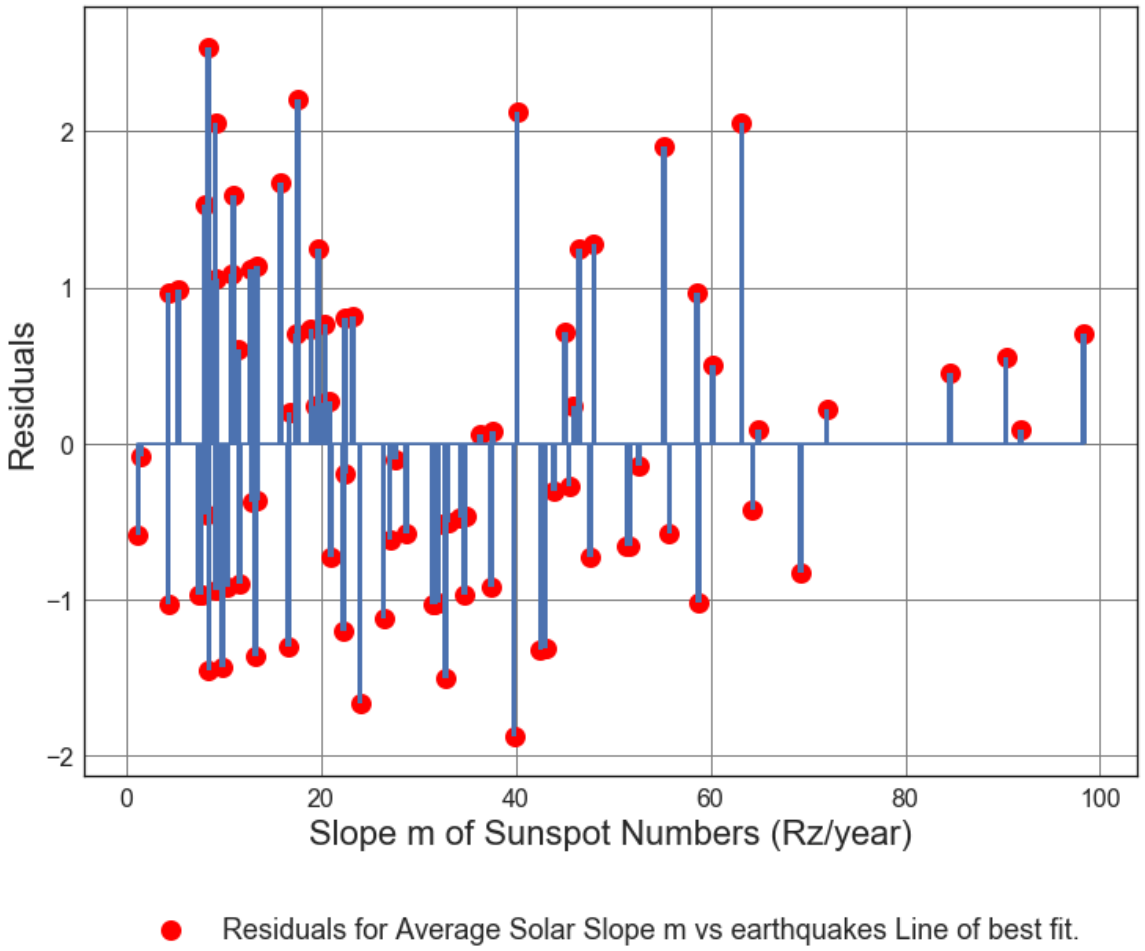

Figure C4.12: Scatter Plot of Solar cycle slope (from 1964 to 2017) vs. Average number of 7.5M and up Earthquakes/6months. Line of best fit, y = -0.01851x + (2.616), mean x = 31.16 +/- 22.09, mean y = 2.039 +/- 1.115, R = -0.3668, R squared = 0.1345, p-value = 0.0004069.

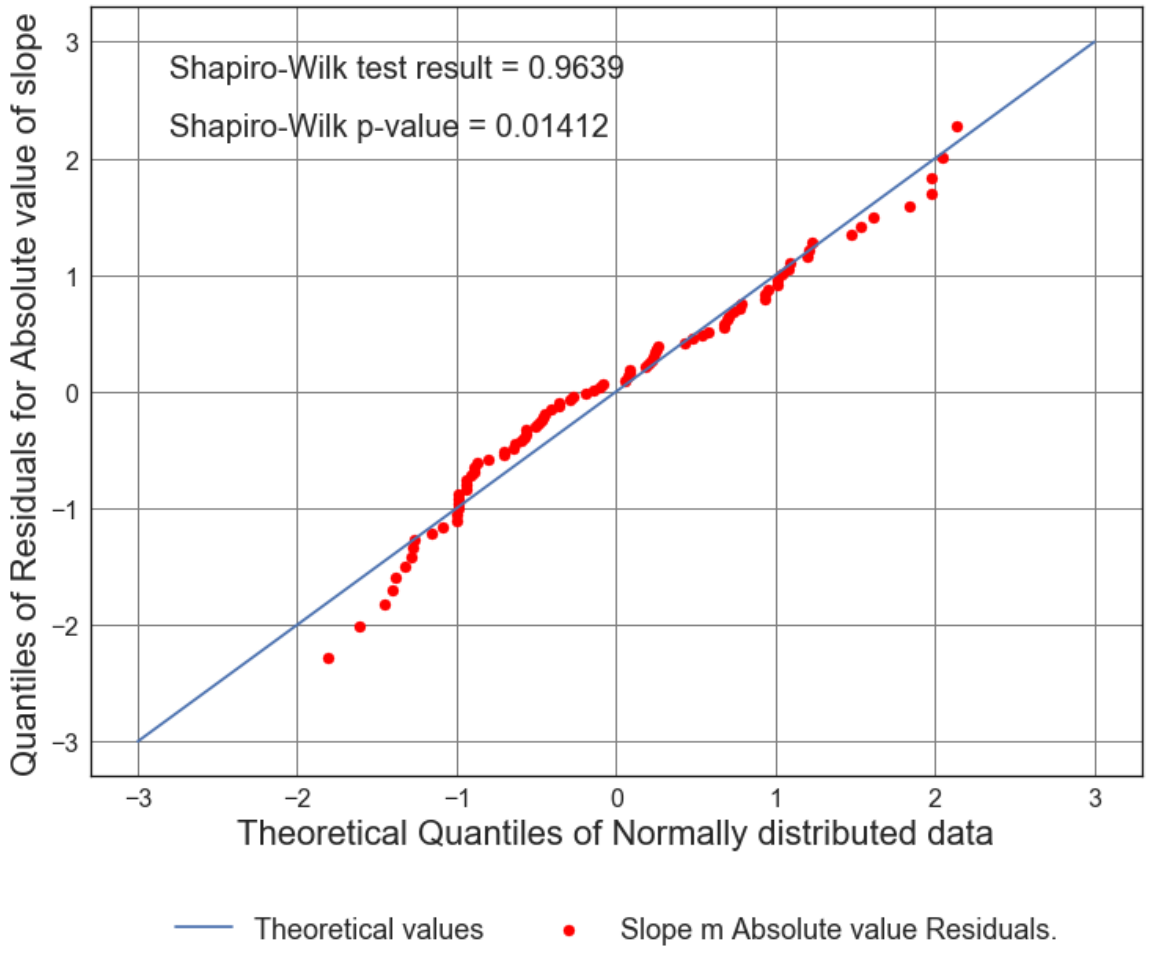

Figure C4.13: Scatter Plot of Solar cycle slope (from 1964 to 2017) vs. Average number of 7.5M and up Earthquakes/6months. Line of best fit, y = -0.01851x + (2.616), mean x = 31.16 +/- 22.09, mean y = 2.039 +/- 1.115, R = -0.3668, R squared = 0.1345, p-value = 0.0004069.

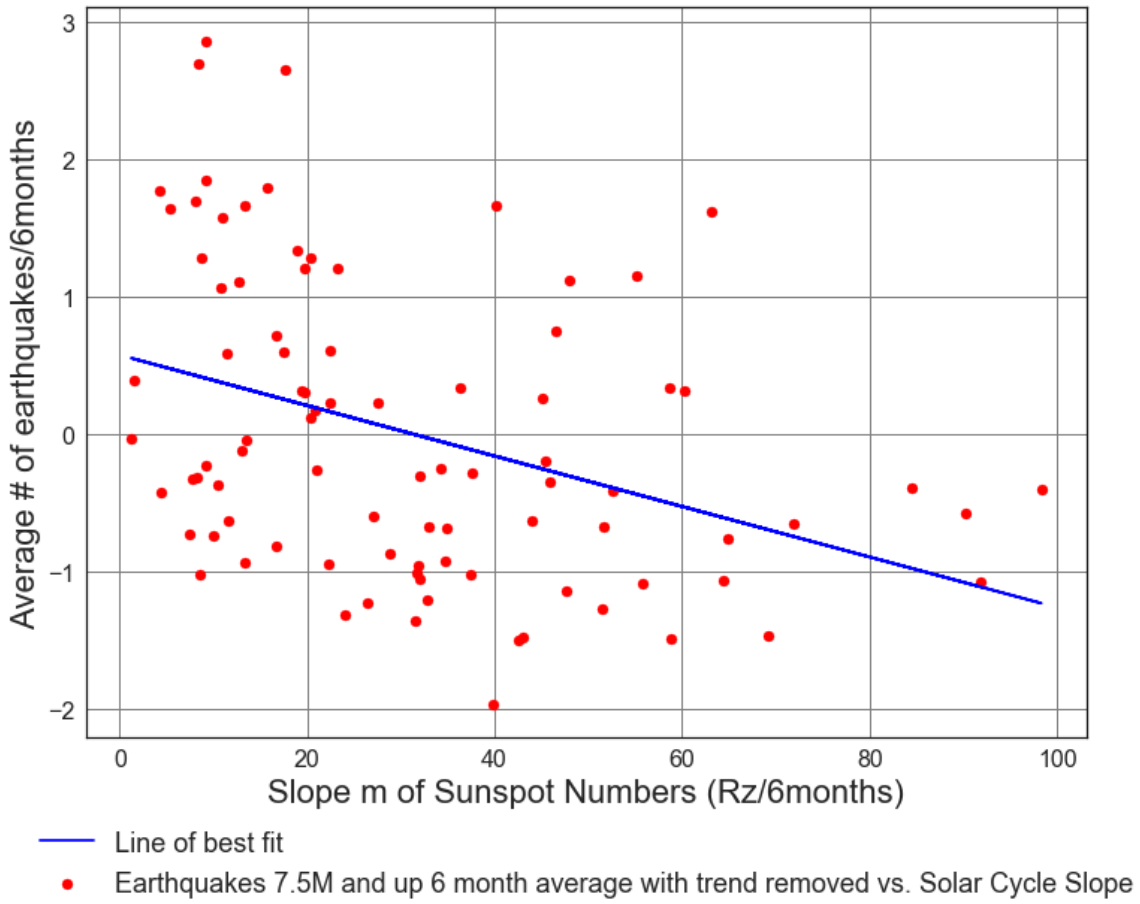

Figure C4.14: Scatter Plot of Solar cycle absolute value slope (from 1964 to 2017) vs. Average number of 7.5M and up Earthquakes/6months with trend removed. Line of best fit, y = -0.01838x + (0.5728), mean x = 31.16 +/- 22.09, mean y = 1.836e-15 +/- 1.091, R = -0.3724, R squared = 0.1387, p-value = 0.000326.

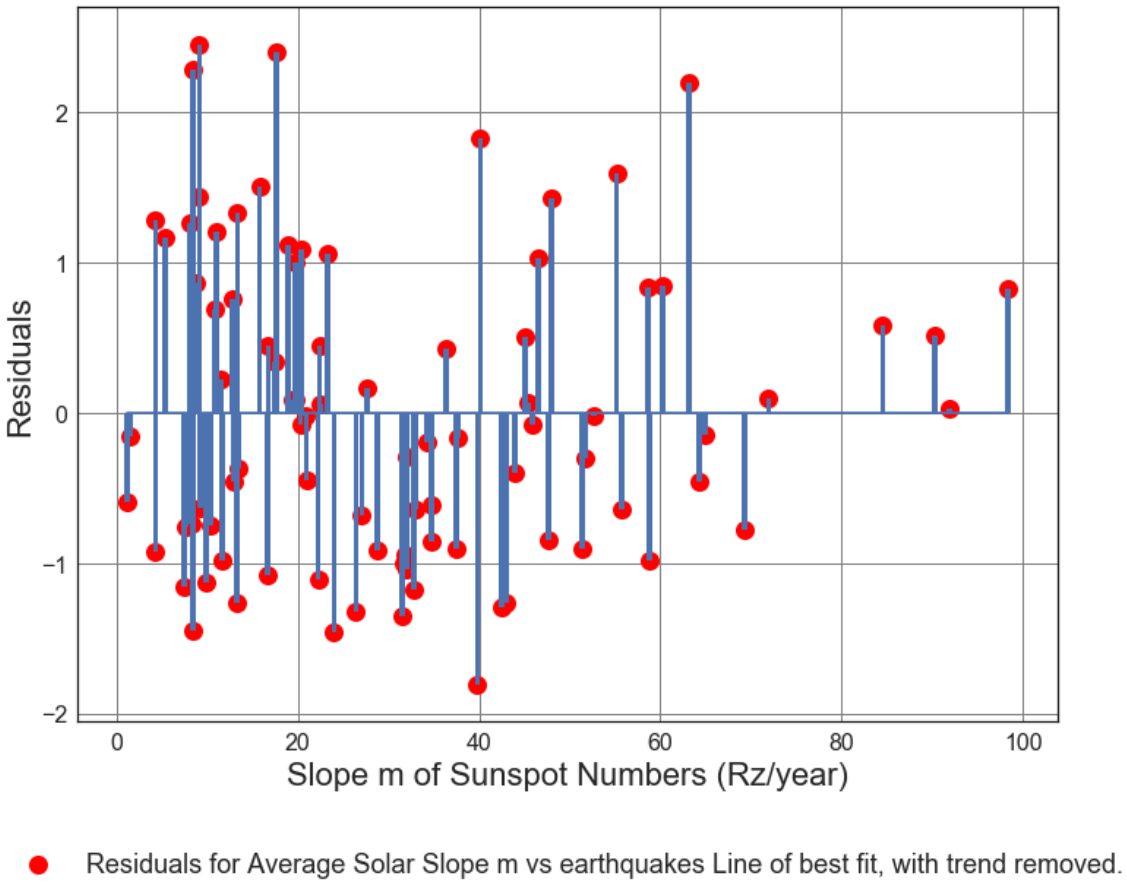

Figure C4.15: Scatter Plot of Solar cycle absolute value slope (from 1964 to 2017) vs. Average number of 7.5M and up Earthquakes/6months with trend removed. Line of best fit, y = -0.01838x + (0.5728), mean x = 31.16 +/- 22.09, mean y = 1.836e-15 +/- 1.091, R = -0.3724, R squared = 0.1387, p-value = 0.000326.

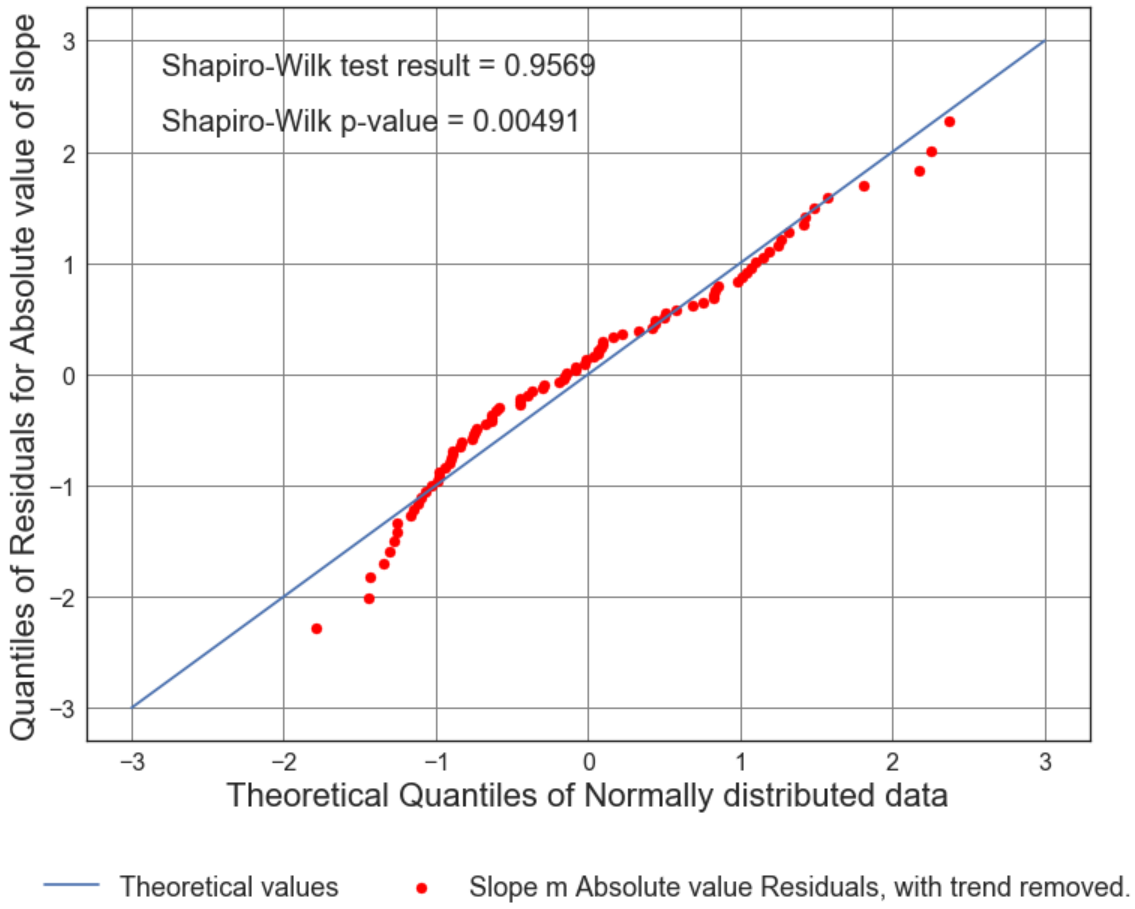

Figure C4.16: Scatter Plot of Solar cycle absolute value slope (from 1964 to 2017) vs. Average number of 7.5M and up Earthquakes/6months with trend removed. Line of best fit, y = -0.01838x + (0.5728), mean x = 31.16 +/- 22.09, mean y = 1.836e-15 +/- 1.091, R = -0.3724, R squared = 0.1387, p-value = 0.000326.

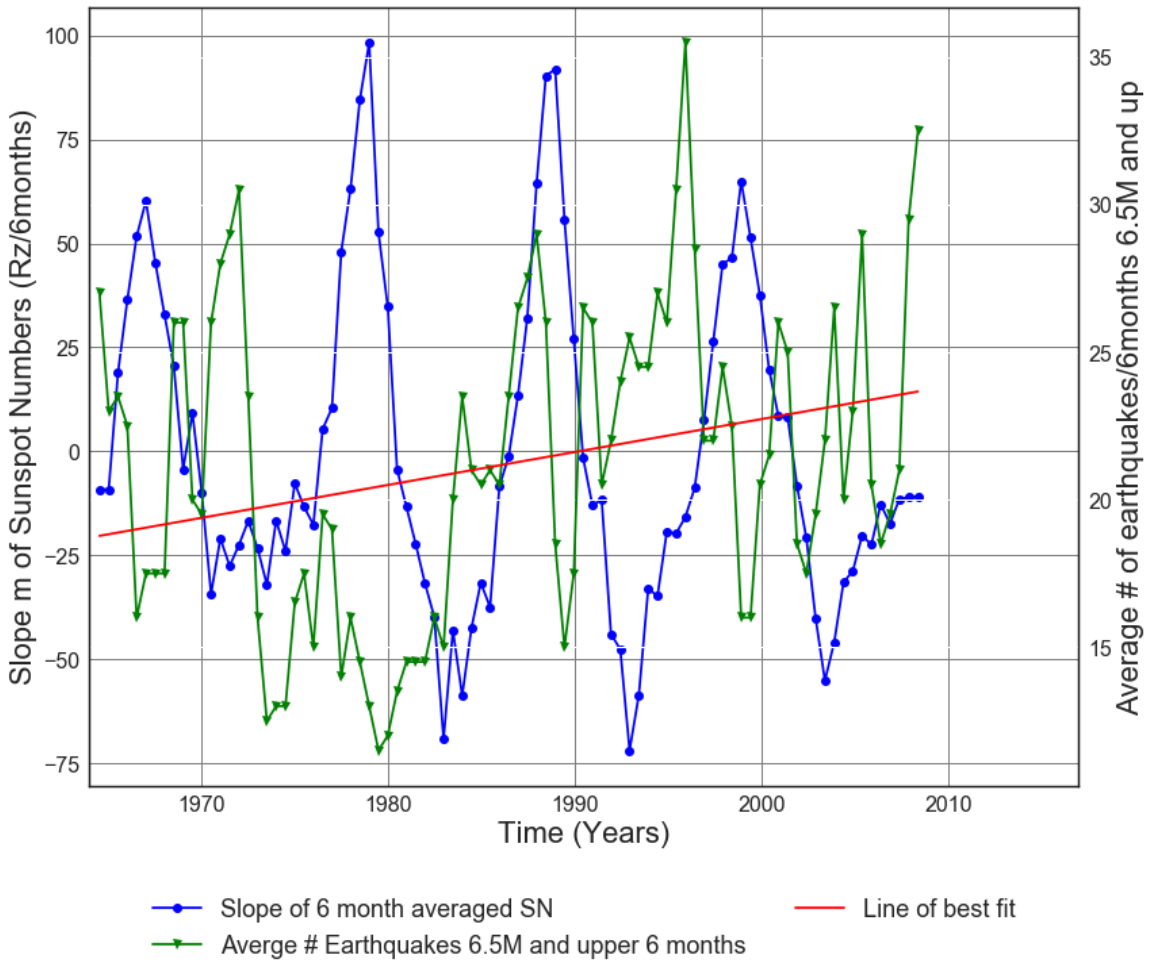

Figure C4.17: Slope of Solar cycle from 1964 to 2017 vs. Average number of 6.5M and up Earthquakes.

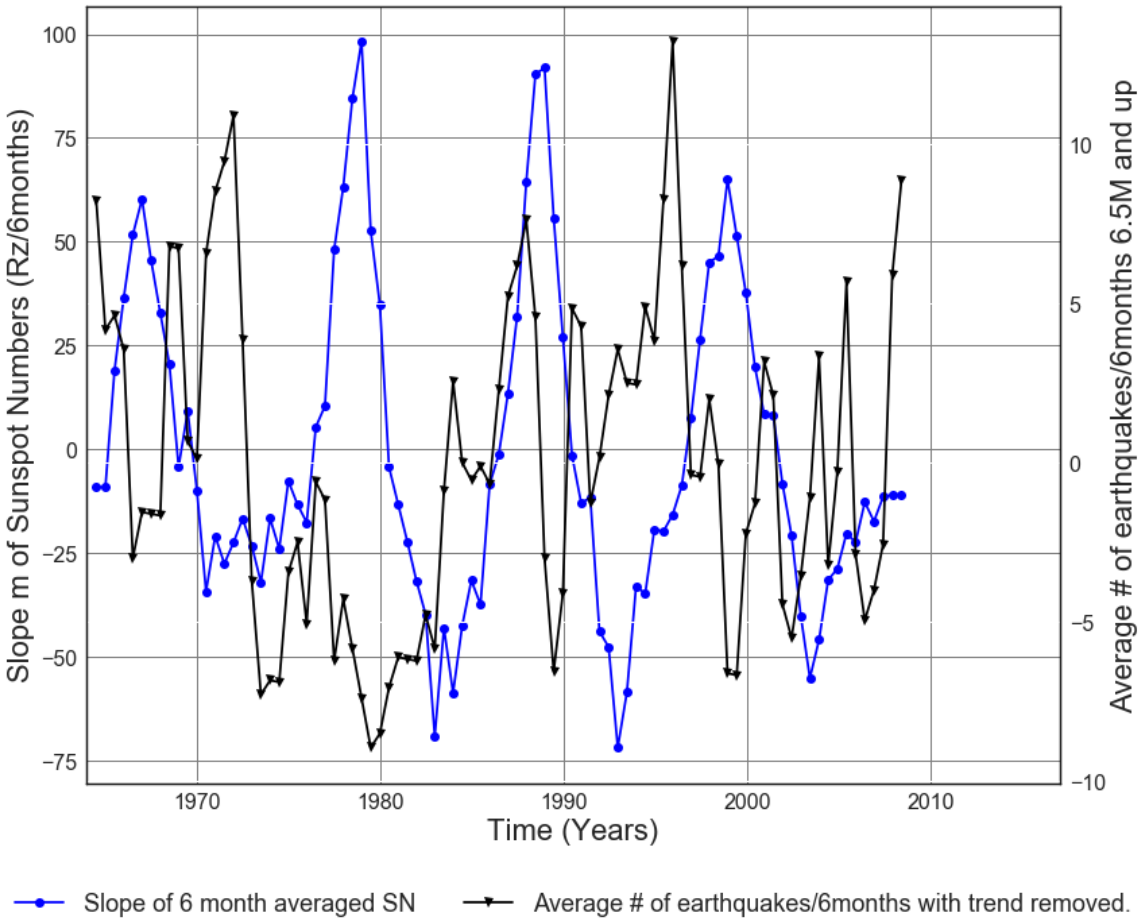

Figure C4.18: Slope of 6 month averaged SN 1964 to 2017 vs. Average number of 6.5M and up Earthquakes with trend removed. Line of best fit, y = 0.1116x + (-200.5), mean x = 1.986e+03 +/- 12.8, mean y = 21.22 +/- 5.289

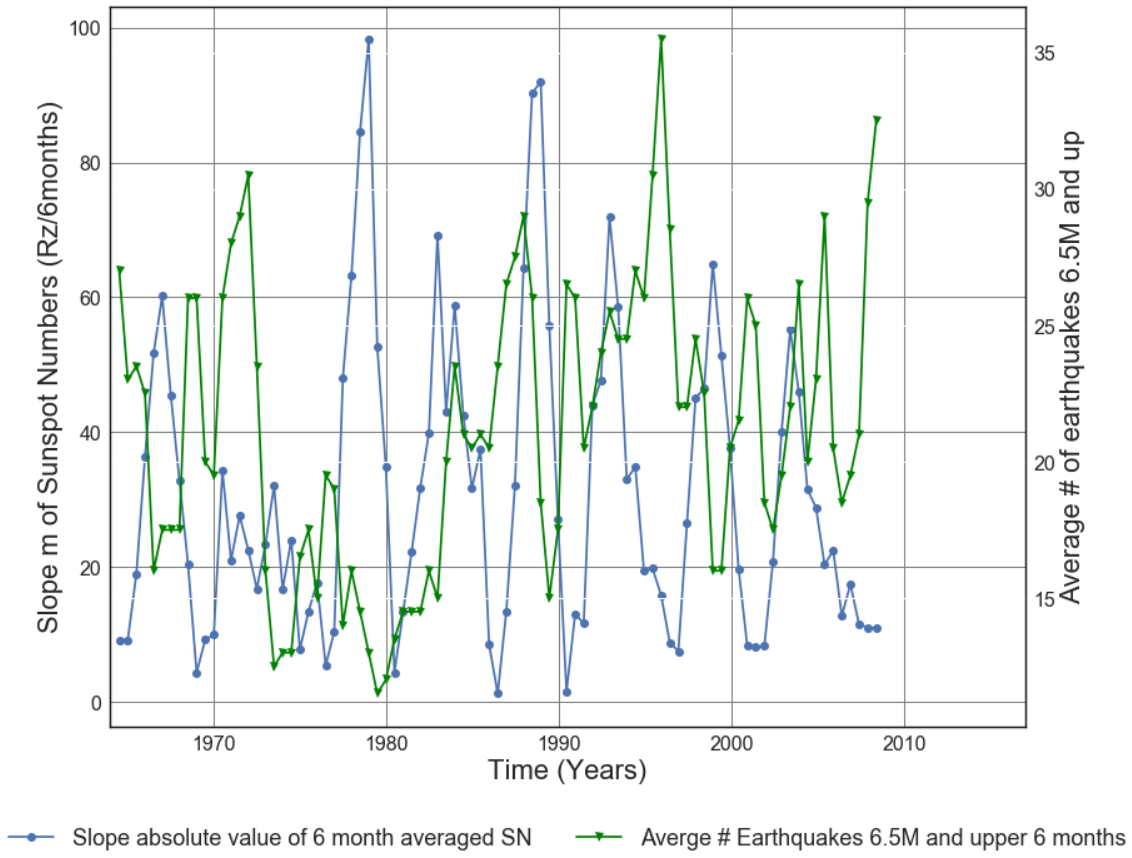

Figure C4.19: Slope Absolute value of Solar cycle from 1964 to 2017 vs. Average number of 6.5M and up Earthquakes.

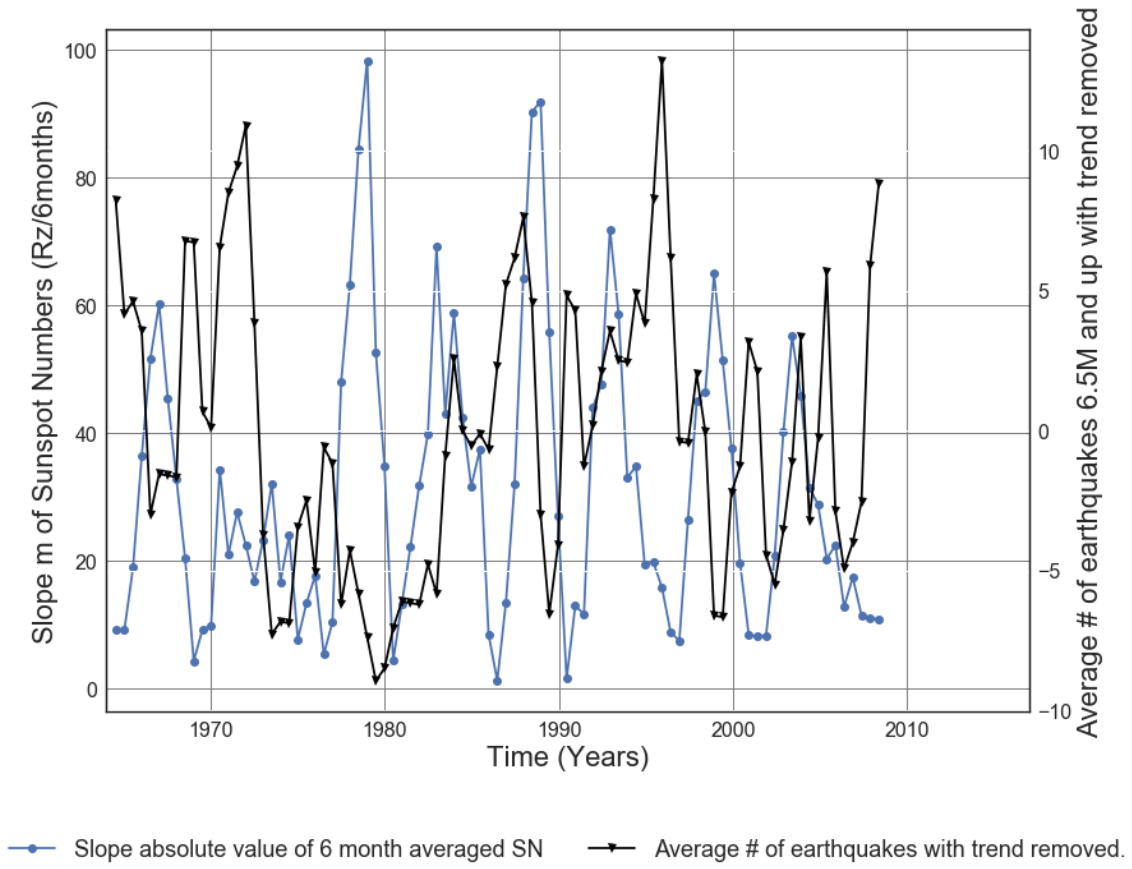

Figure C4.20: Slope Absolute value of Solar cycle from 1964 to 2017 vs. Average number of 6.5M and up earthquakes with trend removed.

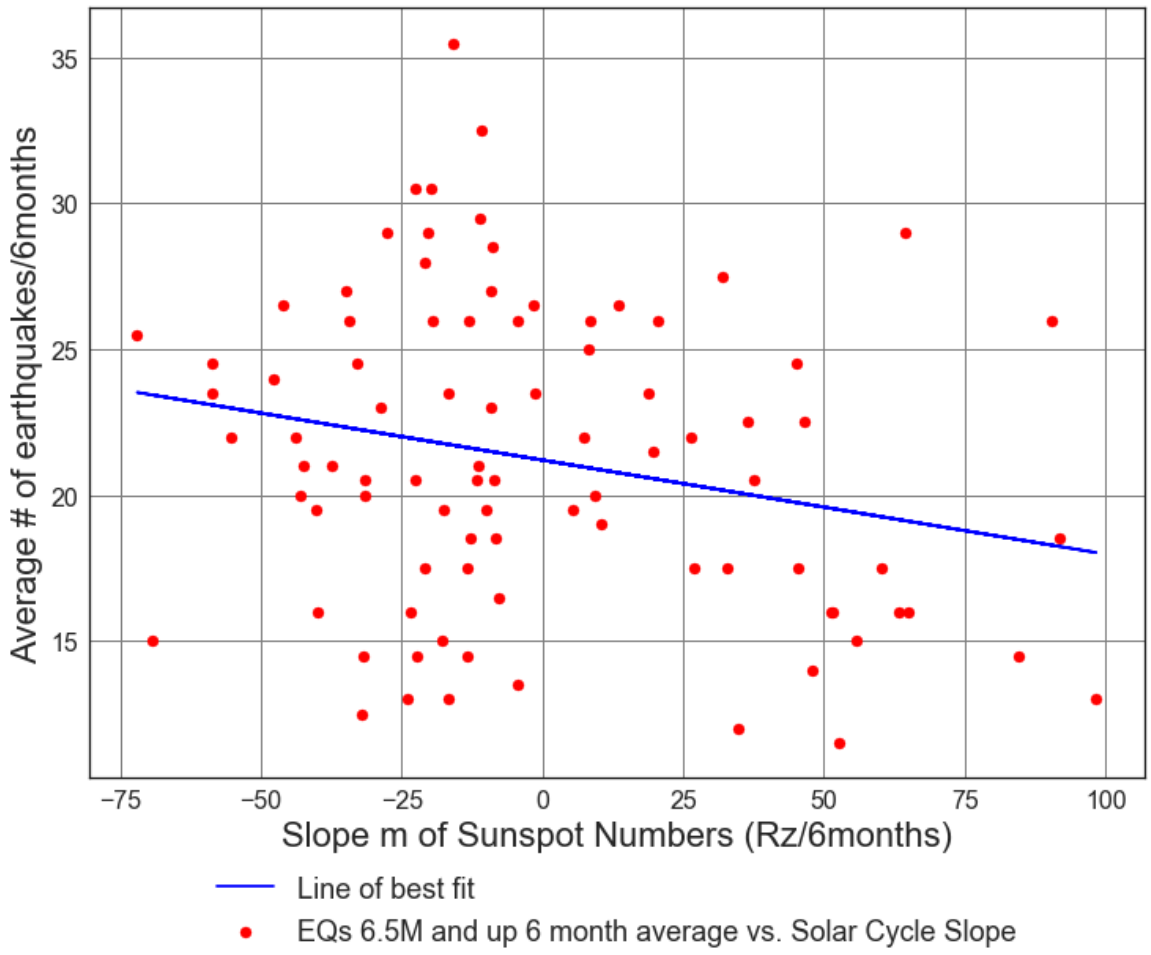

Figure C4.21: Scatter Plot of Solar cycle slope (from 1964 to 2017) vs. Average number of 6.5M and up Earthquakes/6months. Line of best fit, y = -0.03225x + (21.2), mean x = -0.5303 +/- 38.19, mean y = 21.22 +/- 5.289, R = -0.2329, R squared = 0.05424, p-value = 0.02806.

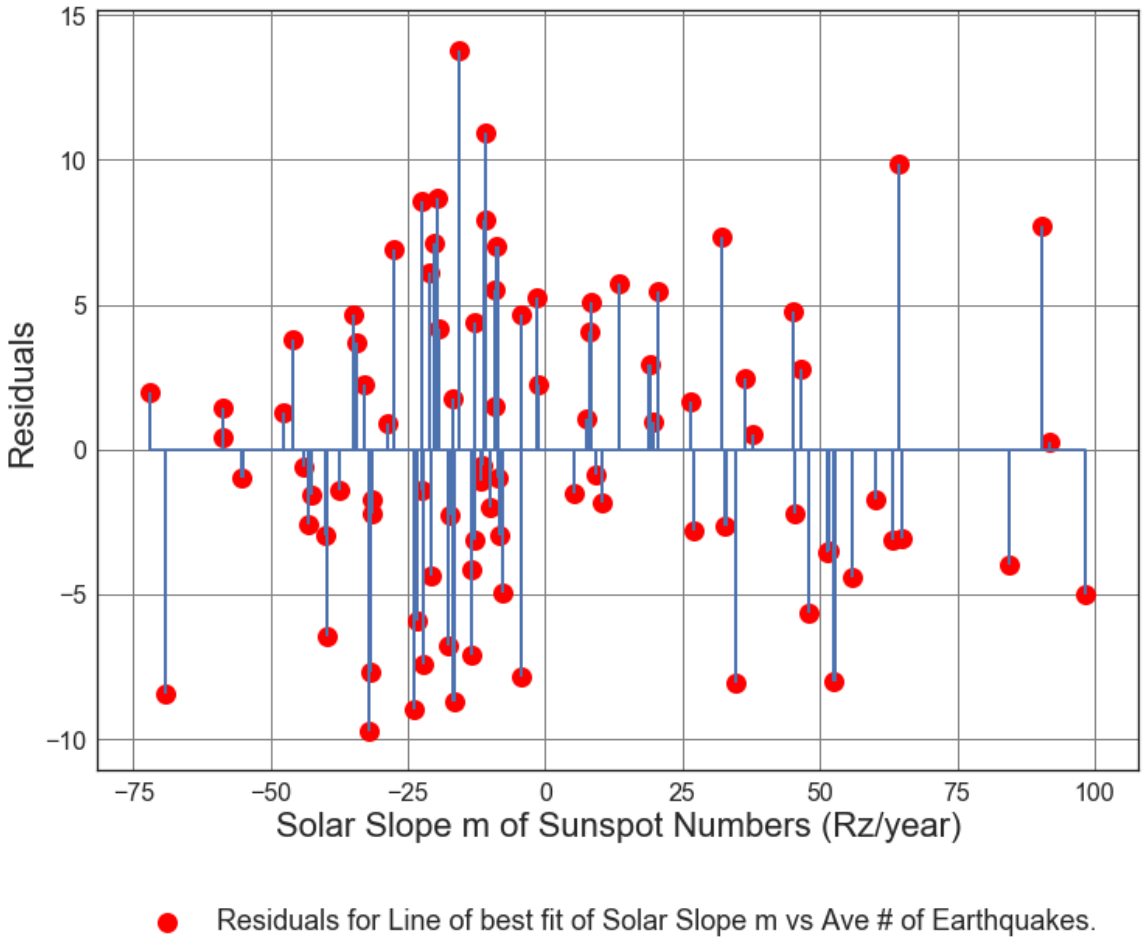

Figure C4.22: Residuals Plot of Solar cycle slope (from 1964 to 2017) vs. Average number of 6.5M and up Earthquakes/6months. Line of best fit, y = -0.03225x + (21.2), mean x = -0.5303 +/- 38.19, mean y = 21.22 +/- 5.289, R = -0.2329, R squared = 0.05424, p-value = 0.02806.

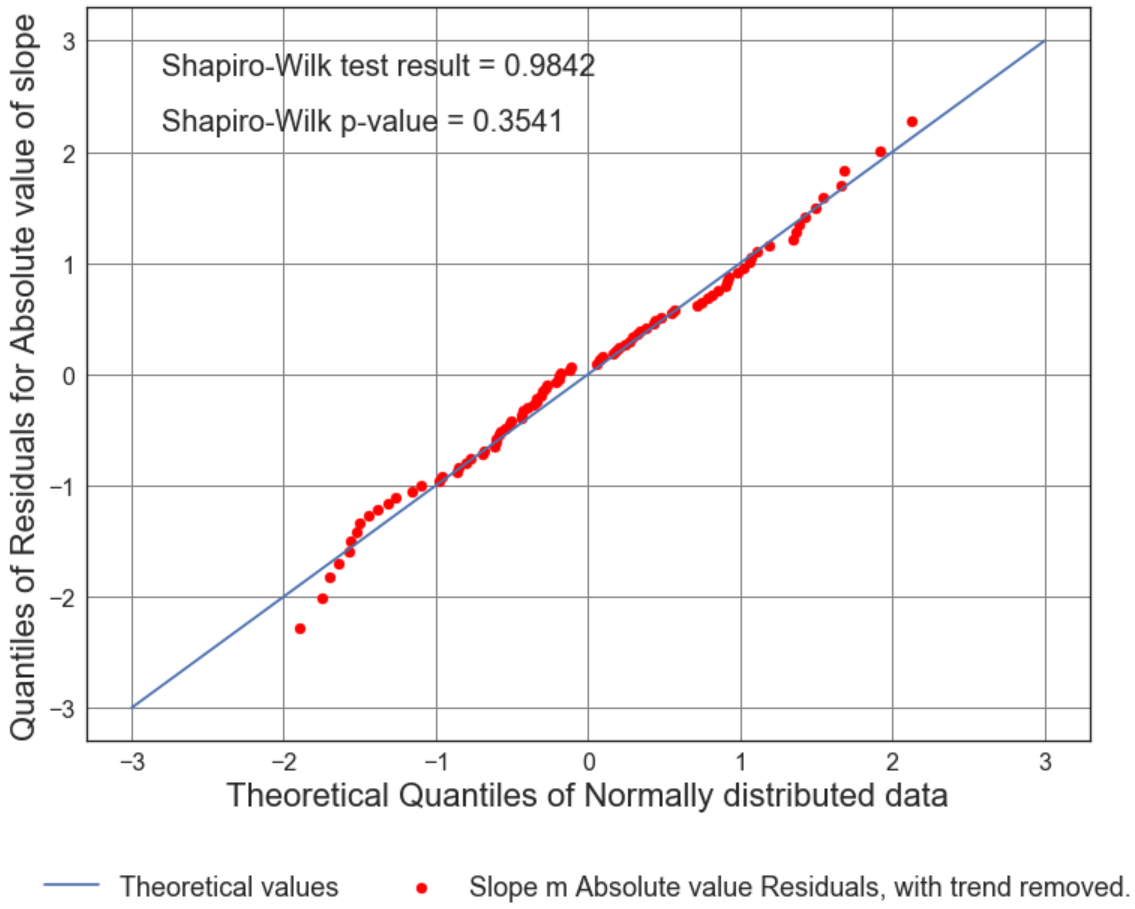

Figure C4.23: Residuals Plot of Solar cycle slope (from 1964 to 2017) vs. Average number of 6.5M and up Earthquakes/6months. Line of best fit, y = -0.03225x + (21.2), mean x = -0.5303 +/- 38.19, mean y = 21.22 +/- 5.289, R = -0.2329, R squared = 0.05424, p-value = 0.02806.

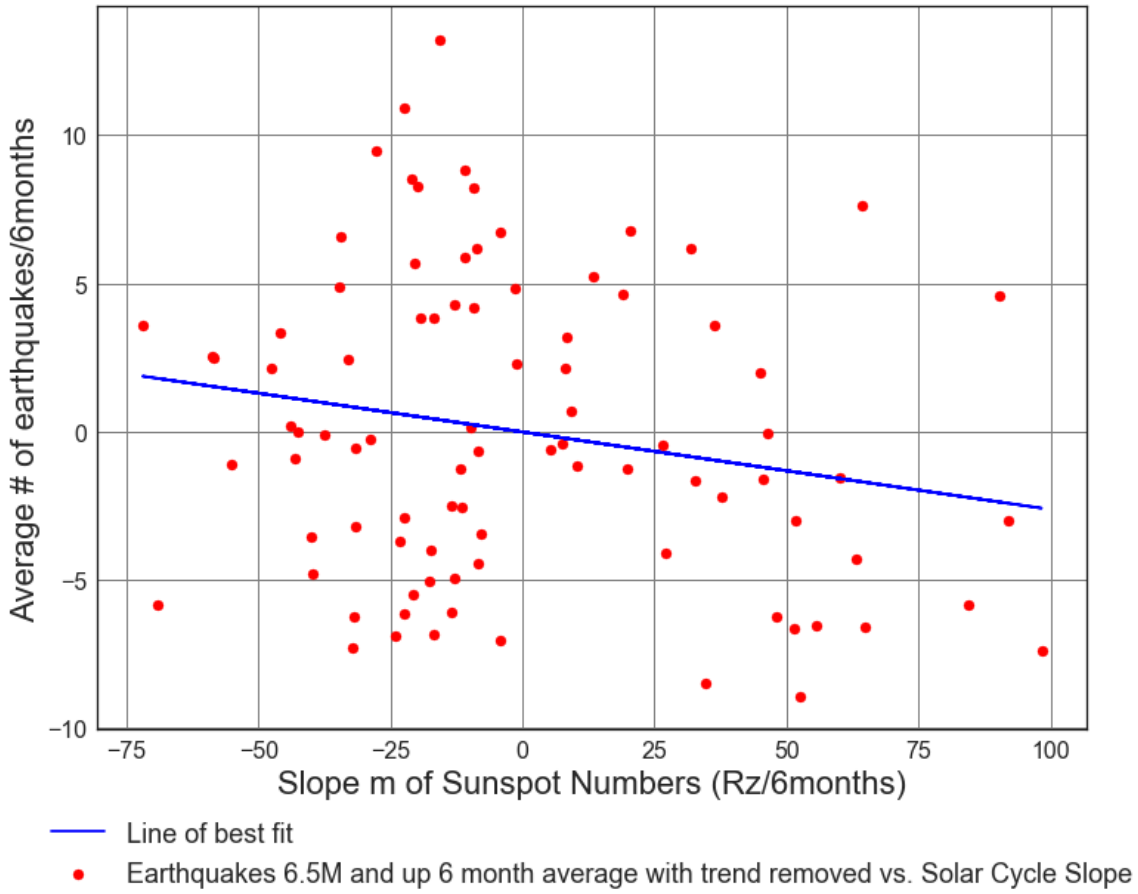

Figure C4.24: Scatter Plot of Solar cycle slope (from 1964 to 2017) vs. Average number of 6.5M and up Earthquakes/6months with trend removed. Line of best fit, y = -0.02614x + (-0.01386), mean x = -0.5303 +/- 38.19, mean y = -1.693e-14 +/- 5.092, R = -0.1961, R squared = 0.03845, p-value = 0.06552.

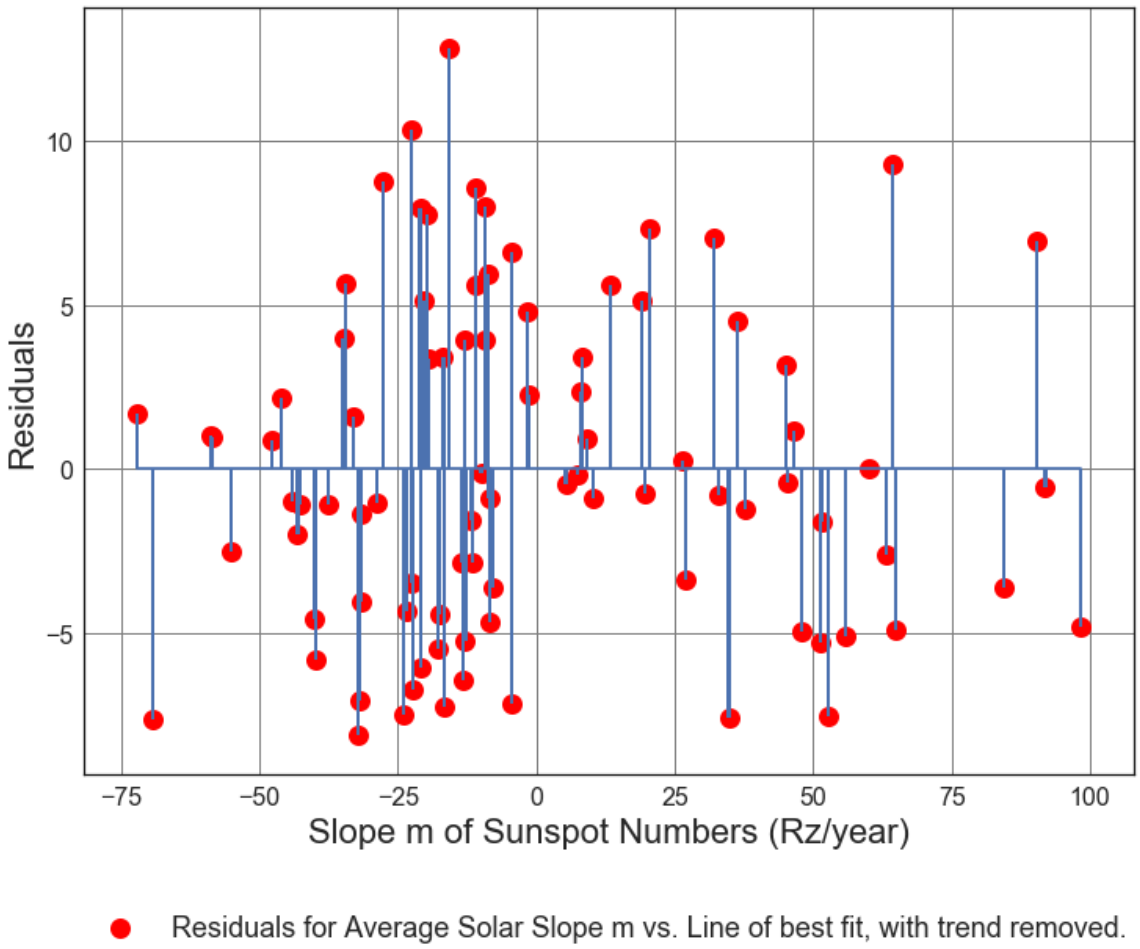

Figure C4.25: Scatter Plot of Solar cycle slope (from 1964 to 2017) vs. Average number of 6.5M and up Earthquakes/6months with trend removed. Line of best fit, y = -0.02614x + (-0.01386), mean x = -0.5303 +/- 38.19, mean y = -1.693e-14 +/- 5.092, R = -0.1961, R squared = 0.03845, p-value = 0.06552.

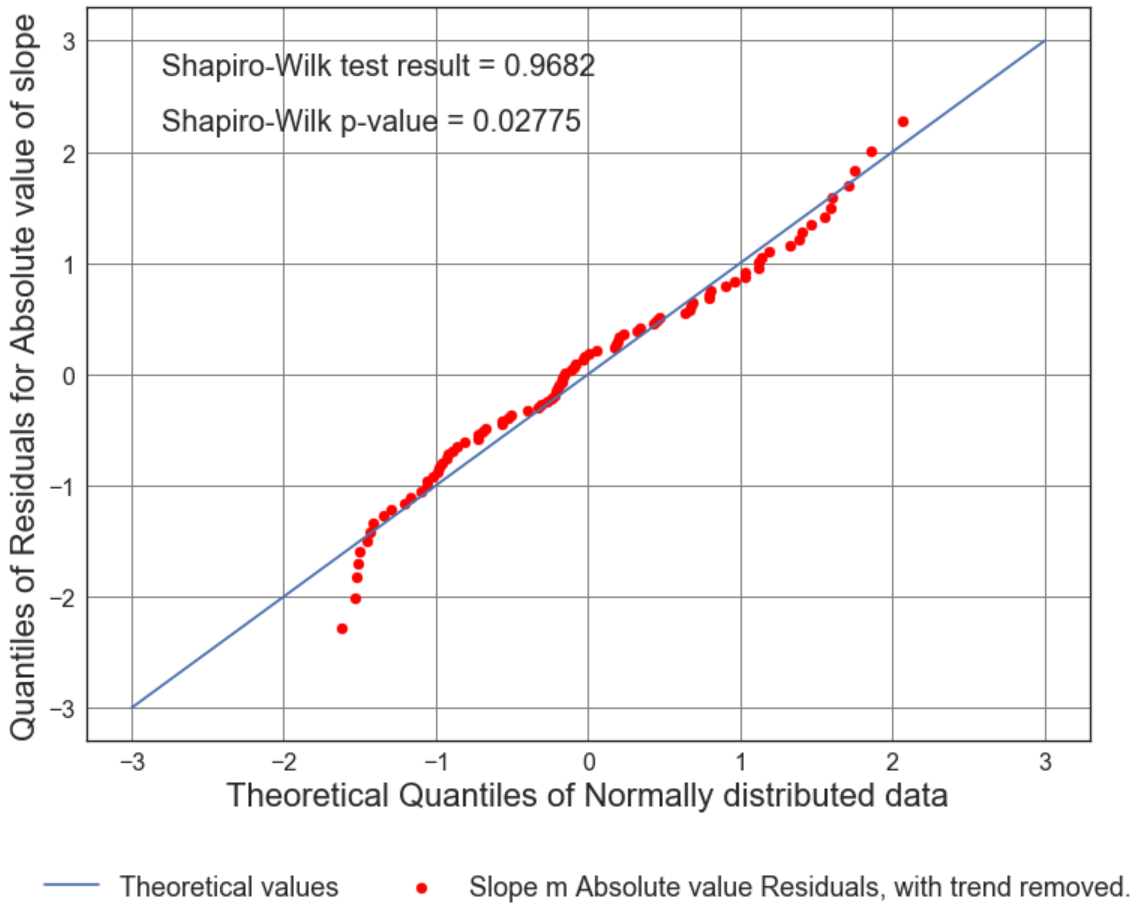

Figure C4.26: Scatter Plot of Solar cycle slope (from 1964 to 2017) vs. Average number of 6.5M and up Earthquakes/6months with trend removed. Line of best fit, y = -0.02614x + (-0.01386), mean x = -0.5303 +/- 38.19, mean y = -1.693e-14 +/- 5.092, R = -0.1961, R squared = 0.03845, p-value = 0.06552.

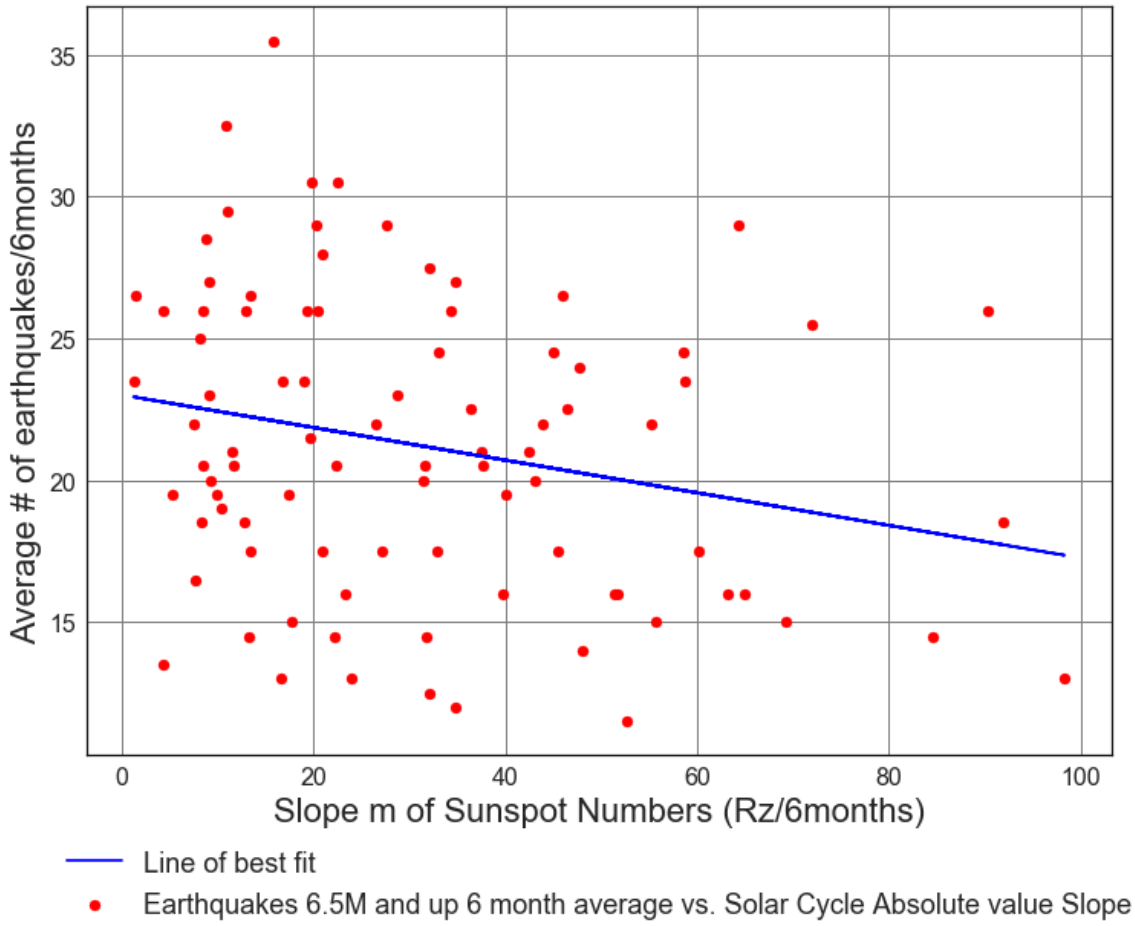

Figure C4.27: Scatter Plot of Solar cycle slope (from 1964 to 2017) vs. Average number of 6.5M and up Earthquakes/6months. Line of best fit, y = -0.0575x + (23.01), mean x = 31.16 +/- 22.09, mean y = 21.22 +/- 5.289, R = -0.2402, R squared = 0.0577, p-value = 0.02337.

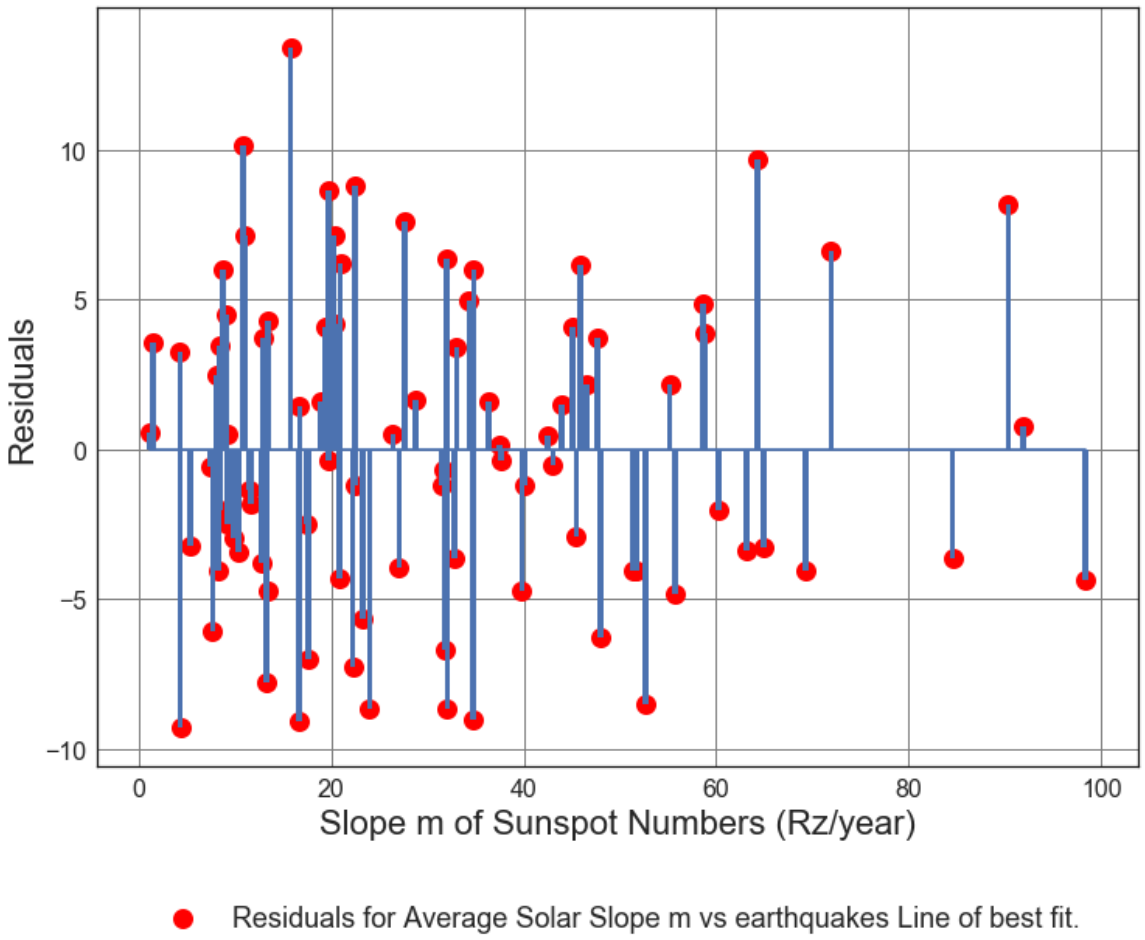

Figure C4.28: Scatter Plot of Solar cycle slope (from 1964 to 2017) vs. Average number of 6.5M and up Earthquakes/6months. Line of best fit, y = -0.0575x + (23.01), mean x = 31.16 +/- 22.09, mean y = 21.22 +/- 5.289, R = -0.2402, R squared = 0.0577, p-value = 0.02337.

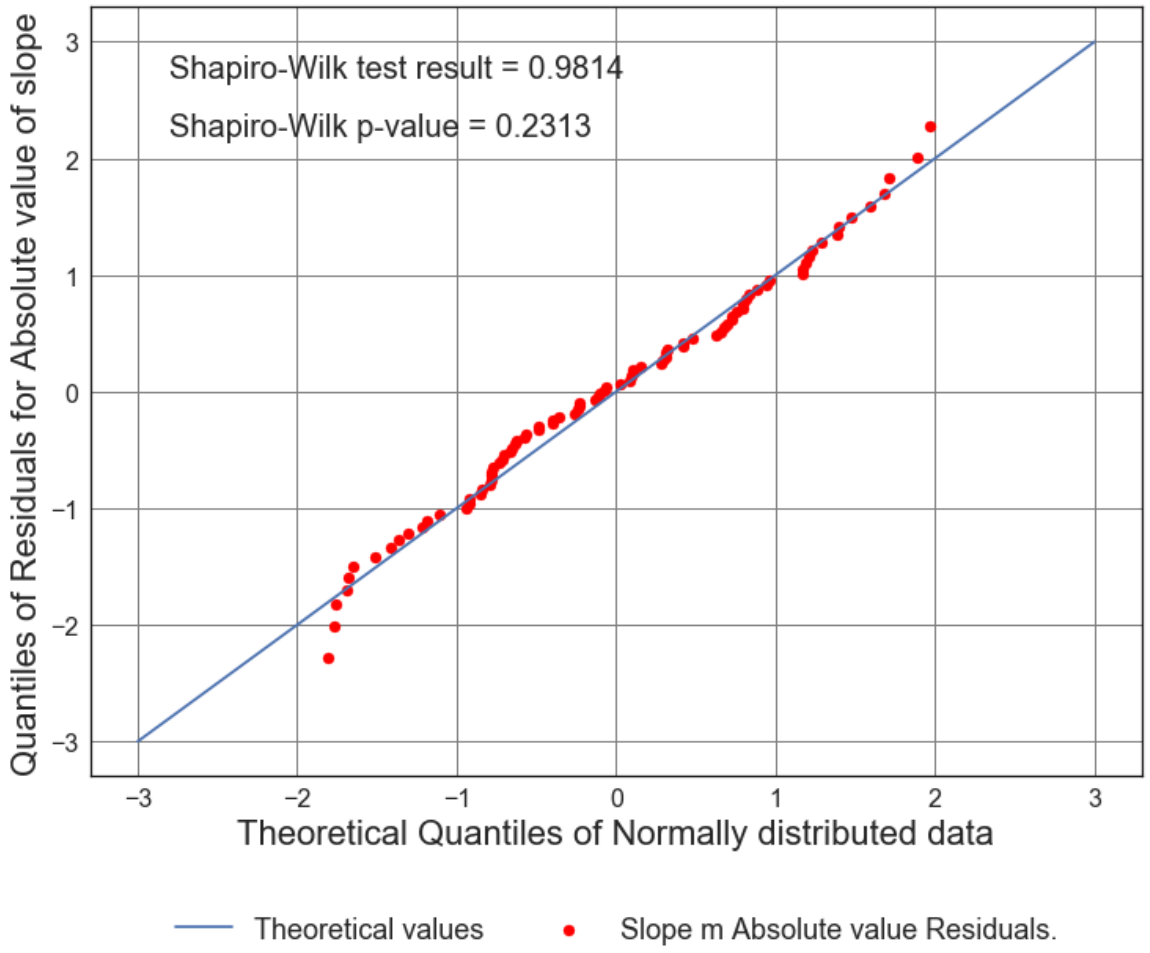

Figure C4.29: Scatter Plot of Solar cycle slope (from 1964 to 2017) vs. Average number of 6.5M and up Earthquakes/6months. Line of best fit, y = -0.0575x + (23.01), mean x = 31.16 +/- 22.09, mean y = 21.22 +/- 5.289, R = -0.2402, R squared = 0.0577, p-value = 0.02337.

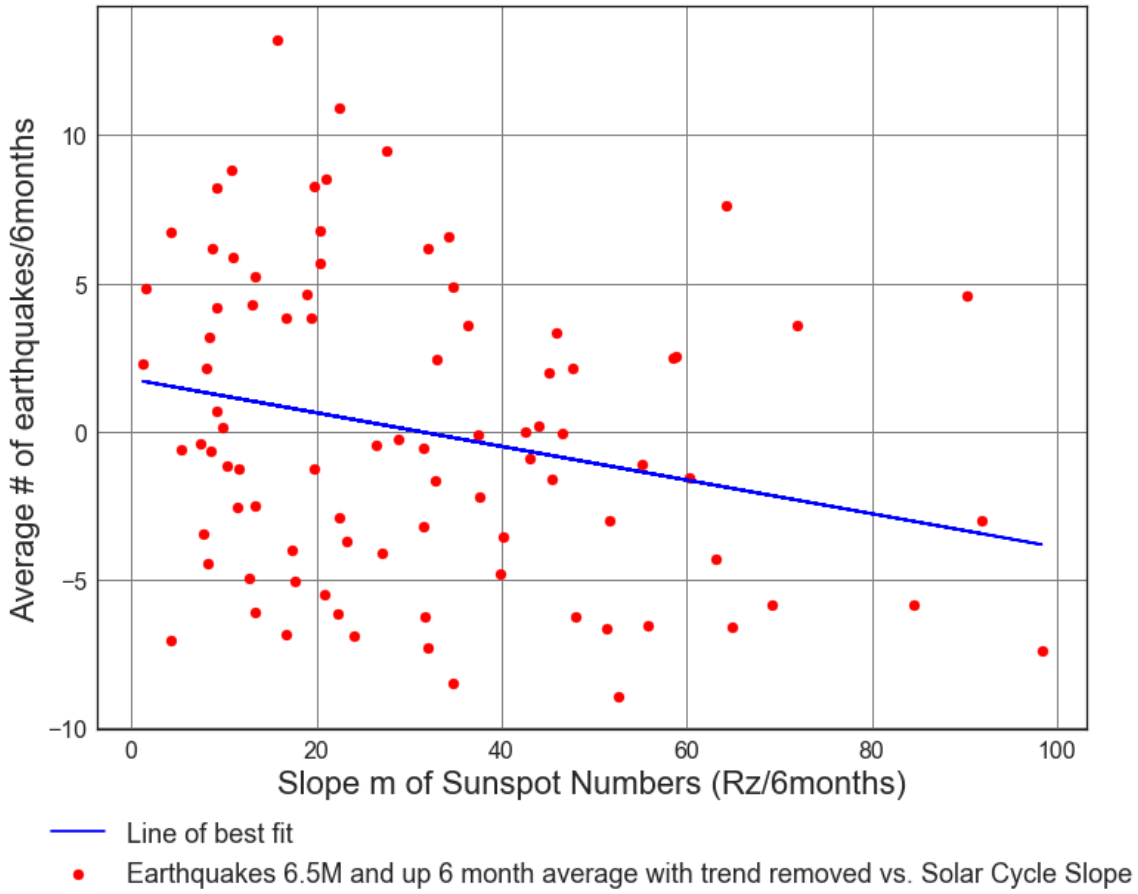

Figure C4.30: Scatter Plot of Solar cycle absolute value slope (from 1964 to 2017) vs. Average number of 6.5M and up Earthquakes/6months with trend removed. Line of best fit, y = -0.05672x + (1.767), mean x = 31.16 +/- 22.09, mean y = -1.693e-14 +/- 5.092, R = -0.2461, R squared = 0.06057, p-value = 0.02008.

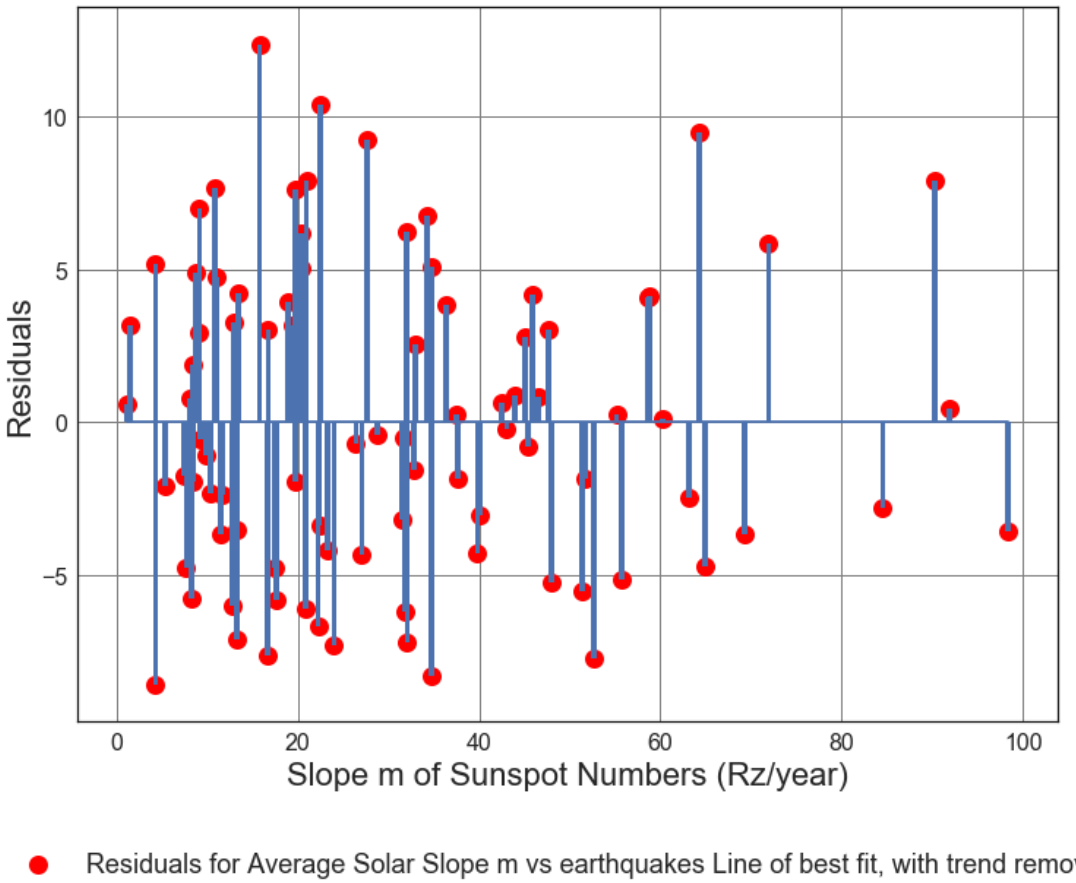

Figure C4.31: Scatter Plot of Solar cycle absolute value slope (from 1964 to 2017) vs. Average number of 6.5M and up Earthquakes/6months with trend removed. Line of best fit, y = -0.05672x + (1.767), mean x = 31.16 +/- 22.09, mean y = -1.693e-14 +/- 5.092, R = -0.2461, R squared = 0.06057, p-value = 0.02008.

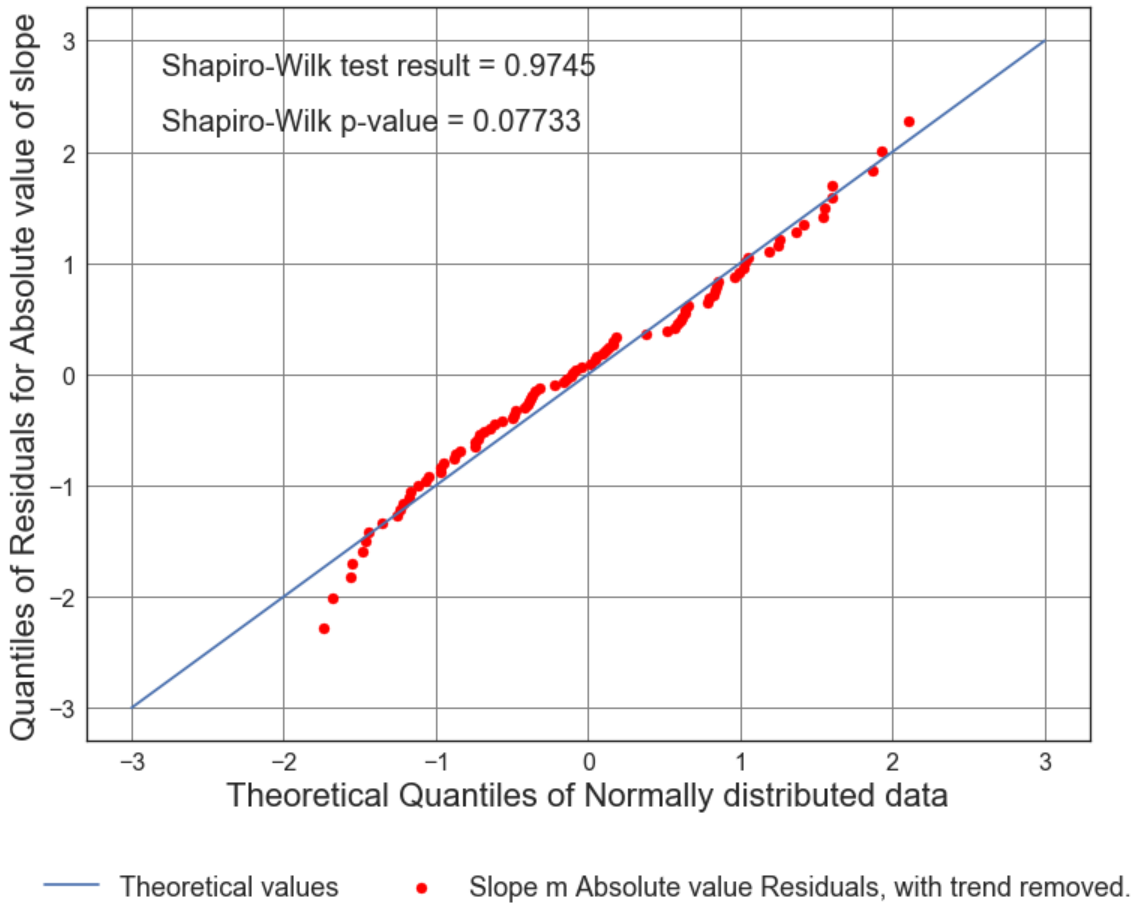

Figure C4.32: Scatter Plot of Solar cycle absolute value slope (from 1964 to 2017) vs. Average number of 6.5M and up Earthquakes/6months with trend removed. Line of best fit, y = -0.05672x + (1.767), mean x = 31.16 +/- 22.09, mean y = -1.693e-14 +/- 5.092, R = -0.2461, R squared = 0.06057, p-value = 0.02008.

Appendix D1: ISC Time Series Analysis Part 1 - Average # of Earthquakes per Rise and Decline of Solar cycle slope.

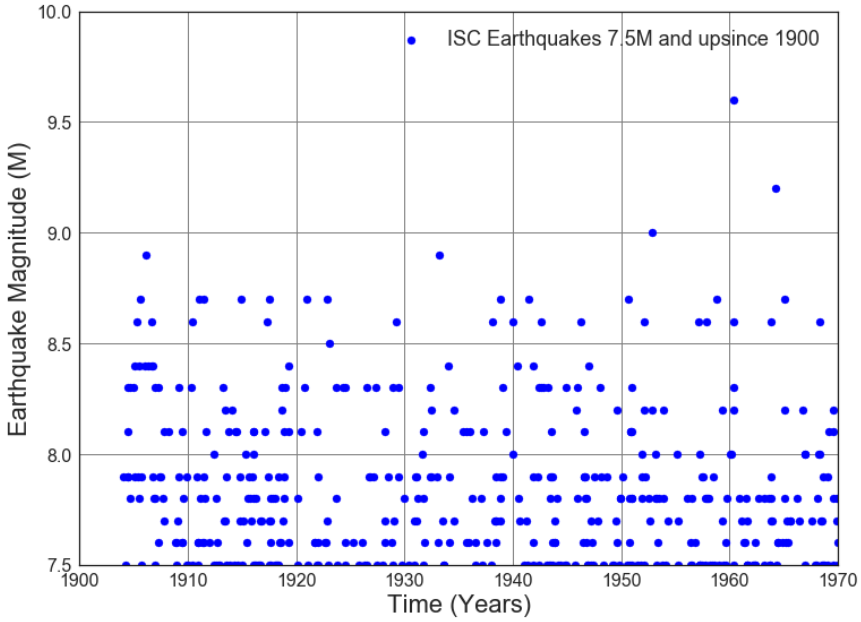

Figure D1.1: Scatter plot of ISC earthquakes 7.5M and up magnitudes 1900 to 1970

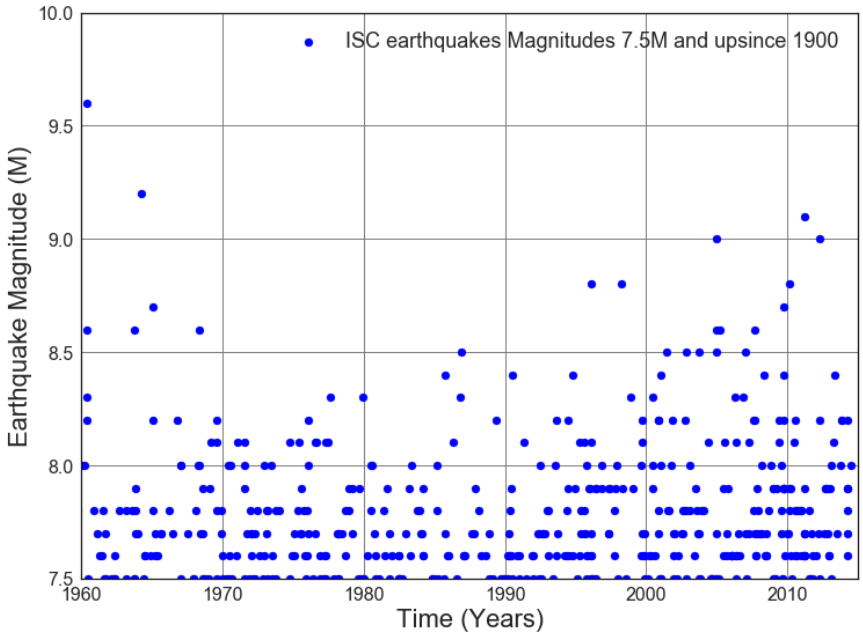

Figure D1.2: Scatter plot of ISC earthquakes 7.5M and up Magnitudes 1960 to 2017

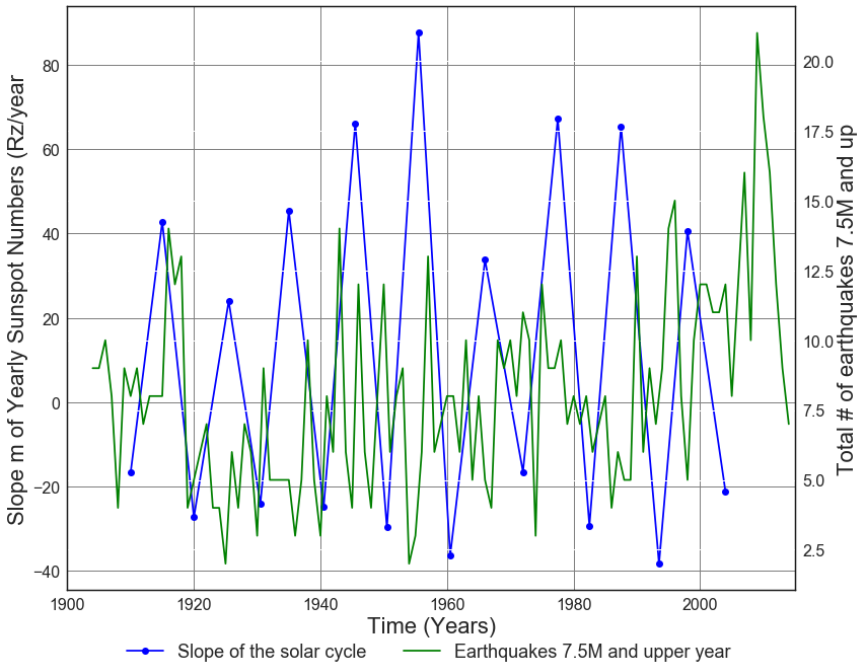

Figure D1.3: Slope of Solar cycle from 1900 to 2014 vs. Average number of 7.5M and up Earthquakes.

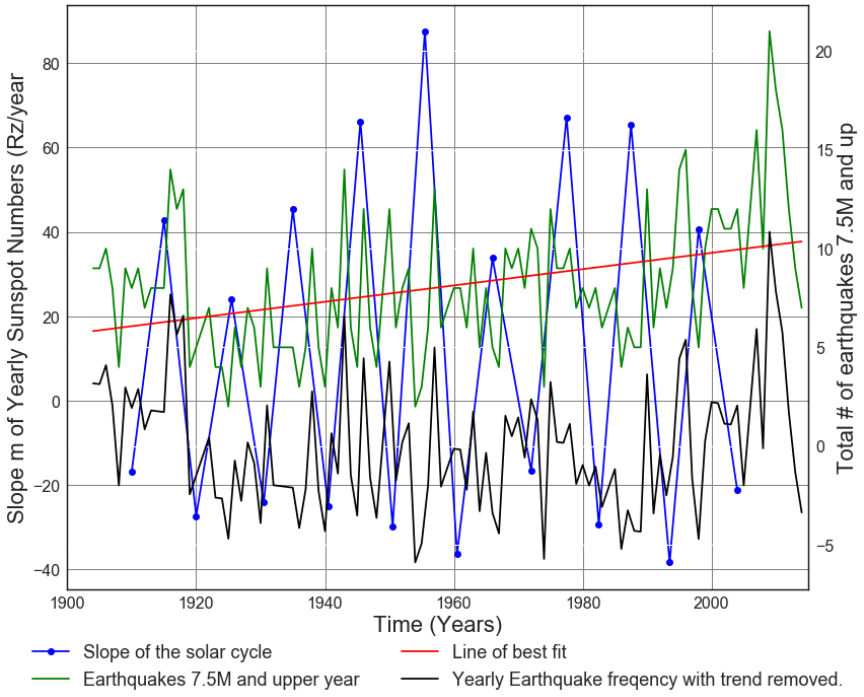

Figure D1.4: Slope of Solar cycle from 1900 to 2014 vs. Average number of 7.5M and up Earthquakes. Line of best fit, y = 0.04123x + (-72.69), mean x = 1.959e+03 +/- 32.04, mean y = 8.09 +/- 3.497

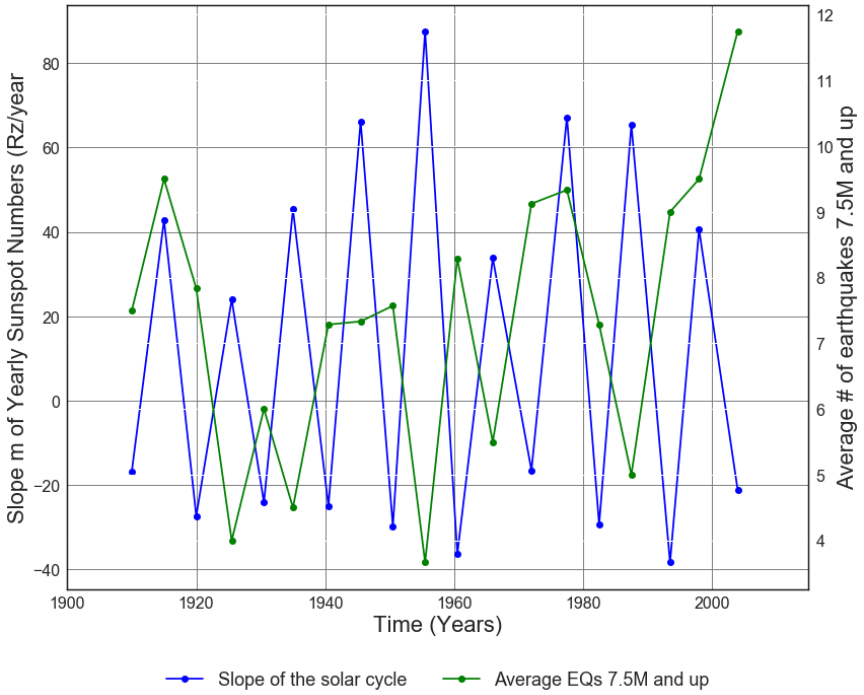

Figure D1.5: Slope of Solar cycle from 1900 to 2014 vs. Average number of 7.5M and up Earthquakes.

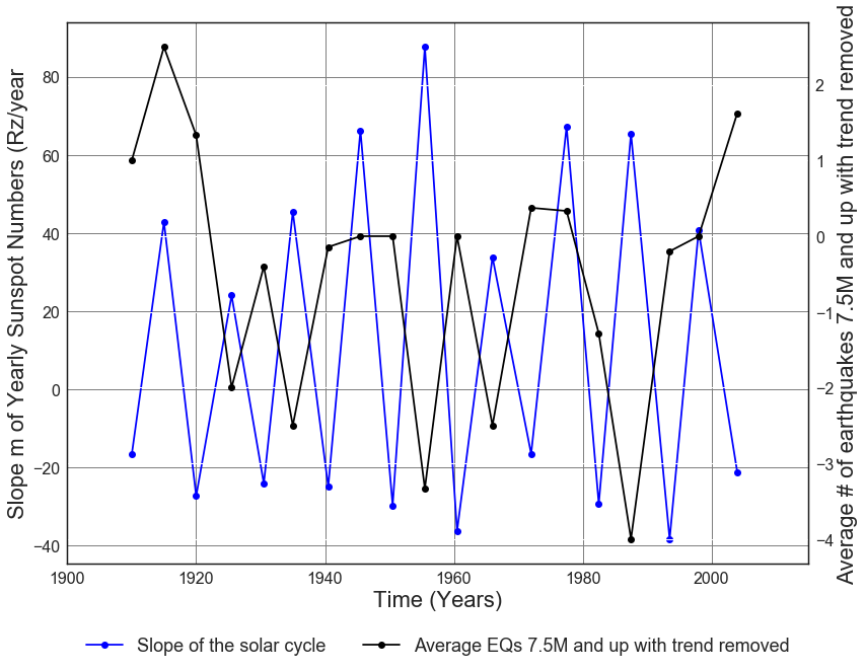

Figure D1.6: Slope of Solar cycle from 1900 to 2014 vs. Average number of 7.5M and up earthquakes.

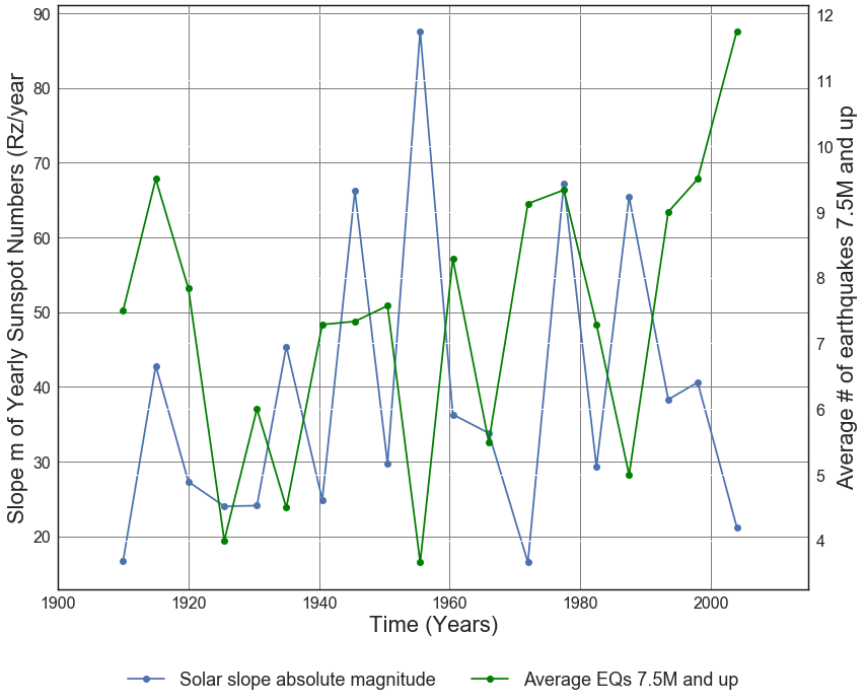

Figure D1.7: Absolute value of Solar cycle slope from 1900 to 2014 vs. Average number of 7.5M and up Earthquakes.

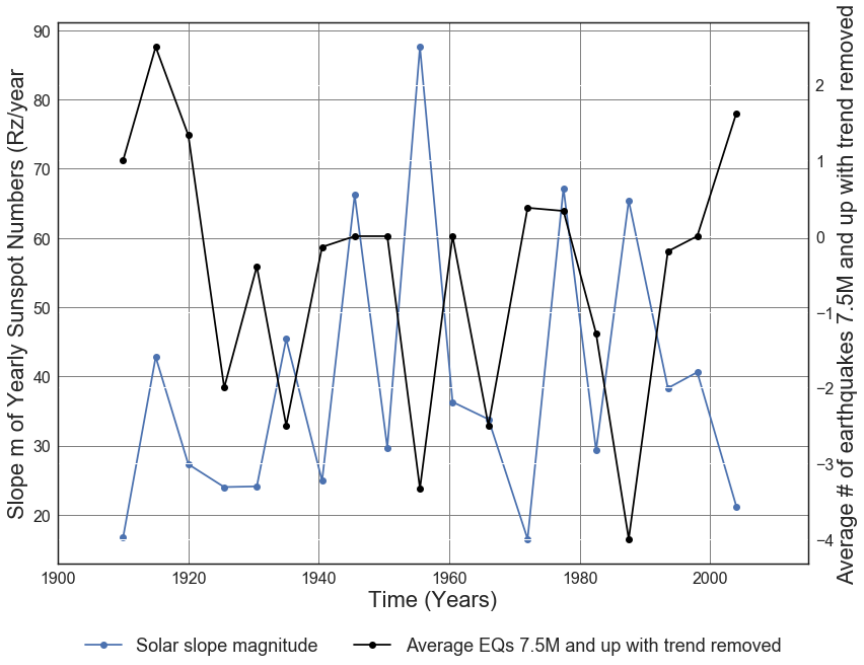

Figure D1.8: Absolute value of solar cycle slope from 1900 to 2014 vs. Average number of 7.5M and up Earthquakes with trend removed.

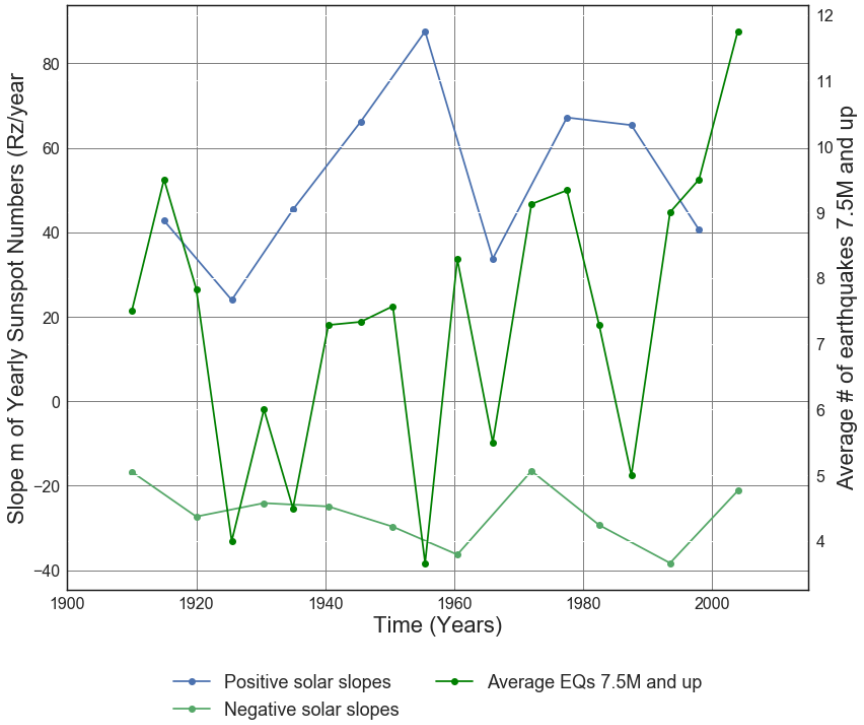

Figure D1.9: Positive and negative solar cycle slopes from 1900 to 2014 vs. Average number of 7.5M and up Earthquakes.

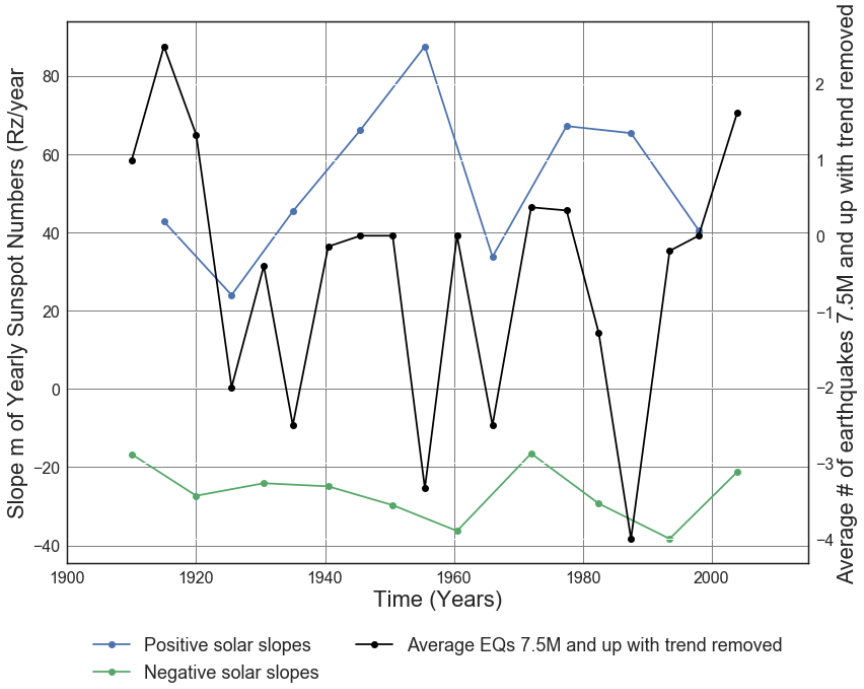

Figure D1.10: Positive and negative solar cycle slopes from 1900 to 2014 vs. Average number of 7.5M and up Earthquakes with trend removed.

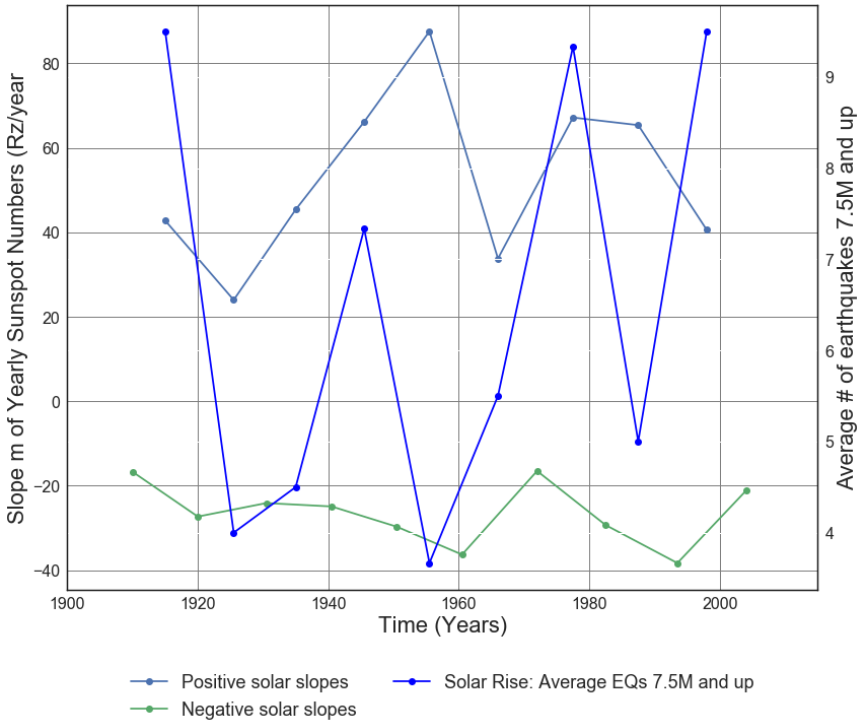

Figure D1.11: Positive and negative solar cycle slopes from 1900 to 2014 vs. Solar Rise: Average number of 7.5M and up Earthquakes.

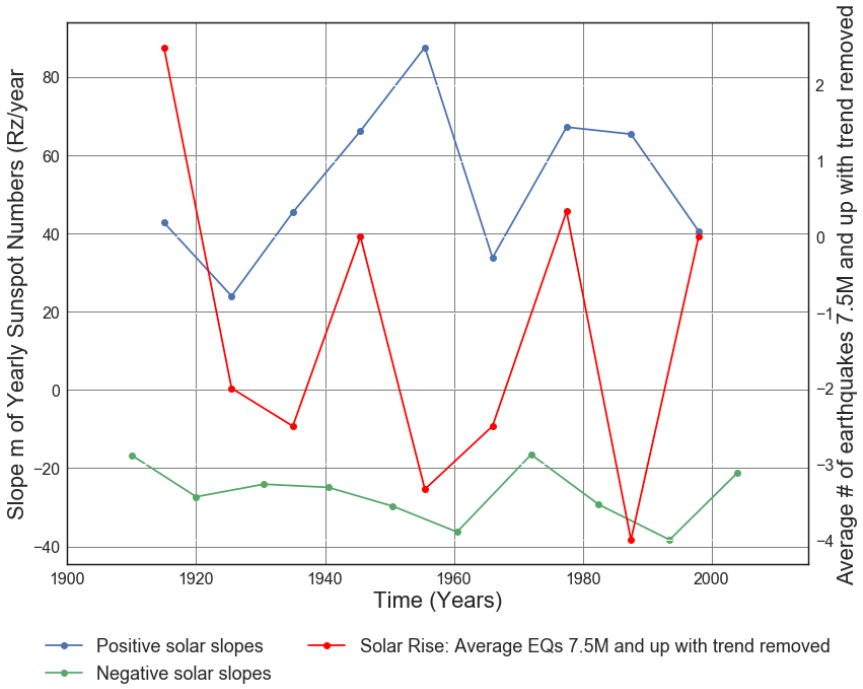

Figure D1.12: Positive and negative solar cycle slopes from 1900 to 2014 vs. Solar Rise: Average number of 7.5M and up Earthquakes with trend removed.

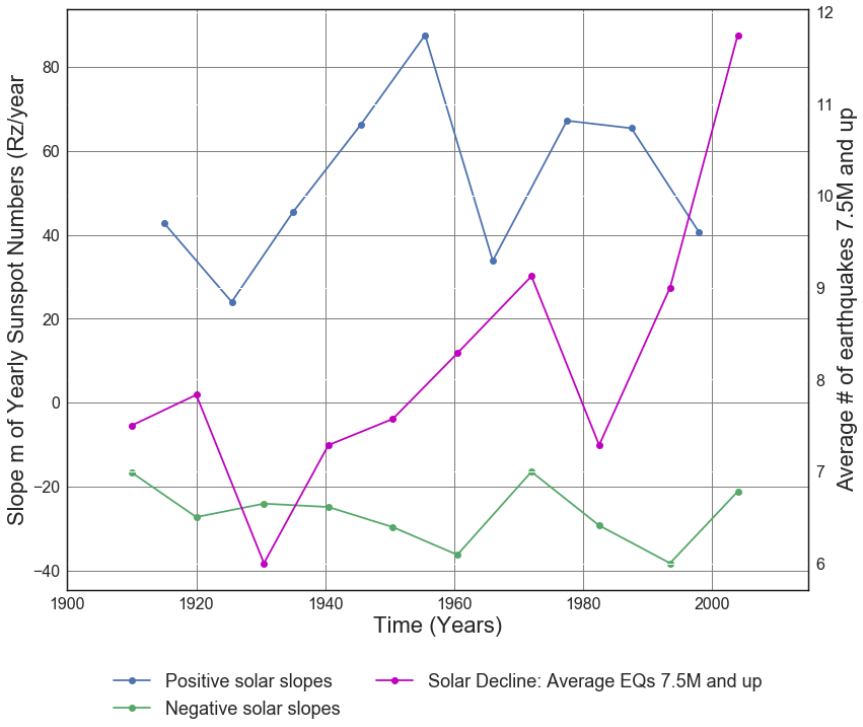

Figure D1.13: Positive and negative solar cycle slopes from 1900 to 2014 vs. Solar Decline: Average number of 7.5M and up Earthquakes.

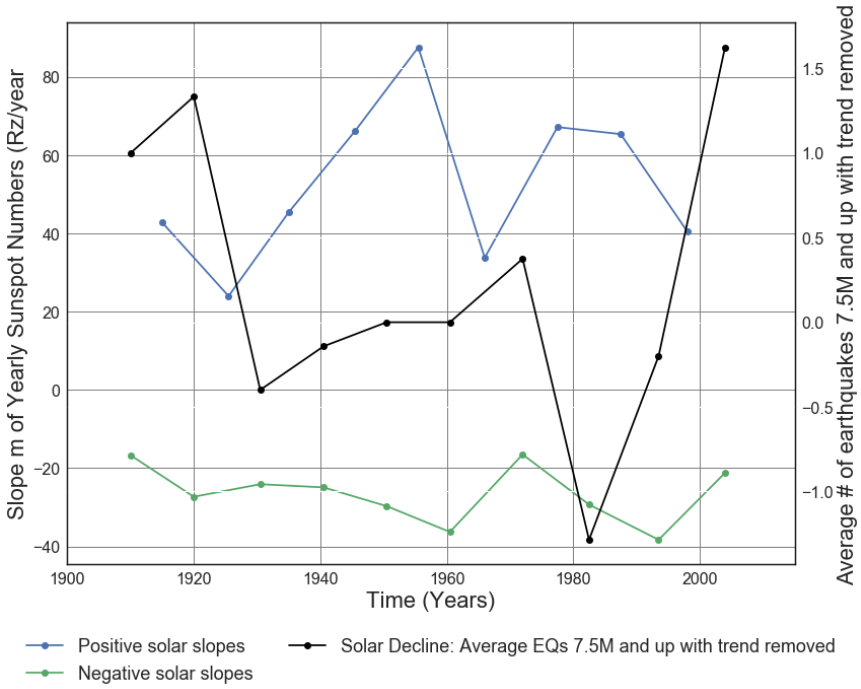

Figure D1.14: Positive and negative solar cycle slopes from 1900 to 2014 vs. Solar Rise: Average number of 7.5M and up Earthquakes.

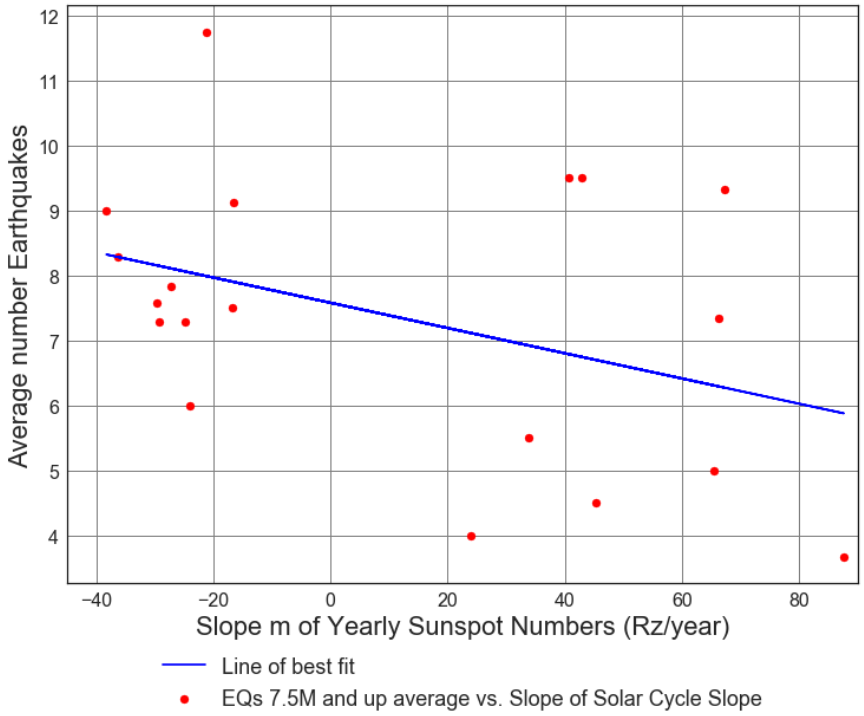

Figure D1.15: Scatter Plot of Slope m of Solar cycle (from 1900 to 2014) vs. Average number of 7.5M and up Earthquakes. Line of best fit, y = -0.01943x + (7.58), mean x = 10.98 +/- 41.86, mean y = 7.367 +/- 2.094, R = -0.3884, R squared = 0.1509, p-value = 0.1003.

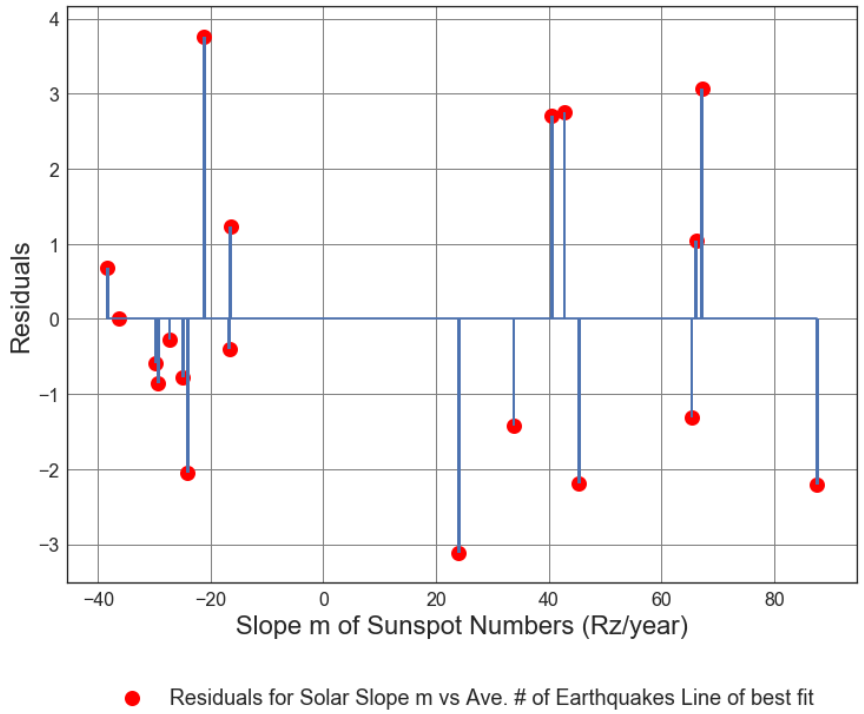

Figure D1.16: Residuals Plot of Average Solar Cycle Slope m (from 1900 to 2014) vs. Average number of 7.5M and up Earthquakes. Line of best fit, y = -0.01943x + (7.58), mean x = 10.98 +/- 41.86, mean y = 7.367 +/- 2.094, R = -0.3884, R squared = 0.1509, p-value = 0.1003.

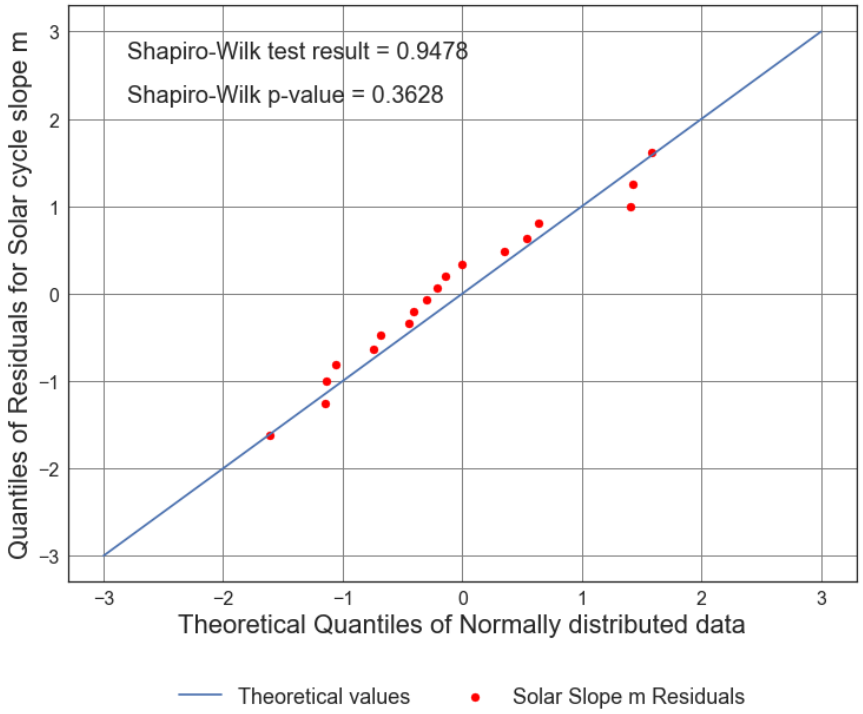

Figure D1.17: Quantile-Quantile Plot of the resisuales of Slope of Solar cycle m (from 1900 to 2014) vs. Average number of 7.5M and up Earthquakes. Line of best fit, y = -0.01943x + (7.58), mean x = 10.98 +/- 41.86, mean y = 7.367 +/- 2.094, R = -0.3884, R squared = 0.1509, p-value = 0.1003.

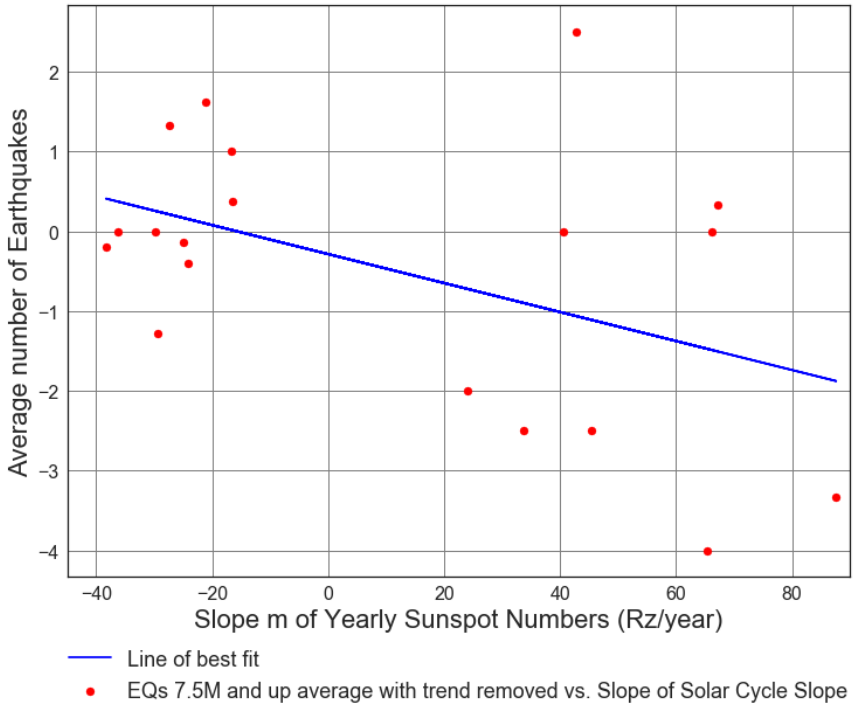

Figure D1.18: Scatter Plot of Slope m of Solar cycle (from 1900 to 2014) vs. Average number of 7.5M and up Earthquakes with trend removed. Line of best fit, y = -0.01816x + (-0.2845), mean x = 10.98 +/- 41.86, mean y = -0.484 +/- 1.669, R = -0.4552, R squared = 0.2072, p-value = 0.05017.

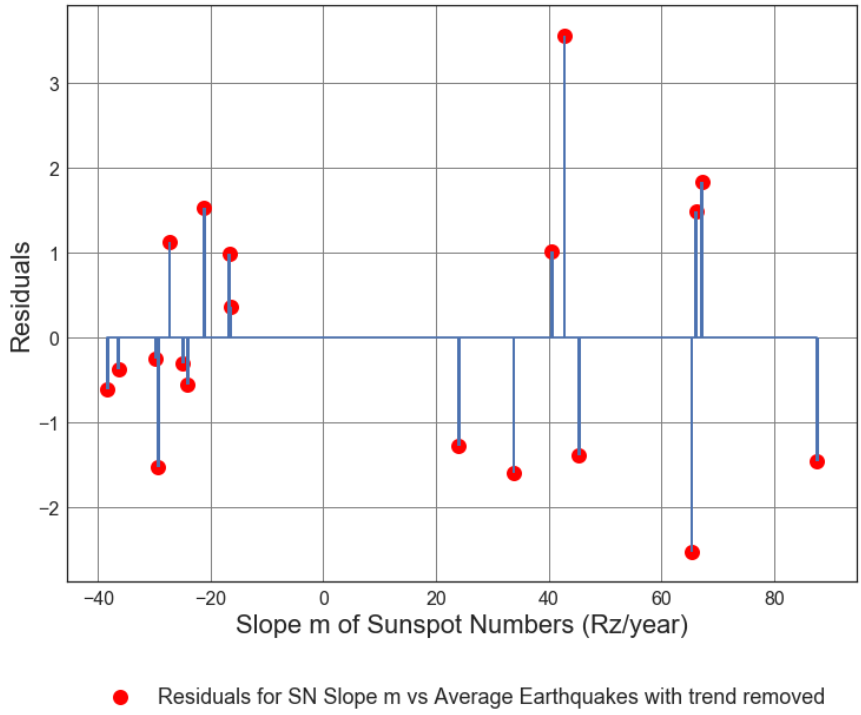

Figure D1.19: Residuals Plot of the Slope of Solar cycle (from 1900 to 2014) vs. Average number of 7.5M and up Earthquakes with trend removed. Line of best fit, y = -0.01816x + (-0.2845), mean x = 10.98 +/- 41.86, mean y = -0.484 +/- 1.669, R = -0.4552, R squared = 0.2072, p-value = 0.05017.

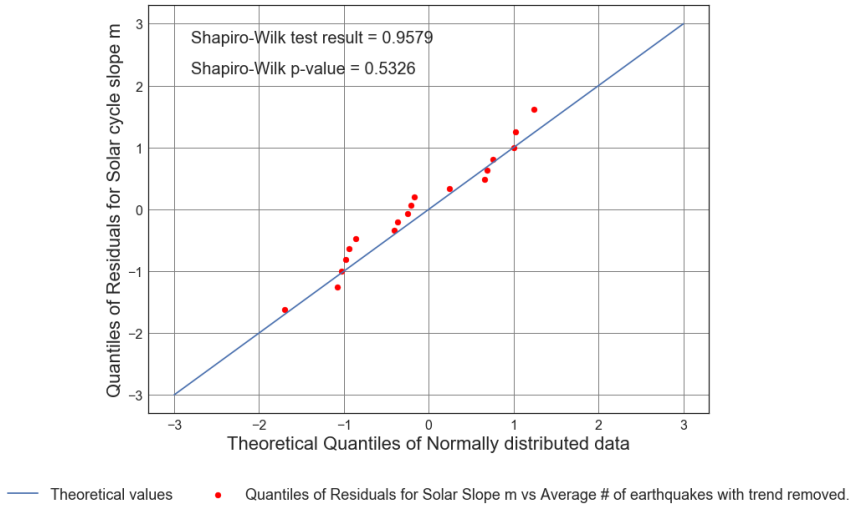

Figure D1.20: Scatter Plot of Absolute Magnitude of the Slope of Solar cycle (from 1900 to 2014) vs. Average number of 7.5M and up Earthquakes. Line of best fit, y = -0.01816x + (-0.2845), mean x = 10.98 +/- 41.86, mean y = -0.484 +/- 1.669, R = -0.4552, R squared = 0.2072, p-value = 0.05017.

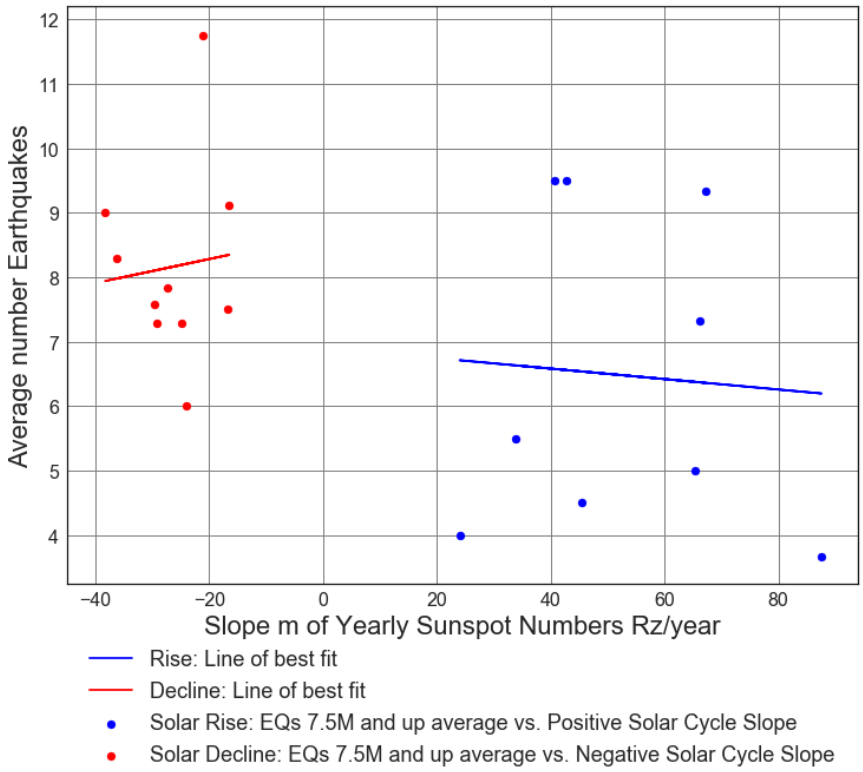

Figure D1.21: Scatter Plot of Slope of Solar cycle (from 1900 to 2014) vs. Average number of 7.5M and up Earthquakes. Rise: Line of best fit, y = -0.008115x + (6.908), mean x = 52.56 +/- 19.0, mean y = 6.481 +/- 2.315, R = -0.1921, R squared = 0.0369, p-value = 0.595. Decline: Line of best fit, y = 0.01865x + 8.657, mean x = -26.43 +/- 6.974, mean y = 8.164 +/- 1.47, R = 0.08846, R squared = 0.007826, p-value = 0.808.

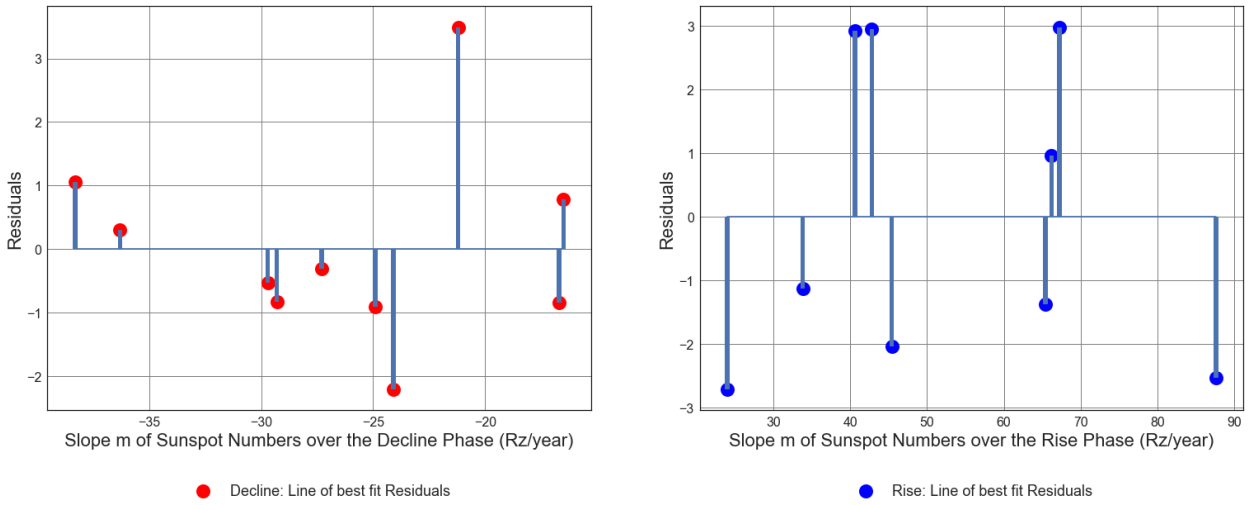

Figure D1.22: Residuals centered about zero, plot of Slope of Solar cycle (from 1900 to 2014) vs. Average number of 7.5M and up Earthquakes. Rise: Line of best fit, y = -0.008115x + (6.908), mean x = 52.56 +/- 19.0, mean y = 6.481 +/- 2.315, R = -0.1921, R squared = 0.0369, p-value = 0.595. Decline: Line of best fit, y = 0.01865x + 8.657, mean x = -26.43 +/- 6.974, mean y = 8.164 +/- 1.47, R = 0.08846, R squared = 0.007826, p-value = 0.808.

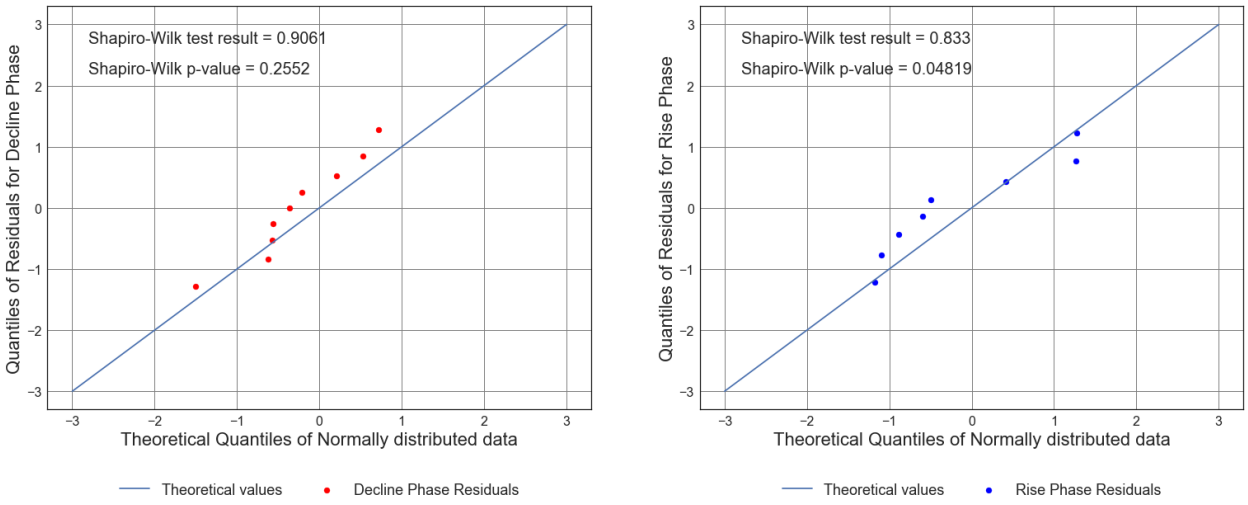

Figure D1.23: Quartile-Quartile Plot of Residuals for the Rise and Decline phase Slope of Solar cycle (from 1900 to 2014) vs. Average number of 7.5M and up Earthquakes. Rise: Line of best fit, y = -0.008115x + (6.908), mean x = 52.56 +/- 19.0, mean y = 6.481 +/- 2.315, R = -0.1921, R squared =

0.0369, p-value = 0.595. Decline: Line of best fit, y = 0.01865x + 8.657, mean x = -26.43 +/- 6.974, mean y = 8.164 +/- 1.47, R = 0.08846, R squared = 0.007826, p-value = 0.808.

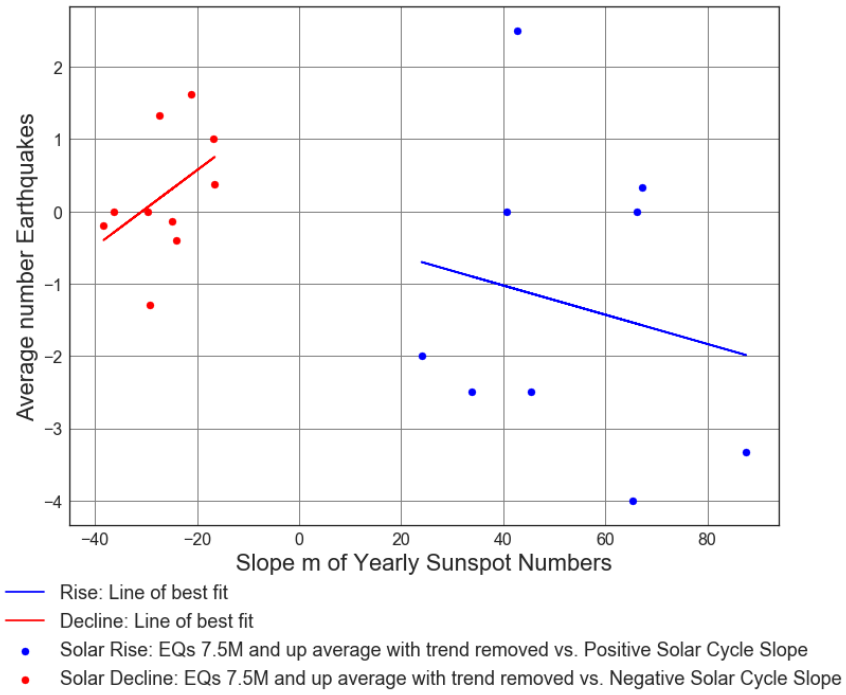

Figure D1.24: Scatter Plot of Slope of Solar cycle (from 1900 to 2014) vs. with trend removed Average number of 7.5M and up Earthquakes. Rise: Line of best fit, y = -0.02025x + (-0.2136), mean x = 52.56 +/- 19.0, mean y = -1.278 +/- 1.98, R = -0.1944, R squared = 0.03777, p-value = 0.6163. Decline: Line of best fit, y = 0.05285x + 1.627, mean x = -26.43 +/- 6.974, mean y = 0.2305 +/- 0.8307, R = 0.4437, R squared = 0.1969, p-value = 0.199.

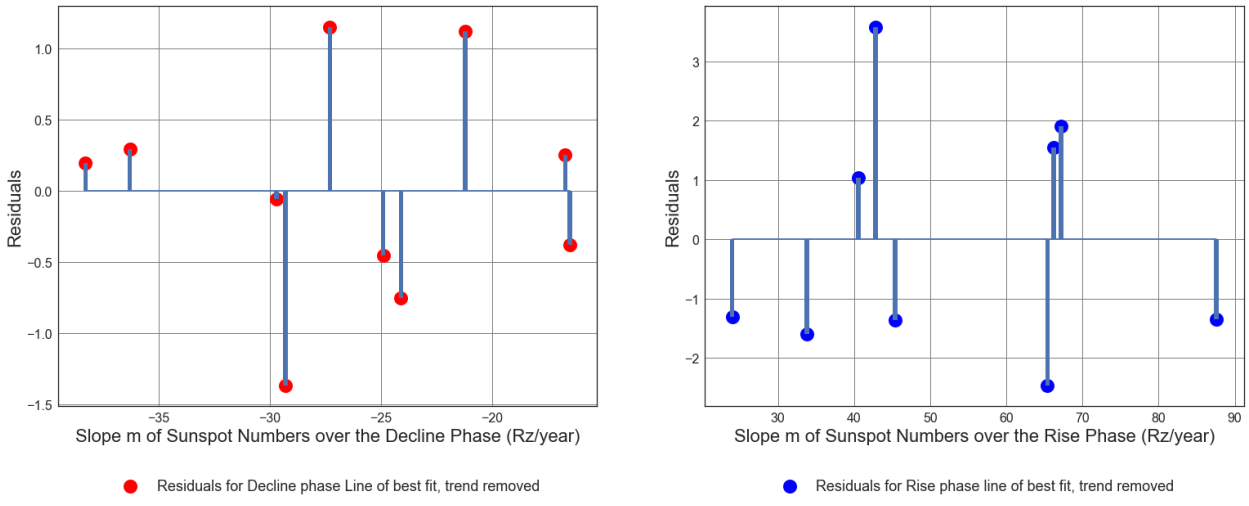

Figure D1.25: Residuals centered about zero, plot of Slope of Solar cycle (from 1900 to 2014) vs. Average number of 7.5M and up Earthquakes with trend removed. Rise: Line of best fit, y =

-0.02025x + (-0.2136), mean x = 52.56 +/- 19.0, mean y = -1.278 +/- 1.98, R = -0.1944, R squared = 0.03777, p-value = 0.6163. Decline: Line of best fit, y = 0.05285x + 1.627, mean x = -26.43 +/- 6.974, mean y = 0.2305 +/- 0.8307, R = 0.4437, R squared = 0.1969, p-value = 0.199.

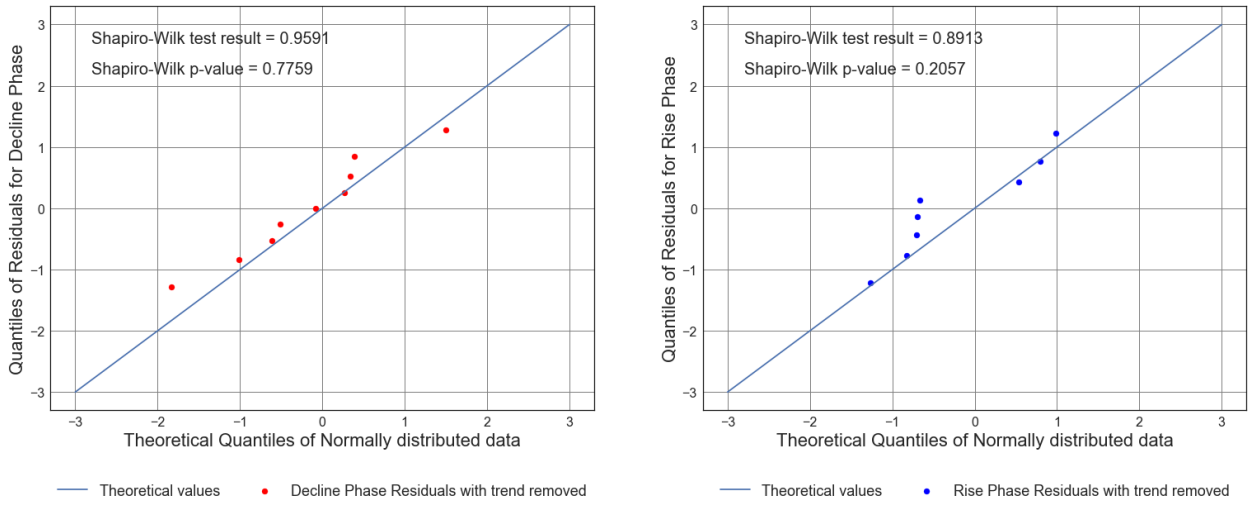

Figure D1.26: Quartile-Quartile Plot of Residuals for the Rise and Decline phase Slope of Solar cycle (from 1900 to 2014) vs. Average number of 7.5M and up Earthquakes with trend removed. Rise: Line of best fit, y = -0.02025x + (-0.2136), mean x = 52.56 +/- 19.0, mean y = -1.278 +/- 1.98, R = -0.1944, R squared = 0.03777, p-value = 0.6163. Decline: Line of best fit, y = 0.05285x + 1.627, mean x = -26.43 +/- 6.974, mean y = 0.2305 +/- 0.8307, R = 0.4437, R squared = 0.1969, p-value = 0.199.

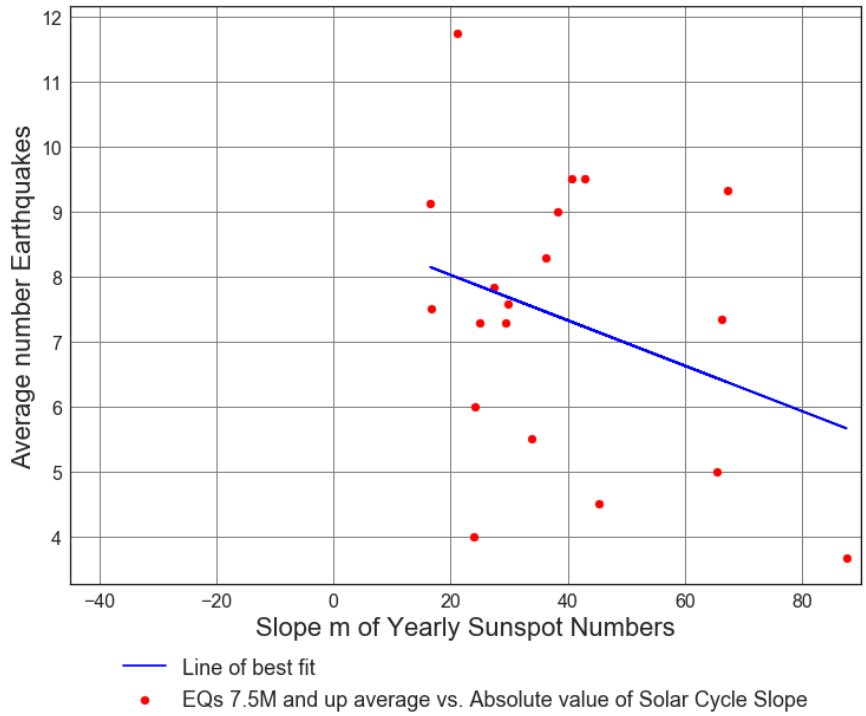

Figure D1.27: Scatter Plot of Absolute Value of the Slope of Solar cycle (from 1900 to 2014) vs. Average number of 7.5M and up Earthquakes. Line of best fit, y = -0.03495x + (8.723), mean x = 38.81 +/- 19.15, mean y = 7.367 +/- 2.094, R = -0.3198, R squared = 0.1023, p-value = 0.182.

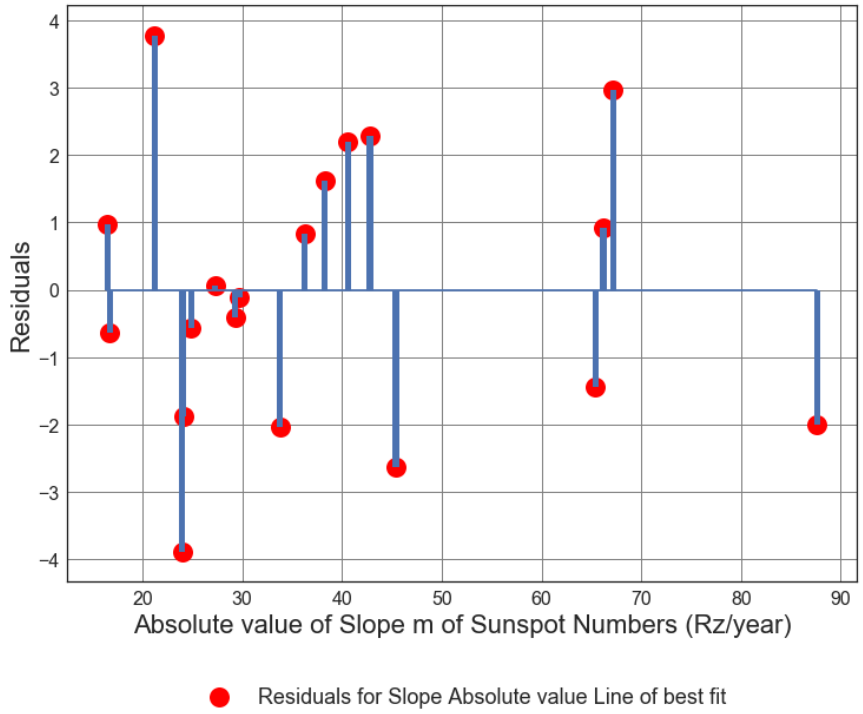

Figure D1.28: Residuals Plot of Absolute Magnitude of the Slope of Solar cycle (from 1900 to 2014) vs. Average number of 7.5M and up Earthquakes. Line of best fit, y = -0.03495x + (8.723), mean x = 38.81 +/- 19.15, mean y = 7.367 +/- 2.094, R = -0.3198, R squared = 0.1023, p-value = 0.182.

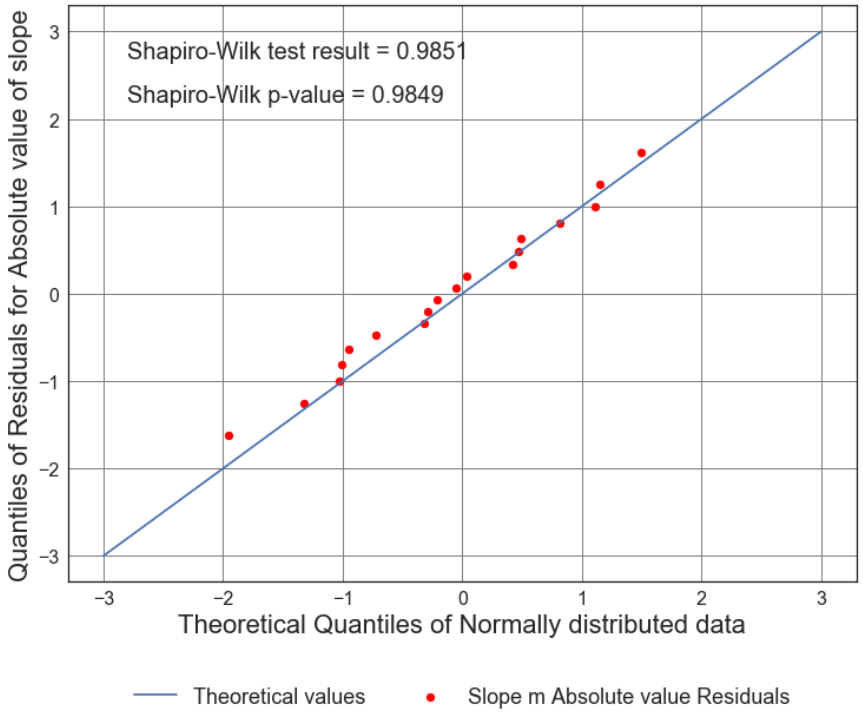

Figure D1.29: Scatter Plot of Absolute Magnitude of the Slope of Solar cycle (from 1900 to 2014) vs. Average number of 7.5M and up Earthquakes. Line of best fit, y = -0.03495x + (8.723), mean x = 38.81 +/- 19.15, mean y = 7.367 +/- 2.094, R = -0.3198, R squared = 0.1023, p-value = 0.182.

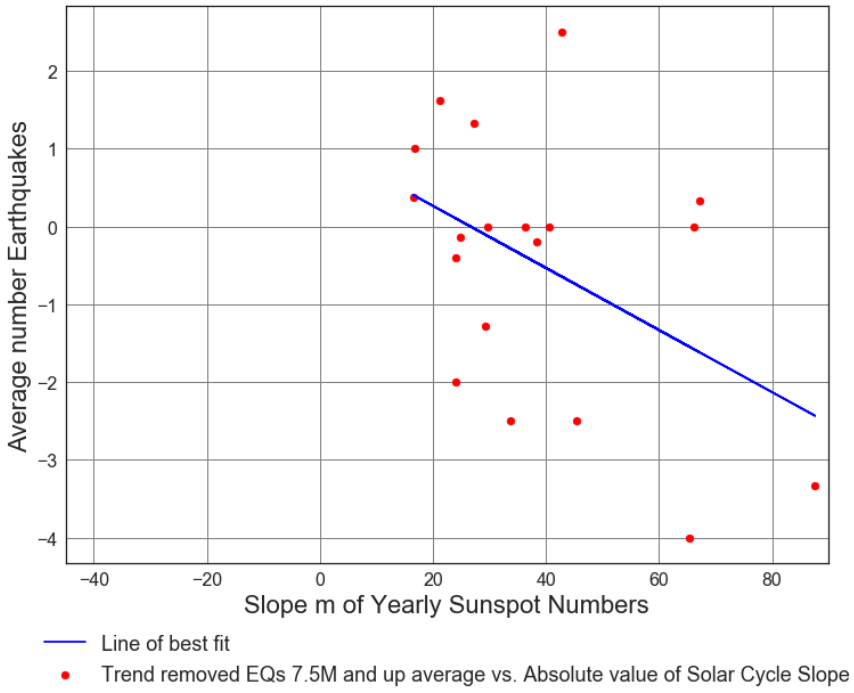

Figure D1.30: Scatter Plot of Absolute Slope Magnitude of the Solar cycle (from 1900 to 2014) vs. Trend removed Average number of 7.5M and up Earthquakes. Line of best fit, y = -0.03991x + (1.065), mean x = 38.81 +/- 19.15, mean y = -0.484 +/- 1.669, R = -0.4579, R squared = 0.2096, p-value = 0.04869.

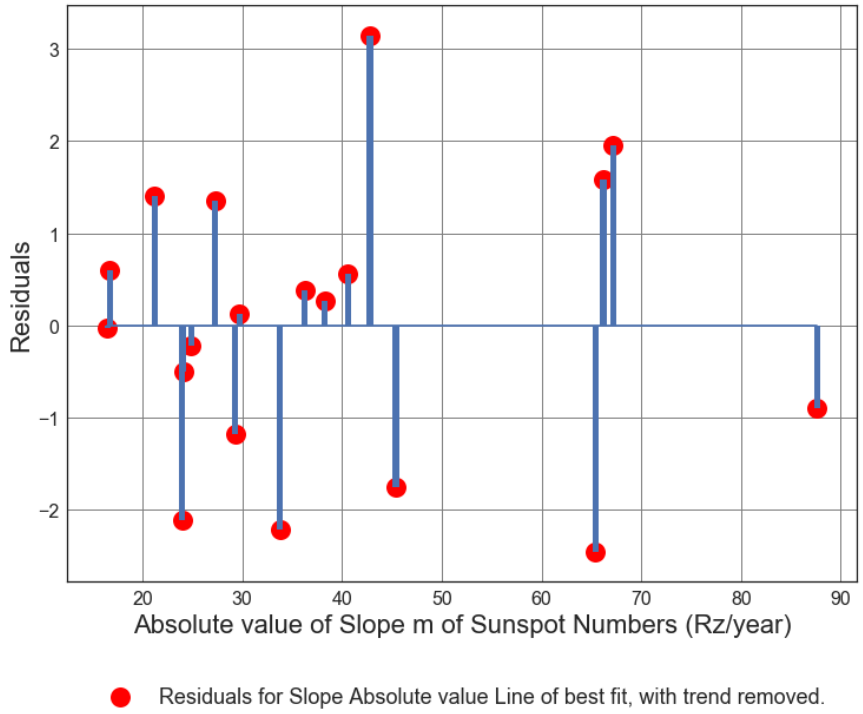

Figure D1.31: Scatter Plot of Absolute Slope Magnitude of the Solar cycle (from 1900 to 2014) vs. Trend removed Average number of 7.5M and up Earthquakes. Line of best fit, y = -0.03991x + (1.065), mean x = 38.81 +/- 19.15, mean y = -0.484 +/- 1.669, R = -0.4579, R squared = 0.2096, p-value = 0.04869.

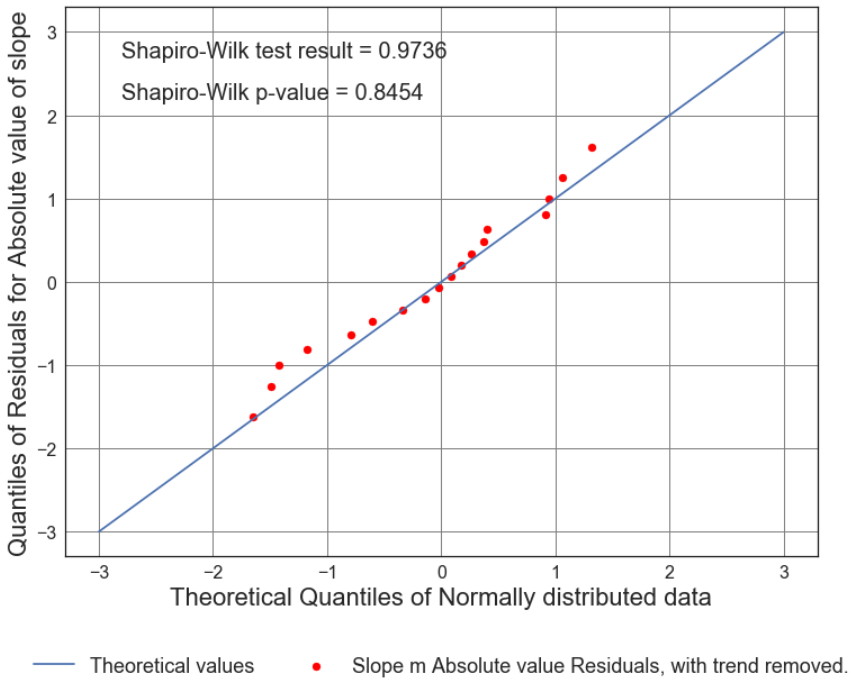

Figure D1.32: Scatter Plot of Absolute Slope Magnitude of the Solar cycle (from 1900 to 2014) vs. Trend removed Average number of 7.5M and up Earthquakes. Line of best fit, y = -0.03991x + (1.065), mean x = 38.81 +/- 19.15, mean y = -0.484 +/- 1.669, R = -0.4579, R squared = 0.2096, p-value = 0.04869.

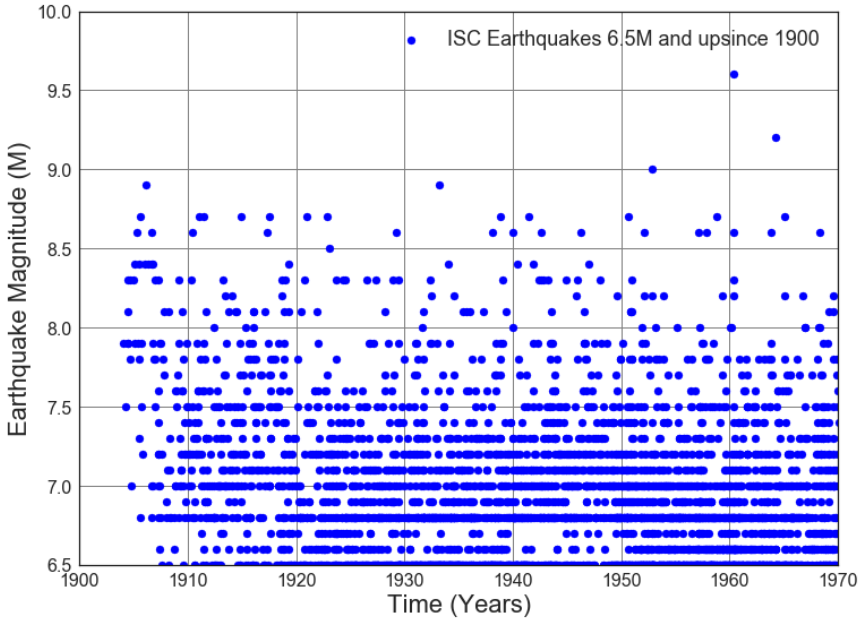

Figure D1.33: Scatter plot of ISC earthquakes 6.5M and up magnitudes 1900 to 1970

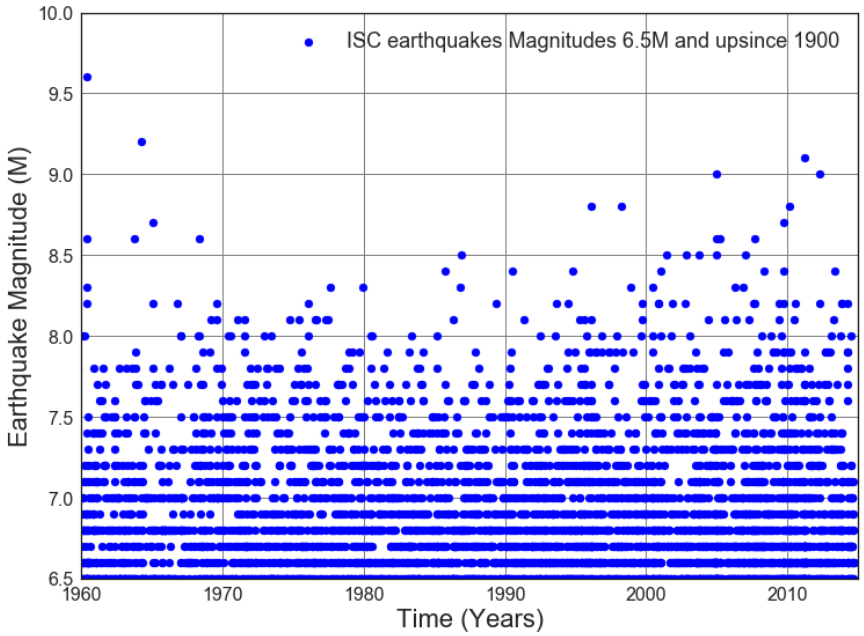

Figure D1.34: Scatter plot of ISC earthquakes 6.5M and up Magnitudes 1960 to 2017

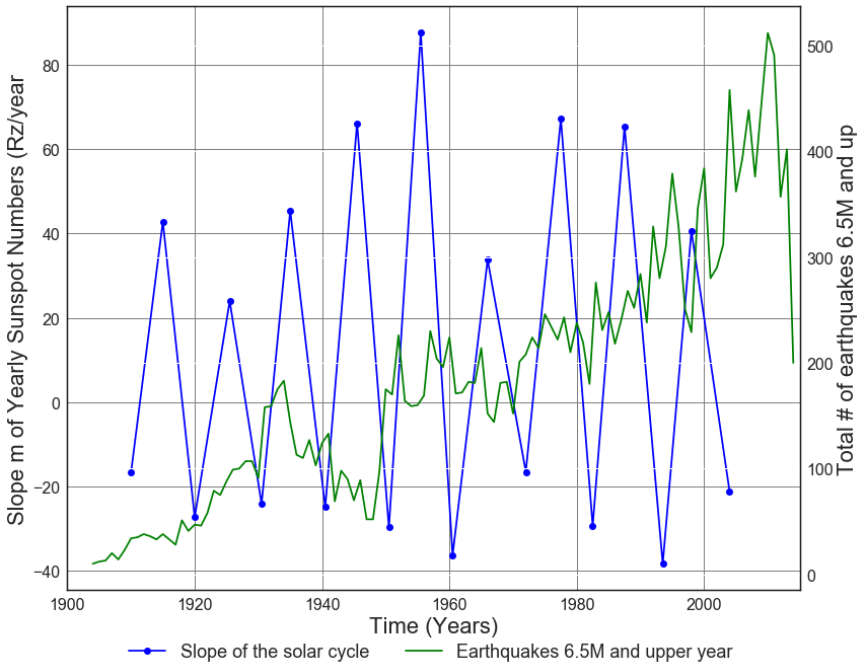

Figure D1.35: Slope of Solar cycle from 1900 to 2014 vs. Average number of 6.5M and up Earthquakes.

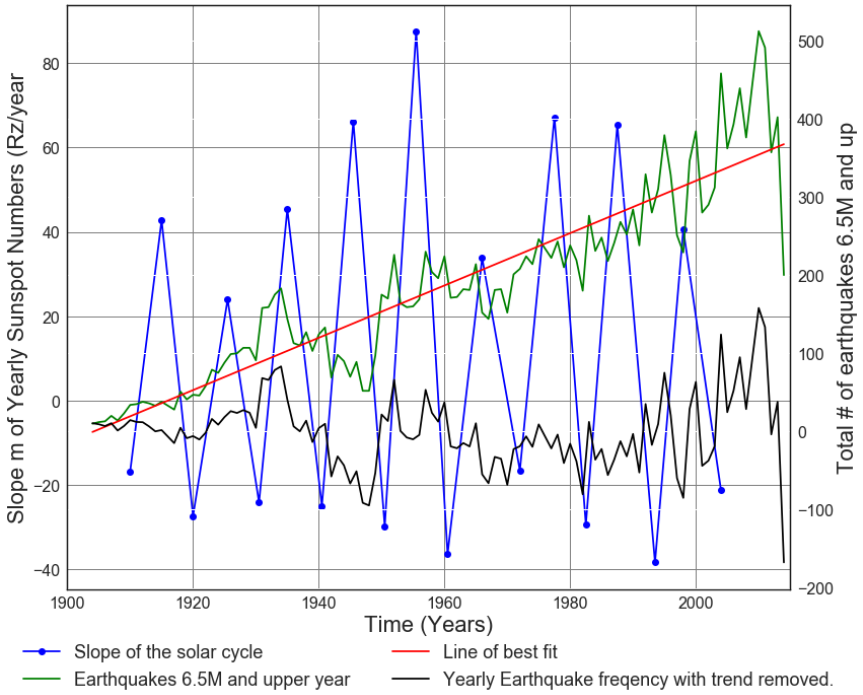

Figure D1.36: Slope of Solar cycle from 1900 to 2014 vs. Average number of 6.5M and up Earthquakes. Line of best fit, y = 3.346x + (-6.371e+03), mean x = 1.959e+03 +/- 32.04, mean y = 183.4 +/- 117.1

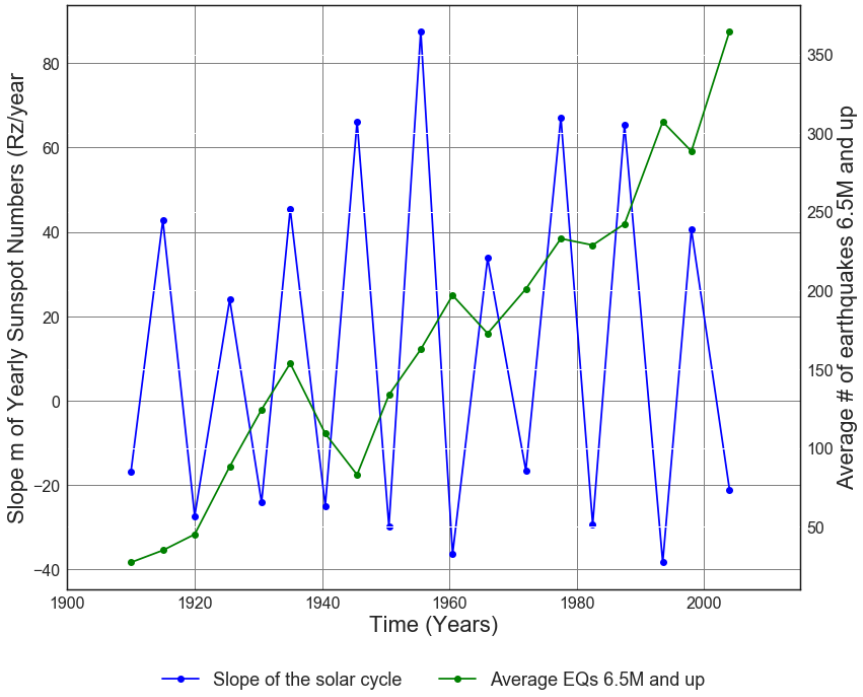

Figure D1.37: Slope of Solar cycle from 1900 to 2014 vs. Average number of 6.5M and up Earthquakes.

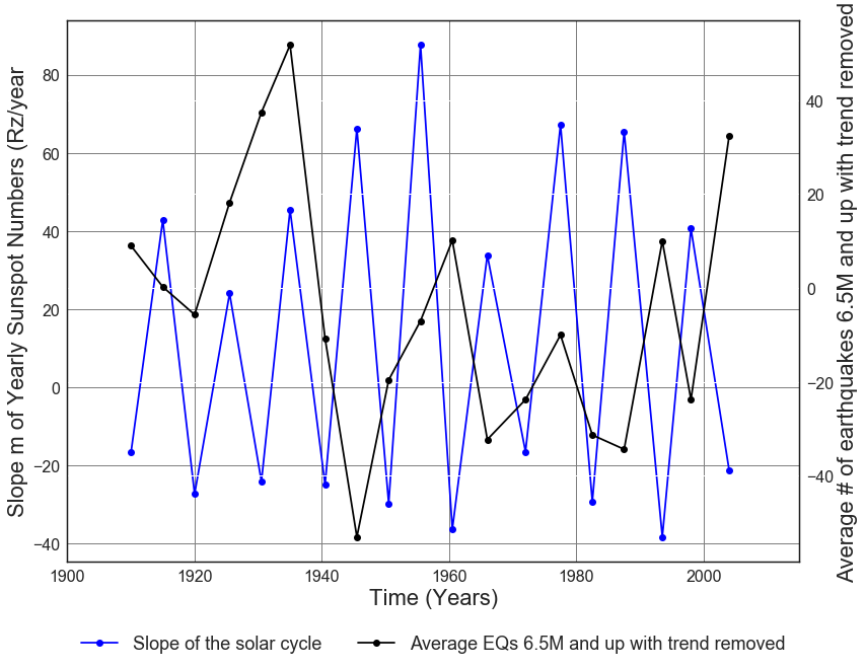

Figure D1.38: Slope of Solar cycle from 1900 to 2014 vs. Average number of 6.5M and up earthquakes.

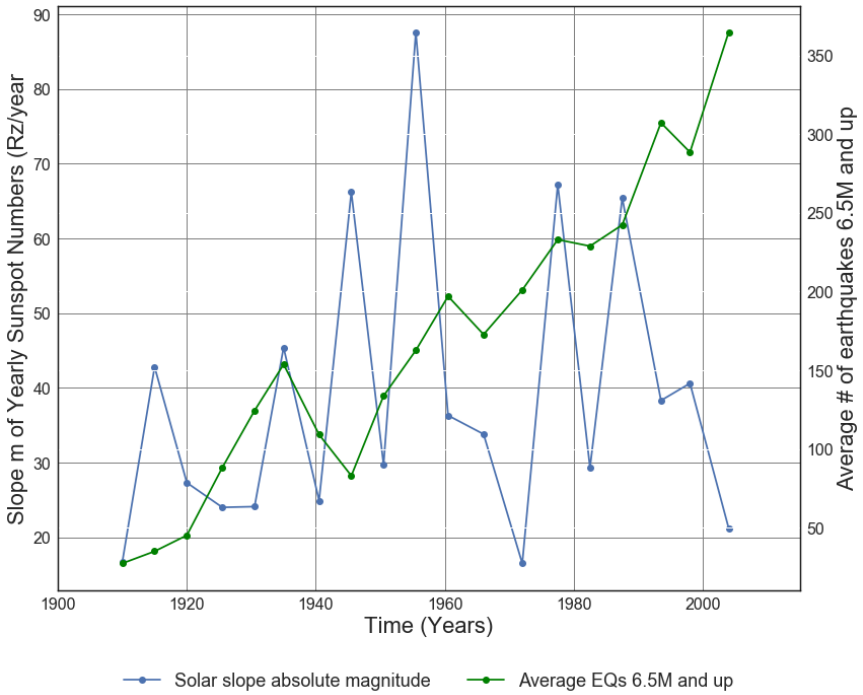

Figure D1.39: Absolute value of Solar cycle slope from 1900 to 2014 vs. Average number of 6.5M and up Earthquakes.

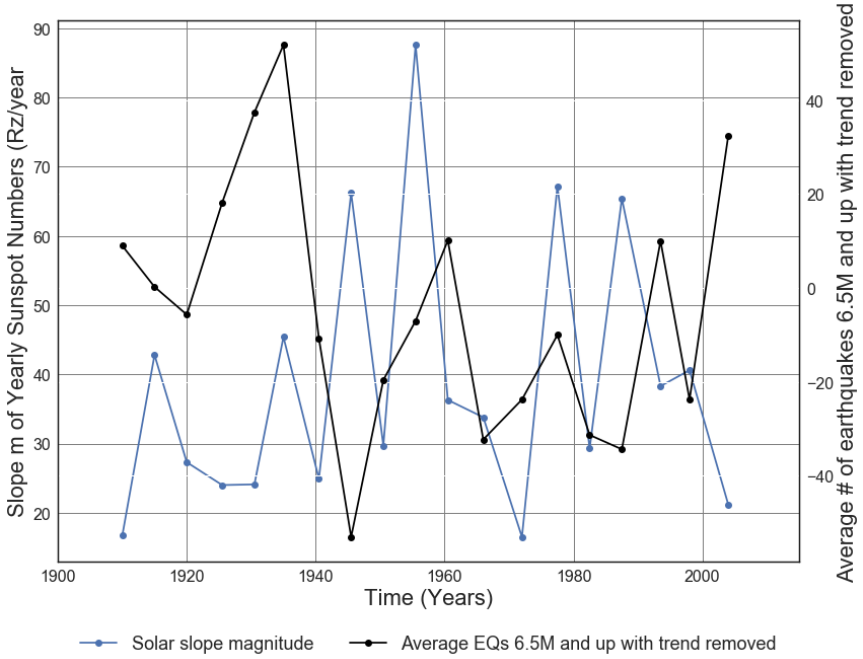

Figure D1.40: Absolute value of solar cycle slope from 1900 to 2014 vs. Average number of 6.5M and up Earthquakes with trend removed.

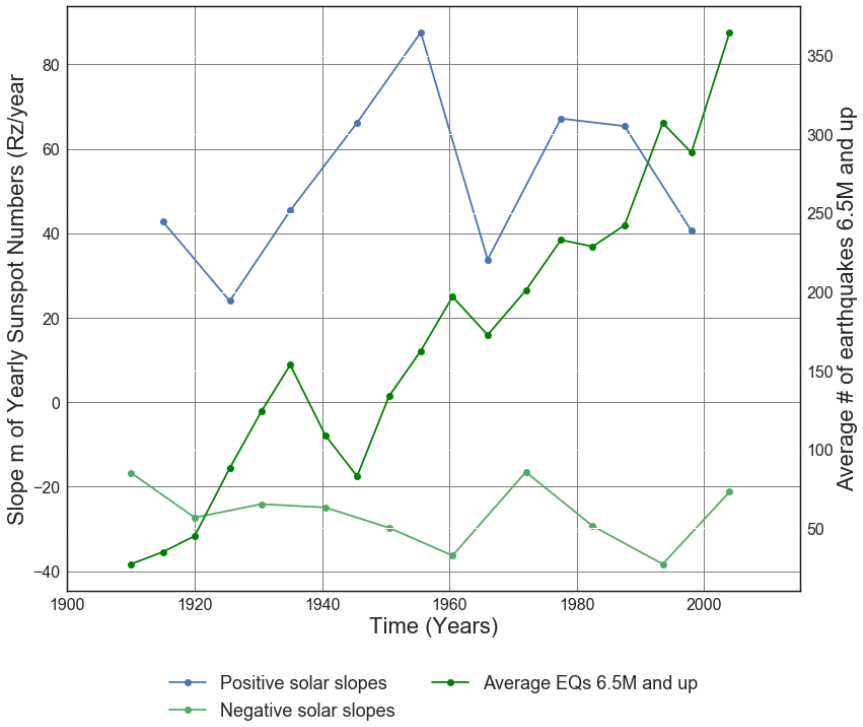

Figure D1.41: Positive and negative solar cycle slopes from 1900 to 2014 vs. Average number of 6.5M and up Earthquakes.

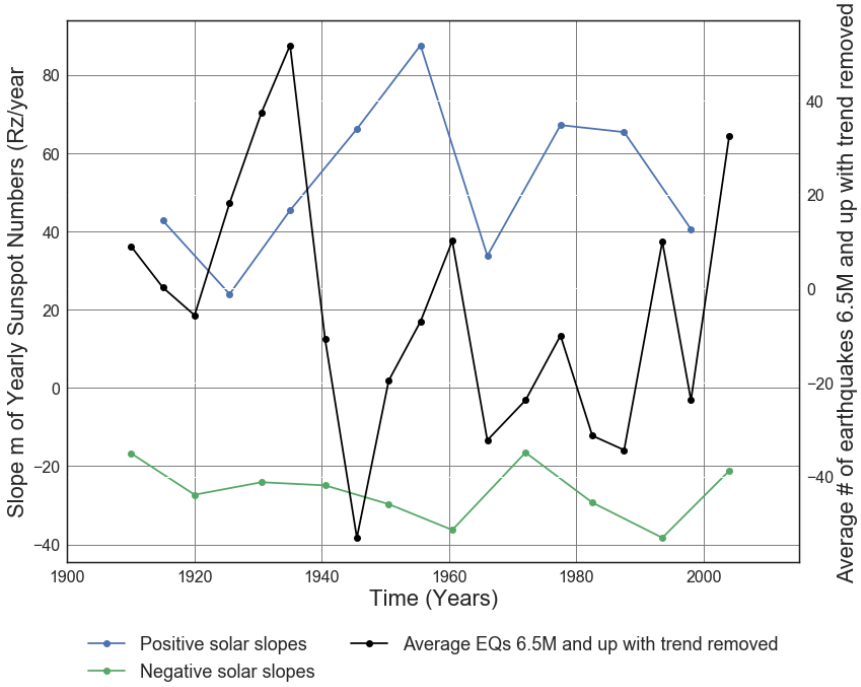

Figure D1.42: Positive and negative solar cycle slopes from 1900 to 2014 vs. Average number of 6.5M and up Earthquakes with trend removed.

Figure D1.43: Positive and negative solar cycle slopes from 1900 to 2014 vs. Solar Rise: Average number of 6.5M and up Earthquakes.

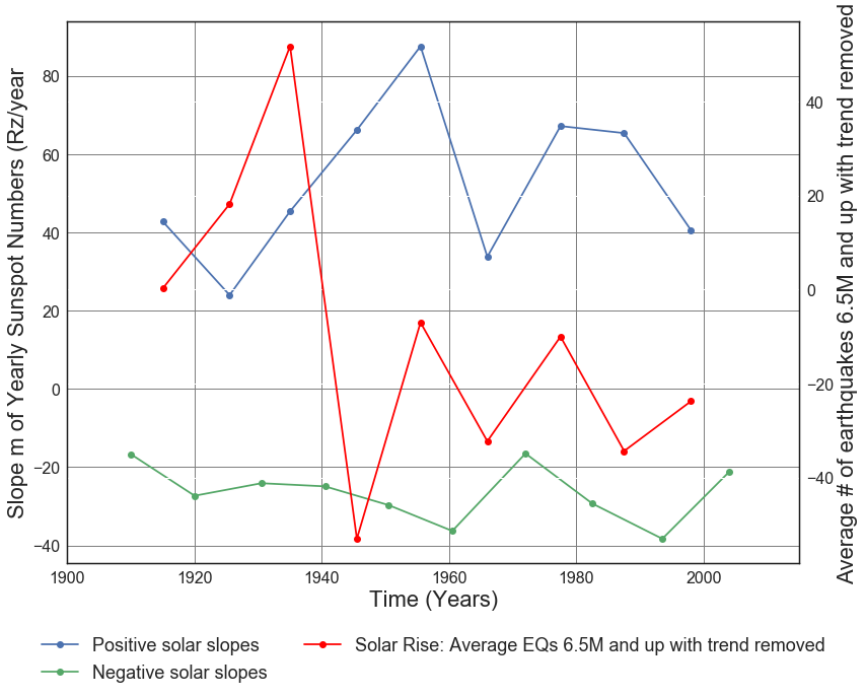

Figure D1.44: Positive and negative solar cycle slopes from 1900 to 2014 vs. Solar Rise: Average number of 6.5M and up Earthquakes with trend removed.

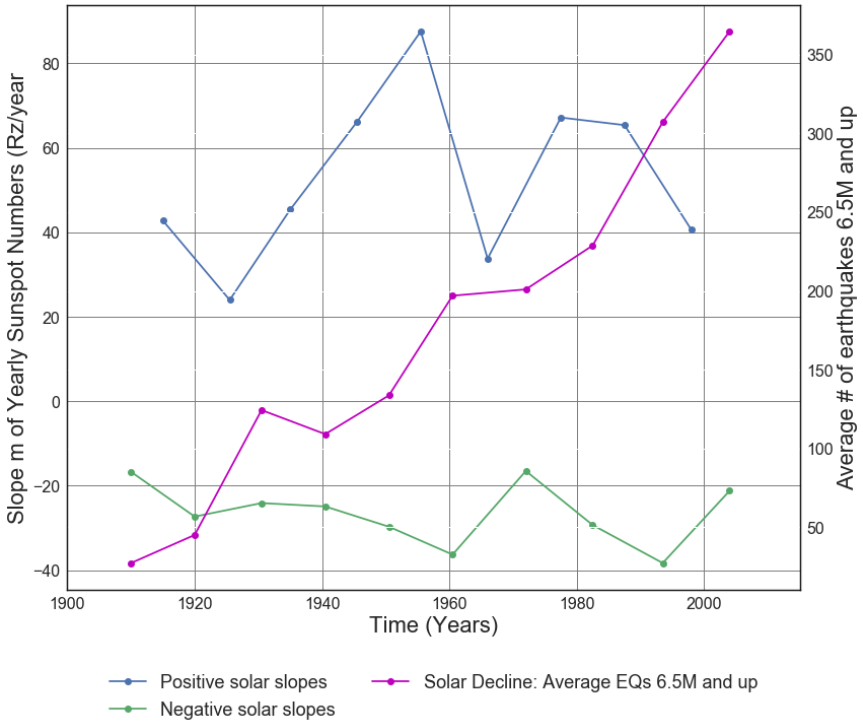

Figure D1.45: Positive and negative solar cycle slopes from 1900 to 2014 vs. Solar Decline: Average number of 6.5M and up Earthquakes.

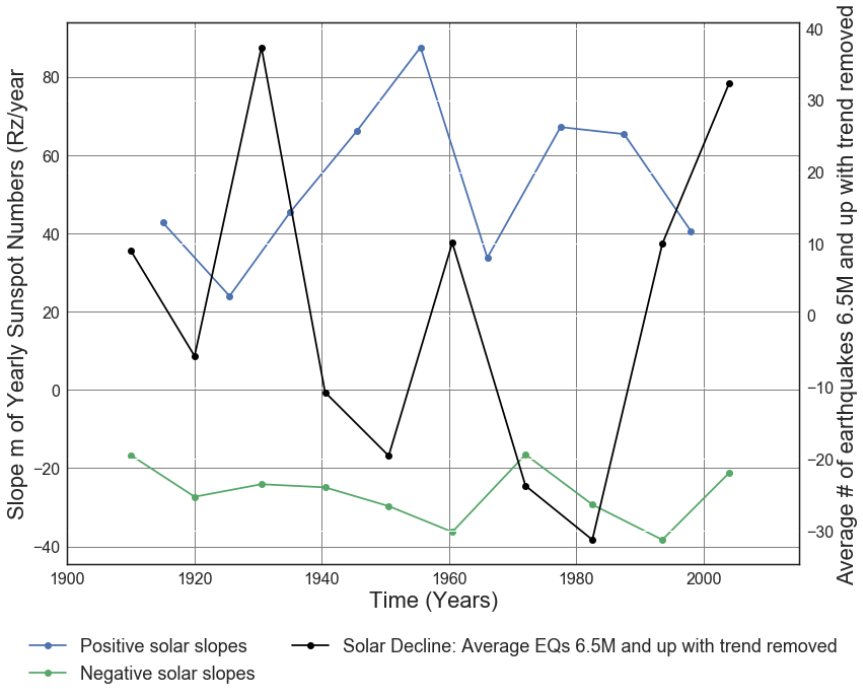

Figure D1.46: Positive and negative solar cycle slopes from 1900 to 2014 vs. Solar Rise: Average number of 6.5M and up Earthquakes.

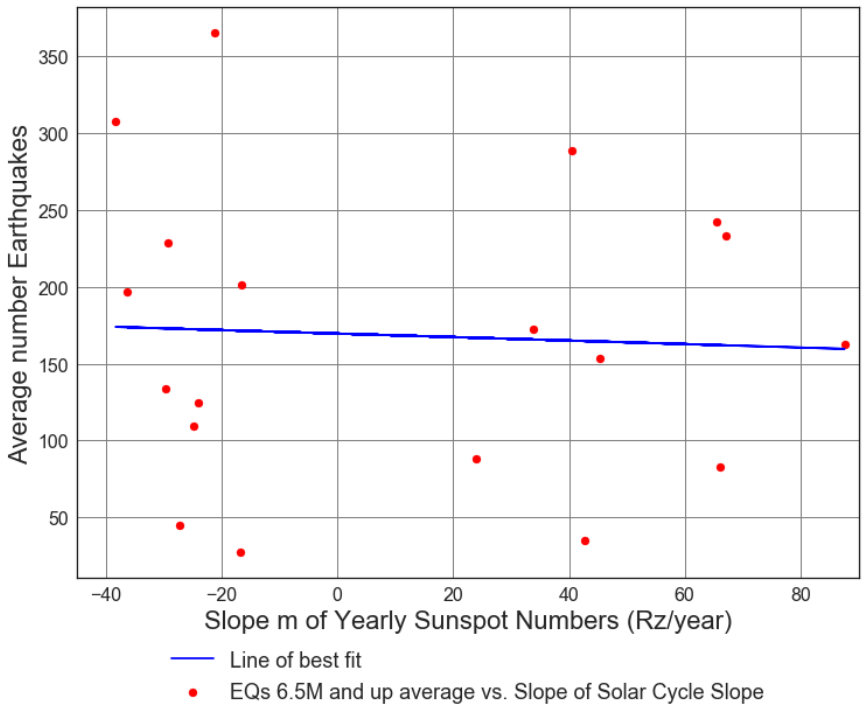

Figure D1.47: Scatter Plot of Slope m of Solar cycle (from 1900 to 2014) vs. Average number of 6.5M and up Earthquakes. Line of best fit, y = -0.1134x + (169.5), mean x = 10.98 +/- 41.86, mean y = 168.3 +/- 92.04, R = -0.05158, R squared = 0.002661, p-value = 0.8339.

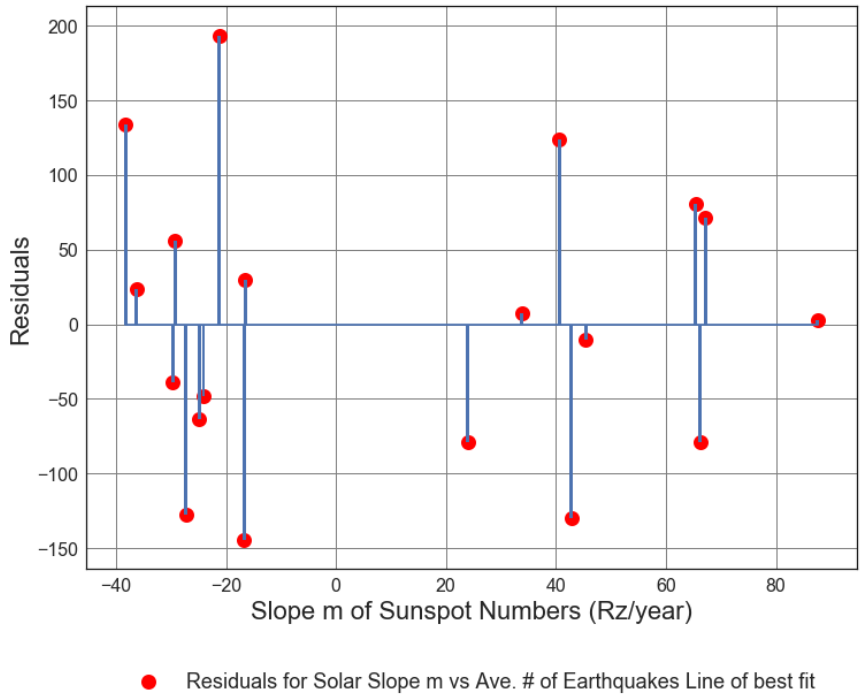

Figure D1.48: Residuals Plot of Average Solar Cycle Slope m (from 1900 to 2014) vs. Average number of 6.5M and up Earthquakes. Line of best fit, y = -0.1134x + (169.5), mean x = 10.98 +/- 41.86, mean y = 168.3 +/- 92.04, R = -0.05158, R squared = 0.002661, p-value = 0.8339.

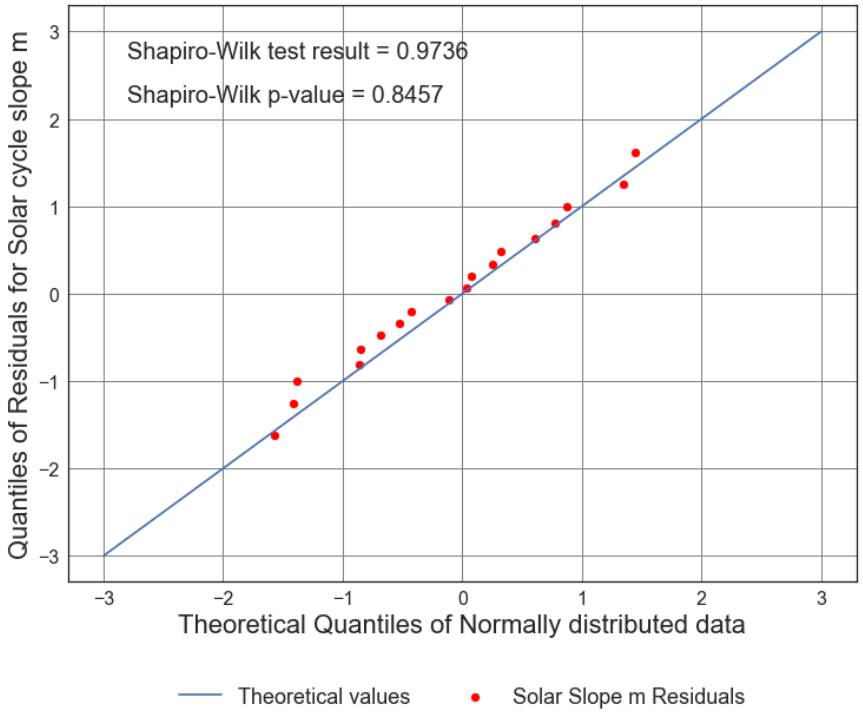

Figure D1.49: Quantile-Quantile Plot of the resisuales of Slope of Solar cycle m (from 1900 to 2014) vs. Average number of 6.5M and up Earthquakes. Line of best fit, y = -0.1134x + (169.5), mean x = 10.98 +/- 41.86, mean y = 168.3 +/- 92.04, R = -0.05158, R squared = 0.002661, p-value = 0.8339.

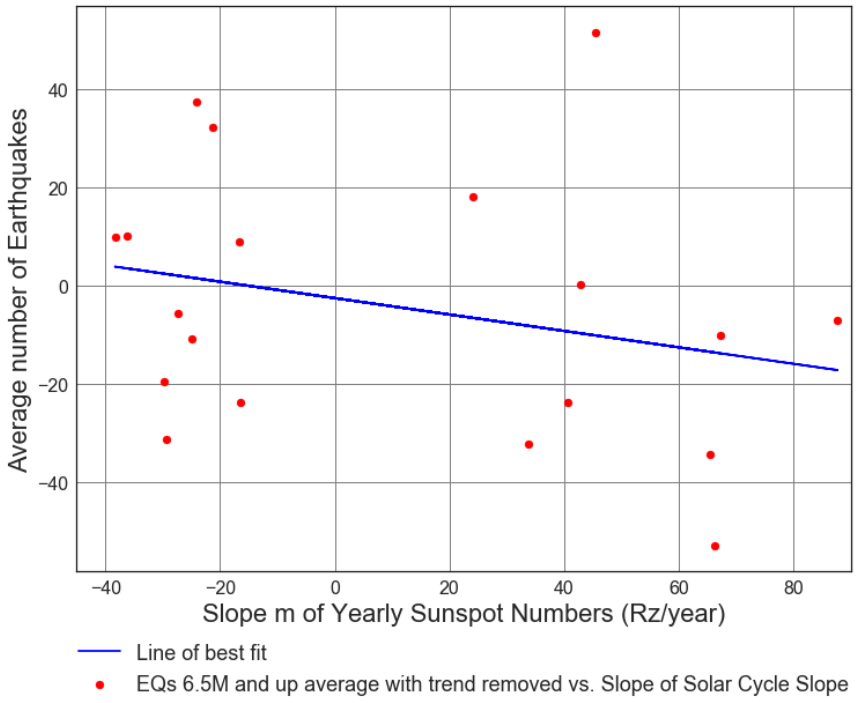

Figure D1.50: Scatter Plot of Slope m of Solar cycle (from 1900 to 2014) vs. Average number of 6.5M and up Earthquakes with trend removed. Line of best fit, y = -0.1674x + (-2.488), mean x = 10.98 +/- 41.86, mean y = -4.327 +/- 26.36, R = -0.2658, R squared = 0.07065, p-value = 0.2714.

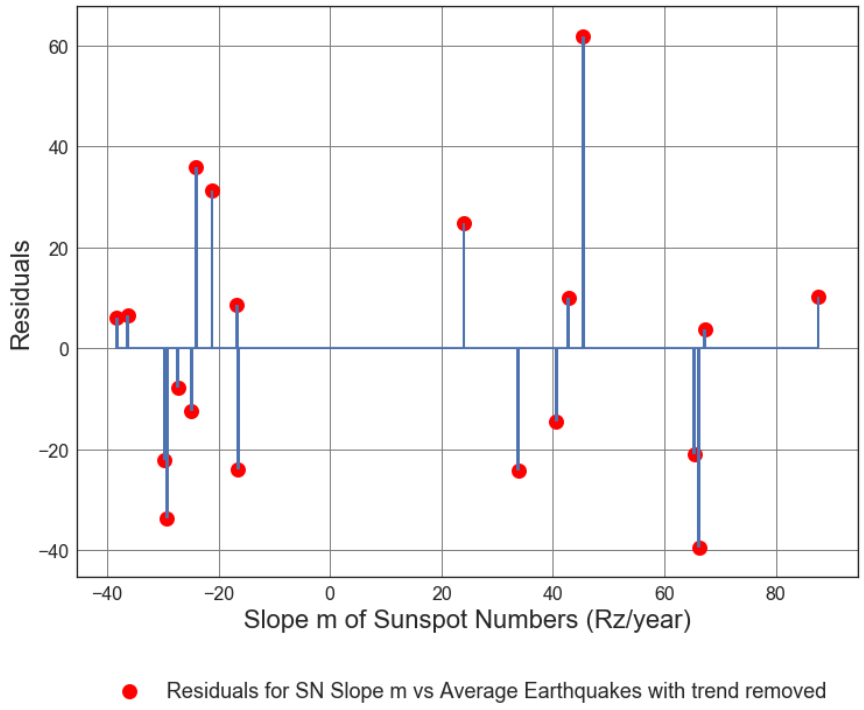

Figure D1.51: Residuals Plot of the Slope of Solar cycle (from 1900 to 2014) vs. Average number of 6.5M and up Earthquakes with trend removed. Line of best fit, y = -0.1674x + (-2.488), mean x = 10.98 +/- 41.86, mean y = -4.327 +/- 26.36, R = -0.2658, R squared = 0.07065, p-value = 0.2714.

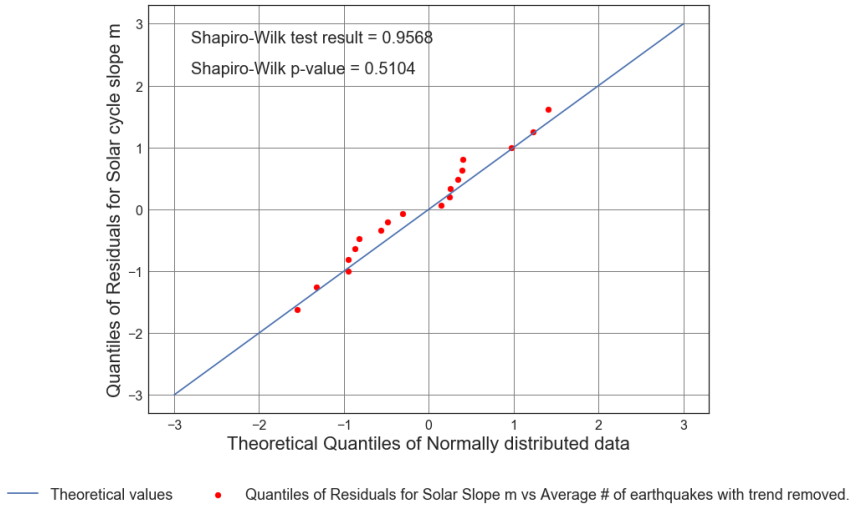

Figure D1.52: Scatter Plot of Absolute Magnitude of the Slope of Solar cycle (from 1900 to 2014) vs. Average number of 6.5M and up Earthquakes. Line of best fit, y = -0.1674x + (-2.488), mean x = 10.98 +/- 41.86, mean y = -4.327 +/- 26.36, R = -0.2658, R squared = 0.07065, p-value = 0.2714.

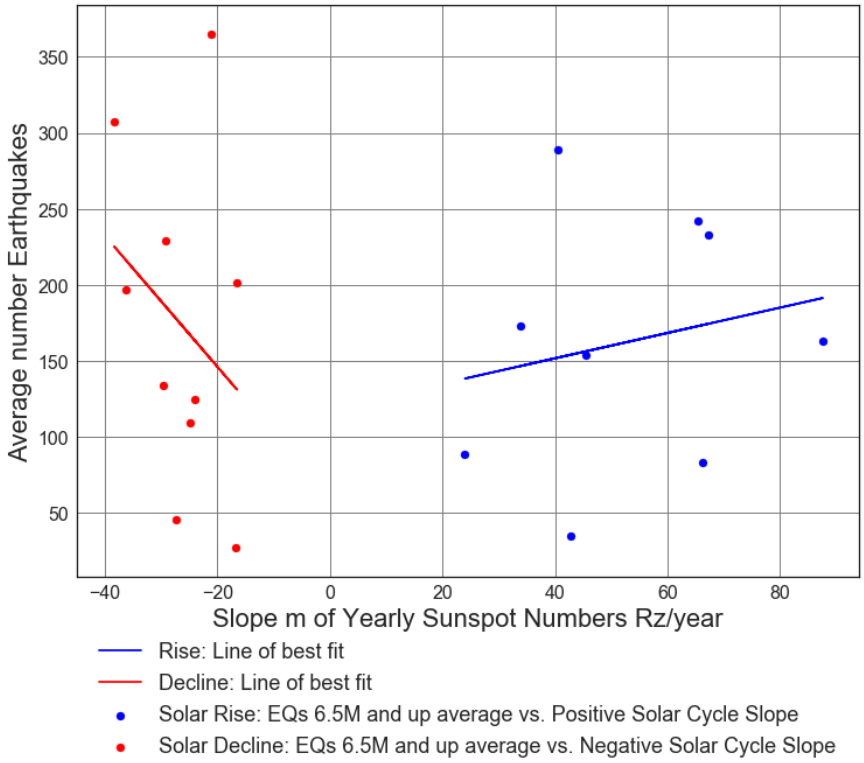

Figure D1.53: Scatter Plot of Slope of Solar cycle (from 1900 to 2014) vs. Average number of 6.5M and up Earthquakes. Rise: Line of best fit, y = 0.8333x + (118.3), mean x = 52.56 +/- 19.0, mean y = 162.1 +/- 78.53, R = 0.3729, R squared = 0.1391, p-value = 0.2885. Decline: Line of best fit, y = -4.313x + 59.86, mean x = -26.43 +/- 6.974, mean y = 173.9 +/- 102.4, R = -0.2938, R squared = 0.08634, p-value = 0.4099.

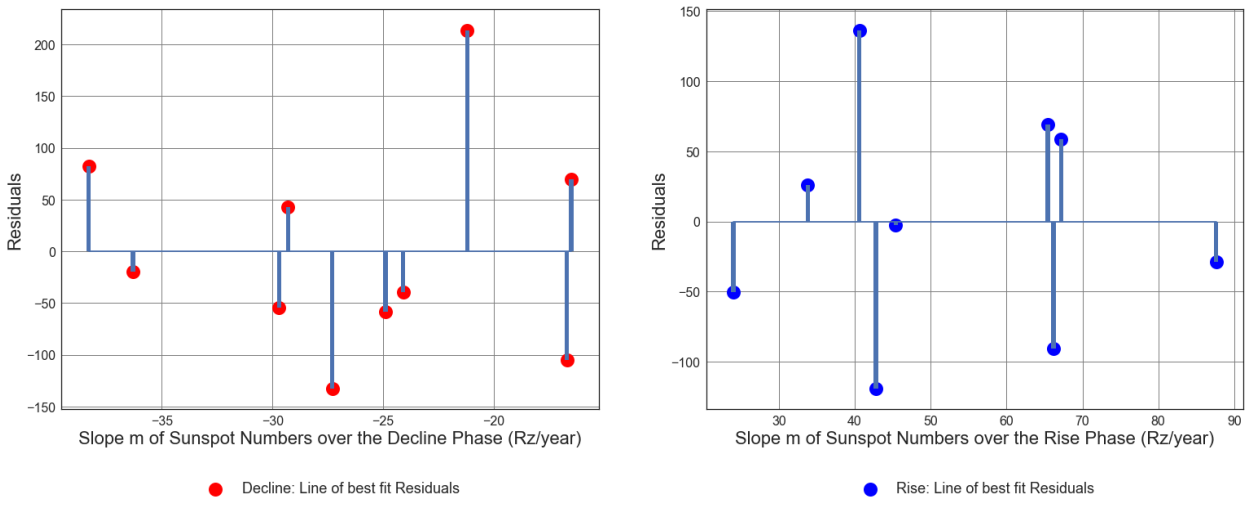

Figure D1.54: Residuals centered about zero, plot of Slope of Solar cycle (from 1900 to 2014) vs. Average number of 6.5M and up Earthquakes. Rise: Line of best fit, y = 0.8333x + (118.3), mean x = 52.56 +/- 19.0, mean y = 162.1 +/- 78.53, R = 0.3729, R squared = 0.1391, p-value = 0.2885. Decline: Line of best fit, y = -4.313x + 59.86, mean x = -26.43 +/- 6.974, mean y = 173.9 +/- 102.4, R = -0.2938, R squared = 0.08634, p-value = 0.4099.

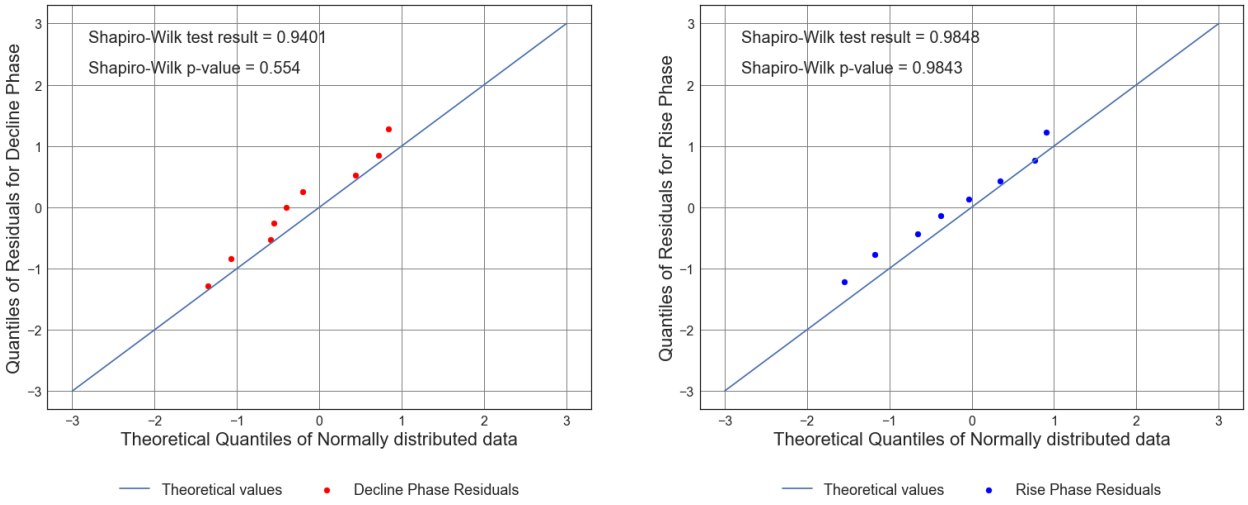

Figure D1.55: Quartile-Quartile Plot of Residuals for the Rise and Decline phase Slope of Solar cycle (from 1900 to 2014) vs. Average number of 6.5M and up Earthquakes. Rise: Line of best fit, y = 0.8333x + (118.3), mean x = 52.56 +/- 19.0, mean y = 162.1 +/- 78.53, R = 0.3729, R squared = 0.1391, p-value = 0.2885. Decline: Line of best fit, y = -4.313x + 59.86, mean x = -26.43 +/- 6.974, mean y = 173.9 +/- 102.4, R = -0.2938, R squared = 0.08634, p-value = 0.4099.

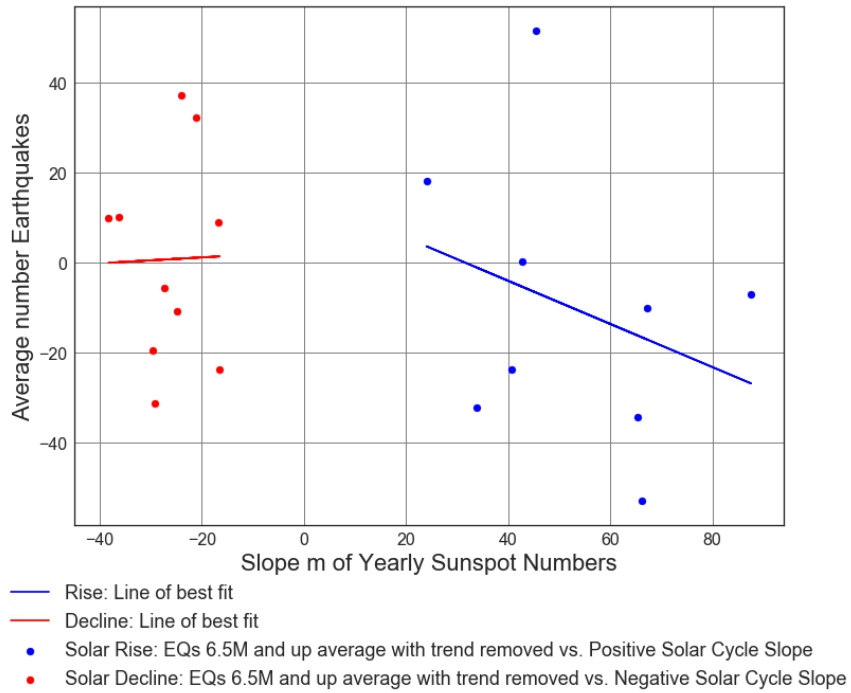

Figure D1.56: Scatter Plot of Slope of Solar cycle (from 1900 to 2014) vs. with trend removed Average number of 6.5M and up Earthquakes. Rise: Line of best fit, y = -0.4798x + (15.2), mean x = 52.56 +/- 19.0, mean y = -10.01 +/- 29.53, R = -0.3088, R squared = 0.09536, p-value = 0.4188. Decline: Line of best fit, y = 0.0652x + 2.516, mean x = -26.43 +/- 6.974, mean y = 0.793 +/- 21.9, R = 0.02076, R squared = 0.000431, p-value = 0.9546.

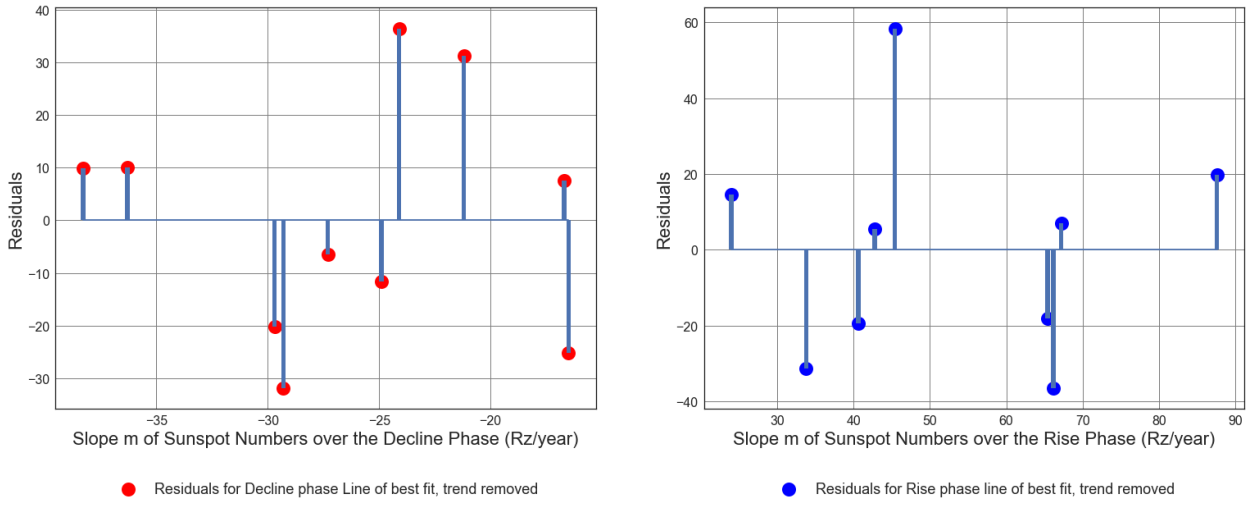

Figure D1.57: Residuals centered about zero, plot of Slope of Solar cycle (from 1900 to 2014) vs. Average number of 6.5M and up Earthquakes with trend removed. Rise: Line of best fit, y = -0.4798x + (15.2), mean x = 52.56 +/- 19.0, mean y = -10.01 +/- 29.53, R = -0.3088, R squared = 0.09536,

p-value = 0.4188. Decline: Line of best fit, y = 0.0652x + 2.516, mean x = -26.43 +/- 6.974, mean y = 0.793 +/- 21.9, R = 0.02076, R squared = 0.000431, p-value = 0.9546.

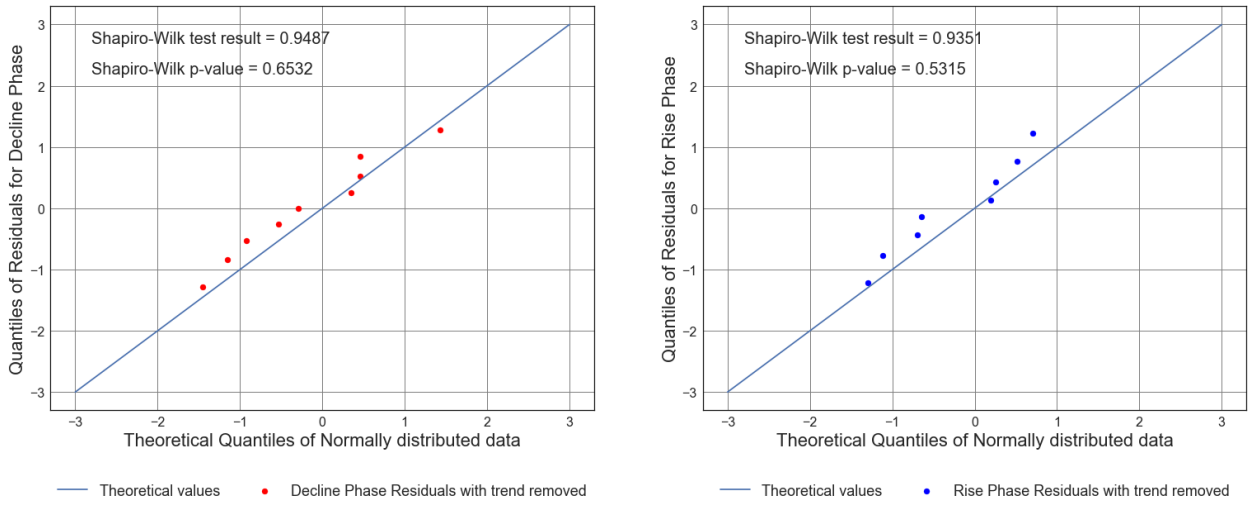

Figure D1.58: Quartile-Quartile Plot of Residuals for the Rise and Decline phase Slope of Solar cycle (from 1900 to 2014) vs. Average number of 6.5M and up Earthquakes with trend removed. Rise: Line of best fit, y = -0.4798x + (15.2), mean x = 52.56 +/- 19.0, mean y = -10.01 +/- 29.53, R = -0.3088, R squared = 0.09536, p-value = 0.4188. Decline: Line of best fit, y = 0.0652x + 2.516, mean x = -26.43 +/- 6.974, mean y = 0.793 +/- 21.9, R = 0.02076, R squared = 0.000431, p-value = 0.9546.

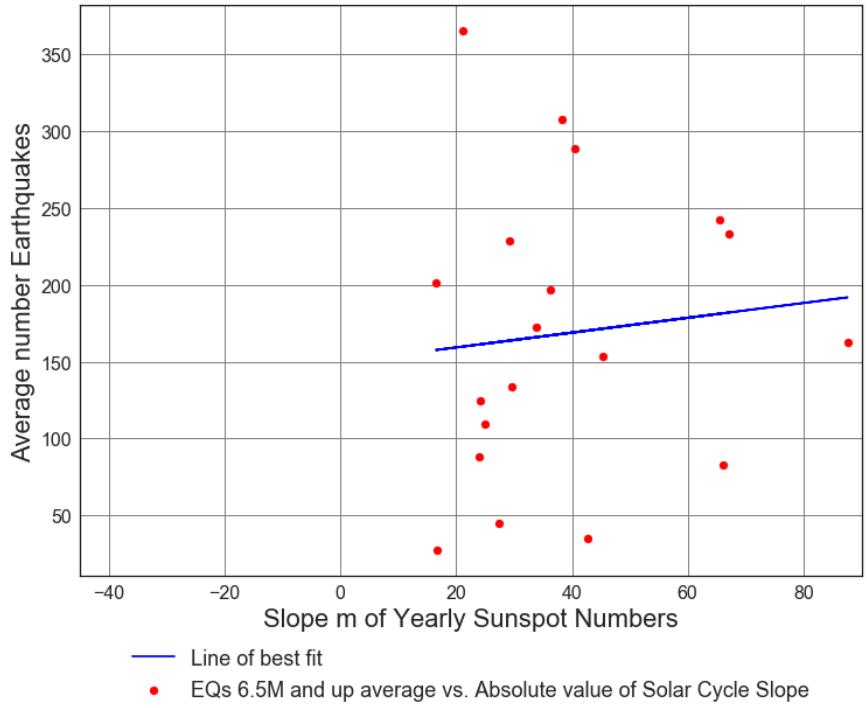

Figure D1.59: Scatter Plot of Absolute Value of the Slope of Solar cycle (from 1900 to 2014) vs. Average number of 6.5M and up Earthquakes. Line of best fit, y = 0.4814x + (149.6), mean x = 38.81 +/- 19.15, mean y = 168.3 +/- 92.04, R = 0.1002, R squared = 0.01004, p-value = 0.6832.

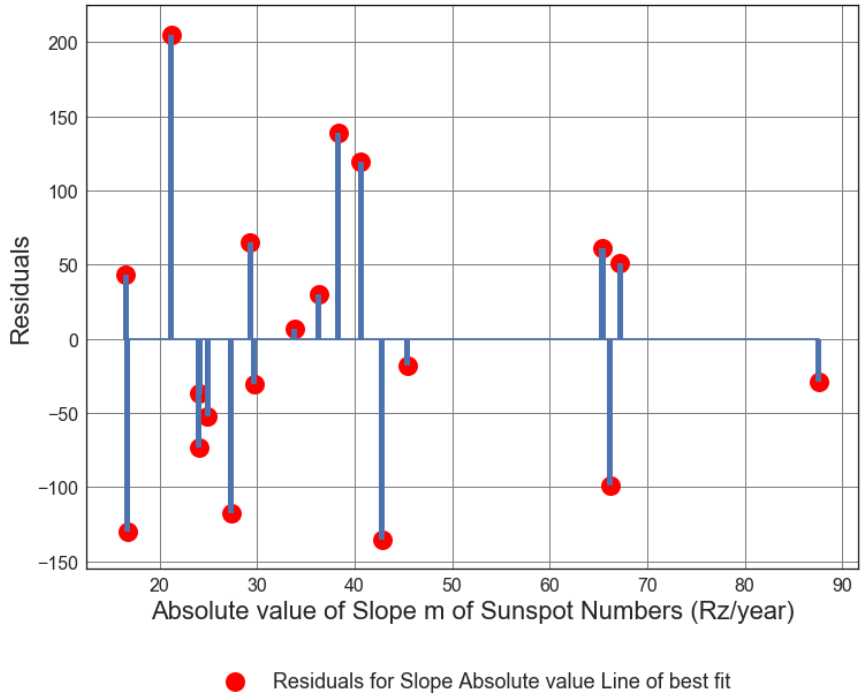

Figure D1.60: Residuals Plot of Absolute Magnitude of the Slope of Solar cycle (from 1900 to 2014) vs. Average number of 6.5M and up Earthquakes. Line of best fit, y = 0.4814x + (149.6), mean x = 38.81 +/- 19.15, mean y = 168.3 +/- 92.04, R = 0.1002, R squared = 0.01004, p-value = 0.6832.

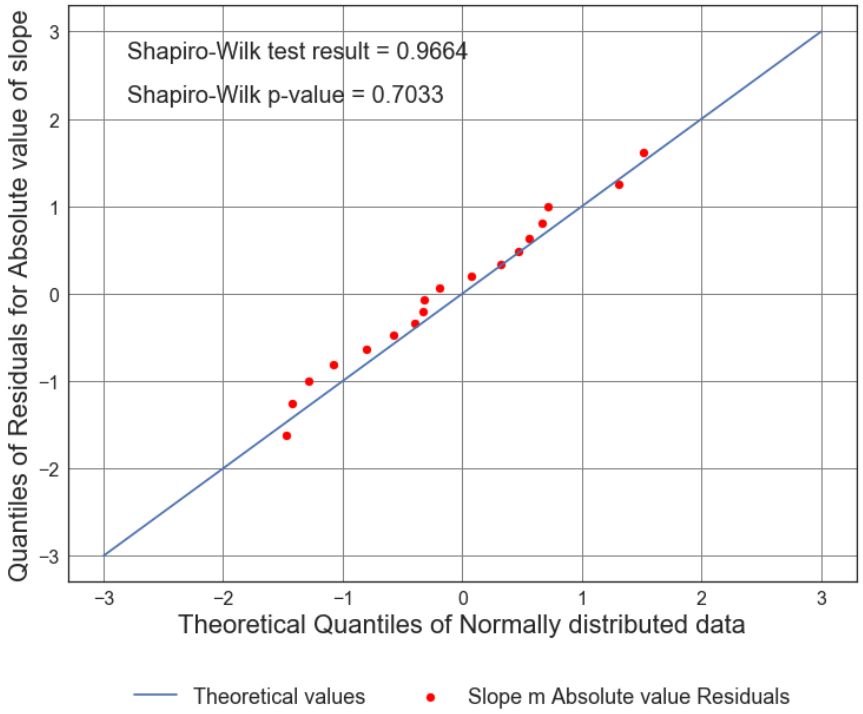

Figure D1.61: Scatter Plot of Absolute Magnitude of the Slope of Solar cycle (from 1900 to 2014) vs. Average number of 6.5M and up Earthquakes. Line of best fit, y = 0.4814x + (149.6), mean x = 38.81 +/- 19.15, mean y = 168.3 +/- 92.04, R = 0.1002, R squared = 0.01004, p-value = 0.6832.

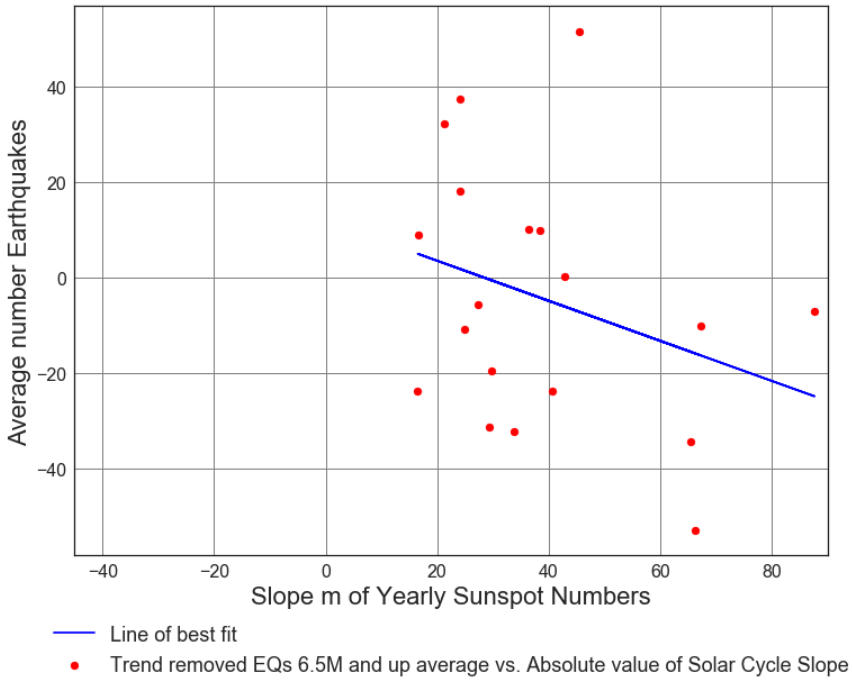

Figure D1.62: Scatter Plot of Absolute Slope Magnitude of the Solar cycle (from 1900 to 2014) vs. Trend removed Average number of 6.5M and up Earthquakes. Line of best fit, y = -0.4202x + (11.98), mean x = 38.81 +/- 19.15, mean y = -4.327 +/- 26.36, R = -0.3054, R squared = 0.09325, p-value = 0.2036.

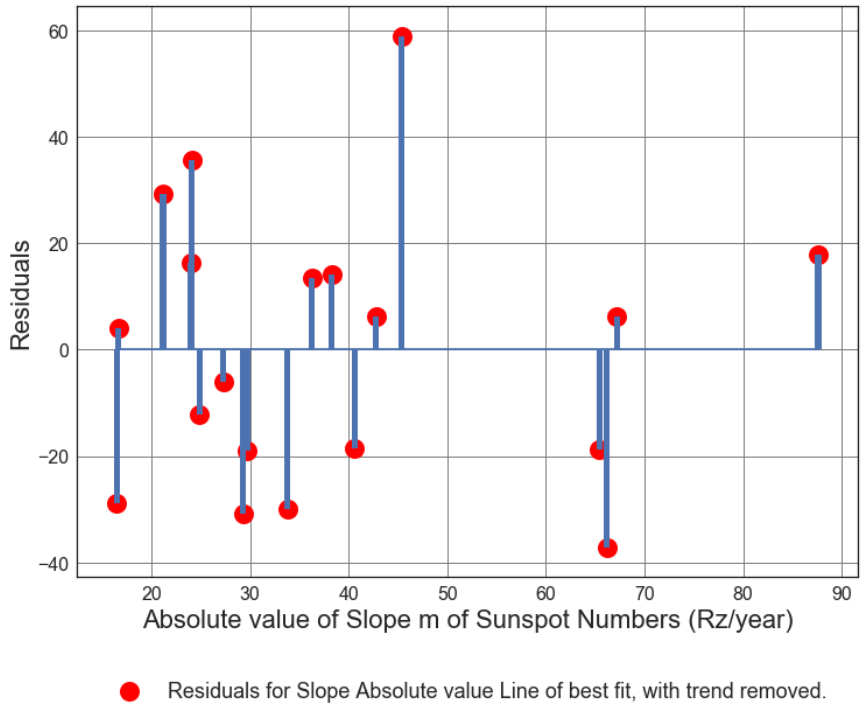

Figure D1.63: Scatter Plot of Absolute Slope Magnitude of the Solar cycle (from 1900 to 2014) vs. Trend removed Average number of 6.5M and up Earthquakes. Line of best fit, y = -0.4202x + (11.98), mean x = 38.81 +/- 19.15, mean y = -4.327 +/- 26.36, R = -0.3054, R squared = 0.09325, p-value = 0.2036.

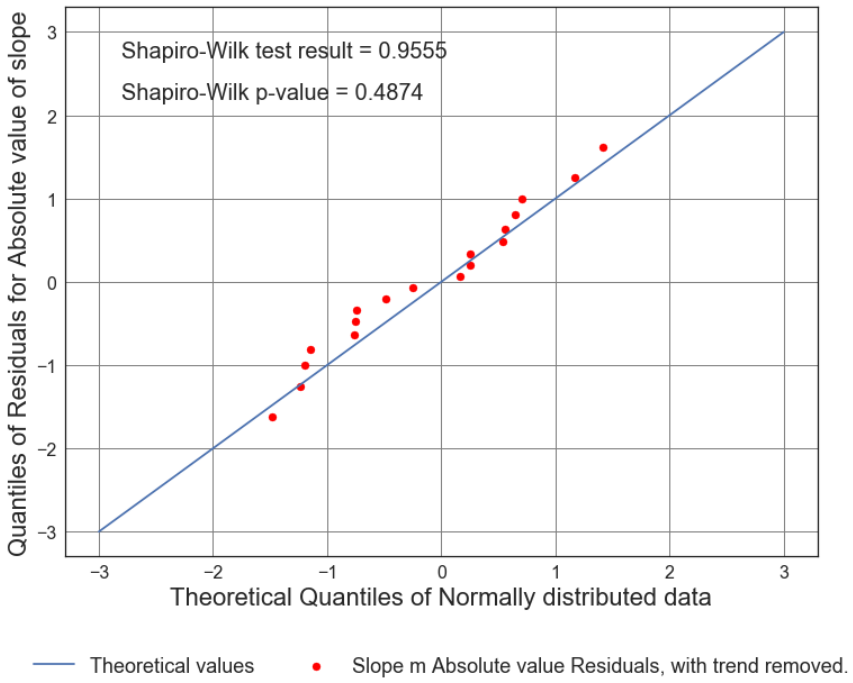

Figure D1.64: Scatter Plot of Absolute Slope Magnitude of the Solar cycle (from 1900 to 2014) vs. Trend removed Average number of 6.5M and up Earthquakes. Line of best fit, y = -0.4202x + (11.98), mean x = 38.81 +/- 19.15, mean y = -4.327 +/- 26.36, R = -0.3054, R squared = 0.09325, p-value = 0.2036.

Appendix D2: ISC Time Series Analysis Part 2 - Six Month Averaged Earthquake and Sunspot Data.

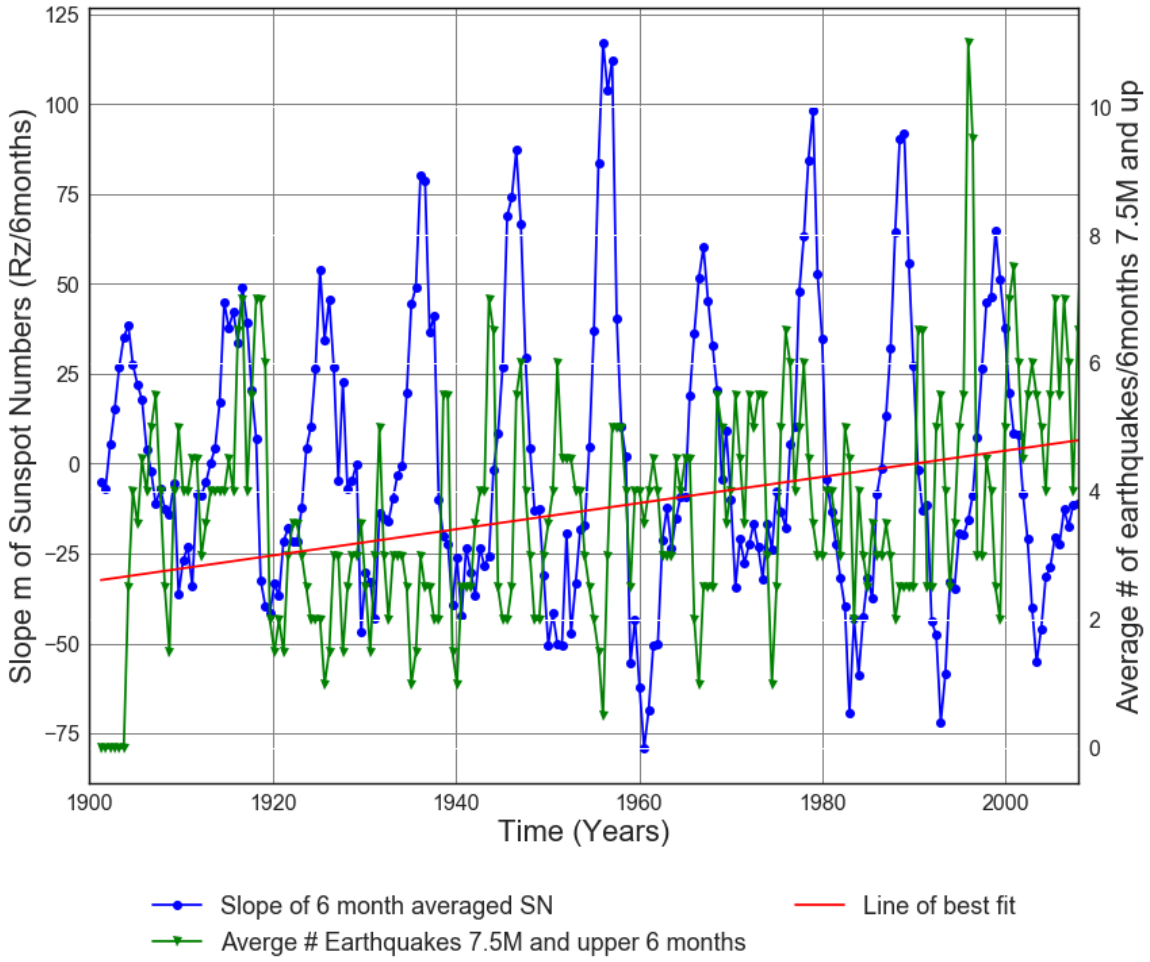

Figure D2.1: Slope of Solar cycle from 1900 to 2017 vs. Average number of 7.5M and up Earthquakes.

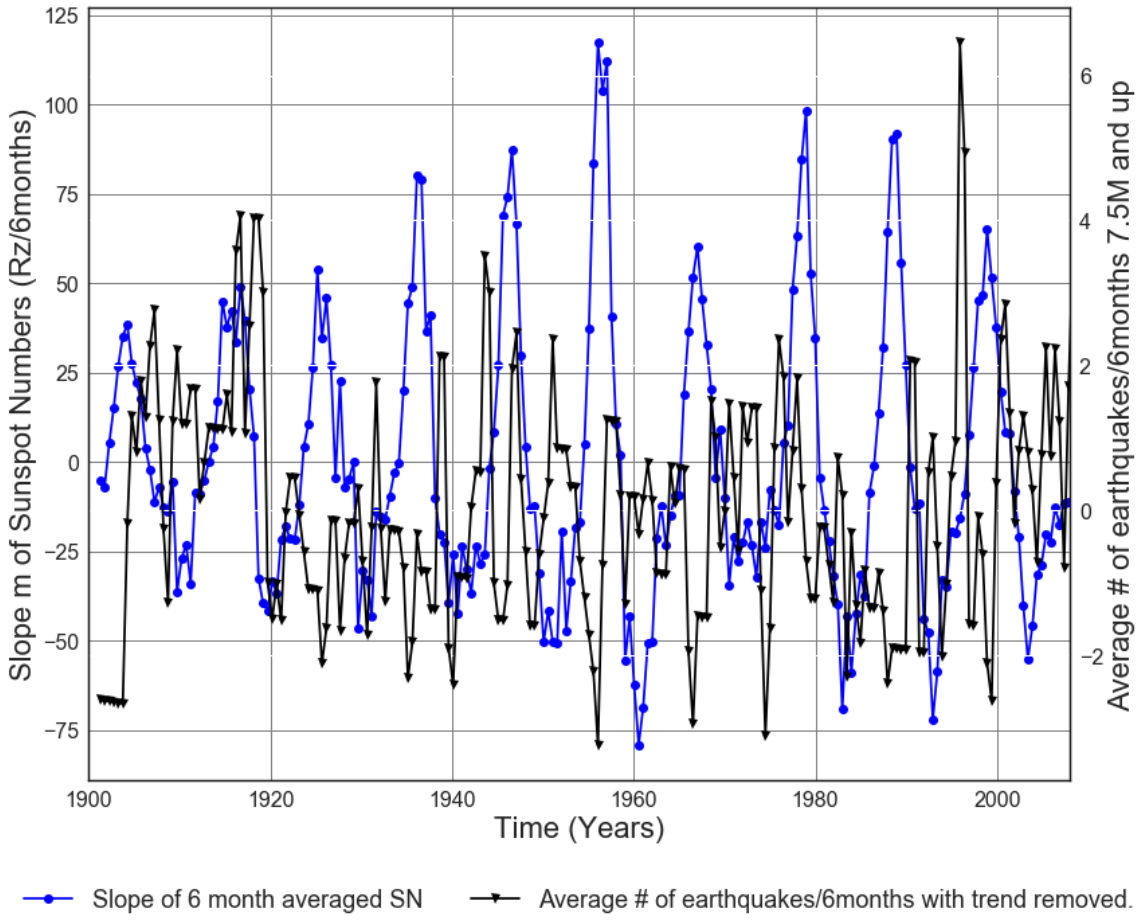

Figure D2.2: Slope of 6 month averaged SN 1900 to 2017 vs. Average number of 7.5M and up Earthquakes with trend removed. Line of best fit, y = 0.02043x + (-36.21), mean x = 1.955e+03 +/- 31.21, mean y = 3.71 +/- 1.759

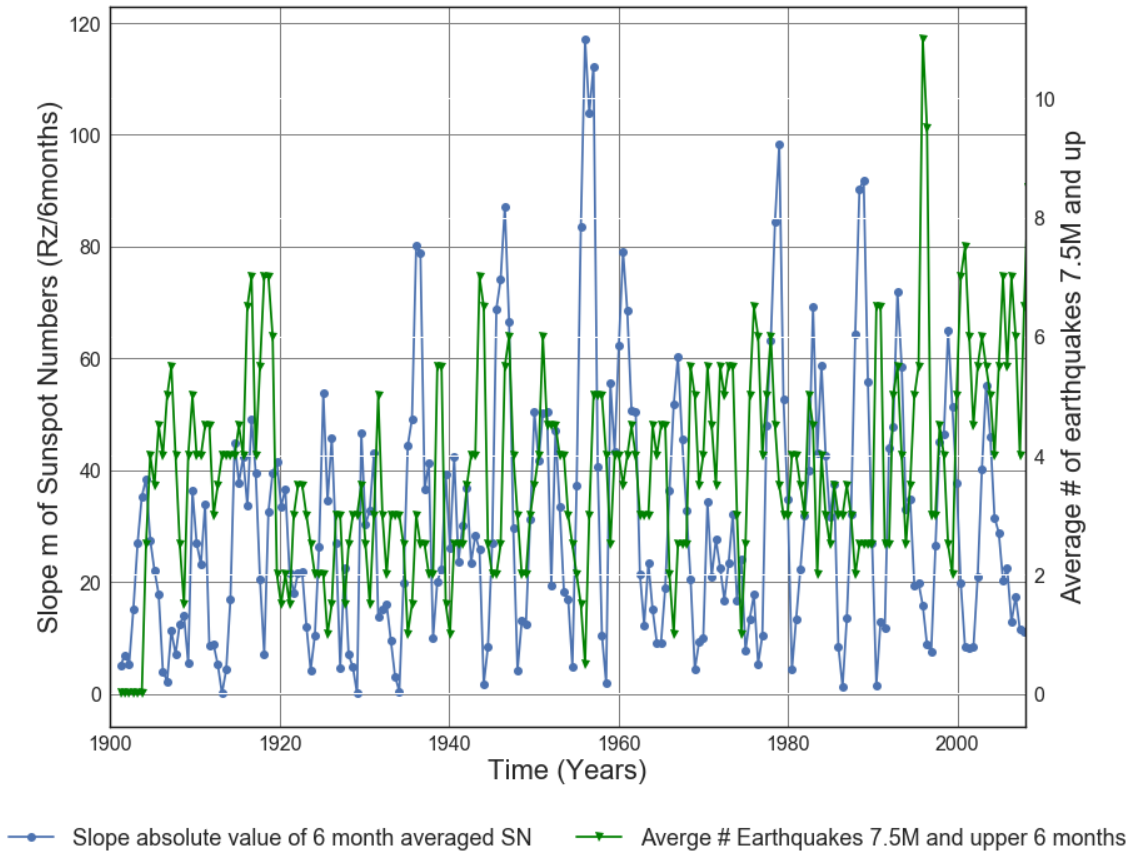

Figure D2.3: Slope Absolute value of Solar cycle from 1900 to 2017 vs. Average number of 7.5M and up Earthquakes.

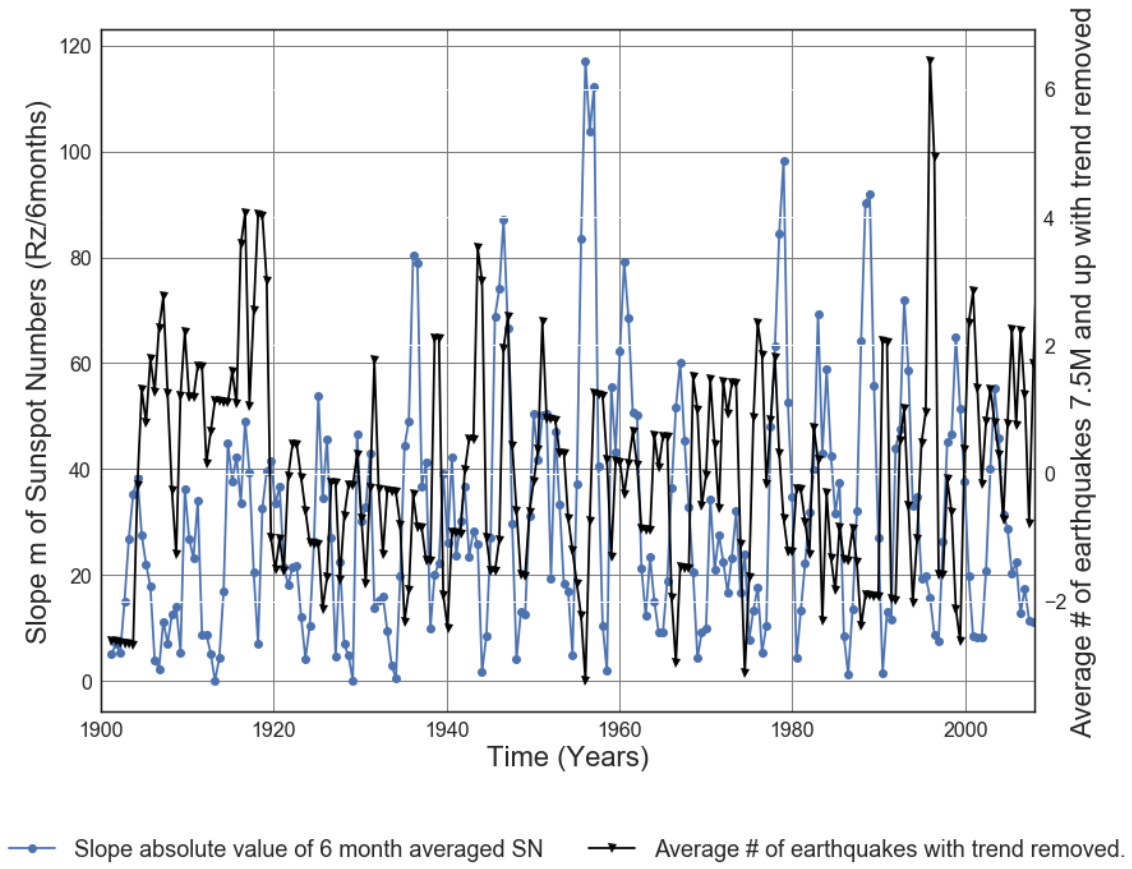

Figure D2.4: Slope Absolute value of Solar cycle from 1900 to 2017 vs. Average number of 7.5M and up earthquakes with trend removed.

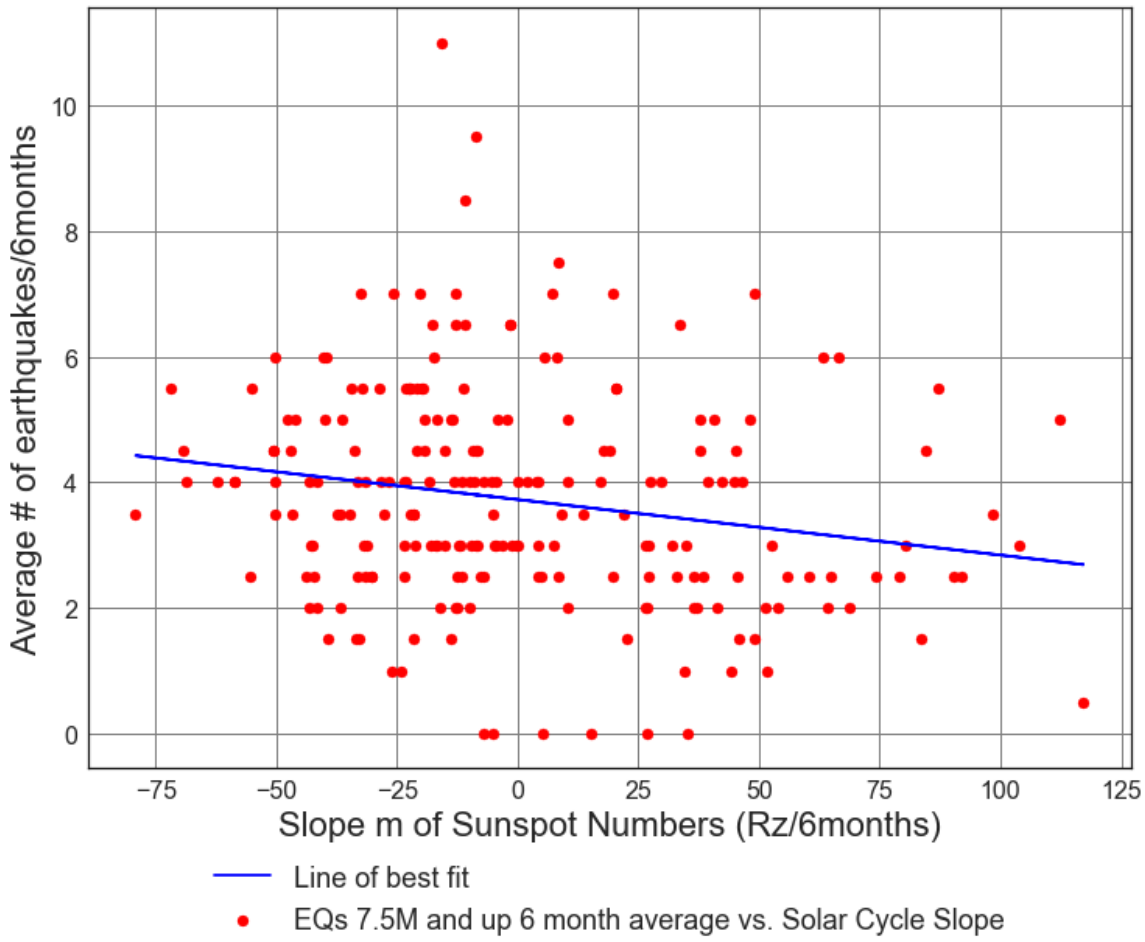

Figure D2.5: Scatter Plot of Solar cycle slope (from 1900 to 2017) vs. Average number of 7.5M and up Earthquakes/6months. Line of best fit, y = -0.008843x + (3.726), mean x = -0.07013 +/- 38.33, mean y = 3.727 +/- 1.745, R = -0.1943, R squared = 0.03775, p-value = 0.004152.

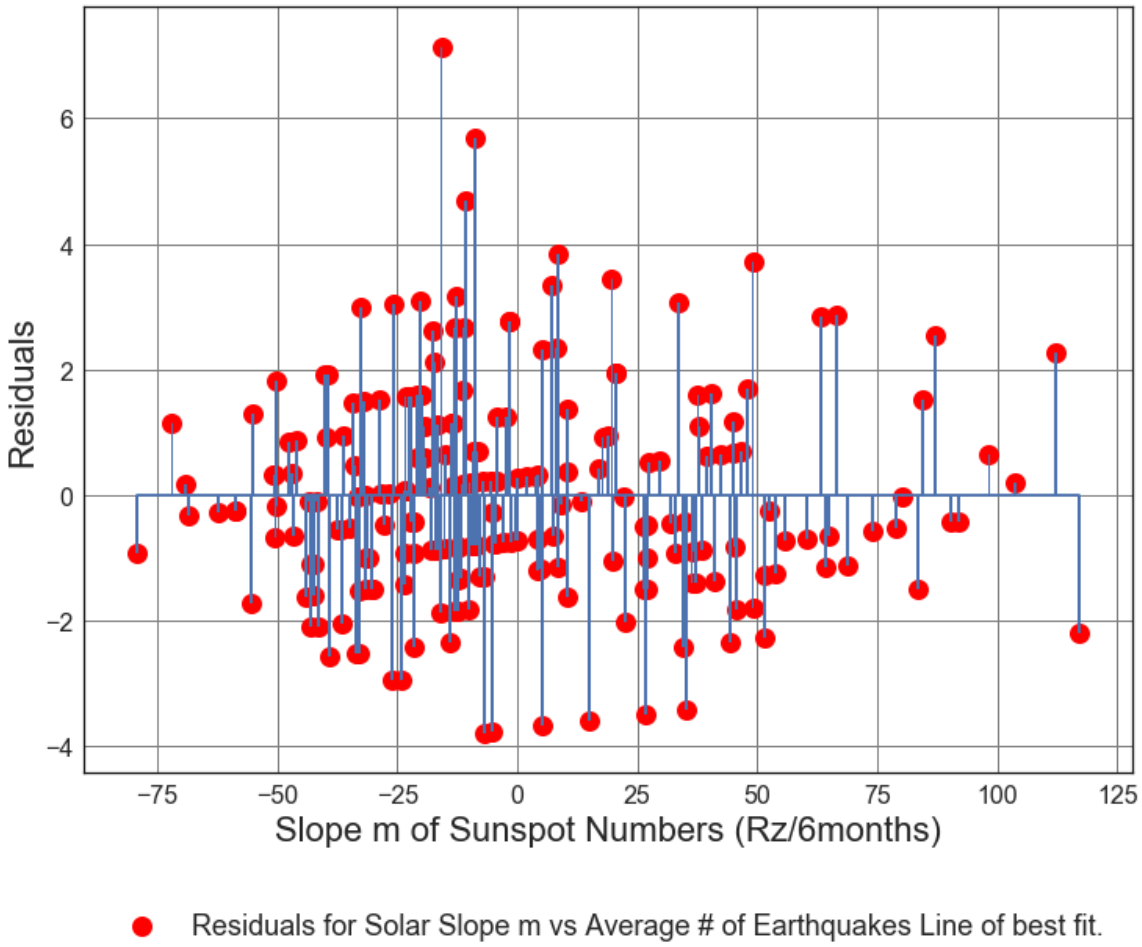

Figure D2.6: Residuals Plot of Solar cycle slope (from 1900 to 2017) vs. Average number of 7.5M and up Earthquakes/6months. Line of best fit, y = -0.008843x + (3.726), mean x = -0.07013 +/- 38.33, mean y = 3.727 +/- 1.745, R = -0.1943, R squared = 0.03775, p-value = 0.004152.

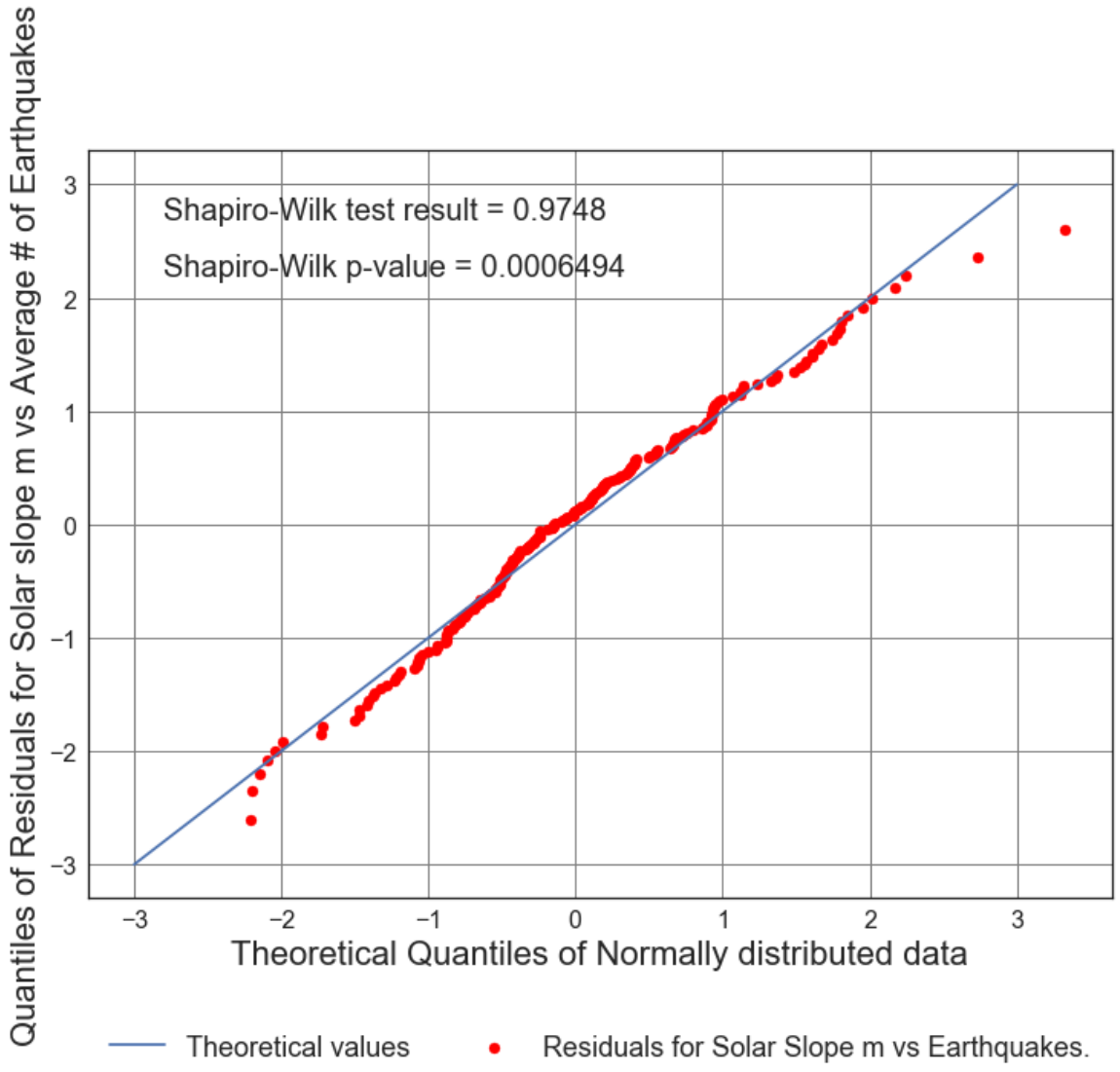

Figure D2.7: Residuals Plot of Solar cycle slope (from 1900 to 2017) vs. Average number of 7.5M and up Earthquakes/6months. Line of best fit, y = -0.008843x + (3.726), mean x = -0.07013 +/- 38.33, mean y = 3.727 +/- 1.745, R = -0.1943, R squared = 0.03775, p-value = 0.004152.

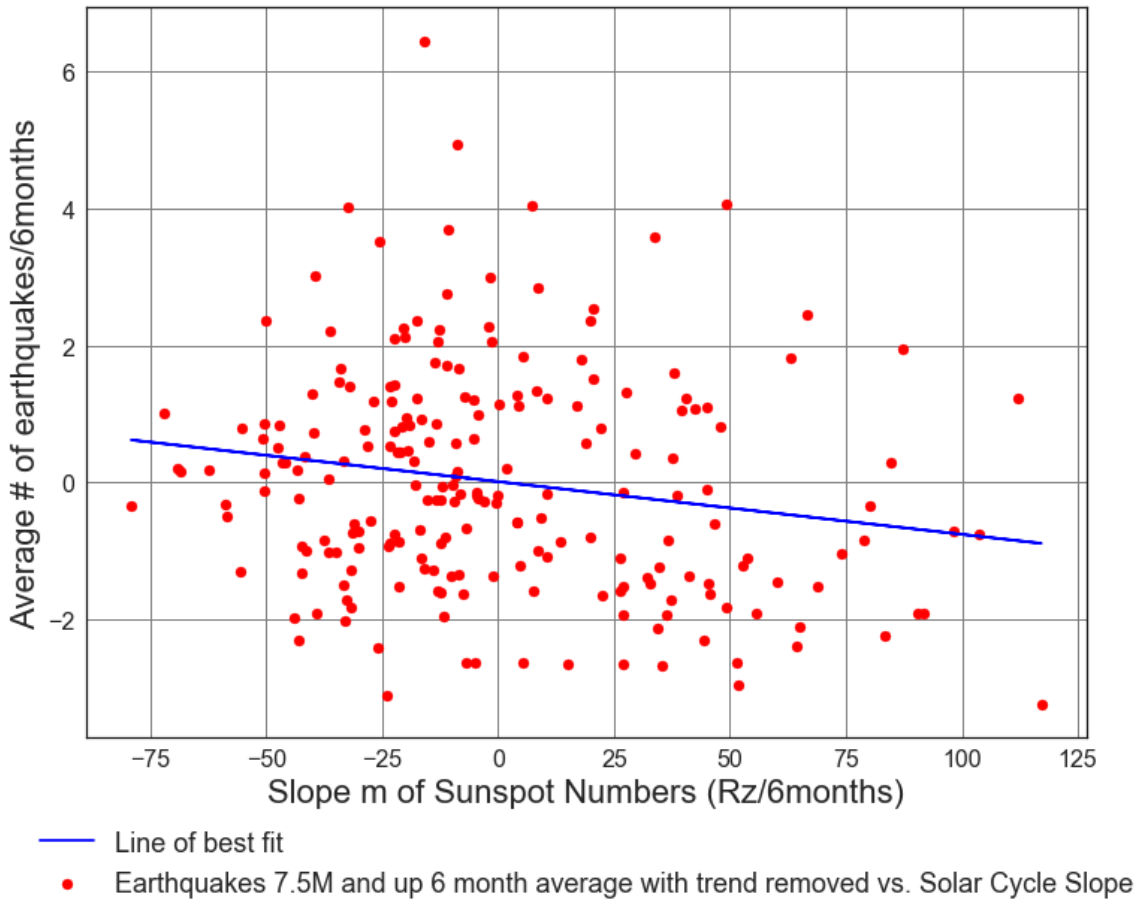

Figure D2.8: Scatter Plot of Solar cycle slope (from 1900 to 2017) vs. Average number of 7.5M and up Earthquakes/6months with trend removed. Line of best fit, y = -0.007695x + (0.01155), mean x = -0.07013 +/- 38.33, mean y = 0.01209 +/- 1.633, R = -0.1806, R squared = 0.03261, p-value = 0.0078.

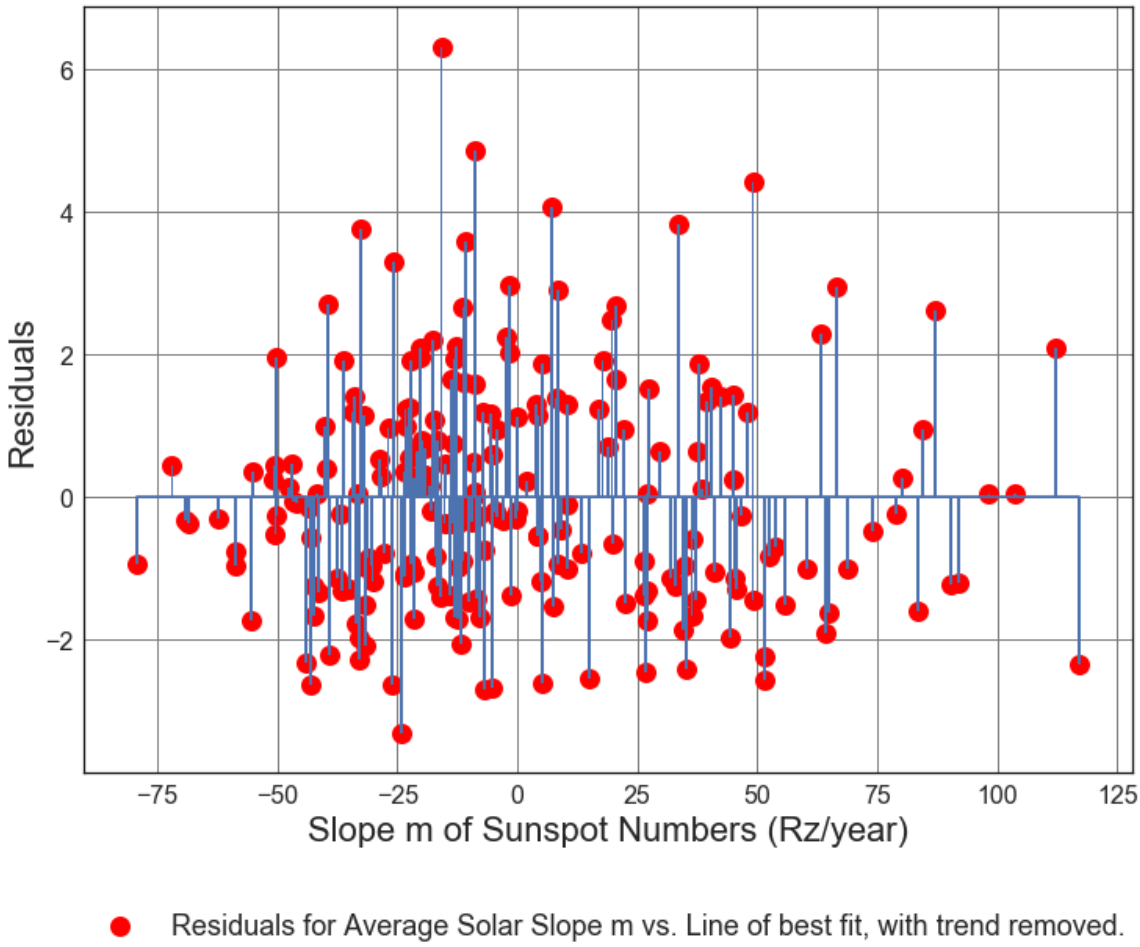

Figure D2.9: Scatter Plot of Solar cycle slope (from 1900 to 2017) vs. Average number of 7.5M and up Earthquakes/6months with trend removed. Line of best fit, y = -0.007695x + (0.01155), mean x = -0.07013 +/- 38.33, mean y = 0.01209 +/- 1.633, R = -0.1806, R squared = 0.03261, p-value = 0.0078.

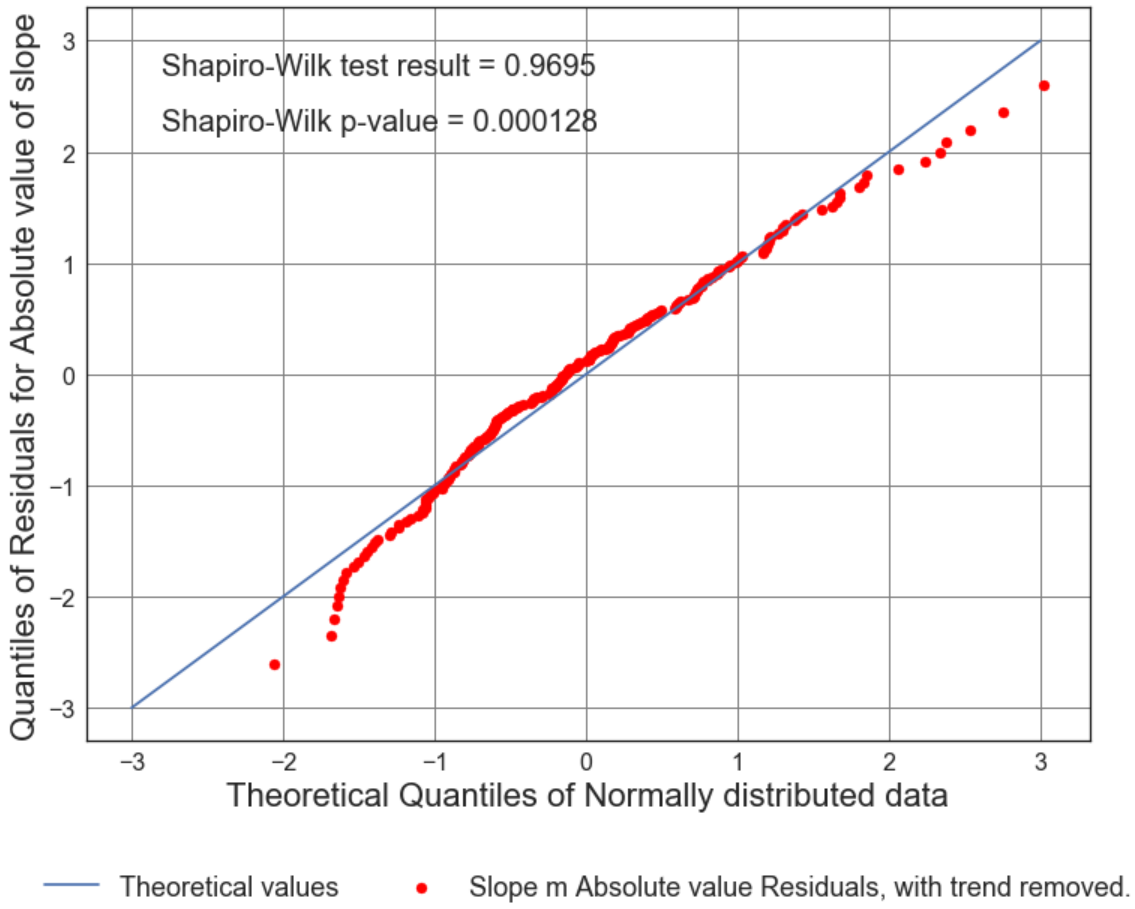

Figure D2.10: Scatter Plot of Solar cycle slope (from 1900 to 2017) vs. Average number of 7.5M and up Earthquakes/6months with trend removed. Line of best fit, y = -0.007695x + (0.01155), mean x = -0.07013 +/- 38.33, mean y = 0.01209 +/- 1.633, R = -0.1806, R squared = 0.03261, p-value = 0.0078.

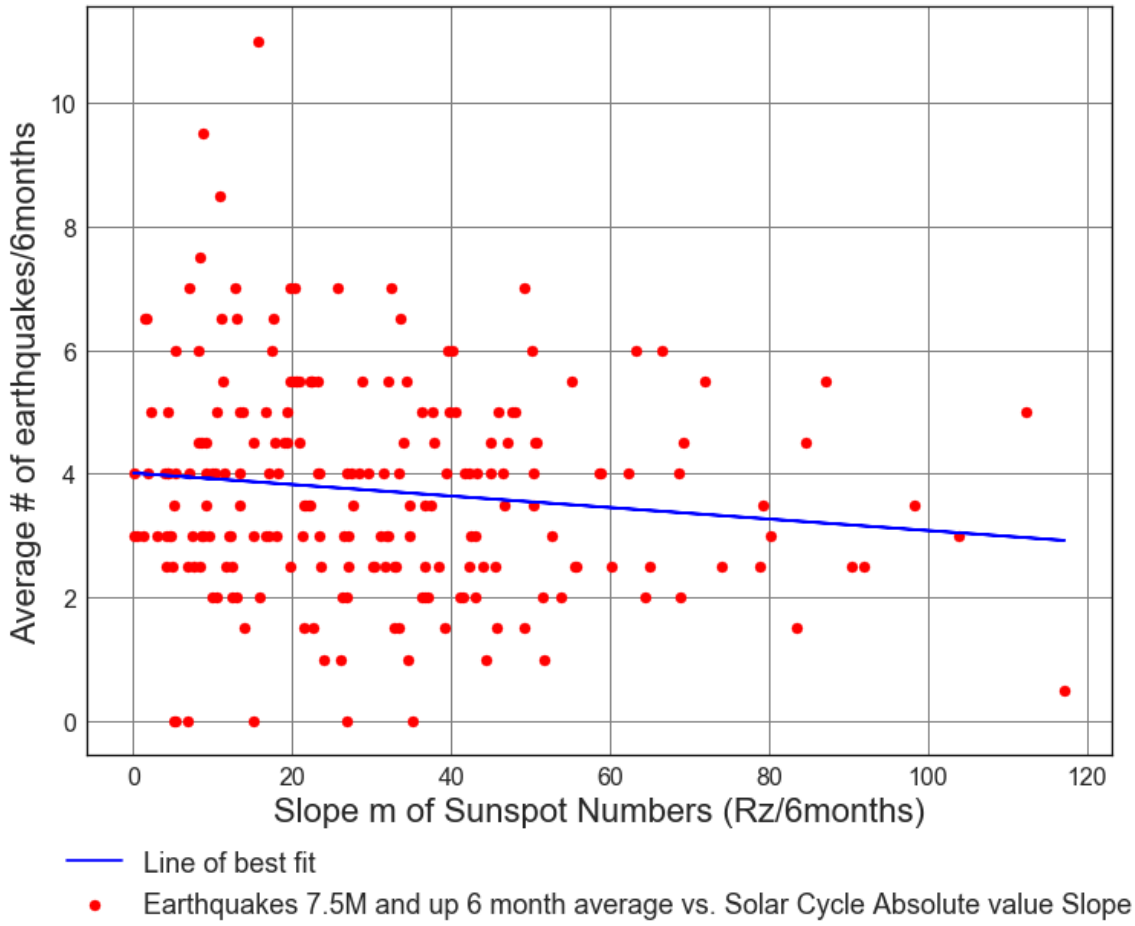

Figure D2.11: Scatter Plot of Solar cycle slope (from 1900 to 2017) vs. Average number of 7.5M and up Earthquakes/6months. Line of best fit, y = -0.009309x + (4.012), mean x = 30.66 +/- 23.0, mean y = 3.727 +/- 1.745, R = -0.1227, R squared = 0.01506, p-value = 0.07184.

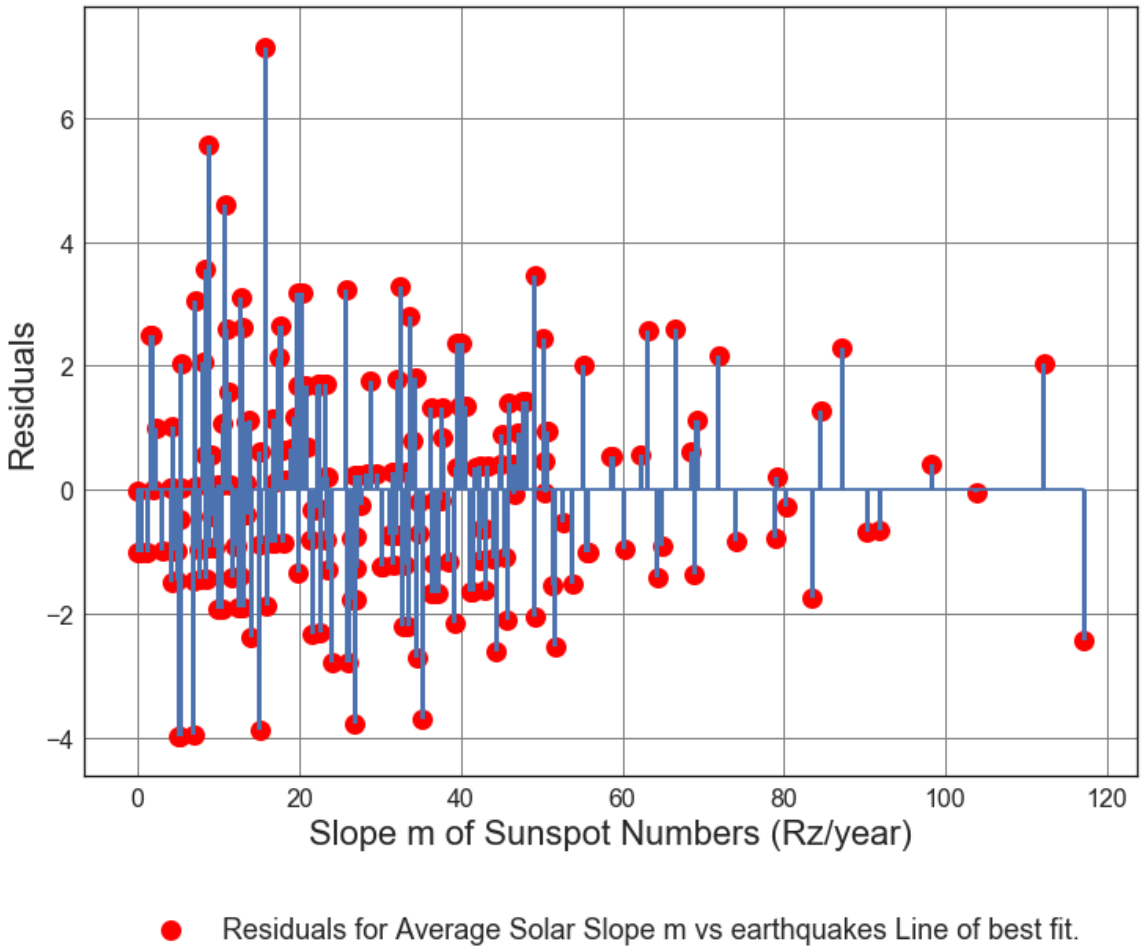

Figure D2.12: Scatter Plot of Solar cycle slope (from 1900 to 2017) vs. Average number of 7.5M and up Earthquakes/6months. Line of best fit, y = -0.009309x + (4.012), mean x = 30.66 +/- 23.0, mean y = 3.727 +/- 1.745, R = -0.1227, R squared = 0.01506, p-value = 0.07184.

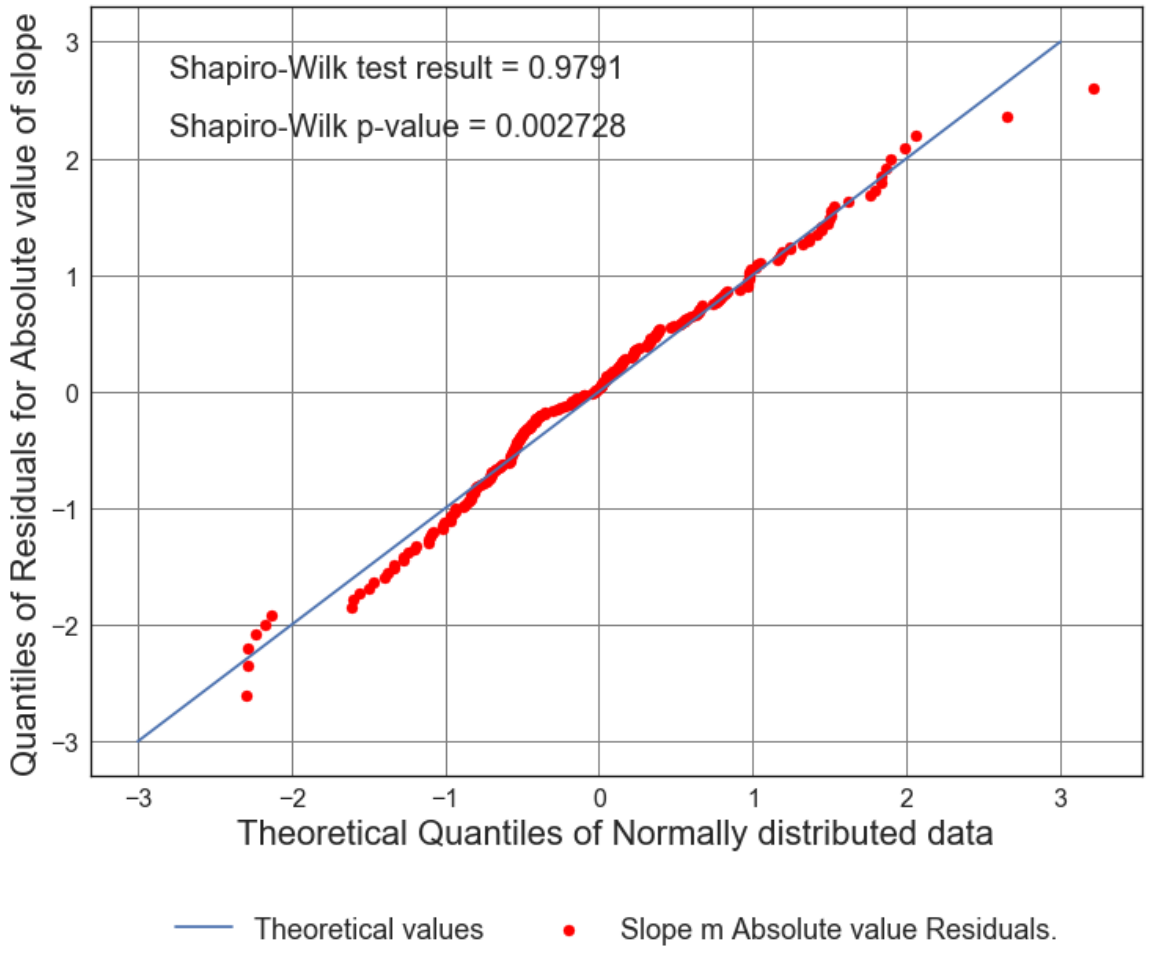

Figure D2.13: Scatter Plot of Solar cycle slope (from 1900 to 2017) vs. Average number of 7.5M and up Earthquakes/6months. Line of best fit, y = -0.009309x + (4.012), mean x = 30.66 +/- 23.0, mean y = 3.727 +/- 1.745, R = -0.1227, R squared = 0.01506, p-value = 0.07184.

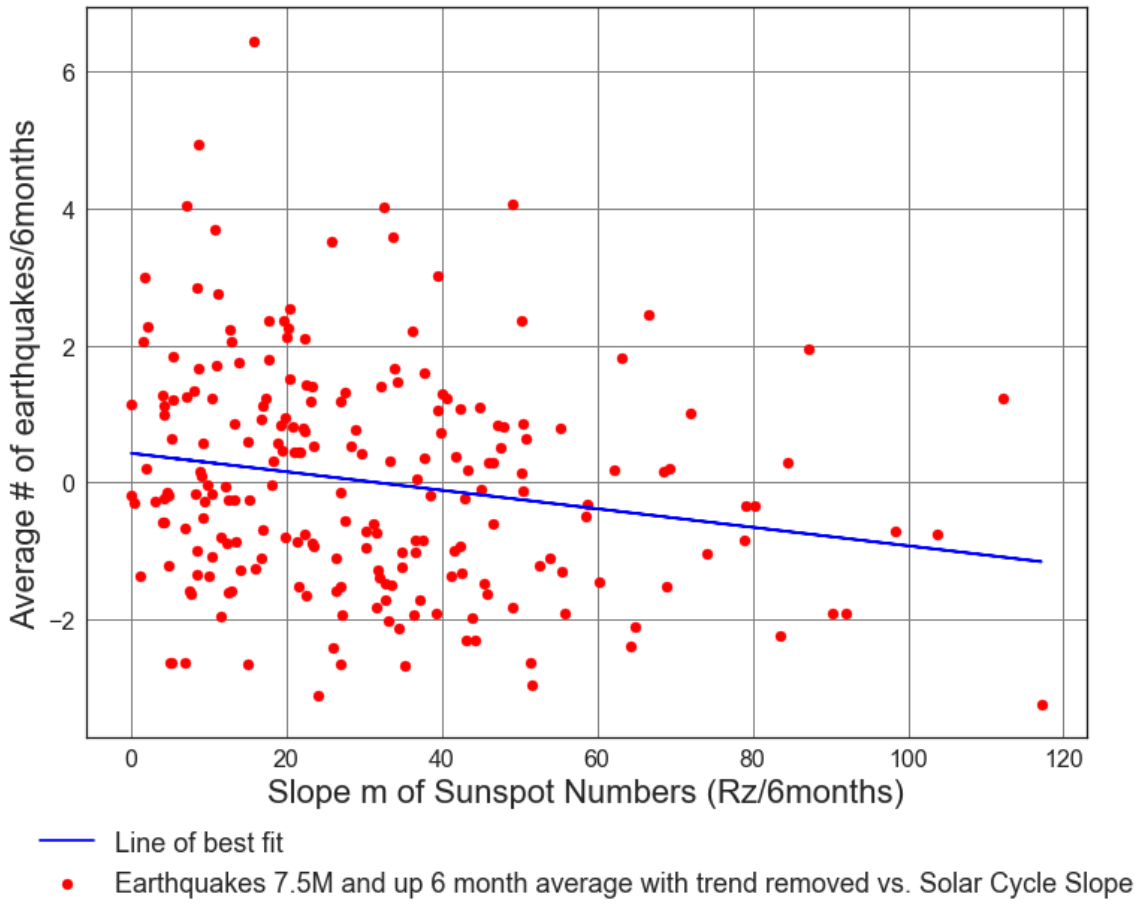

Figure D2.14: Scatter Plot of Solar cycle absolute value slope (from 1900 to 2017) vs. Average number of 7.5M and up Earthquakes/6months with trend removed. Line of best fit, y = -0.01352x + (0.4266), mean x = 30.66 +/- 23.0, mean y = 0.01209 +/- 1.633, R = -0.1904, R squared = 0.03625, p-value = 0.004991.

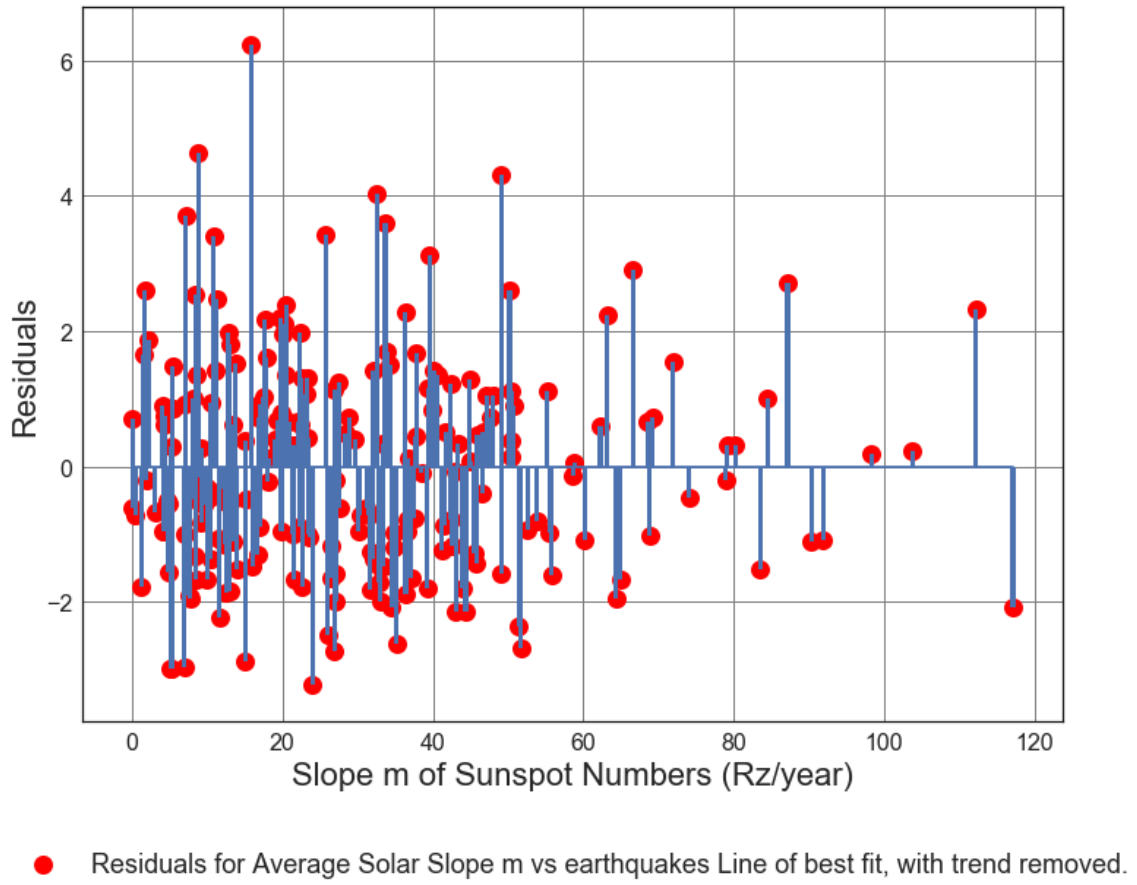

Figure D2.15: Scatter Plot of Solar cycle absolute value slope (from 1900 to 2017) vs. Average number of 7.5M and up Earthquakes/6months with trend removed. Line of best fit, y = -0.01352x + (0.4266), mean x = 30.66 +/- 23.0, mean y = 0.01209 +/- 1.633, R = -0.1904, R squared = 0.03625, p-value = 0.004991.

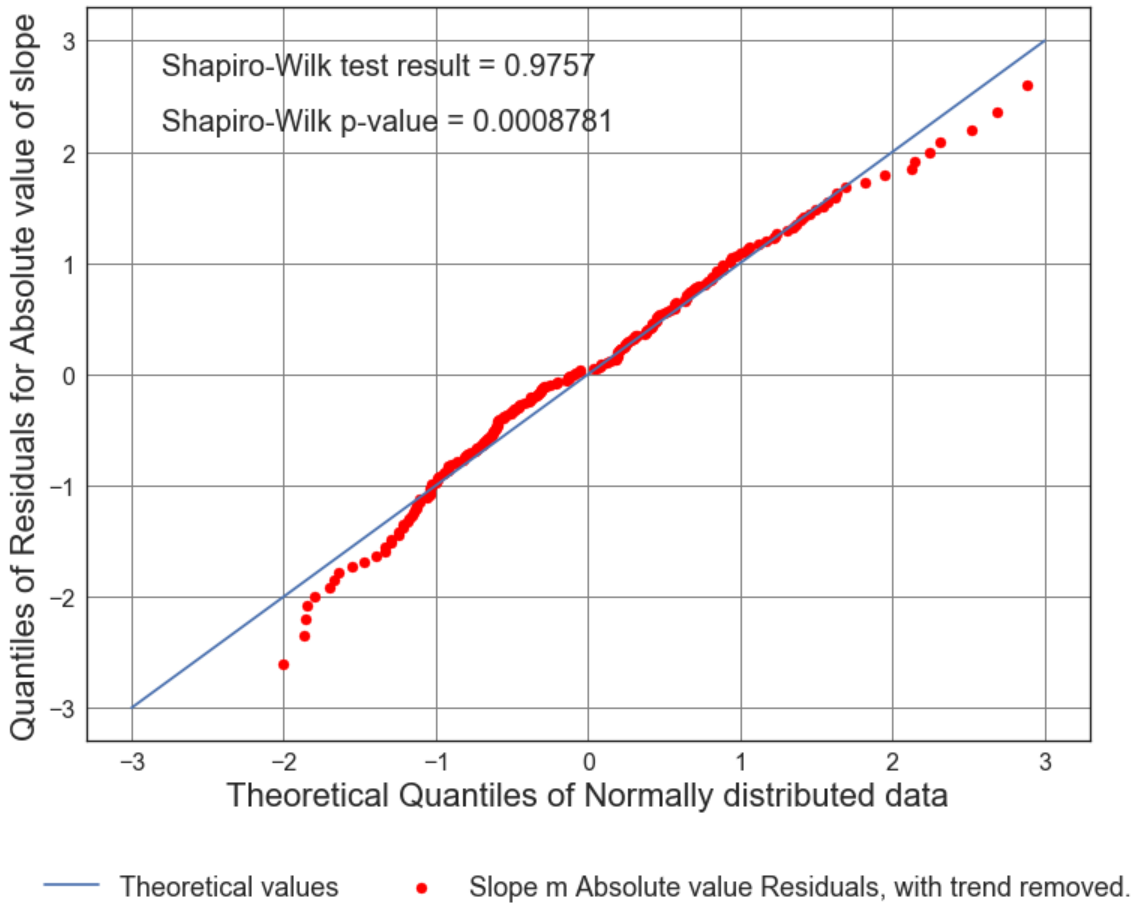

Figure D2.16: Scatter Plot of Solar cycle absolute value slope (from 1900 to 2017) vs. Average number of 7.5M and up Earthquakes/6months with trend removed. Line of best fit, y = -0.01352x + (0.4266), mean x = 30.66 +/- 23.0, mean y = 0.01209 +/- 1.633, R = -0.1904, R squared = 0.03625, p-value = 0.004991.

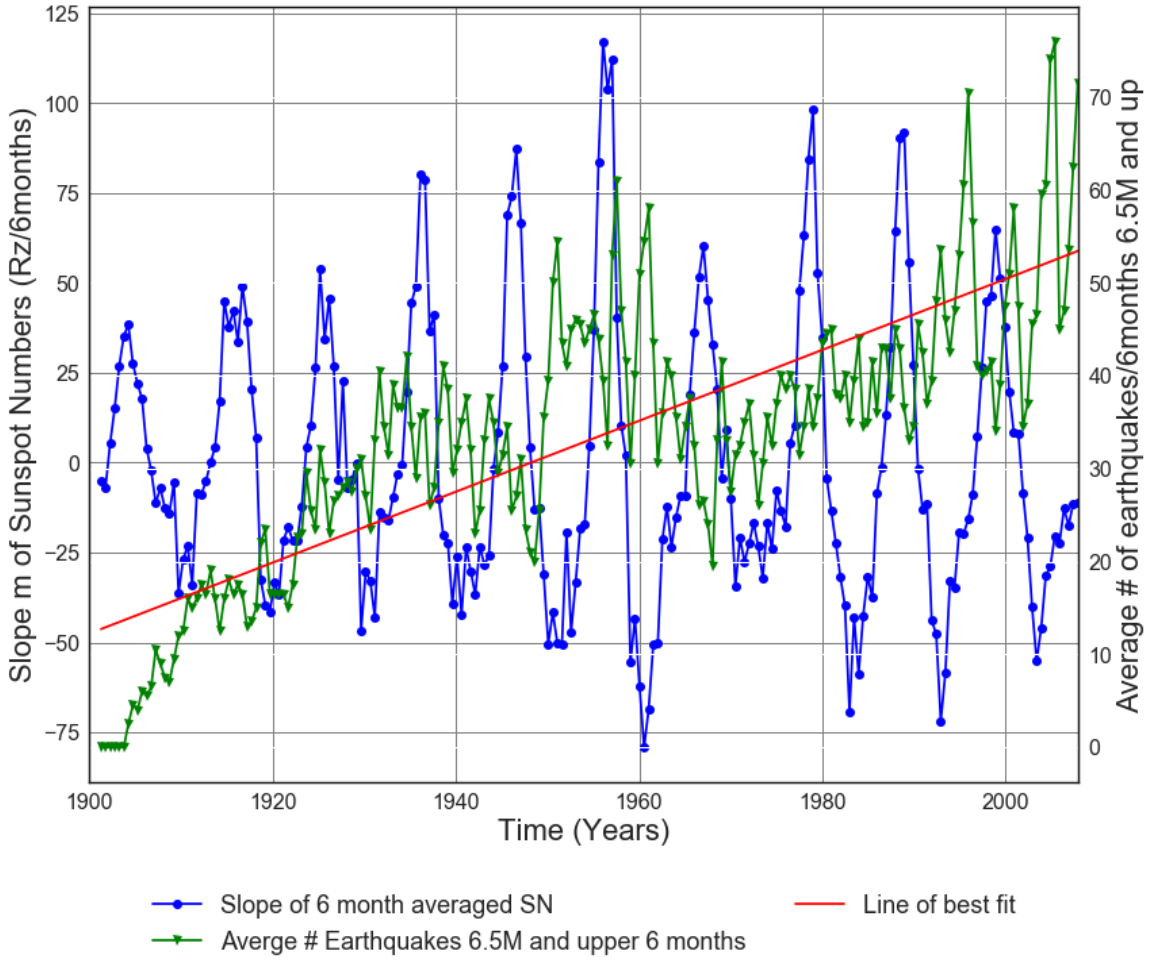

Figure D2.17: Slope of Solar cycle from 1900 to 2017 vs. Average number of 6.5M and up Earthquakes.

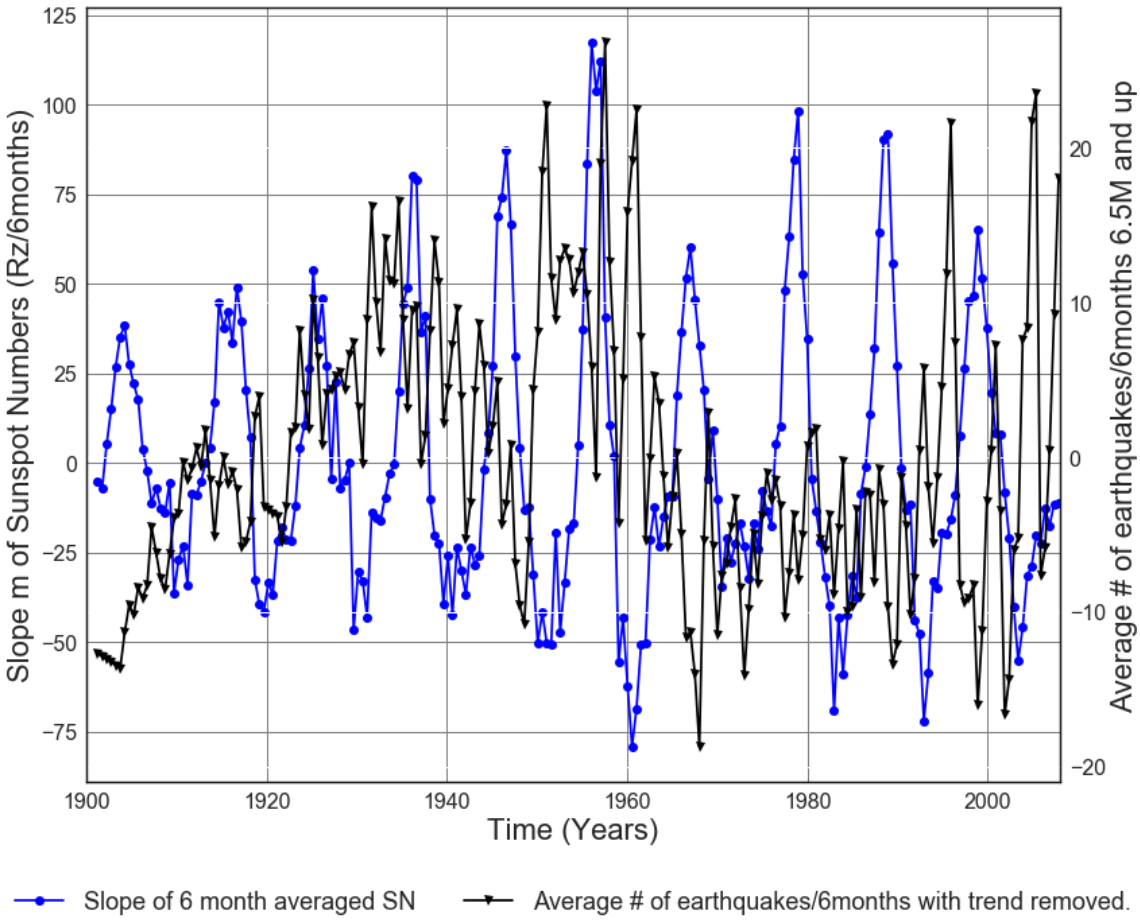

Figure D2.18: Slope of 6 month averaged SN 1900 to 2017 vs. Average number of 6.5M and up Earthquakes with trend removed. Line of best fit, y = 0.3819x + (-713.4), mean x = 1.955e+03 +/- 31.21, mean y = 33.08 +/- 14.89

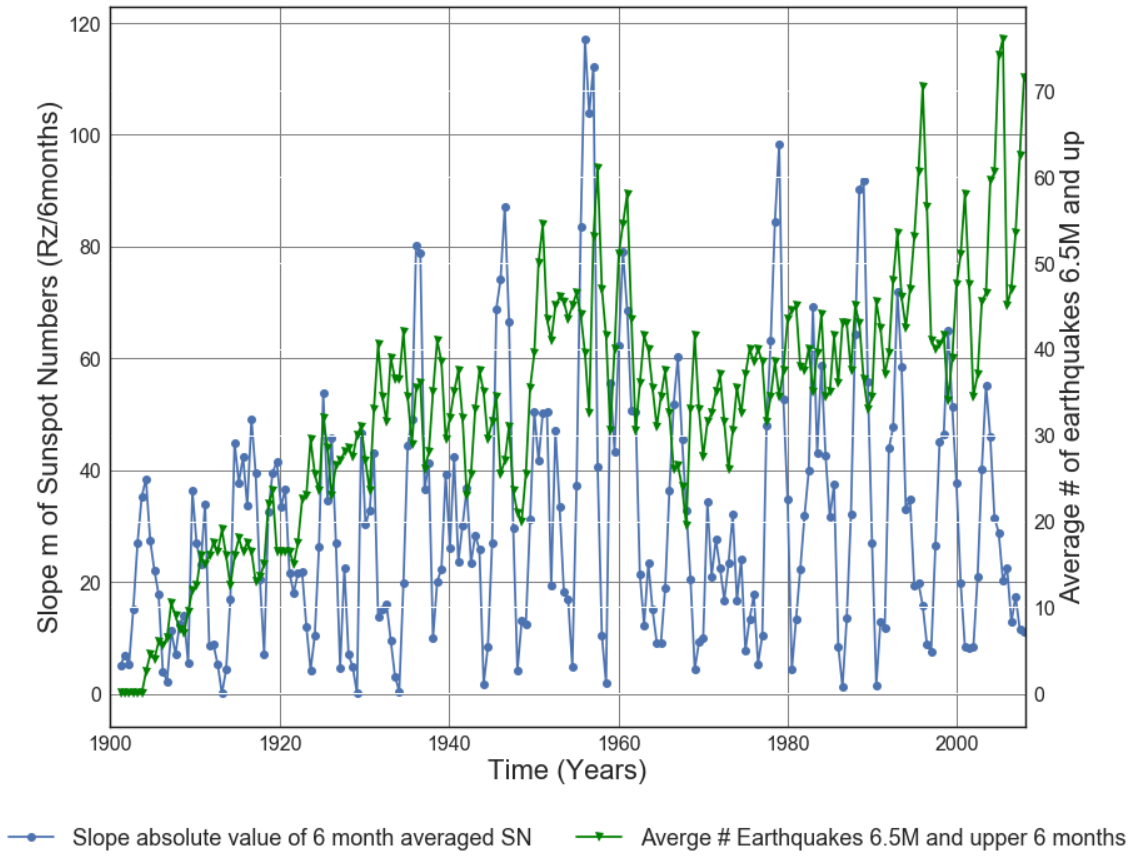

Figure D2.19: Slope Absolute value of Solar cycle from 1900 to 2017 vs. Average number of 6.5M and up Earthquakes.

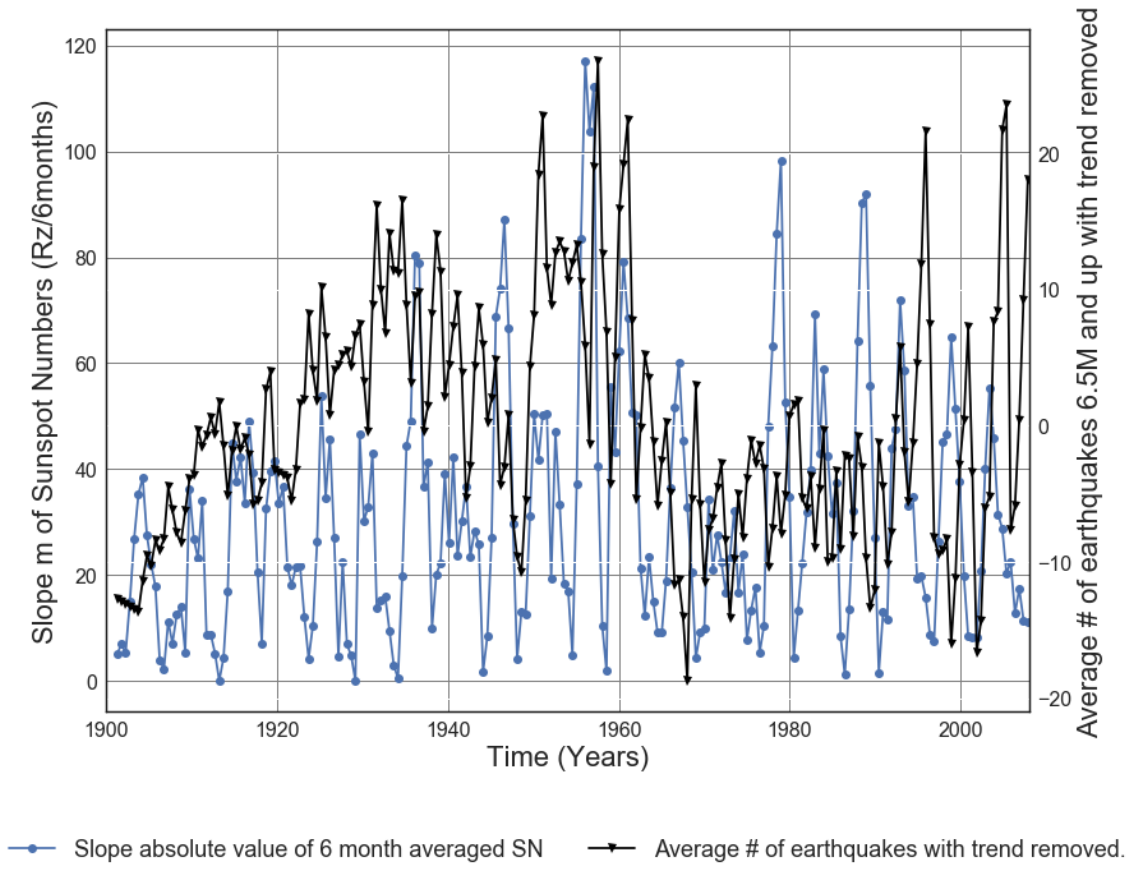

Figure D2.20: Slope Absolute value of Solar cycle from 1900 to 2017 vs. Average number of 6.5M and up earthquakes with trend removed.

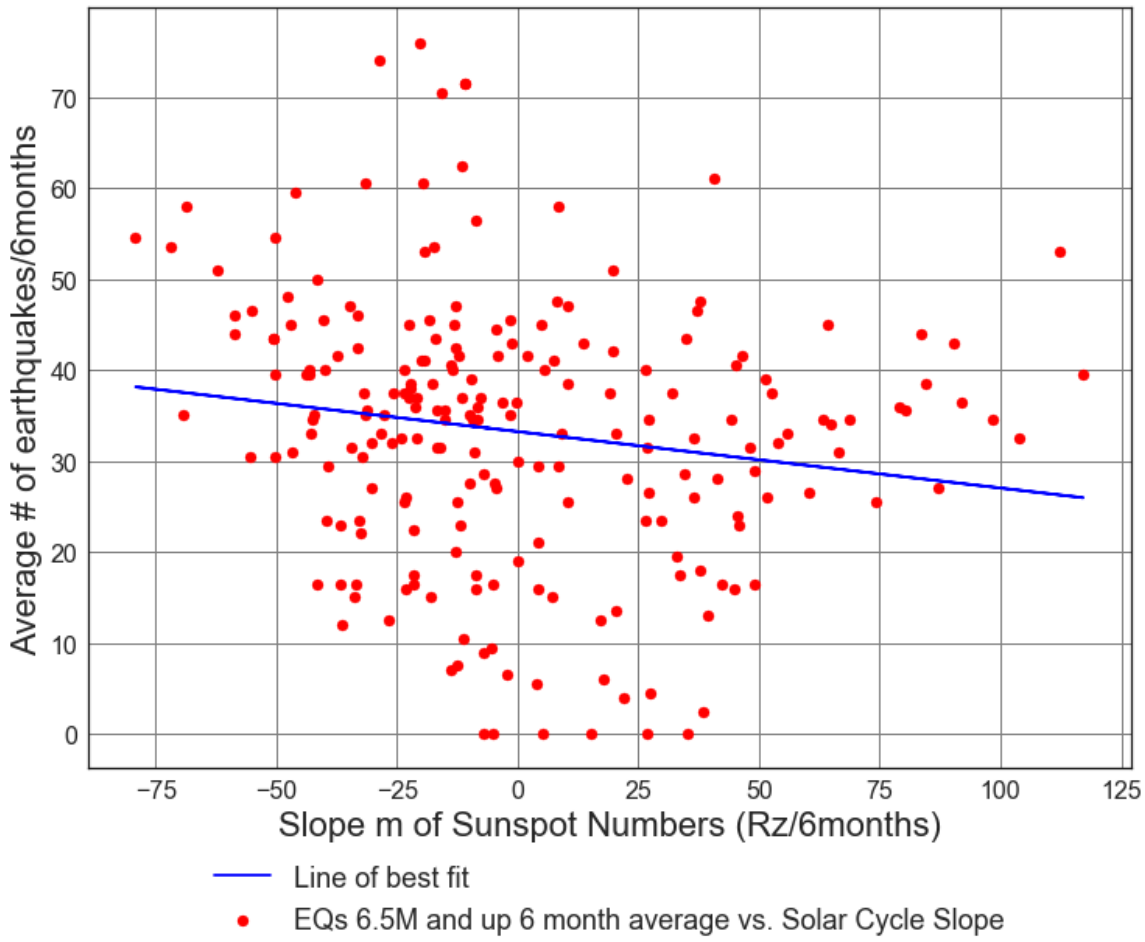

Figure D2.21: Scatter Plot of Solar cycle slope (from 1900 to 2017) vs. Average number of 6.5M and up Earthquakes/6months. Line of best fit, y = -0.06203x + (33.23), mean x = -0.07013 +/- 38.33, mean y = 33.23 +/- 14.75, R = -0.1611, R squared = 0.02596, p-value = 0.01779.

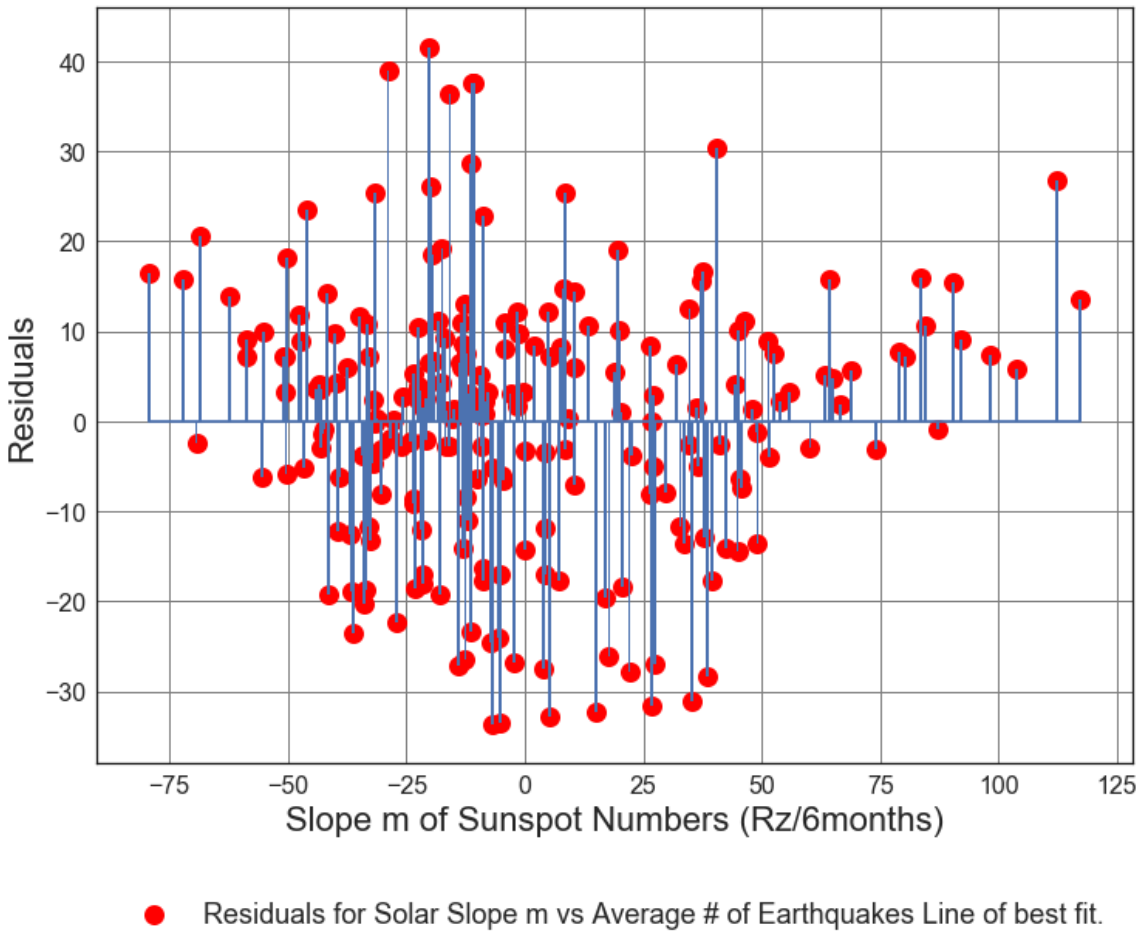

Figure D2.22: Residuals Plot of Solar cycle slope (from 1900 to 2017) vs. Average number of 6.5M and up Earthquakes/6months. Line of best fit, y = -0.06203x + (33.23), mean x = -0.07013 +/- 38.33, mean y = 33.23 +/- 14.75, R = -0.1611, R squared = 0.02596, p-value = 0.01779.

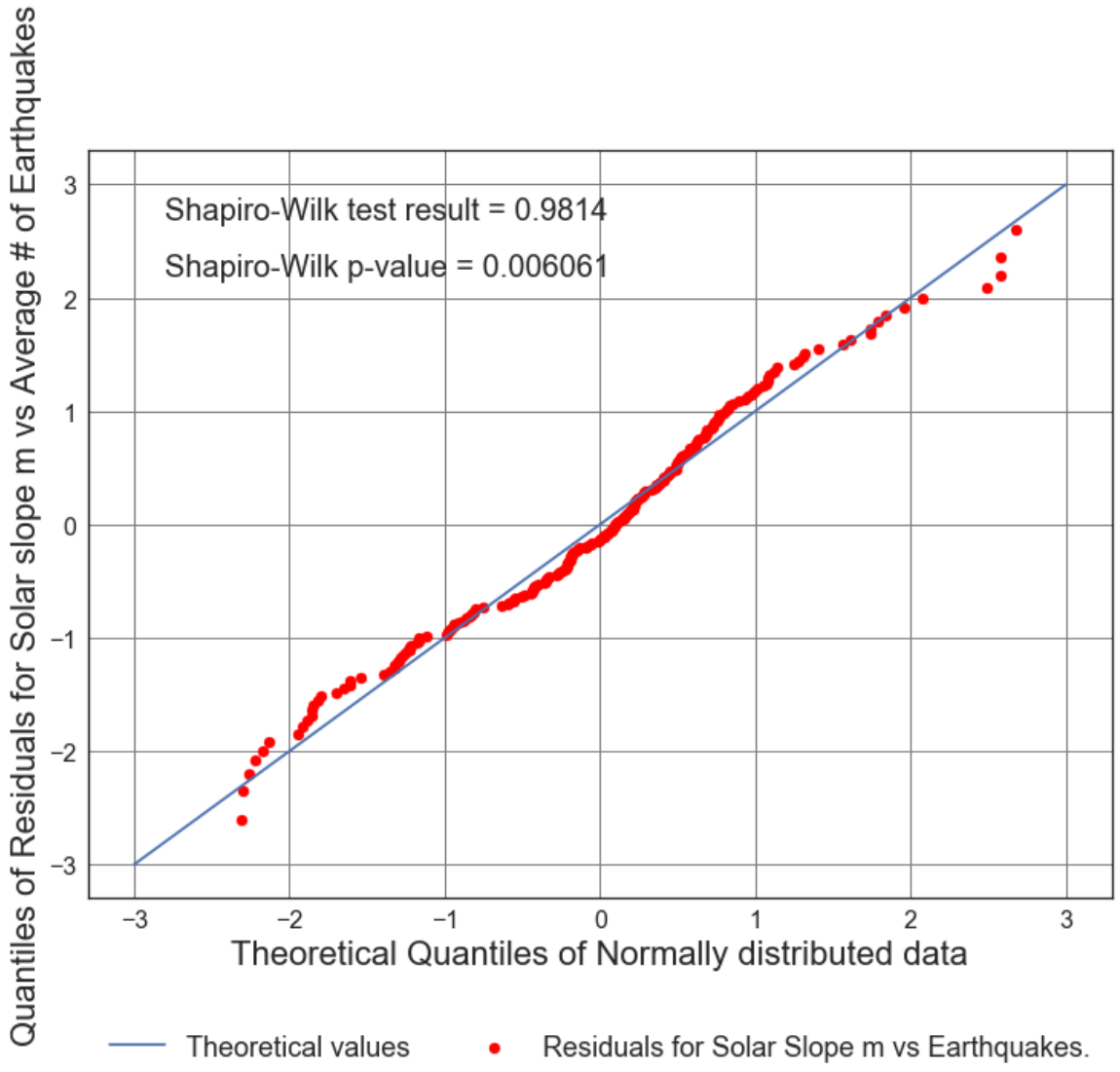

Figure D2.23: Residuals Plot of Solar cycle slope (from 1900 to 2017) vs. Average number of 6.5M and up Earthquakes/6months. Line of best fit, y = -0.06203x + (33.23), mean x = -0.07013 +/- 38.33, mean y = 33.23 +/- 14.75, R = -0.1611, R squared = 0.02596, p-value = 0.01779.

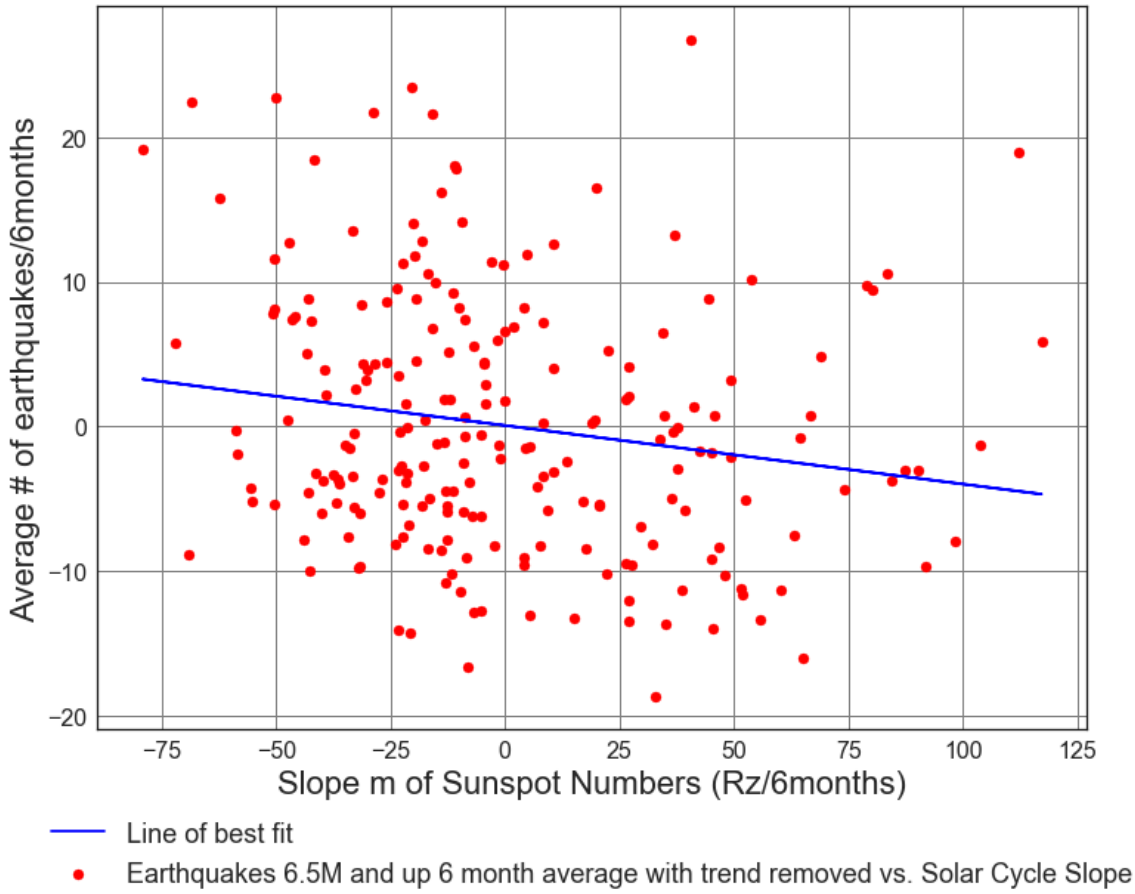

Figure D2.24: Scatter Plot of Solar cycle slope (from 1900 to 2017) vs. Average number of 6.5M and up Earthquakes/6months with trend removed. Line of best fit, y = -0.04055x + (0.05514), mean x = -0.07013 +/- 38.33, mean y = 0.05799 +/- 8.905, R = -0.1746, R squared = 0.03047, p-value = 0.01016.

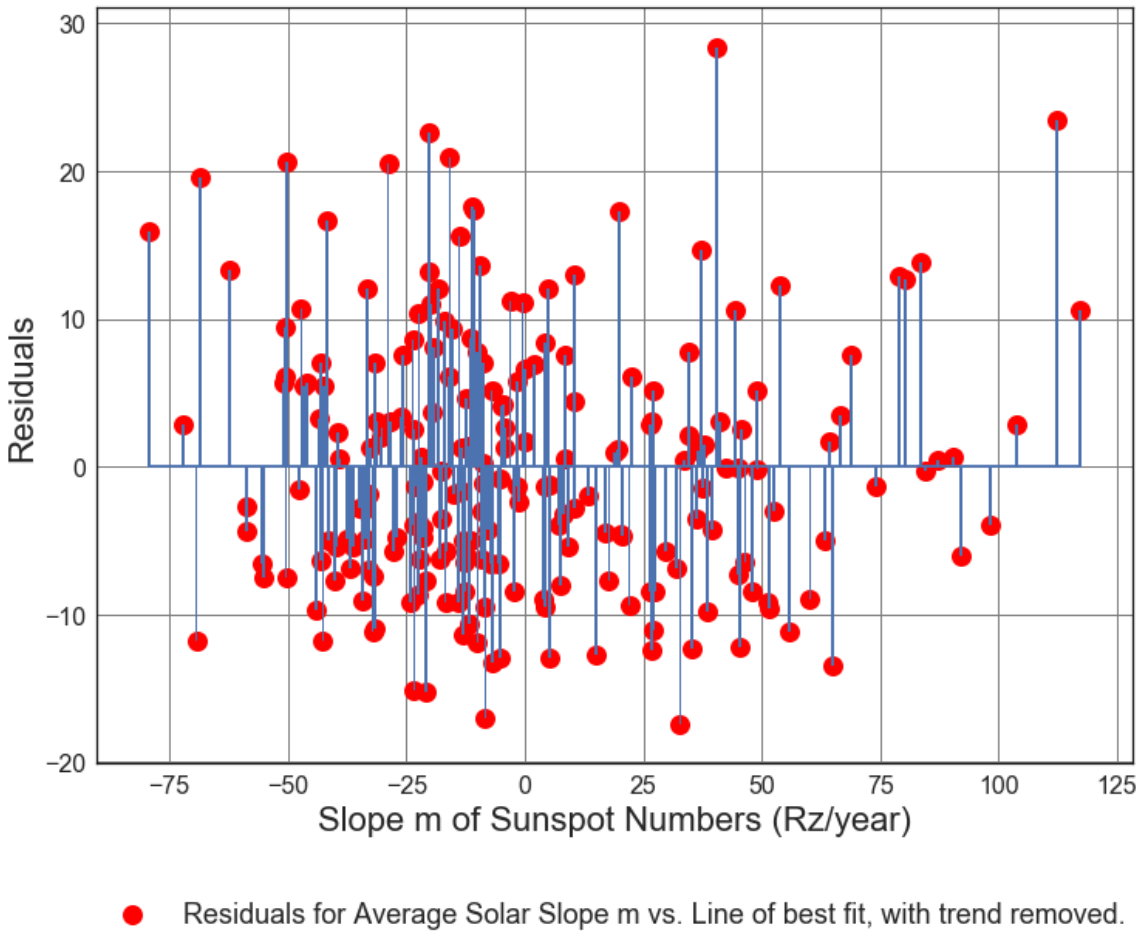

Figure D2.25: Scatter Plot of Solar cycle slope (from 1900 to 2017) vs. Average number of 6.5M and up Earthquakes/6months with trend removed. Line of best fit, y = -0.04055x + (0.05514), mean x = -0.07013 +/- 38.33, mean y = 0.05799 +/- 8.905, R = -0.1746, R squared = 0.03047, p-value = 0.01016.

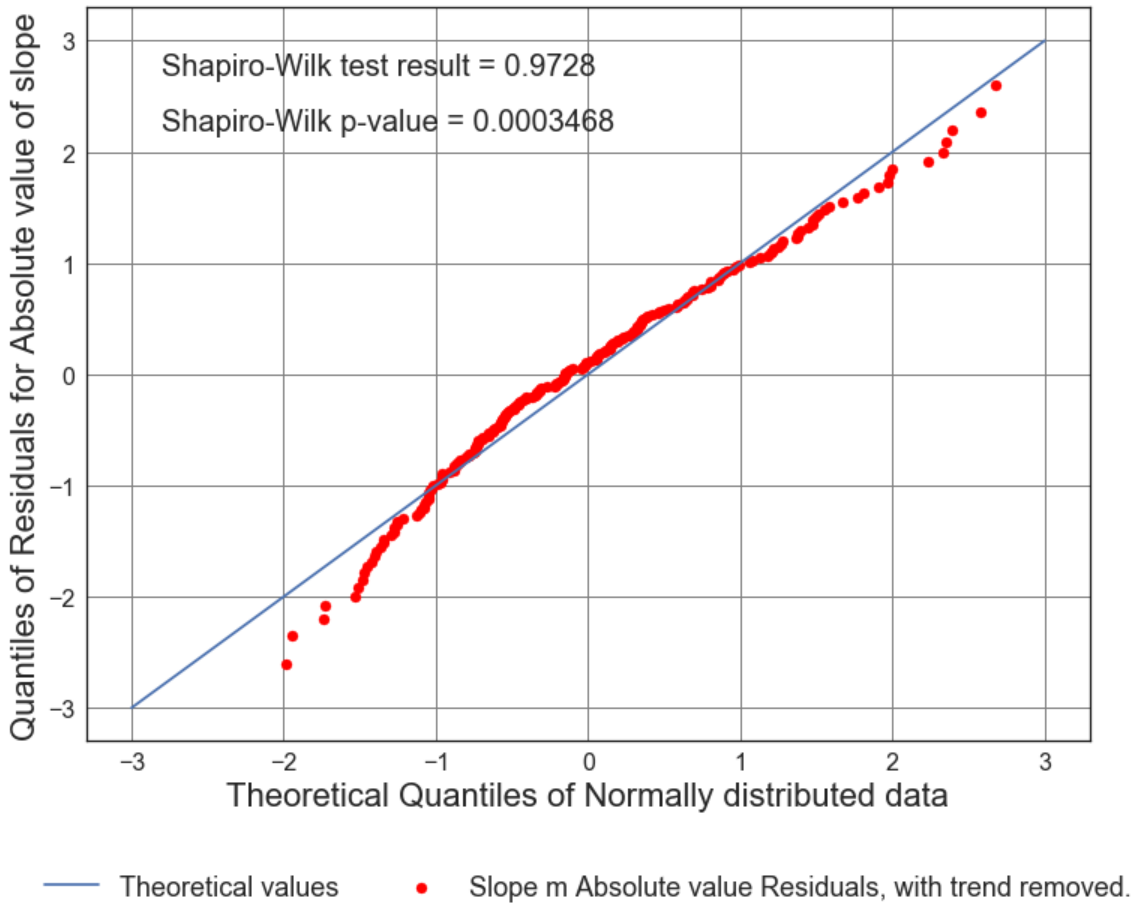

Figure D2.26: Scatter Plot of Solar cycle slope (from 1900 to 2017) vs. Average number of 6.5M and up Earthquakes/6months with trend removed. Line of best fit, y = -0.04055x + (0.05514), mean x = -0.07013 +/- 38.33, mean y = 0.05799 +/- 8.905, R = -0.1746, R squared = 0.03047, p-value = 0.01016.

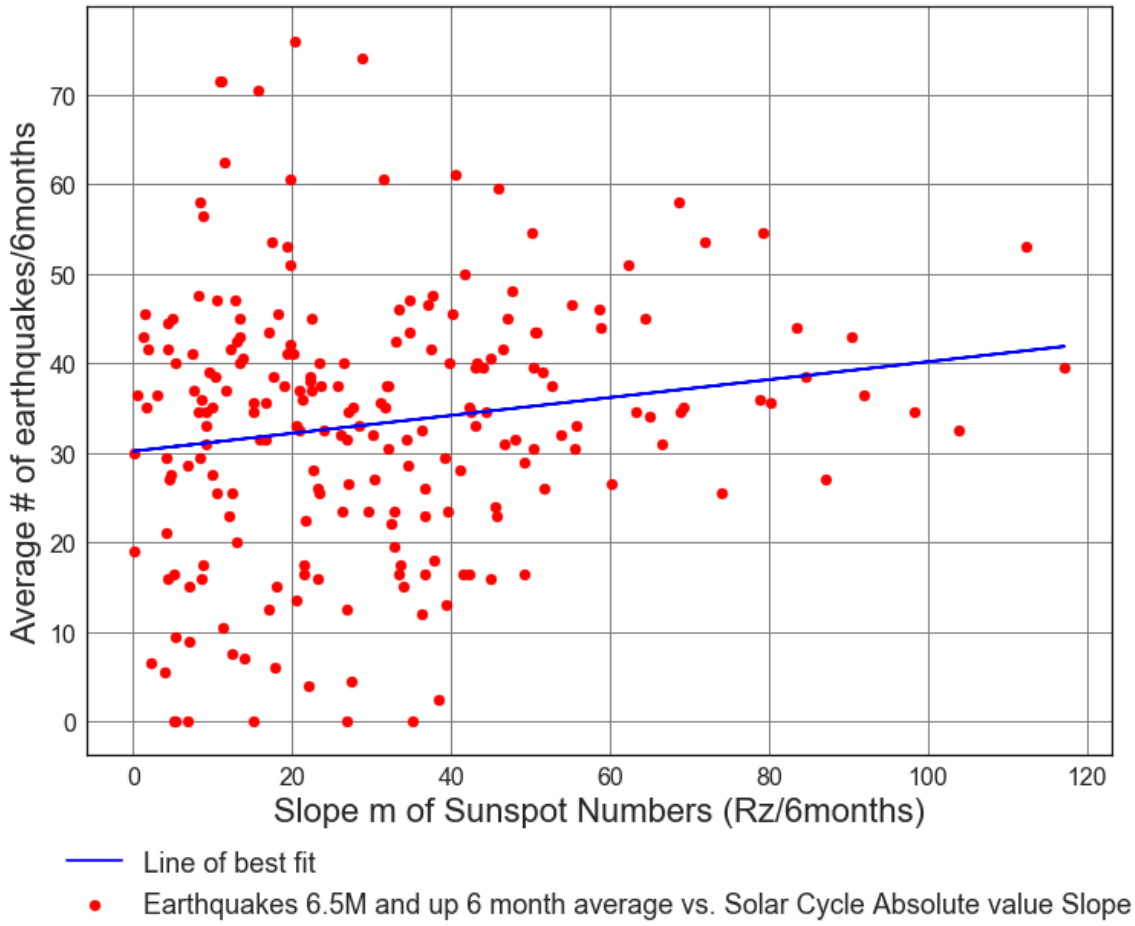

Figure D2.27: Scatter Plot of Solar cycle slope (from 1900 to 2017) vs. Average number of 6.5M and up Earthquakes/6months. Line of best fit, y = 0.09991x + (30.17), mean x = 30.66 +/- 23.0, mean y = 33.23 +/- 14.75, R = 0.1557, R squared = 0.02426, p-value = 0.02204.

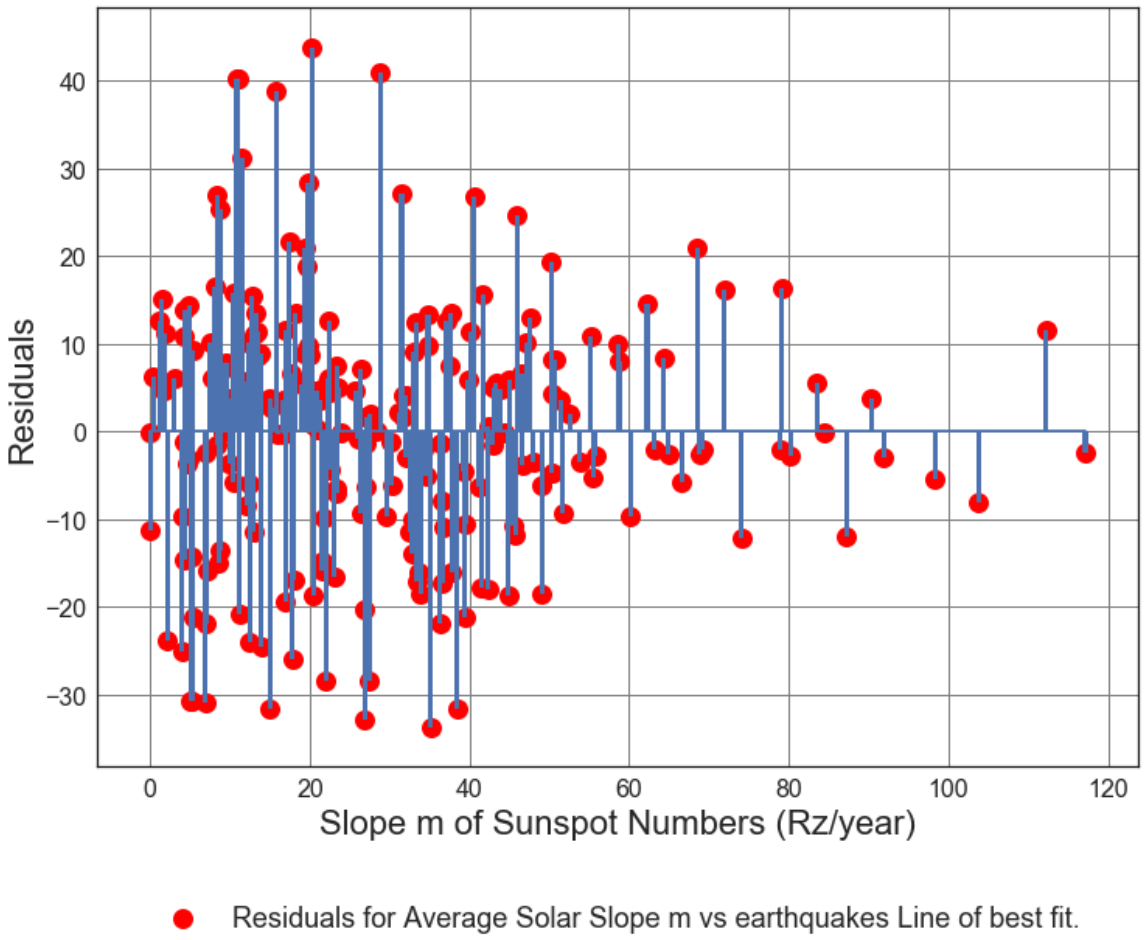

Figure D2.28: Scatter Plot of Solar cycle slope (from 1900 to 2017) vs. Average number of 6.5M and up Earthquakes/6months. Line of best fit, y = 0.09991x + (30.17), mean x = 30.66 +/- 23.0, mean y = 33.23 +/- 14.75, R = 0.1557, R squared = 0.02426, p-value = 0.02204.

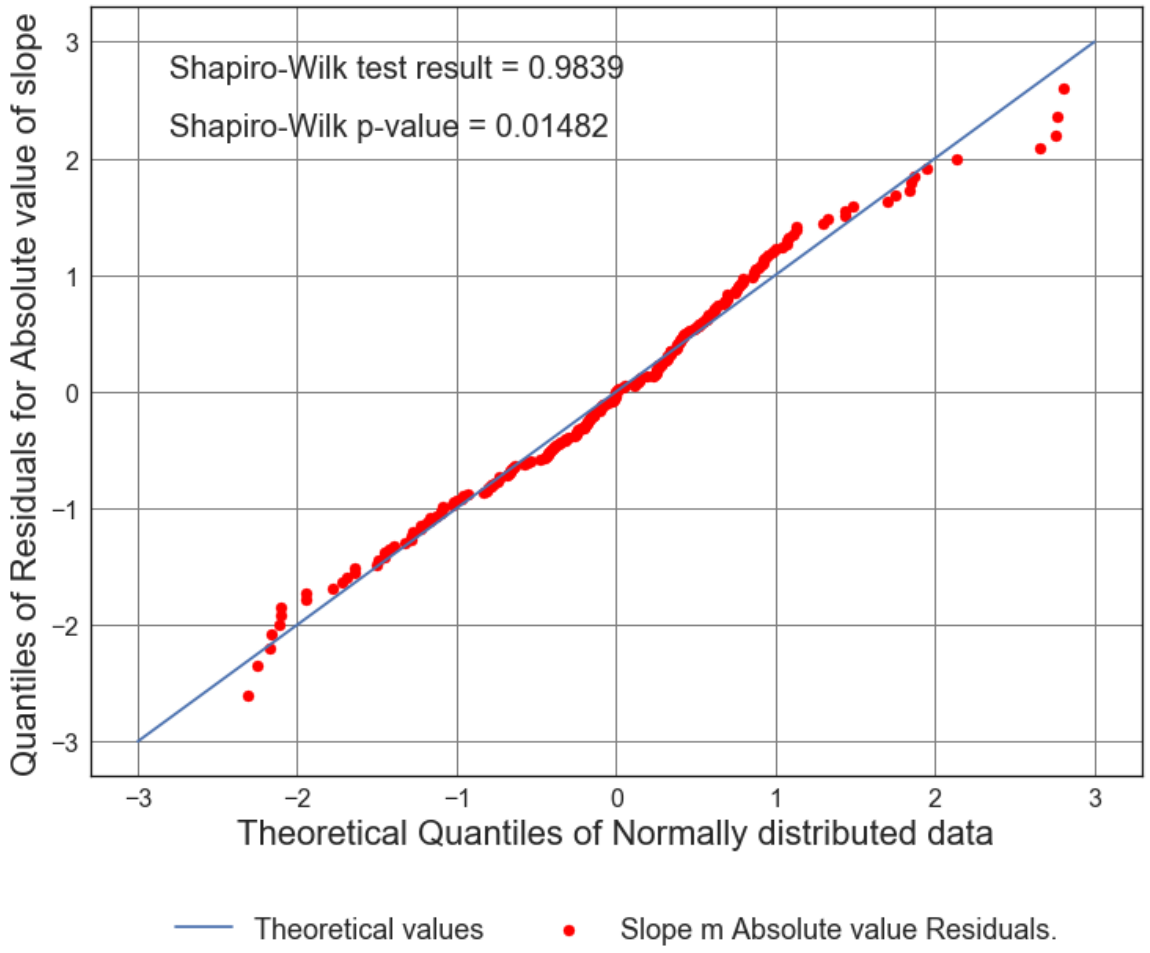

Figure D2.29: Scatter Plot of Solar cycle slope (from 1900 to 2017) vs. Average number of 6.5M and up Earthquakes/6months. Line of best fit, y = 0.09991x + (30.17), mean x = 30.66 +/- 23.0, mean y = 33.23 +/- 14.75, R = 0.1557, R squared = 0.02426, p-value = 0.02204.

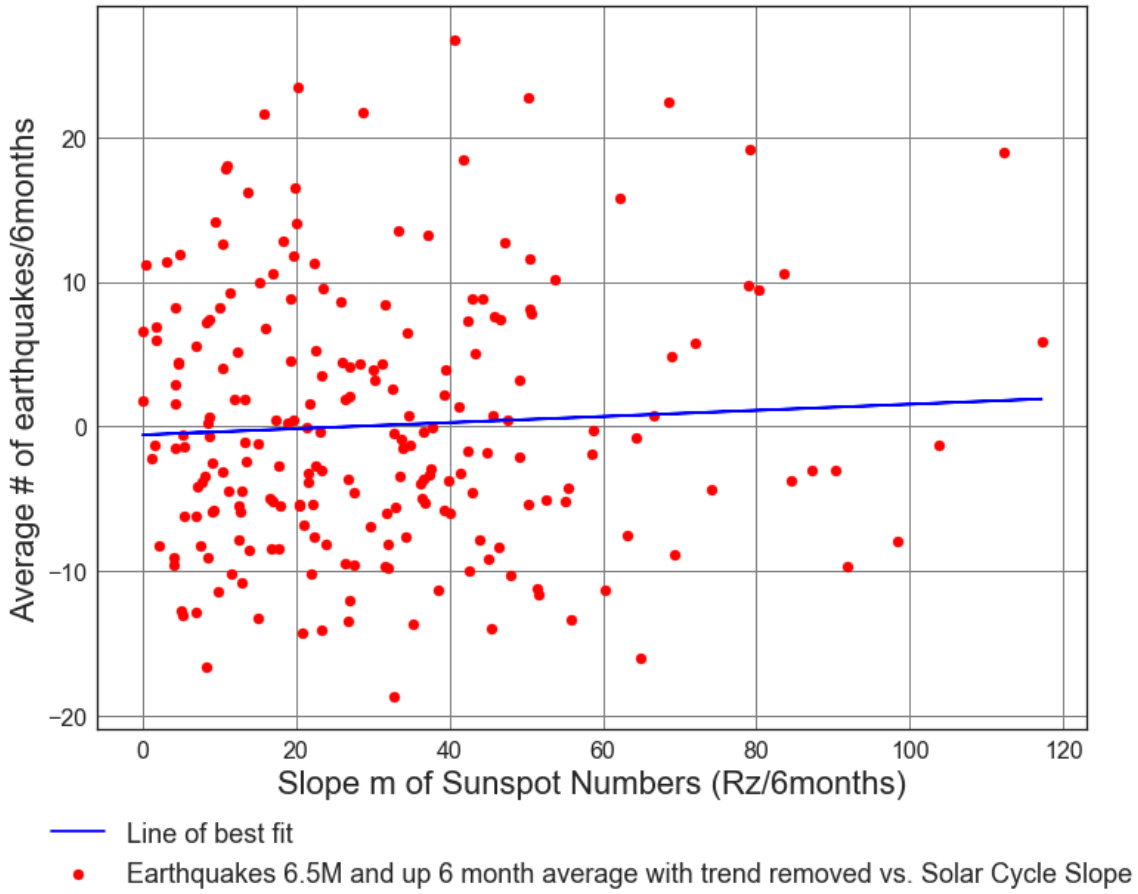

Figure D2.30: Scatter Plot of Solar cycle absolute value slope (from 1900 to 2017) vs. Average number of 6.5M and up Earthquakes/6months with trend removed. Line of best fit, y = 0.02119x + (-0.5919), mean x = 30.66 +/- 23.0, mean y = 0.05799 +/- 8.905, R = 0.05474, R squared = 0.002997, p-value = 0.4234.

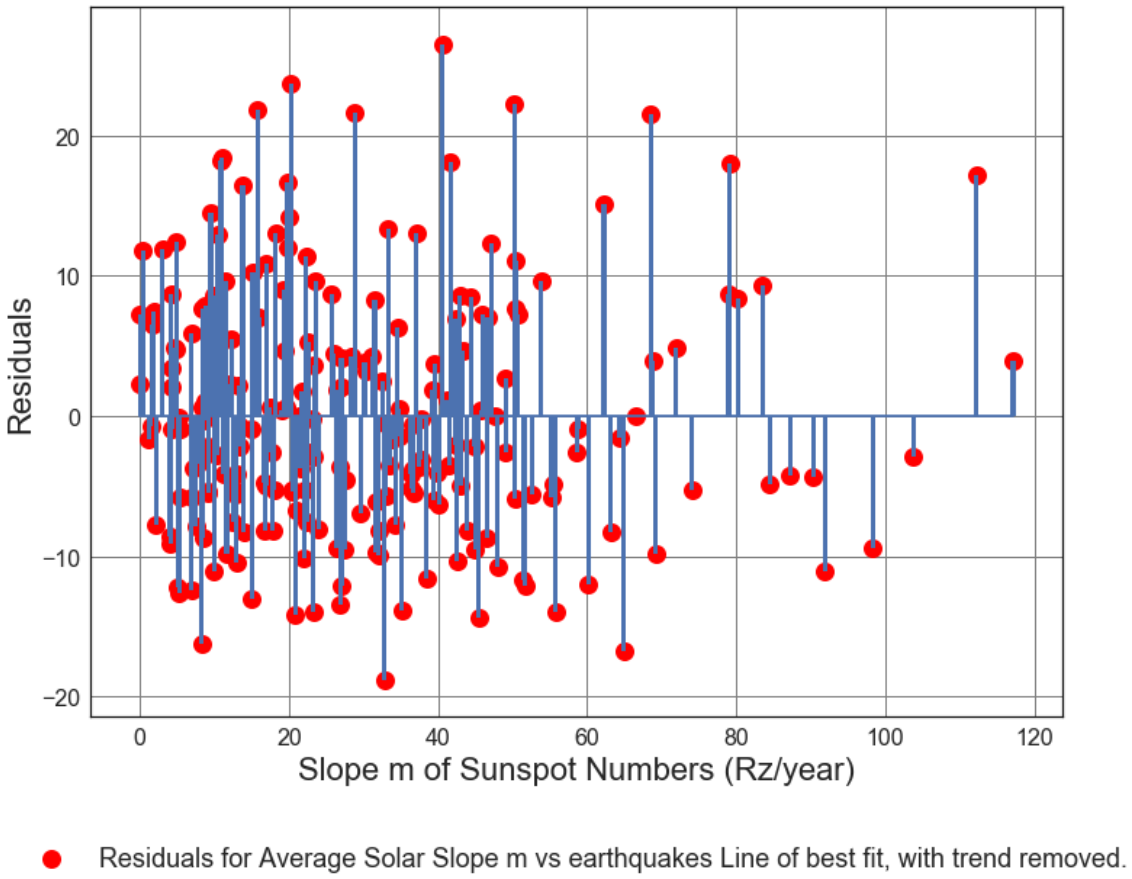

Figure D2.31: Scatter Plot of Solar cycle absolute value slope (from 1900 to 2017) vs. Average number of 6.5M and up Earthquakes/6months with trend removed. Line of best fit, y = 0.02119x + (-0.5919), mean x = 30.66 +/- 23.0, mean y = 0.05799 +/- 8.905, R = 0.05474, R squared = 0.002997, p-value = 0.4234.

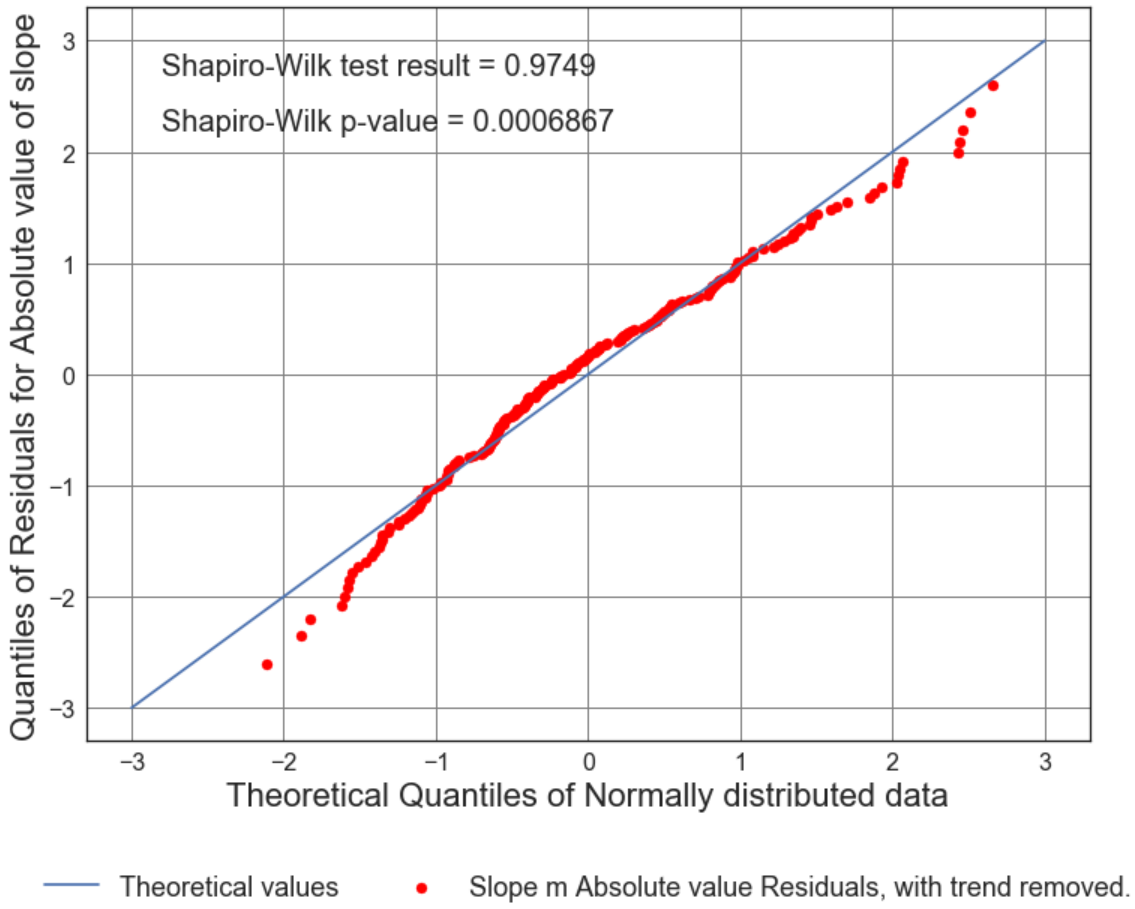

Figure D2.32: Scatter Plot of Solar cycle absolute value slope (from 1900 to 2017) vs. Average number of 6.5M and up Earthquakes/6months with trend removed. Line of best fit, y = 0.02119x + (-0.5919), mean x = 30.66 +/- 23.0, mean y = 0.05799 +/- 8.905, R = 0.05474, R squared = 0.002997, p-value = 0.4234.

Appendix D3: ISC Time Series Analysis Part 3 - Pre 1964 (Historical period) Six Month Averaged Earthquake and Sunspot Data.

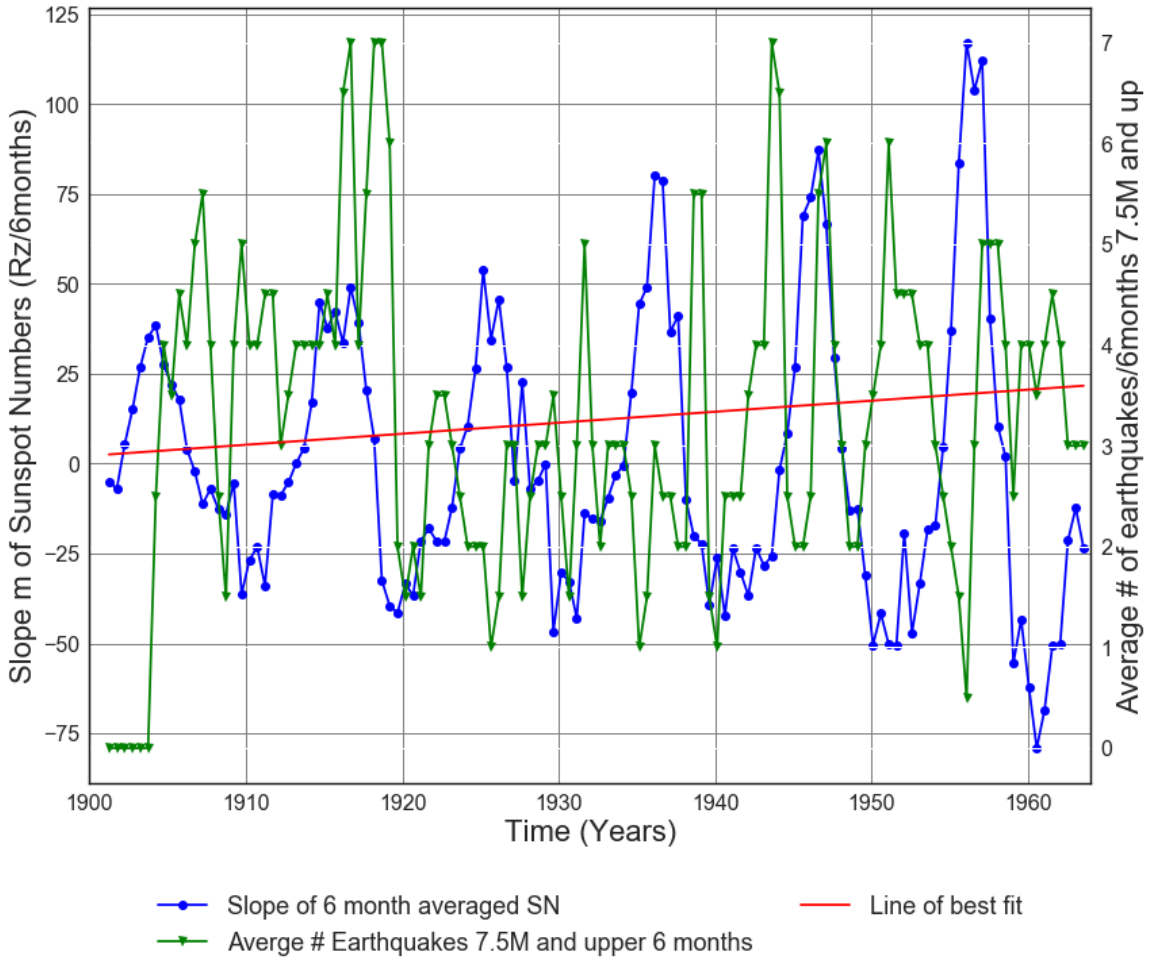

Figure D3.1: Slope of Solar cycle from 1900 to 1964 vs. Average number of 7.5M and up Earthquakes.

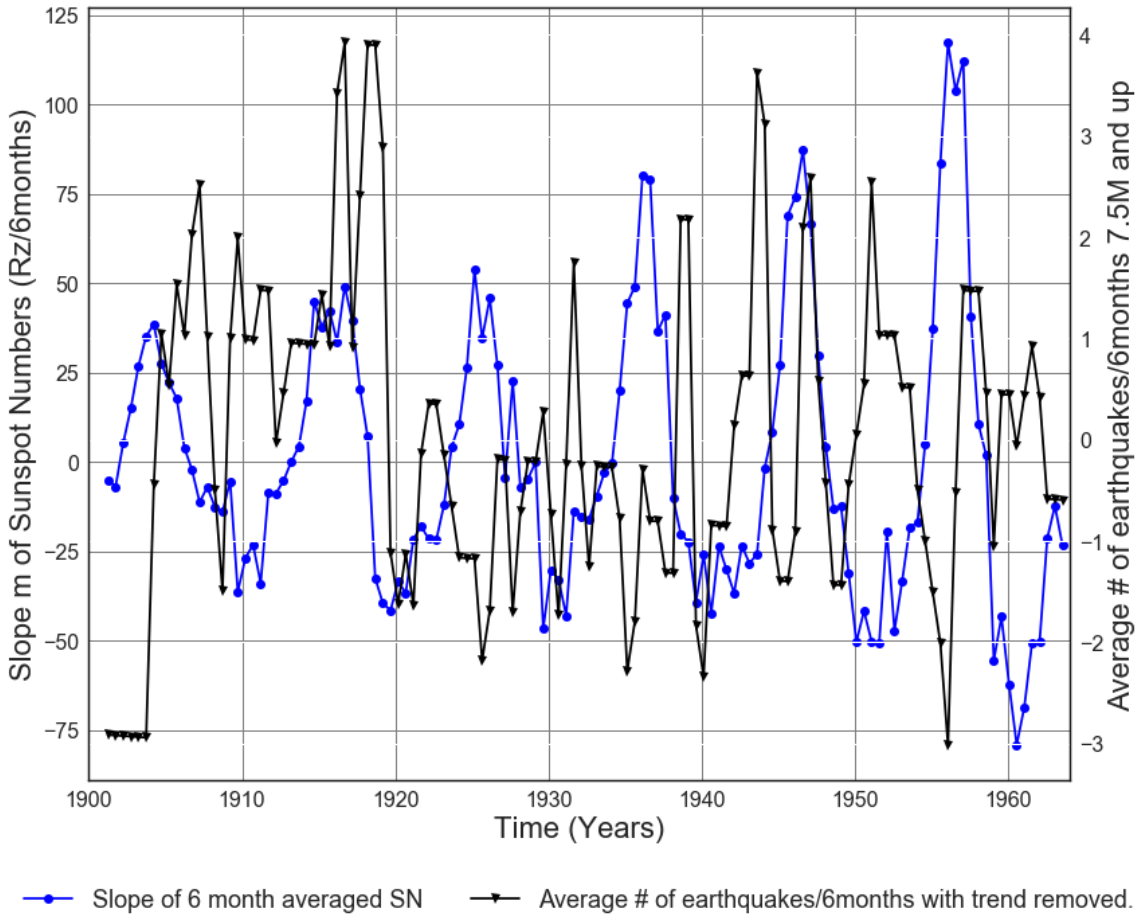

Figure D3.2: Slope of 6 month averaged SN 1900 to 1964 vs. Average number of 7.5M and up Earthquakes with trend removed. Line of best fit, y = 0.01094x + (-17.89), mean x = 1.932e+03 +/- 18.27, mean y = 3.252 +/- 1.597

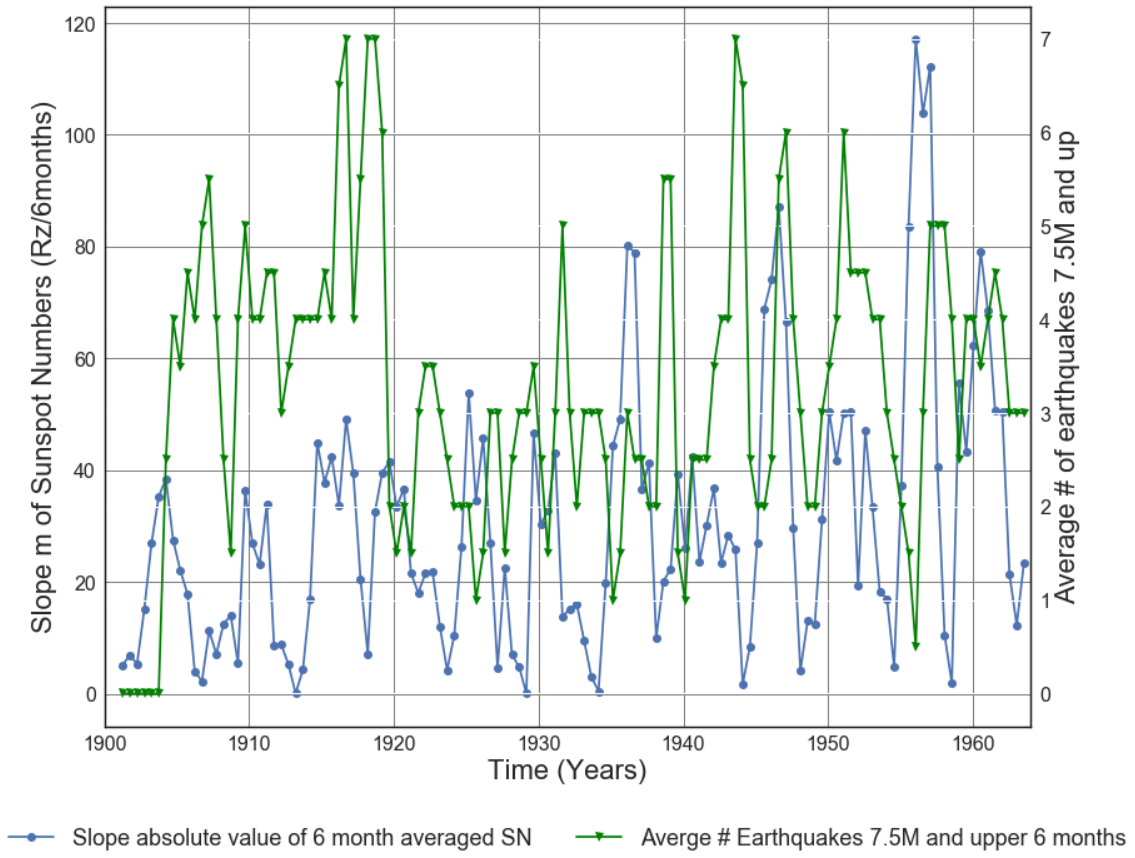

Figure D3.3: Slope Absolute value of Solar cycle from 1900 to 1964 vs. Average number of 7.5M and up Earthquakes.

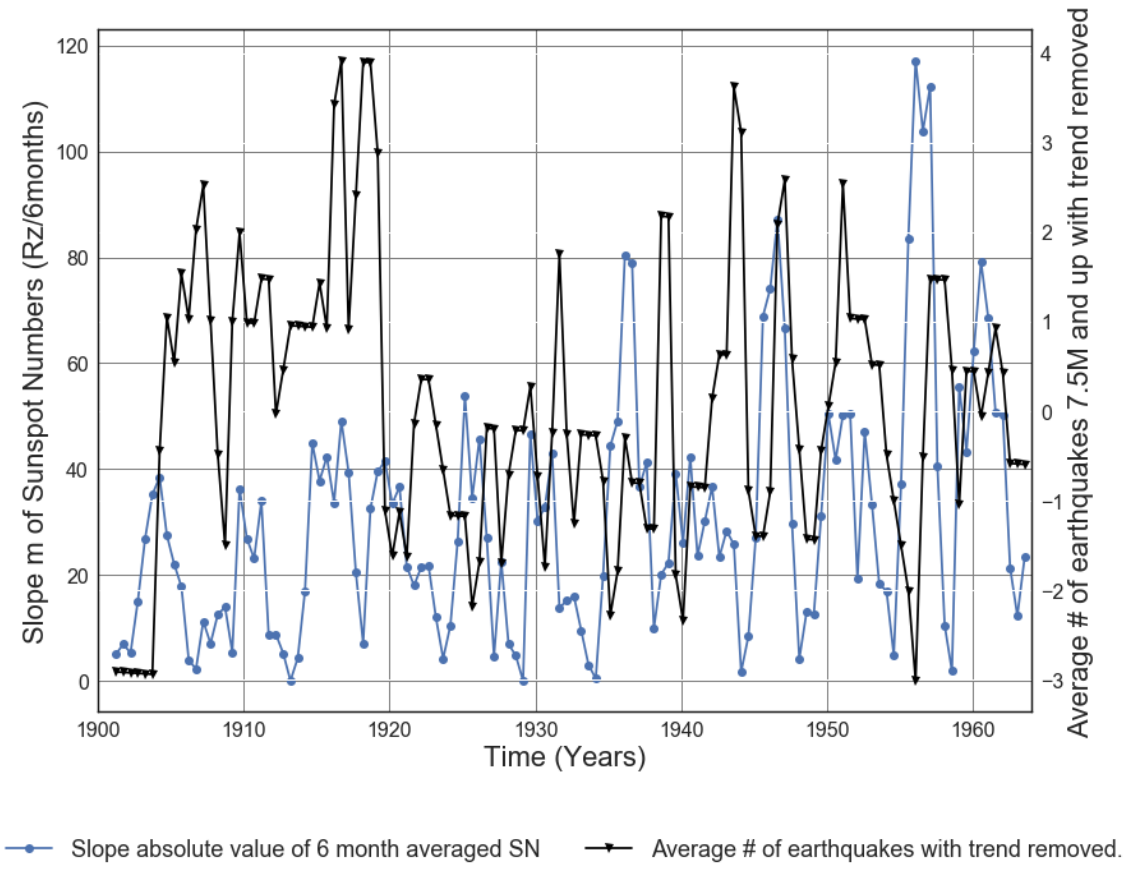

Figure D3.4: Slope Absolute value of Solar cycle from 1900 to 1964 vs. Average number of 7.5M and up earthquakes with trend removed.

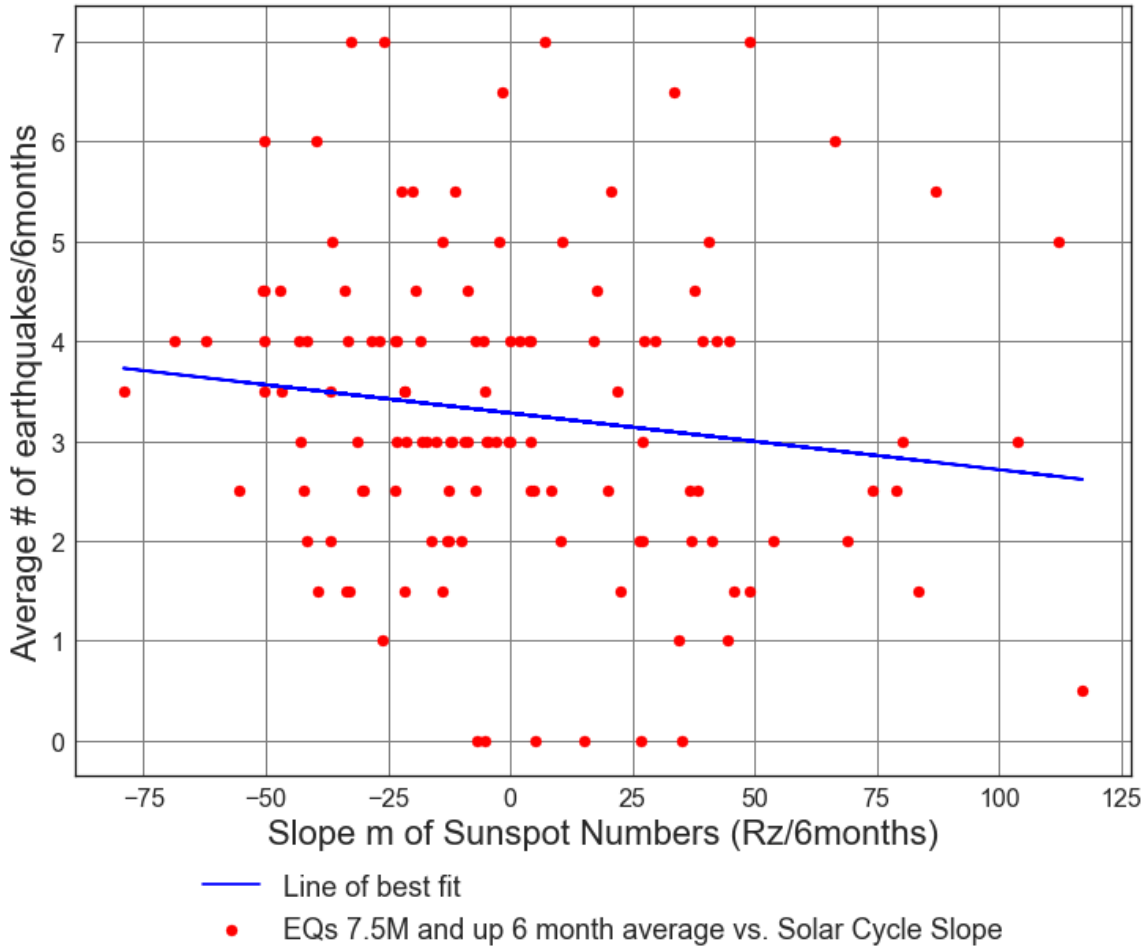

Figure D3.5: Scatter Plot of Solar cycle slope (from 1900 to 1964) vs. Average number of 7.5M and up Earthquakes/6months. Line of best fit, y = -0.005669x + (3.28), mean x = 0.3737 +/- 38.55, mean y = 3.278 +/- 1.577, R = -0.1386, R squared = 0.01921, p-value = 0.1217.

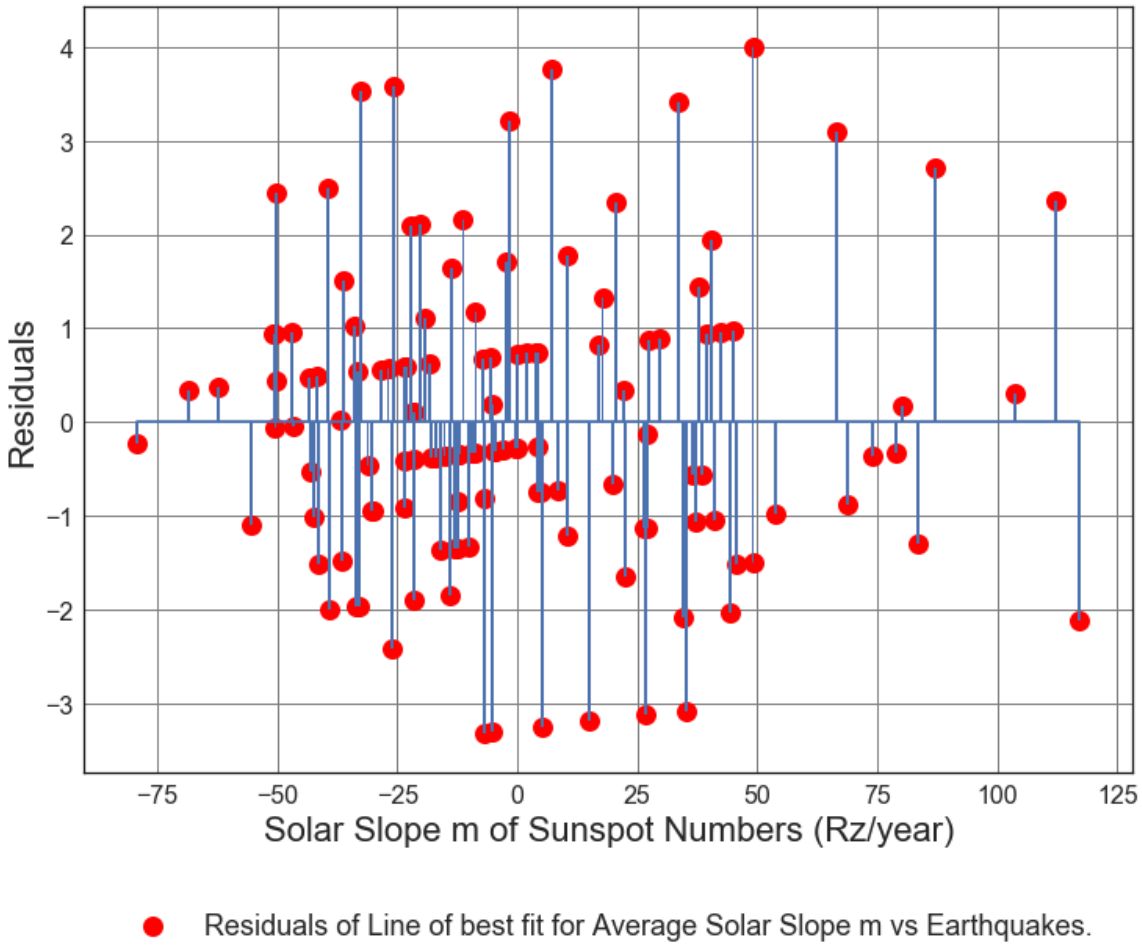

Figure D3.6: Residuals Plot of Solar cycle slope (from 1900 to 1964) vs. Average number of 7.5M and up Earthquakes/6months. Line of best fit, y = -0.005669x + (3.28), mean x = 0.3737 +/- 38.55, mean y = 3.278 +/- 1.577, R = -0.1386, R squared = 0.01921, p-value = 0.1217.

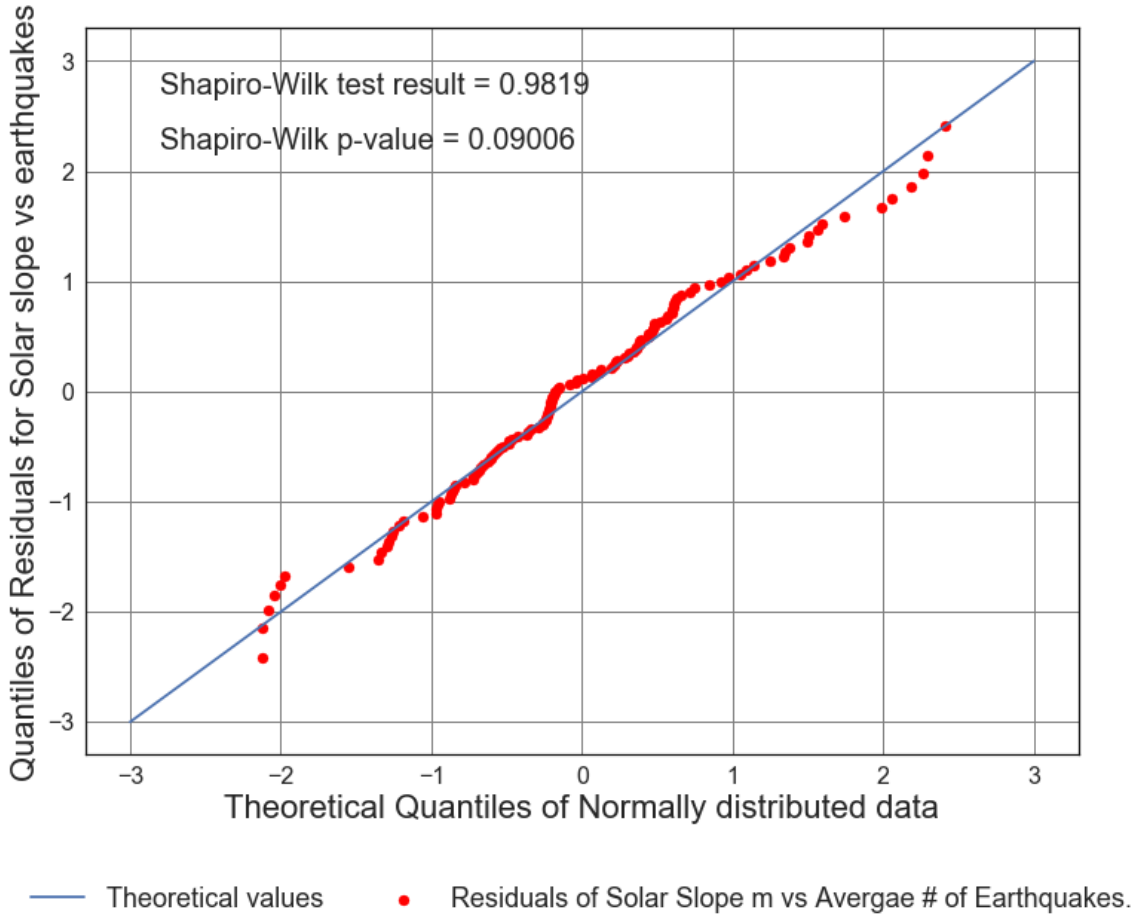

Figure D3.7: Residuals Plot of Solar cycle slope (from 1900 to 1964) vs. Average number of 7.5M and up Earthquakes/6months. Line of best fit, y = -0.005669x + (3.28), mean x = 0.3737 +/- 38.55, mean y = 3.278 +/- 1.577, R = -0.1386, R squared = 0.01921, p-value = 0.1217.

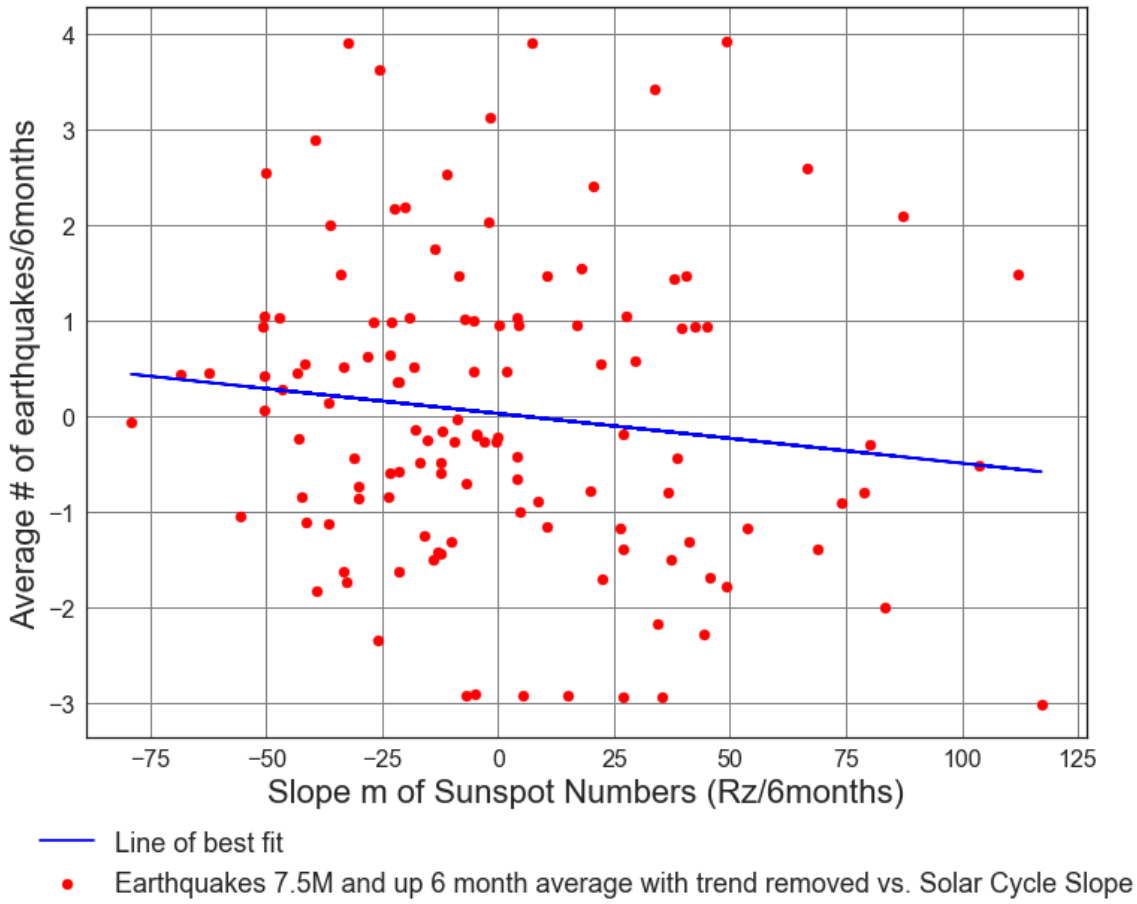

Figure D3.8: Scatter Plot of Solar cycle slope (from 1900 to 1964) vs. Average number of 7.5M and up Earthquakes/6months with trend removed. Line of best fit, y = -0.005199x + (0.02503), mean x = 0.3737 +/- 38.55, mean y = 0.02308 +/- 1.569, R = -0.1277, R squared = 0.01631, p-value = 0.1542.

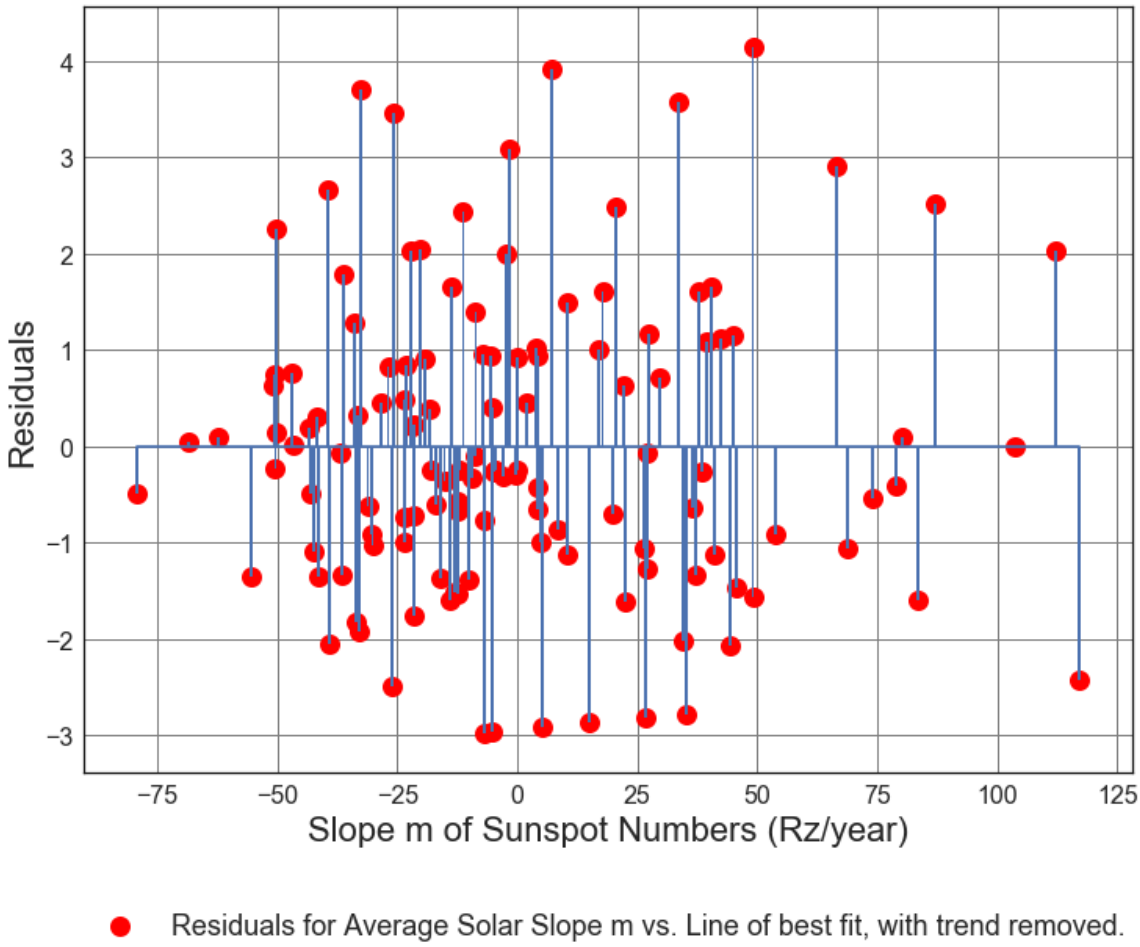

Figure D3.9: Scatter Plot of Solar cycle slope (from 1900 to 1964) vs. Average number of 7.5M and up Earthquakes/6months with trend removed. Line of best fit, y = -0.005199x + (0.02503), mean x = 0.3737 +/- 38.55, mean y = 0.02308 +/- 1.569, R = -0.1277, R squared = 0.01631, p-value = 0.1542.

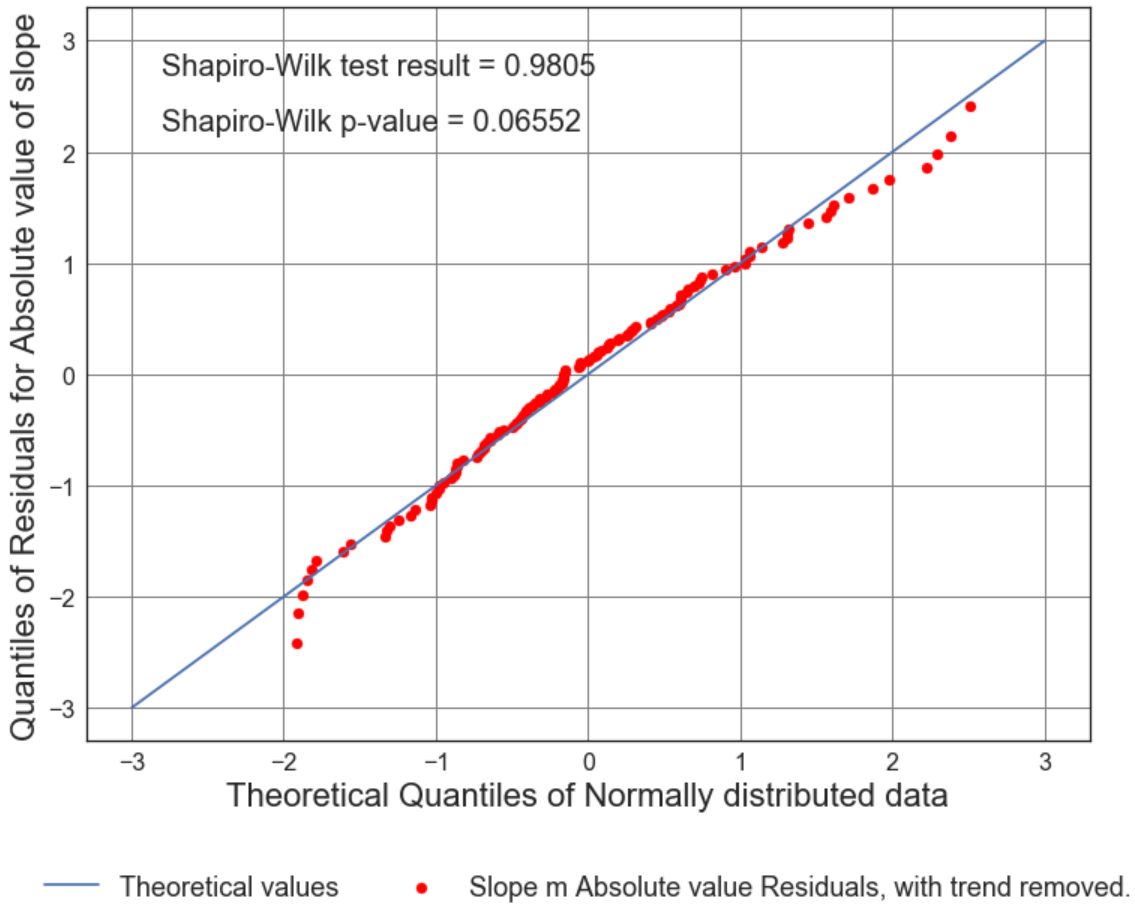

Figure D3.10: Scatter Plot of Solar cycle slope (from 1900 to 1964) vs. Average number of 7.5M and up Earthquakes/6months with trend removed. Line of best fit, y = -0.005199x + (0.02503), mean x = 0.3737 +/- 38.55, mean y = 0.02308 +/- 1.569, R = -0.1277, R squared = 0.01631, p-value = 0.1542.

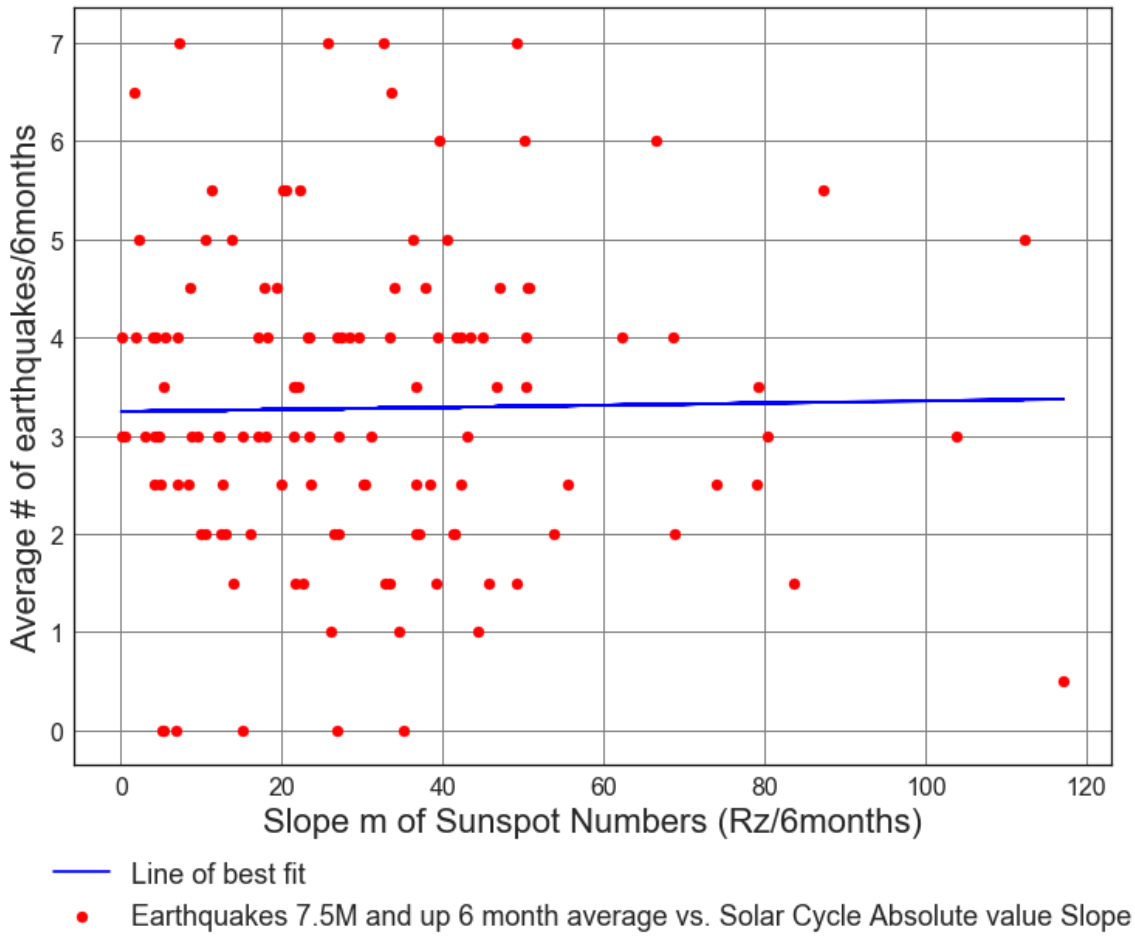

Figure D3.11: Scatter Plot of Solar cycle slope (from 1900 to 1964) vs. Average number of 7.5M and up Earthquakes/6months. Line of best fit, y = 0.001085x + (3.245), mean x = 30.43 +/- 23.66, mean y = 3.278 +/- 1.577, R = 0.01628, R squared = 0.0002651, p-value = 0.8564.

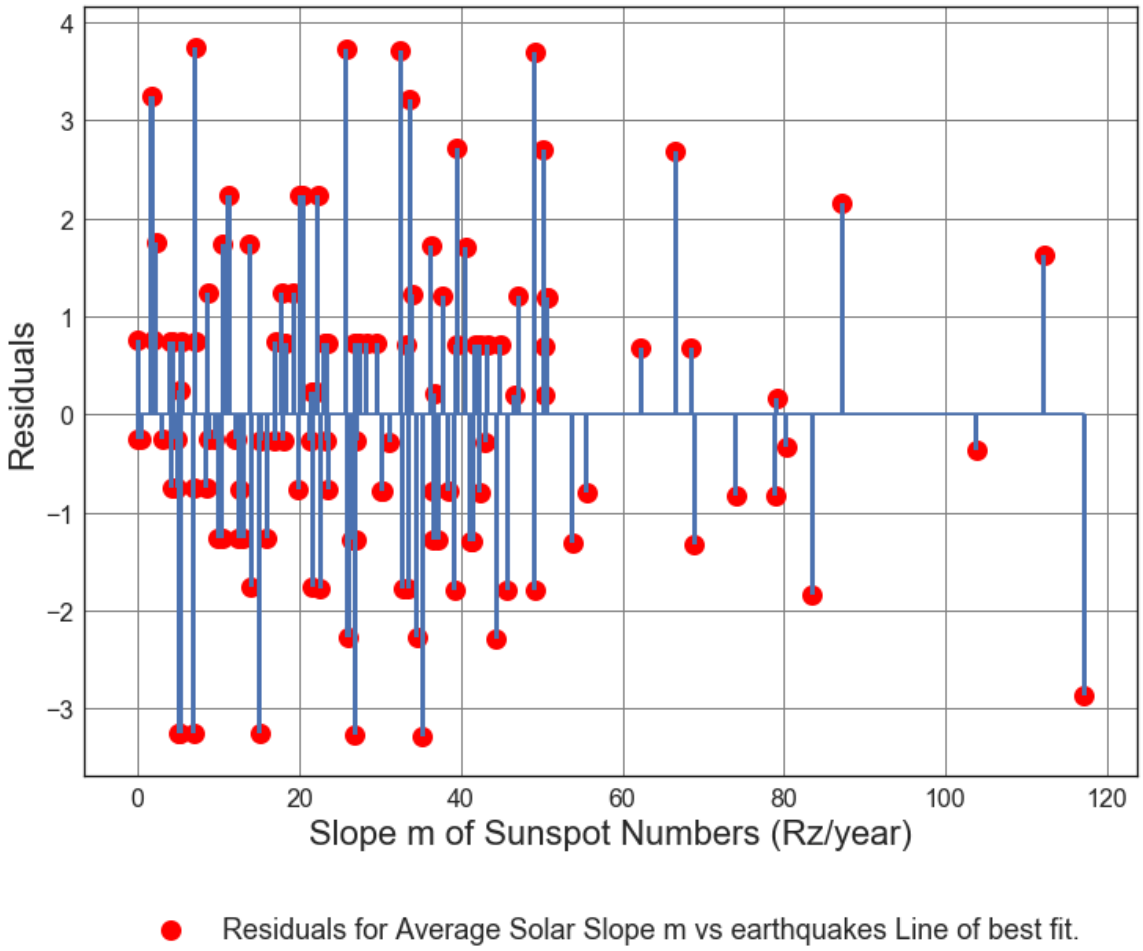

Figure D3.12: Scatter Plot of Solar cycle slope (from 1900 to 1964) vs. Average number of 7.5M and up Earthquakes/6months. Line of best fit, y = 0.001085x + (3.245), mean x = 30.43 +/- 23.66, mean y = 3.278 +/- 1.577, R = 0.01628, R squared = 0.0002651, p-value = 0.8564.

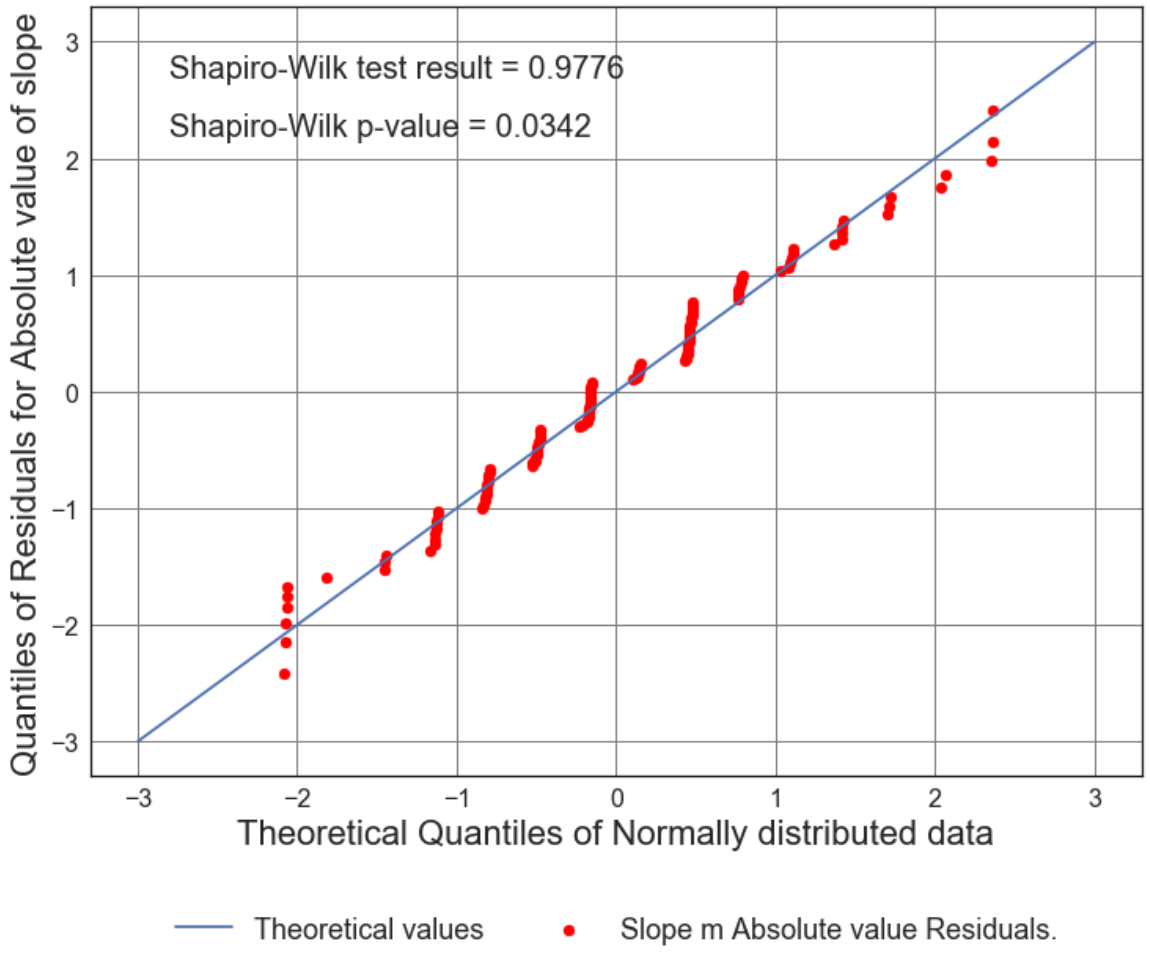

Figure D3.13: Scatter Plot of Solar cycle slope (from 1900 to 1964) vs. Average number of 7.5M and up Earthquakes/6months. Line of best fit, y = 0.001085x + (3.245), mean x = 30.43 +/- 23.66, mean y = 3.278 +/- 1.577, R = 0.01628, R squared = 0.0002651, p-value = 0.8564.

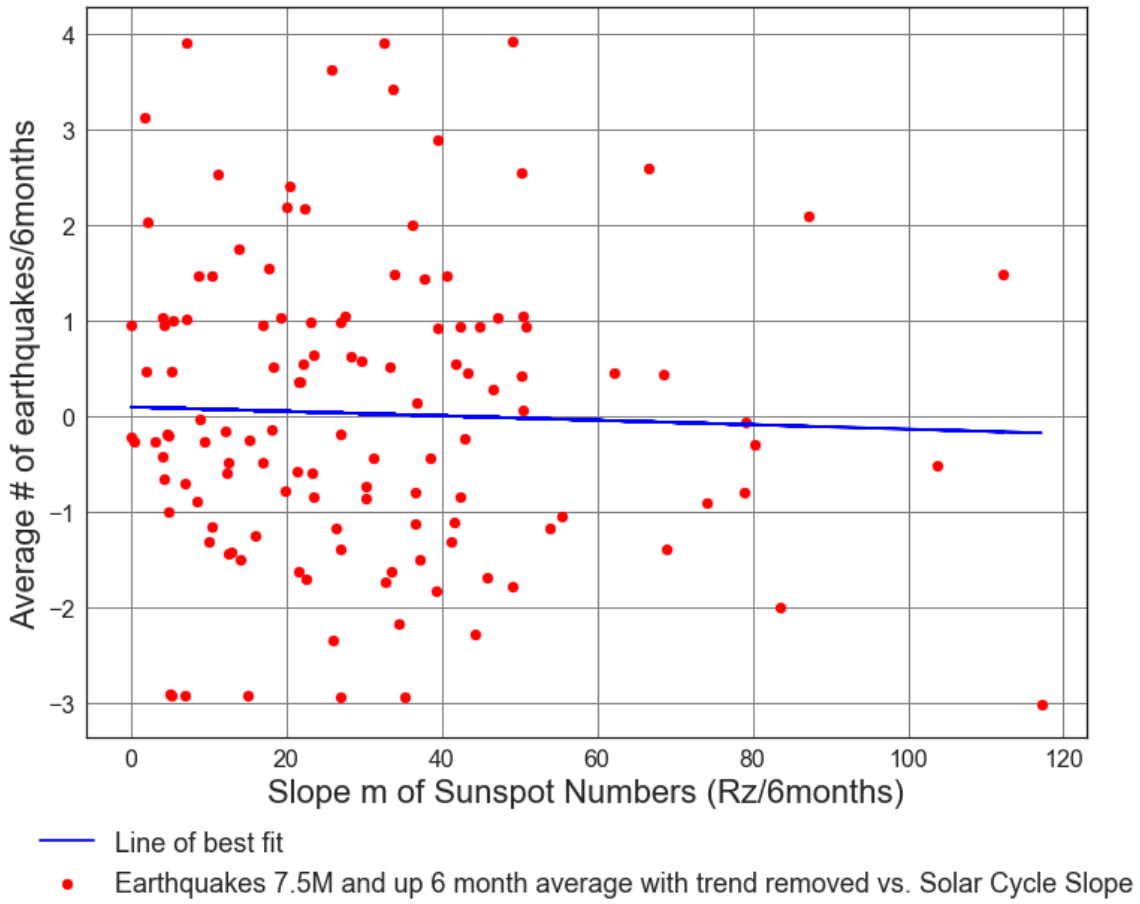

Figure D3.14: Scatter Plot of Solar cycle absolute value slope (from 1900 to 1964) vs. Average number of 7.5M and up Earthquakes/6months with trend removed. Line of best fit, y = -0.00232x + (0.09368), mean x = 30.43 +/- 23.66, mean y = 0.02308 +/- 1.569, R = -0.03498, R squared = 0.001223, p-value = 0.6974.

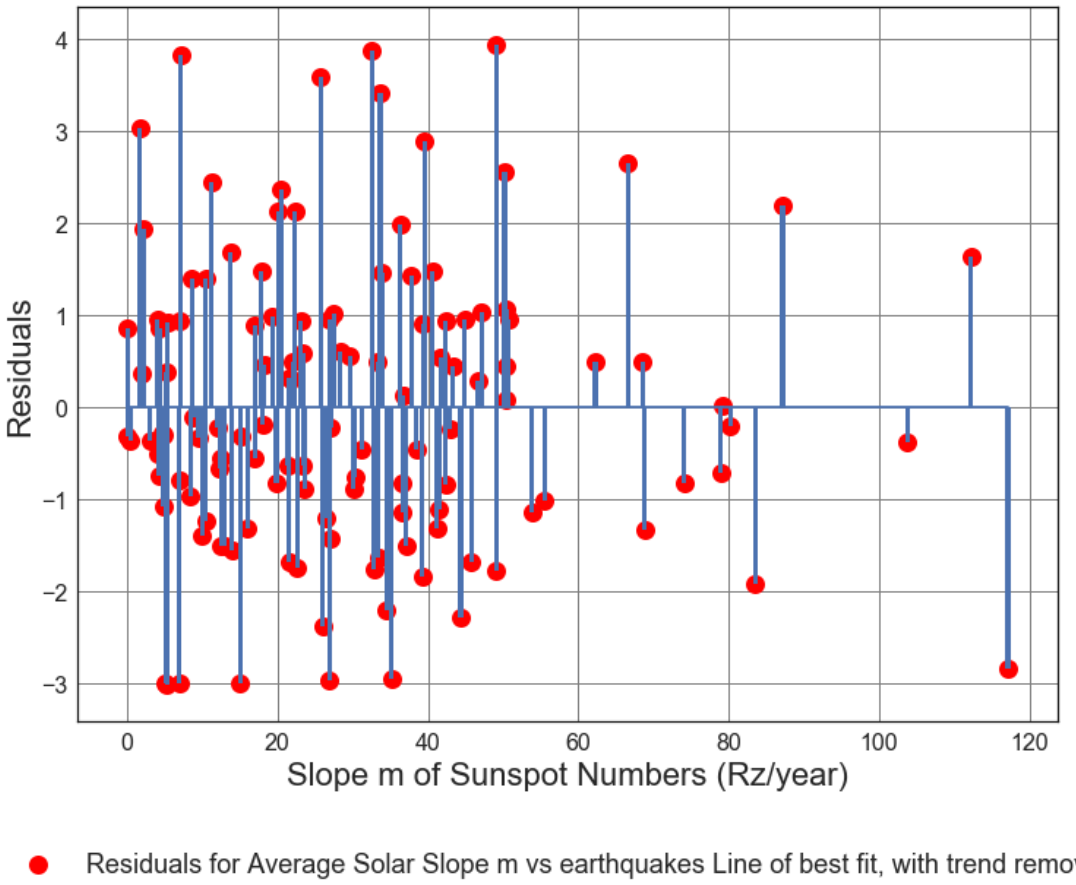

Figure D3.15: Scatter Plot of Solar cycle absolute value slope (from 1900 to 1964) vs. Average number of 7.5M and up Earthquakes/6months with trend removed. Line of best fit, y = -0.00232x + (0.09368), mean x = 30.43 +/- 23.66, mean y = 0.02308 +/- 1.569, R = -0.03498, R squared = 0.001223, p-value = 0.6974.

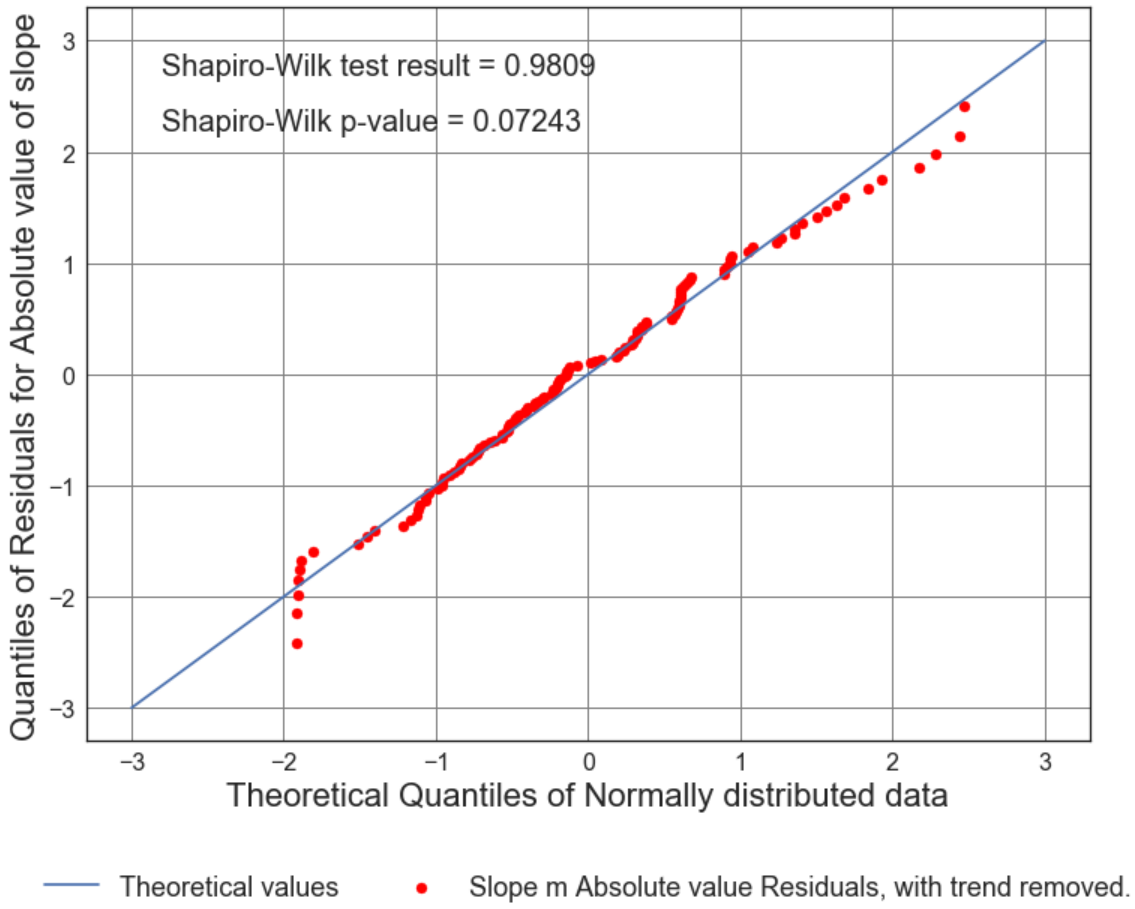

Figure D3.16: Scatter Plot of Solar cycle absolute value slope (from 1900 to 1964) vs. Average number of 7.5M and up Earthquakes/6months with trend removed. Line of best fit, y = -0.00232x + (0.09368), mean x = 30.43 +/- 23.66, mean y = 0.02308 +/- 1.569, R = -0.03498, R squared = 0.001223, p-value = 0.6974.

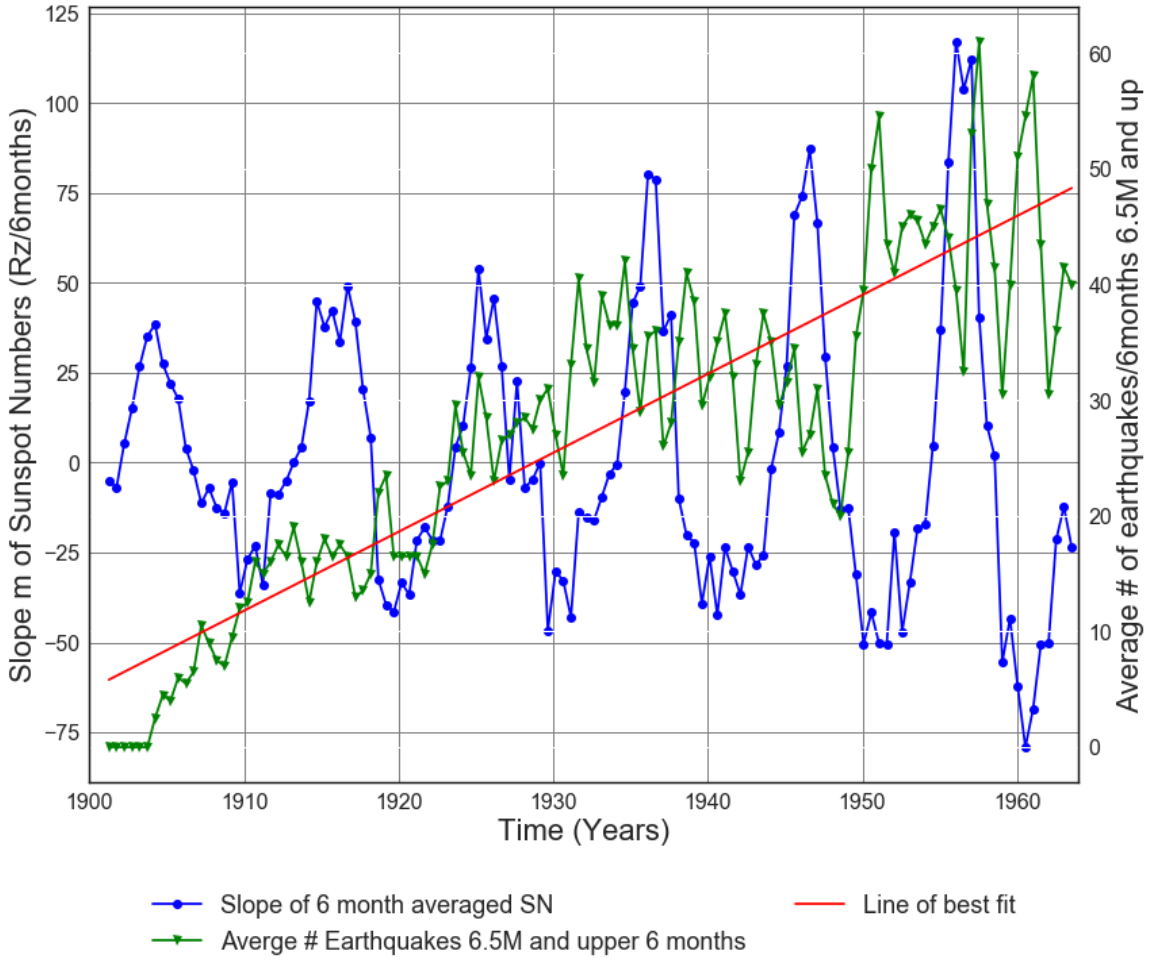

Figure D3.17: Slope of Solar cycle from 1900 to 1964 vs. Average number of 6.5M and up Earthquakes.

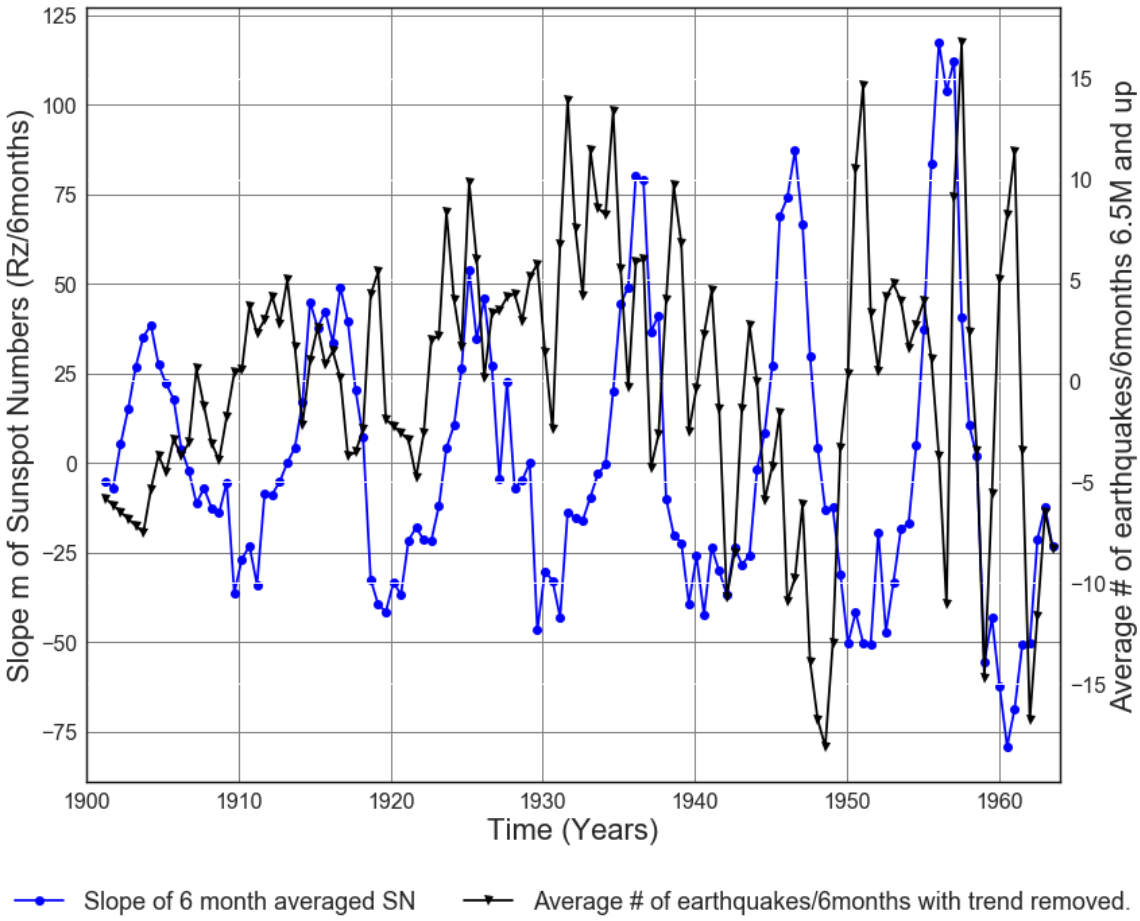

Figure D3.18: Slope of 6 month averaged SN 1900 to 1964 vs. Average number of 6.5M and up Earthquakes with trend removed. Line of best fit, y = 0.6824x + (-1.292e+03), mean x = 1.932e+03 +/- 18.27, mean y = 26.91 +/- 14.11

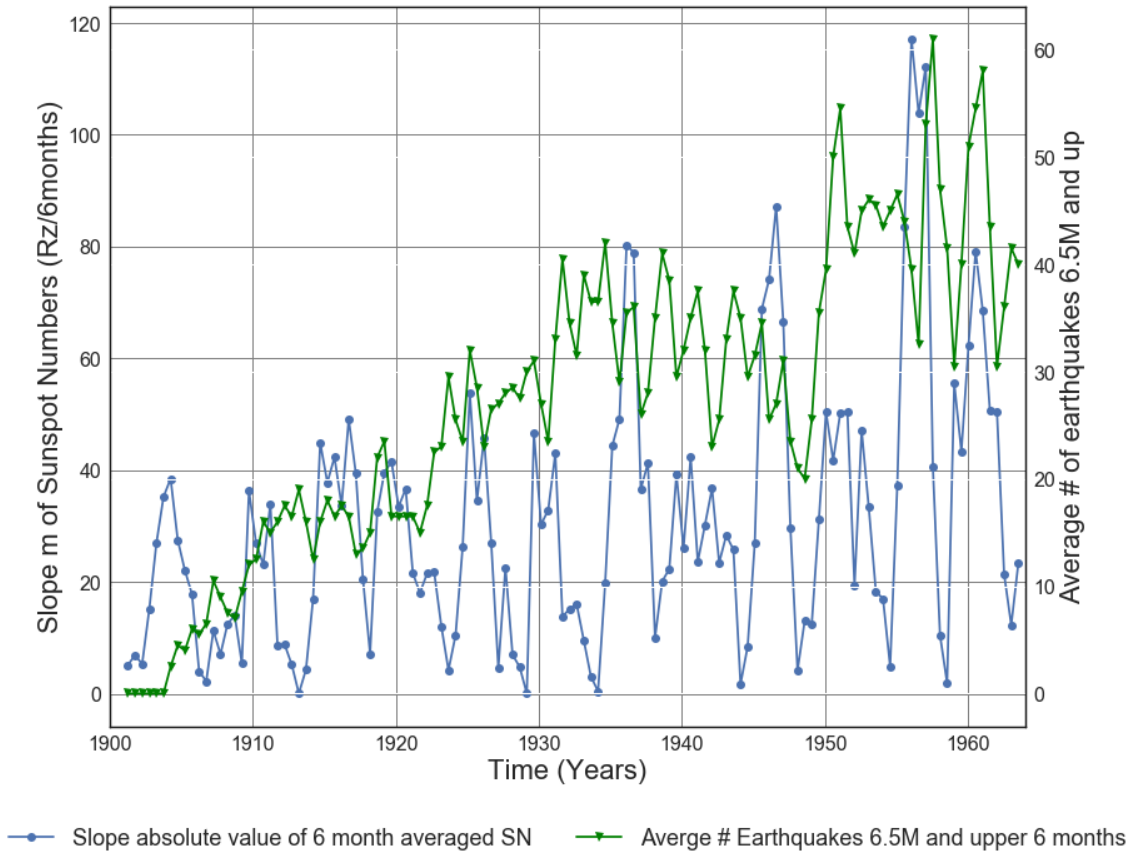

Figure D3.19: Slope Absolute value of Solar cycle from 1900 to 1964 vs. Average number of 6.5M and up Earthquakes.

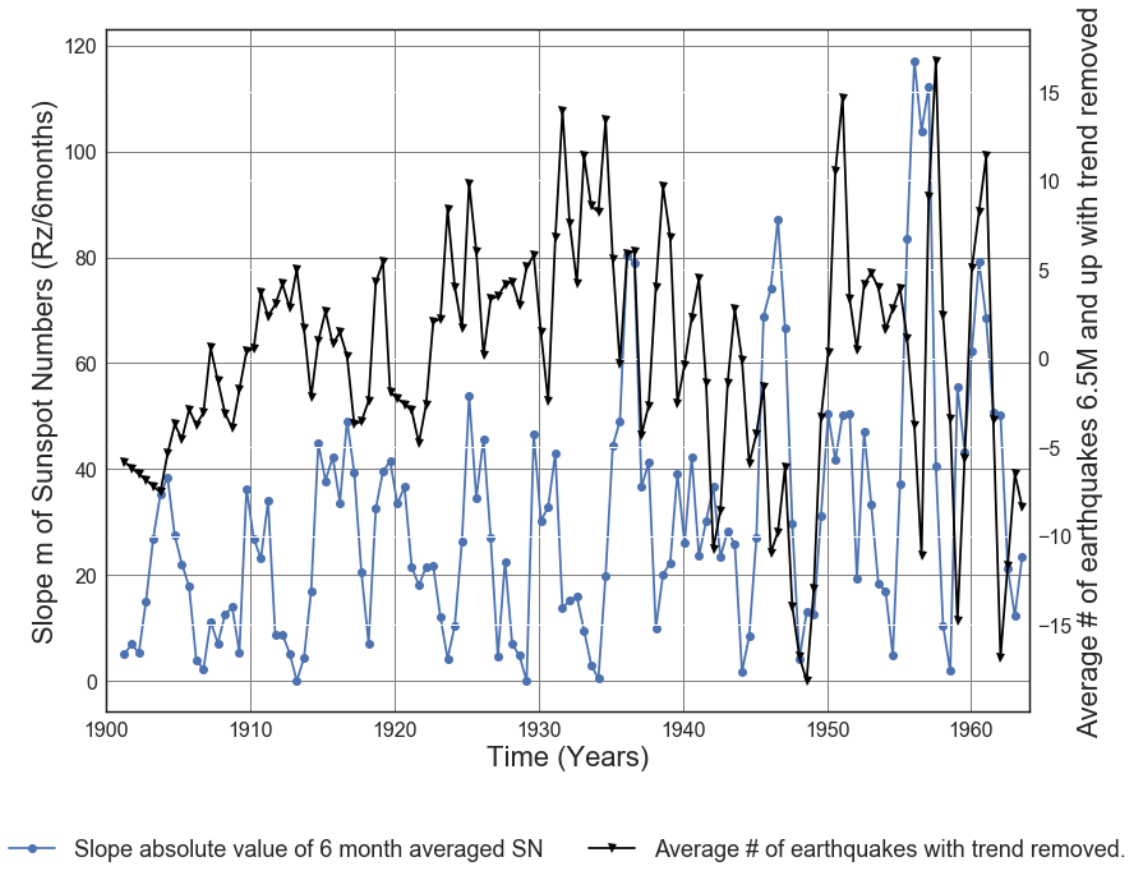

Figure D3.20: Slope Absolute value of Solar cycle from 1900 to 1964 vs. Average number of 6.5M and up earthquakes with trend removed.

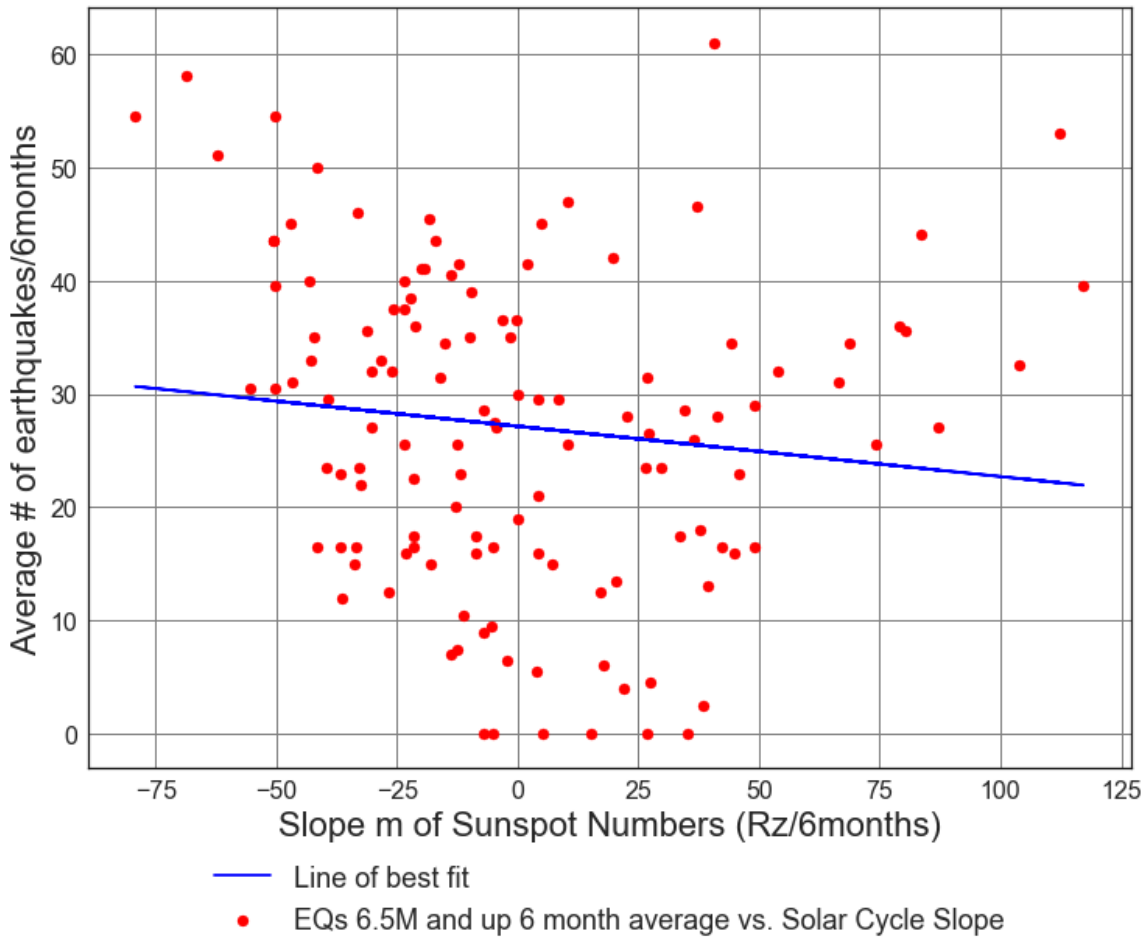

Figure D3.21: Scatter Plot of Solar cycle slope (from 1900 to 1964) vs. Average number of 6.5M and up Earthquakes/6months. Line of best fit, y = -0.04436x + (27.14), mean x = 0.3737 +/- 38.55, mean y = 27.12 +/- 13.96, R = -0.1225, R squared = 0.01501, p-value = 0.1717.

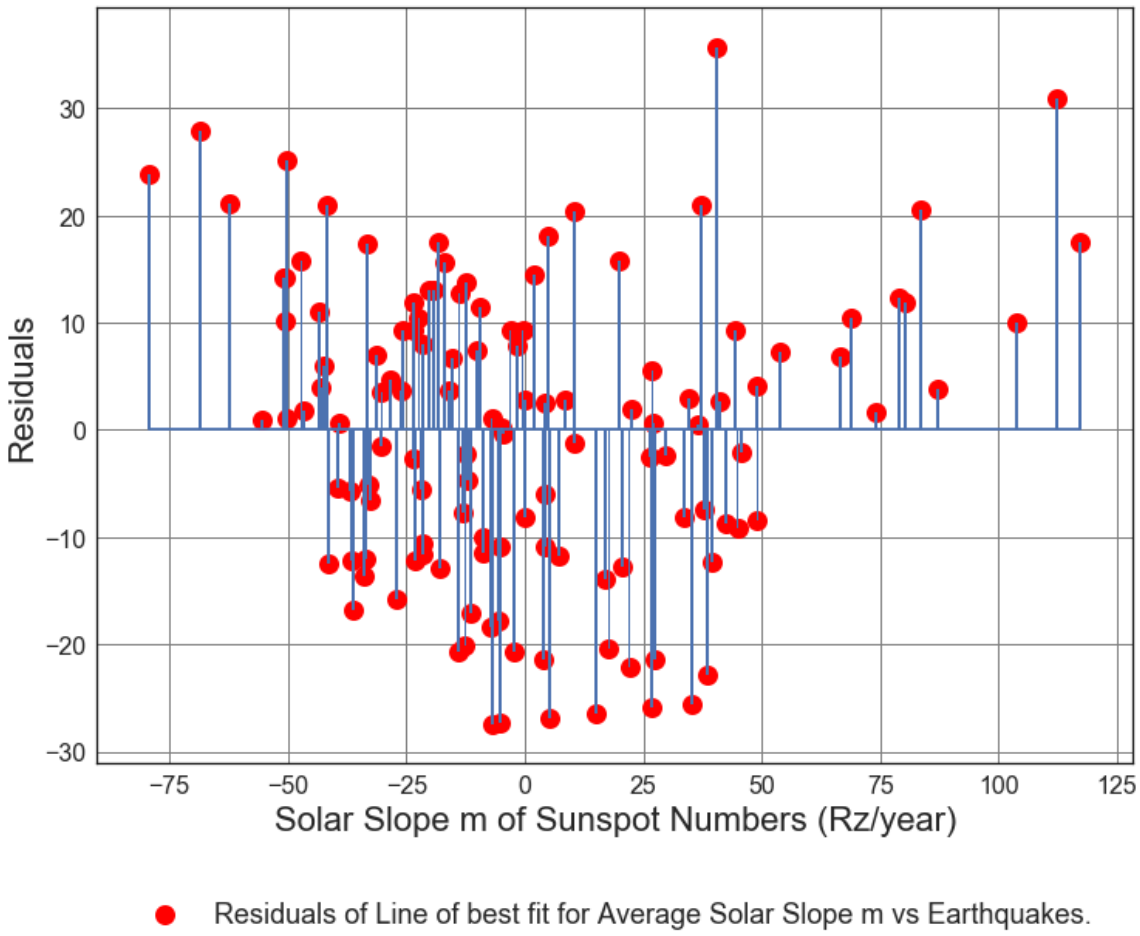

Figure D3.22: Residuals Plot of Solar cycle slope (from 1900 to 1964) vs. Average number of 6.5M and up Earthquakes/6months. Line of best fit, y = -0.04436x + (27.14), mean x = 0.3737 +/- 38.55, mean y = 27.12 +/- 13.96, R = -0.1225, R squared = 0.01501, p-value = 0.1717.

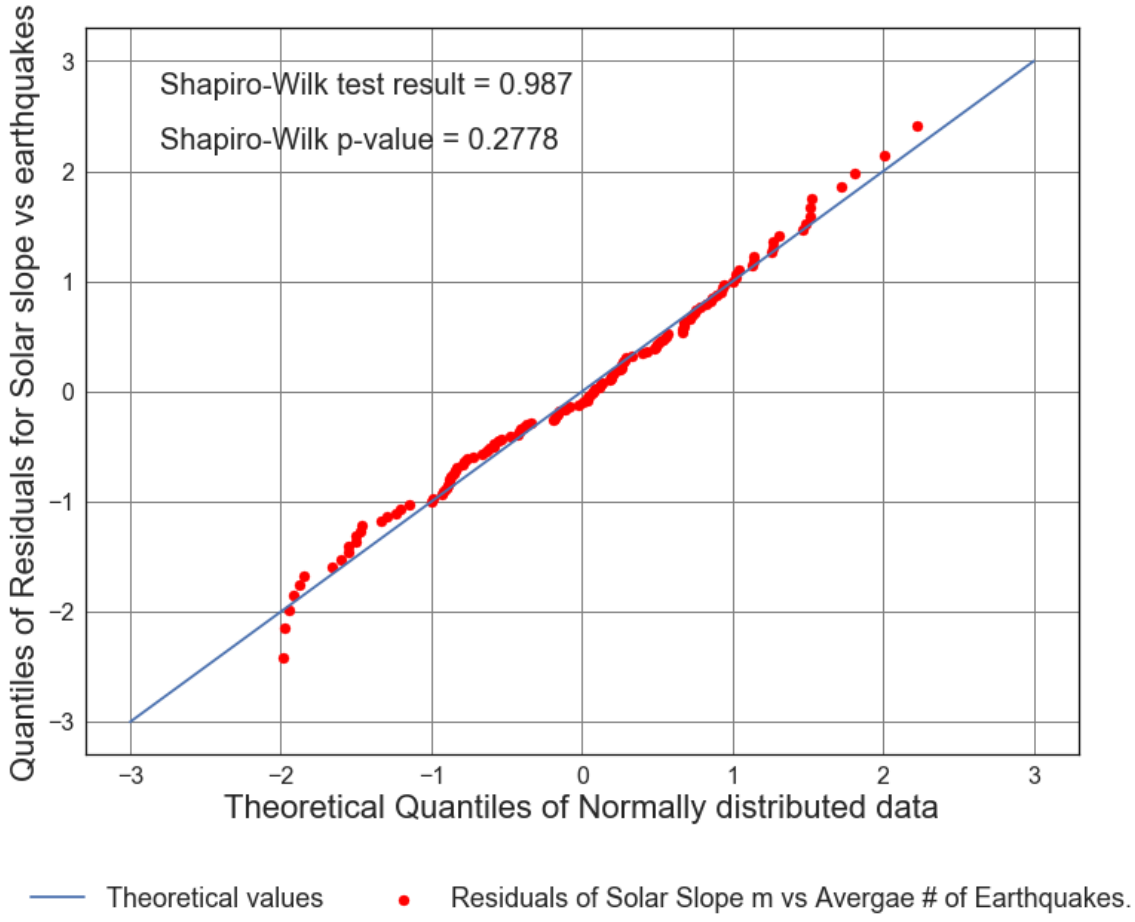

Figure D3.23: Residuals Plot of Solar cycle slope (from 1900 to 1964) vs. Average number of 6.5M and up Earthquakes/6months. Line of best fit, y = -0.04436x + (27.14), mean x = 0.3737 +/- 38.55, mean y = 27.12 +/- 13.96, R = -0.1225, R squared = 0.01501, p-value = 0.1717.

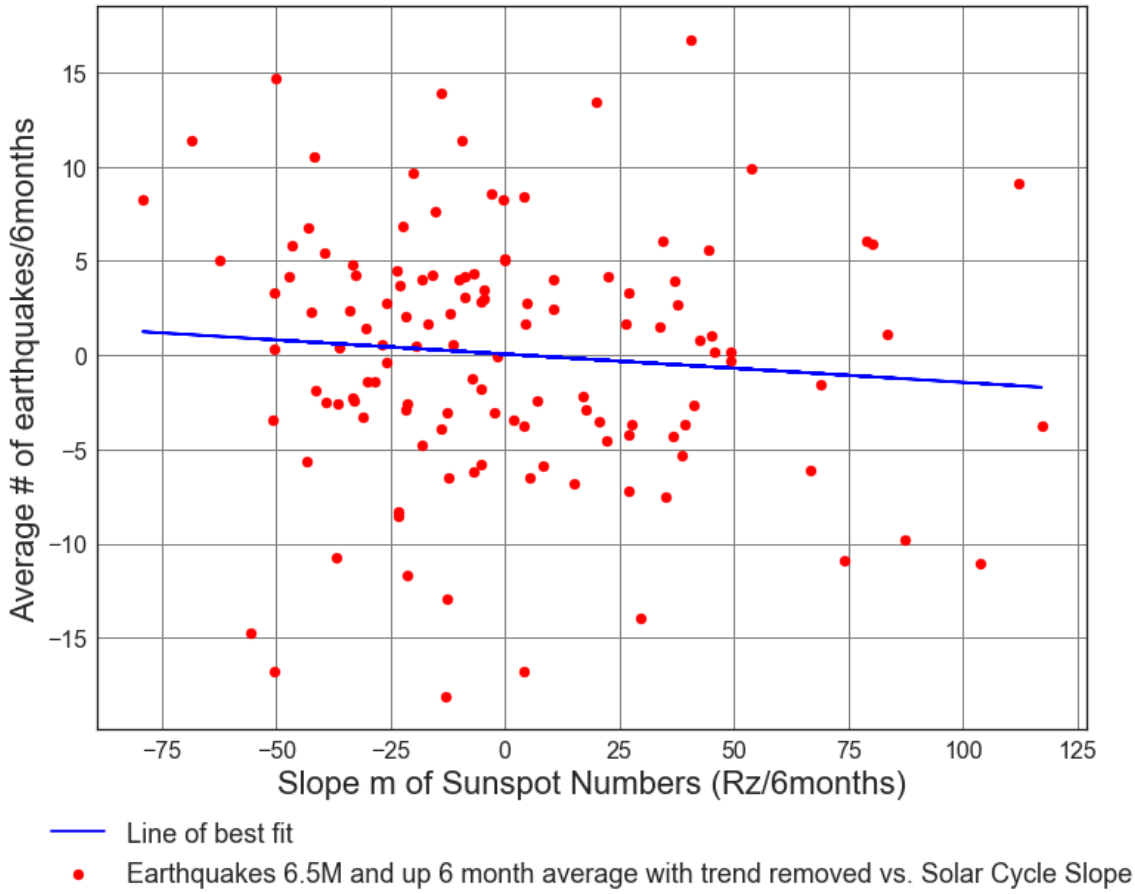

Figure D3.24: Scatter Plot of Solar cycle slope (from 1900 to 1964) vs. Average number of 6.5M and up Earthquakes/6months with trend removed. Line of best fit, y = -0.01502x + (0.04915), mean x = 0.3737 +/- 38.55, mean y = 0.04354 +/- 6.617, R = -0.08748, R squared = 0.007653, p-value = 0.33.

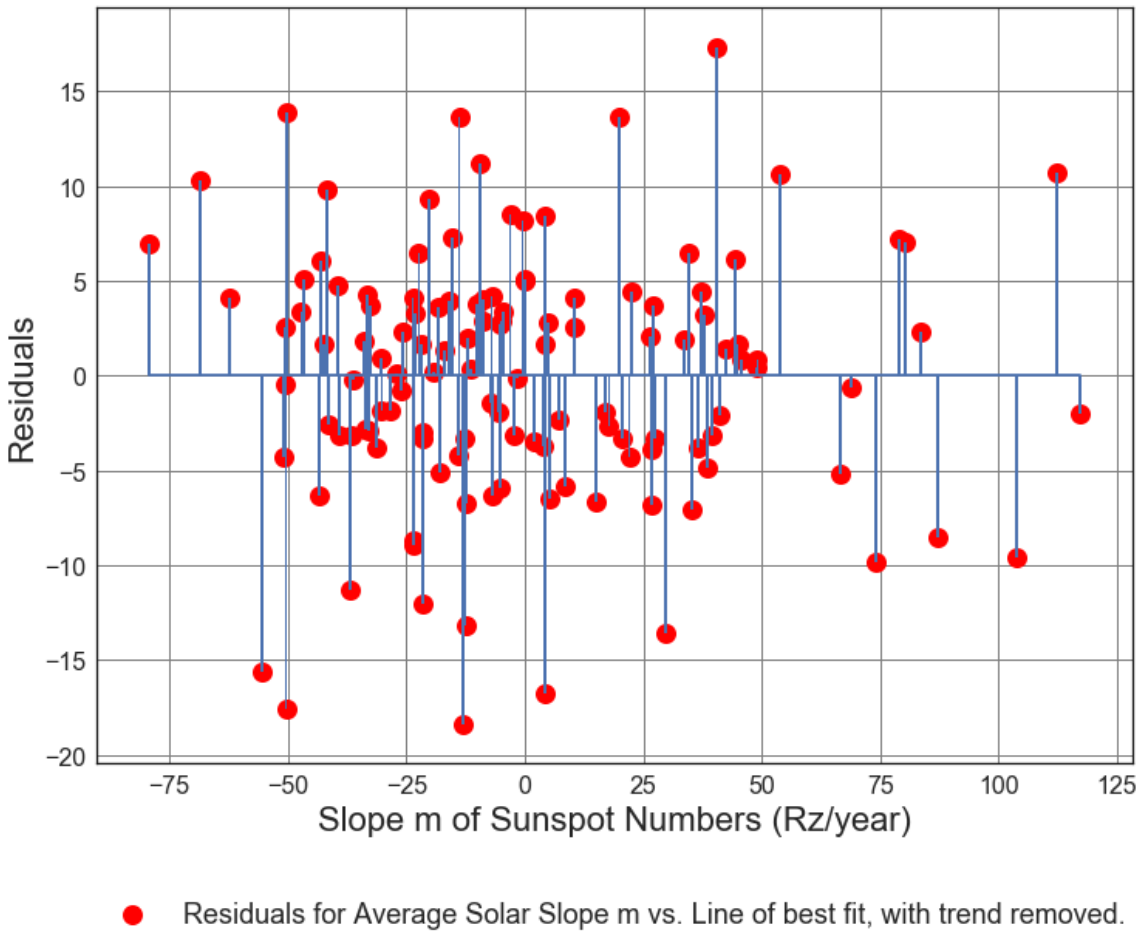

Figure D3.25: Scatter Plot of Solar cycle slope (from 1900 to 1964) vs. Average number of 6.5M and up Earthquakes/6months with trend removed. Line of best fit, y = -0.01502x + (0.04915), mean x = 0.3737 +/- 38.55, mean y = 0.04354 +/- 6.617, R = -0.08748, R squared = 0.007653, p-value = 0.33.

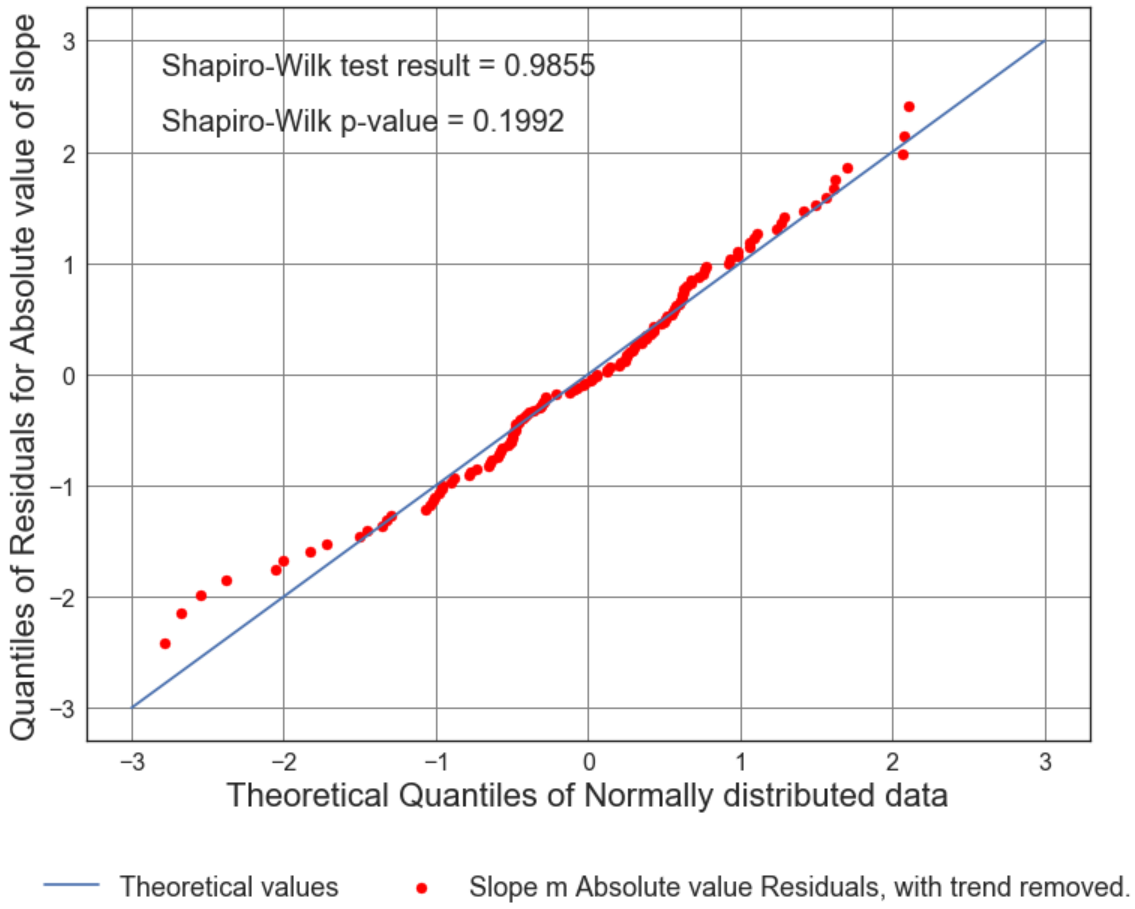

Figure D3.26: Scatter Plot of Solar cycle slope (from 1900 to 1964) vs. Average number of 6.5M and up Earthquakes/6months with trend removed. Line of best fit, y = -0.01502x + (0.04915), mean x = 0.3737 +/- 38.55, mean y = 0.04354 +/- 6.617, R = -0.08748, R squared = 0.007653, p-value = 0.33.

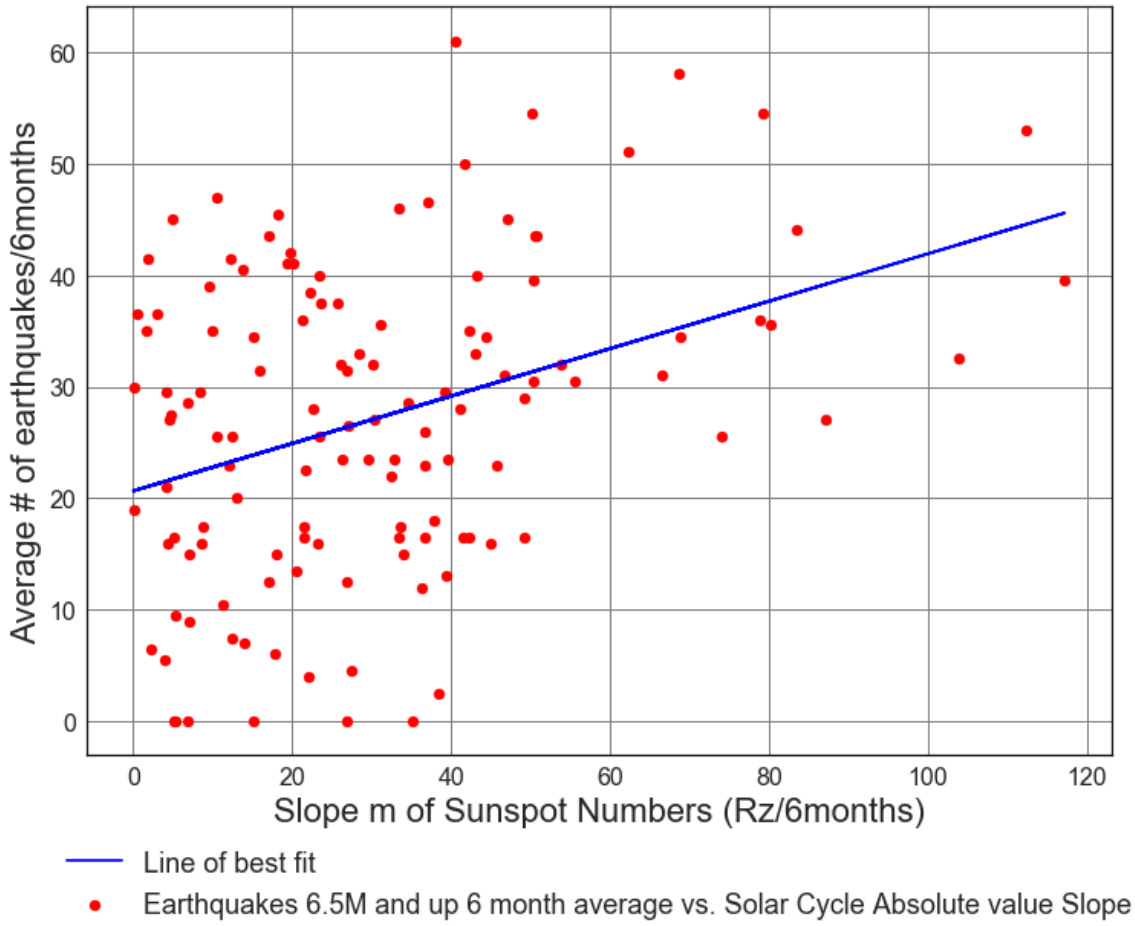

Figure D3.27: Scatter Plot of Solar cycle slope (from 1900 to 1964) vs. Average number of 6.5M and up Earthquakes/6months. Line of best fit, y = 0.2126x + (20.65), mean x = 30.43 +/- 23.66, mean y = 27.12 +/- 13.96, R = 0.3604, R squared = 0.1299, p-value = 3.385e-05.

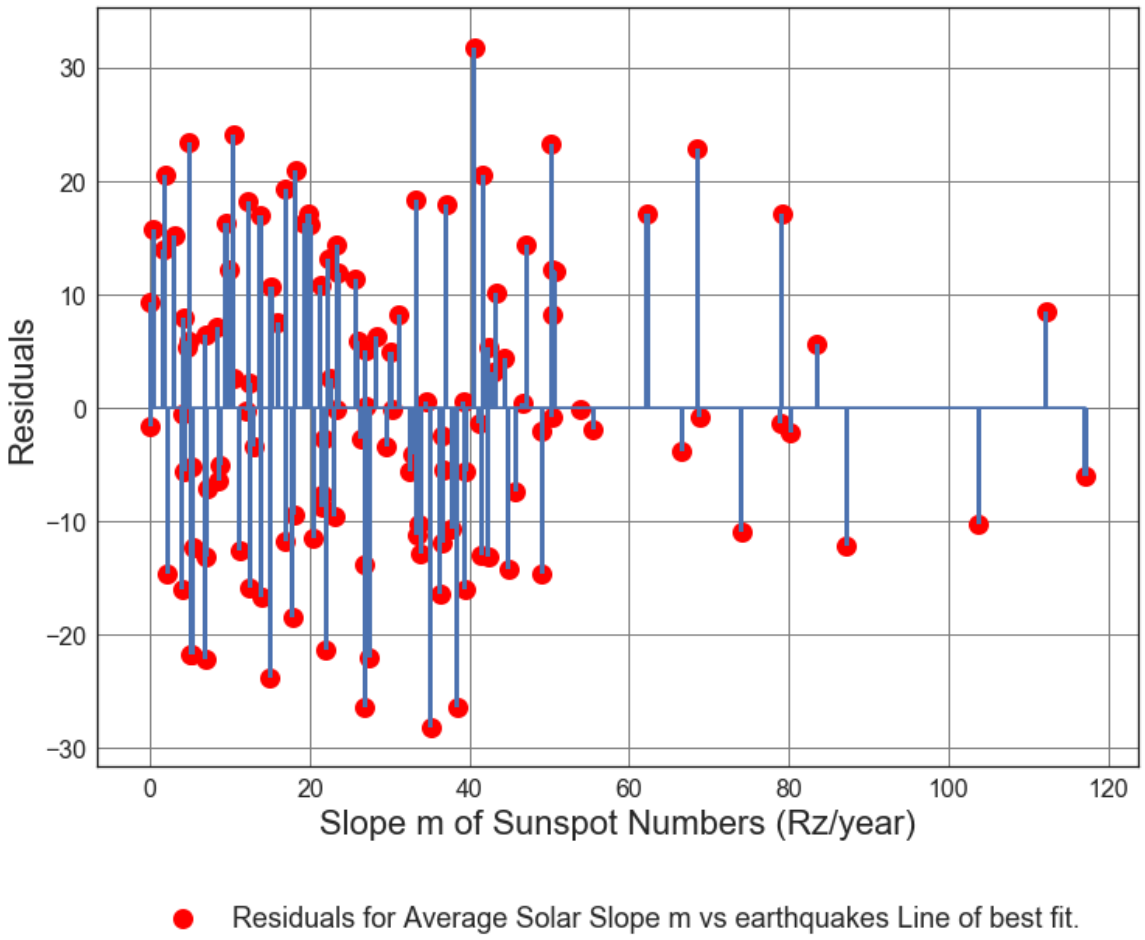

Figure D3.28: Scatter Plot of Solar cycle slope (from 1900 to 1964) vs. Average number of 6.5M and up Earthquakes/6months. Line of best fit, y = 0.2126x + (20.65), mean x = 30.43 +/- 23.66, mean y = 27.12 +/- 13.96, R = 0.3604, R squared = 0.1299, p-value = 3.385e-05.

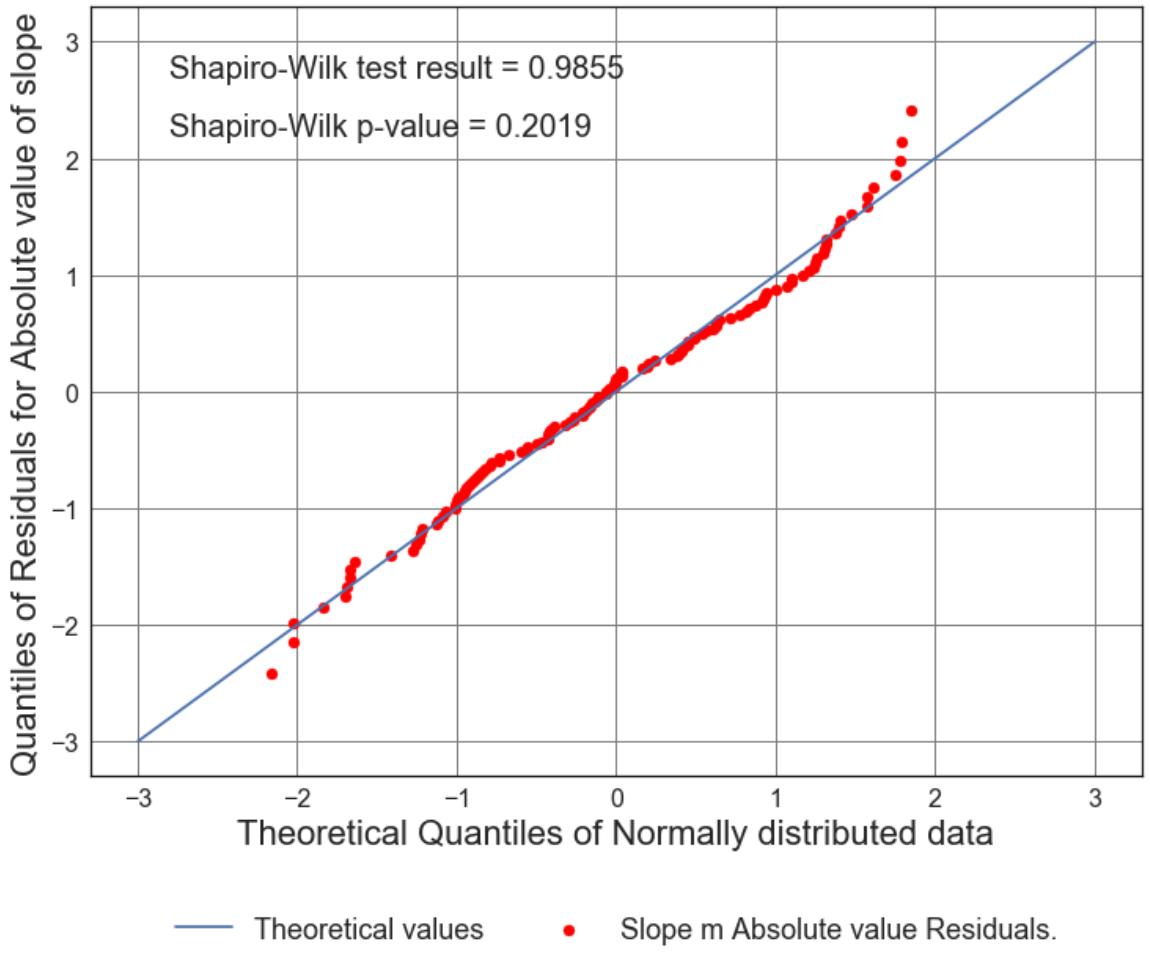

Figure D3.29: Scatter Plot of Solar cycle slope (from 1900 to 1964) vs. Average number of 6.5M and up Earthquakes/6months. Line of best fit, y = 0.2126x + (20.65), mean x = 30.43 +/- 23.66, mean y = 27.12 +/- 13.96, R = 0.3604, R squared = 0.1299, p-value = 3.385e-05.

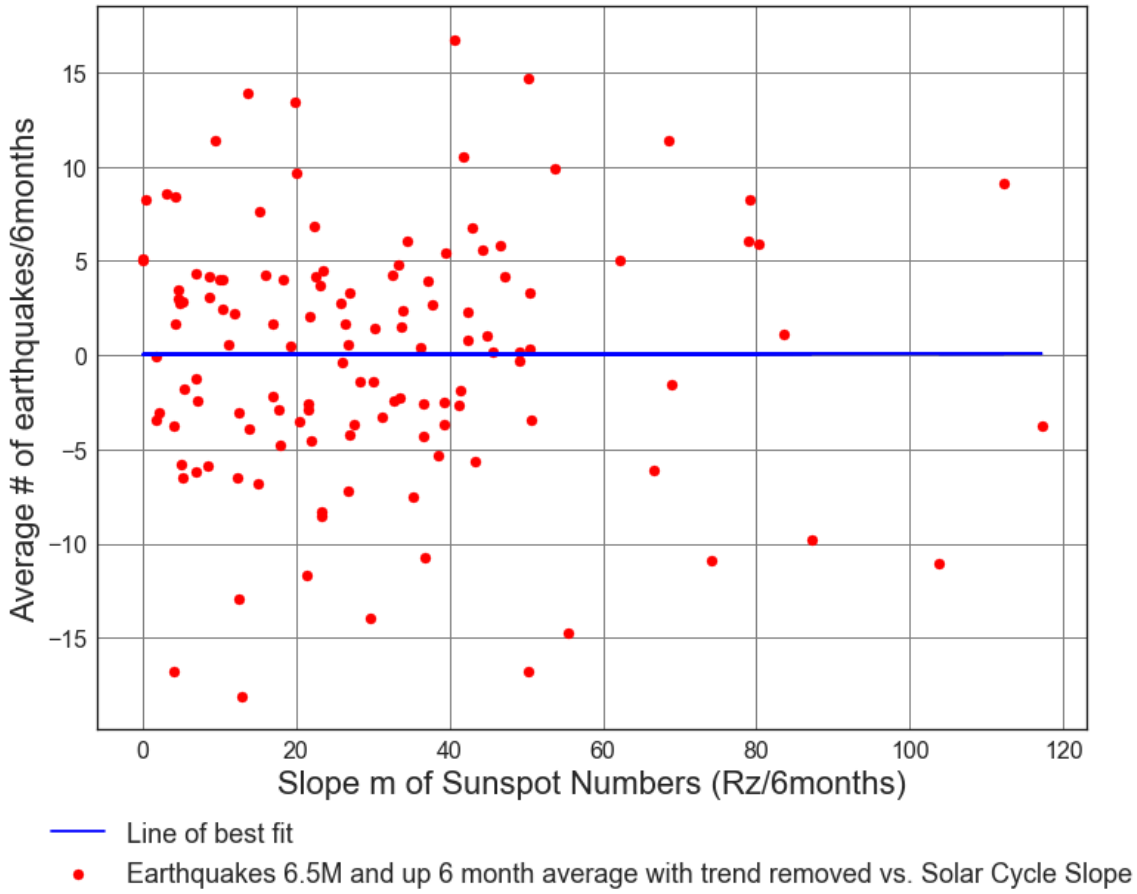

Figure D3.30: Scatter Plot of Solar cycle absolute value slope (from 1900 to 1964) vs. Average number of 6.5M and up Earthquakes/6months with trend removed. Line of best fit, y = 0.0002686x + (0.03537), mean x = 30.43 +/- 23.66, mean y = 0.04354 +/- 6.617, R = 0.0009605, R squared = 9.225e-07, p-value = 0.9915.

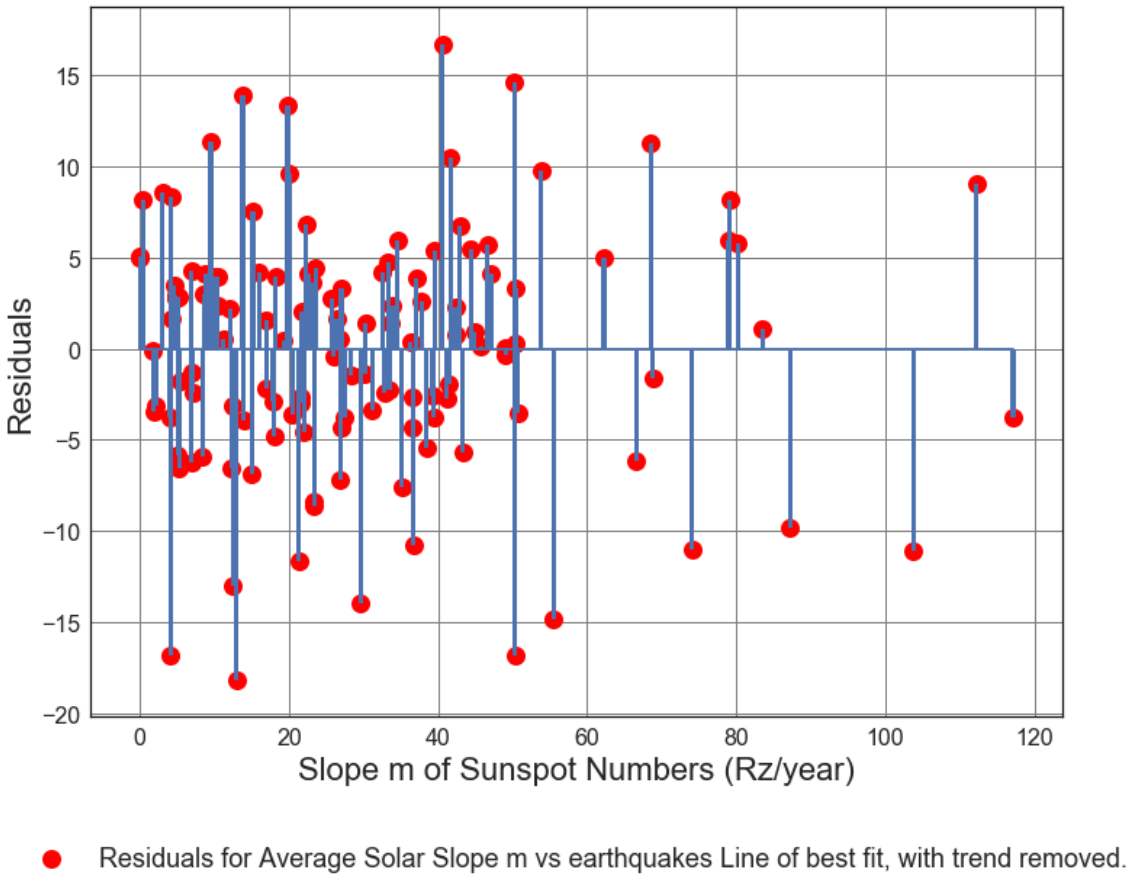

Figure D3.31: Scatter Plot of Solar cycle absolute value slope (from 1900 to 1964) vs. Average number of 6.5M and up Earthquakes/6months with trend removed. Line of best fit, y = 0.0002686x + (0.03537), mean x = 30.43 +/- 23.66, mean y = 0.04354 +/- 6.617, R = 0.0009605, R squared = 9.225e-07, p-value = 0.9915.

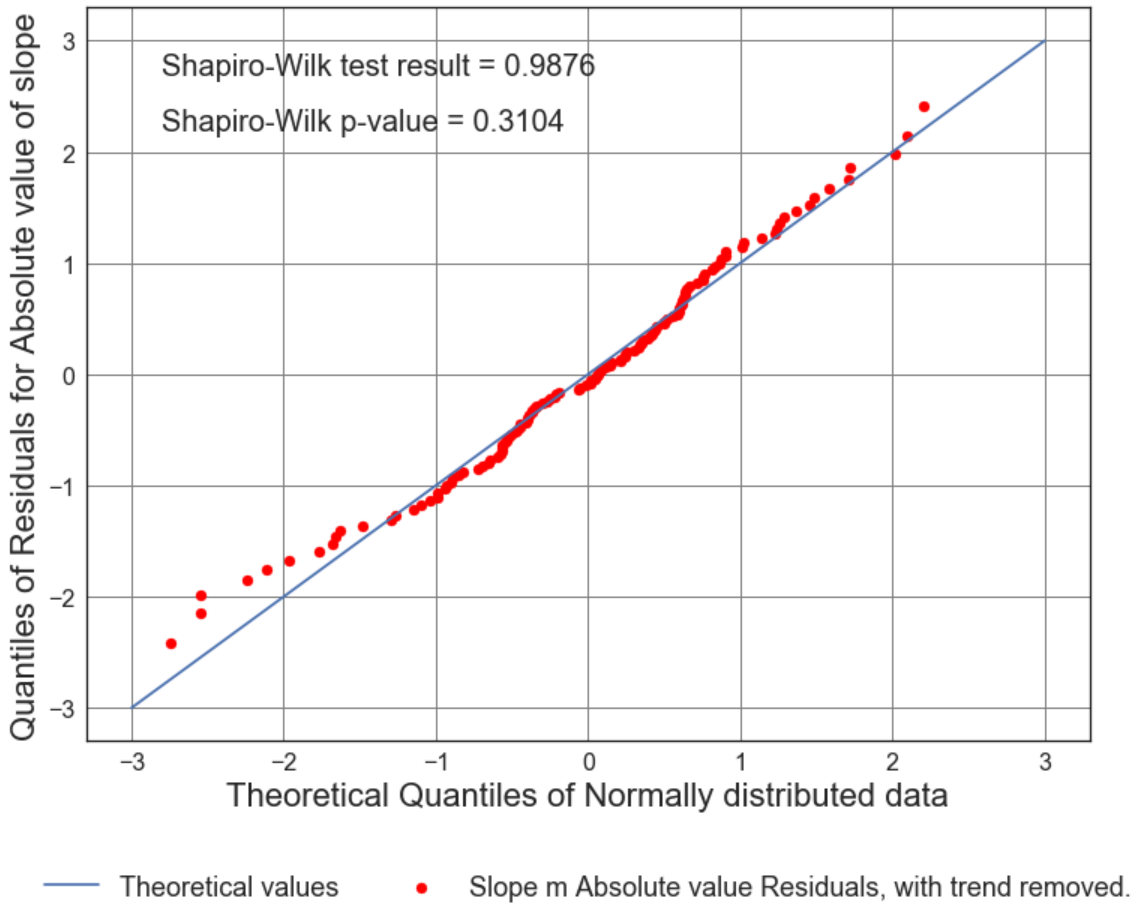

Figure D3.32: Scatter Plot of Solar cycle absolute value slope (from 1900 to 1964) vs. Average number of 6.5M and up Earthquakes/6months with trend removed. Line of best fit, y = 0.0002686x + (0.03537), mean x = 30.43 +/- 23.66, mean y = 0.04354 +/- 6.617, R = 0.0009605, R squared = 9.225e-07, p-value = 0.9915.

Appendix D4: ISC Time Series Analysis Part 4 - Modern Era Post 1964 Six Month Averaged Earthquake and Sunspot Data.

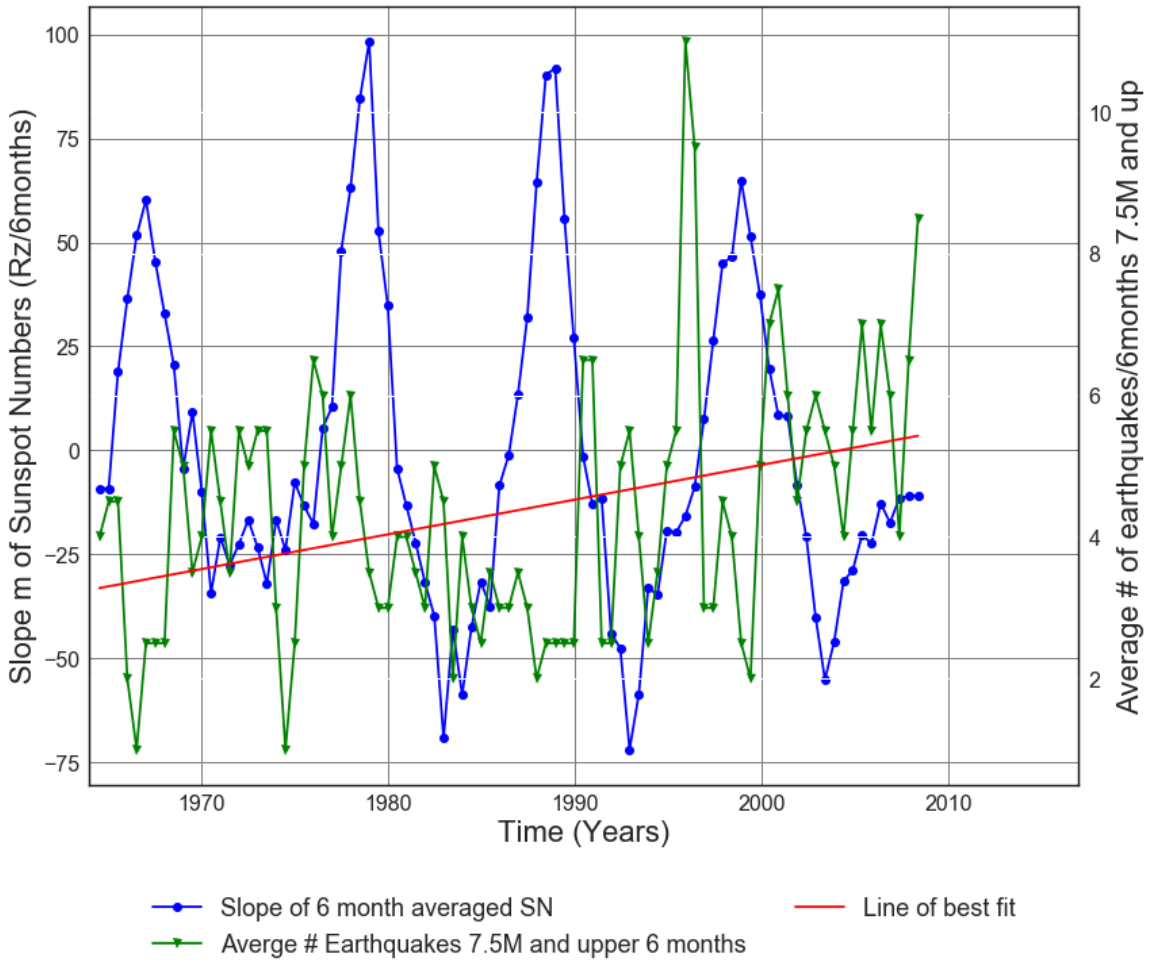

Figure D4.1: Slope of Solar cycle from 1964 to 2017 vs. Average number of 7.5M and up Earthquakes.

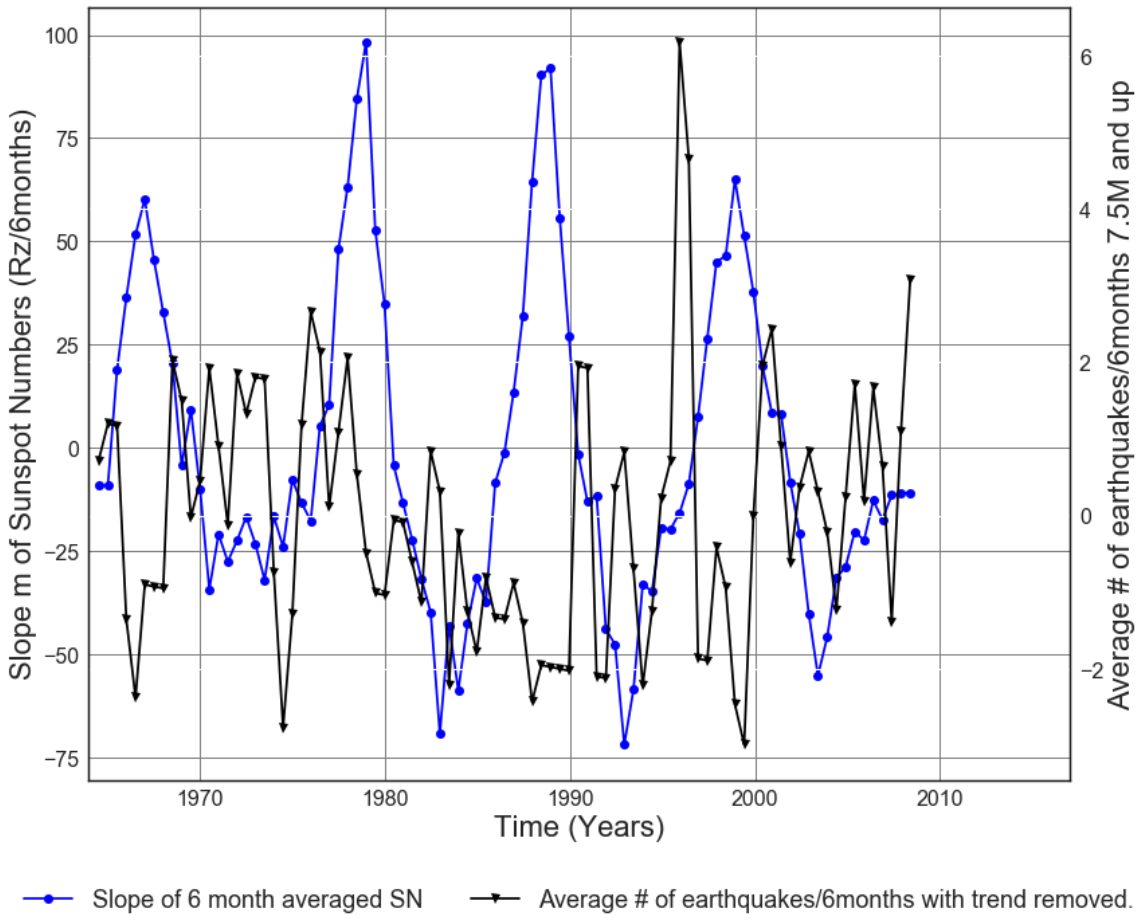

Figure D4.2: Slope of 6 month averaged SN 1964 to 2017 vs. Average number of 7.5M and up Earthquakes with trend removed. Line of best fit, y = 0.04904x + (-93.07), mean x = 1.986e+03 +/- 12.8, mean y = 4.354 +/- 1.784

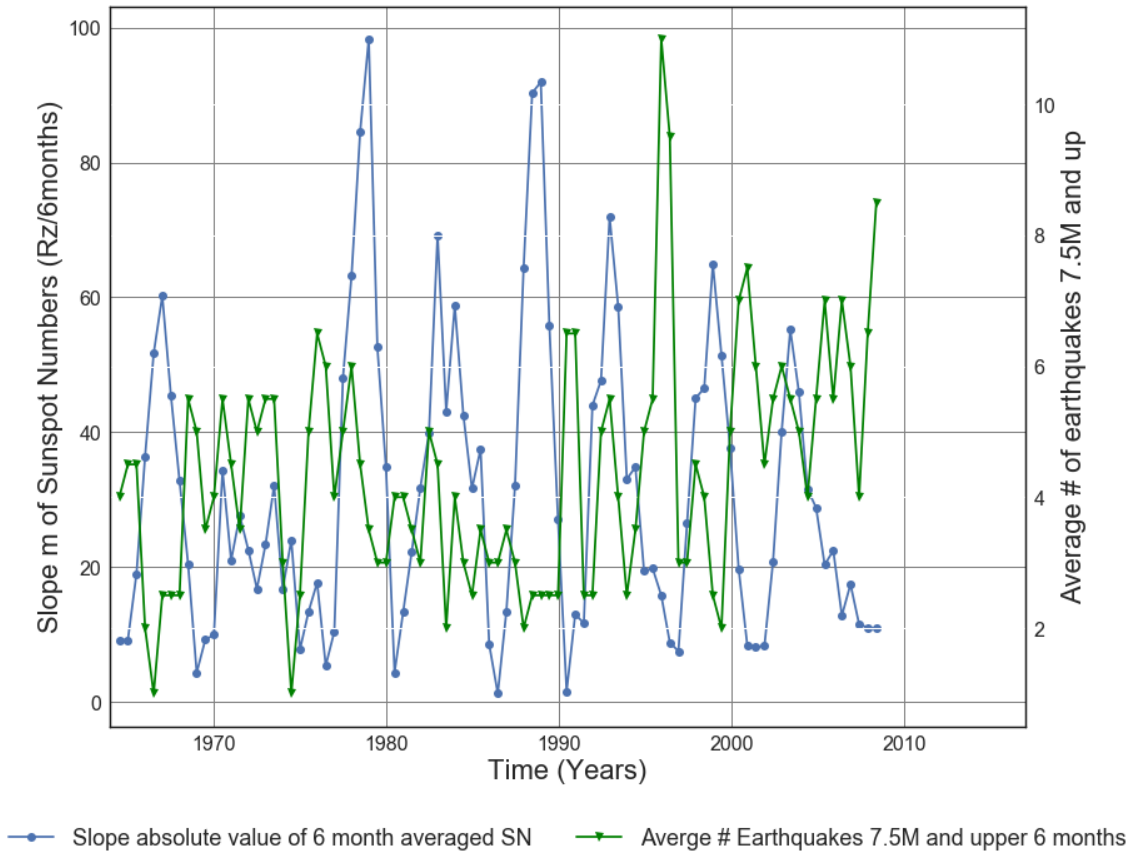

Figure D4.3: Slope Absolute value of Solar cycle from 1964 to 2017 vs. Average number of 7.5M and up Earthquakes.

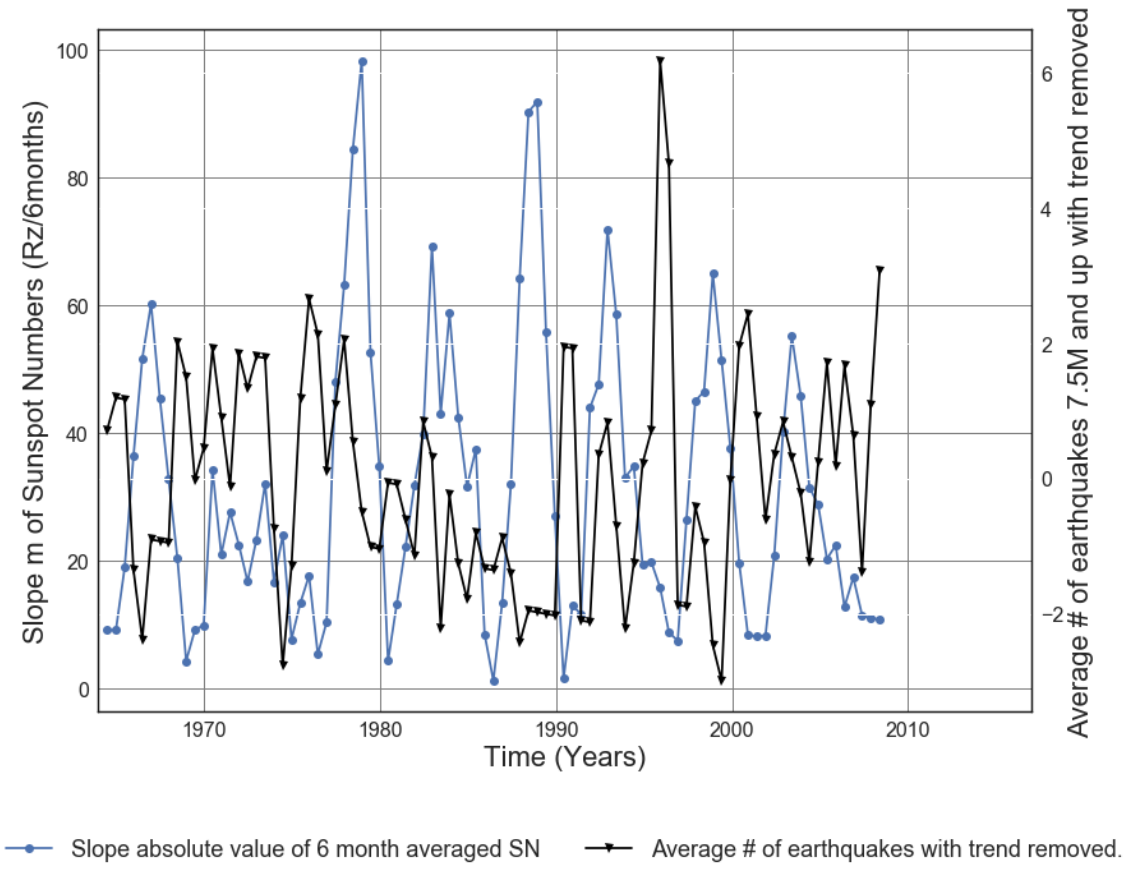

Figure D4.4: Slope Absolute value of Solar cycle from 1964 to 2017 vs. Average number of 7.5M and up earthquakes with trend removed.

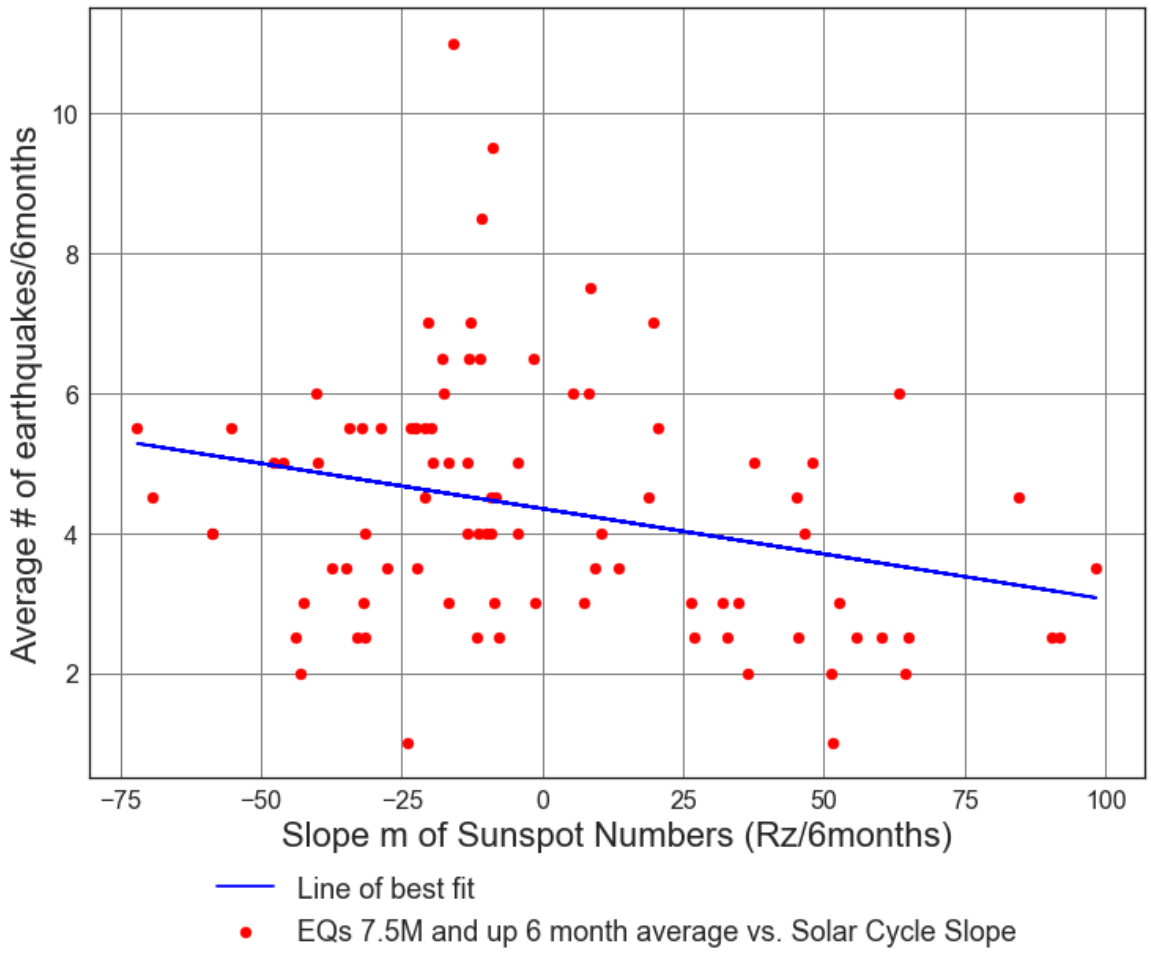

Figure D4.5: Scatter Plot of Solar cycle slope (from 1964 to 2017) vs. Average number of 7.5M and up Earthquakes/6months. Line of best fit, y = -0.01296x + (4.347), mean x = -0.5303 +/- 38.19, mean y = 4.354 +/- 1.784, R = -0.2775, R squared = 0.07701, p-value = 0.008465.

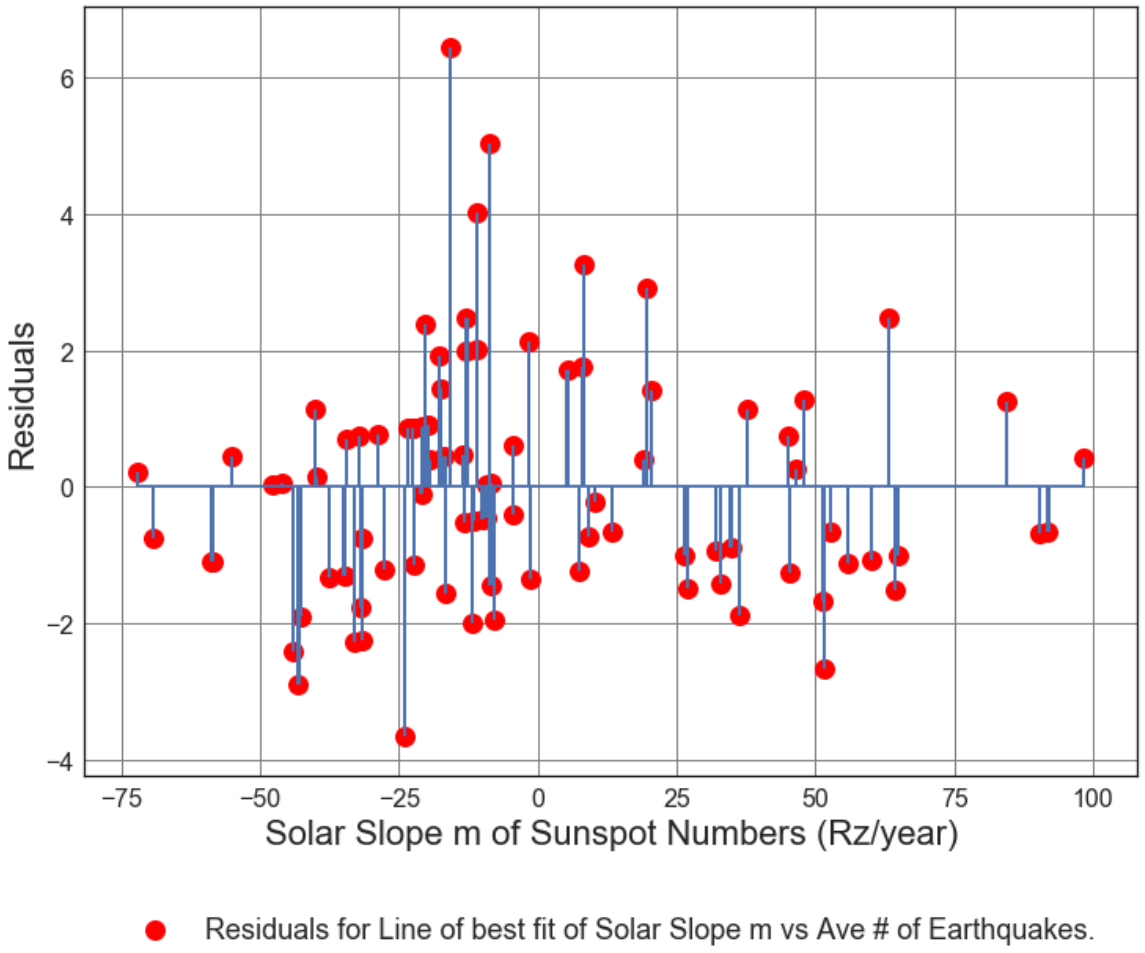

Figure D4.6: Residuals Plot of Solar cycle slope (from 1964 to 2017) vs. Average number of 7.5M and up Earthquakes/6months. Line of best fit, y = -0.01296x + (4.347), mean x = -0.5303 +/- 38.19, mean y = 4.354 +/- 1.784, R = -0.2775, R squared = 0.07701, p-value = 0.008465.

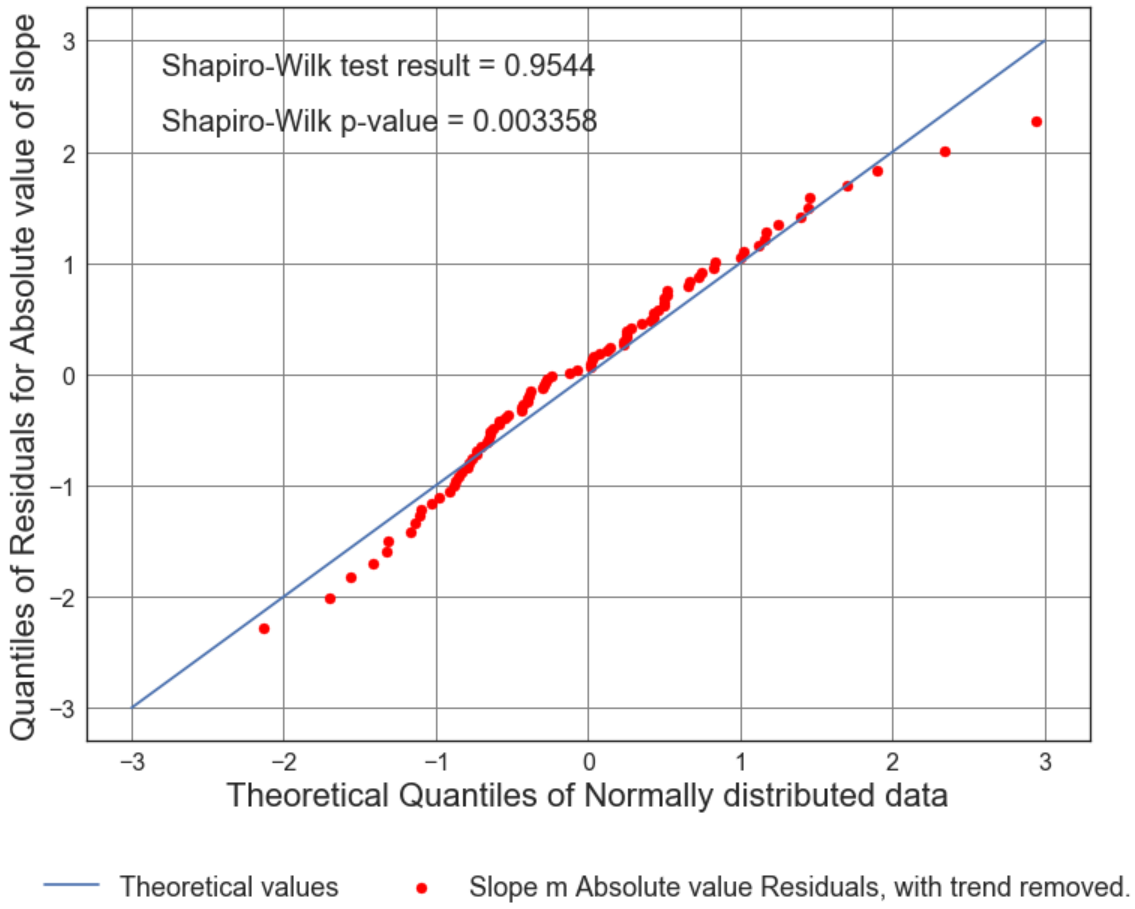

Figure D4.7: Residuals Plot of Solar cycle slope (from 1964 to 2017) vs. Average number of 7.5M and up Earthquakes/6months. Line of best fit, y = -0.01296x + (4.347), mean x = -0.5303 +/- 38.19, mean y = 4.354 +/- 1.784, R = -0.2775, R squared = 0.07701, p-value = 0.008465.

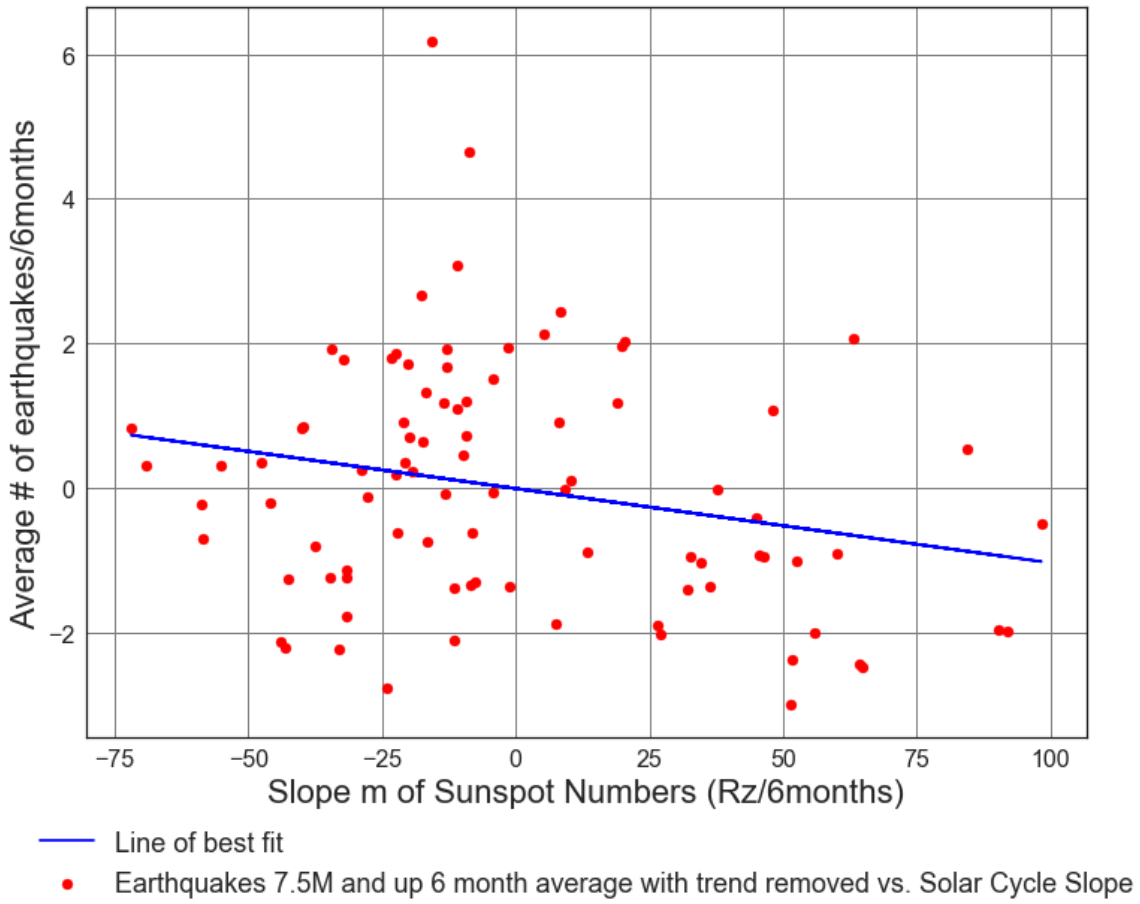

Figure D4.8: Scatter Plot of Solar cycle slope (from 1964 to 2017) vs. Average number of 7.5M and up Earthquakes/6months with trend removed. Line of best fit, y = -0.01028x + (-0.005449), mean x = -0.5303 +/- 38.19, mean y = -1.277e-15 +/- 1.669, R = -0.2351, R squared = 0.05527, p-value = 0.02657.

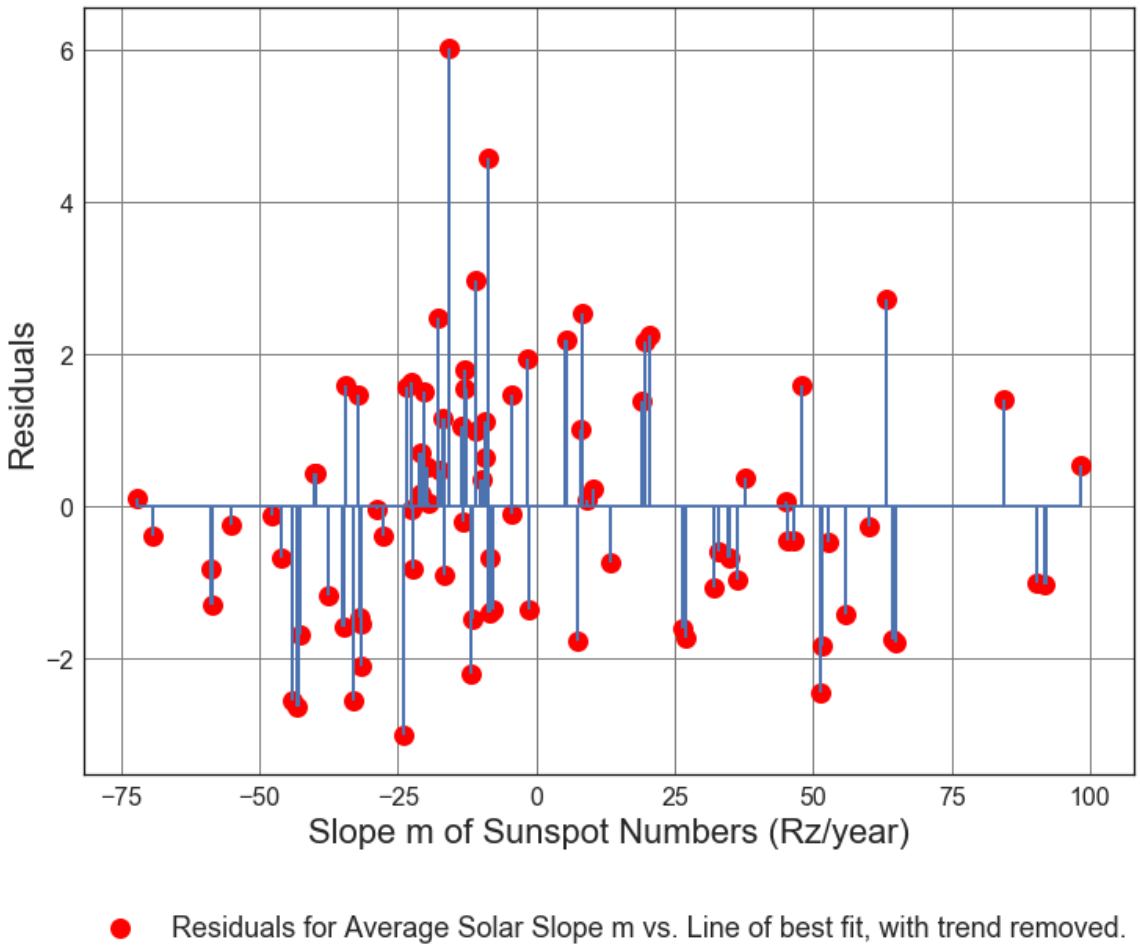

Figure D4.9: Scatter Plot of Solar cycle slope (from 1964 to 2017) vs. Average number of 7.5M and up Earthquakes/6months with trend removed. Line of best fit, y = -0.01028x + (-0.005449), mean x = -0.5303 +/- 38.19, mean y = -1.277e-15 +/- 1.669, R = -0.2351, R squared = 0.05527, p-value = 0.02657.

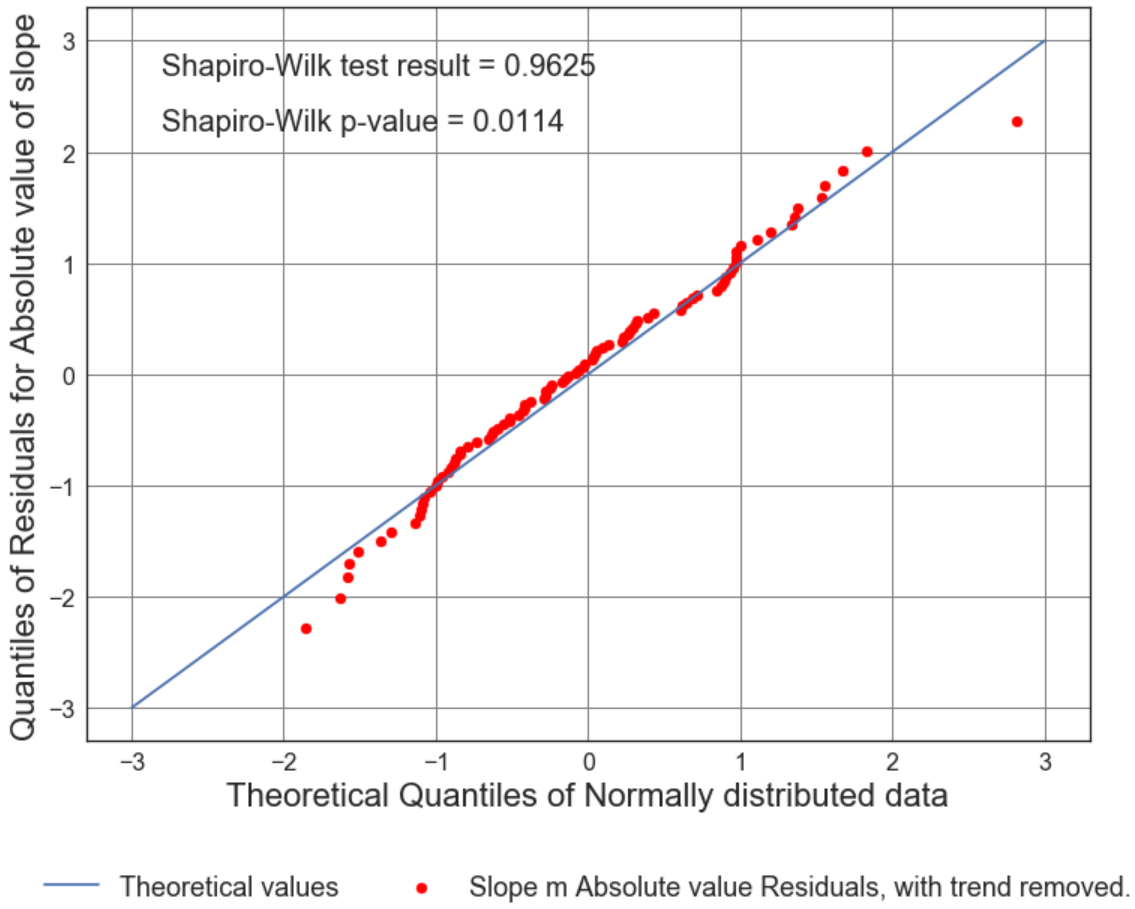

Figure D4.10: Scatter Plot of Solar cycle slope (from 1964 to 2017) vs. Average number of 7.5M and up Earthquakes/6months with trend removed. Line of best fit, y = -0.01028x + (-0.005449), mean x = -0.5303 +/- 38.19, mean y = -1.277e-15 +/- 1.669, R = -0.2351, R squared = 0.05527, p-value = 0.02657.

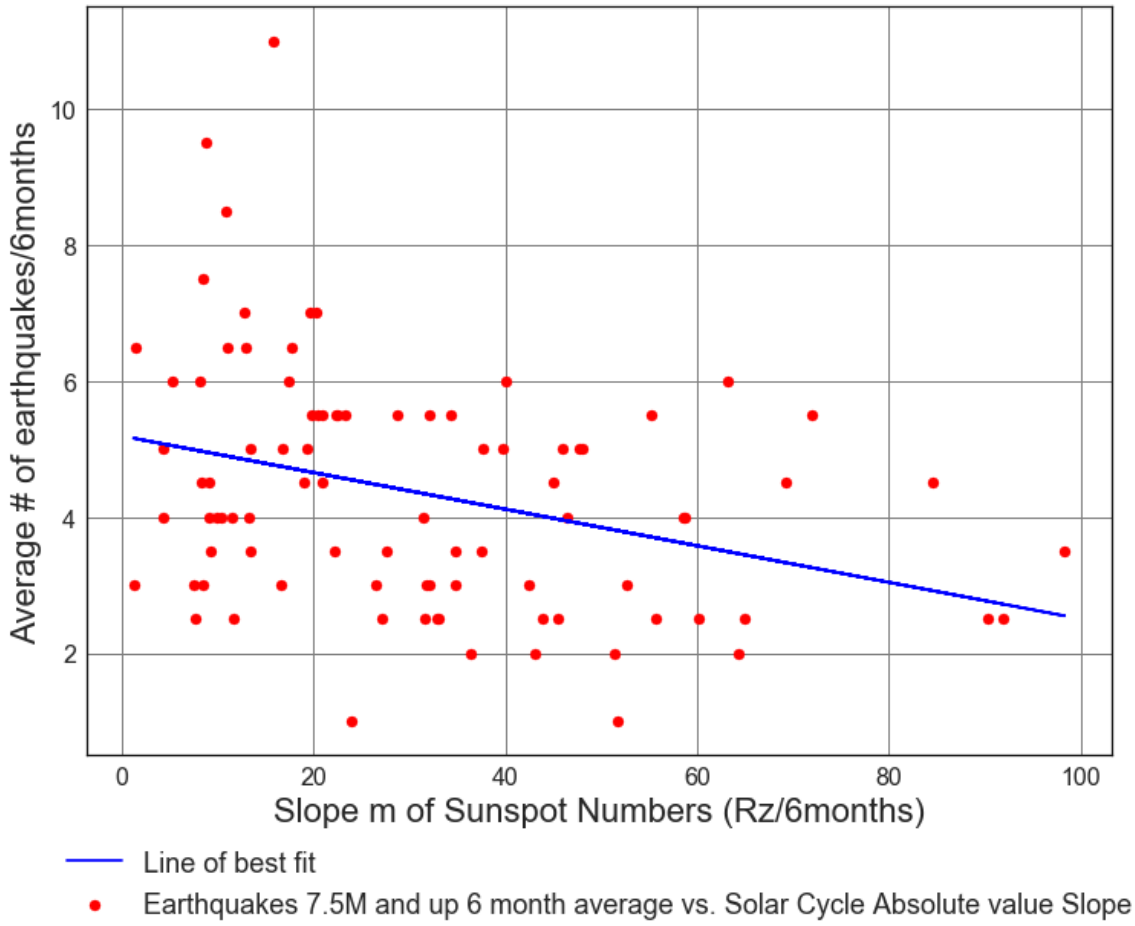

Figure D4.11: Scatter Plot of Solar cycle slope (from 1964 to 2017) vs. Average number of 7.5M and up Earthquakes/6months. Line of best fit, y = -0.0269x + (5.192), mean x = 31.16 +/- 22.09, mean y = 4.354 +/- 1.784, R = -0.3333, R squared = 0.1111, p-value = 0.001416.

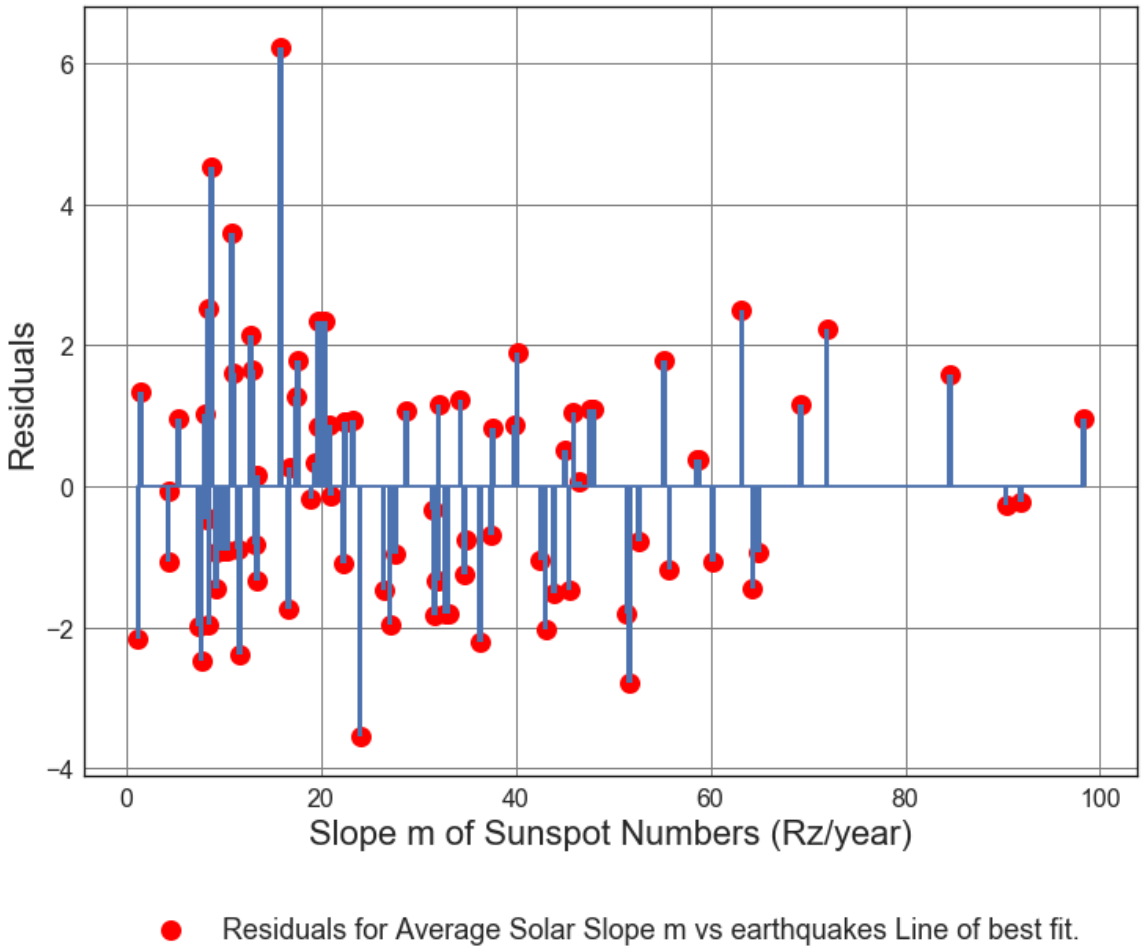

Figure D4.12: Scatter Plot of Solar cycle slope (from 1964 to 2017) vs. Average number of 7.5M and up Earthquakes/6months. Line of best fit, y = -0.0269x + (5.192), mean x = 31.16 +/- 22.09, mean y = 4.354 +/- 1.784, R = -0.3333, R squared = 0.1111, p-value = 0.001416.

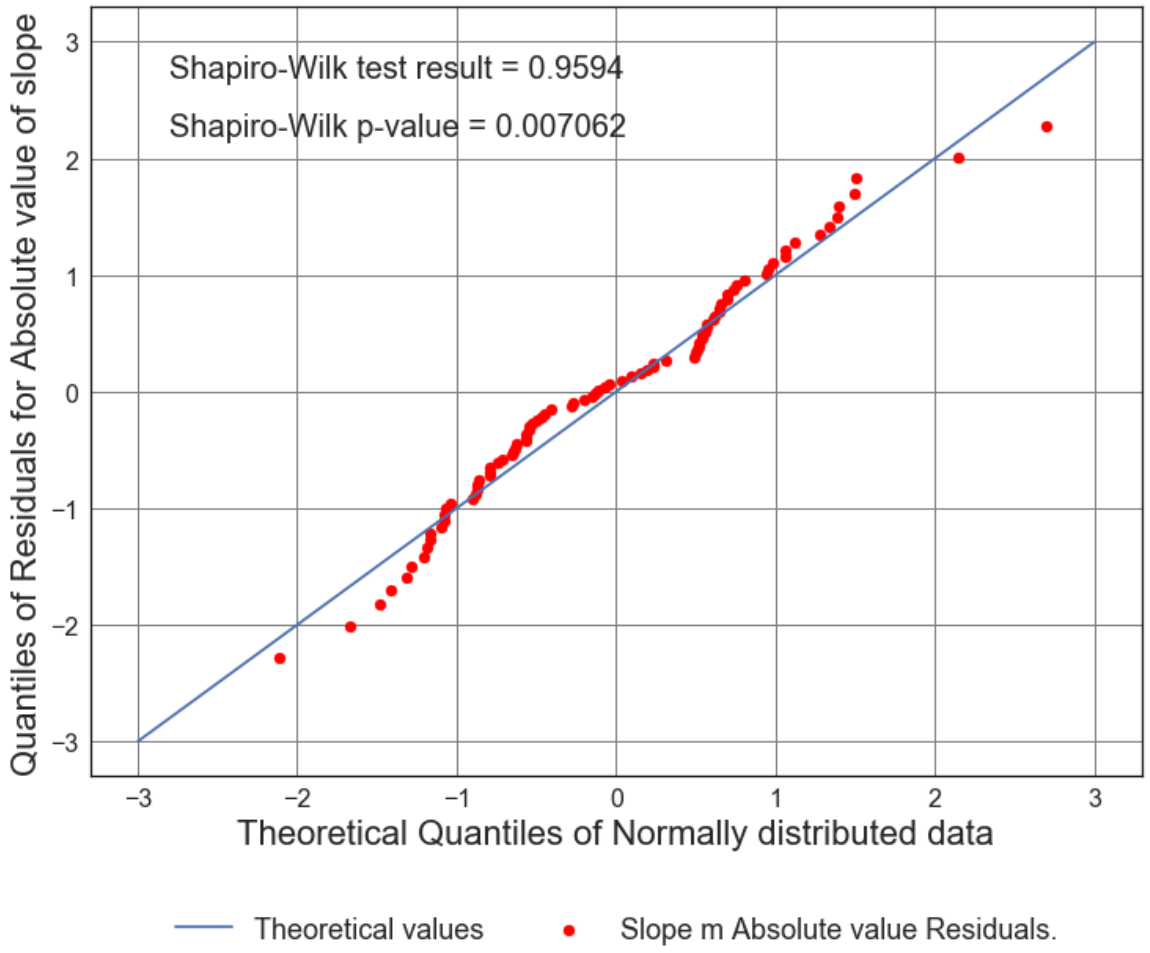

Figure D4.13: Scatter Plot of Solar cycle slope (from 1964 to 2017) vs. Average number of 7.5M and up Earthquakes/6months. Line of best fit, y = -0.0269x + (5.192), mean x = 31.16 +/- 22.09, mean y = 4.354 +/- 1.784, R = -0.3333, R squared = 0.1111, p-value = 0.001416.

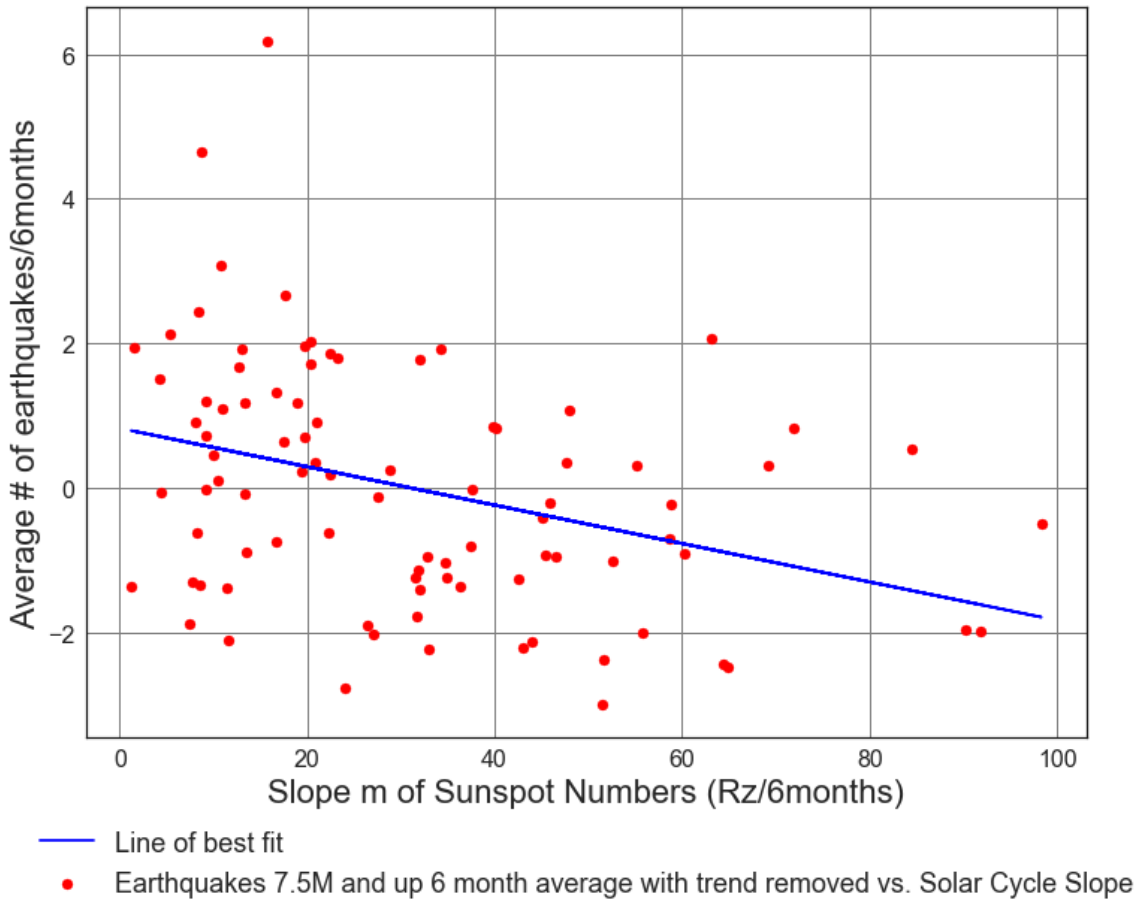

Figure D4.14: Scatter Plot of Solar cycle absolute value slope (from 1964 to 2017) vs. Average number of 7.5M and up Earthquakes/6months with trend removed. Line of best fit, y = -0.02656x + (0.8277), mean x = 31.16 +/- 22.09, mean y = -1.277e-15 +/- 1.669, R = -0.3516, R squared = 0.1236, p-value = 0.0007294.

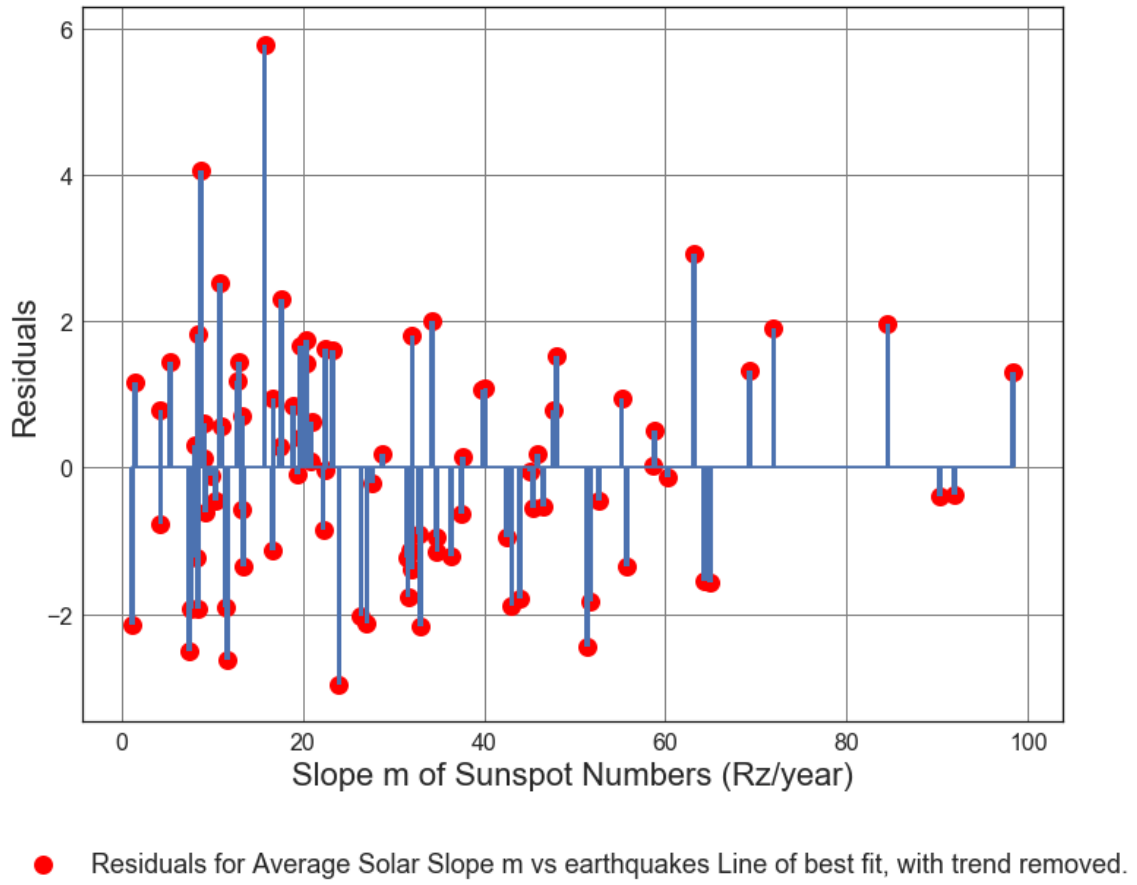

Figure D4.15: Scatter Plot of Solar cycle absolute value slope (from 1964 to 2017) vs. Average number of 7.5M and up Earthquakes/6months with trend removed. Line of best fit, y = -0.02656x + (0.8277), mean x = 31.16 +/- 22.09, mean y = -1.277e-15 +/- 1.669, R = -0.3516, R squared = 0.1236, p-value = 0.0007294.

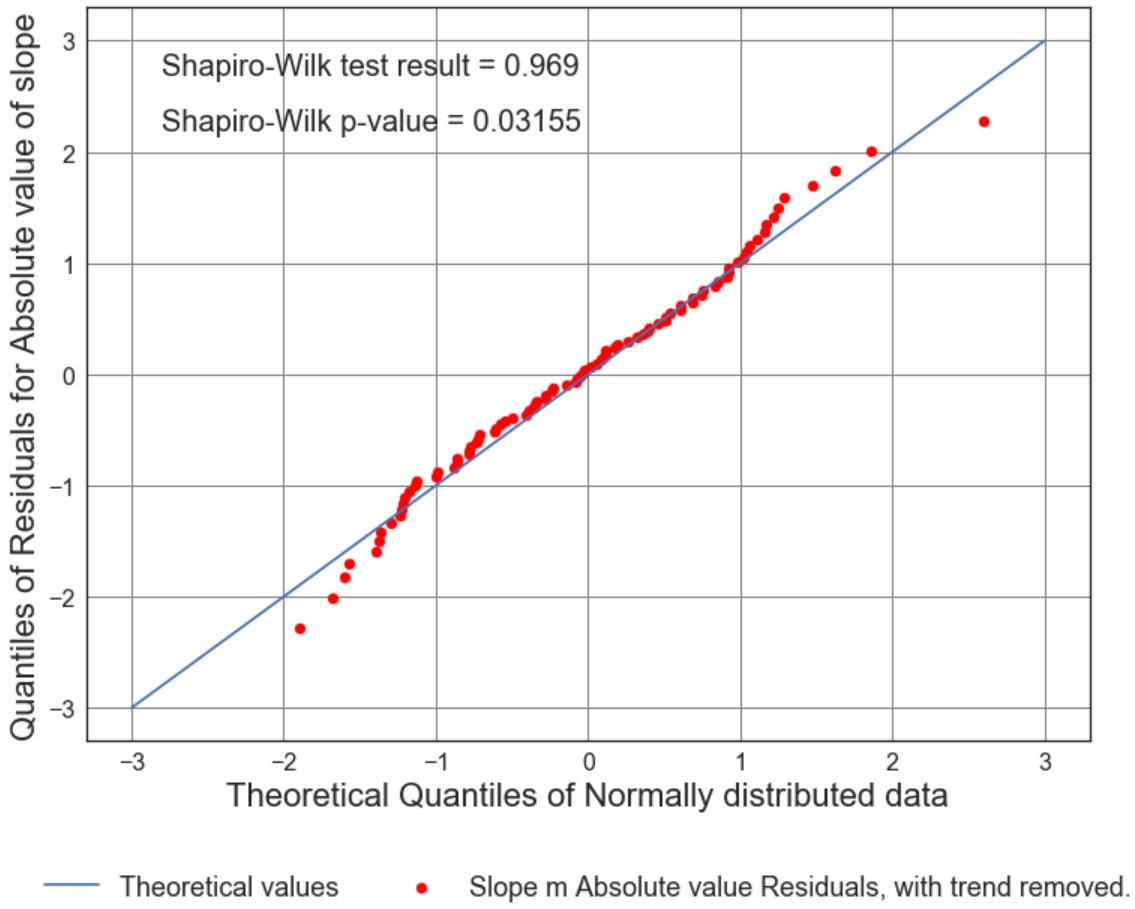

Figure D4.16: Scatter Plot of Solar cycle absolute value slope (from 1964 to 2017) vs. Average number of 7.5M and up Earthquakes/6months with trend removed. Line of best fit, y = -0.02656x + (0.8277), mean x = 31.16 +/- 22.09, mean y = -1.277e-15 +/- 1.669, R = -0.3516, R squared = 0.1236, p-value = 0.0007294.

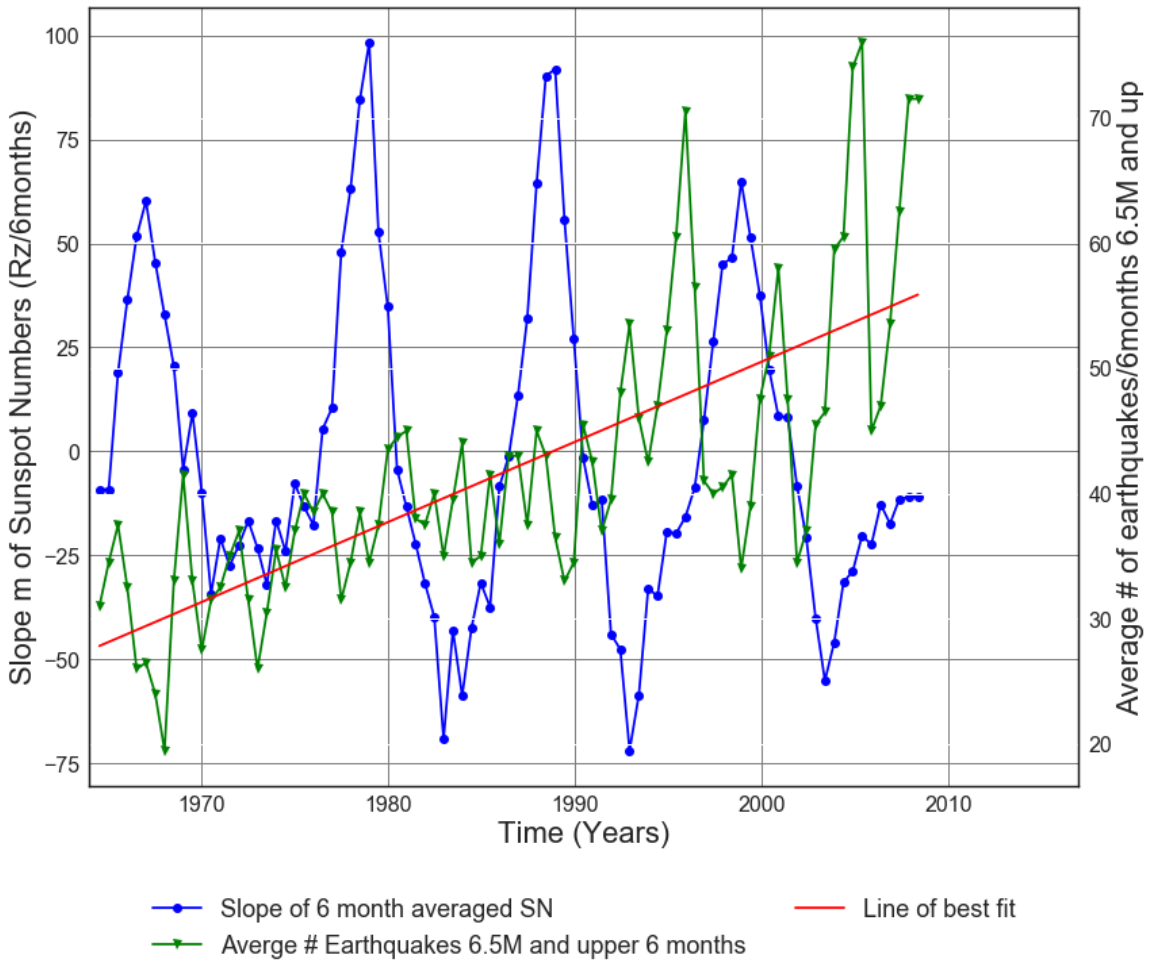

Figure D4.17: Slope of Solar cycle from 1964 to 2017 vs. Average number of 6.5M and up Earthquakes.

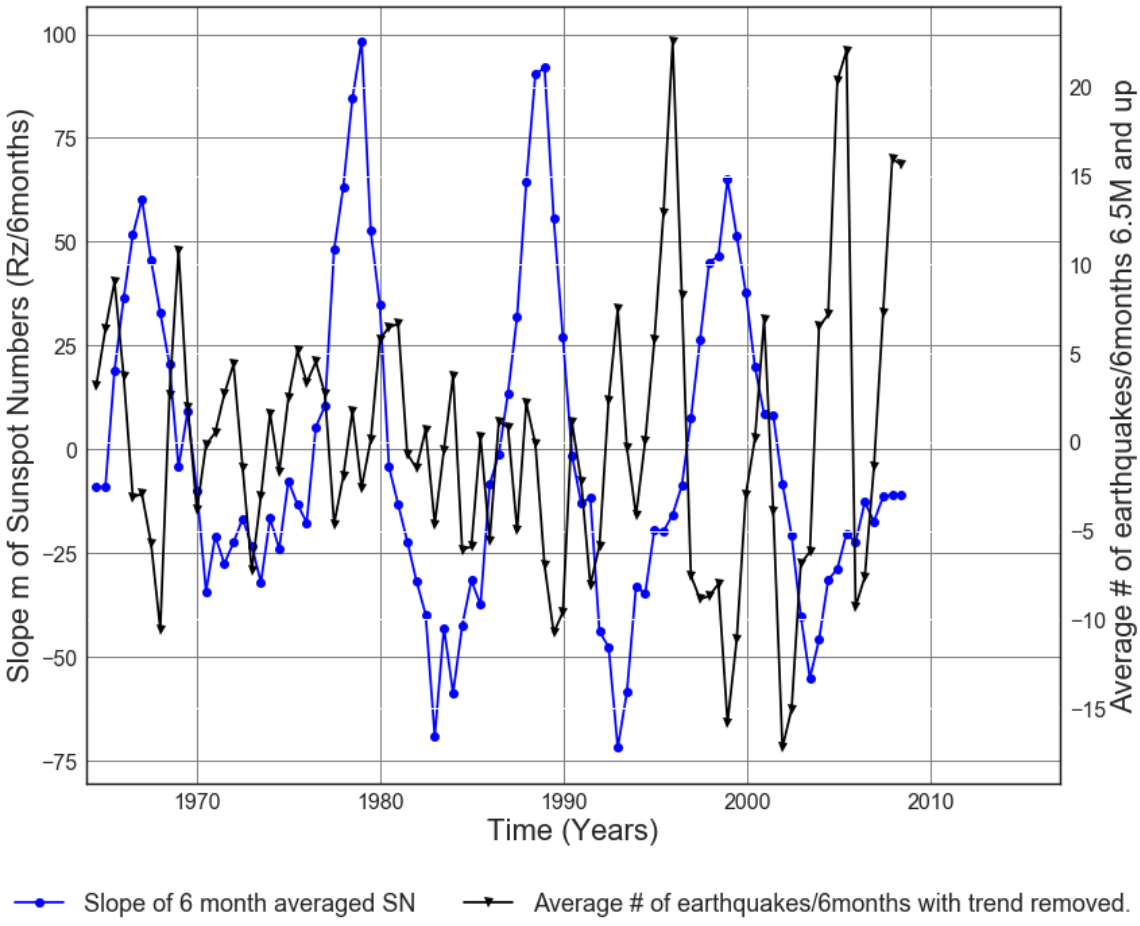

Figure D4.18: Slope of 6 month averaged SN 1964 to 2017 vs. Average number of 6.5M and up Earthquakes with trend removed. Line of best fit, y = 0.6394x + (-1.228e+03), mean x = 1.986e+03 +/- 12.8, mean y = 41.85 +/- 11.19

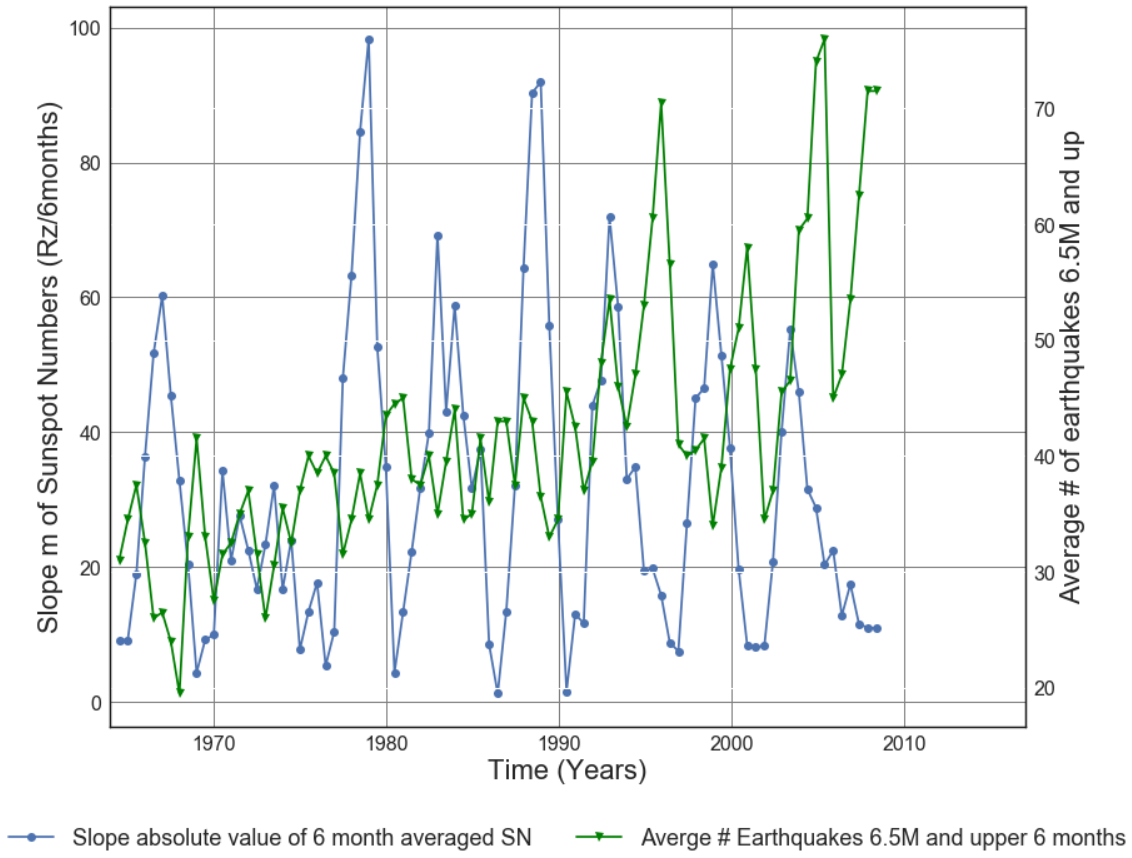

Figure D4.19: Slope Absolute value of Solar cycle from 1964 to 2017 vs. Average number of 6.5M and up Earthquakes.

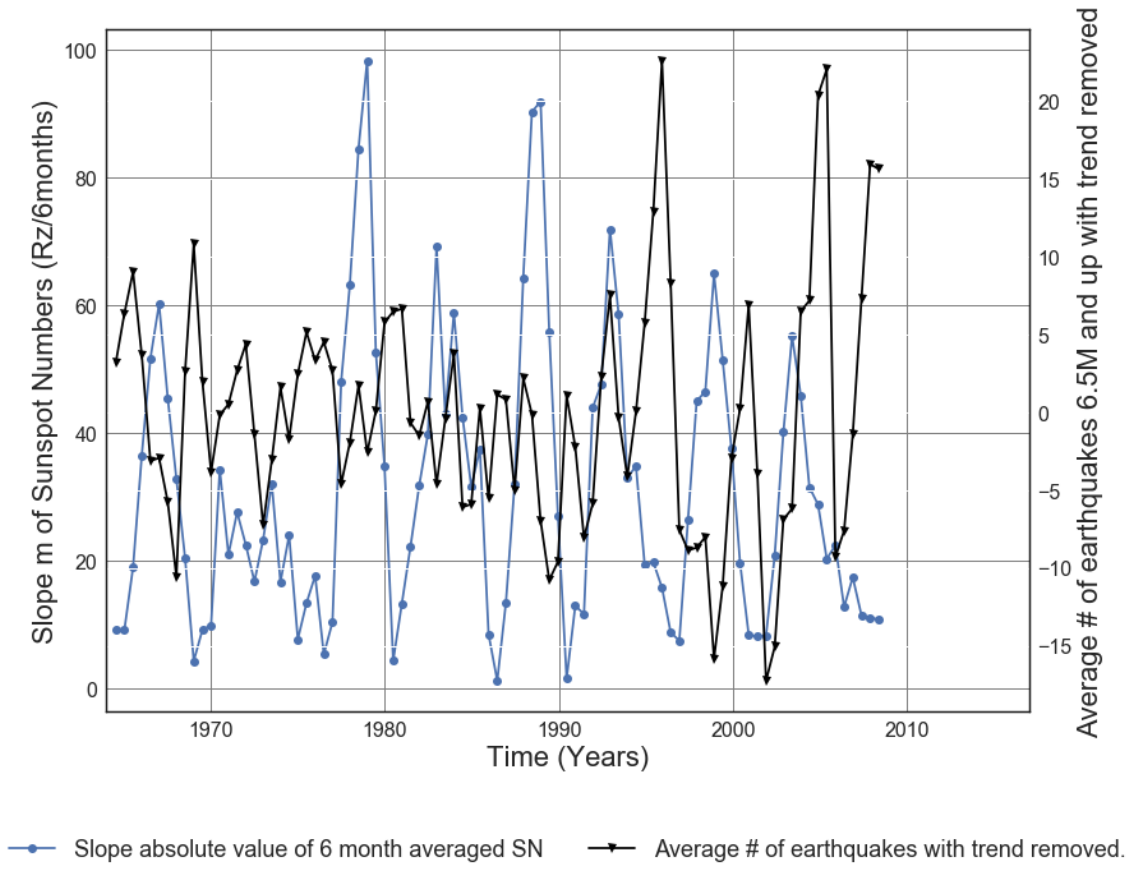

Figure D4.20: Slope Absolute value of Solar cycle from 1964 to 2017 vs. Average number of 6.5M and up earthquakes with trend removed.

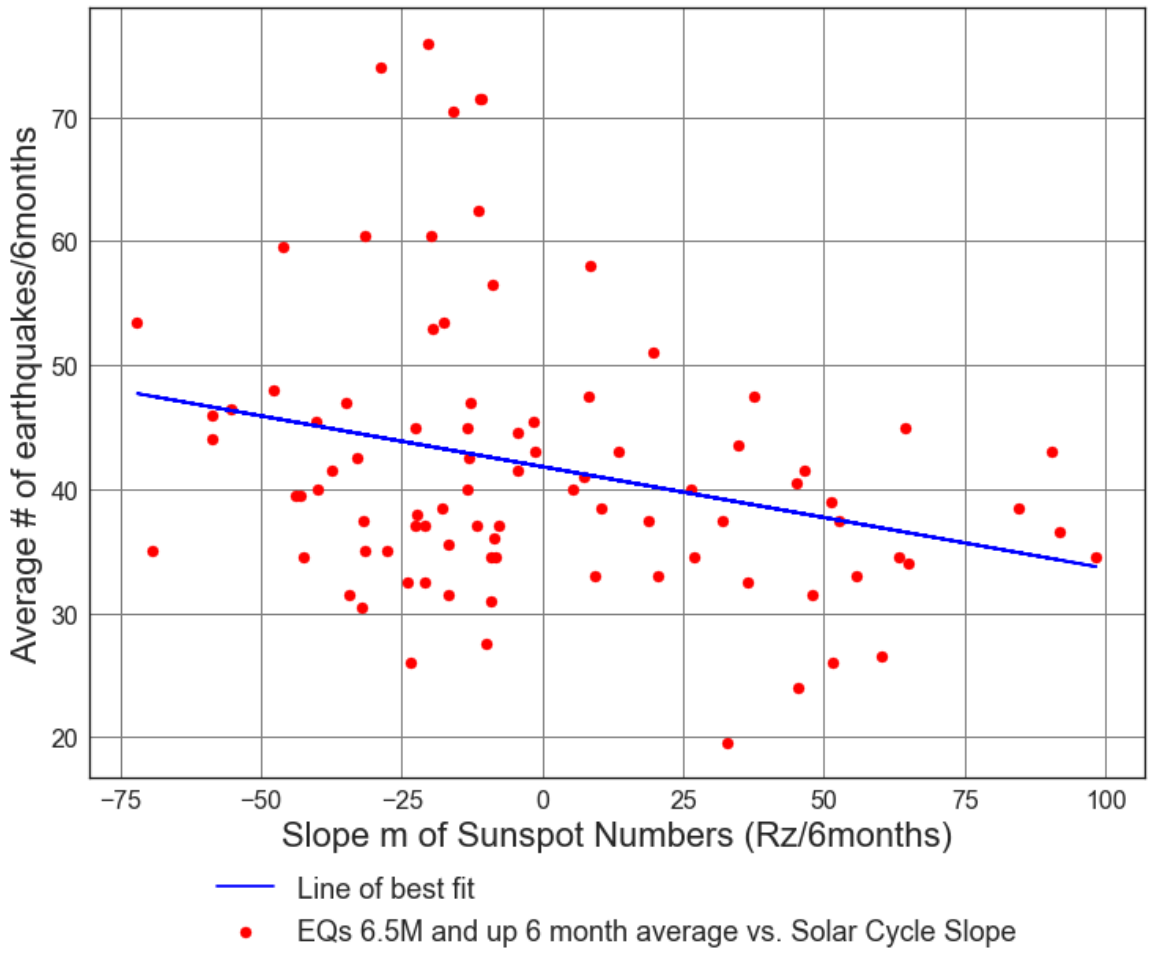

Figure D4.21: Scatter Plot of Solar cycle slope (from 1964 to 2017) vs. Average number of 6.5M and up Earthquakes/6months. Line of best fit, y = -0.08202x + (41.81), mean x = -0.5303 +/- 38.19, mean y = 41.85 +/- 11.19, R = -0.2799, R squared = 0.07835, p-value = 0.007892.

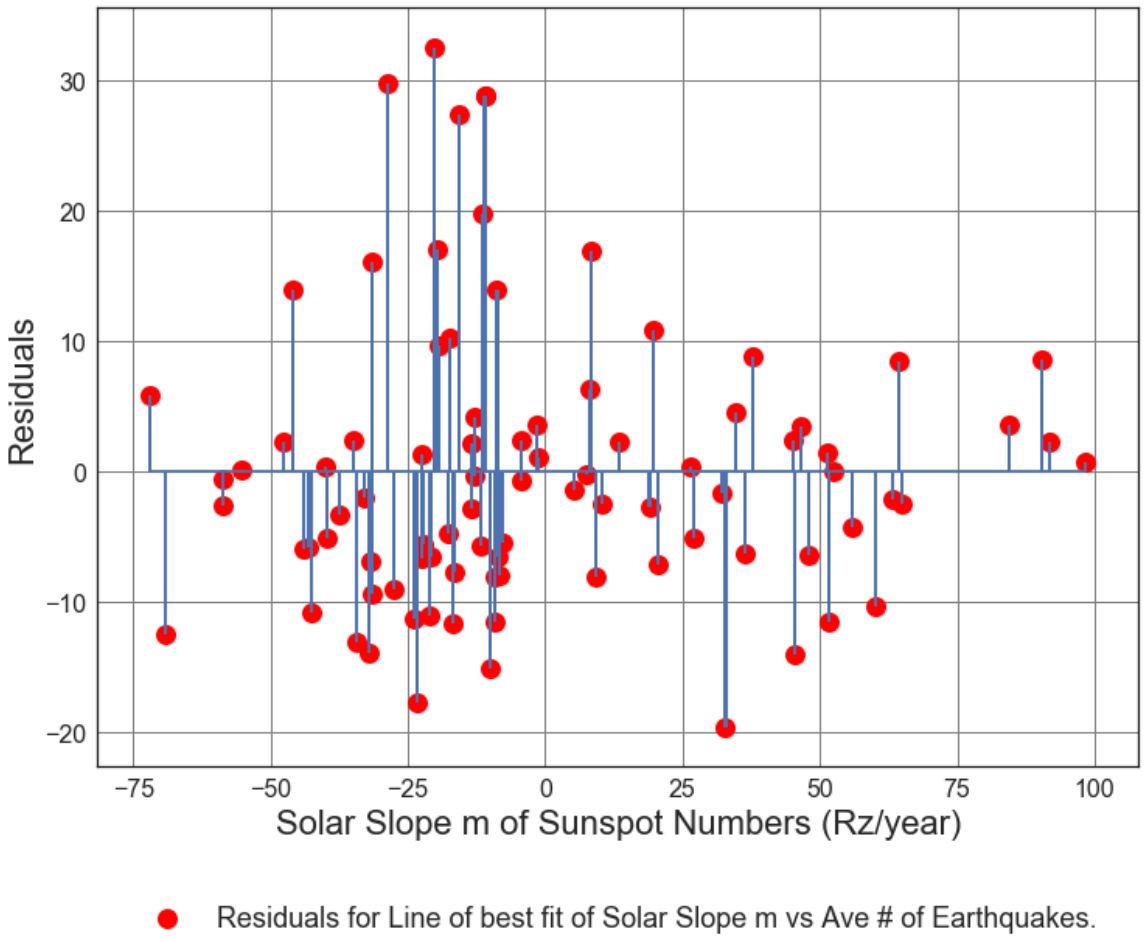

Figure D4.22: Residuals Plot of Solar cycle slope (from 1964 to 2017) vs. Average number of 6.5M and up Earthquakes/6months. Line of best fit, y = -0.08202x + (41.81), mean x = -0.5303 +/- 38.19, mean y = 41.85 +/- 11.19, R = -0.2799, R squared = 0.07835, p-value = 0.007892.

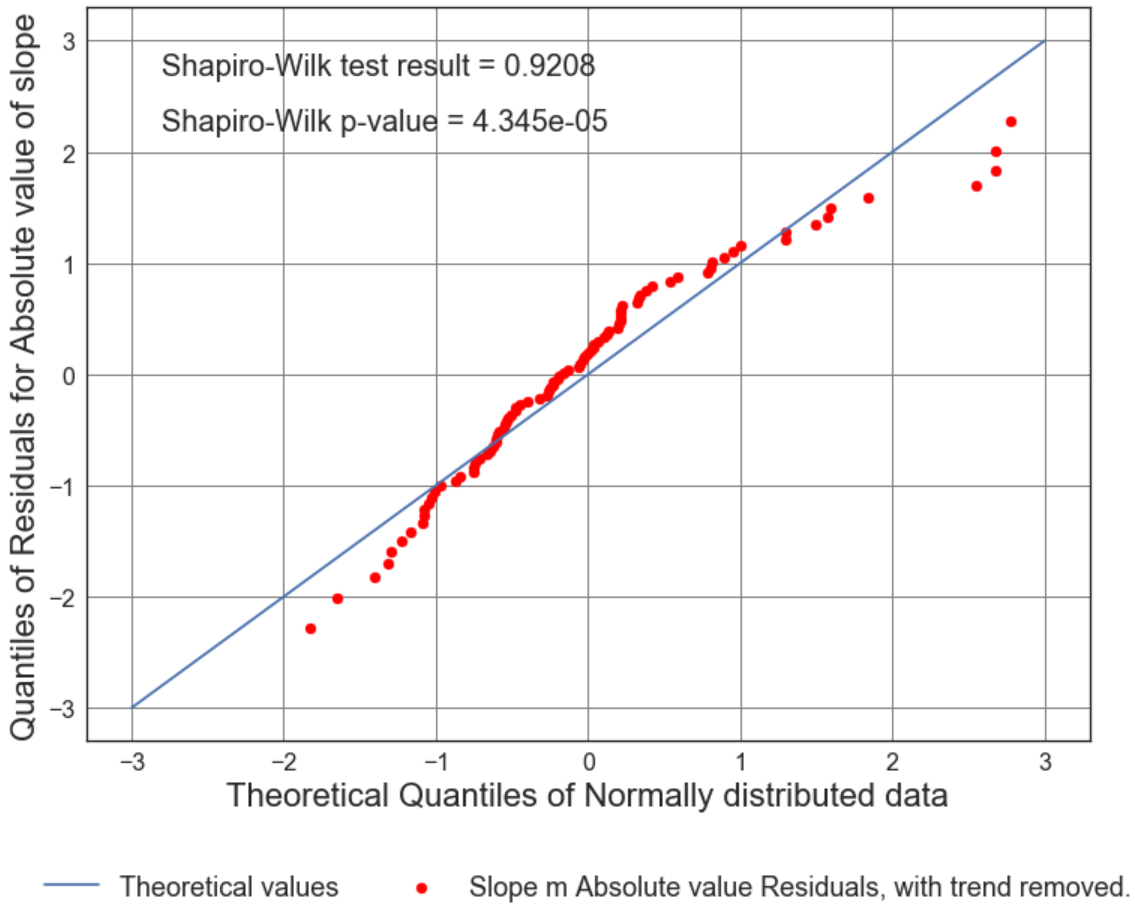

Figure D4.23: Residuals Plot of Solar cycle slope (from 1964 to 2017) vs. Average number of 6.5M and up Earthquakes/6months. Line of best fit, y = -0.08202x + (41.81), mean x = -0.5303 +/- 38.19, mean y = 41.85 +/- 11.19, R = -0.2799, R squared = 0.07835, p-value = 0.007892.

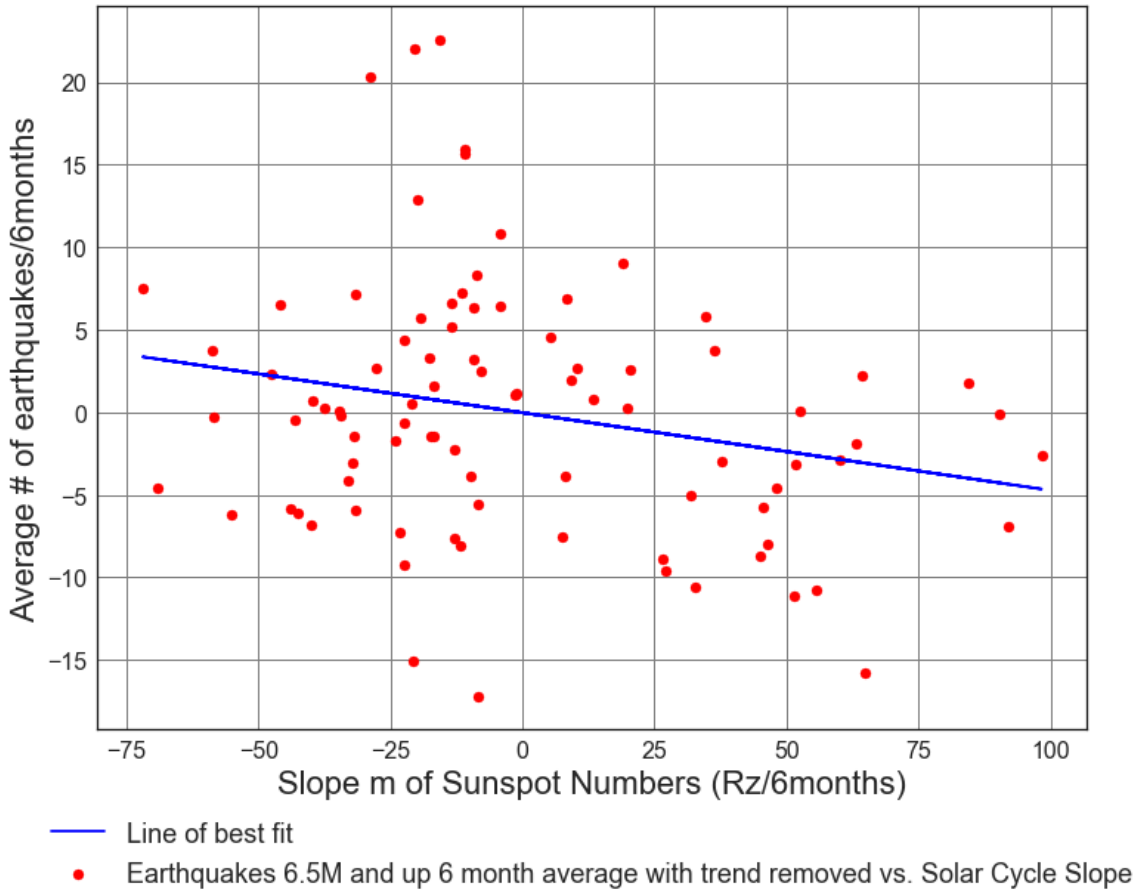

Figure D4.24: Scatter Plot of Solar cycle slope (from 1964 to 2017) vs. Average number of 6.5M and up Earthquakes/6months with trend removed. Line of best fit, y = -0.04704x + (-0.02494), mean x = -0.5303 +/- 38.19, mean y = 3.066e-14 +/- 7.633, R = -0.2354, R squared = 0.05541, p-value = 0.02638.

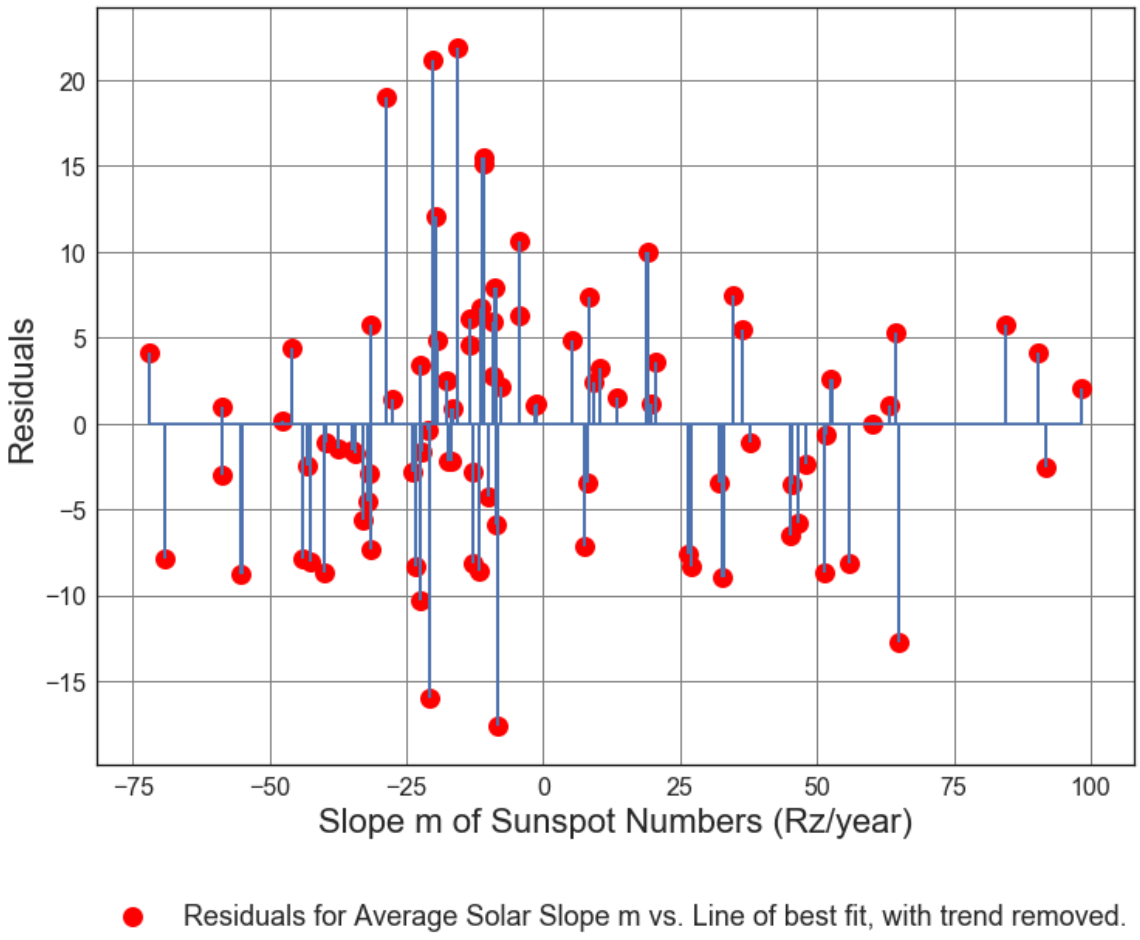

Figure D4.25: Scatter Plot of Solar cycle slope (from 1964 to 2017) vs. Average number of 6.5M and up Earthquakes/6months with trend removed. Line of best fit, y = -0.04704x + (-0.02494), mean x = -0.5303 +/- 38.19, mean y = 3.066e-14 +/- 7.633, R = -0.2354, R squared = 0.05541, p-value = 0.02638.

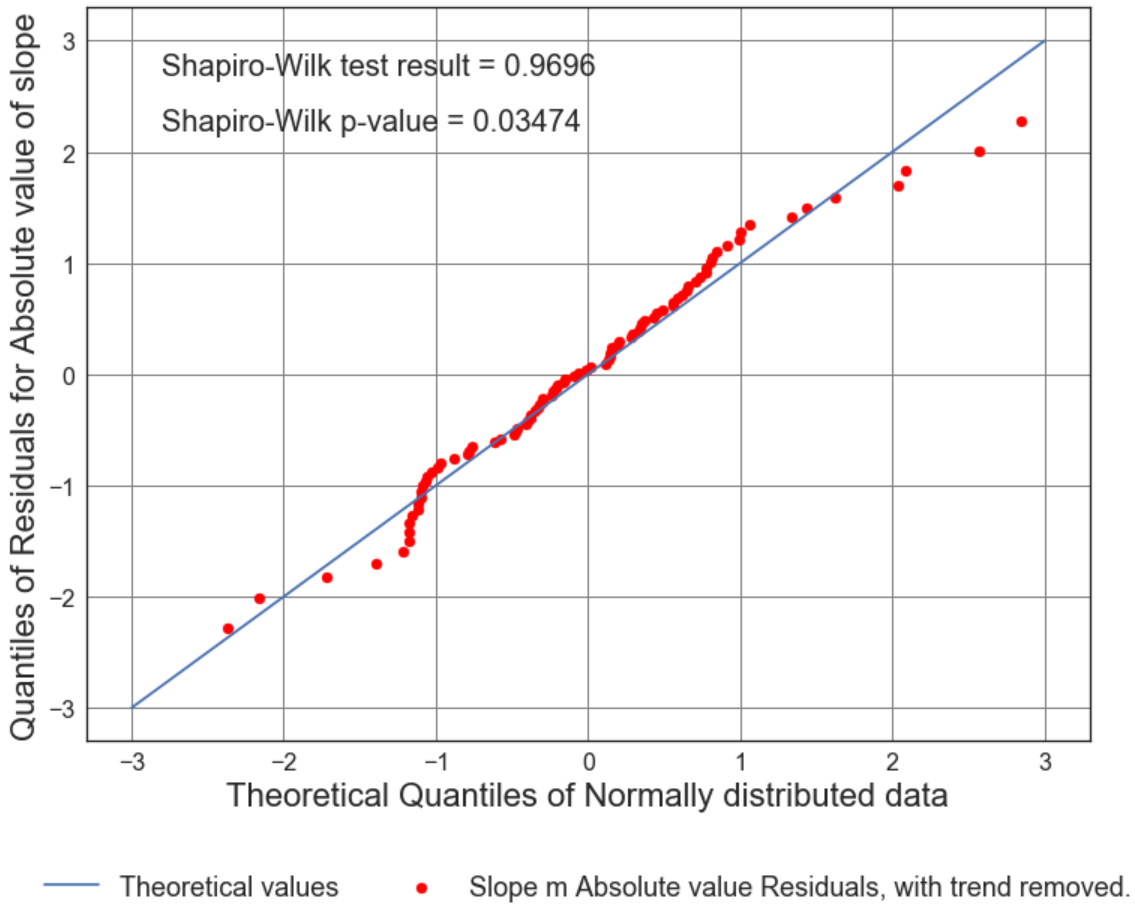

Figure D4.26: Scatter Plot of Solar cycle slope (from 1964 to 2017) vs. Average number of 6.5M and up Earthquakes/6months with trend removed. Line of best fit, y = -0.04704x + (-0.02494), mean x = -0.5303 +/- 38.19, mean y = 3.066e-14 +/- 7.633, R = -0.2354, R squared = 0.05541, p-value = 0.02638.

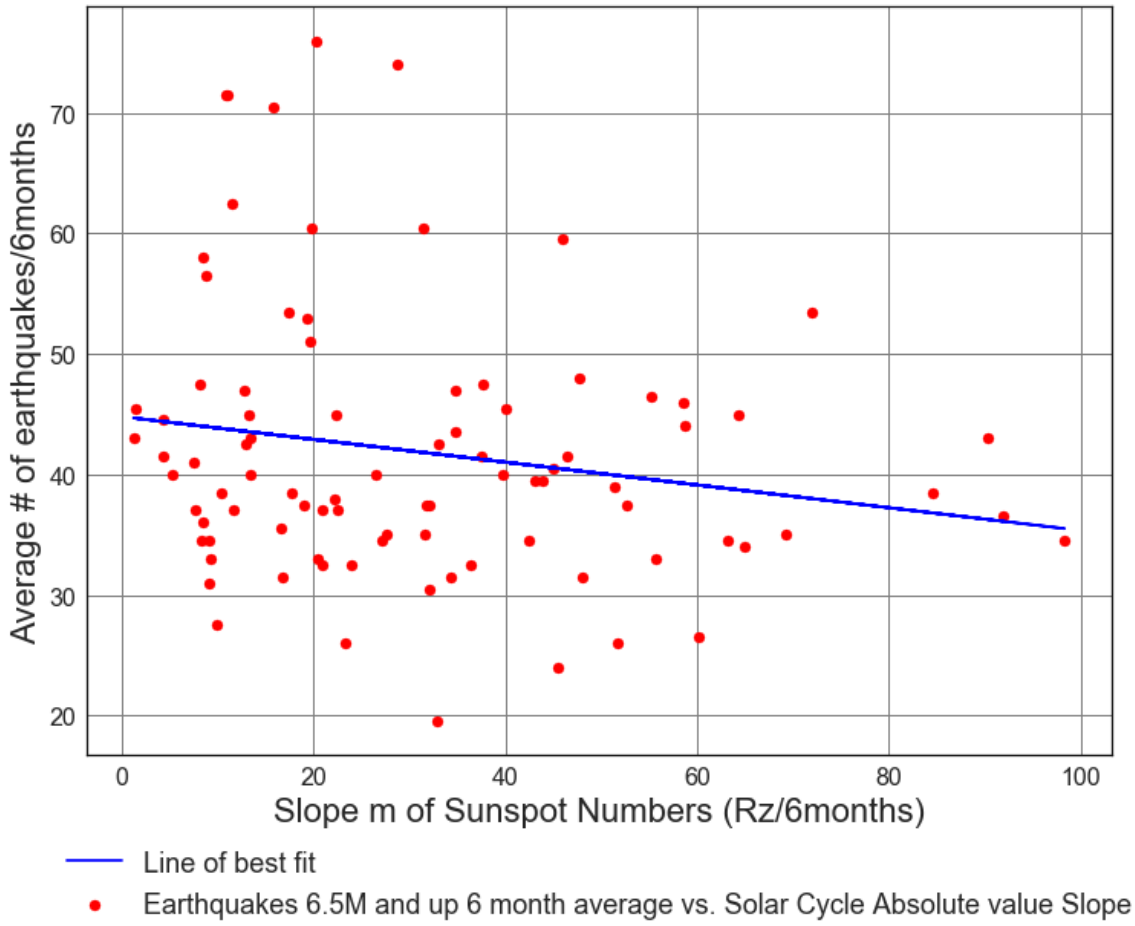

Figure D4.27: Scatter Plot of Solar cycle slope (from 1964 to 2017) vs. Average number of 6.5M and up Earthquakes/6months. Line of best fit, y = -0.09451x + (44.8), mean x = 31.16 +/- 22.09, mean y = 41.85 +/- 11.19, R = -0.1866, R squared = 0.03481, p-value = 0.07999.

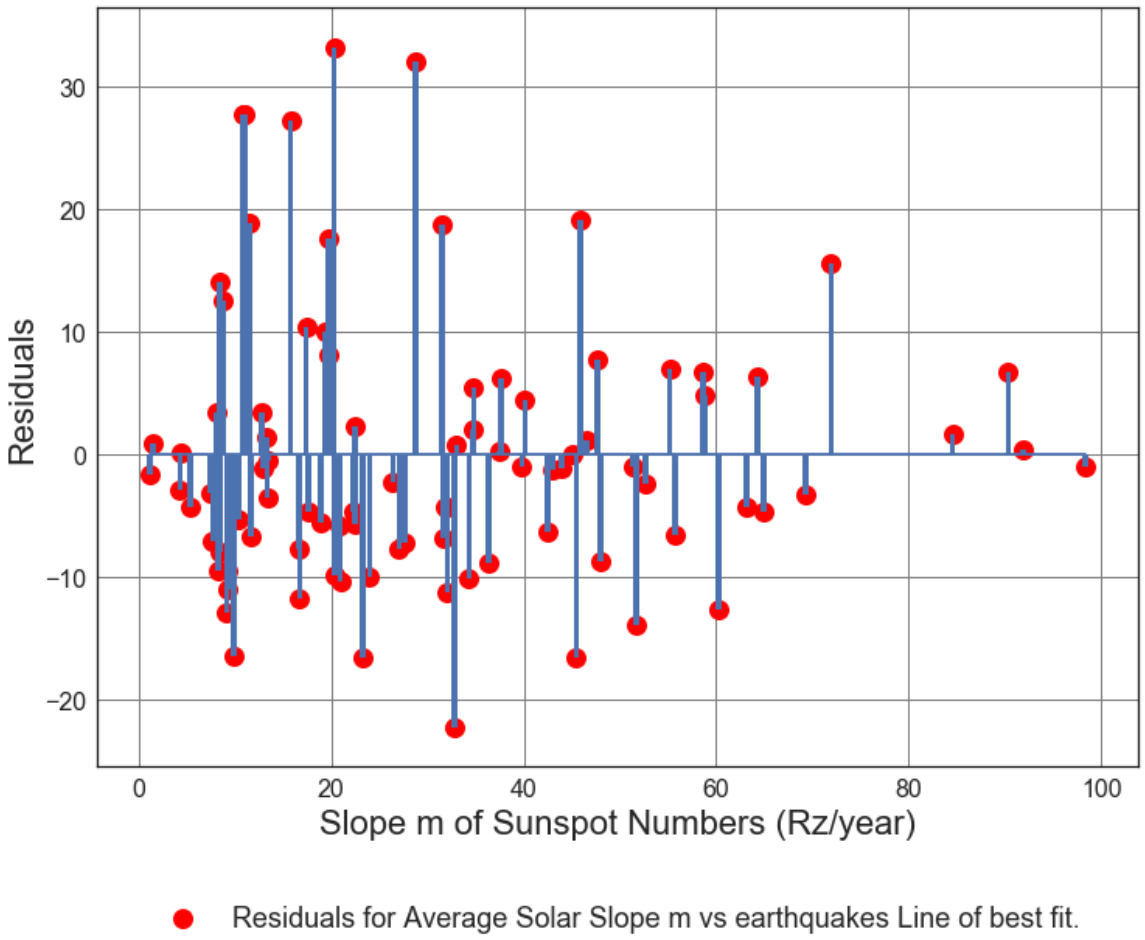

Figure D4.28: Scatter Plot of Solar cycle slope (from 1964 to 2017) vs. Average number of 6.5M and up Earthquakes/6months. Line of best fit, y = -0.09451x + (44.8), mean x = 31.16 +/- 22.09, mean y = 41.85 +/- 11.19, R = -0.1866, R squared = 0.03481, p-value = 0.07999.

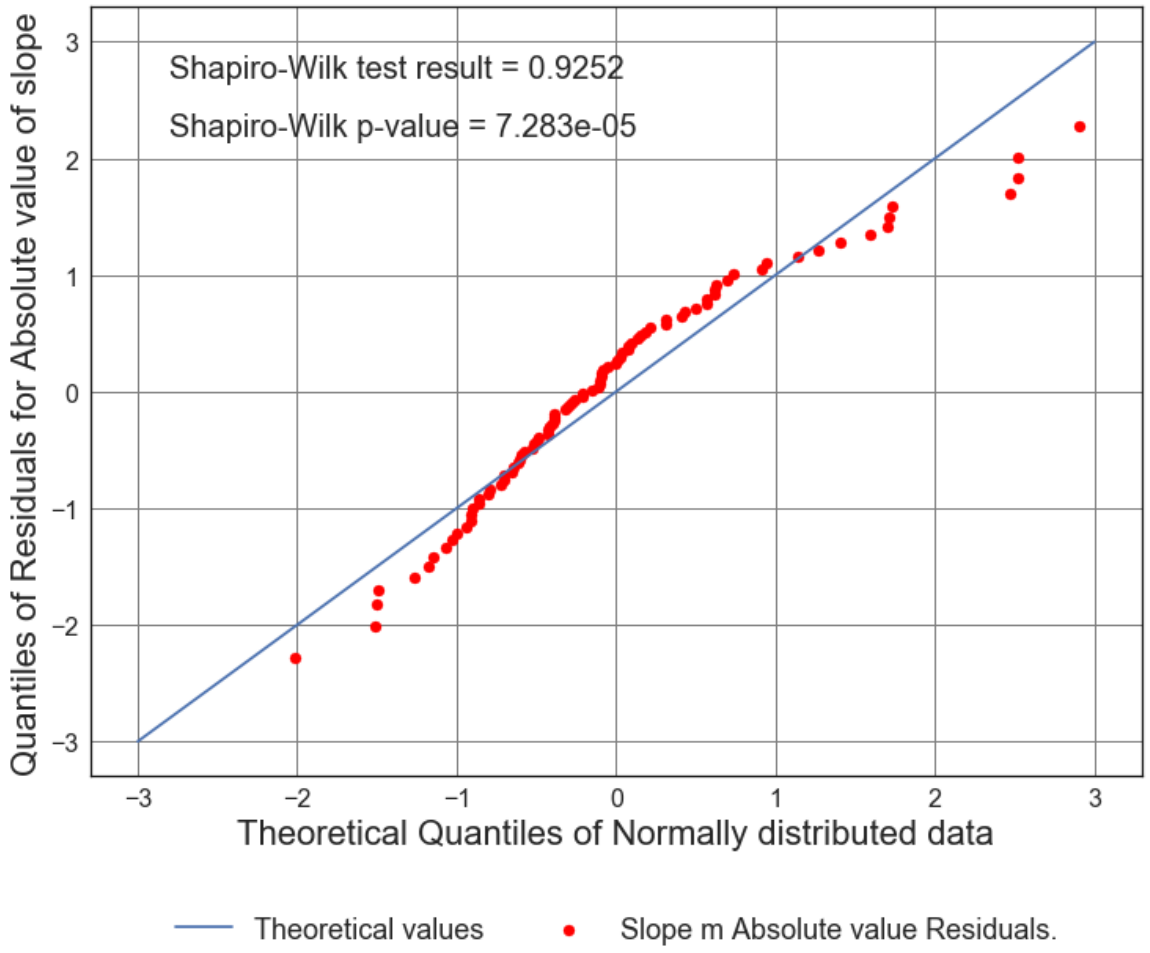

Figure D4.29: Scatter Plot of Solar cycle slope (from 1964 to 2017) vs. Average number of 6.5M and up Earthquakes/6months. Line of best fit, y = -0.09451x + (44.8), mean x = 31.16 +/- 22.09, mean y = 41.85 +/- 11.19, R = -0.1866, R squared = 0.03481, p-value = 0.07999.

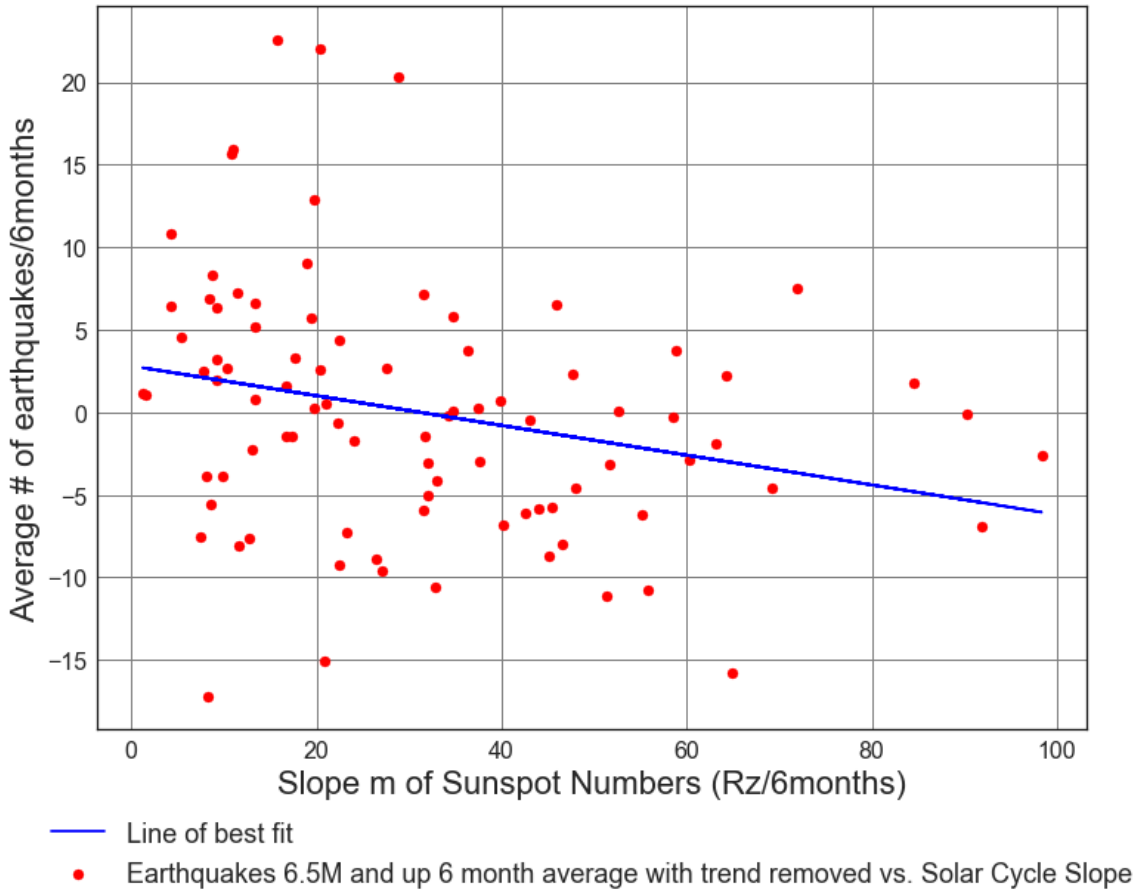

Figure D4.30: Scatter Plot of Solar cycle absolute value slope (from 1964 to 2017) vs. Average number of 6.5M and up Earthquakes/6months with trend removed. Line of best fit, y = -0.09007x + (2.807), mean x = 31.16 +/- 22.09, mean y = 3.066e-14 +/- 7.633, R = -0.2607, R squared = 0.06799, p-value = 0.01359.

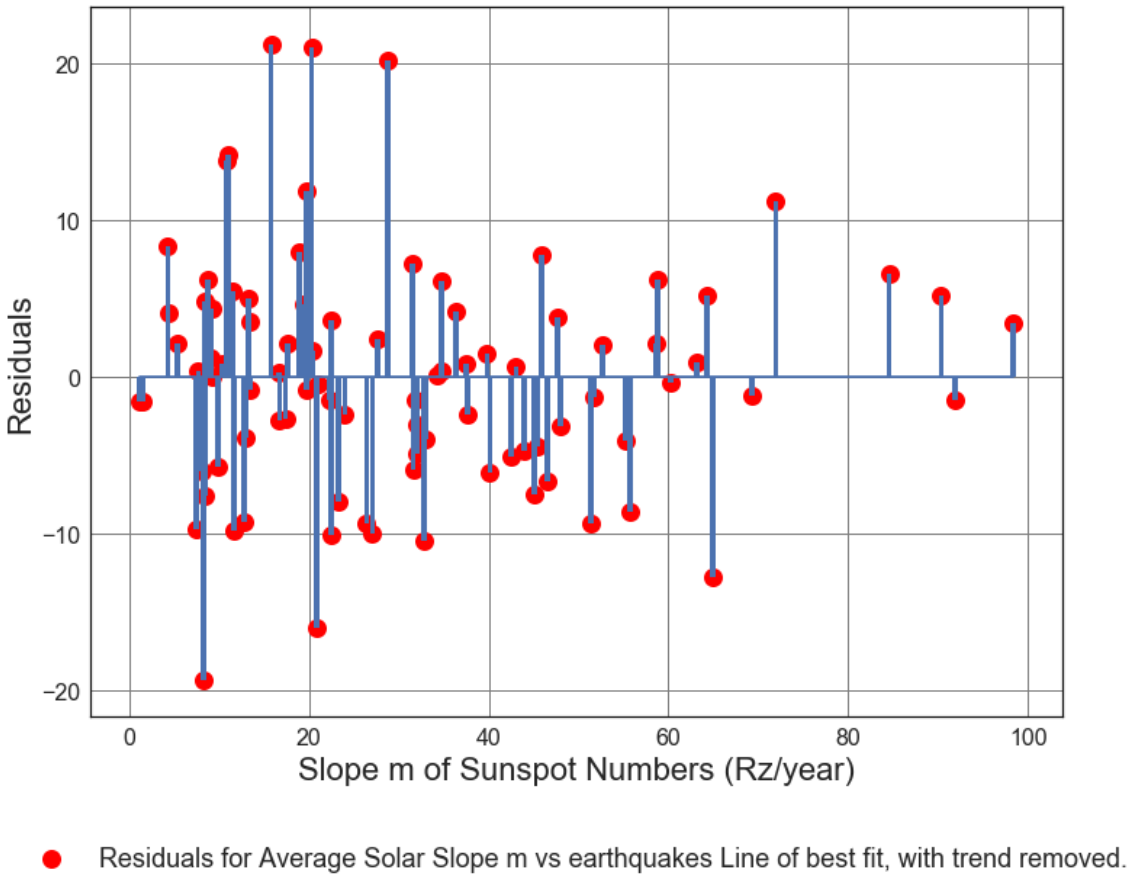

Figure D4.31: Scatter Plot of Solar cycle absolute value slope (from 1964 to 2017) vs. Average number of 6.5M and up Earthquakes/6months with trend removed. Line of best fit, y = -0.09007x + (2.807), mean x = 31.16 +/- 22.09, mean y = 3.066e-14 +/- 7.633, R = -0.2607, R squared = 0.06799, p-value = 0.01359.

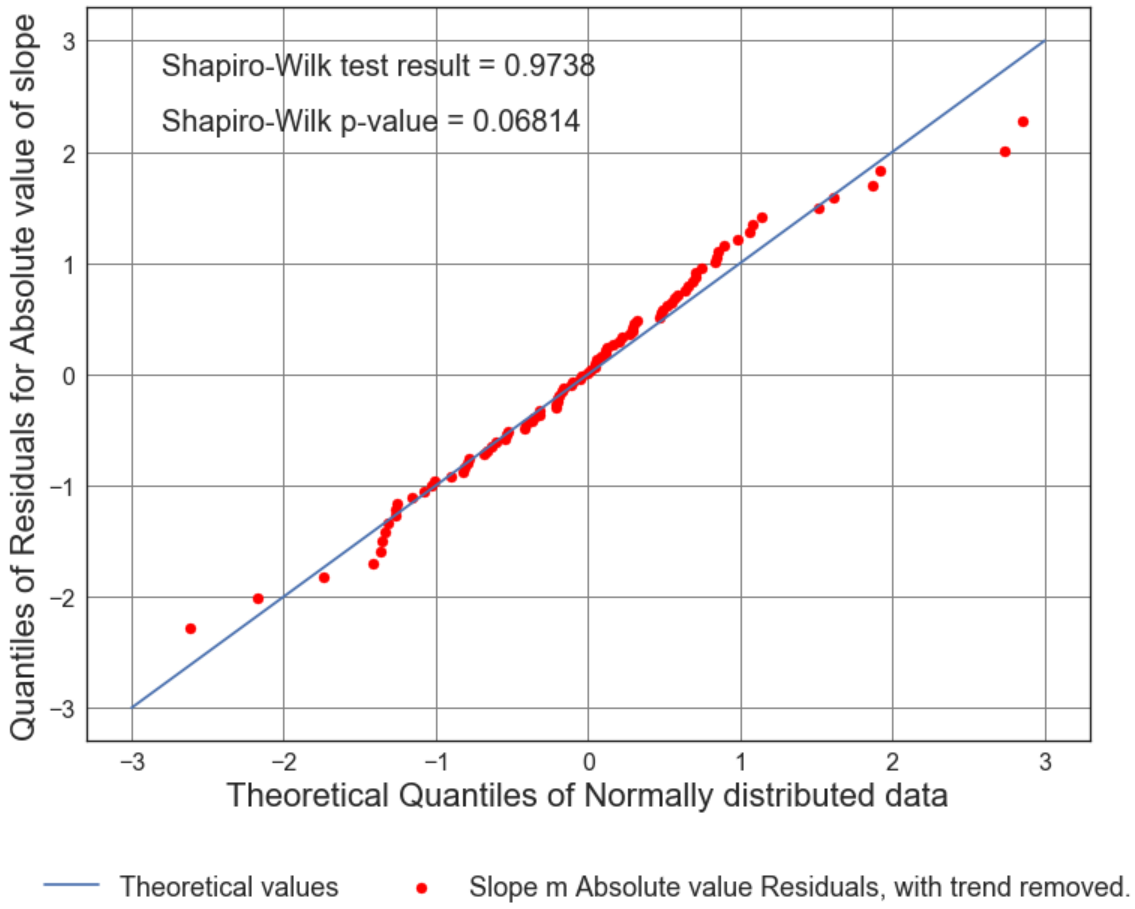

Figure D4.32: Scatter Plot of Solar cycle absolute value slope (from 1964 to 2017) vs. Average number of 6.5M and up Earthquakes/6months with trend removed. Line of best fit, y = -0.09007x + (2.807), mean x = 31.16 +/- 22.09, mean y = 3.066e-14 +/- 7.633, R = -0.2607, R squared = 0.06799, p-value = 0.01359.

Appendix E1: Fast Fourier Transform Magnitude Spectra Comparison of Averaged (ISC, USGS, and Centennial) Earthquake Frequencies with Solar Cycle frequencies. Part 1 - Earthquake Counts and Energy Released in Joules.

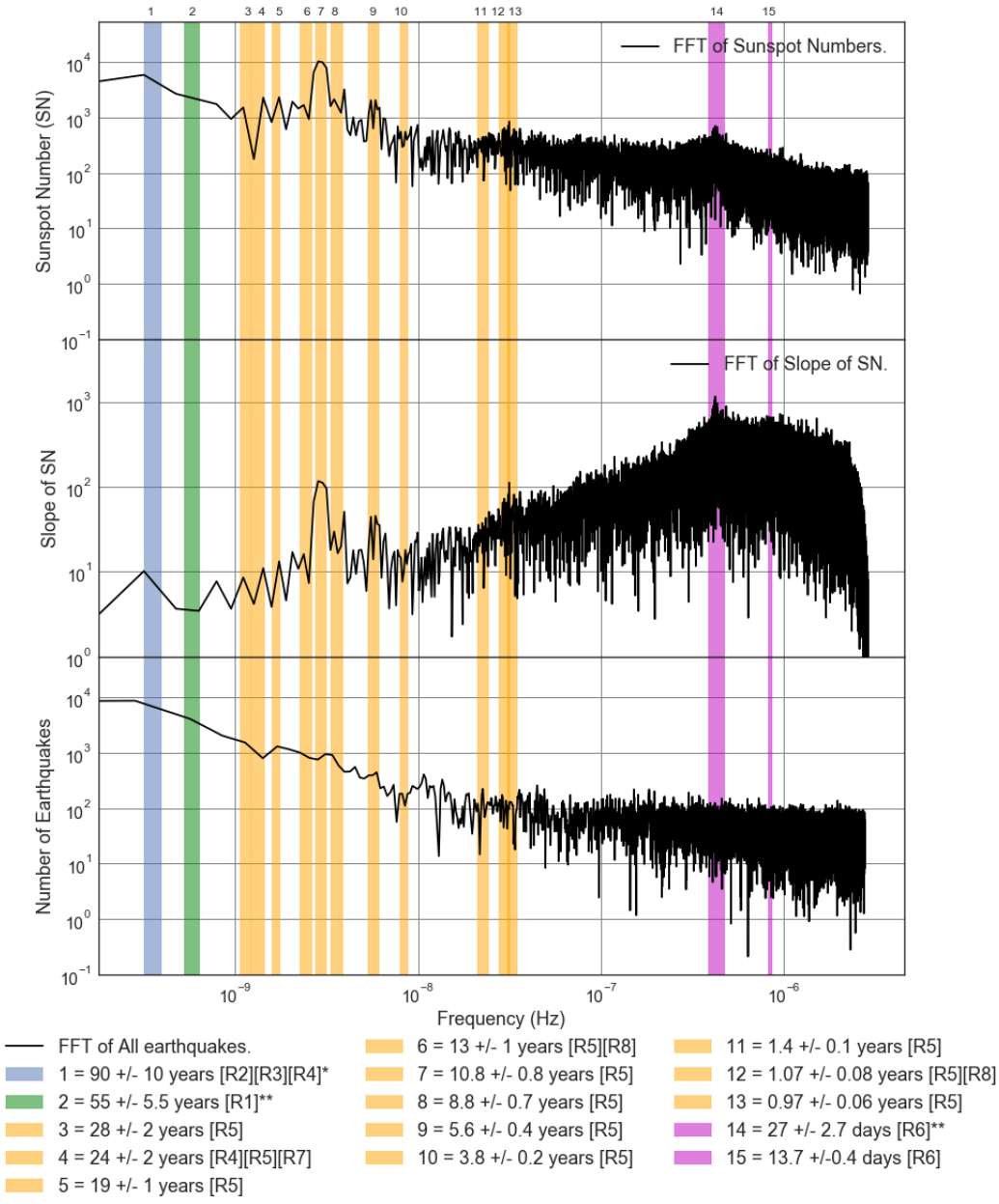

Figure E1.1: FFT Loglog Comparison Plot of number of Averaged All Earthquakes, Sunspot number (SN) and slope from 1818 to 2017. Additional meaning of the legend colors: Blue = Various Analysis techniques, Green = Meyer wavelet, Orange = Instantly maximal wavelet skeleton spectra, Magenta = Periodram and Linear phase finite impulse response.

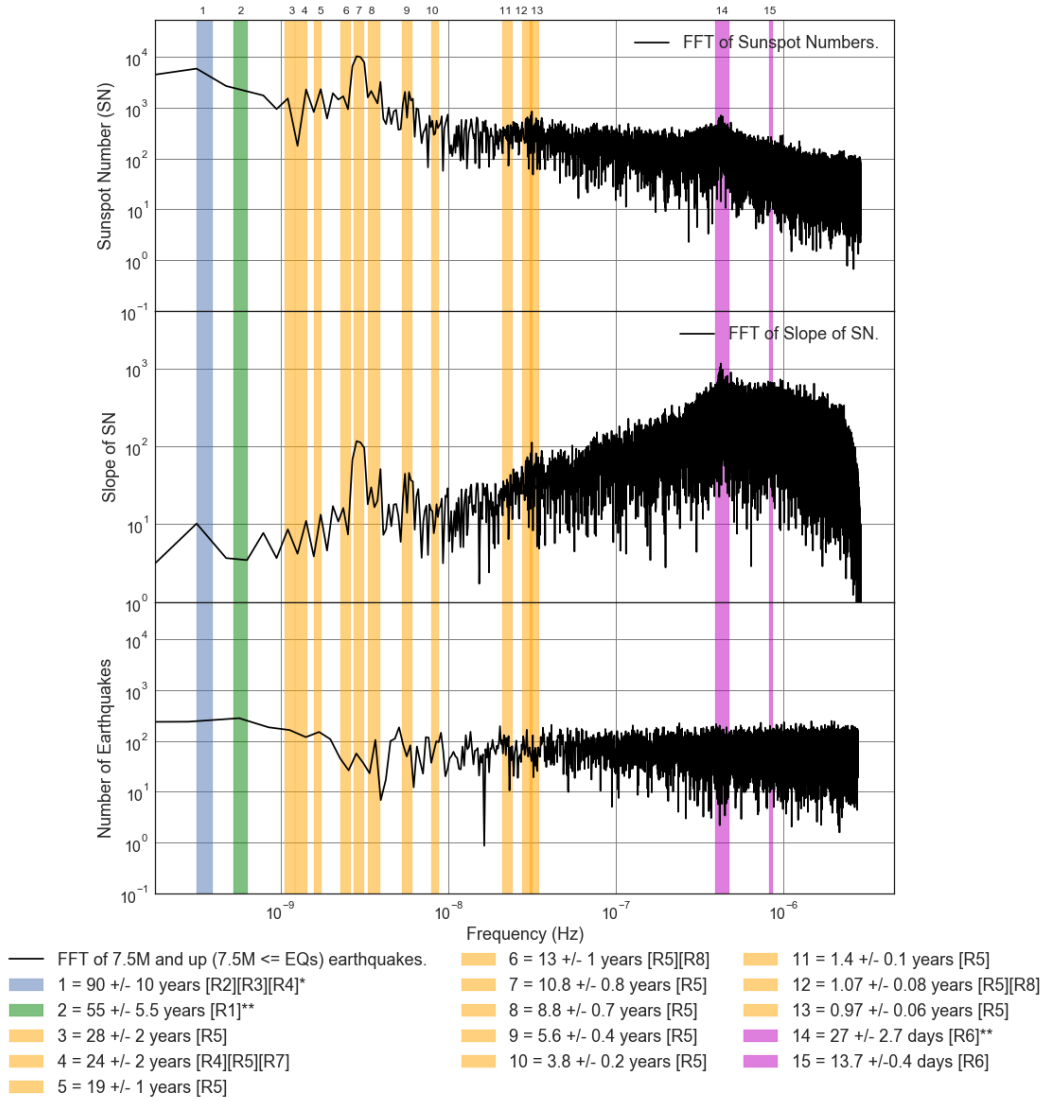

Figure E1.2: FFT Loglog Comparison Plot of number of Averaged 7.5M and up (7.5M <= EQs) Earthquakes, Sunspot number (SN) and slope from 1818 to 2017. Additional meaning of the legend colors: Blue = Various Analysis techniques, Green = Meyer wavelet, Orange = Instantly maximal wavelet skeleton spectra, Magenta = Periodram and Linear phase finite impulse response.

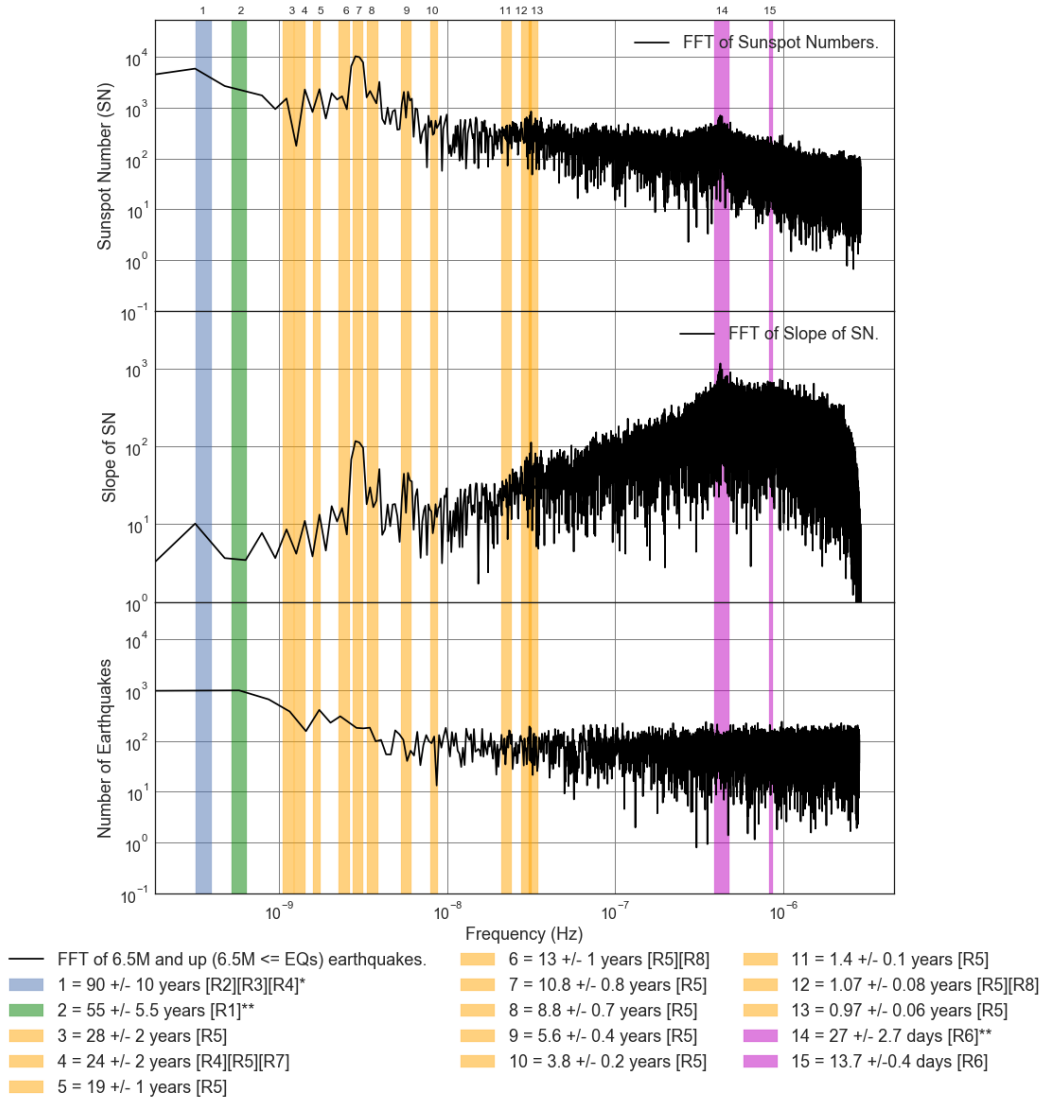

Figure E1.3: FFT Loglog Comparison Plot of number of Averaged 6.5M and up (6.5M <= EQs) Earthquakes, Sunspot number (SN) and slope from 1818 to 2017. Additional meaning of the legend colors: Blue = Various Analysis techniques, Green = Meyer wavelet, Orange = Instantly maximal wavelet skeleton spectra, Magenta = Periodram and Linear phase finite impulse response.

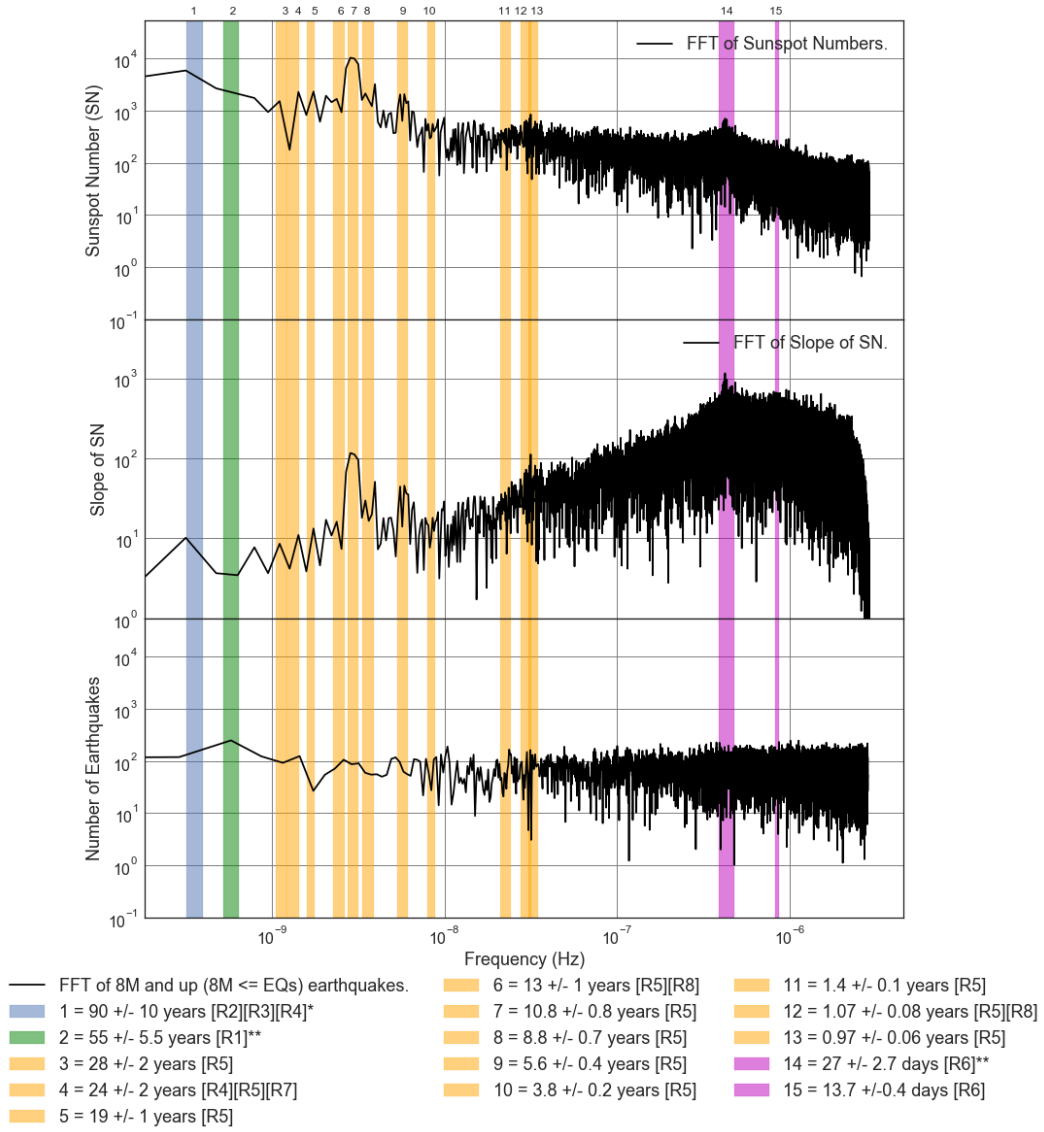

Figure E1.4: FFT Loglog Comparison Plot of number of Averaged 8M and up (8M <= EQs) Earthquakes, Sunspot number (SN) and slope from 1818 to 2017. Additional meaning of the legend colors: Blue = Various Analysis techniques, Green = Meyer wavelet, Orange = Instantly maximal wavelet skeleton spectra, Magenta = Periodram and Linear phase finite impulse response.

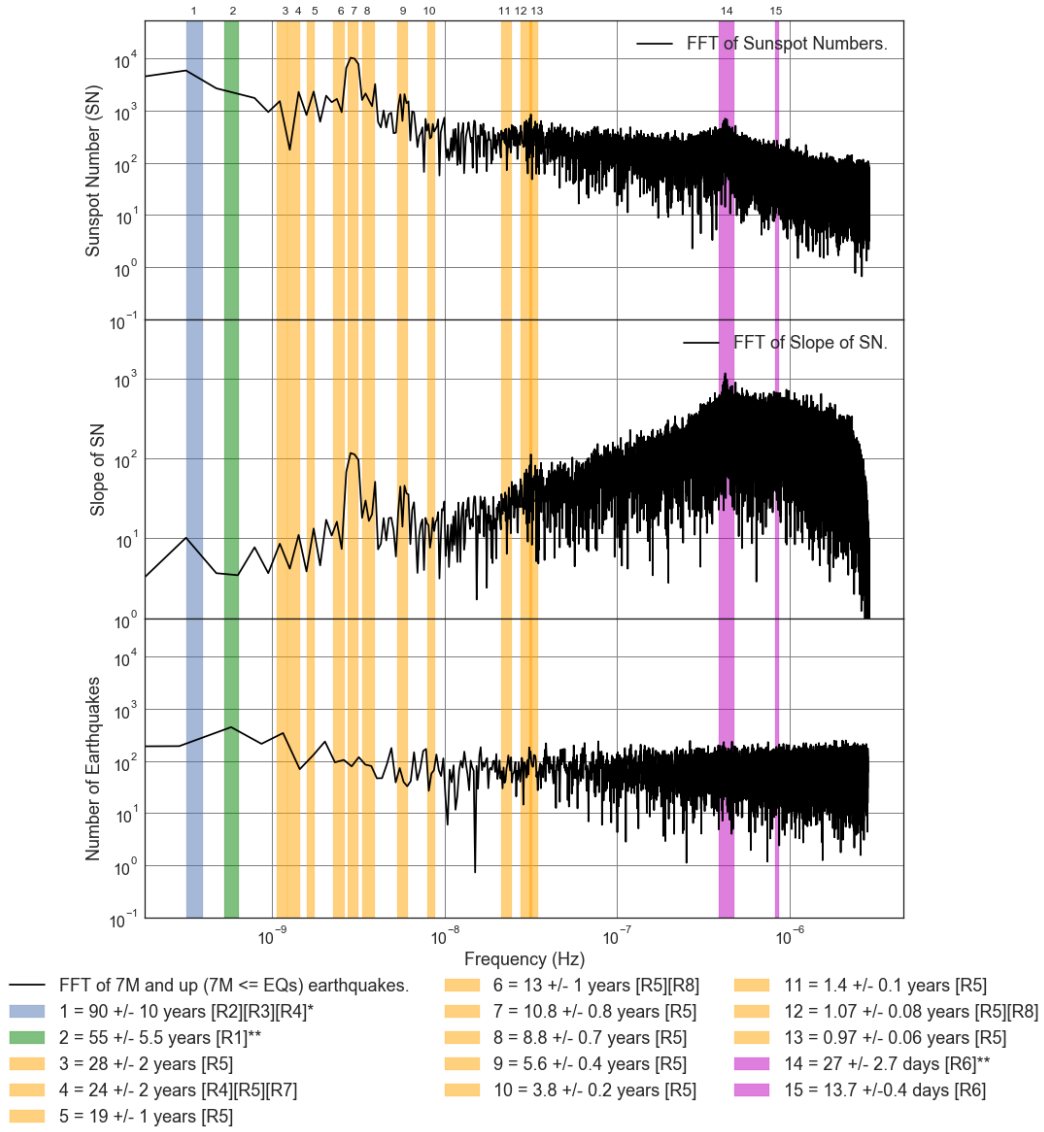

Figure E1.5: FFT Loglog Comparison Plot of number of Averaged 7M and up (7M <= EQs) Earthquakes, Sunspot number (SN) and slope from 1818 to 2017. Additional meaning of the legend colors: Blue = Various Analysis techniques, Green = Meyer wavelet, Orange = Instantly maximal wavelet skeleton spectra, Magenta = Periodram and Linear phase finite impulse response.

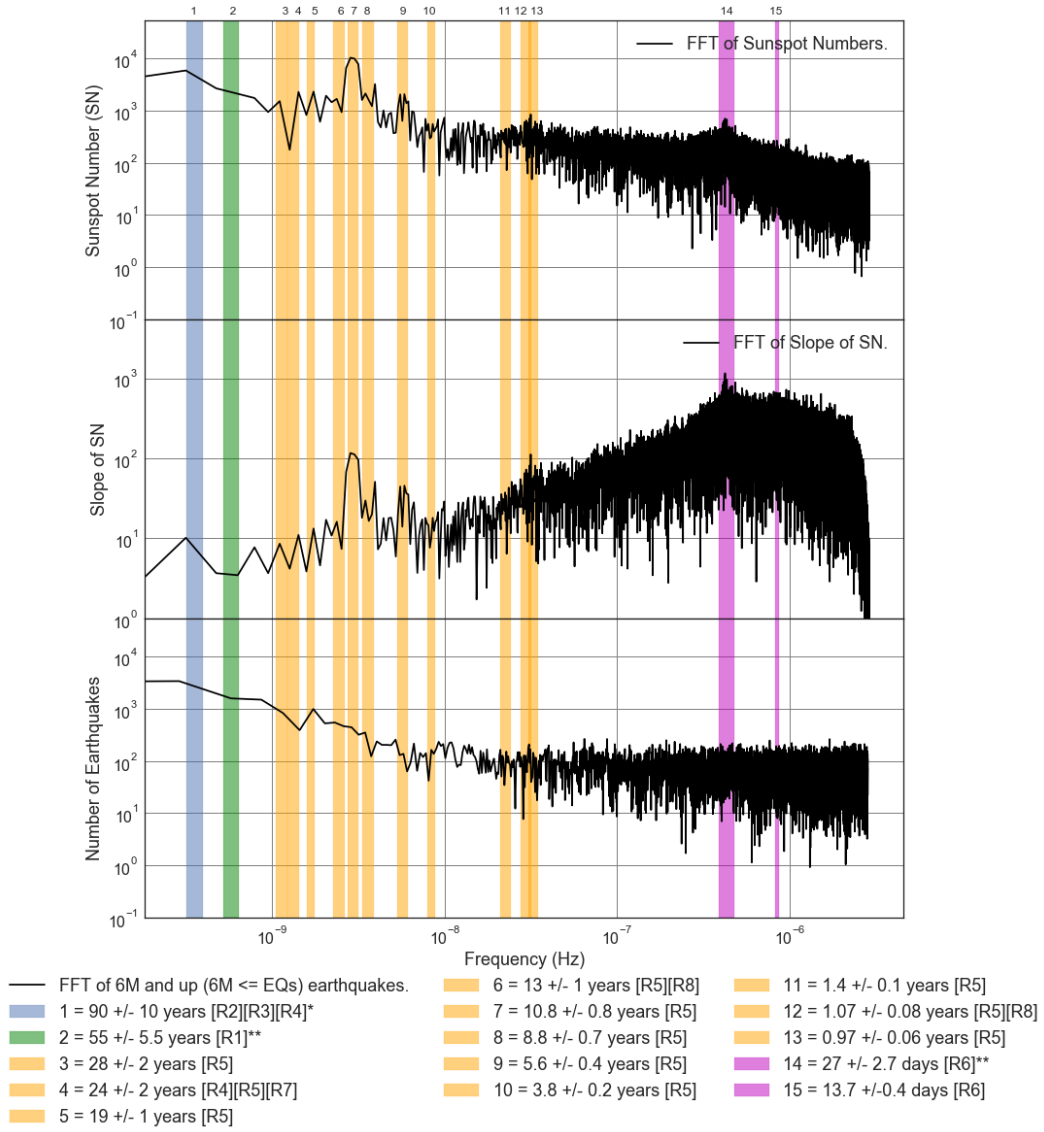

Figure E1.6: FFT Loglog Comparison Plot of number of Averaged 6M and up (6M <= EQs) Earthquakes, Sunspot number (SN) and slope from 1818 to 2017. Additional meaning of the legend colors: Blue = Various Analysis techniques, Green = Meyer wavelet, Orange = Instantly maximal wavelet skeleton spectra, Magenta = Periodram and Linear phase finite impulse response.

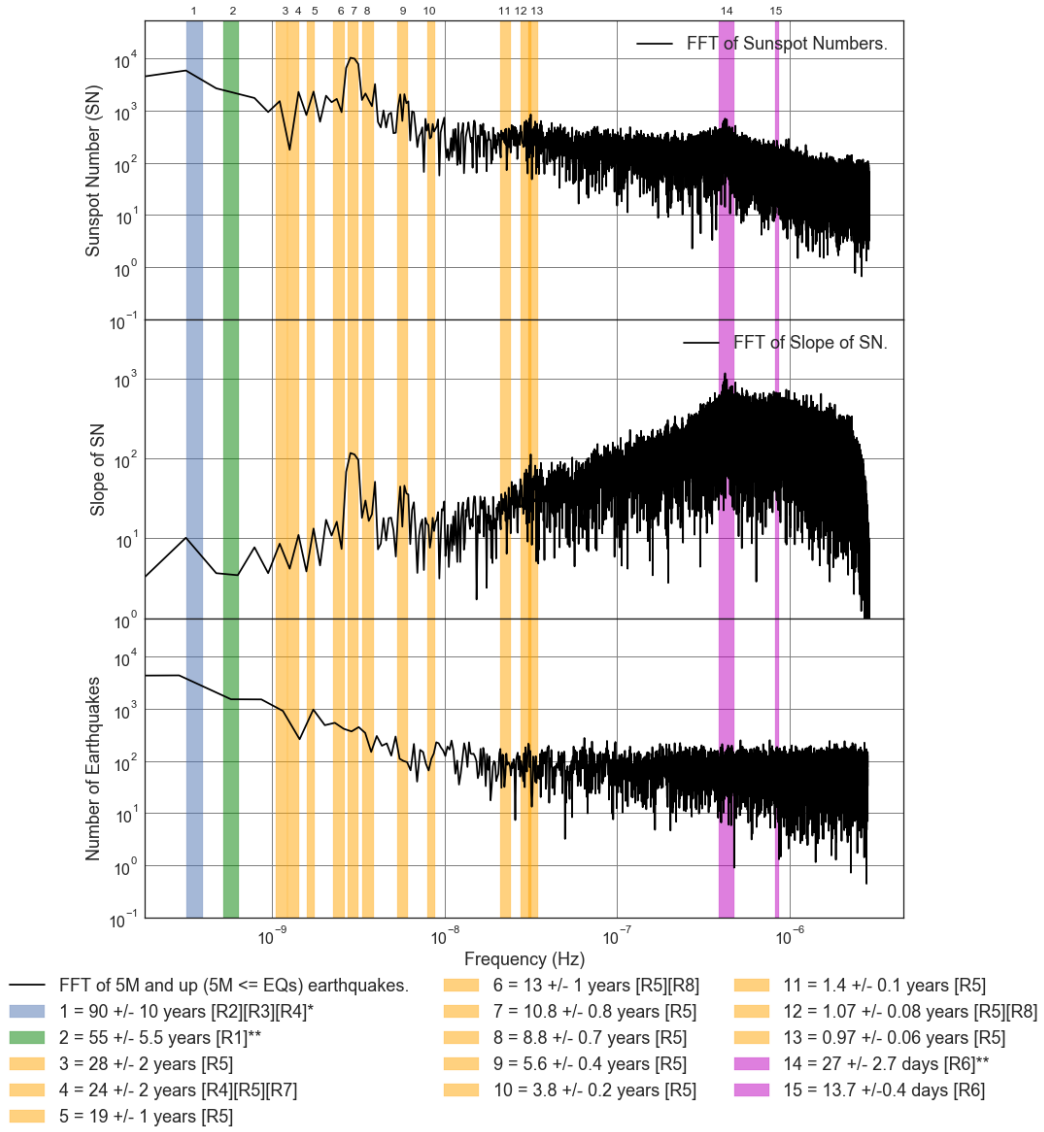

Figure E1.7: FFT Loglog Comparison Plot of number of Averaged 5M and up (5M <= EQs) Earthquakes, Sunspot number (SN) and slope from 1818 to 2017. Additional meaning of the legend colors: Blue = Various Analysis techniques, Green = Meyer wavelet, Orange = Instantly maximal wavelet skeleton spectra, Magenta = Periodram and Linear phase finite impulse response.

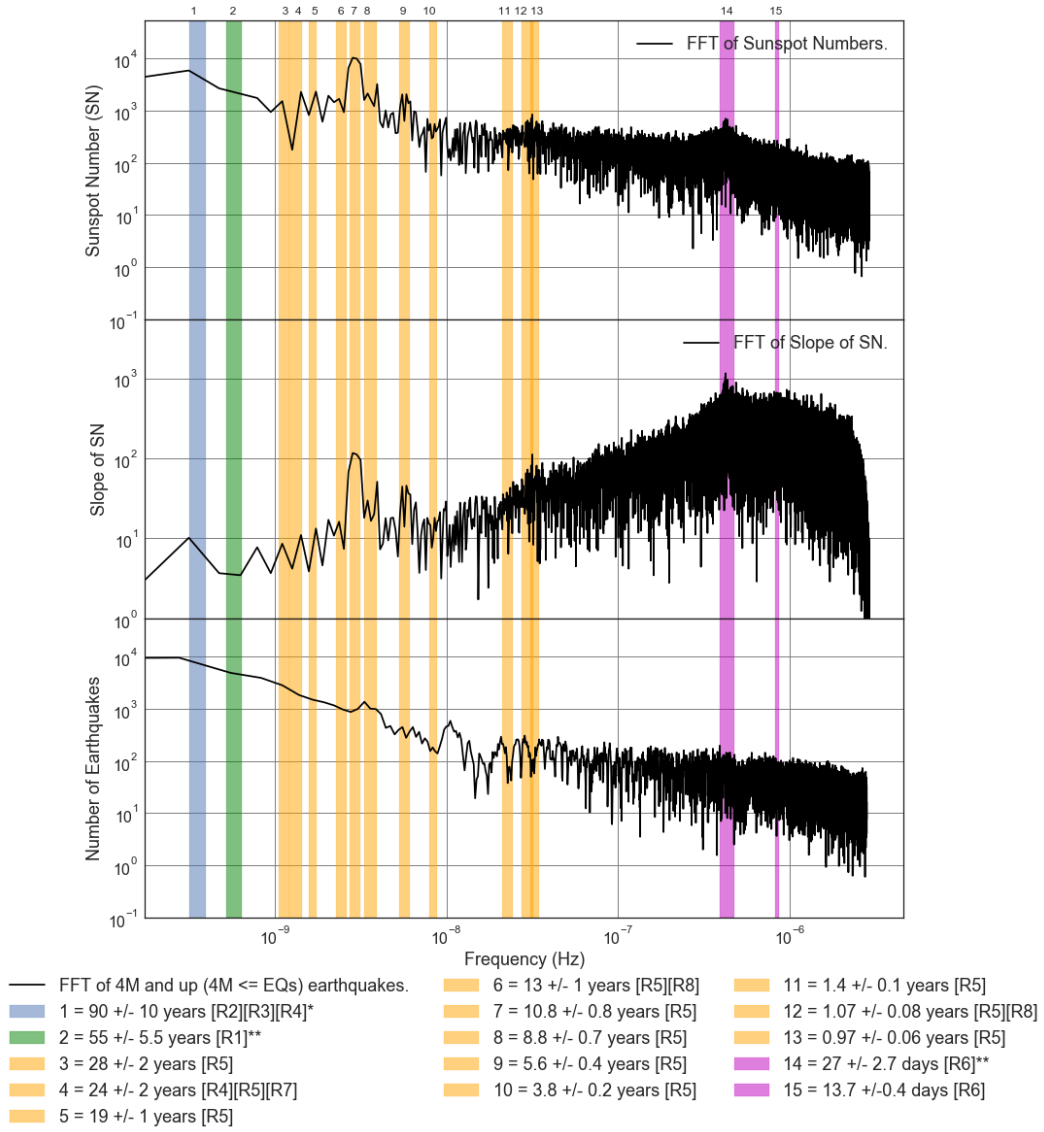

Figure E1.8: FFT Loglog Comparison Plot of number of Averaged 4M and up (4M <= EQs) Earthquakes, Sunspot number (SN) and slope from 1818 to 2017. Additional meaning of the legend colors: Blue = Various Analysis techniques, Green = Meyer wavelet, Orange = Instantly maximal wavelet skeleton spectra, Magenta = Periodram and Linear phase finite impulse response.

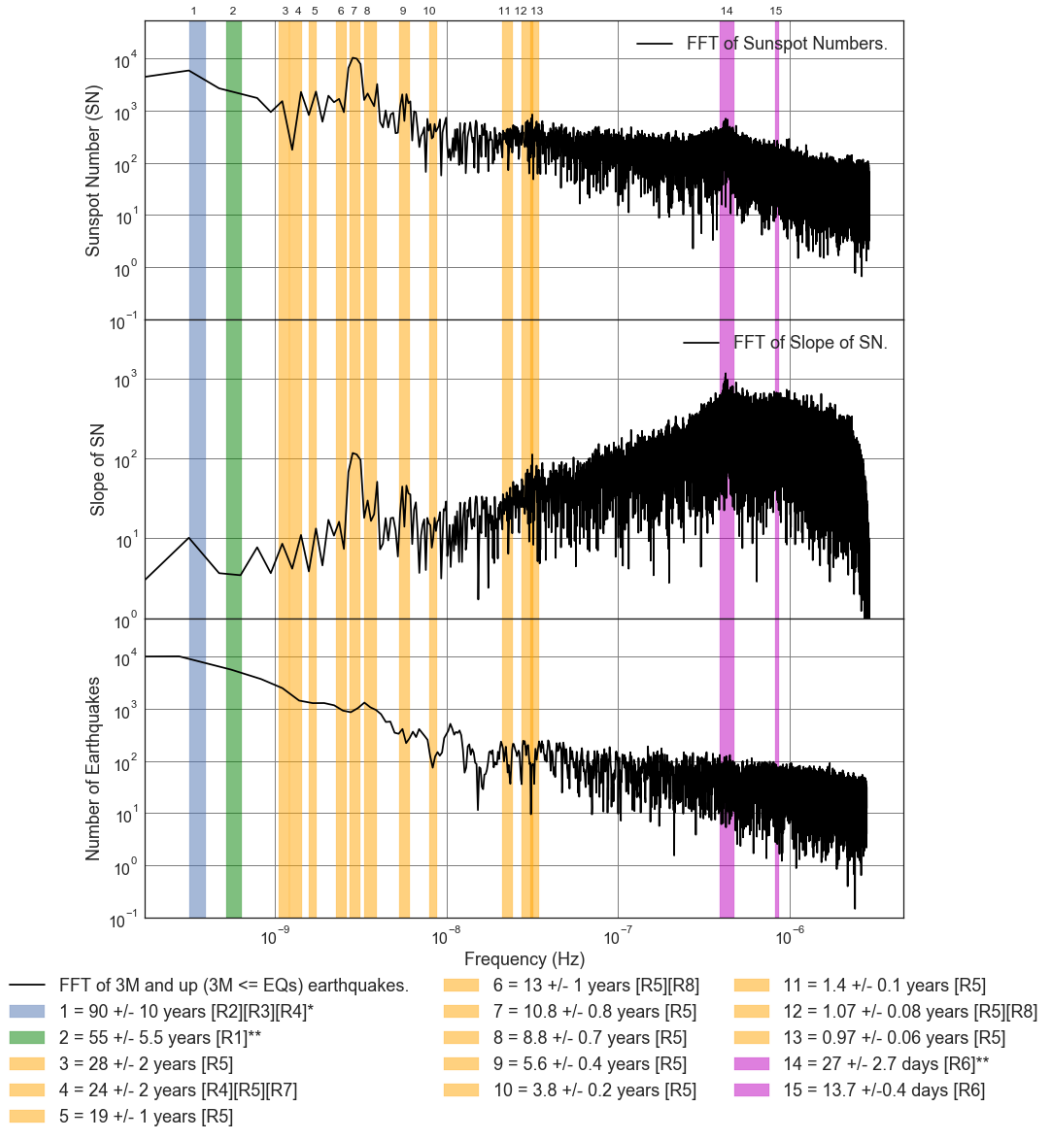

Figure E1.9: FFT Loglog Comparison Plot of number of Averaged 3M and up (3M <= EQs) Earthquakes, Sunspot number (SN) and slope from 1818 to 2017. Additional meaning of the legend colors: Blue = Various Analysis techniques, Green = Meyer wavelet, Orange = Instantly maximal wavelet skeleton spectra, Magenta = Periodram and Linear phase finite impulse response.

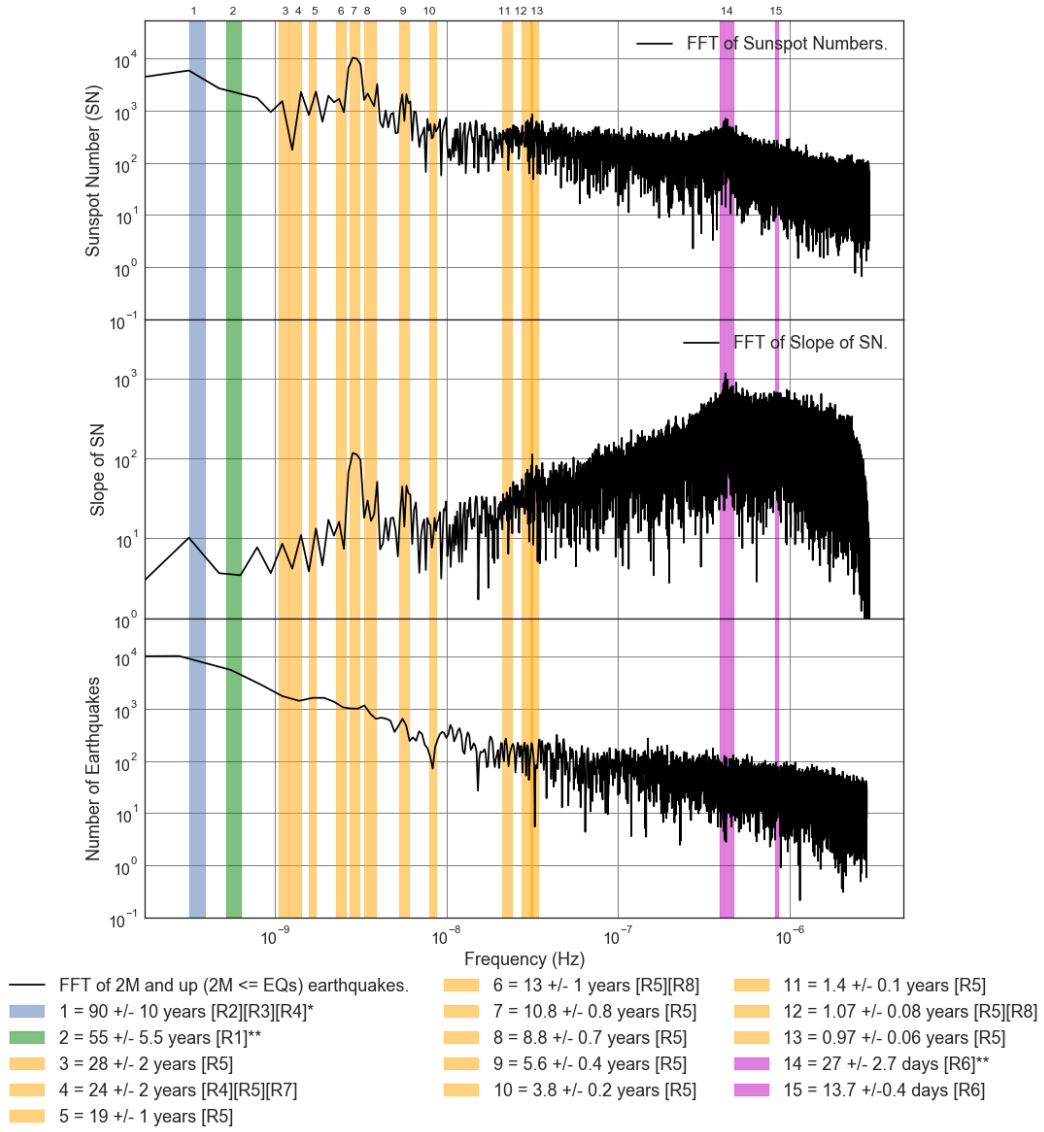

Figure E1.10: FFT Loglog Comparison Plot of number of Averaged 2M and up (2M <= EQs) Earthquakes, Sunspot number (SN) and slope from 1818 to 2017. Additional meaning of the legend colors: Blue = Various Analysis techniques, Green = Meyer wavelet, Orange = Instantly maximal wavelet skeleton spectra, Magenta = Periodram and Linear phase finite impulse response.

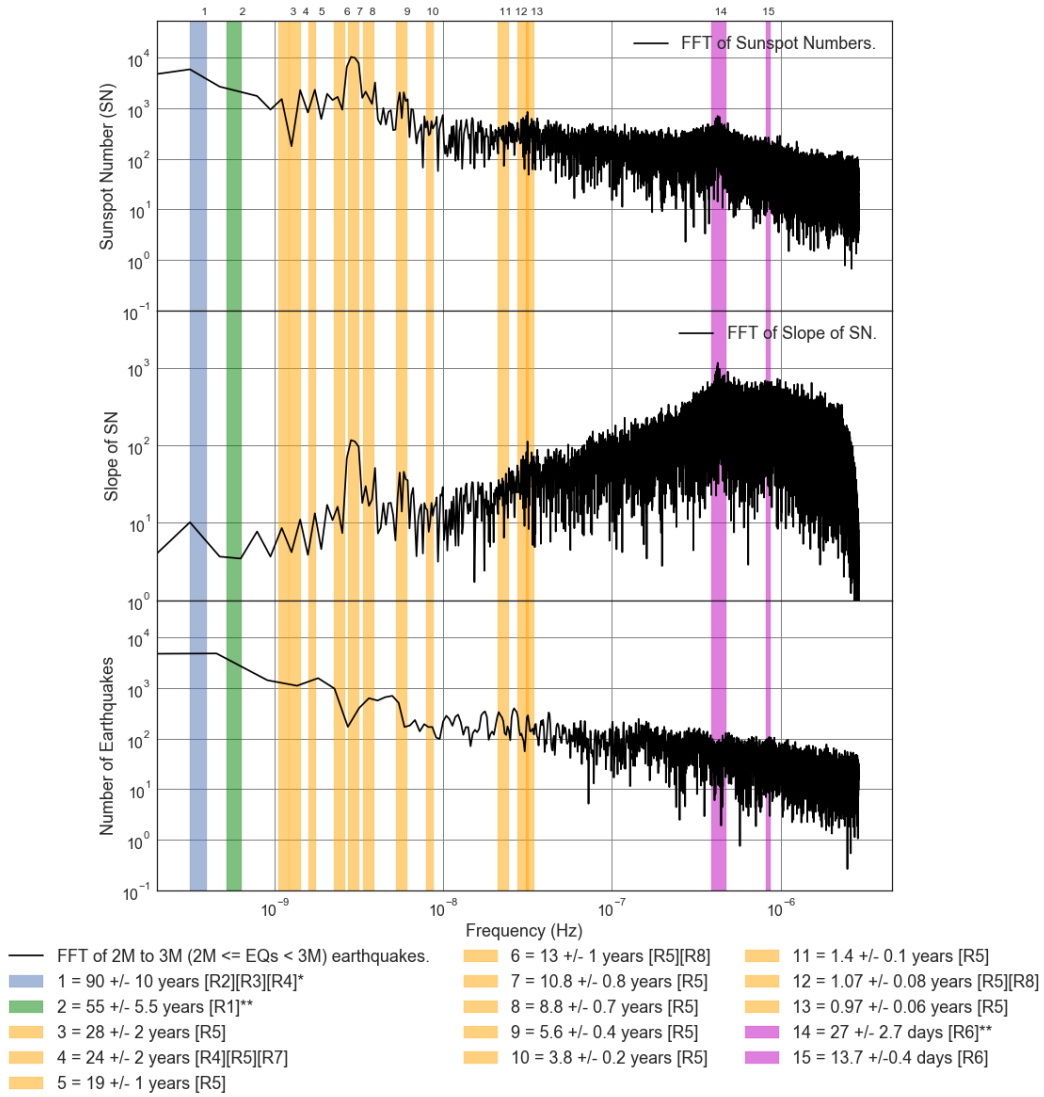

Figure E1.11: FFT Loglog Comparison Plot of number of Averaged 2M to 3M (2M <= EQs < 3M) Earthquakes, Sunspot number (SN) and slope from 1818 to 2017. Additional meaning of the legend colors: Blue = Various Analysis techniques, Green = Meyer wavelet, Orange = Instantly maximal wavelet skeleton spectra, Magenta = Periodram and Linear phase finite impulse response.

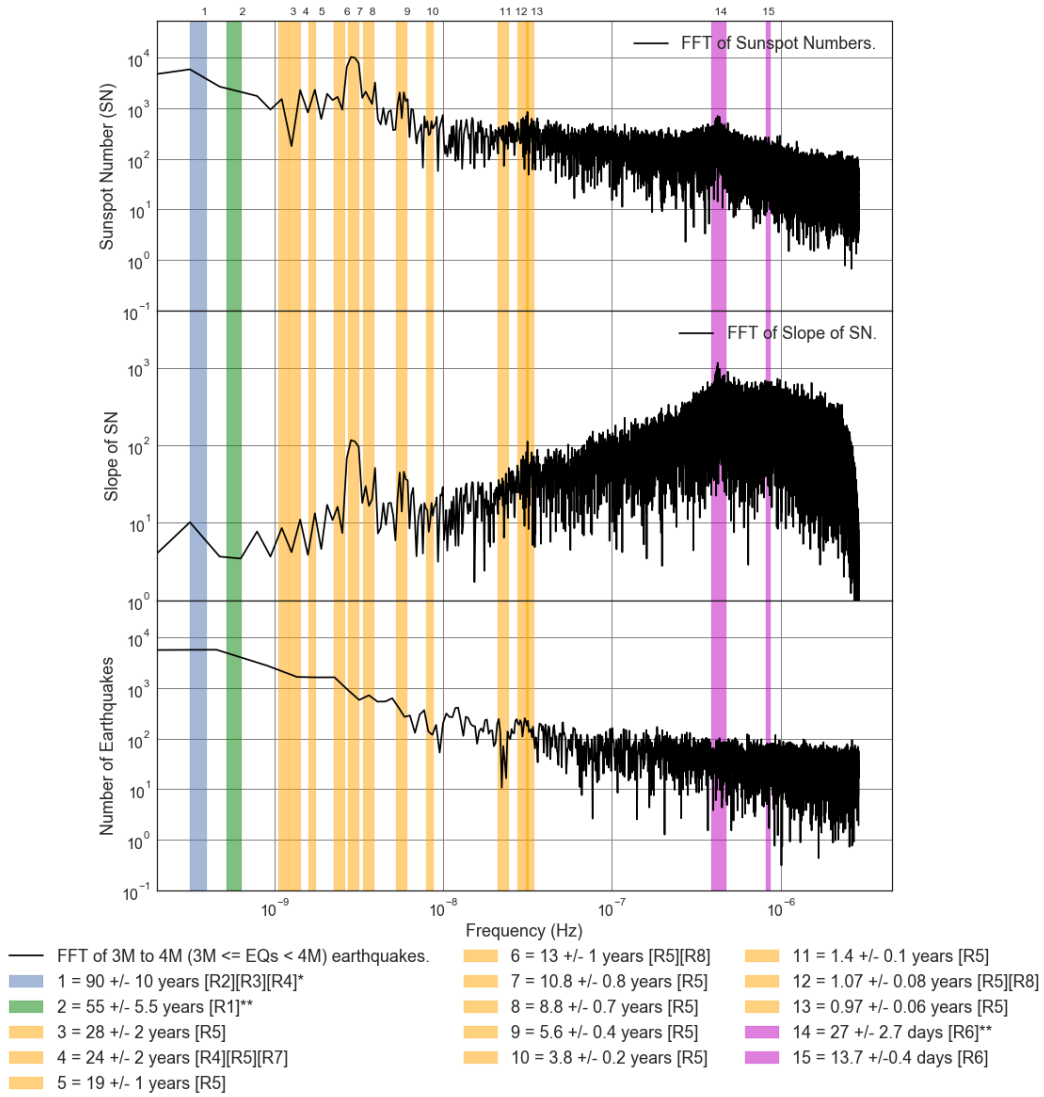

Figure E1.12: FFT Loglog Comparison Plot of number of Averaged 3M to 4M (3M <= EQs < 4M) Earthquakes, Sunspot number (SN) and slope from 1818 to 2017. Additional meaning of the legend colors: Blue = Various Analysis techniques, Green = Meyer wavelet, Orange = Instantly maximal wavelet skeleton spectra, Magenta = Periodram and Linear phase finite impulse response.

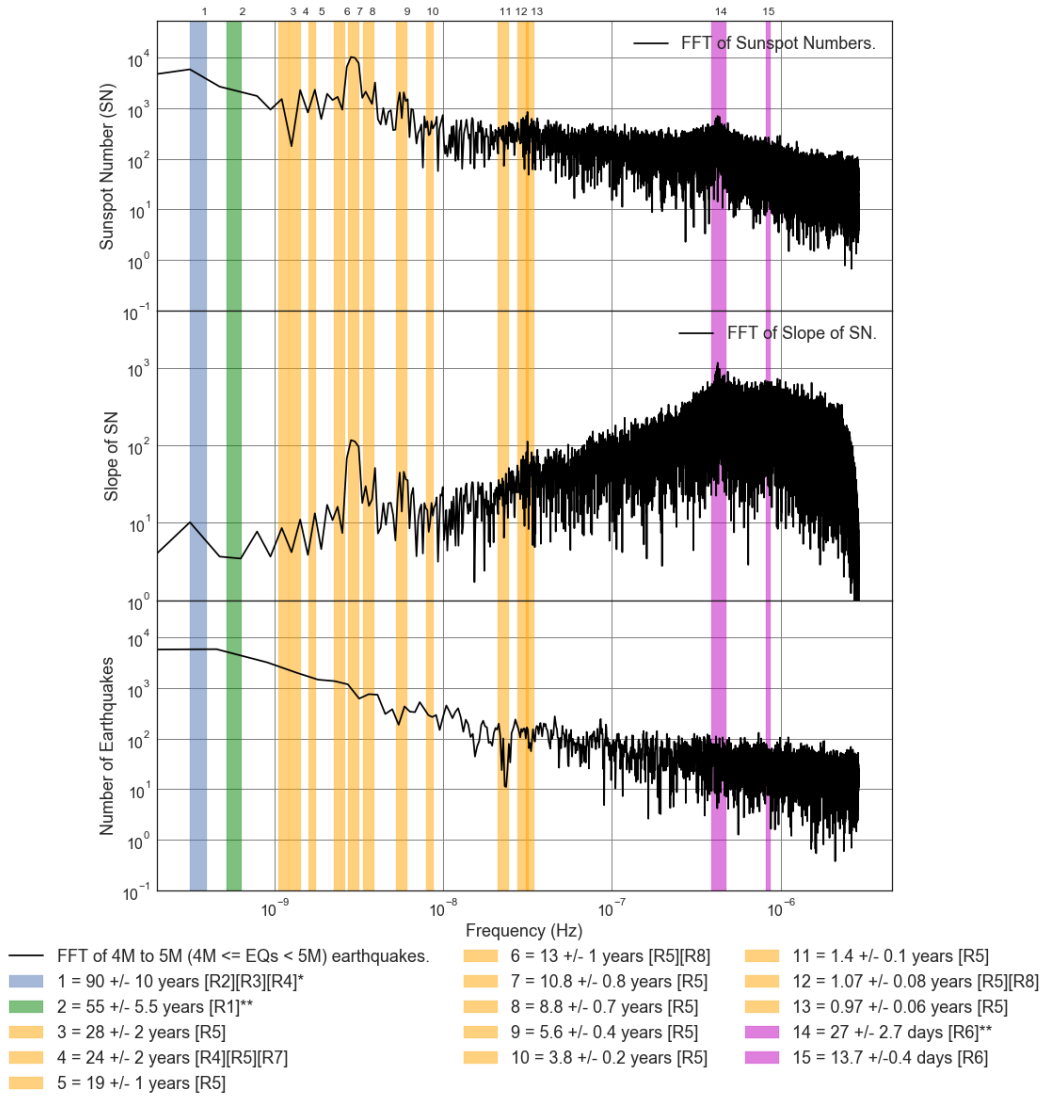

Figure E1.13: FFT Loglog Comparison Plot of number of Averaged 4M to 5M (4M <= EQs < 5M) Earthquakes, Sunspot number (SN) and slope from 1818 to 2017. Additional meaning of the legend colors: Blue = Various Analysis techniques, Green = Meyer wavelet, Orange = Instantly maximal wavelet skeleton spectra, Magenta = Periodram and Linear phase finite impulse response.

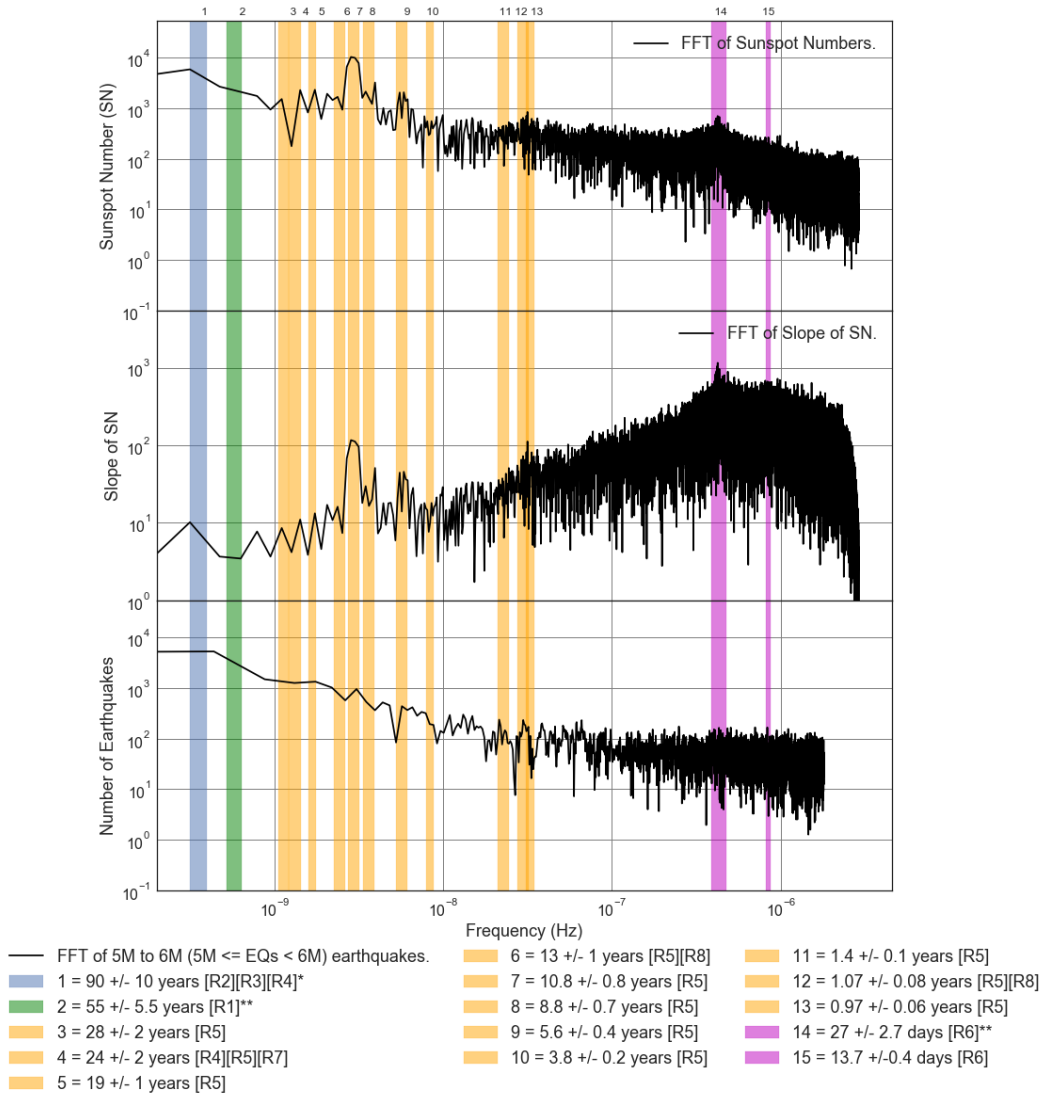

Figure E1.14: FFT Loglog Comparison Plot of number of Averaged 5M to 6M (5M <= EQs < 6M) Earthquakes, Sunspot number (SN) and slope from 1818 to 2017. Additional meaning of the legend colors: Blue = Various Analysis techniques, Green = Meyer wavelet, Orange = Instantly maximal wavelet skeleton spectra, Magenta = Periodram and Linear phase finite impulse response.

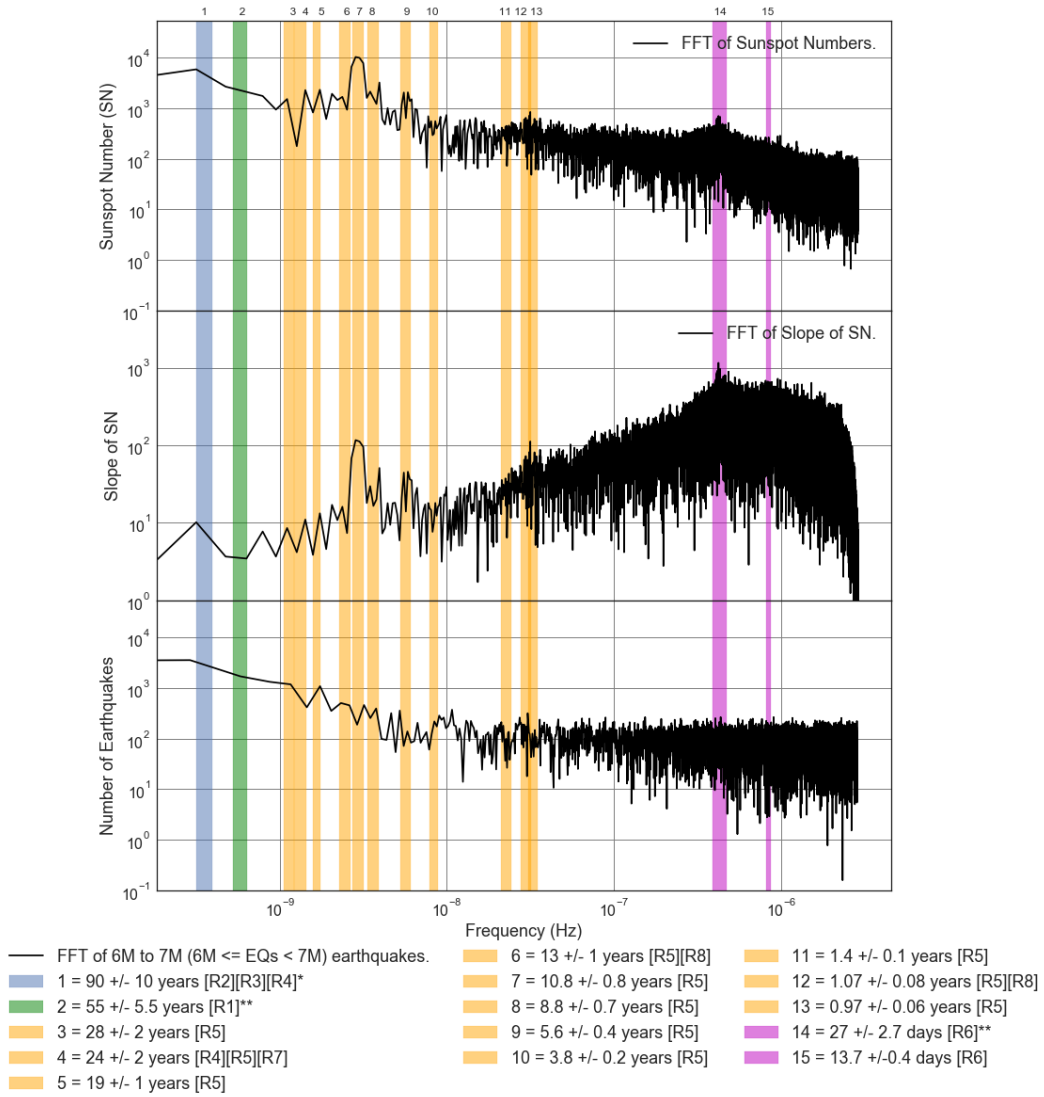

Figure E1.15: FFT Loglog Comparison Plot of number of Averaged 6M to 7M (6M <= EQs < 7M) Earthquakes, Sunspot number (SN) and slope from 1818 to 2017. Additional meaning of the legend colors: Blue = Various Analysis techniques, Green = Meyer wavelet, Orange = Instantly maximal wavelet skeleton spectra, Magenta = Periodram and Linear phase finite impulse response.

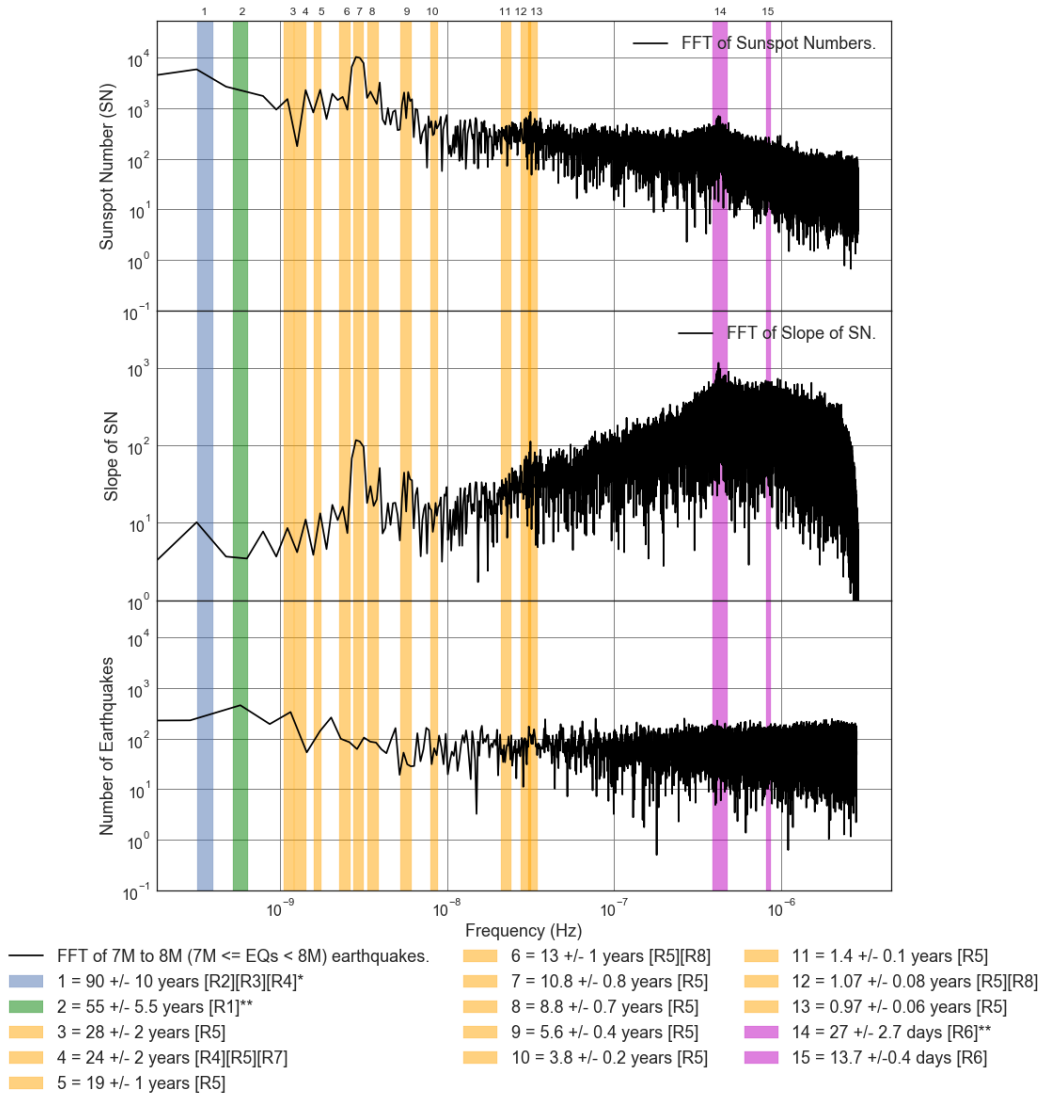

Figure E1.16: FFT Loglog Comparison Plot of number of Averaged 7M to 8M (7M <= EQs < 8M) Earthquakes, Sunspot number (SN) and slope from 1818 to 2017. Additional meaning of the legend colors: Blue = Various Analysis techniques, Green = Meyer wavelet, Orange = Instantly maximal wavelet skeleton spectra, Magenta = Periodram and Linear phase finite impulse response.

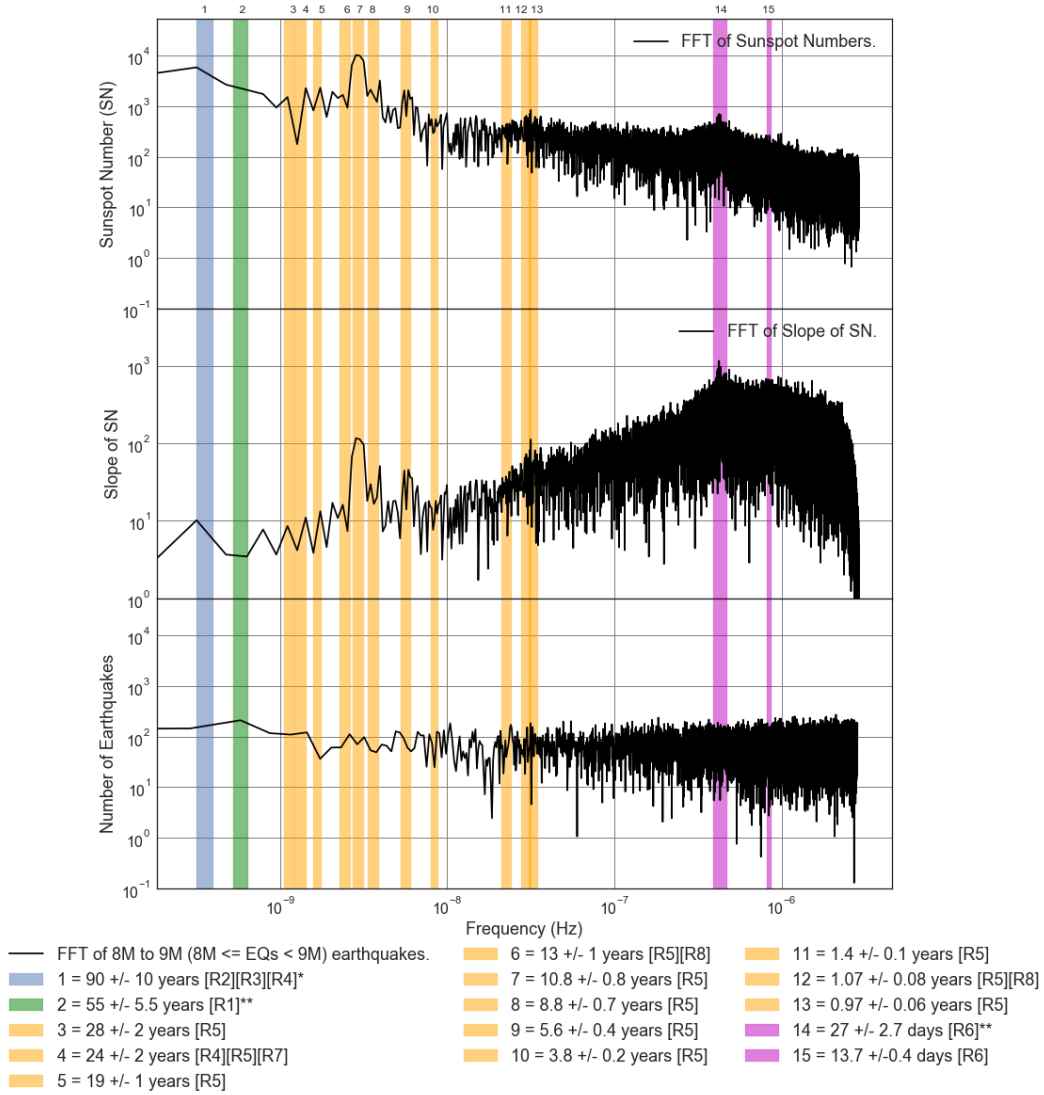

Figure E1.17: FFT Loglog Comparison Plot of number of Averaged 8M to 9M (8M <= EQs < 9M) Earthquakes, Sunspot number (SN) and slope from 1818 to 2017. Additional meaning of the legend colors: Blue = Various Analysis techniques, Green = Meyer wavelet, Orange = Instantly maximal wavelet skeleton spectra, Magenta = Periodram and Linear phase finite impulse response.

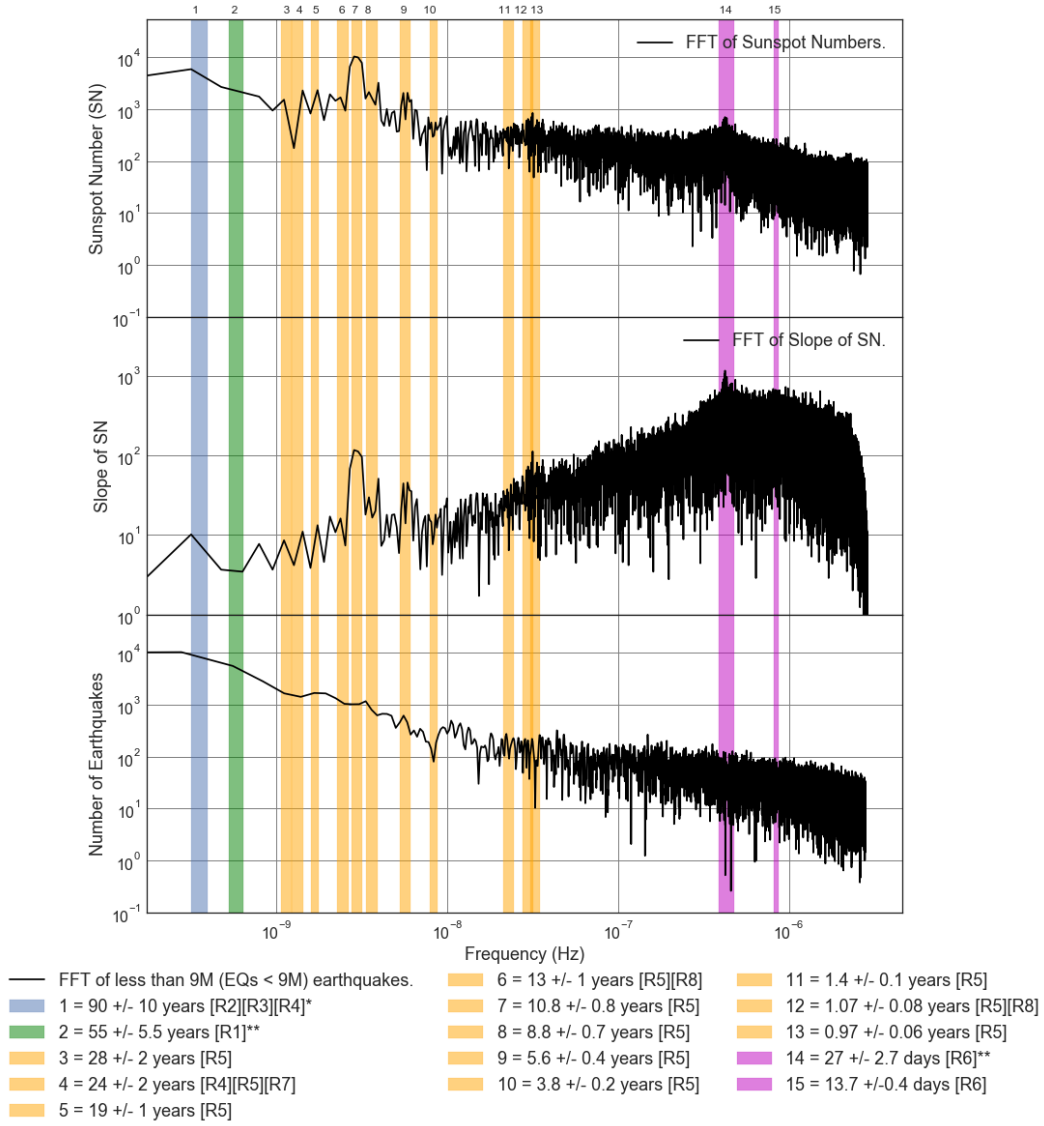

Figure E1.18: FFT Loglog Comparison Plot of number of Averaged less than 9M (EQs < 9M) Earthquakes, Sunspot number (SN) and slope from 1818 to 2017. Additional meaning of the legend colors: Blue = Various Analysis techniques, Green = Meyer wavelet, Orange = Instantly maximal wavelet skeleton spectra, Magenta = Periodram and Linear phase finite impulse response.

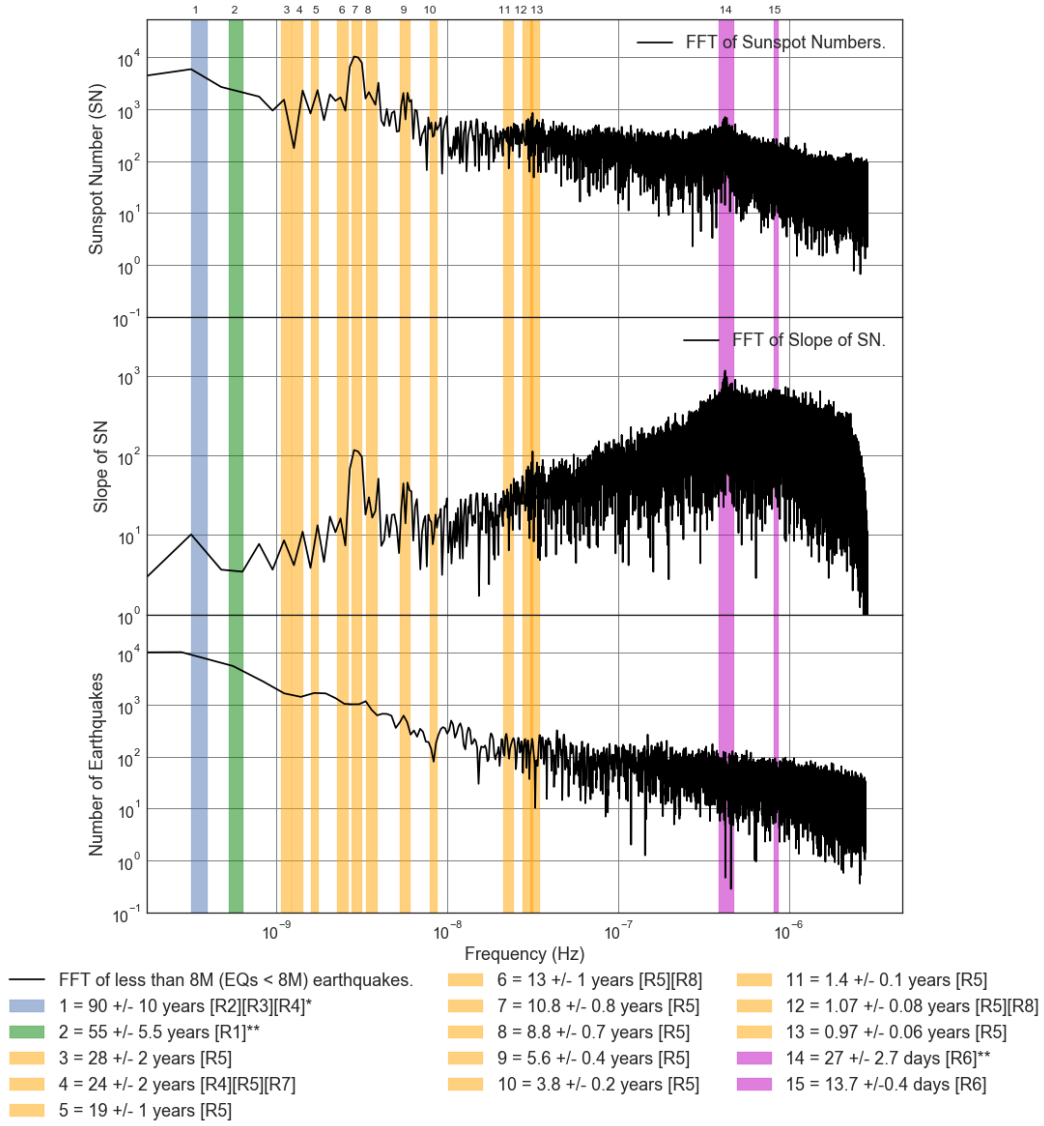

Figure E1.19: FFT Loglog Comparison Plot of number of Averaged less than 8M (EQs < 8M) Earthquakes, Sunspot number (SN) and slope from 1818 to 2017. Additional meaning of the legend colors: Blue = Various Analysis techniques, Green = Meyer wavelet, Orange = Instantly maximal wavelet skeleton spectra, Magenta = Periodram and Linear phase finite impulse response.

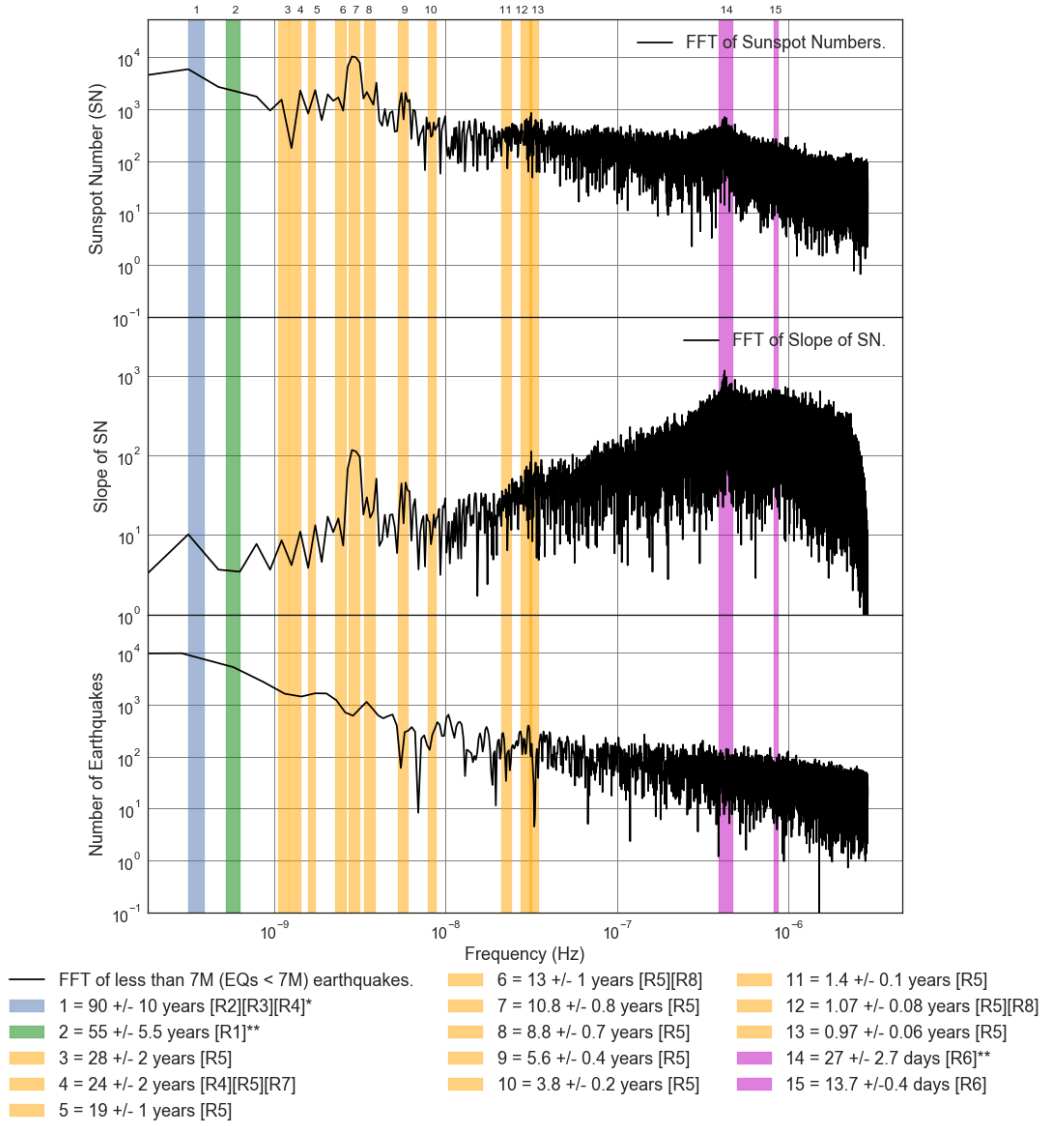

Figure E1.20: FFT Loglog Comparison Plot of number of Averaged less than 7M (EQs < 7M) Earthquakes, Sunspot number (SN) and slope from 1818 to 2017. Additional meaning of the legend colors: Blue = Various Analysis techniques, Green = Meyer wavelet, Orange = Instantly maximal wavelet skeleton spectra, Magenta = Periodram and Linear phase finite impulse response.

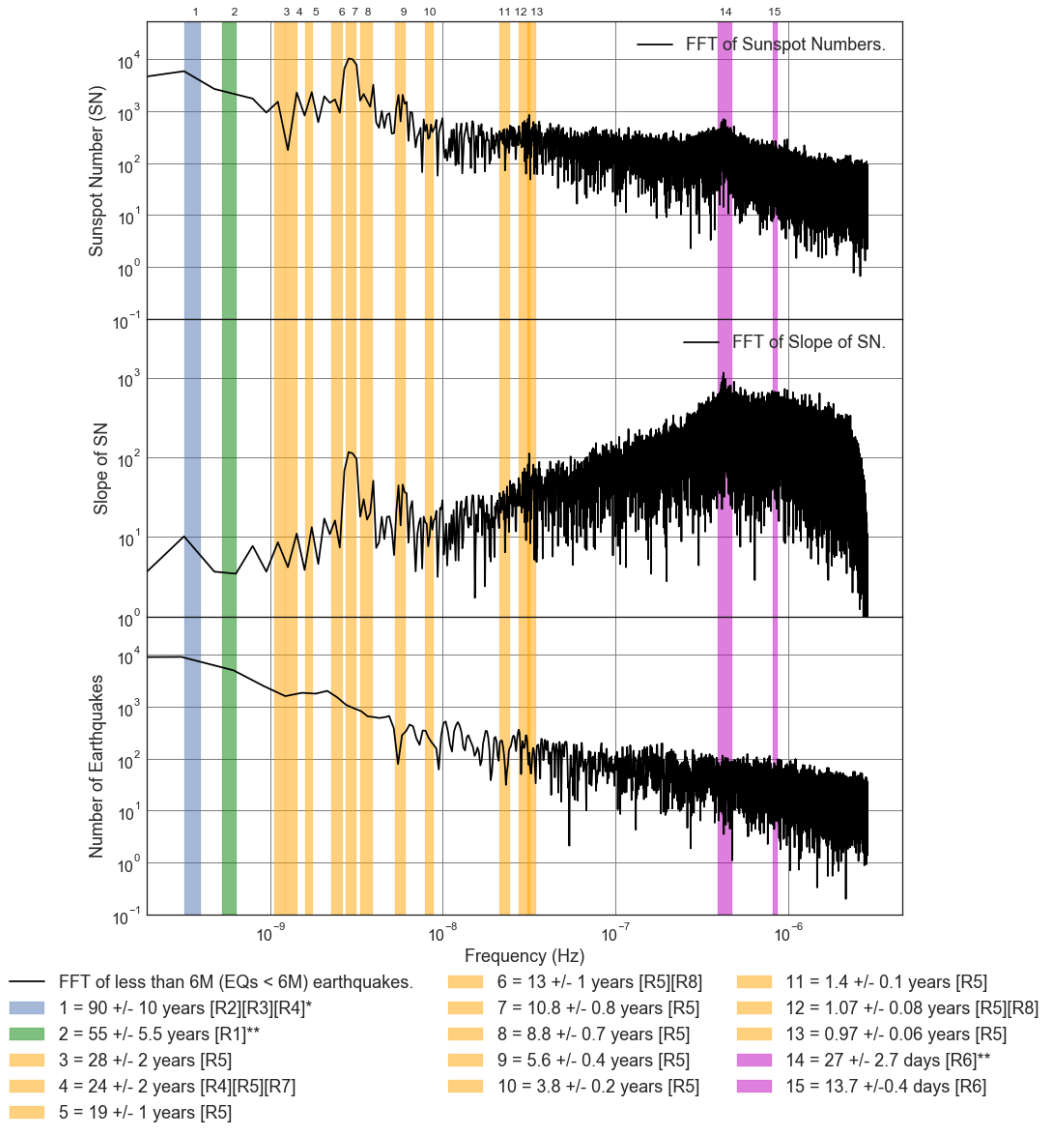

Figure E1.21: FFT Loglog Comparison Plot of number of Averaged less than 6M (EQs < 6M) Earthquakes, Sunspot number (SN) and slope from 1818 to 2017. Additional meaning of the legend colors: Blue = Various Analysis techniques, Green = Meyer wavelet, Orange = Instantly maximal wavelet skeleton spectra, Magenta = Periodram and Linear phase finite impulse response.

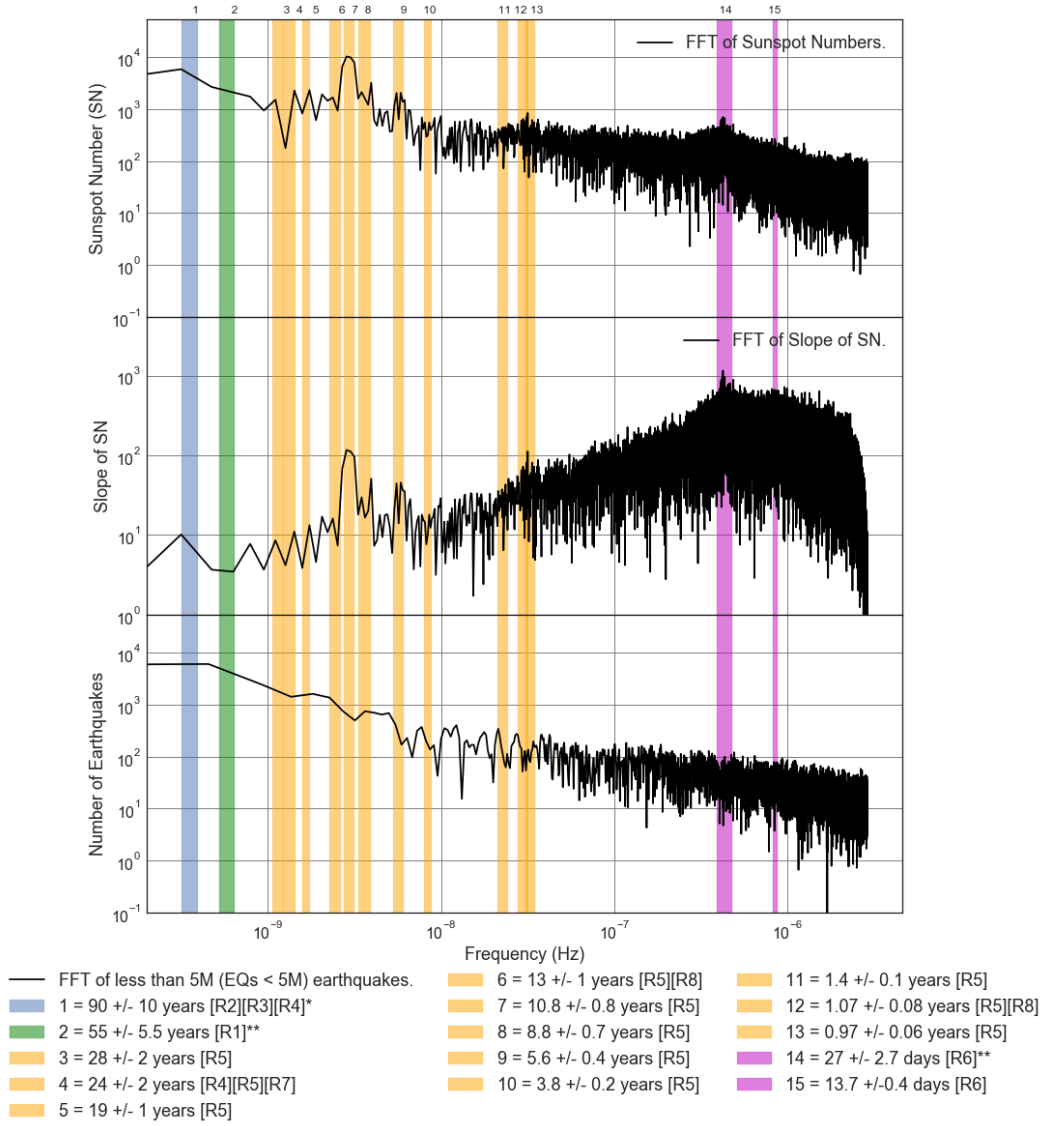

Figure E1.22: FFT Loglog Comparison Plot of number of Averaged less than 5M (EQs < 5M) Earthquakes, Sunspot number (SN) and slope from 1818 to 2017. Additional meaning of the legend colors: Blue = Various Analysis techniques, Green = Meyer wavelet, Orange = Instantly maximal wavelet skeleton spectra, Magenta = Periodram and Linear phase finite impulse response.

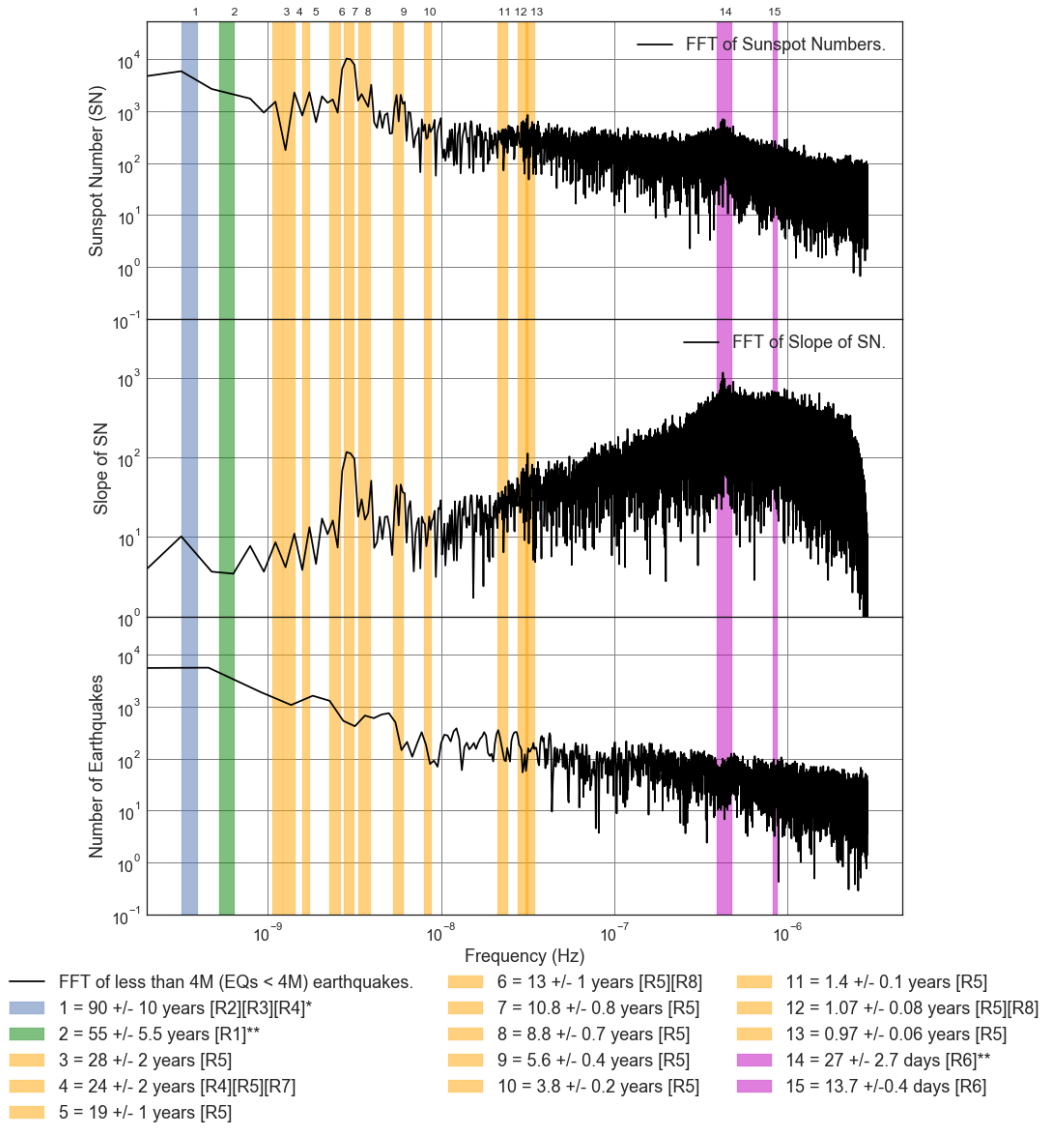

Figure E1.23: FFT Loglog Comparison Plot of number of Averaged less than 4M (EQs < 4M) Earthquakes, Sunspot number (SN) and slope from 1818 to 2017. Additional meaning of the legend colors: Blue = Various Analysis techniques, Green = Meyer wavelet, Orange = Instantly maximal wavelet skeleton spectra, Magenta = Periodram and Linear phase finite impulse response.

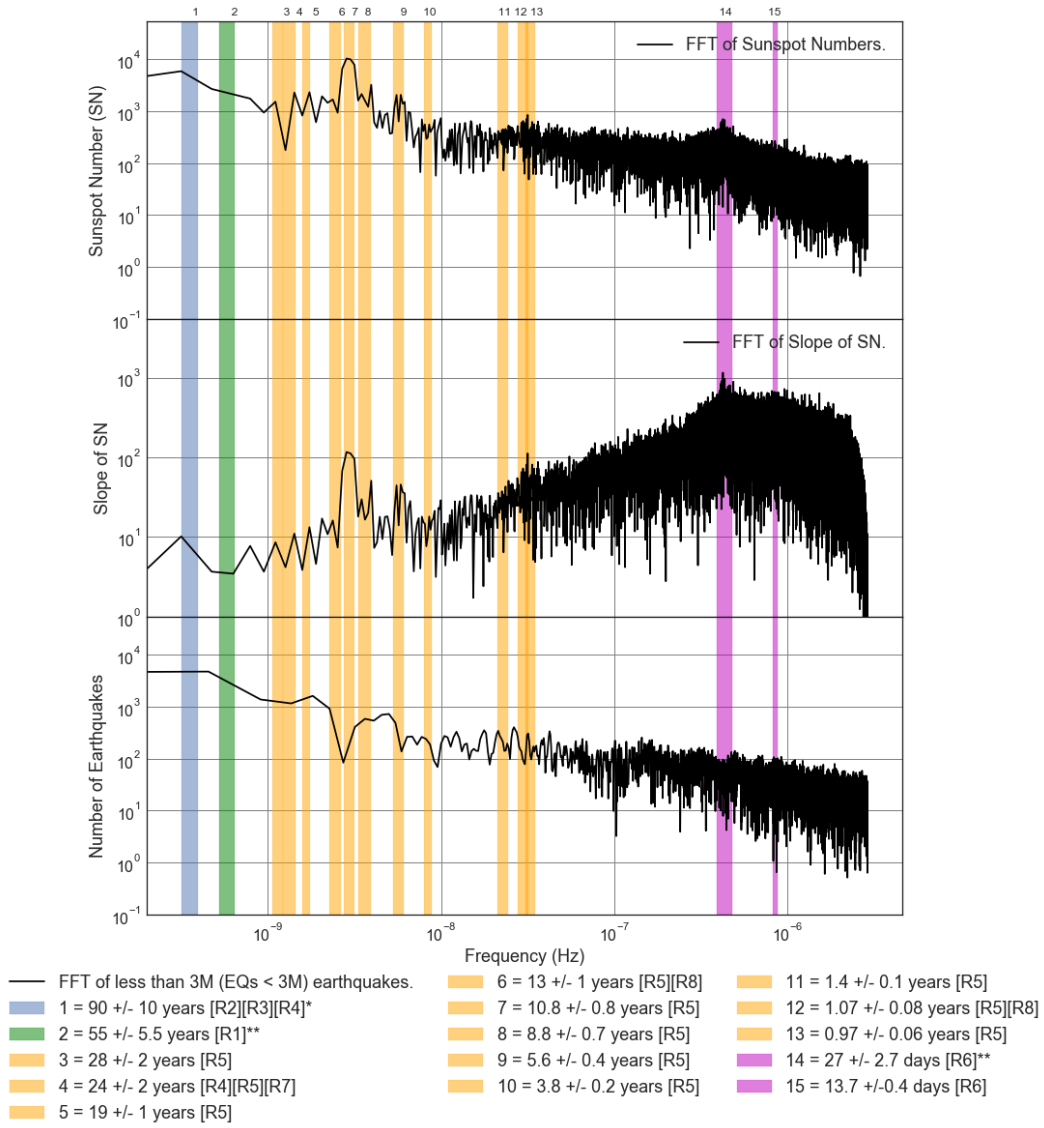

Figure E1.24: FFT Loglog Comparison Plot of number of Averaged less than 3M (EQs < 3M) Earthquakes, Sunspot number (SN) and slope from 1818 to 2017. Additional meaning of the legend colors: Blue = Various Analysis techniques, Green = Meyer wavelet, Orange = Instantly maximal wavelet skeleton spectra, Magenta = Periodram and Linear phase finite impulse response.

Comparison Plots of Averaged FFT Earthquake Spectra for Earthquake Energy Released

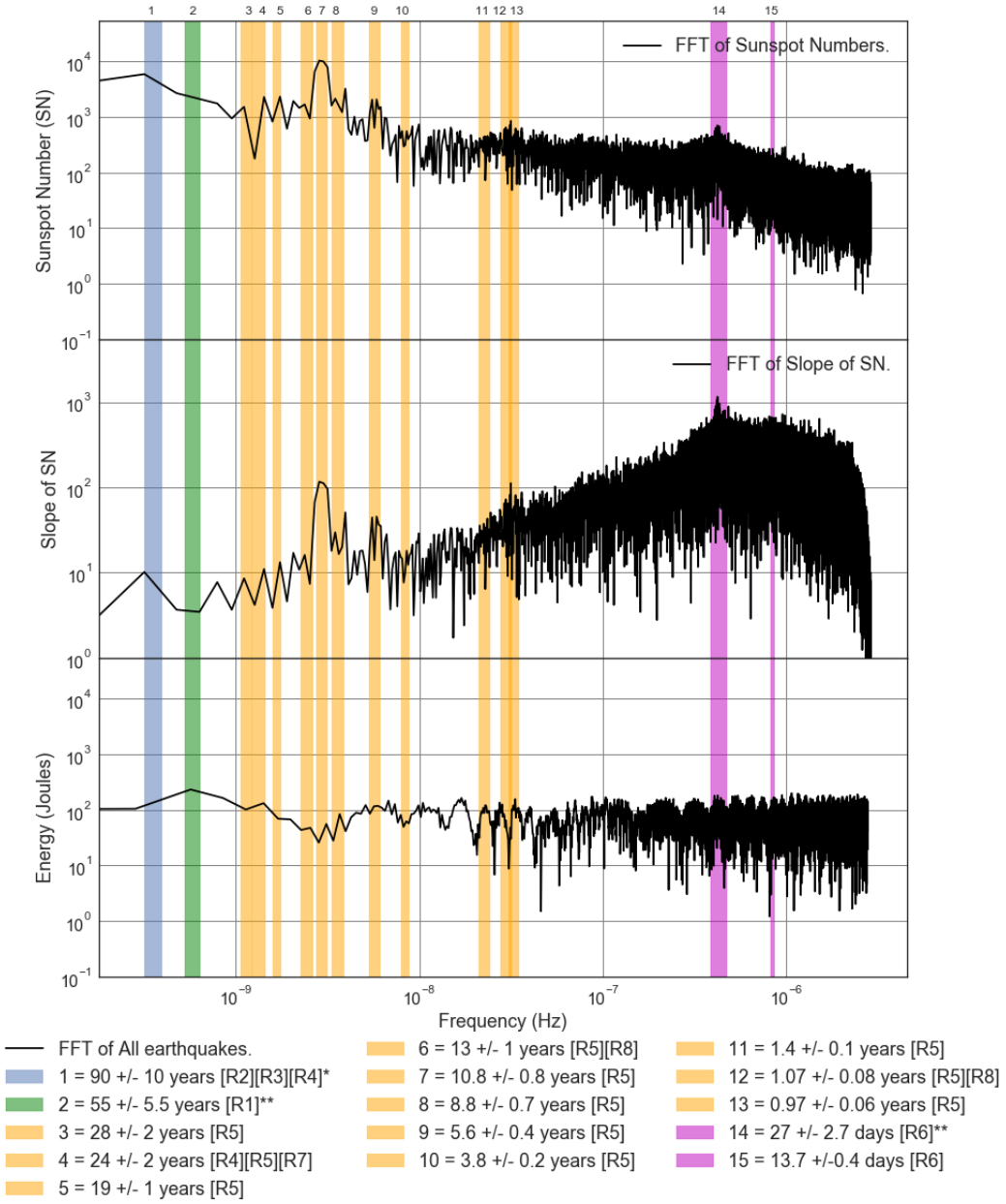

Figure E1.25: FFT Loglog Comparison Plot of Averaged All Earthquake (EQ) total energy released, 2 Day Sunspot number and slope from 1818 to 2017. Additional meaning of the legend colors: Blue = Various Analysis techniques, Green = Meyer wavelet, Orange = Instantly maximal wavelet skeleton spectra, Magenta = Periodram and Linear phase finite impulse response.

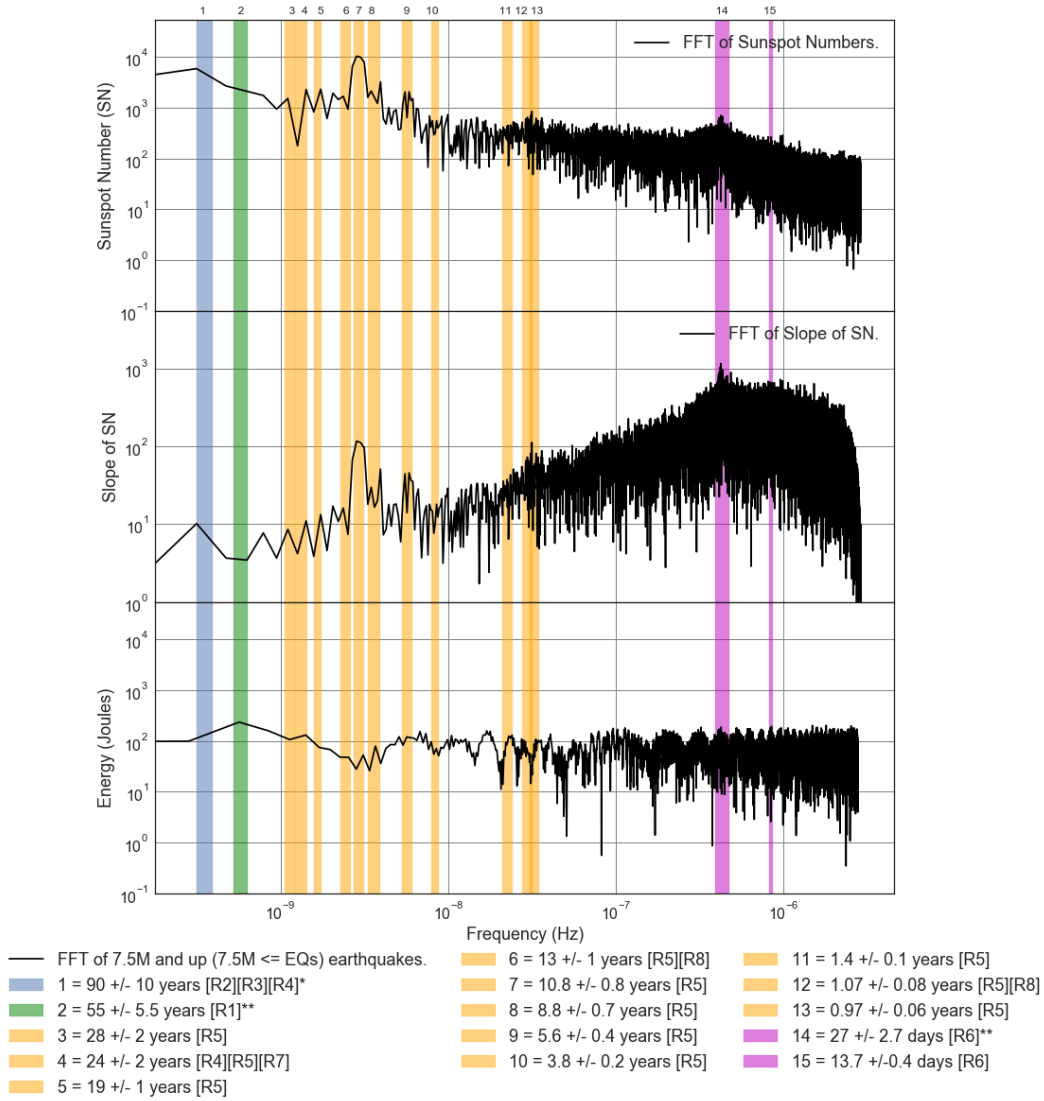

Figure E1.26: FFT Loglog Comparison Plot of Averaged 7.5M and up (7.5M <= EQs) Earthquake (EQ) total energy released, 2 Day Sunspot number and slope from 1818 to 2017. Additional meaning of the legend colors: Blue = Various Analysis techniques, Green = Meyer wavelet, Orange = Instantly maximal wavelet skeleton spectra, Magenta = Periodram and Linear phase finite impulse response.

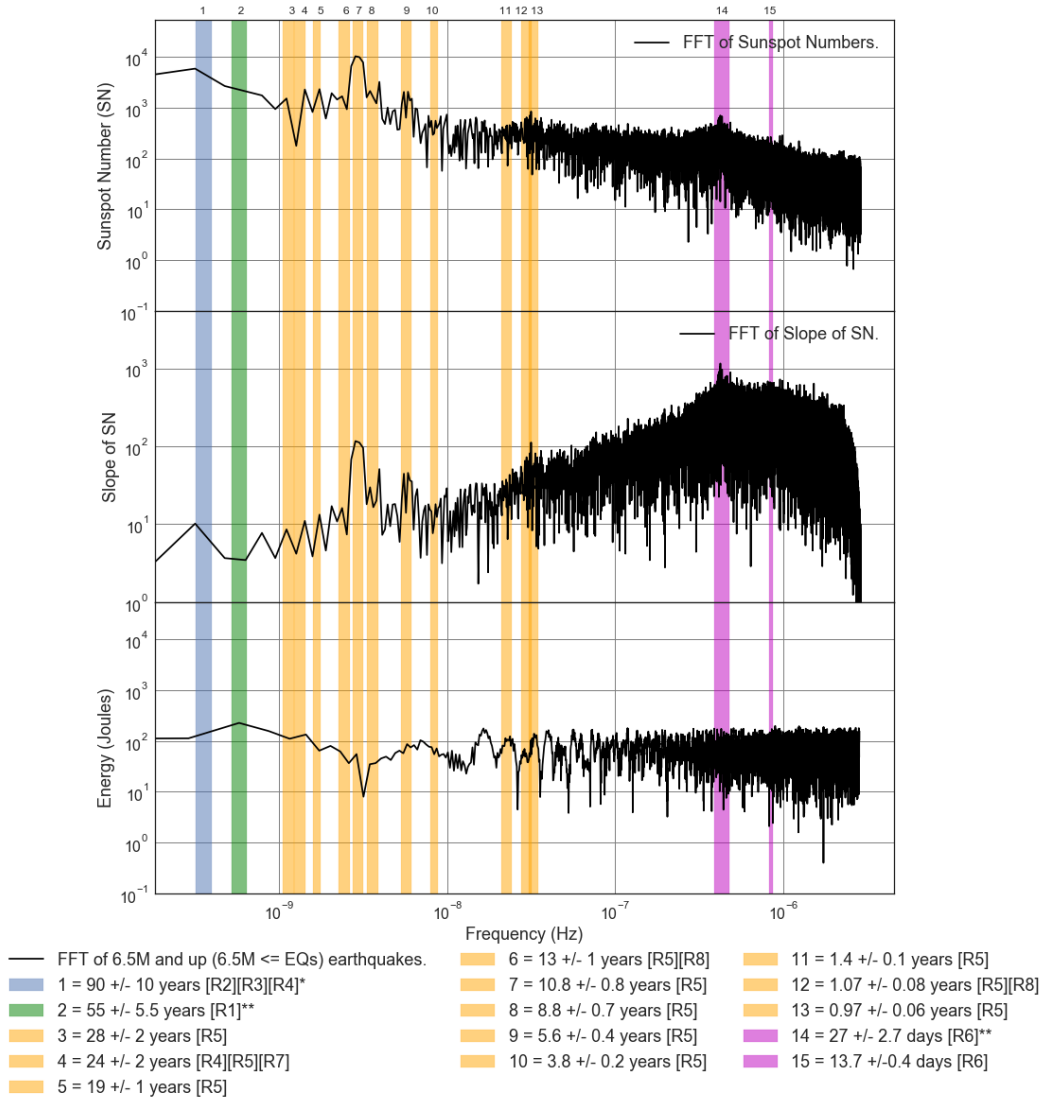

Figure E1.27: FFT Loglog Comparison Plot of Averaged 6.5M and up (6.5M <= EQs) Earthquake (EQ) total energy released, 2 Day Sunspot number and slope from 1818 to 2017. Additional meaning of the legend colors: Blue = Various Analysis techniques, Green = Meyer wavelet, Orange = Instantly maximal wavelet skeleton spectra, Magenta = Periodram and Linear phase finite impulse response.

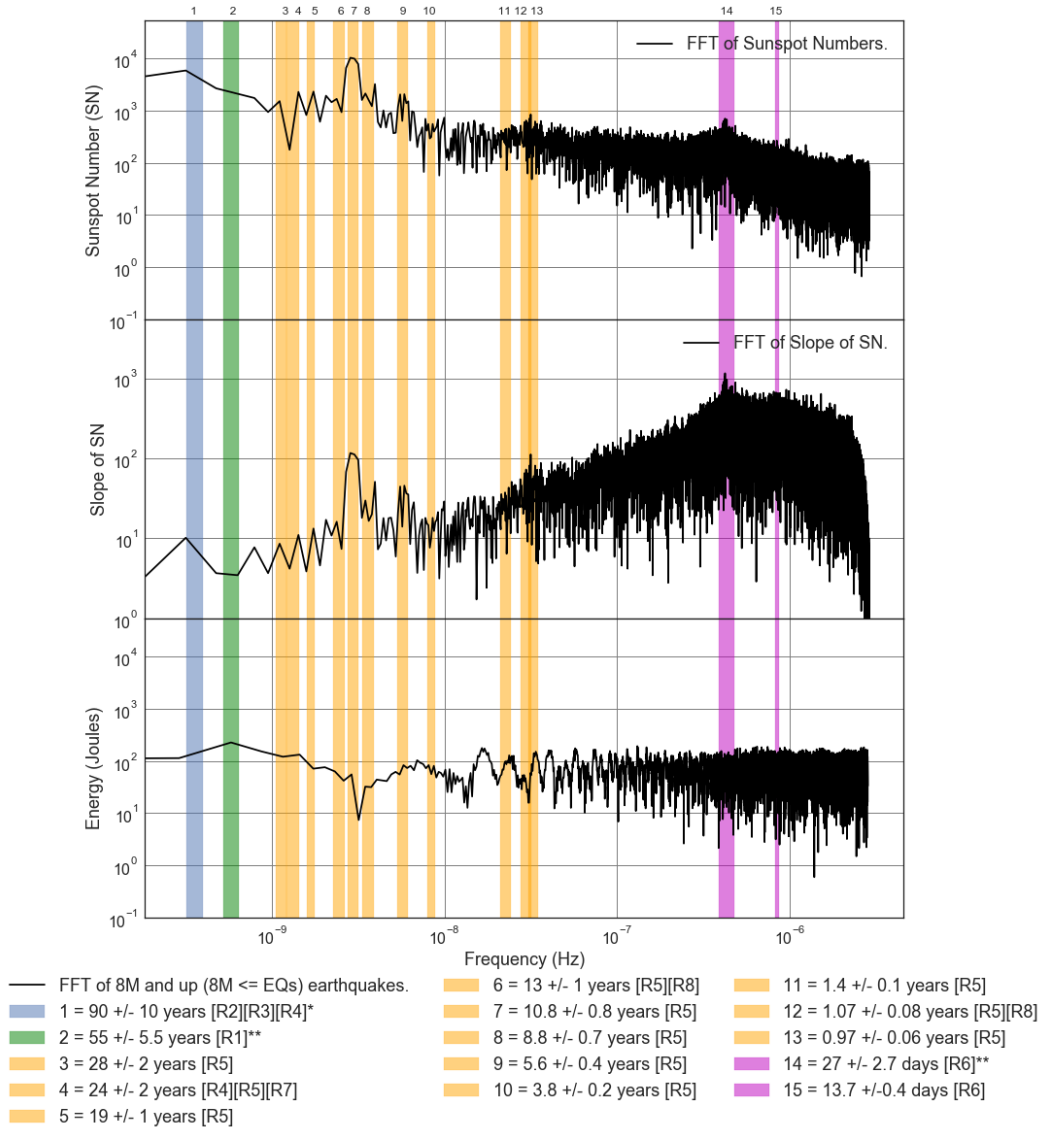

Figure E1.28: FFT Loglog Comparison Plot of Averaged 8M and up (8M <= EQs) Earthquake (EQ) total energy released, 2 Day Sunspot number and slope from 1818 to 2017. Additional meaning of the legend colors: Blue = Various Analysis techniques, Green = Meyer wavelet, Orange = Instantly maximal wavelet skeleton spectra, Magenta = Periodram and Linear phase finite impulse response.

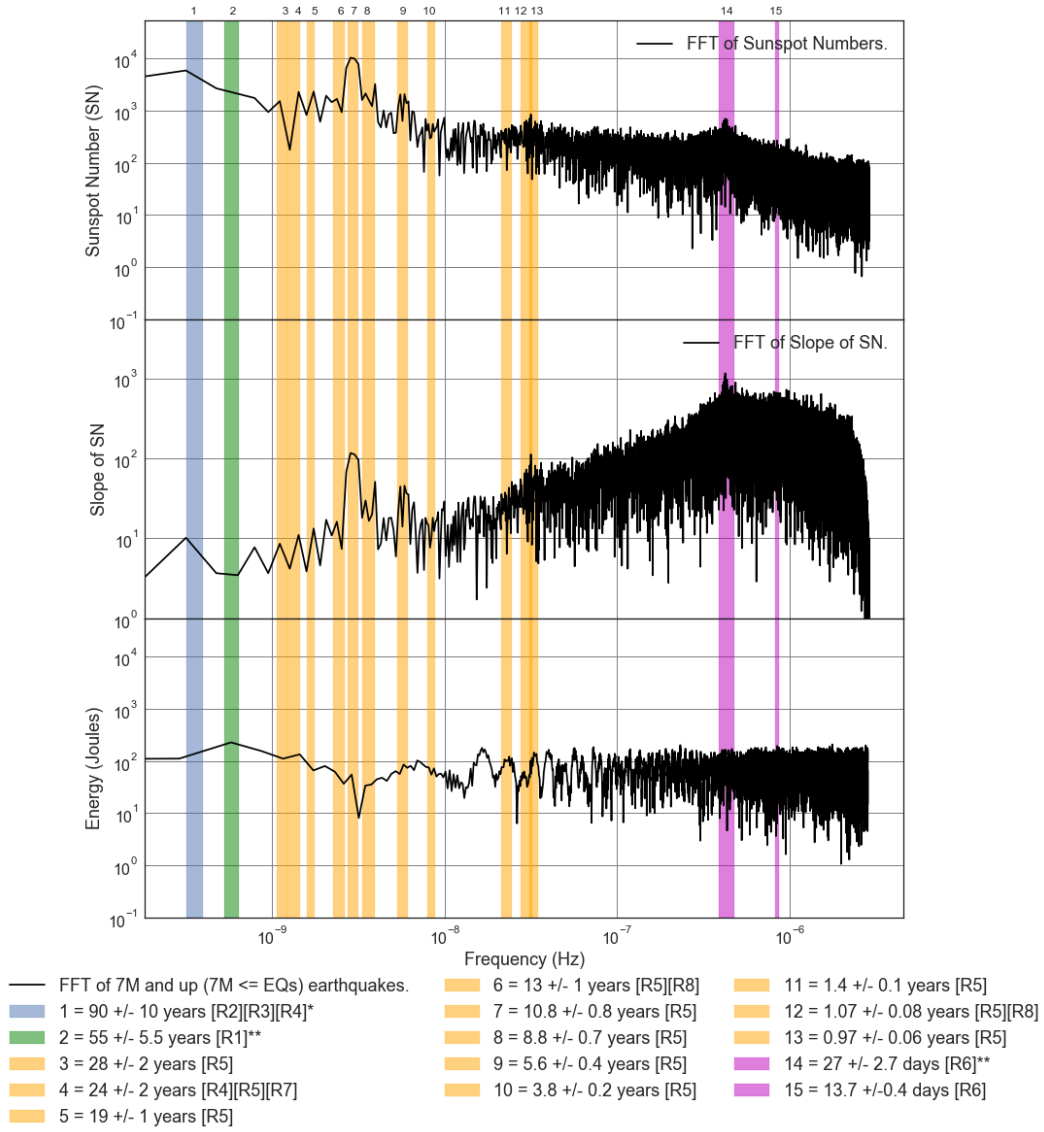

Figure E1.29: FFT Loglog Comparison Plot of Averaged 7M and up (7M <= EQs) Earthquake (EQ) total energy released, 2 Day Sunspot number and slope from 1818 to 2017. Additional meaning of the legend colors: Blue = Various Analysis techniques, Green = Meyer wavelet, Orange = Instantly maximal wavelet skeleton spectra, Magenta = Periodram and Linear phase finite impulse response.

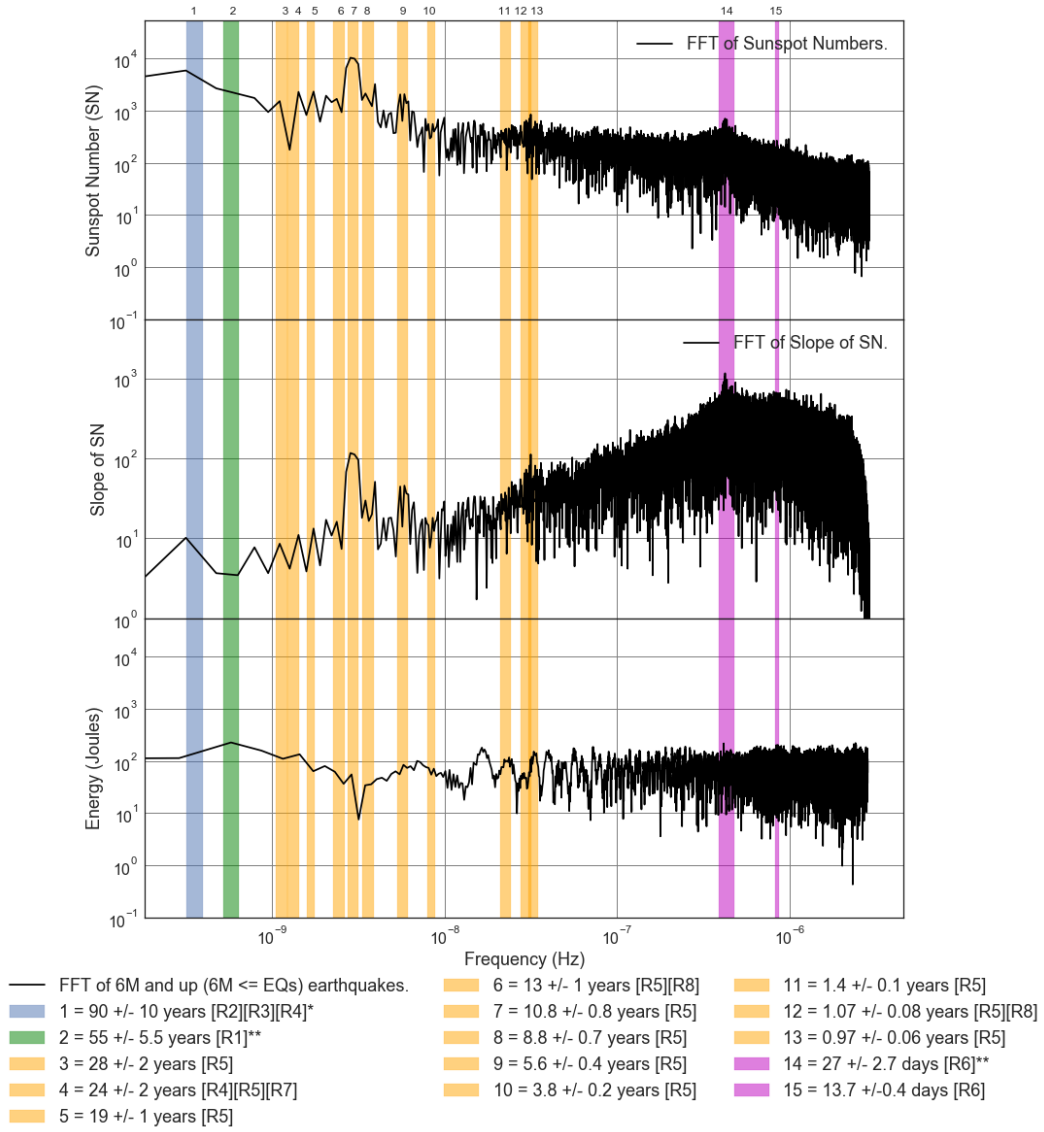

Figure E1.30: FFT Loglog Comparison Plot of Averaged 6M and up (6M <= EQs) Earthquake (EQ) total energy released, 2 Day Sunspot number and slope from 1818 to 2017. Additional meaning of the legend colors: Blue = Various Analysis techniques, Green = Meyer wavelet, Orange = Instantly maximal wavelet skeleton spectra, Magenta = Periodram and Linear phase finite impulse response.

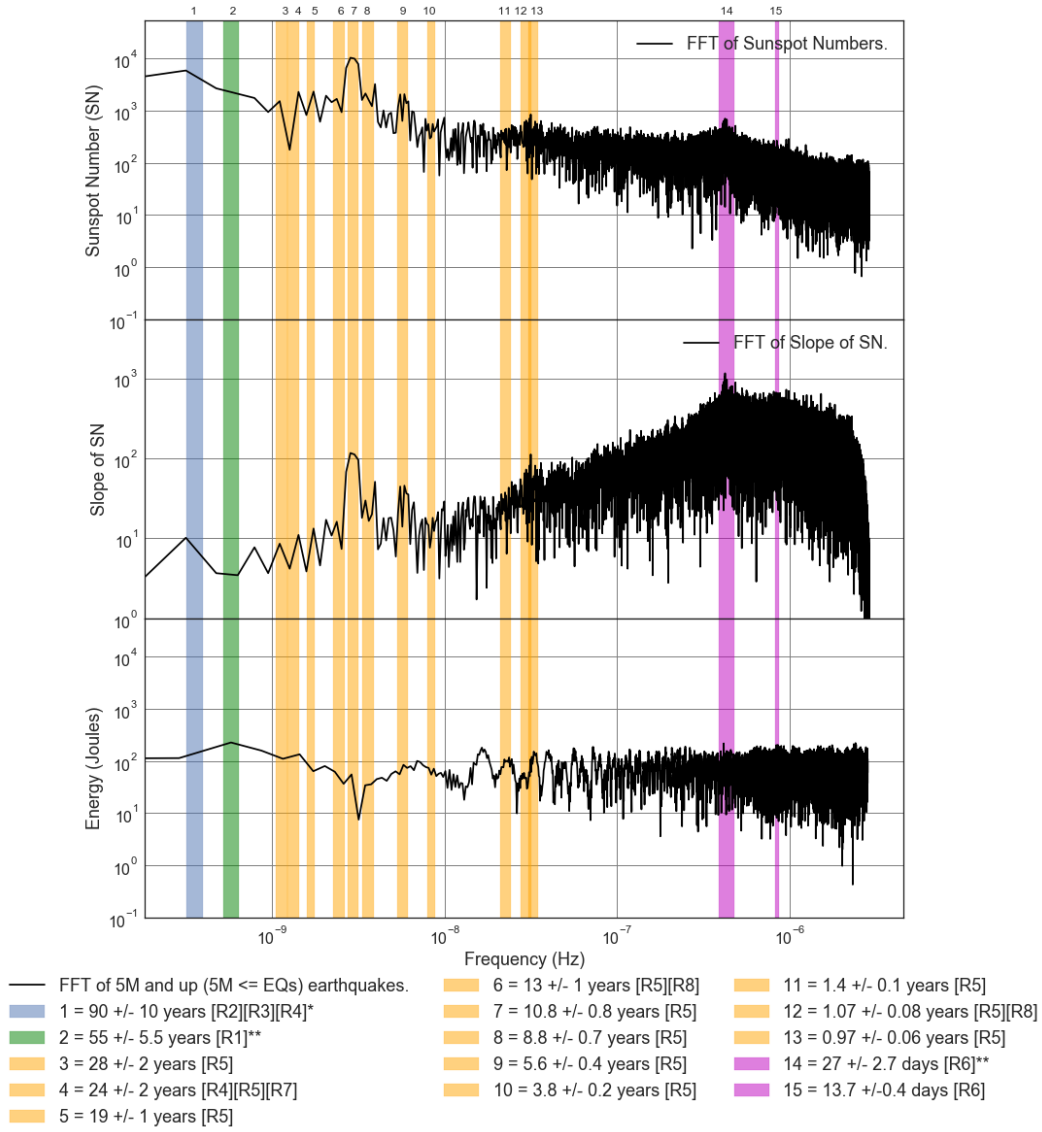

Figure E1.31: FFT Loglog Comparison Plot of Averaged 5M and up (5M <= EQs) Earthquake (EQ) total energy released, 2 Day Sunspot number and slope from 1818 to 2017. Additional meaning of the legend colors: Blue = Various Analysis techniques, Green = Meyer wavelet, Orange = Instantly maximal wavelet skeleton spectra, Magenta = Periodram and Linear phase finite impulse response.

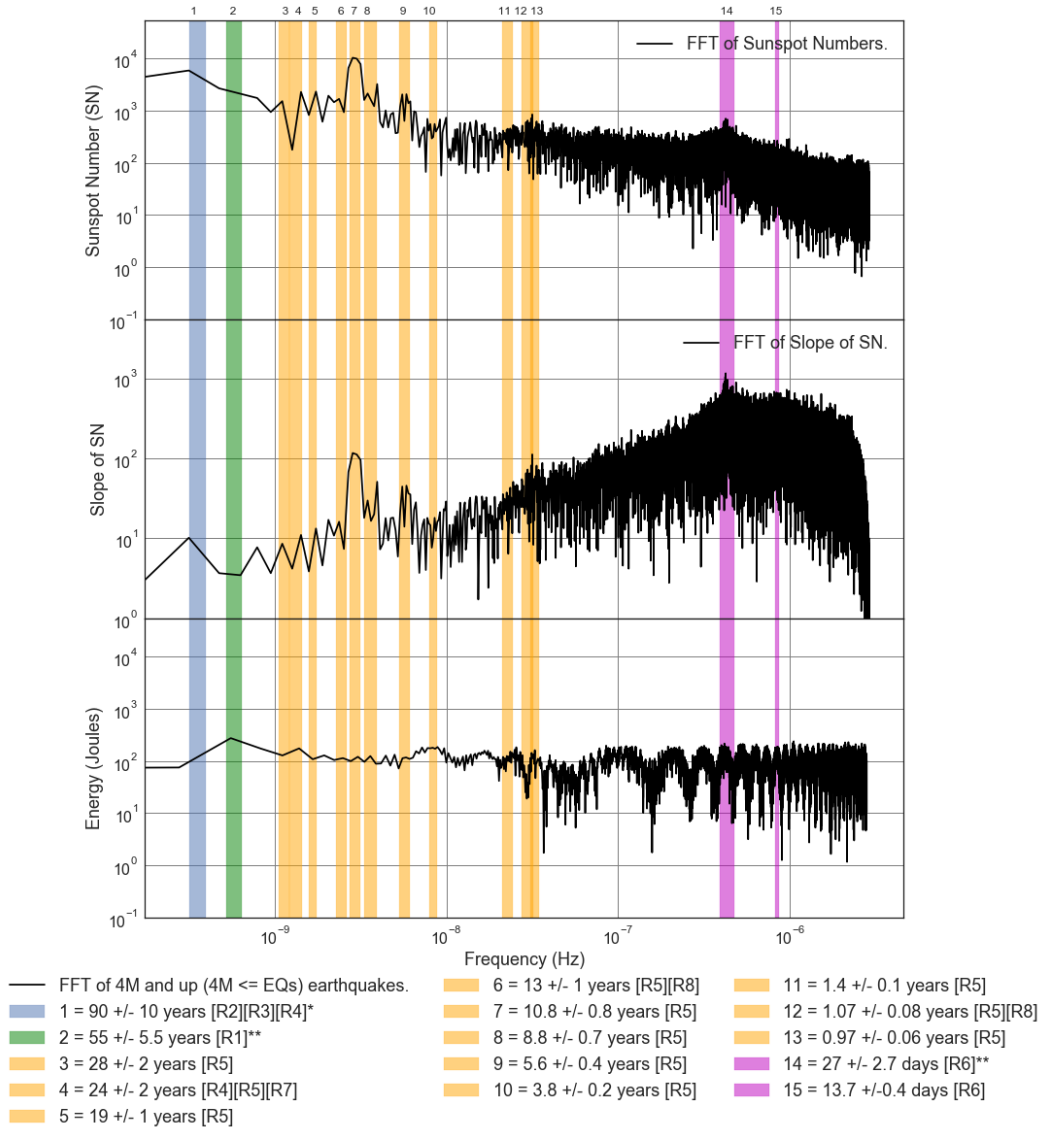

Figure E1.32: FFT Loglog Comparison Plot of Averaged 4M and up (4M <= EQs) Earthquake (EQ) total energy released, 2 Day Sunspot number and slope from 1818 to 2017. Additional meaning of the legend colors: Blue = Various Analysis techniques, Green = Meyer wavelet, Orange = Instantly maximal wavelet skeleton spectra, Magenta = Periodram and Linear phase finite impulse response.

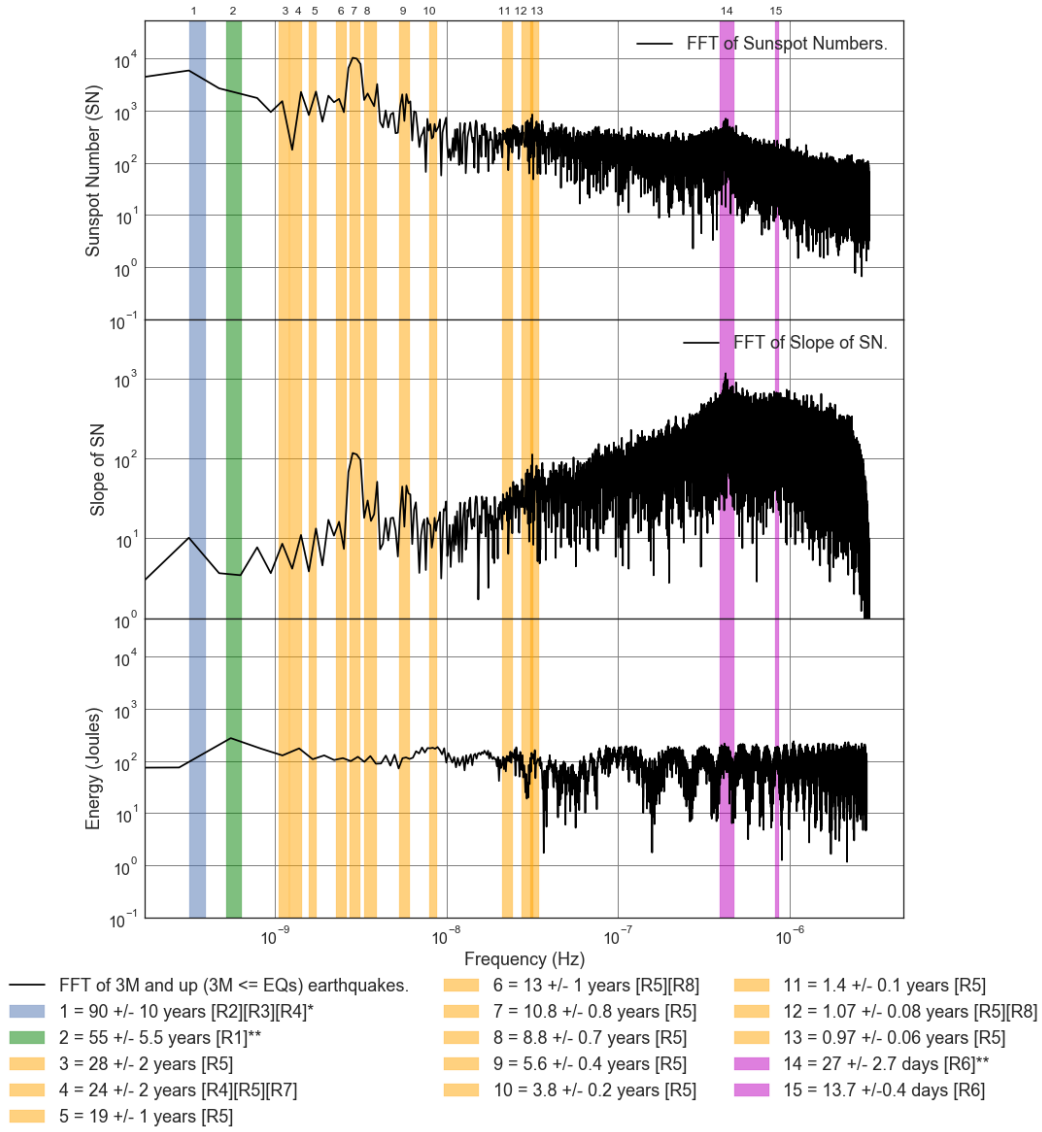

Figure E1.33: FFT Loglog Comparison Plot of Averaged 3M and up (3M <= EQs) Earthquake (EQ) total energy released, 2 Day Sunspot number and slope from 1818 to 2017. Additional meaning of the legend colors: Blue = Various Analysis techniques, Green = Meyer wavelet, Orange = Instantly maximal wavelet skeleton spectra, Magenta = Periodram and Linear phase finite impulse response.

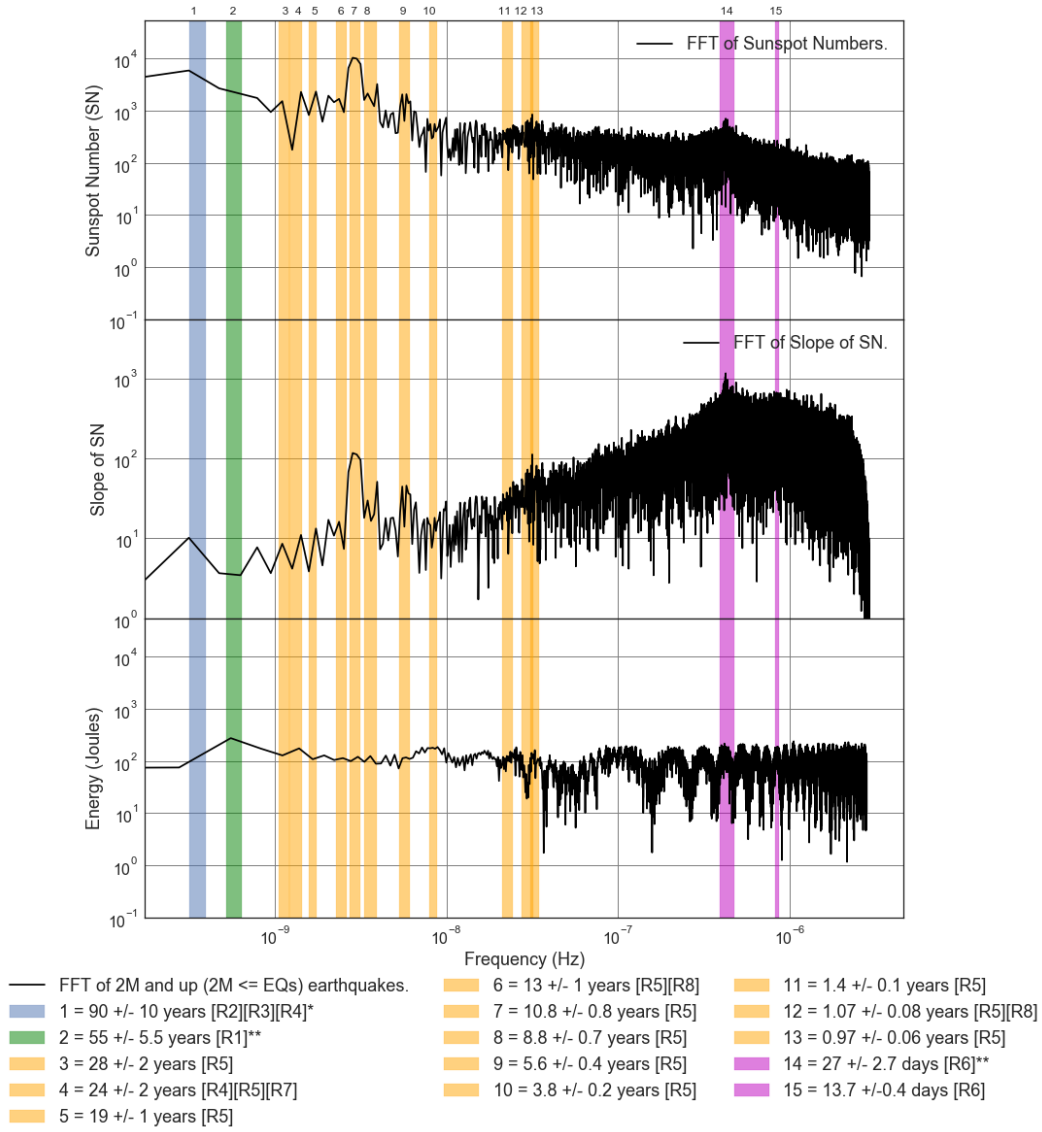

Figure E1.34: FFT Loglog Comparison Plot of Averaged 2M and up (2M <= EQs) Earthquake (EQ) total energy released, 2 Day Sunspot number and slope from 1818 to 2017. Additional meaning of the legend colors: Blue = Various Analysis techniques, Green = Meyer wavelet, Orange = Instantly maximal wavelet skeleton spectra, Magenta = Periodram and Linear phase finite impulse response.

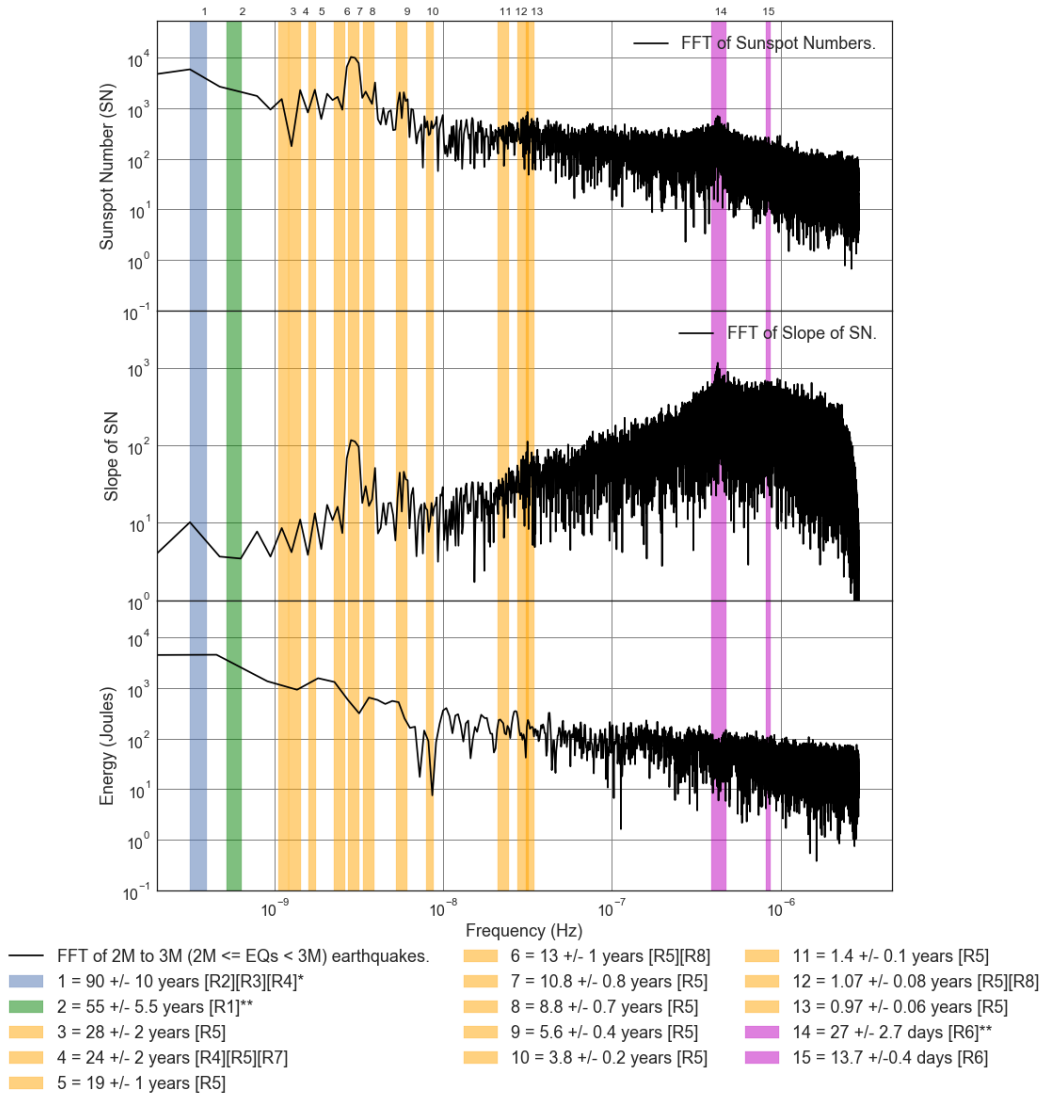

Figure E1.35: FFT Loglog Comparison Plot of Averaged 2M to 3M (2M <= EQs < 3M) Earthquake (EQ) total energy released, 2 Day Sunspot number and slope from 1818 to 2017. Additional meaning of the legend colors: Blue = Various Analysis techniques, Green = Meyer wavelet, Orange = Instantly maximal wavelet skeleton spectra, Magenta = Periodram and Linear phase finite impulse response.

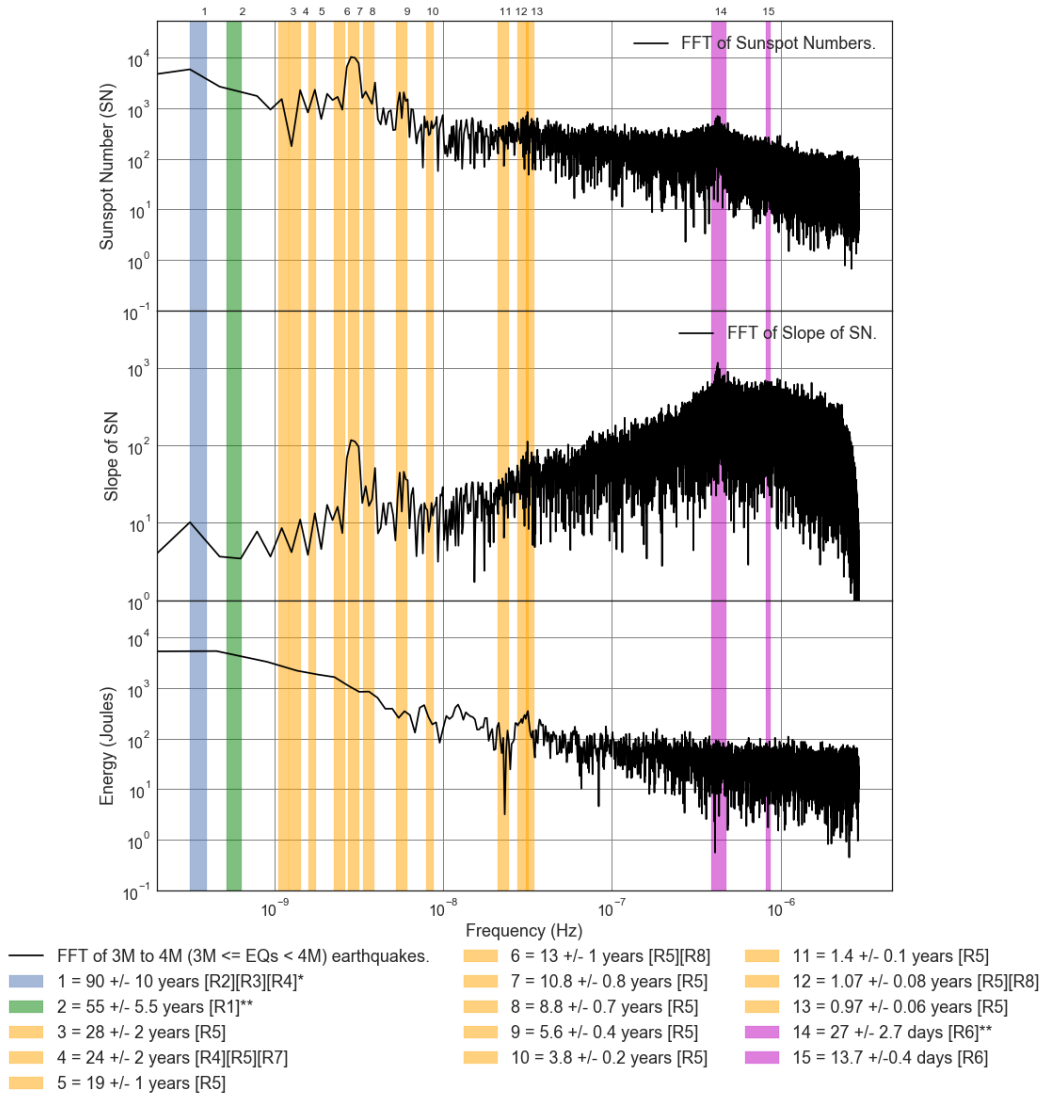

Figure E1.36: FFT Loglog Comparison Plot of Averaged 3M to 4M (3M <= EQs < 4M) Earthquake (EQ) total energy released, 2 Day Sunspot number and slope from 1818 to 2017. Additional meaning of the legend colors: Blue = Various Analysis techniques, Green = Meyer wavelet, Orange = Instantly maximal wavelet skeleton spectra, Magenta = Periodram and Linear phase finite impulse response.

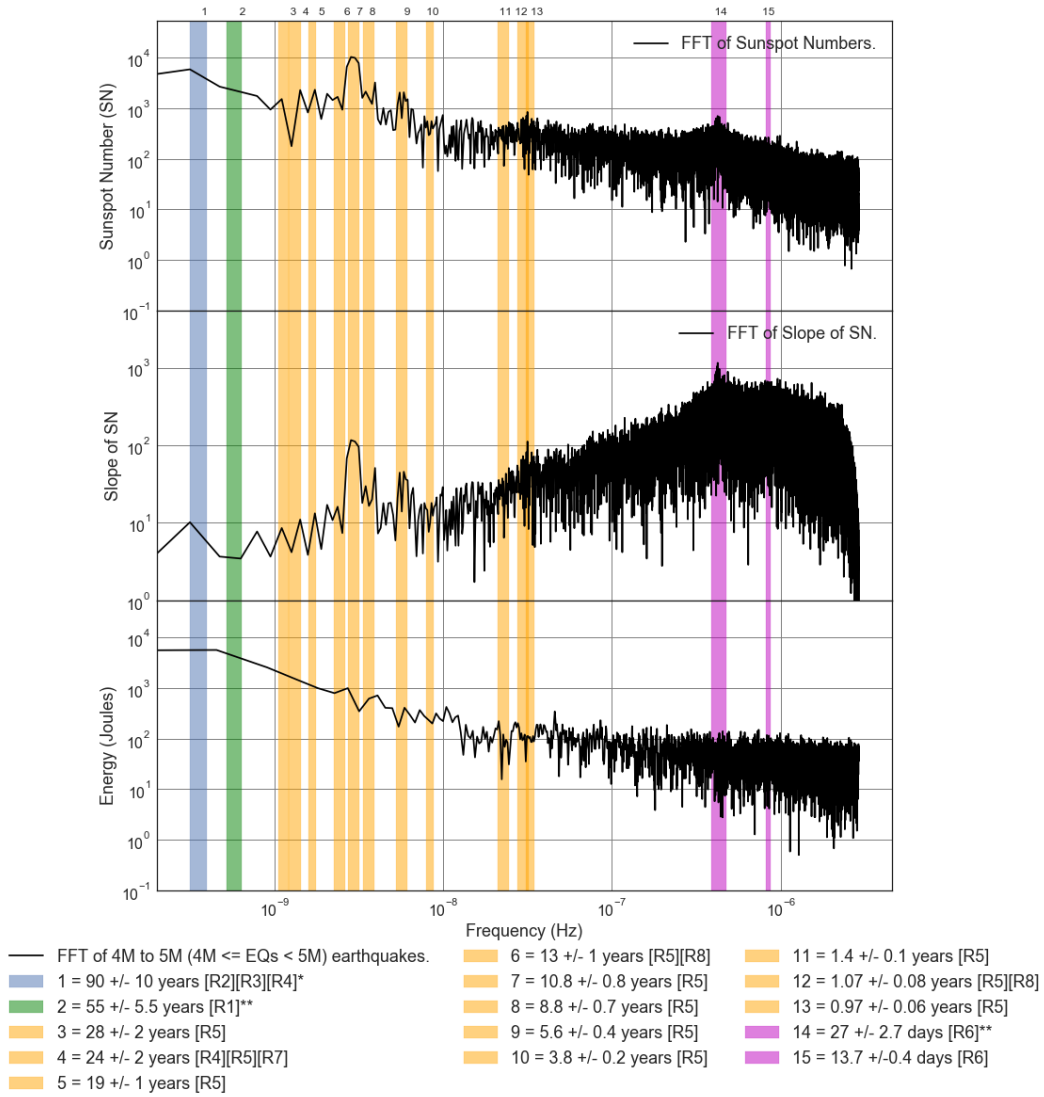

Figure E1.37: FFT Loglog Comparison Plot of Averaged 4M to 5M (4M <= EQs < 5M) Earthquake (EQ) total energy released, 2 Day Sunspot number and slope from 1818 to 2017. Additional meaning of the legend colors: Blue = Various Analysis techniques, Green = Meyer wavelet, Orange = Instantly maximal wavelet skeleton spectra, Magenta = Periodram and Linear phase finite impulse response.

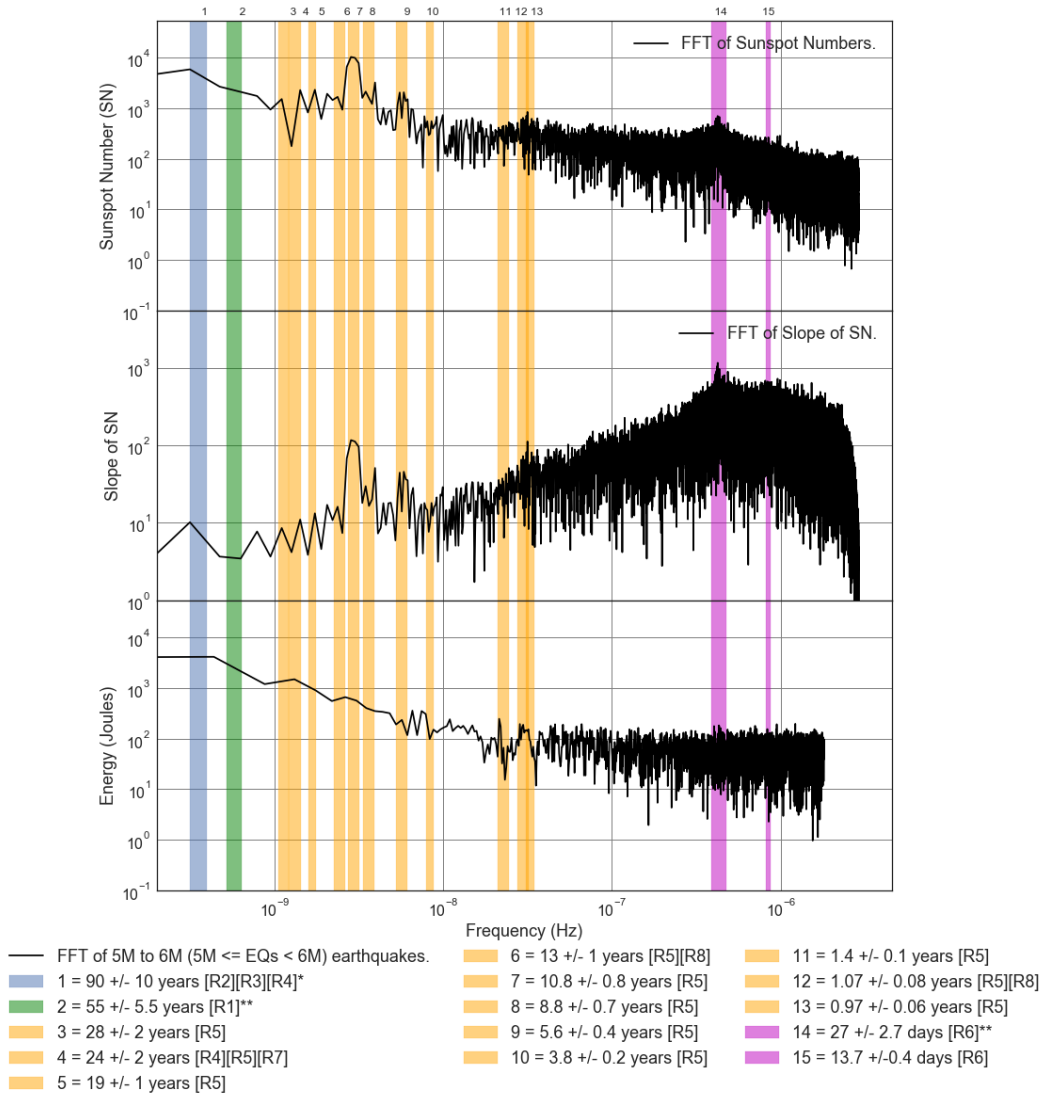

Figure E1.38: FFT Loglog Comparison Plot of Averaged 5M to 6M (5M <= EQs < 6M) Earthquake (EQ) total energy released, 2 Day Sunspot number and slope from 1818 to 2017. Additional meaning of the legend colors: Blue = Various Analysis techniques, Green = Meyer wavelet, Orange = Instantly maximal wavelet skeleton spectra, Magenta = Periodram and Linear phase finite impulse response.

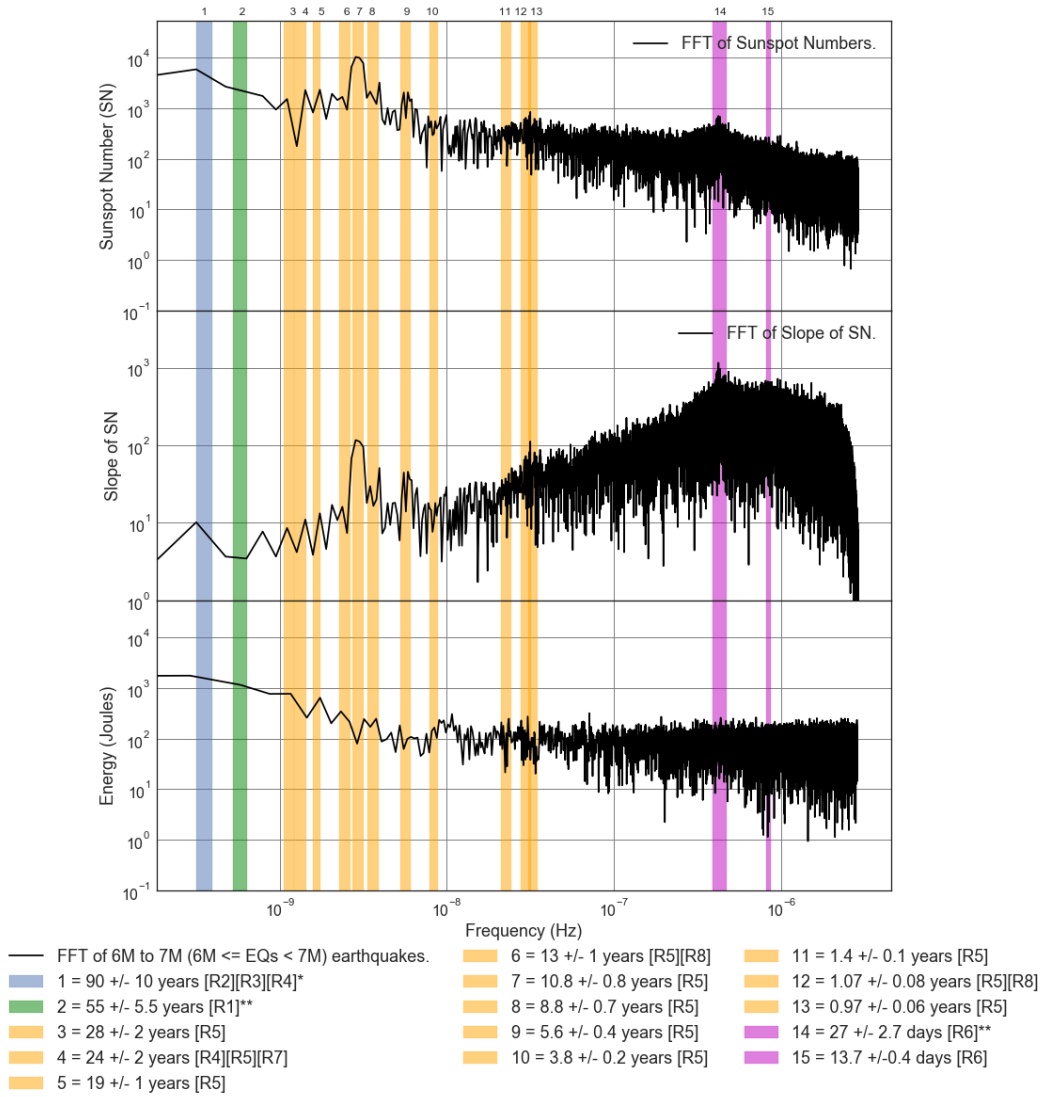

Figure E1.39: FFT Loglog Comparison Plot of Averaged 6M to 7M (6M <= EQs < 7M) Earthquake (EQ) total energy released, 2 Day Sunspot number and slope from 1818 to 2017. Additional meaning of the legend colors: Blue = Various Analysis techniques, Green = Meyer wavelet, Orange = Instantly maximal wavelet skeleton spectra, Magenta = Periodram and Linear phase finite impulse response.

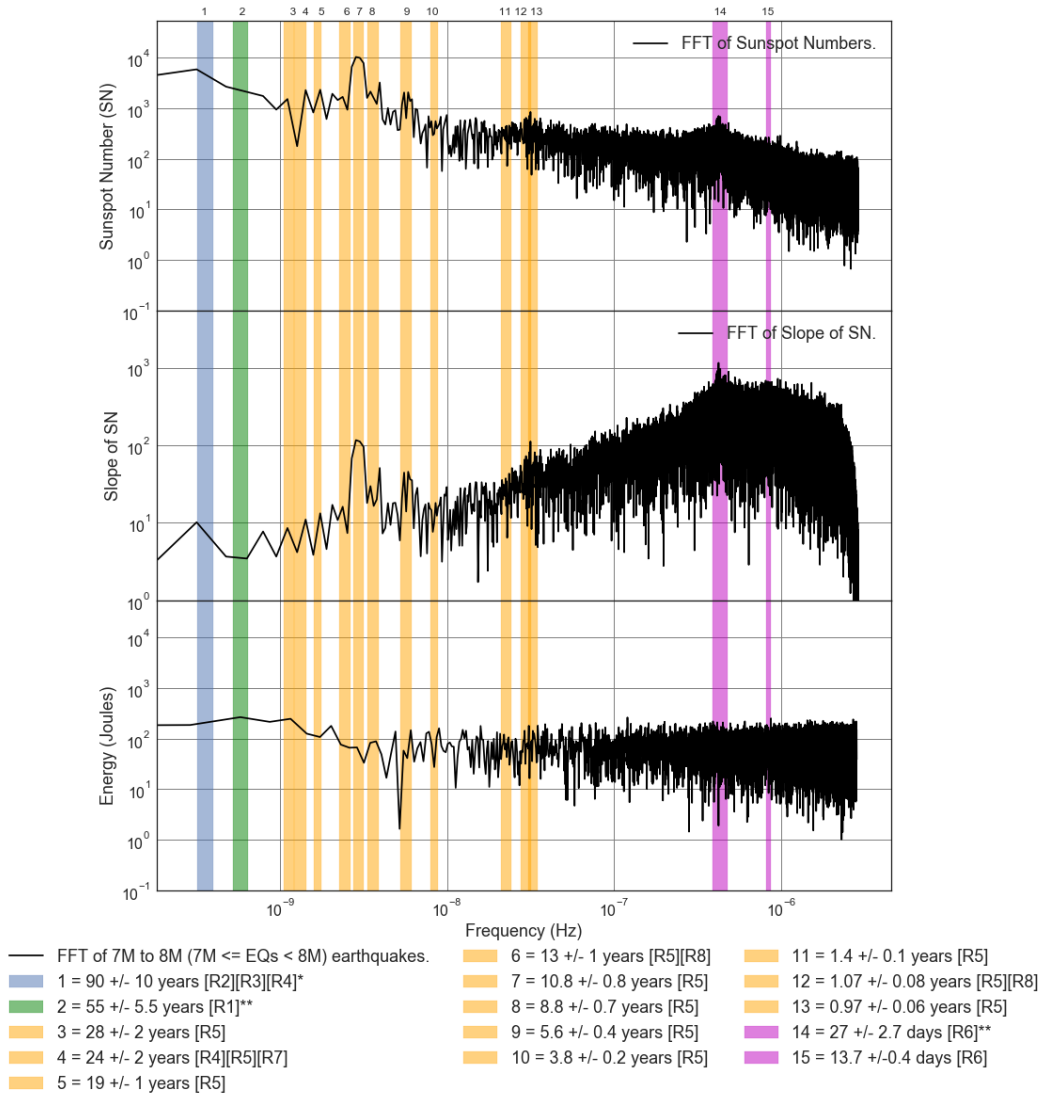

Figure E1.40: FFT Loglog Comparison Plot of Averaged 7M to 8M (7M <= EQs < 8M) Earthquake (EQ) total energy released, 2 Day Sunspot number and slope from 1818 to 2017. Additional meaning of the legend colors: Blue = Various Analysis techniques, Green = Meyer wavelet, Orange = Instantly maximal wavelet skeleton spectra, Magenta = Periodram and Linear phase finite impulse response.

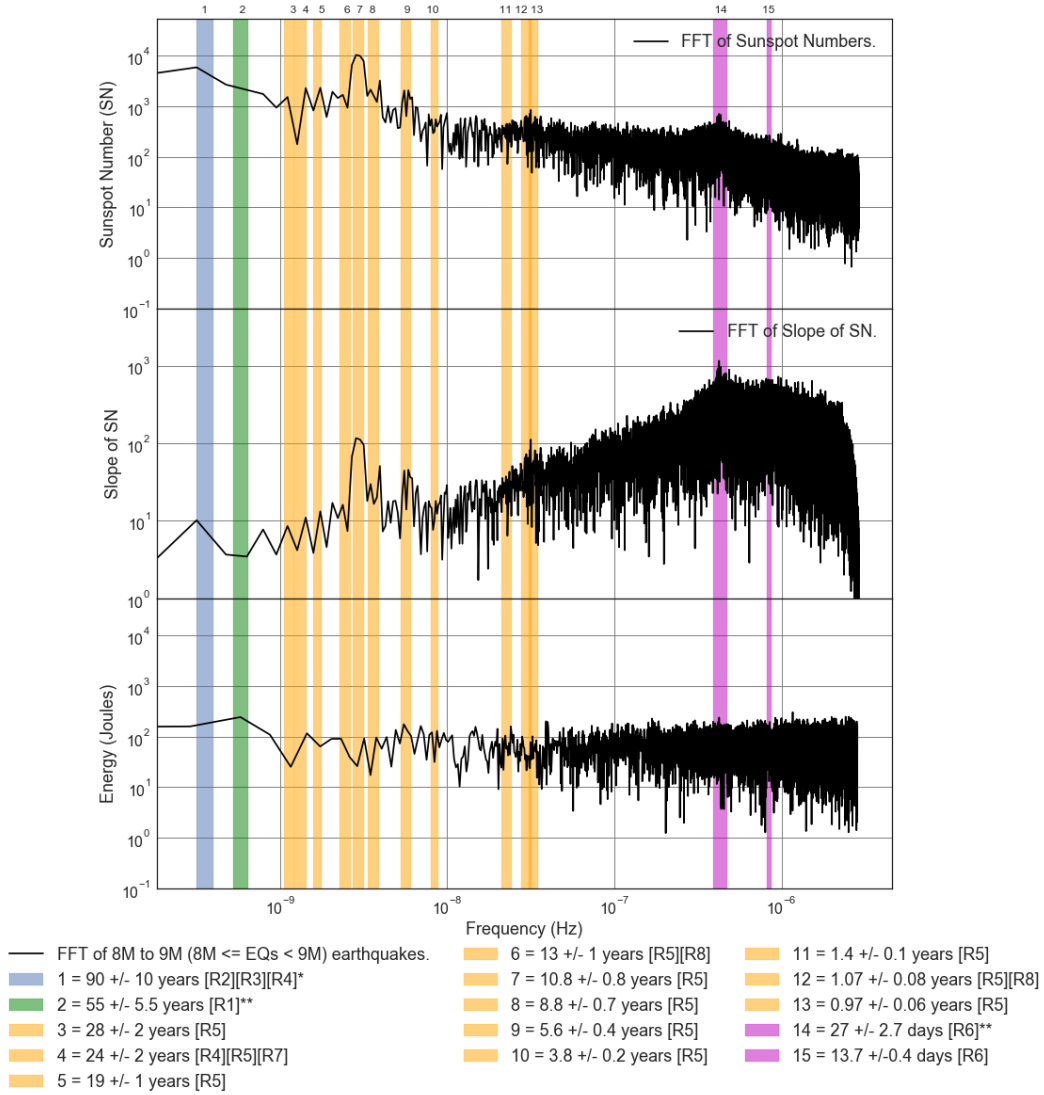

Figure E1.41: FFT Loglog Comparison Plot of Averaged 8M to 9M (8M <= EQs < 9M) Earthquake (EQ) total energy released, 2 Day Sunspot number and slope from 1818 to 2017. Additional meaning of the legend colors: Blue = Various Analysis techniques, Green = Meyer wavelet, Orange = Instantly maximal wavelet skeleton spectra, Magenta = Periodram and Linear phase finite impulse response.

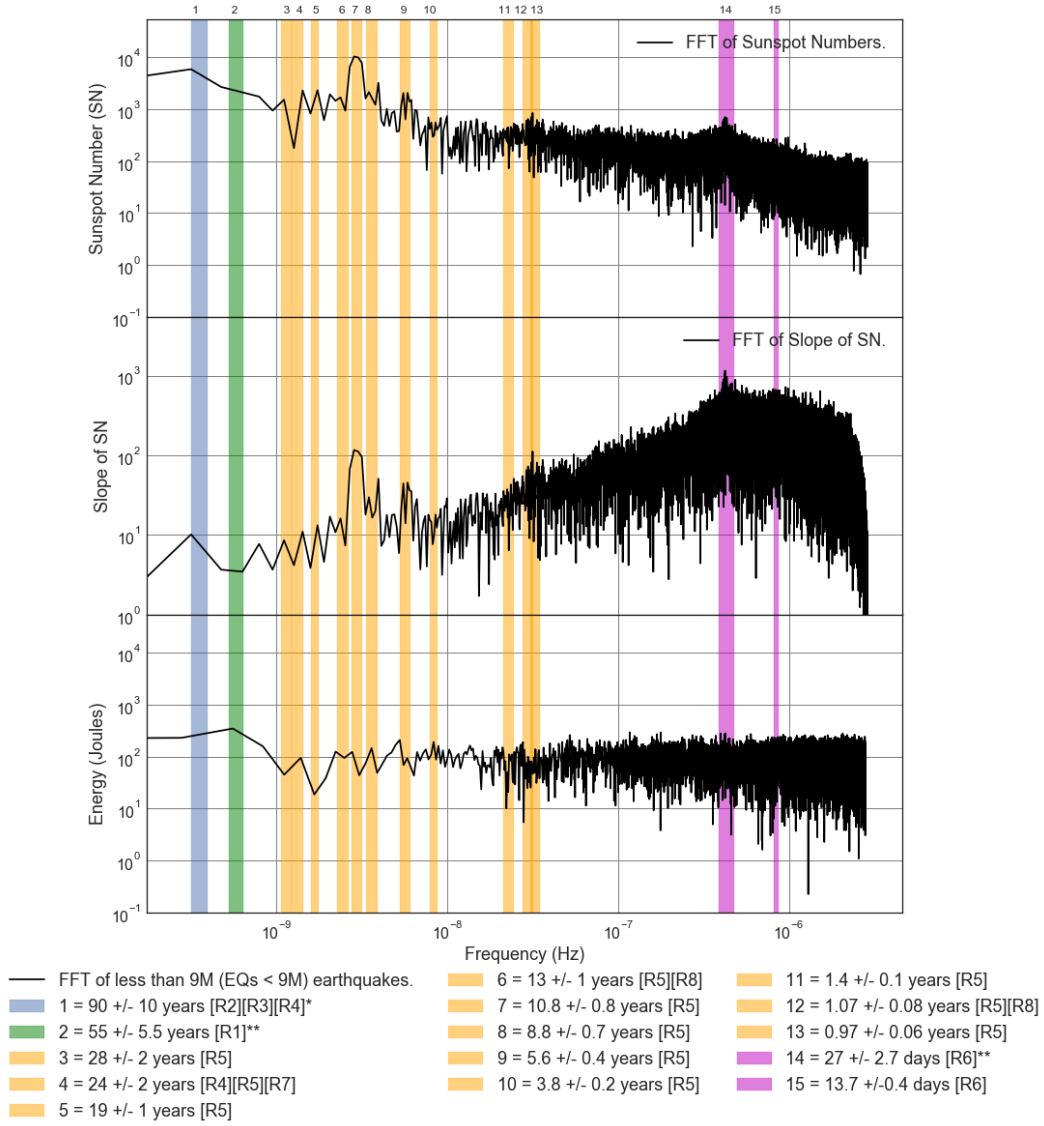

Figure E1.42: FFT Loglog Comparison Plot of Averaged less than 9M (EQs < 9M) Earthquake (EQ) total energy released, 2 Day Sunspot number and slope from 1818 to 2017. Additional meaning of the legend colors: Blue = Various Analysis techniques, Green = Meyer wavelet, Orange = Instantly maximal wavelet skeleton spectra, Magenta = Periodram and Linear phase finite impulse response.

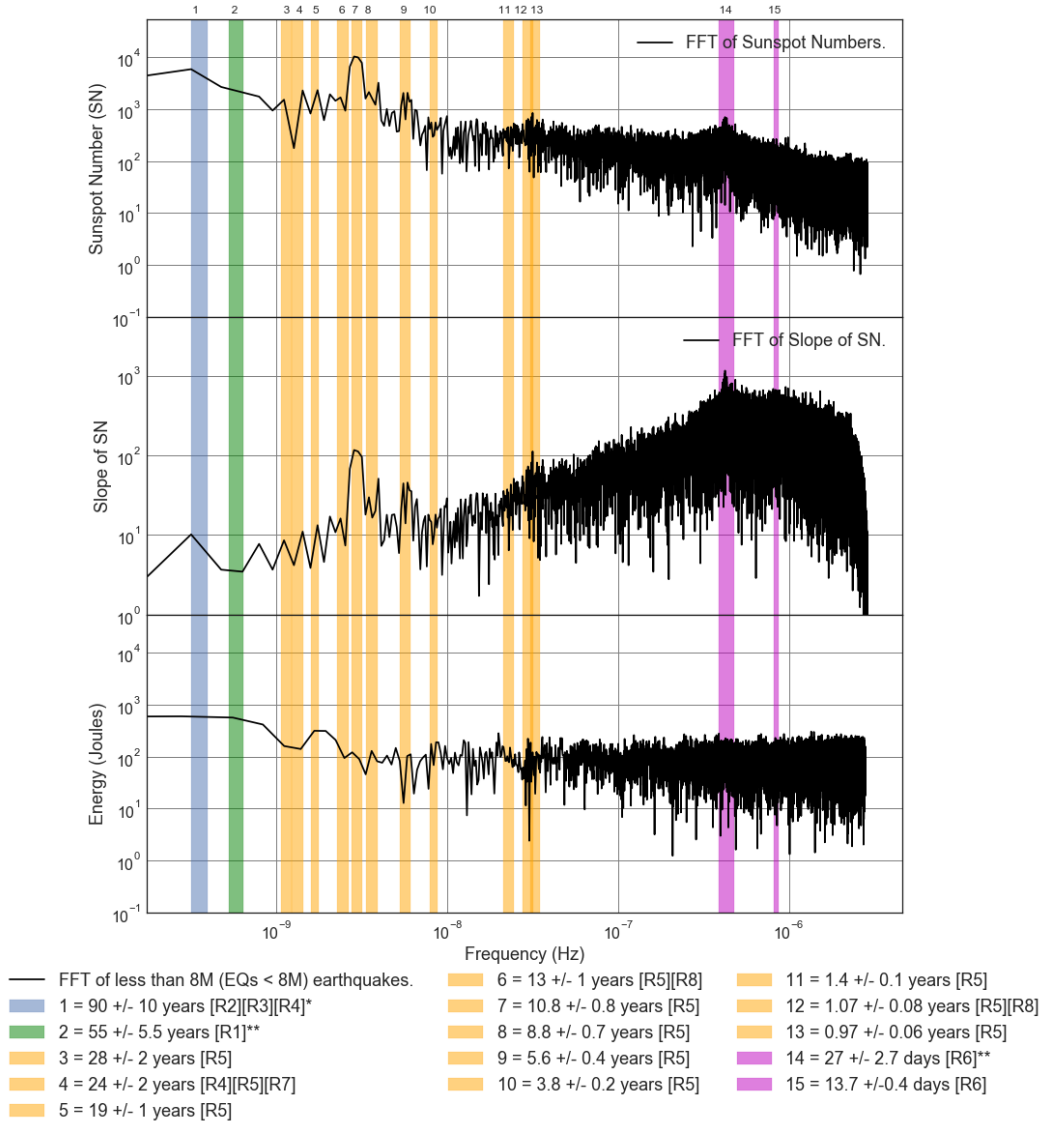

Figure E1.43: FFT Loglog Comparison Plot of Averaged less than 8M (EQs < 8M) Earthquake (EQ) total energy released, 2 Day Sunspot number and slope from 1818 to 2017. Additional meaning of the legend colors: Blue = Various Analysis techniques, Green = Meyer wavelet, Orange = Instantly maximal wavelet skeleton spectra, Magenta = Periodram and Linear phase finite impulse response.

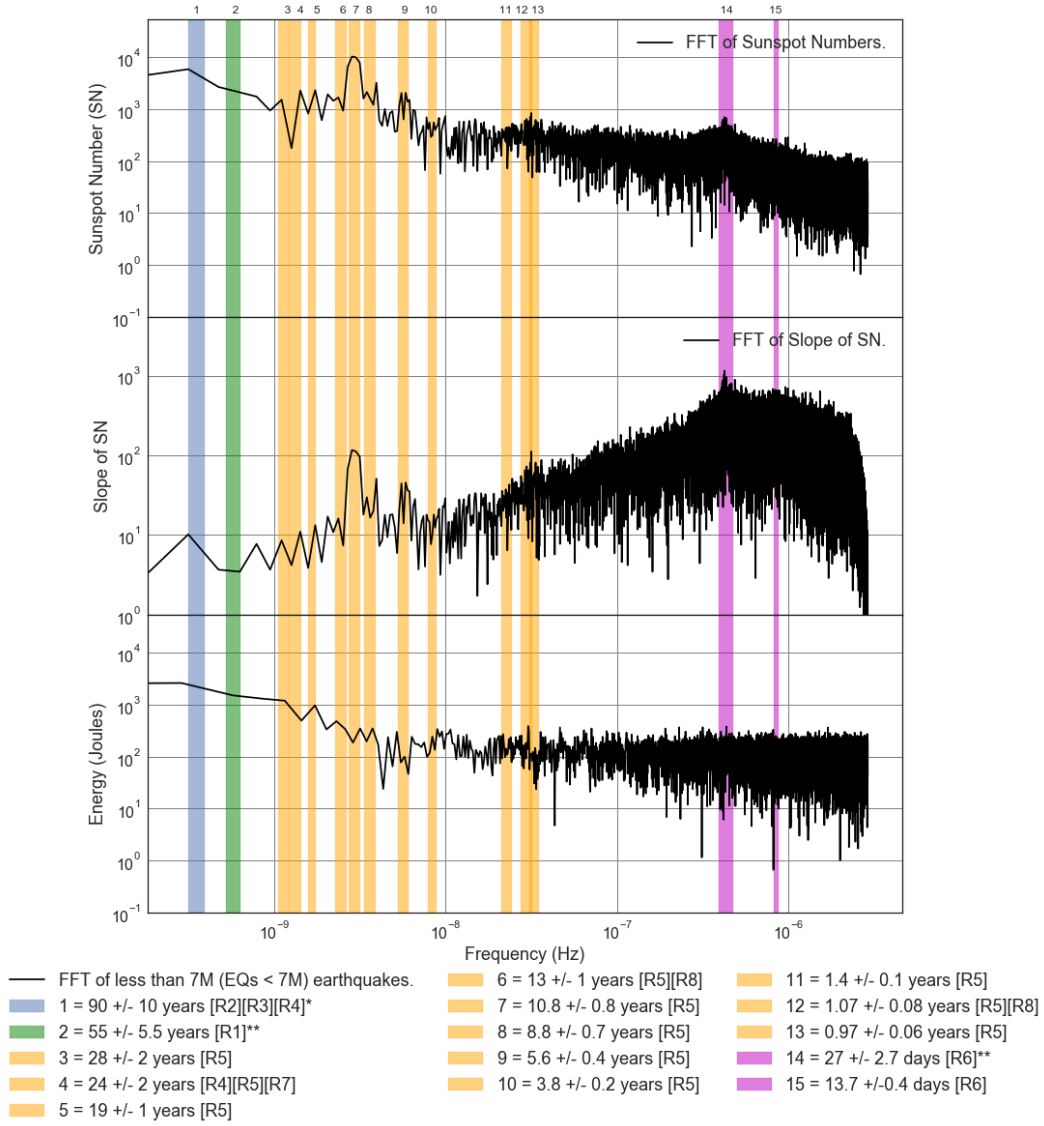

Figure E1.44: FFT Loglog Comparison Plot of Averaged less than 7M (EQs < 7M) Earthquake (EQ) total energy released, 2 Day Sunspot number and slope from 1818 to 2017. Additional meaning of the legend colors: Blue = Various Analysis techniques, Green = Meyer wavelet, Orange = Instantly maximal wavelet skeleton spectra, Magenta = Periodram and Linear phase finite impulse response.

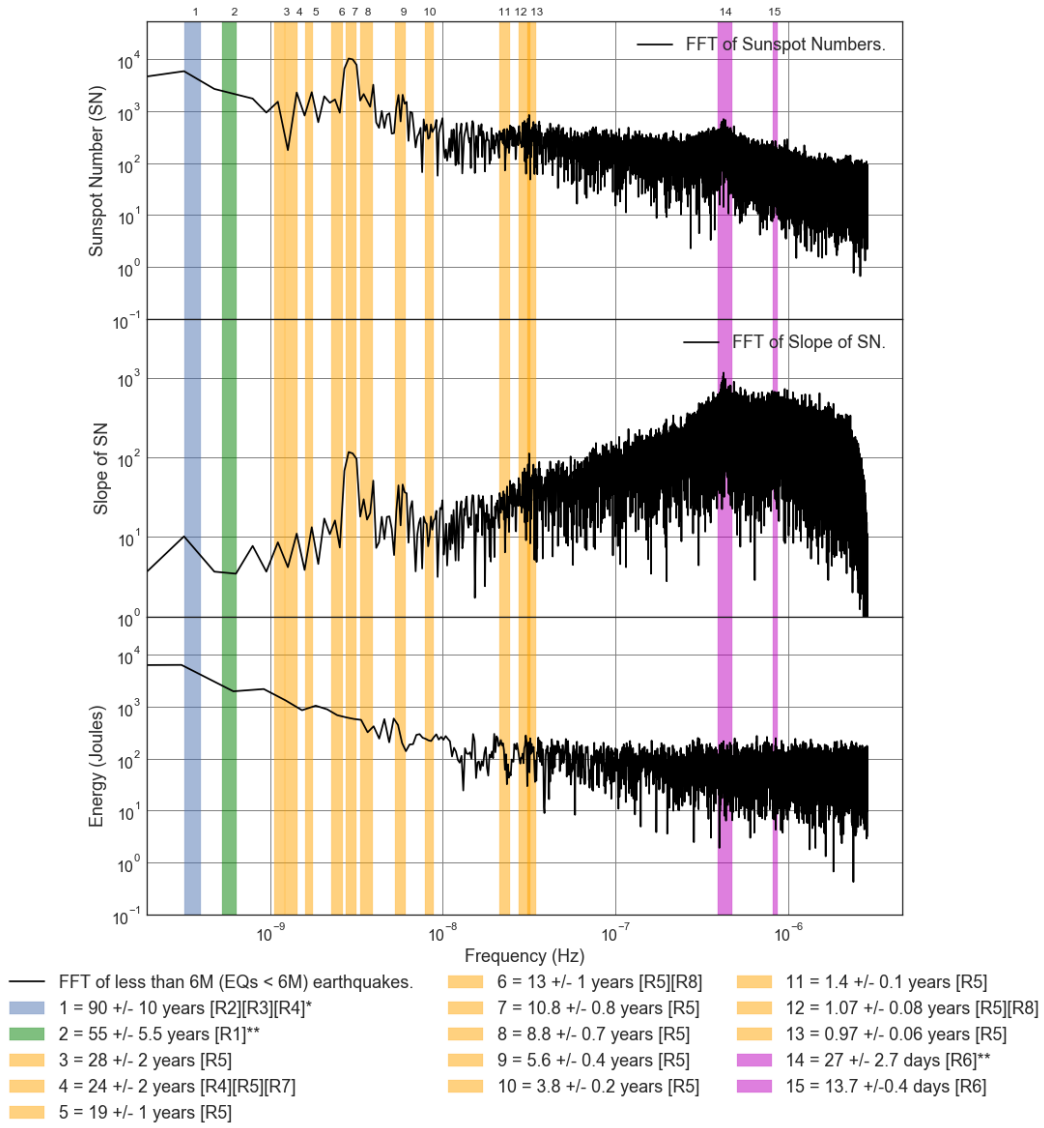

Figure E1.45: FFT Loglog Comparison Plot of Averaged less than 6M (EQs < 6M) Earthquake (EQ) total energy released, 2 Day Sunspot number and slope from 1818 to 2017. Additional meaning of the legend colors: Blue = Various Analysis techniques, Green = Meyer wavelet, Orange = Instantly maximal wavelet skeleton spectra, Magenta = Periodram and Linear phase finite impulse response.

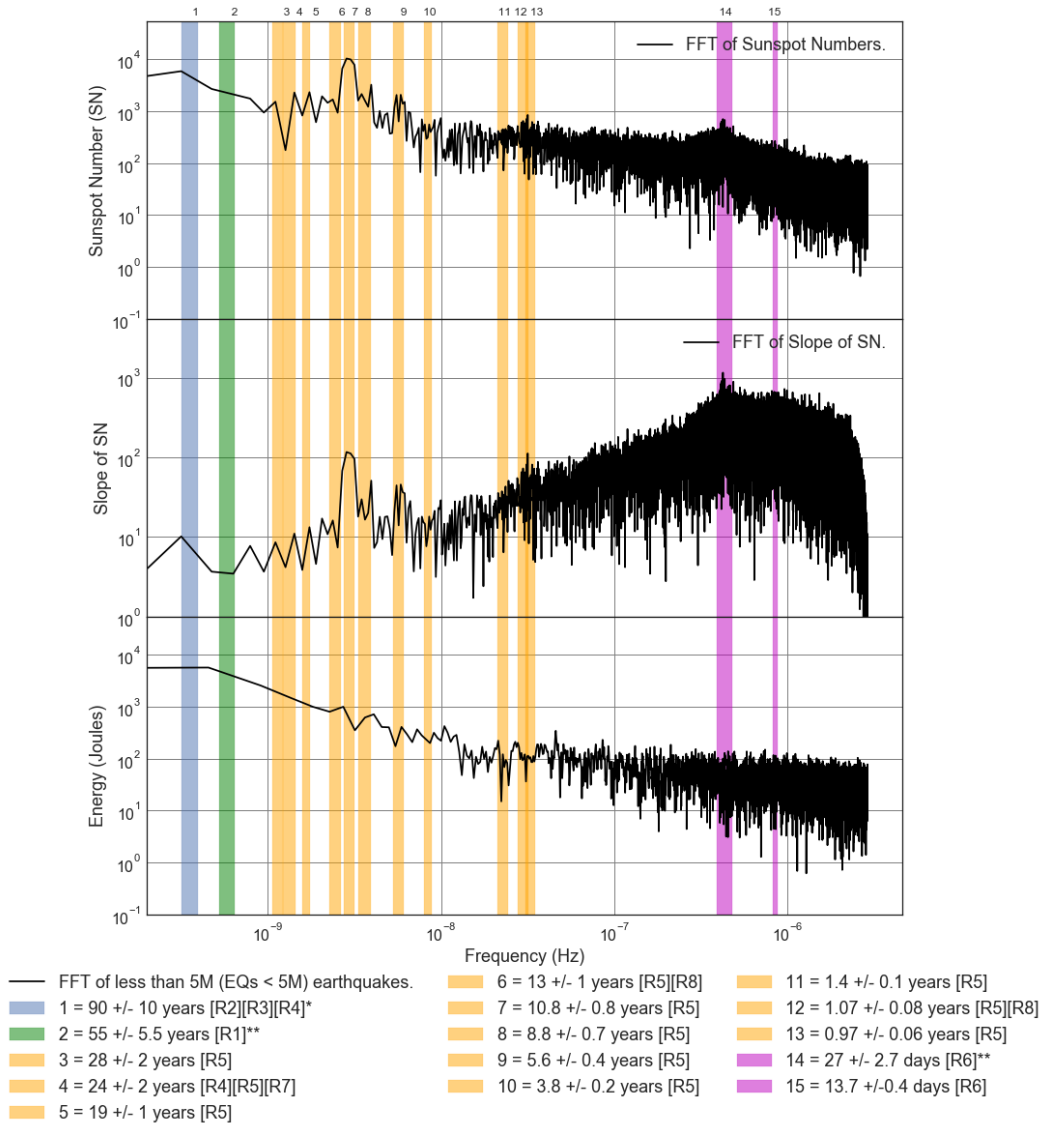

Figure E1.46: FFT Loglog Comparison Plot of Averaged less than 5M (EQs < 5M) Earthquake (EQ) total energy released, 2 Day Sunspot number and slope from 1818 to 2017. Additional meaning of the legend colors: Blue = Various Analysis techniques, Green = Meyer wavelet, Orange = Instantly maximal wavelet skeleton spectra, Magenta = Periodram and Linear phase finite impulse response.

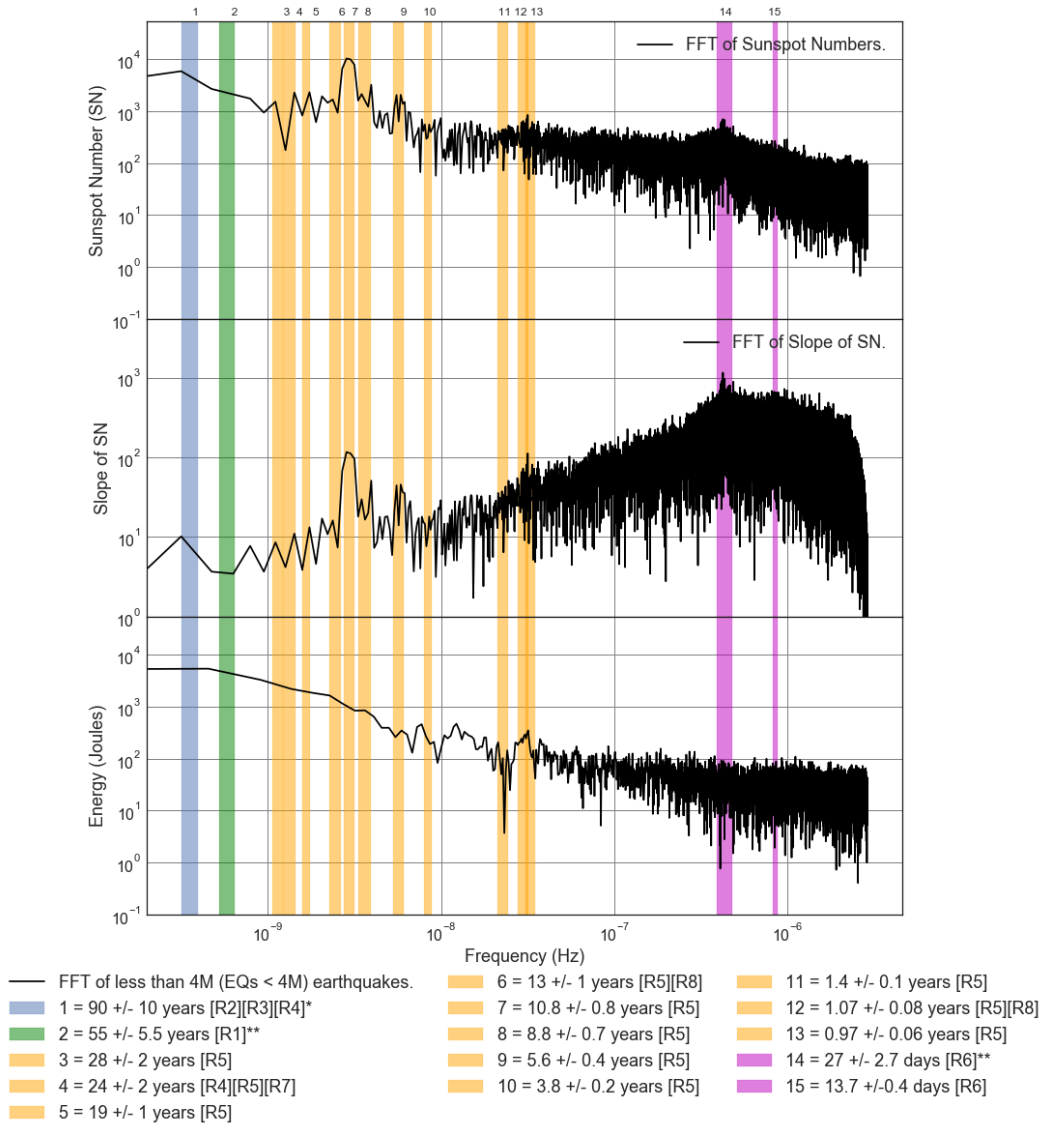

Figure E1.47: FFT Loglog Comparison Plot of Averaged less than 4M (EQs < 4M) Earthquake (EQ) total energy released, 2 Day Sunspot number and slope from 1818 to 2017. Additional meaning of the legend colors: Blue = Various Analysis techniques, Green = Meyer wavelet, Orange = Instantly maximal wavelet skeleton spectra, Magenta = Periodram and Linear phase finite impulse response.

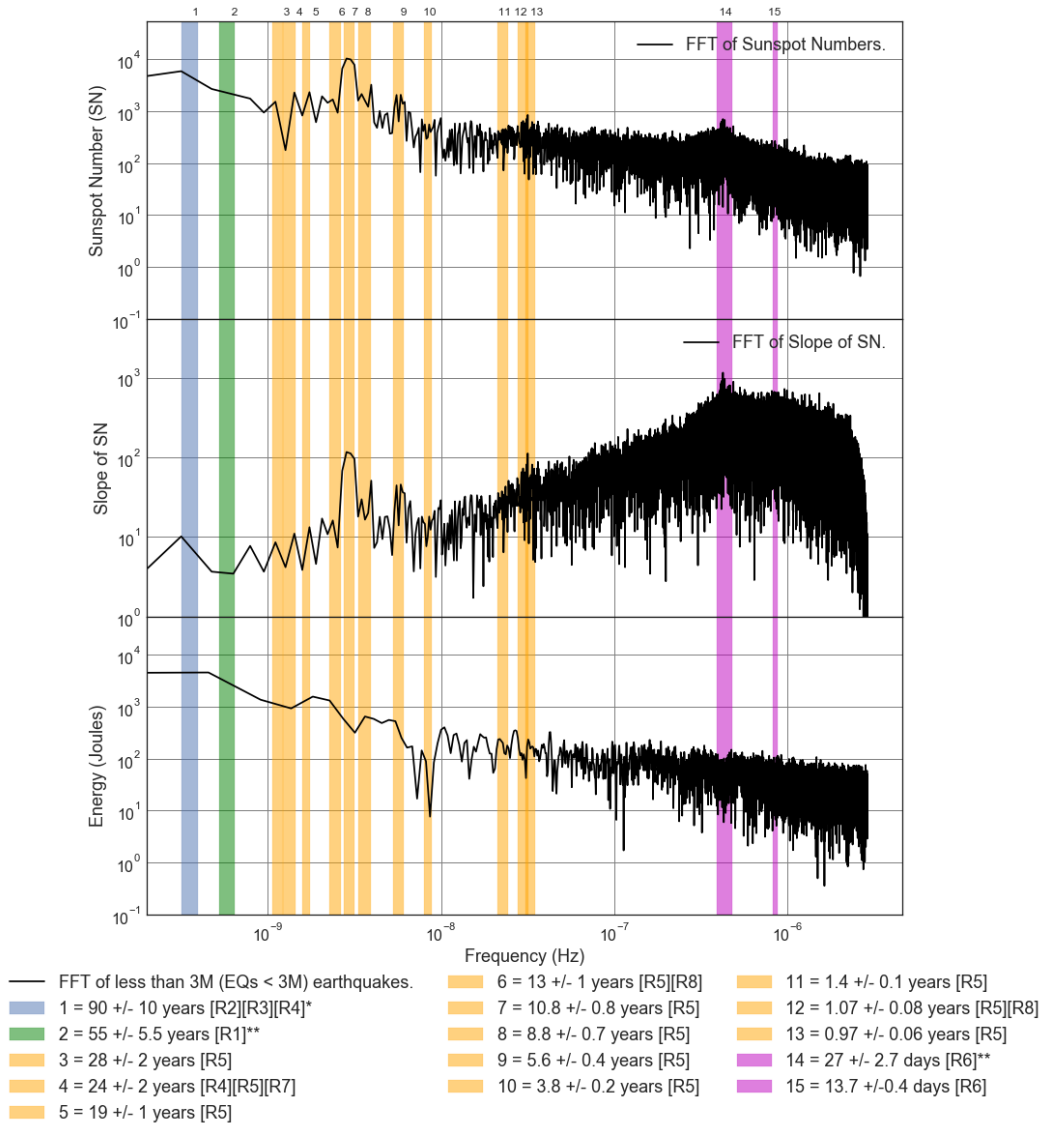

Figure E1.48: FFT Loglog Comparison Plot of Averaged less than 3M (EQs < 3M) Earthquake (EQ) total energy released, 2 Day Sunspot number and slope from 1818 to 2017. Additional meaning of the legend colors: Blue = Various Analysis techniques, Green = Meyer wavelet, Orange = Instantly maximal wavelet skeleton spectra, Magenta = Periodram and Linear phase finite impulse response.

Appendix E2: Fast Fourier Transform Magnitude Spectra Comparison of Averaged (ISC, USGS, and Centennial) Earthquake Frequencies with Solar Cycle frequencies. Part 2 - Slope of Earthquake Counts and Slope of Earthquake Energy in Joules.

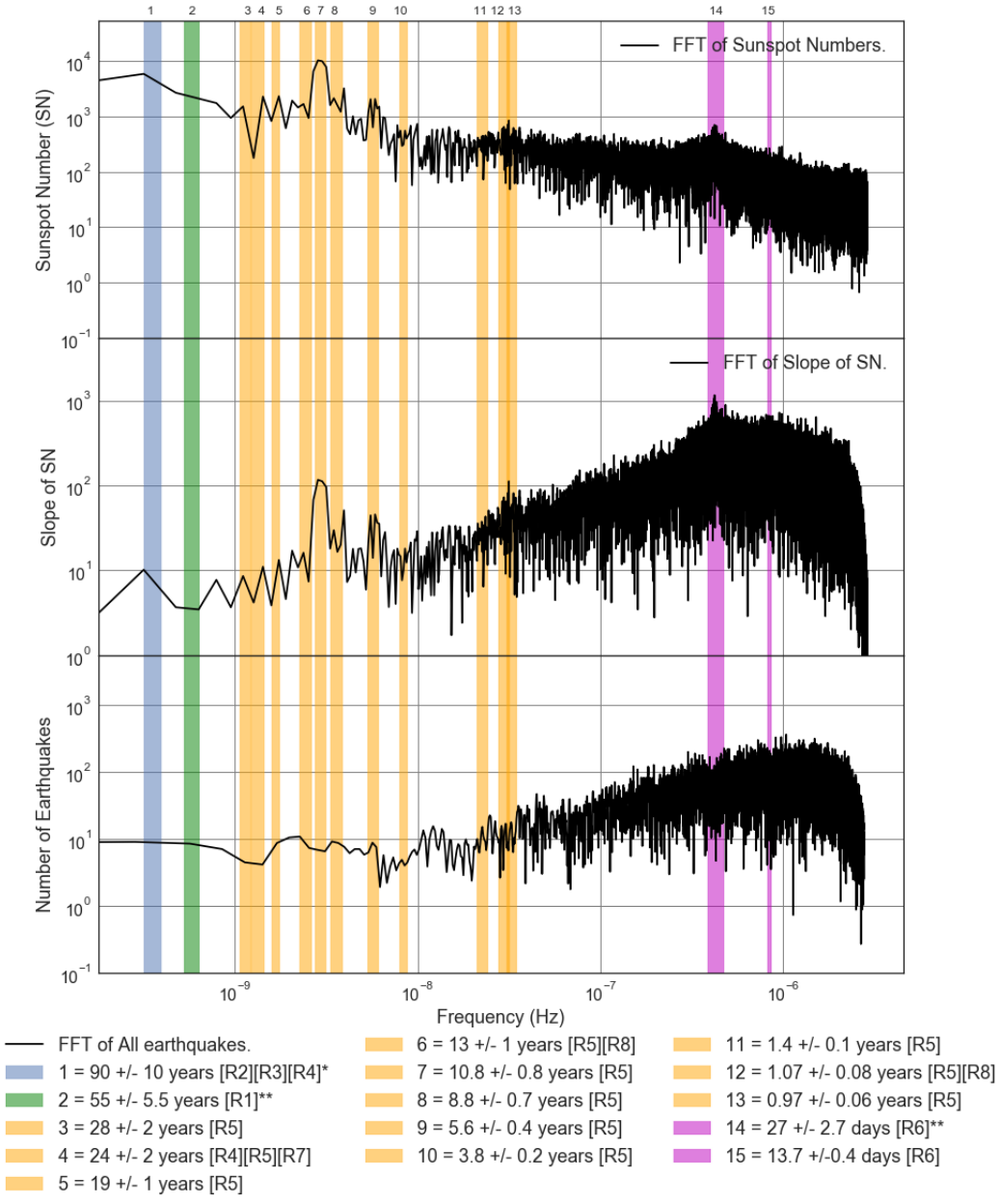

Figure E2.1: FFT Loglog Comparison Plot: Slope of Averaged All Earthquake counts, Sunspot number (SN) and slope from 1818 to 2017. Additional meaning of the legend colors: Blue = Various Analysis techniques, Green = Meyer wavelet, Orange = Instantly maximal wavelet skeleton spectra, Magenta = Periodram and Linear phase finite impulse response.

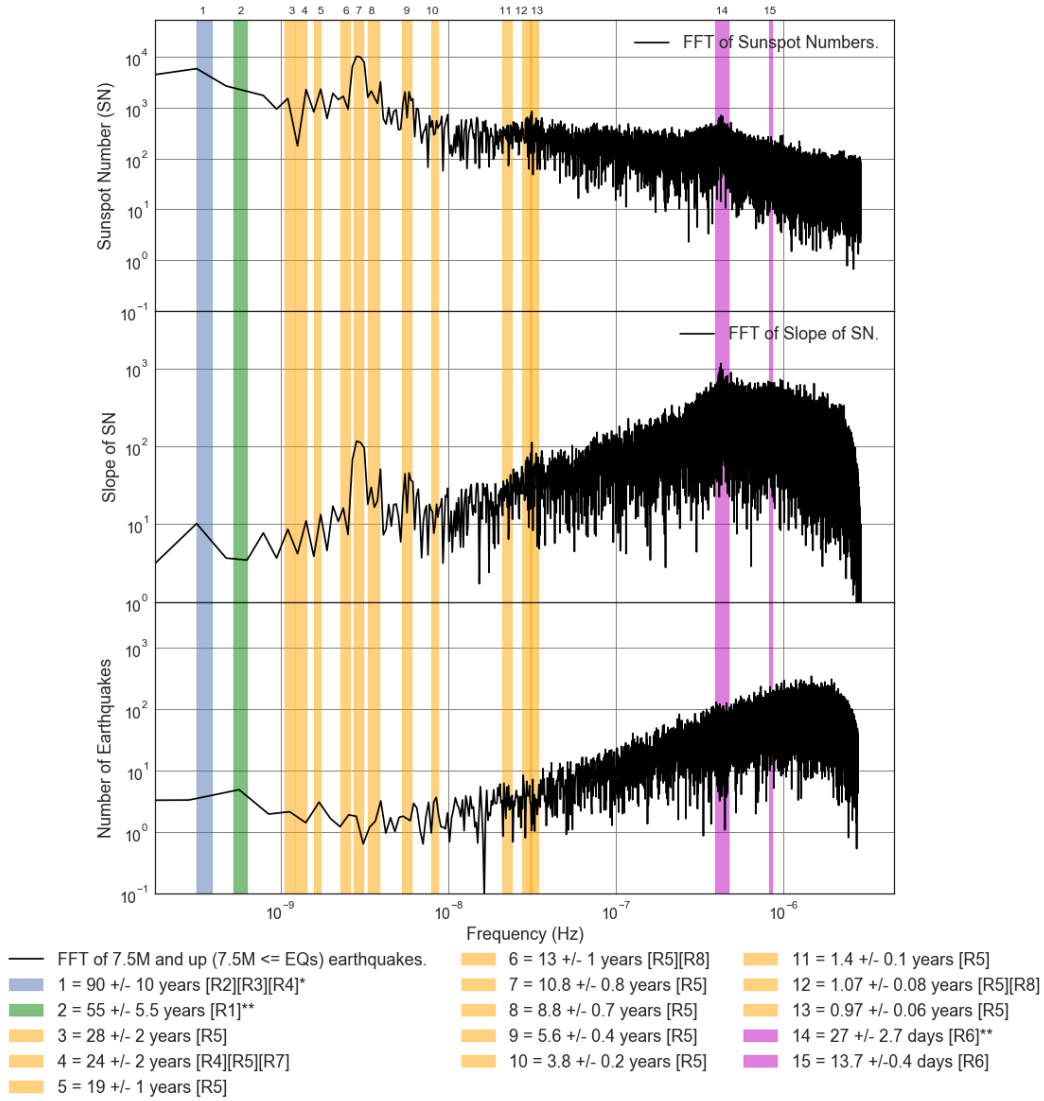

Figure E2.2: FFT Loglog Comparison Plot: Slope of Averaged 7.5M and up (7.5M <= EQs) Earthquake counts, Sunspot number (SN) and slope from 1818 to 2017. Additional meaning of the legend colors: Blue = Various Analysis techniques, Green = Meyer wavelet, Orange = Instantly maximal wavelet skeleton spectra, Magenta = Periodram and Linear phase finite impulse response.

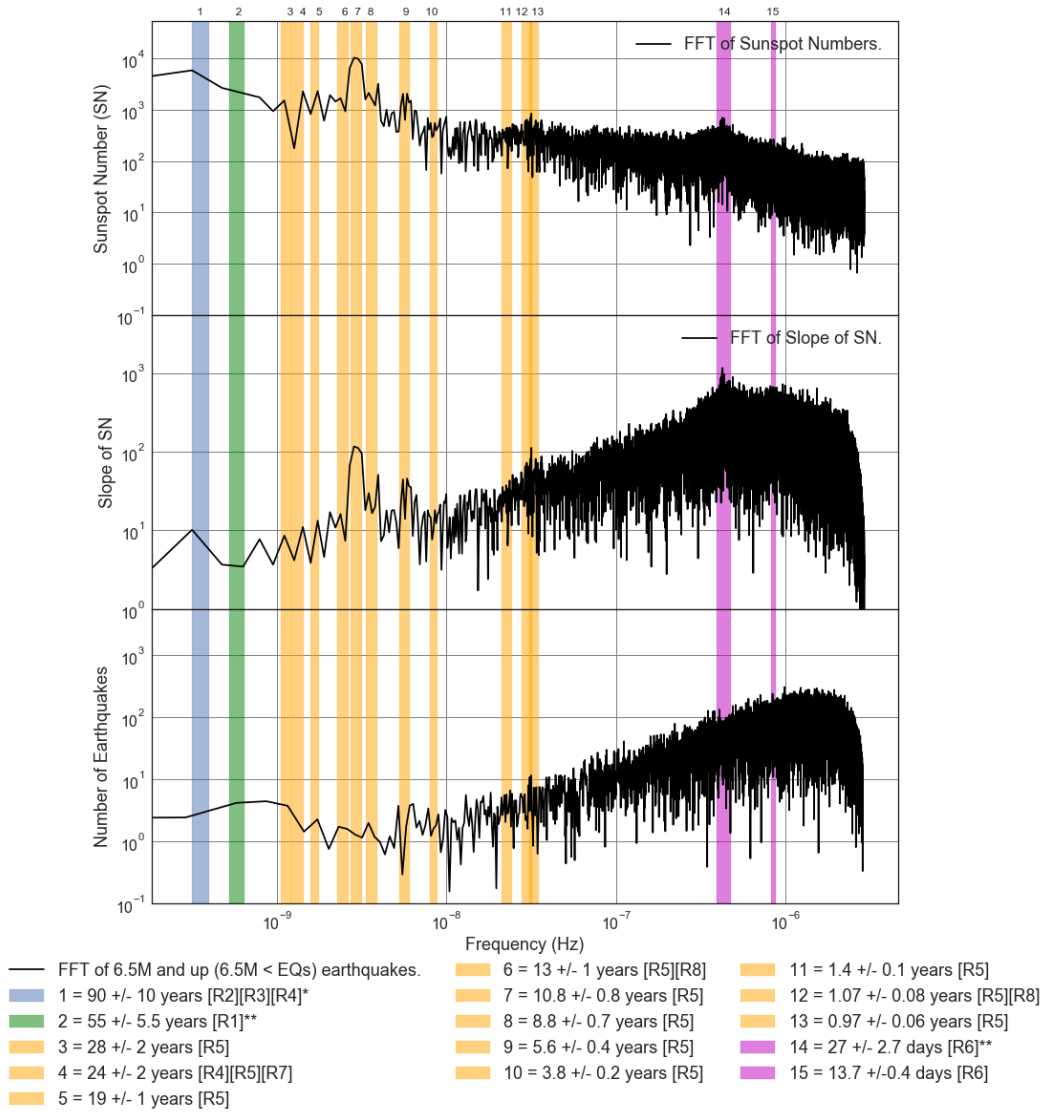

Figure E2.3: FFT Loglog Comparison Plot: Slope of Averaged 6.5M and up (6.5M < EQs) Earthquake counts, Sunspot number (SN) and slope from 1818 to 2017. Additional meaning of the legend colors: Blue = Various Analysis techniques, Green = Meyer wavelet, Orange = Instantly maximal wavelet skeleton spectra, Magenta = Periodram and Linear phase finite impulse response.

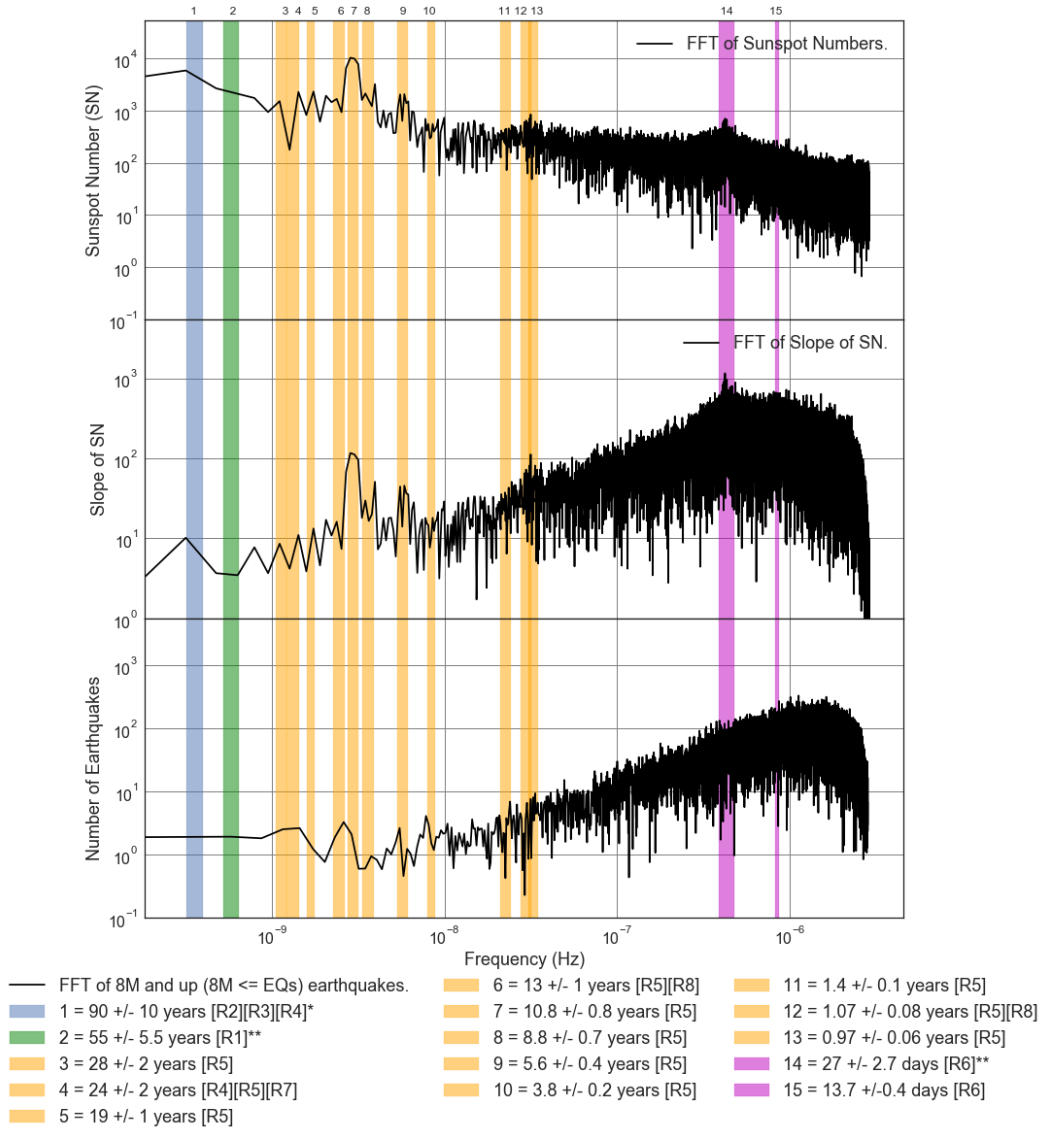

Figure E2.4: FFT Loglog Comparison Plot: Slope of Averaged 8M and up (8M <= EQs) Earthquake counts, Sunspot number (SN) and slope from 1818 to 2017. Additional meaning of the legend colors: Blue = Various Analysis techniques, Green = Meyer wavelet, Orange = Instantly maximal wavelet skeleton spectra, Magenta = Periodram and Linear phase finite impulse response.

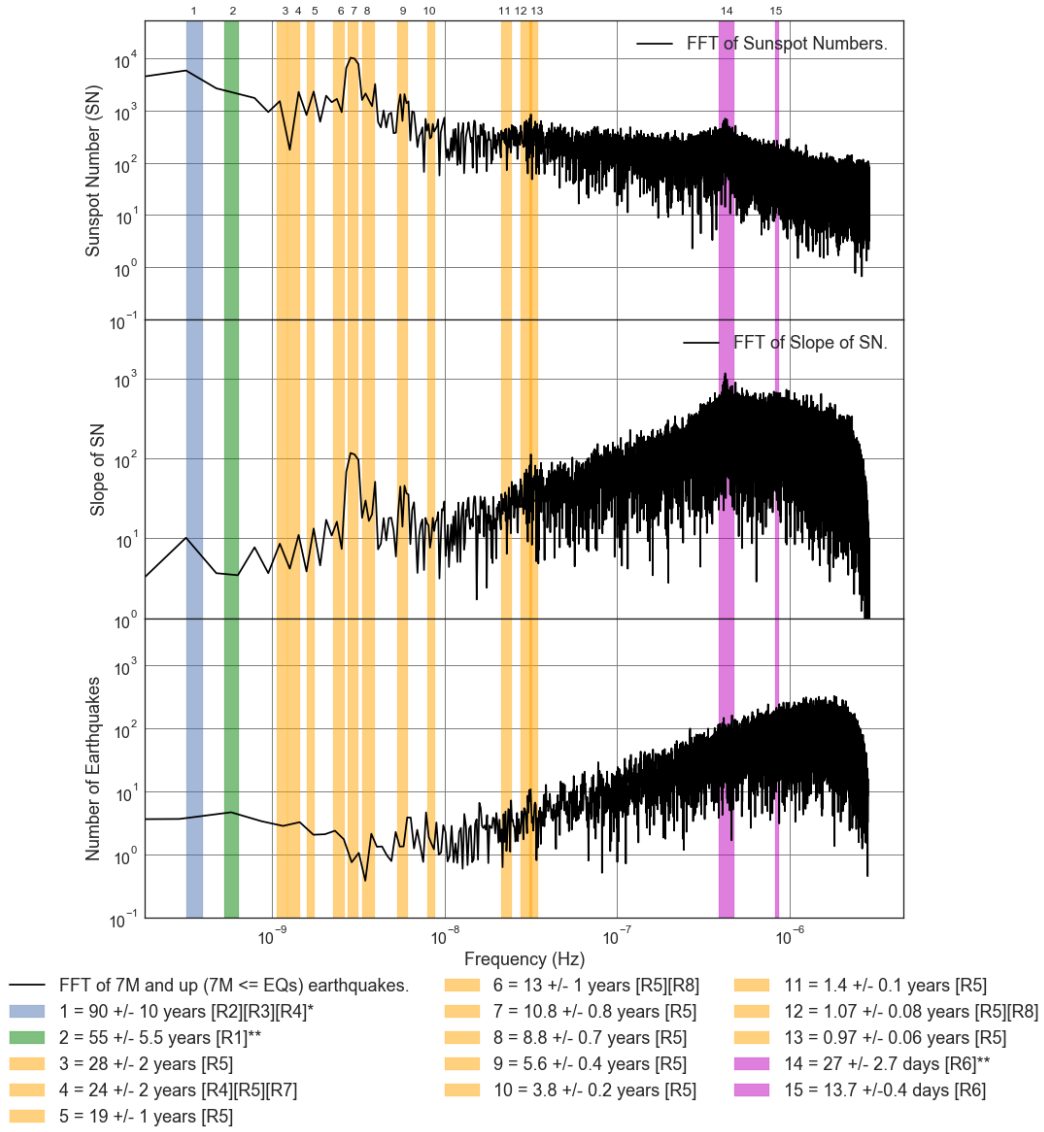

Figure E2.5: FFT Loglog Comparison Plot: Slope of Averaged 7M and up (7M <= EQs) Earthquake counts, Sunspot number (SN) and slope from 1818 to 2017. Additional meaning of the legend colors: Blue = Various Analysis techniques, Green = Meyer wavelet, Orange = Instantly maximal wavelet skeleton spectra, Magenta = Periodram and Linear phase finite impulse response.

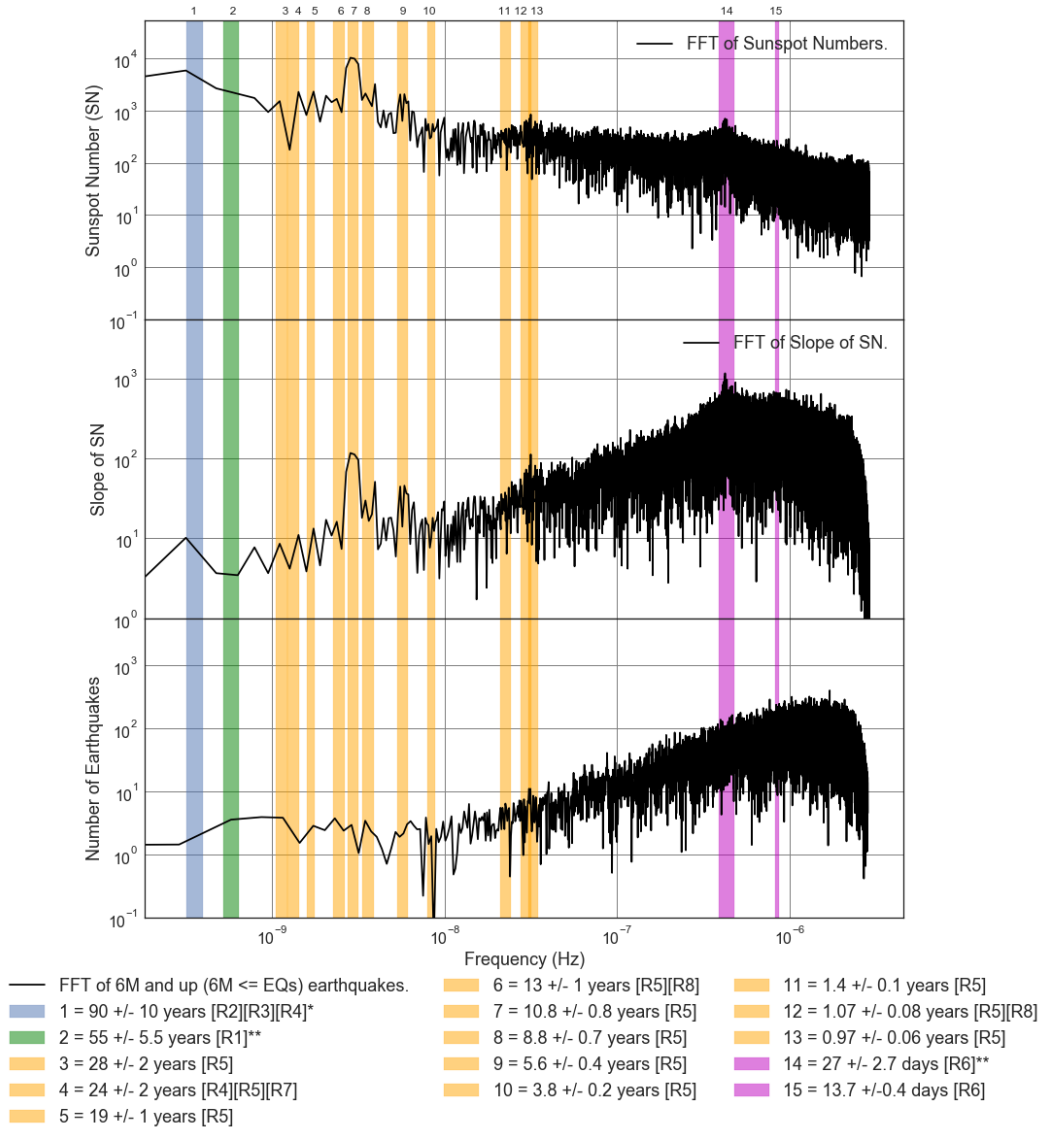

Figure E2.6: FFT Loglog Comparison Plot: Slope of Averaged 6M and up (6M <= EQs) Earthquake counts, Sunspot number (SN) and slope from 1818 to 2017. Additional meaning of the legend colors: Blue = Various Analysis techniques, Green = Meyer wavelet, Orange = Instantly maximal wavelet skeleton spectra, Magenta = Periodram and Linear phase finite impulse response.

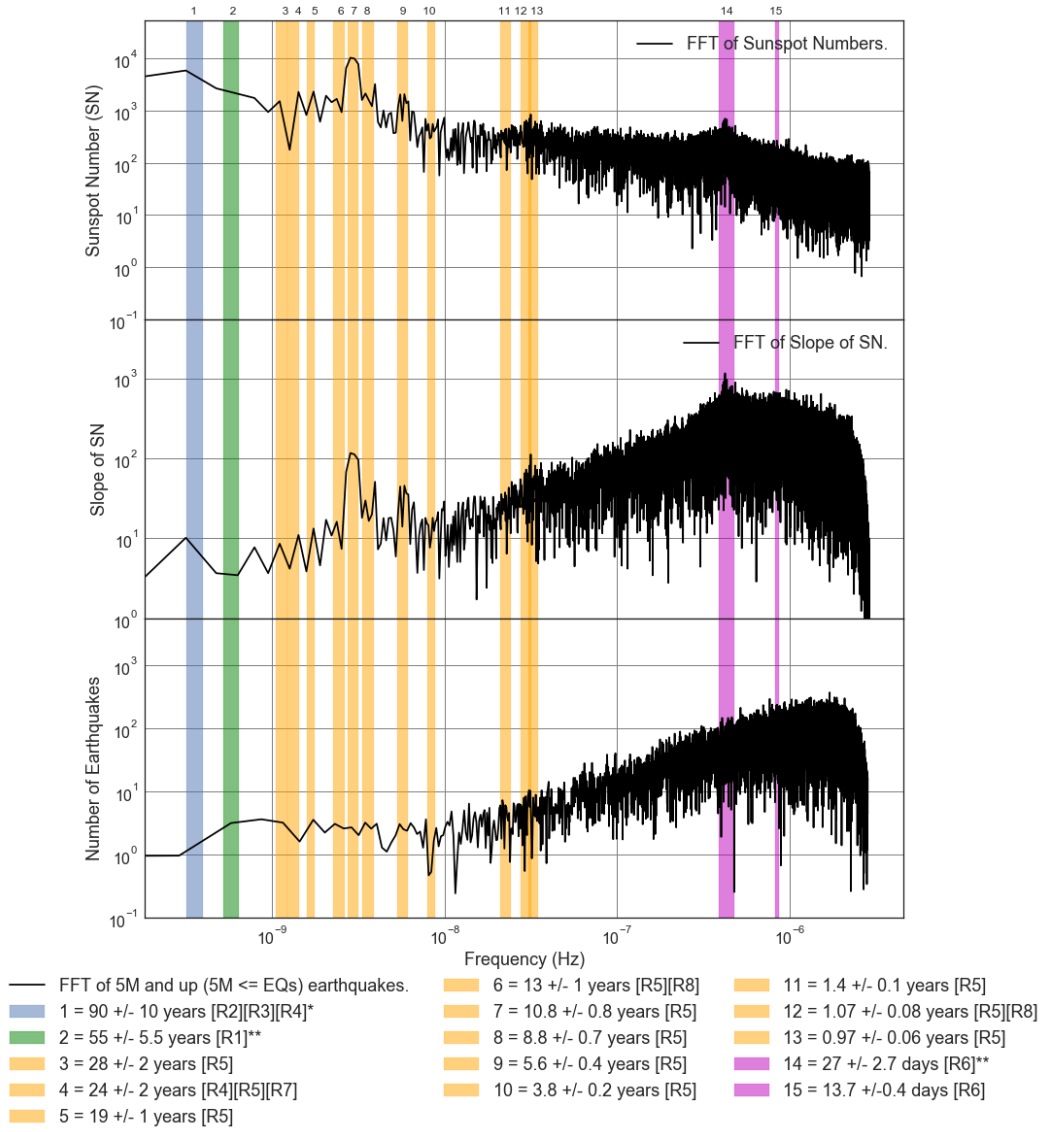

Figure E2.7: FFT Loglog Comparison Plot: Slope of Averaged 5M and up (5M <= EQs) Earthquake counts, Sunspot number (SN) and slope from 1818 to 2017. Additional meaning of the legend colors: Blue = Various Analysis techniques, Green = Meyer wavelet, Orange = Instantly maximal wavelet skeleton spectra, Magenta = Periodram and Linear phase finite impulse response.

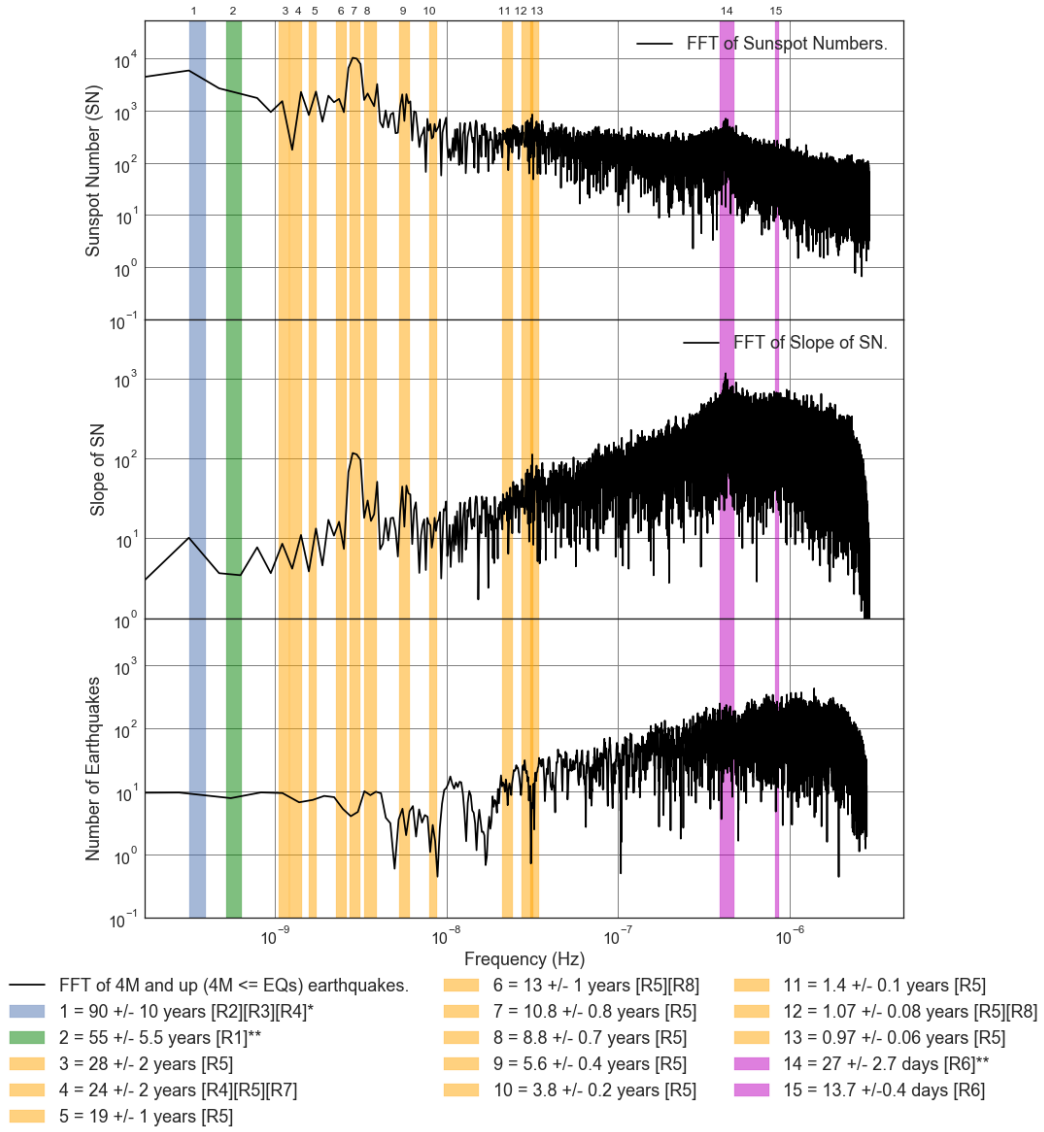

Figure E2.8: FFT Loglog Comparison Plot: Slope of Averaged 4M and up (4M <= EQs) Earthquake counts, Sunspot number (SN) and slope from 1818 to 2017. Additional meaning of the legend colors: Blue = Various Analysis techniques, Green = Meyer wavelet, Orange = Instantly maximal wavelet skeleton spectra, Magenta = Periodram and Linear phase finite impulse response.

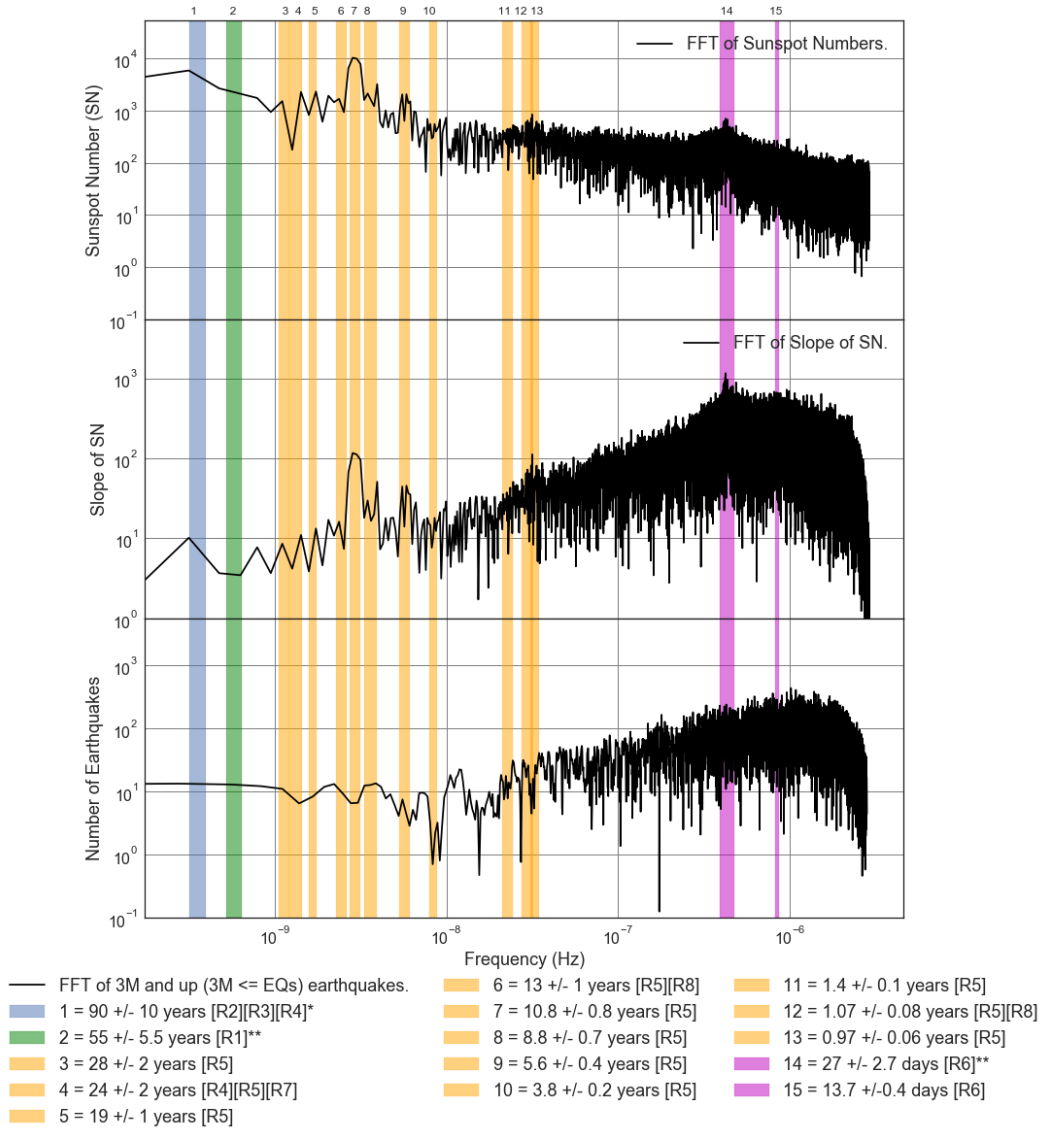

Figure E2.9: FFT Loglog Comparison Plot: Slope of Averaged 3M and up (3M <= EQs) Earthquake counts, Sunspot number (SN) and slope from 1818 to 2017. Additional meaning of the legend colors: Blue = Various Analysis techniques, Green = Meyer wavelet, Orange = Instantly maximal wavelet skeleton spectra, Magenta = Periodram and Linear phase finite impulse response.

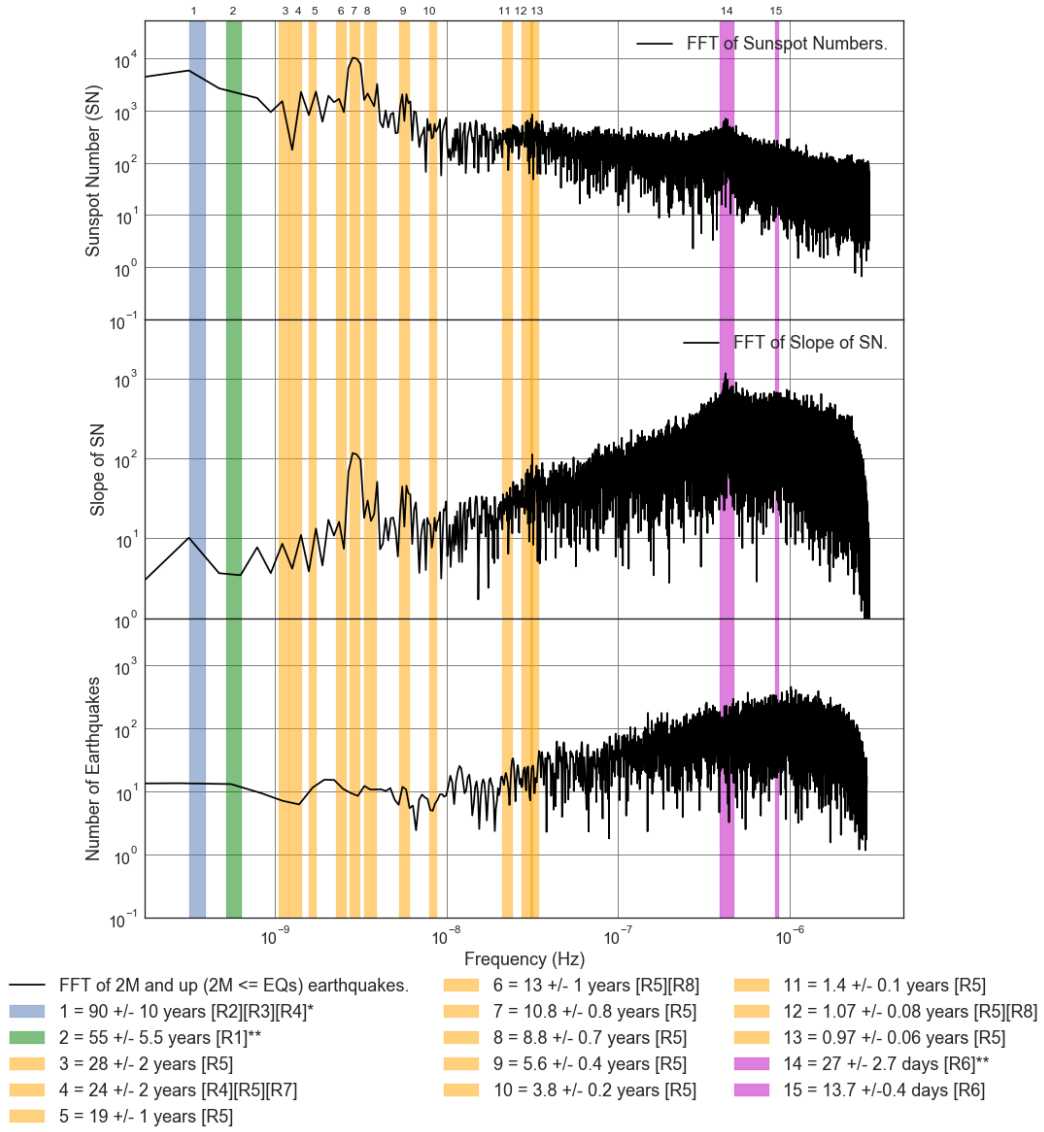

Figure E2.10: FFT Loglog Comparison Plot: Slope of Averaged 2M and up (2M <= EQs) Earthquake counts, Sunspot number (SN) and slope from 1818 to 2017. Additional meaning of the legend colors: Blue = Various Analysis techniques, Green = Meyer wavelet, Orange = Instantly maximal wavelet skeleton spectra, Magenta = Periodram and Linear phase finite impulse response.

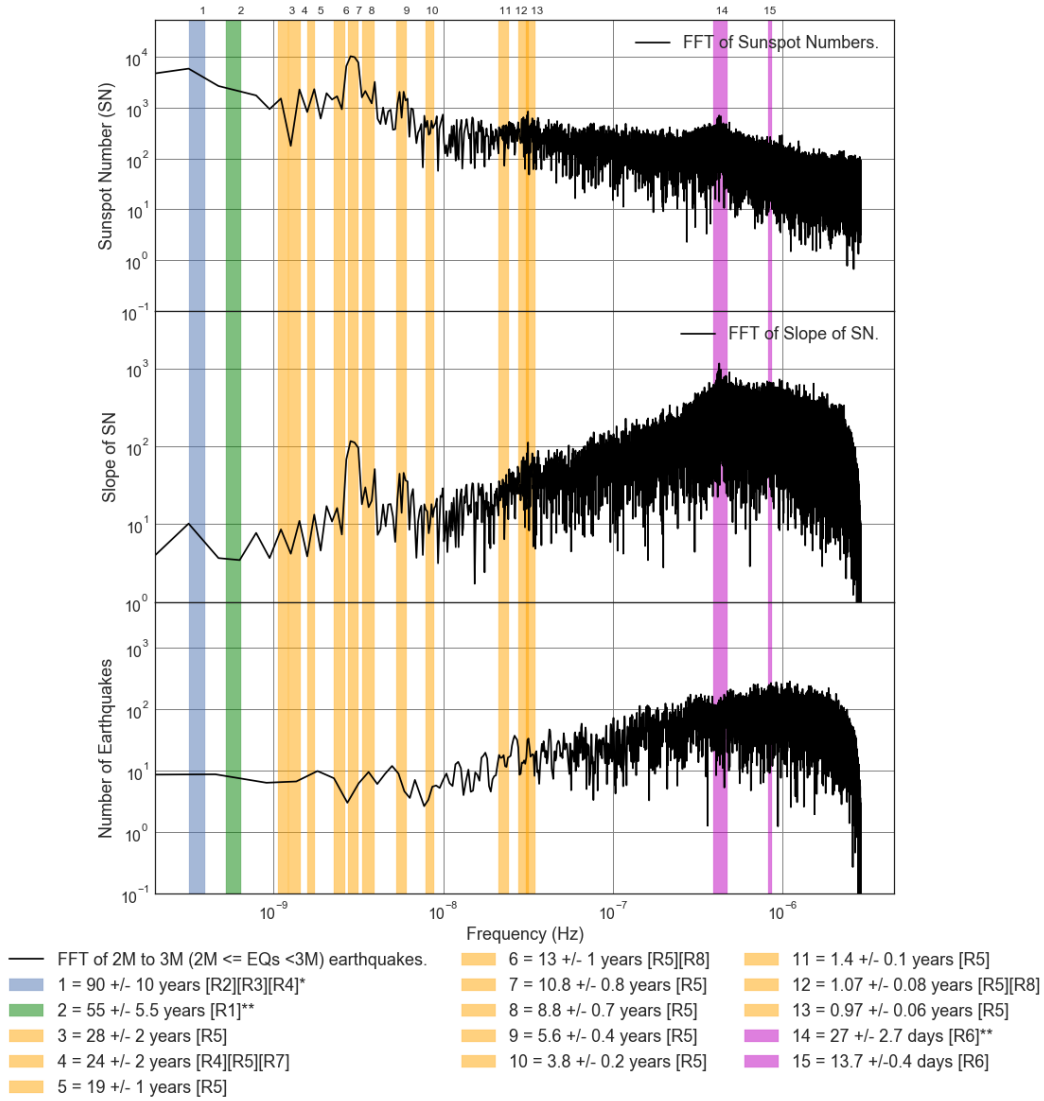

Figure E2.11: FFT Loglog Comparison Plot: Slope of Averaged 2M to 3M (2M <= EQs <3M) Earthquake counts, Sunspot number (SN) and slope from 1818 to 2017. Additional meaning of the legend colors: Blue = Various Analysis techniques, Green = Meyer wavelet, Orange = Instantly maximal wavelet skeleton spectra, Magenta = Periodram and Linear phase finite impulse response.

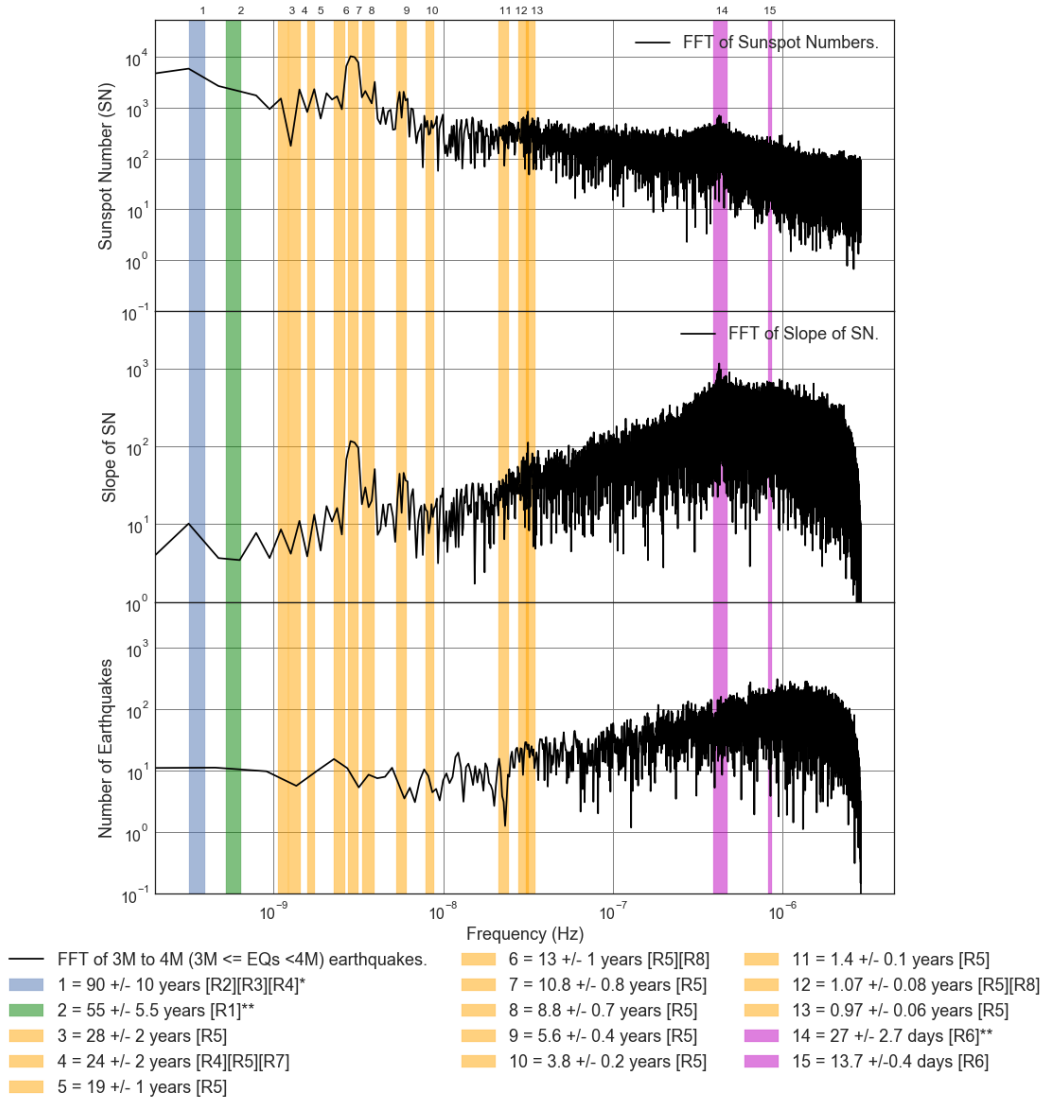

Figure E2.12: FFT Loglog Comparison Plot: Slope of Averaged 3M to 4M (3M <= EQs <4M) Earthquake counts, Sunspot number (SN) and slope from 1818 to 2017. Additional meaning of the legend colors: Blue = Various Analysis techniques, Green = Meyer wavelet, Orange = Instantly maximal wavelet skeleton spectra, Magenta = Periodram and Linear phase finite impulse response.

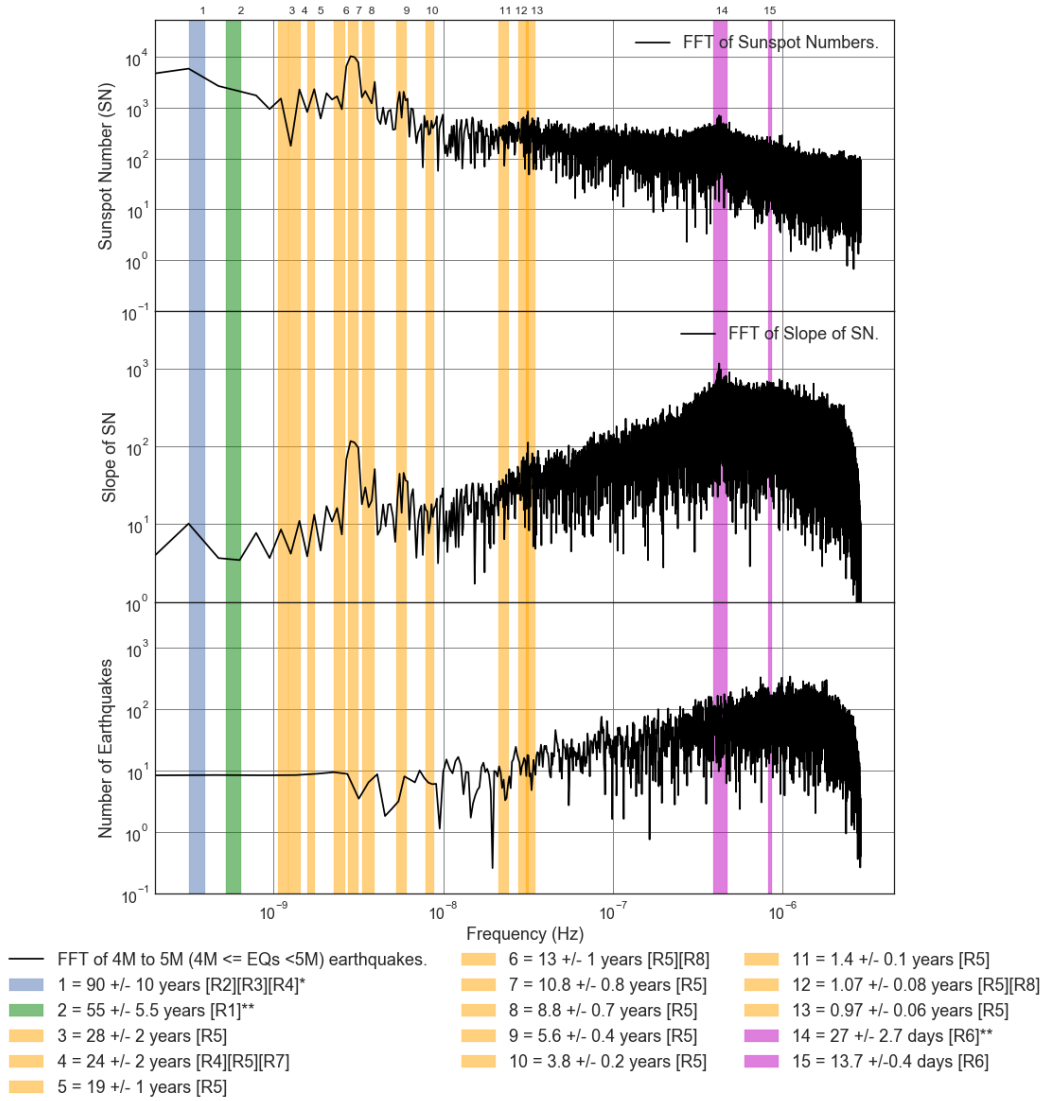

Figure E2.13: FFT Loglog Comparison Plot: Slope of Averaged 4M to 5M (4M <= EQs <5M) Earthquake counts, Sunspot number (SN) and slope from 1818 to 2017. Additional meaning of the legend colors: Blue = Various Analysis techniques, Green = Meyer wavelet, Orange = Instantly maximal wavelet skeleton spectra, Magenta = Periodram and Linear phase finite impulse response.

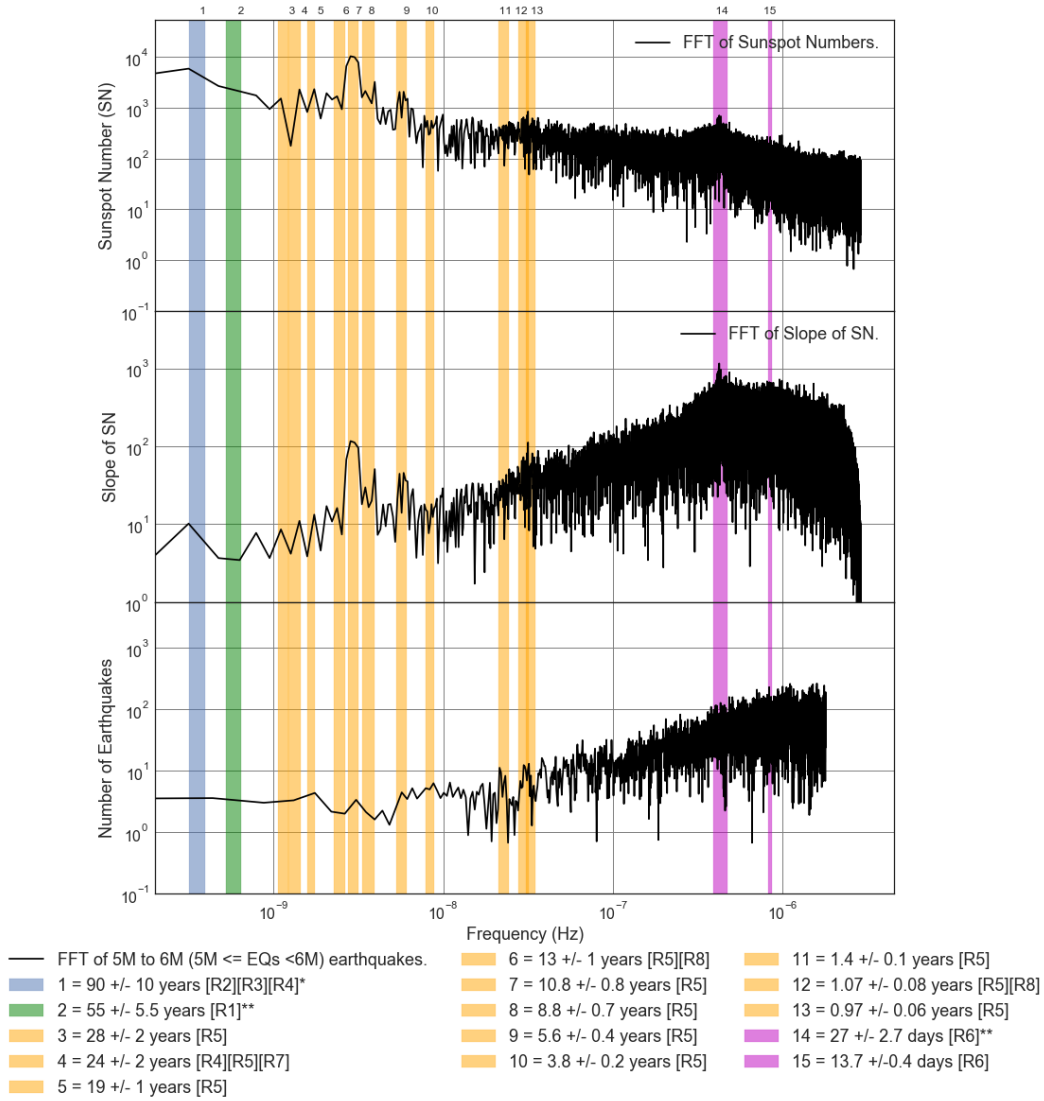

Figure E2.14: FFT Loglog Comparison Plot: Slope of Averaged 5M to 6M (5M <= EQs <6M) Earthquake counts, Sunspot number (SN) and slope from 1818 to 2017. Additional meaning of the legend colors: Blue = Various Analysis techniques, Green = Meyer wavelet, Orange = Instantly maximal wavelet skeleton spectra, Magenta = Periodram and Linear phase finite impulse response.

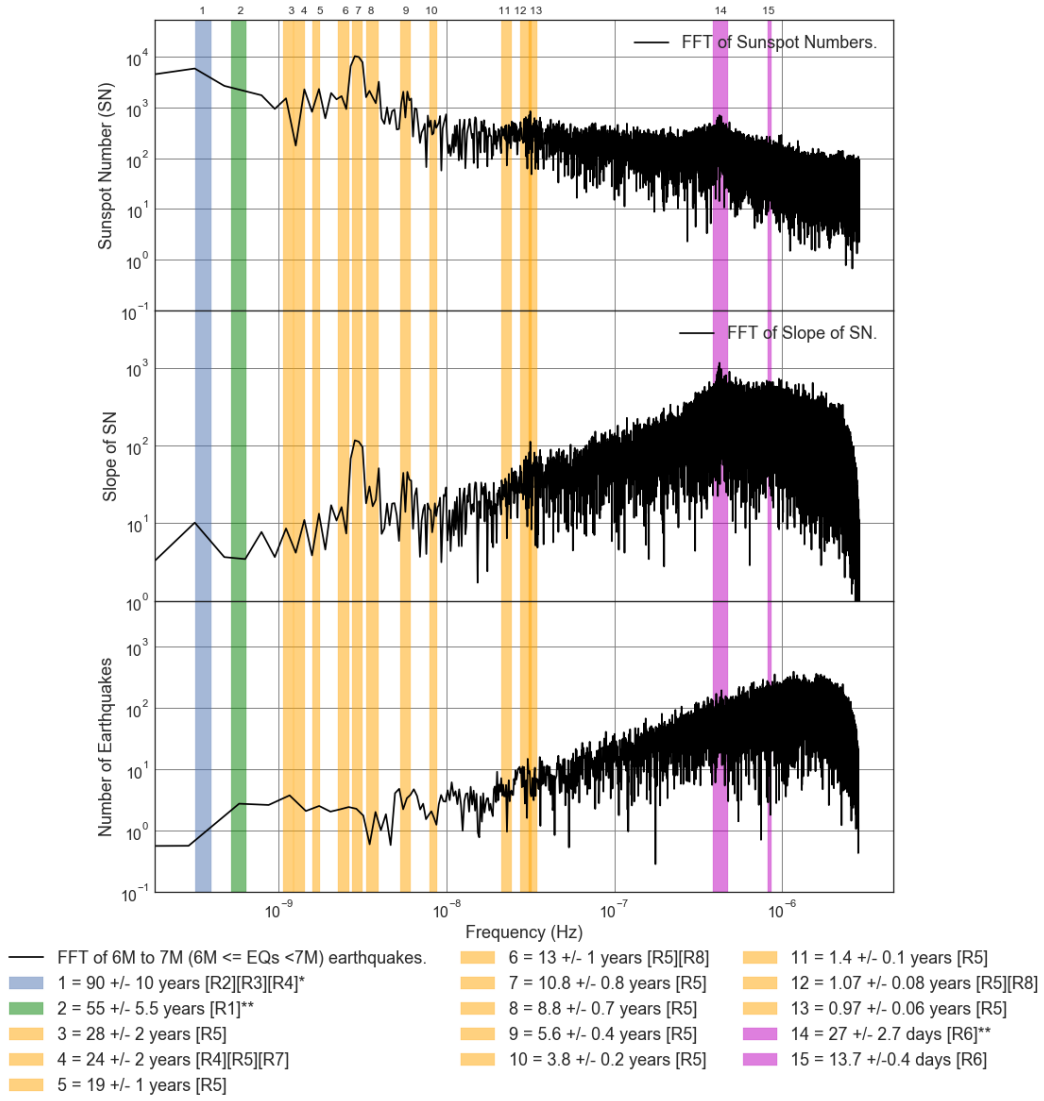

Figure E2.15: FFT Loglog Comparison Plot: Slope of Averaged 6M to 7M (6M <= EQs <7M) Earthquake counts, Sunspot number (SN) and slope from 1818 to 2017. Additional meaning of the legend colors: Blue = Various Analysis techniques, Green = Meyer wavelet, Orange = Instantly maximal wavelet skeleton spectra, Magenta = Periodram and Linear phase finite impulse response.

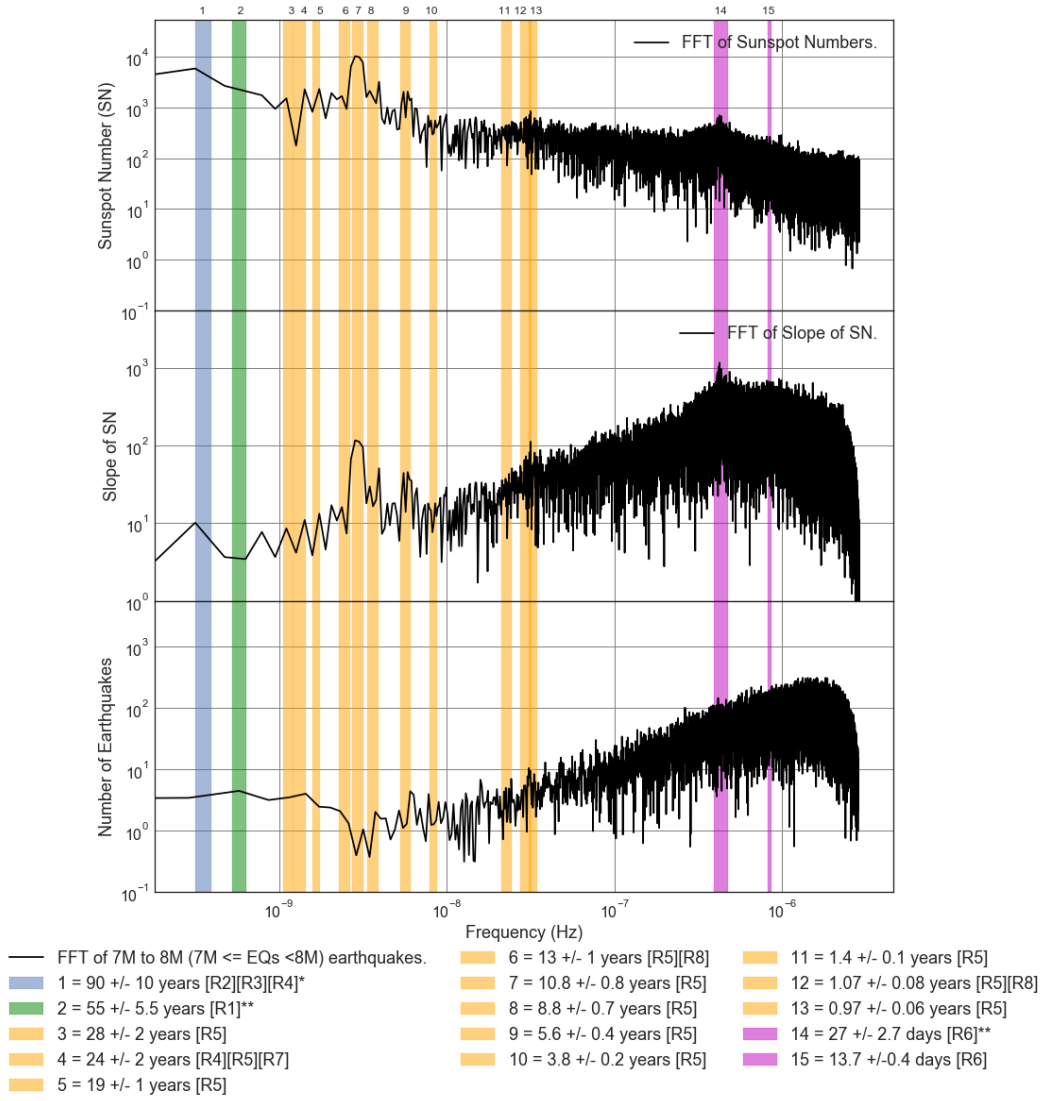

Figure E2.16: FFT Loglog Comparison Plot: Slope of Averaged 7M to 8M (7M <= EQs <8M) Earthquake counts, Sunspot number (SN) and slope from 1818 to 2017. Additional meaning of the legend colors: Blue = Various Analysis techniques, Green = Meyer wavelet, Orange = Instantly maximal wavelet skeleton spectra, Magenta = Periodram and Linear phase finite impulse response.

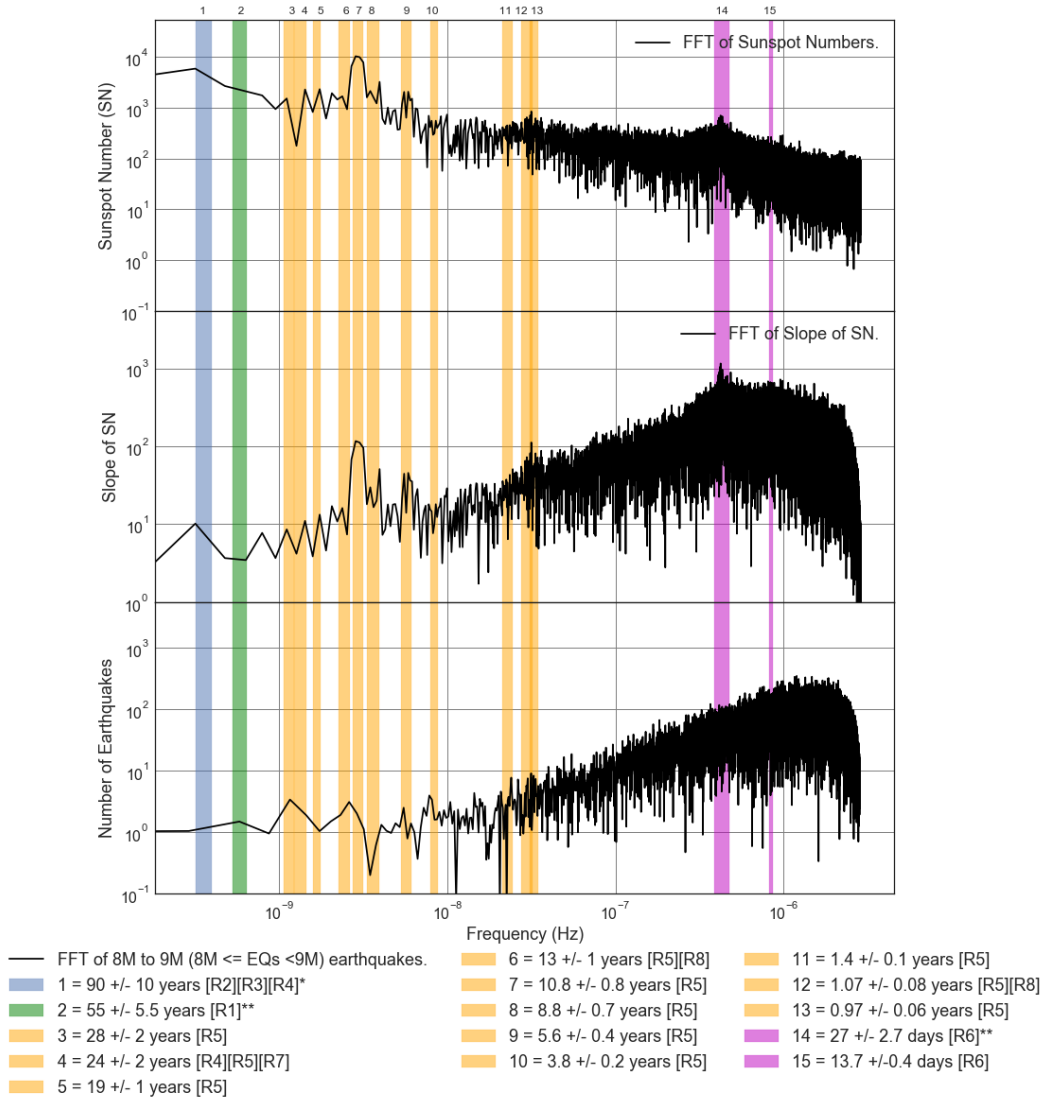

Figure E2.17: FFT Loglog Comparison Plot: Slope of Averaged 8M to 9M (8M <= EQs <9M) Earthquake counts, Sunspot number (SN) and slope from 1818 to 2017. Additional meaning of the legend colors: Blue = Various Analysis techniques, Green = Meyer wavelet, Orange = Instantly maximal wavelet skeleton spectra, Magenta = Periodram and Linear phase finite impulse response.

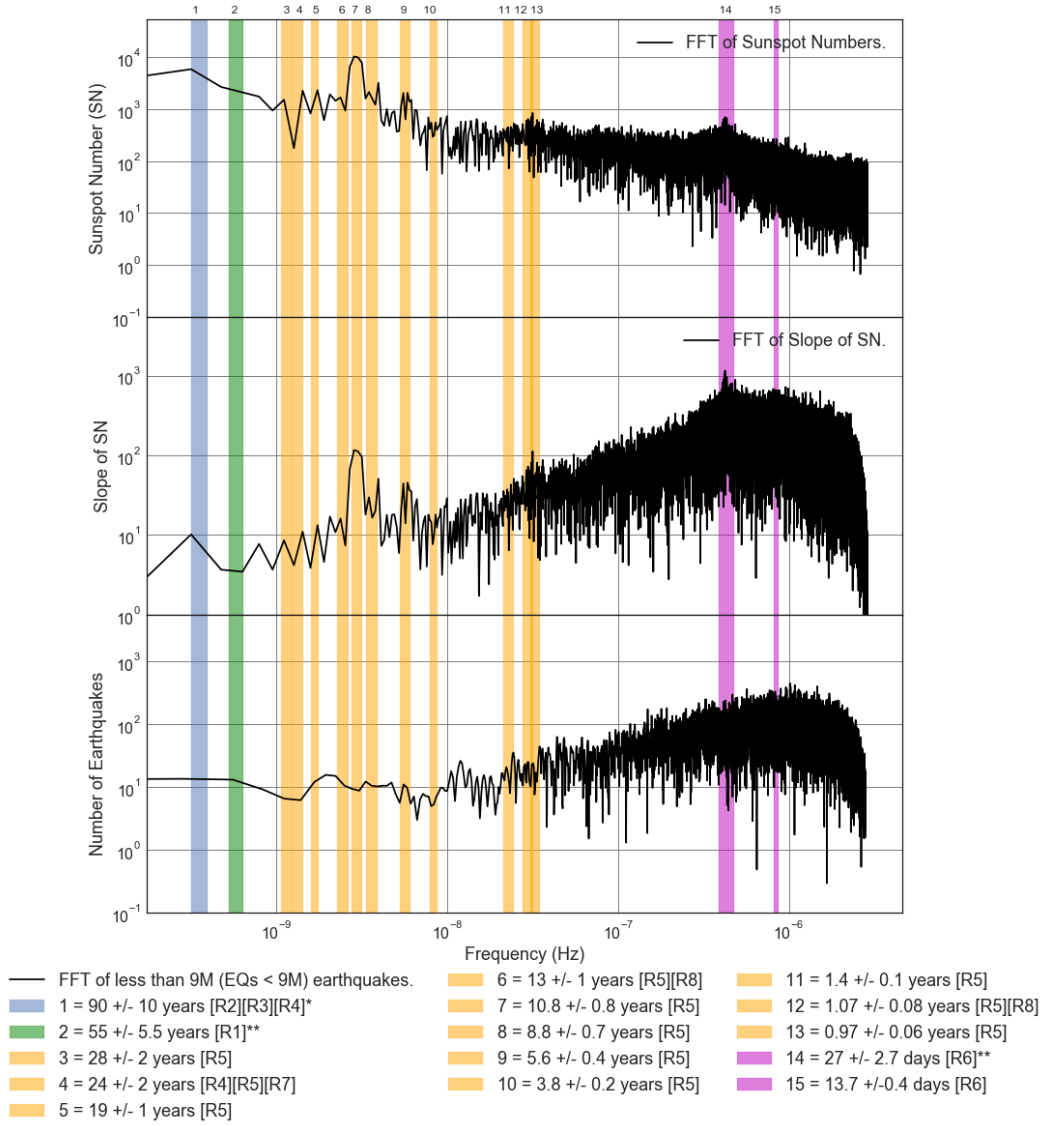

Figure E2.18: FFT Loglog Comparison Plot: Slope of Averaged less than 9M (EQs < 9M) Earthquake counts, Sunspot number (SN) and slope from 1818 to 2017. Additional meaning of the legend colors: Blue = Various Analysis techniques, Green = Meyer wavelet, Orange = Instantly maximal wavelet skeleton spectra, Magenta = Periodram and Linear phase finite impulse response.

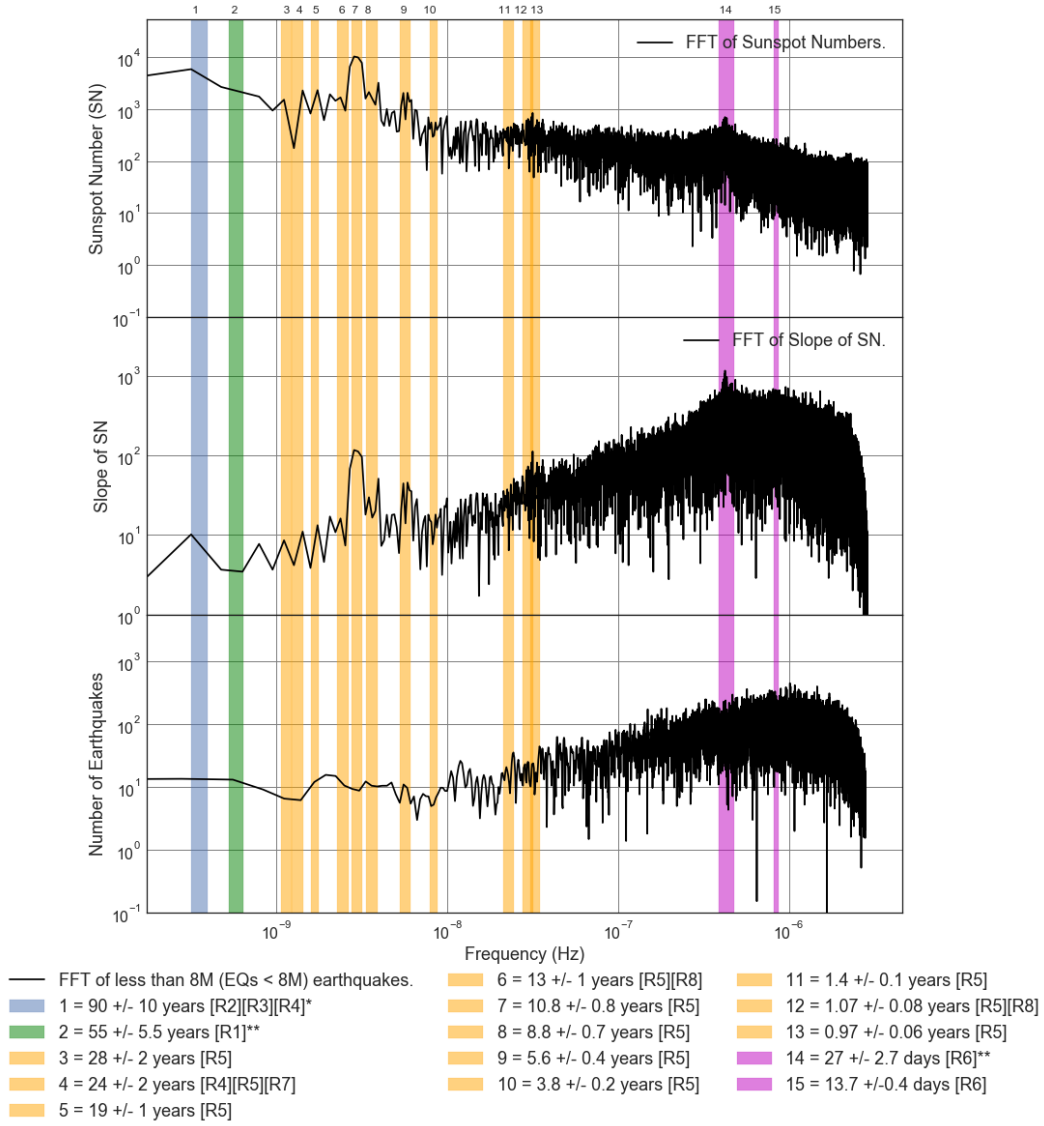

Figure E2.19: FFT Loglog Comparison Plot: Slope of Averaged less than 8M (EQs < 8M) Earthquake counts, Sunspot number (SN) and slope from 1818 to 2017. Additional meaning of the legend colors: Blue = Various Analysis techniques, Green = Meyer wavelet, Orange = Instantly maximal wavelet skeleton spectra, Magenta = Periodram and Linear phase finite impulse response.

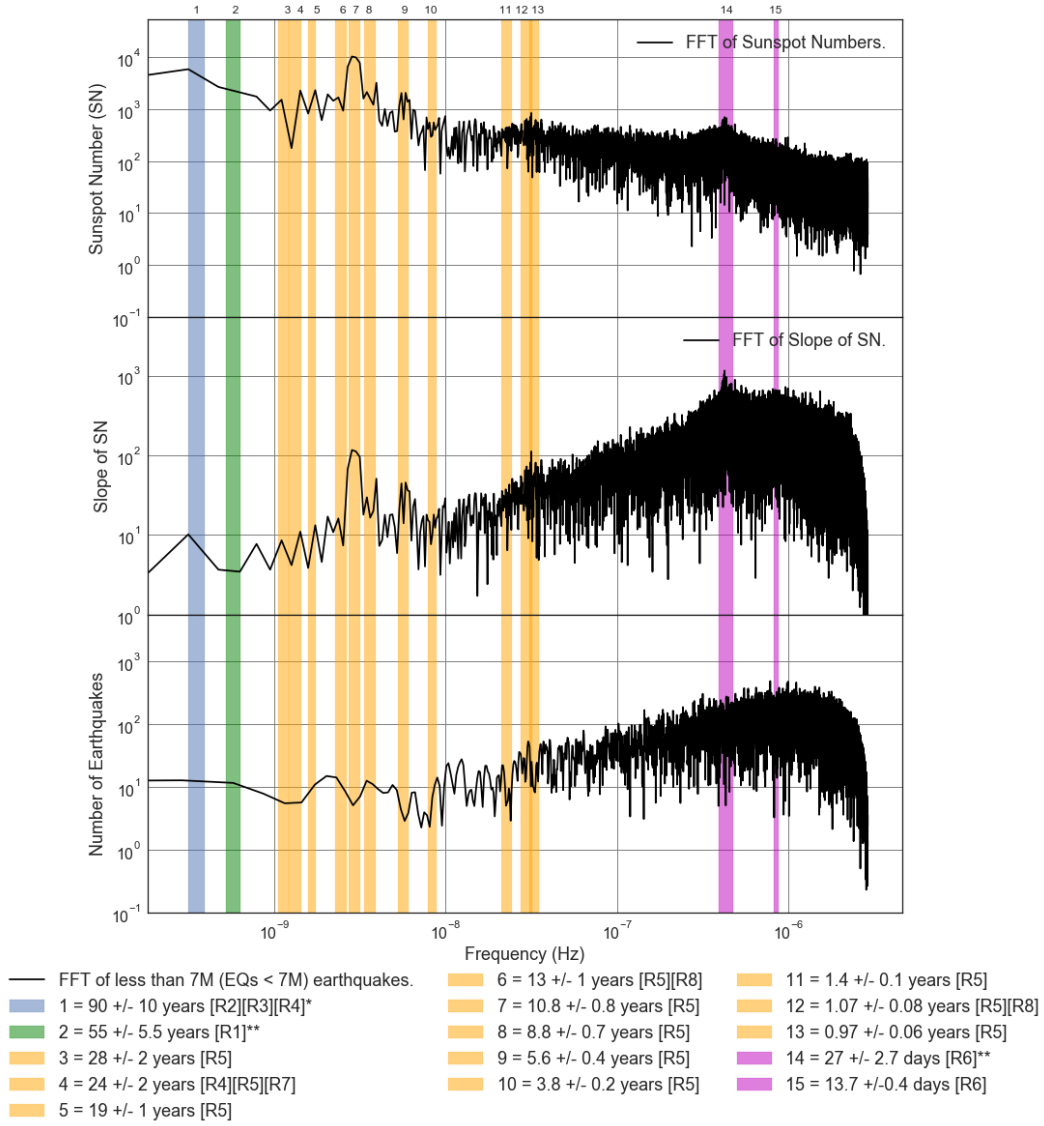

Figure E2.20: FFT Loglog Comparison Plot: Slope of Averaged less than 7M (EQs < 7M) Earthquake counts, Sunspot number (SN) and slope from 1818 to 2017. Additional meaning of the legend colors: Blue = Various Analysis techniques, Green = Meyer wavelet, Orange = Instantly maximal wavelet skeleton spectra, Magenta = Periodram and Linear phase finite impulse response.

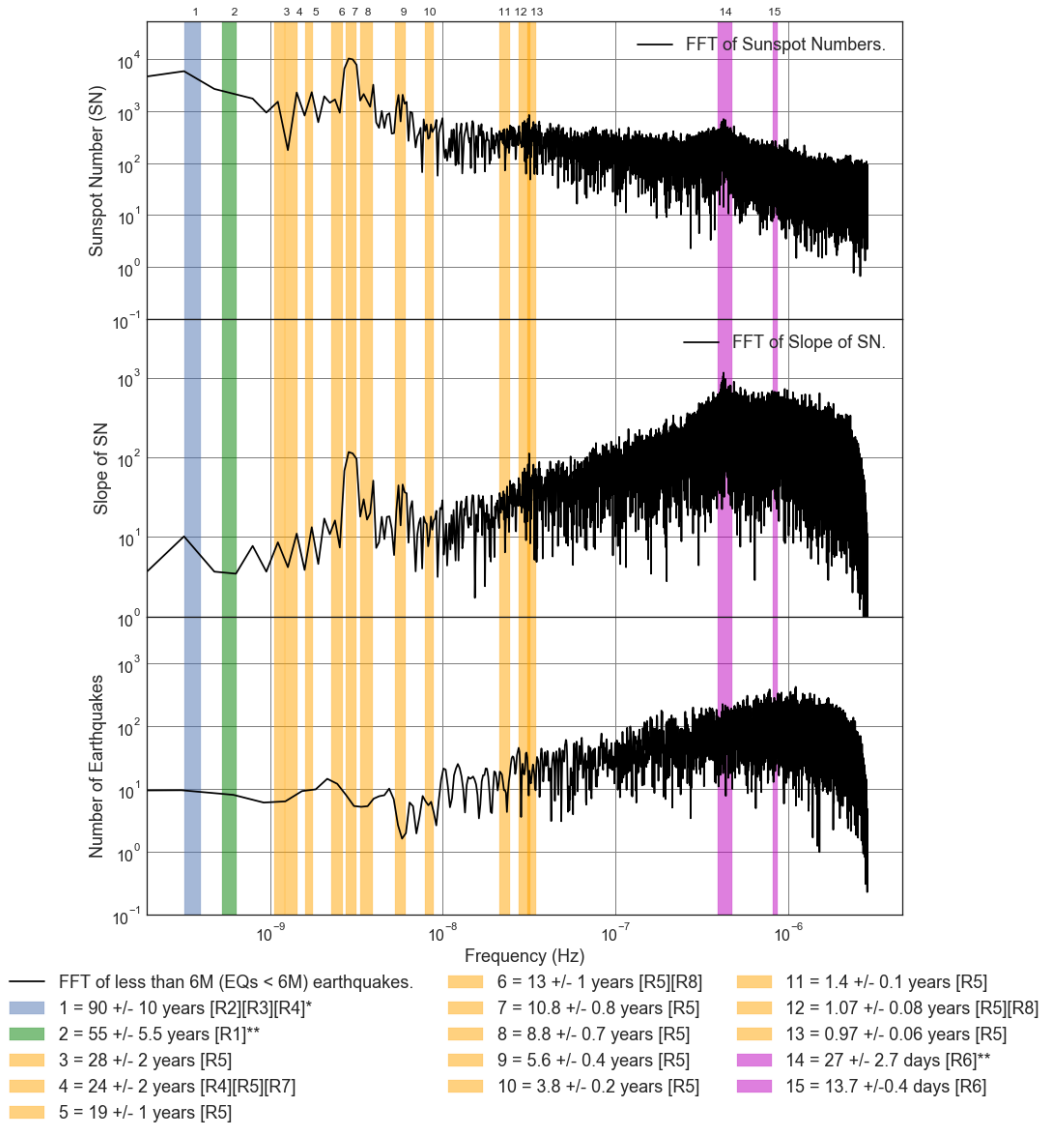

Figure E2.21: FFT Loglog Comparison Plot: Slope of Averaged less than 6M (EQs < 6M) Earthquake counts, Sunspot number (SN) and slope from 1818 to 2017. Additional meaning of the legend colors: Blue = Various Analysis techniques, Green = Meyer wavelet, Orange = Instantly maximal wavelet skeleton spectra, Magenta = Periodram and Linear phase finite impulse response.

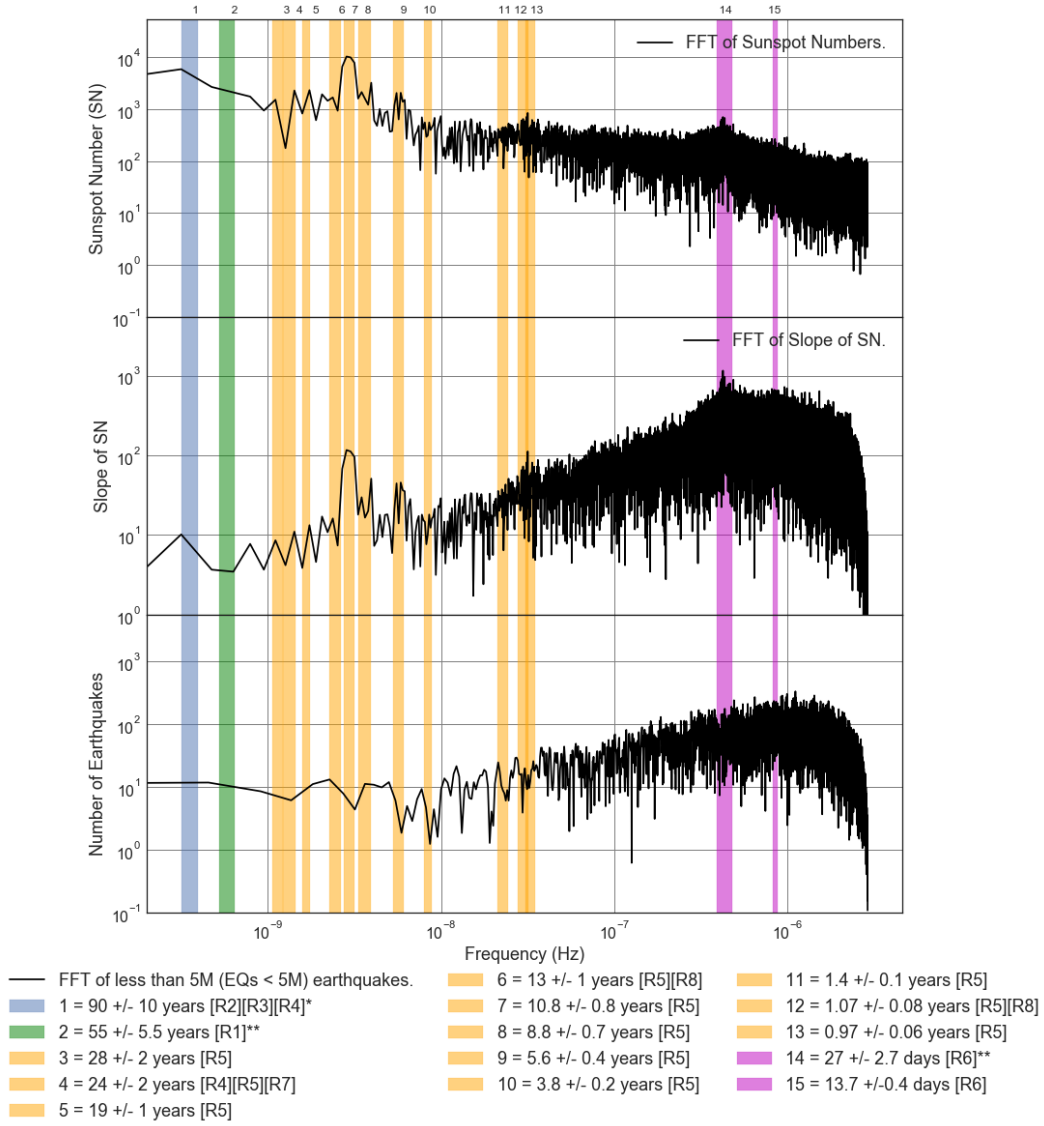

Figure E2.22: FFT Loglog Comparison Plot: Slope of Averaged less than 5M (EQs < 5M) Earthquake counts, Sunspot number (SN) and slope from 1818 to 2017. Additional meaning of the legend colors: Blue = Various Analysis techniques, Green = Meyer wavelet, Orange = Instantly maximal wavelet skeleton spectra, Magenta = Periodram and Linear phase finite impulse response.

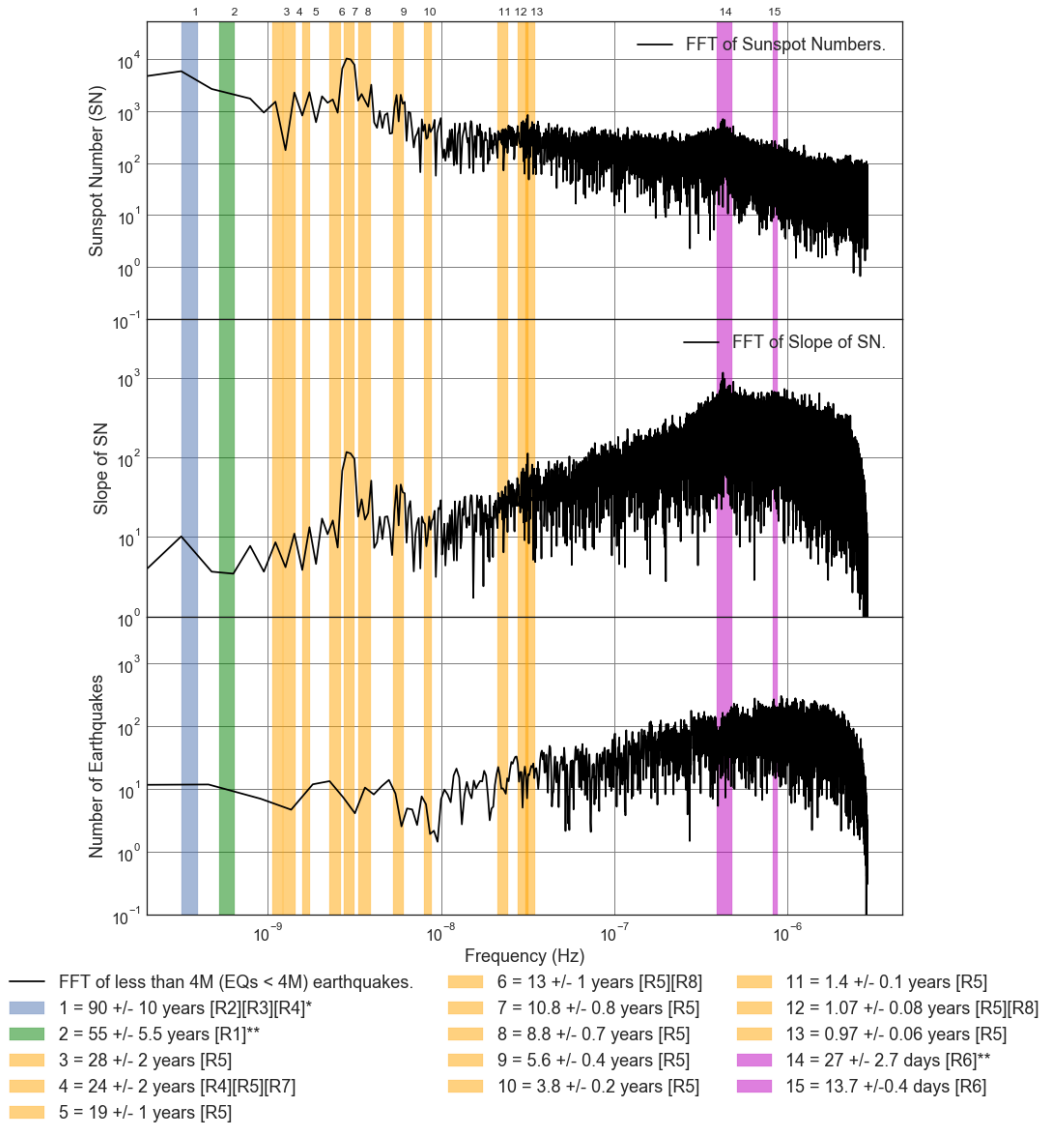

Figure E2.23: FFT Loglog Comparison Plot: Slope of Averaged less than 4M (EQs < 4M) Earthquake counts, Sunspot number (SN) and slope from 1818 to 2017. Additional meaning of the legend colors: Blue = Various Analysis techniques, Green = Meyer wavelet, Orange = Instantly maximal wavelet skeleton spectra, Magenta = Periodram and Linear phase finite impulse response.

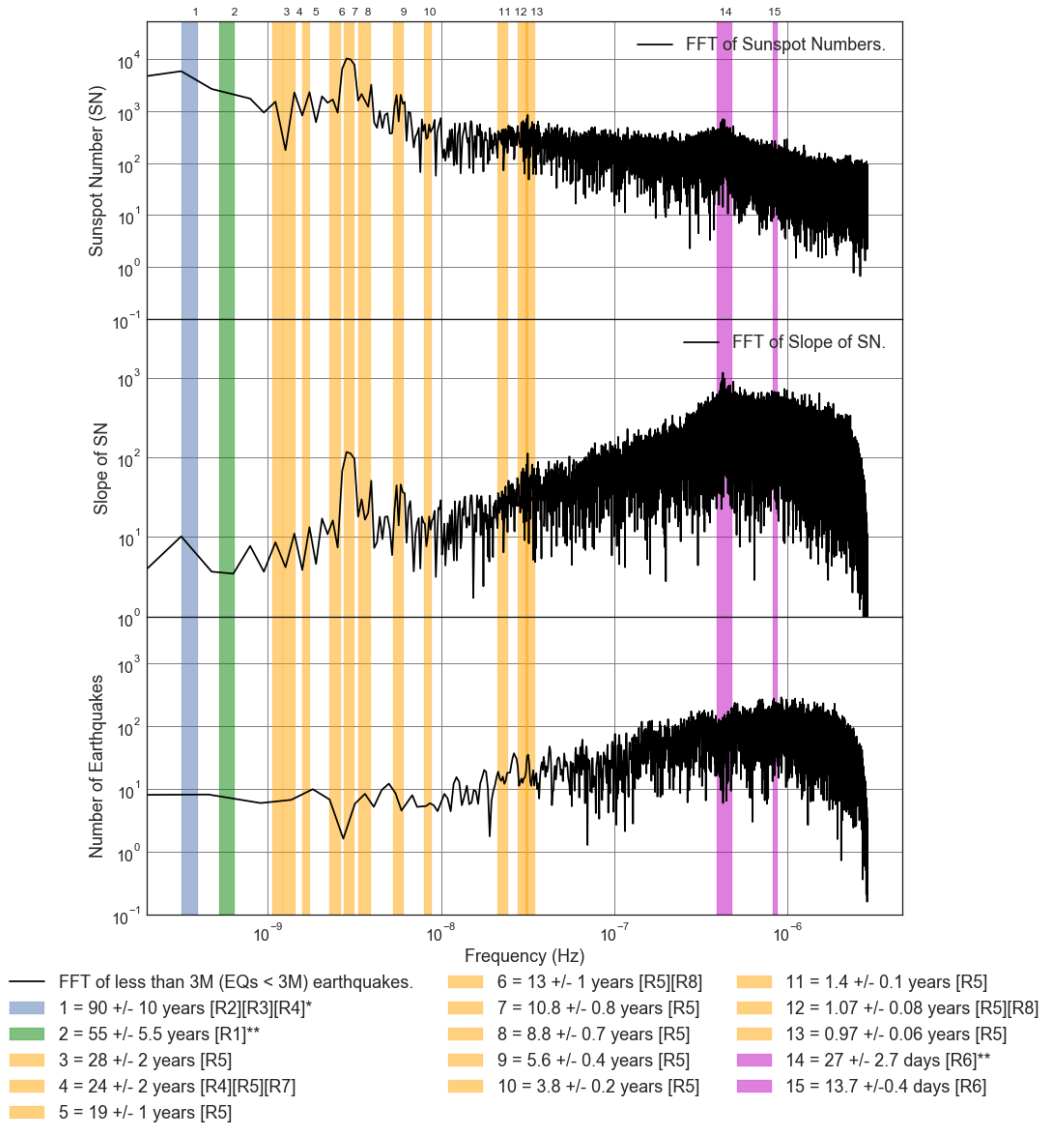

Figure E2.24: FFT Loglog Comparison Plot: Slope of Averaged less than 3M (EQs < 3M) Earthquake counts, Sunspot number (SN) and slope from 1818 to 2017. Additional meaning of the legend colors: Blue = Various Analysis techniques, Green = Meyer wavelet, Orange = Instantly maximal wavelet skeleton spectra, Magenta = Periodram and Linear phase finite impulse response.

Comparison Plots of Averaged FFT Earthquake Spectra for Slope of Earthquake Energy Released

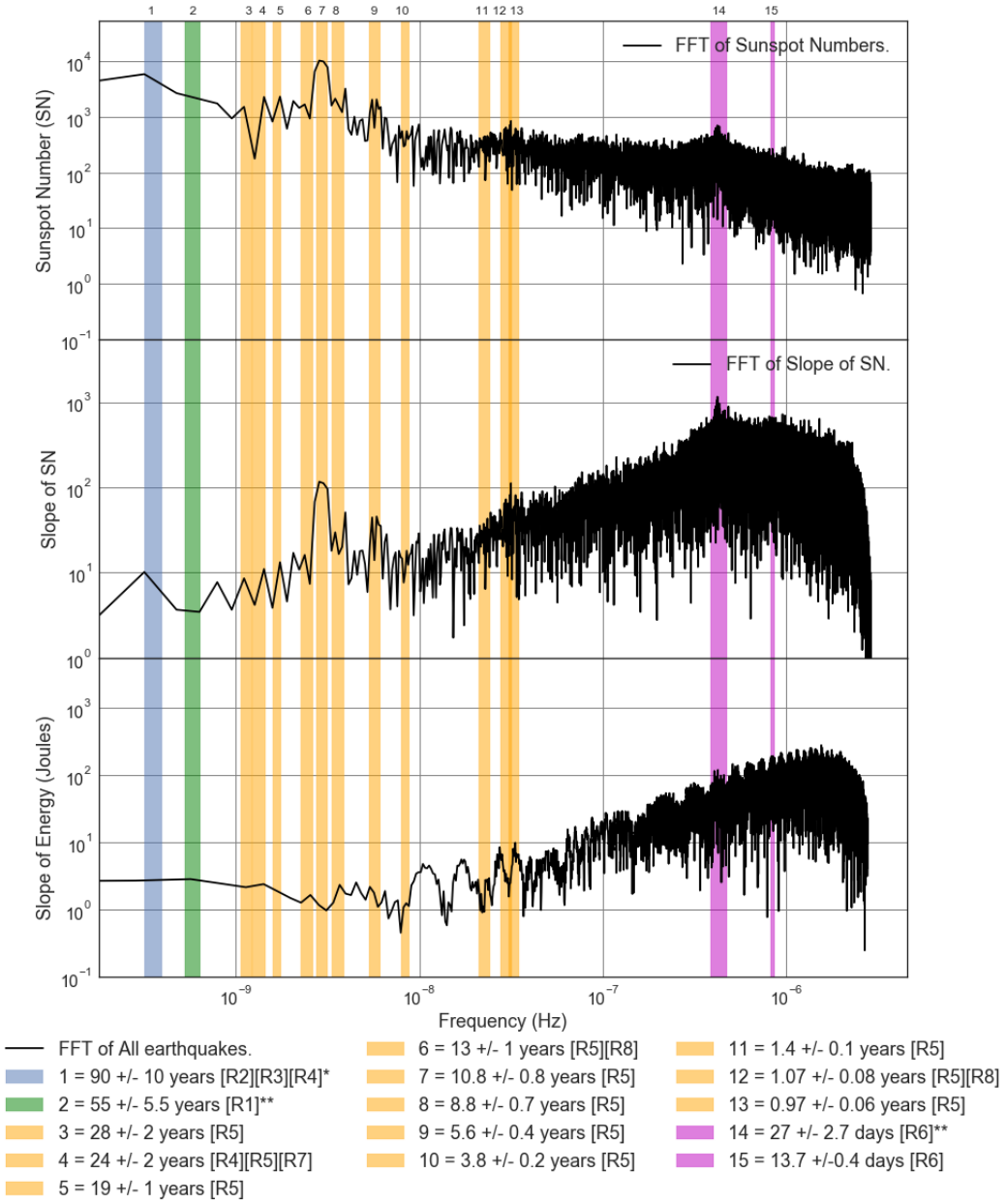

Figure E2.25: FFT Loglog Comparison Plot: Slope of Averaged All Earthquake (EQ) total energy released, 2 Day Sunspot number and slope from 1818 to 2017. Additional meaning of the legend colors: Blue = Various Analysis techniques, Green = Meyer wavelet, Orange = Instantly maximal wavelet skeleton spectra, Magenta = Periodram and Linear phase finite impulse response.

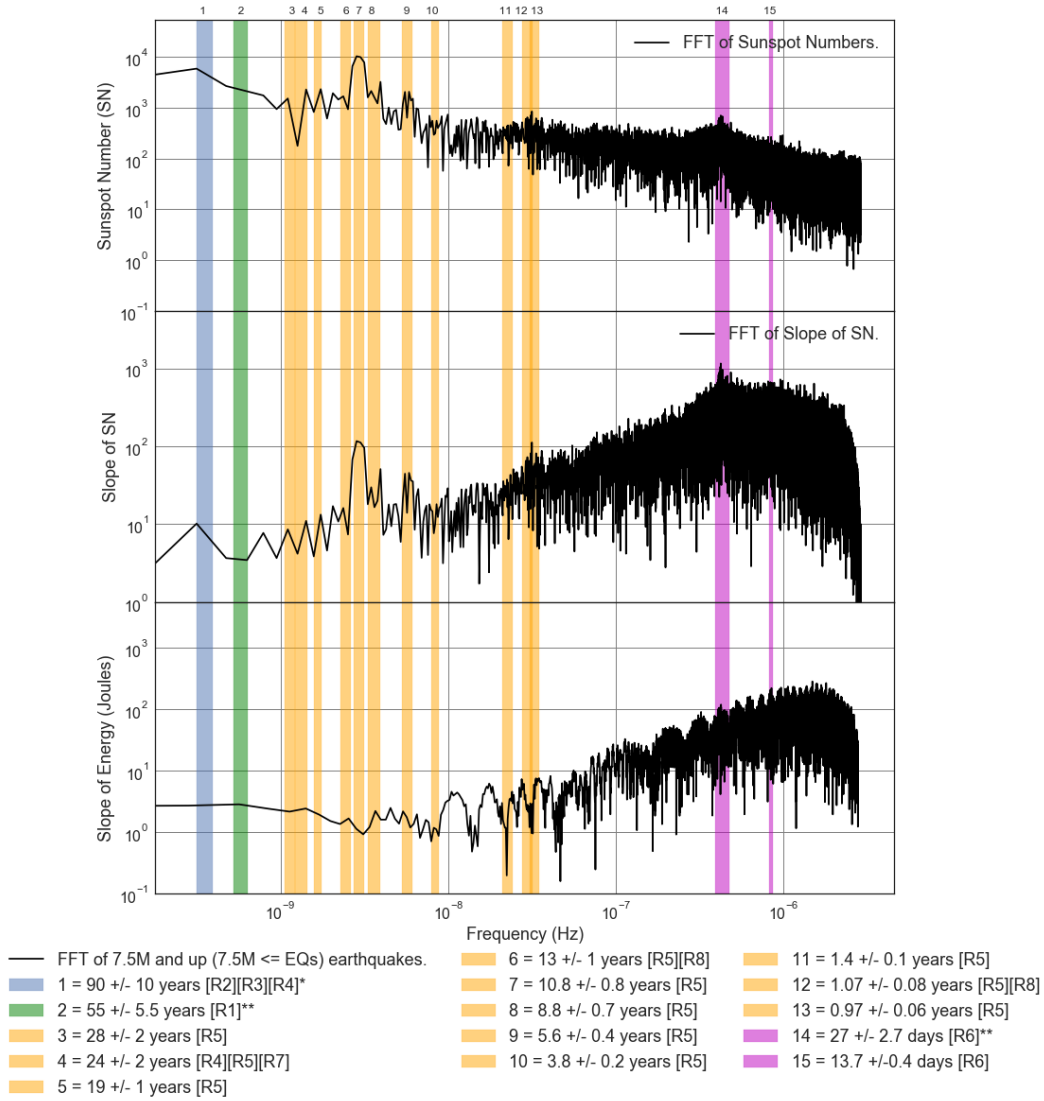

Figure E2.26: FFT Loglog Comparison Plot: Slope of Averaged 7.5M and up (7.5M <= EQs) Earthquake (EQ) total energy released, 2 Day Sunspot number and slope from 1818 to 2017. Additional meaning of the legend colors: Blue = Various Analysis techniques, Green = Meyer wavelet, Orange = Instantly maximal wavelet skeleton spectra, Magenta = Periodram and Linear phase finite impulse response.

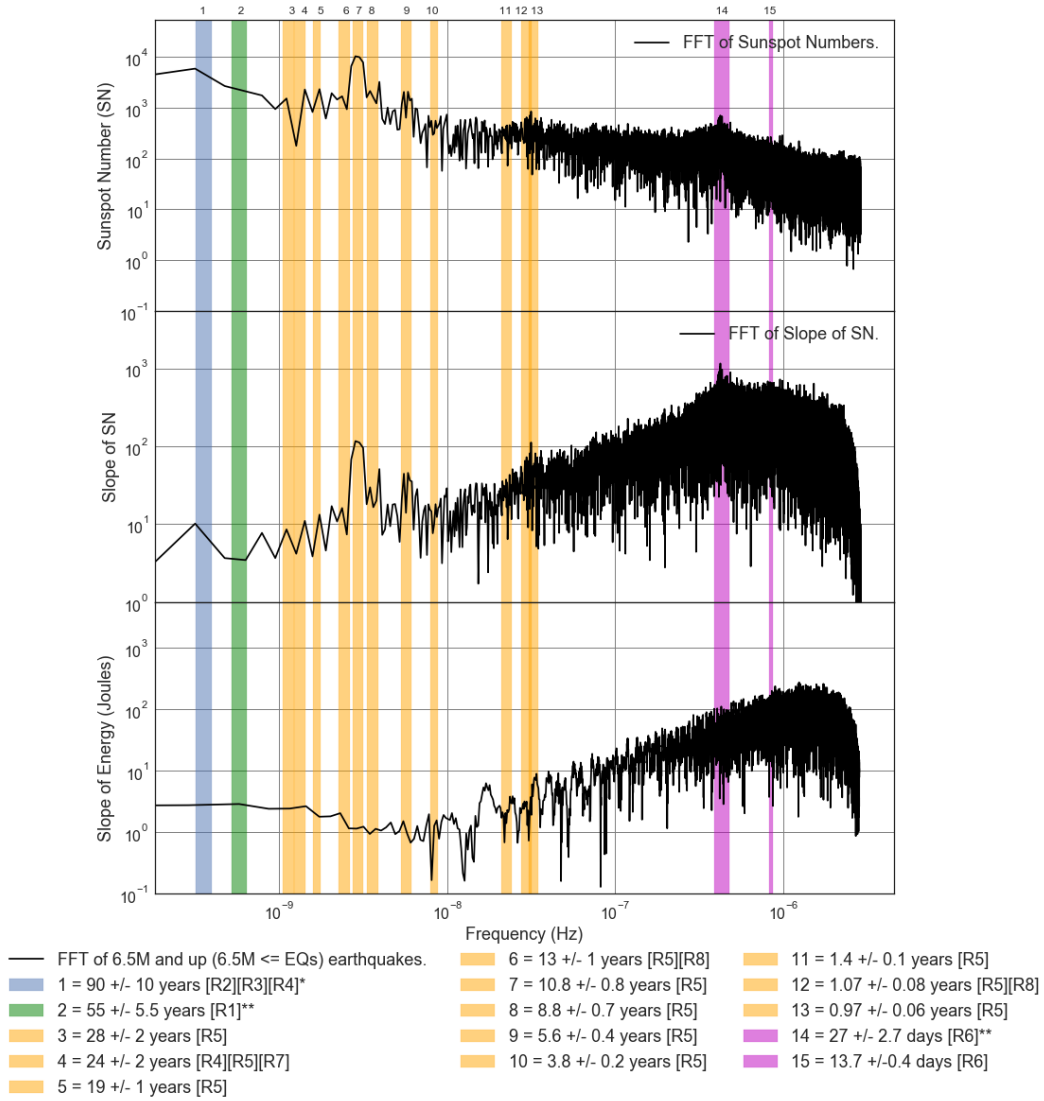

Figure E2.27: FFT Loglog Comparison Plot: Slope of Averaged 6.5M and up (6.5M <= EQs) Earthquake (EQ) total energy released, 2 Day Sunspot number and slope from 1818 to 2017. Additional meaning of the legend colors: Blue = Various Analysis techniques, Green = Meyer wavelet, Orange = Instantly maximal wavelet skeleton spectra, Magenta = Periodram and Linear phase finite impulse response.

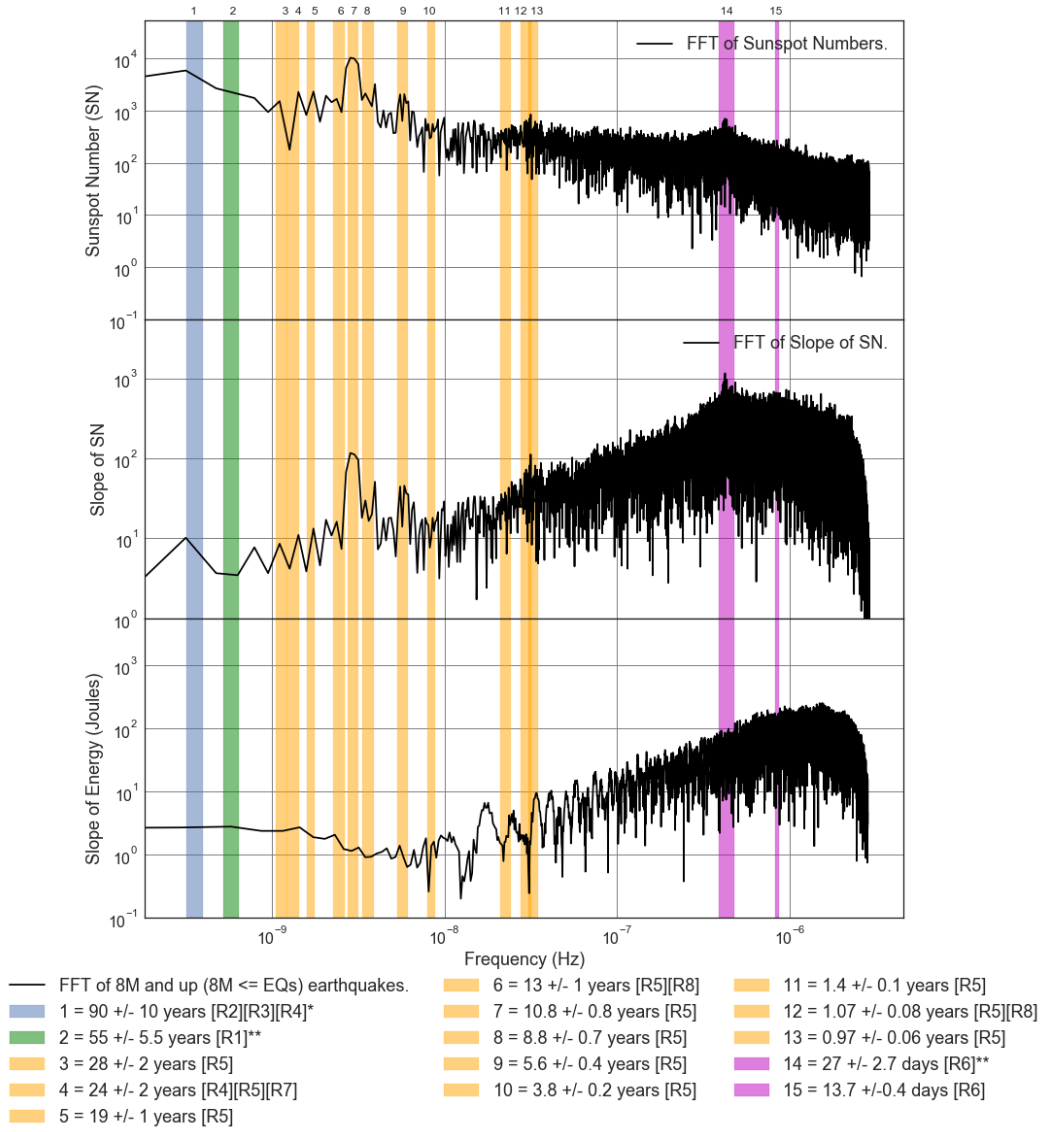

Figure E2.28: FFT Loglog Comparison Plot: Slope of Averaged 8M and up (8M <= EQs) Earthquake (EQ) total energy released, 2 Day Sunspot number and slope from 1818 to 2017. Additional meaning of the legend colors: Blue = Various Analysis techniques, Green = Meyer wavelet, Orange = Instantly maximal wavelet skeleton spectra, Magenta = Periodram and Linear phase finite impulse response.

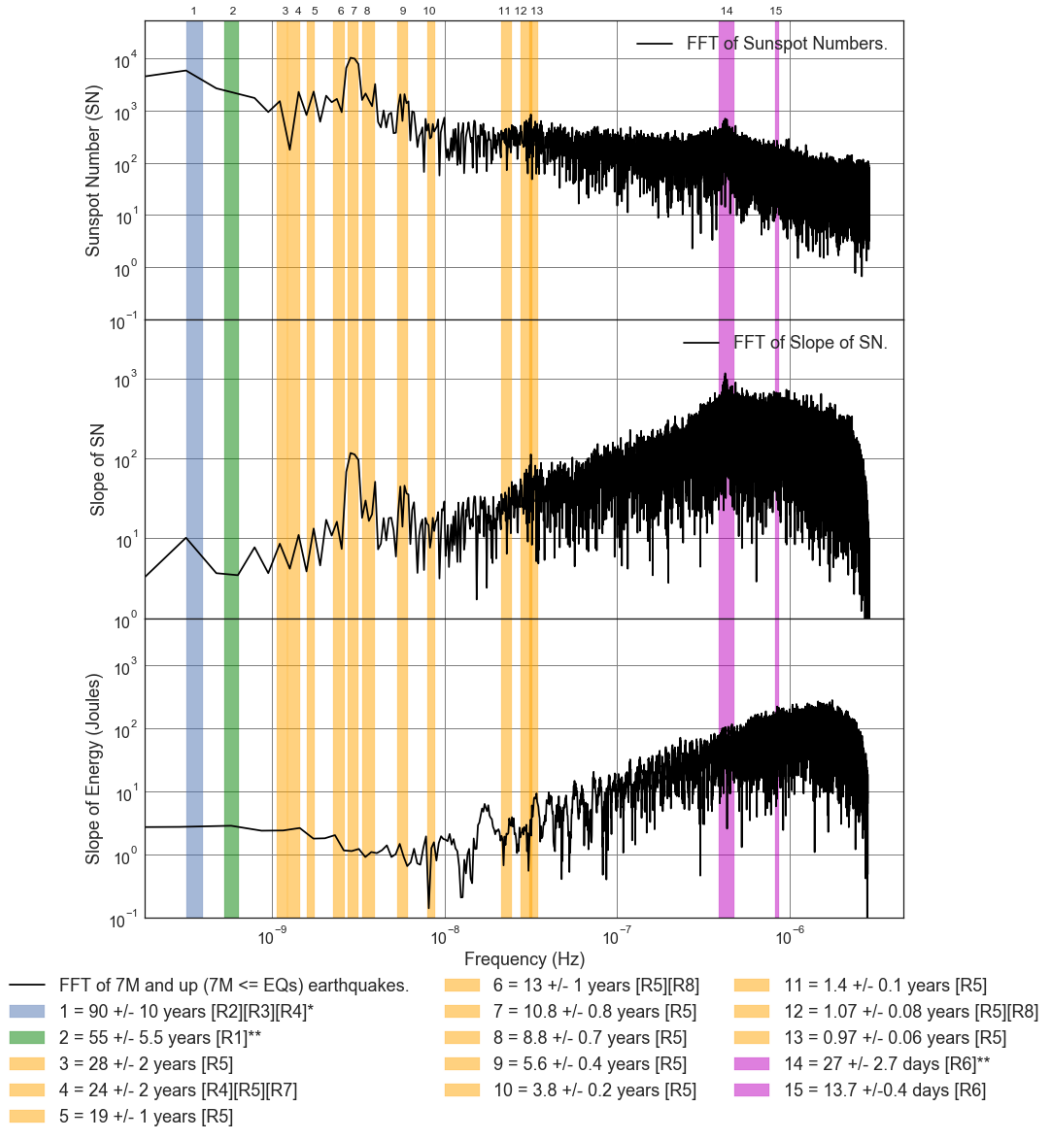

Figure E2.29: FFT Loglog Comparison Plot: Slope of Averaged 7M and up (7M <= EQs) Earthquake (EQ) total energy released, 2 Day Sunspot number and slope from 1818 to 2017. Additional meaning of the legend colors: Blue = Various Analysis techniques, Green = Meyer wavelet, Orange = Instantly maximal wavelet skeleton spectra, Magenta = Periodram and Linear phase finite impulse response.

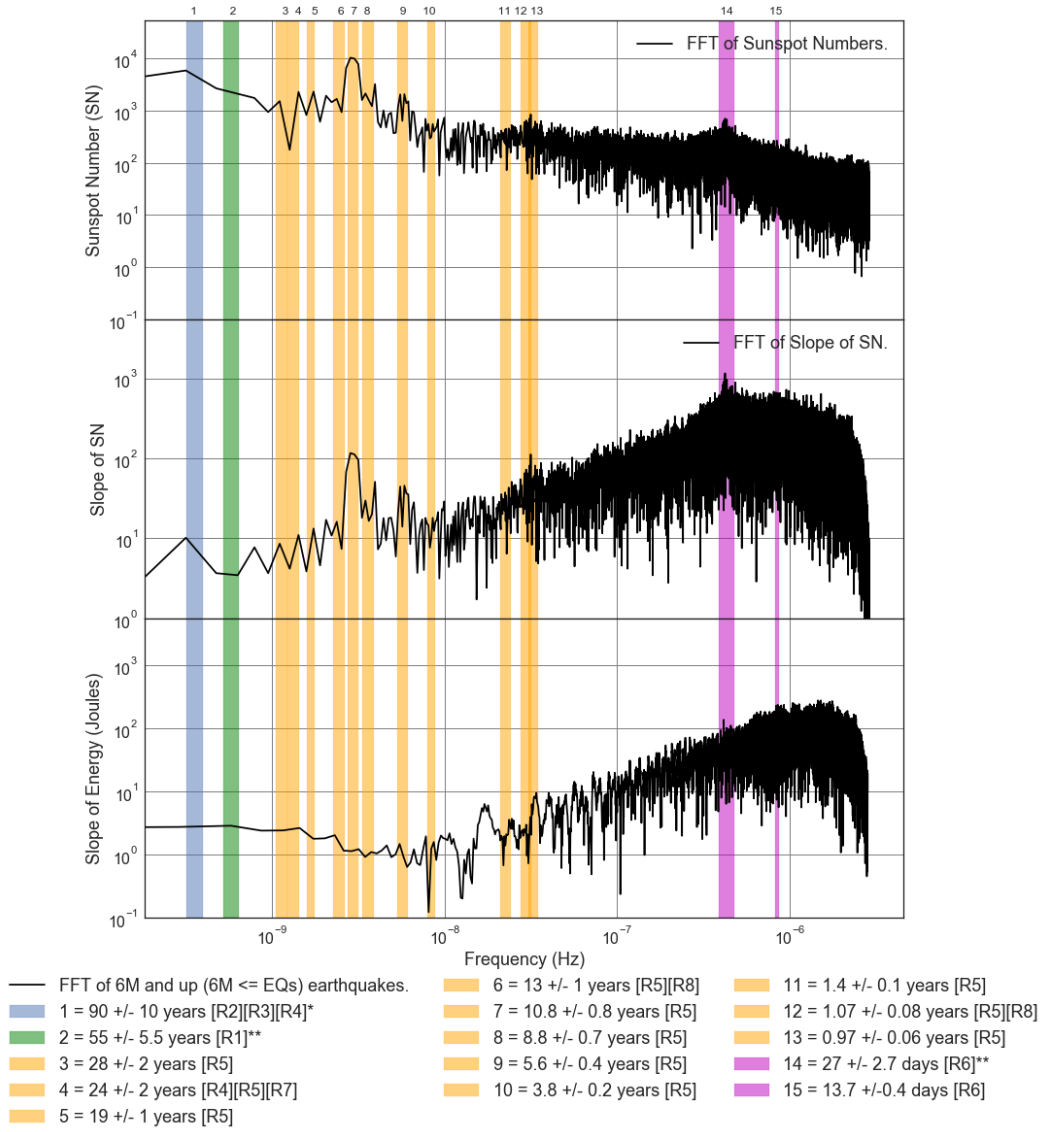

Figure E2.30: FFT Loglog Comparison Plot: Slope of Averaged 6M and up (6M <= EQs) Earthquake (EQ) total energy released, 2 Day Sunspot number and slope from 1818 to 2017. Additional meaning of the legend colors: Blue = Various Analysis techniques, Green = Meyer wavelet, Orange = Instantly maximal wavelet skeleton spectra, Magenta = Periodram and Linear phase finite impulse response.

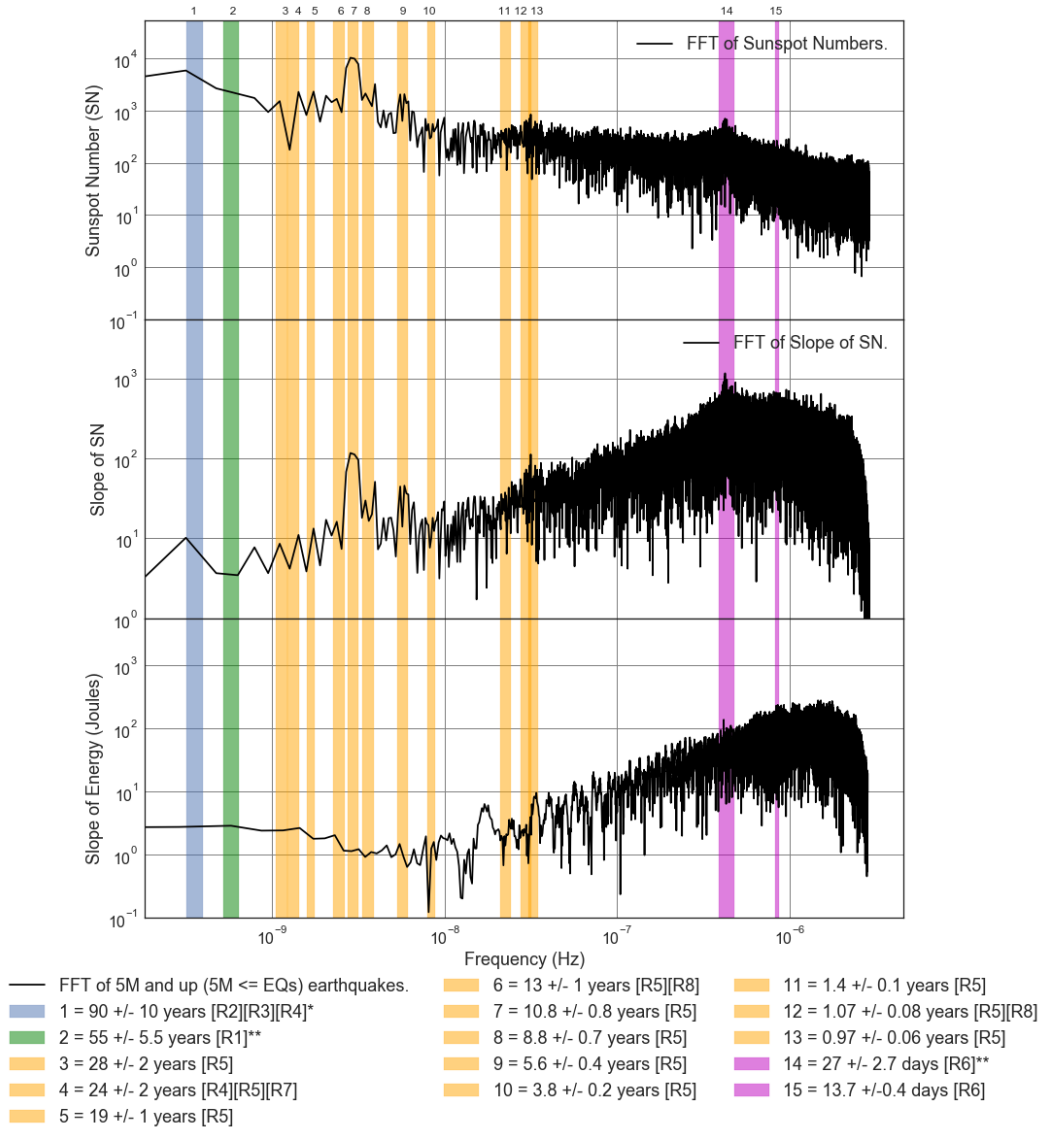

Figure E2.31: FFT Loglog Comparison Plot: Slope of Averaged 5M and up (5M <= EQs) Earthquake (EQ) total energy released, 2 Day Sunspot number and slope from 1818 to 2017. Additional meaning of the legend colors: Blue = Various Analysis techniques, Green = Meyer wavelet, Orange = Instantly maximal wavelet skeleton spectra, Magenta = Periodram and Linear phase finite impulse response.

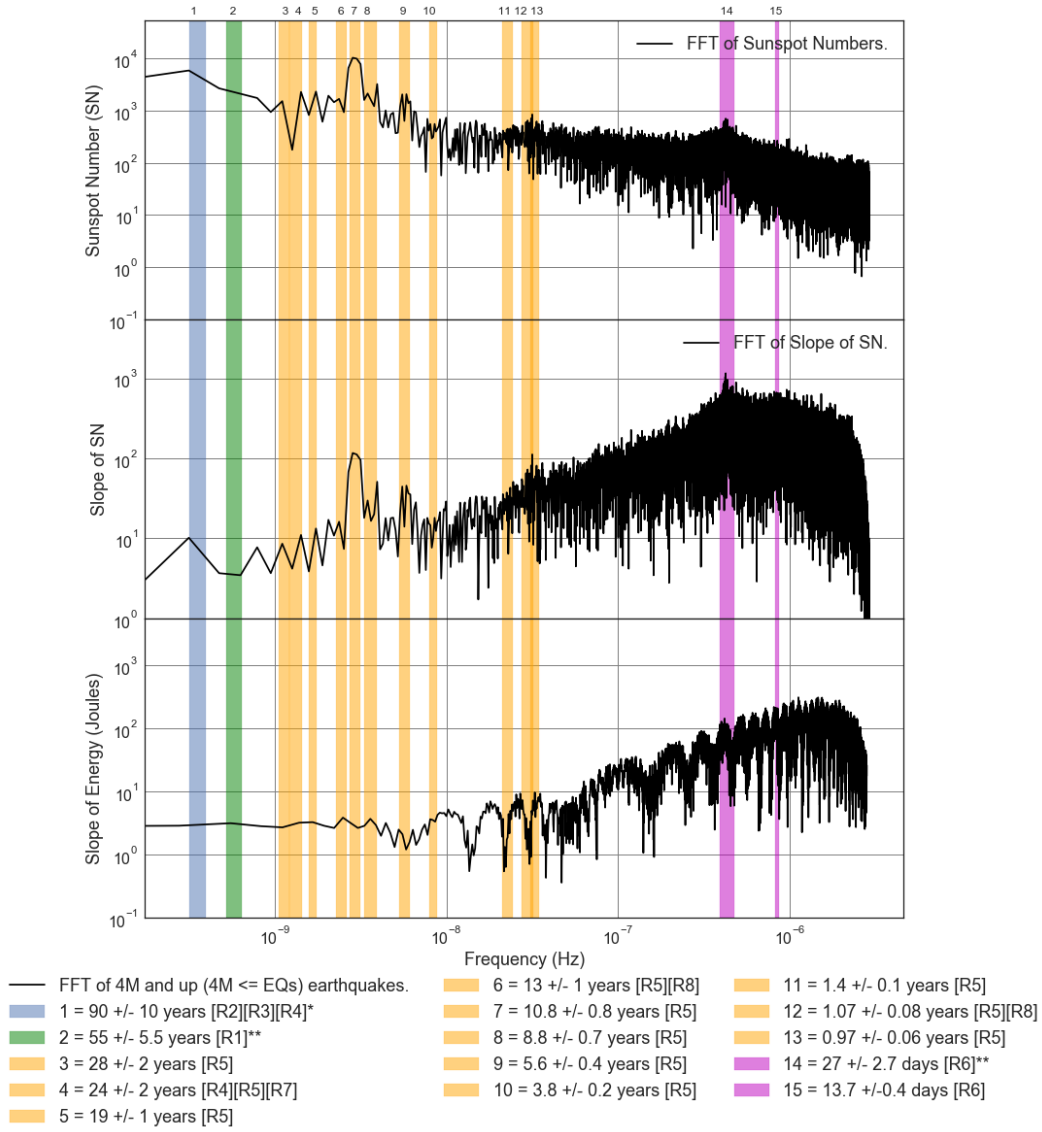

Figure E2.32: FFT Loglog Comparison Plot: Slope of Averaged 4M and up (4M <= EQs) Earthquake (EQ) total energy released, 2 Day Sunspot number and slope from 1818 to 2017. Additional meaning of the legend colors: Blue = Various Analysis techniques, Green = Meyer wavelet, Orange = Instantly maximal wavelet skeleton spectra, Magenta = Periodram and Linear phase finite impulse response.

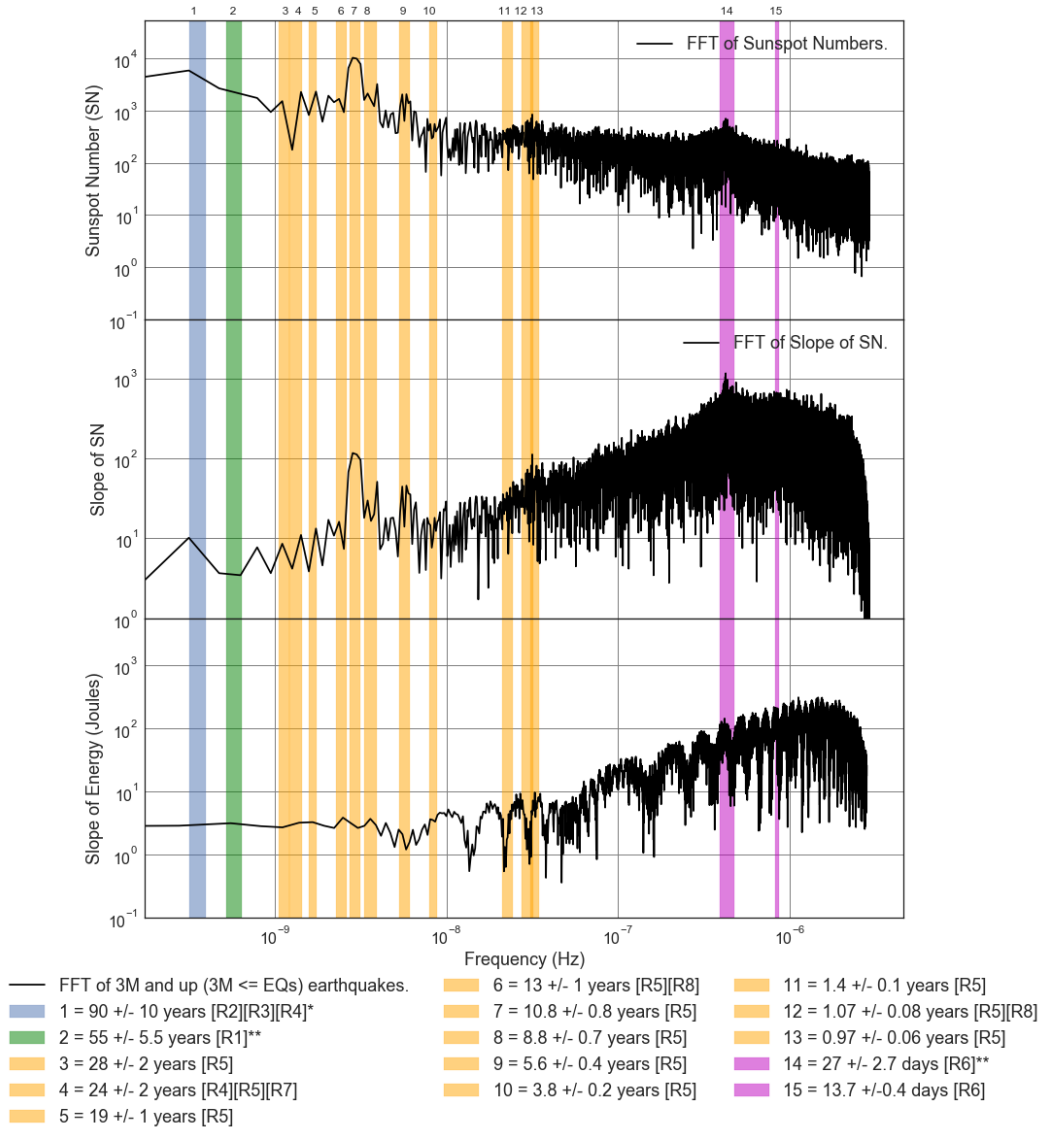

Figure E2.33: FFT Loglog Comparison Plot: Slope of Averaged 3M and up (3M <= EQs) Earthquake (EQ) total energy released, 2 Day Sunspot number and slope from 1818 to 2017. Additional meaning of the legend colors: Blue = Various Analysis techniques, Green = Meyer wavelet, Orange = Instantly maximal wavelet skeleton spectra, Magenta = Periodram and Linear phase finite impulse response.

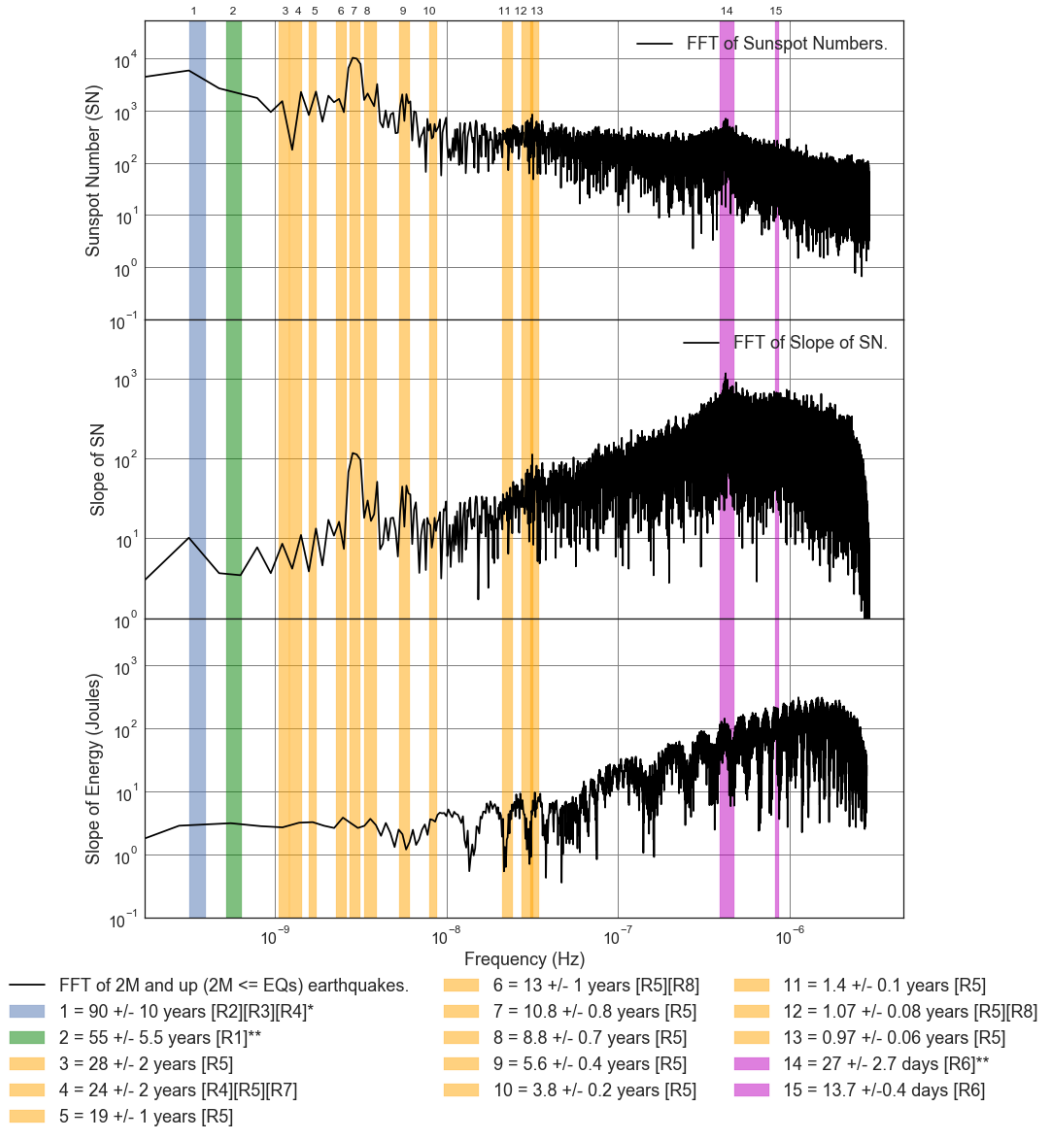

Figure E2.34: FFT Loglog Comparison Plot: Slope of Averaged 2M and up (2M <= EQs) Earthquake (EQ) total energy released, 2 Day Sunspot number and slope from 1818 to 2017. Additional meaning of the legend colors: Blue = Various Analysis techniques, Green = Meyer wavelet, Orange = Instantly maximal wavelet skeleton spectra, Magenta = Periodram and Linear phase finite impulse response.

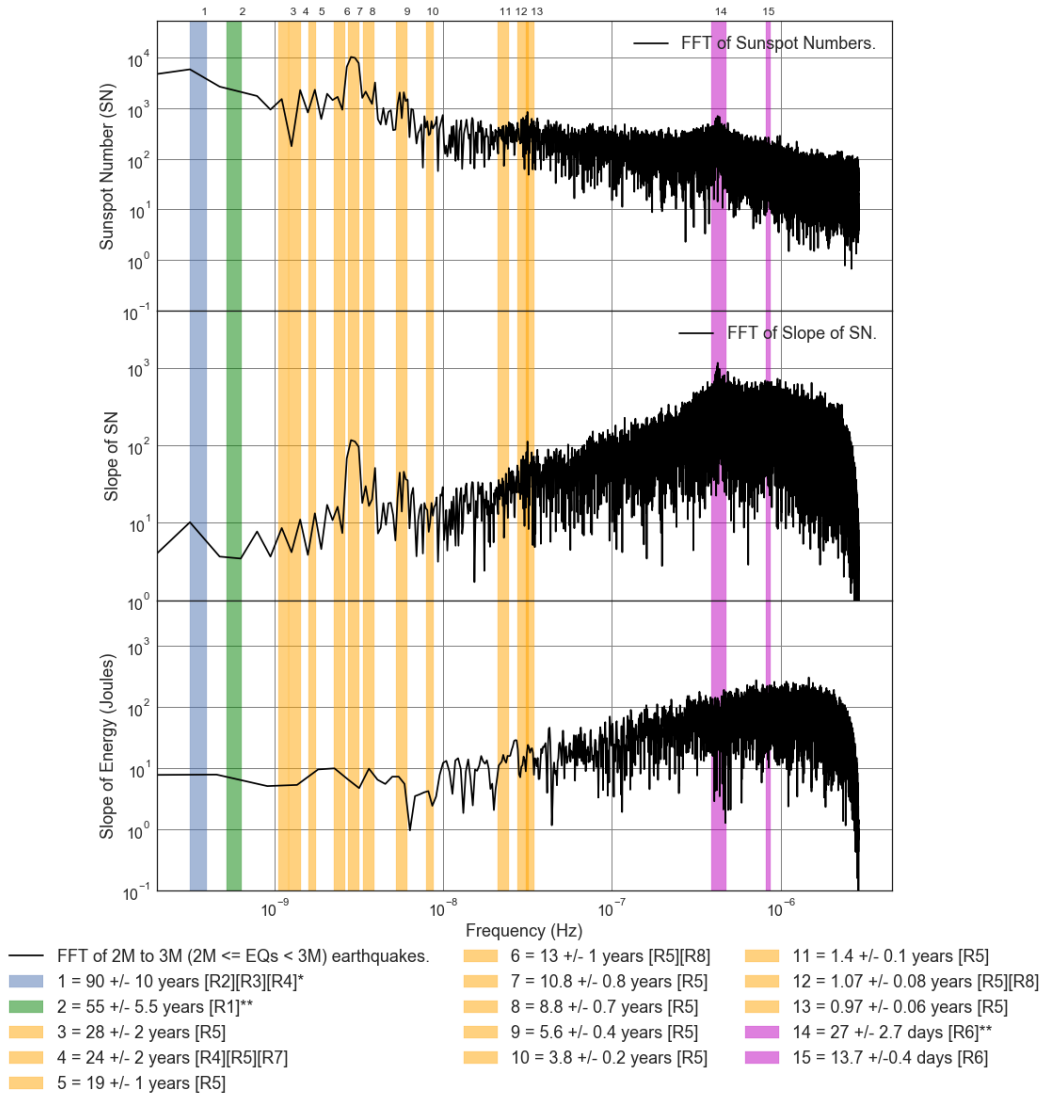

Figure E2.35: FFT Loglog Comparison Plot: Slope of Averaged 2M to 3M (2M <= EQs < 3M) Earthquake (EQ) total energy released, 2 Day Sunspot number and slope from 1818 to 2017. Additional meaning of the legend colors: Blue = Various Analysis techniques, Green = Meyer wavelet, Orange = Instantly maximal wavelet skeleton spectra, Magenta = Periodram and Linear phase finite impulse response.

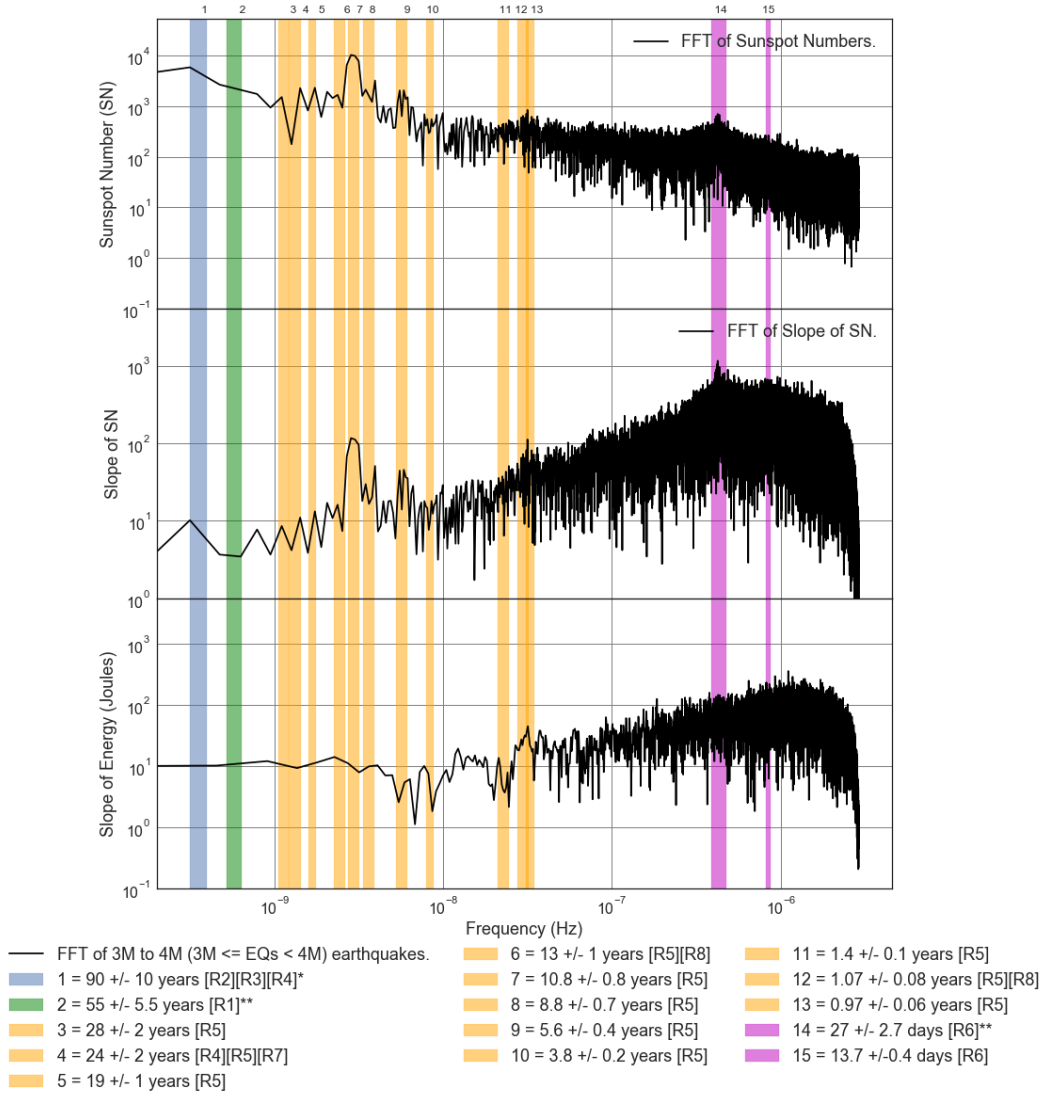

Figure E2.36: FFT Loglog Comparison Plot: Slope of Averaged 3M to 4M (3M <= EQs < 4M) Earthquake (EQ) total energy released, 2 Day Sunspot number and slope from 1818 to 2017. Additional meaning of the legend colors: Blue = Various Analysis techniques, Green = Meyer wavelet, Orange = Instantly maximal wavelet skeleton spectra, Magenta = Periodram and Linear phase finite impulse response.

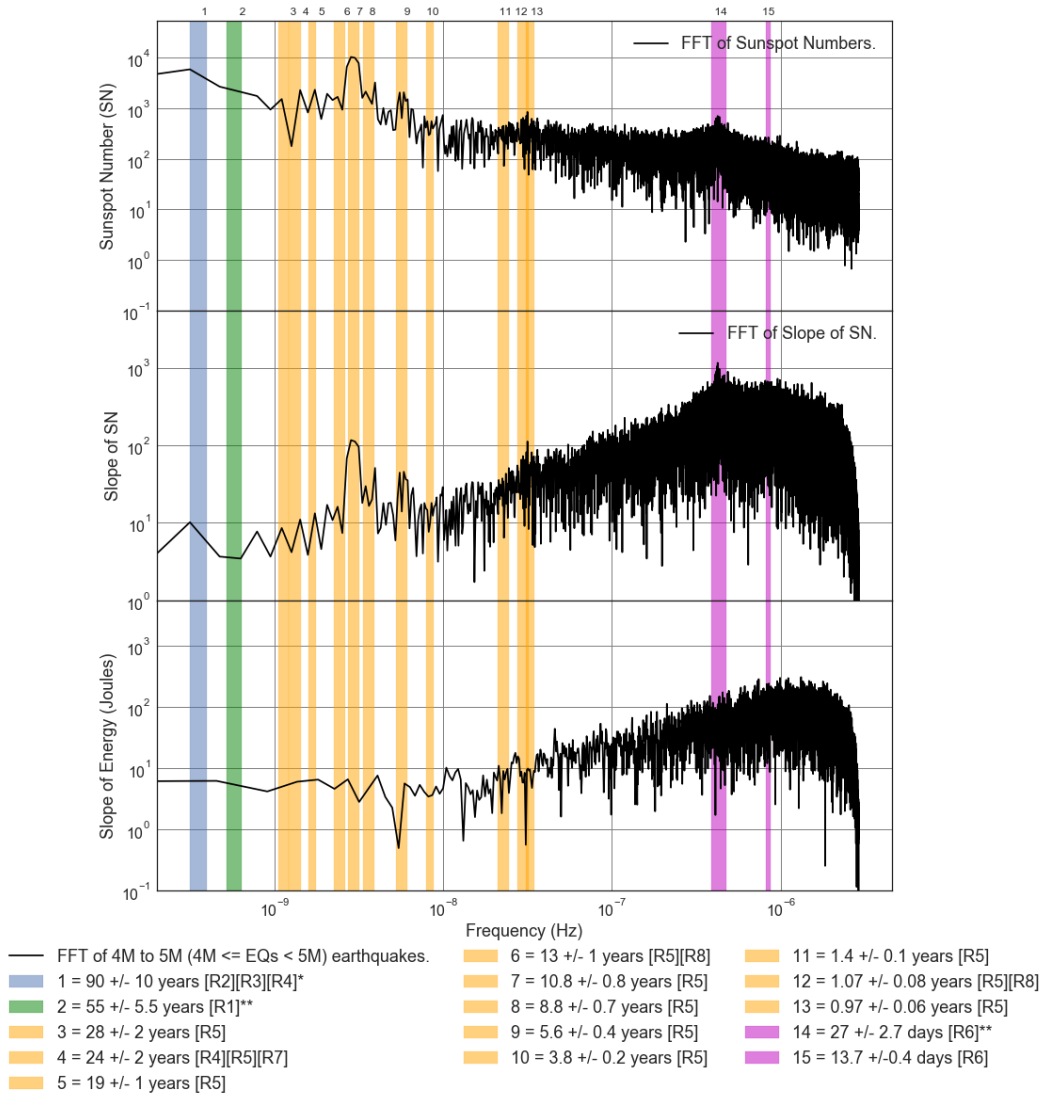

Figure E2.37: FFT Loglog Comparison Plot: Slope of Averaged 4M to 5M (4M <= EQs < 5M) Earthquake (EQ) total energy released, 2 Day Sunspot number and slope from 1818 to 2017. Additional meaning of the legend colors: Blue = Various Analysis techniques, Green = Meyer wavelet, Orange = Instantly maximal wavelet skeleton spectra, Magenta = Periodram and Linear phase finite impulse response.

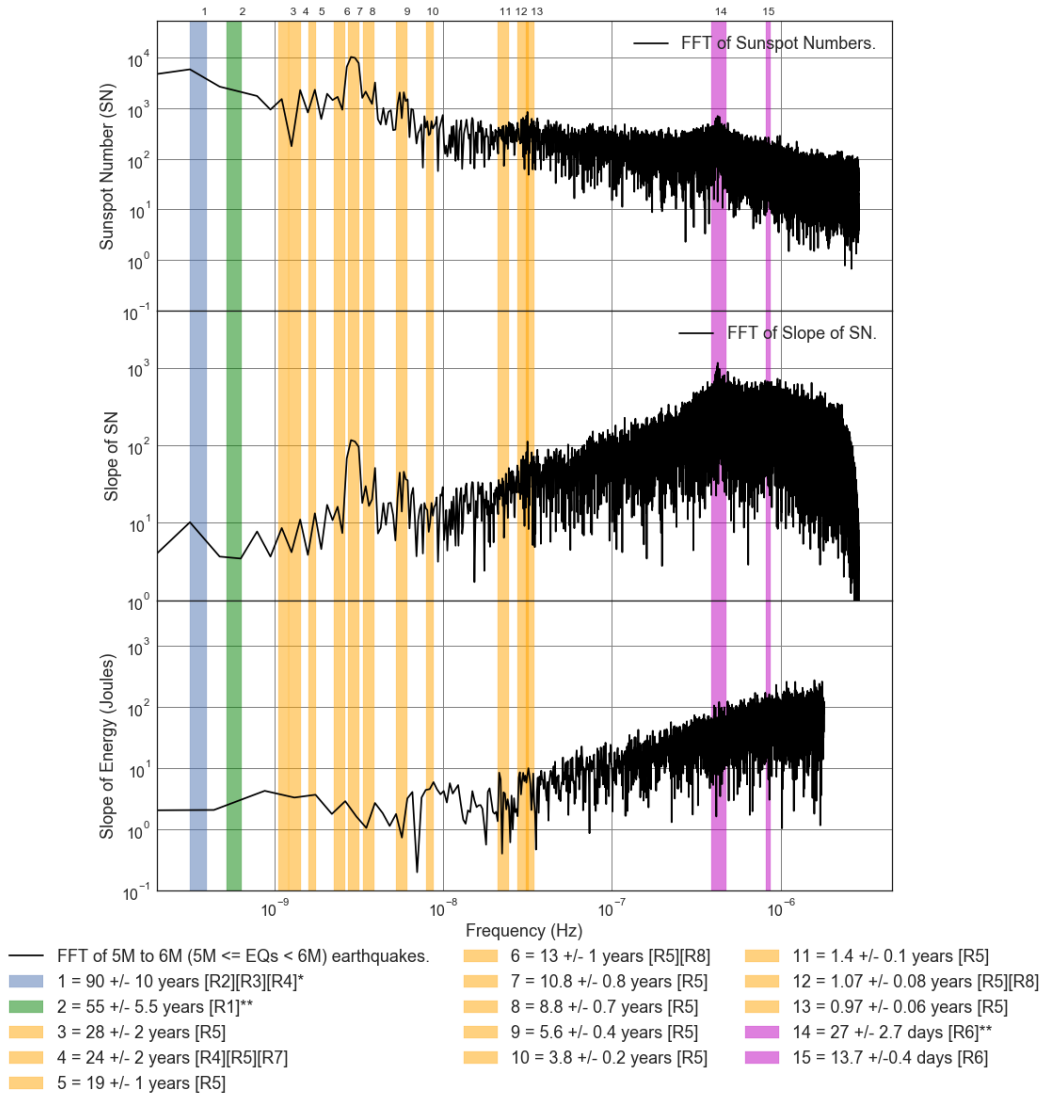

Figure E2.38: FFT Loglog Comparison Plot: Slope of Averaged 5M to 6M (5M <= EQs < 6M) Earthquake (EQ) total energy released, 2 Day Sunspot number and slope from 1818 to 2017. Additional meaning of the legend colors: Blue = Various Analysis techniques, Green = Meyer wavelet, Orange = Instantly maximal wavelet skeleton spectra, Magenta = Periodram and Linear phase finite impulse response.

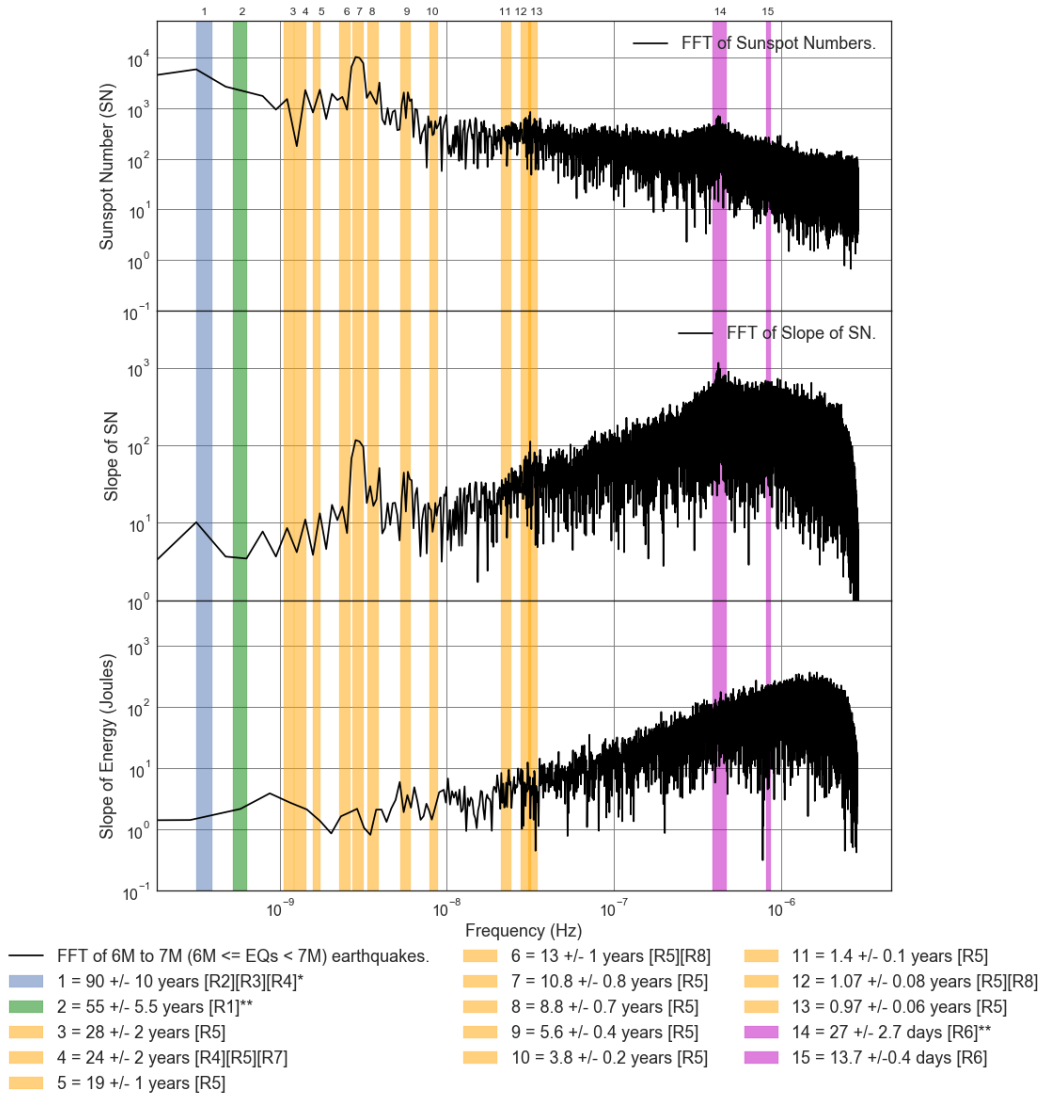

Figure E2.39: FFT Loglog Comparison Plot: Slope of Averaged 6M to 7M (6M <= EQs < 7M) Earthquake (EQ) total energy released, 2 Day Sunspot number and slope from 1818 to 2017. Additional meaning of the legend colors: Blue = Various Analysis techniques, Green = Meyer wavelet, Orange = Instantly maximal wavelet skeleton spectra, Magenta = Periodram and Linear phase finite impulse response.

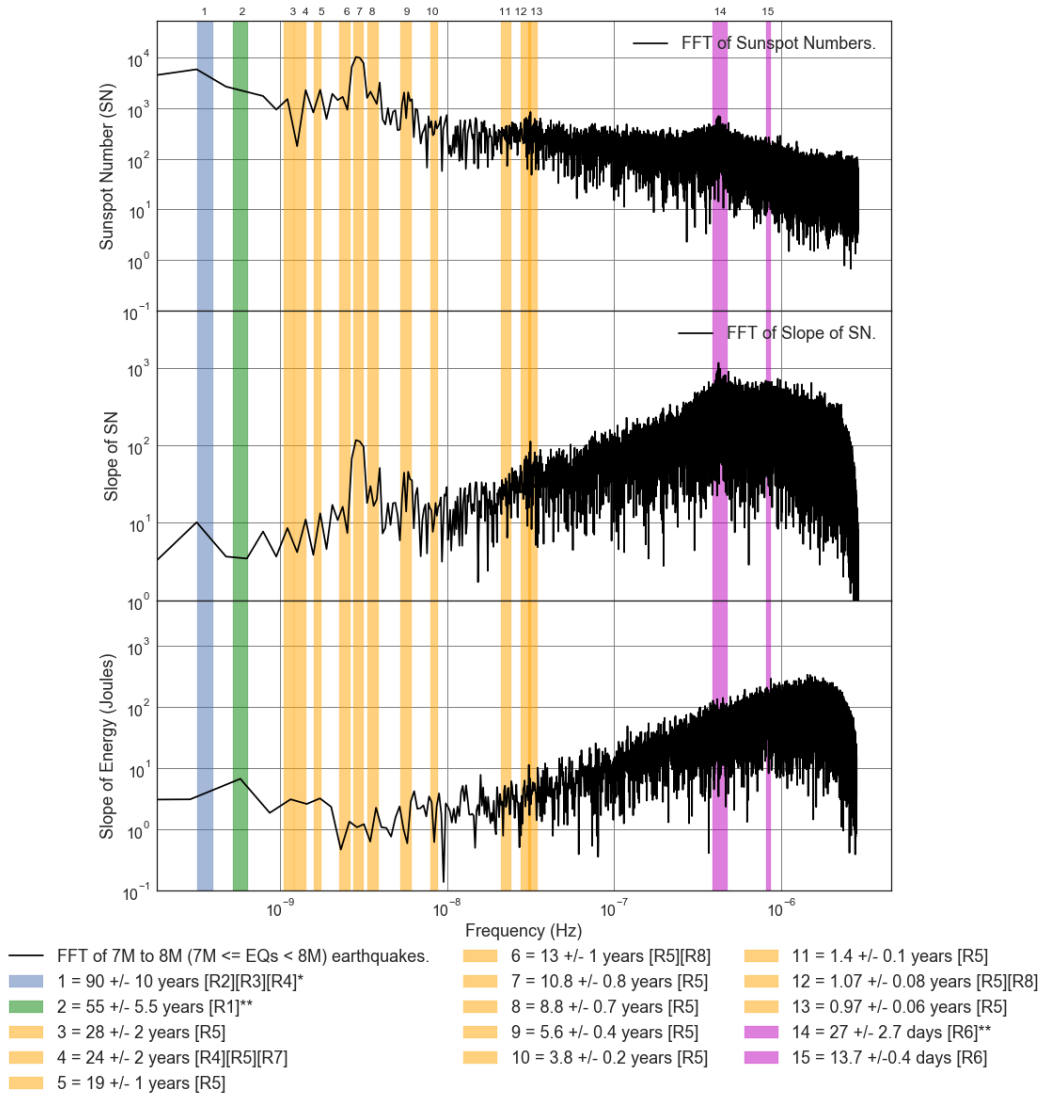

Figure E2.40: FFT Loglog Comparison Plot: Slope of Averaged 7M to 8M (7M <= EQs < 8M) Earthquake (EQ) total energy released, 2 Day Sunspot number and slope from 1818 to 2017. Additional meaning of the legend colors: Blue = Various Analysis techniques, Green = Meyer wavelet, Orange = Instantly maximal wavelet skeleton spectra, Magenta = Periodram and Linear phase finite impulse response.

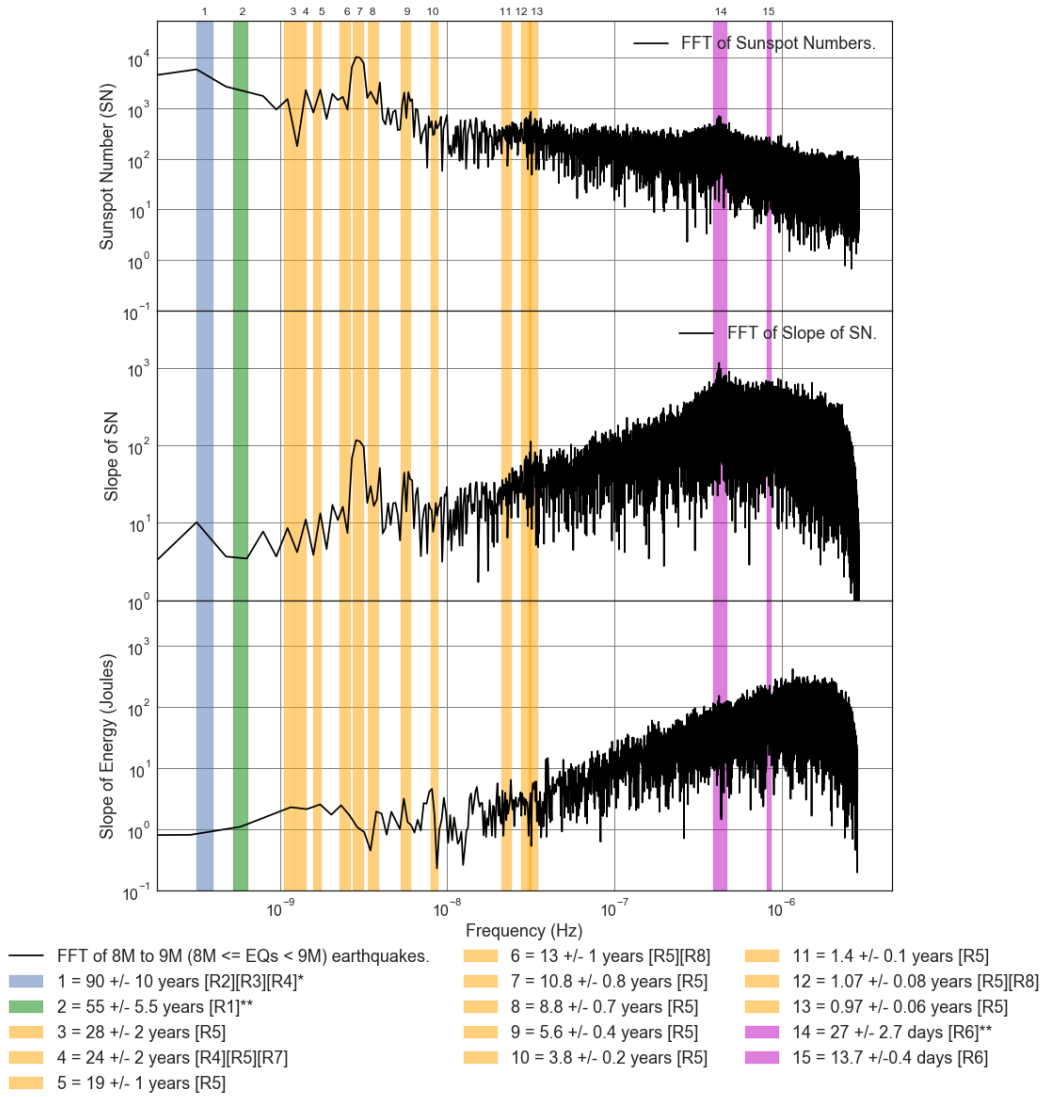

Figure E2.41: FFT Loglog Comparison Plot: Slope of Averaged 8M to 9M (8M <= EQs < 9M) Earthquake (EQ) total energy released, 2 Day Sunspot number and slope from 1818 to 2017. Additional meaning of the legend colors: Blue = Various Analysis techniques, Green = Meyer wavelet, Orange = Instantly maximal wavelet skeleton spectra, Magenta = Periodram and Linear phase finite impulse response.

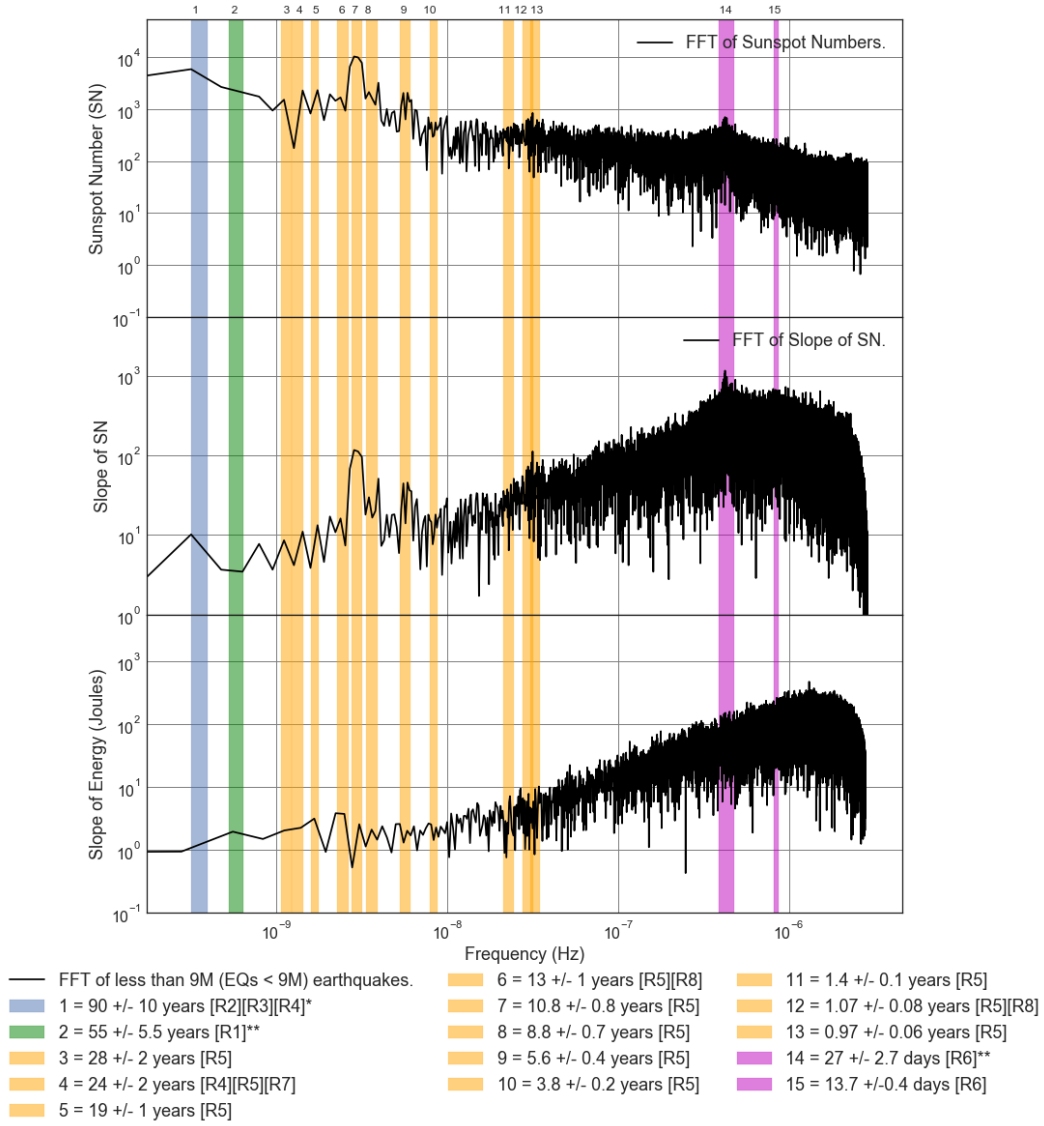

Figure E2.42: FFT Loglog Comparison Plot: Slope of Averaged less than 9M (EQs < 9M) Earthquake (EQ) total energy released, 2 Day Sunspot number and slope from 1818 to 2017. Additional meaning of the legend colors: Blue = Various Analysis techniques, Green = Meyer wavelet, Orange = Instantly maximal wavelet skeleton spectra, Magenta = Periodram and Linear phase finite impulse response.

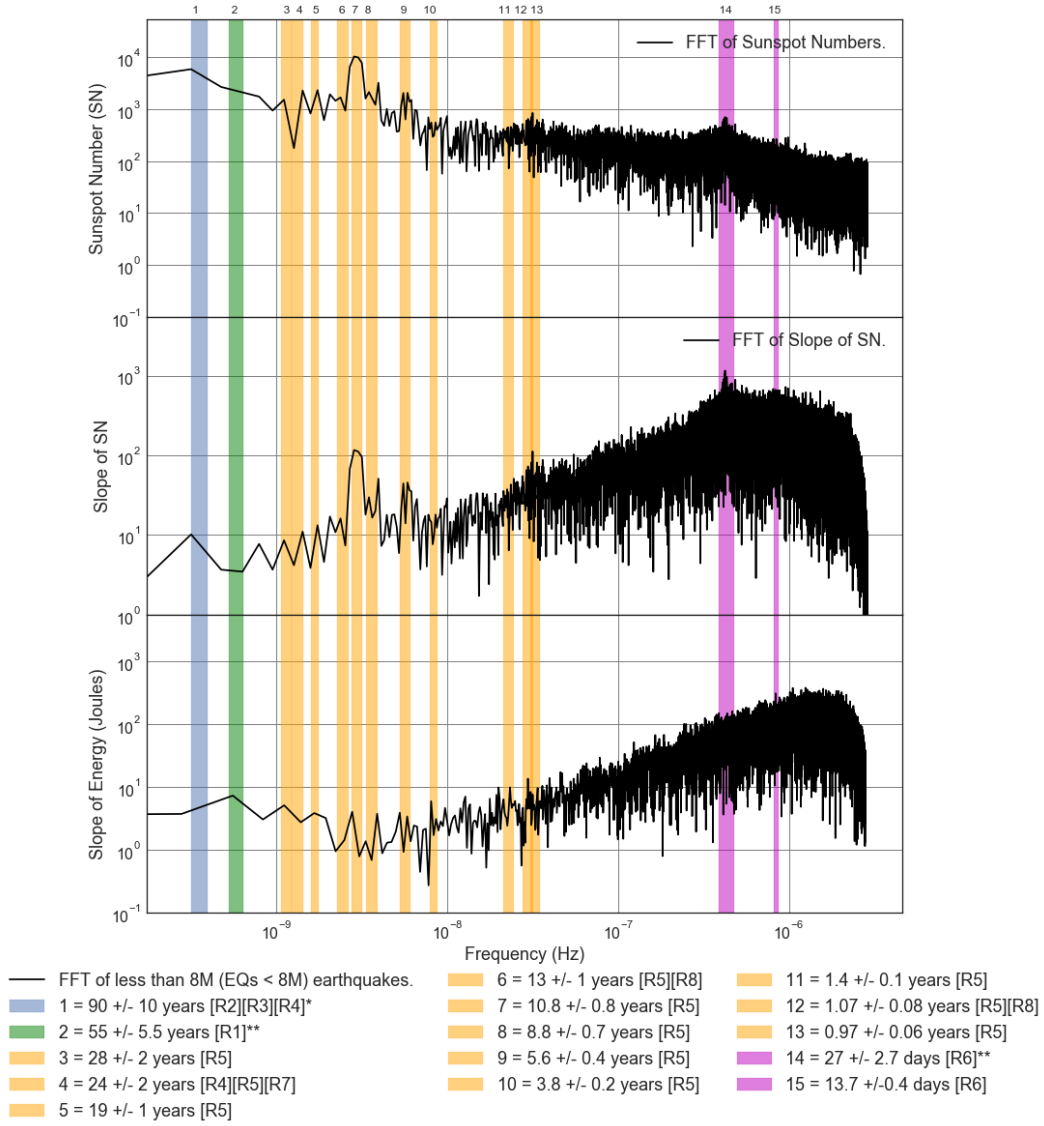

Figure E2.43: FFT Loglog Comparison Plot: Slope of Averaged less than 8M (EQs < 8M) Earthquake (EQ) total energy released, 2 Day Sunspot number and slope from 1818 to 2017. Additional meaning of the legend colors: Blue = Various Analysis techniques, Green = Meyer wavelet, Orange = Instantly maximal wavelet skeleton spectra, Magenta = Periodram and Linear phase finite impulse response.

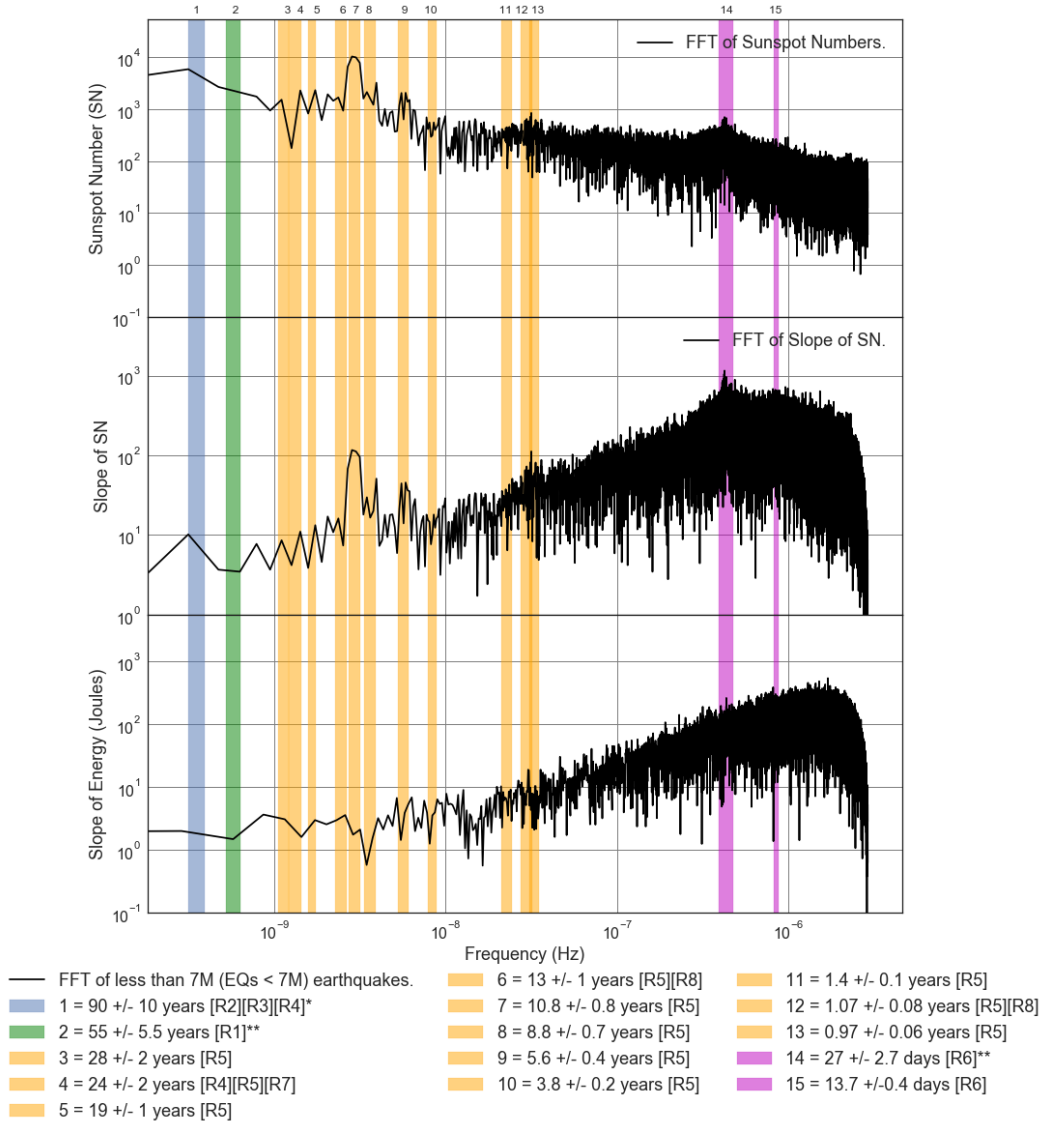

Figure E2.44: FFT Loglog Comparison Plot: Slope of Averaged less than 7M (EQs < 7M) Earthquake (EQ) total energy released, 2 Day Sunspot number and slope from 1818 to 2017. Additional meaning of the legend colors: Blue = Various Analysis techniques, Green = Meyer wavelet, Orange = Instantly maximal wavelet skeleton spectra, Magenta = Periodram and Linear phase finite impulse response.

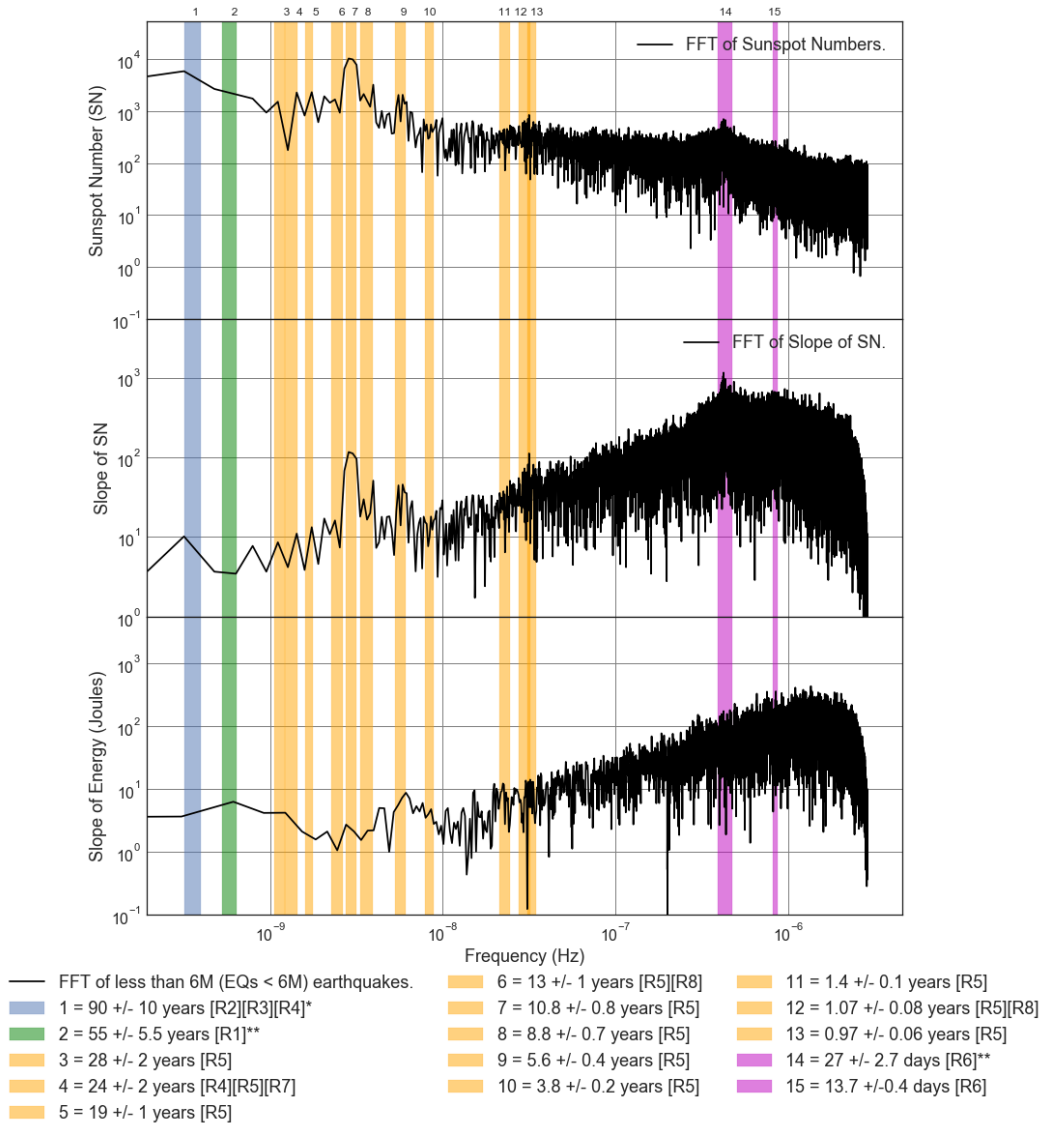

Figure E2.45: FFT Loglog Comparison Plot: Slope of Averaged less than 6M (EQs < 6M) Earthquake (EQ) total energy released, 2 Day Sunspot number and slope from 1818 to 2017. Additional meaning of the legend colors: Blue = Various Analysis techniques, Green = Meyer wavelet, Orange = Instantly maximal wavelet skeleton spectra, Magenta = Periodram and Linear phase finite impulse response.

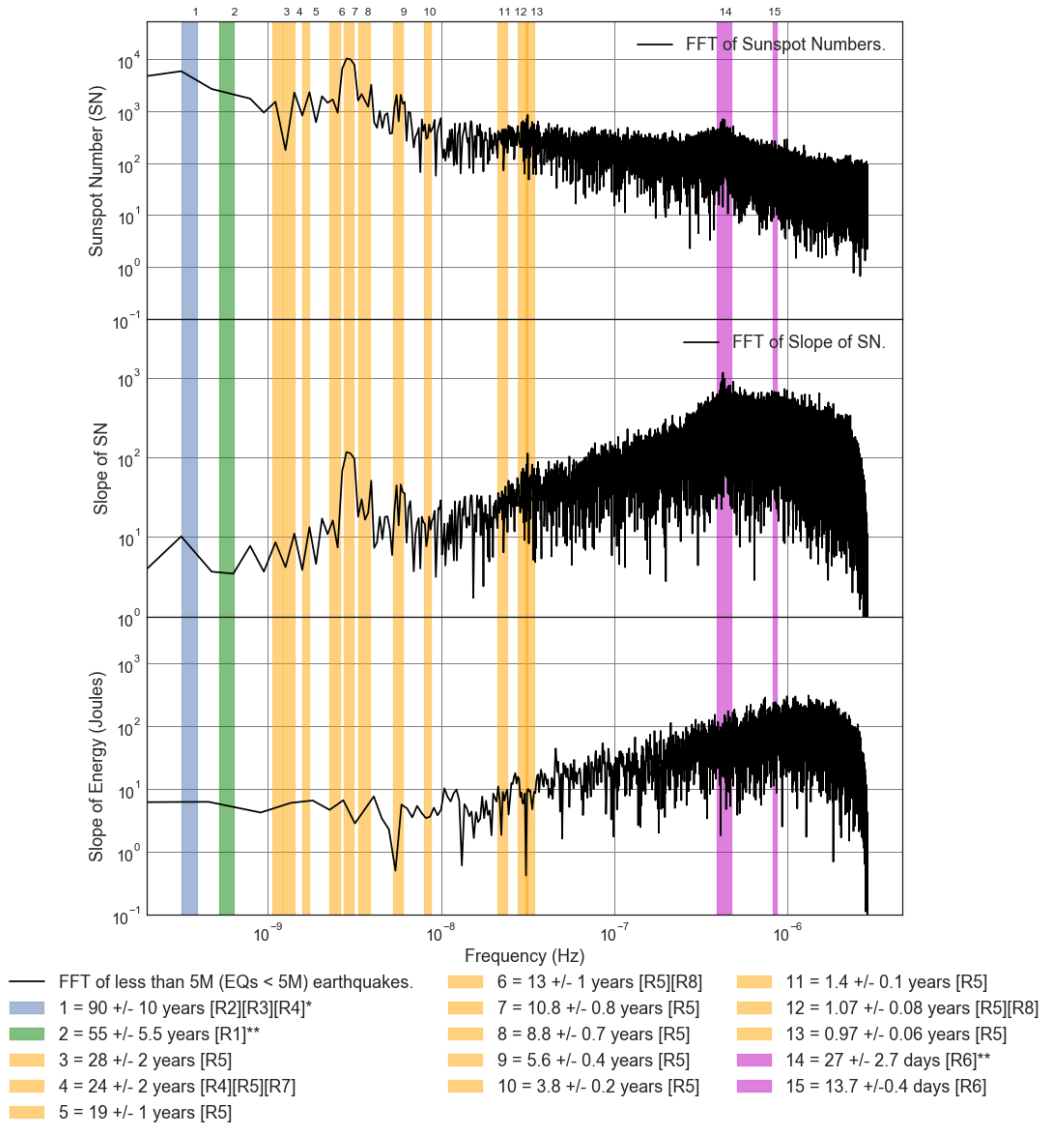

Figure E2.46: FFT Loglog Comparison Plot: Slope of Averaged less than 5M (EQs < 5M) Earthquake (EQ) total energy released, 2 Day Sunspot number and slope from 1818 to 2017. Additional meaning of the legend colors: Blue = Various Analysis techniques, Green = Meyer wavelet, Orange = Instantly maximal wavelet skeleton spectra, Magenta = Periodram and Linear phase finite impulse response.

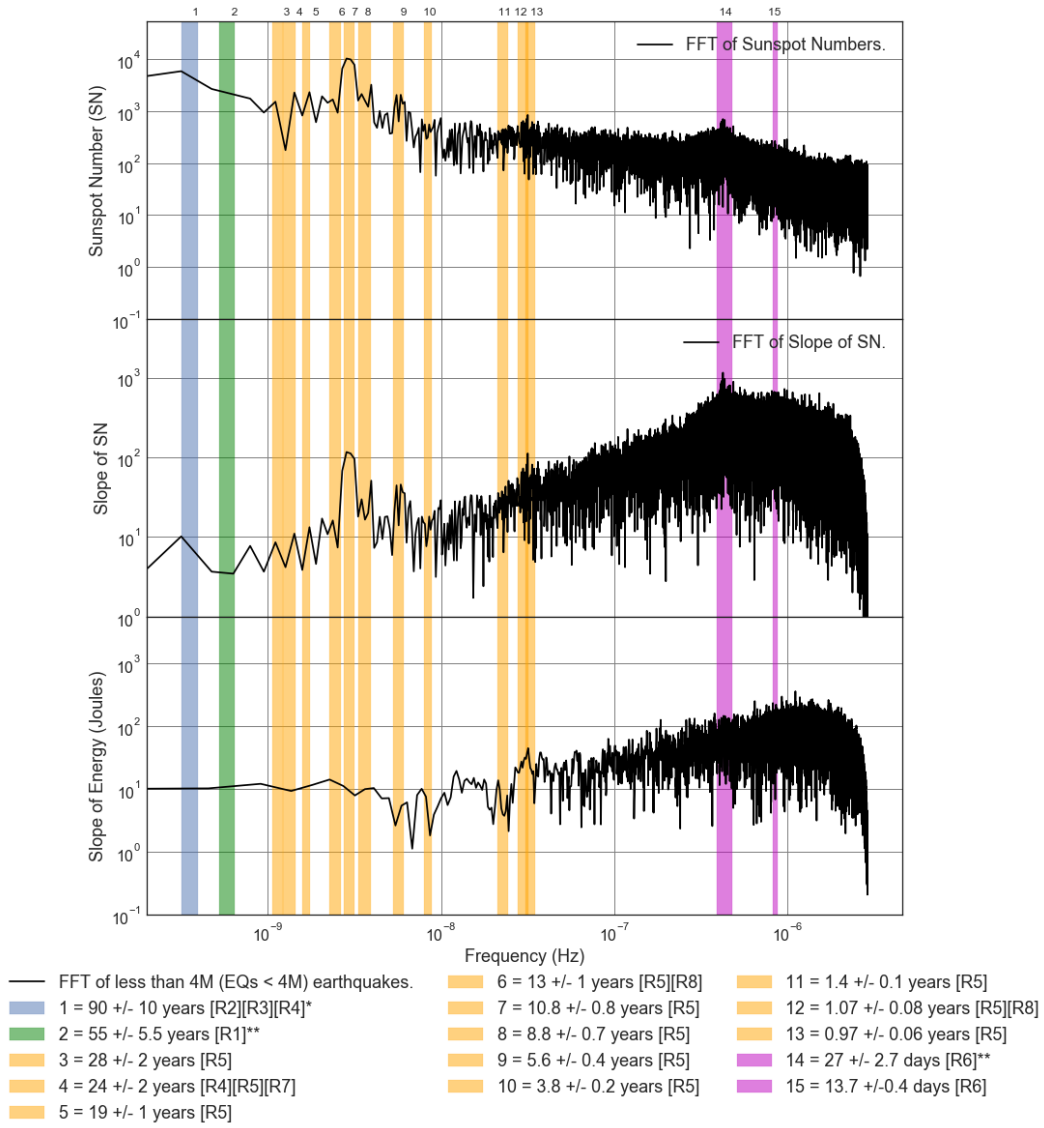

Figure E2.47: FFT Loglog Comparison Plot: Slope of Averaged less than 4M (EQs < 4M) Earthquake (EQ) total energy released, 2 Day Sunspot number and slope from 1818 to 2017. Additional meaning of the legend colors: Blue = Various Analysis techniques, Green = Meyer wavelet, Orange = Instantly maximal wavelet skeleton spectra, Magenta = Periodram and Linear phase finite impulse response.

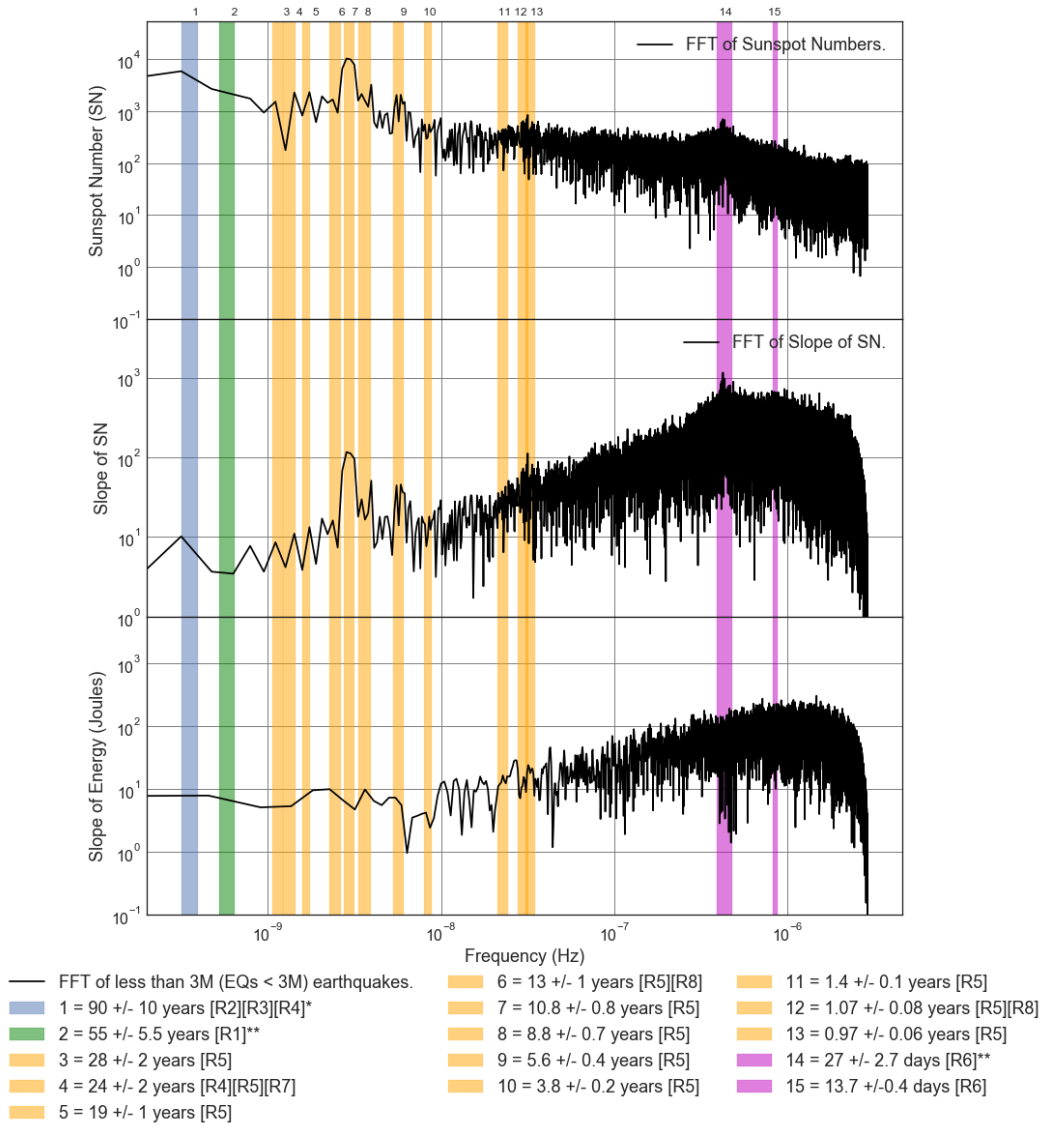

Figure E2.48: FFT Loglog Comparison Plot: Slope of Averaged less than 3M (EQs < 3M) Earthquake (EQ) total energy released, 2 Day Sunspot number and slope from 1818 to 2017. Additional meaning of the legend colors: Blue = Various Analysis techniques, Green = Meyer wavelet, Orange = Instantly maximal wavelet skeleton spectra, Magenta = Periodram and Linear phase finite impulse response.

Appendix F: Fast Fourier Transform Magnitude Spectra Comparison of Averaged (ISC, USGS, and Centennial) Earthquake Frequencies with each Earthquake dataset.

Comparison of ISC, USGS, and Centennial Y2K of FFT Earthquake Counts Plots

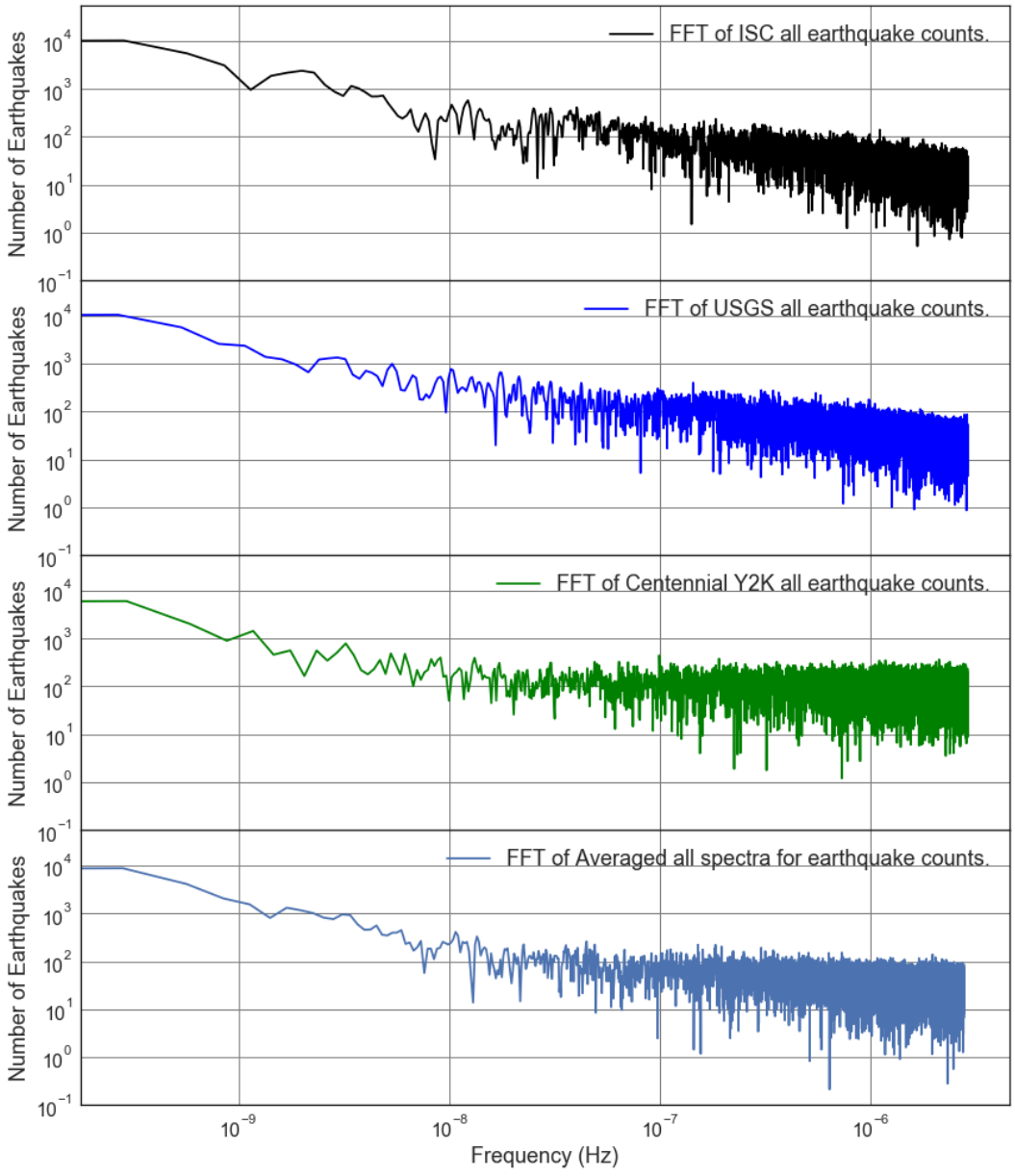

Figure F1.1: FFT Loglog Comparison Plot of number of all Earthquakes from the ISC, USGS, and Centennial Y2K datasets.

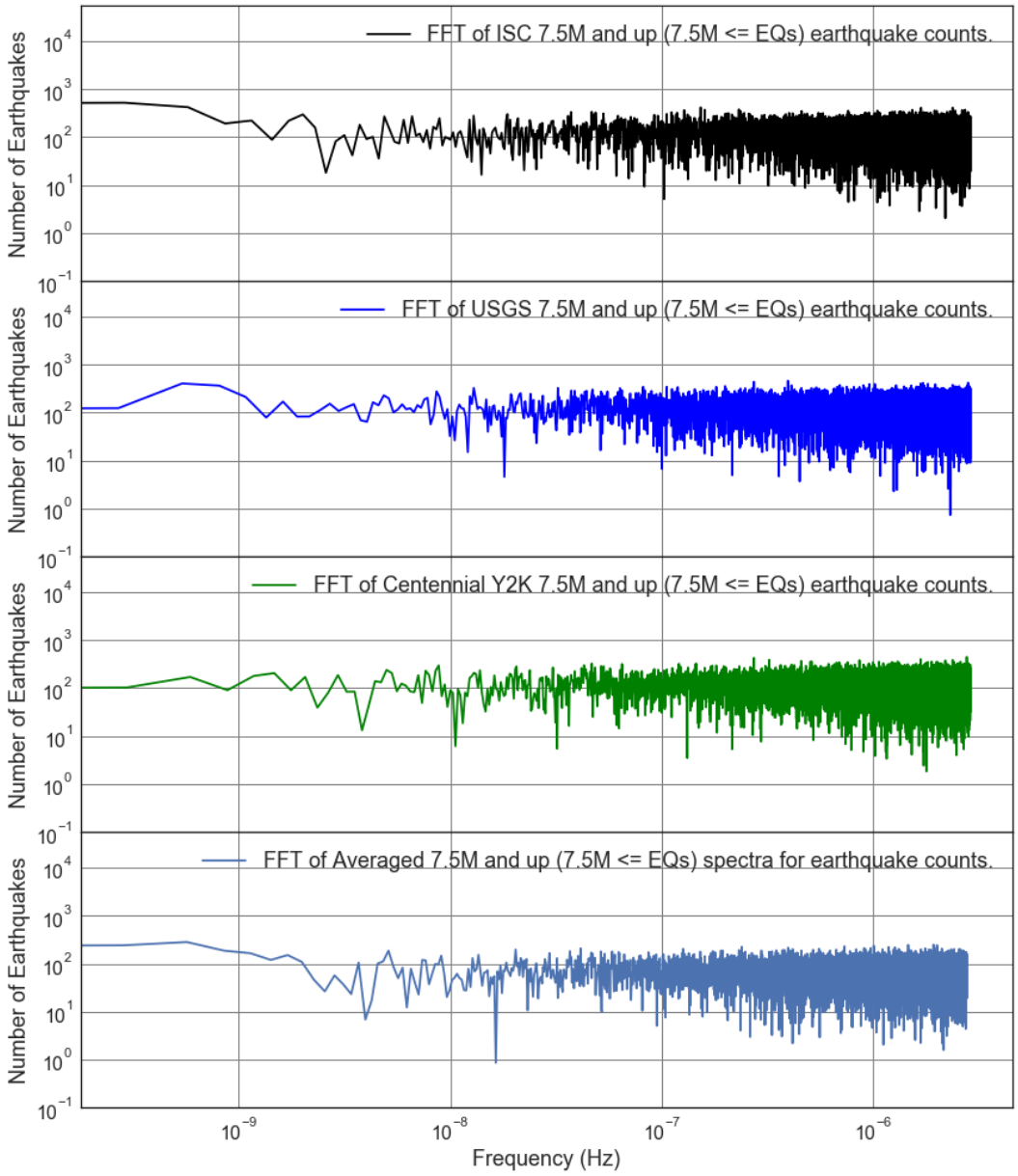

Figure F1.2: FFT Loglog Comparison Plot of number of 7.5M and up (7.5M <= EQs) Earthquakes from the ISC, USGS, and Centennial Y2K datasets.

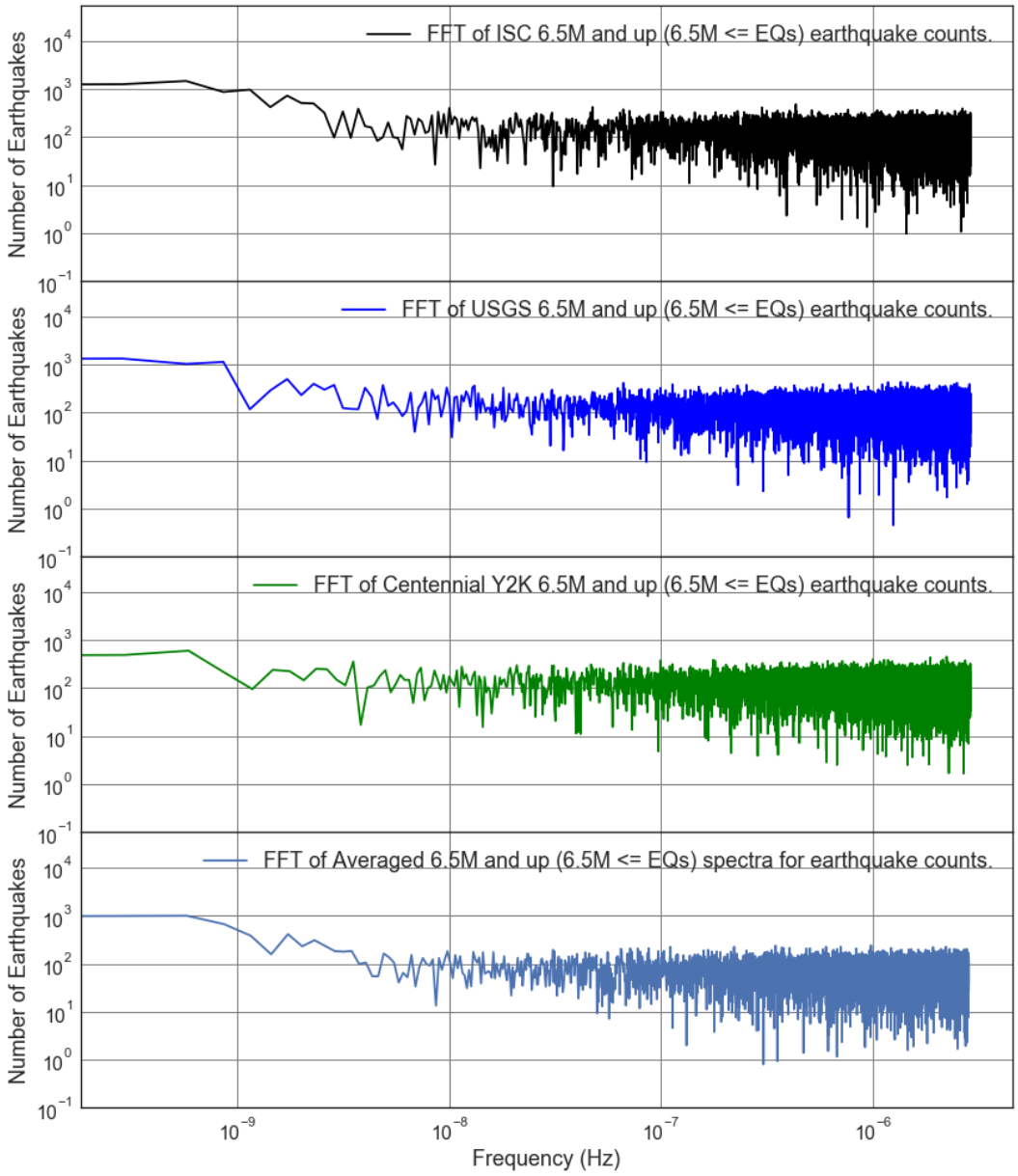

Figure F1.3: FFT Loglog Comparison Plot of number of 6.5M and up (6.5M <= EQs) Earthquakes from the ISC, USGS, and Centennial Y2K datasets.

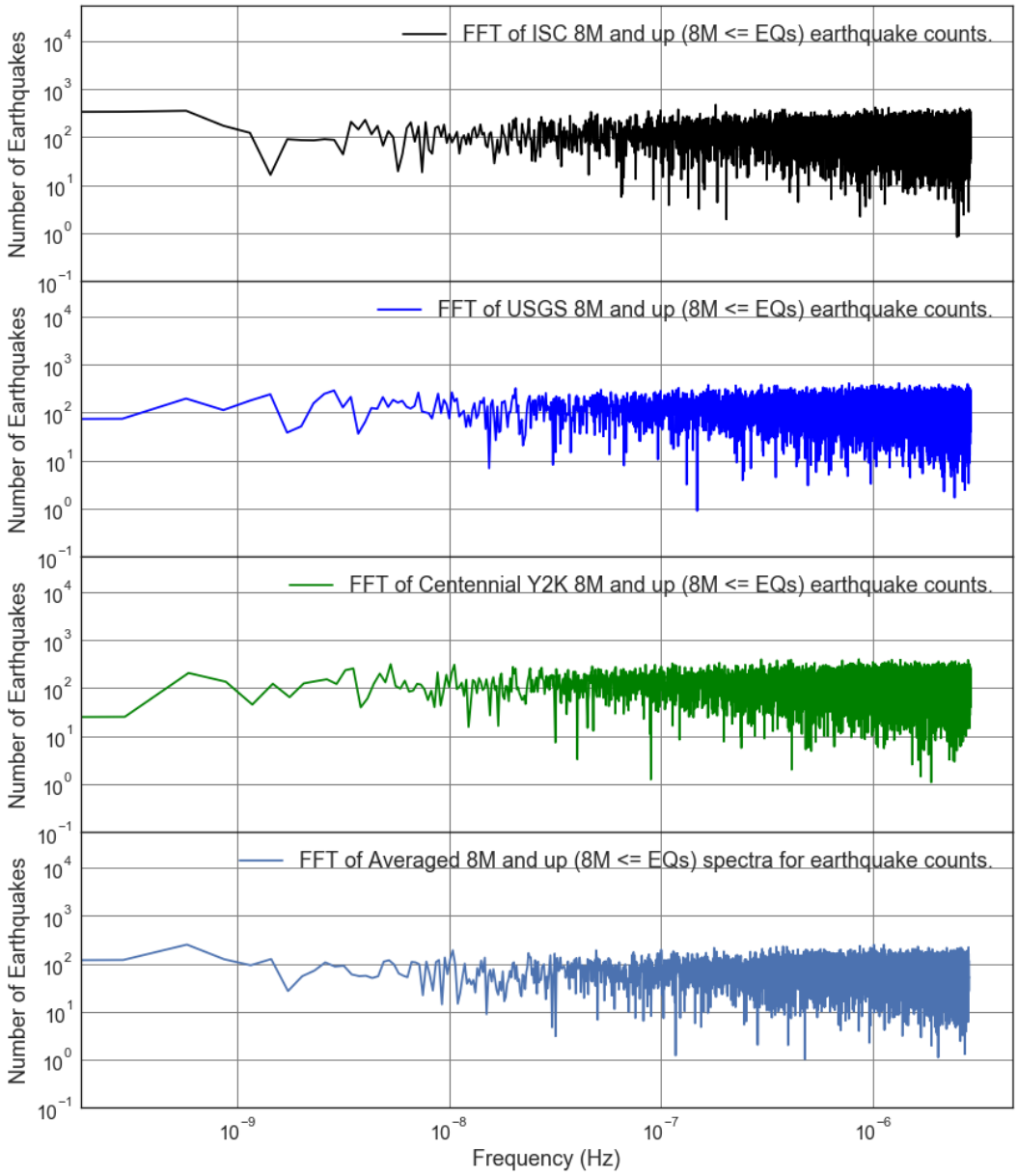

Figure F1.4: FFT Loglog Comparison Plot of number of 8M and up (8M <= EQs) Earthquakes from the ISC, USGS, and Centennial Y2K datasets.

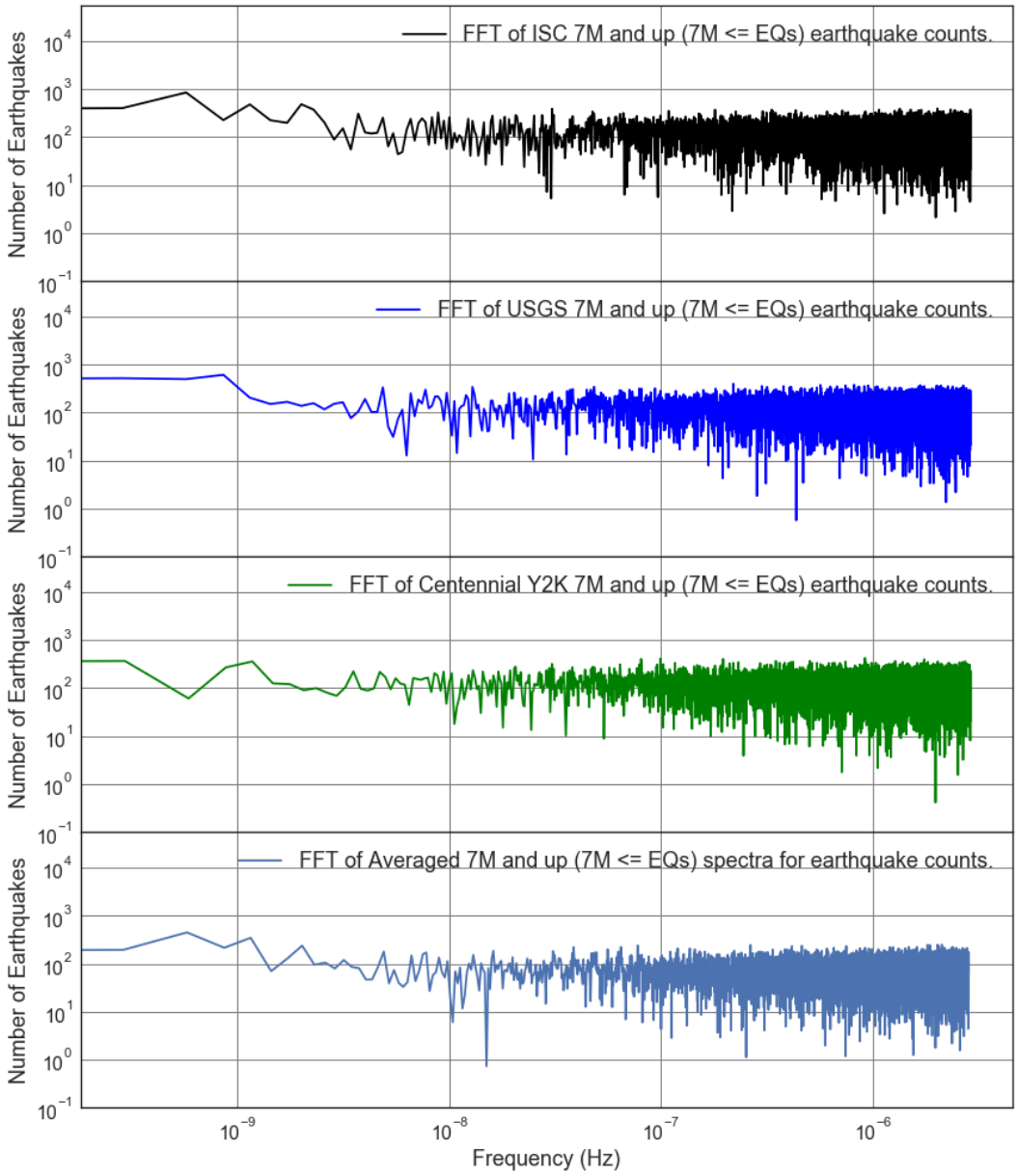

Figure F1.5: FFT Loglog Comparison Plot of number of 7M and up (7M <= EQs) Earthquakes from the ISC, USGS, and Centennial Y2K datasets.

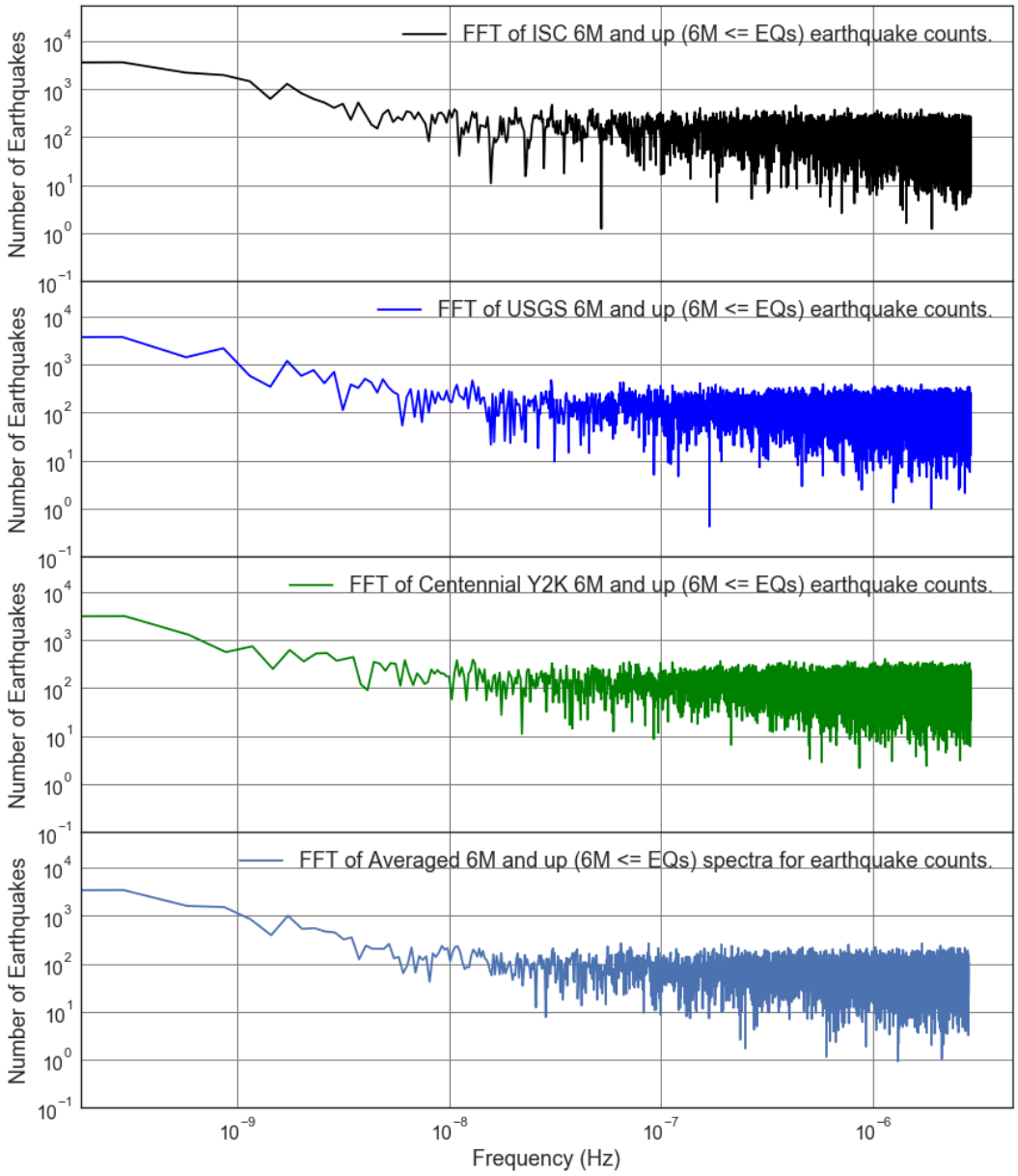

Figure F1.6: FFT Loglog Comparison Plot of number of 6M and up (6M <= EQs) Earthquakes from the ISC, USGS, and Centennial Y2K datasets.

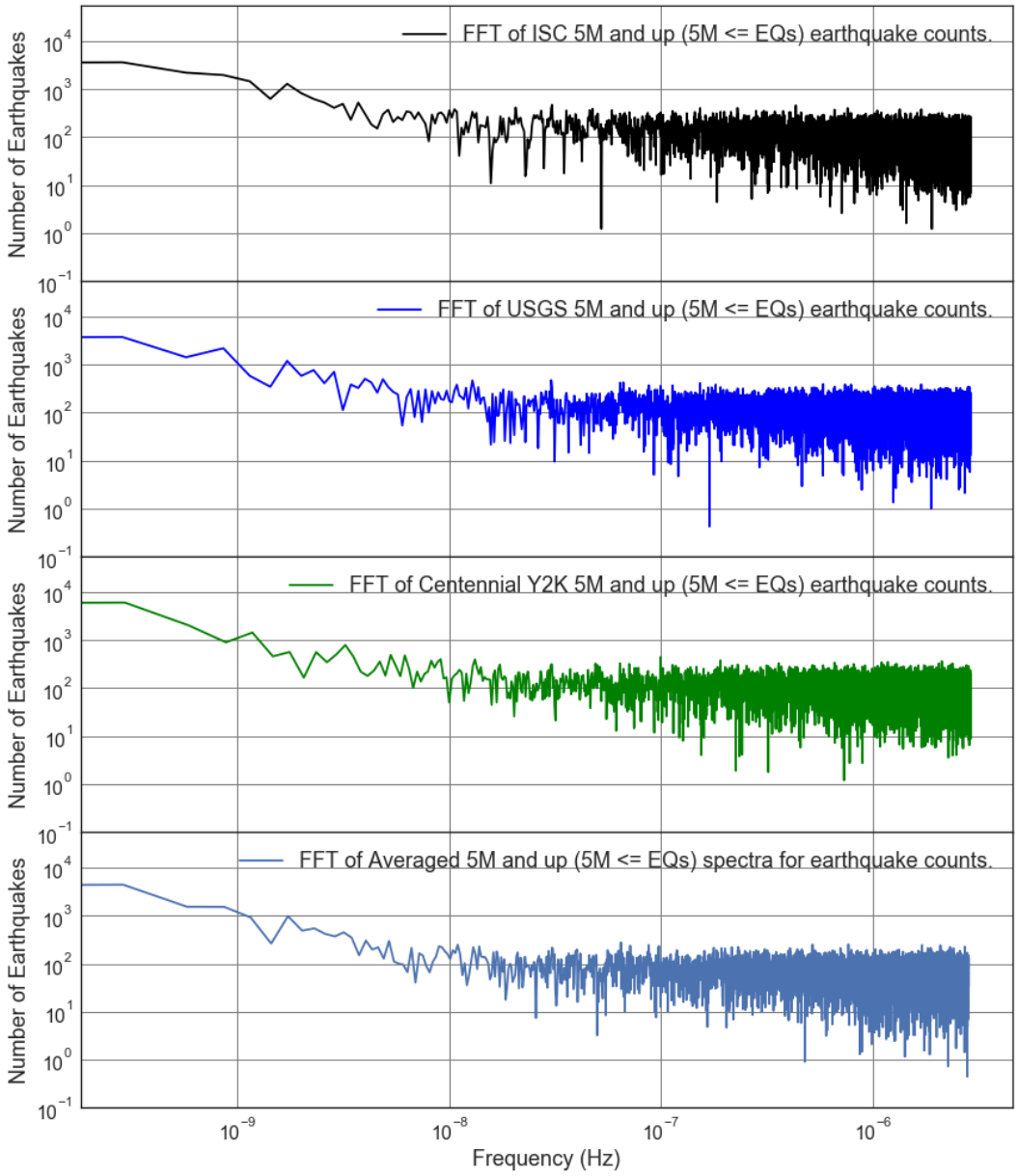

Figure F1.7: FFT Loglog Comparison Plot of number of 5M and up (5M <= EQs) Earthquakes from the ISC, USGS, and Centennial Y2K datasets.

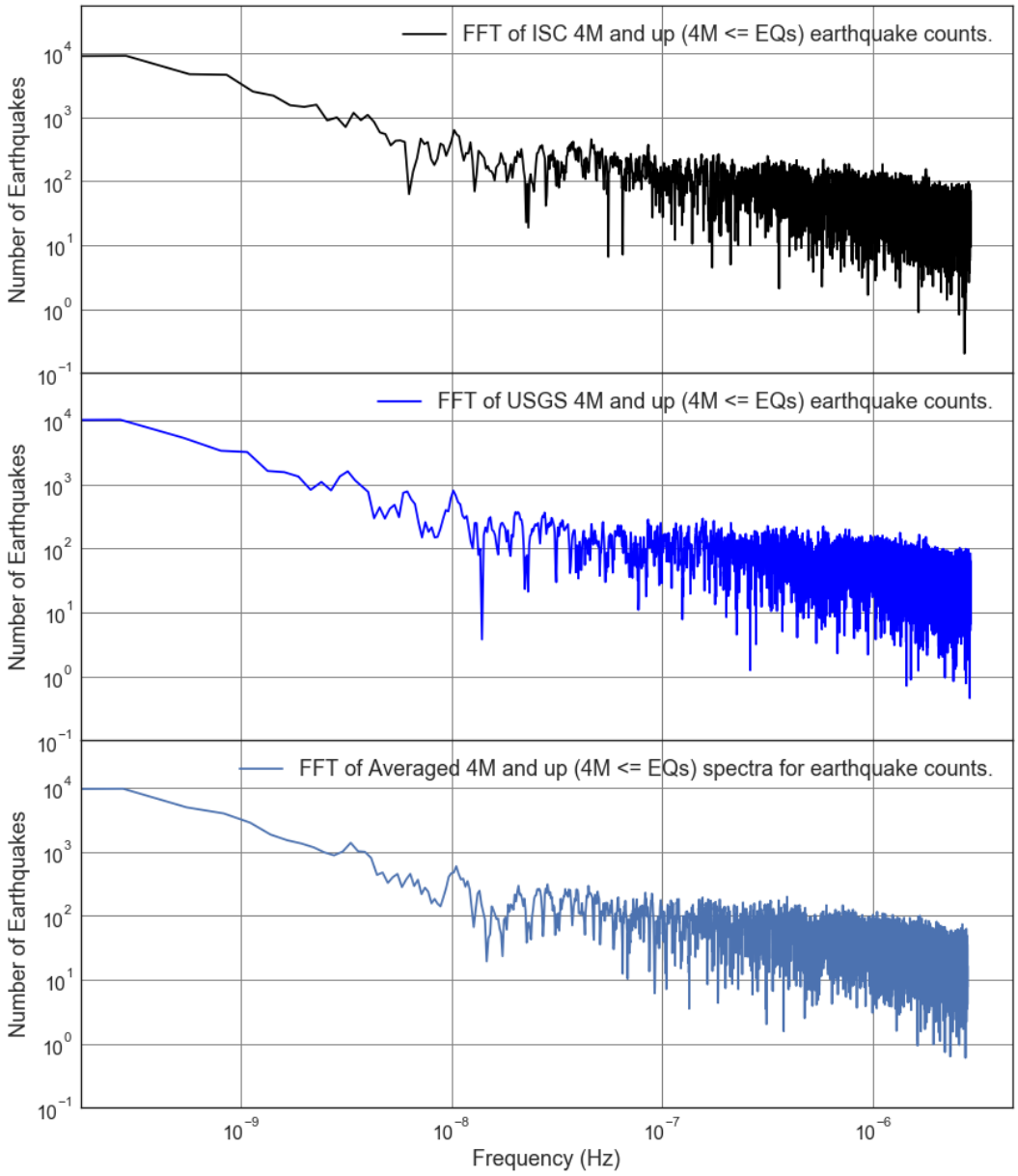

Figure F1.8: FFT Loglog Comparison Plot of number of 4M and up (4M <= EQs) Earthquakes from the ISC, USGS, and Centennial Y2K datasets.

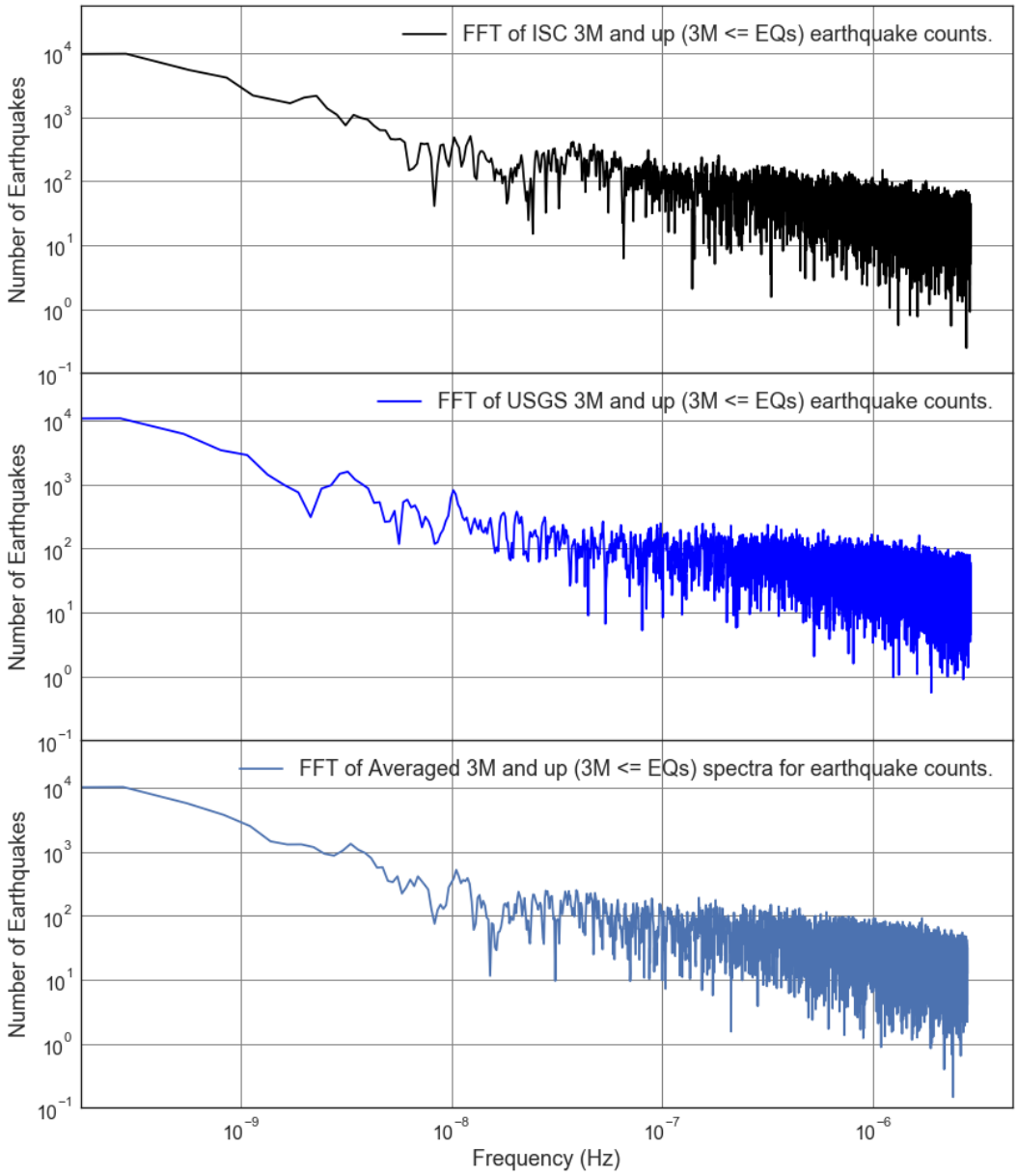

Figure F1.9: FFT Loglog Comparison Plot of number of 3M and up (3M <= EQs) Earthquakes from the ISC, USGS, and Centennial Y2K datasets.

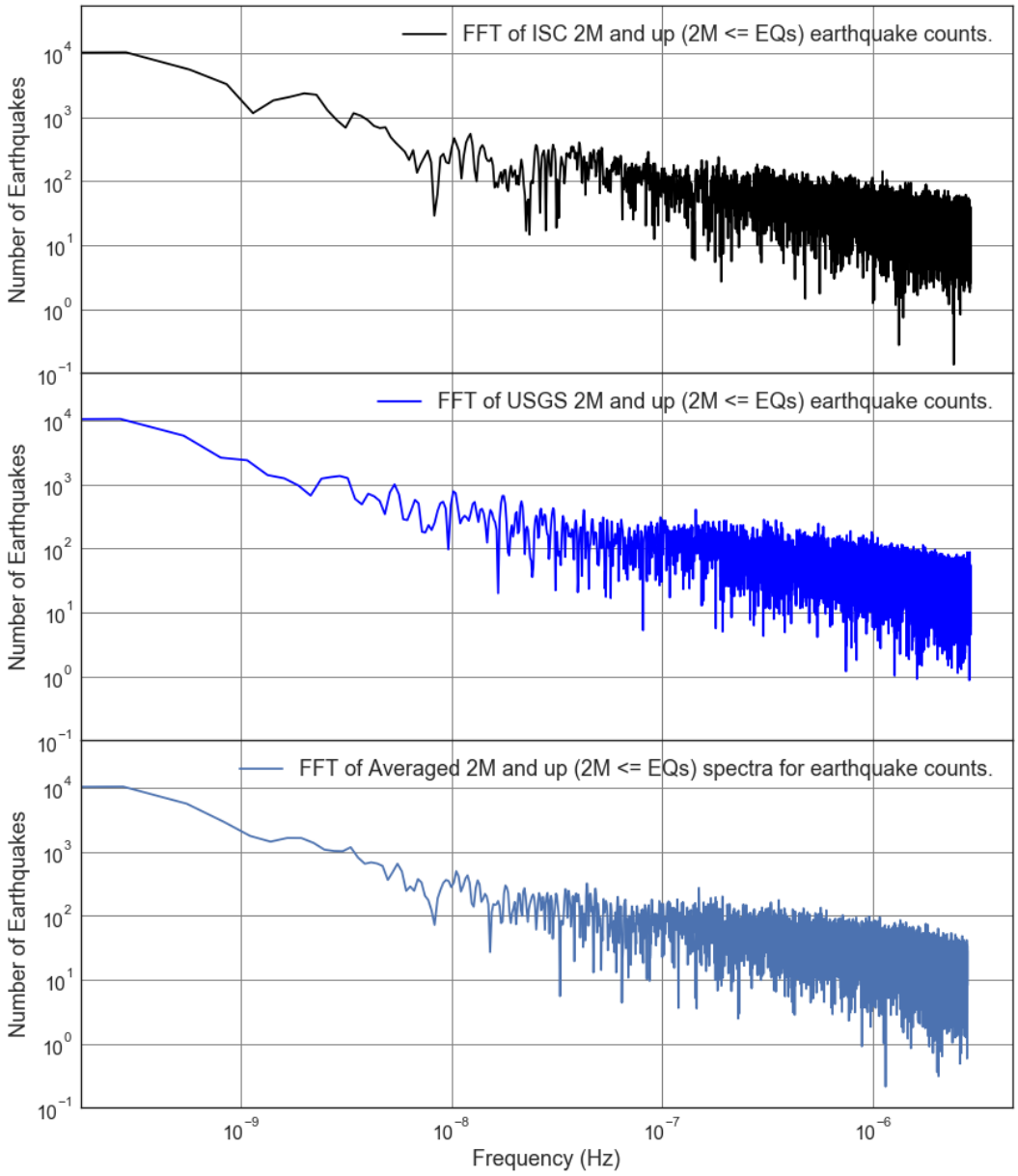

Figure F1.10: FFT Loglog Comparison Plot of number of 2M and up (2M <= EQs) Earthquakes from the ISC, USGS, and Centennial Y2K datasets.

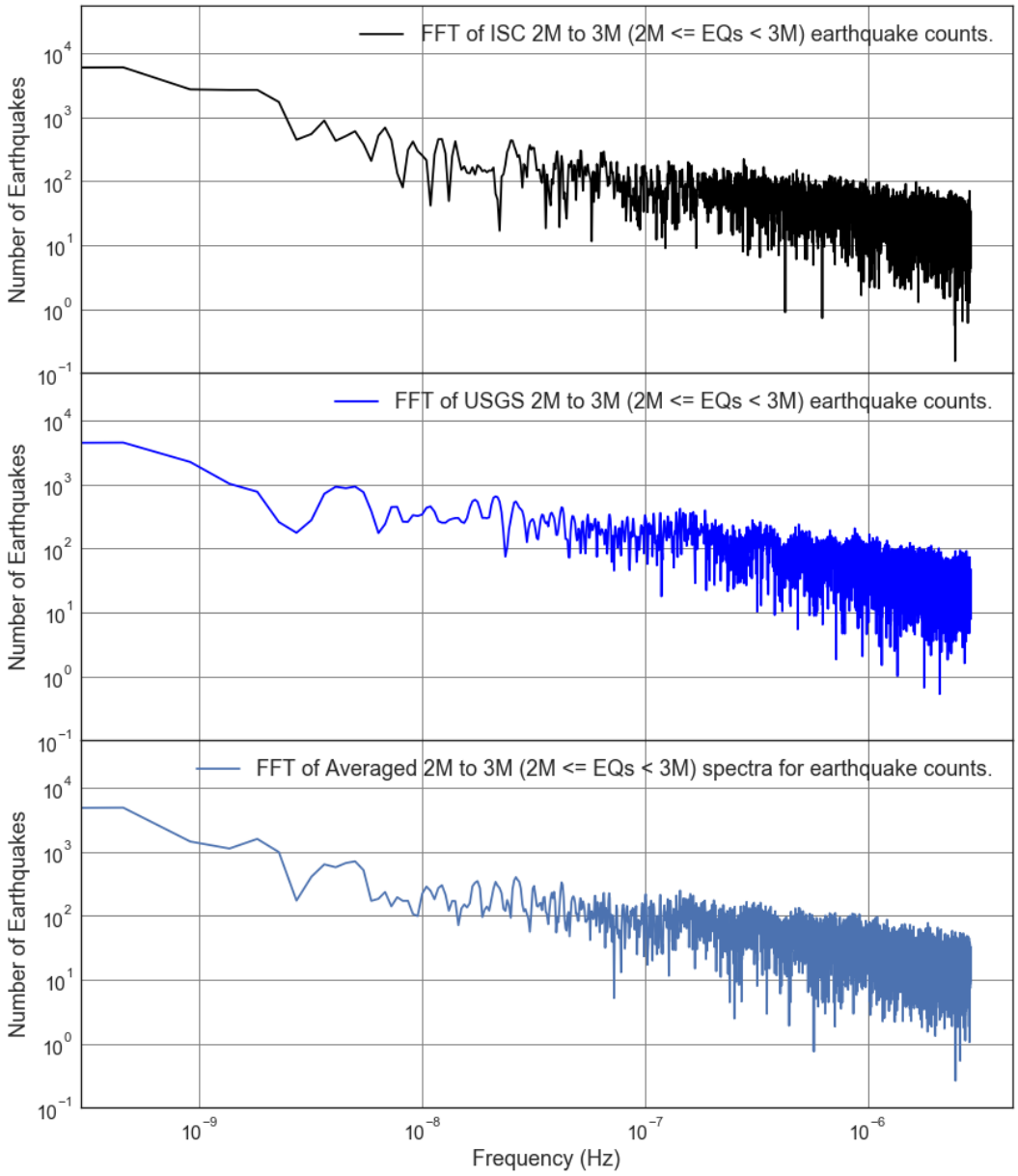

Figure F1.11: FFT Loglog Comparison Plot of number of 2M to 3M (2M <= EQs < 3M) Earthquakes from the ISC and USGS datasets.

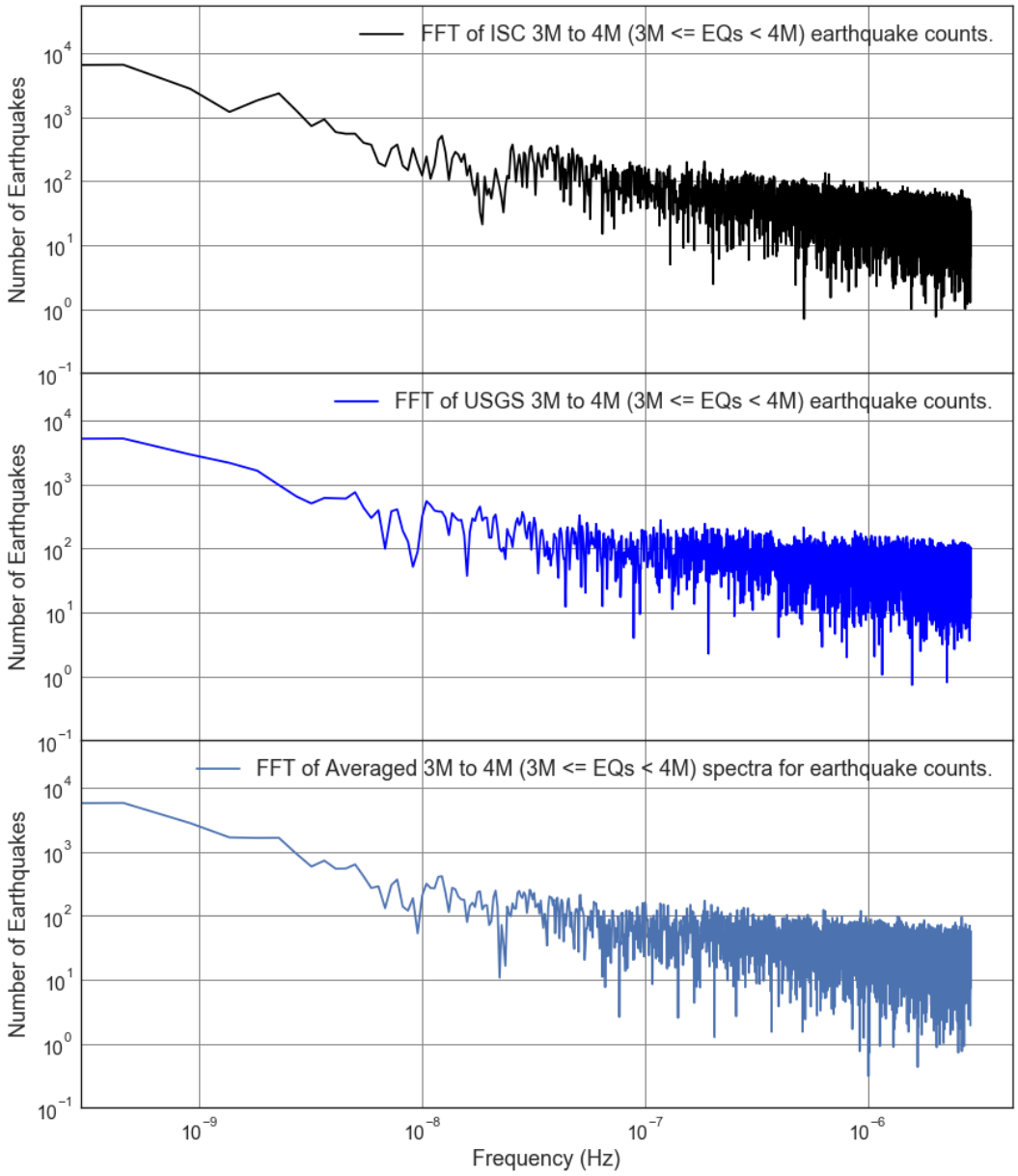

Figure F1.12: FFT Loglog Comparison Plot of number of 3M to 4M (3M <= EQs < 4M) Earthquakes from the ISC and USGS datasets.

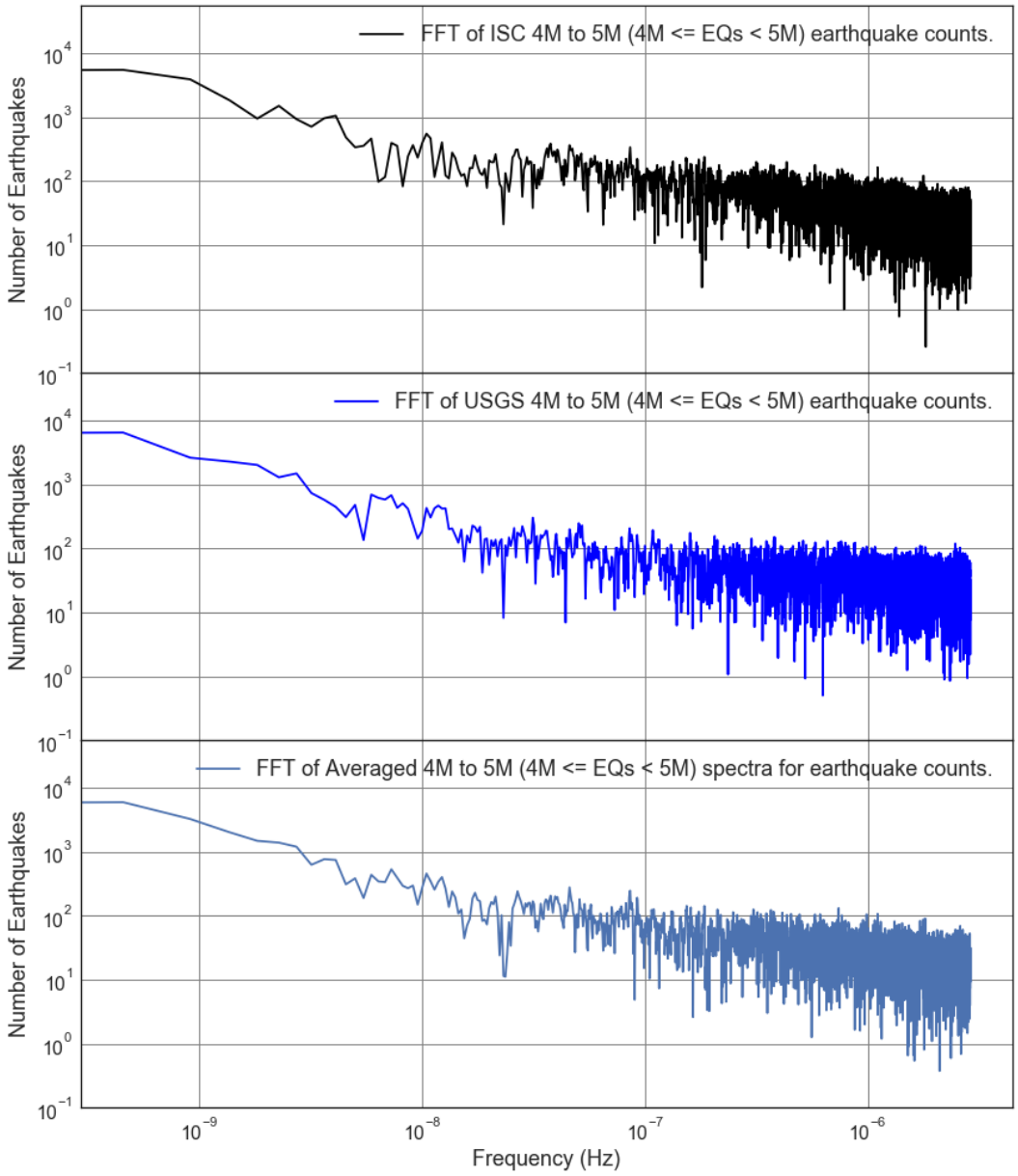

Figure F1.13: FFT Loglog Comparison Plot of number of 4M to 5M (4M <= EQs < 5M) Earthquakes from the ISC and USGS datasets.

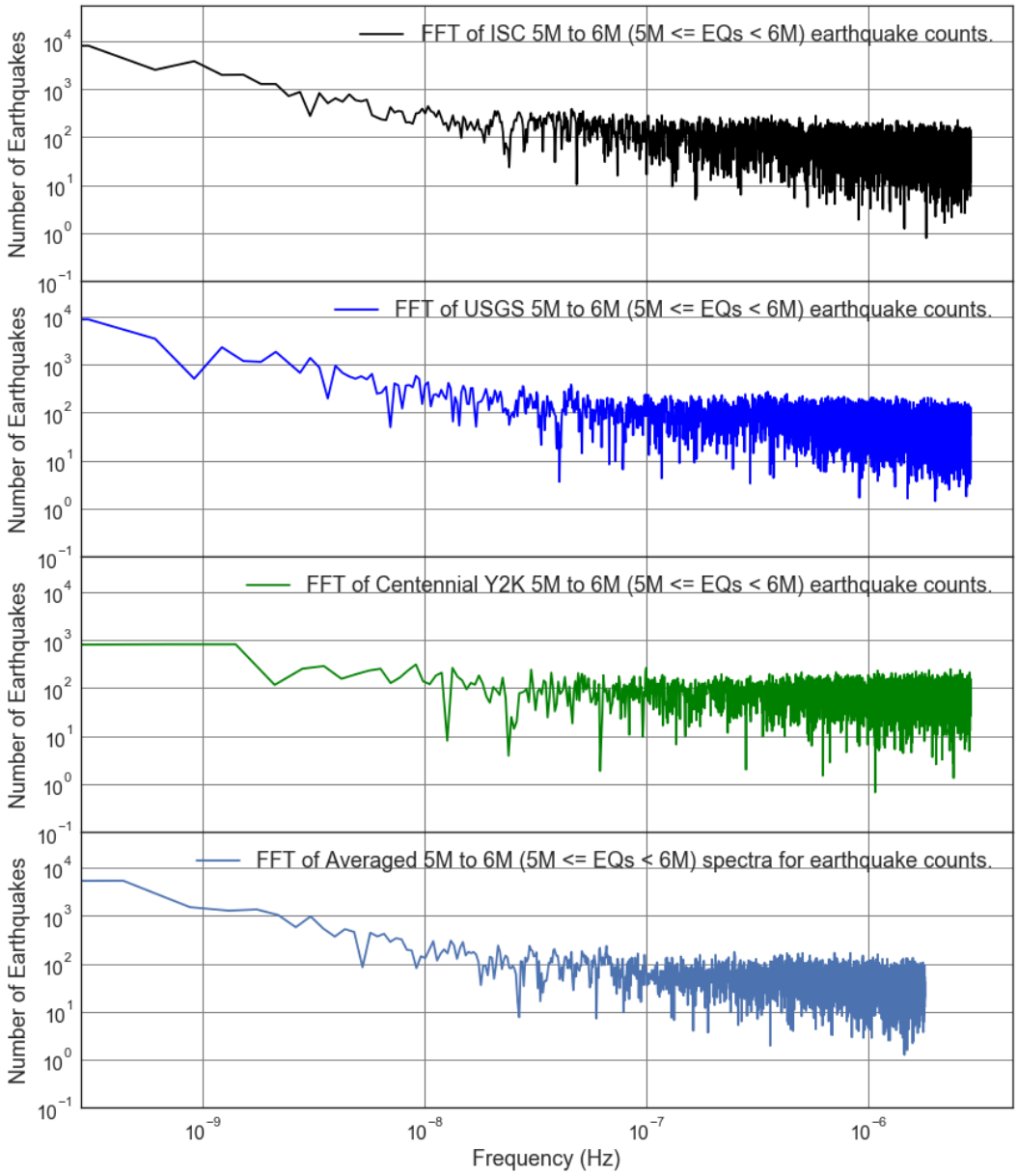

Figure F1.14: FFT Loglog Comparison Plot of number of 5M to 6M (5M <= EQs < 6M) Earthquakes from the ISC, USGS, and Centennial Y2K datasets.

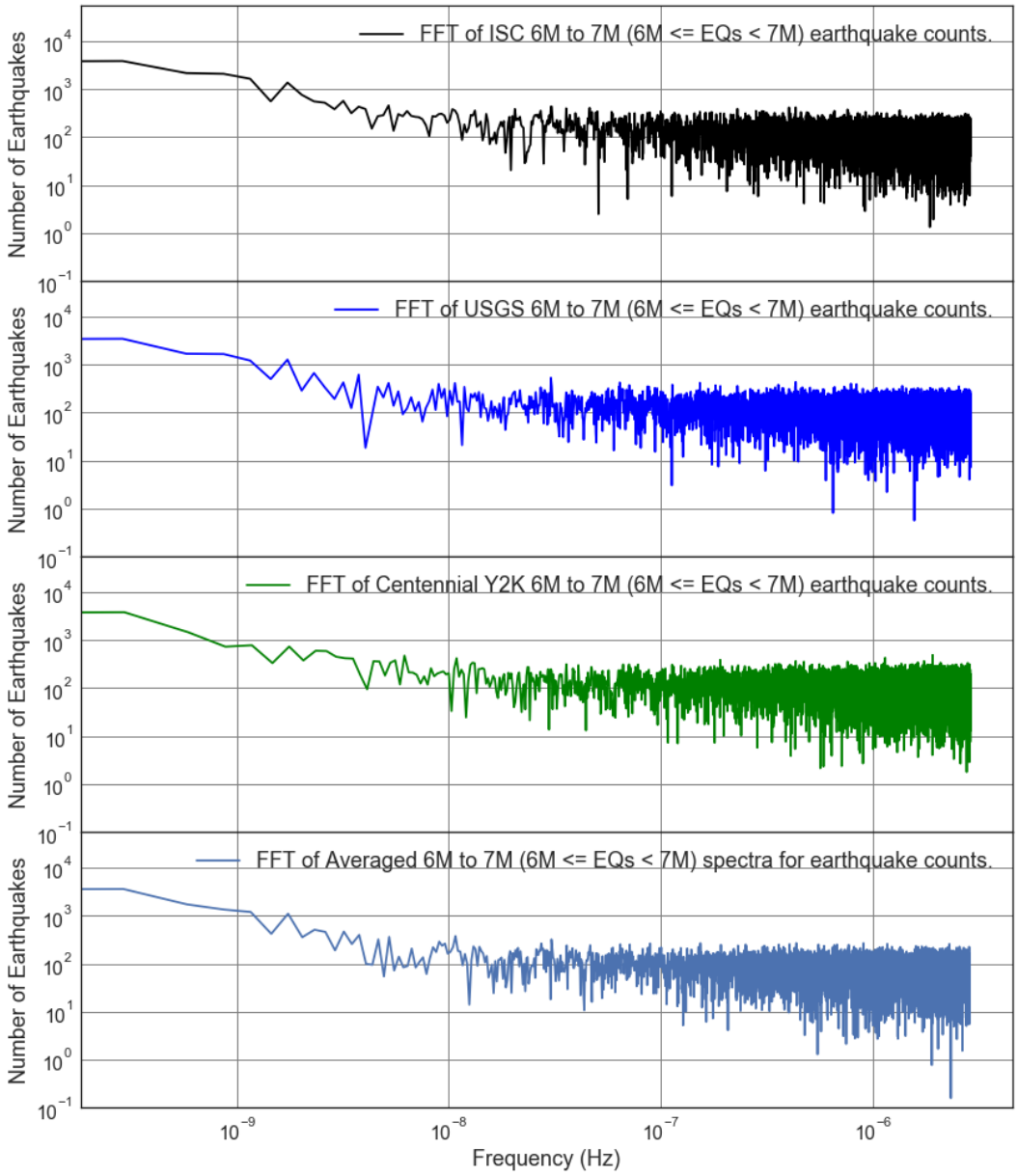

Figure F1.15: FFT Loglog Comparison Plot of number of 6M to 7M (6M <= EQs < 7M) Earthquakes from the ISC, USGS, and Centennial Y2K datasets.

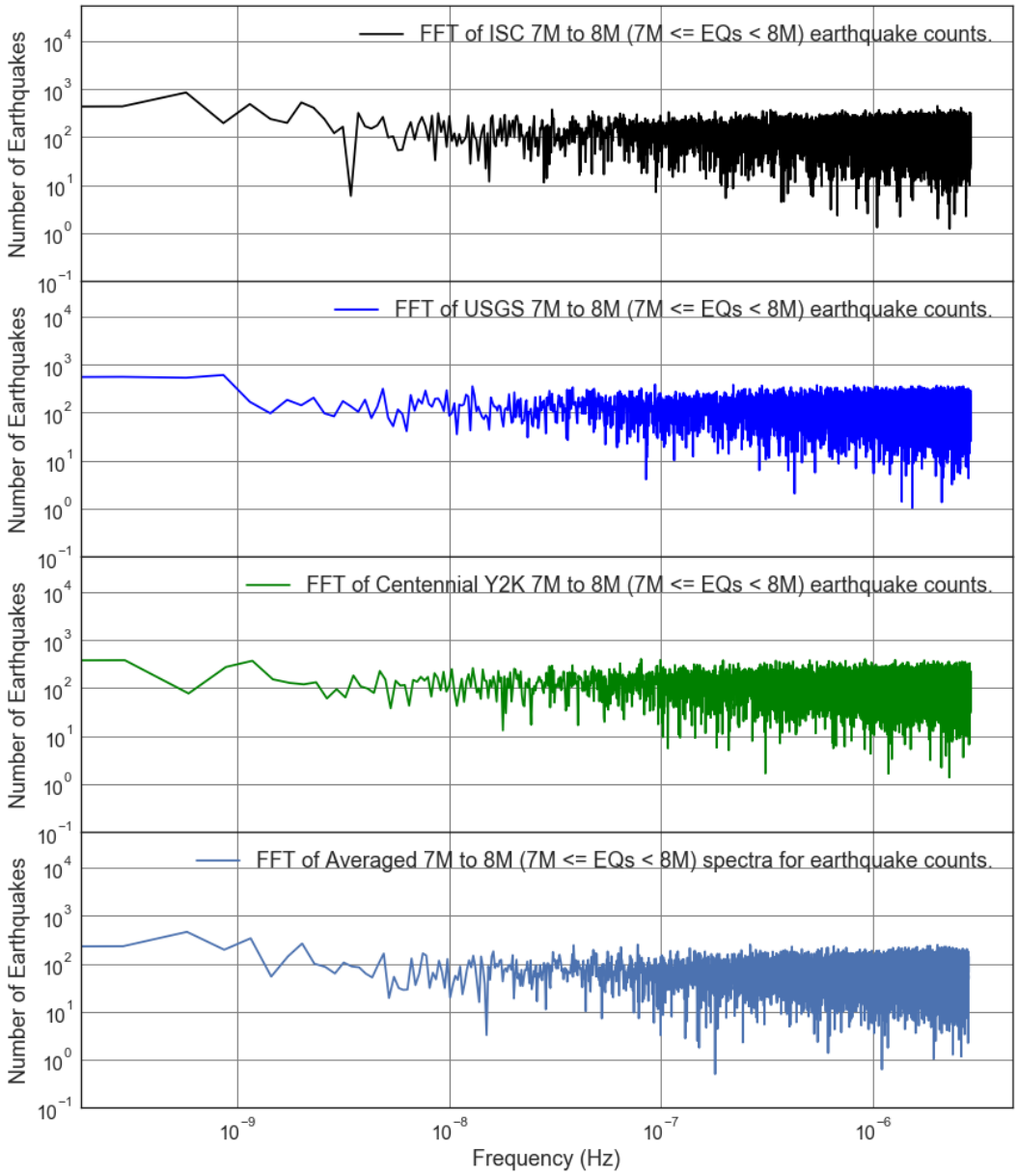

Figure F1.16: FFT Loglog Comparison Plot of number of 7M to 8M (7M <= EQs < 8M) Earthquakes from the ISC, USGS, and Centennial Y2K datasets.

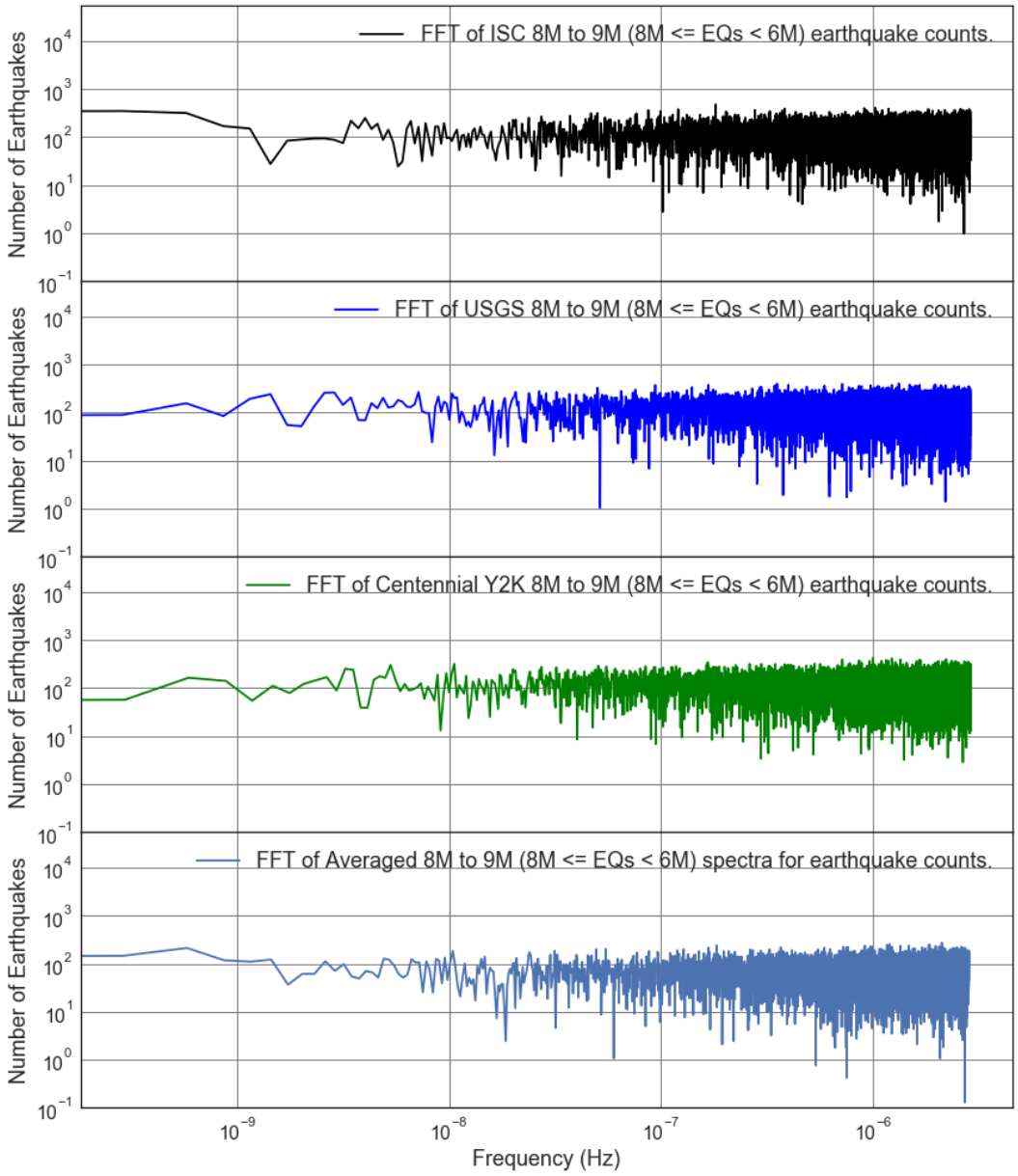

Figure F1.17: FFT Loglog Comparison Plot of number of 8M to 9M (8M <= EQs < 6M) Earthquakes from the ISC, USGS, and Centennial Y2K datasets.

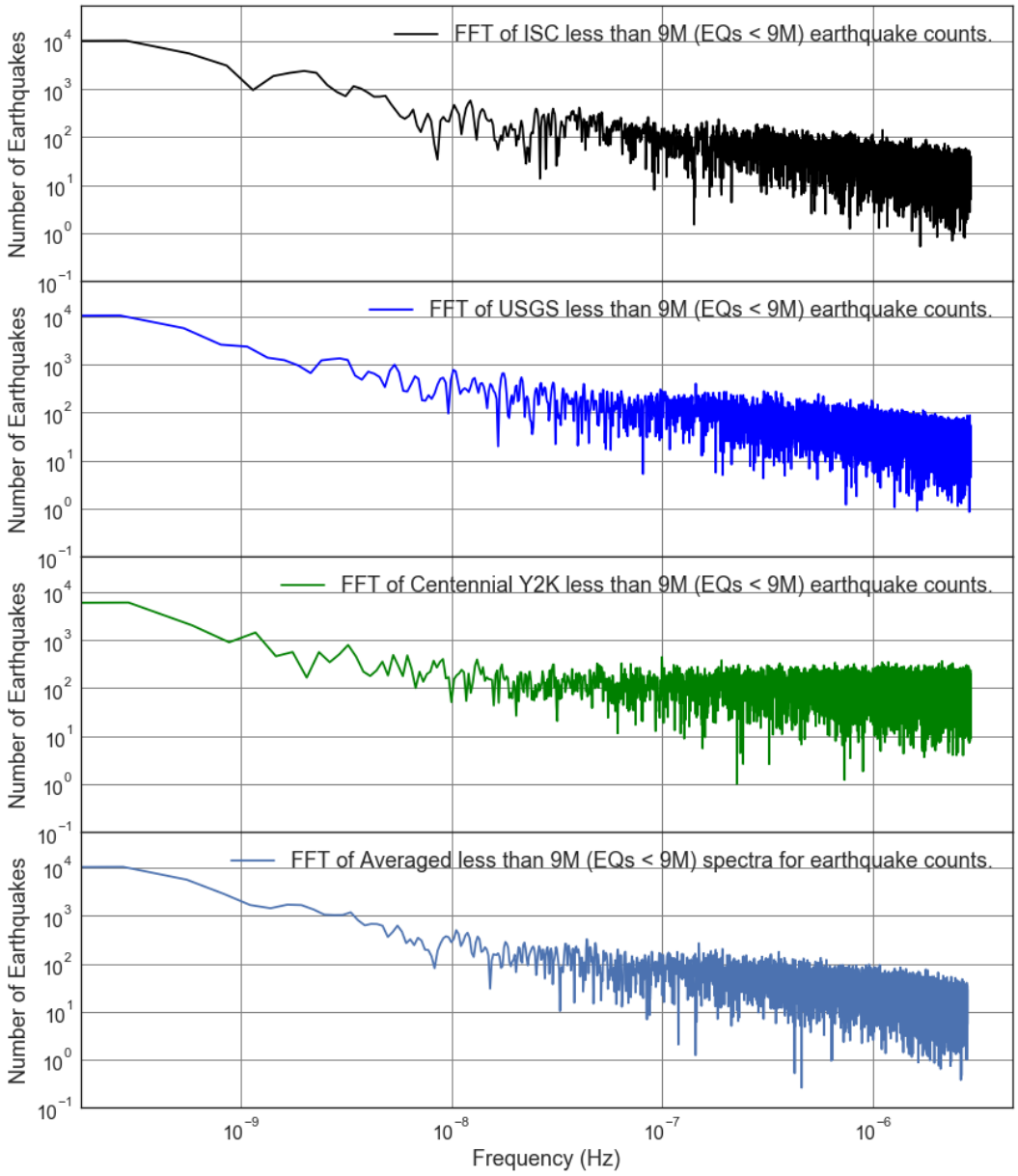

Figure F1.18: FFT Loglog Comparison Plot of number of Earthquakes less than 9M (EQs < 9M) from the ISC, USGS, and Centennial Y2K datasets.

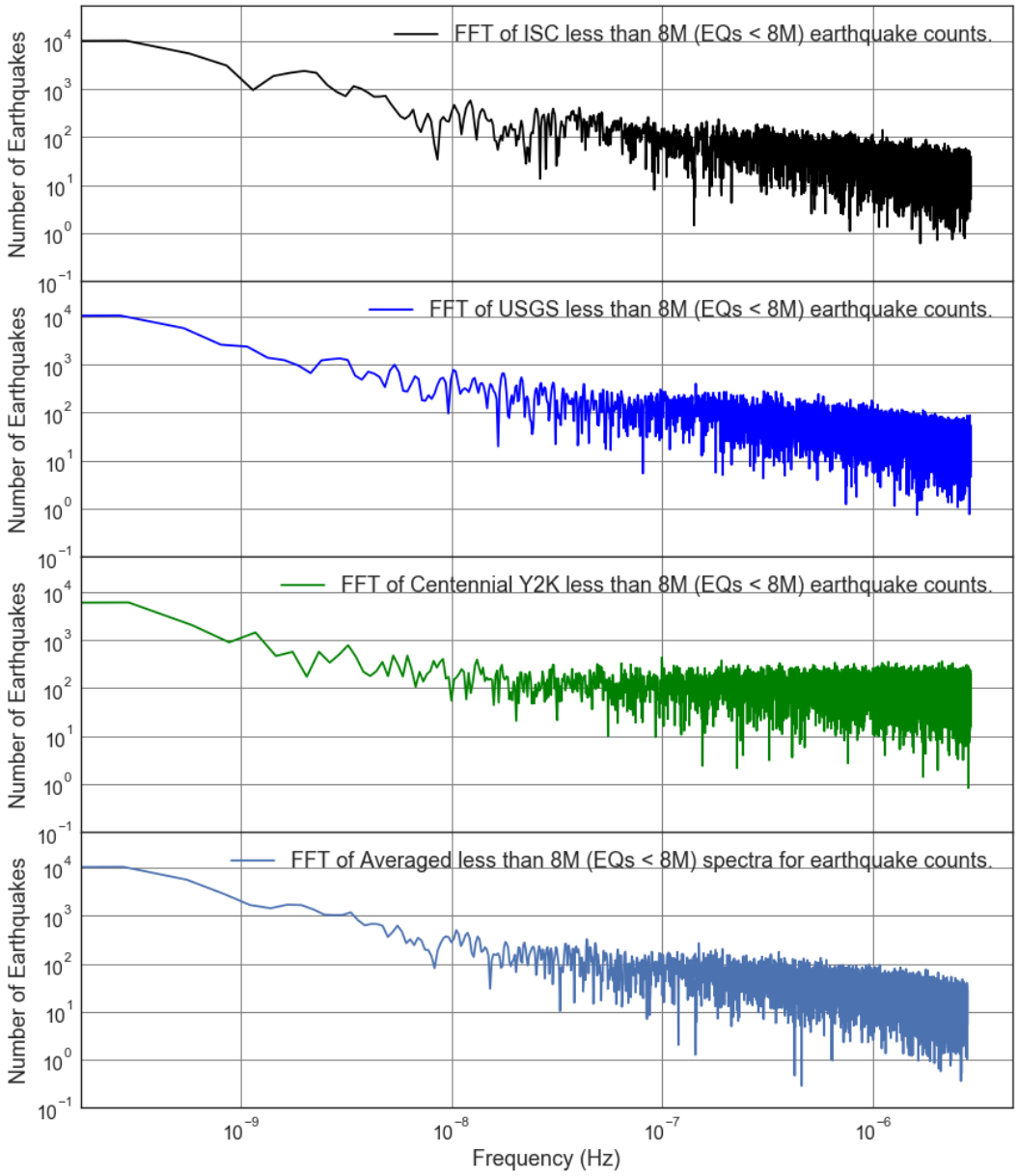

Figure F1.19: FFT Loglog Comparison Plot of number of Earthquakes less than less than 8M (EQs < 8M) from the ISC, USGS, and Centennial Y2K datasets.

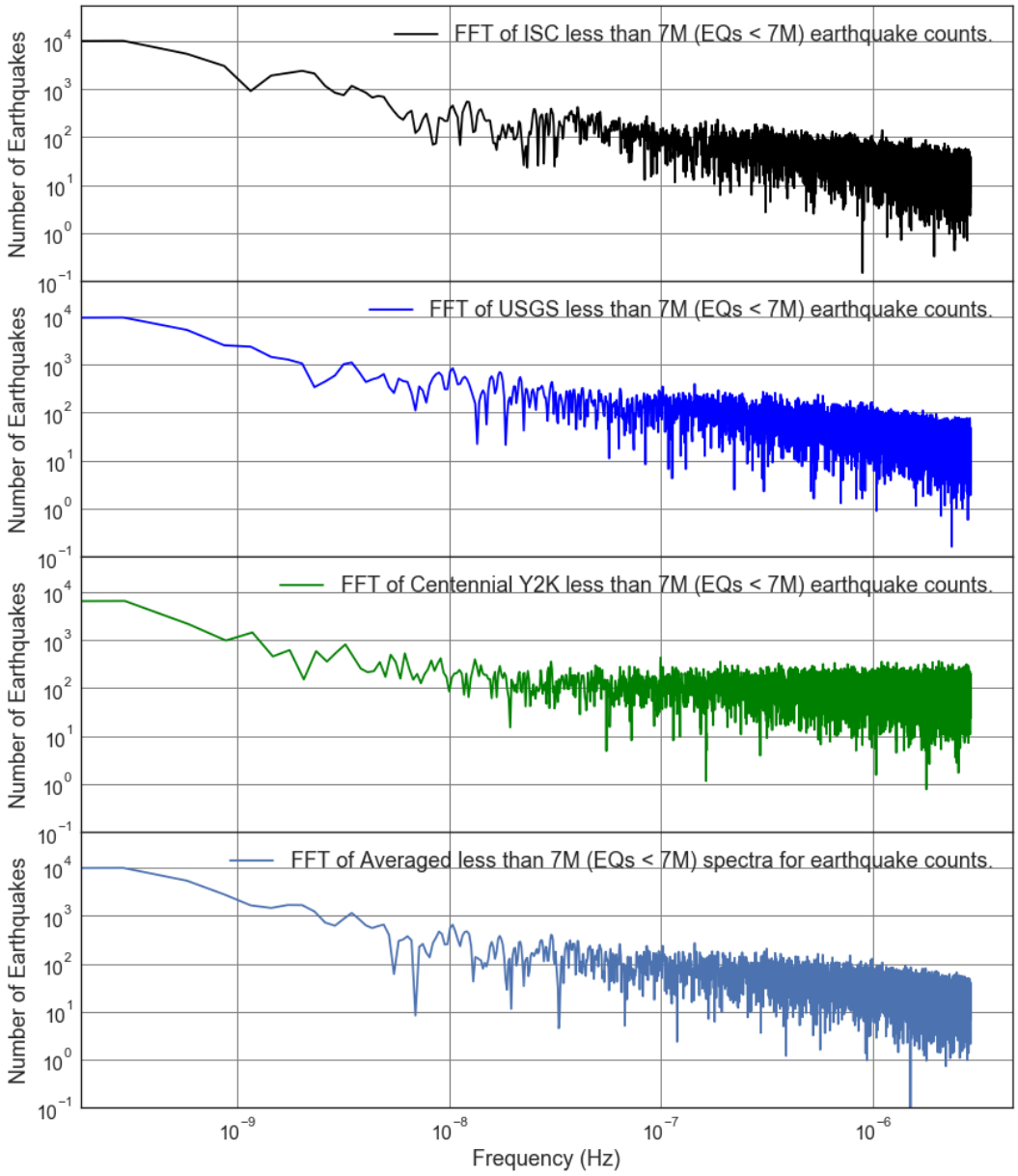

Figure F1.20: FFT Loglog Comparison Plot of number of Earthquakes less than less than 7M (EQs < 7M) from the ISC, USGS, and Centennial Y2K datasets.

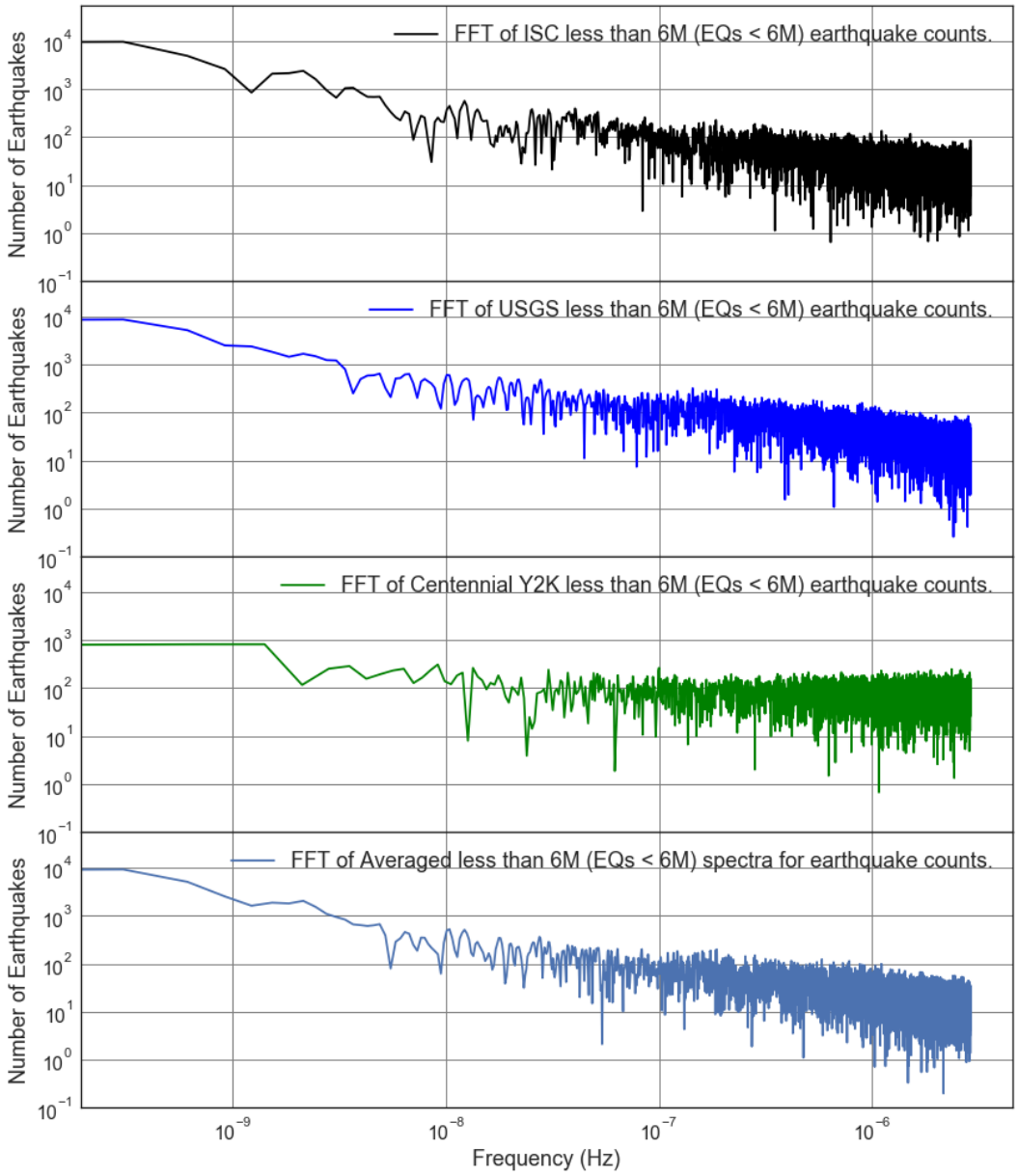

Figure F1.21: FFT Loglog Comparison Plot of number of Earthquakes less than less than 6M (EQs < 6M) from the ISC, USGS, and Centennial Y2K datasets.

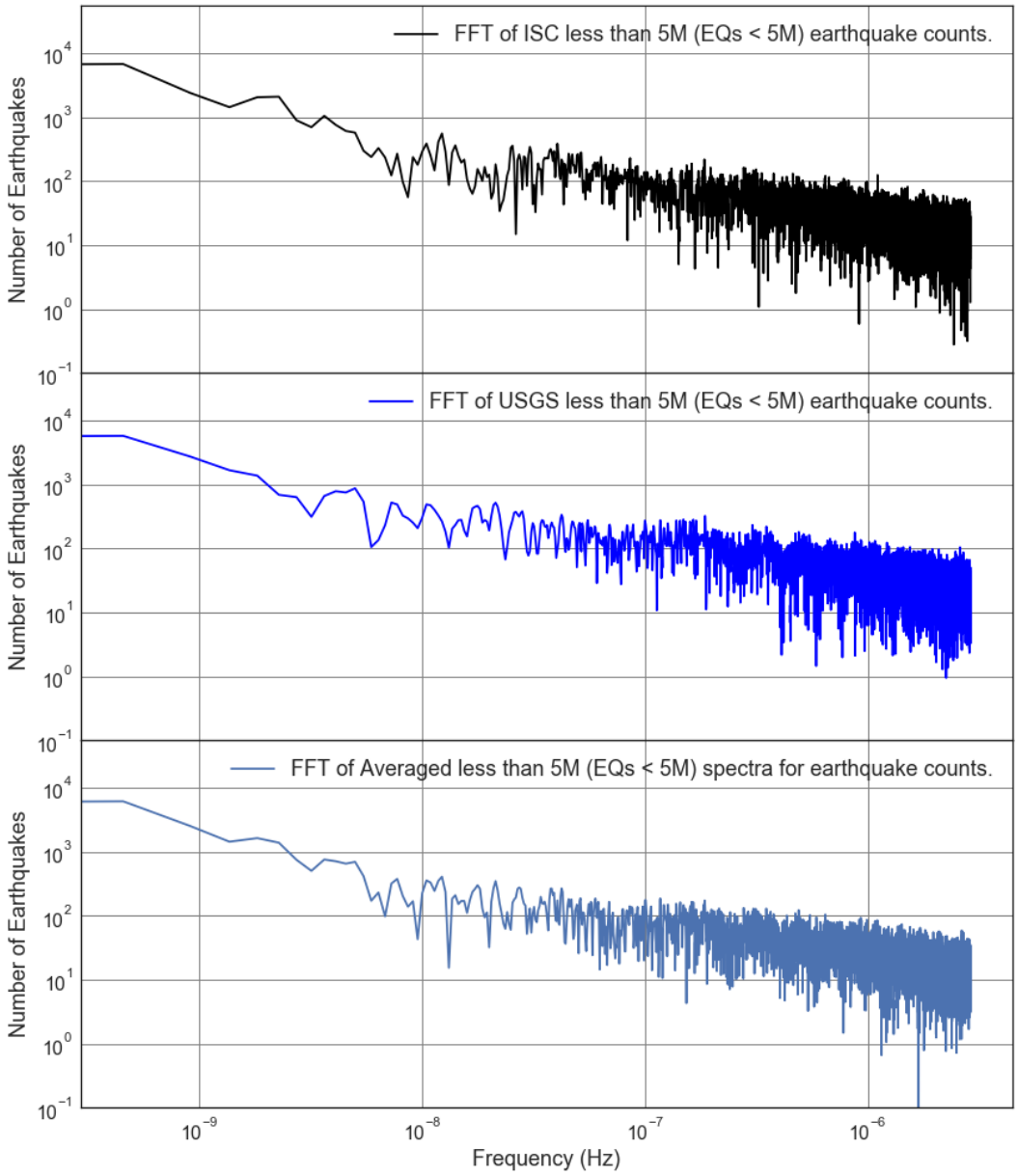

Figure F1.22: FFT Loglog Comparison Plot of number of Earthquakes less than 5M (EQs < 5M) from the ISC and USGS datasets.

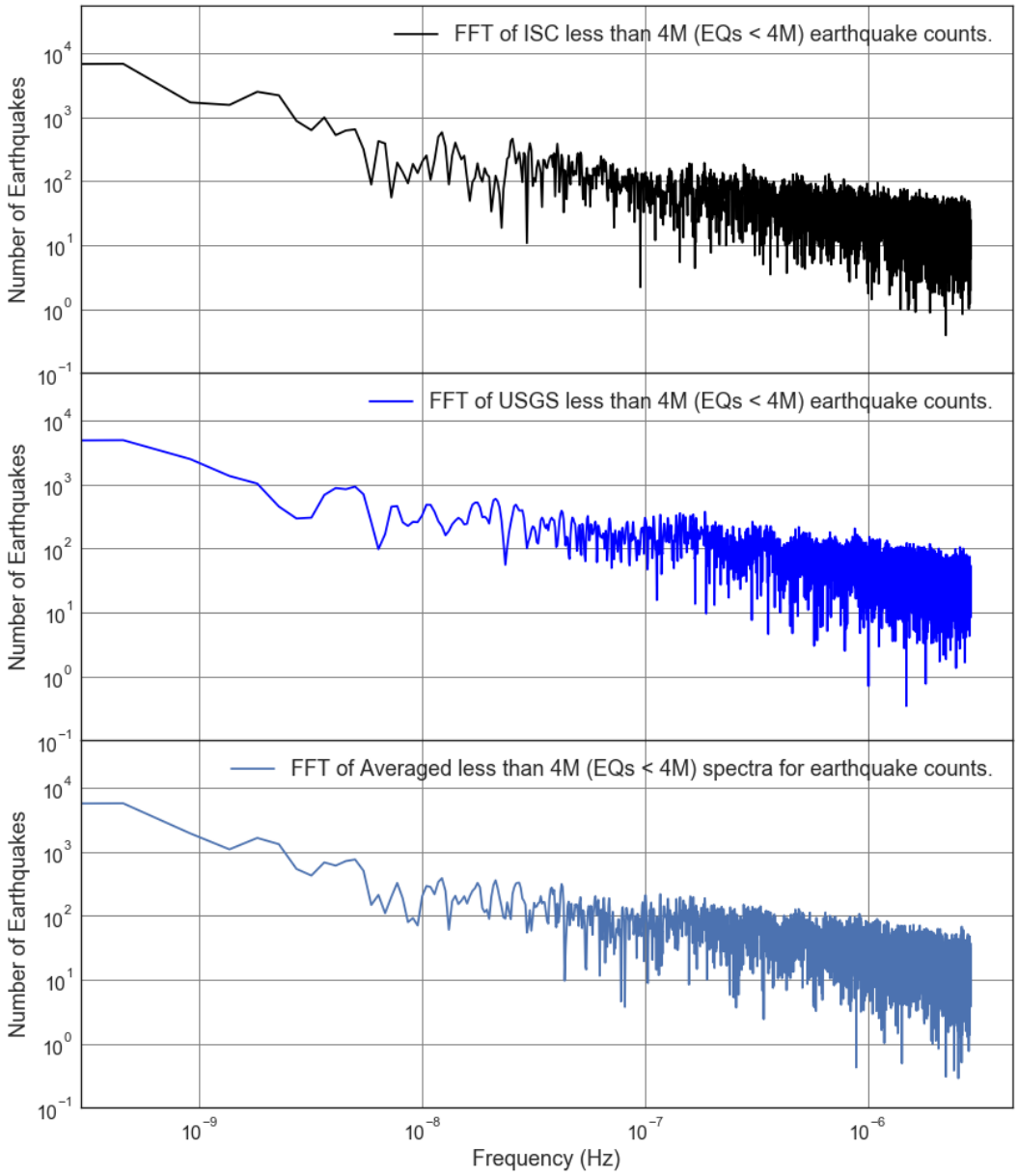

Figure F1.23: FFT Loglog Comparison Plot of number of Earthquakes less than 4M (EQs < 4M) from the ISC and USGS datasets.

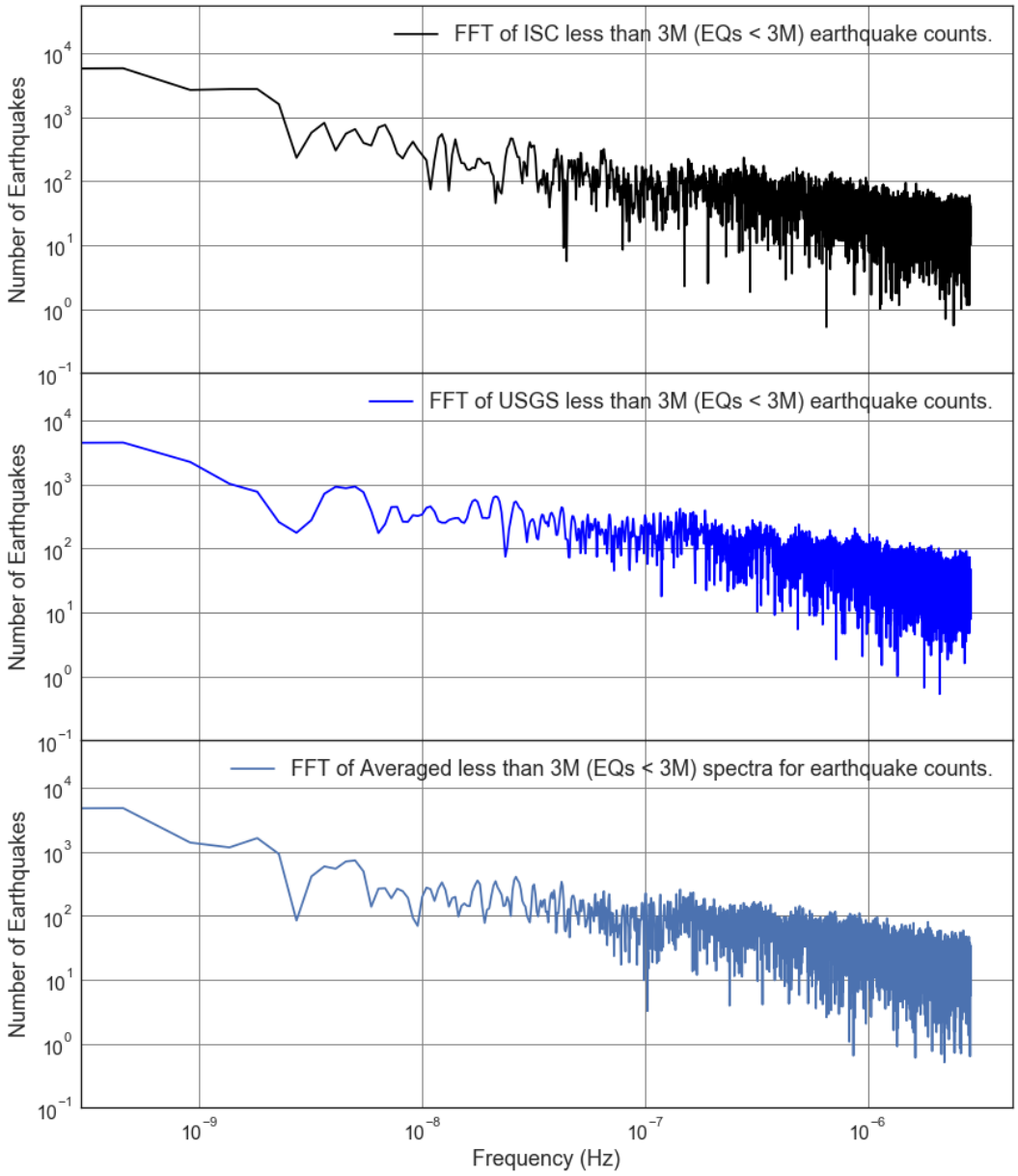

Figure F1.24: FFT Loglog Comparison Plot of number of Earthquakes less than 3M (EQs < 3M) from the ISC and USGS datasets.

Comparison of Averaged, ISC, USGS, and Centennial Y2K FFT of Earthquake Energy Plots

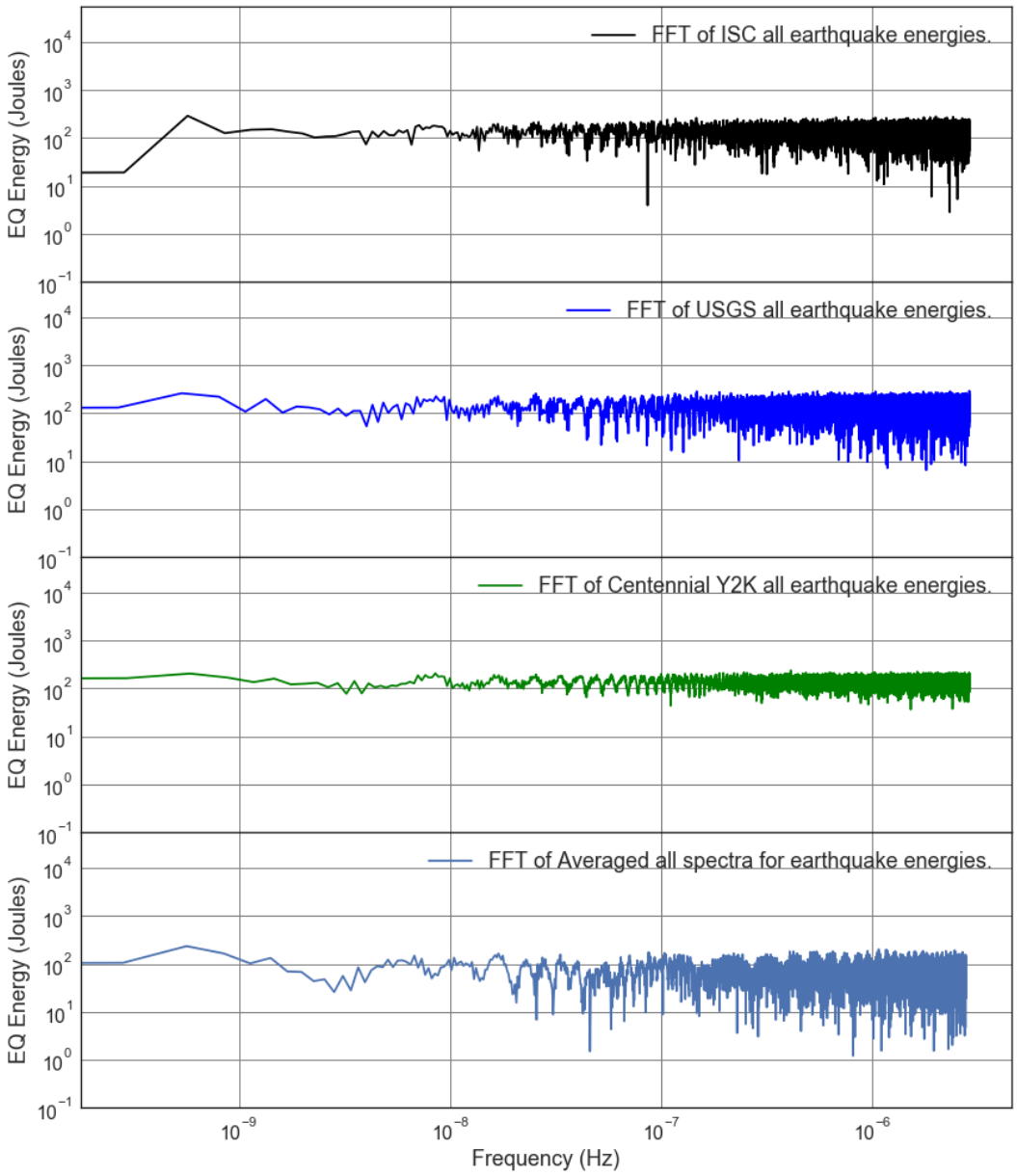

Figure F1.25: FFT Loglog Comparison Plot of number of all Earthquake Energies from the ISC, USGS, and Centennial Y2K datasets.

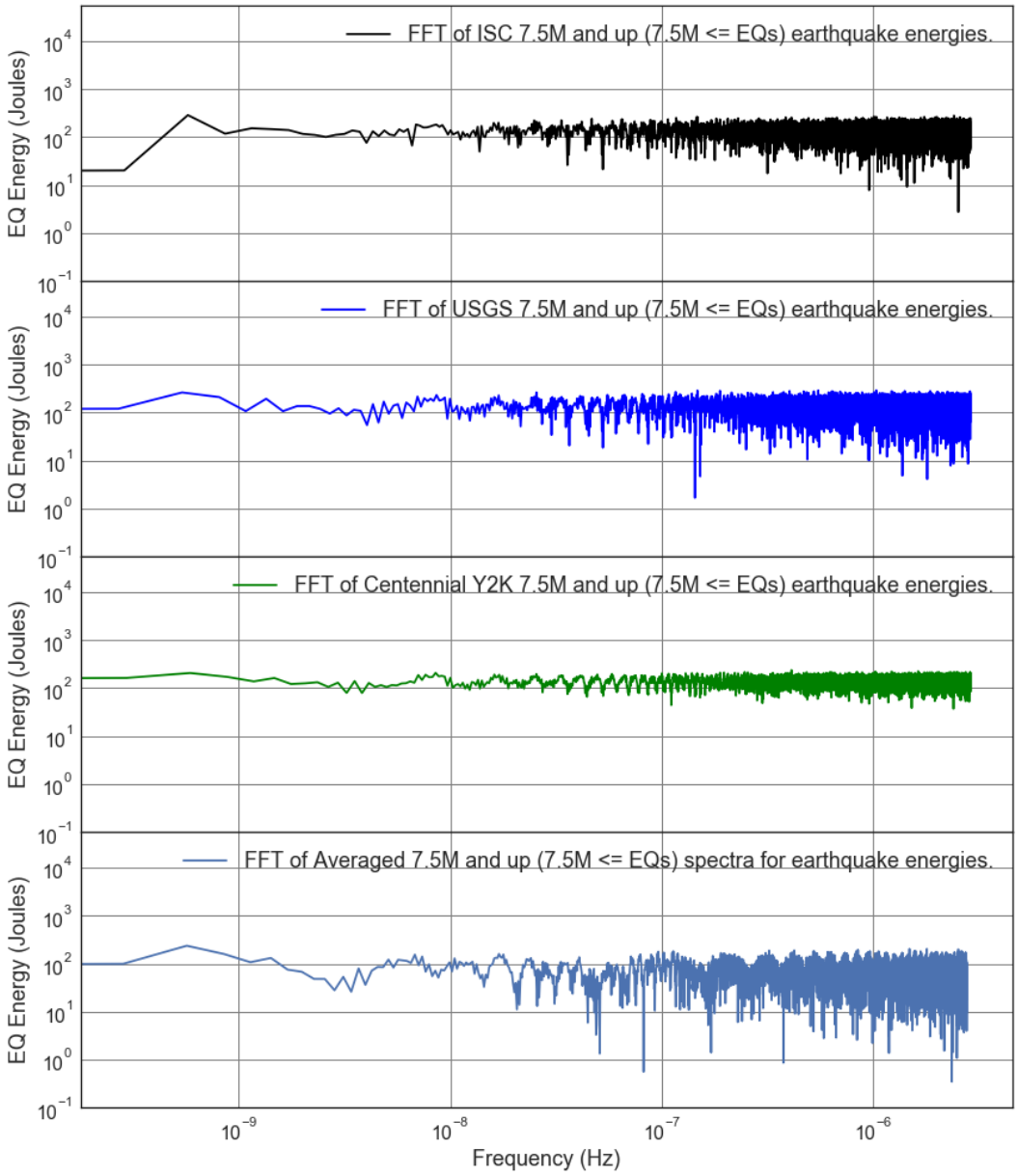

Figure F1.26: FFT Loglog Comparison Plot of Estimated Total 7.5M and up (7.5M <= EQs) Earthquake Energies Released from the ISC, USGS, and Centennial Y2K datasets.

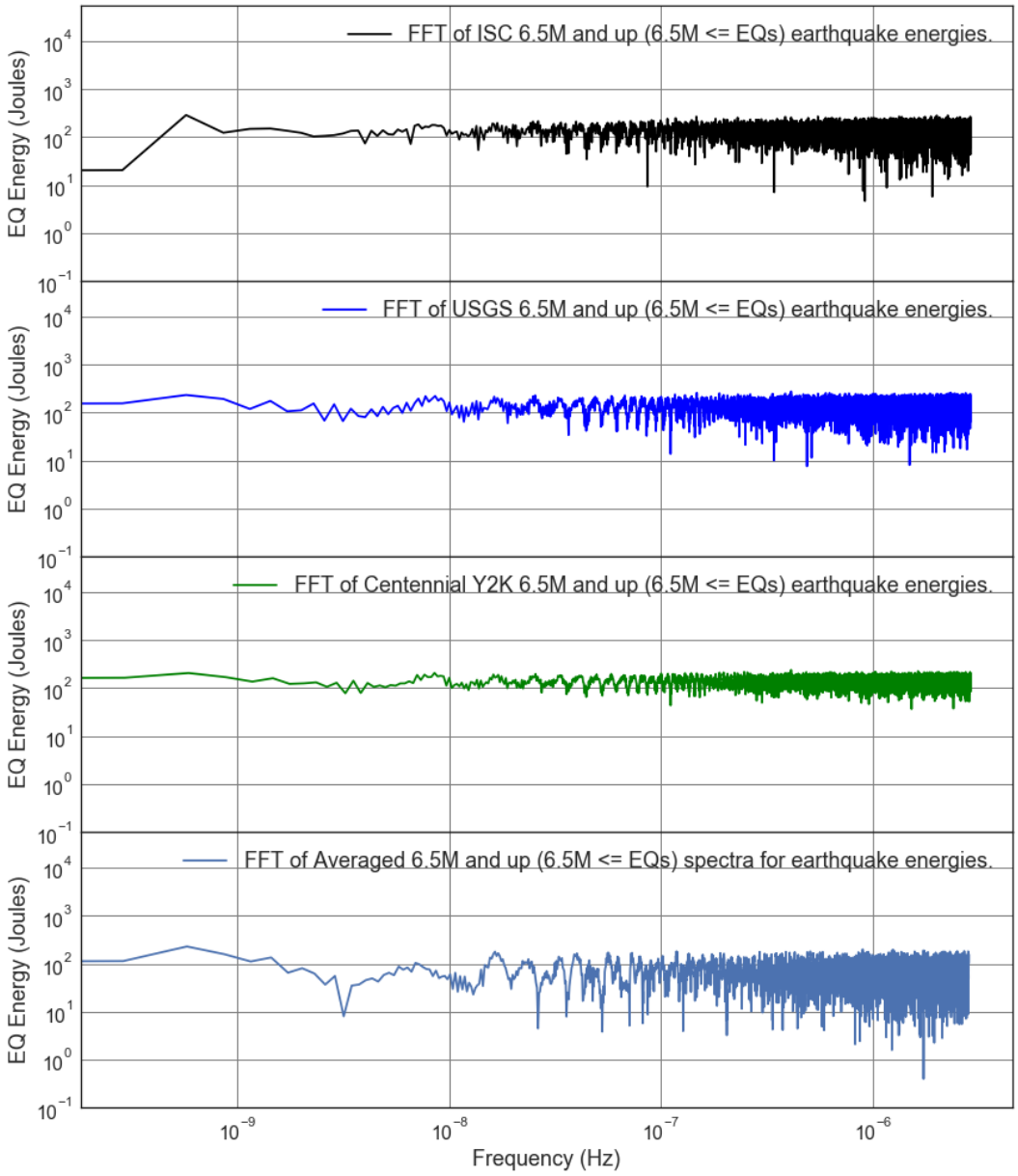

Figure F1.27: FFT Loglog Comparison Plot of Estimated Total 6.5M and up (6.5M <= EQs) Earthquake Energies Released from the ISC, USGS, and Centennial Y2K datasets.

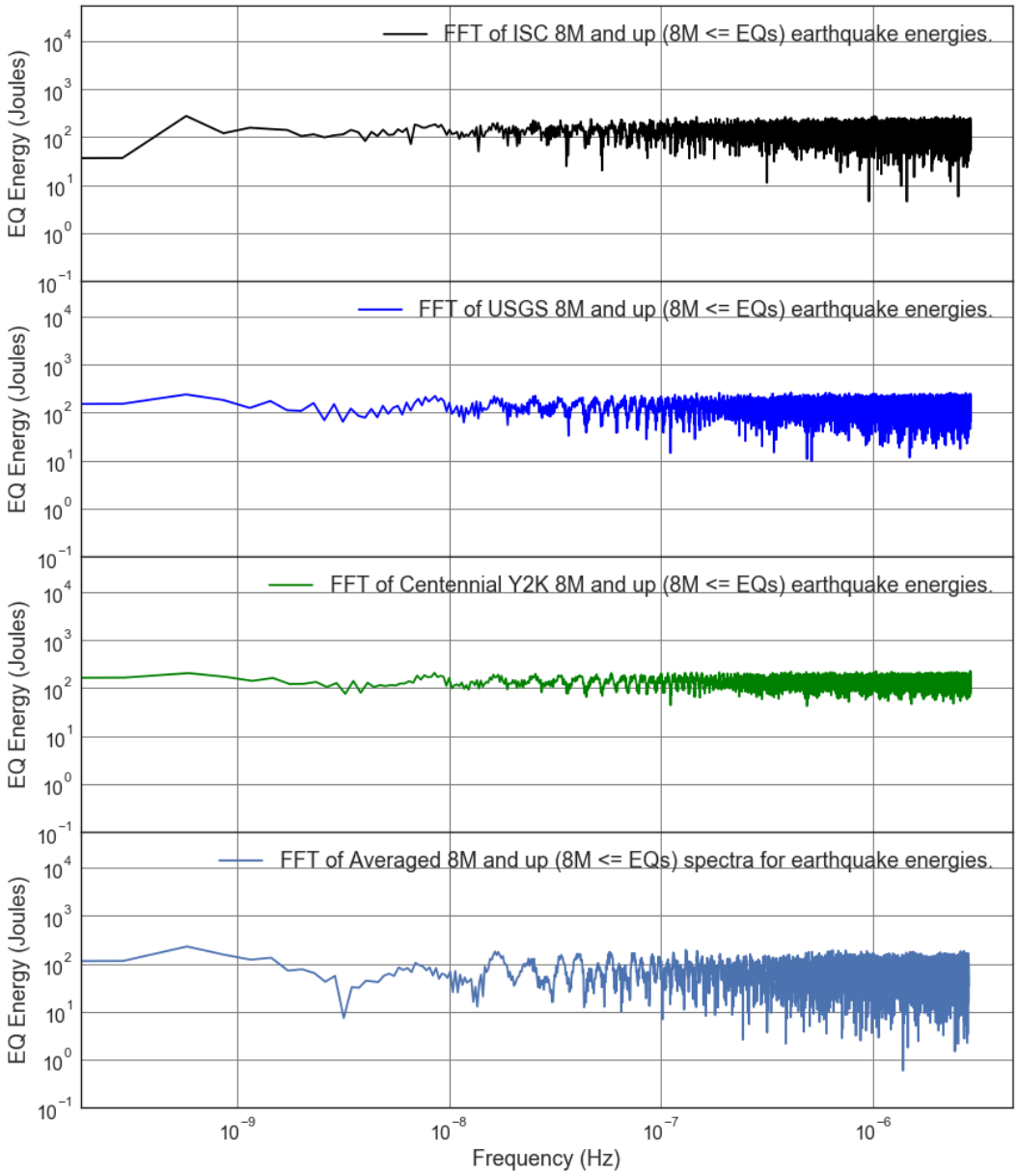

Figure F1.28: FFT Loglog Comparison Plot of Estimated Total 8M and up (8M <= EQs) Earthquake Energies Released from the ISC, USGS, and Centennial Y2K datasets.

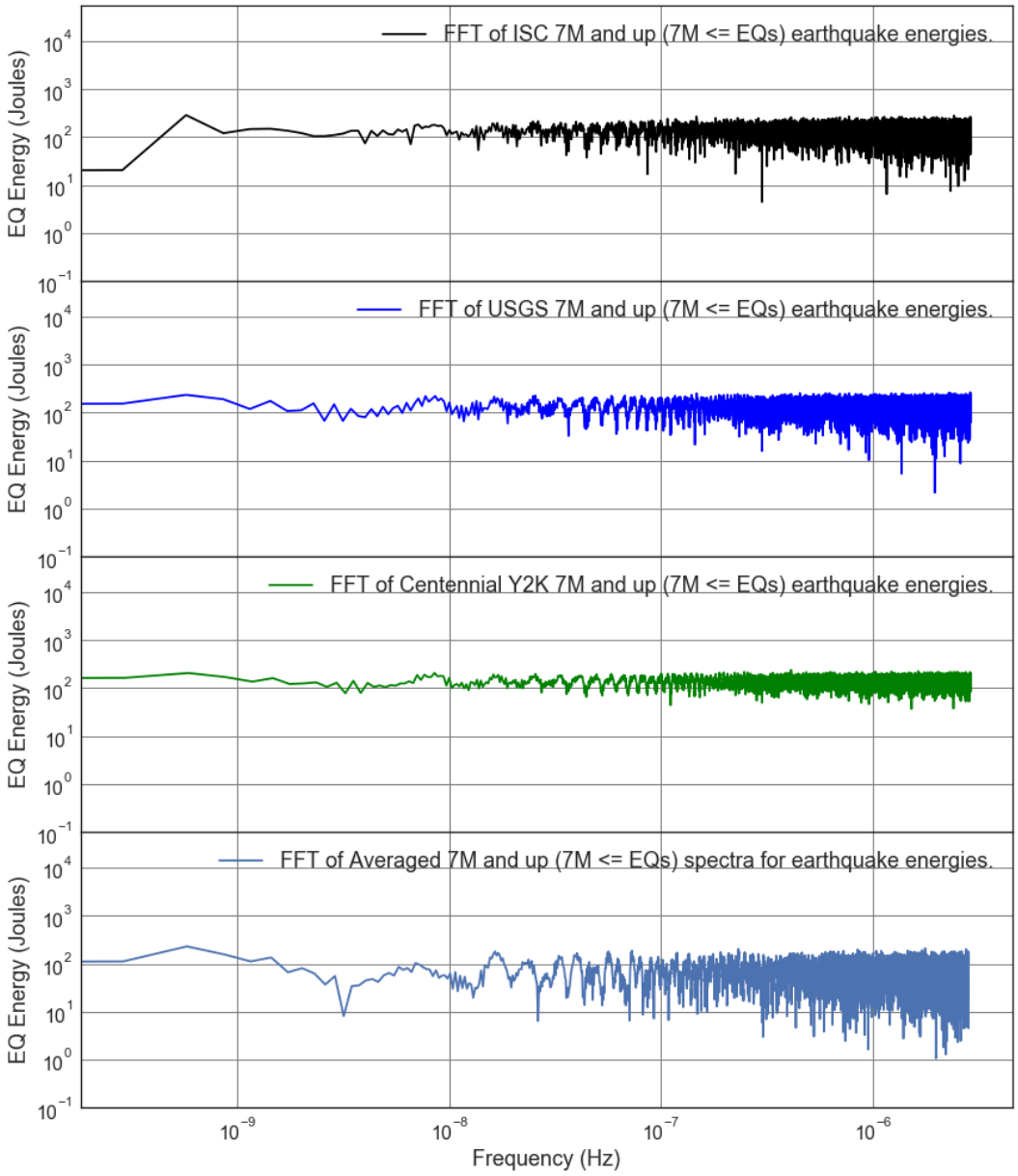

Figure F1.29: FFT Loglog Comparison Plot of Estimated Total 7M and up (7M <= EQs) Earthquake Energies Released from the ISC, USGS, and Centennial Y2K datasets.

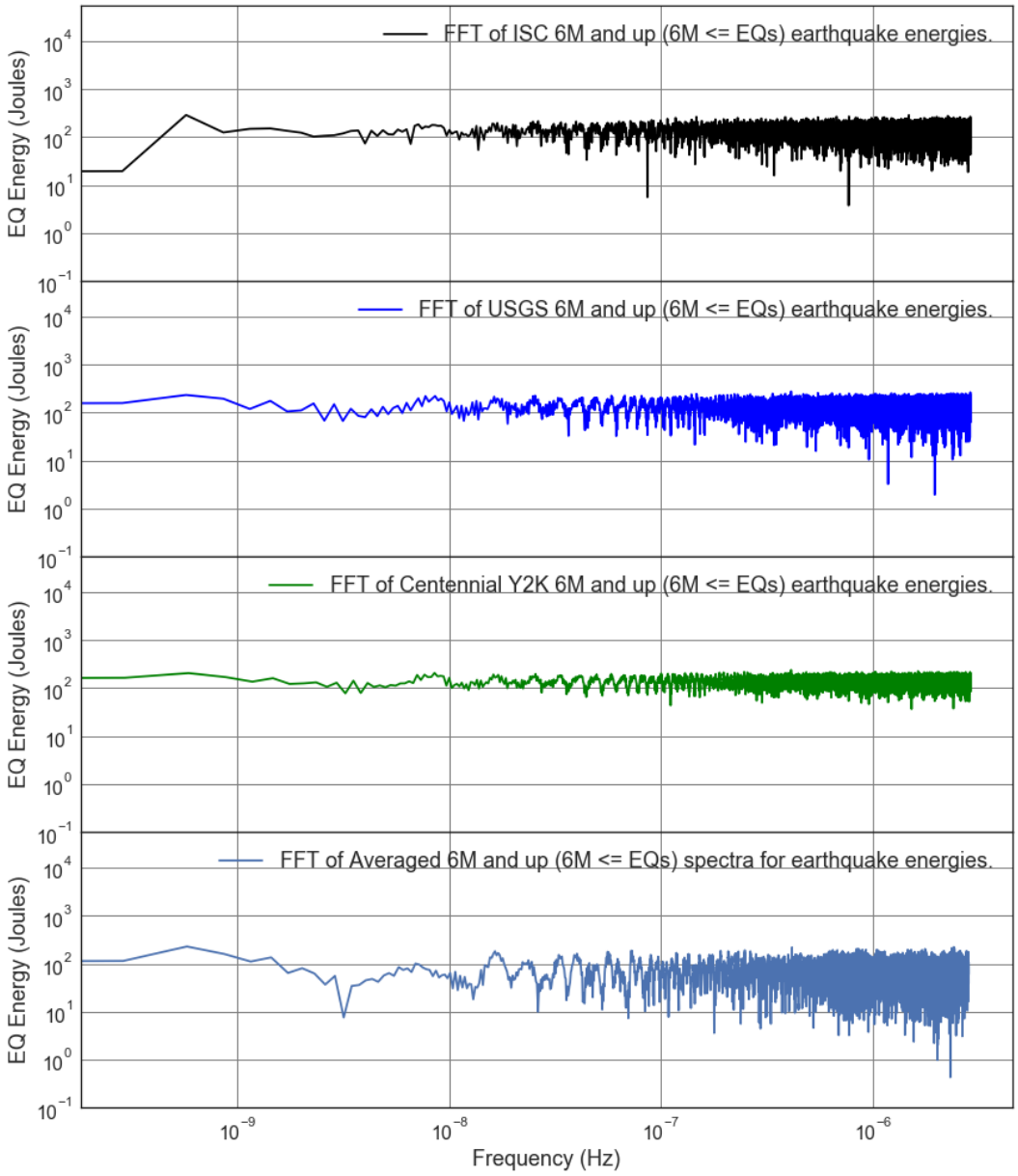

Figure F1.30: FFT Loglog Comparison Plot of Estimated Total 6M and up (6M <= EQs) Earthquake Energies Released from the ISC, USGS, and Centennial Y2K datasets.

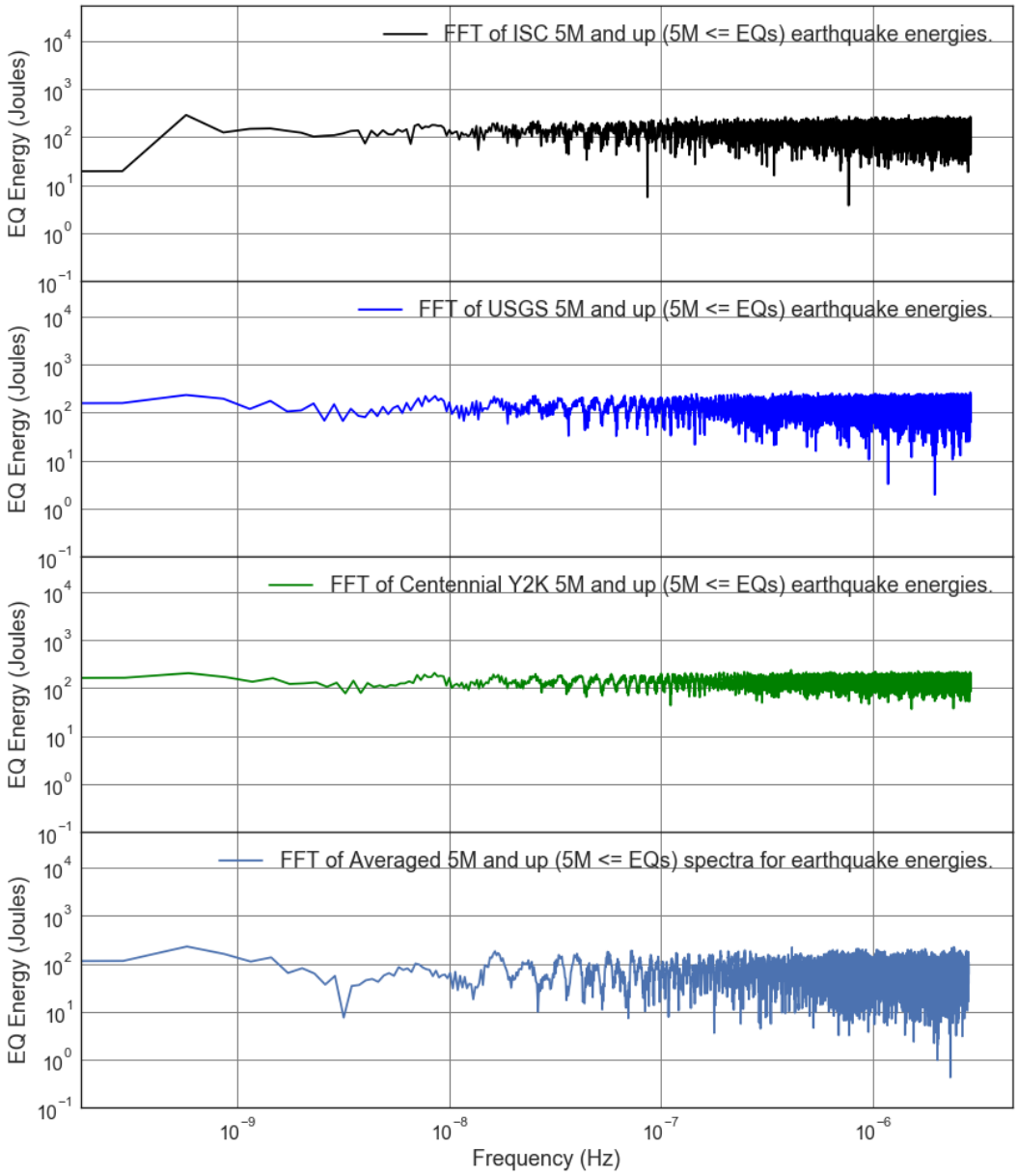

Figure F1.31: FFT Loglog Comparison Plot of Estimated Total 5M and up (5M <= EQs) Earthquake Energies Released from the ISC, USGS, and Centennial Y2K datasets.

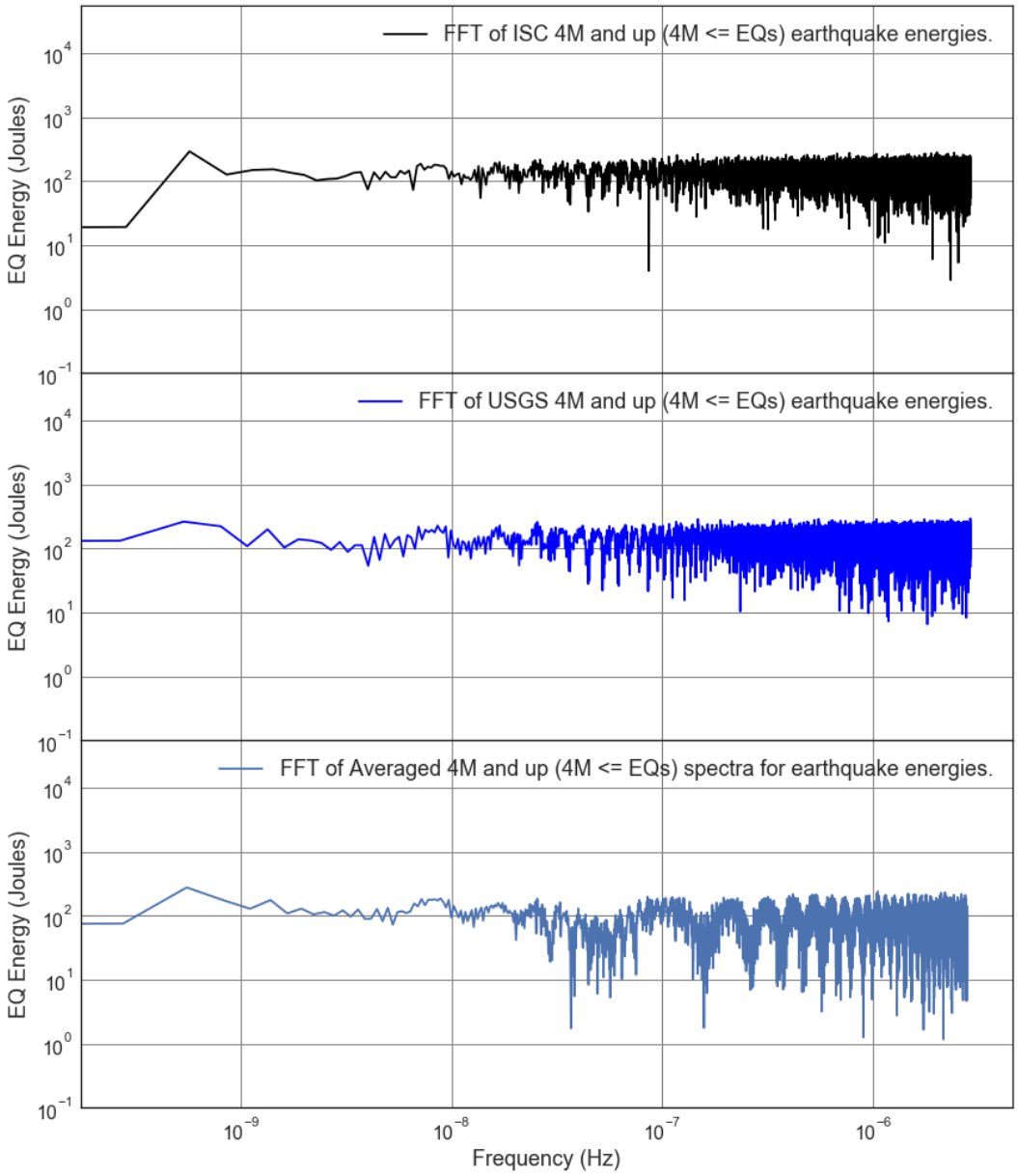

Figure F1.32: FFT Loglog Comparison Plot of Estimated Total 4M and up (4M <= EQs) Earthquake Energies Released from the ISC, USGS, and Centennial Y2K datasets.

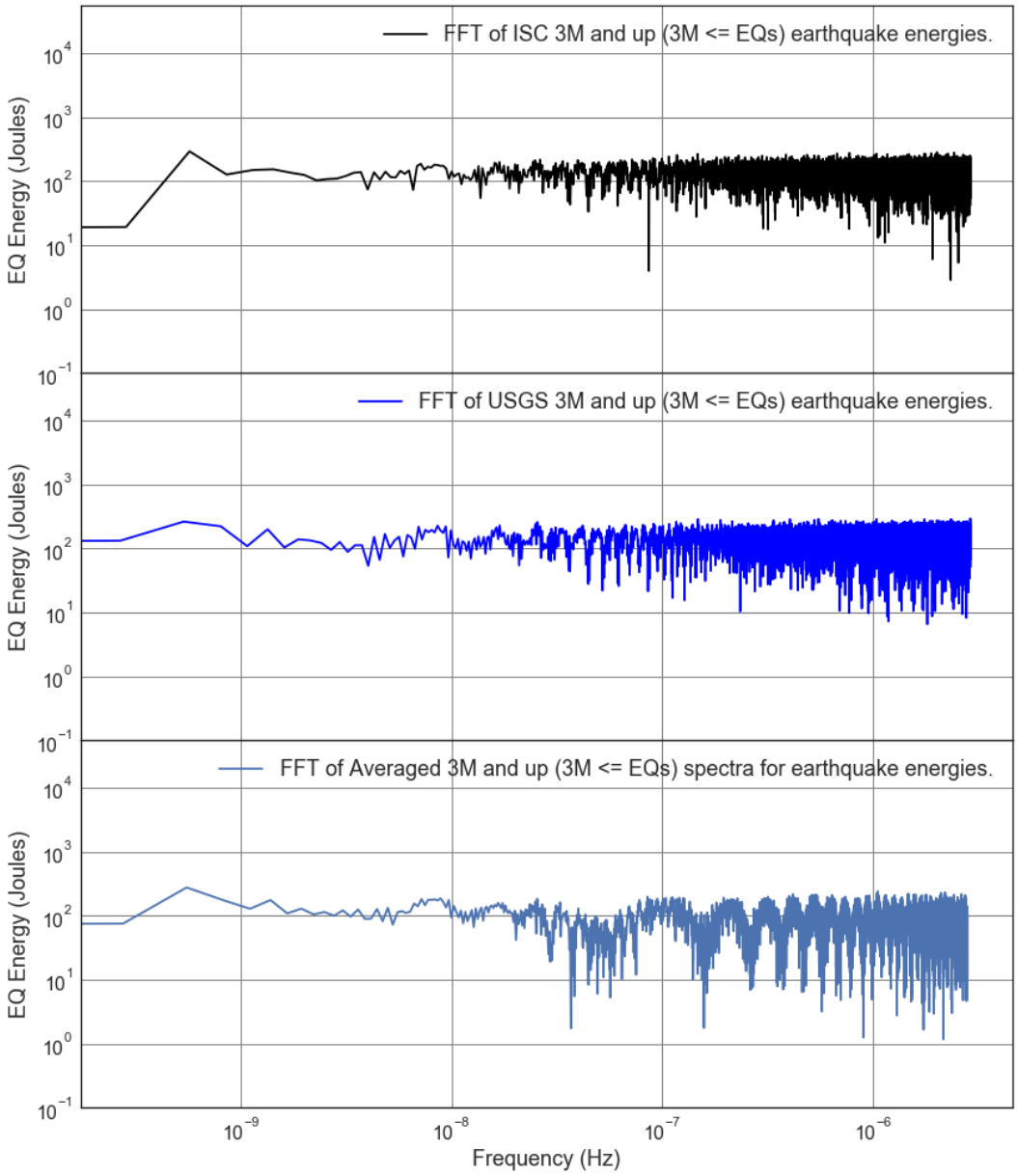

Figure F1.33: FFT Loglog Comparison Plot of Estimated Total 3M and up (3M <= EQs) Earthquake Energies Released from the ISC, USGS, and Centennial Y2K datasets.

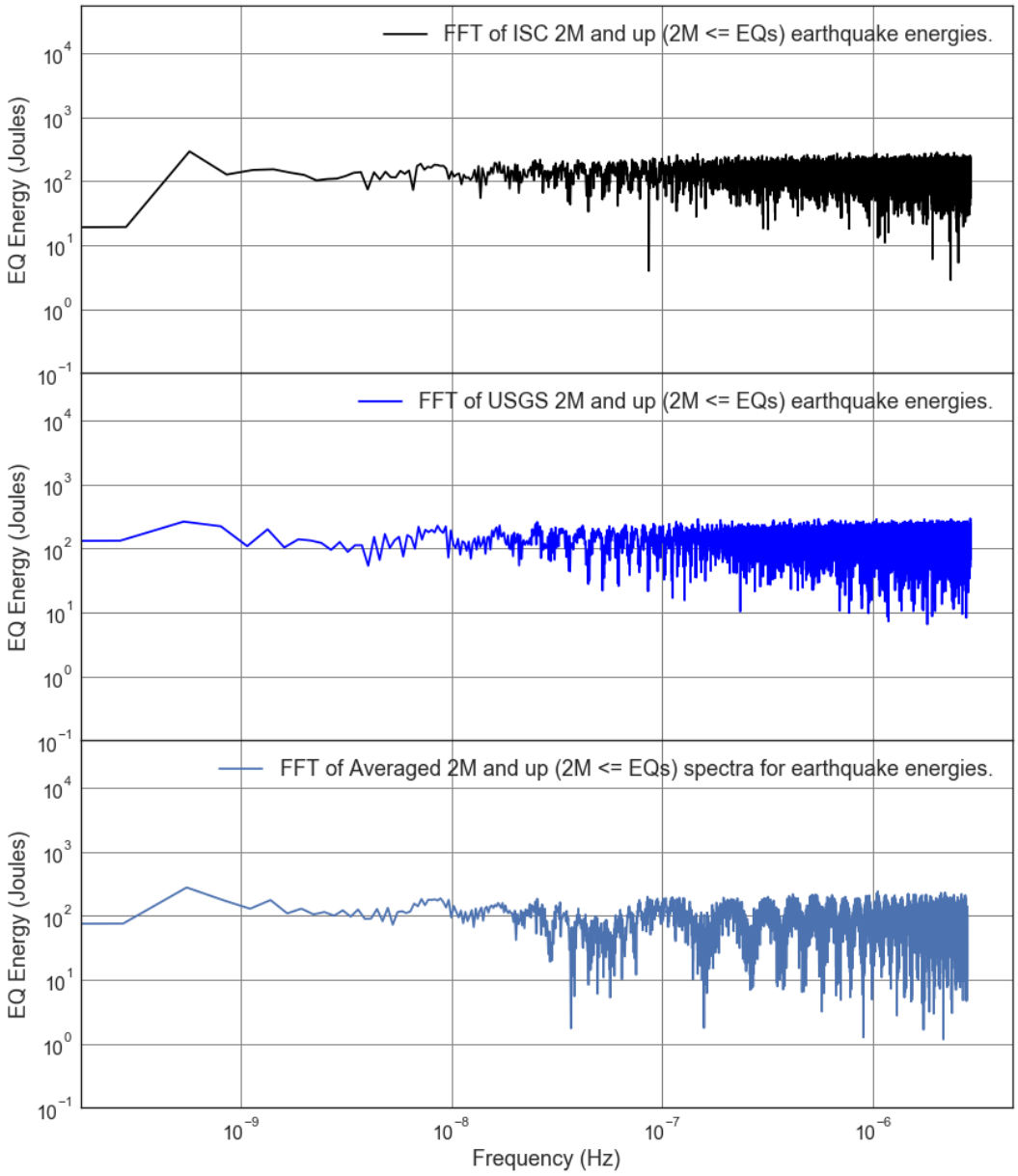

Figure F1.34: FFT Loglog Comparison Plot of Estimated Total 2M and up (2M <= EQs) Earthquake Energies Released from the ISC, USGS, and Centennial Y2K datasets.

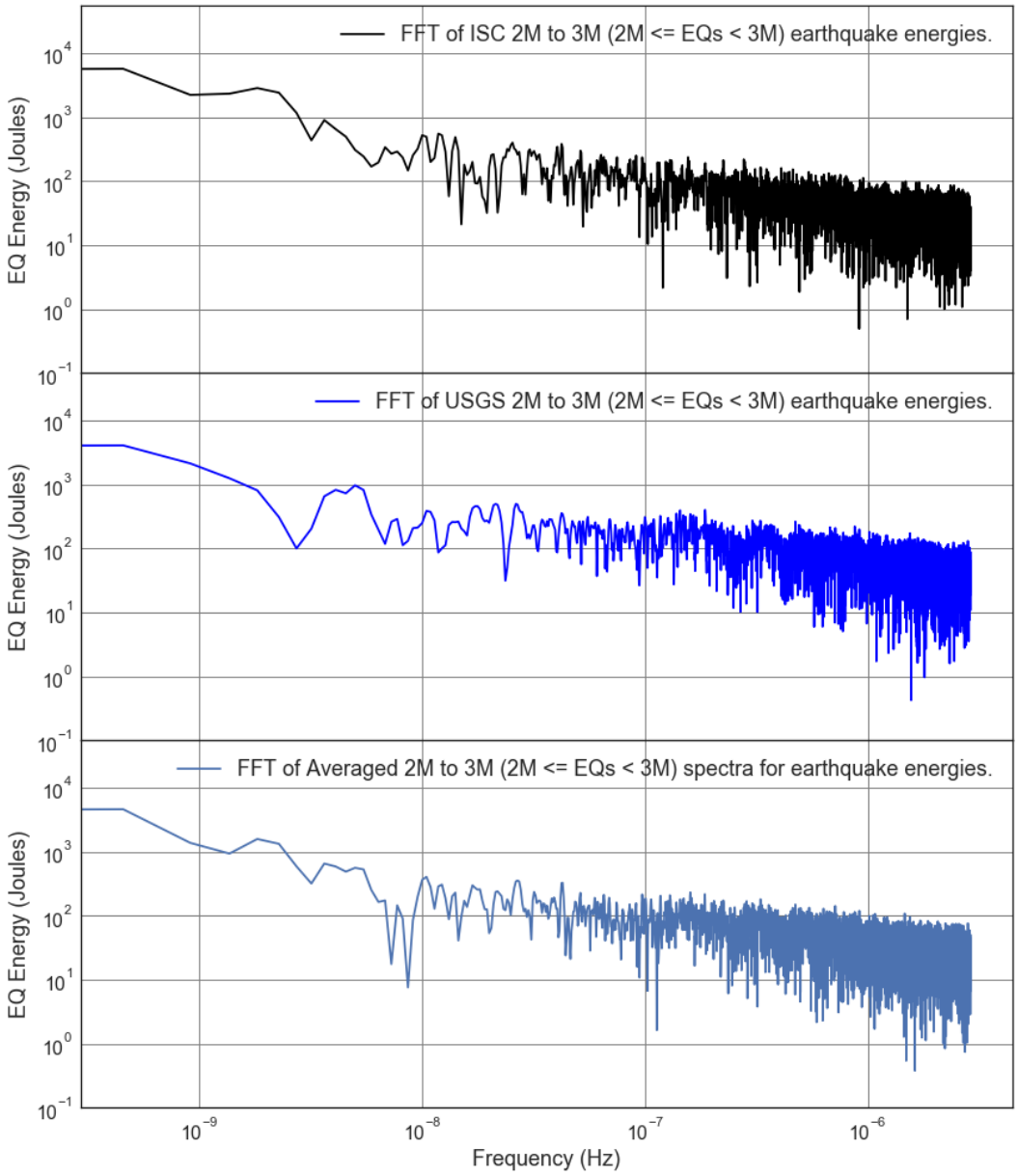

Figure F1.35: FFT Loglog Comparison Plot of Estimated Total 2M to 3M (2M <= EQs < 3M) Earthquake Energies Released from the ISC, USGS, and Centennial Y2K datasets.

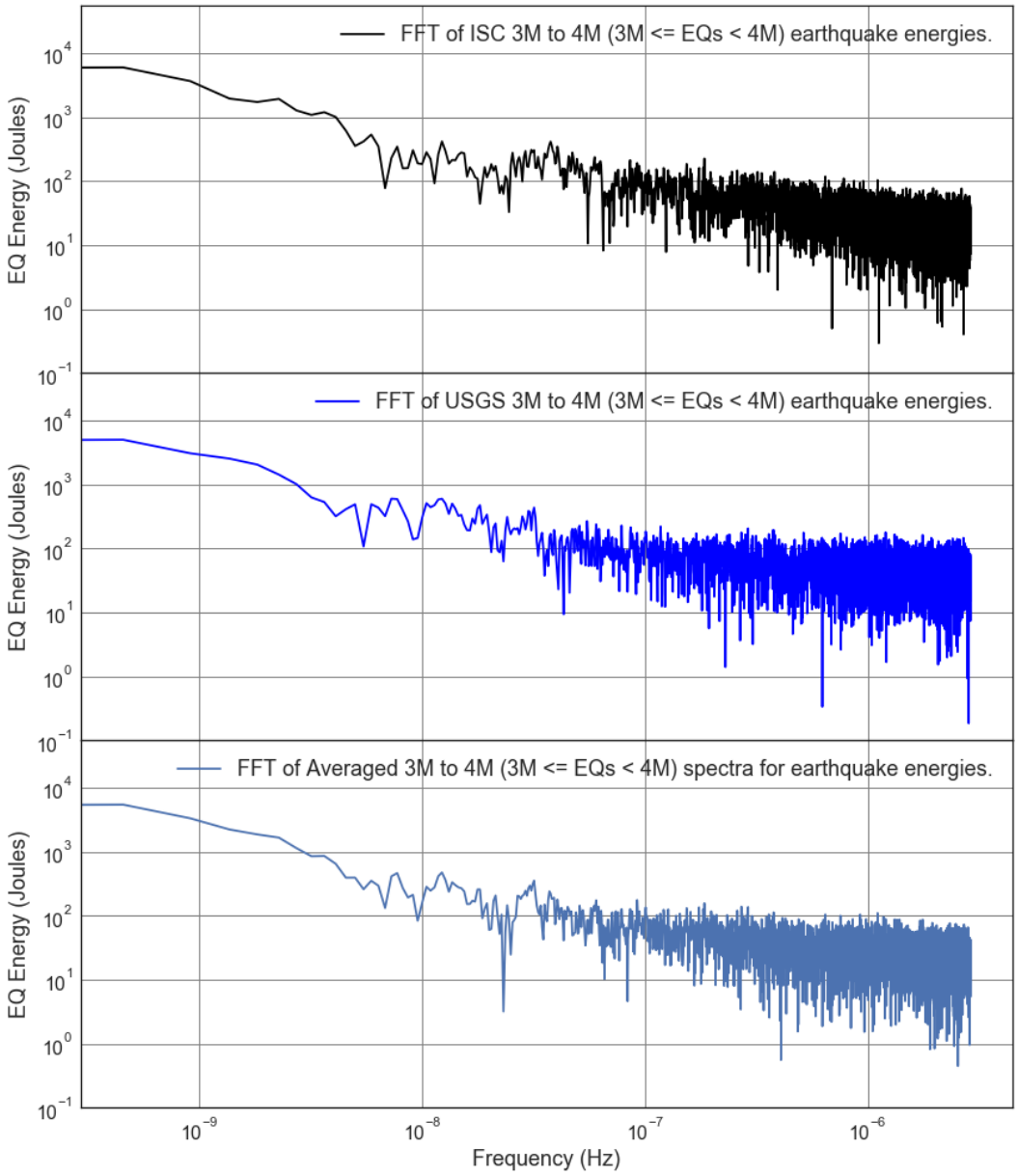

Figure F1.36: FFT Loglog Comparison Plot of Estimated Total 3M to 4M (3M <= EQs < 4M) Earthquake Energies Released from the ISC, USGS, and Centennial Y2K datasets.

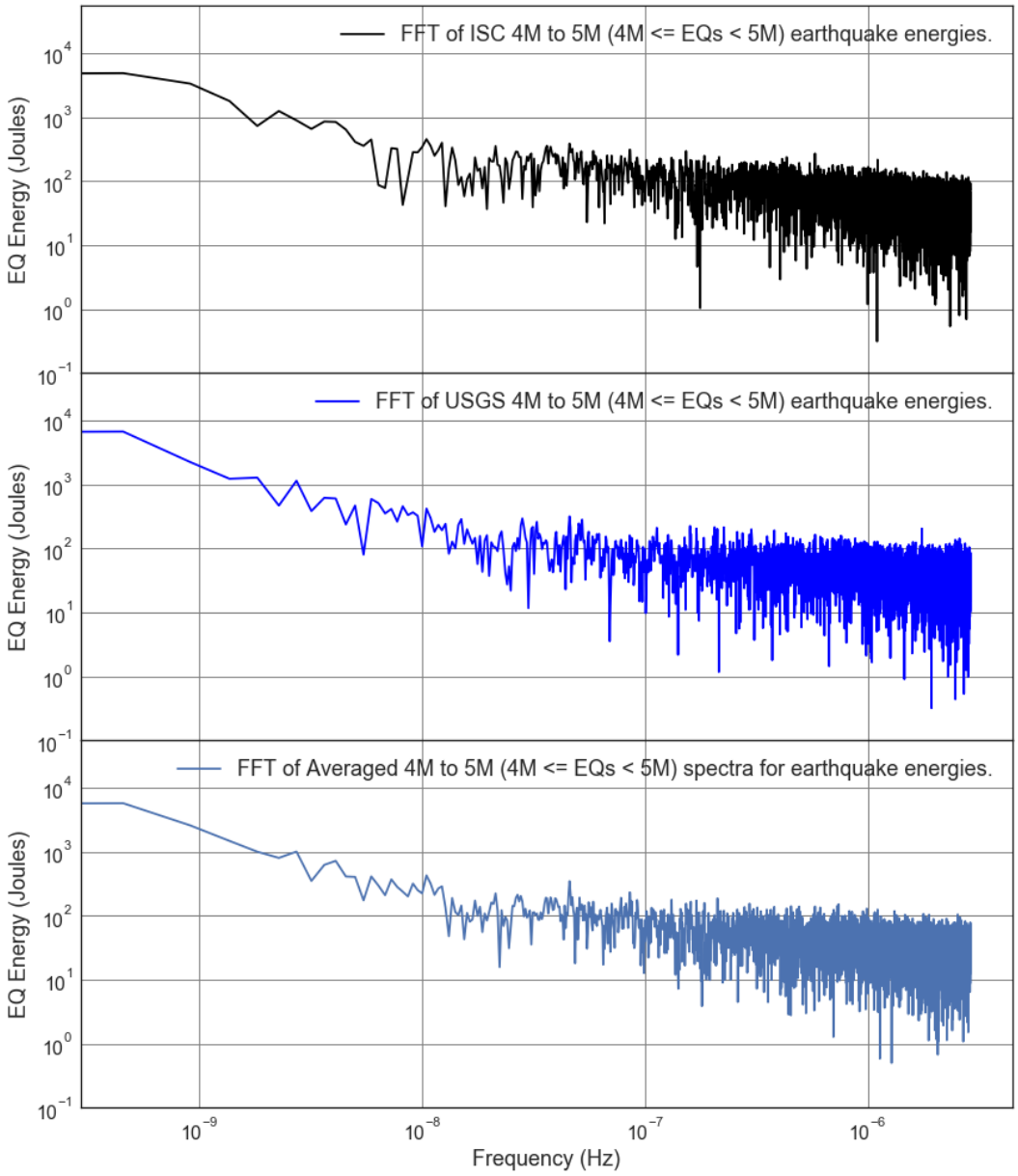

Figure F1.37: FFT Loglog Comparison Plot of Estimated Total 4M to 5M (4M <= EQs < 5M) Earthquake Energies Released from the ISC, USGS, and Centennial Y2K datasets.

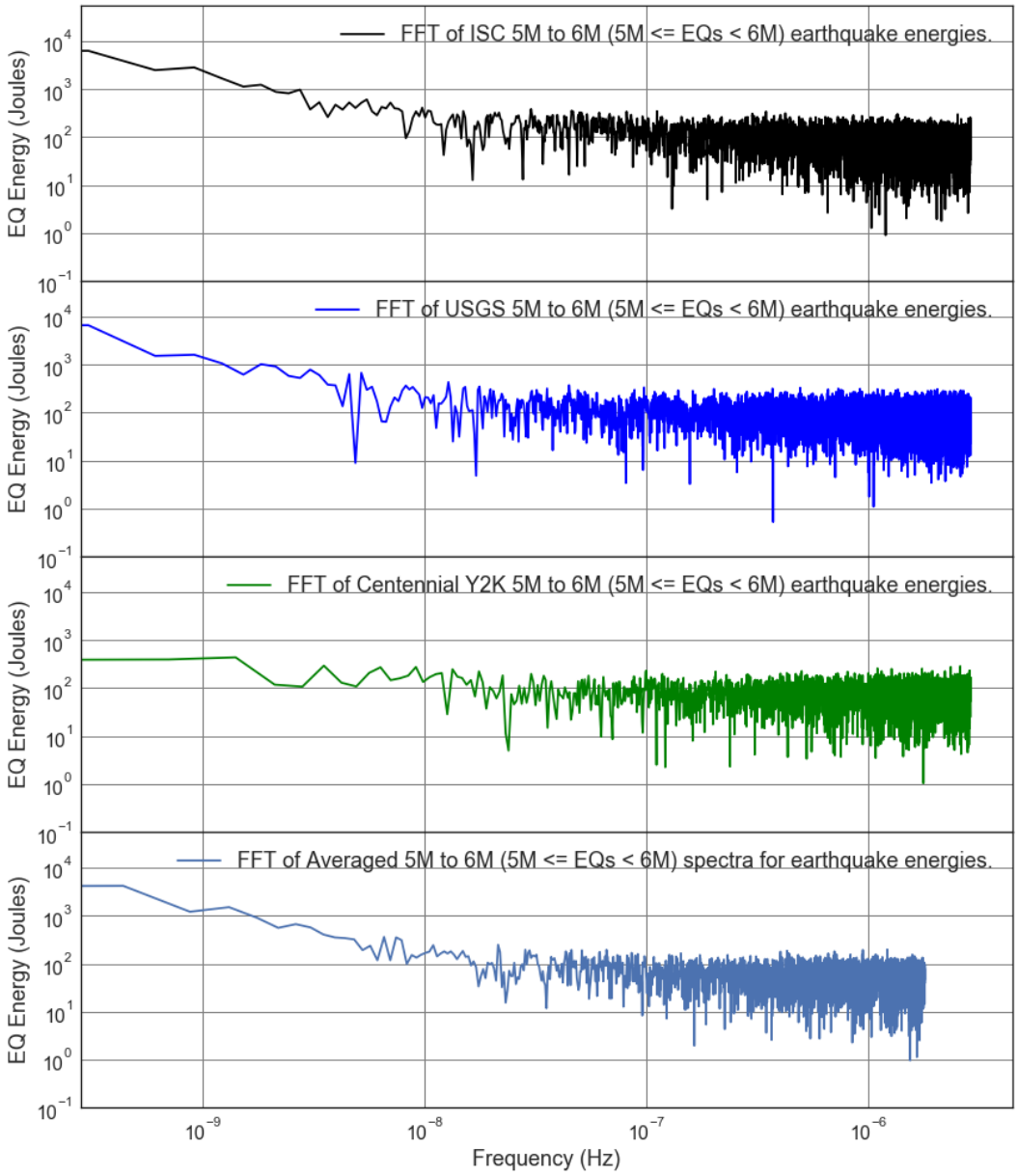

Figure F1.38: FFT Loglog Comparison Plot of Estimated Total 5M to 6M (5M <= EQs < 6M) Earthquake Energies Released from the ISC, USGS, and Centennial Y2K datasets.

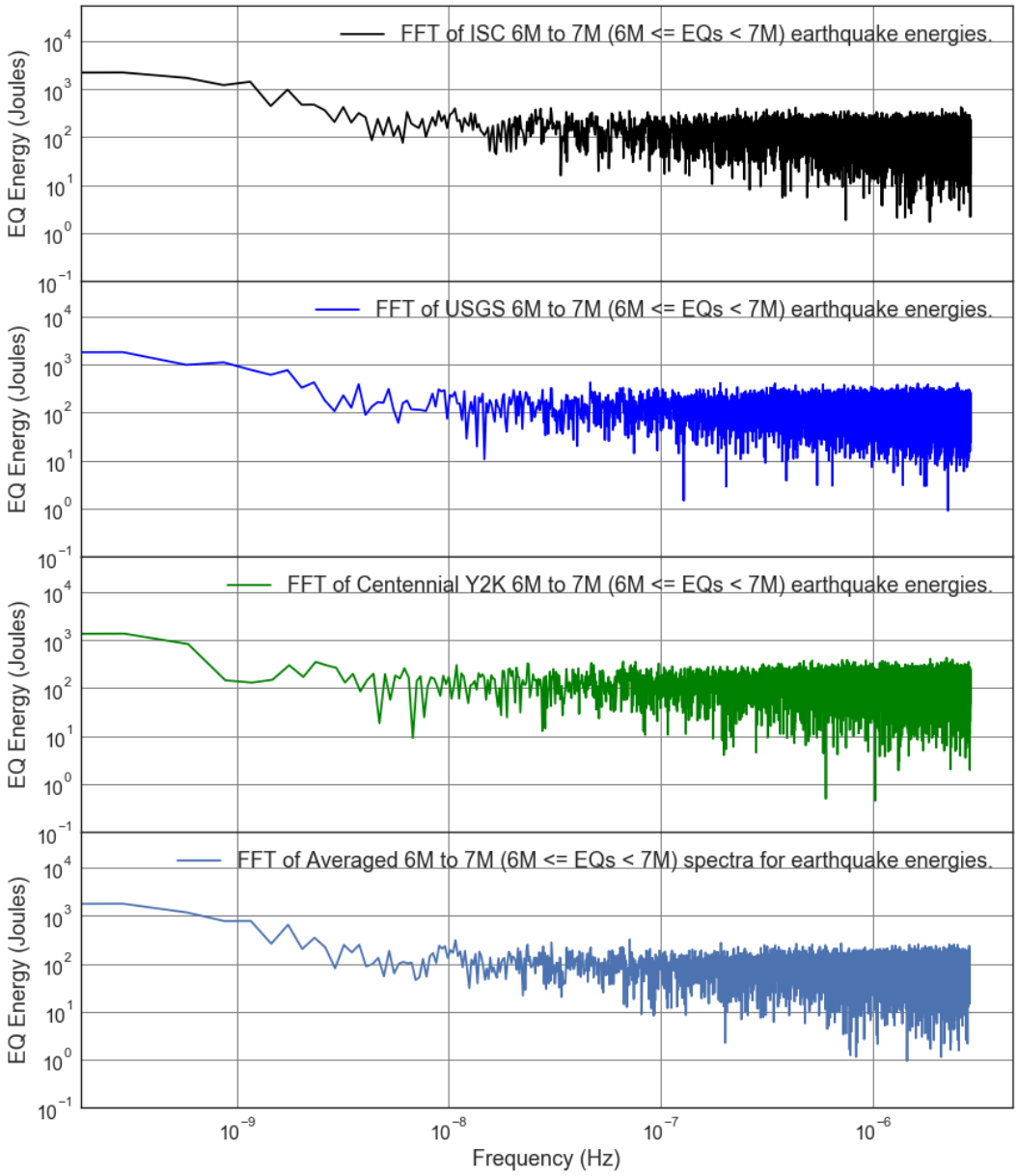

Figure F1.39: FFT Loglog Comparison Plot of Estimated Total 6M to 7M (6M <= EQs < 7M) Earthquake Energies Released from the ISC, USGS, and Centennial Y2K datasets.

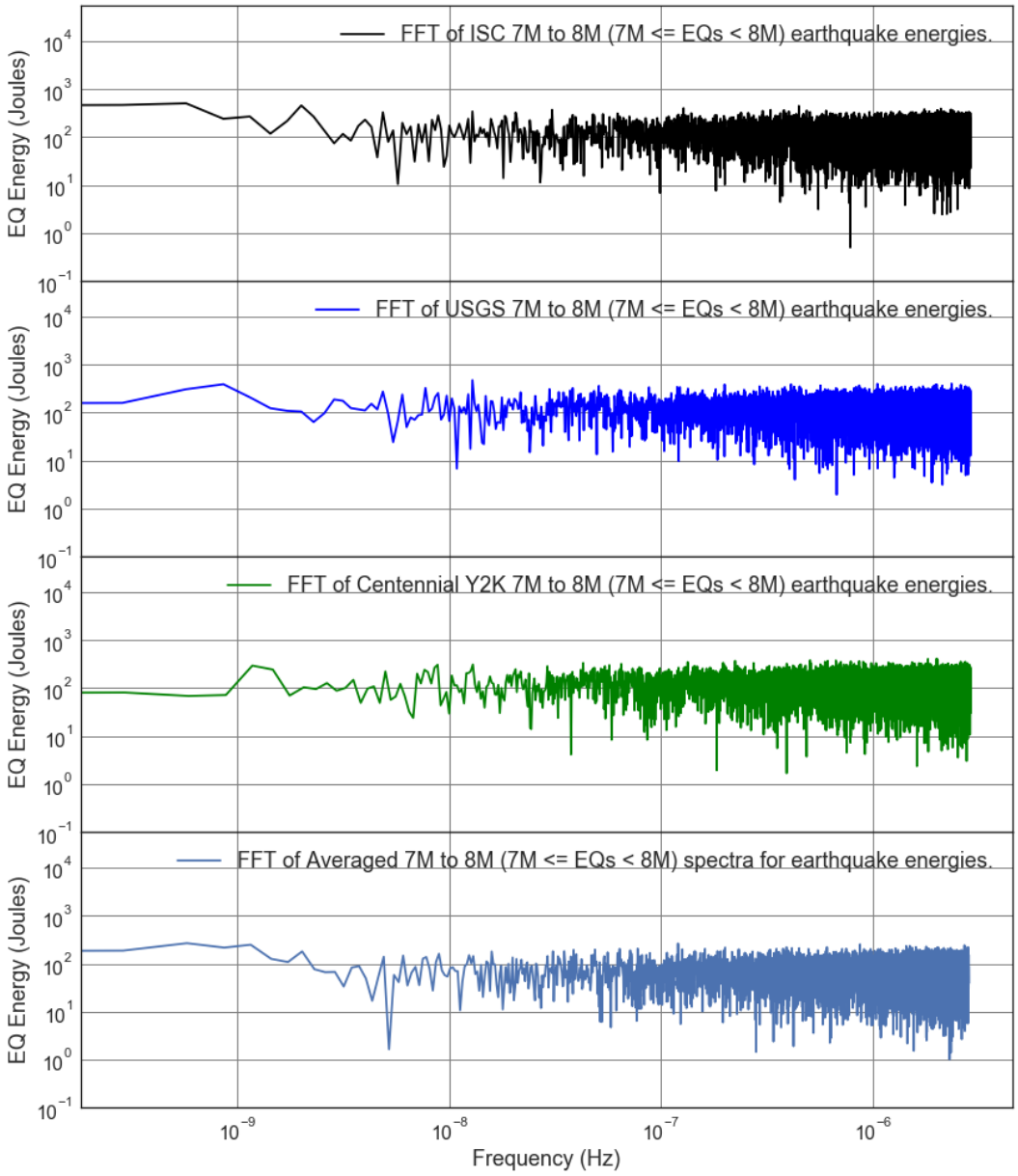

Figure F1.40: FFT Loglog Comparison Plot of Estimated Total 7M to 8M (7M <= EQs < 8M) Earthquake Energies Released from the ISC, USGS, and Centennial Y2K datasets.

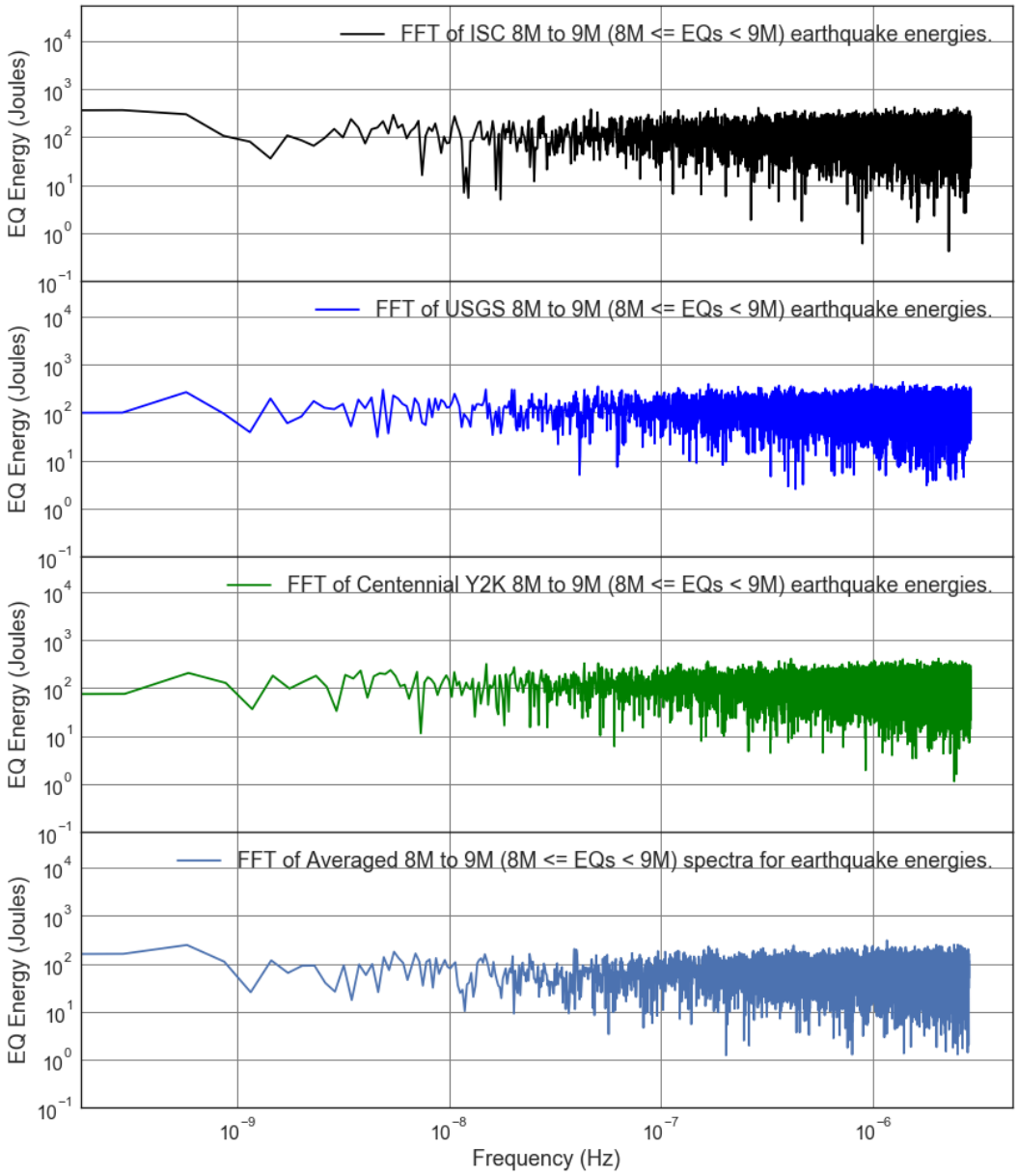

Figure F1.41: FFT Loglog Comparison Plot of Estimated Total 8M to 9M (8M <= EQs < 9M) Earthquake Energies Released from the ISC, USGS, and Centennial Y2K datasets.

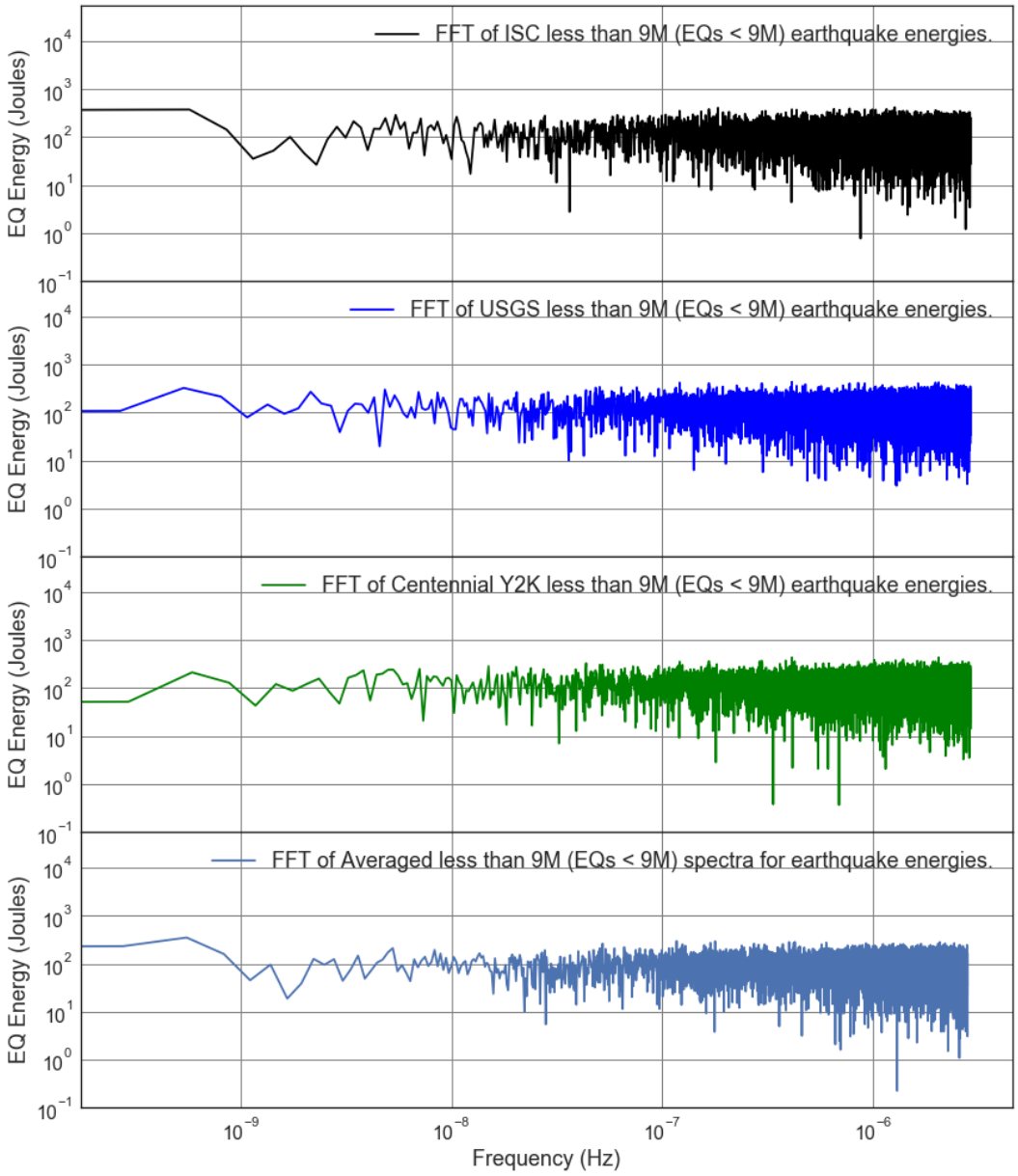

Figure F1.42: FFT Loglog Comparison Plot of Estimated Total of Earthquake Energies Released for less than 9M (EQs < 9M) from the ISC, USGS, and Centennial Y2K datasets.

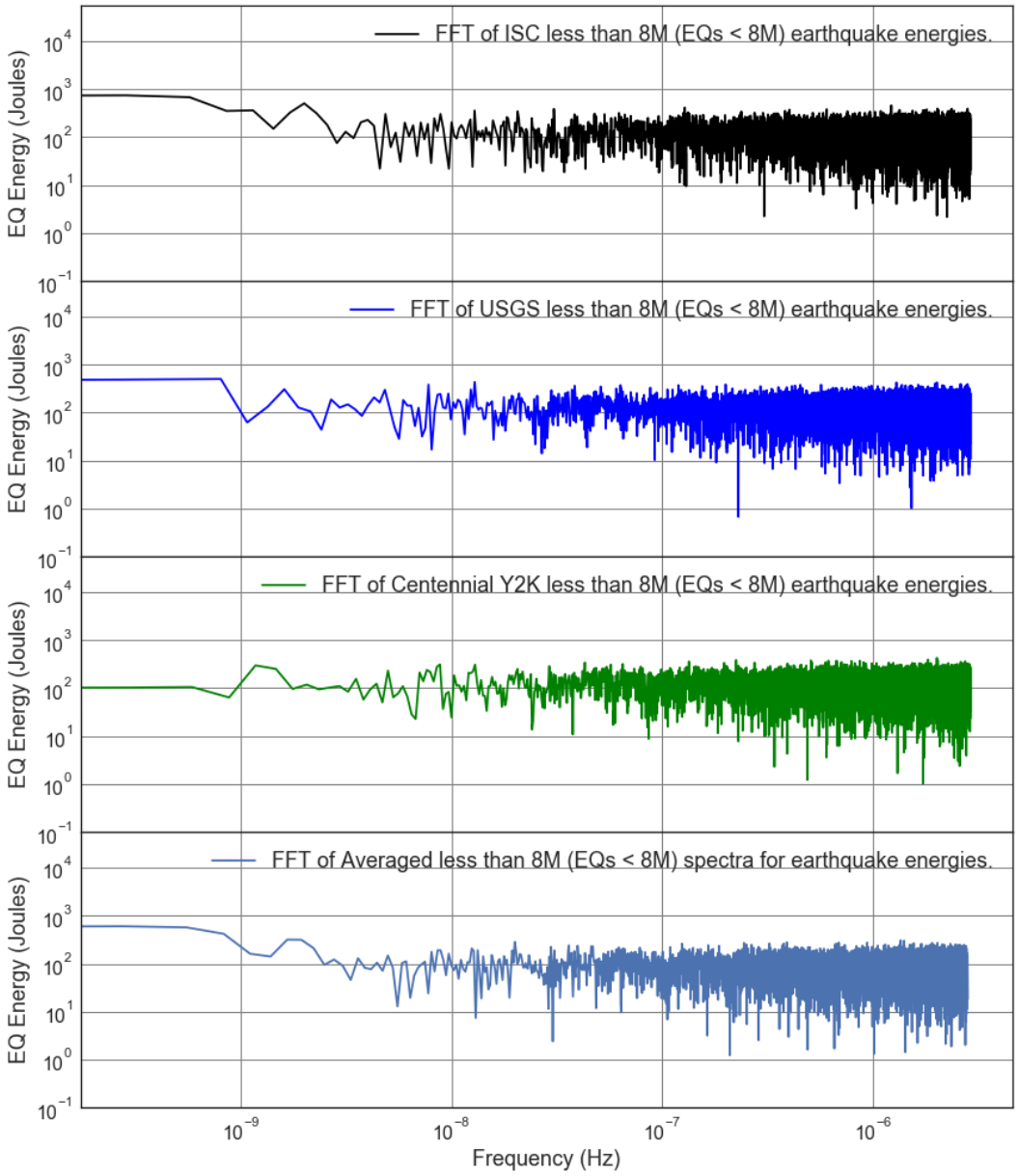

Figure F1.43: FFT Loglog Comparison Plot of Estimated Total of Earthquake Energies Released for less than 8M (EQs < 8M) from the ISC, USGS, and Centennial Y2K datasets.

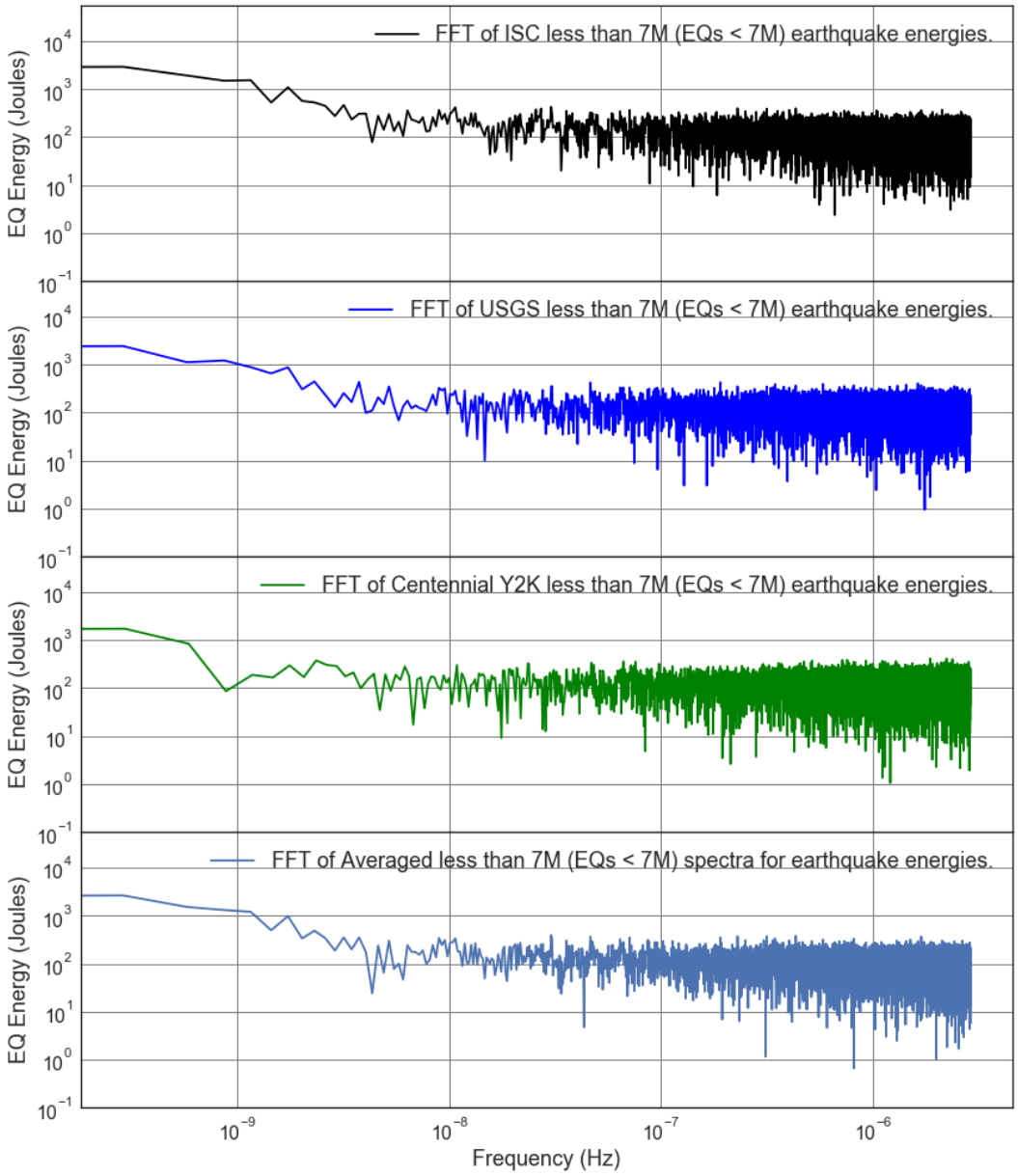

Figure F1.44: FFT Loglog Comparison Plot of Estimated Total of Earthquake Energies Released for less than 7M (EQs < 7M) from the ISC, USGS, and Centennial Y2K datasets.

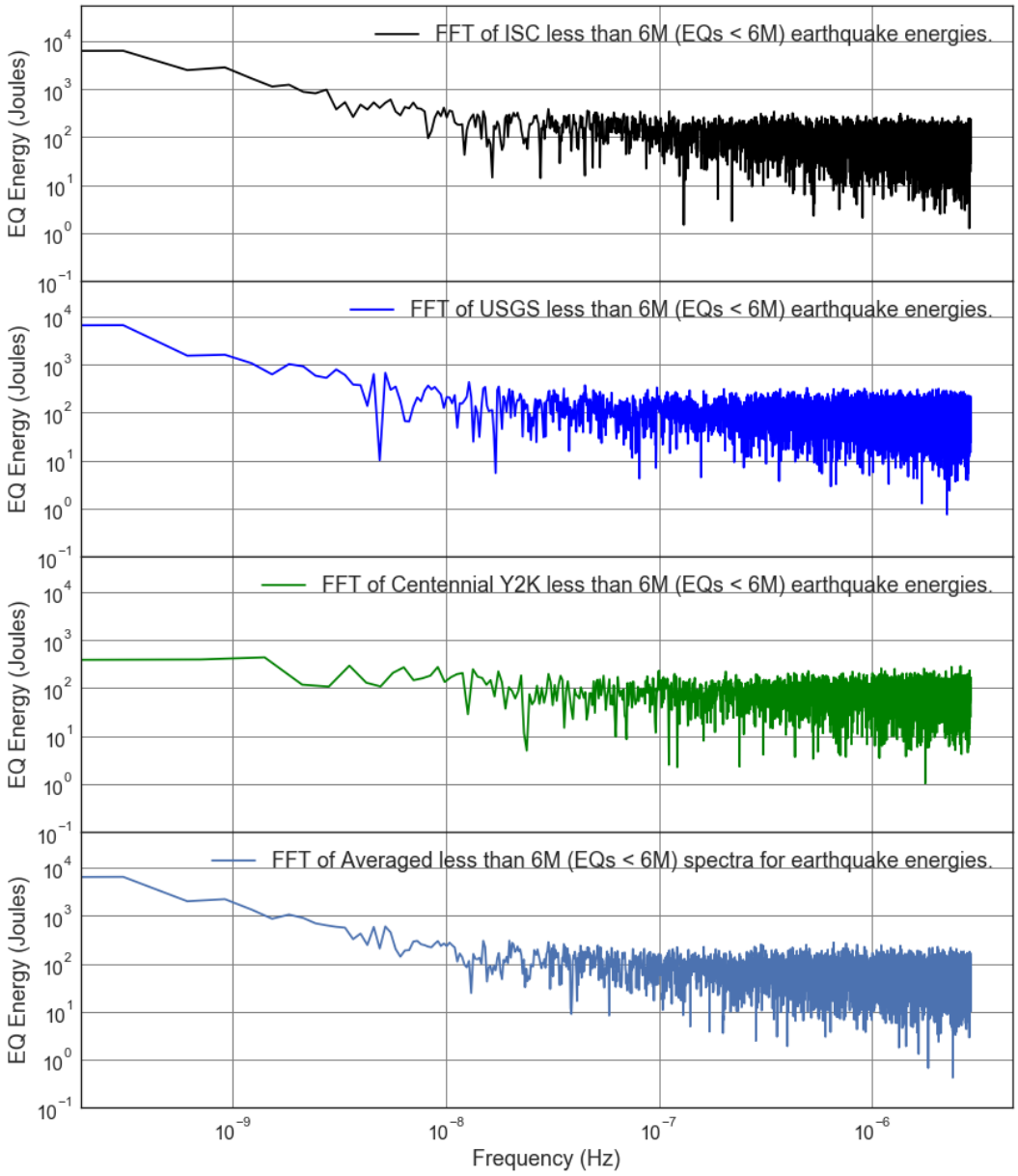

Figure F1.45: FFT Loglog Comparison Plot of Estimated Total of Earthquake Energies Released for less than 6M (EQs < 6M) from the ISC, USGS, and Centennial Y2K datasets.

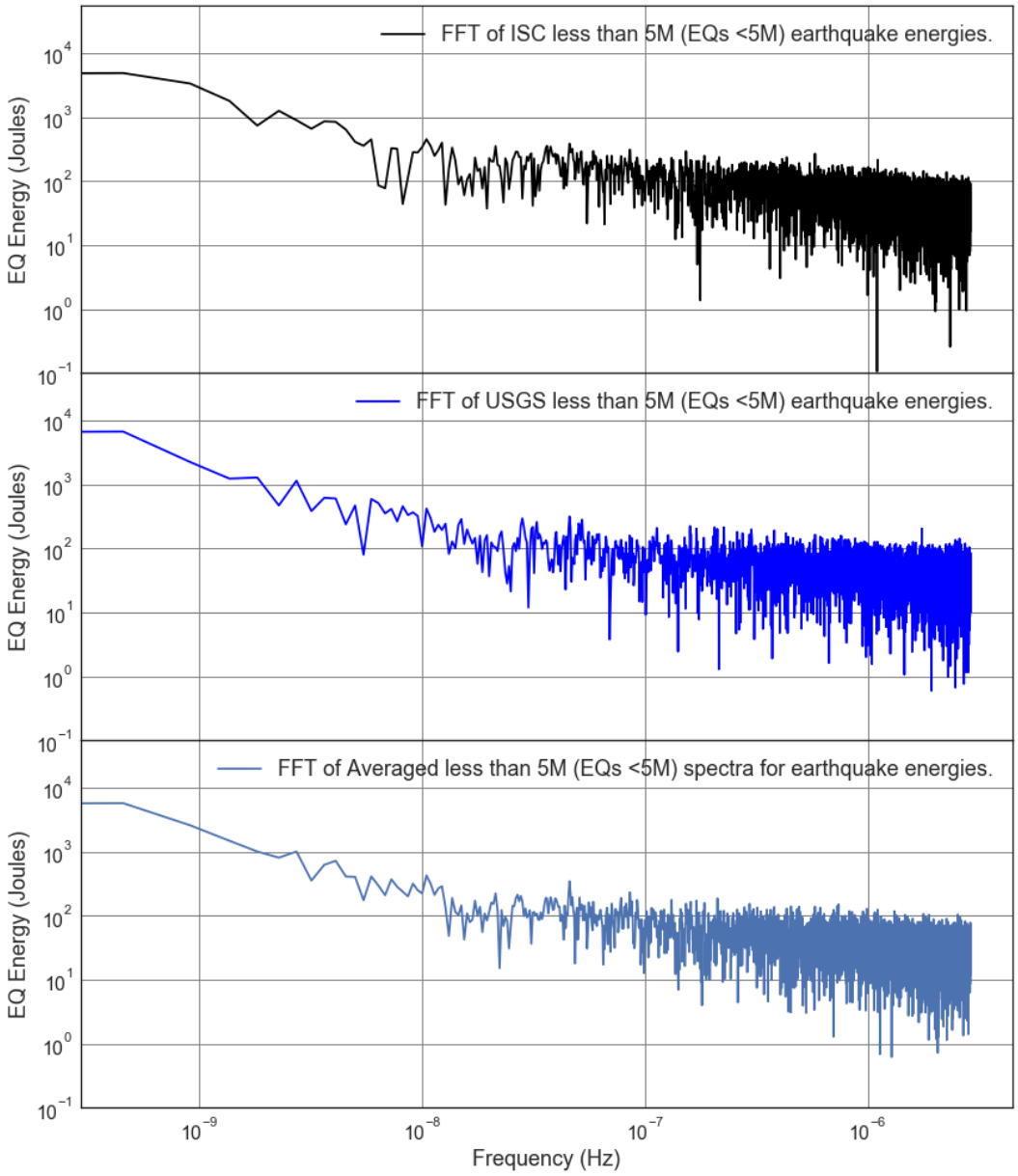

Figure F1.46: FFT Loglog Comparison Plot of Estimated Total of Earthquake Energies Released for less than 5M (EQs <5M) from the ISC, USGS, and Centennial Y2K datasets.

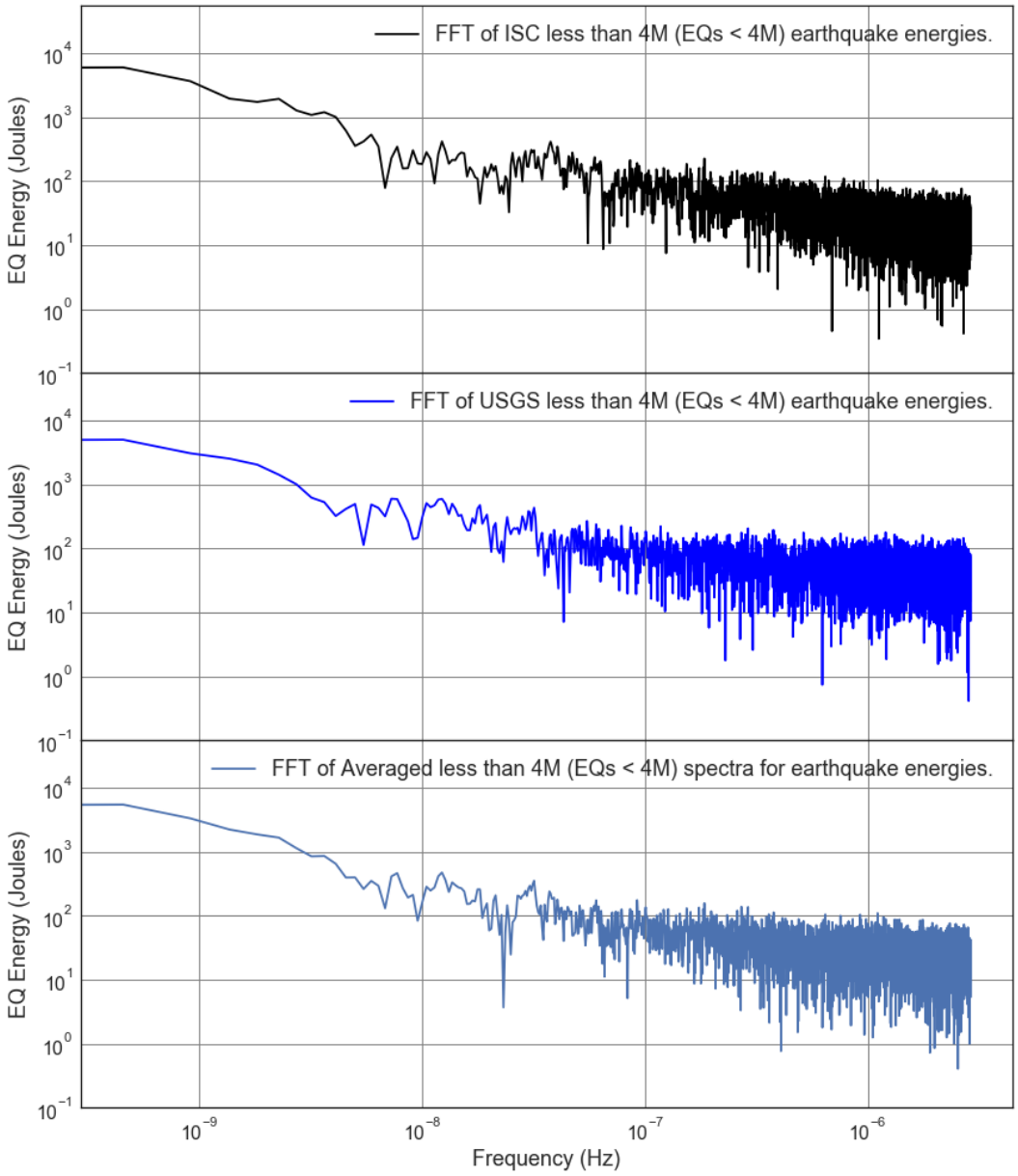

Figure F1.47: FFT Loglog Comparison Plot of Estimated Total of Earthquake Energies Released for less than 4M (EQs < 4M) from the ISC, USGS, and Centennial Y2K datasets.

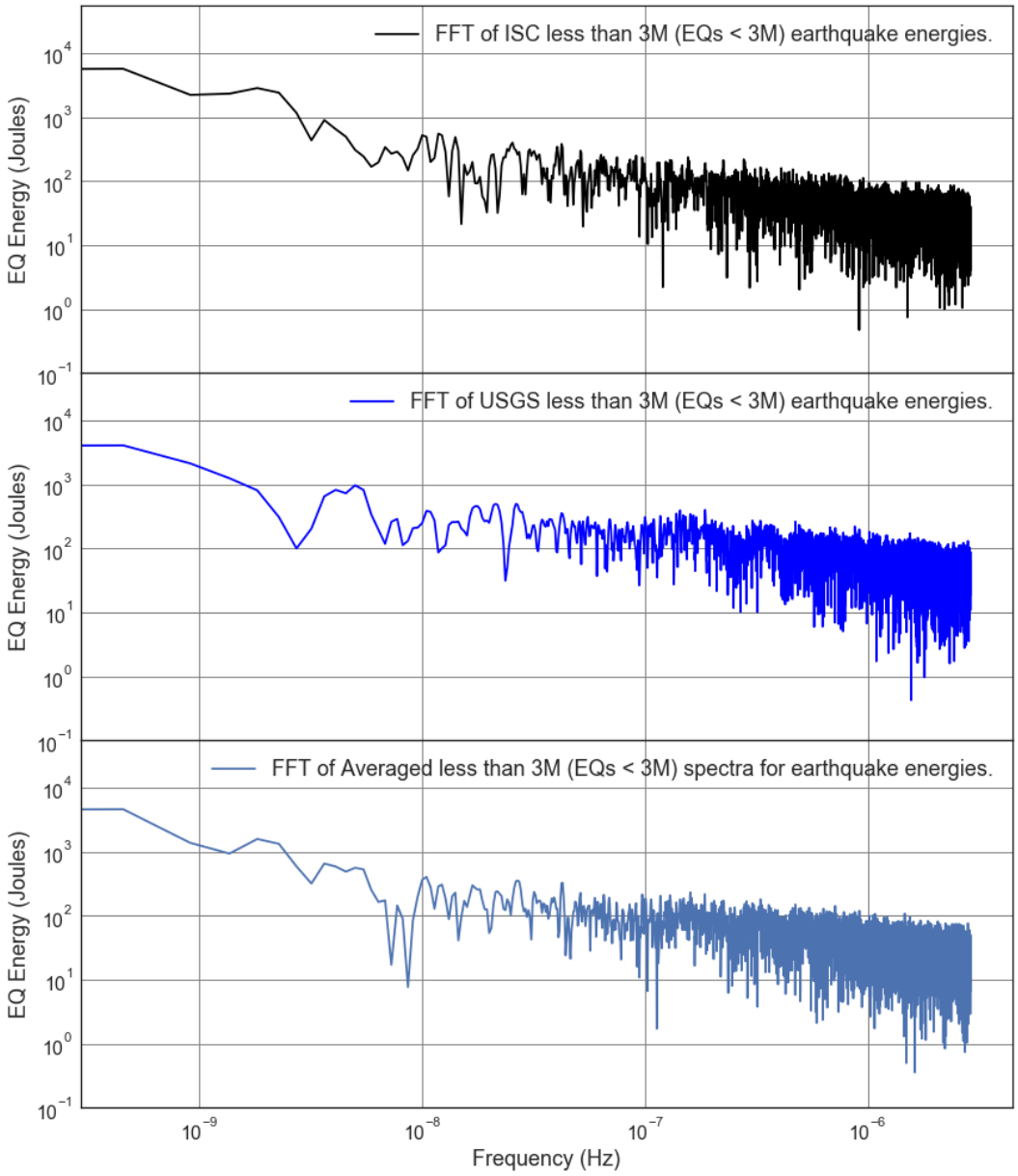

Figure F1.48: FFT Loglog Comparison Plot of Estimated Total of Earthquake Energies Released for less than 3M (EQs < 3M) from the ISC, USGS, and Centennial Y2K datasets.

Comparison of ISC, USGS, and Centennial Y2K of FFT Earthquake Slope Counts Plots

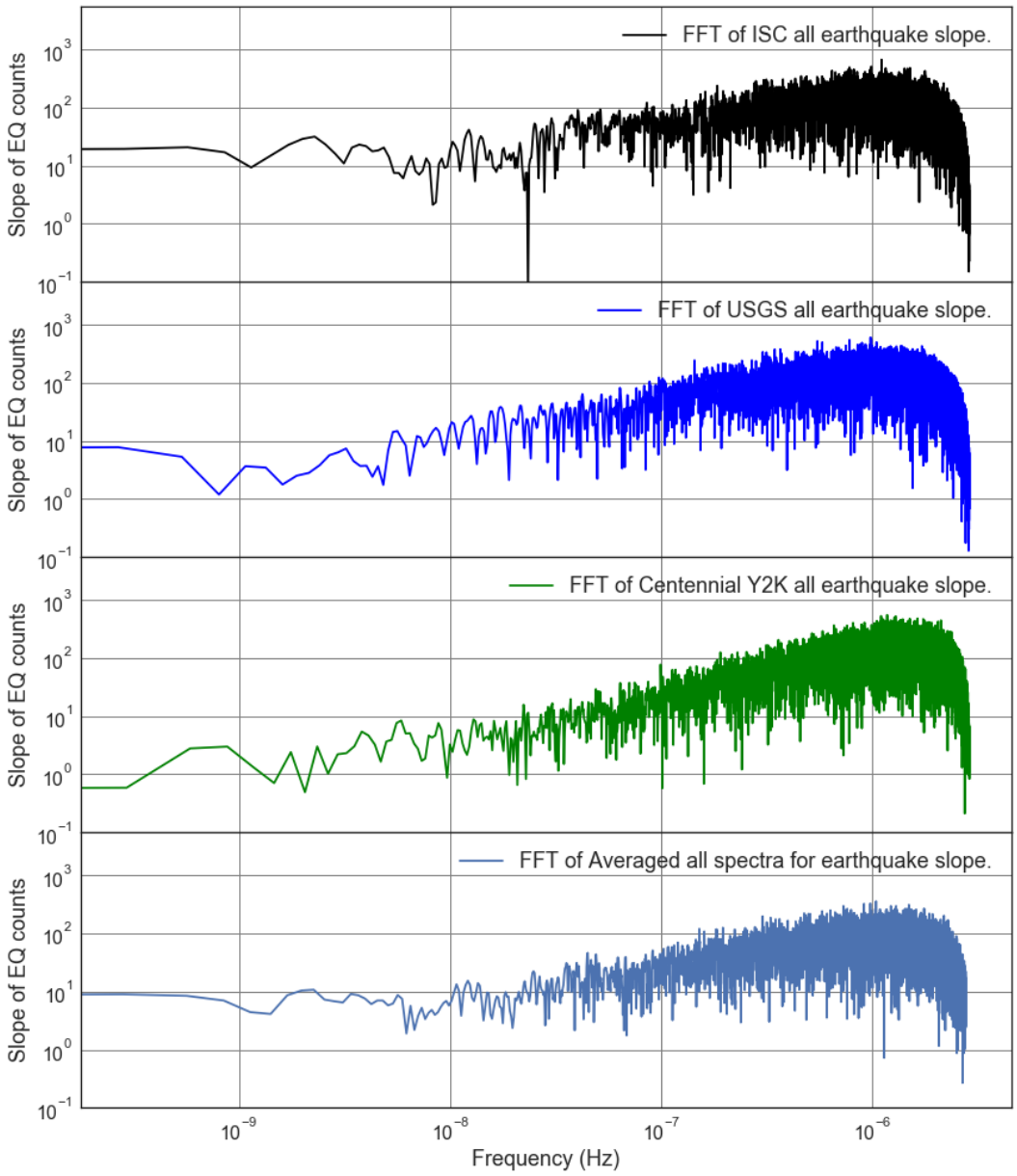

Figure 2.1: FFT Loglog Comparison Plot of Earthquake Count Slope for all Earthquakes from the ISC, USGS, and Centennial Y2K datasets.

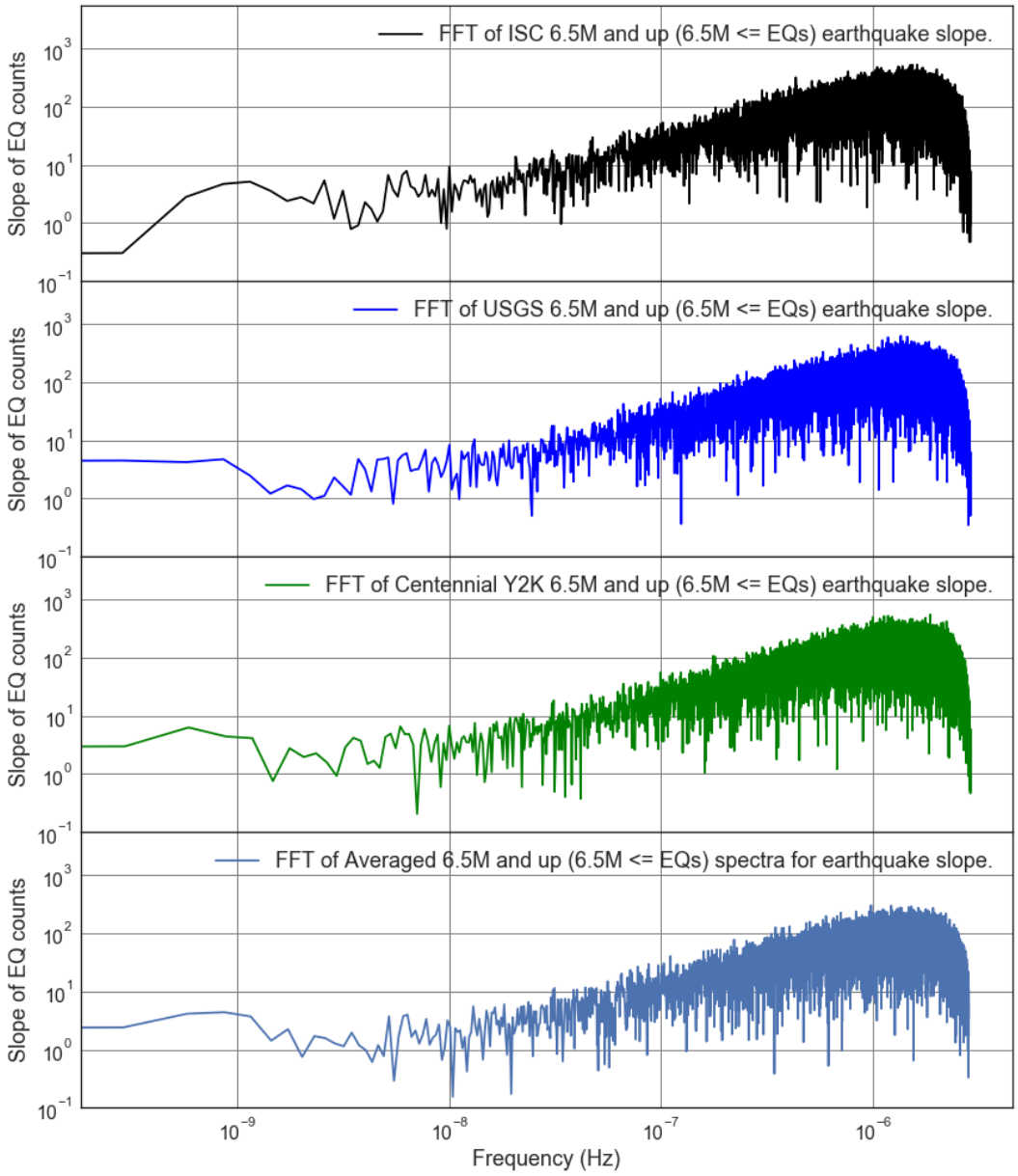

Figure 2.2: FFT Loglog Comparison Plot of Earthquake Count Slope for 6.5M and up (6.5M <= EQs) Earthquakes from the ISC, USGS, and Centennial Y2K datasets.

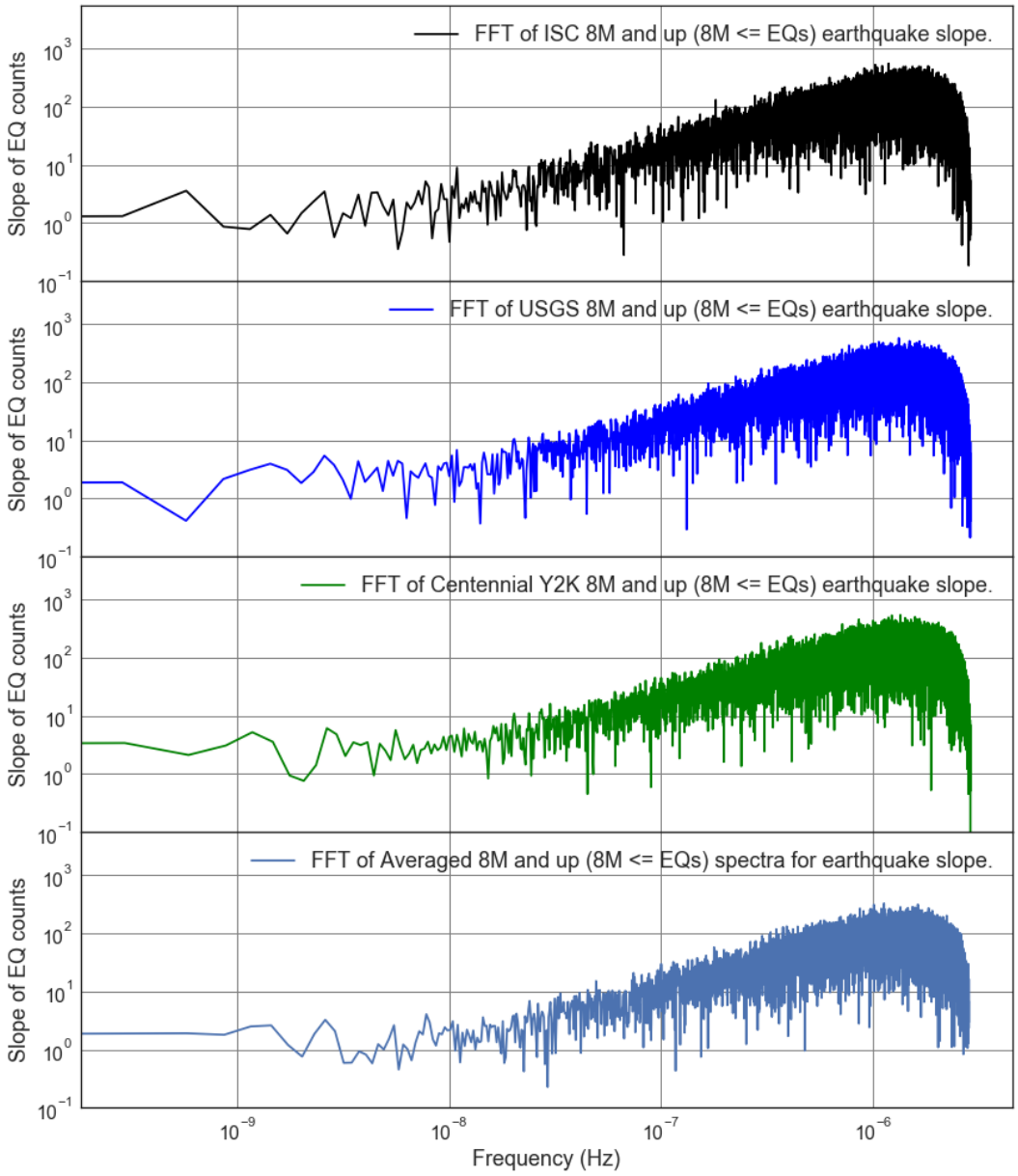

Figure 2.3: FFT Loglog Comparison Plot of Earthquake Count Slope for 8M and up (8M <= EQs) Earthquakes from the ISC, USGS, and Centennial Y2K datasets.

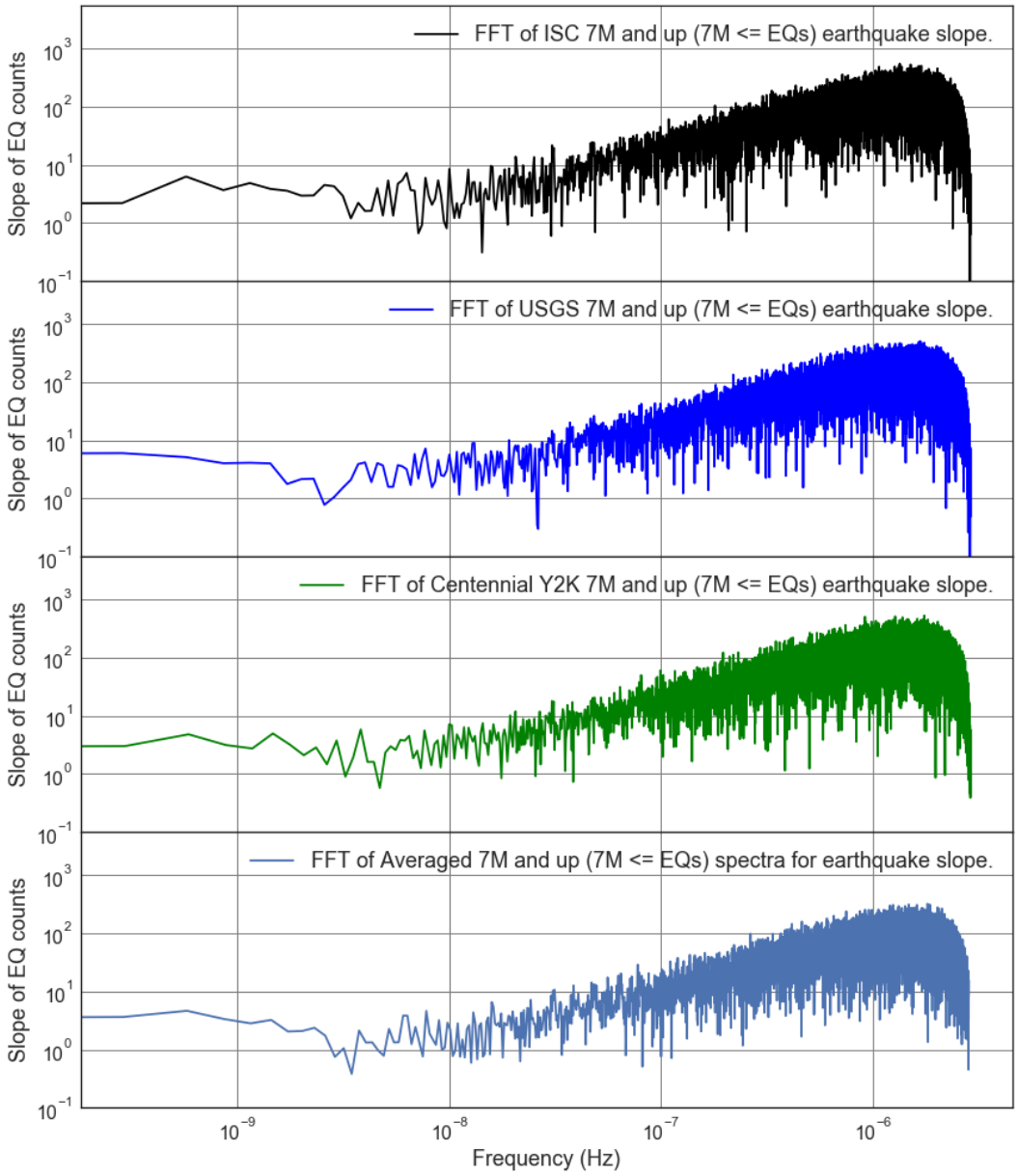

Figure 2.4: FFT Loglog Comparison Plot of Earthquake Count Slope for 7M and up (7M <= EQs) Earthquakes from the ISC, USGS, and Centennial Y2K datasets.

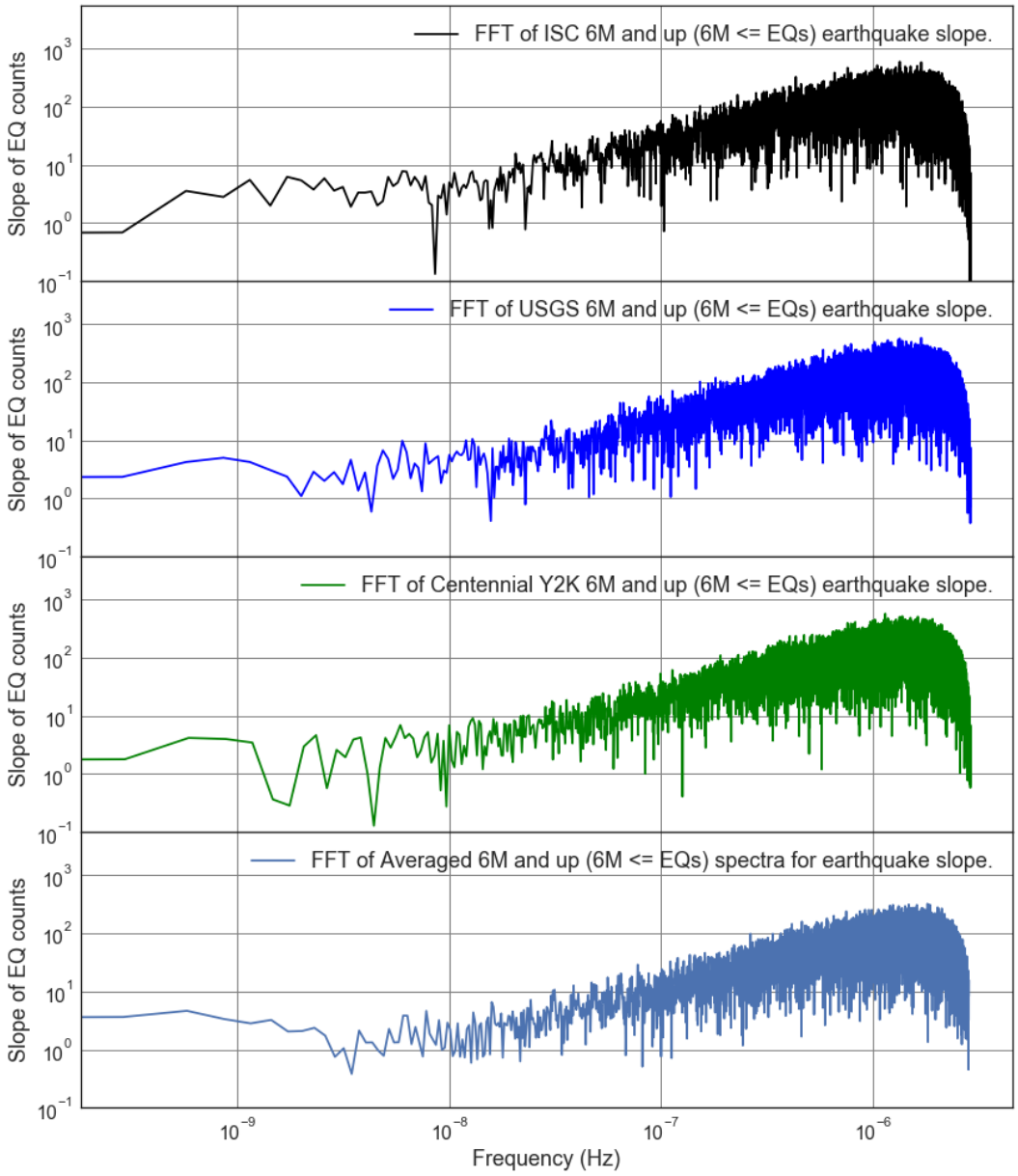

Figure 2.5: FFT Loglog Comparison Plot of Earthquake Count Slope for 6M and up (6M <= EQs) Earthquakes from the ISC, USGS, and Centennial Y2K datasets.

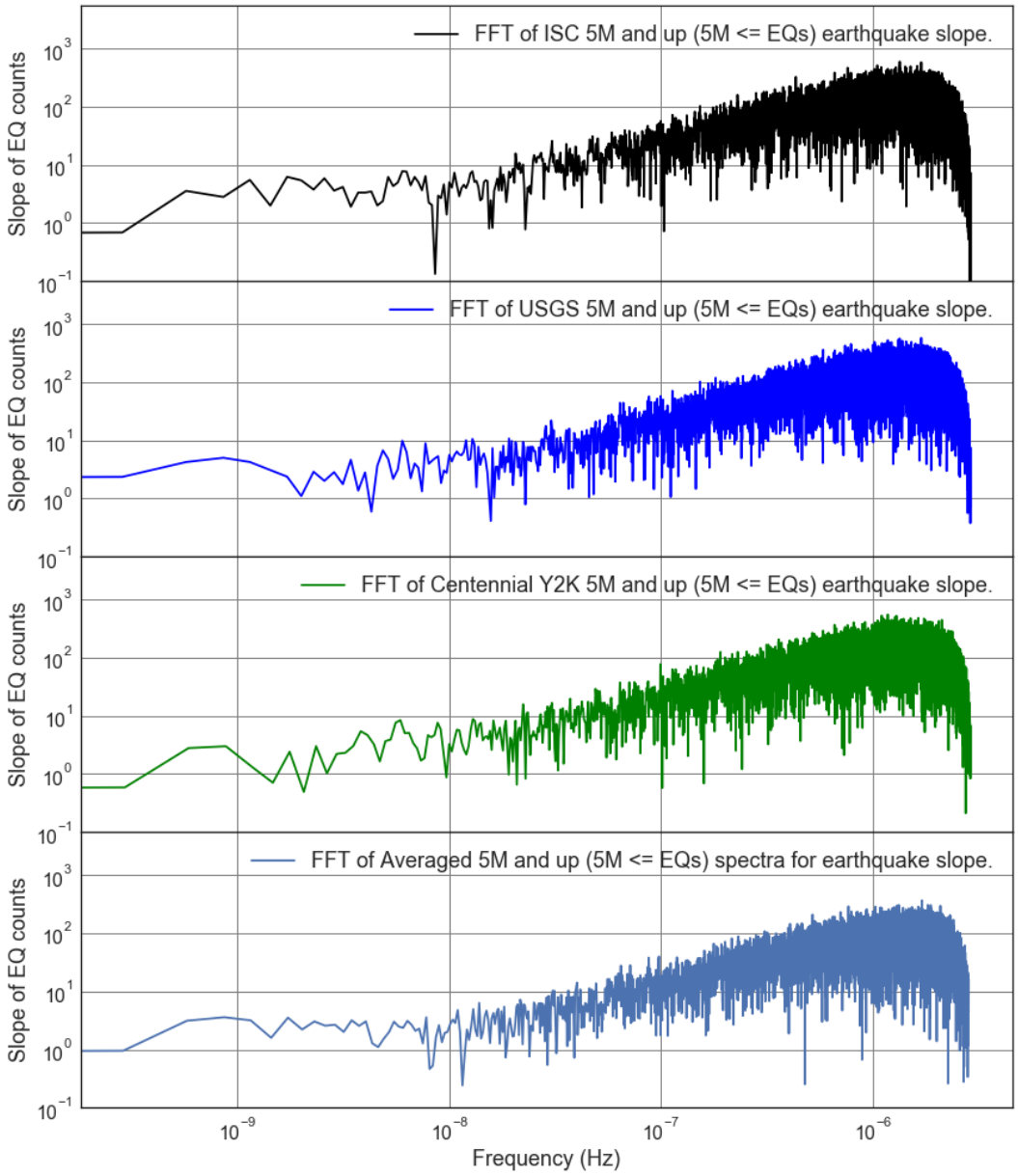

Figure 2.6: FFT Loglog Comparison Plot of Earthquake Count Slope for 5M and up (5M <= EQs) Earthquakes from the ISC, USGS, and Centennial Y2K datasets.

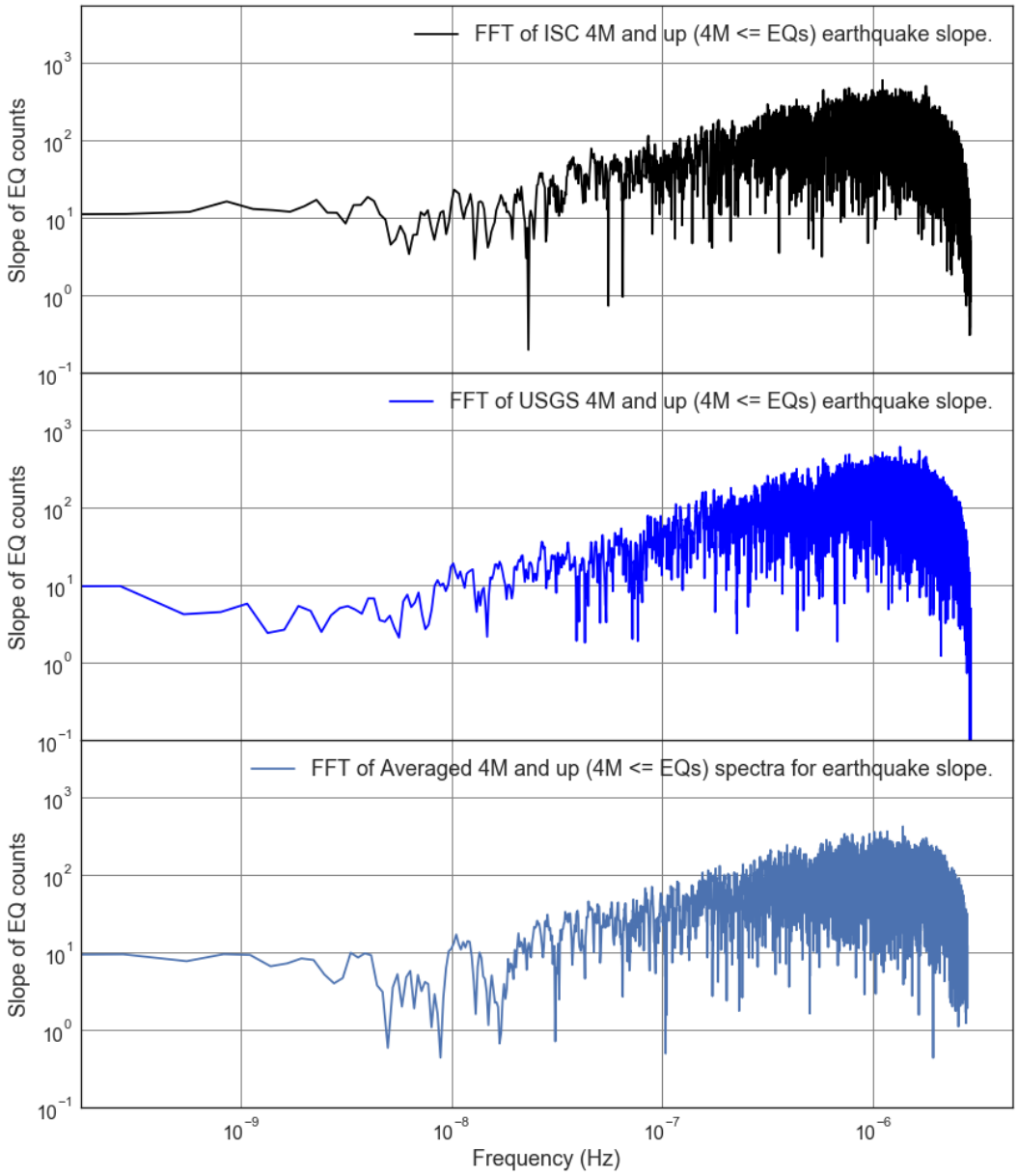

Figure 2.7: FFT Loglog Comparison Plot of Earthquake Count Slope for 4M and up (4M <= EQs) Earthquakes from the ISC, USGS, and Centennial Y2K datasets.

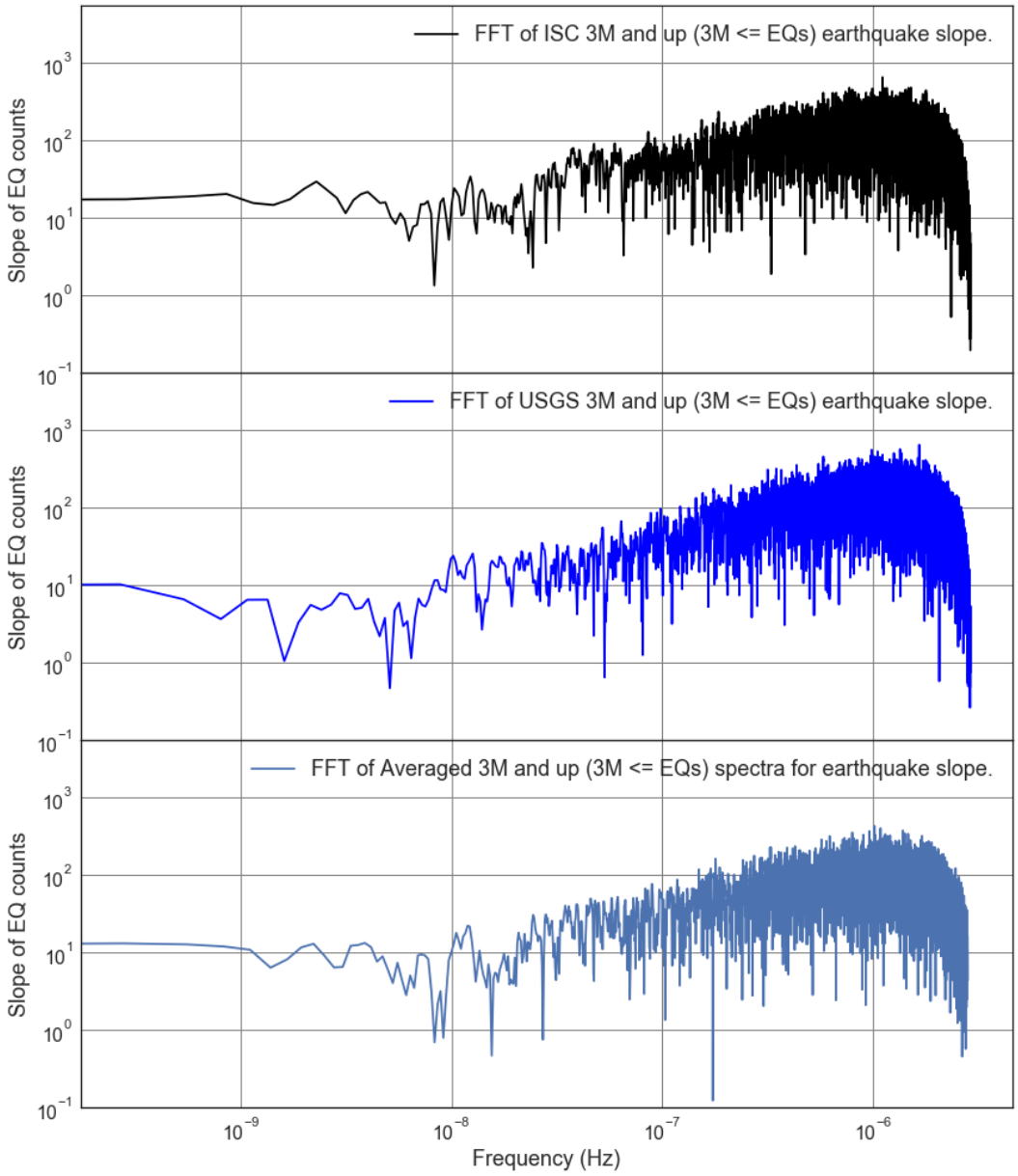

Figure 2.8: FFT Loglog Comparison Plot of Earthquake Count Slope for 3M and up (3M <= EQs) Earthquakes from the ISC, USGS, and Centennial Y2K datasets.

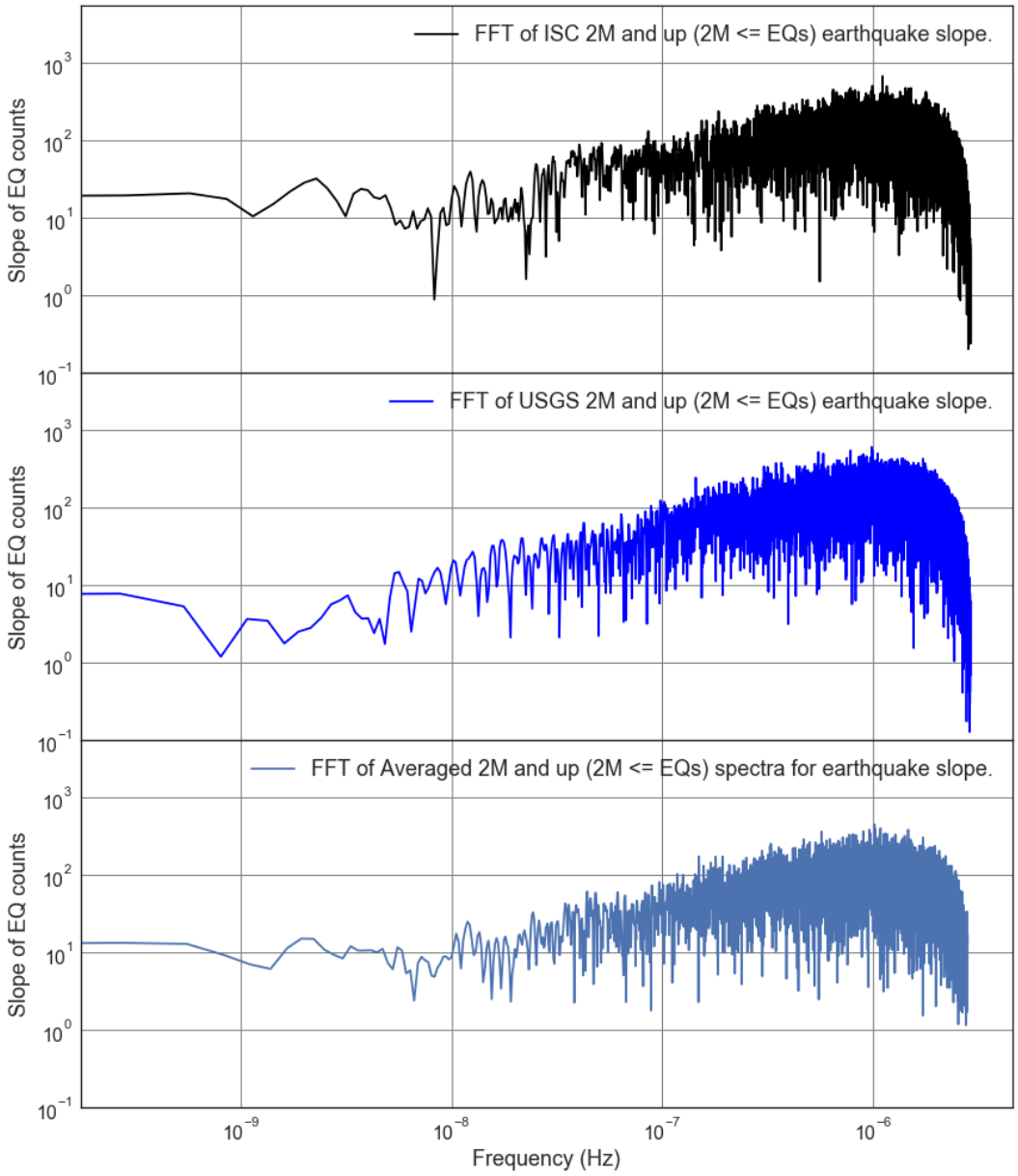

Figure 2.9: FFT Loglog Comparison Plot of Earthquake Count Slope for 2M and up (2M <= EQs) Earthquakes from the ISC, USGS, and Centennial Y2K datasets.

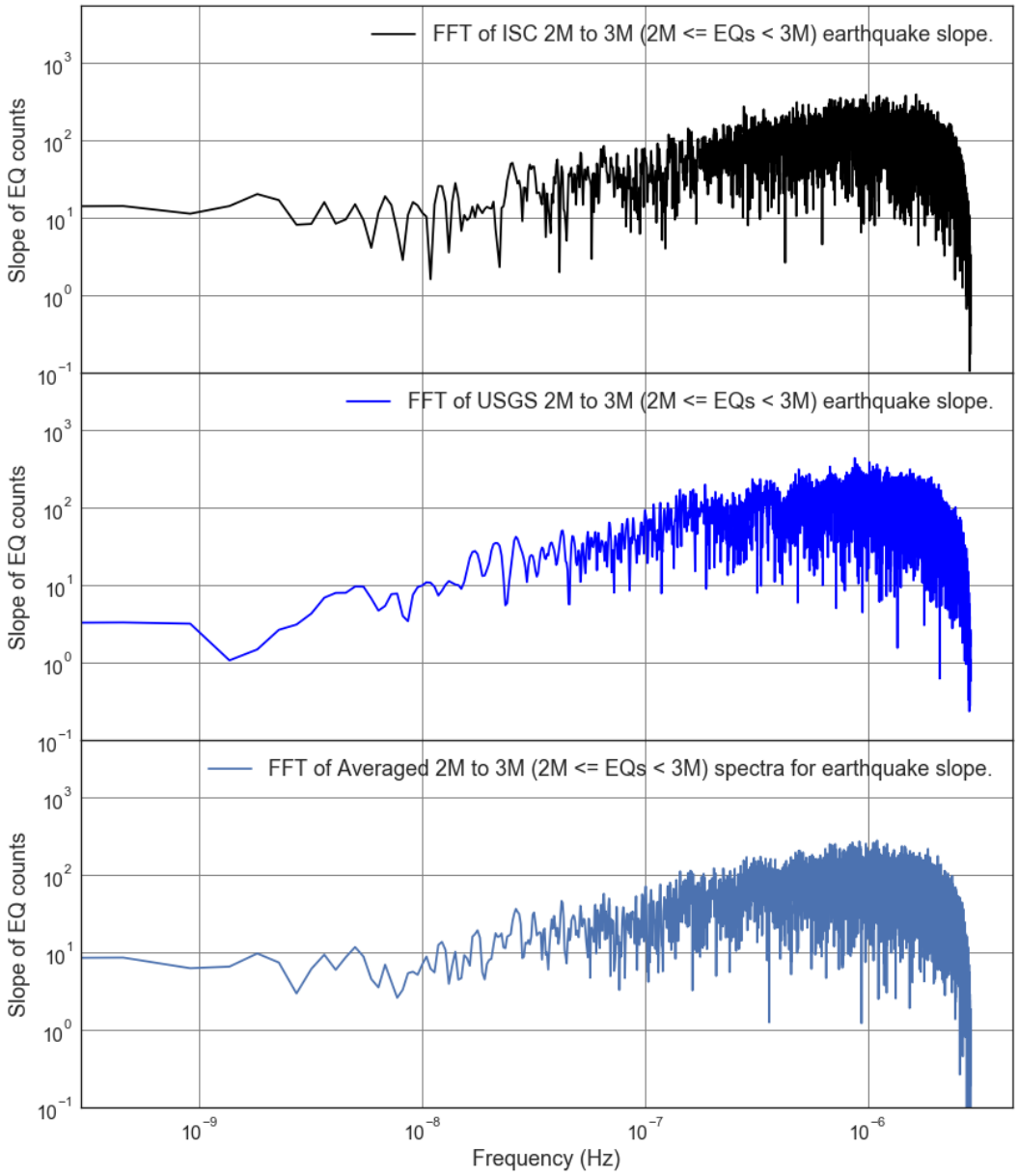

Figure 2.10: FFT Loglog Comparison Plot of Earthquake Count Slope for 2M to 3M (2M <= EQs < 3M) Earthquakes from the ISC, USGS, and Centennial Y2K datasets.

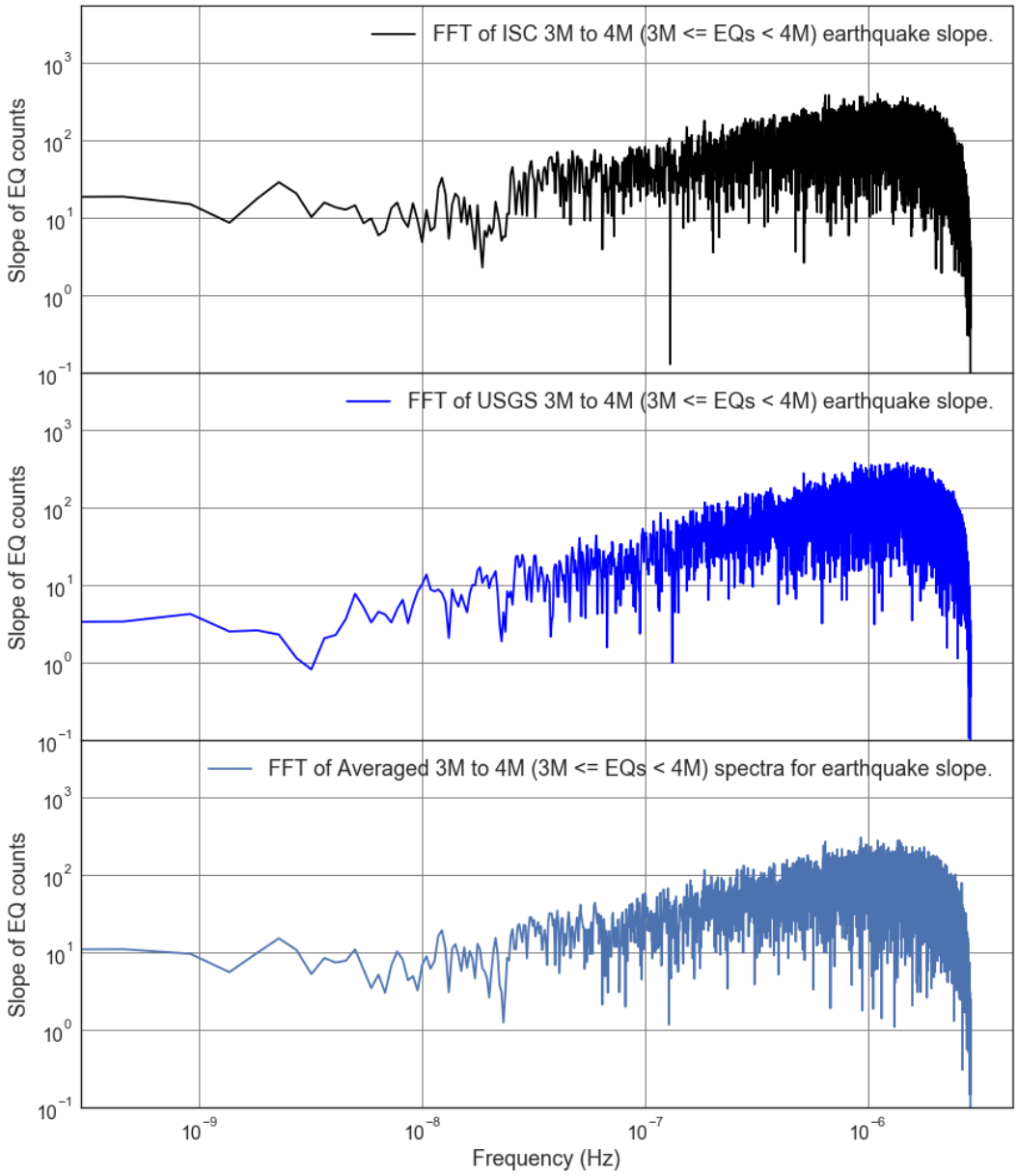

Figure 2.11: FFT Loglog Comparison Plot of Earthquake Count Slope for 3M to 4M (3M <= EQs < 4M) Earthquakes from the ISC, USGS, and Centennial Y2K datasets.

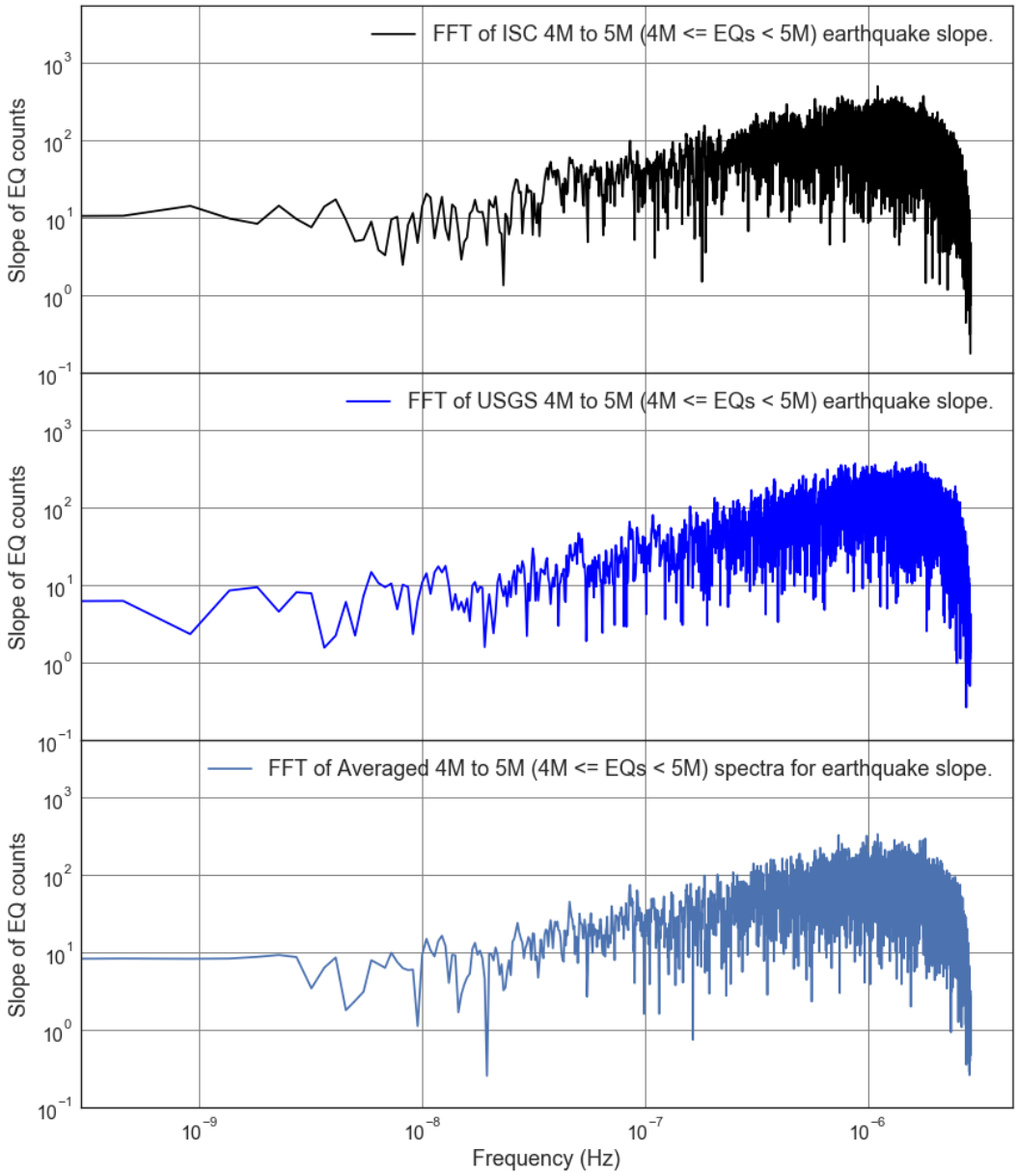

Figure 2.12: FFT Loglog Comparison Plot of Earthquake Count Slope for 4M to 5M (4M <= EQs < 5M) Earthquakes from the ISC, USGS, and Centennial Y2K datasets.

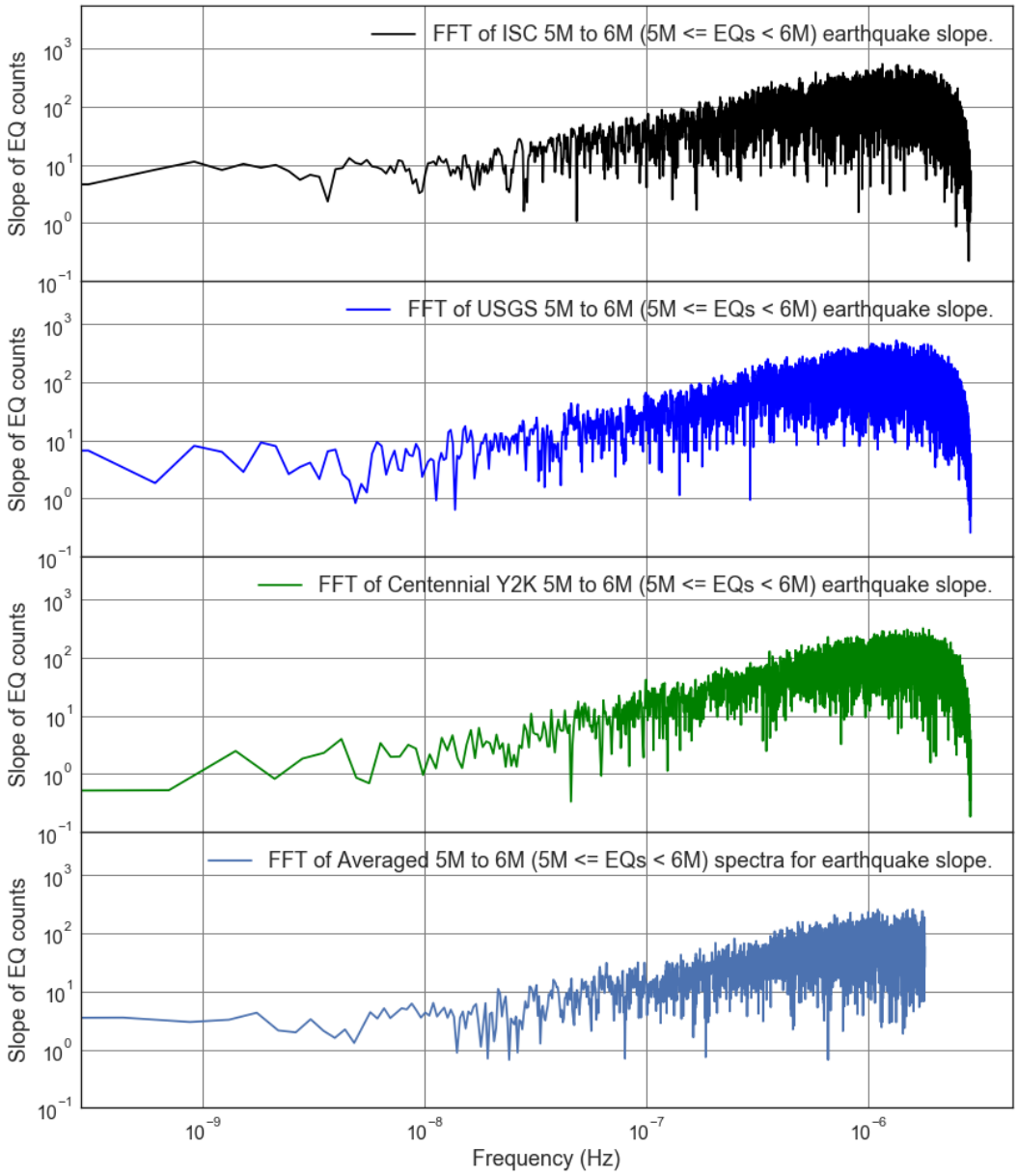

Figure 2.13: FFT Loglog Comparison Plot of Earthquake Count Slope for 5M to 6M (5M <= EQs < 6M) Earthquakes from the ISC, USGS, and Centennial Y2K datasets.

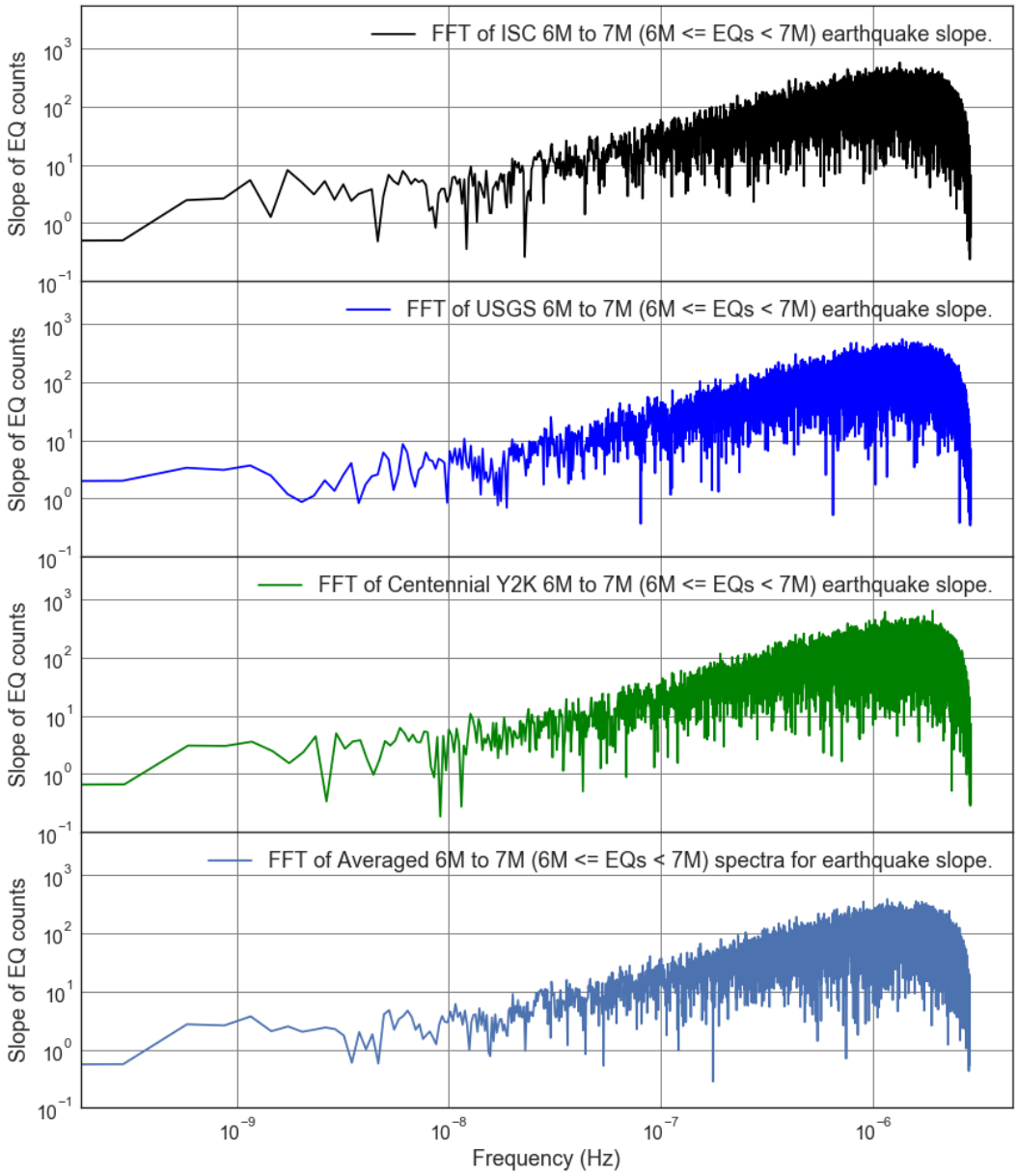

Figure 2.14: FFT Loglog Comparison Plot of Earthquake Count Slope for 6M to 7M (6M <= EQs < 7M) Earthquakes from the ISC, USGS, and Centennial Y2K datasets.

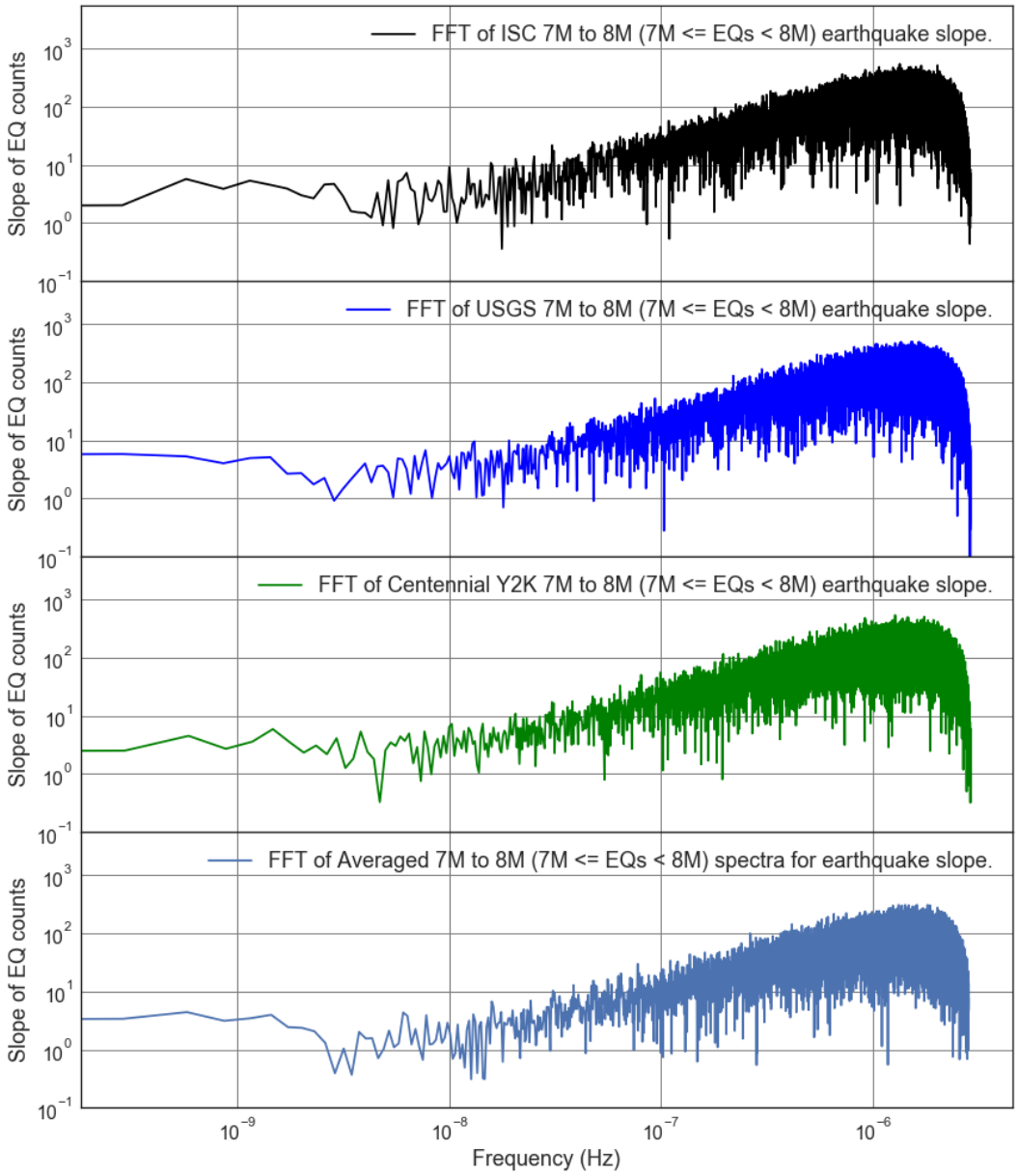

Figure 2.15: FFT Loglog Comparison Plot of Earthquake Count Slope for 7M to 8M (7M <= EQs < 8M) Earthquakes from the ISC, USGS, and Centennial Y2K datasets.

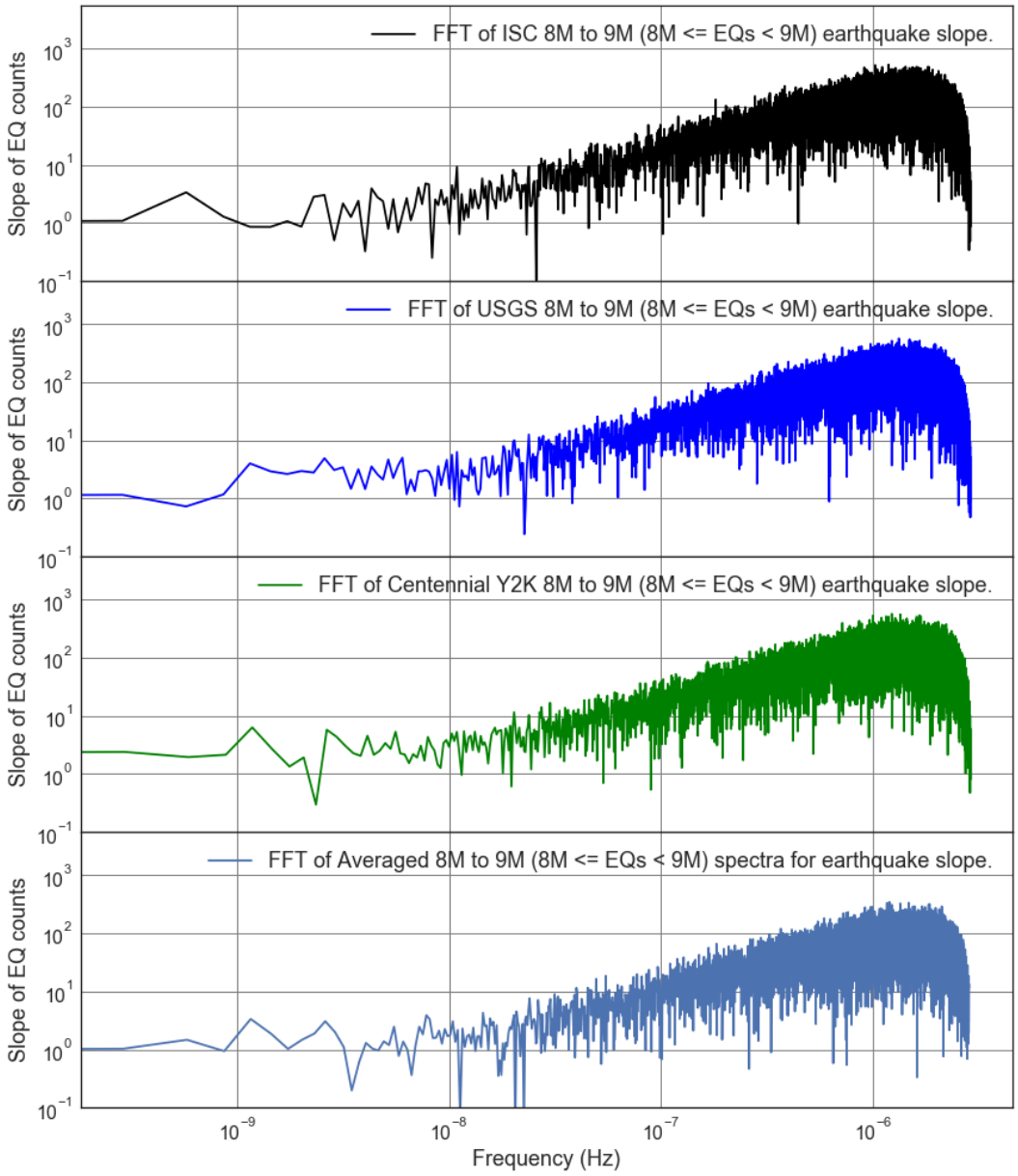

Figure 2.16: FFT Loglog Comparison Plot of Earthquake Count Slope for 8M to 9M (8M <= EQs < 9M) Earthquakes from the ISC, USGS, and Centennial Y2K datasets.

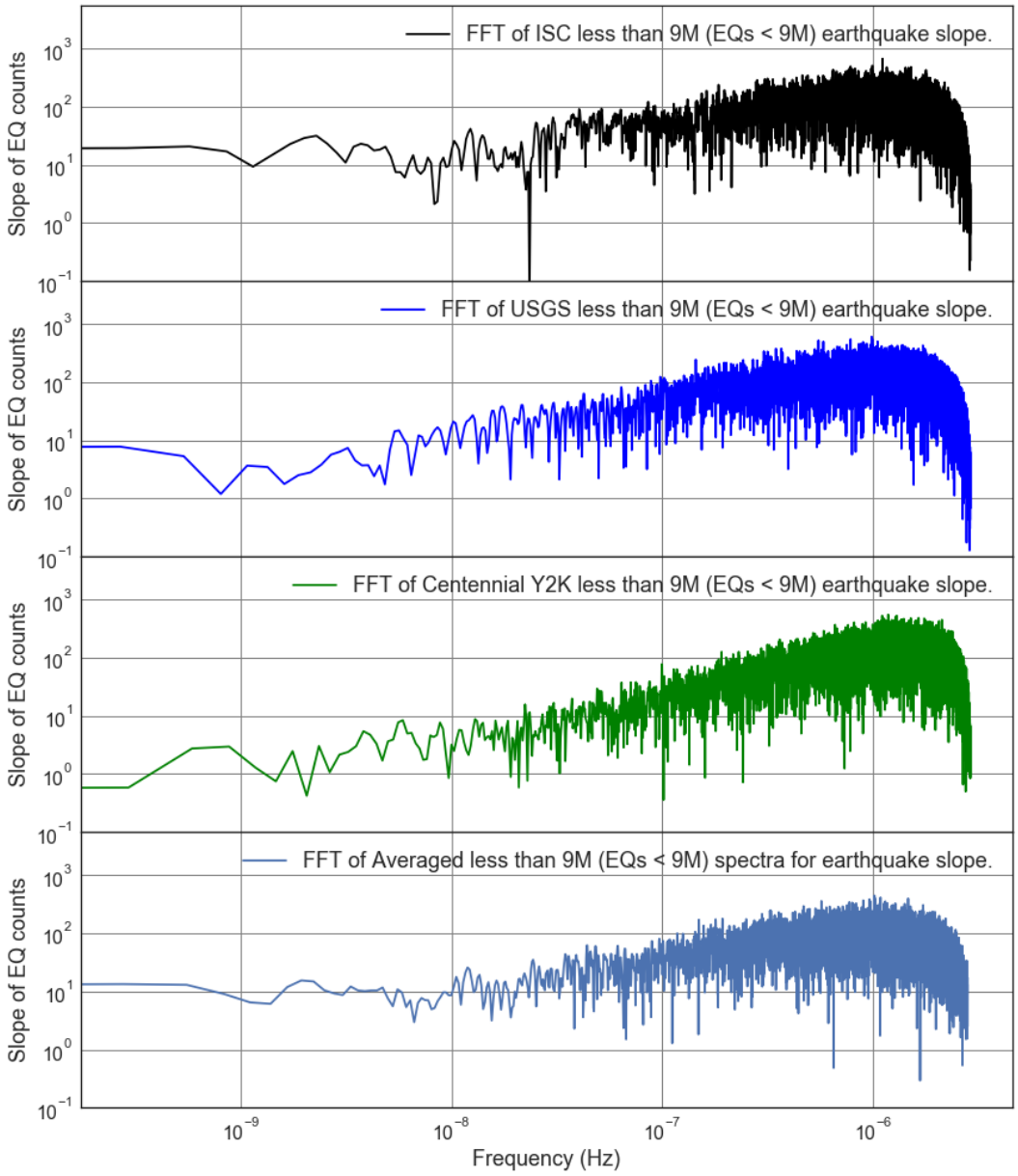

Figure 2.17: FFT Loglog Comparison Plot of Earthquake Count Slope for less than 9M (EQs < 9M) Earthquakes from the ISC, USGS, and Centennial Y2K datasets.

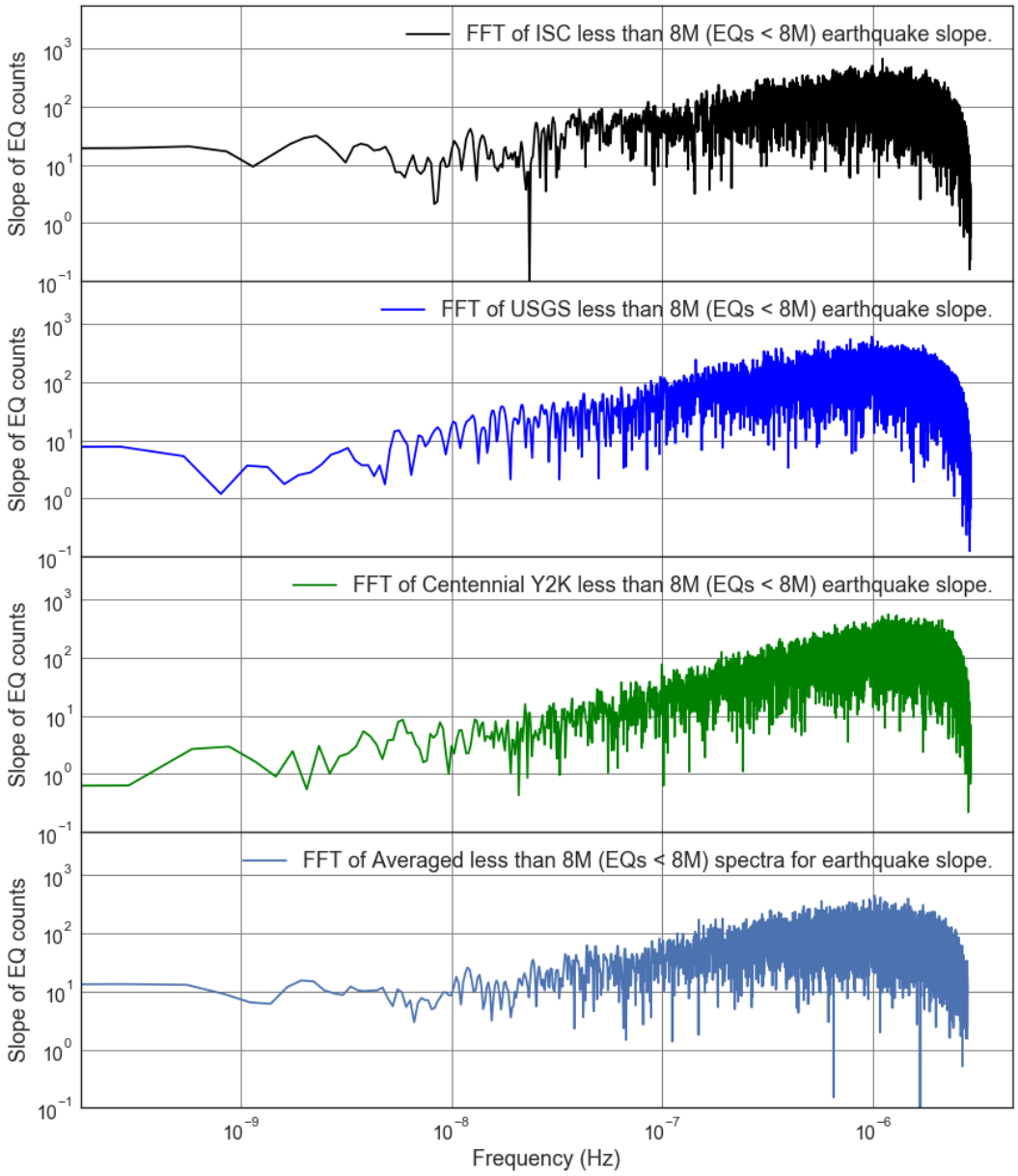

Figure 2.18: FFT Loglog Comparison Plot of Earthquake Count Slope for less than 8M (EQs < 8M) Earthquakes from the ISC, USGS, and Centennial Y2K datasets.

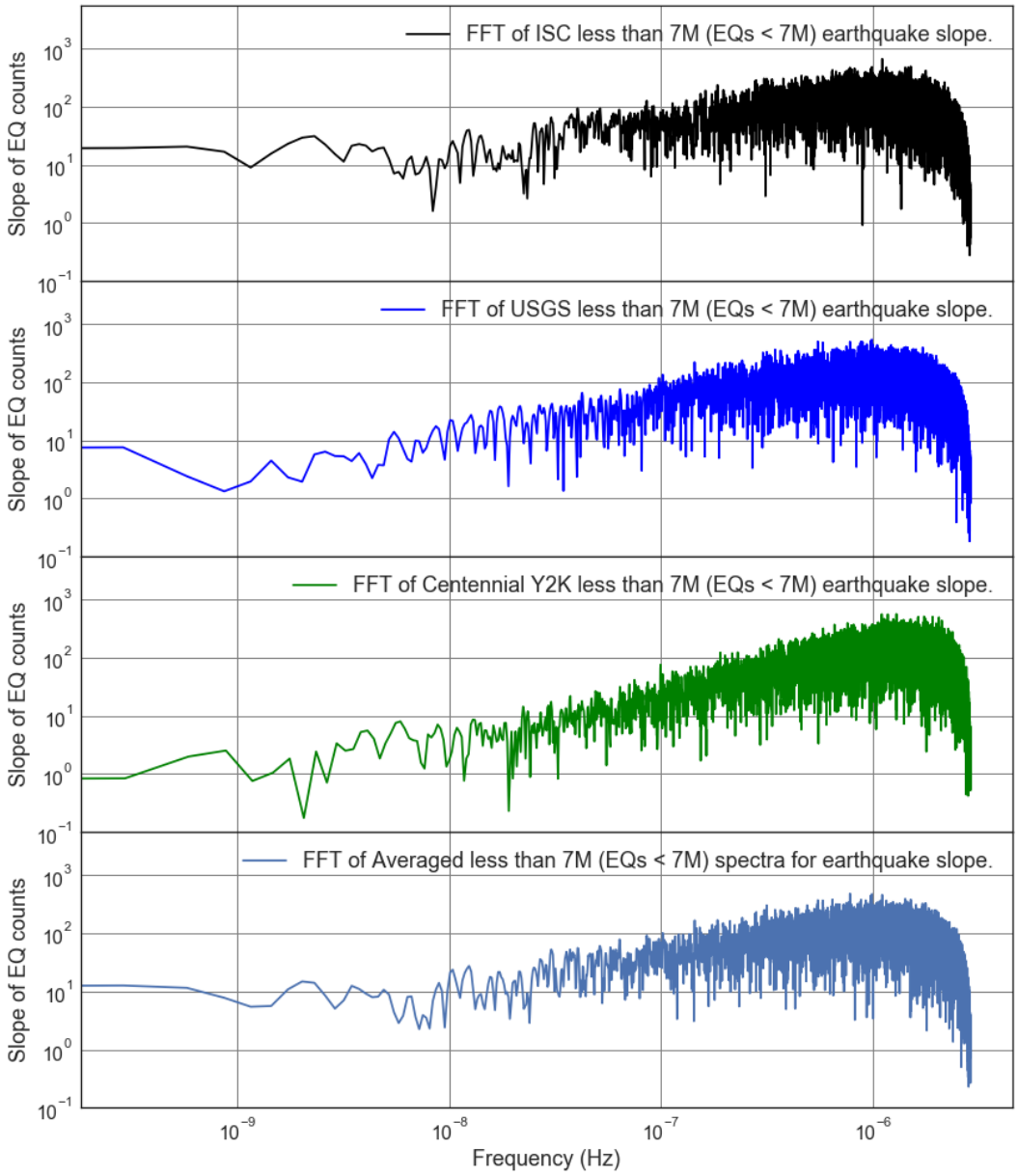

Figure 2.19: FFT Loglog Comparison Plot of Earthquake Count Slope for less than 7M (EQs < 7M) Earthquakes from the ISC, USGS, and Centennial Y2K datasets.

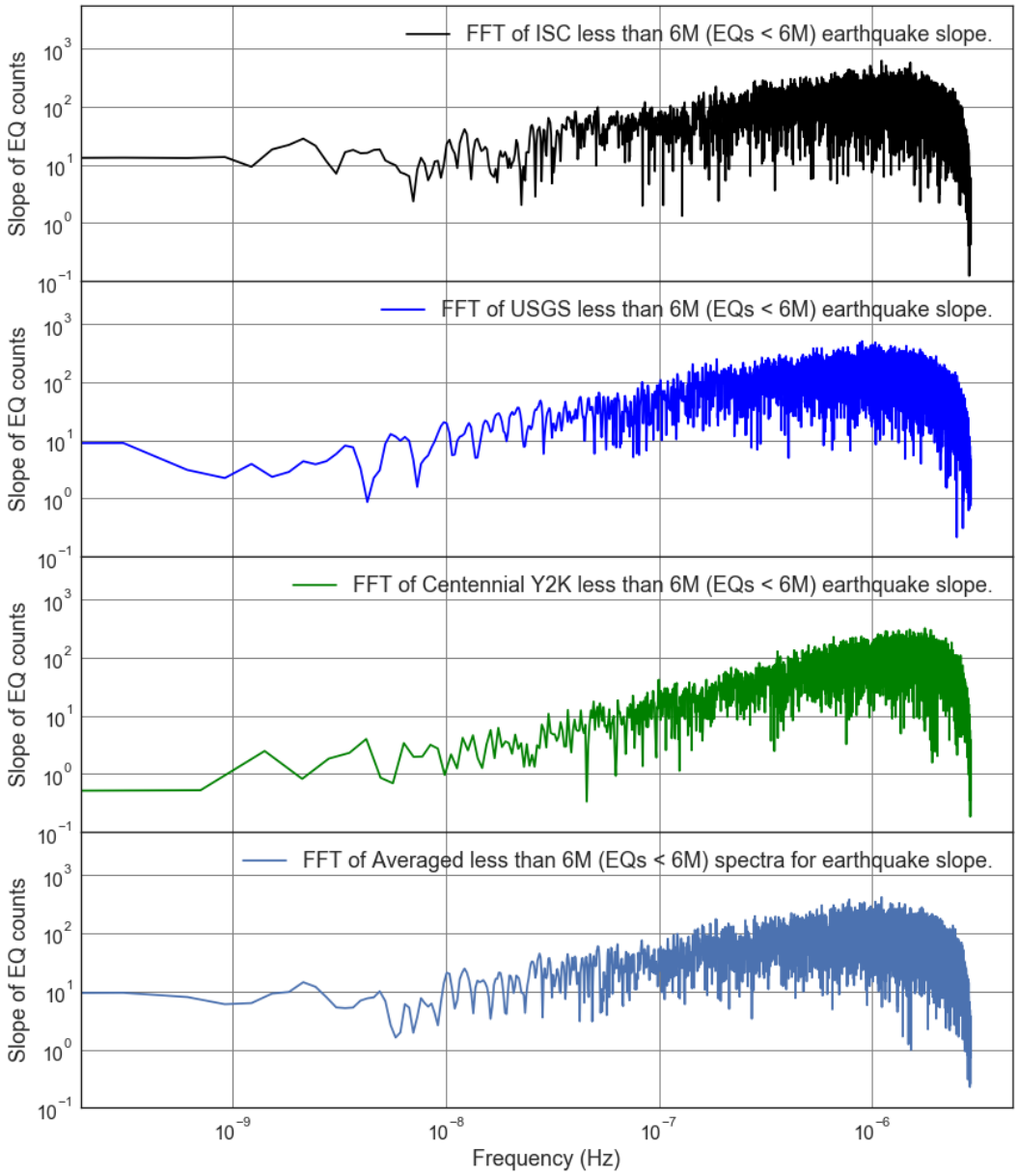

Figure 2.20: FFT Loglog Comparison Plot of Earthquake Count Slope for less than 6M (EQs < 6M) Earthquakes from the ISC, USGS, and Centennial Y2K datasets.

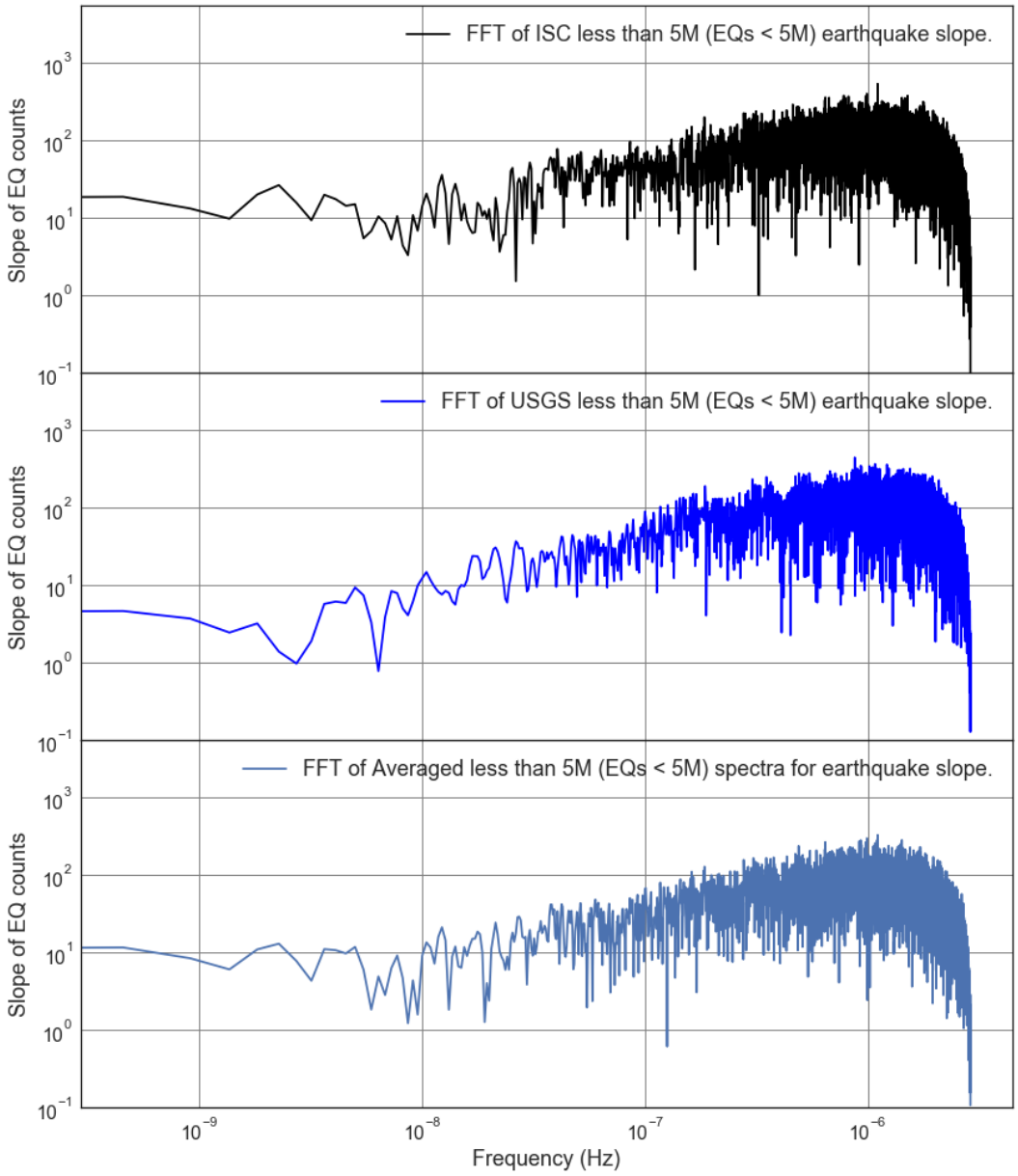

Figure 2.21: FFT Loglog Comparison Plot of Earthquake Count Slope for less than 5M (EQs < 5M) Earthquakes from the ISC, USGS, and Centennial Y2K datasets.

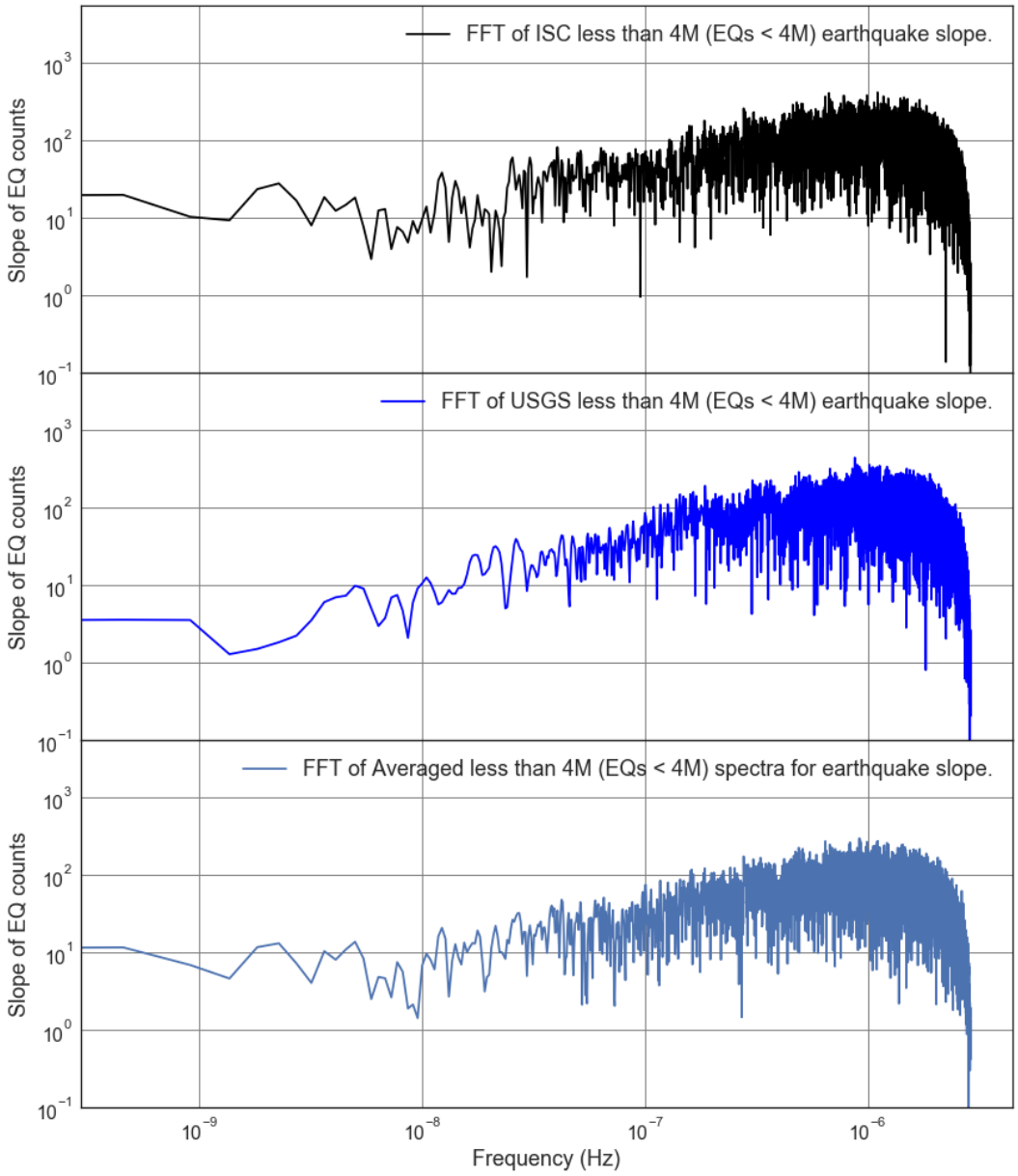

Figure 2.22: FFT Loglog Comparison Plot of Earthquake Count Slope for less than 4M (EQs < 4M) Earthquakes from the ISC, USGS, and Centennial Y2K datasets.

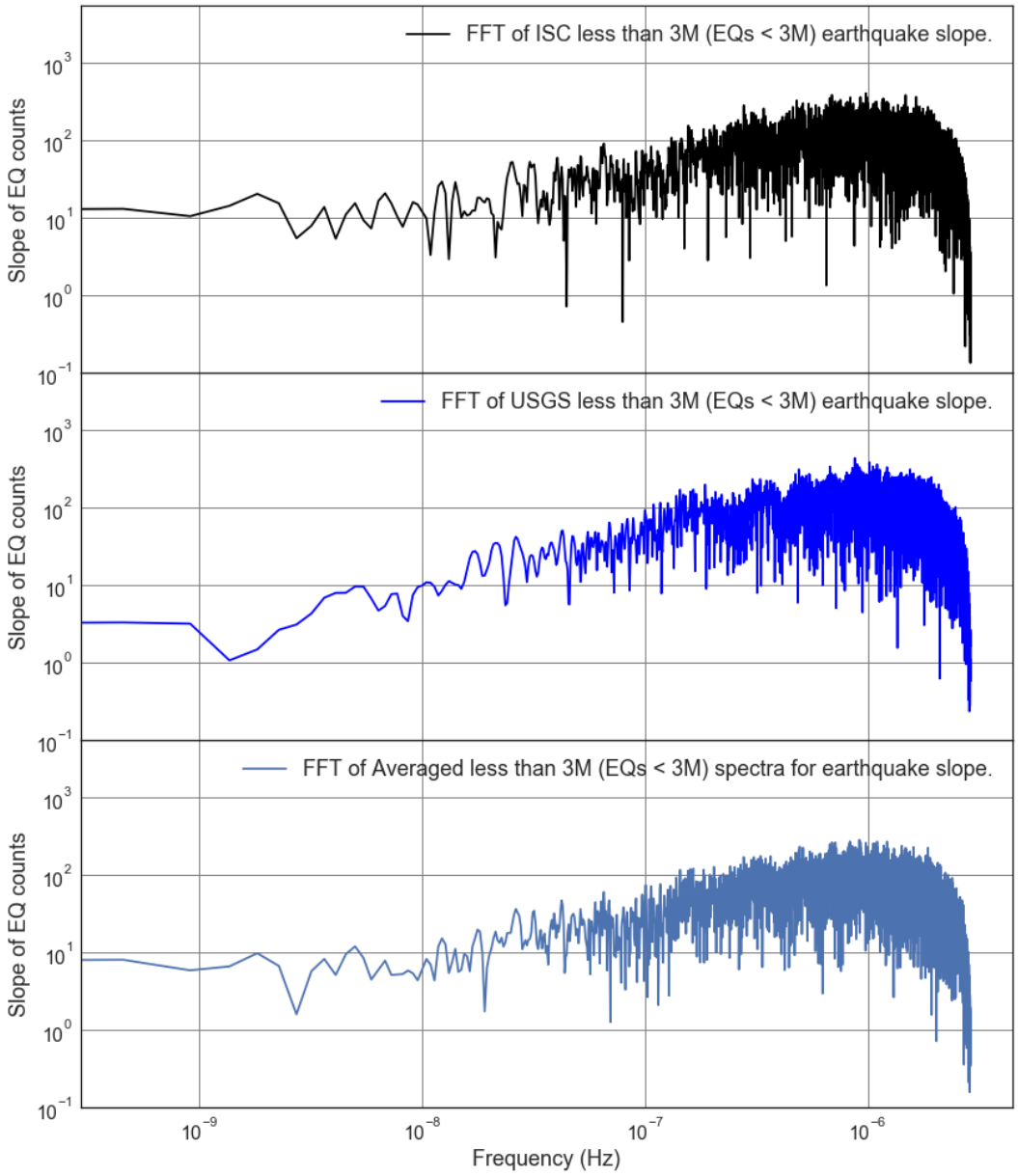

Figure 2.23: FFT Loglog Comparison Plot of Earthquake Count Slope for less than 3M (EQs < 3M) Earthquakes from the ISC, USGS, and Centennial Y2K datasets.

Comparison of ISC, USGS, and Centennial Y2K FFT of Slope of Earthquake Energy Plots

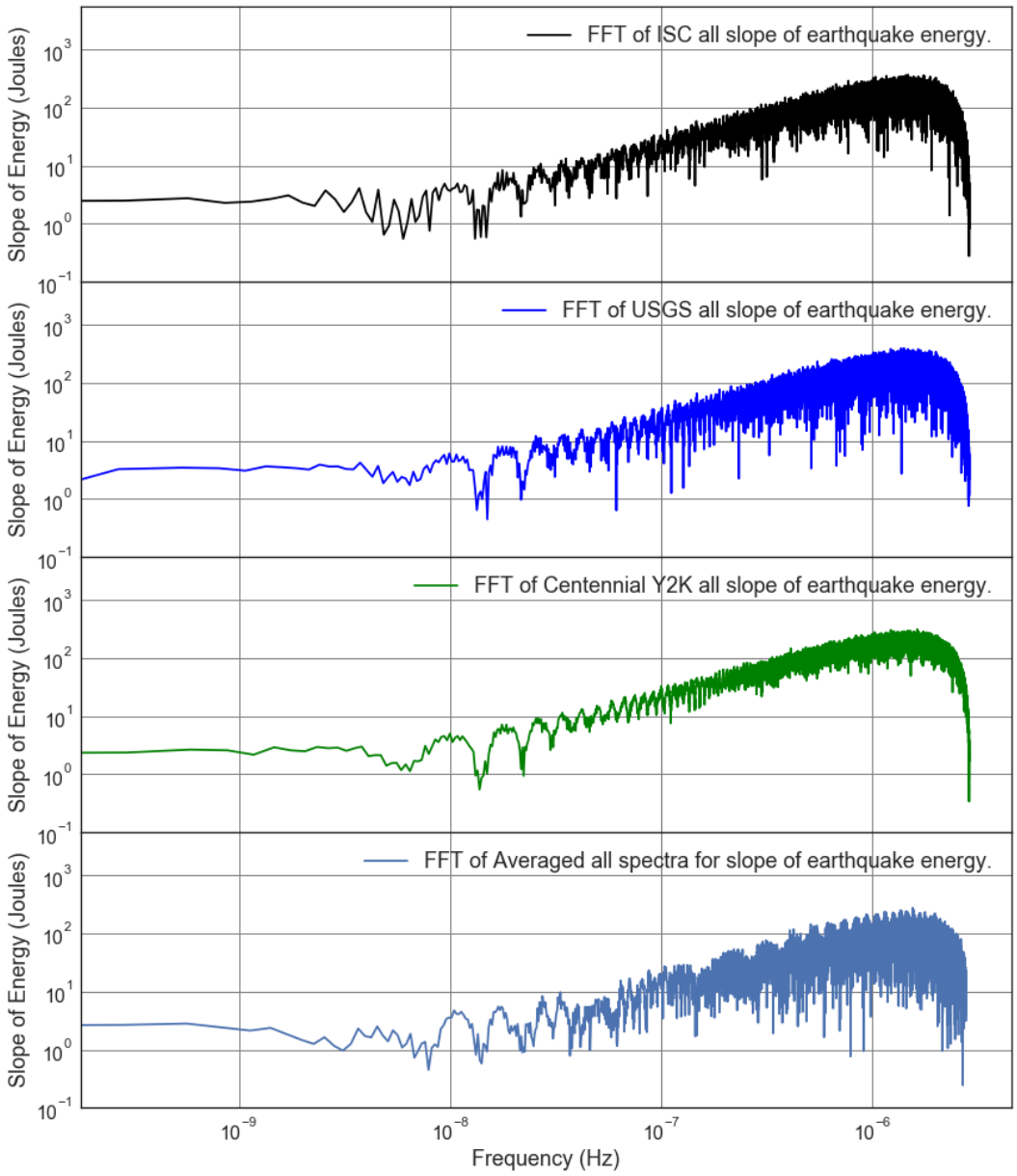

Figure 2.24: FFT Loglog Comparison Plot: Slope of all Earthquake Energy from the ISC, USGS, and Centennial Y2K datasets.

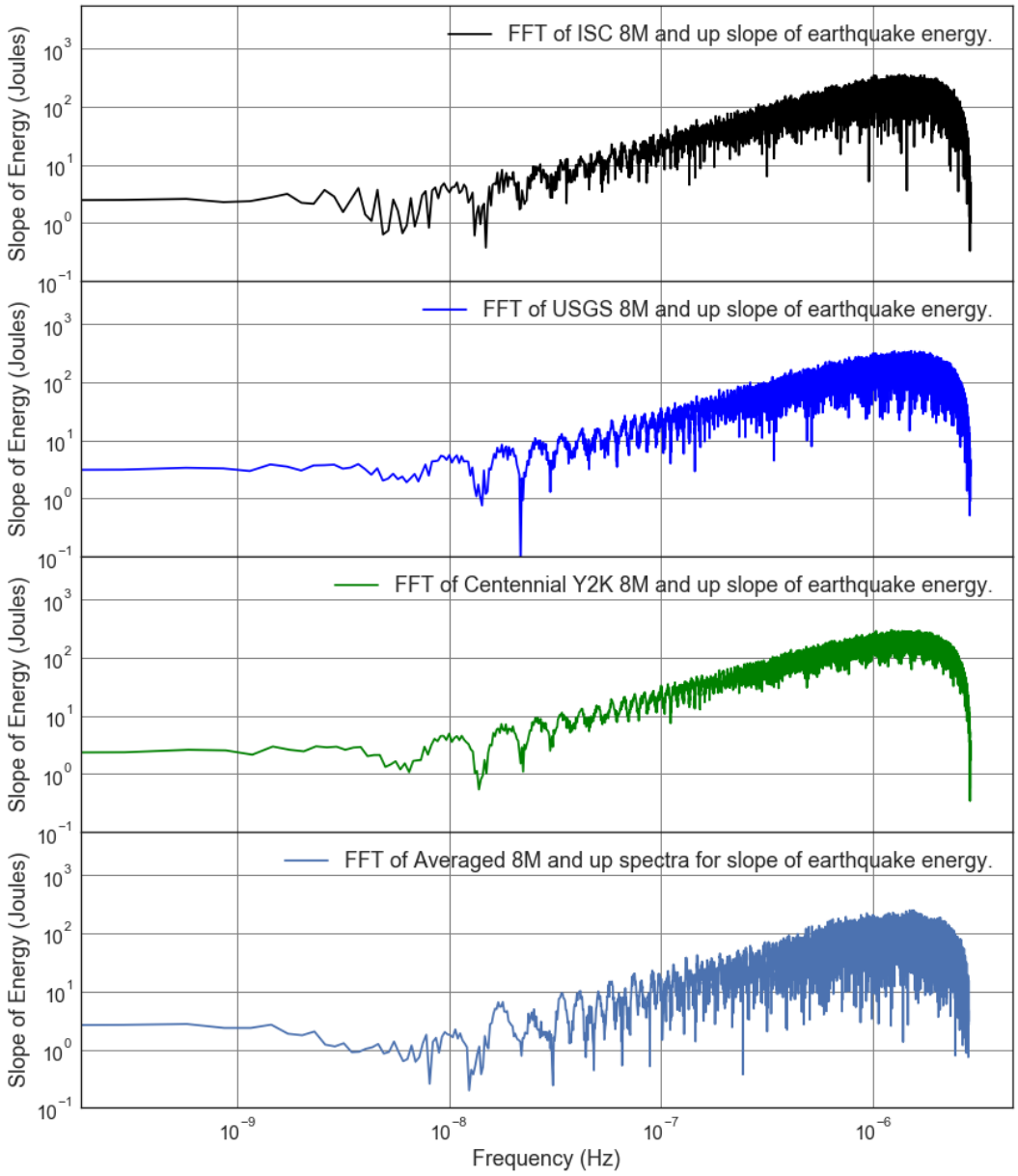

Figure 2.25: FFT Loglog Comparison Plot: Slope of 8M and up Earthquake Energy from the ISC, USGS, and Centennial Y2K datasets.

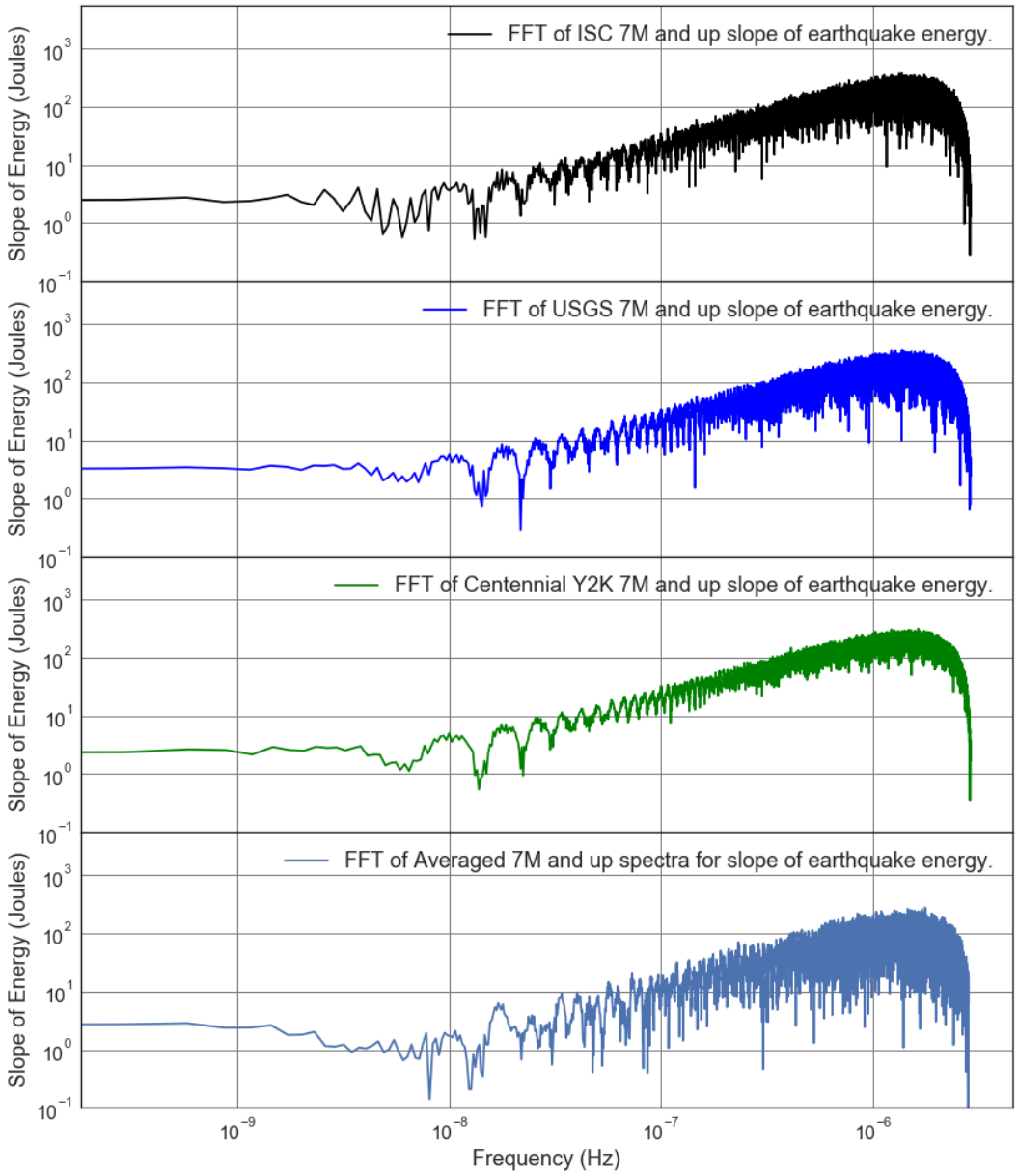

Figure 2.26: FFT Loglog Comparison Plot: Slope of 7M and up Earthquake Energy from the ISC, USGS, and Centennial Y2K datasets.

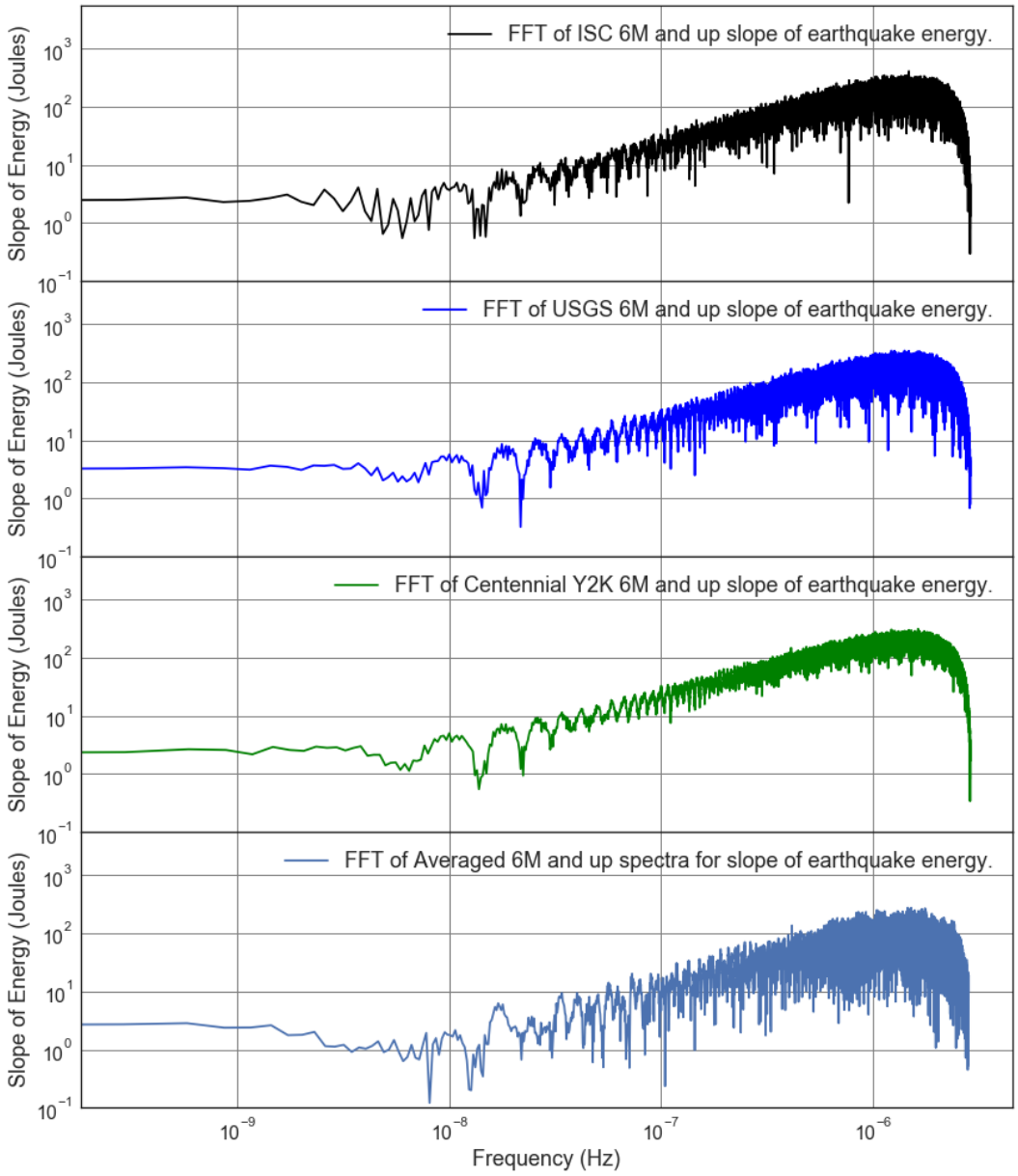

Figure 2.27: FFT Loglog Comparison Plot: Slope of 6M and up Earthquake Energy from the ISC, USGS, and Centennial Y2K datasets.

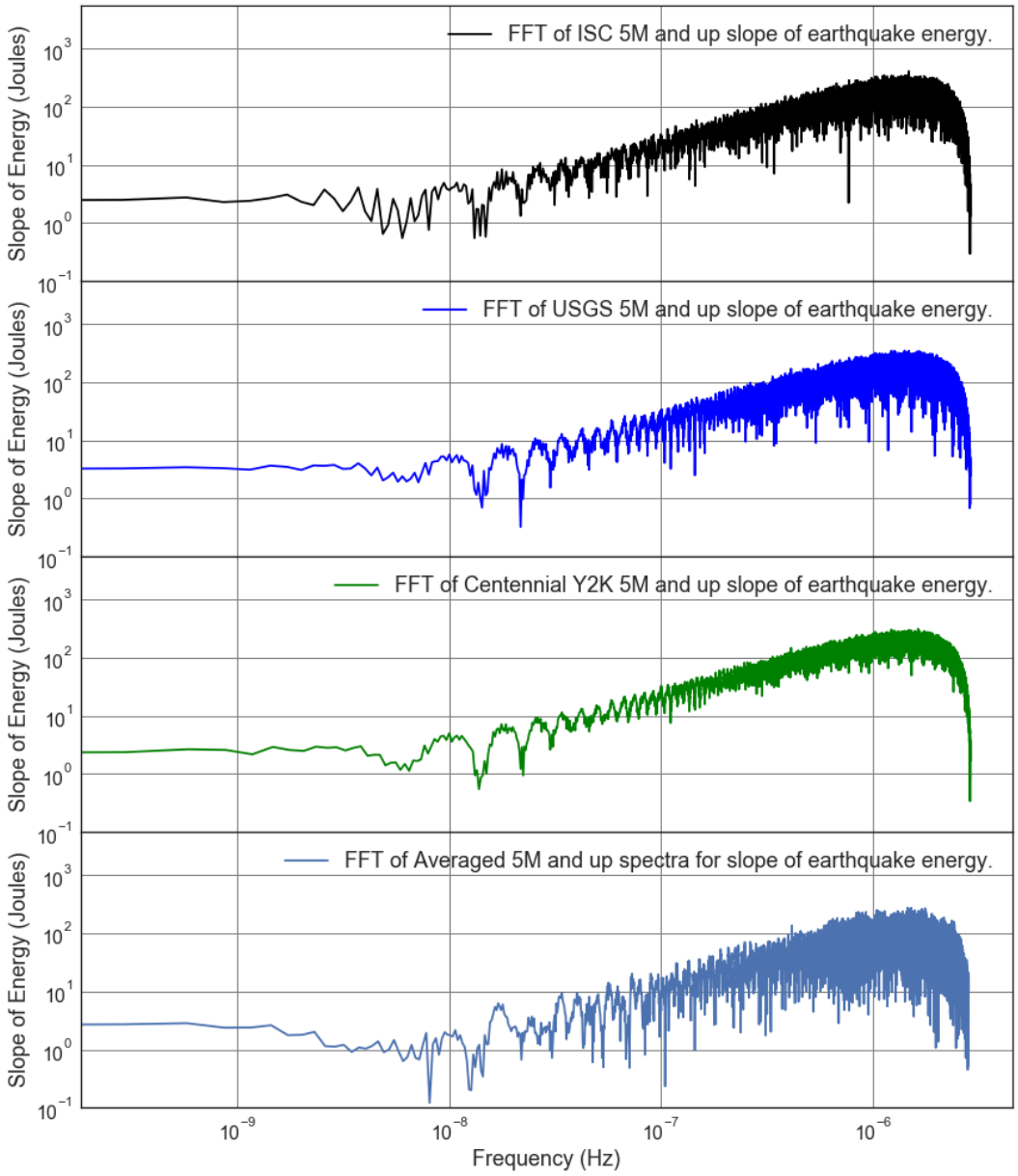

Figure 2.28: FFT Loglog Comparison Plot: Slope of 5M and up Earthquake Energy from the ISC, USGS, and Centennial Y2K datasets.

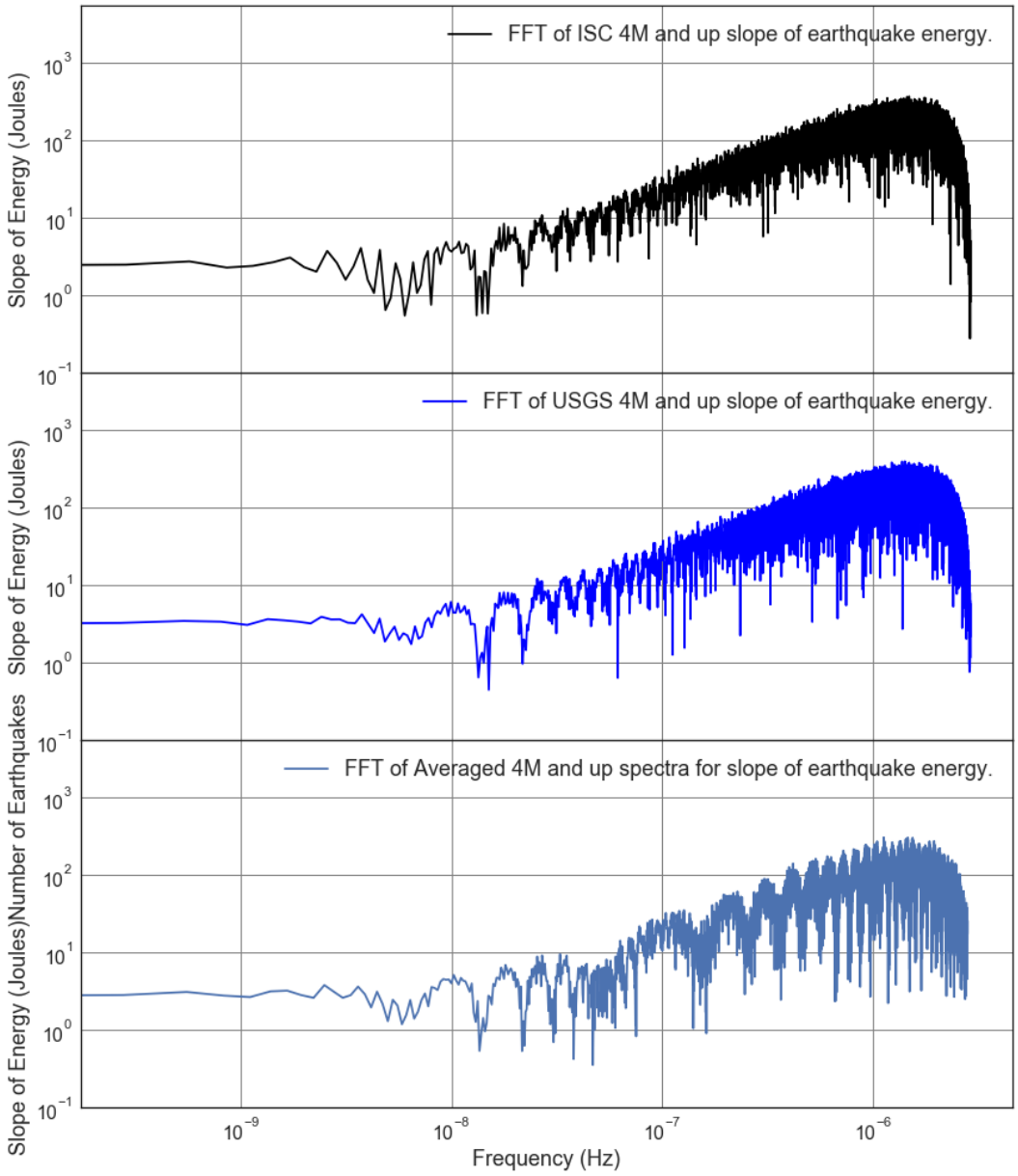

Figure 2.29: FFT Loglog Comparison Plot: Slope of 4M and up Earthquake Energy from the ISC, USGS, and Centennial Y2K datasets.

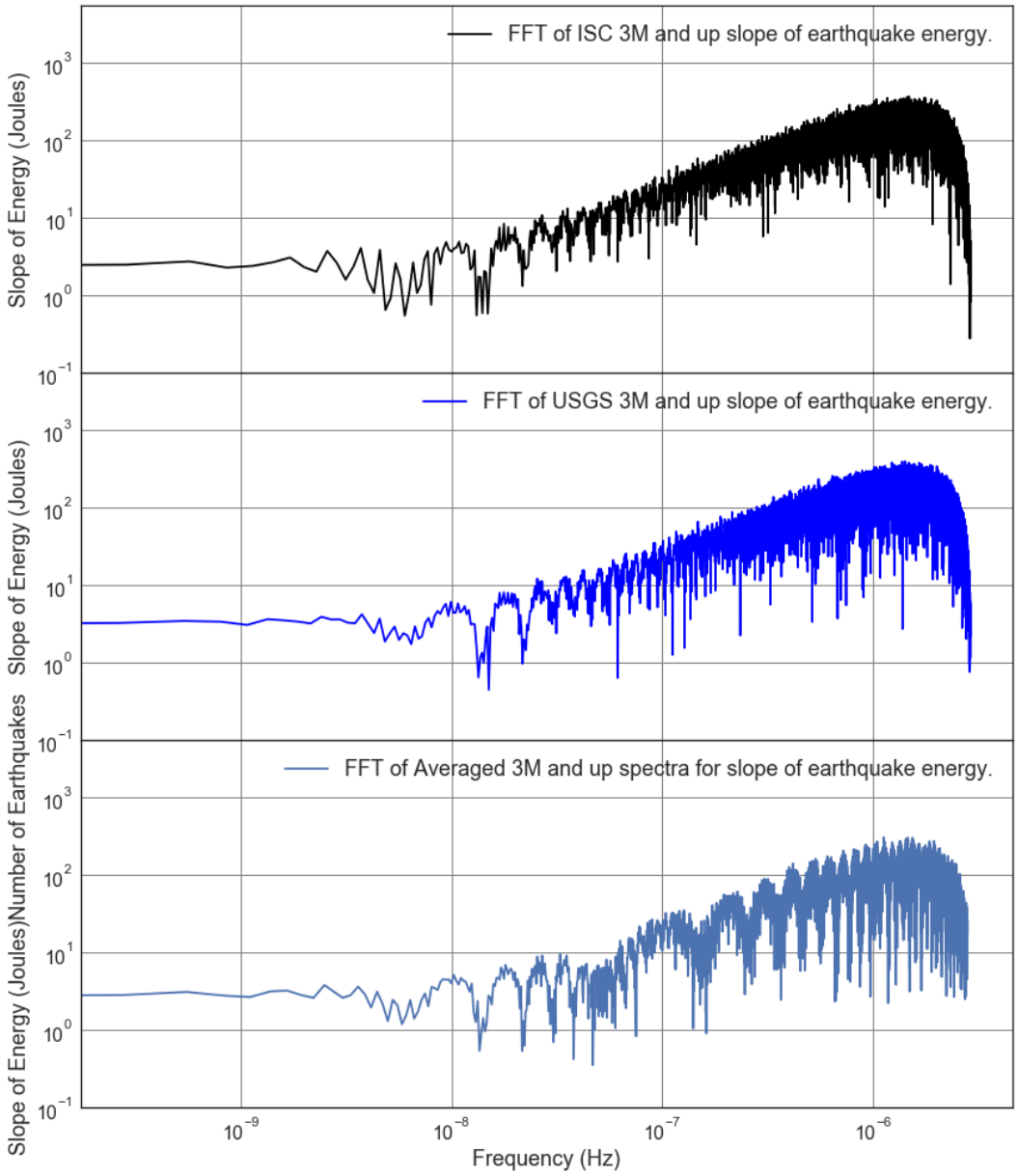

Figure 2.30: FFT Loglog Comparison Plot: Slope of 3M and up Earthquake Energy from the ISC, USGS, and Centennial Y2K datasets.

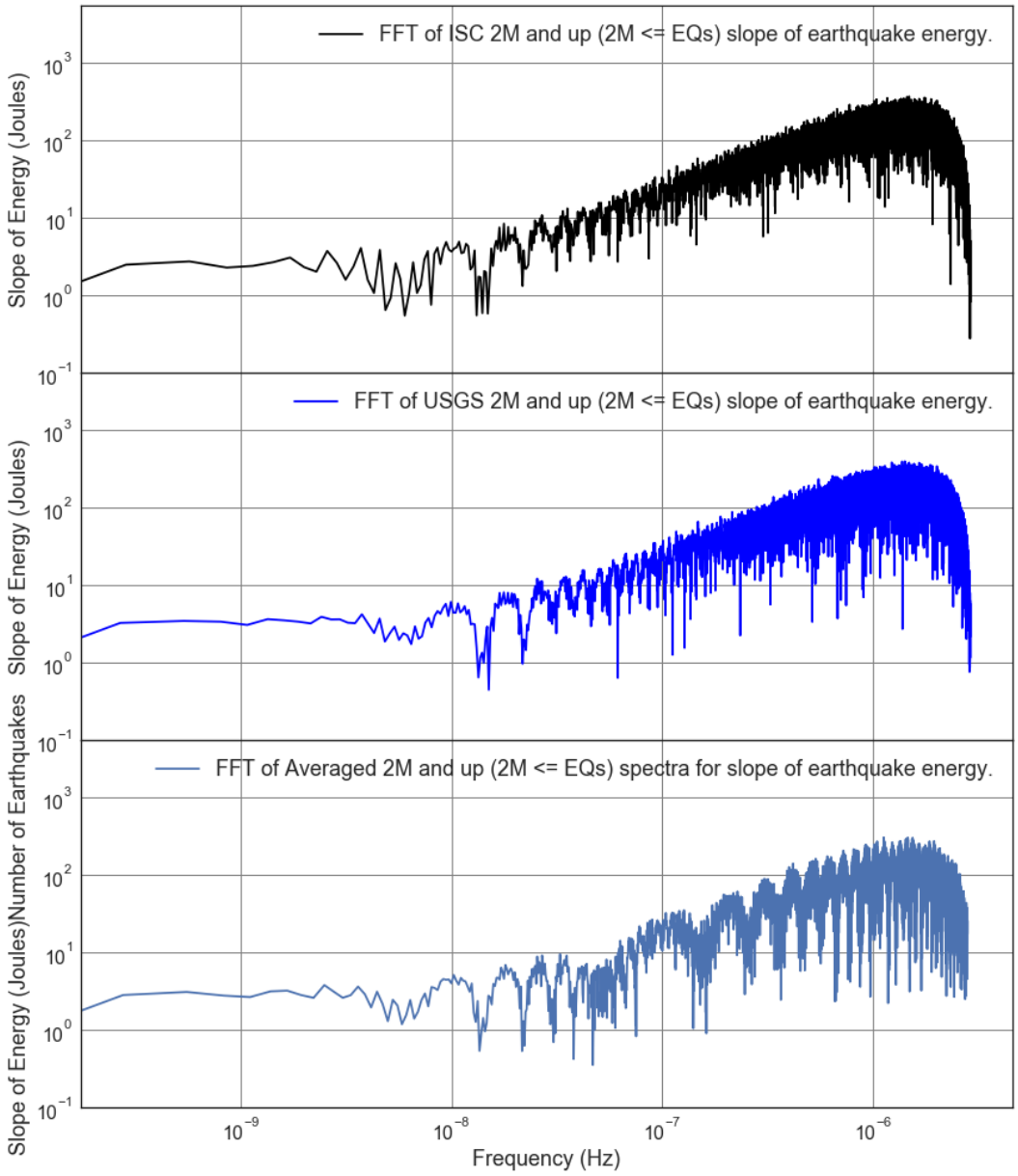

Figure 2.31: FFT Loglog Comparison Plot: Slope of 2M and up (2M <= EQs) Earthquake Energy from the ISC, USGS, and Centennial Y2K datasets.

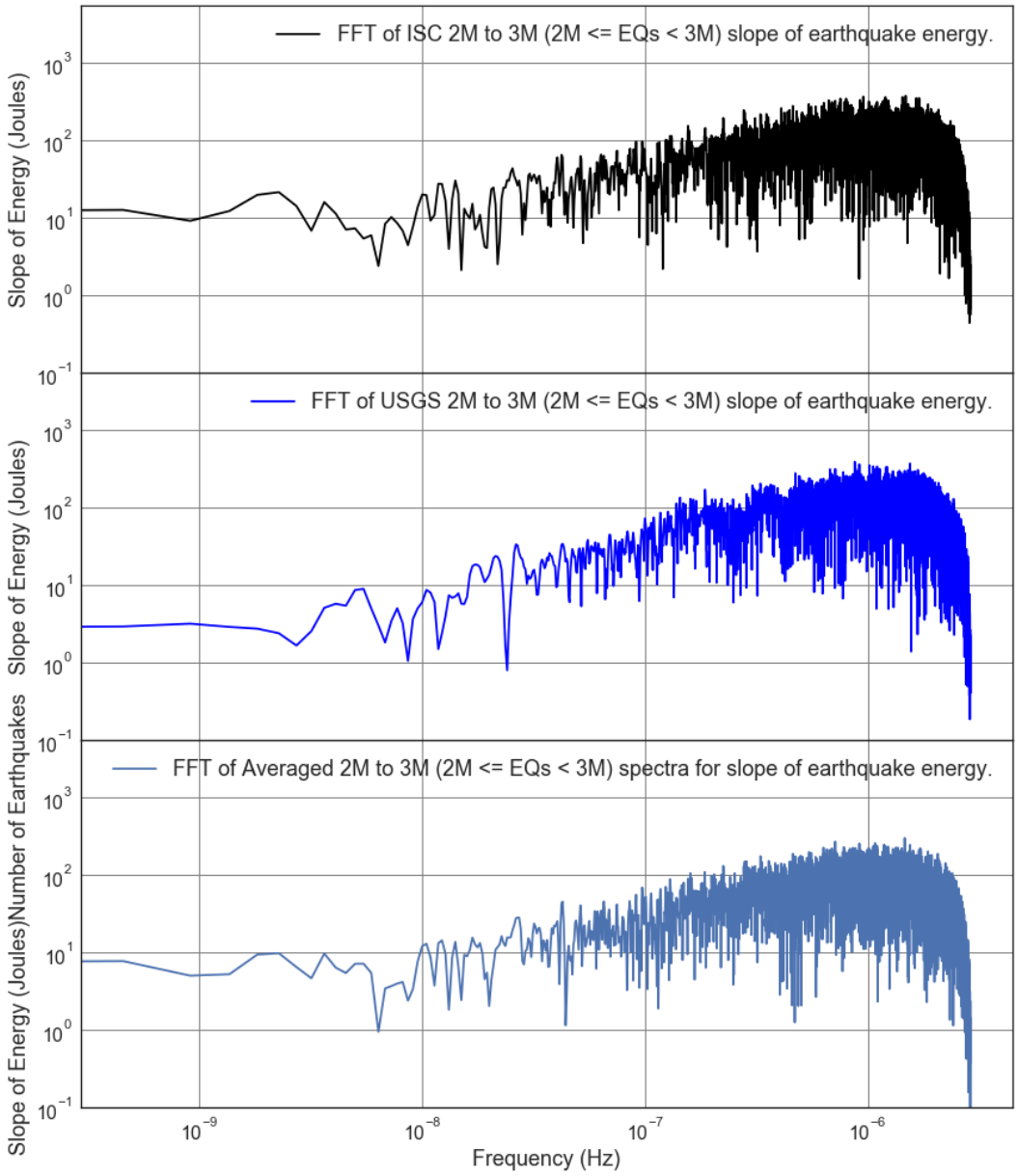

Figure 2.32: FFT Loglog Comparison Plot: Slope of 2M to 3M (2M <= EQs < 3M) Earthquake Energy from the ISC, USGS, and Centennial Y2K datasets.

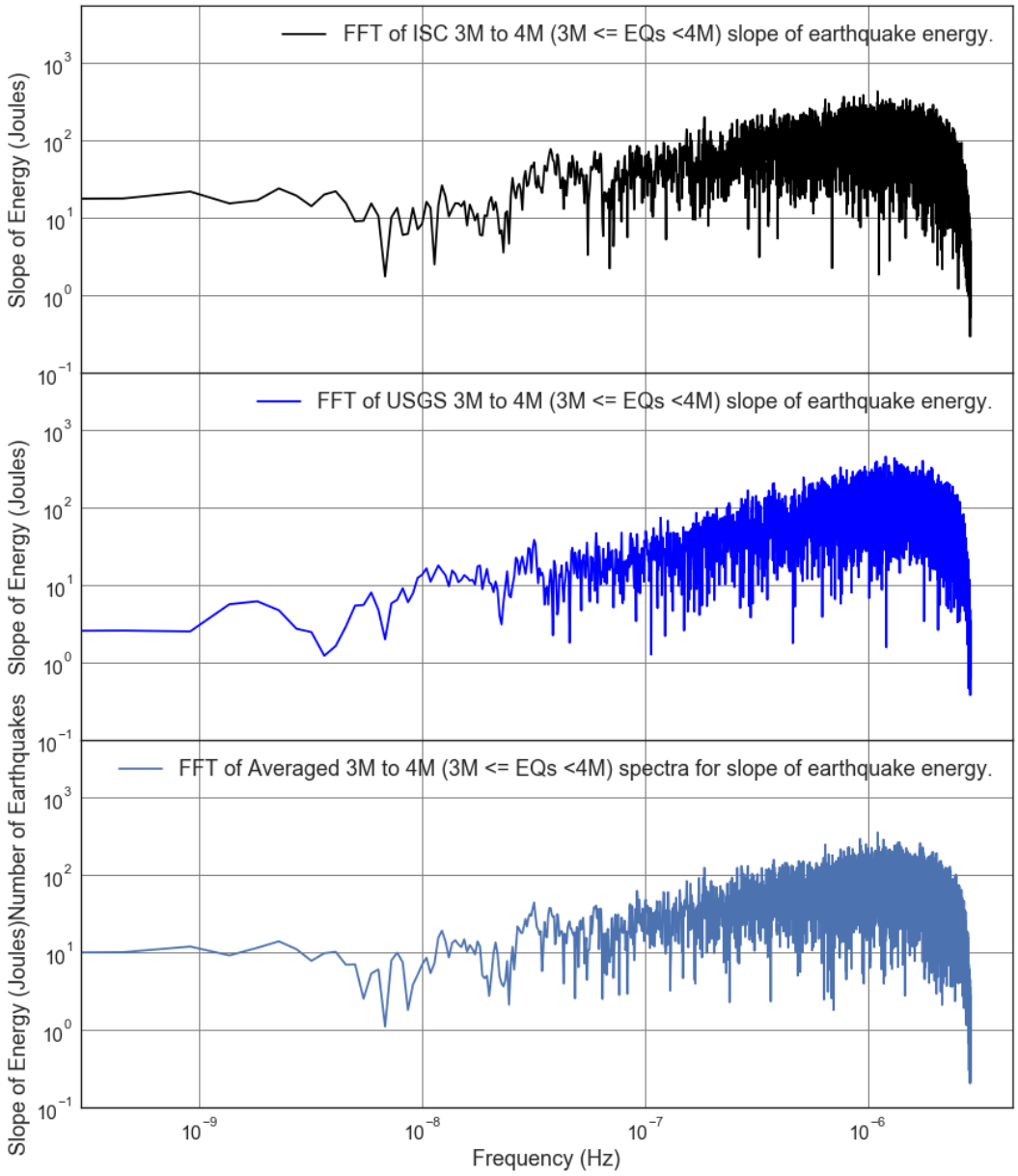

Figure 2.33: FFT Loglog Comparison Plot: Slope of 3M to 4M (3M <= EQs <4M) Earthquake Energy from the ISC, USGS, and Centennial Y2K datasets.

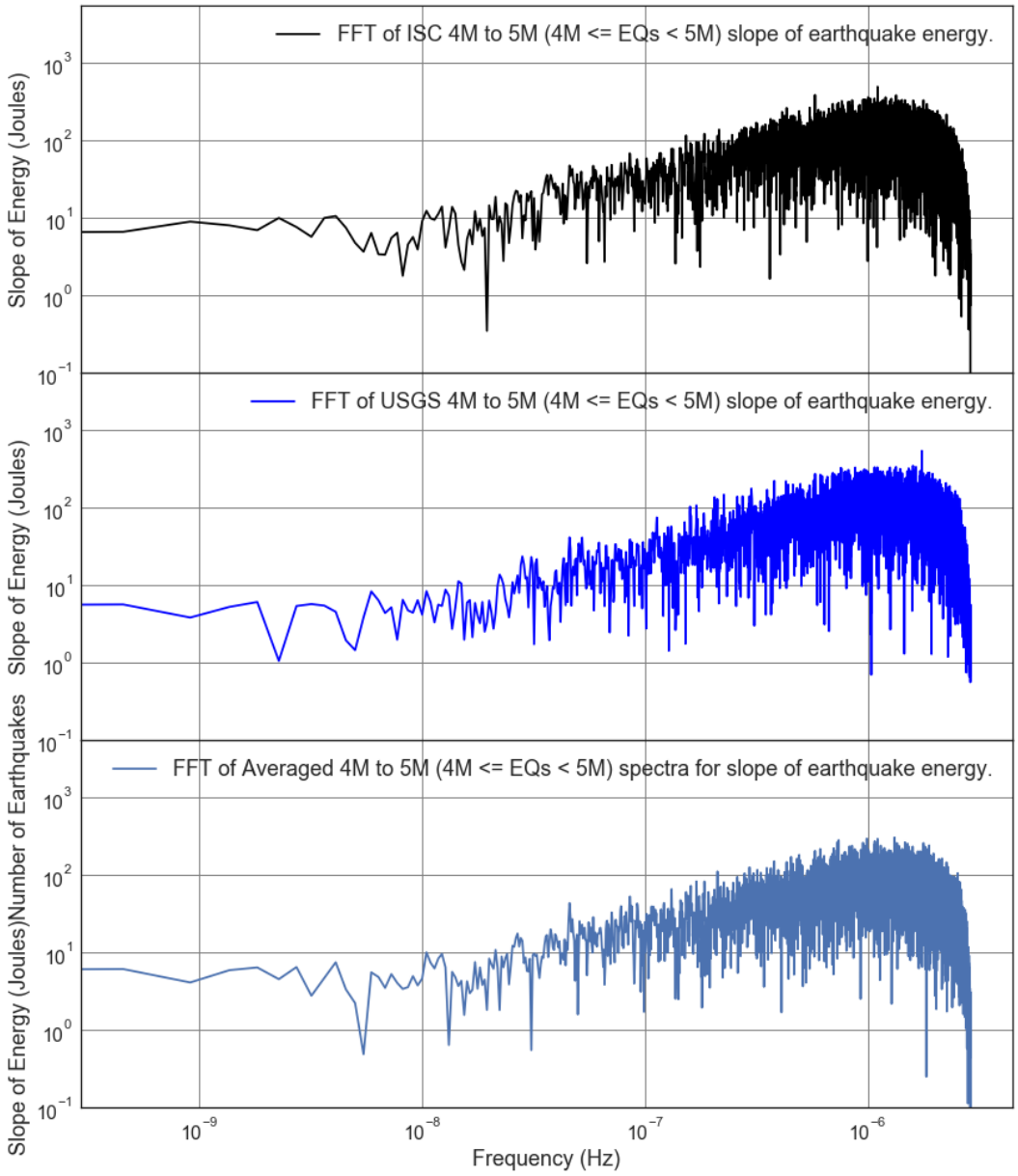

Figure 2.34: FFT Loglog Comparison Plot: Slope of 4M to 5M (4M <= EQs < 5M) Earthquake Energy from the ISC, USGS, and Centennial Y2K datasets.

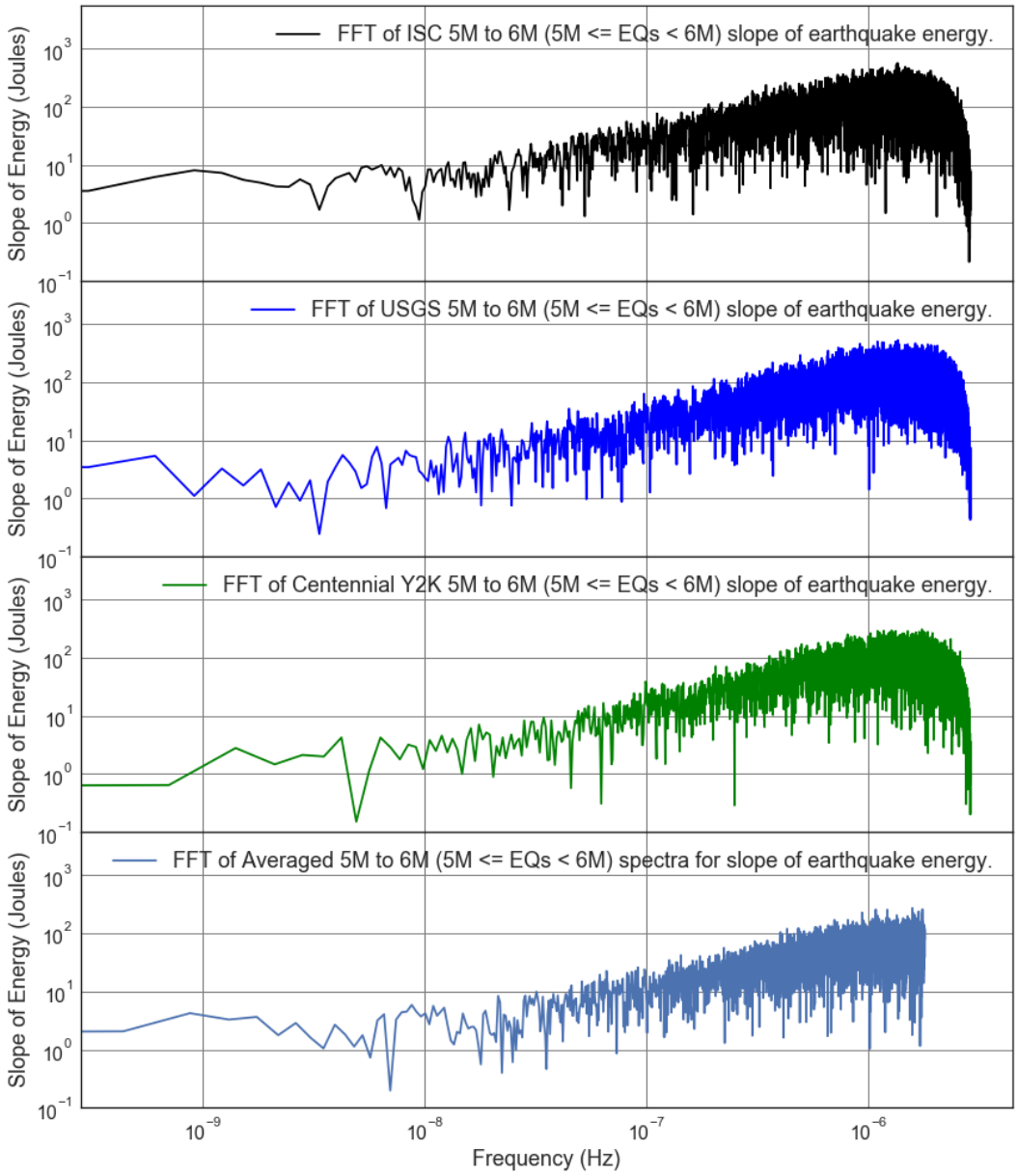

Figure 2.35: FFT Loglog Comparison Plot: Slope of 5M to 6M (5M <= EQs < 6M) Earthquake Energy from the ISC, USGS, and Centennial Y2K datasets.

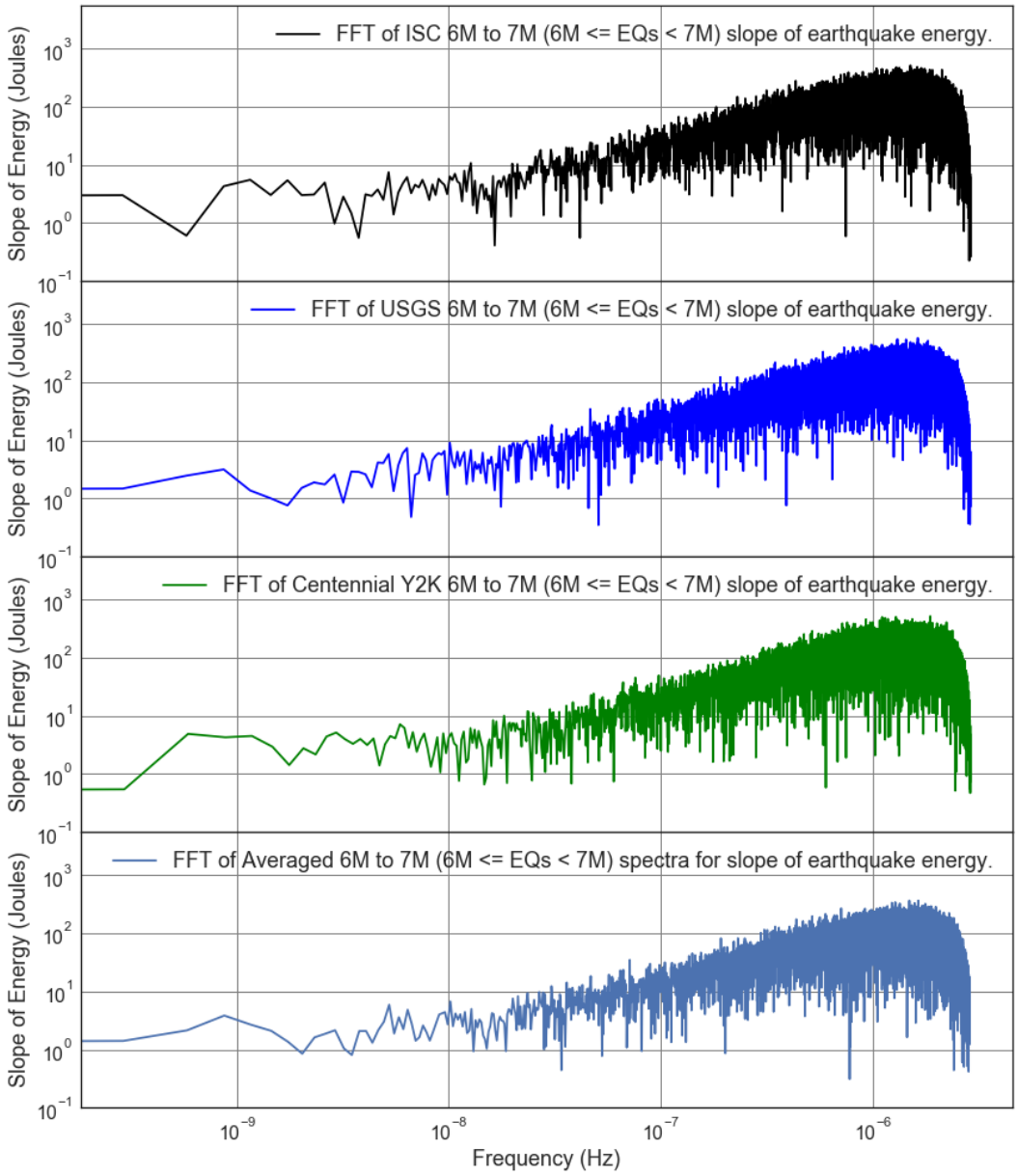

Figure 2.36: FFT Loglog Comparison Plot: Slope of 6M to 7M (6M <= EQs < 7M) Earthquake Energy from the ISC, USGS, and Centennial Y2K datasets.

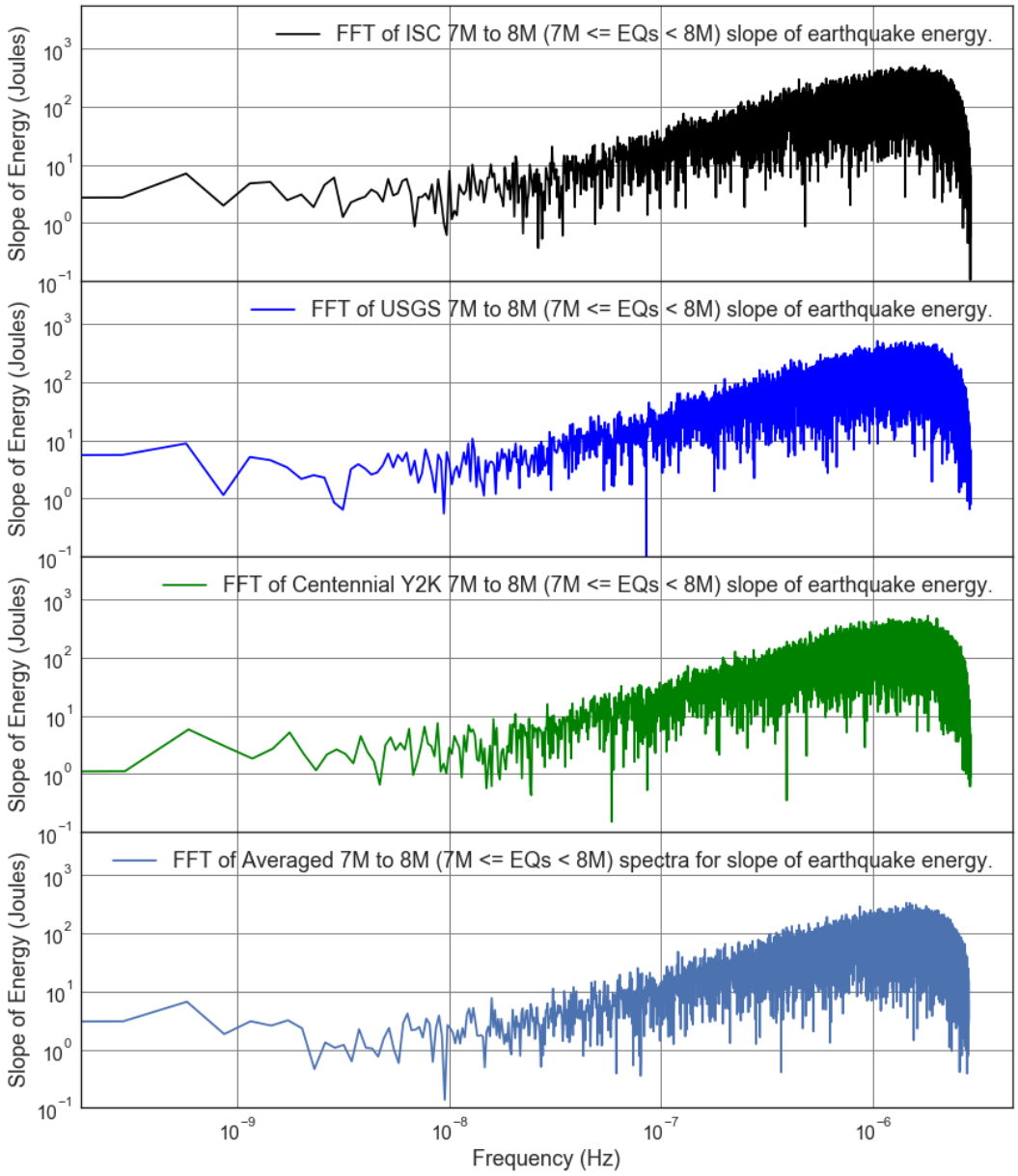

Figure 2.37: FFT Loglog Comparison Plot: Slope of 7M to 8M (7M <= EQs < 8M) Earthquake Energy from the ISC, USGS, and Centennial Y2K datasets.

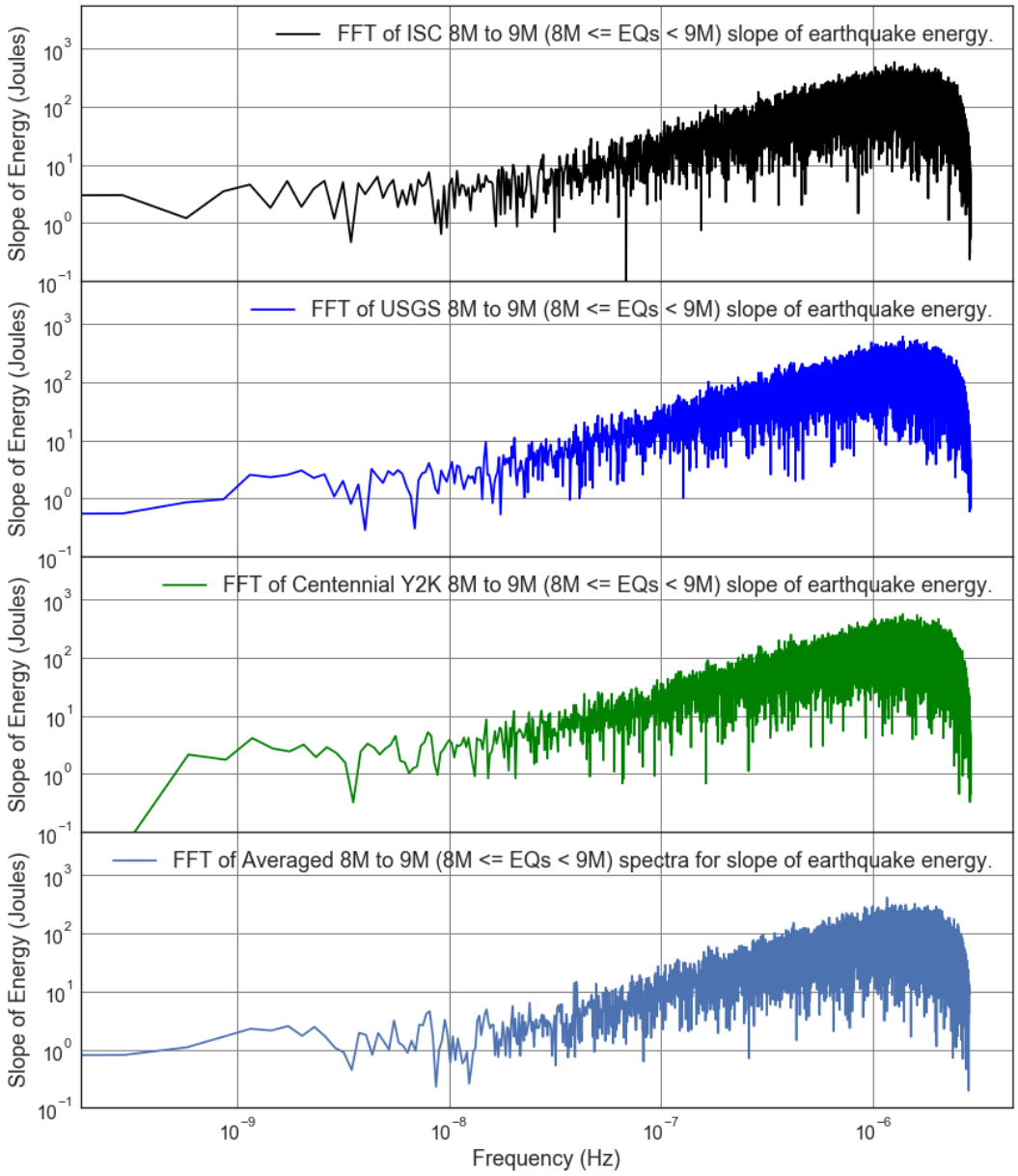

Figure 2.38: FFT Loglog Comparison Plot: Slope of 8M to 9M (8M <= EQs < 9M) Earthquake Energy from the ISC, USGS, and Centennial Y2K datasets.

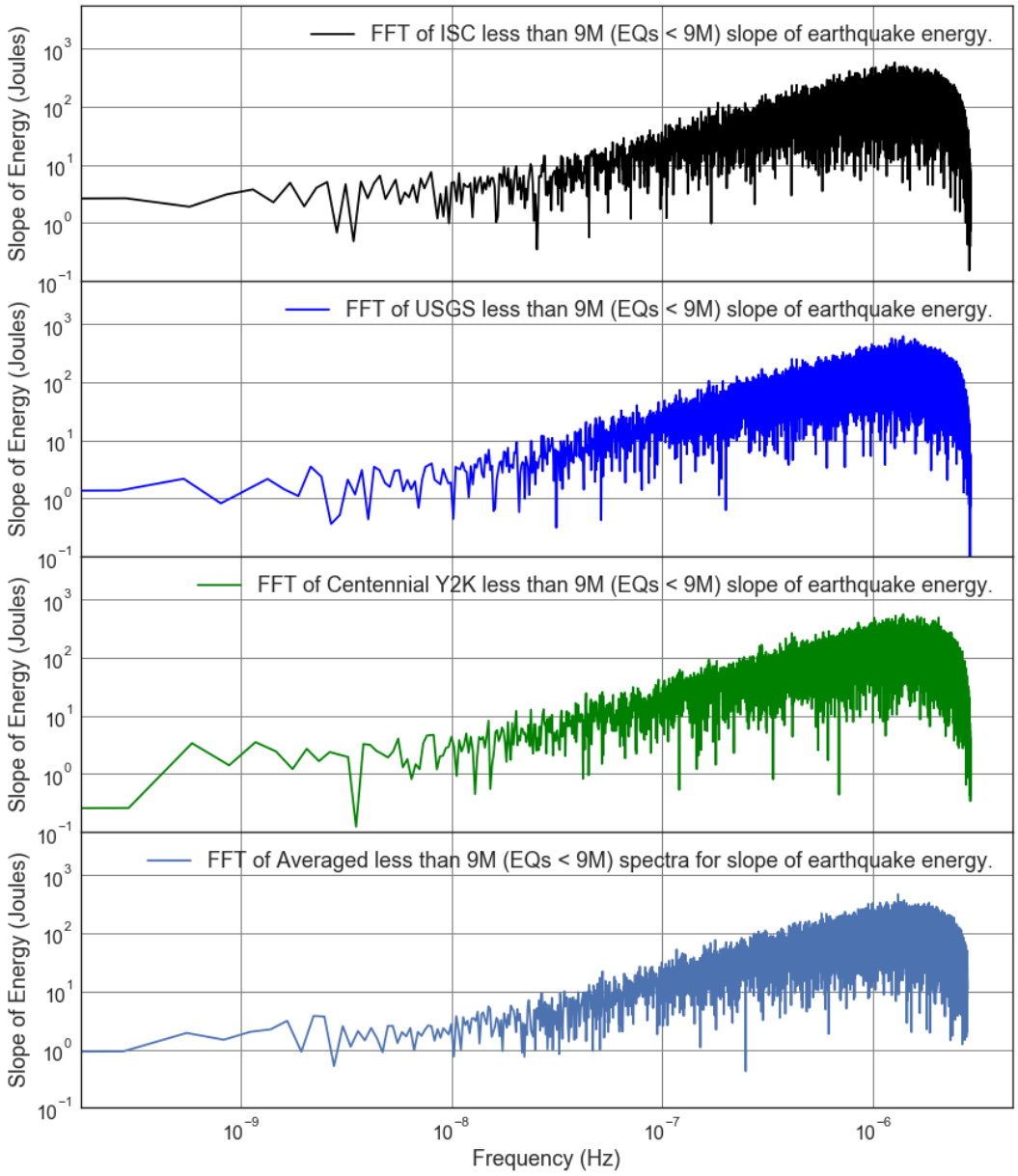

Figure 2.39: FFT Loglog Comparison Plot: Slope of less than 9M (EQs < 9M) Earthquake Energy from the ISC, USGS, and Centennial Y2K datasets.

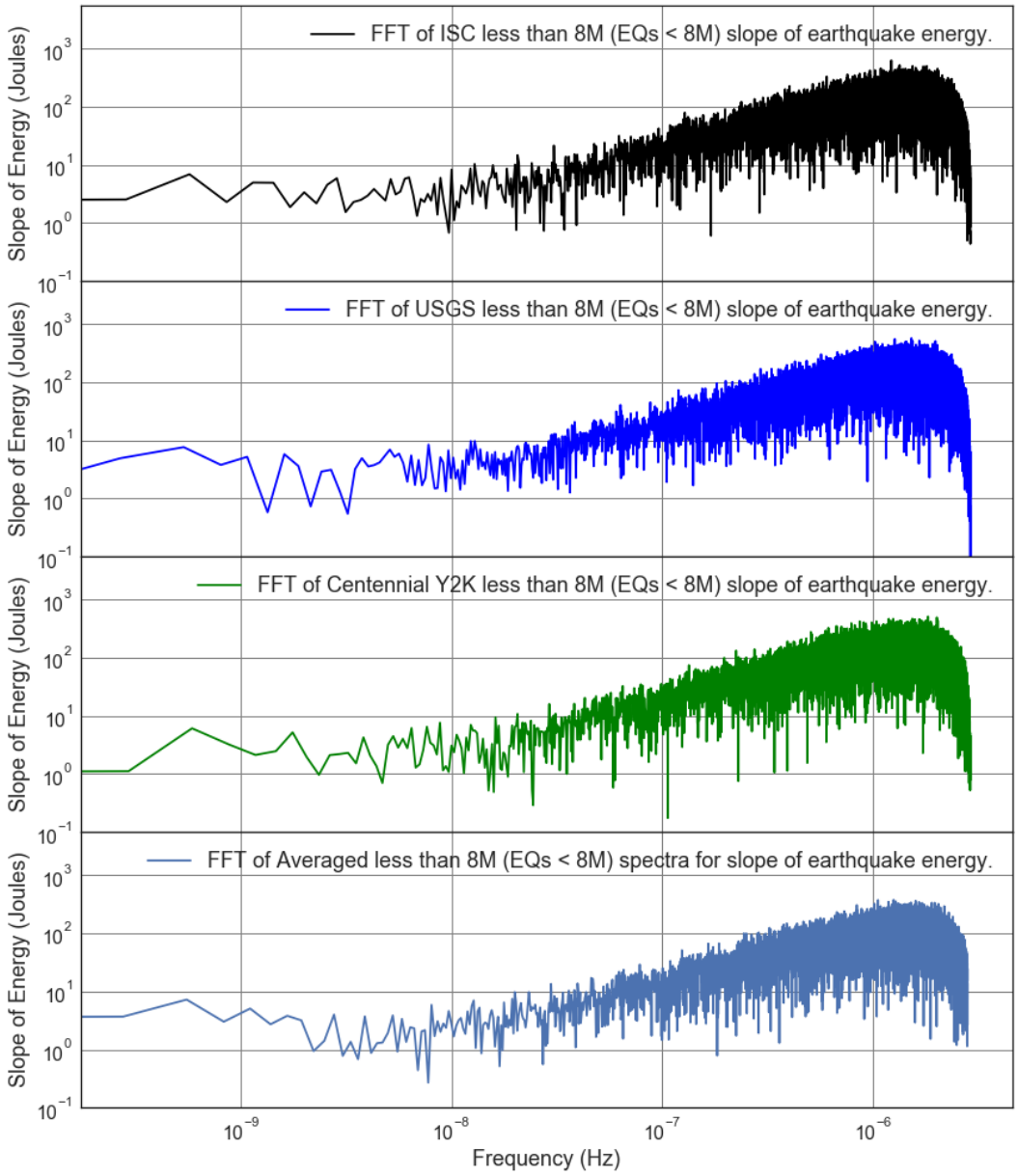

Figure 2.40: FFT Loglog Comparison Plot: Slope of less than 8M (EQs < 8M) Earthquake Energy from the ISC, USGS, and Centennial Y2K datasets.

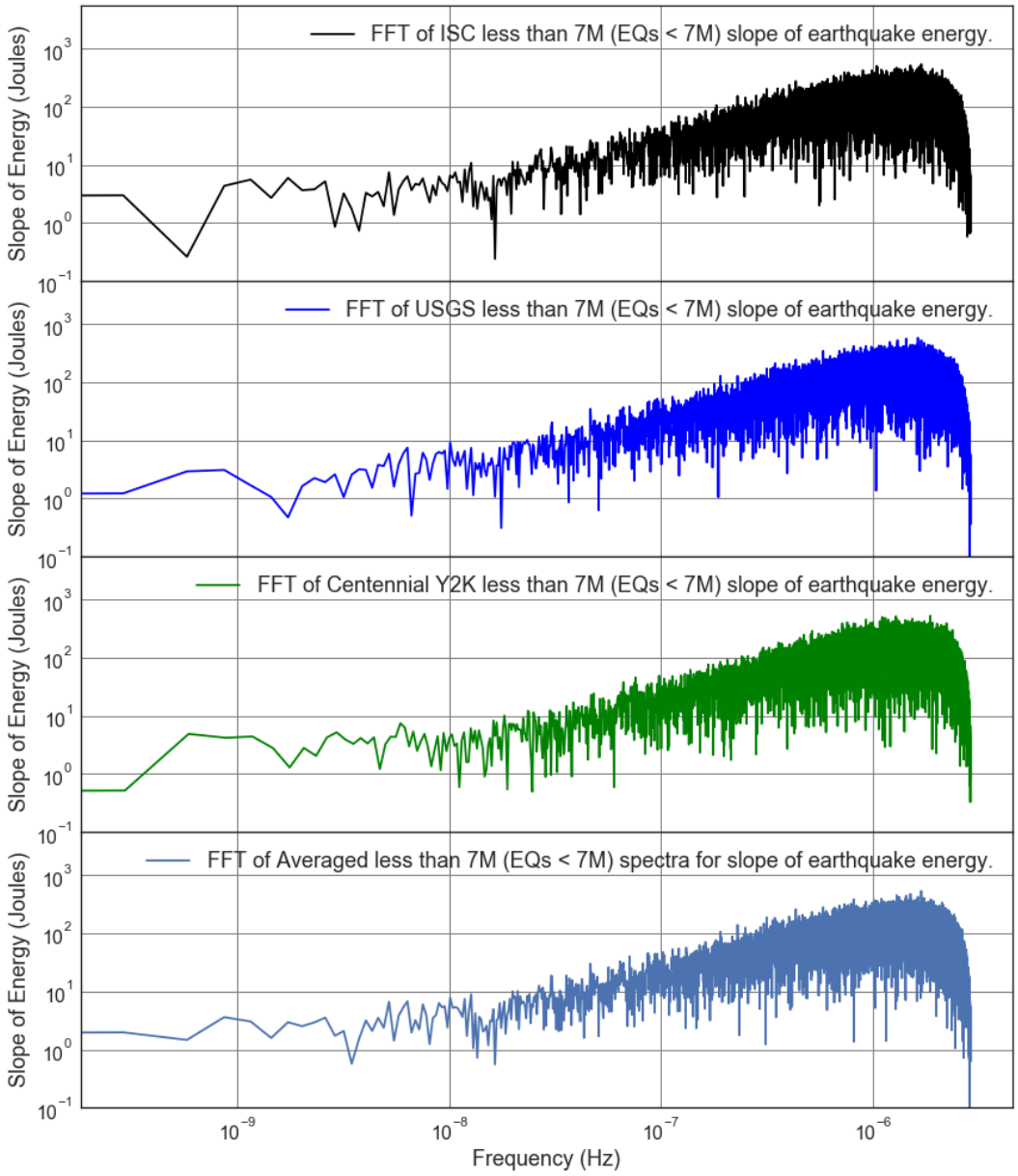

Figure 2.41: FFT Loglog Comparison Plot: Slope of less than 7M (EQs < 7M) Earthquake Energy from the ISC, USGS, and Centennial Y2K datasets.

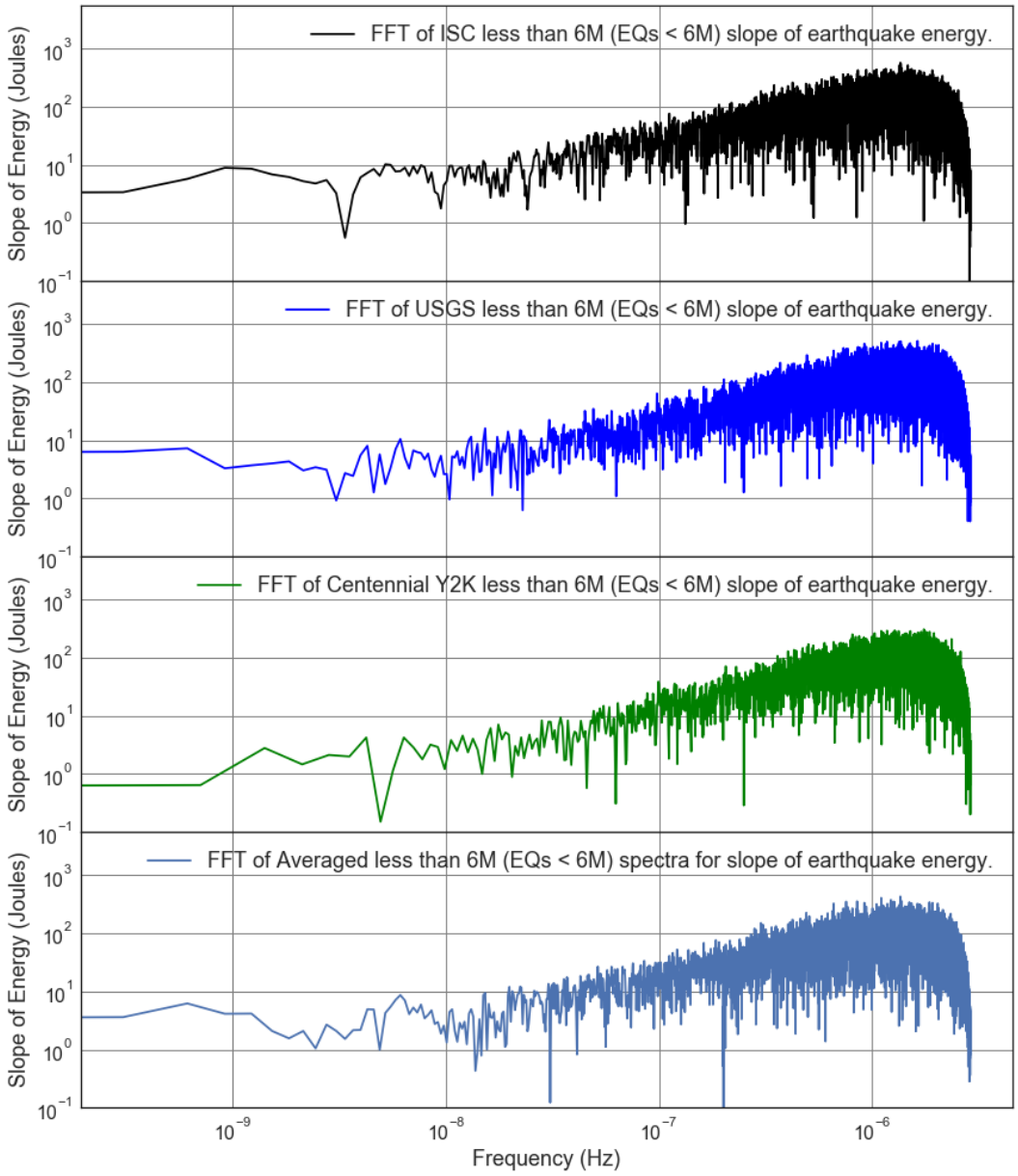

Figure 2.42: FFT Loglog Comparison Plot: Slope of less than 6M (EQs < 6M) Earthquake Energy from the ISC, USGS, and Centennial Y2K datasets.

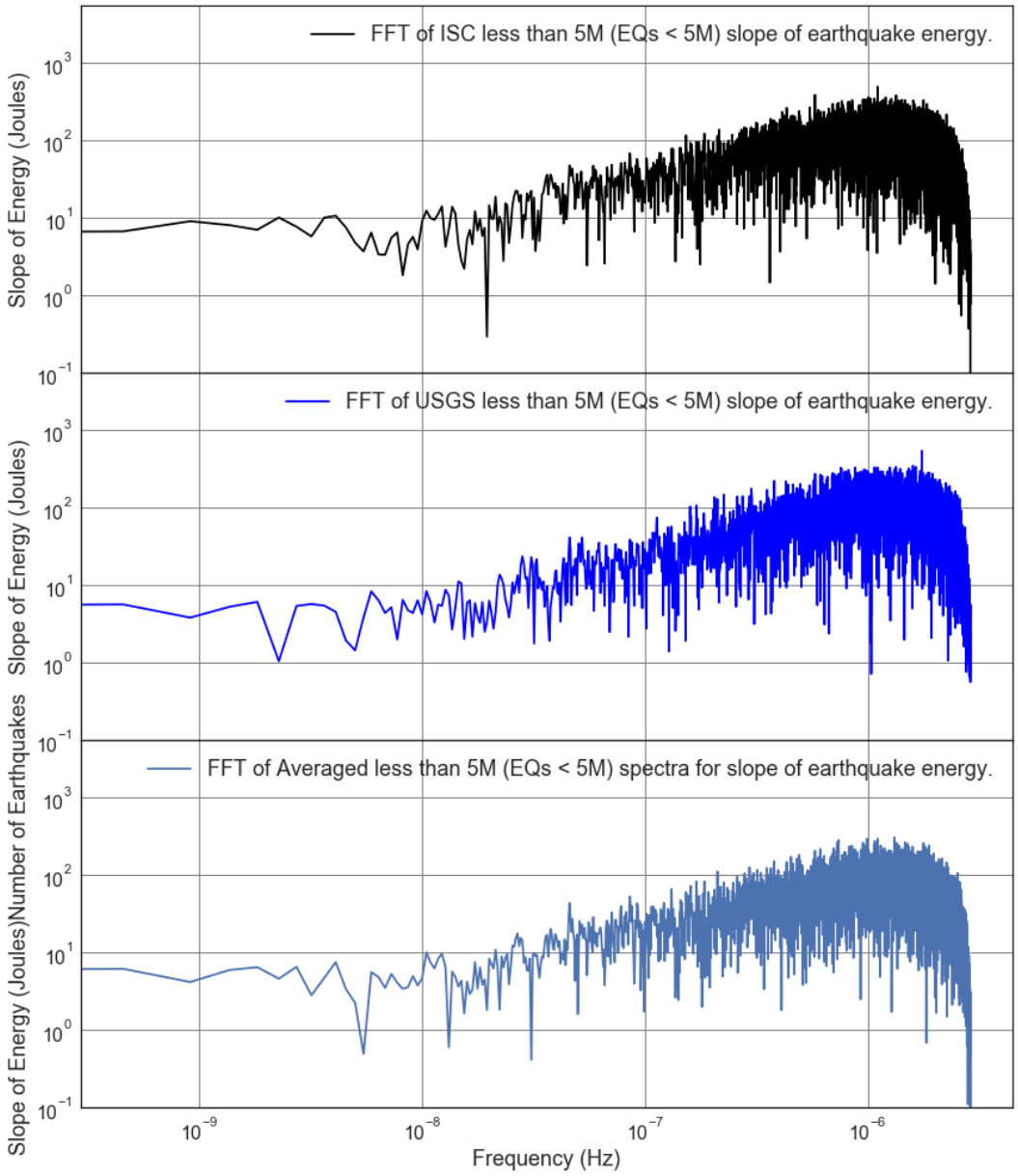

Figure 2.43: FFT Loglog Comparison Plot: Slope of less than 5M (EQs < 5M) Earthquake Energy from the ISC, USGS, and Centennial Y2K datasets.

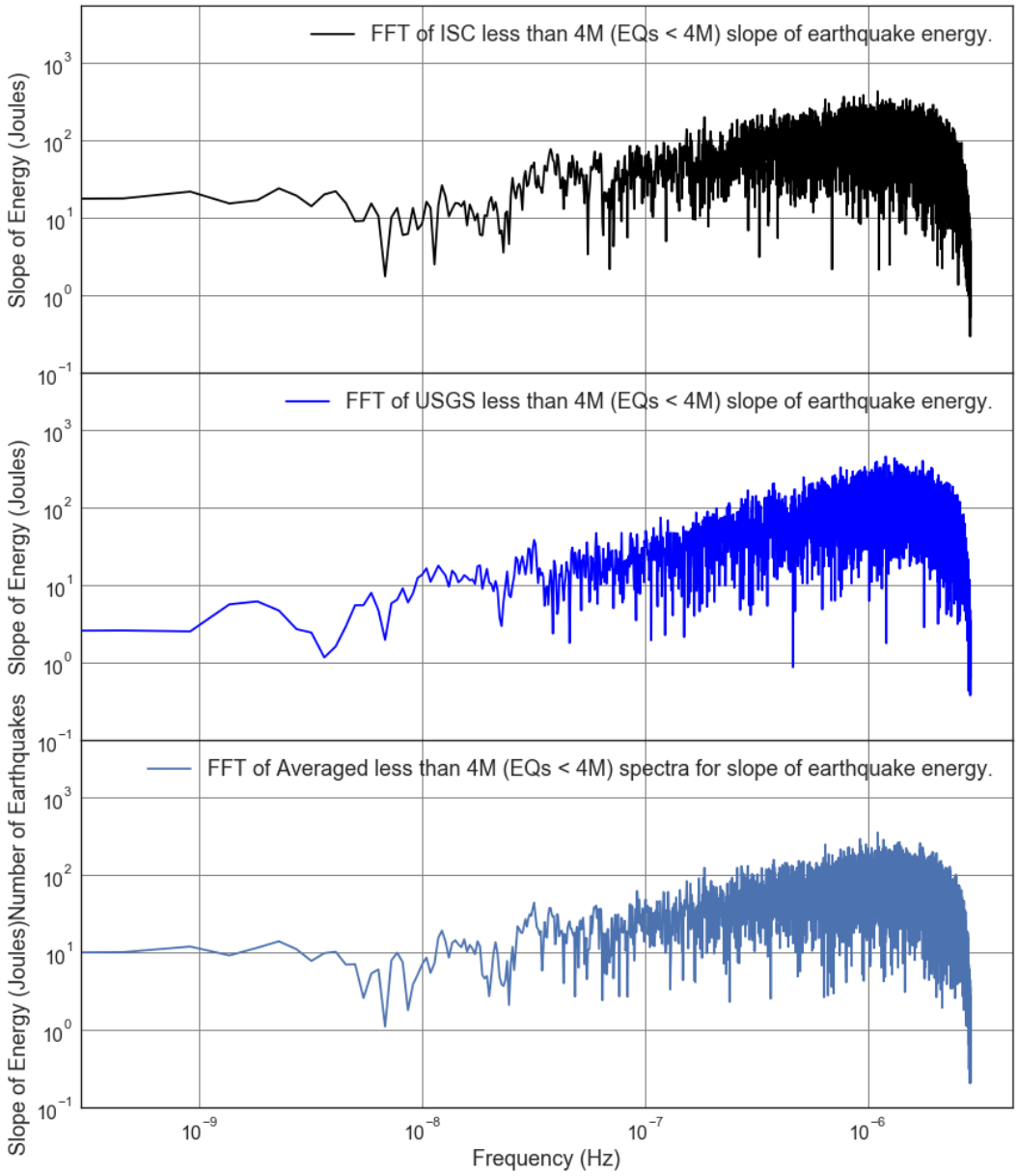

Figure 2.44: FFT Loglog Comparison Plot: Slope of less than 4M (EQs < 4M) Earthquake Energy from the ISC, USGS, and Centennial Y2K datasets.

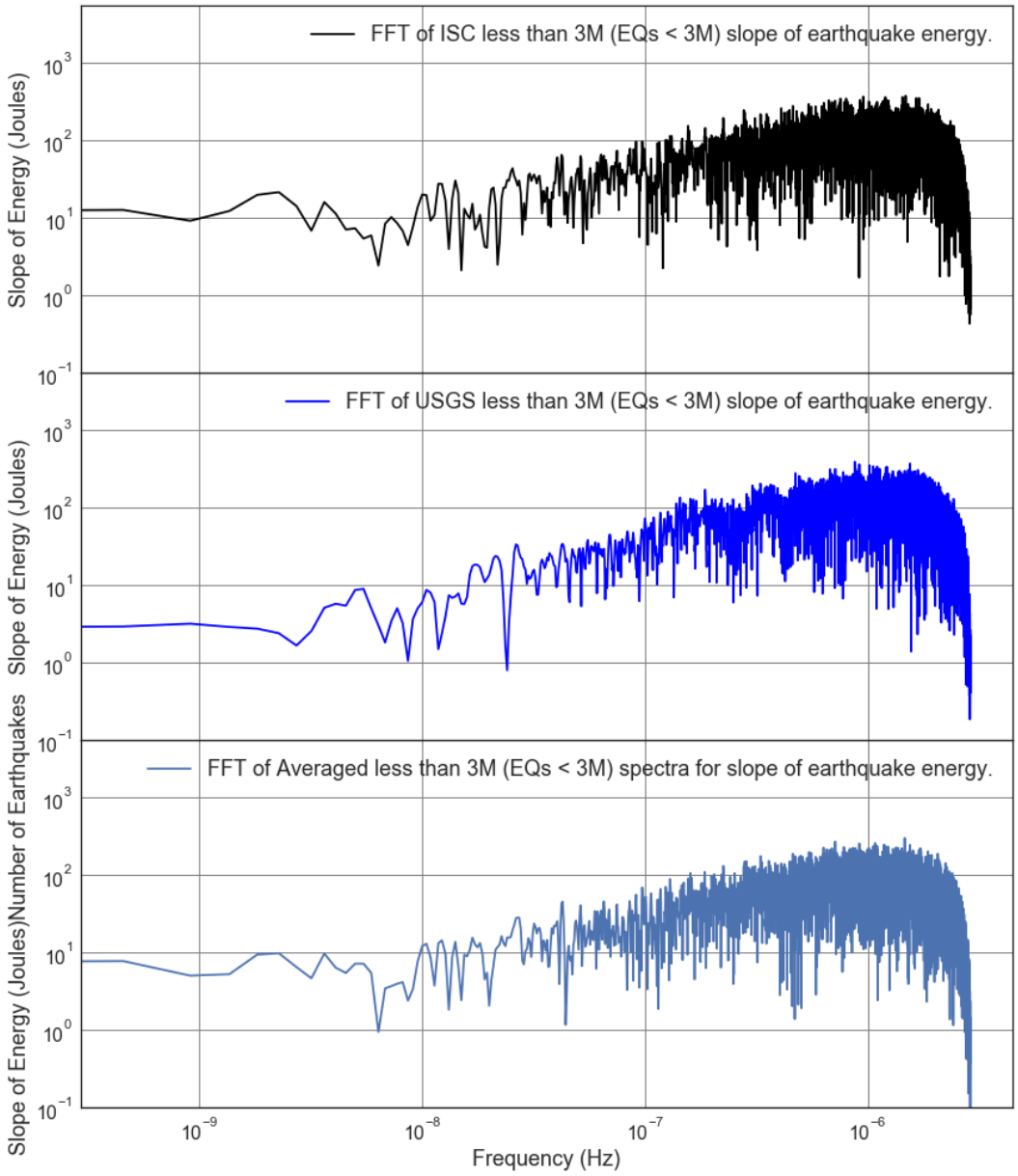

Figure 2.45: FFT Loglog Comparison Plot: Slope of less than 3M (EQs < 3M) Earthquake Energy from the ISC, USGS, and Centennial Y2K datasets.